NASA/CR—1999-208690

Validation Results for LEWICE 2.0

William B. Wright
Dynacs Engineering Company, Inc., Brookpark, Ohio

Adam Rutkowski
Case Western Reserve University, Cleveland, Ohio

January 1999

The NASA STI Program Office . . . in Profile

Since its founding, NASA has been dedicated to the advancement of aeronautics and space science. The NASA Scientific and Technical Information (STI) Program Office plays a key part in helping NASA maintain this important role.

The NASA STI Program Office is operated by Langley Research Center, the Lead Center for NASA's scientific and technical information. The NASA STI Program Office provides access to the NASA STI Database, the largest collection of aeronautical and space science STI in the world. The Program Office is also NASA's institutional mechanism for disseminating the results of its research and development activities. These results are published by NASA in the NASA STI Report Series, which includes the following report types:

- TECHNICAL PUBLICATION. Reports of completed research or a major significant phase of research that present the results of NASA programs and include extensive data or theoretical analysis. Includes compilations of significant scientific and technical data and information deemed to be of continuing reference value. NASA's counterpart of peer-reviewed formal professional papers but has less stringent limitations on manuscript length and extent of graphic presentations.

- TECHNICAL MEMORANDUM. Scientific and technical findings that are preliminary or of specialized interest, e.g., quick release reports, working papers, and bibliographies that contain minimal annotation. Does not contain extensive analysis.

- CONTRACTOR REPORT. Scientific and technical findings by NASA-sponsored contractors and grantees.

- CONFERENCE PUBLICATION. Collected papers from scientific and technical conferences, symposia, seminars, or other meetings sponsored or cosponsored by NASA.

- SPECIAL PUBLICATION. Scientific, technical, or historical information from NASA programs, projects, and missions, often concerned with subjects having substantial public interest.

- TECHNICAL TRANSLATION. English-language translations of foreign scientific and technical material pertinent to NASA's mission.

Specialized services that complement the STI Program Office's diverse offerings include creating custom thesauri, building customized data bases, organizing and publishing research results . . . even providing videos.

For more information about the NASA STI Program Office, see the following:

- Access the NASA STI Program Home Page at ***http://www.sti.nasa.gov***

- E-mail your question via the Internet to help@sti.nasa.gov

- Fax your question to the NASA Access Help Desk at (301) 621-0134

- Telephone the NASA Access Help Desk at (301) 621-0390

- Write to:
  NASA Access Help Desk
  NASA Center for AeroSpace Information
  7121 Standard Drive
  Hanover, MD 21076

NASA/CR—1999-208690

Validation Results for LEWICE 2.0

William B. Wright
Dynacs Engineering Company, Inc., Brookpark, Ohio

Adam Rutkowski
Case Western Reserve University, Cleveland, Ohio

Prepared under Contract NAS3–98022

National Aeronautics and
Space Administration

Lewis Research Center

January 1999

Acknowledgments

The authors would like to thank the NASA Lewis Icing Branch for their continued support of this research, both financially and for their help with this report. Special recognition goes to the researchers who generated the experimental data included in this report, to Dr. Mark Potapczuk for his insights into this work and especially to Tammy Langhals for digitizing all of the experimental ice tracings in this report.

Available from

NASA Center for Aerospace Information
7121 Standard Drive
Hanover, MD 21076
Price Code: A99

National Technical Information Service
5285 Port Royal Road
Springfield, VA 22100
Price Code: A99

Validation Results for LEWICE 2.0

William B. Wright
Dynacs Engineering Co., Inc.
Brook Park, OH

Adam Rutkowski
Case Western Reserve University
Cleveland, OH

I. Abstract

A research project is underway at NASA Lewis to produce a computer code which can accurately predict ice growth under any meteorological conditions for any aircraft surface. This report will present results from version 2.0 of this code, which is called LEWICE. This version differs from previous releases due to its robustness and its ability to reproduce results accurately for different spacing and time step criteria across computing platform. It also differs in the extensive amount of effort undertaken to compare the results in a quantified manner against the database of ice shapes which have been generated in the NASA Lewis Icing Research Tunnel (IRT). The results of the shape comparisons are analyzed to determine the range of meteorological conditions under which LEWICE 2.0 is within the experimental repeatability. This comparison shows that the average variation of LEWICE 2.0 from the experimental data is 7.2% while the overall variability of the experimental data is 2.5%.

II. Introduction

The Icing Branch at NASA Lewis has undertaken a research project to produce a computer code capable of accurately predicting ice growth under a wide range of meteorological conditions for any aircraft surface. The most recent release of this code is LEWICE 2.0. which is well documented in the new user manual.[1] This report will not go into the details of the capabilities of this code, as those features are well-described by the user manual.

The purpose of this report is to present the complete set of data used for validation of this code as well as identify and assess criteria which are used to validate the NASA icing codes. The measurement techniques used in this report are not necessarily the only criteria which can be used for validation but they represent one possible path.

The process for validation of an icing code is quite challenging and consists of many steps, one of which is the comparison of code results to some known solution whether experimental or analytical. This testing activity is complicated by the fact that no predefined acceptance criteria have been identified. To date, previous evaluation of the performance of ice prediction codes has been based on subjective judgements of the visual appearance of comparisons between ice shapes generated by the code and ice shapes measured in an experimental facility[2-9].

In order to accurately determine the capabilities of a prediction code it is necessary to develop quantitative measures for assessing the similarity between two ice shapes. The measurement used to make the comparison should be based on the characteristics considered most important for the purposes of the simulation process. For example, design of a thermal ice protection system may dictate that icing limits, accumulation rates, and total collection efficiency are the most important parameters to be simulated while certification of a wing for flight with an ice accretion may require that the performance characteristics of the ice shape be modeled accurately. Due to the large number of shapes, an aerodynamic performance analysis was not performed at this time.

In past reports[10-15], LEWICE has been compared to shapes created in the NASA Lewis Icing Research Tunnel (IRT). While these qualitative comparisons have been favorable, they do not demonstrate a validation process that quantitatively determines the accuracy of an ice prediction code. Comparisons are made in this report using a large subset of the data which has been generated in the IRT. The test entries which were not used for comparison represent ice shapes from proprietary tests or those tests for which the ice shapes were not digitized. The results are examined from a more quantitative approach than has been undertaken in previous efforts. Measured quantities are horn length, horn

angle, stagnation point thickness, ice shape cross section area and icing limits. This report will define the differences between experimental ice shapes and LEWICE 2.0 ice shapes as well as the differences between two experimental ice shapes, where applicable. A spreadsheet of all of the quantifiable measurements is presented along with summary tables and charts to illustrate overall comparisons.

The report is divided into seven sections. The first section will provide a brief description of LEWICE and the LEWICE 2.0 model. The second section will provide a description of the experimental data presented in this report. The third section will describe the quantitative parameters chosen and how they were measured. The fourth section presents results of the quantitative comparison. Comparison of LEWICE 2.0 with the experimental average is presented as well as the comparison of individual experimental ice shapes against the average. Spanwise variability and repeat condition variability are presented as well as the variability due to the technique used by the researcher to trace the ice shape. The fifth section presents LEWICE runs made to asses the sensitivity of the code to various inputs. The sixth section provides a description of the data on the accompanying CD-ROMs which contain the experimental data and LEWICE 2.0 predictions for this effort. The last section, given in an appendix, provides printed copies of ice shape and ice thickness plots comparing LEWICE 2.0 with the experimental data to provide the reader with the standard qualitative comparisons of the predictions.

III. LEWICE 2.0

The computer code LEWICE embodies an analytical ice accretion model that evaluates the thermodynamics of the freezing process that occurs when supercooled droplets impinge on a body. The atmospheric parameters of temperature, pressure, and velocity, and the meteorological parameters of liquid water content (LWC), droplet diameter, and relative humidity are specified and used to determine the shape of the ice accretion. The surface of the clean (un-iced) geometry is defined by segments joining a set of discrete body coordinates. The code consists of four major modules. They are 1) the flow field calculation, 2) the particle trajectory and impingement calculation, 3) the thermodynamic and ice growth calculation, and 4) the modification of the current geometry by addition of the ice growth.

LEWICE applies a time-stepping procedure to "grow" the ice accretion. Initially, the flow field and droplet impingement characteristics are determined for the clean geometry. The ice growth rate on each segment defining the surface is then determined by applying the thermodynamic model. When a time increment is specified, this growth rate can be interpreted as an ice thickness and the body coordinates are adjusted to account for the accreted ice. This procedure is repeated, beginning with the calculation of the flow field about the iced geometry, then continued until the desired icing time has been reached.

LEWICE 2.0 is different from its predecessors not through wholesale changes in the physical models but rather through an extensive effort to adjust, test and document the code to ensure: that the code runs correctly for all of the cases shown; that the quality of output is maintained across platforms and compilers; that the effects of time step and spacing have been minimized and demonstrated; that the code inputs and outputs are consistent and easy to understand; that the structure and documentation within the code makes it readily modifiable to those outside the standard LEWICE development team; and that the code has been validated in a quantified manner against the largest possible amount of experimental data. This last statement forms the basis of the comparisons in this report.

IV. Description of the Experimental Data

The experimental data described in this report and provided on the CD-ROMs are the result of a wide variety of tests performed in the NASA Lewis Icing Research Tunnel (IRT) in recent years.[16-23] Seven airfoils were selected for this comparison. These airfoils and the accompanying ice shapes represent the complete set of publicly available data which has been generated in the IRT and digitized for single element airfoils. There is some data available on multi-element airfoils, but it was considered to be an insufficient amount for validation purposes. There are a total of 400 IRT runs analyzed for this validation report, of which 169 are repeats of previous runs in the IRT. There are 442 digitized tracings at off-center-

line locations for a total of 842 experimental ice shapes.

The seven airfoils analyzed are listed as follows, in the order in which they are given in the matrix of results. The first airfoil is a modified NACA230XX series airfoil with a slight spanwise taper and sweep. At the mid-span of the test section, the thickness is 14.5% chord and increases in thickness from the floor to the ceiling of the test section. In this report, it is listed as a modified NACA23014 airfoil, as the thickness is closer to 14% at the lower end of the model. This data was originally presented in references 17-20. The cross-section at the mid-span of the test section is given in Figure 1. The database for this airfoil is comprised of 62 IRT runs, of which 22 are repeats of previous conditions. Due to the spanwise variation of the model, only 8 tracings have been digitized at off-centerline locations for a total of 70 ice shapes.

The second airfoil listed is shown in Figure 2. It is representative of a Large Transport Horizontal Stabilizer and is listed in the matrix with the abbreviation LTHS. This data was originally reported in reference 17. There are 28 IRT cases, of which only one is a repeat of a previous run. There are 52 tracings digitized at off-centerline locations for a total of 80 ice shapes.

The third airfoil in the database is representative of a business jet airfoil and given the designation GLC305. It is shown in Figure 3. This data was originally reported in reference 17. There are 84 IRT cases, of which only eight are repeats of a previous run. There are 36 tracings digitized at off-centerline locations for a total of 120 ice shapes.

The fourth airfoil in the database is the NACA0012. This airfoil has been used in several test entries over the years[16, 24, 25] in order to document the uniformity and repeatability of the IRT, especially after the tunnel has undergone modifications which could potentially alter the tunnel calibration. This airfoil is shown in Figure 4. The data from this airfoil encompasses the highest number of ice shapes which have been created in the IRT. There are 183 IRT cases, of which 126 are repeats of a previous run. There are 307 tracings digitized at off-centerline locations for a total of 490 ice shapes.

The fifth airfoil in the database is a modified NACA4415 airfoil and is shown in Figure 5. This airfoil is representative of an airfoil used in past regional aircraft design. The data was originally presented in reference 19. There are 29 IRT cases, of which 11 are repeats of a previous run. There are 39 tracings digitized at off-centerline locations for a total of 68 ice shapes.

The sixth airfoil presented is an NLF-0414 airfoil and is representative of a laminar flow design for general aviation. It is shown in Figure 6. This data comes from a very recent test in the IRT[21]. Due to time constraints, only eight cases from this test entry have been digitized and analyzed for this comparison. It was included in this report in order to add more variety to the database. Additional test points from this airfoil will be included for future validation efforts.

The last airfoil entry in the database is for a NACA0015 airfoil used for scaling studies. This airfoil is shown in Figure 7. This data is also from a very recent test entry in the IRT and will be presented in an upcoming report[23]. Again due to time constraints only six cases were processed for this report, one of which is a repeat case.

The data is taken in the IRT by cutting out a small section of the ice growth and tracing the contour of the ice shape onto a cardboard template with a pencil. The pencil tracing is then transformed into digital coordinates with a hand-held digitizer. Recently, a flat-bed scanner with digitizing software has been available to accelerate the data acquisition process. For any given IRT test run, up to five spanwise sections of the ice shape are traced and digitized in this manner. There are several steps within this process which can potentially cause experimental error. Those which can be quantified by the current technique are the spanwise variability, the repeatability error, and errors involved in the tracing technique.

Spanwise Variability

Except for the NACA23014(mod) model, all of the models used for this comparison are two-dimensional models. This means that they have a constant cross-section in the spanwise direction and are mounted in the test section without any sweep angle. Even with a two-dimensional model, the ice shape produced in the tunnel will have some spanwise variability due to the random nature of the ice accretion process. One means which has been used in the IRT to assess this variability is to take ice tracings at sev-

eral spanwise sections. In the reports mentioned previously, the variability was assessed in the same qualitative manner as comparisons of predicted ice shapes. One technique often used was to visually inspect the ice shape and the cardboard tracings for similarity in the spanwise direction. The shapes may also be digitized at each tracing location and plotted to assess the variability. This report applies the quantitative scale described in section V for assessing both LEWICE predictions and the spanwise variability of the test condition. In both cases, the reported difference will be the difference between a measurement on a given ice shape and the average of the experimental measurements for that condition.

Repeatability

Several tests in the IRT have also assessed experimental error by running the same flow and spray conditions for the same airfoil multiple times. Cases analyzed for this report have been repeated by immediately running the same condition again, by running the same condition on a different night than the original test and by running the same condition in a different test entry with the same model. In the past for each of these cases, the researcher would apply the same qualitative assessment as described earlier to assess the repeatability of the condition. This report will apply the quantitative scale described in section V for assessing LEWICE predictions for assessing the repeatability of the ice shape in the IRT.

Tracing Technique

There are several potential errors involved in the ice tracing and digitization process which were often difficult to quantify. Some of these errors are the quality of the template, the technique used by the researcher to trace the ice shape, and the digitization process.

The template is a rectangular piece of cardboard which has the contour of the airfoil cut into it. This is illustrated in Figure 8. As can be seen from this figure, if the ice shape extends beyond the dimensions of the template, it cannot be traced. Additionally, in the past the contour of the airfoil was not always cut precisely into the template so the template may not have fit squarely onto the airfoil. More recent tracing techniques use registration marks to ensure a precise fit.

The technique used by the researcher also may have an effect on the final digitized ice shape. The template may not be placed squarely on the airfoil, the researcher may only trace the tops of ice feathers or not trace feathers at all, as the ice feather may break off due to the pressure applied by the pencil. The researcher may not always trace a single continuous line for the ice shape, making the digitalization process more difficult. In order to assess these potential errors, researchers may trace the ice shape more than once or have more than one person trace the same ice shape. In the past, these tracings were then compared in the same qualitative manner as used for spanwise variability and repeatability.

Multiple tracings of the same ice shape are rarely performed in the IRT and even more rarely are both tracings digitized. Those which have been digitized are included in this report to provide a more quantitative assessment of the errors involved in the data acquisition process. It will be shown that despite the problems listed here, the quantitative errors due to tracing issues are minor in comparison to other sources of error.

V. Description of Comparison Method

This section describes the methodology used to make the quantitative measurements on experimental and predicted ice shapes. This methodology has been incorporated into a computer code called THICK which calculates and outputs the parameters described. This code was created in order to process the large number of ice shapes presented in this report. This program reads two geometry files: one for the clean airfoil and one containing an ice shape. The following sections describe the calculations made by this program.

Calculation of Ice Thickness

The ice thickness distribution for both experimental ice shapes and LEWICE ice shapes is determined by using a combination of two measurement techniques. The thickness is first measured by calculating the minimum distance from each point on the ice shape to a point on the clean surface. If the distribution of points on the clean surface is sufficiently con-

centrated, this procedure will provide a good approximation to the actual ice thickness. For this effort, each clean airfoil geometry contained over 5000 points to ensure the quality of the calculation.

An approach using the unit normal from the ice shape or from the surface will fail to determine ice thickness at every location on complex ice shapes. This is illustrated in Figure 9. As seen in this figure, the unit normal from the surface diverges outward. Even for a geometry with over 5000 surface points, a unit normal approach could not accurately capture thickness on the large and complex ice shapes presented in this report. This is especially true of experimental ice shapes which have a large amount of detail.

The minimum distance approach will very accurately determine large ice thicknesses. For very small ice thicknesses, however, the accuracy is lessened as the thickness nears the resolution of the surface geometry. This is illustrated in Figure 10.

The procedure used is to first calculate the thickness using the minimum distance approach. When this thickness becomes less than the segment length of either the iced or clean surface, it is then recalculated using the unit normal approach. Using the approach described, a unique ice thickness is determined for each point on the ice shape. At each point on the clean surface, however, it is possible to have regions where there is no recorded thickness or for a point to have more than one thickness value. This is illustrated in Figure 11.

In the first case where there is no thickness recorded, a thickness value at the clean surface can be interpolated from the values which have been obtained. In the second case where more than one value exists, the max. ice thickness value is recorded.

Determination of Icing Limits

The upper and lower limits of ice accretion for both experimental shapes and LEWICE shapes are easily found from the ice thickness distribution. They are located at the points on the clean airfoil where the ice thickness first changes from zero as measured from the trailing edge. Experimental ice shapes may have sections where parts of the ice (ice feathers) are isolated from the main ice shape. This definition extends the icing limit to include this section of the ice shape. It should also be noted that the definition used in this report for icing limit is distinct from the impingement limit, which only refers to the extent of water collection on the airfoil. Both the wrap distance from the leading edge and the x-distance are recorded for each icing limit. The icing limits are illustrated in Figure 12 on a sample ice shape. Figure 13 shows the icing limits on the ice thickness plot for this ice shape.

Determination of Maximum and Minimum Thicknesses

Three ice thicknesses were selected for the quantitative analysis, the upper surface max. thickness, the lower surface max. thickness and the min. thickness between these two maxima. These thicknesses are illustrated in Figure 14. In this illustration, the upper surface and lower surface maxima clearly correspond to the classic definition of a glaze ice horn. For other conditions this may not be the case, hence the use of the term "max. thickness" rather than "horn thickness". This differentiation is usually found on smaller ice shape for which the max. thickness is not easily seen. This is illustrated in Figure 15.

For the upper surface and lower surface max. thickness, the x,y locations at the maxima are also saved for calculation of a max. thickness angle. The min. thickness between the two maxima is also recorded. This thickness is often termed the "stagnation point thickness", but the aerodynamic stagnation point is not necessarily at this location. In this report, the term "min. leading edge thickness" is used instead.

For a rime ice shape, the term "horn" does not apply, nor are there two distinct maxima to record. For this case, only the max. ice thickness and the x,y location at this maxima are recorded.

Determination of Max. Thickness Angle

The max. thickness alone does not adequately capture all of the necessary quantitative attributes desired. Some indication of where that max. thickness occurred is also desirable. In this report, the x,y locations at the max. thickness were recorded for each ice shape, both experimental and for LEWICE. An angle at the max. thickness is then calculated. The reference location for all cases is the center of

the inscribed circular cylinder at the leading edge for each airfoil. This is illustrated in Figure 16.

Again note the terminology of "max. thickness angle". As discussed earlier, not all ice shapes have a classic glaze ice "horn" but every ice shape has a max. thickness. Where a glaze ice horn does exist, however, this measurement does define the "horn angle".

Determination of Ice Area

The iced area calculated for this report is not a true area. A more simplified calculation was performed by integrating the ice thickness calculated with respect to the wrap distance, as given by Equation 1. The approach used is valuable for quantitatively assessing ice shape features such as horn width which are not included in the other parameters.

$$A = \int t\,ds \tag{1}$$

For the large number of points used on the clean surface of each airfoil, the calculation given is a reasonable approximation of area. Three areas are recorded: the total iced area, the lower surface area and the upper surface area. The lower surface area is defined as the ice area below the leading edge and the upper surface ice area is calculated by subtracting the lower surface value from the total. For complex ice shapes where the ice thickness is multiply defined as is shown in Figure 11, this method for calculating ice area will result in an overstatement of the actual ice area. However the methodology is consistent for both experimental ice shapes and for LEWICE ice shapes.

VI. Procedure for the LEWICE Runs

There are 231 cases which were run with LEWICE for this validation report. This is the complete set of unique conditions, as 169 of the 400 test entries are repeat conditions. All of the cases run for this validation test were performed using the same procedure on a Silicon Graphics Indigo2 to ensure the consistency of the LEWICE predictions. It is well known that a user of an ice accretion code may alter the ice shape prediction by varying the time step and/or the panel spacing until a desired prediction is achieved. This procedure was not followed for these validation runs. For every run, the point spacing was fixed at a value of $4*10^{-4}$ (dimensionless). This was the smallest value which could be used for the array sizes in the program. The time step for all runs was 1 minute for cases where the accretion time was 15 minutes or less. For longer runs, an automated procedure was implemented based on accumulation parameter. When the accumulation parameter exceeded 0.01 for that time step, a new time step was started. The number of time steps is calculated internally in the program by Equation 2.

$$N = \frac{(LWC)(V)(Time)}{(chord)(\rho_{ice})(0.01)} \tag{2}$$

where

LWC = liquid water content (g/m^3)
V = velocity (m/s)
Time = accretion time (s)
chord = airfoil chord (m)
ρ_{ice} = ice density = $9.17*10^5$ g/m^3

The variability of LEWICE results for various time steps and point spacings is discussed in the section on Numerical Variability in this report. The LEWICE cases had an additional correction due to the use of a potential flow code for the flow solution. As illustrated in Figure 17, a potential flow code will overpredict lift coefficient especially at high angles of attack. To compensate for this, all LEWICE cases are run using a corrected angle of attack. This correction is determined by equating the lift coefficient predicted by LEWICE on the clean airfoil for a given case with the lift coefficient on the airfoil at the angle of attack run in the tunnel.

VII. Quantitative Results

For each of the 842 experimental ice shapes and 231 predicted ice shapes, the quantitative measurements described in a previous section were taken and then entered into a Microsoft Excel® spreadsheet. A description of the exact contents of this spreadsheet is given in the description of the contents of the CD-ROMs which accompany this report. Each of the 231 ice shapes is plotted against the tunnel centerline ice shape for that condition. The ice thickness distribution is also plotted. These figures are listed in the appendix and a brief description of the plots is presented there. This section will describe the quantitative comparison between the LEWICE

predicted shape and the experimental average as well as the comparison of individual experimental ice shapes to this average. In each case, the experimental average for a given quantity is the average of all experimental ice shapes at that condition. Measurements for repeat runs and off-centerline measurements are averaged with the centerline measurement to arrive at this value.

Icing Limits

The icing limits are the chordwise locations on the ice shape on the upper and lower surface where the ice shape merges with the airfoil. Both the wrap distance from the leading edge and the x-distance are recorded for each icing limit. The results presented here are for the wrap distance values. Results for the x-distance values can be easily calculated in the spreadsheet if the user prefers that reference.

Figure 18 shows the results of these measurements for both the experimental ice shapes and for LEWICE. These results are presented as a percentage of chord in order to normalize the results for different cases. This figure shows that the experimental variation in the lower icing limit is 2% of chord while the LEWICE result lies within 6% of chord from the experimental average value. This result uses the absolute error for each case in order to compute the average. Contrary to popular belief, in the majority of cases LEWICE underpredicts rather than overpredicts the icing limit as compared to the experimental data. This result can likely be attributed to the use of a monodispersed drop size when obtaining the predicted result.

Max. Ice Thickness (Horns)

The details of the ice thickness calculation were presented in the section on Description of Comparison Method. As discussed in this section, the measurement of a max. thickness is not necessarily the thickness of a glaze ice horn. Where the ice shape does have a glaze ice horn, the max. thickness does give the horn thickness. In order to compare different conditions with different chord lengths and accretion conditions, the individual ice thicknesses were nondimensionalized by the maximum accumulation thickness as given in Equation 3.

$$t_{max} = \frac{(LWC)(V)(Time)}{\rho_{ice}} \quad (3)$$

Figure 19 shows the dimensionless difference in ice thickness for the three ice thickness measurements made in this report. Results are presented for the variation of tunnel repeatability, spanwise variability, tracing error as well as for the overall experimental error and for LEWICE. This figure shows that the max. thicknesses can be measured to within 5% and that the average difference between LEWICE and the experimental average value is 11% for max. thickness.

Ice Area

The comparison of ice area for the different cases also poses a problem. A fair comparison across the varied conditions and airfoil sizes is difficult. In this report, the area difference has been nondimensionalized by the maximum accumulation thickness given earlier and by the airfoil thickness. It should be noted that the absolute values for ice area are maintained in the Excel® spreadsheet so that the users of this data can make their own comparisons.

Figure 20 shows the results for the ice area comparison. Values for the upper surface ice area, lower surface ice area and overall ice area are shown for each of the categories described earlier. This figure shows that the experimental difference in ice area is less than 4% on the scale given while for the LEWICE results the variation from the experimental average is approximately 10%.

Angle at Max. Thickness (Horn Angle)

As described earlier, the horn angle was measured with respect to a horizontal line which goes through the center of the inscribed cylinder at the leading edge. This angle was measured for all ice shapes whether or not they fit the classical definition of having a glaze ice horn. Many experimental ice shapes were in the form of distributed roughness with several peaks which can cause a large amount of scatter in the experimental results shown.

Figure 21 shows the variation between the max. thickness angle for LEWICE and for the experimental average value as well as the variation for individual experimental ice shapes to the same average using the categories described earlier. Results are pre-

sented in degrees. This figure shows that the variation in the experimental data is 6 degrees for the upper angle, 10 degrees for the lower angle and 13 degrees for the difference between these angles. The LEWICE difference from the experimental average are 16 degrees for the upper angle, 30 degrees for the lower angle and 33 degrees for the angle difference.

Overall Assessment

Once the individual measurements are taken for each ice shape, it becomes useful to create an overall assessment of the ice shape prediction. Since each measurement is different, several methods could be used to assess the overall difference between two ice shapes. Eight of the 11 measured values presented in this report have been nondimensionalized. Angles do not have a characteristic measure to use for nondimensionalization, so the three angle criteria are reported in degrees. Since not all of the measured quantities can be nondimensionalized, two overall assessment factors have been calculated. The first overall assessment was determined by an average of the eight individual dimensionless values and the three angle criteria in degrees. The second overall assessment was calculated by using only the eight dimensionless measurements.

Figure 22 shows the comparison of the first overall assessment for each of the experimental errors and for LEWICE. This calculation shows an average overall difference of approximately 4.4 for the experimental data base and 12.5 for LEWICE. Since the angle criteria are not dimensionless, these numbers cannot be considered a percent difference. Figure 23 shows the comparison using the second overall assessment. This second calculation shows an average overall difference of 2.5% for the experimental data and 7.2% for LEWICE. In order to determine if this simple average is a good assessment of the variation, plots were made of the average variation for the experimental shapes and for the LEWICE shapes.

Figure 24 shows an example of two ice shapes which are near the overall experimental average. This plot shows the spanwise variability from a data point in the NACA4415(mod) database. The qualitative comparison of these two ice shapes suggests that the overall assessment parameter is a reasonable approximation. Similarly, Figure 25 shows an example which is at the average variation for the LEWICE cases. The qualitative assessment of this comparison also agrees with the overall assessment parameter used.

Improvements to methodology

The technique used in this report for quantitative comparison of ice shapes represents only one possible path for quantitative validation of code results. Ruff[26] proposed an alternate methodology for creating an overall assessment of ice shape prediction. Other methods can also be tested for creating an overall assessment of ice shape prediction. Due to the number of cases in this database, an important consideration is the efficiency at which quantitative measurements can be taken and entered into a spreadsheet for analysis. The current technique used a stand alone utility program to generate the ice thickness distributions. This code was very useful in generating the data needed for this comparison, but the process of transferring the information to the spreadsheet was time consuming. More efficient methods for acquiring the quantitative parameters will be developed in the future.

The definition of max. thickness angle used in this report is not the only possible definition. Other possible definitions could use the chord line of the airfoil instead of a horizontal line. The reference point could be selected as the leading edge of the airfoil or the point on the clean surface where the ice thickness was defined. Due to time constraints, the definition presented in this report was the only one calculated from the ice shapes.

It was stated in the introduction of this report that a quantitative analysis is only one facet of the code validation process. Once the comparison of ice shape has been made, it would be useful to quantify the difference in aeroperformance based on the quantitative difference in geometry. This process would be very time consuming to perform on the entire database even at the fast processor speeds available now. A comparison of a selected number of these cases is being planned at this time. This comparison would calculate the difference in predicted aeroperformance for a given difference in ice shape, using both experimental ice shapes and predicted ice shapes from LEWICE. For example, this comparison would try to determine if the difference in aeroperformance for two ice shapes which are 10% different is

consistently greater than the difference in aeroperformance for two ice shapes which are only 5% different.

VIII. Numerical Variability

This section of the report will describe the additional LEWICE cases which were performed to determine robustness of the code and variability to various parameters. The parameters shown are not necessarily input variables to LEWICE 2.0 but represent advanced features which could be utilized by sophisticated users who wish to recompile the source code.

Variability of Code to User Inputs

This section will illustrate the differences in output generated by LEWICE 2.0 due to user inputs. The inputs selected were the point spacing (parameter DSMN), the time step, and the droplet distribution. Due to time constrains, only qualitative comparisons of the variability can be made in this report.

Point Spacing

All of the cases performed for the quantitative comparison used a spacing of $4*10^{-4}$. This is listed in the input file as variable DSMN. Twelve additional cases were ran to assess the variability of LEWICE to this parameter. The cases were selected by choosing the largest ice accretions for each airfoil as these cases were considered to be the most susceptible to variation. Some smaller ice accretions were chosen to test this hypothesis. The ice shapes and ice thickness plots are shown in Figures 26-41. Most of the cases show only a slight variation in ice shape due to point spacing in the range studied. A range of $2*10^{-4}$ to $8*10^{-4}$ was chosen for this comparison. The largest variation in ice shape due to point spacing was seen in Run 103 from the LTHS database.

Time Step

All of the cases ran for the quantitative comparison used a automated time step procedure for those cases. An additional 18 runs were made to illustrate the variation when different time steps are used. Most of the cases were longer ice accretions as these cases were again considered more susceptible to variation. These cases are shown in Figures 42-59. These cases show a large variation in ice shape prediction due to time step, although the variation decreases as the number of time steps increase. This illustrates the need to use a sufficient number of time steps in order to reduce the variation due to this effect. In LEWICE 2.0, the automated time step procedure has been adopted as the default case. If the user does not wish to use this feature, it can be turned off with an input flag. A warning message will be issued at the start of the run advising the user as to the proper number of time steps recommended for this run.

Droplet Distribution

All of the cases used for the quantitative comparison used a monodispersed drop size distribution. There were 21 cases out of the 231 conditions which were then repeated using a Langmuir "D" dropsize distribution. The Langmuir "D" distribution for a 20 micron MVD is given in Table 1. The conditions selected were chosen to provide an example of the range of drop sized ran for that airfoil.

Table 1: Langmuir "D" Drop Size Distribution

%LWC	Ratio	Drop size
0.05	0.31	6.2
0.10	0.52	10.4
0.20	0.71	14.2
0.30	1.00	20.0
0.20	1.37	27.4
0.10	1.74	34.8
0.05	2.22	44.4

The ice shape and ice thickness for these runs are compared to the baseline monodispersed case and are shown in Figures 60-101. Qualitatively, there is very little difference in the shape of the ice due to the droplet distribution. The ice thickness plots illustrate the quantitative difference which occurs mostly in the icing limits, which is to be expected. The maximum increase in icing limit for these cases was 4.5" for Run 120r5 in the NACA23014(mod) database.

Variability of Code for Advanced Features

This section describes the variability of LEWICE for advanced features which can only be selected by modifying the code itself. These inputs were removed

from the input due to their effect on the ice shape as will be illustrated in this section. This data is being shown for users who may wish to modify the code. The features selected are smoothing, case study, maximum point spacing and angle criteria.

Modification of the LEWICE code is undertaken by the user at their own discretion. NASA cannot assume responsibility for any such modification of the code or for support of user modified versions of LEWICE.

Maximum Point Spacing and Angle Criteria

In LEWICE version 1.6, the user had control of three variables which determined point spacing on the body. Those were the minimum point spacing (DSMN), the maximum point spacing (DSMAX) and a panel angle criteria (DDANG). The current scheme used in LEWICE 2.0 for point distribution uses only the minimum criteria DSMN. To illustrate this, eight additional cases were ran to show the effects of the other variables. The ice shapes for these cases are plotted in Figures 102-109. As seen in these plots, the ice shape is completely unaffected by these parameters. The inputs for these variables have been removed for the release of version 2.0.

Smoothing

The ability of an ice accretion code to automatically add ice in a consistent manner for multiple time steps may be enhanced by smoothing the iced surface prior to the next time step. A smoother ice shape can also be used to create molds for experimental entries investigating performance effects and can be more easily gridded for use in Naviér-Stokes flow solvers. For these reasons, techniques are being developed to smooth the ice shape.

One such method has been named "blanket" smoothing because it overlays a smooth layer on top of the existing rough ice shape. The details of this method will not be presented here. The routines for this method have been made inactive in the official release of version 2.0 but can easily be reactivated by users who understand the effects these methods can have on the ice shape.

Six additional cases have been run with the blanket smoothing activated to show its effect on ice shape prediction. The ice shapes and ice thickness distributions are plotted versus the LEWICE predictions without smoothing in Figures 110-121. Three of these cases show little effect of the ice shape due to smoothing, but the other three show that this smoothing technique can significantly alter the ice shape prediction and artificially add a significant amount of ice to the surface. It is for this reason that this methodology was inactive for all of the validation runs in this report and has been inactivated in the LEWICE 2.0 release. Further research is under way to develop improved methods for smoothing the ice shape.

Case Study

A feature existed in LEWICE version 1.6 to run a parameter study on a given variable. For example, all variables could be held constant except temperature to study temperature variations on a particular ice shape.However, it was discovered that the ice shapes generated using this case study did not always match the prediction when that case was ran alone.

A case study was run using time step as the varying parameter. This means that LEWICE ran four cases consecutively with each case using a different time step. These results were compared to previous cases where the four cases were each ran separately. This is shown in Figures 122-129. These figures show that the predicted ice shape ran using the case study is different from the ice shape predicted when a case study was not used. For this reason, this feature has been made inactive in version 2.0.

Compiler and Platform Uniformity

This section demonstrates the differences in output generated by LEWICE 2.0 when it is run on different machines and compilers. The three computers used for this purpose were an SGI Indigo2 running IRIX 6.2 and MIPSPro Fortran 7.2, a Gateway2000 Pentium II running Windows 95, and a Compaq Presario Pentium running Windows 95. The PC compilers used were Absoft Pro Fortran 1.0.2, Digital Virtual Fortran 5.0.A, and Lahey Fortran 90 v4.5. The Microsoft PowerStation compiler was not used as that product had been sold to Digital and that company offers Virtual Fortran 5.0 as an upgrade to PowerStation owners. It is believed that results for those two compilers should be comparable.

The use of specific computers or compilers is not meant as an endorsement of any particular product, but are mentioned for demonstration purposes. It was desired to ensure that LEWICE could run accu-

rately on various computers and compilers due to the likelihood that users would have hardware that was different from that used to develop the program.

Sixteen cases were run for each possible combination of compiler and platform. Fifteen of these cases represent cases which can be compared to the experimental data on the CD-ROM. The other case was generated using a cylinder as some users reported a platform variability for cylinder cases with previous versions of the code. The results of this comparison are shown in Figures 130-161. All of the cases ran successfully on each computer. In general, the results are satisfactory, with only slight differences in the ice shapes generated. The largest variation was seen in Figure 141.

IX. Contents of the CD-ROM

This report includes two CD-ROMs of data which were used for the code validation process. The data includes ice shapes for both experiment and for LEWICE, all of the input and output files for the LEWICE cases, JPG files of all plots generated, an electronic copy of this report, and a Microsoft Excel® spreadsheet containing all of the quantitative measurements taken. The first part of this section describes the file structure on the CD-ROMs. The second section describes the contents of the information in the files, including an explanation of the contents of the Excel® spreadsheet and formulas used.

Description of files and folders

The top level directories are named LewInput, LewOutput, ExpData and jpgfiles. The top level directory also contains an electronic copy of this report and a copy of the Excel® database with the quantitative measurements. LewInput contains all of the LEWICE 2.0 input files used to generate the data in this report. LewOutput contains all of the LEWICE 2.0 output files generated for this report and the analysis output files of the final LEWICE ice shape prediction. The analysis output files were generated to create the quantitative comparison with the experimental data. ExpData contains the digitized ice shape from the IRT and output analysis files used for the quantitative comparison. The directory jpgfiles contains all of the JPG format files of the printed ice shape and ice thickness comparison plots.

Within each of these directories are subdirectories named for each of the seven airfoils included in this report. The seven airfoils are: GLC305, LTHS, NACA0012, NACA0015, NACA23014(mod), NACA4415(mod) and NLF414.

The directory LewInput also contains a subdirectory named Geometry containing the input geometries for LEWICE 2.0 and the input geometries for the program used for creating the ice thickness profiles (program THICK). These two sets of inputs are in subdirectories Lewice and thick inside the directory Geometry (LewInput\Geometry\thick and LewInput\Geometry\Lewice). The airfoil subdirectories within LewInput contain the main LEWICE 2.0 input file for each of the LEWICE 2.0 cases ran. The information in the input file is described in the LEWICE 2.0 User Manual. The names of each file correspond to the IRT run number for that condition.

The directory LewOutput also contains a subdirectory named numerics containing LEWICE 2.0 cases ran for determining the robustness of the program and the variability of the output to various factors. These cases are described in the section on numerical variability. The airfoil subdirectories within LewOutput contain a directory for each LEWICE 2.0 run. The name of the directory corresponds to the IRT run number for that condition.

Each LEWICE 2.0 run produces the following 10 files: beta.dat, final.dat, flow.dat, htc.dat, ice1.dat, imp.dat, junk.dat, misc.dat, pres.dat, and xkinit.dat. In addition, each of these directories also contain output from the program THICK. These files are named clean.dat, echo.dat and iced.dat. A JPG format screen shot of the interactive graphics used on an SGI machine is also included in this directory and is named snap.jpg. The output from the program THICK is generated using the input files in the directory LewInput\Geometry\thick and the file final.dat containing the final ice shape predicted by LEWICE 2.0.

The airfoil subdirectories contained within the directory ExpData contain a directory for each digitized ice shape. The subdirectory names correspond to the IRT Run number for that condition followed by the spanwise location of the tracing as measured from the tunnel floor. Each of these subdirectories contains the original digitized ice shape for that run and location. The digitized ice shape file will be ASCII format (.txt). A single number at the top of this file

denotes the number of data points in the file and the remaining lines contain the x,y coordinates of the ice shape in inches. The digitized ice shape is also present in spreadsheet format (.xls,.wk1,.wk3) for most cases. The subdirectories will also contain output files from the ice thickness analysis program THICK. These three output files (clean.dat, iced.dat, and echo.dat) are the output generated when running THICK with the input file in directory Geometry\LewInput\thick and the text format of the digitized ice shape file.

The directory jpgfiles contains the seven airfoil subdirectories and subdirectory numerics. The airfoil subdirectories contain plots comparing LEWICE 2.0 with the experimental data. Both ice shape and ice thickness comparison plots are present. The name of the files correspond to the IRT Run number for that case plus "ice" to denote an ice shape plot or "thick" to denote an ice thickness plot. The subdirectory numerics contains plots of the LEWICE 2.0 runs made to determine robustness and variability of the program to selected inputs. The inputs selected will be described in the section on numerical variability.

File Contents

This section will give a brief description of the data within a given file name.

LEWICE Output Files

This list contains a description of the LEWICE output files included in this report. There are other output files which the user can activate such as a printout of the individual trajectories which are not included in this list. Refer to the upcoming LEWICE 2.0 User Manual for a complete listing of input and output files. The value in parenthesis is the title used for that column of data in the output file.

beta.dat - collection efficiency output for each time step. Columns are dimensionless wrap distance from the stagnation point (labeled S/C) and collection efficiency (labeled BETA). The actual tests in this report were ran on an alpha version of LEWICE 2.0. The output data for the official version will be very similar, but the format has been changed. Additional columns for the official release include dimensionless wrap distance as measured from the airfoil hilite, and the dimensionless x,y coordinates of the airfoil.

final.dat - contains the final ice shape produced by LEWICE. The first row contains the number of points on the ice shape and the remaining lines contain the x,y coordinates of the ice shape in inches. This file format can be used as input to the utility program THICK.

flow.dat - contains the output from the potential flow solution at each time step. Columns contain the panel index (I), dimensionless x,y coordinates (X, Y) at the panel center (not at the endpoints as with other files), wrap distance as measured from the lower surface trailing edge (S), dimensionless tangent velocity (VT), pressure coefficient (CP), a separate panel index for each body (J), the panel source/sink value (SIGMA), and the dimensionless normal velocity (VN). For each time step, two flow solutions are generated and an additional flow solution is generated on the final ice shape before the program exits. This will be discussed in more detail in the upcoming Users Manual.

htc.dat - contains the convective heat transfer coefficient at each time step. Columns are segment number (SEG), dimensionless wrap distance from stagnation (S), heat transfer coefficient (HTC) in W/m^2/K, and Frössling Number.

ice1.dat - contains the ice shape for the first body at each time step. Columns contain the coordinates of the ice shape (X,Y) in inches, ice thickness (THICK) in inches and wrap distance from the stagnation point (S) in inches. Data is output in inches as all of the experimental data is taken in inches. As of this writing, it has not been decided if the official 2.0 release will contain inches in the output or dimensionless units.

imp.dat - contains information related to the impingement limit for each time step. Columns are droplet size (microns), dimensionless x-coordinate of the lower impingement limit (XLOW), dimensionless y-coordinate of the lower impingement limit (YLOW), dimensionless wrap distance from stagnation of the lower impingement limit (SLOW), dimensionless wrap distance from the leading edge of the lower impingement limit (SLOWLE), dimensionless x-coordinate of the upper impingement limit (XHI), dimensionless y-coordinate of the upper impingement limit (YHI), dimensionless wrap distance from stagnation of the upper impingement limit (SHI), dimensionless wrap distance from the leading edge of the upper impingement limit (SHILE)

junk.dat - contains information useful for debugging the code and any screen outputs including

warning or error messages. By default in version 2.0, much of this printout is turned OFF.

misc.dat - contains miscellaneous information about the run including lift coefficient and the starting and ending locations of individual drops.

pres.dat - contains the compressible flow solution at the edge of the boundary layer. Columns are segment number (SEG), dimensionless wrap distance from stagnation (S), dimensionless velocity at the edge of the boundary layer (VE), dimensionless temperature at the edge of the boundary layer (TE), dimensionless pressure at the edge of the boundary layer (PRESS) and dimensionless density at the edge of the boundary layer (RA). Reference variables which were used to non-dimensionalize these quantities are chord length, ambient velocity, freestream total temperature, freestream total pressure and freestream total density, calculated from the equation

$$\rho_o = \frac{P_o}{RT_o} \tag{4}$$

xkinit.dat - contains the predicted sand-grain roughness at each time step. Columns are time in seconds (TIME), and two predictions for sand-grain roughness which are calculated by different sets of equations (XKINIT). LEWICE 2.0 uses the last value listed on each line as the sand-grain roughness, which is also dimensionless.

snap.jpg - this file is a JPG format file containing a screen snapshot of various LEWICE parameters which are plotted interactively during a LEWICE run on a Silicon Graphics Indigo2 workstation. The routines create the following plot windows while LEWICE runs: BETA, VEDGE, GEOM, HTC, FFRAC, ICE THICKNESS and ICE GROWTH. The variables plotted in these windows are the collection efficiency on the airfoil (BETA), the velocity at the edge of the boundary layer of the airfoil (VEDGE), the iced geometry (GEOM), the external convective heat transfer coefficient (HTC), the freezing fraction (FFRAC), the amount of ice which will be added in each time step (ICE THICKNESS), and a magnified view of the ice shape at the leading edge of the airfoil (ICE GROWTH). In order to use this package, the user must have a Silicon Graphics Workstation, a FORTRAN compiler on this workstation, a C compiler on this workstation and the GL libraries. Future revisions of LEWICE may include this function for other platforms.

THICK Utility Output Files

This list contains a description of the output files from the utility program THICK. The value in parenthesis is the title used for that column of data in the output file.

clean.dat - contains the ice thickness output relative to the clean airfoil coordinates. Columns are the x-coordinate of the clean airfoil (XSAV) in inches, the y-coordinate of the clean airfoil (YSAV) in inches, the ice thickness from the clean surface (DITOT) in inches, the cumulative ice area (AREA) in square inches, and the wrap distance as measured from the leading edge (S) in inches.

iced.dat - contains the ice shape and ice thickness output. Columns are the x-coordinate of the ice shape (XICE) in inches, the y-coordinate of the ice shape (YICE) in inches, and the ice thickness from that point to the clean surface (YPTOT) in inches.

echo.dat - contains a copy of information printed to the screen. Data includes the icing limits in inches, the total ice area and the maximum ice thickness. Data was printed to this smaller file to expedite transfer of the quantitative measurements to the spreadsheet.

Description of Excel Matrix and Formulas

This section will describe the data input into a Microsoft Excel spreadsheet for the quantitative comparison presented earlier. A complete printout of this matrix has not been included as it is over 200 pages in size. Each spreadsheet row contains one data point for the comparison or values for the experimental average. Blank lines were included to separate different test entries and the data was organized by airfoil.

The spreadsheet columns contain conditions for the run, measured and calculated parameters for the experimental data point, measured and calculated parameters for the associated LEWICE run, percent differences for LEWICE compared to the experimental data and experimental averages, percent differences for the experimental data compared to the experimental average, the absolute differences for LEWICE compared to the experiment and experimental averages and the absolute differences for the experimental data compared to the experimental average. Each category will be discussed in detail.

Spreadsheet Columns

Column 1: Contains the last name of the icing researcher who took the data. This is provided for informational purposes.

Column 2: Contains the name of the airfoil. Data for each airfoil are grouped together in this matrix.

Column 3: Contains the test date (month and year only).

Column 4: Contains the airfoil chord length in inches.

Column 5: Contains the NASA Run number used by the researcher. Each researcher has their own unique number scheme which will not be elaborated on here. Future tests are expected to have a more uniform convention for numbering runs.

Column 6: Contains the spanwise location (measured from the tunnel floor) for the experimental data. In addition, some rows contain averages of the other columns. Rows where this column is labeled 'Average' contain the spanwise average for that run. For every case which has more than one spanwise location where an ice shape was traced and digitized, a spanwise average was calculated.

Where this column contains '36" Avg.', that row will contain the repeatability average at the 36" span location for that run. Other labels such as '24" Avg.' or '48" Avg.' will contain the experimental repeatability average at that spanwise location for that condition. If the column is labeled 'Repeat Avg.', there is only one spanwise location available for which to calculate a repeatability average.

Every case which contains a repeat condition will have a repeatability average at every spanwise location where data is available. The repeat conditions will contain a spanwise average for that run as described earlier, but the repeatability information is listed only under the first run for that condition. The repeatability averages weight each ice shape the same rather than weighting each spanwise location the same. For example, consider a condition with five repeat runs in which the first two cases had three spanwise ice shapes traced while in the other three cases only the mid-span location was traced. There are a total of nine ice shapes for the overall average which are equally weighted.

Certain cases contain two sets of data where two different researchers both traced the same ice shape. These are identified in this matrix by listing each researcher individually under Column 1. An average value for that run is labeled "Tracer Avg." in this column. This average is distinct from both spanwise average and the repeatability average. In any condition where there are two or more types of averages (for example both a spanwise average and a repeatability average exist), then an overall average is calculated for that condition and labeled "Overall Avg." in this column. The bottom row for each airfoil also contains the average differences and percent differences for that airfoil. This column is then labeled "Airfoil Avg". The last row of the matrix contains the average differences and percent differences for the entire spreadsheet. This row is labeled "Total Avg.".

Column 7: If the condition listed is a repeat of a run listed earlier in the matrix, this column will contain the NASA Run number of the first entry for that set of conditions. If the condition is not a repeat condition, this column is blank. Each repeat case is referenced to the first entry in the matrix for that condition.

Column 8: Contains the tunnel velocity in knots. The velocity was recorded by some researchers in knots and by others in miles per hour. In the second case, values were converted to knots for listing in this table.

Column 9: Contains the tunnel velocity in meters per second. LEWICE uses meters per second as input units for velocity, so both set of units were listed.

Column 10: Contains the tunnel total temperature in degrees Fahrenheit. Most of the data for total temperature was recorded in degrees Fahrenheit. Some researchers recorded total temperature in degrees Celsius which was converted for listing in this table.

Column 11: Contains *static* temperature in degrees Kelvin. LEWICE uses Kelvin as its input unit for static temperature, hence the inclusion of this column in the matrix.

Column 12: Contains the angle of the airfoil with respect to the tunnel air flow.

Column 13: Contains the corrected angle of attack for input into LEWICE. Since the flow in LEWICE is calculated by a potential flow code, the lift predicted on the clean airfoil will be higher than the actual value (and by inference on the iced airfoil as well). Therefore it is necessary, especially for high angle of attack conditions, to use a corrected value for the LEWICE predictions. This correction is determined by selecting the angle of attack in LEWICE which will match the experimental lift coefficient for

the clean airfoil at that actual angle of attack. No additional corrections are made if the iced airfoil predicts a lift coefficient higher than expected since not enough data is available to make that determination.

Column 14: Contains the Liquid Water Content of the water sprayed at the model in the IRT. All data is reported in grams per cubic meter.

Column 15: Contains the Median Volume Diameter of the water sprayed at the model in the IRT. For all of the baseline conditions in this matrix ran with LEWICE, a mono-dispersed drop distribution using this MVD value was chosen. Cases using a droplet distribution are shown in the section on numerical variability earlier in this report.

Column 16: Contains the duration of the water spray for the tunnel condition in minutes. It should be noted that LEWICE uses time in seconds as input to the code. A separate column listing time in seconds was considered unnecessary.

Columns 17-30: Contains the measured data for the experimental ice shape. The parameters measured are explained in the section titled "Description of Comparison Method" earlier in this report. That explanation will not be repeated here. The columns as listed in this matrix are:

Lower Icing Limit (x-value)
Upper Icing Limit (x-value)
Lower Icing Limit (wrap distance)
Upper Icing Limit (wrap distance)
Lower Surface Max. Thickness
Leading Edge Min. Thickness
Upper Surface Max. Thickness
Lower Surface Ice Area
Upper Surface Ice Area
Total Ice Area
x-value at lower max. thickness
y-value at lower max. thickness
x-value at upper max. thickness
y-value at upper max. thickness

For rime ice shapes and other ice shapes with only a single maxima, the Lower Surface Max. Thickness, Leading Edge Min. Thickness, x-value at lower max. thickness and y-value at the lower max. thickness are listed as "N/A" for "not applicable". The single maxima was listed under Upper Surface Max. Thickness regardless of where the max. thickness occurred. One exception was made for a case where there was zero upper surface ice. In this case, the Upper Surface Max. Thickness, Leading Edge Min. Thickness, x-value at upper max. thickness and y-value at upper max. thickness are listed as "N/A". The wrap distance is reported as an absolute value as measured from the leading edge. Some sign conventions would indicate that the lower wrap distance should be listed with a negative distance. This convention was not followed in this matrix.

Columns 31-32: Contains the x,y coordinate at the center of the inscribed circle at the leading edge of the clean airfoil. For a small percentage of the data, the digitized ice shape was found to be offset from other data points. Because of this, the reference point may be different for the same airfoil.

Column 33: Contains the angle at the lower max. thickness. This angle is calculated from the x,y point at the lower max. thickness and the x,y point at the center of the inscribed circle at the leading edge and is referenced to the horizontal axis. The angle is reported as a positive angle between 0° and 360°. Since it is the lower angle, most values lay between 180° and 360°. Because of the reference point chosen, for negative angles of attack it is possible for the angle at the lower max. thickness to be less than 180°.

For rime ice shapes and other conditions with only a single maxima in the ice shape curve, the angle at the lower max. thickness is listed as "#VALUE!" as the columns this value is calculated from is labeled "N/A". One exception was made for a case which had no upper surface ice whatsoever. In this case, the angle at the upper max. thickness was listed as "#VALUE!" and the angle at the lower max. thickness contained the angle at the max. ice thickness.

Note: for rows containing average values for the experimental data, the angle is calculated from the average x,y values at the max. thickness. It is not an average of the calculated angles. This calculation is best expressed by the equations below.

$$\theta_{av} = \operatorname{atan}\left(\frac{y_{av} - y_c}{x_{av} - x_c}\right) \tag{5}$$

where

$$y_{av} = \frac{\sum_{i=1}^{n} y_i}{n} \quad \text{and} \quad x_{av} = \frac{\sum_{i=1}^{n} x_i}{n} \tag{6}$$

x_c and y_c are the x,y values at the center of the inscribed circle and n is the number of points in the average.

Column 34: Contains the angle at the upper max. thickness. This angle is calculated from the x,y point at the upper max. thickness and the x,y point at the center of the inscribed circle at the leading edge and is referenced to the horizontal axis. The angle is reported as a positive angle between 0° and 360°. Since it is the upper angle, most values lay between 0° and 180°. Because of the reference point chosen, for positive angles of attack it is possible for the angle at the upper max. thickness to be greater than 180°. As stated in the previous paragraph, certain cells in this column lists "#VALUE!" since the value it is calculated from is listed as "N/A".

Column 35: Contains the difference between the angle at the upper max. thickness and the angle at the lower max. thickness. If one of these two columns contains a value of "#VALUE!", then this column will be listed as "#VALUE!" as well.

Columns 36 and 37: Contains the lift coefficient predicted by LEWICE for the clean airfoil and for the iced airfoil for the condition listed. The iced airfoil value used is the lift predicted by LEWICE for that condition on the final ice shape. It is interesting to note that for most cases, LEWICE predicts an increase in lift due to ice. This is an artifact of the potential flow code and is **not** considered to be indicative of the actual effect of the ice shape on lift.

Columns 38-54: Contains the measured data for the final ice shape predicted by LEWICE for that condition. The parameters measured are explained in the section titled "Description of Comparison Method" earlier in this report. That explanation will not be repeated here. The columns as listed in this matrix are:

Lower Icing Limit (x-value)
Upper Icing Limit (x-value)
Lower Icing Limit (wrap distance)
Upper Icing Limit (wrap distance)
Lower Surface Max. Thickness
Leading Edge Min. Thickness
Upper Surface Max. Thickness
Lower Surface Ice Area
Upper Surface Ice Area
Total Ice Area
x-value at lower max. thickness
y-value at lower max. thickness
x-value at upper max. thickness
y-value at upper max. thickness
Angle at Lower Max. Thickness
Angle at Upper Max. Thickness
Angle Difference

Each column title also includes the word "Lewice" to differentiate these columns from those containing measured quantities from the experimental data. For rime ice shapes and other ice shapes with only a single maxima, the Lower Surface Max. Thickness, Leading Edge Min. Thickness, x-value at lower max. thickness and y-value at the lower max. thickness are listed as "N/A" for "not applicable". The single maxima was listed under Upper Surface Max. Thickness regardless of where the max. thickness occurred. One exception was made for a case where there was zero upper surface ice. In this case, the Upper Surface Max. Thickness, Leading Edge Min. Thickness, x-value at upper max. thickness and y-value at upper max. thickness are listed as "N/A". The angles for these cases will list a value of "#VALUE!" as explained earlier. The wrap distance is reported as an absolute value as measured from the leading edge. Some sign conventions would indicate that the lower wrap distance should be listed with a negative distance. This convention was not followed in this matrix.

Columns 55-65: Contains the percent difference of the LEWICE result from the experimental data in that row. Where that row contains averages of the experimental data, these columns will show the percent difference of the LEWICE result to the average value. The values for which a percent difference is calculated are:

Lower Icing Limit (wrap distance)
Upper Icing Limit (wrap distance)
Lower Surface Max. Thickness
Leading Edge Min. Thickness
Upper Surface Max. Thickness
Lower Surface Ice Area
Upper Surface Ice Area
Total Ice Area
Angle at Lower Max. Thickness
Angle at Upper Max. Thickness
Angle Difference

Certain cells will contain a value of "#VALUE!" as the column it is calculated from is listed as "N/A" or "#VALUE!" as explained earlier. For cases where the

leading edge min. thickness is zero for the experimental data, the percent difference will yield a result of "#DIV/0!".

Columns 66-76: Contains the percent difference between the measured value for the experimental data and the experimental average. For the rows with experimental measurements, the percent difference shown uses the spanwise average for that run when calculating the percent difference. For the rows containing the experimental averages, a percent difference is calculated by comparing the average value to the overall average for that run. For example, the percent difference columns for a row containing a spanwise average will contain the percent difference of the spanwise average value with respect to the overall average value for that condition. The values for which a percent difference is calculated are:

Lower Icing Limit (wrap distance)
Upper Icing Limit (wrap distance)
Lower Surface Max. Thickness
Leading Edge Min. Thickness
Upper Surface Max. Thickness
Lower Surface Ice Area
Upper Surface Ice Area
Total Ice Area
Angle at Lower Max. Thickness
Angle at Upper Max. Thickness
Angle Difference

Certain cells will contain a value of "#VALUE!" as the column it is calculated from is listed as "N/A" or "#VALUE!" as explained earlier. For cases where the leading edge min. thickness is zero for the experimental data, the percent difference will yield a result of "#DIV/0!".

Column 77: Contains a value for the theoretical max. ice thickness for the condition listed. This is calculated from the following equation:

$$t_{max} = \frac{(LWC)(V)(Time)}{\rho_{ice}} \quad (7)$$

where ρ_{ice} is the ice density which is set equal to 917 kg/m^3. This max. thickness value is used by later columns to nondimensionalize ice thickness and ice area values so that differences from different test entries and airfoils may be compared against each other.

Columns 78-88: Contains the absolute dimensionless difference of the LEWICE result from the experimental data in that row. Where that row contains averages of the experimental data, these columns will show the difference of the LEWICE result to the average value. The values for which an absolute difference is calculated are:

Lower Icing Limit (wrap distance)
Upper Icing Limit (wrap distance)
Lower Surface Max. Thickness
Leading Edge Min. Thickness
Upper Surface Max. Thickness
Lower Surface Ice Area
Upper Surface Ice Area
Total Ice Area
Angle at Lower Max. Thickness
Angle at Upper Max. Thickness
Angle Difference

In order to compare differences for various icing conditions and various airfoils, the differences are nondimensionalized. The two icing limits are nondimensionalized by the chord length and then multiplied by 100 to give a percentage difference. The ice thickness values are nondimensionalized by the theoretical max. thickness for that condition which is listed in column 77 and then multiplied by 100 to give a percentage difference. Ice area values are nondimensionalized by the theoretical max. ice thickness in column 77 and the thickness of the airfoil and then multiplied by 100 to give a percentage difference. The airfoil thickness was believed to provide a more accurate assessment of percent difference than chord length as the entire length of an airfoil is not covered with ice. The angle values are absolute values and are given in degrees.

Columns 89-99: Contains the absolute dimensionless difference of the experimental result from the experimental average. For the rows with experimental measurements, the difference shown uses the spanwise average for that run when calculating the difference. For the rows containing the experimental averages, a difference is calculated by comparing the average value to the overall average for that run. For example, the difference columns for a row containing a spanwise average will contain the difference of the spanwise average value with respect to the overall average value for that term. The values for which an absolute difference is calculated are:

Lower Icing Limit (wrap distance)
Upper Icing Limit (wrap distance)
Lower Surface Max. Thickness
Leading Edge Min. Thickness
Upper Surface Max. Thickness
Lower Surface Ice Area
Upper Surface Ice Area
Total Ice Area
Angle at Lower Max. Thickness
Angle at Upper Max. Thickness
Angle Difference

In order to compare differences for various icing conditions and various airfoils, the differences are nondimensionalized. The two icing limits are nondimensionalized by the chord length and then multiplied by 100 to give a percentage difference. The ice thickness values are nondimensionalized by the theoretical max. thickness for that condition which is listed in column 77 and then multiplied by 100 to give a percentage difference. Ice area values are nondimensionalized by the theoretical max. ice thickness in column 77 and the thickness of the airfoil and then multiplied by 100 to give a percentage difference. The airfoil thickness was believed to provide a more accurate assessment of percent difference than chord length as the entire length of an airfoil is not covered with ice. The angle values are absolute values and are given in degrees.

Column 100: contains the average of the 11 percentage difference calculations in Columns 55-65 between LEWICE and the experimental data for each run. For the rows with experimental measurements, the percent difference shown uses the spanwise average for that run when calculating the percent difference. For the rows containing the experimental averages, a percent difference is calculated by comparing the average value to the overall average for that run.

For example, the percent difference columns for a row containing a spanwise average will contain the percent difference of the spanwise average value with respect to the overall average value for that condition. For conditions where one or more of the individual percentage differences is labeled "#VALUE!" or "#DIV/0!" then the average is calculated from the remaining columns which have numbers.

Column 101: contains the average of the 11 percentage difference calculations in Columns 66-76 between the experimental data for each run and the experimental average. For the rows with experimental measurements, the percent difference shown uses the spanwise average for that run when calculating the percent difference. For the rows containing the experimental averages, a percent difference is calculated by comparing the average value to the overall average for that run.

For example, the percent difference columns for a row containing a spanwise average will contain the percent difference of the spanwise average value with respect to the overall average value for that condition. For conditions where one or more of the individual percentage differences is labeled "#VALUE!" or "#DIV/0!" then the average is calculated from the remaining columns which have numbers.

Column 102: contains the average of the 11 absolute difference calculations in Columns 78-88 between LEWICE and the experimental data for each run. For the rows with experimental measurements, the difference shown uses the spanwise average for that run when calculating the absolute difference. For the rows containing the experimental averages, an absolute difference is calculated by comparing the average value to the overall average for that run.

For example, the absolute difference columns for a row containing a spanwise average will contain the absolute difference of the spanwise average value with respect to the overall average value for that condition. For conditions where one or more of the individual absolute differences is labeled "#VALUE!" or "#DIV/0!" then the average is calculated from the remaining columns which have numbers.

Column 103: contains the average of the 11 absolute difference calculations in Columns 89-99 between the experimental data for each run and the experimental average. For the rows with experimental measurements, the absolute difference shown uses the spanwise average for that run when calculating the absolute difference. For the rows containing the experimental averages, an absolute difference is calculated by comparing the average value to the overall average for that run.

For example, the absolute difference columns for a row containing a spanwise average will contain the absolute difference of the spanwise average value with respect to the overall average value for that condition. For conditions where one or more of the individual percentage differences is labeled "#VALUE!" or "#DIV/0!" then the average is calculated from the remaining columns which have numbers.

Column 104: contains the average of the 8 absolute difference calculations in Columns 78-85 between LEWICE and the experimental data for each run. For the rows with experimental measurements, the difference shown uses the spanwise average for that run when calculating the absolute difference. For the rows containing the experimental averages, an absolute difference is calculated by comparing the average value to the overall average for that run.

For example, the absolute difference columns for a row containing a spanwise average will contain the absolute difference of the spanwise average value with respect to the overall average value for that condition. For conditions where one or more of the individual absolute differences is labeled "#VALUE!" or "#DIV/0!" then the average is calculated from the remaining columns which have numbers.

Column 105: contains the average of the 8 absolute difference calculations in Columns 89-96 between the experimental data for each run and the experimental average. For the rows with experimental measurements, the absolute difference shown uses the spanwise average for that run when calculating the absolute difference. For the rows containing the experimental averages, an absolute difference is calculated by comparing the average value to the overall average for that run.

For example, the absolute difference columns for a row containing a spanwise average will contain the absolute difference of the spanwise average value with respect to the overall average value for that condition. For conditions where one or more of the individual percentage differences is labeled "#VALUE!" or "#DIV/0!" then the average is calculated from the remaining columns which have numbers.

X. Conclusions

This report has presented the quantitative comparisons of several geometric characteristics for a database of over 1000 ice shapes. Measurements of icing limit, ice thickness, ice area and horn angle were made for each ice shape. Comparisons were made for the difference in experimental variations such as tunnel repeatability, spanwise variability and tracing errors. Comparisons were also made for the difference between the predicted ice shape from LEWICE and the average experimental value. Comparisons were made for each individual quantitative criteria. An overall assessment was made for the quantitative comparison as well.

This comparison shows that based on the overall assessment criteria presented in this report, the variation in the experimental data was 4.4% and the LEWICE predicted ice shape differs from the experimental average by 12.5%. The ice shape data and output files from LEWICE which were generated for this report are included on CD-ROMs along with all of the quantitative comparison numbers.

XI. Acknowledgments

The authors would like to thank the NASA Lewis Icing Branch for their continued support of this research, both financially and for their help with this report. Special recognition goes to the researchers who generated the experimental data included in this report, to Dr. Mark Potapczuk for his insights into this work and especially to Tammy Langhals for digitizing all of the experimental ice tracings in this report.

XII. References

1 Wright, W. B., "Users Manual for the NASA Lewis Ice Accretion Code LEWICE 2.0," NASA CR to be published, Jan. 1999.

2 Wright, W. B., Gent, R. W. and Guffond, D., "DRA/NASA/ONERA Collaboration on Icing Research Part II - Prediction of Airfoil Ice Accretion," NASA CR 202349, May 1997.

3 Gent, R. W., "TRAJICE2 - A Combined Water Droplet and Ice Accretion Prediction Codes for Airfoils," RAE TR 90054, 1990.

4 Hedde, T. and Guffond, D., "Improvement of the ONERA 3-D Icing Code, Comparison with 3D Experimental Shapes," AIAA 93-0169, Jan. 1993.

5 Brahimi, M. T., Tran, P., and Paraschivoiu, I., "Numerical Simulation and Thermodynamic Analysis of Ice Accretion on Aircraft Wings," Centre de Développement Technologique de l'École Ploytechnique de Montréal, C.D.T. Project C159, Final Report prepared for Canadair, May, 1994.

6 Tran, P., Brahimi, M. T., Tezok, F. and Paraschivoiu, I., "Numerical Simulation of Ice Accretion

on Multi-Element Configurations", AIAA 96-0869, Jan. 1996.

7 Mingione, G., Brandi, V. and Esposito, B., "Ice Accretion Prediction on Multi-Element Airfoils," AIAA 97-0177, Jan. 1997.

8 Olsen, W., Shaw, R., and Newton, J., "Ice Shapes and the Resulting Drag Increase for a NACA 0012 Airfoil," NASA TM-83556, Jan. 1983.

9 Addy, G.E., Potapczuk, M. G., and Sheldon, D., "Modern Airfoil Ice Accretions," NASA TM (AIAA - 97-0174), Jan. 1997.

10 Wright, W. B. and Potapczuk, M. G., "Comparison of LEWICE 1.6 and LEWICE/NS with IRT Experimental Data from Modern Airfoil Tests," NASA TM (AIAA 97-0175), Jan. 1997.

11 Wright, W. B. and Bidwell, C. S., "Additional Improvements to the NASA Lewis Ice Accretion Code LEWICE," NASA TM (AIAA-95-0752), Jan. 1995.

12 Wright, W.B., "Users Manual for the Improved NASA Lewis Ice Accretion Code LEWICE 1.6," NASA CR 198355,June 1995.

13 Wright, W.B., Bidwell, C. S., Potapczuk, M. G. and Britton, R. K., "Proceedings of the LEWICE Workshop," June 1995.

14 Wright, W.B., "Capabilities of LEWICE 1.6 and Comparison with Experimental Data," presented at the SAE/AHS International Icing Symposium, Sept. 1995.

15 Wright, W.B., and Potapczuk, M. G., "Computational Simulation of Large Droplet Icing," presented at the FAA Phase III Meeting, May 1996.

16 Shin, J and Bond, T.H., "Results of an Icing Test on a NACA0012 Airfoil in the NASA Lewis Icing Research Tunnel," AIAA92-0647, Jan. 1992.

17 Addy, Jr., H.E., Potapczuk, M.G., and Sheldon, D.W., "Modern Airfoil Ice Accretions," AIAA-97-0174, January, 1997.

18 Addy, Jr., H.E., Miller, D.R., and Ide, R.F., "A Study of Large Droplet Ice Accretion in the NASA Lewis IRT at Near-Freezing Conditions; Part 2," NASA TM 107424, May, 1996.

19 Miller, D.R., "Addy, Jr., H.E.,and Ide, R.F., "A Study of Large Droplet Ice Accretion in the NASA Lewis IRT at Near-Freezing Conditions," NASA TM 107142, Jan., 1996.

20 Reehorst, A., Chung, J., Potapczuk, M. and Choo, Y., "The Operational Significance of an Experimental and Numerical Study of Icing Effects on Performance and Controllability," AIAA 99-0374, Jan. 1999.

21 Addy, G., IRT Test Entry, Feb. 1998.

22 Anderson, D. IRT Test Entry, June 1996.

23 Chen, S. and Langhals, T., "Experimental Validation on the Modification Techniques Developed for the New Scaling Methods," AIAA 99-xxxx, Jan. 1999.

24 Addy, G., IRT Test Entry, Feb. 1996.

25 Bidwell, C. S. and VanZante, J. F., IRT Test Entry, Jan. 1998.

26 Ruff, G. A. and Anderson, D. N., "Quantification of Ice Accretions for Icing Scaling Evaluations," AIAA 98-0195, Jan. 1998.

XIII. Appendix: Ice Shape and Ice Thickness Comparison Plots

This section contains plots comparing ice shapes measured in the IRT with LEWICE. A plot is made for each unique condition in the matrix. This means that only the first case of a condition is plotted and repeat conditions are not plotted. The spanwise location of the tracing is given on the plot. Only one spanwise location was plotted. The centerline (36" span) location is shown if available. If it is not available, the closest location to the centerline is plotted. In addition to the ice shape, a comparison plot of the ice thickness distribution generated by the utility program THICK is also given. There are 462 plots in this appendix, Figures 162-623.

There are seven sections to this appendix which correspond to the seven airfoils used for this comparison. Each section is preceded by a table which summarizes the experimental conditions for that airfoil. Individual test entries are separated by blank lines in the table. Definitions of the columns in the table are presented in the section describing the Excel spreadsheet, however there is only one entry for each test condition in this table whereas the spreadsheet data contained an entry for each tracing location. There are seven tables in all, labeled as Tables 2-8.

Each ice shape plot contains as its title the NASA run number of the experimental data and the tracing location. The airfoil is plotted as a solid line, the experimental data as short dashes and the LEWICE prediction as longer dashes. All ice shapes are plotted proportionately, which means that the y-axis and x-axis are the same scale. In addition, the ice shape is plotted to scale if it was small enough to fit on the plot axis, which was 7" horizontally by 5" vertically. Larger ice shapes are plotted 1/2 scale (14" x 10" of ice is plotted on the 7" x 5" plot) or 1/3 scale (21" x 15" of ice is plotted on the 7" x 5" plot).

Each ice thickness plot contains as its title the NASA run number of the experimental data and the tracing location. The experimental data is again plotted as short dashes and the LEWICE prediction as longer dashes. **Important note:** the ice thickness plots are **not** plotted proportionately. This was done so that the details of the ice thickness curves could be seen. Much of this detail is lost on a proportional plot. The horizontal axis is wrap distance from the hilite of the clean airfoil and plotted in inches. The vertical axis is ice thickness in inches from the clean surface. The plot label 'ditot' on the vertical axis is the name of the variable for ice thickness internal to the program THICK.

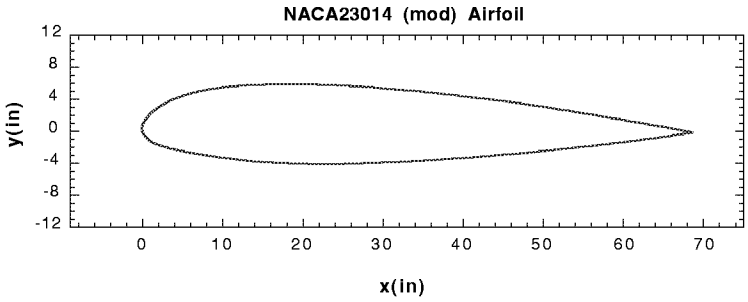

FIGURE 1. NACA 23014(mod) Airfoil

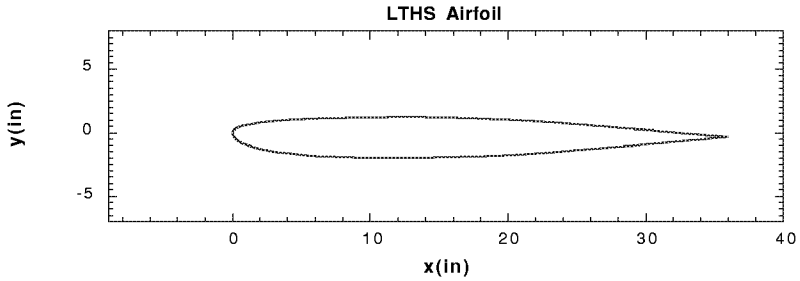

FIGURE 2. LTHS Airfoil

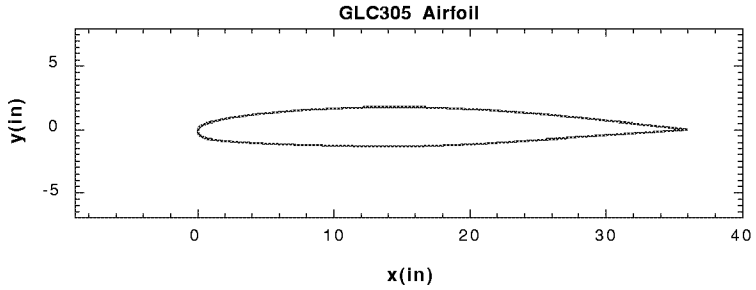

FIGURE 3. GLC305 Airfoil

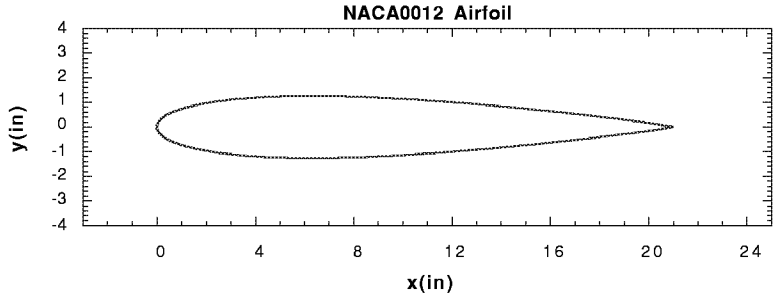

FIGURE 4. NACA0012 Airfoil

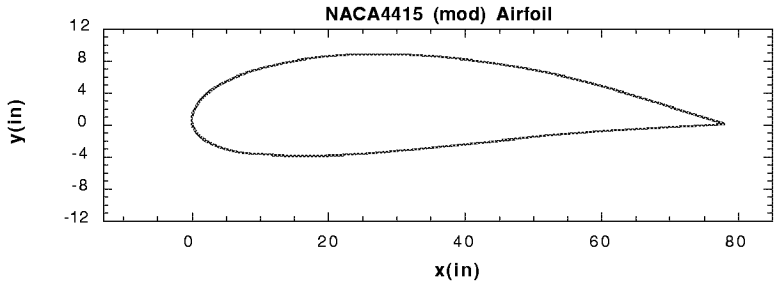

FIGURE 5. NACA 4415(mod) Airfoil

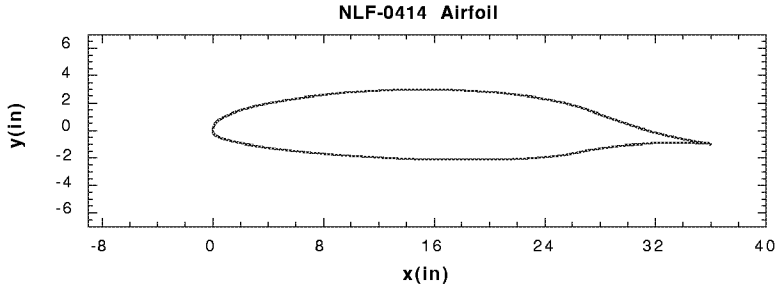

FIGURE 6. NLF-0414 Airfoil

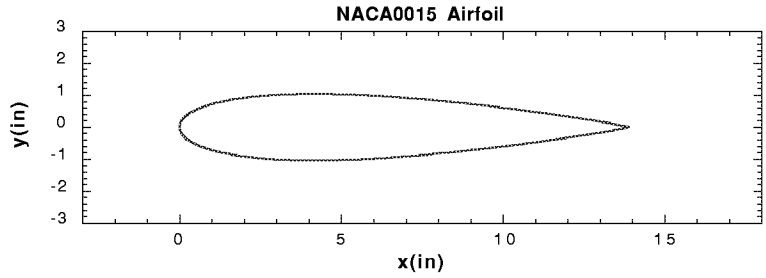

FIGURE 7. NACA0015 Airfoil

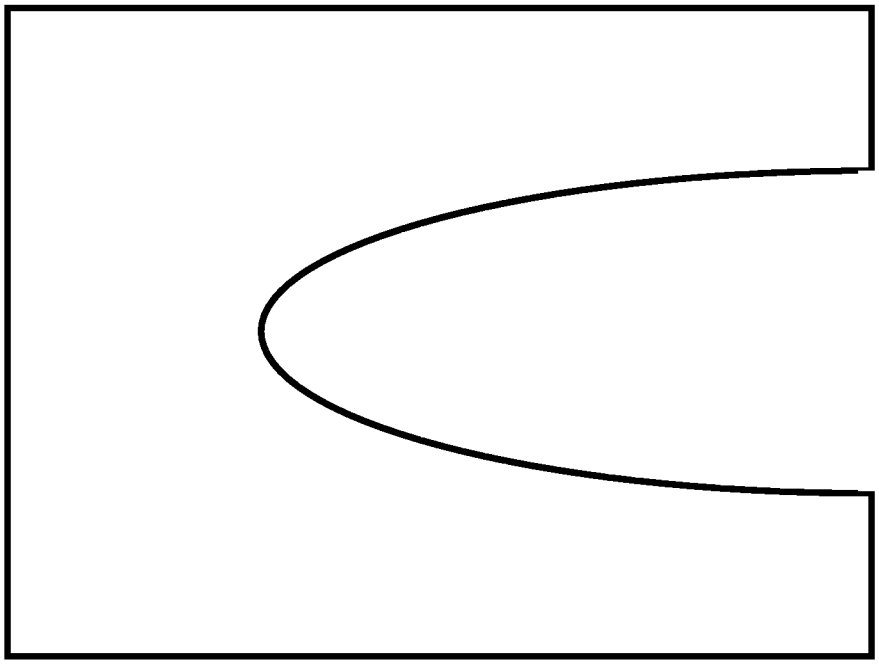

FIGURE 8. Example of a Cardboard Template for Tracing Ice Shapes

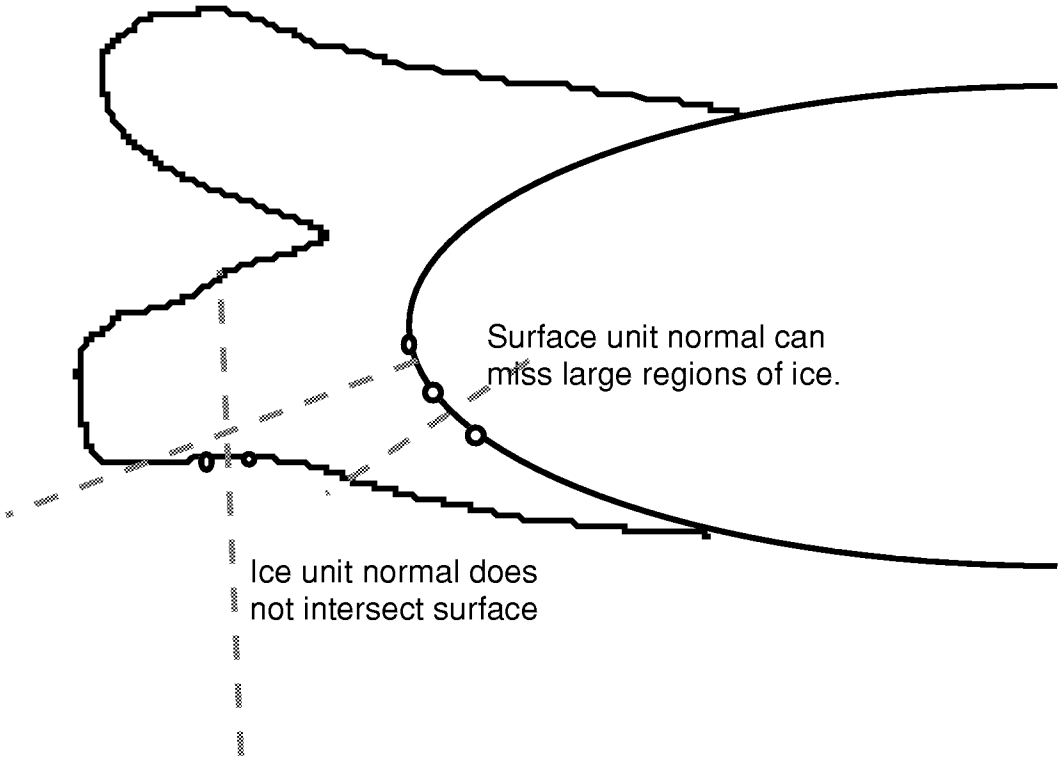

FIGURE 9. Limitations of Unit Normal Approach for Ice Thickness

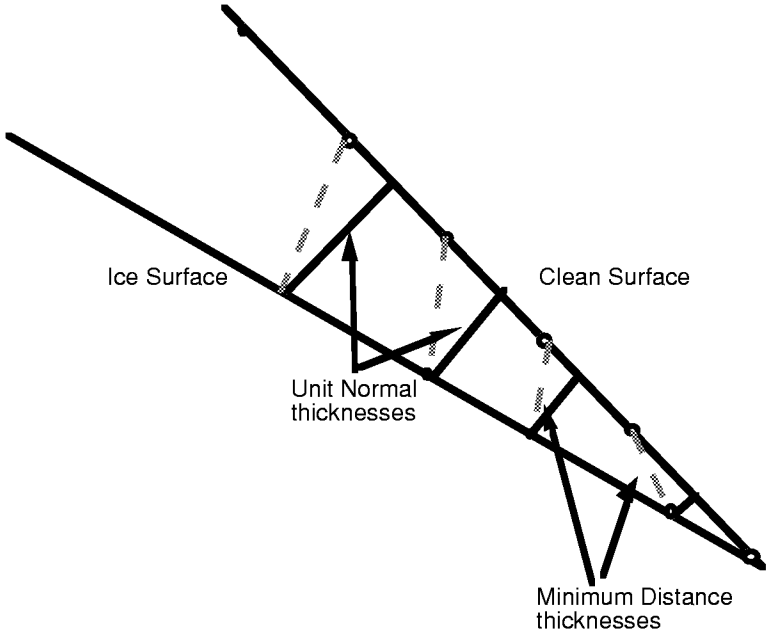

FIGURE 10. Limitations of Minimum Distance Approach

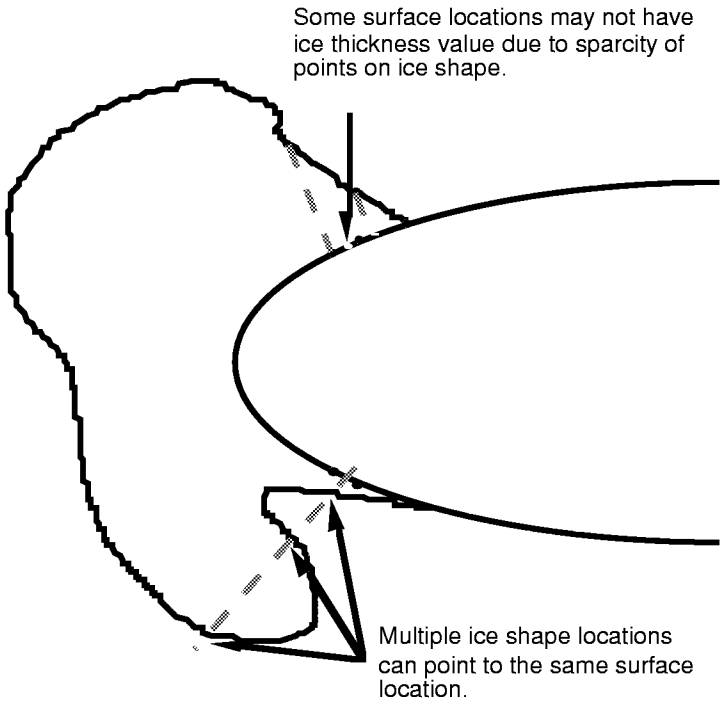

FIGURE 11. Corrections to Ice Thickness Distribution

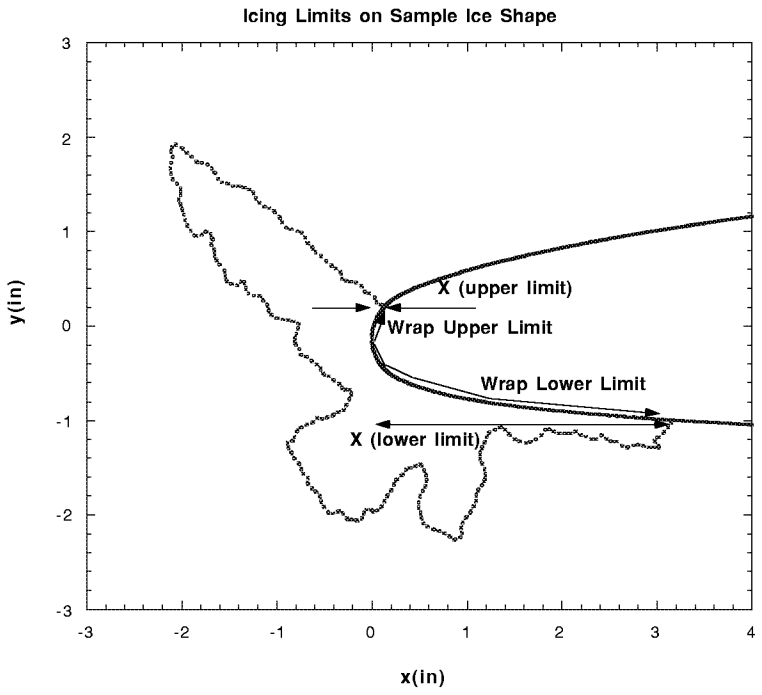

FIGURE 12. Icing Limits on Sample Ice Shape

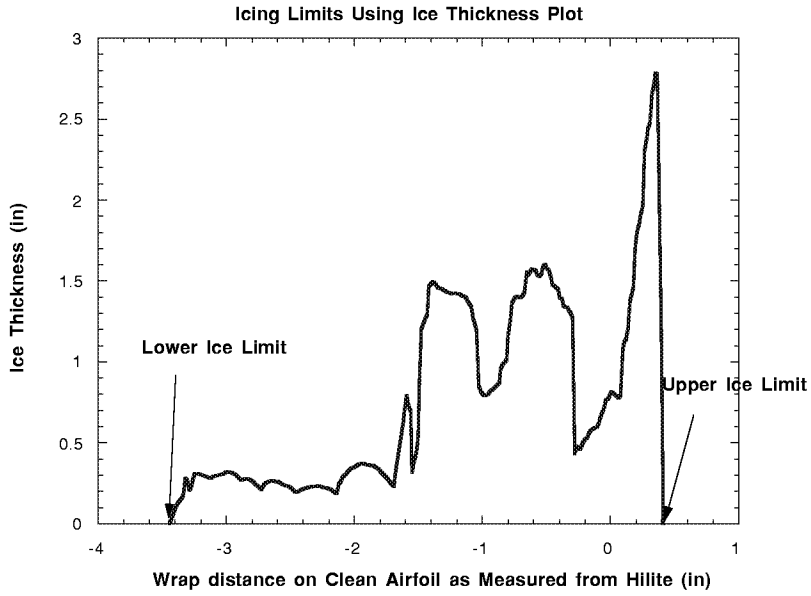

FIGURE 13. Icing Limits Using Ice Thickness Plot

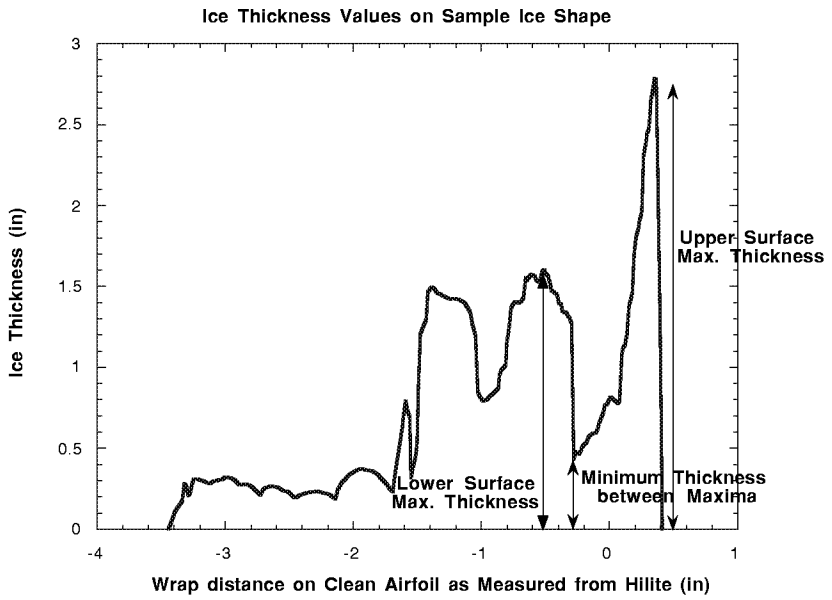

FIGURE 14. Ice Thickness Values on Sample Ice Shape

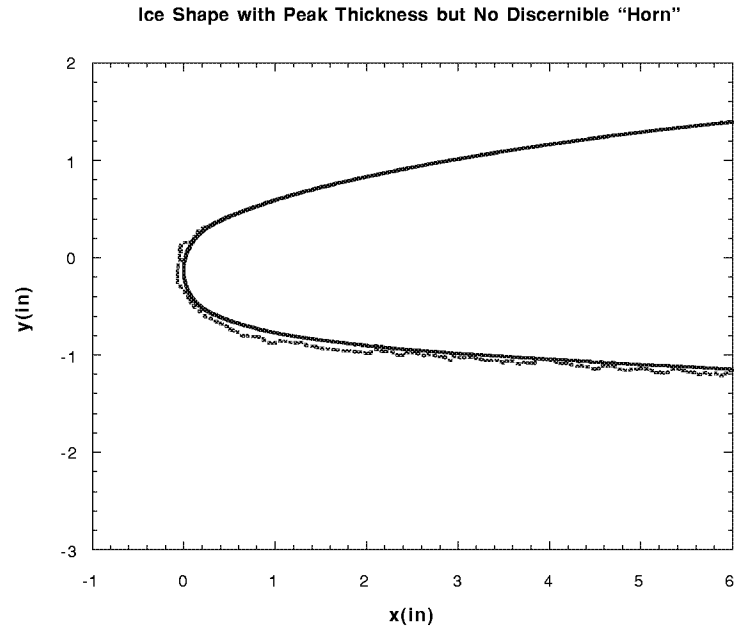

FIGURE 15. Ice Shape with Peak Thickness but No Discernable "Horn"

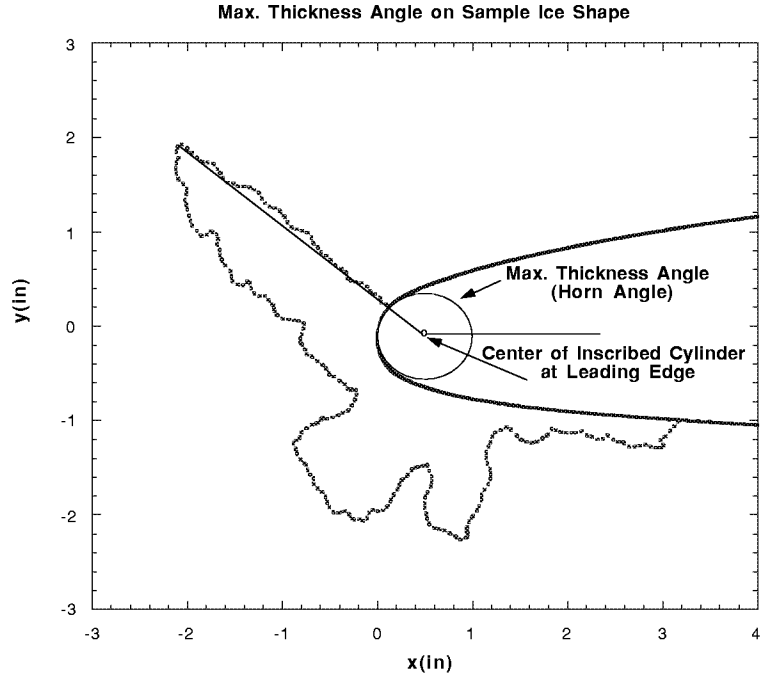

FIGURE 16. Max. Thickness Angle on Sample Ice Shape

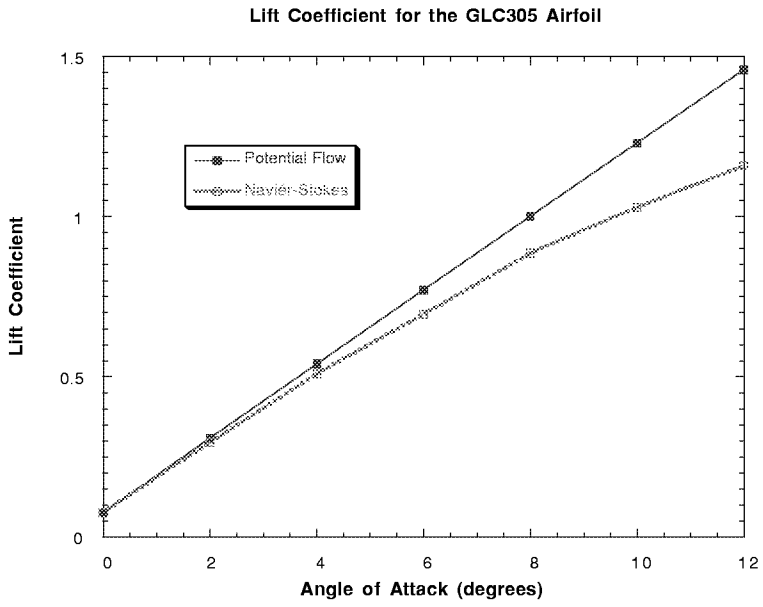

FIGURE 17. Example of Lift Overprediction by Potential Flow

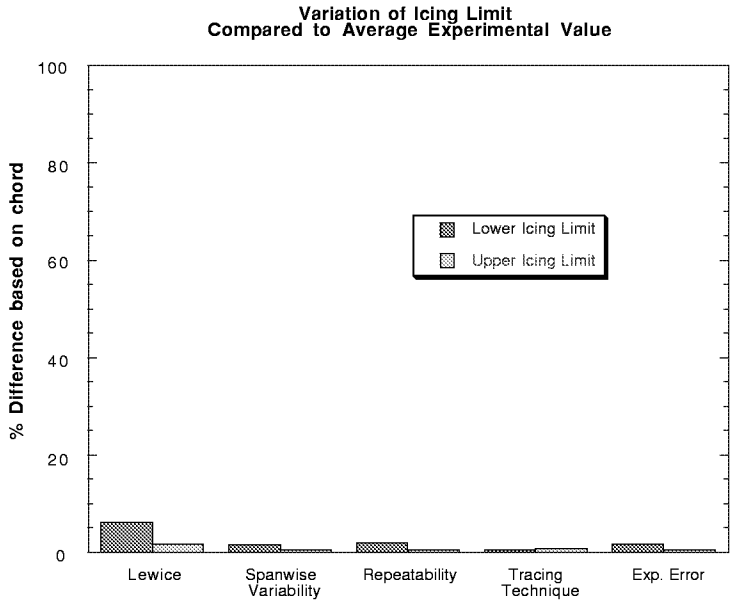

FIGURE 18. Variation of Icing Limit Compared to Average Experimental Value

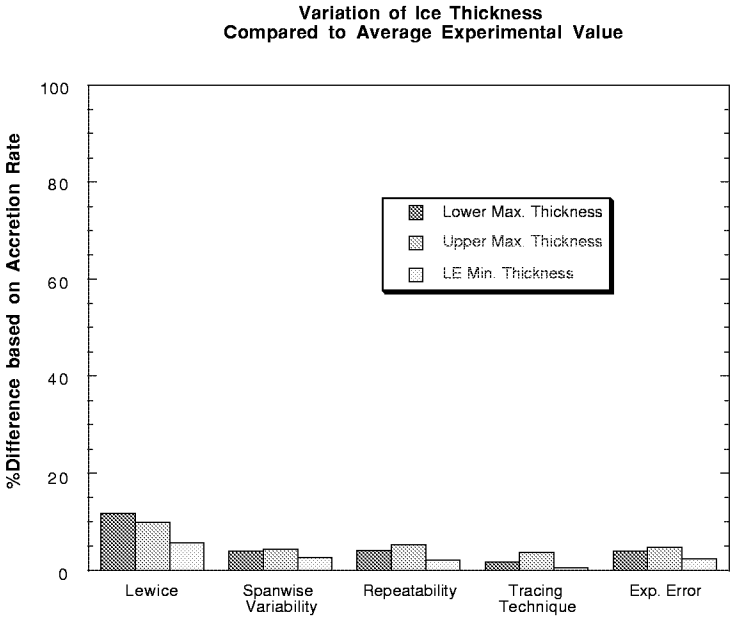

FIGURE 19. Variation of Ice Thickness Compared to Average Experimental Value

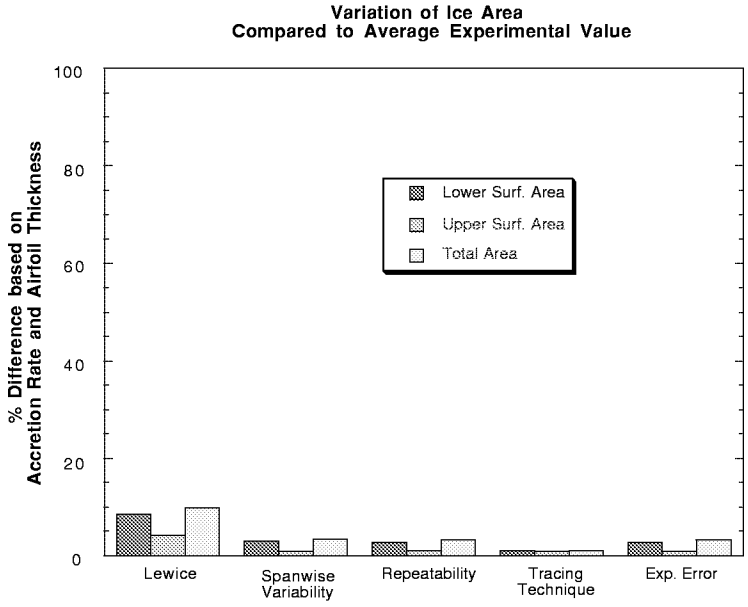

FIGURE 20. Variation of Ice Area Compared to Average Experimental Value

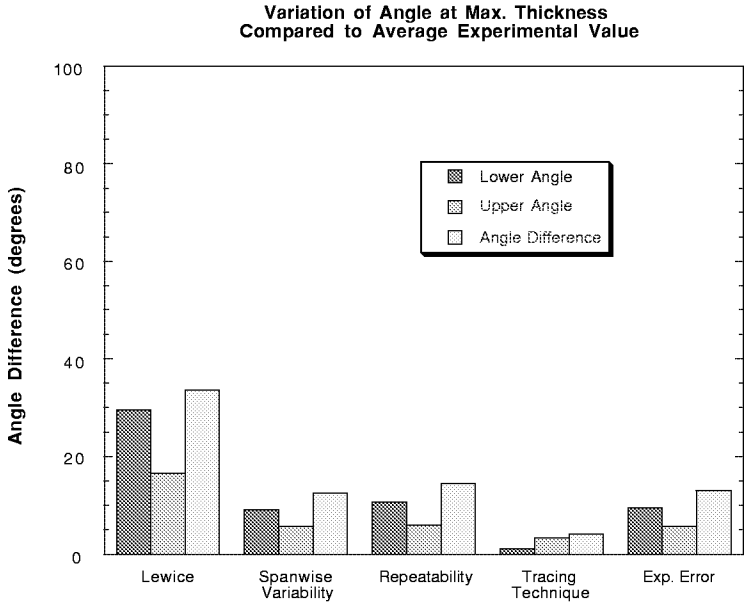

FIGURE 21. Variation of Angle at Max. Thickness Compared to Average Experimental Value

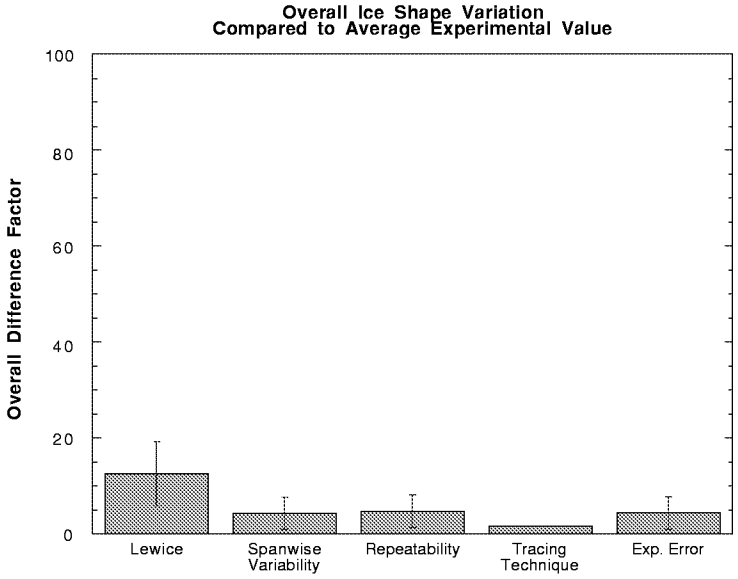

FIGURE 22. Overall Ice Shape Variation Compared to Average Experimental Value

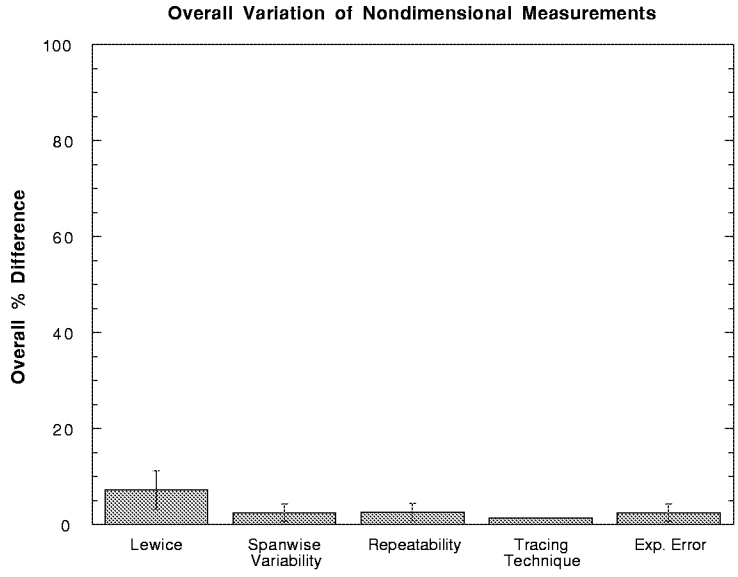

FIGURE 23. Nondimensional Ice Shape Variation Compared to Average Experimental Value

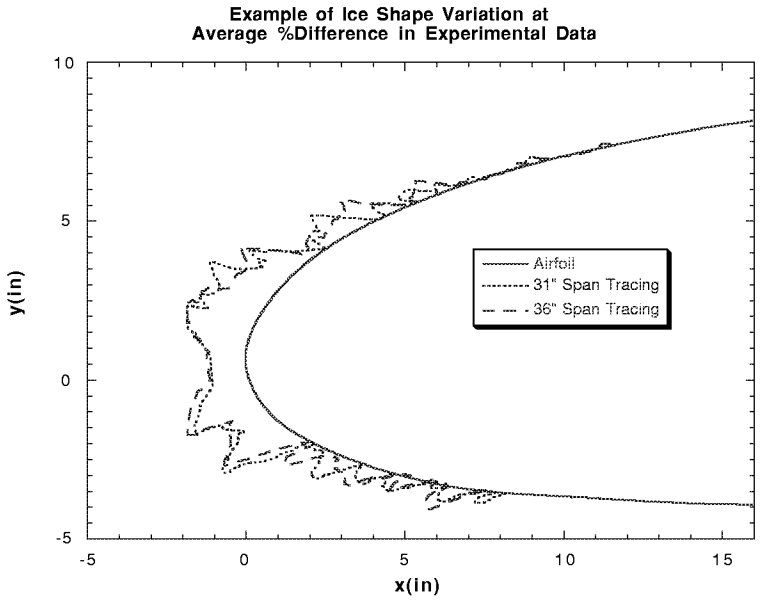

FIGURE 24. Example of Ice Shape Variation at Average %Difference in Experimental Data

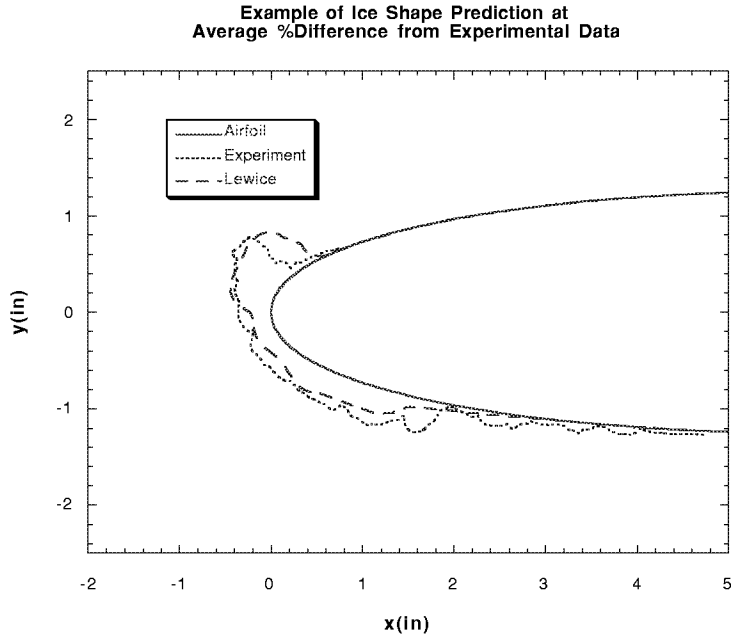

FIGURE 25. Example of Ice Shape Prediction at Average %Difference in Experimental Data

Spacing Cases - DSMN

FIGURE 26

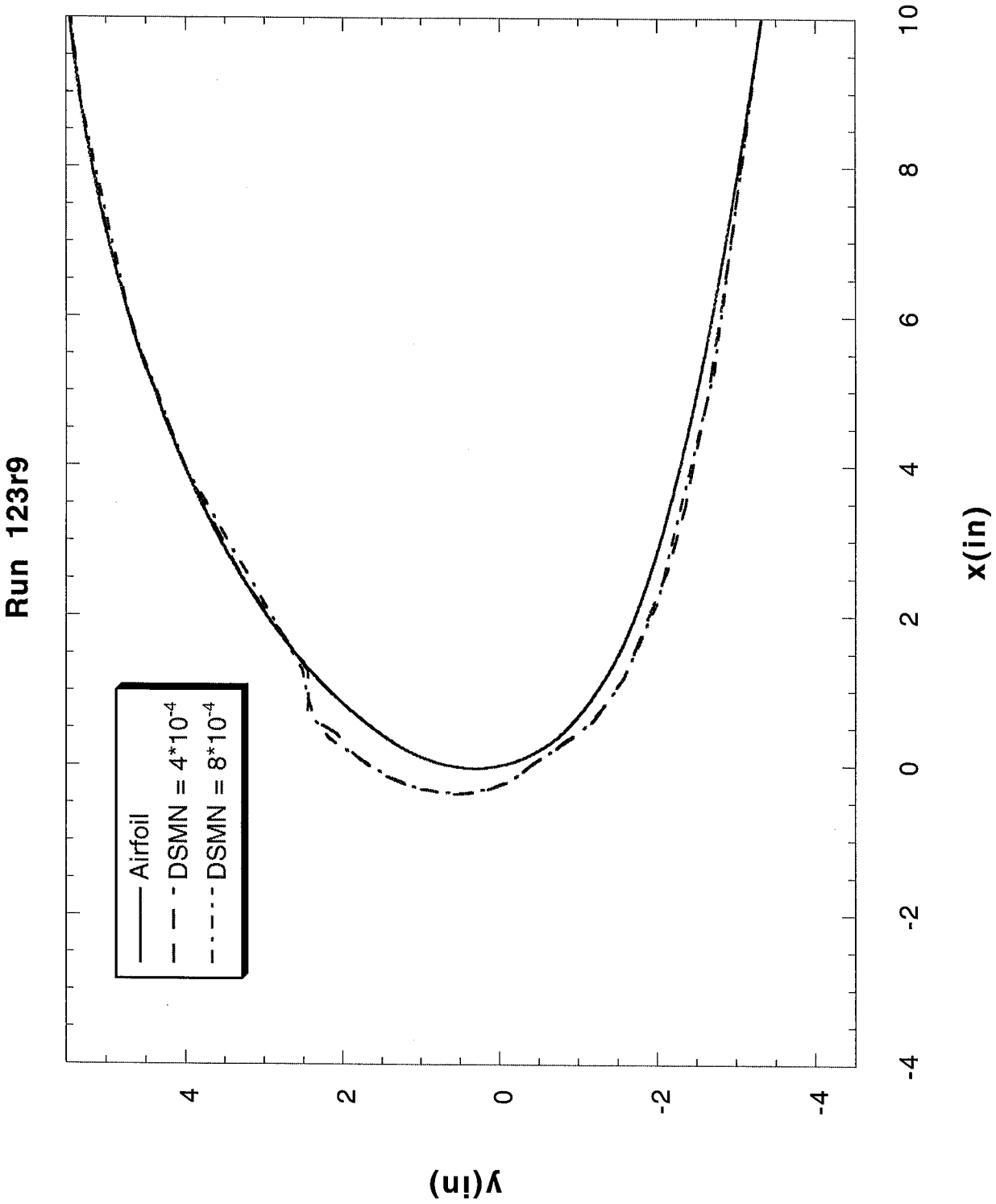
Run 123r9
Airfoil
DSMN = 4*10^-4
DSMN = 8*10^-4
y(in)
4
2
0
-2
-4
x(in)
10
8
6
4
2
0
-2
-4

FIGURE 27

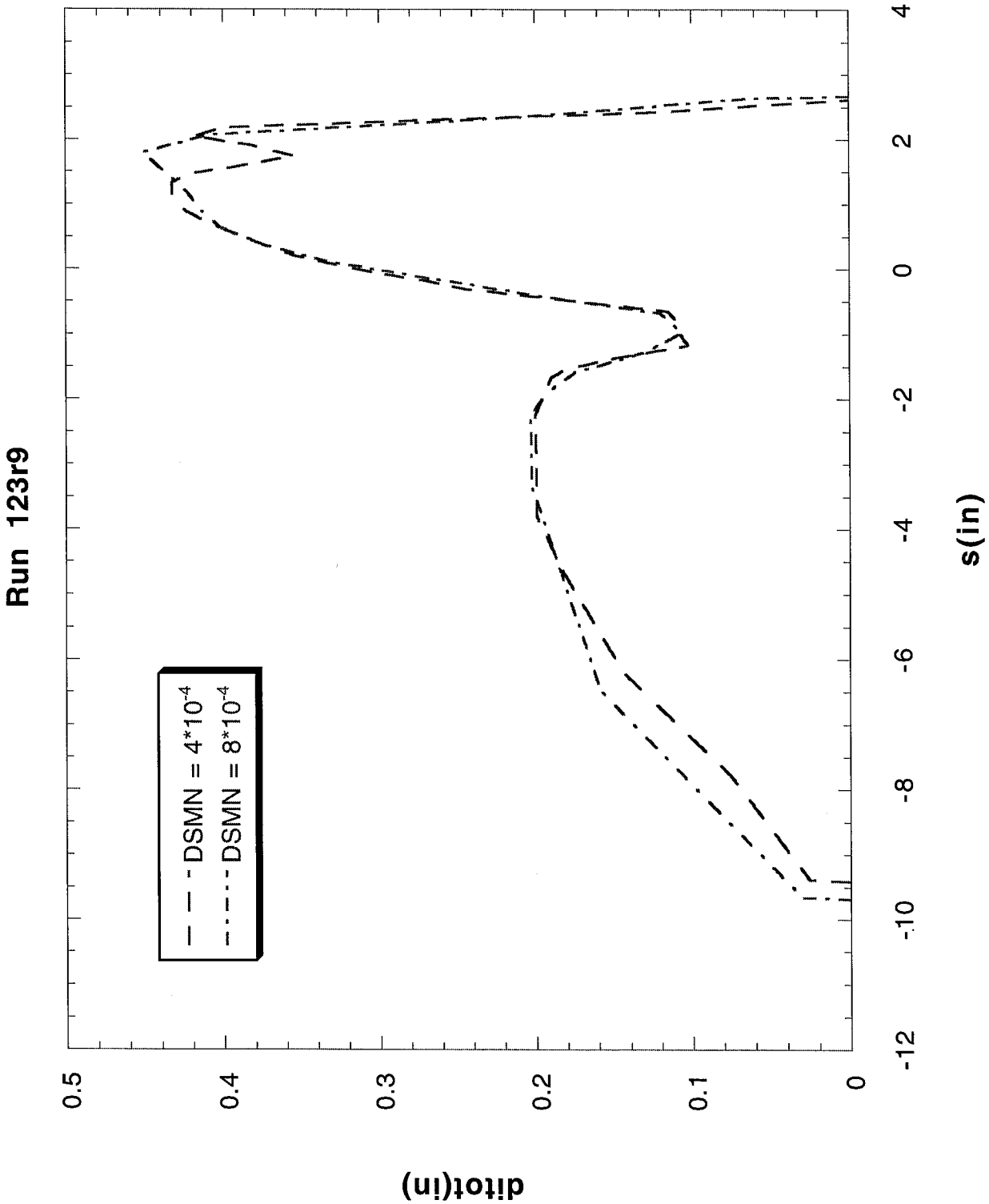
Run 123r9
DSMN = 4*10^-4
DSMN = 8*10^-4
ditot(in)
0.5
0.4
0.3
0.2
0.1
0
s(in)
4
2
0
-2
-4
-6
-8
-10
-12

FIGURE 28

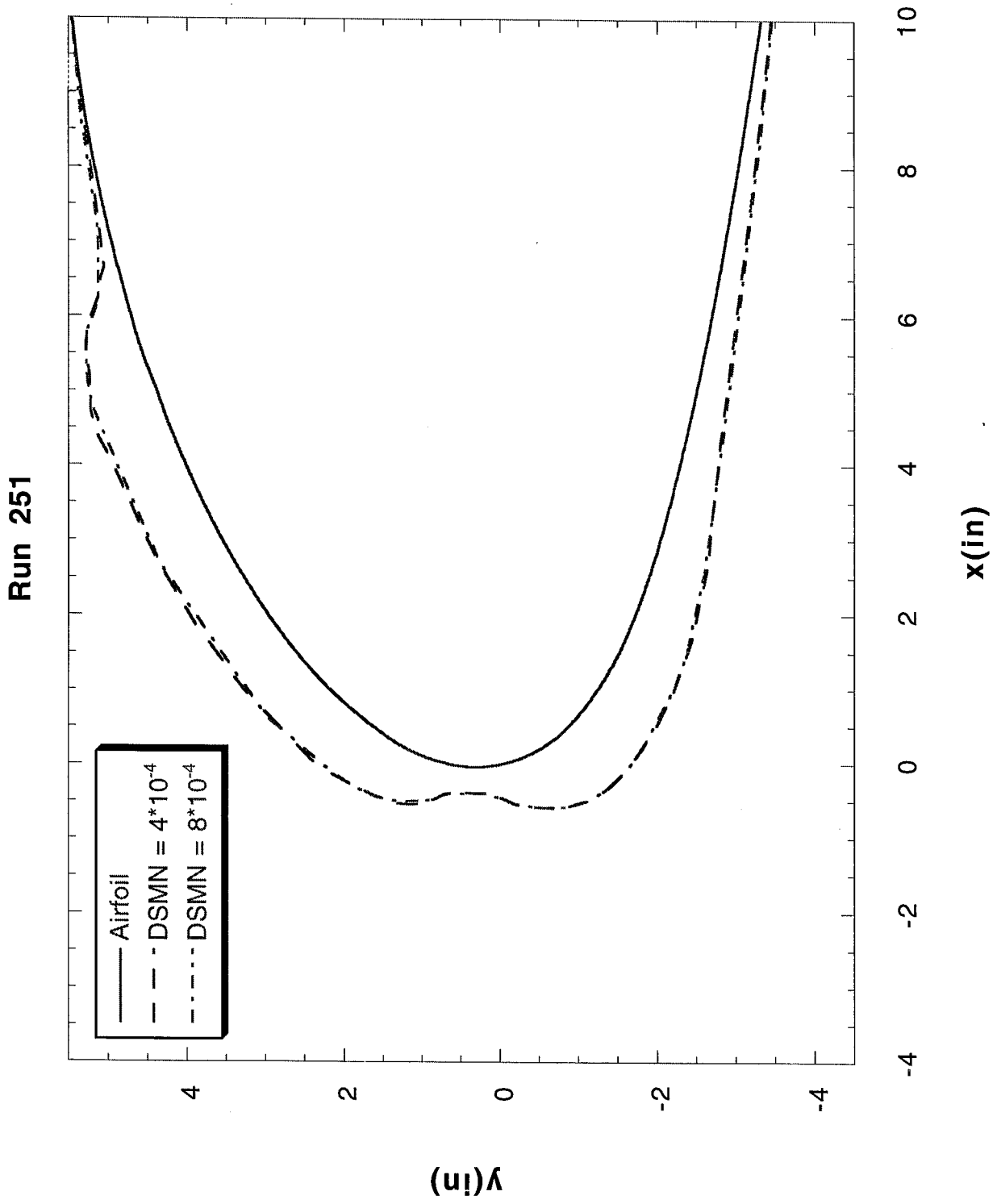

FIGURE 29

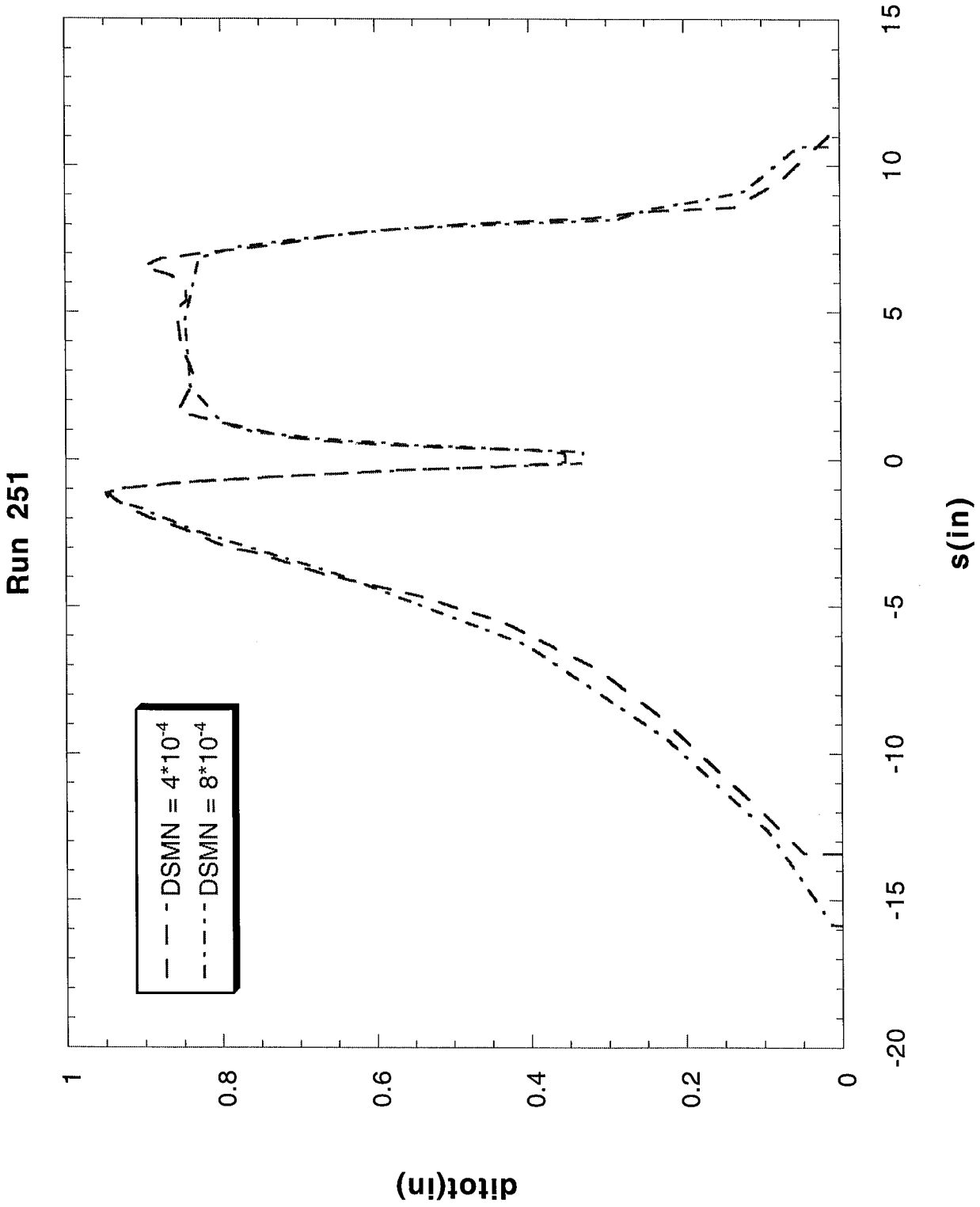
Run 251
ditot(in)
s(in)
DSMN = 4*10^-4
DSMN = 8*10^-4
1
0.8
0.6
0.4
0.2
0
15
10
5
0
-5
-10
-15
-20

FIGURE 30

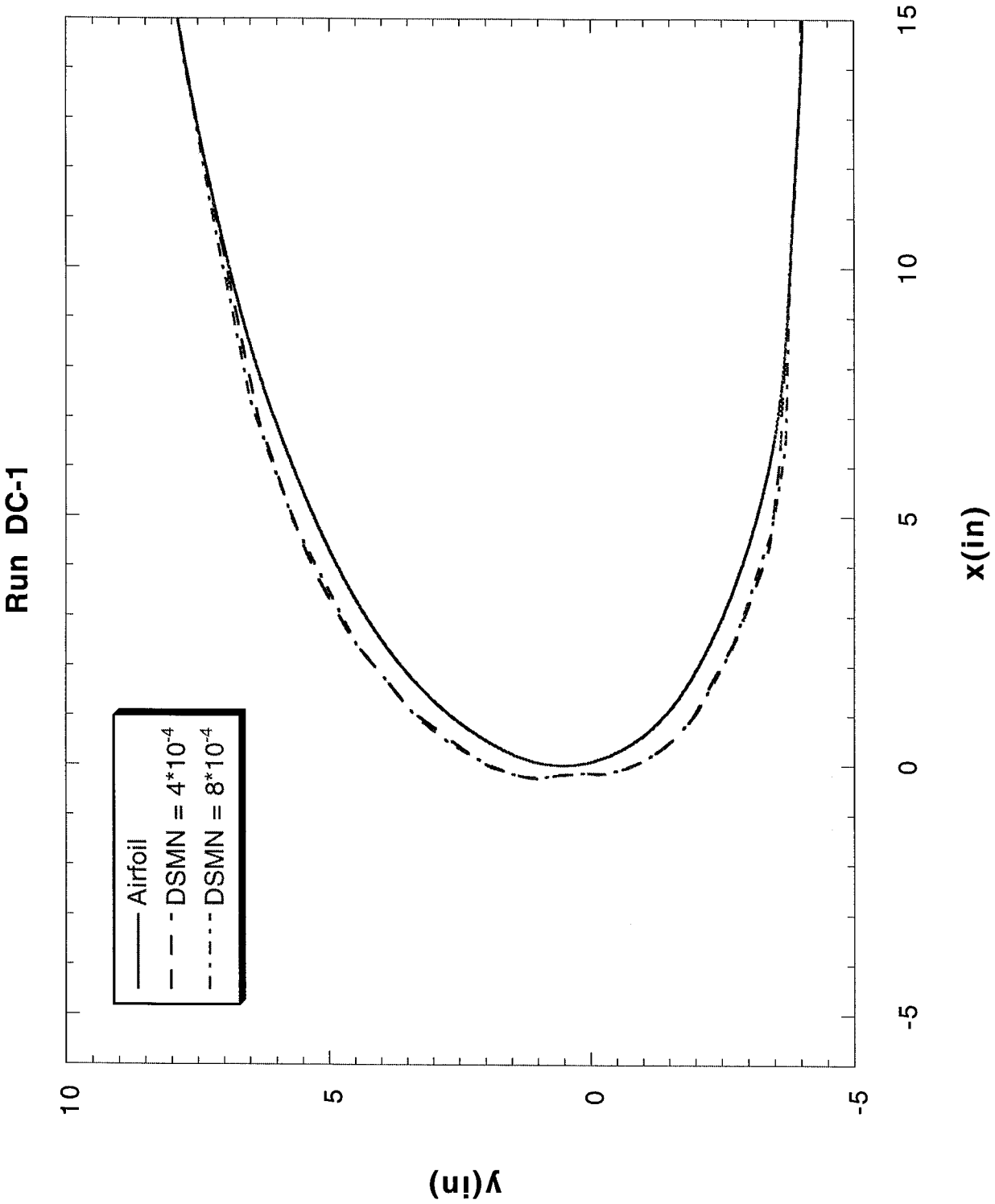

FIGURE 31

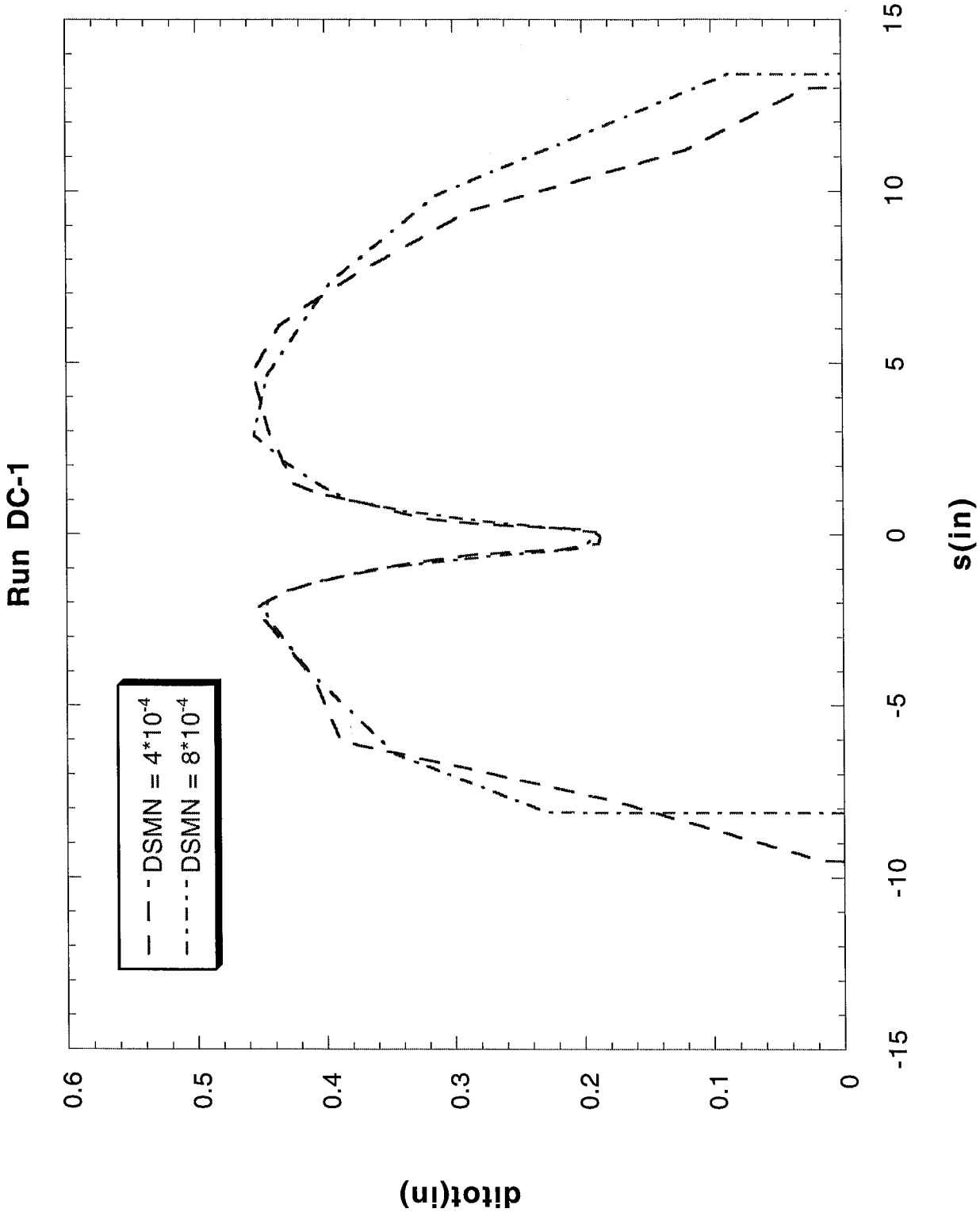
Run DC-1
DSMN = 4*10^-4
DSMN = 8*10^-4
ditot(in)
s(in)
0
0.1
0.2
0.3
0.4
0.5
0.6
-15
-10
-5
0
5
10
15

FIGURE 32

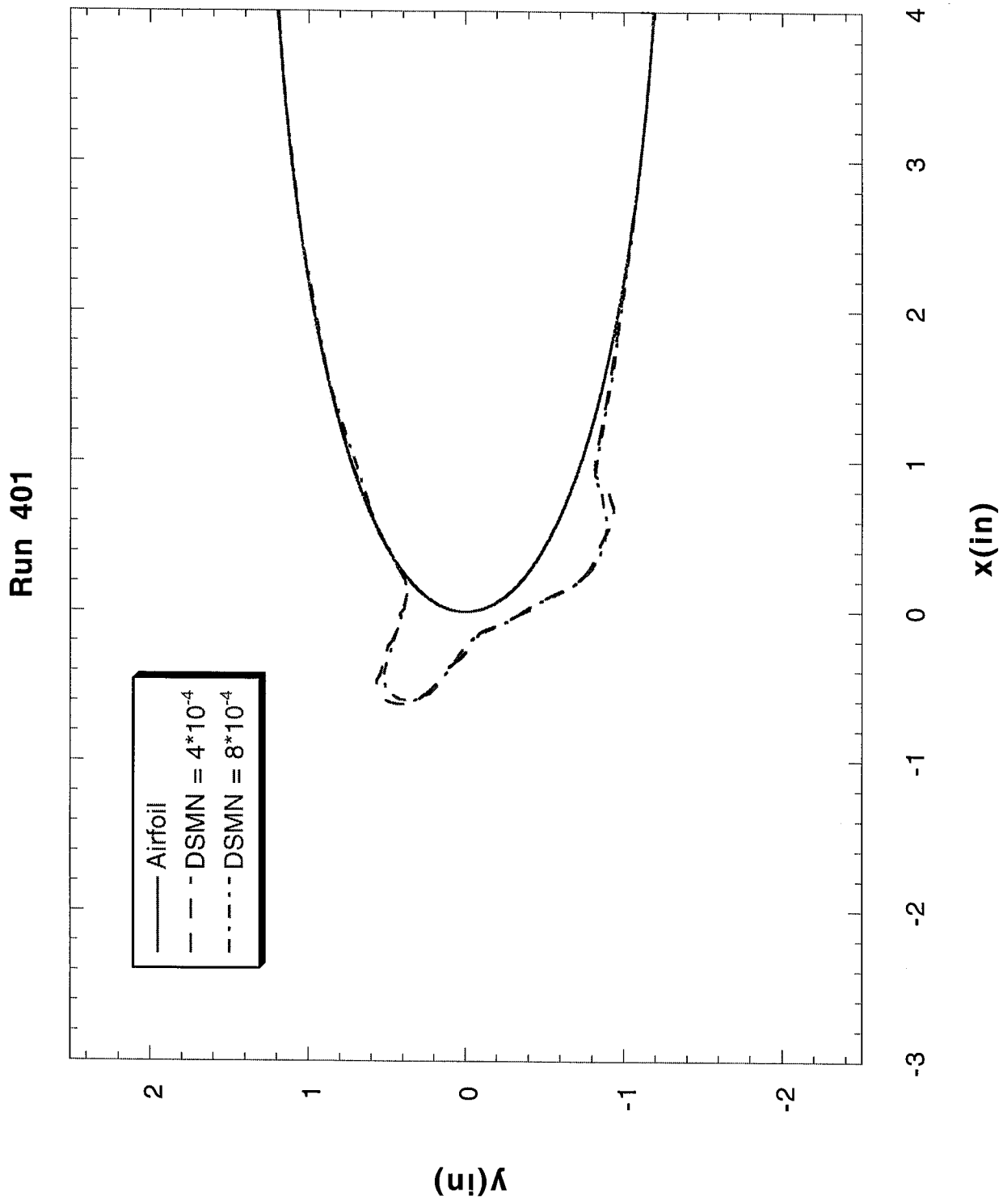

FIGURE 33

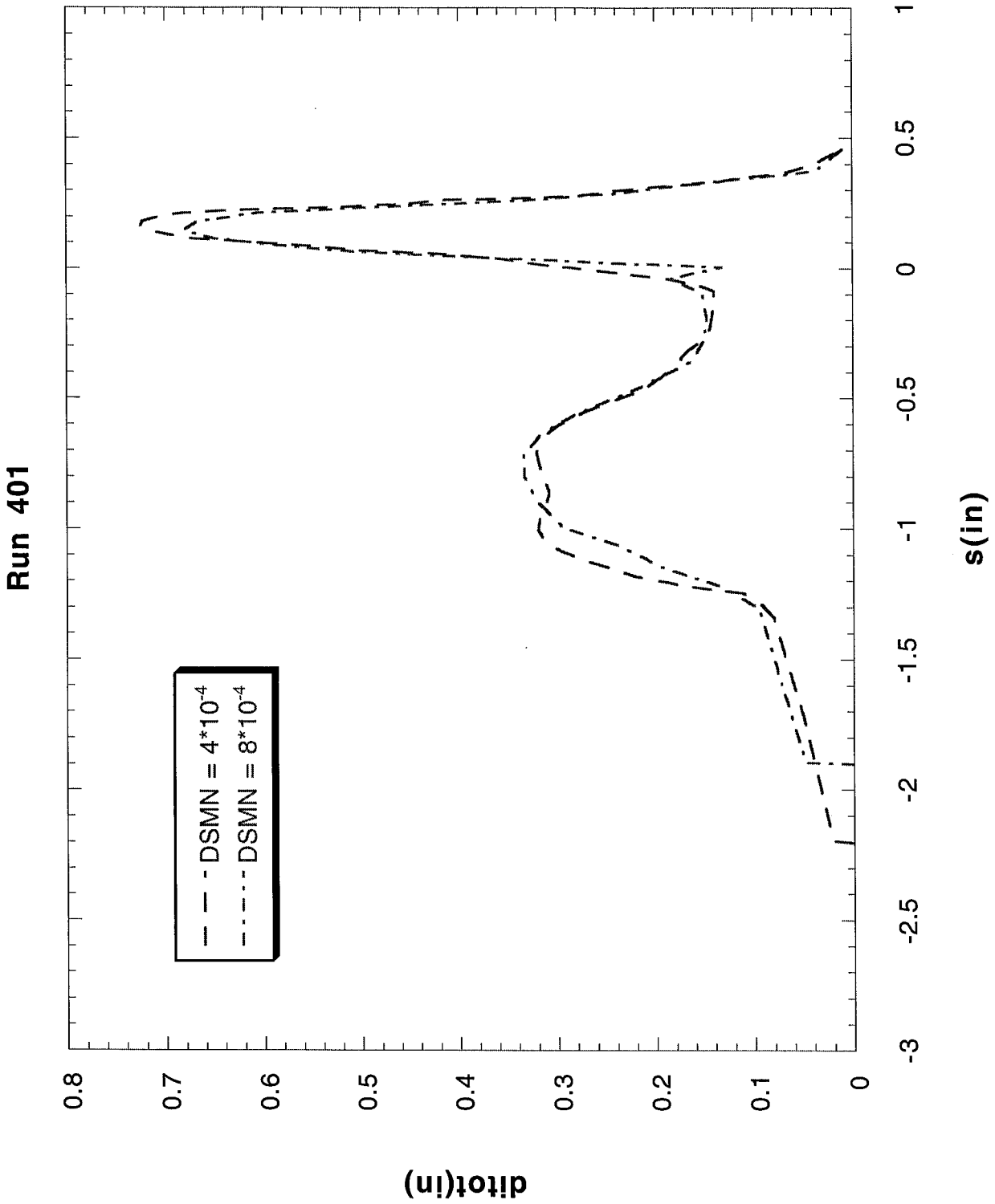
Run 401
dltot(in)
s(in)
DSMN = 4*10^-4
DSMN = 8*10^-4
0.8
0.7
0.6
0.5
0.4
0.3
0.2
0.1
0
-3
-2.5
-2
-1.5
-1
-0.5
0
0.5
1

FIGURE 34

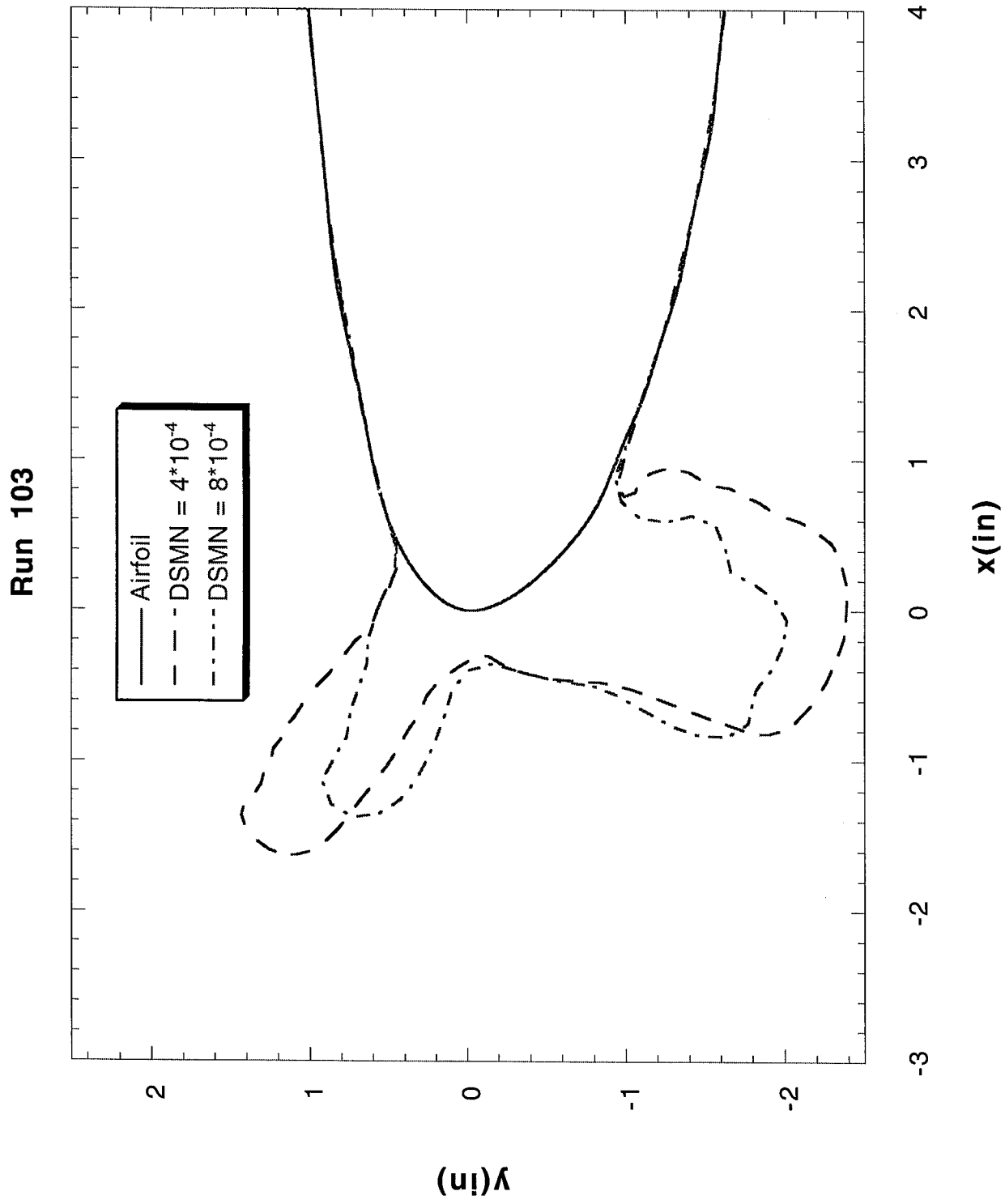

FIGURE 35

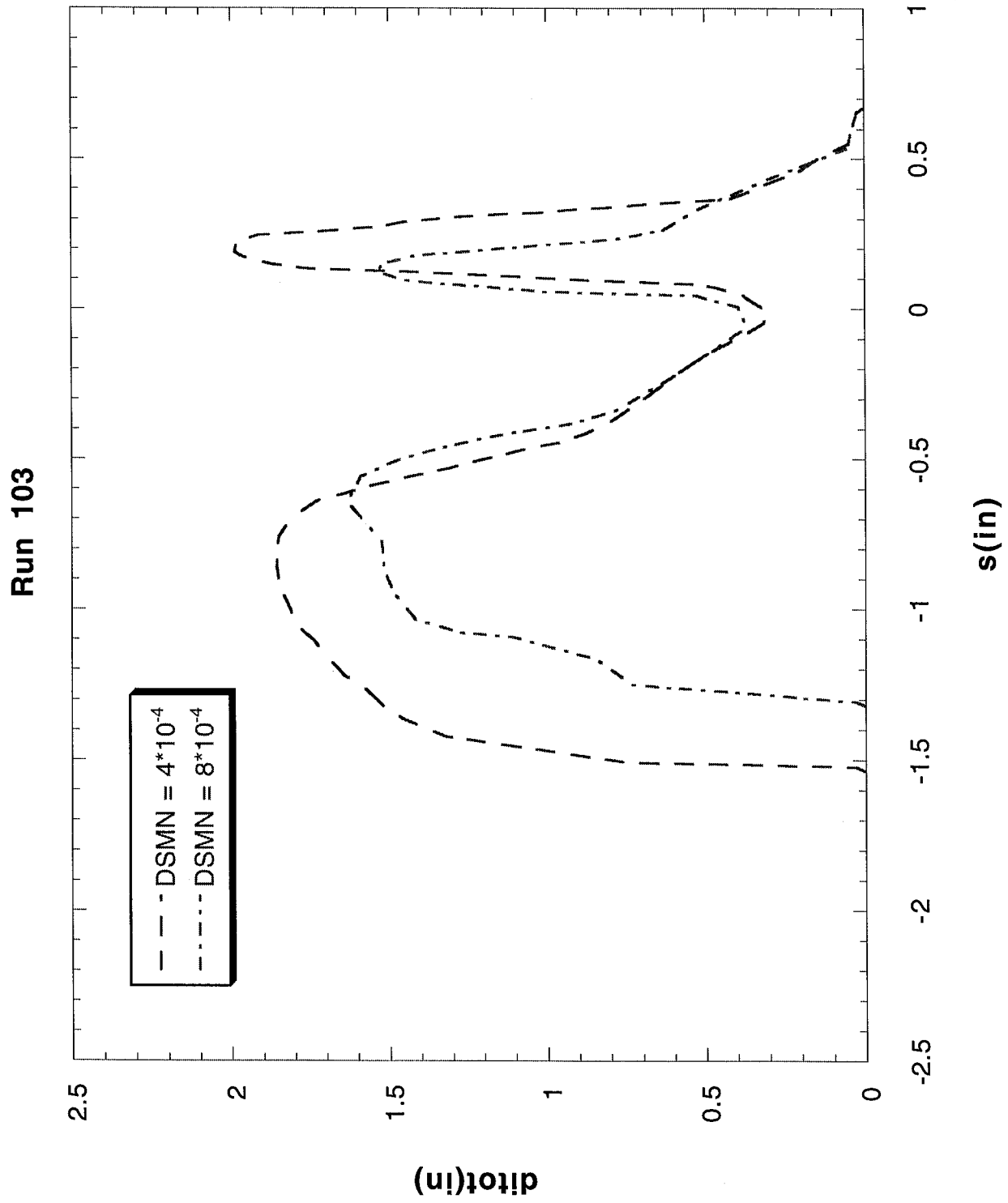
Run 103
DSMN = 4*10^-4
DSMN = 8*10^-4
dltot(in)
s(in)
2.5
2
1.5
1
0.5
0
-2.5
-2
-1.5
-1
-0.5
0
0.5
1

FIGURE 36

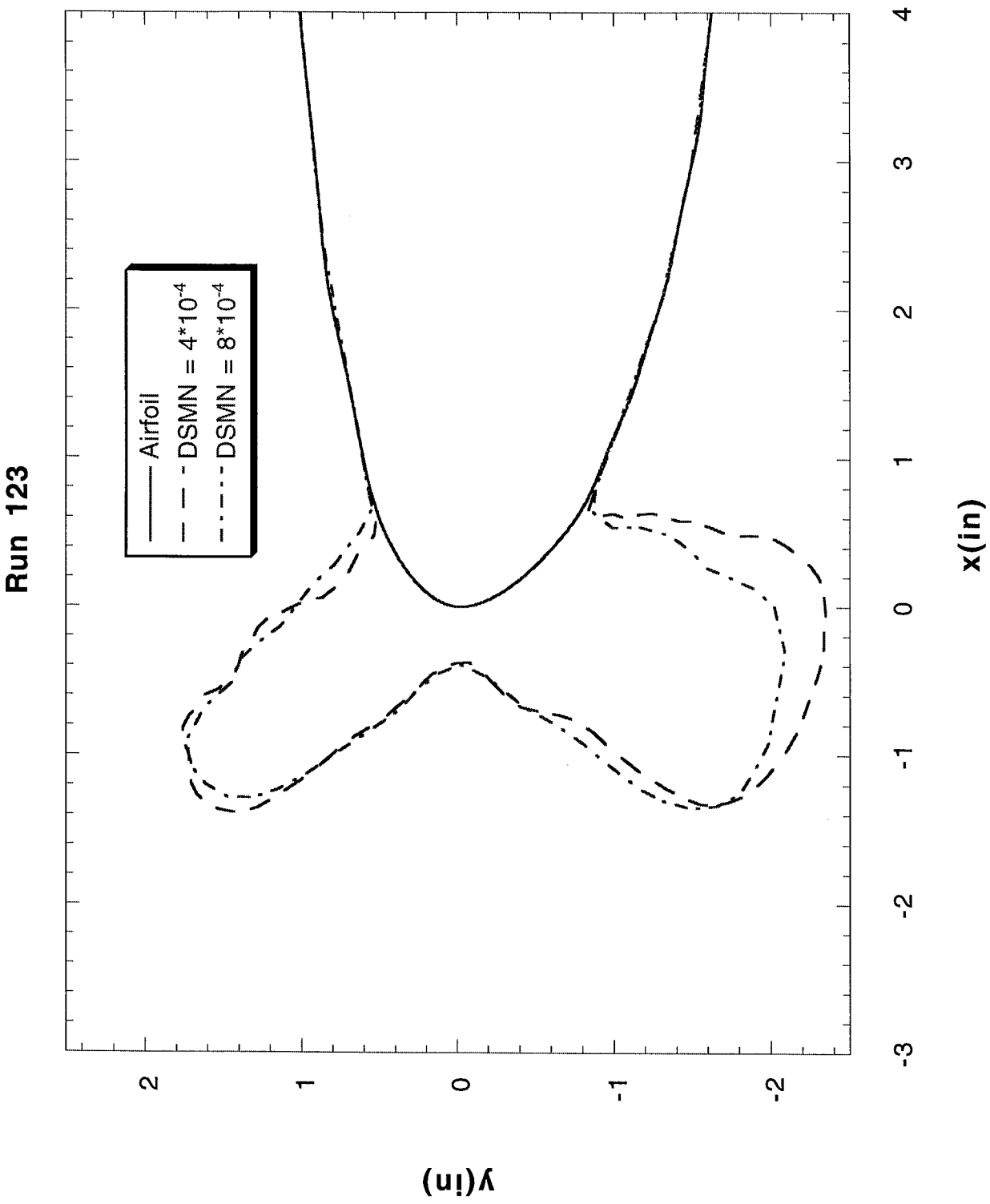

FIGURE 37

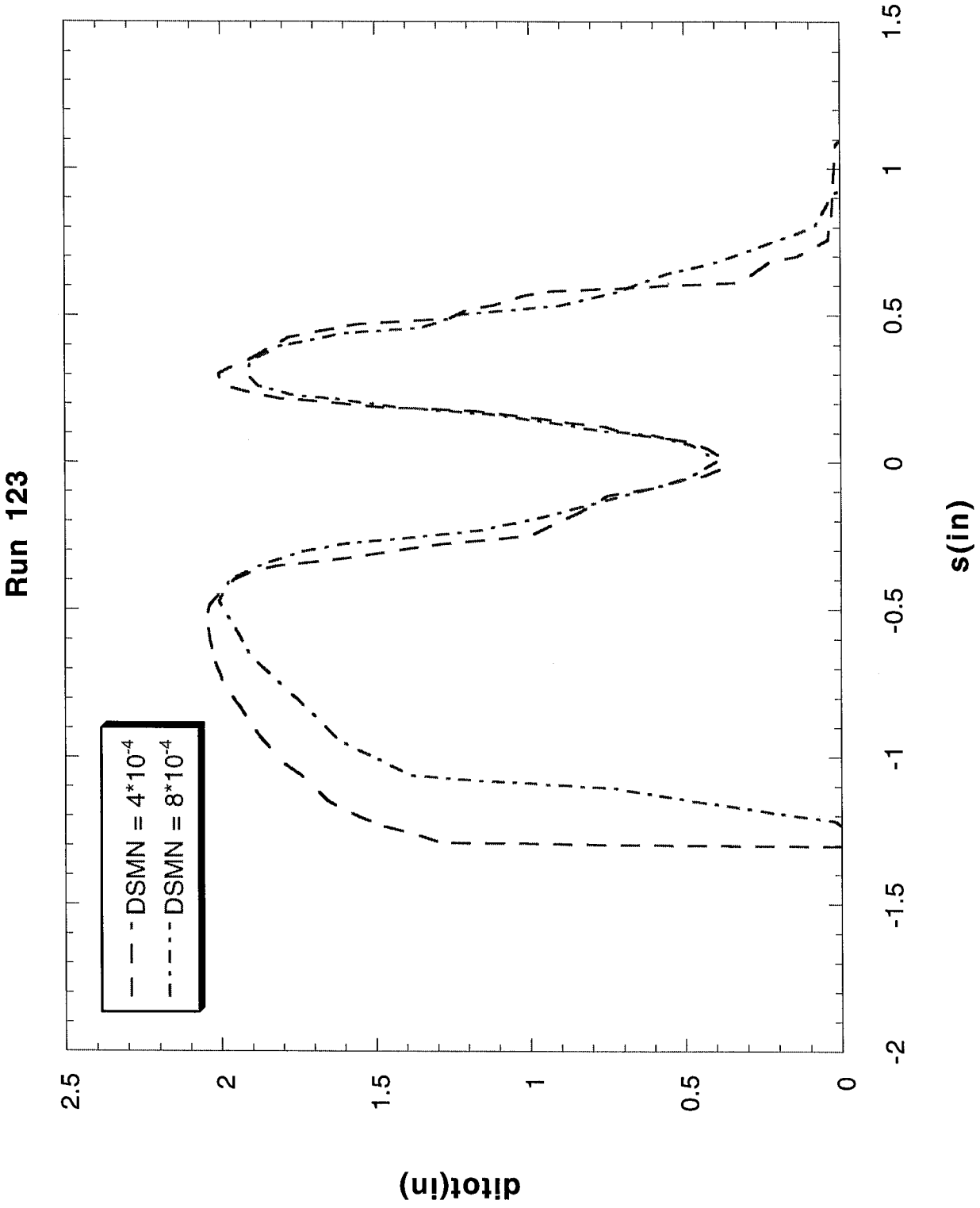
Run 123
dltot(in)
s(in)
- DSMN = 4*10^-4
- DSMN = 8*10^-4
2.5
2
1.5
1
0.5
0
1.5
1
0.5
0
-0.5
-1
-1.5
-2

FIGURE 38

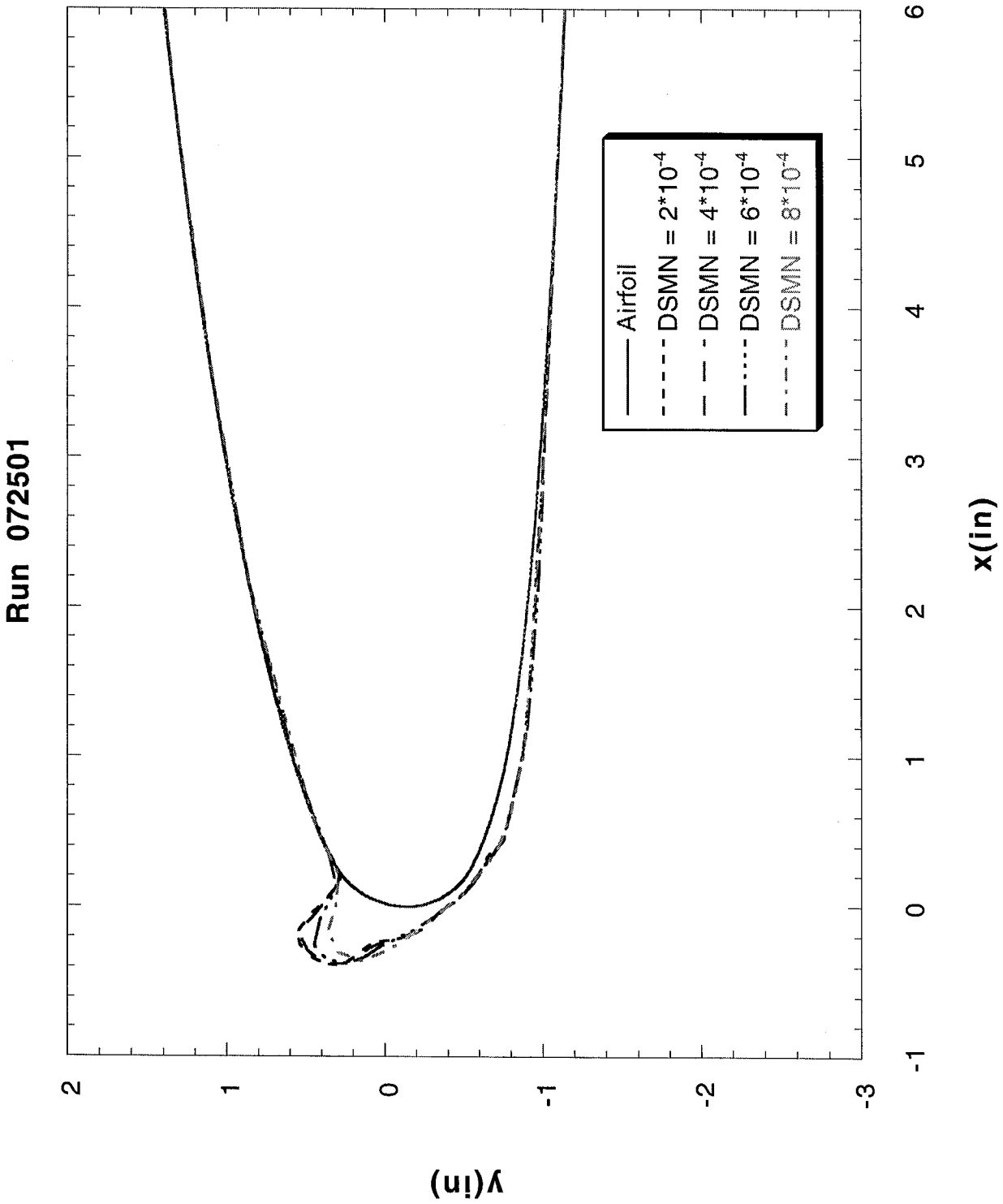
Run 072501
Airfoil
DSMN = 2*10^-4
DSMN = 4*10^-4
DSMN = 6*10^-4
DSMN = 8*10^-4
y(in)
x(in)
2
1
0
-1
-2
-3
-1
0
1
2
3
4
5
6

FIGURE 39

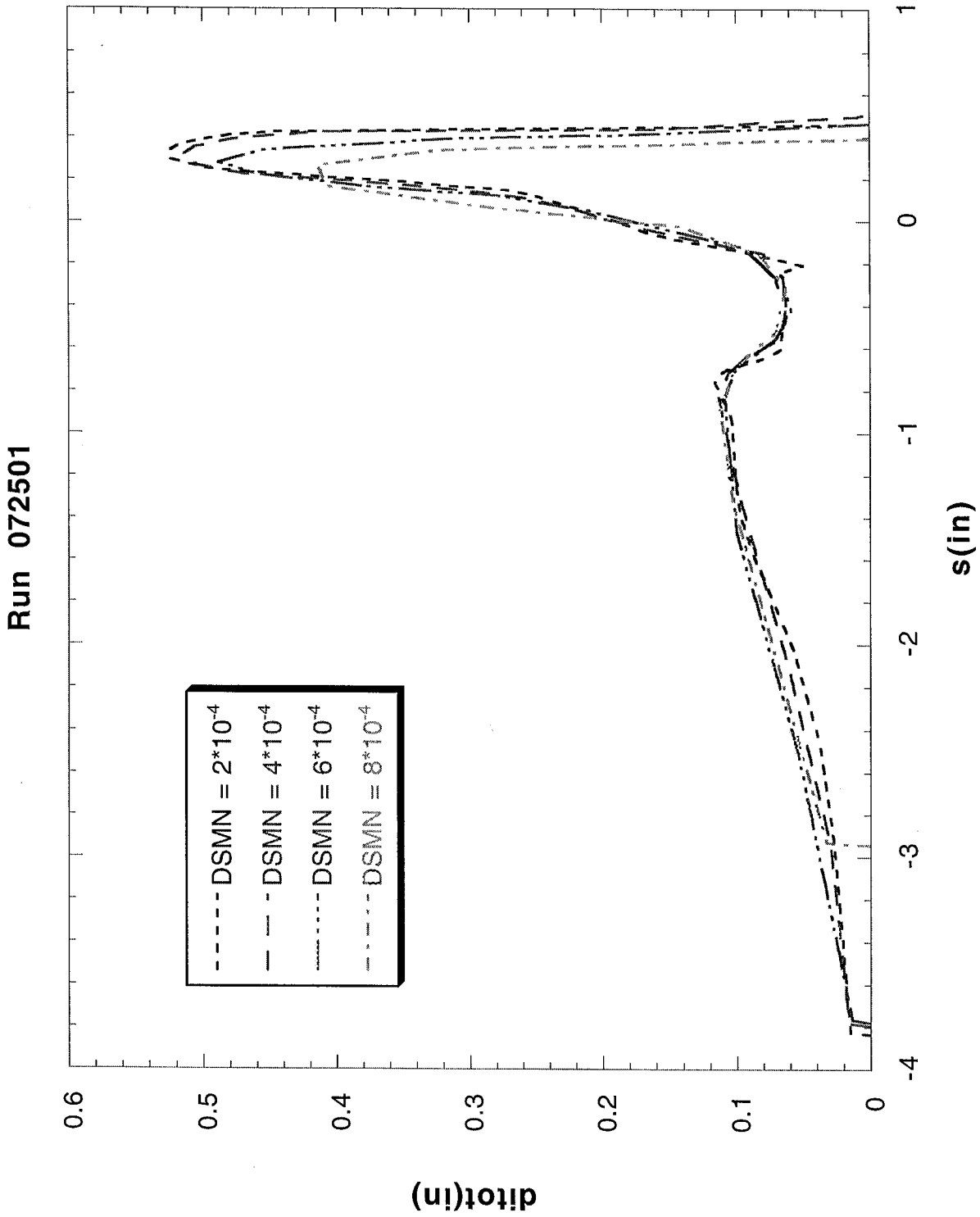
Run 072501
dltot(in)
s(in)
DSMN = 2*10-4
DSMN = 4*10-4
DSMN = 6*10-4
DSMN = 8*10-4
0
0.1
0.2
0.3
0.4
0.5
0.6
-4
-3
-2
-1
0
1

FIGURE 40

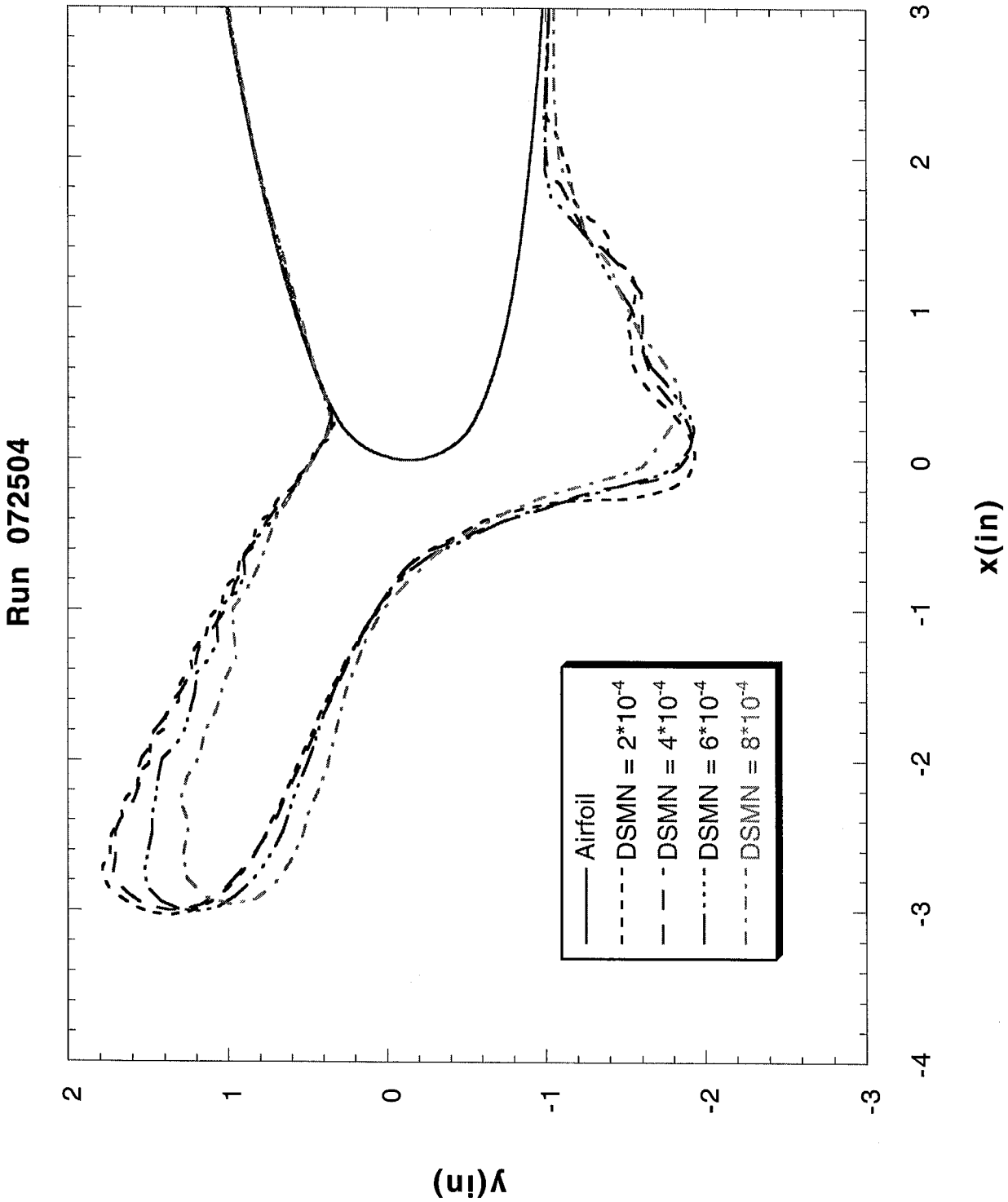
Run 072504
Airfoil
DSMN = 2*10-4
DSMN = 4*10-4
DSMN = 6*10-4
DSMN = 8*10-4
y(in)
x(in)
2
1
0
-1
-2
-3
3
2
1
0
-1
-2
-3
-4

FIGURE 41

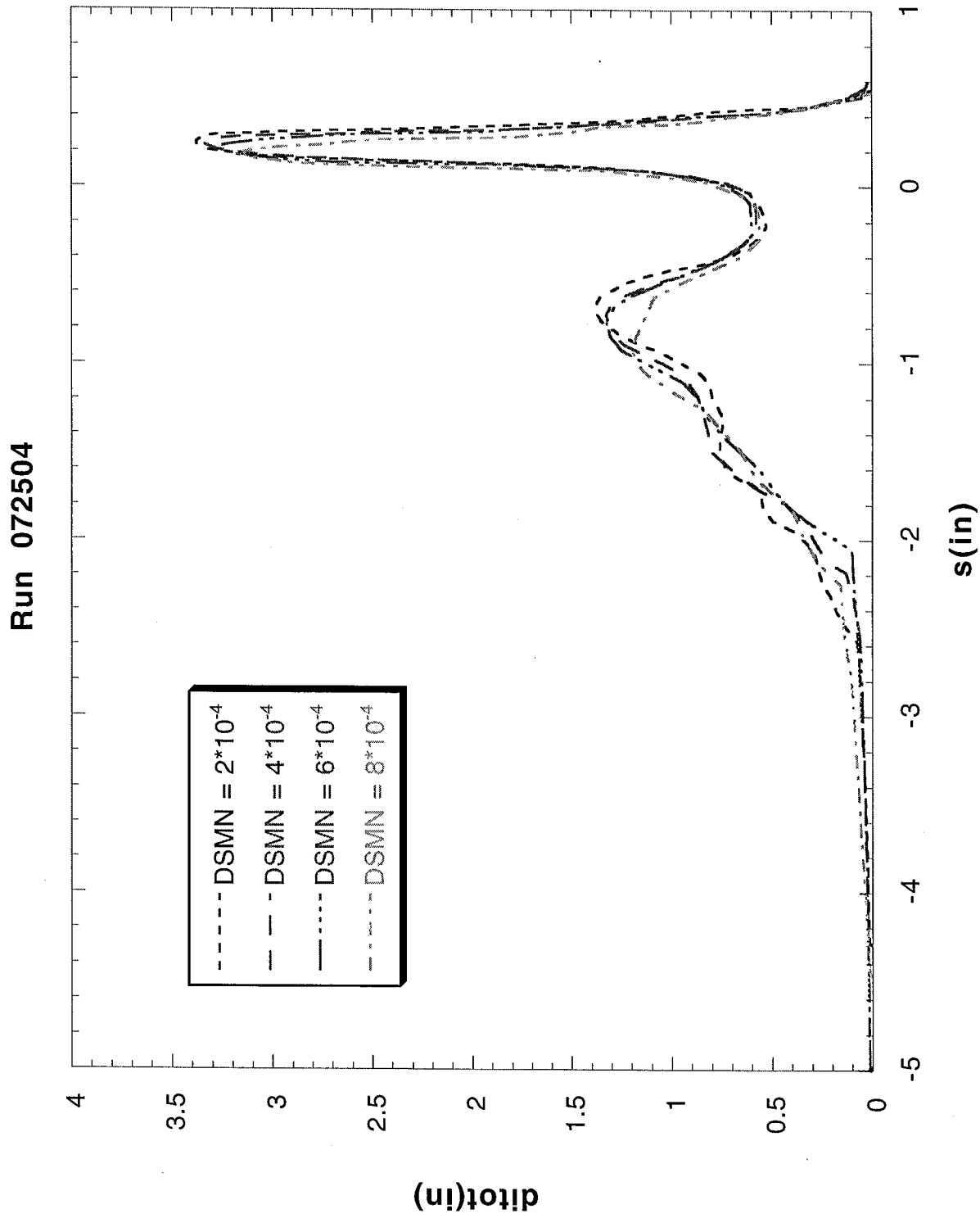
Run 072504
ditot(in)
s(in)
DSMN = 2*10^-4
DSMN = 4*10^-4
DSMN = 6*10^-4
DSMN = 8*10^-4
4
3.5
3
2.5
2
1.5
1
0.5
0
1
0
-1
-2
-3
-4
-5

Time Step Cases

FIGURE 42

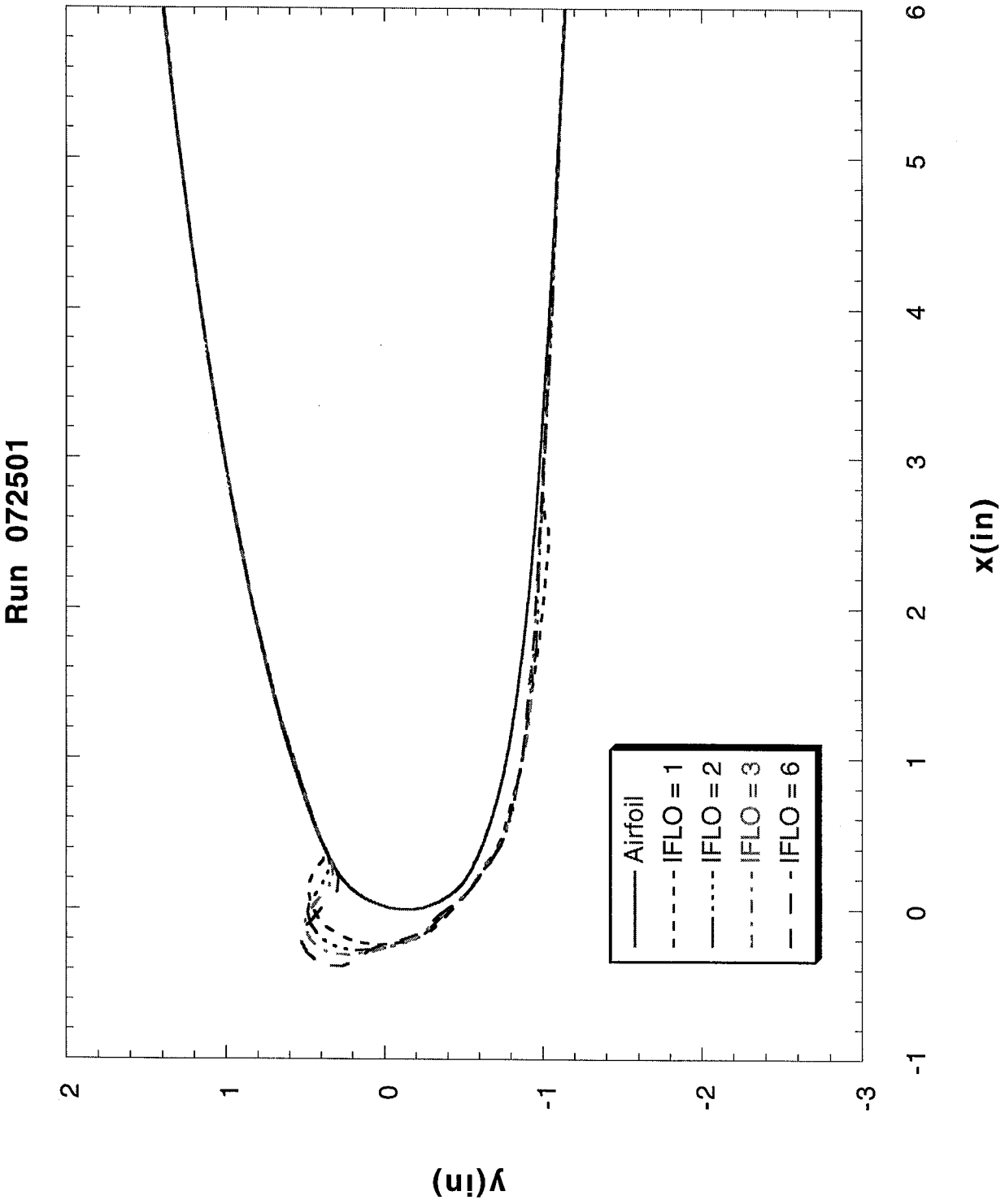
Run 072501
y(in)
x(in)
2
1
0
-1
-2
-3
-1
0
1
2
3
4
5
6
Airfoil
IFLO = 1
IFLO = 2
IFLO = 3
IFLO = 6

FIGURE 43

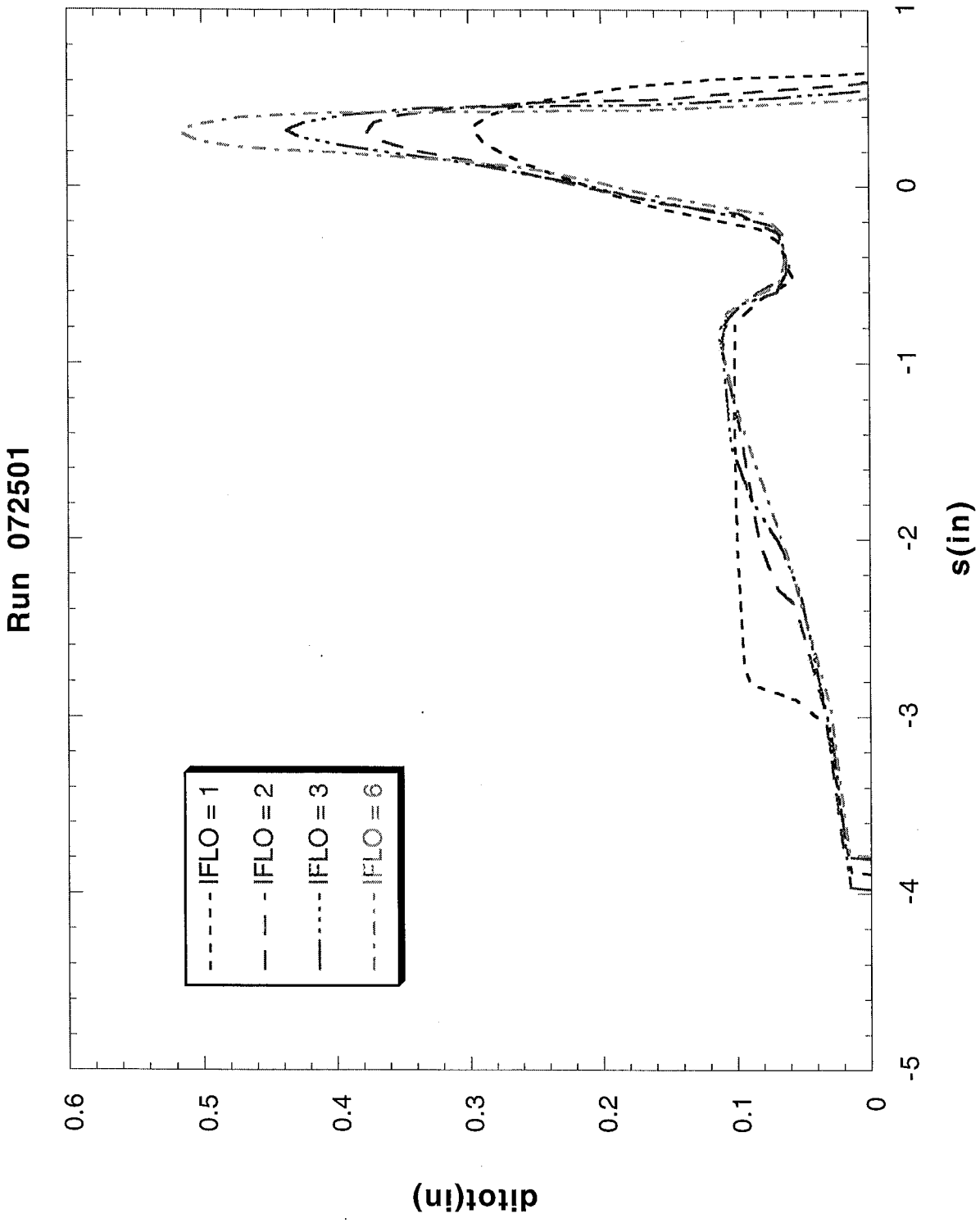
Run 072501
dltot(in)
s(in)
IFLO = 1
IFLO = 2
IFLO = 3
IFLO = 6
0.6
0.5
0.4
0.3
0.2
0.1
0
1
0
-1
-2
-3
-4
-5

FIGURE 44

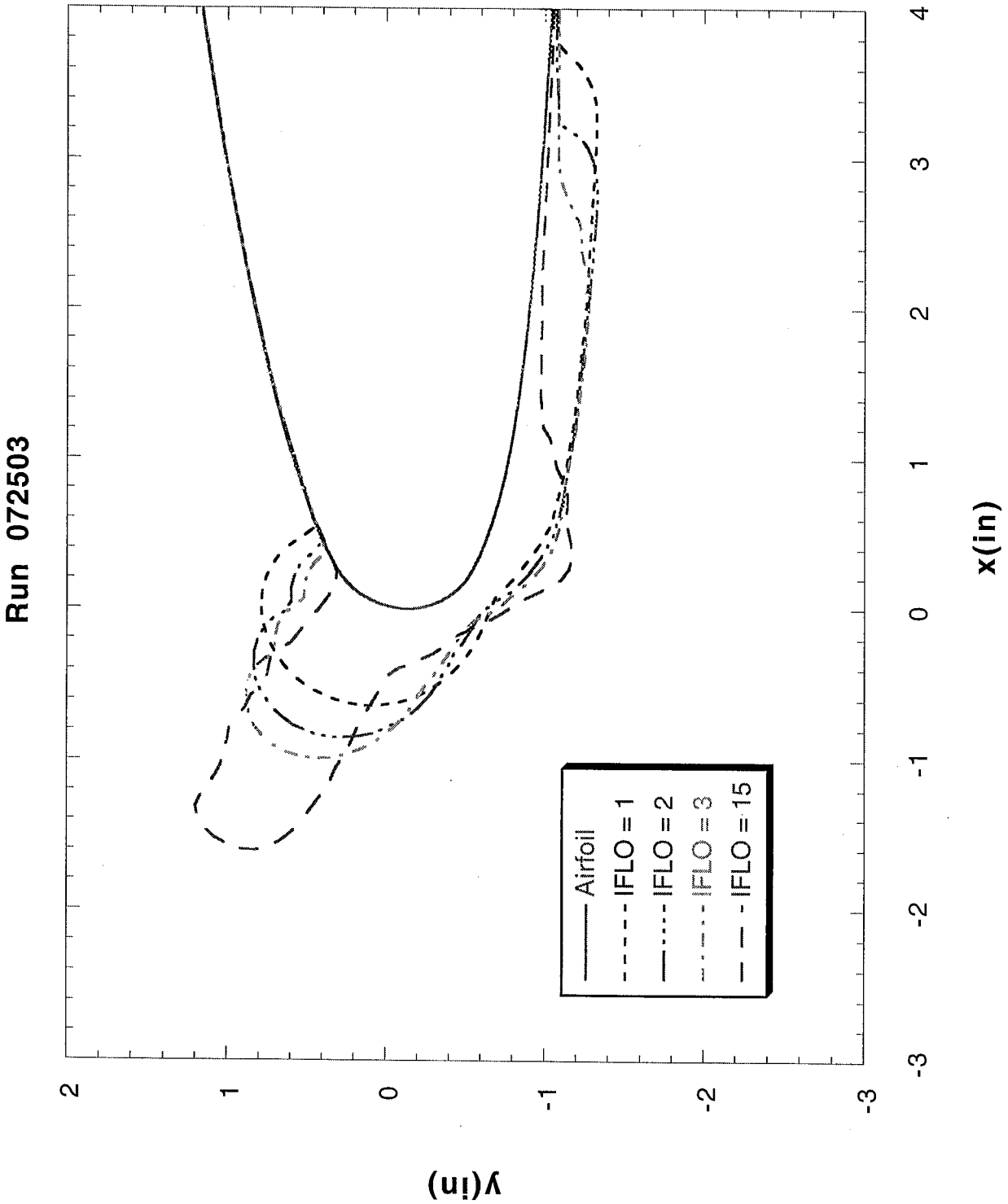
Run 072503
Airfoil
IFLO = 1
IFLO = 2
IFLO = 3
IFLO = 15
y(in)
x(in)
2
1
0
-1
-2
-3
4
3
2
1
0
-1
-2
-3

FIGURE 45

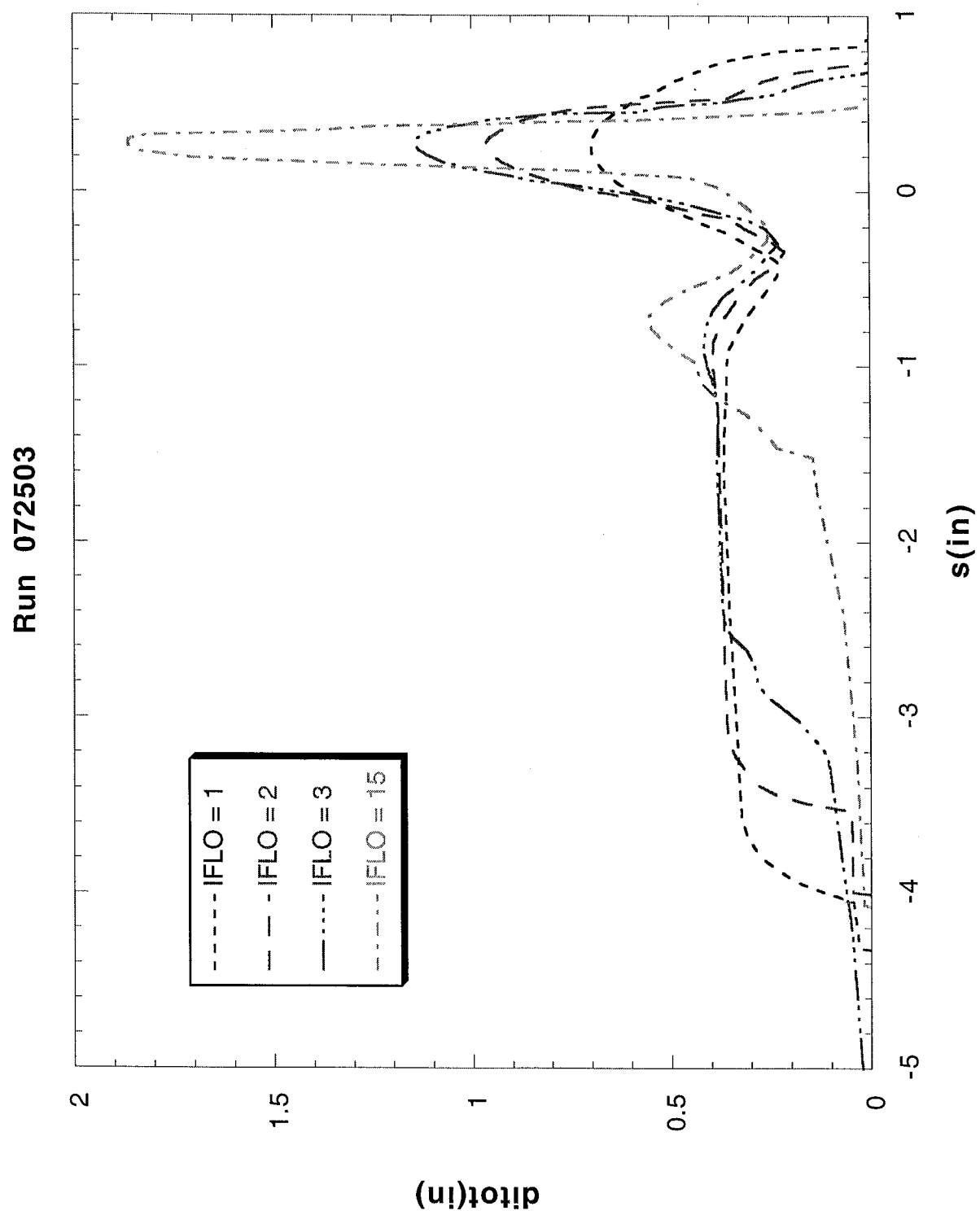
Run 072503
dltot(in)
s(in)
IFLO = 1
IFLO = 2
IFLO = 3
IFLO = 15
2
1.5
1
0.5
0
1
0
-1
-2
-3
-4
-5

FIGURE 46

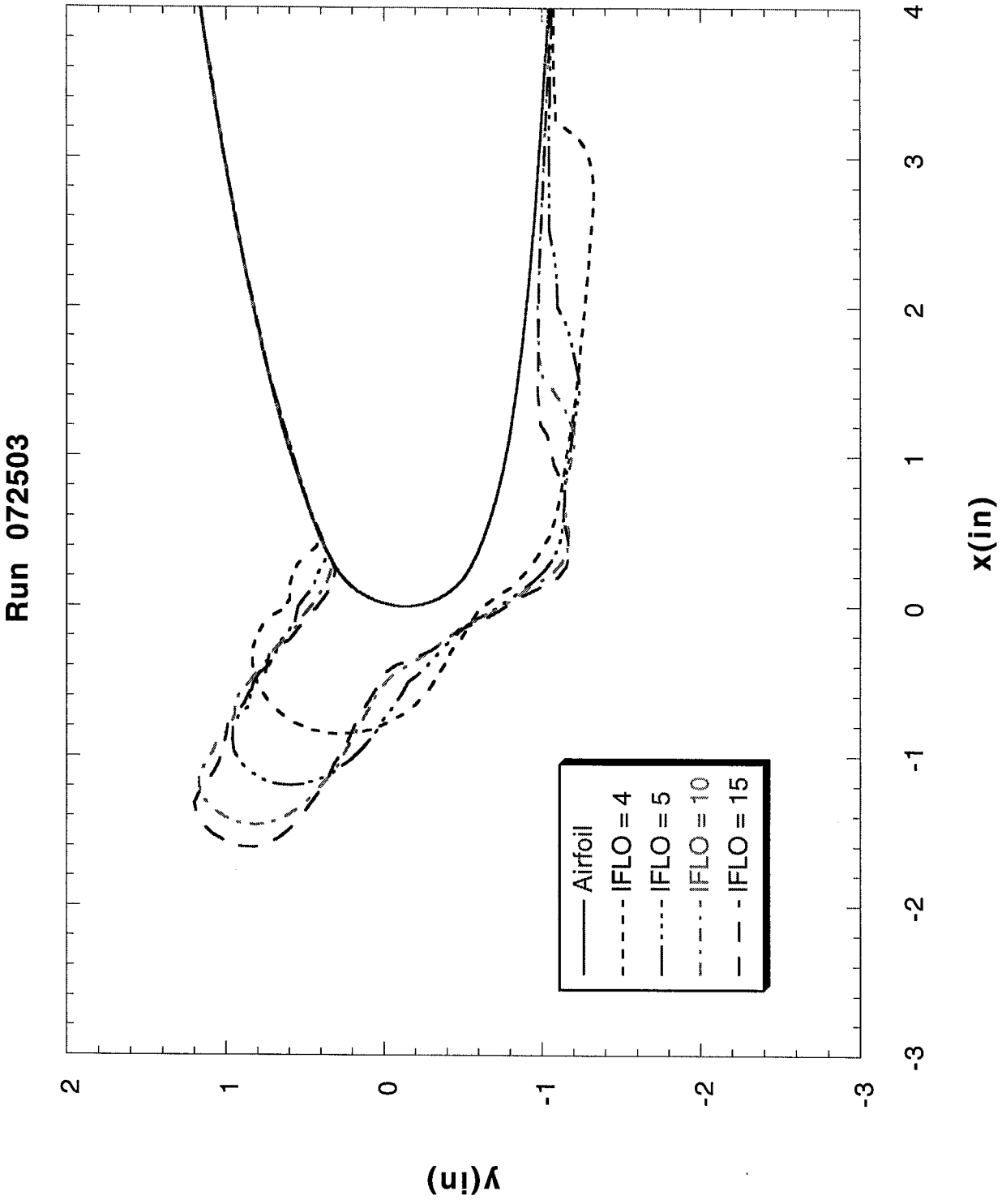
Run 072503
Airfoil
IFLO = 4
IFLO = 5
IFLO = 10
IFLO = 15
y(in)
x(in)
2
1
0
-1
-2
-3
4
3
2
1
0
-1
-2
-3

FIGURE 47

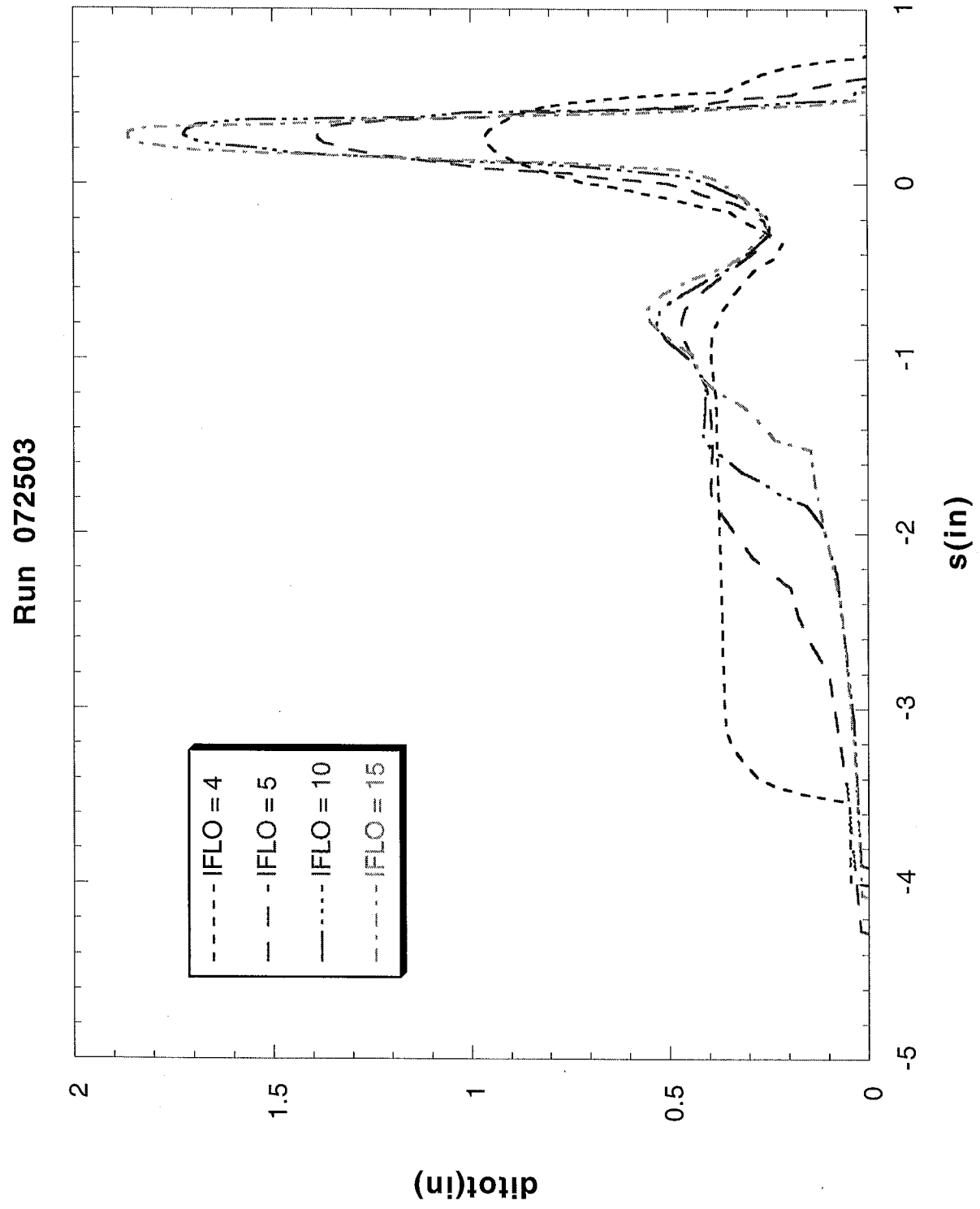
Run 072503
ditot(in)
s(in)
IFLO = 4
IFLO = 5
IFLO = 10
IFLO = 15
2
1.5
1
0.5
0
1
0
-1
-2
-3
-4
-5

FIGURE 48

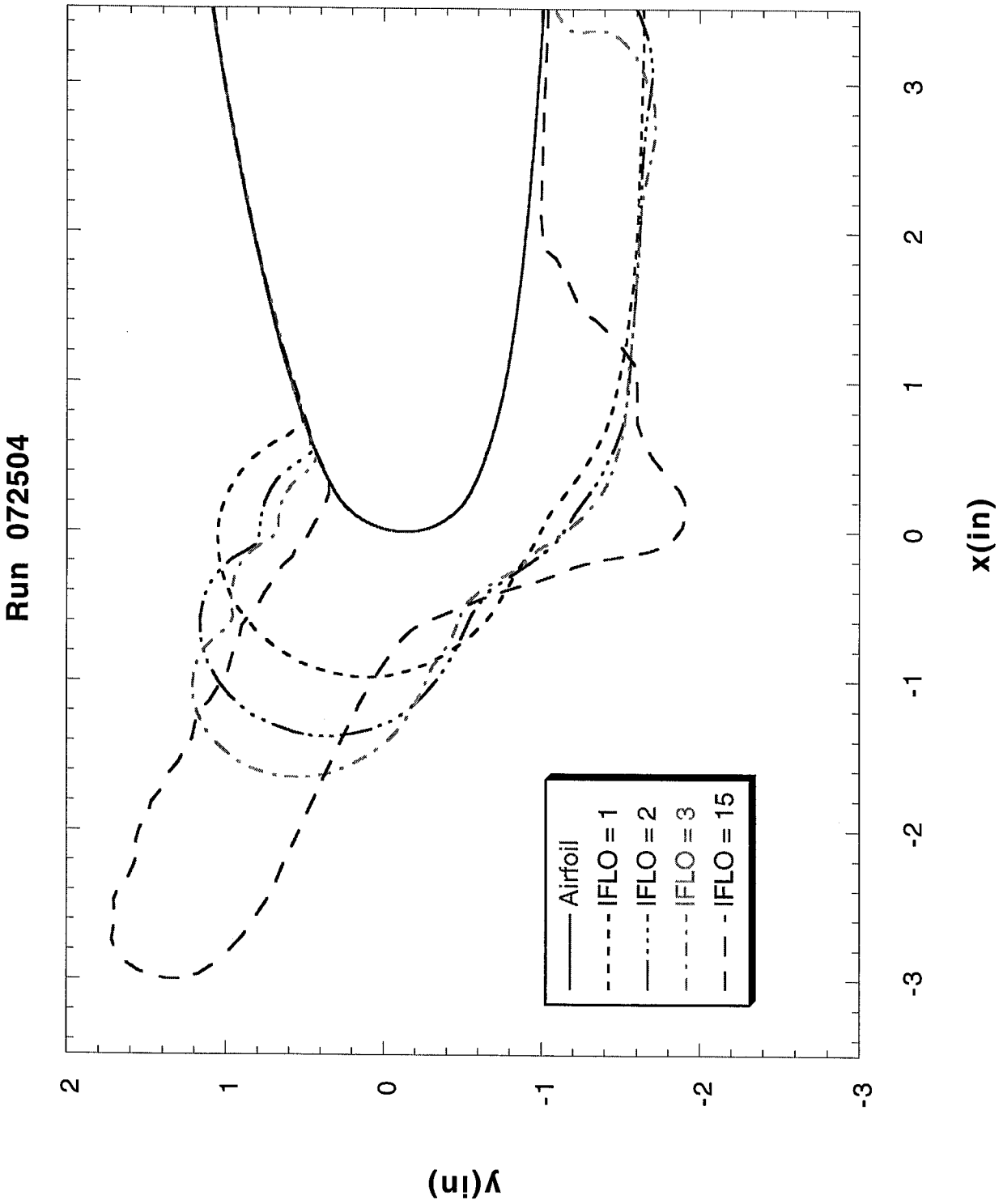
Run 072504
Airfoil
IFLO = 1
IFLO = 2
IFLO = 3
IFLO = 15
y(in)
x(in)
2
1
0
-1
-2
-3
3

FIGURE 49

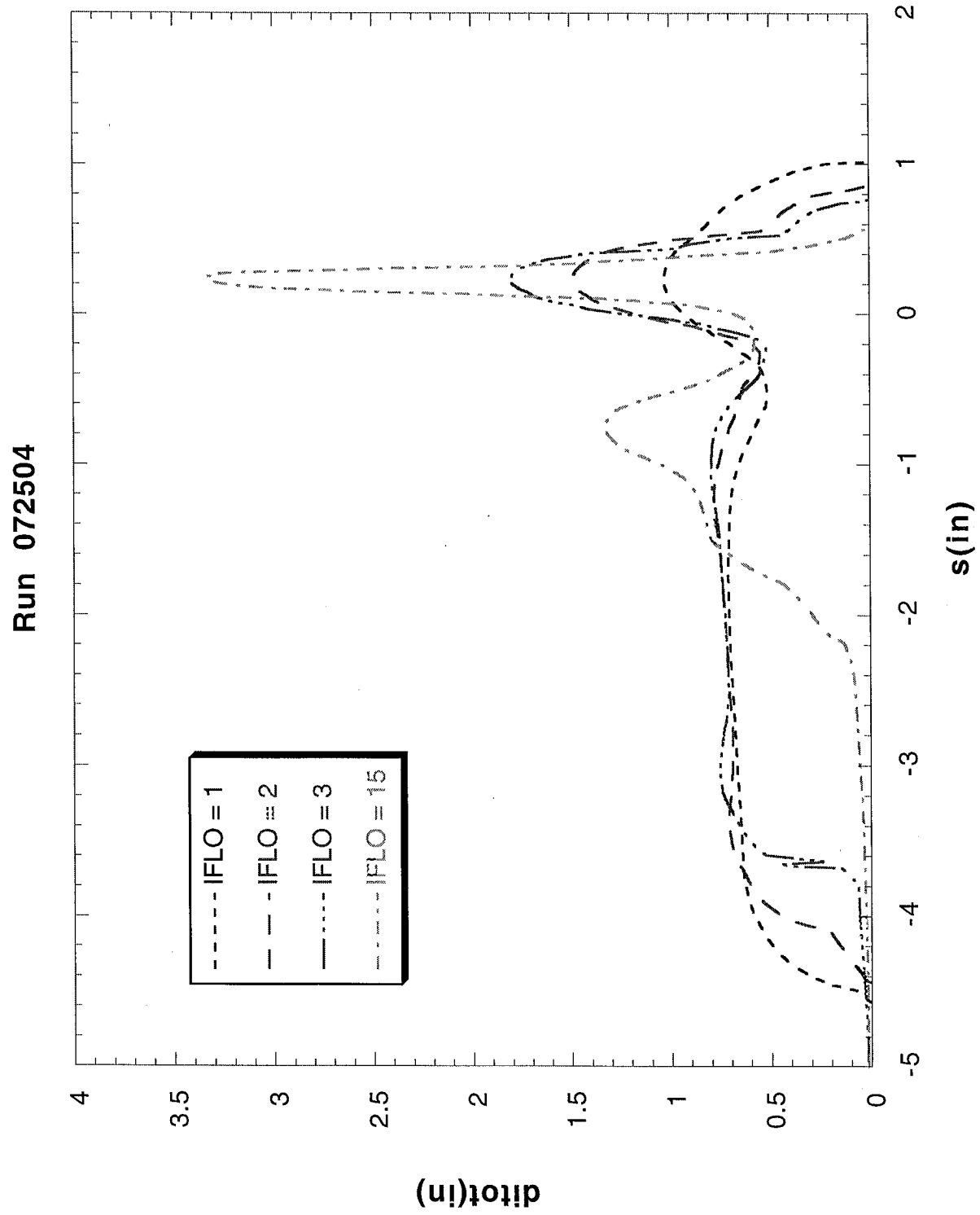
Run 072504
dltot(in)
s(in)
IFLO = 1
IFLO = 2
IFLO = 3
IFLO = 15
4
3.5
3
2.5
2
1.5
1
0.5
0
-5
-4
-3
-2
-1
0
1
2

FIGURE 50

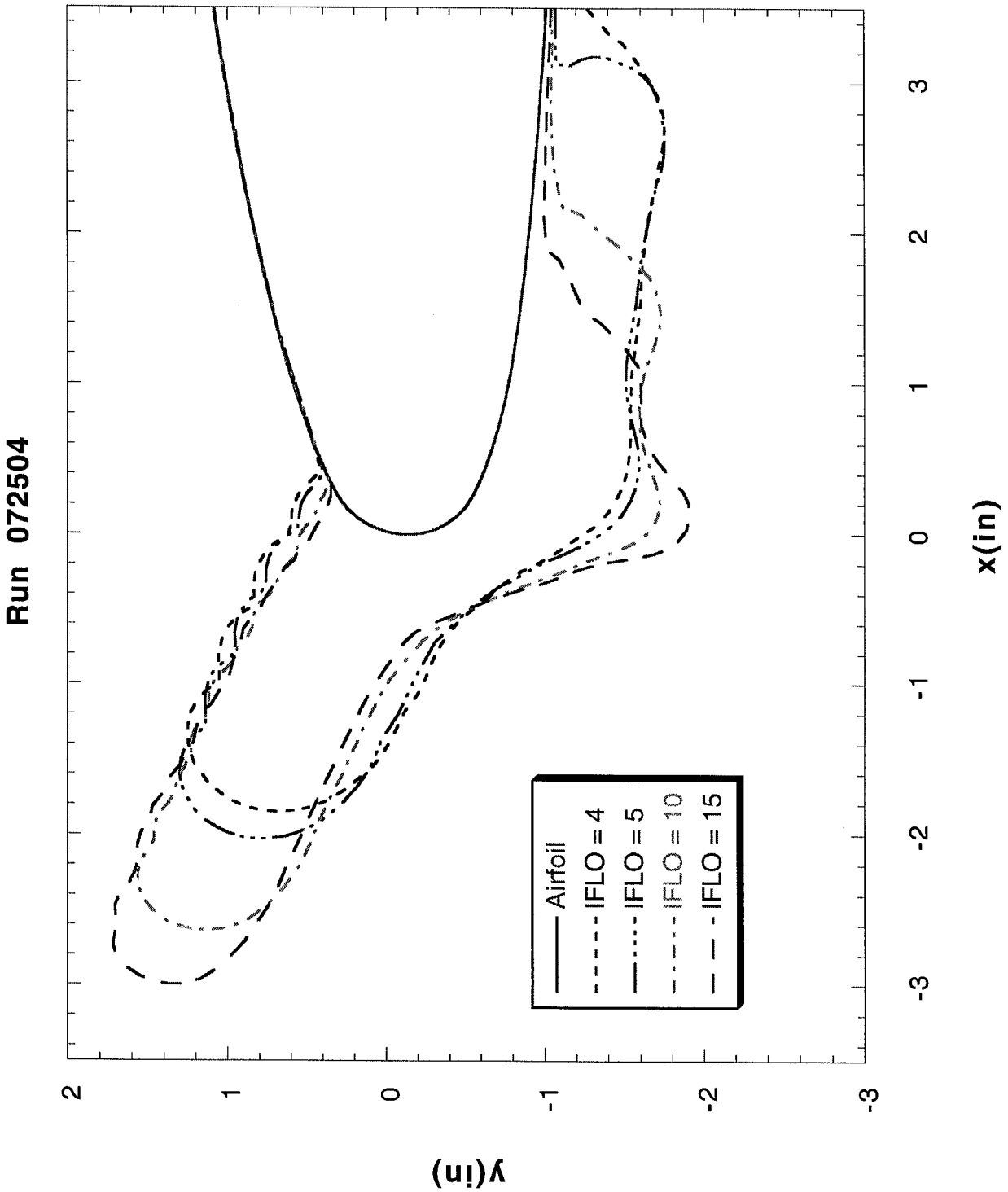
Run 072504
Airfoil
IFLO = 4
IFLO = 5
IFLO = 10
IFLO = 15
y(in)
x(in)
2
1
0
-1
-2
-3
3

FIGURE 51

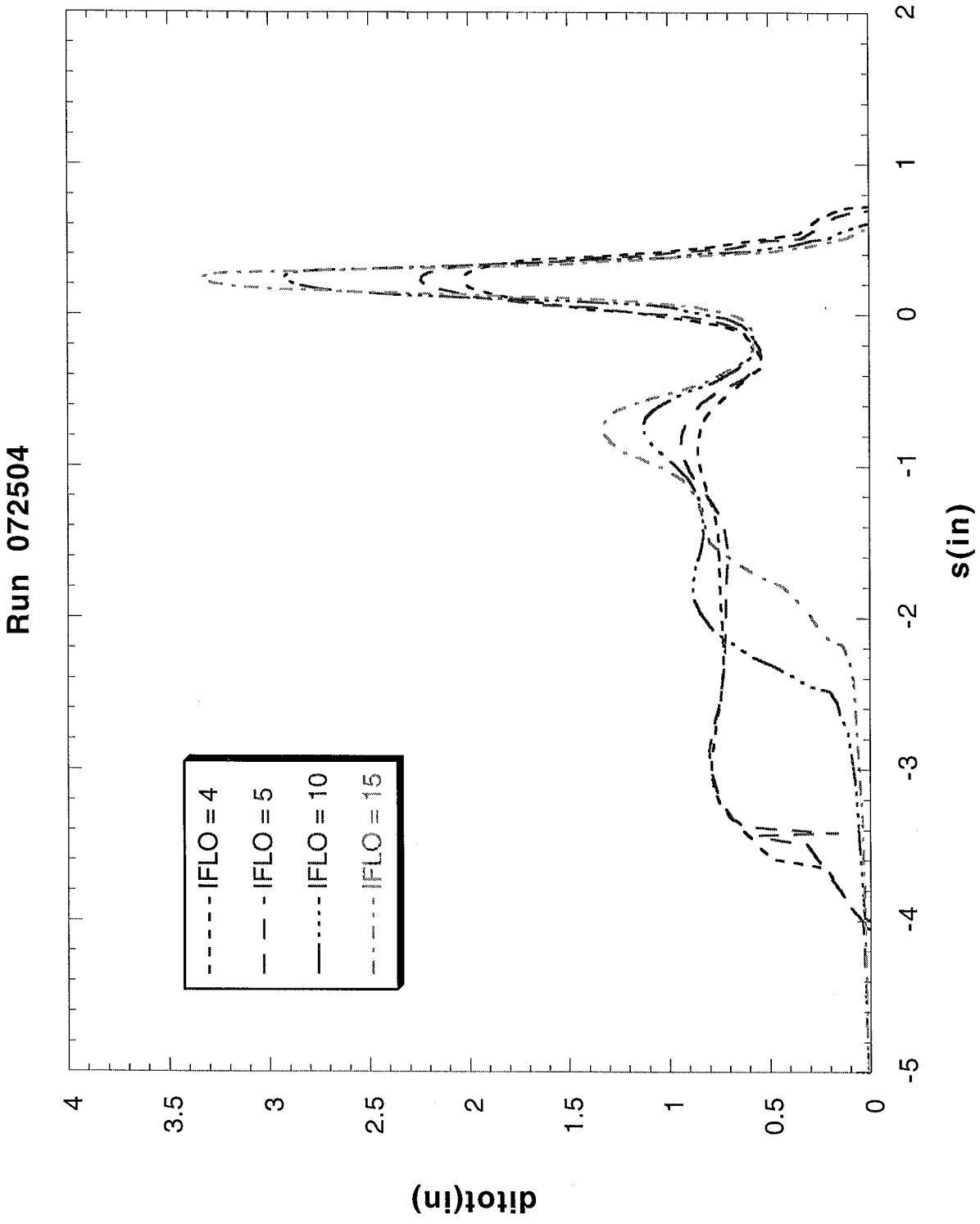
Run 072504
ditot(in)
s(in)
IFLO = 4
IFLO = 5
IFLO = 10
IFLO = 15
4
3.5
3
2.5
2
1.5
1
0.5
0
-5
-4
-3
-2
-1
0
1
2

FIGURE 52

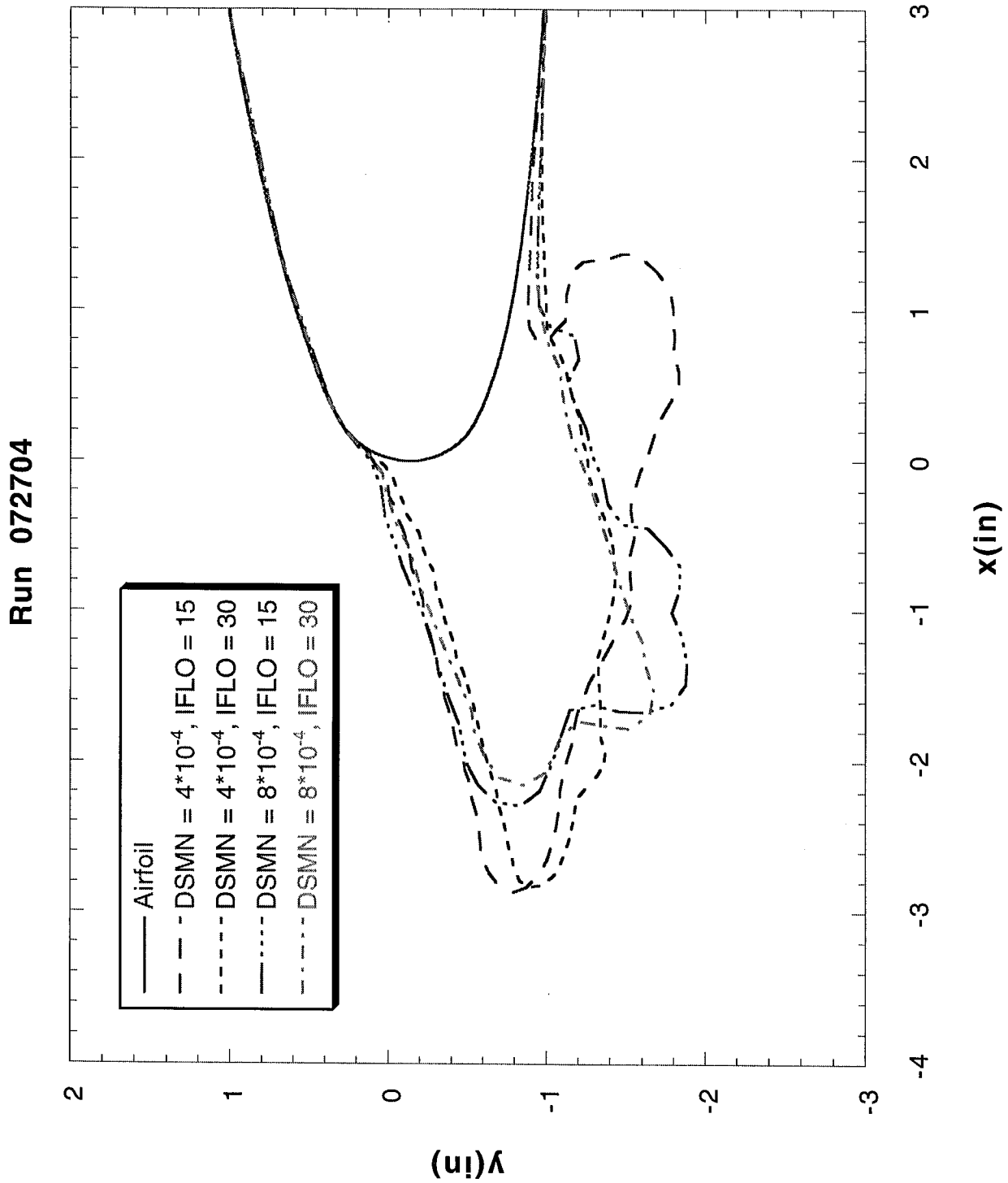
Run 072704
Airfoil
DSMN = 4*10-4, IFLO = 15
DSMN = 4*10-4, IFLO = 30
DSMN = 8*10-4, IFLO = 15
DSMN = 8*10-4, IFLO = 30
y(in)
x(in)
2
1
0
-1
-2
-3
3
2
1
0
-1
-2
-3
-4

FIGURE 53

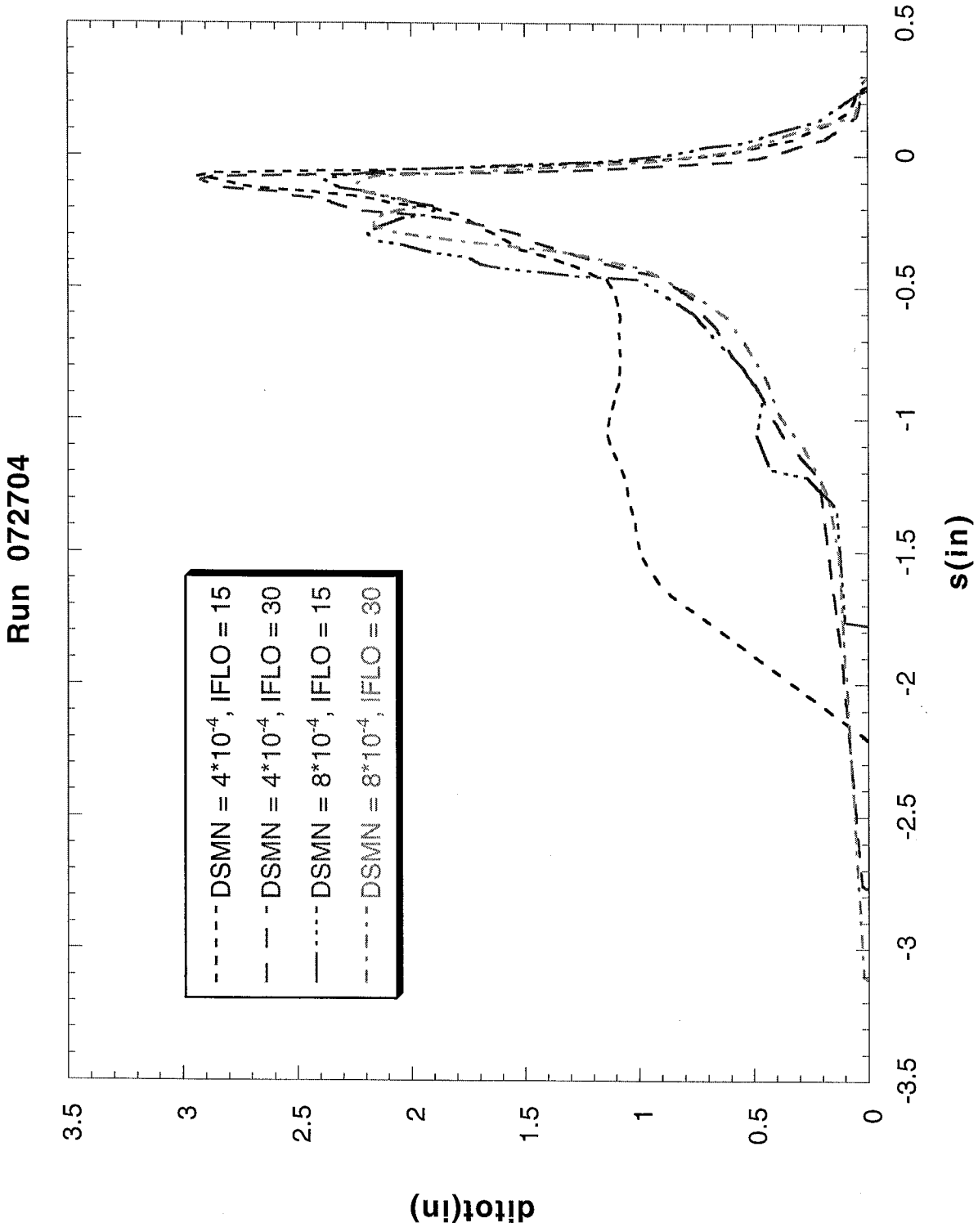
Run 072704
ditot(in)
s(in)
DSMN = 4*10^-4, IFLO = 15
DSMN = 4*10^-4, IFLO = 30
DSMN = 8*10^-4, IFLO = 15
DSMN = 8*10^-4, IFLO = 30
3.5
3
2.5
2
1.5
1
0.5
0
-3.5
-3
-2.5
-2
-1.5
-1
-0.5
0
0.5

FIGURE 54

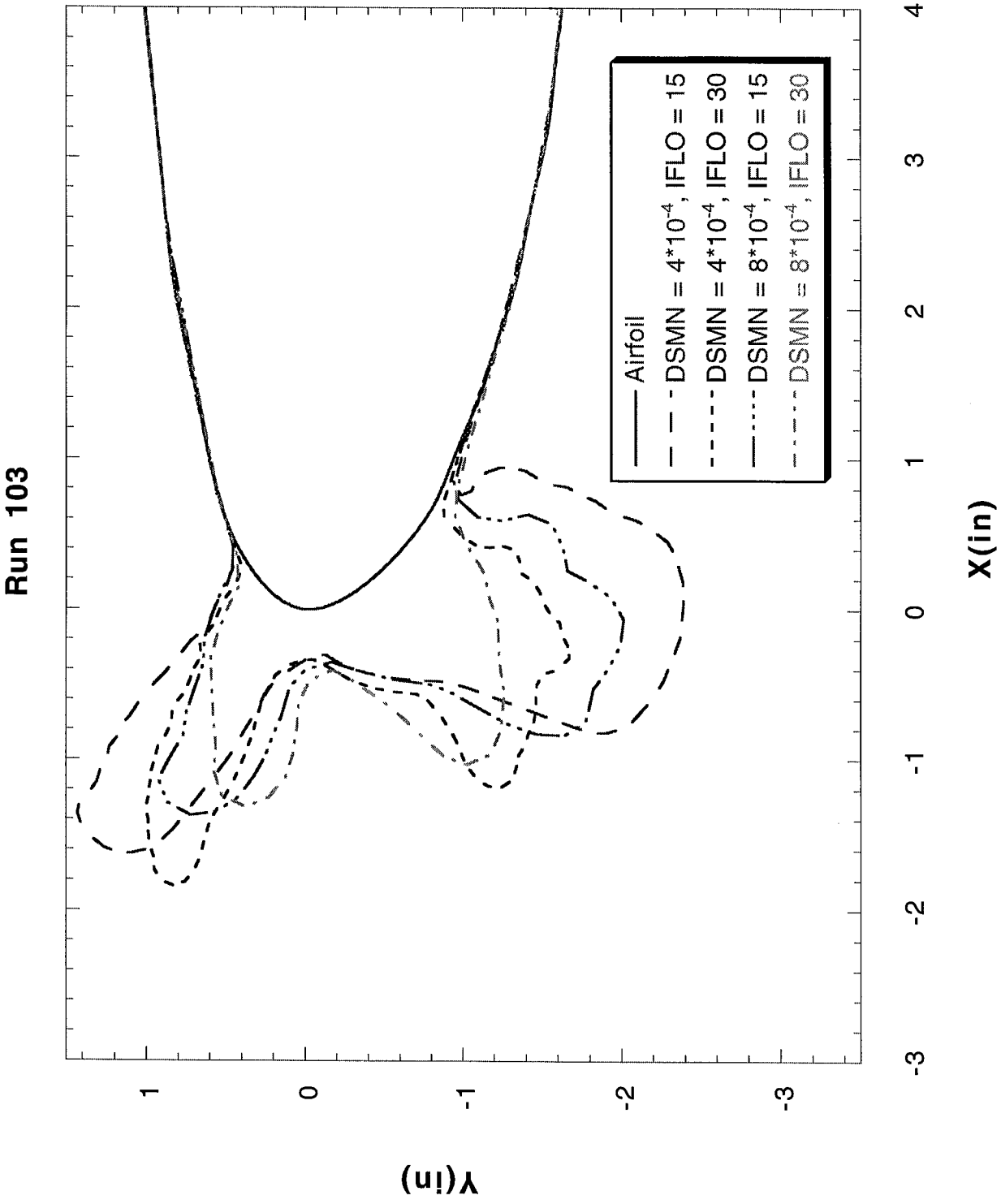
Run 103
Airfoil
DSMN = 4*10-4, IFLO = 15
DSMN = 4*10-4, IFLO = 30
DSMN = 8*10-4, IFLO = 15
DSMN = 8*10-4, IFLO = 30
Y(in)
X(in)
1
0
-1
-2
-3
4
3
2
1
0
-1
-2
-3

FIGURE 55

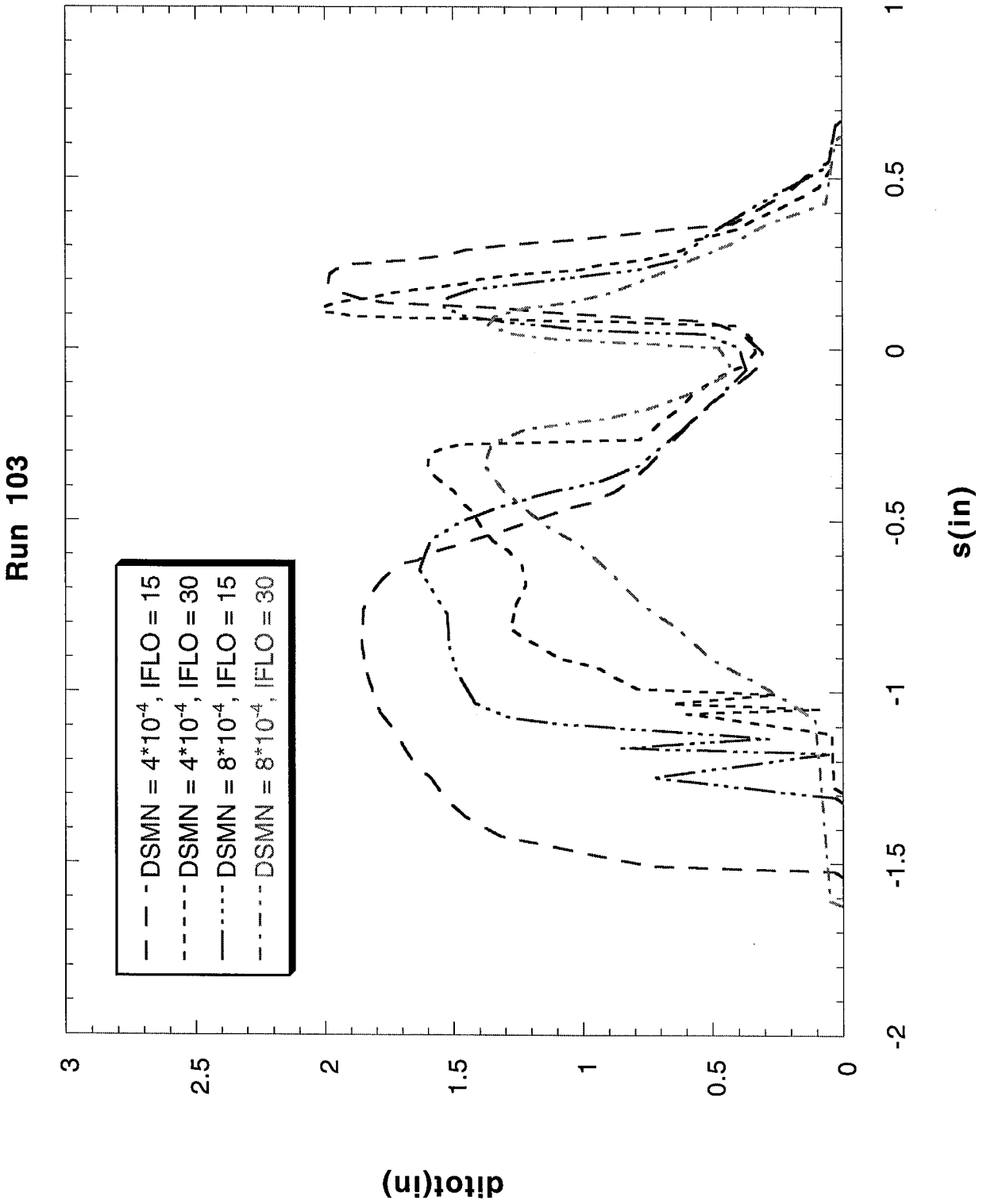
Run 103
DSMN = 4*10^-4, IFLO = 15
DSMN = 4*10^-4, IFLO = 30
DSMN = 8*10^-4, IFLO = 15
DSMN = 8*10^-4, IFLO = 30
ditot(in)
s(in)
3
2.5
2
1.5
1
0.5
0
-2
-1.5
-1
-0.5
0
0.5
1

FIGURE 56

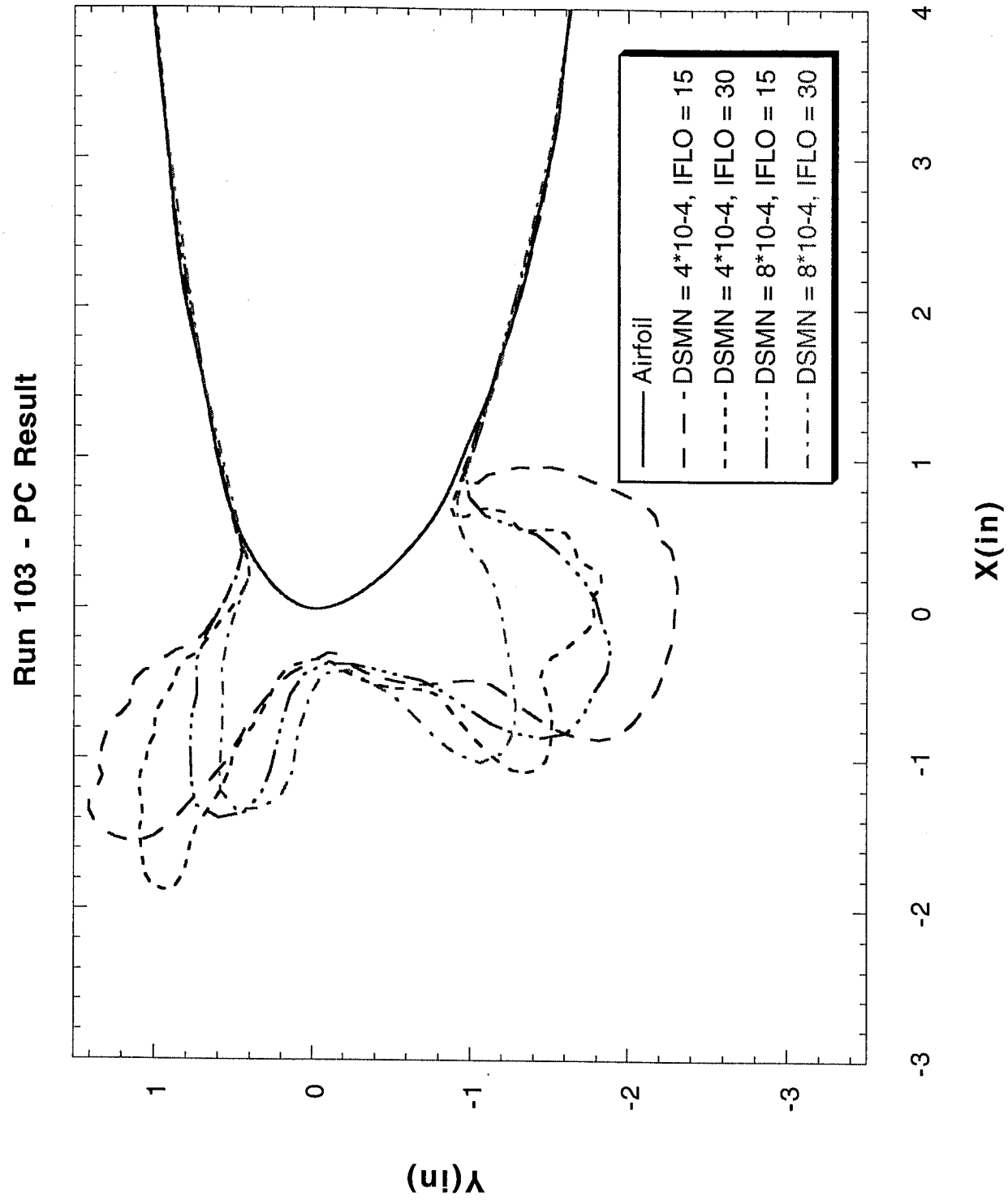
Run 103 - PC Result
Airfoil
DSMN = 4*10-4, IFLO = 15
DSMN = 4*10-4, IFLO = 30
DSMN = 8*10-4, IFLO = 15
DSMN = 8*10-4, IFLO = 30
X(in)
Y(in)
4
3
2
1
0
-1
-2
-3

FIGURE 57

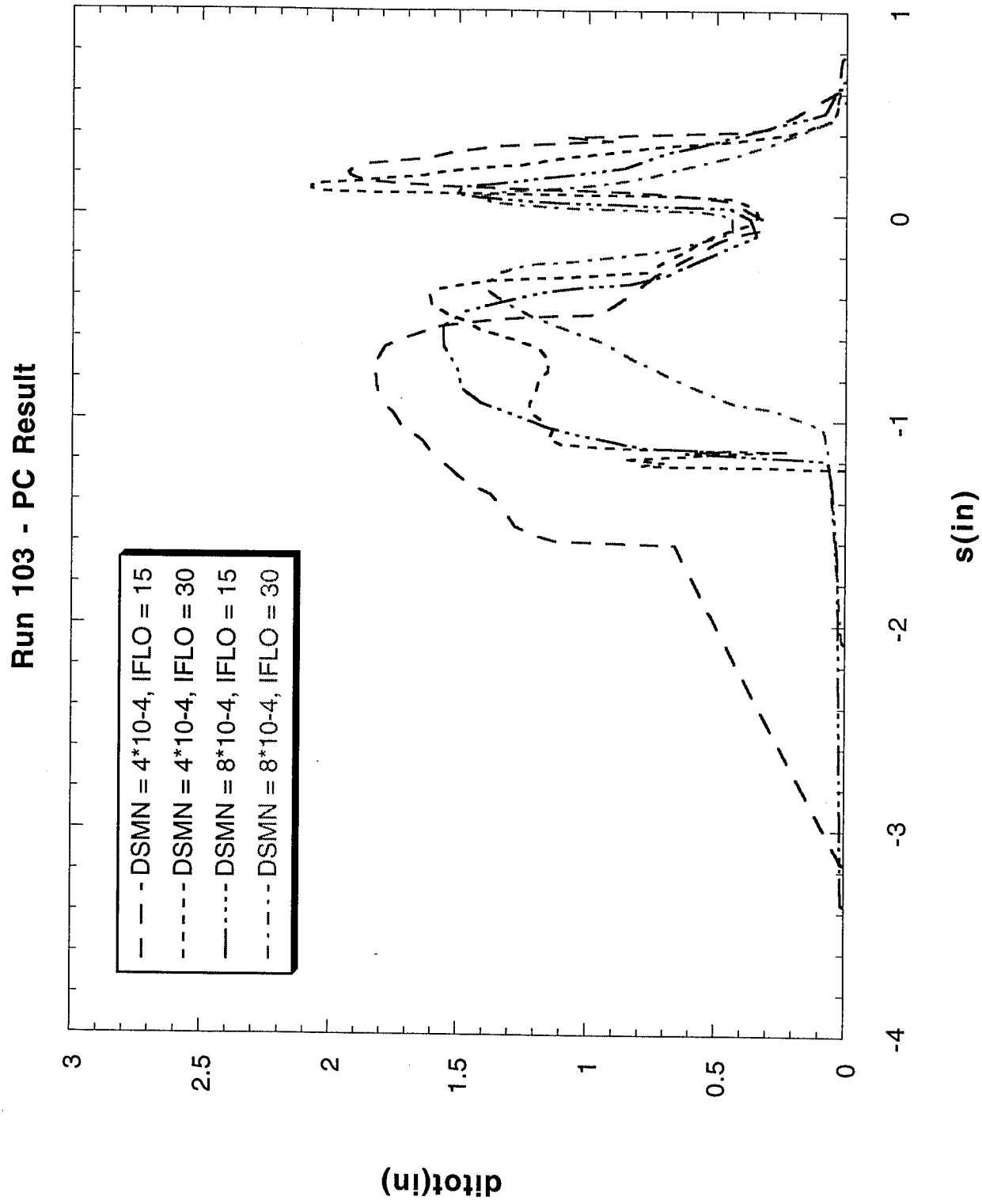
Run 103 - PC Result
DSMN = 4*10-4, IFLO = 15
DSMN = 4*10-4, IFLO = 30
DSMN = 8*10-4, IFLO = 15
DSMN = 8*10-4, IFLO = 30
ditot(in)
s(in)
3
2.5
2
1.5
1
0.5
0
1
0
-1
-2
-3
-4

FIGURE 58

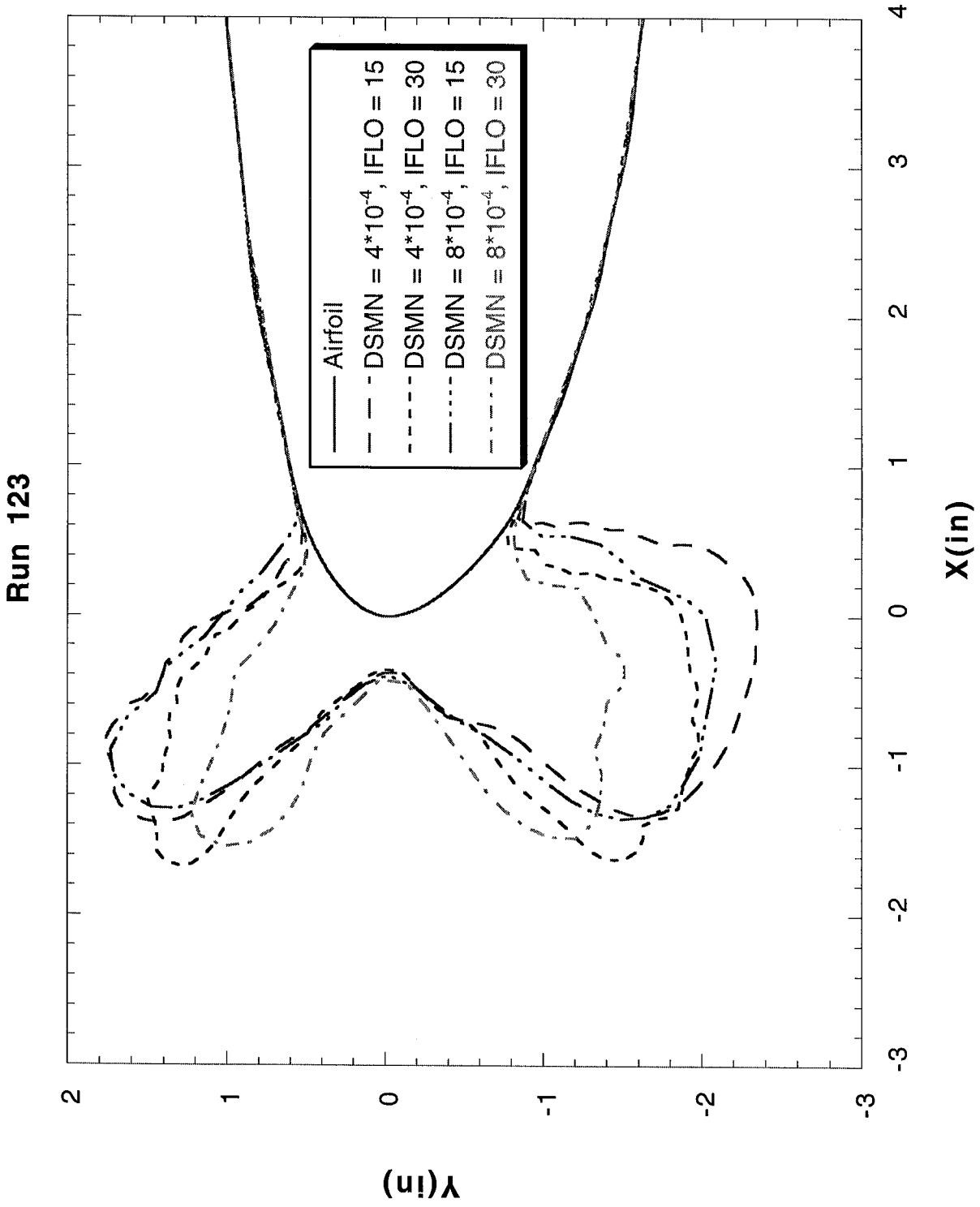
Run 123
Airfoil
DSMN = 4*10^-4, IFLO = 15
DSMN = 4*10^-4, IFLO = 30
DSMN = 8*10^-4, IFLO = 15
DSMN = 8*10^-4, IFLO = 30
Y(in)
X(in)
2
1
0
-1
-2
-3
4
3
2
1
0
-1
-2
-3

FIGURE 59

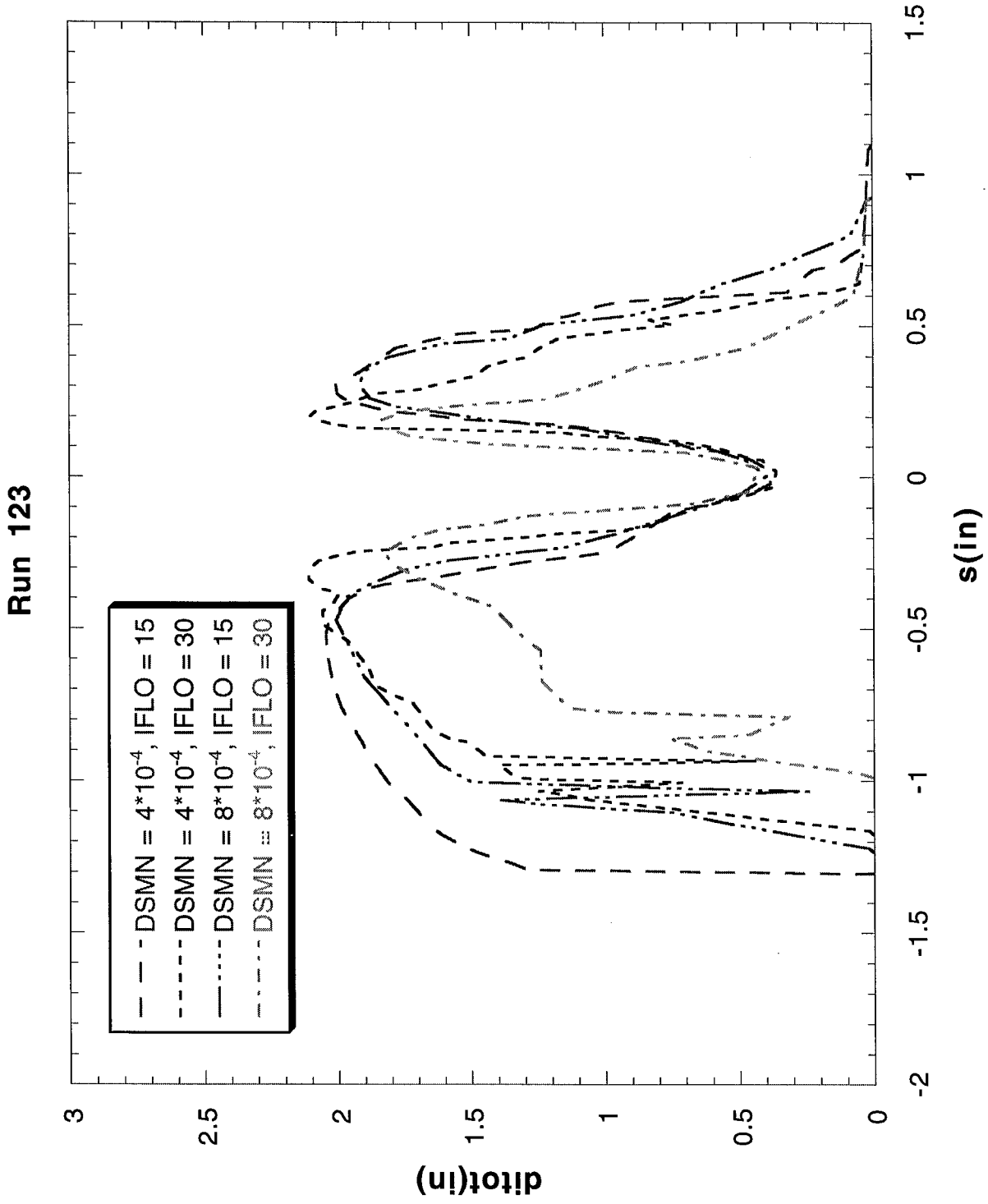
Run 123
DSMN = 4*10^-4, IFLO = 15
DSMN = 4*10^-4, IFLO = 30
DSMN = 8*10^-4, IFLO = 15
DSMN = 8*10^-4, IFLO = 30
ditot(in)
s(in)
3
2.5
2
1.5
1
0.5
0
-2
-1.5
-1
-0.5
0
0.5
1
1.5

Langmuir 'D' Cases

FIGURE 60

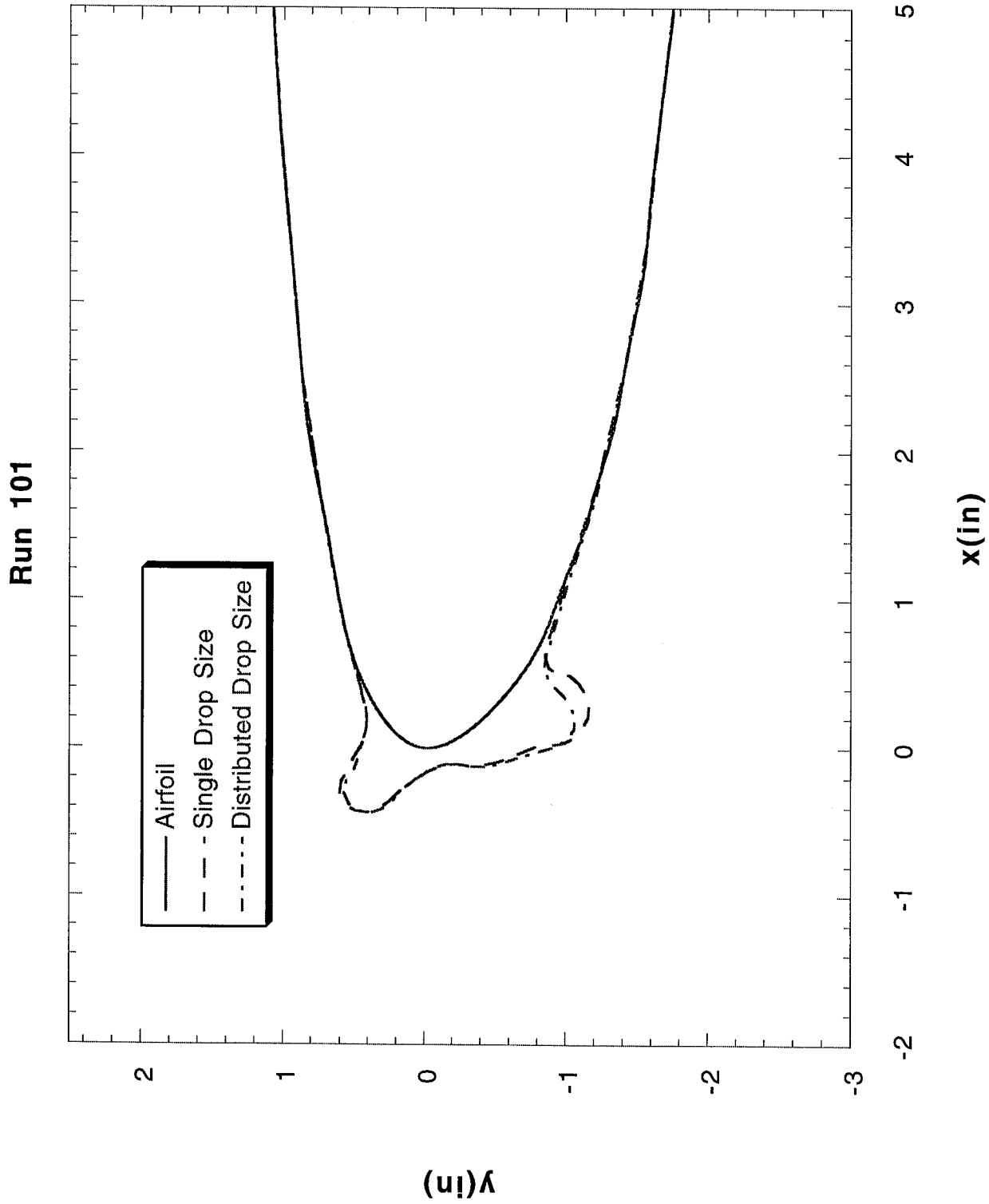
Run 101
Airfoil
Single Drop Size
Distributed Drop Size
y(in)
x(in)
2
1
0
-1
-2
-3
5
4
3
2
1
0
-1
-2

FIGURE 61

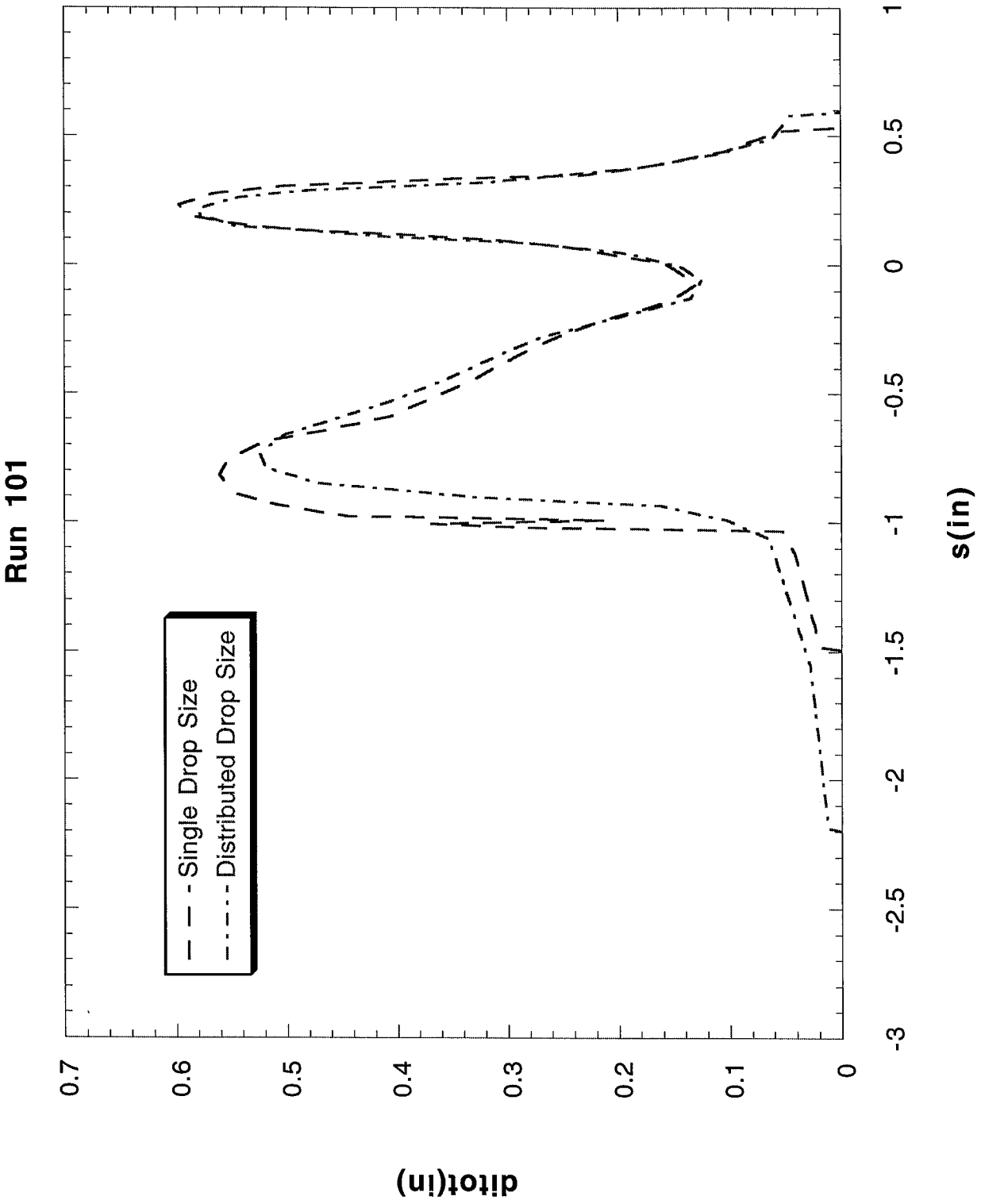
Run 101
Single Drop Size
Distributed Drop Size
ditot(in)
s(in)
0.7
0.6
0.5
0.4
0.3
0.2
0.1
0
1
0.5
0
-0.5
-1
-1.5
-2
-2.5
-3

FIGURE 62

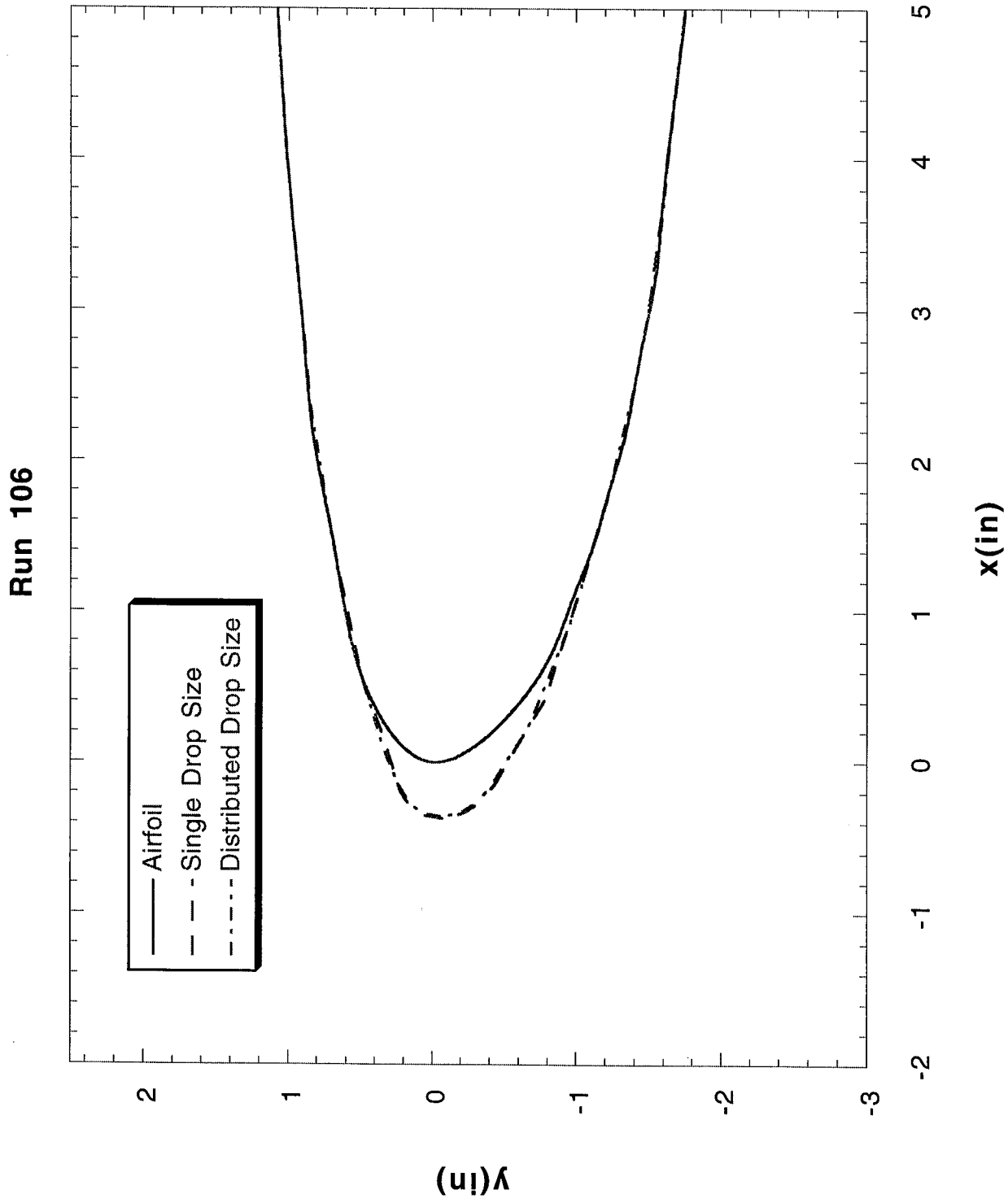
Run 106
Airfoil
Single Drop Size
Distributed Drop Size
y(in)
x(in)
2
1
0
-1
-2
-3
5
4
3
2
1
0
-1
-2

FIGURE 63

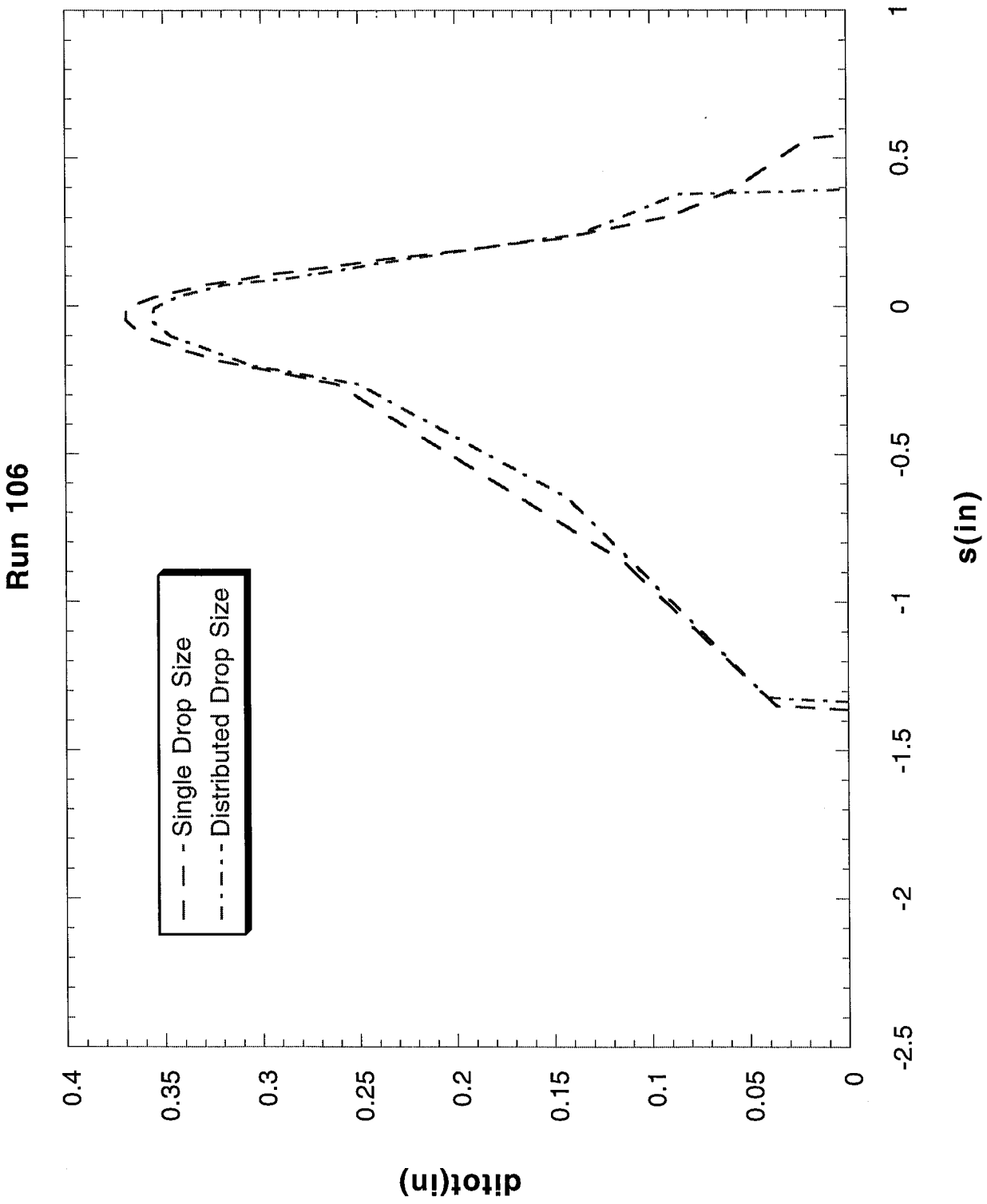
Run 106
Single Drop Size
Distributed Drop Size
ditot(in)
s(in)
0.4
0.35
0.3
0.25
0.2
0.15
0.1
0.05
0
-2.5
-2
-1.5
-1
-0.5
0
0.5
1

FIGURE 64

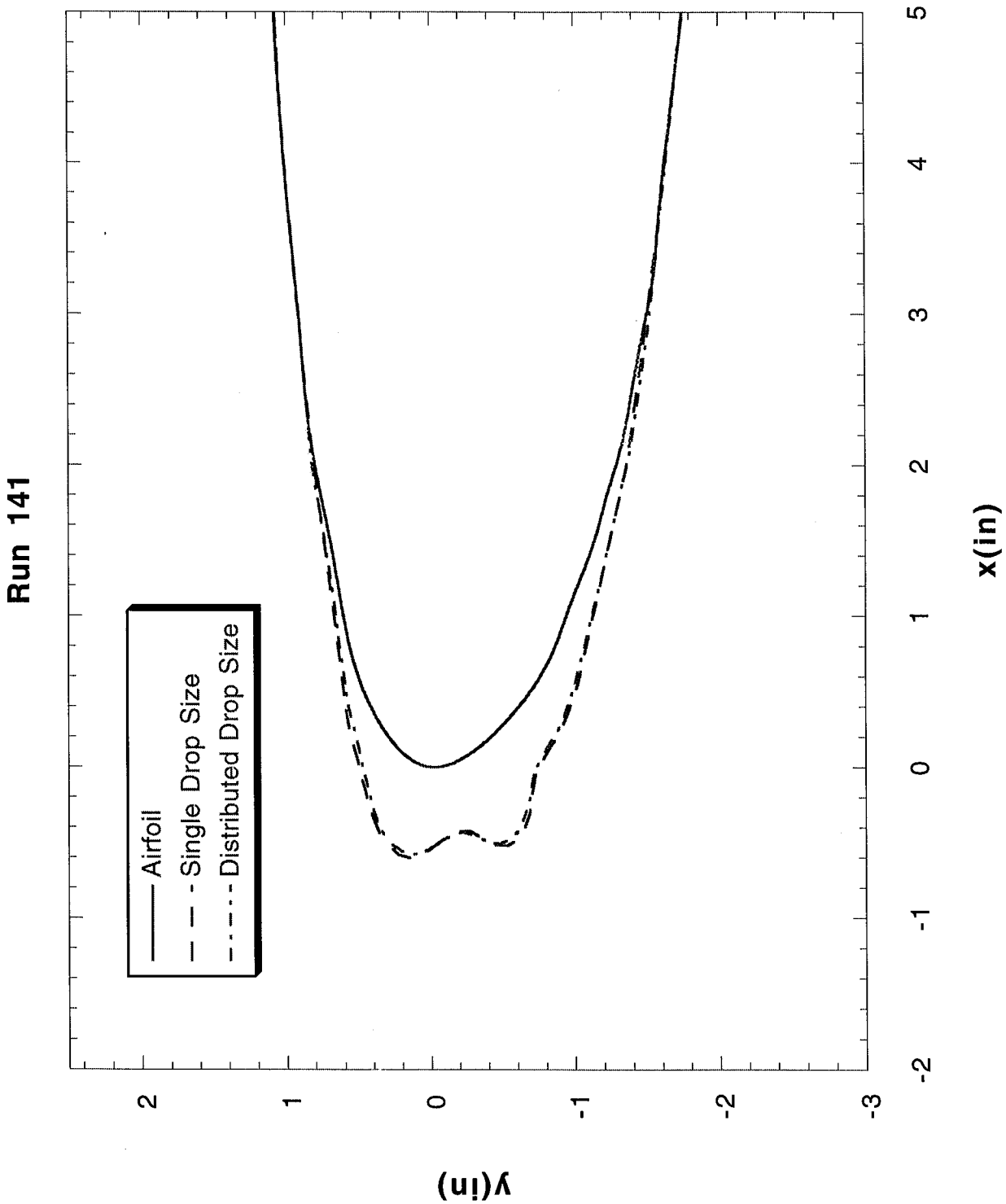
Run 141
Airfoil
- Single Drop Size
- Distributed Drop Size
y(in)
x(in)
2
1
0
-1
-2
-3
5
4
3
2
1
0
-1
-2

FIGURE 65

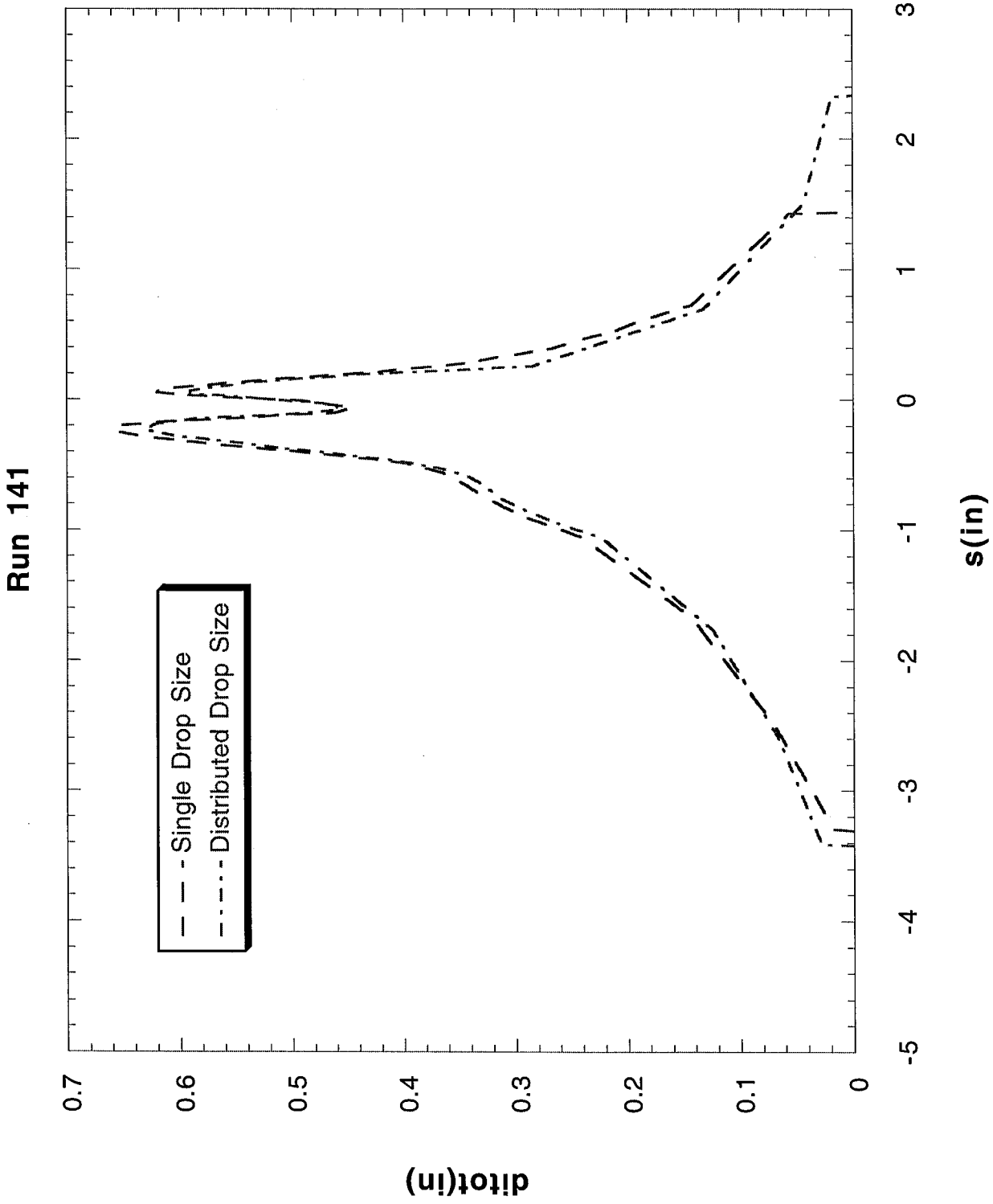
Run 141
Single Drop Size
Distributed Drop Size
ditot(in)
0.7
0.6
0.5
0.4
0.3
0.2
0.1
0
s(in)
3
2
1
0
-1
-2
-3
-4
-5

FIGURE 66

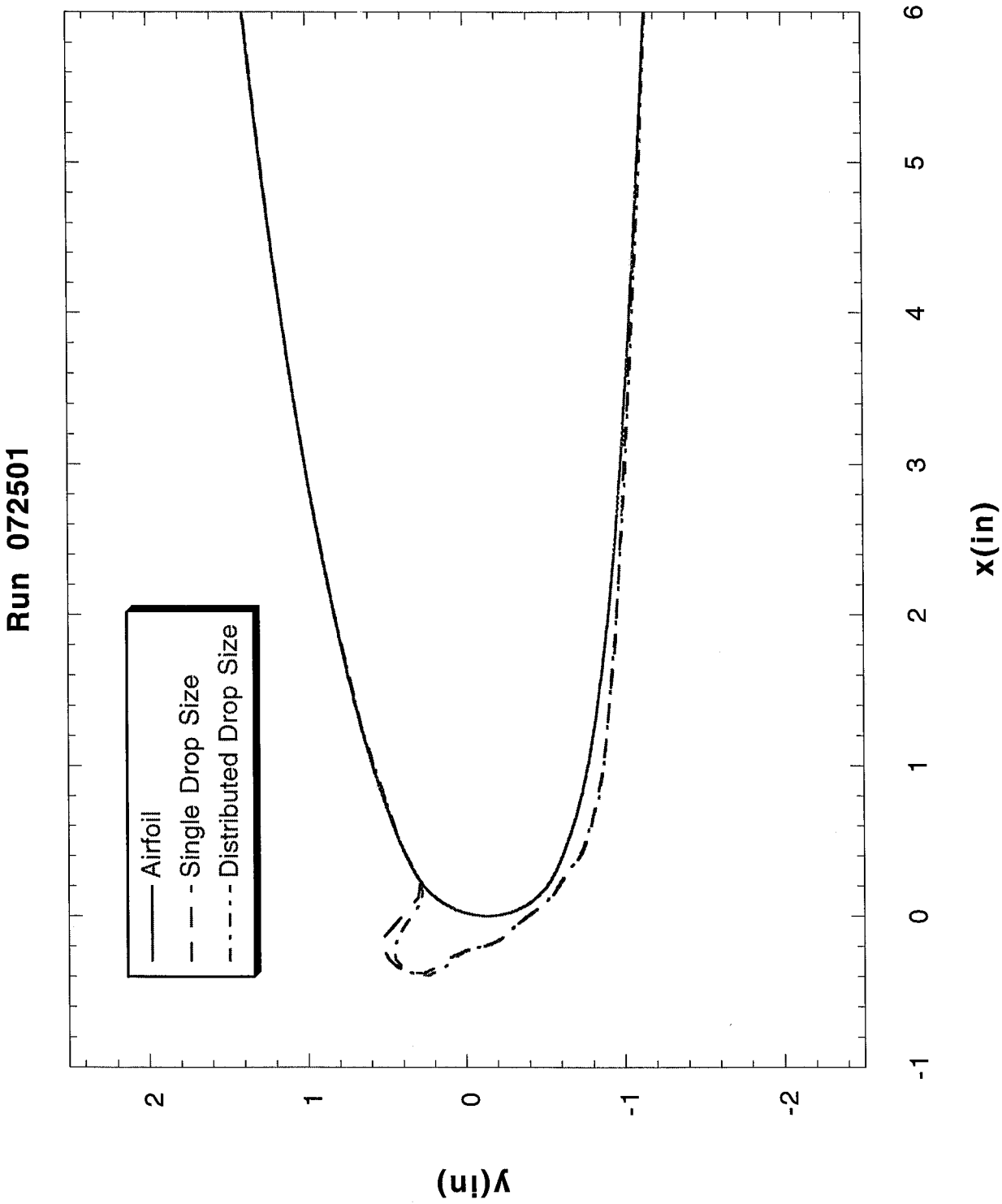
Run 072501
Airfoil
Single Drop Size
Distributed Drop Size
y(in)
2
1
0
-1
-2
x(in)
-1
0
1
2
3
4
5
6

FIGURE 67

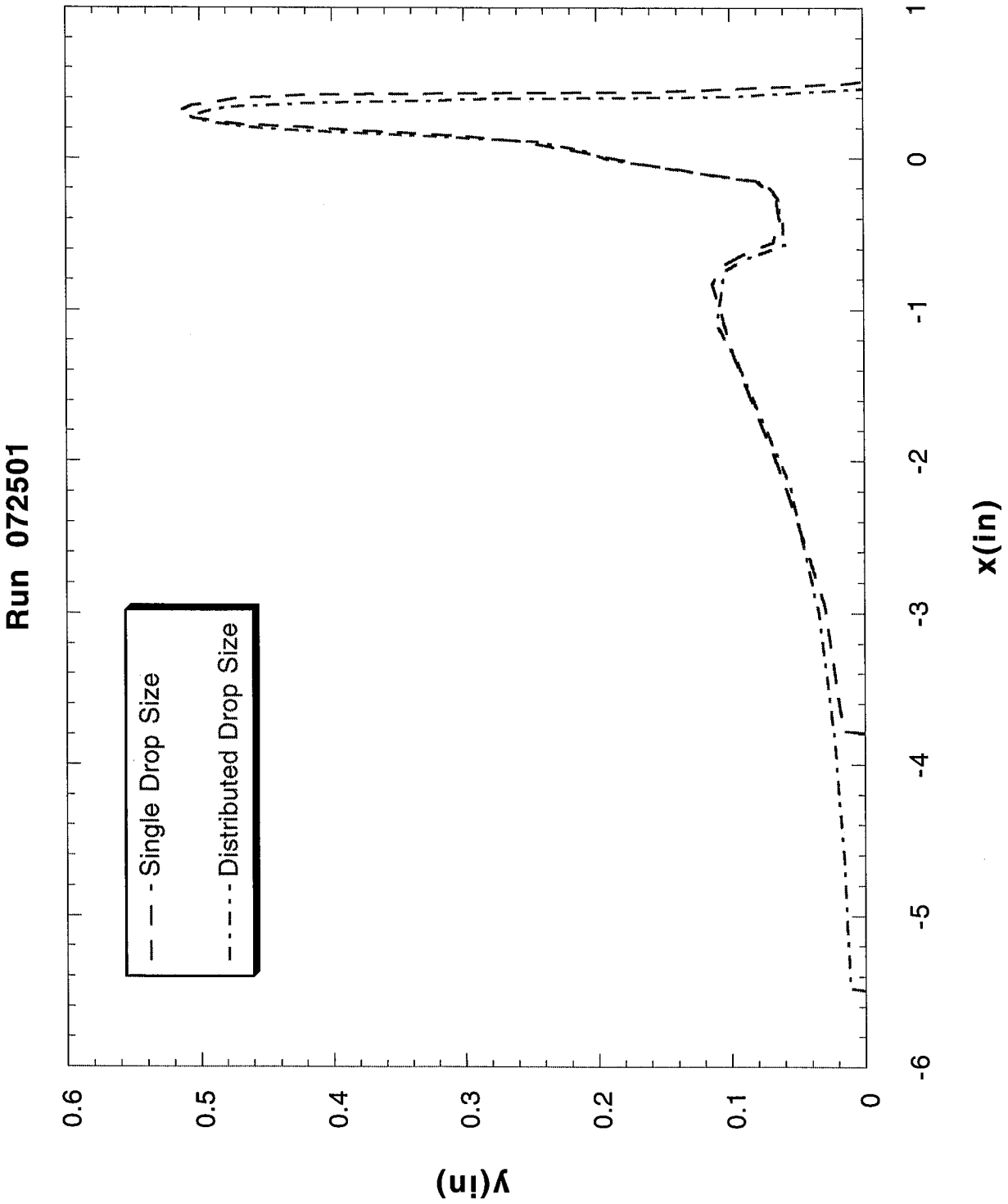
Run 072501
Single Drop Size
Distributed Drop Size
y(in)
0.6
0.5
0.4
0.3
0.2
0.1
0
x(in)
1
0
-1
-2
-3
-4
-5
-6

FIGURE 68

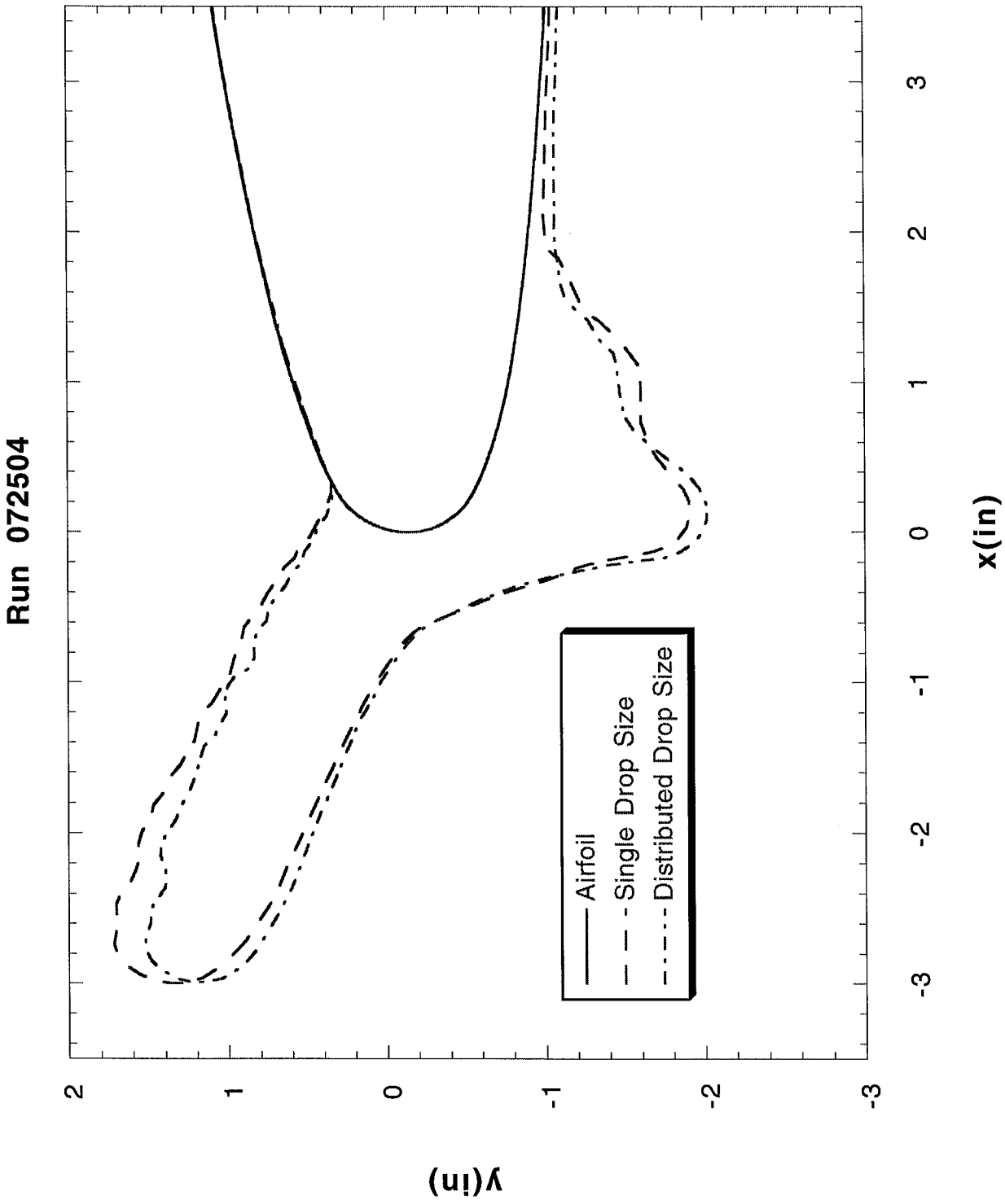
Run 072504
Airfoil
Single Drop Size
Distributed Drop Size
y(in)
x(in)
2
1
0
-1
-2
-3
3

FIGURE 69

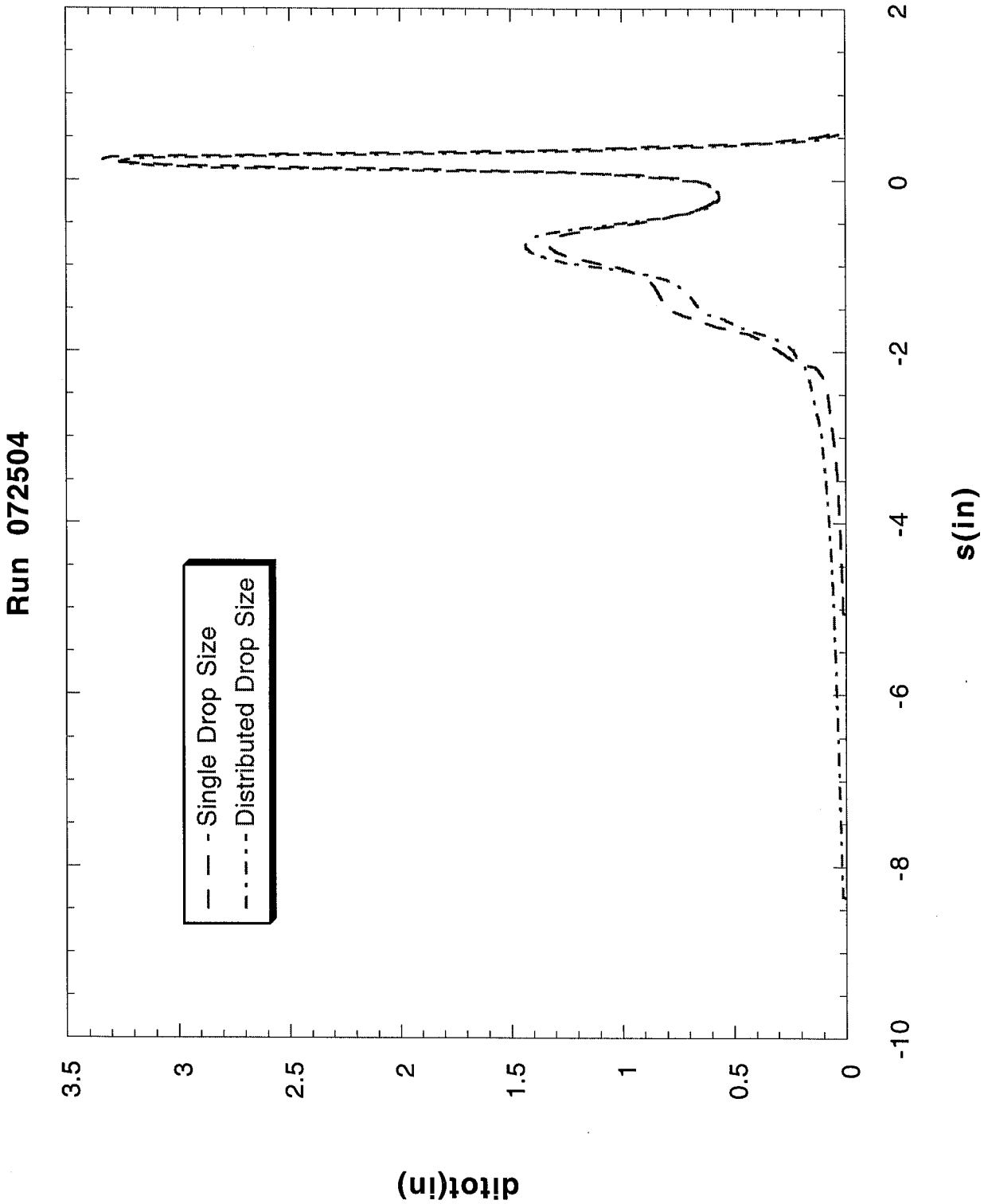
Run 072504
Single Drop Size
Distributed Drop Size
ditot(in)
s(in)
3.5
3
2.5
2
1.5
1
0.5
0
2
0
-2
-4
-6
-8
-10

FIGURE 70

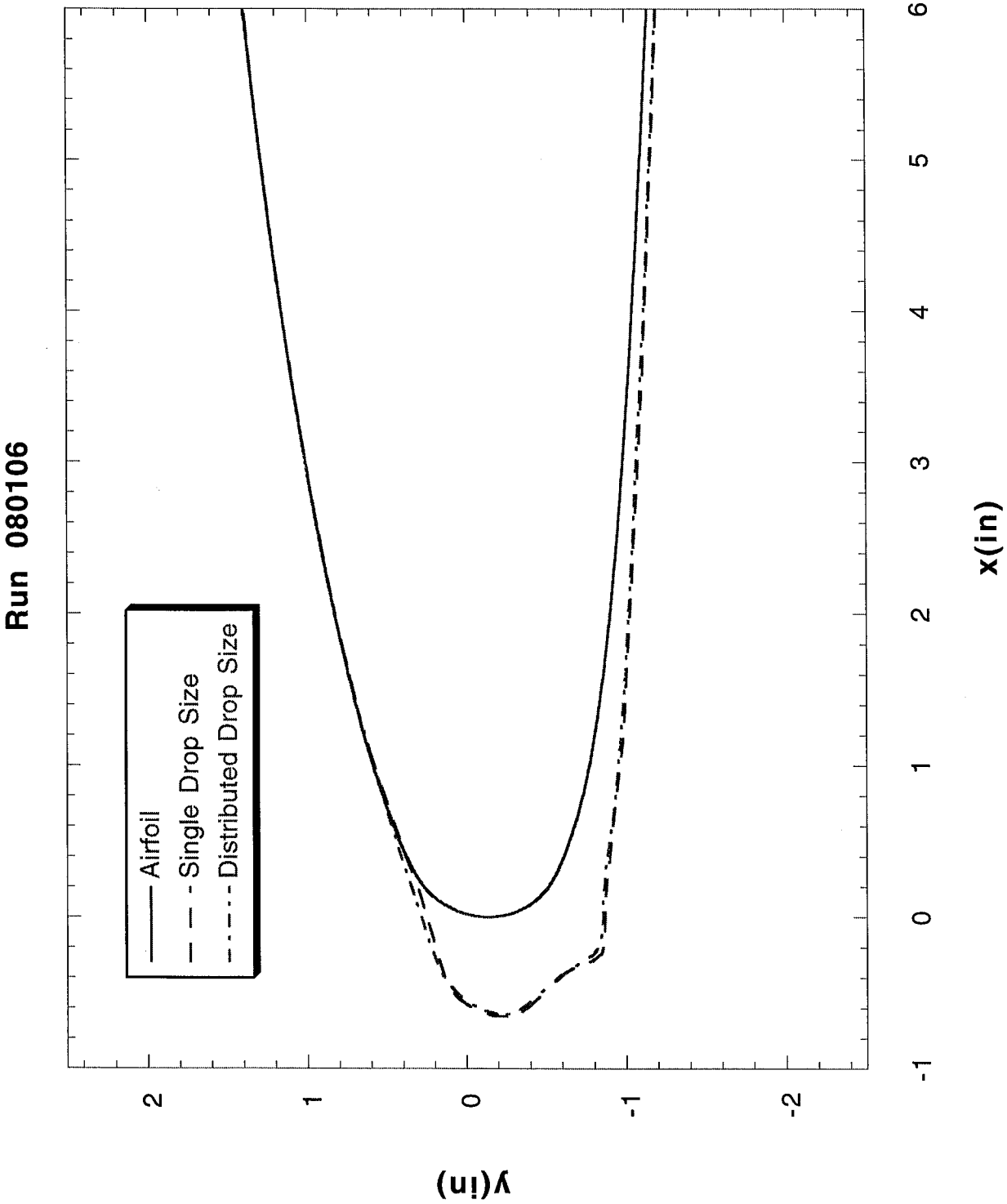
Run 080106
Airfoil
Single Drop Size
Distributed Drop Size
y(in)
x(in)
2
1
0
-1
-2
-1
0
1
2
3
4
5
6

FIGURE 71

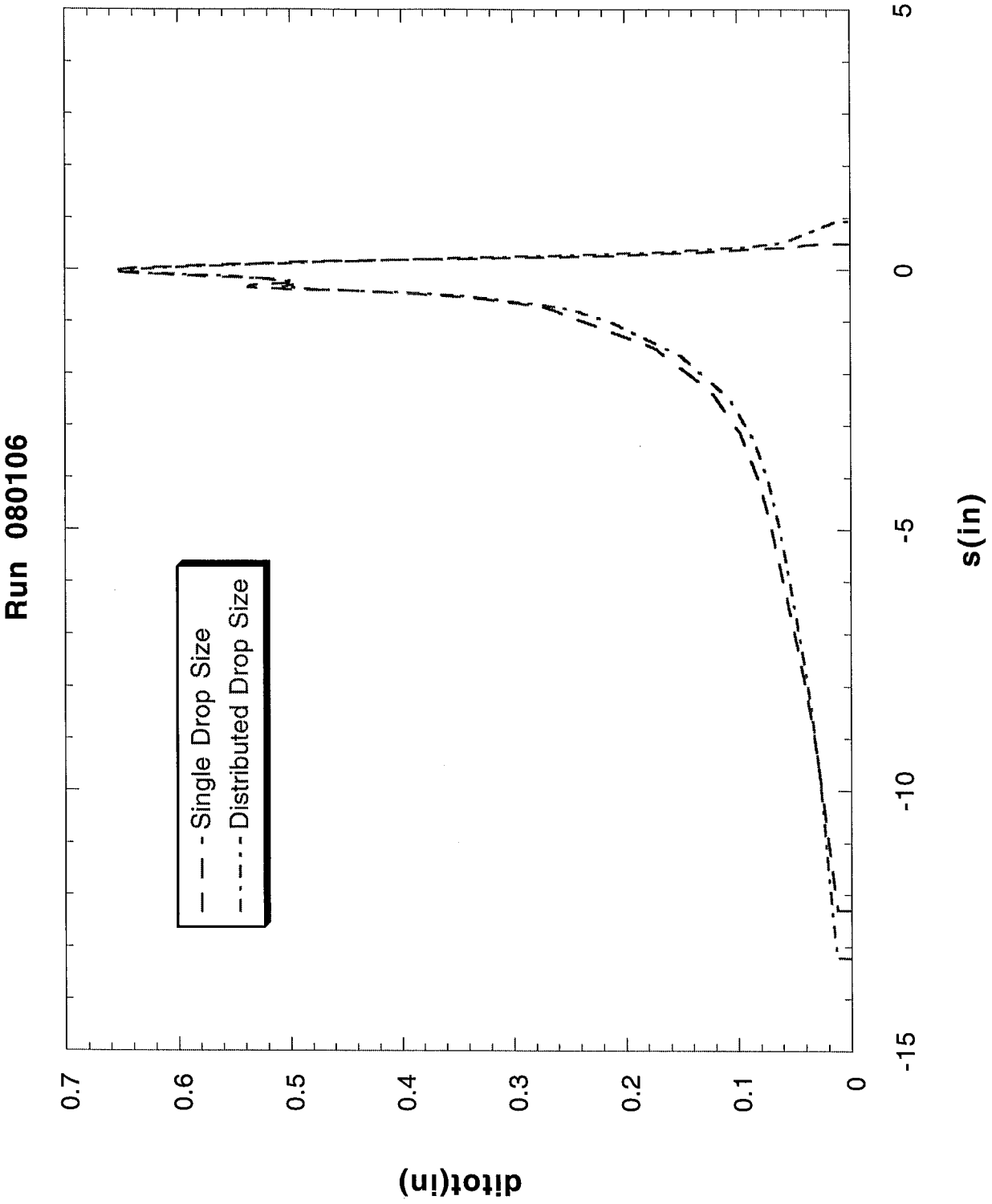
Run 080106
Single Drop Size
Distributed Drop Size
ditot(in)
0.7
0.6
0.5
0.4
0.3
0.2
0.1
0
s(in)
5
0
-5
-10
-15

FIGURE 72

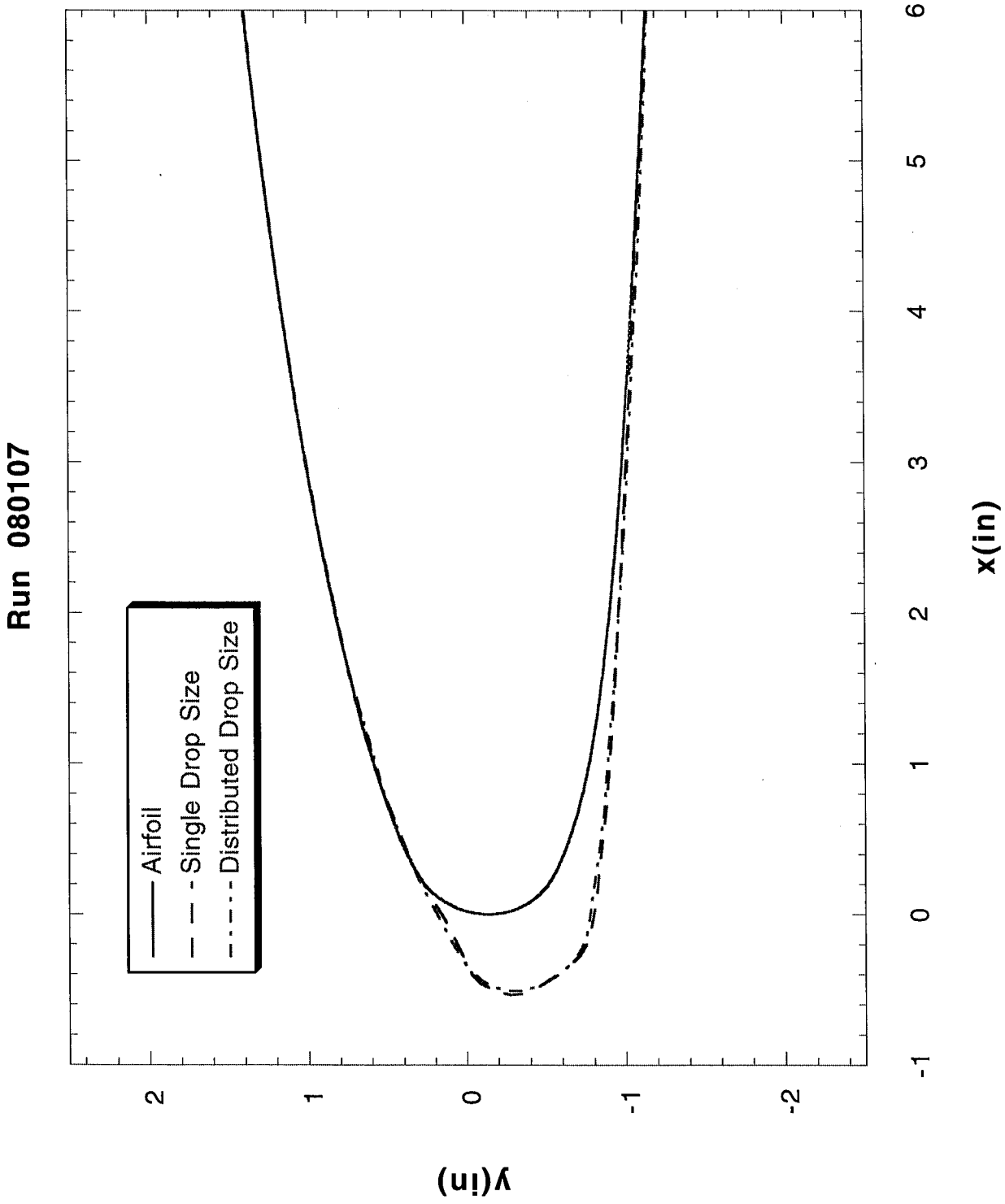
Run 080107
Airfoil
Single Drop Size
Distributed Drop Size
y(in)
2
1
0
-1
-2
x(in)
-1
0
1
2
3
4
5
6

FIGURE 73

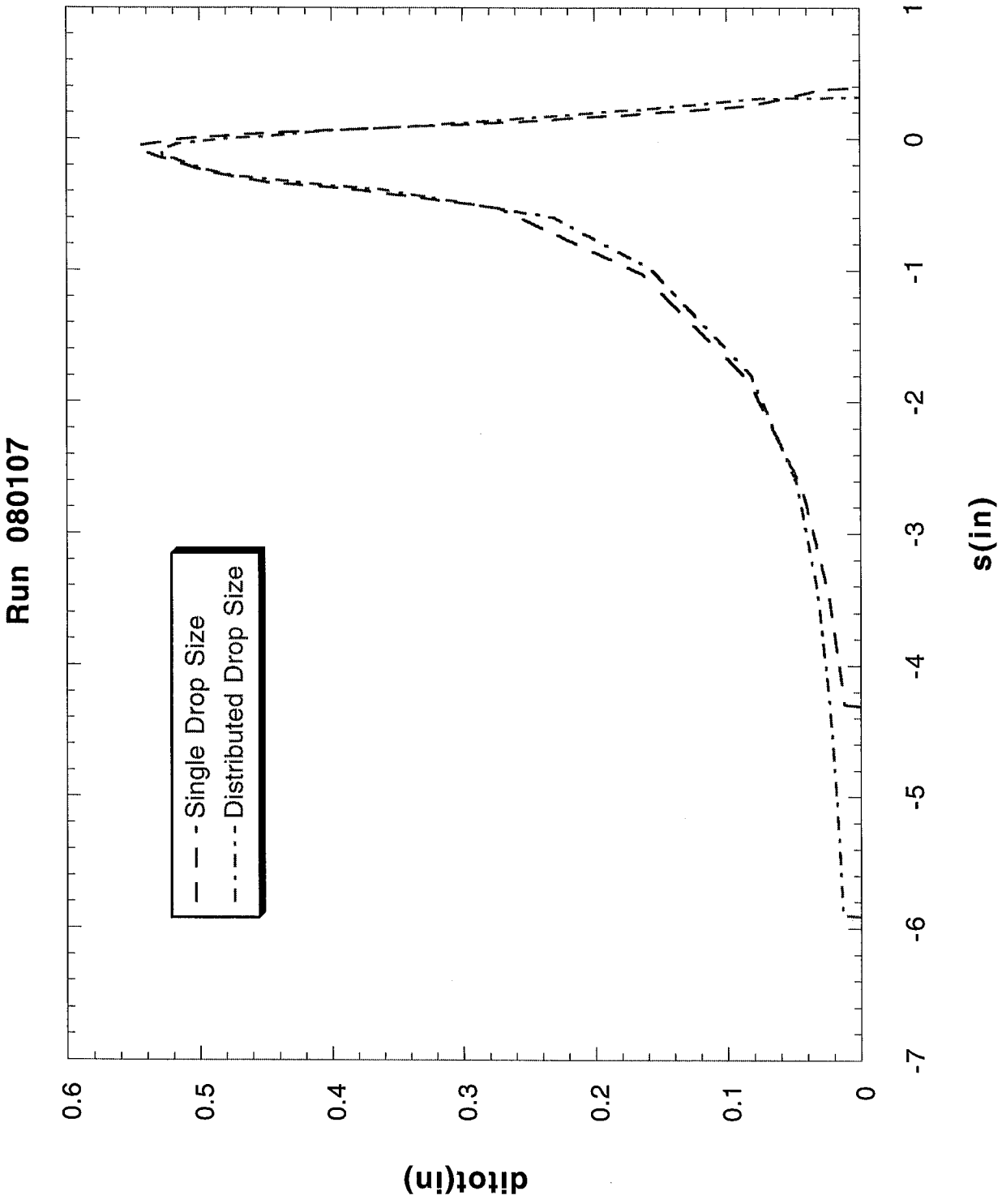
Run 080107
Single Drop Size
Distributed Drop Size
ditot(in)
0.6
0.5
0.4
0.3
0.2
0.1
0
s(in)
1
0
-1
-2
-3
-4
-5
-6
-7

FIGURE 74

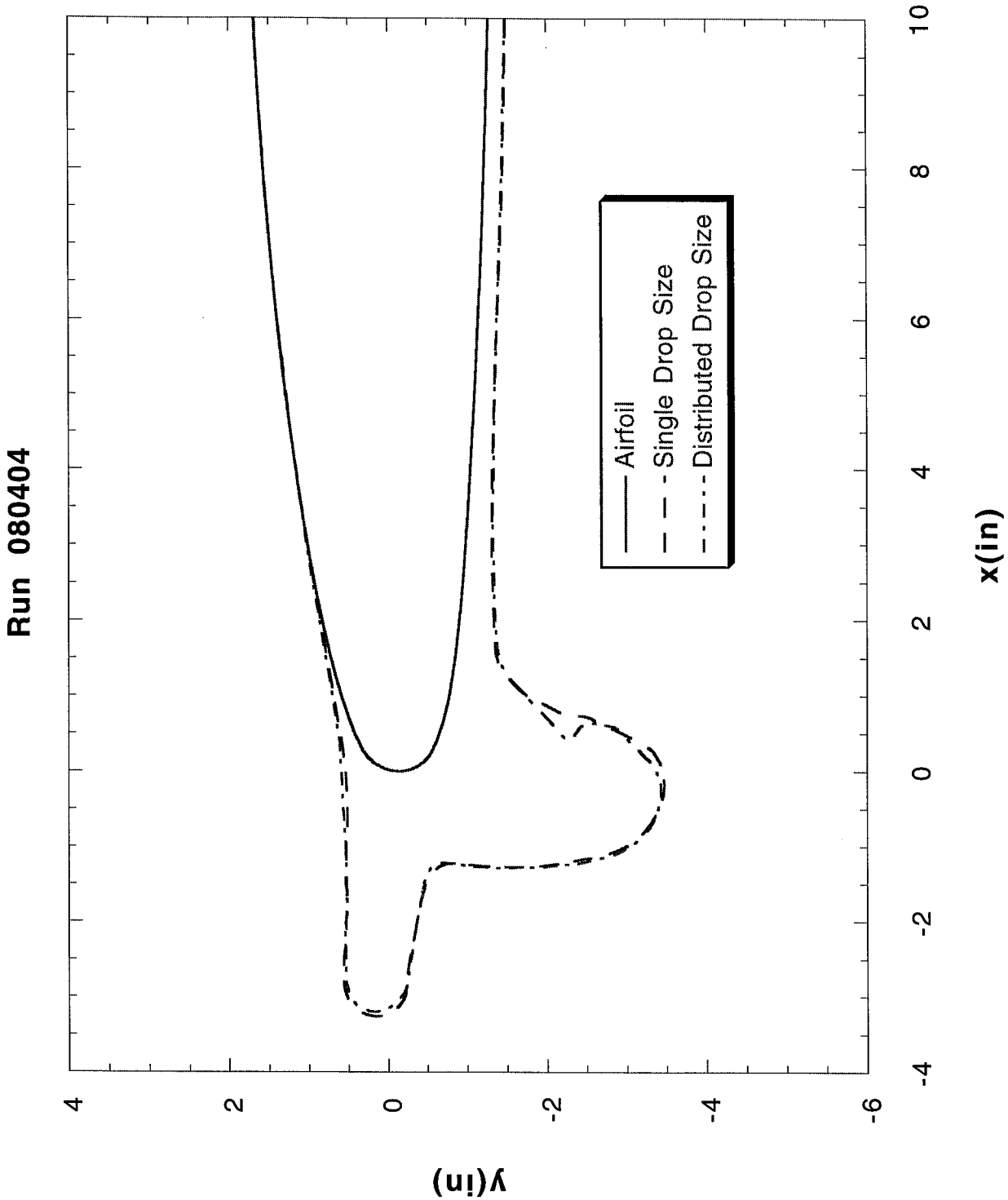
Run 080404
Airfoil
Single Drop Size
Distributed Drop Size
y(in)
x(in)
4
2
0
-2
-4
-6
10
8
6
4
2
0
-2
-4

FIGURE 75

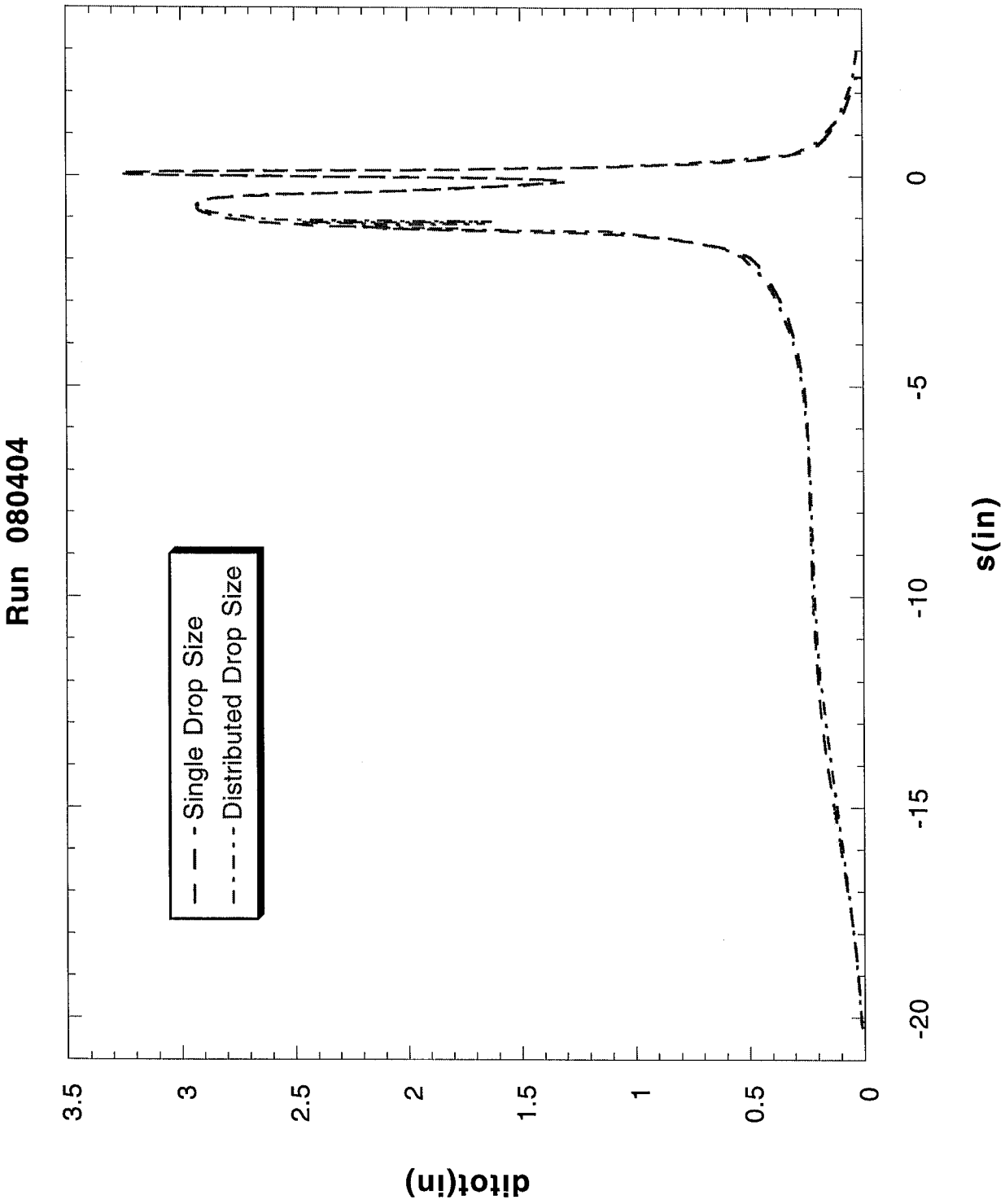
Run 080404
Single Drop Size
Distributed Drop Size
ditot(in)
3.5
3
2.5
2
1.5
1
0.5
0
s(in)
0
-5
-10
-15
-20

FIGURE 76

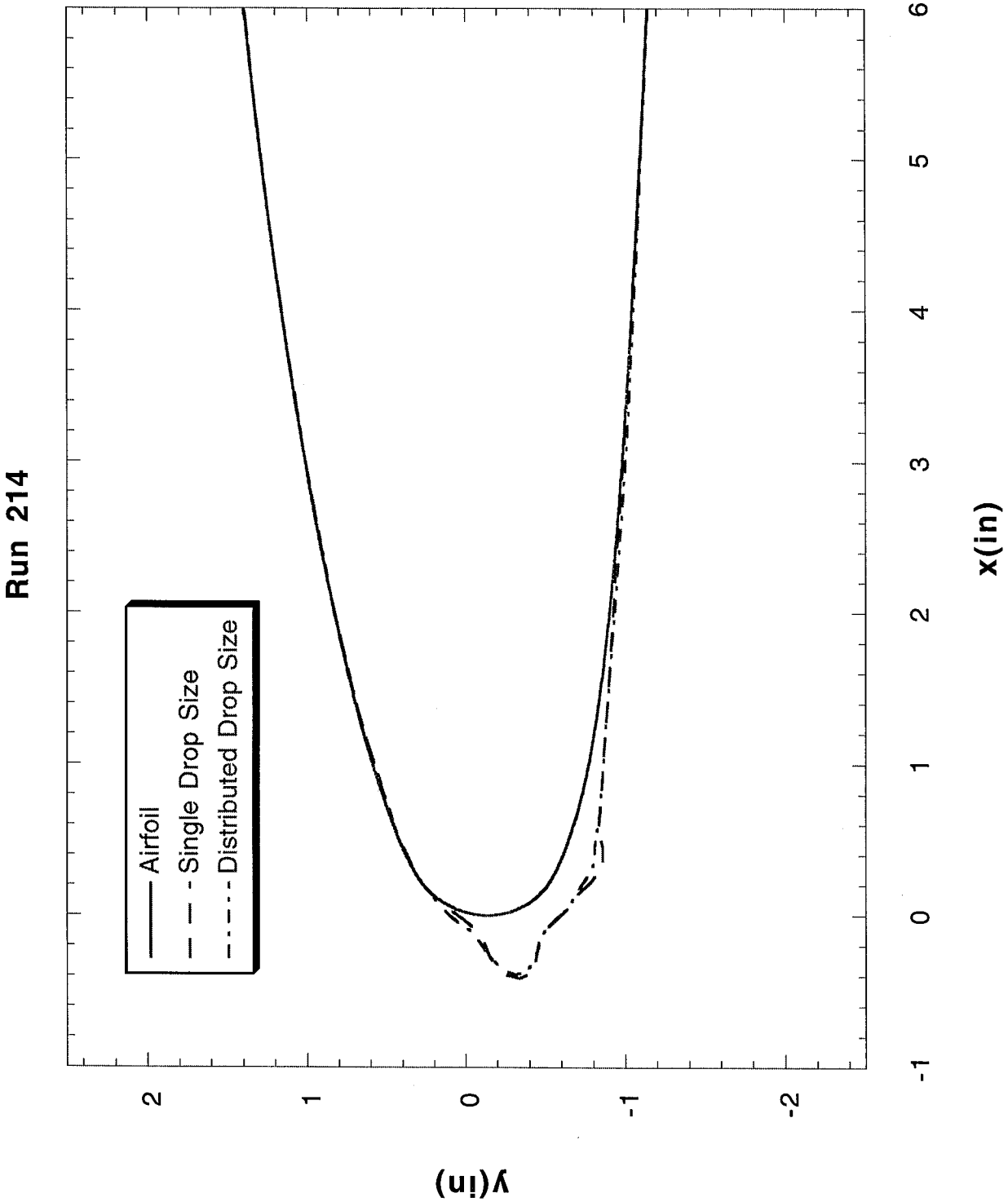
Run 214
Airfoil
Single Drop Size
Distributed Drop Size
y(in)
x(in)
2
1
0
-1
-2
-1
0
1
2
3
4
5
6

FIGURE 77

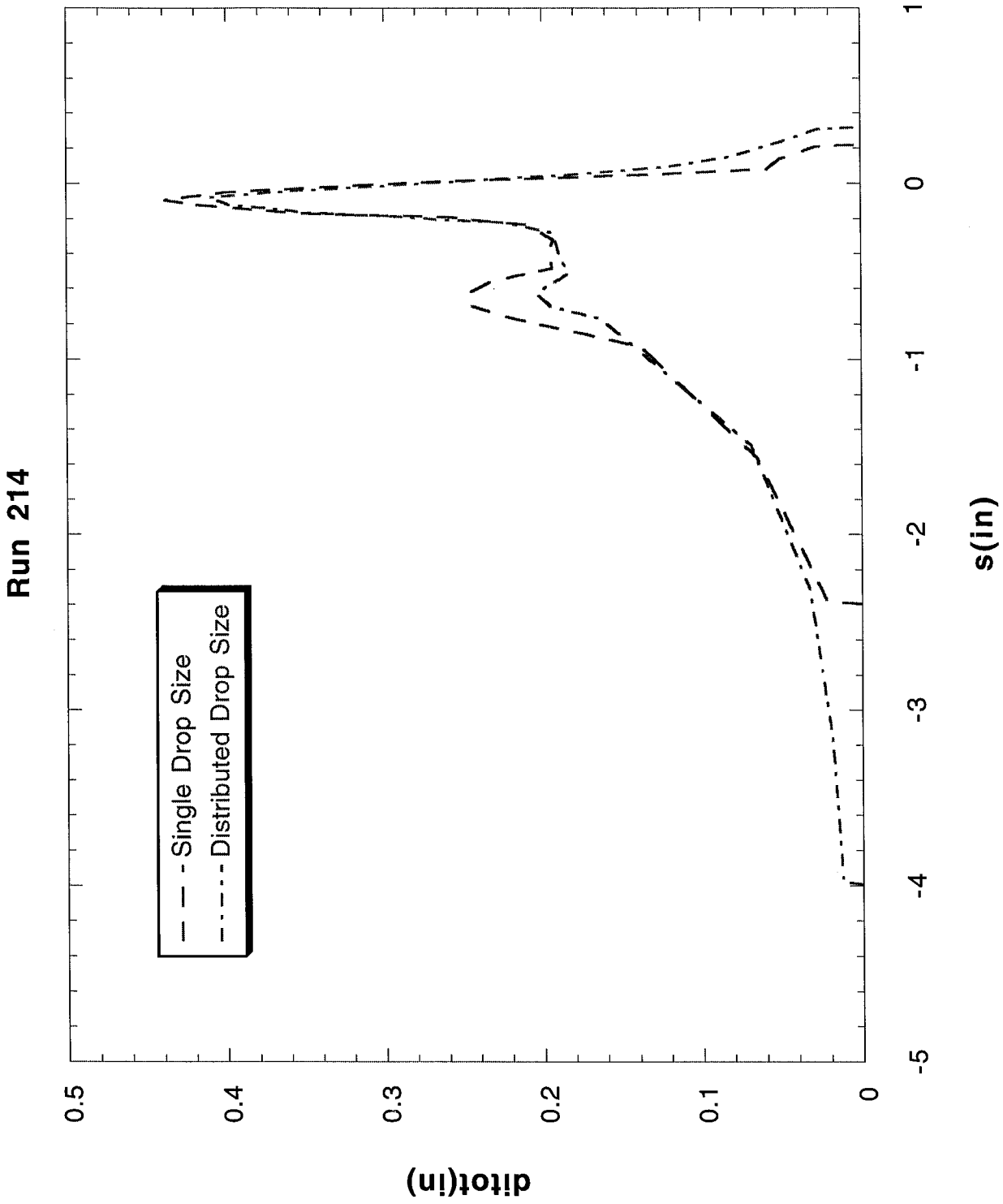
Run 214
Single Drop Size
Distributed Drop Size
ditot(in)
0.5
0.4
0.3
0.2
0.1
0
s(in)
1
0
-1
-2
-3
-4
-5

FIGURE 78

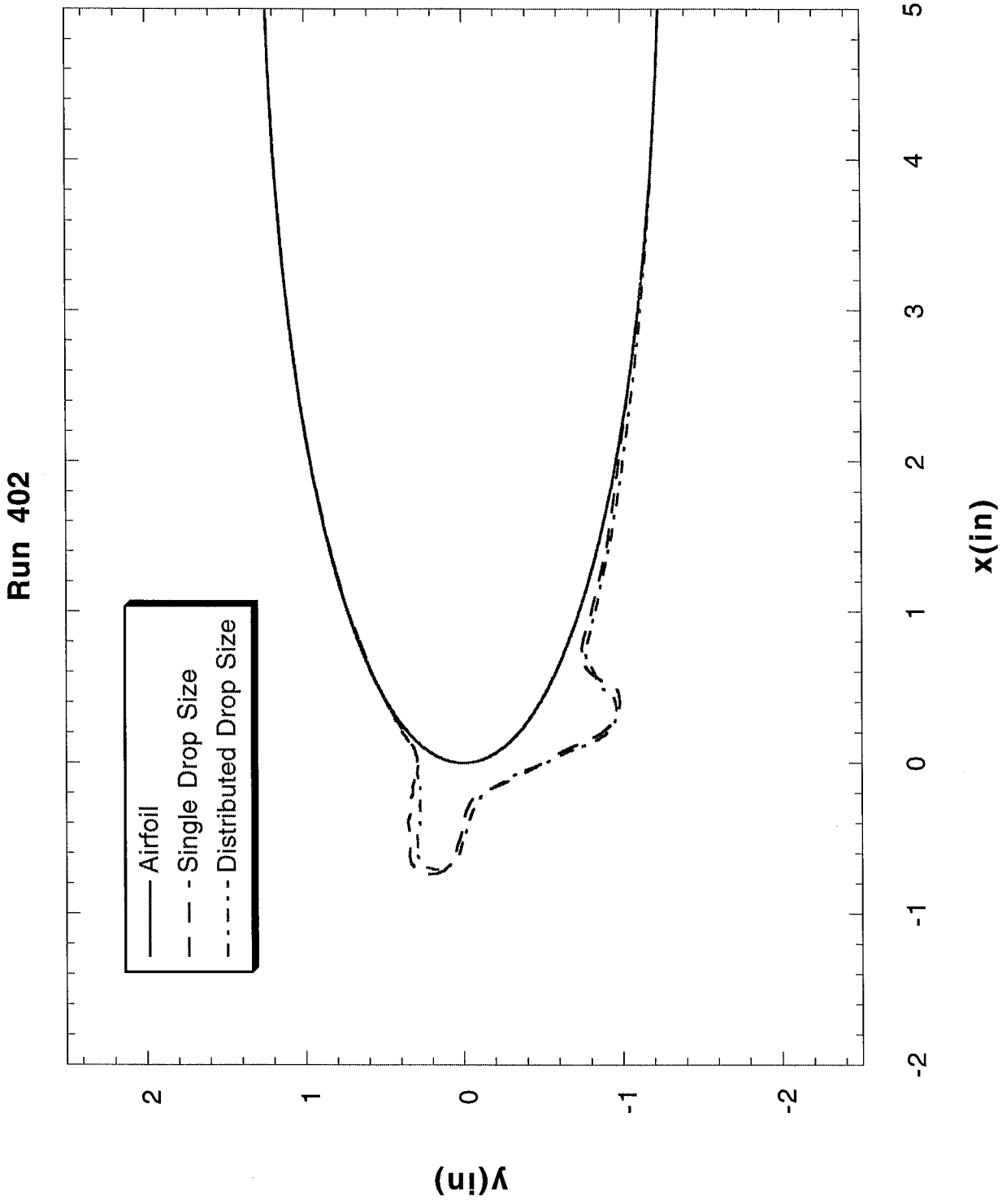
Run 402
Airfoil
Single Drop Size
Distributed Drop Size
y(in)
2
1
0
-1
-2
x(in)
-2
-1
0
1
2
3
4
5

FIGURE 79

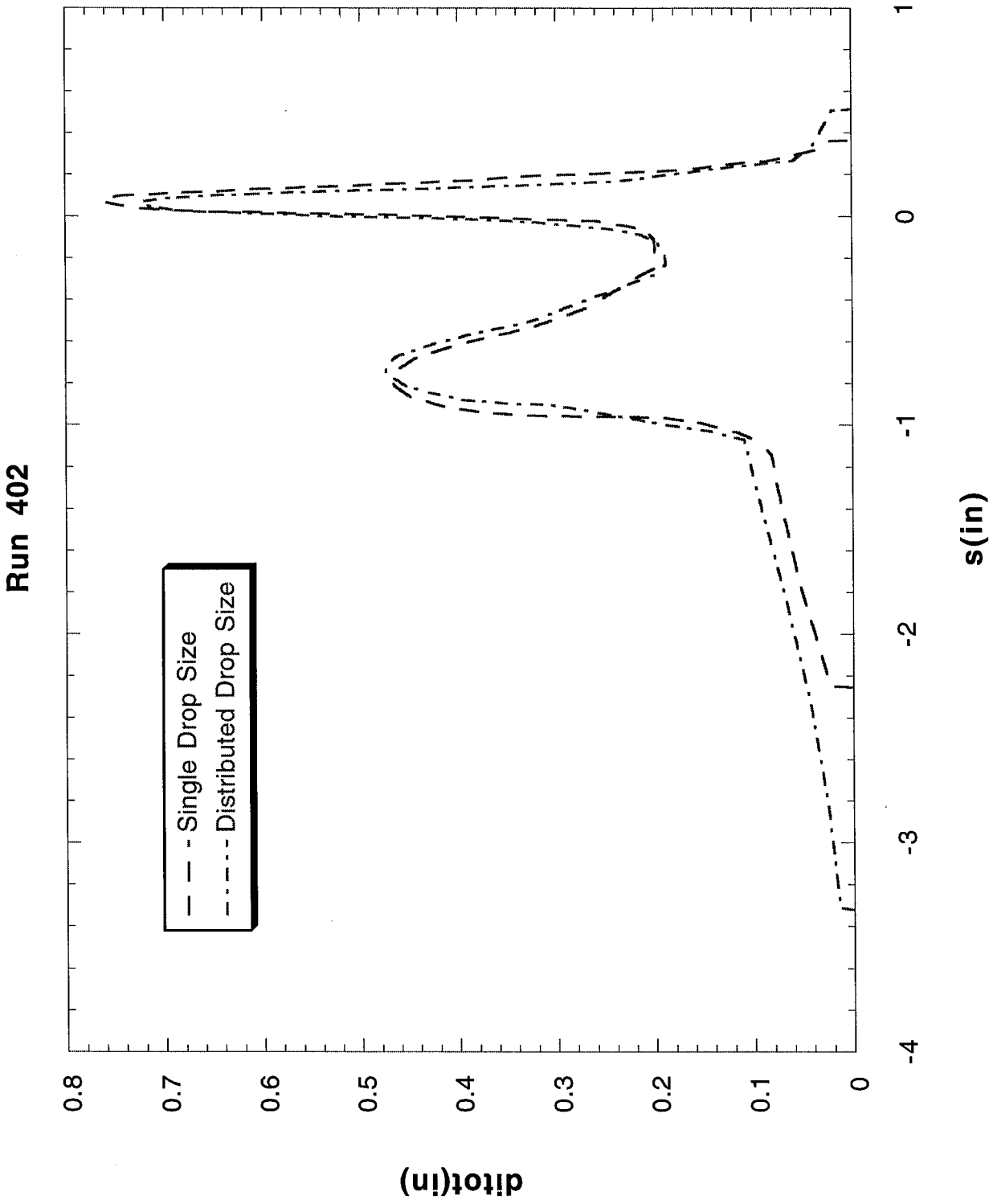
Run 402
Single Drop Size
Distributed Drop Size
ditot(in)
0.8
0.7
0.6
0.5
0.4
0.3
0.2
0.1
0
s(in)
1
0
-1
-2
-3
-4

FIGURE 80

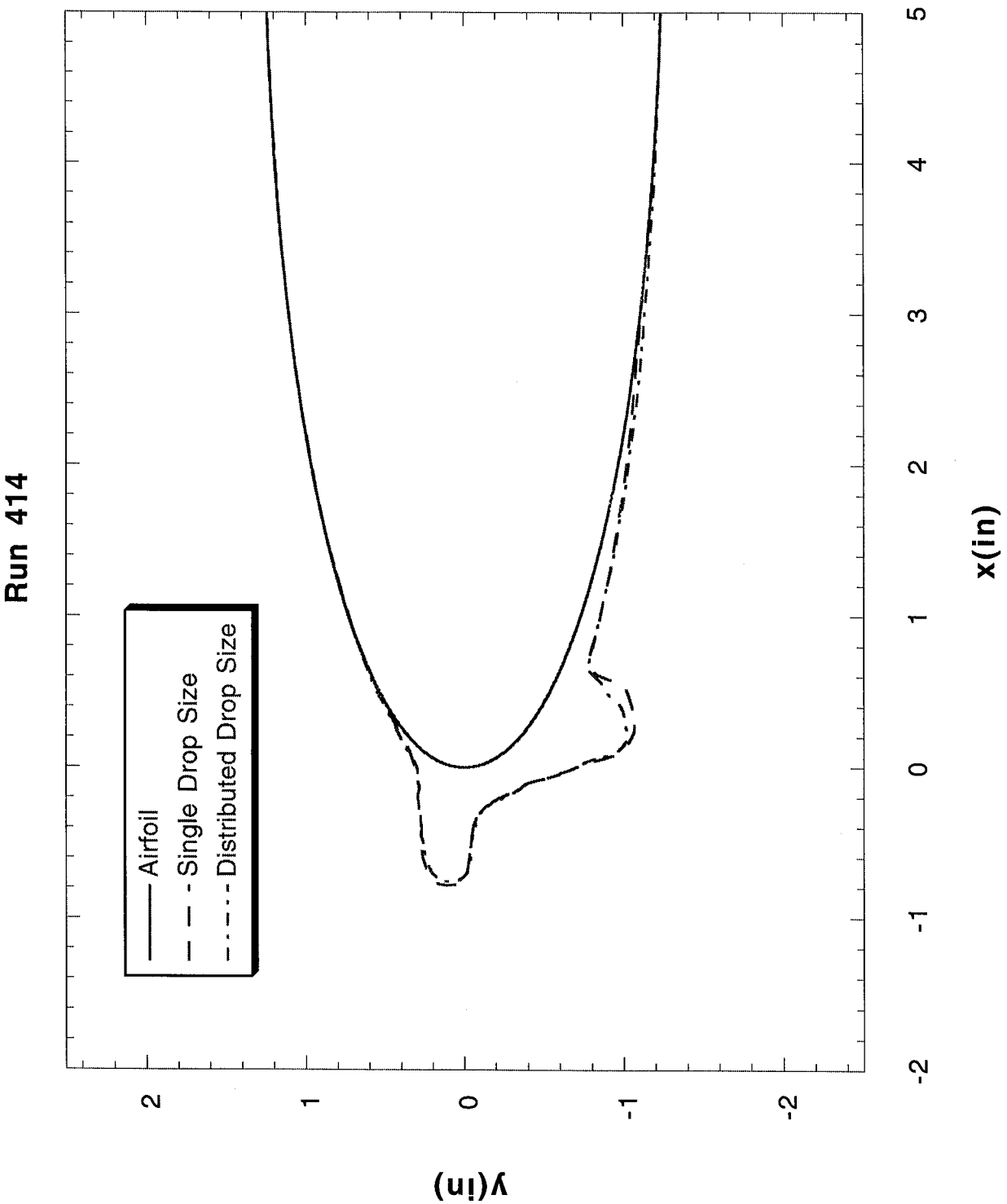
Run 414
Airfoil
Single Drop Size
Distributed Drop Size
y(in)
x(in)
2
1
0
-1
-2
5
4
3
2
1
0
-1
-2

FIGURE 81

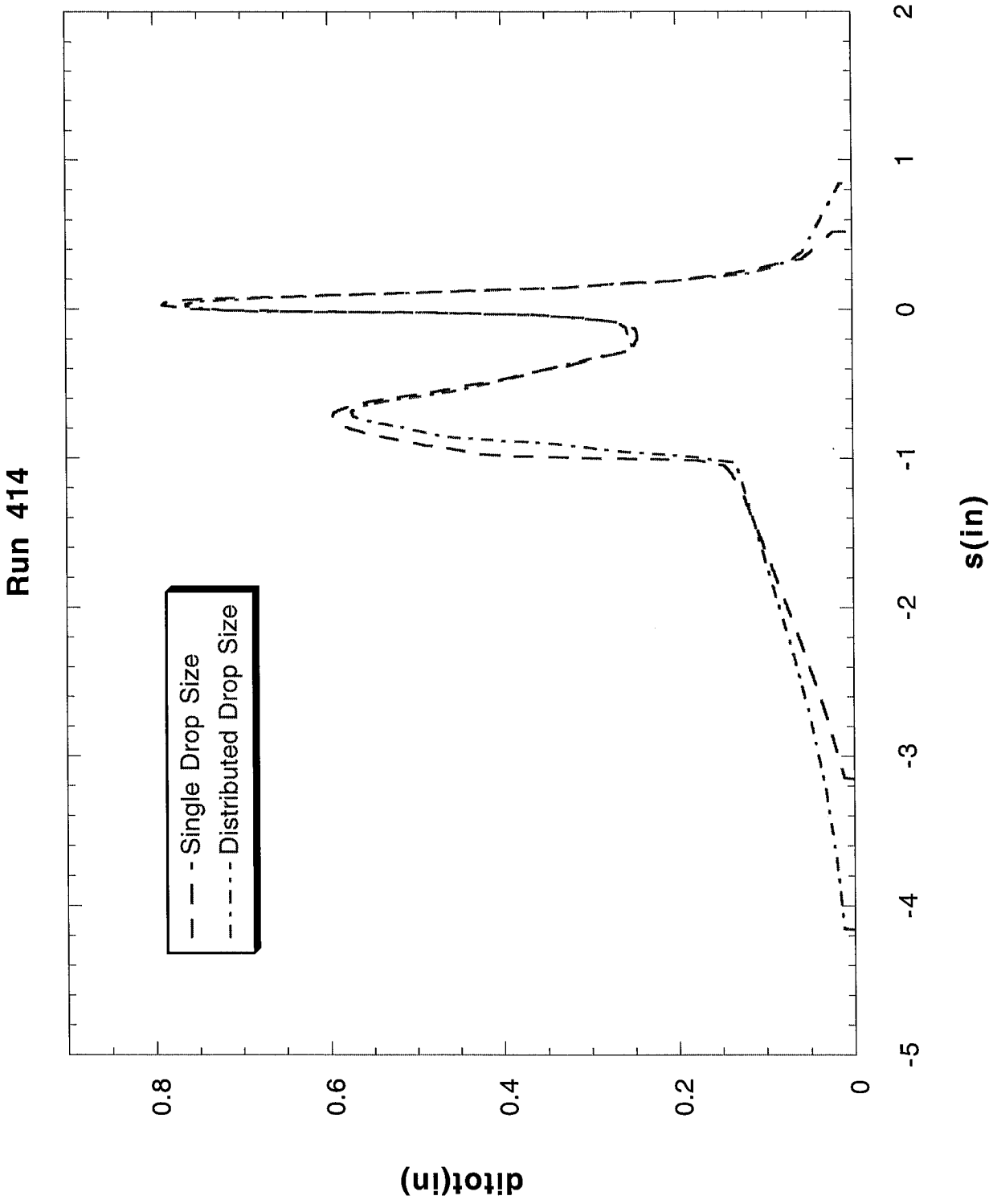
Run 414
Single Drop Size
Distributed Drop Size
dltot(in)
0.8
0.6
0.4
0.2
0
s(in)
2
1
0
-1
-2
-3
-4
-5

FIGURE 82

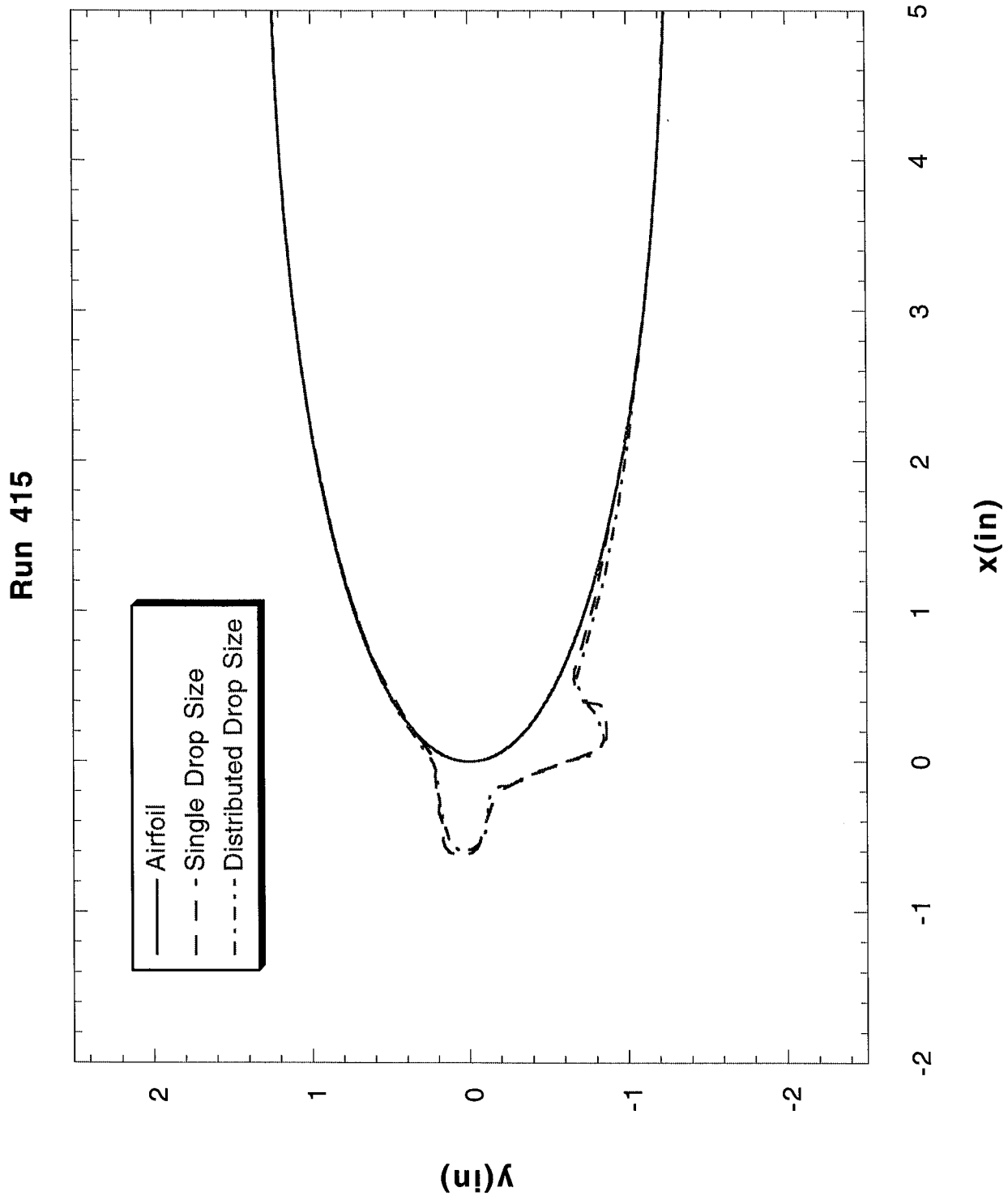
Run 415
Airfoil
Single Drop Size
Distributed Drop Size
y(in)
x(in)
2
1
0
-1
-2
-2
-1
0
1
2
3
4
5

FIGURE 83

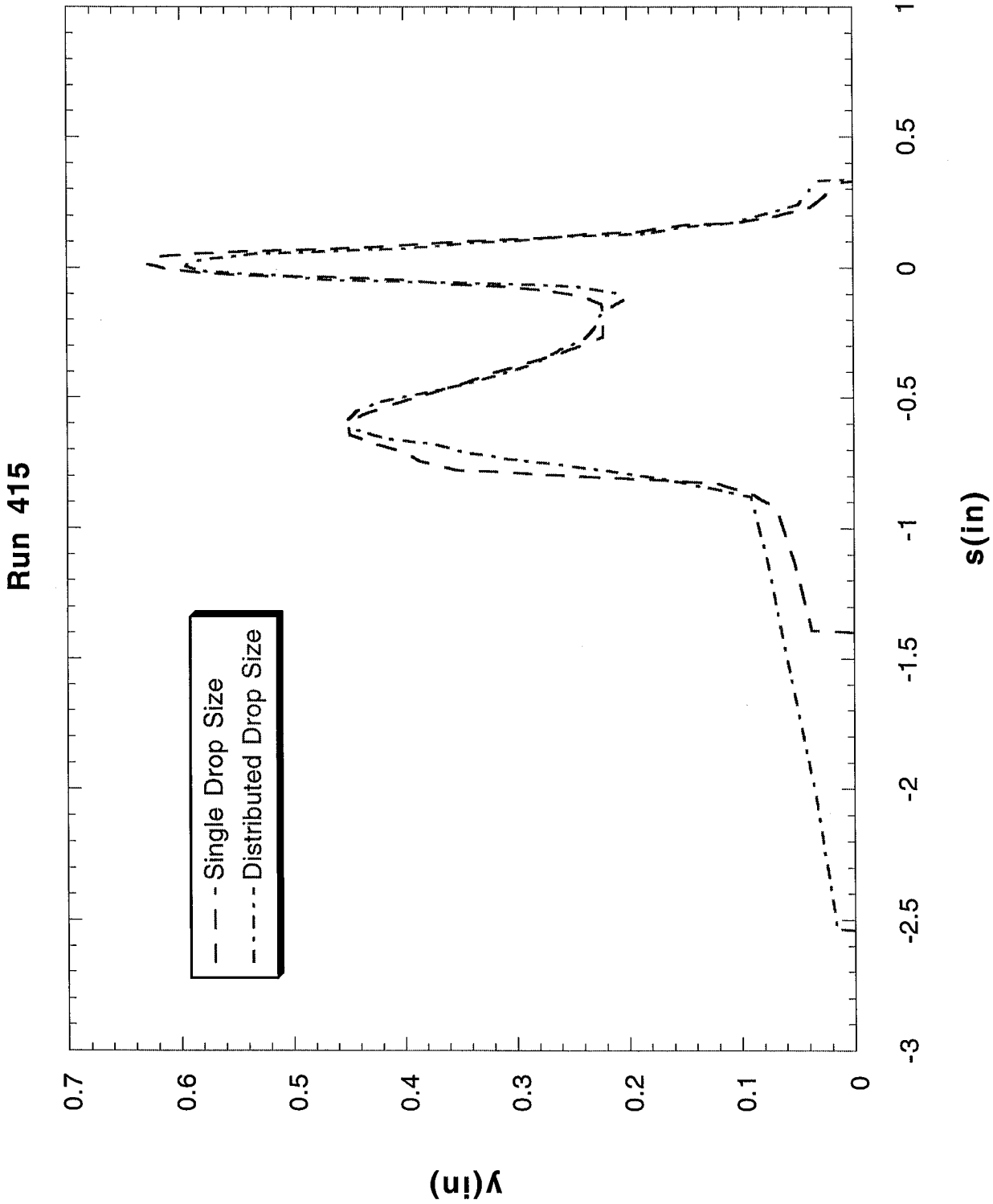
Run 415
Single Drop Size
Distributed Drop Size
y(in)
s(in)
0.7
0.6
0.5
0.4
0.3
0.2
0.1
0
-3
-2.5
-2
-1.5
-1
-0.5
0
0.5
1

FIGURE 84

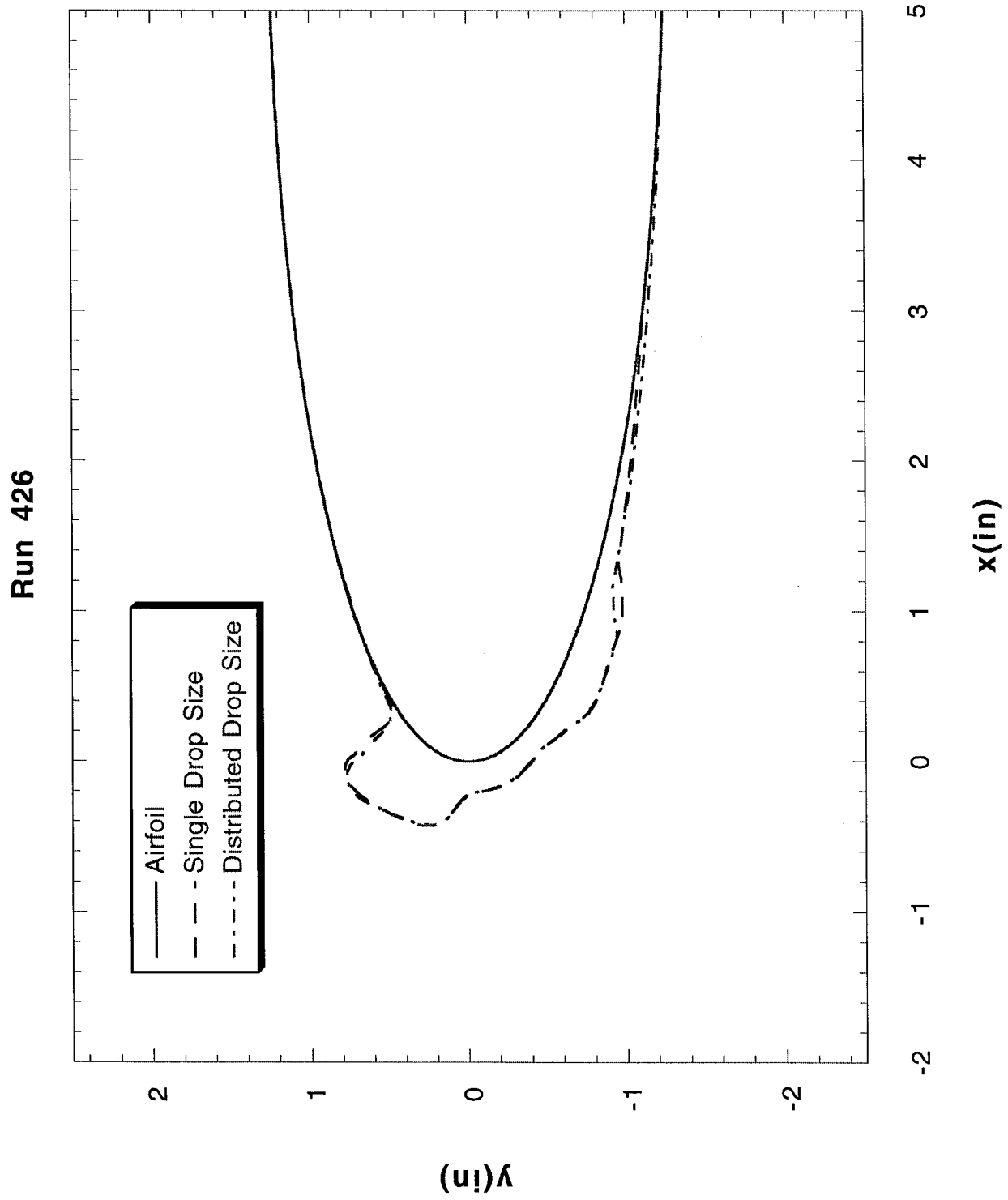
Run 426
Airfoil
Single Drop Size
Distributed Drop Size
y(in)
2
1
0
-1
-2
x(in)
-2
-1
0
1
2
3
4
5

FIGURE 85

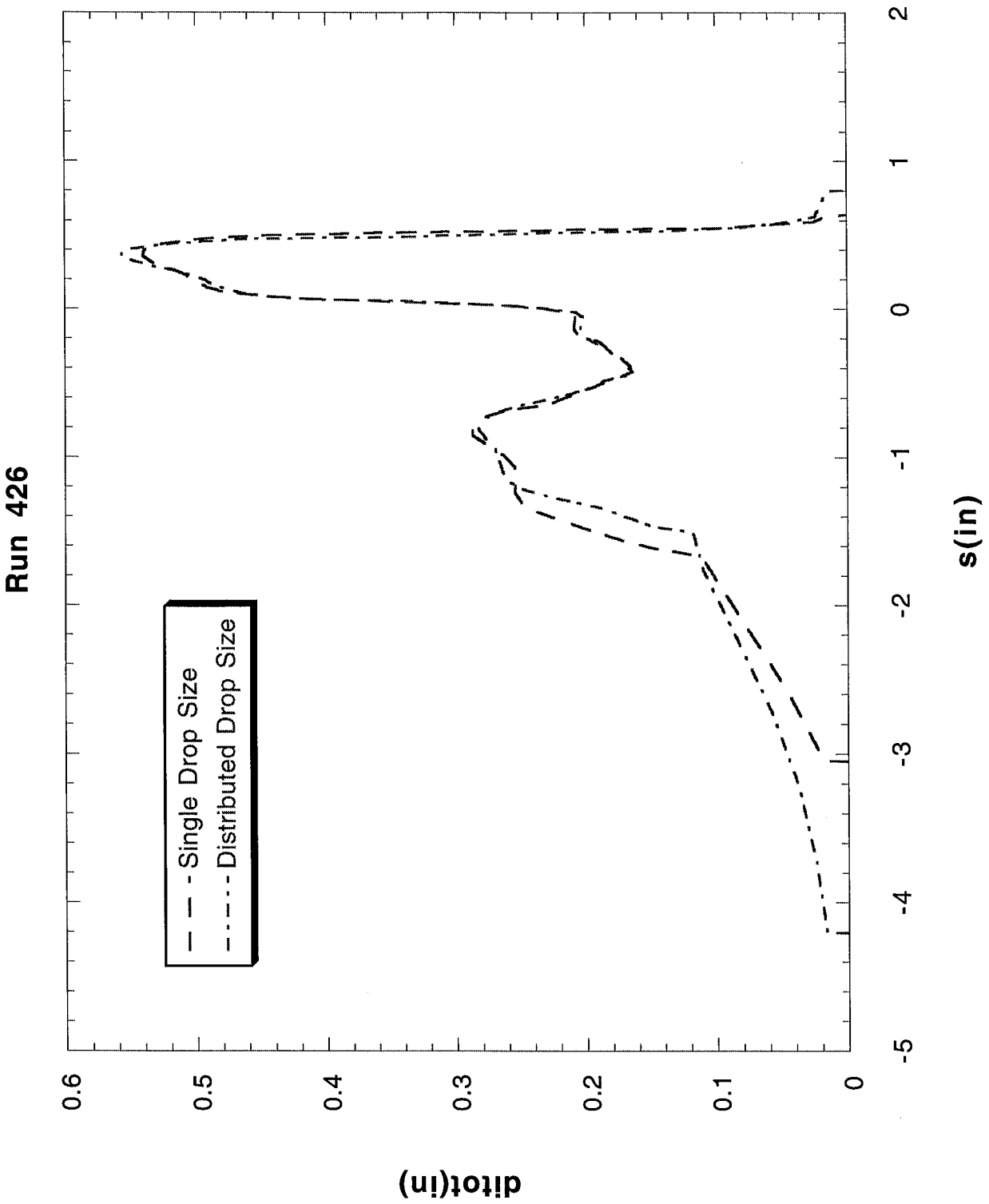
Run 426
Single Drop Size
Distributed Drop Size
ditot(in)
0.6
0.5
0.4
0.3
0.2
0.1
0
s(in)
2
1
0
-1
-2
-3
-4
-5

FIGURE 86

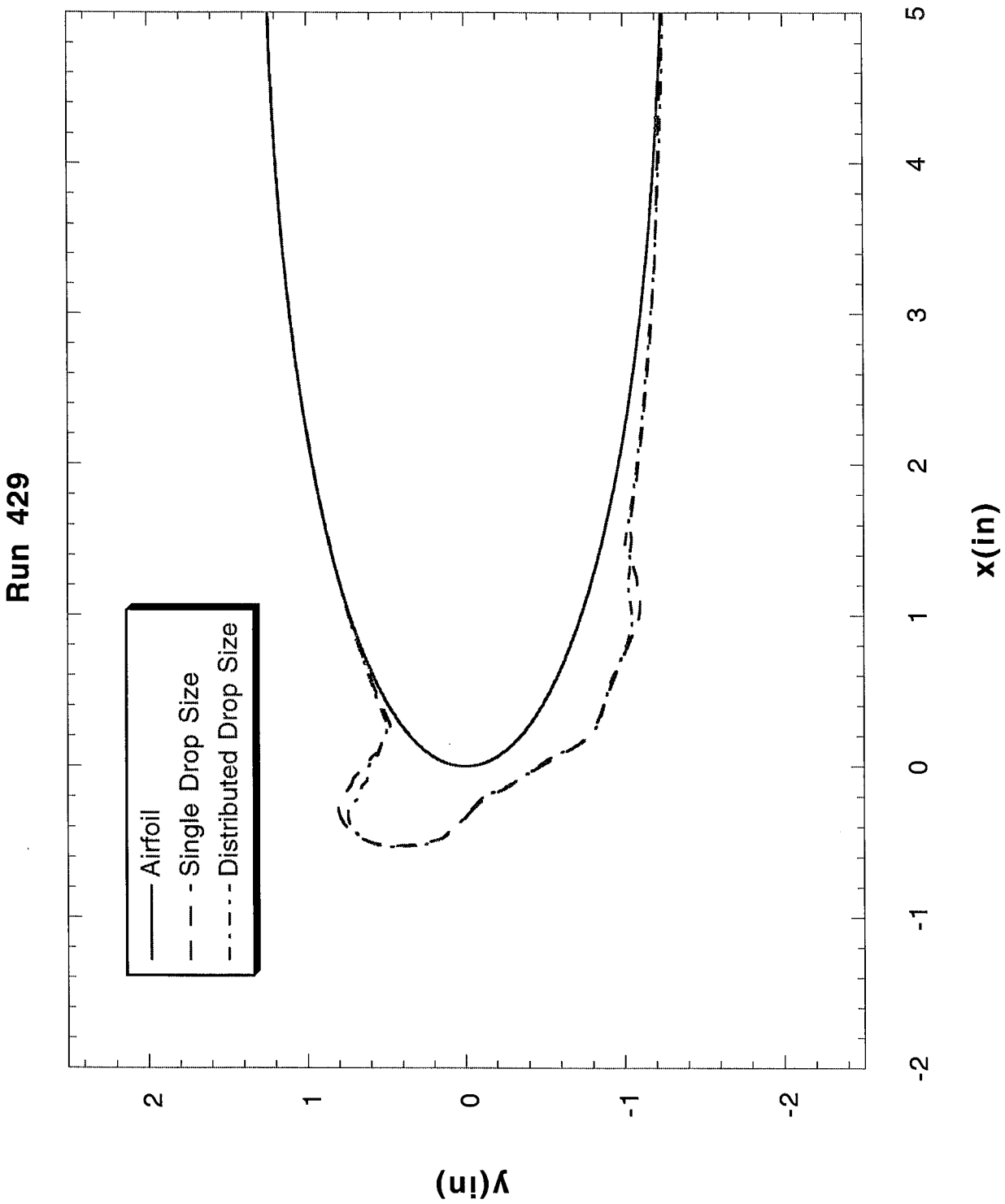
Run 429
Airfoil
Single Drop Size
Distributed Drop Size
y(in)
2
1
0
-1
-2
x(in)
-2
-1
0
1
2
3
4
5

FIGURE 87

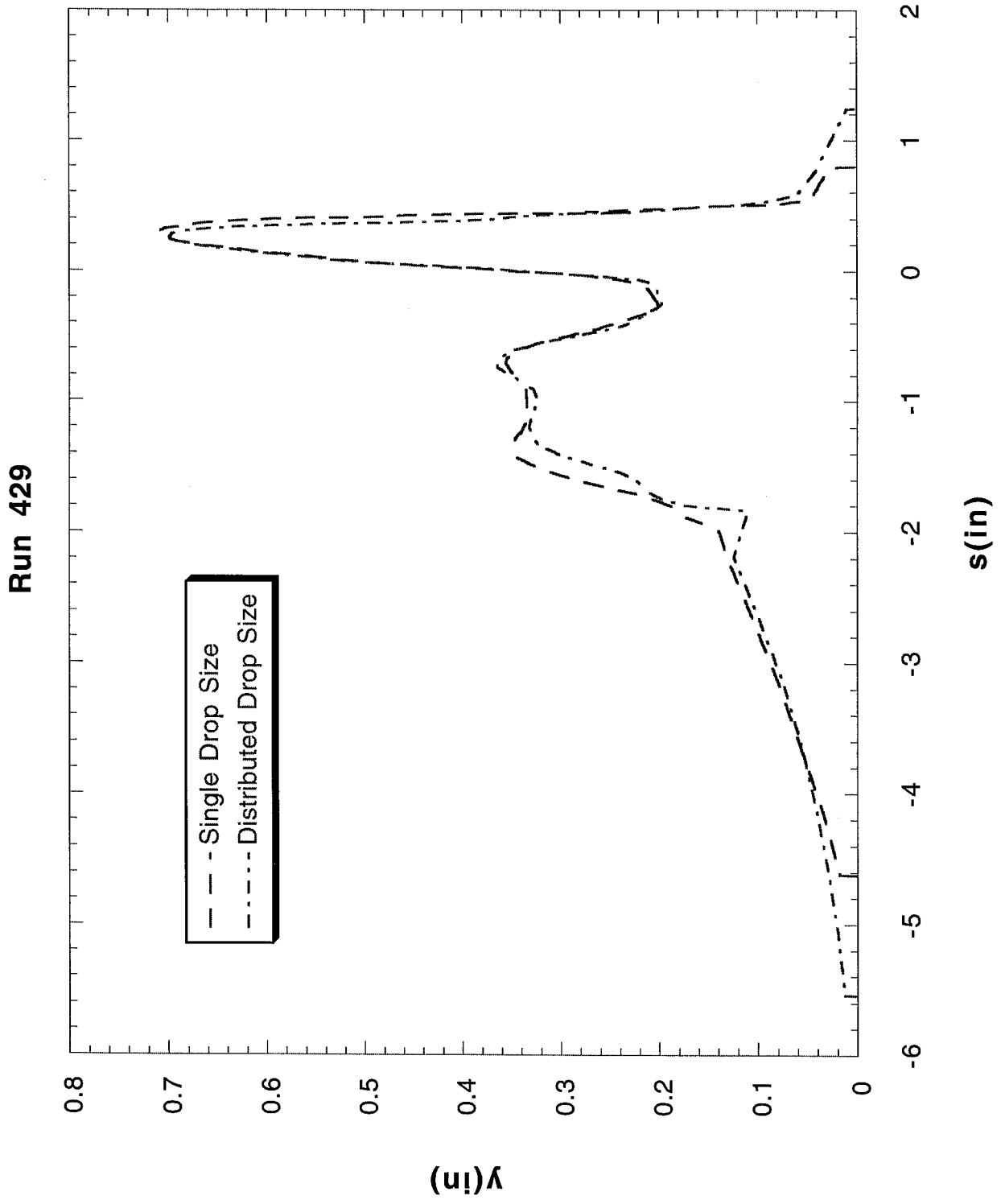
Run 429
Single Drop Size
Distributed Drop Size
y(in)
s(in)
0.8
0.7
0.6
0.5
0.4
0.3
0.2
0.1
0
2
1
0
-1
-2
-3
-4
-5
-6

FIGURE 88

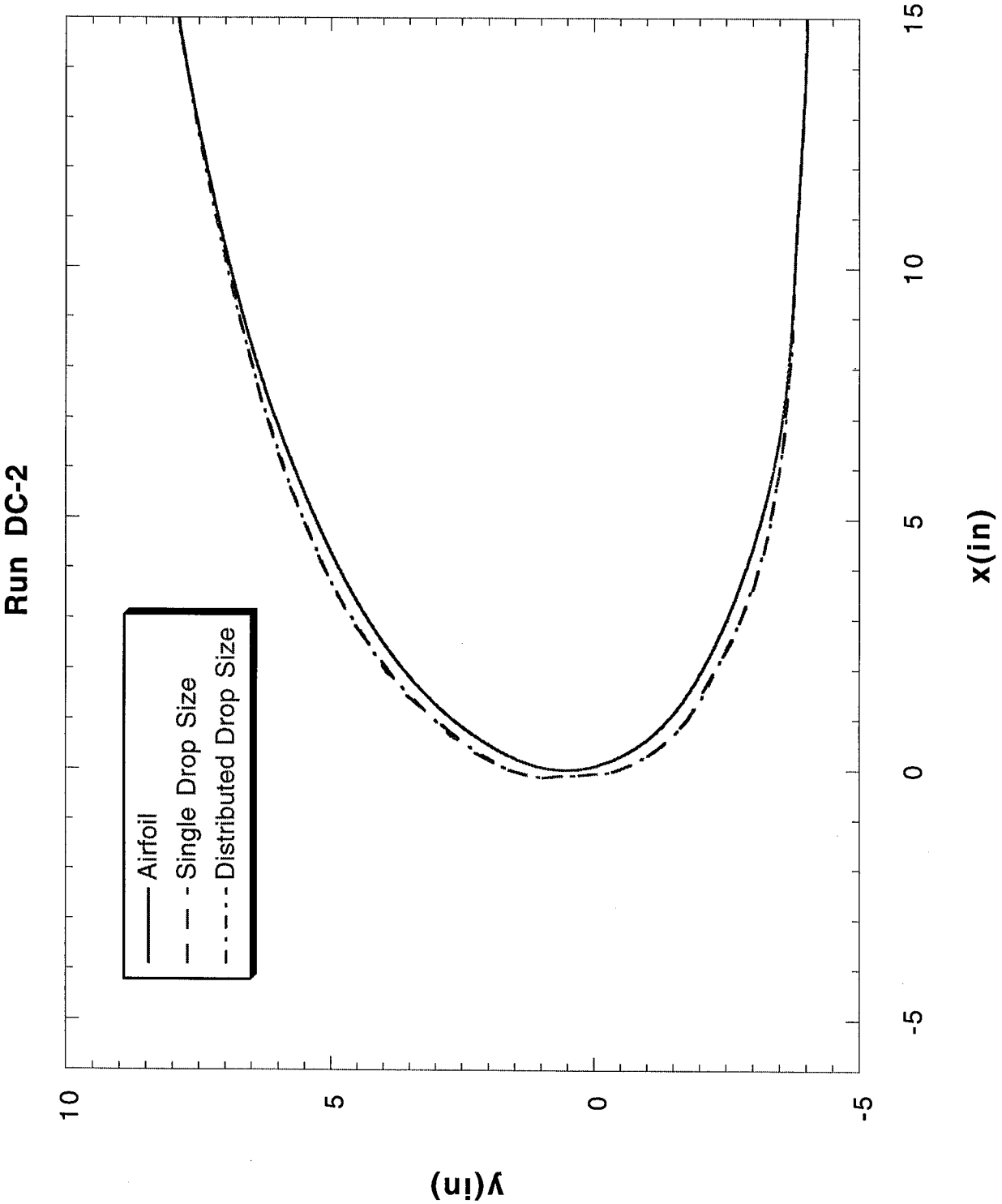
Run DC-2
Airfoil
Single Drop Size
Distributed Drop Size
y(in)
10
5
0
-5
x(in)
-5
0
5
10
15

FIGURE 89

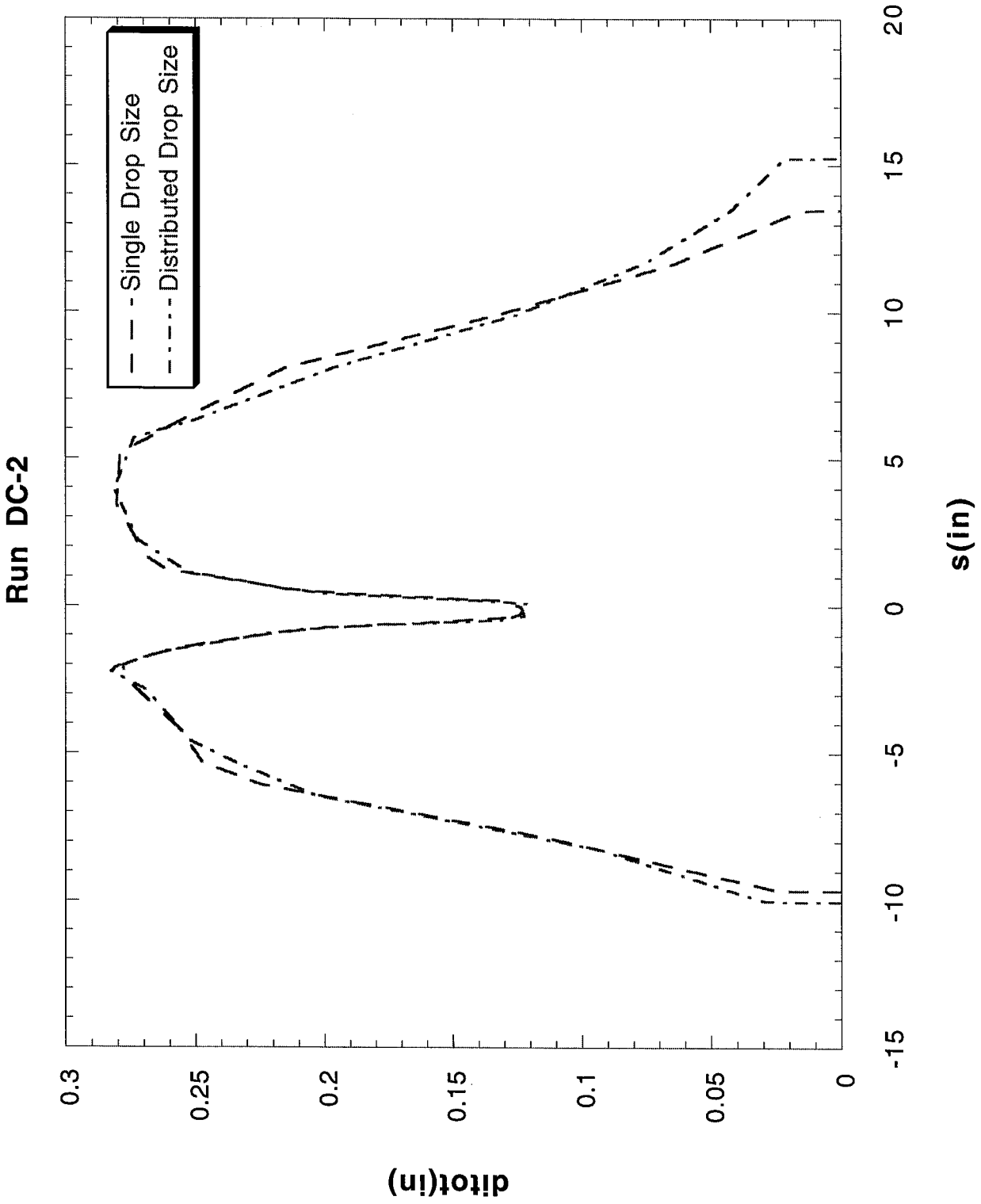
Run DC-2
Single Drop Size
Distributed Drop Size
ditot(in)
0.3
0.25
0.2
0.15
0.1
0.05
0
s(in)
20
15
10
5
0
-5
-10
-15

FIGURE 90

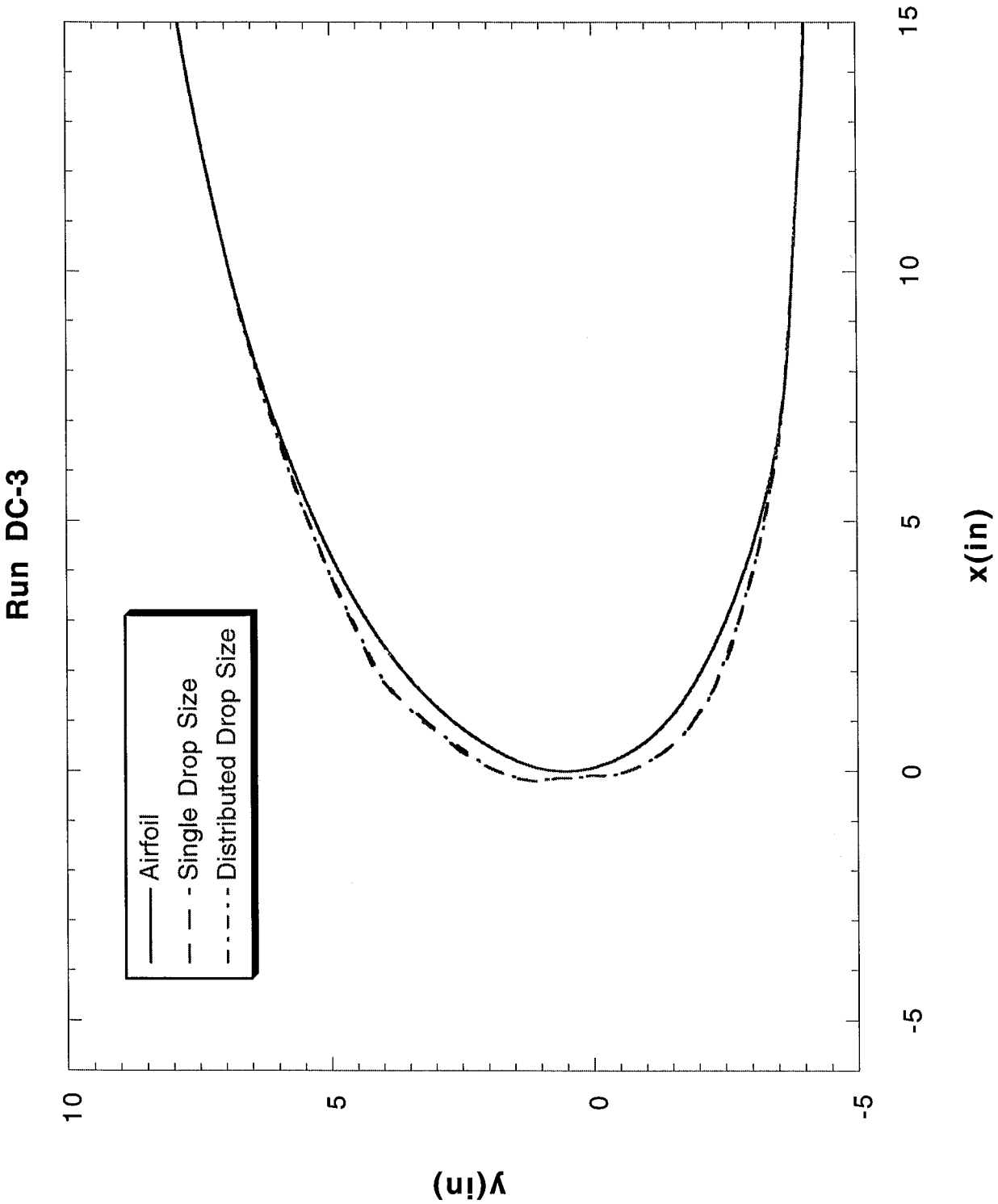
Run DC-3
Airfoil
Single Drop Size
Distributed Drop Size
y(in)
10
5
0
-5
x(in)
-5
0
5
10
15

FIGURE 91

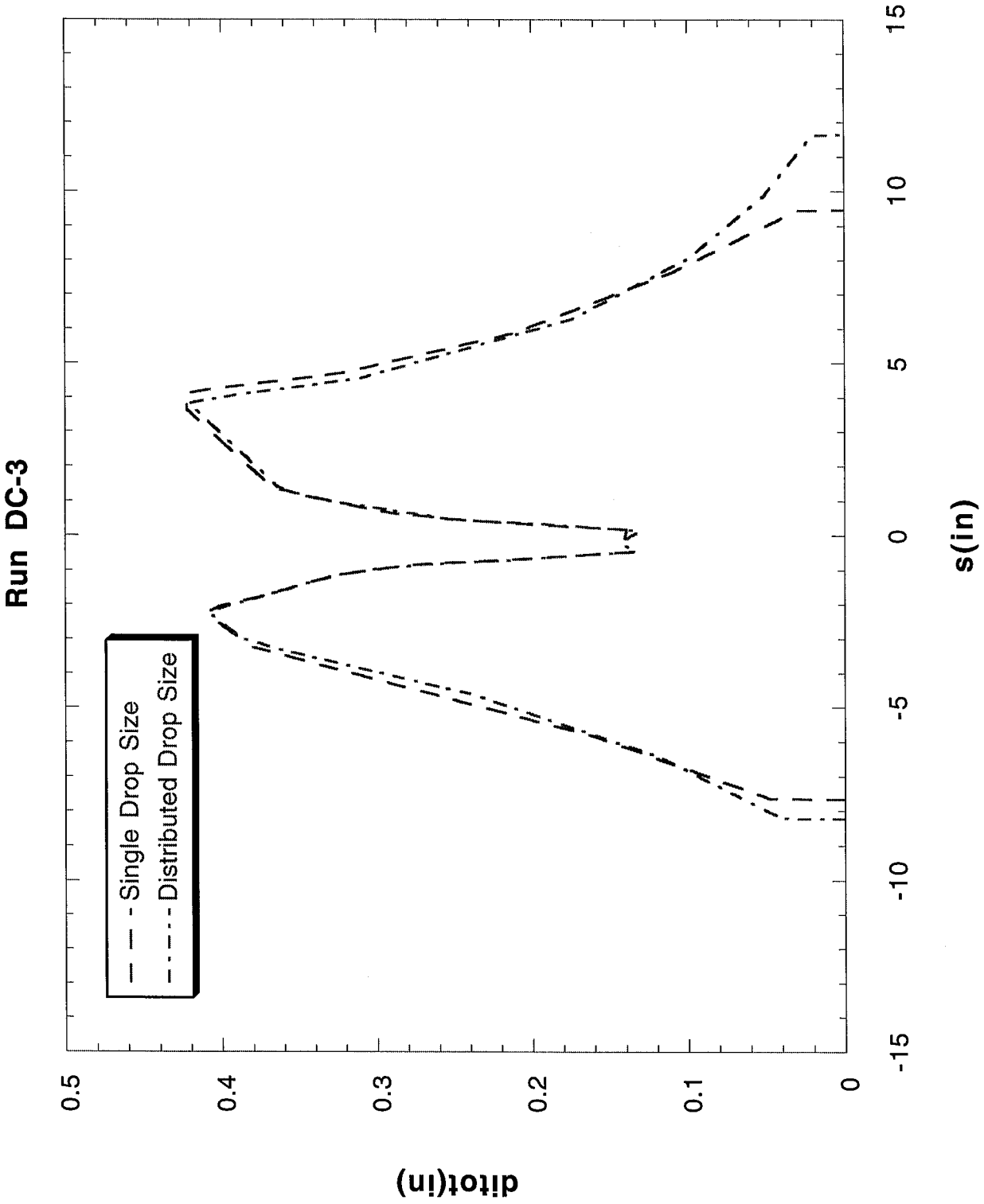
Run DC-3
Single Drop Size
Distributed Drop Size
ditot(in)
0.5
0.4
0.3
0.2
0.1
0
s(in)
15
10
5
0
-5
-10
-15

FIGURE 92

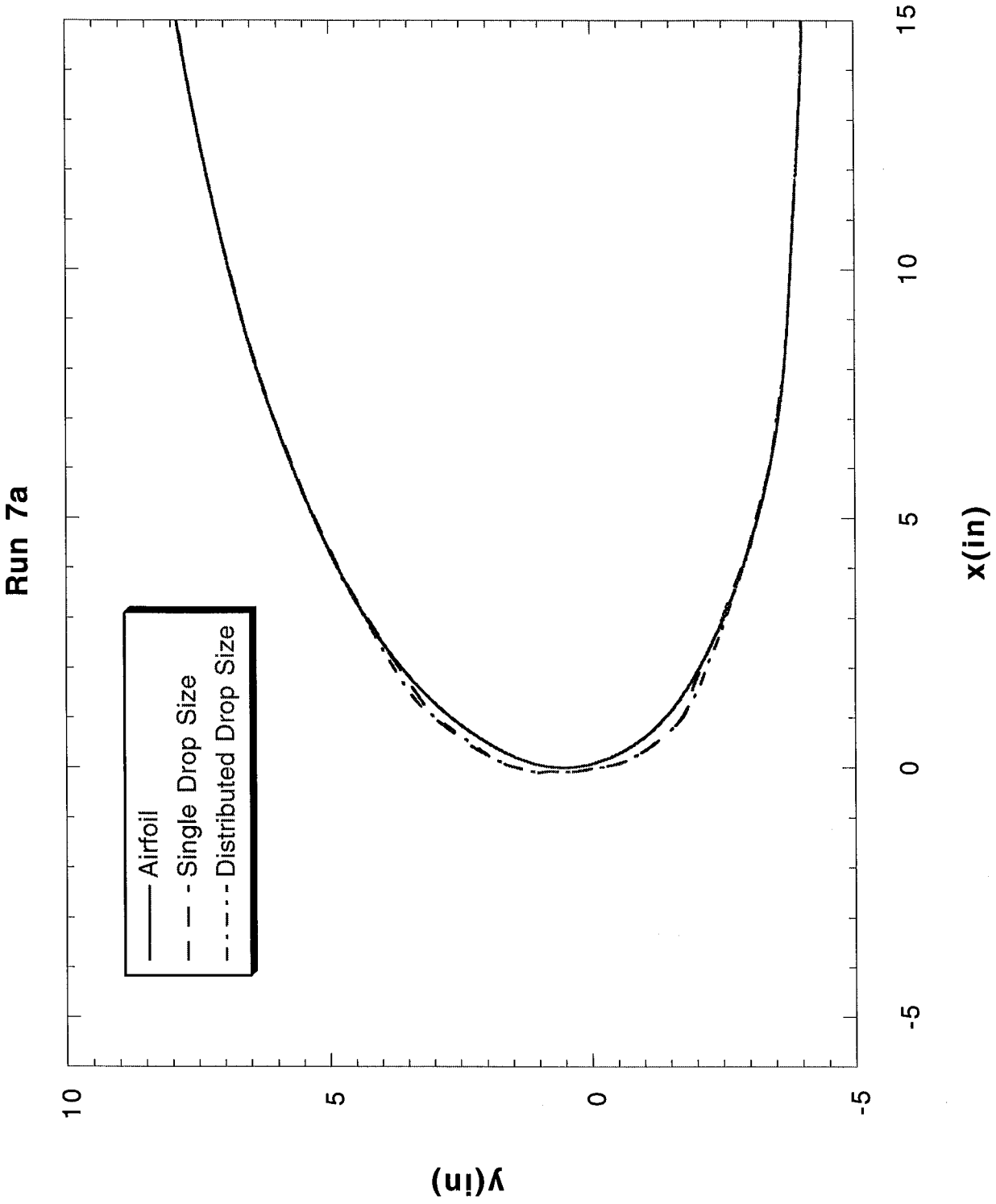
Run 7a
Airfoil
Single Drop Size
Distributed Drop Size
y(in)
10
5
0
-5
x(in)
-5
0
5
10
15

FIGURE 93

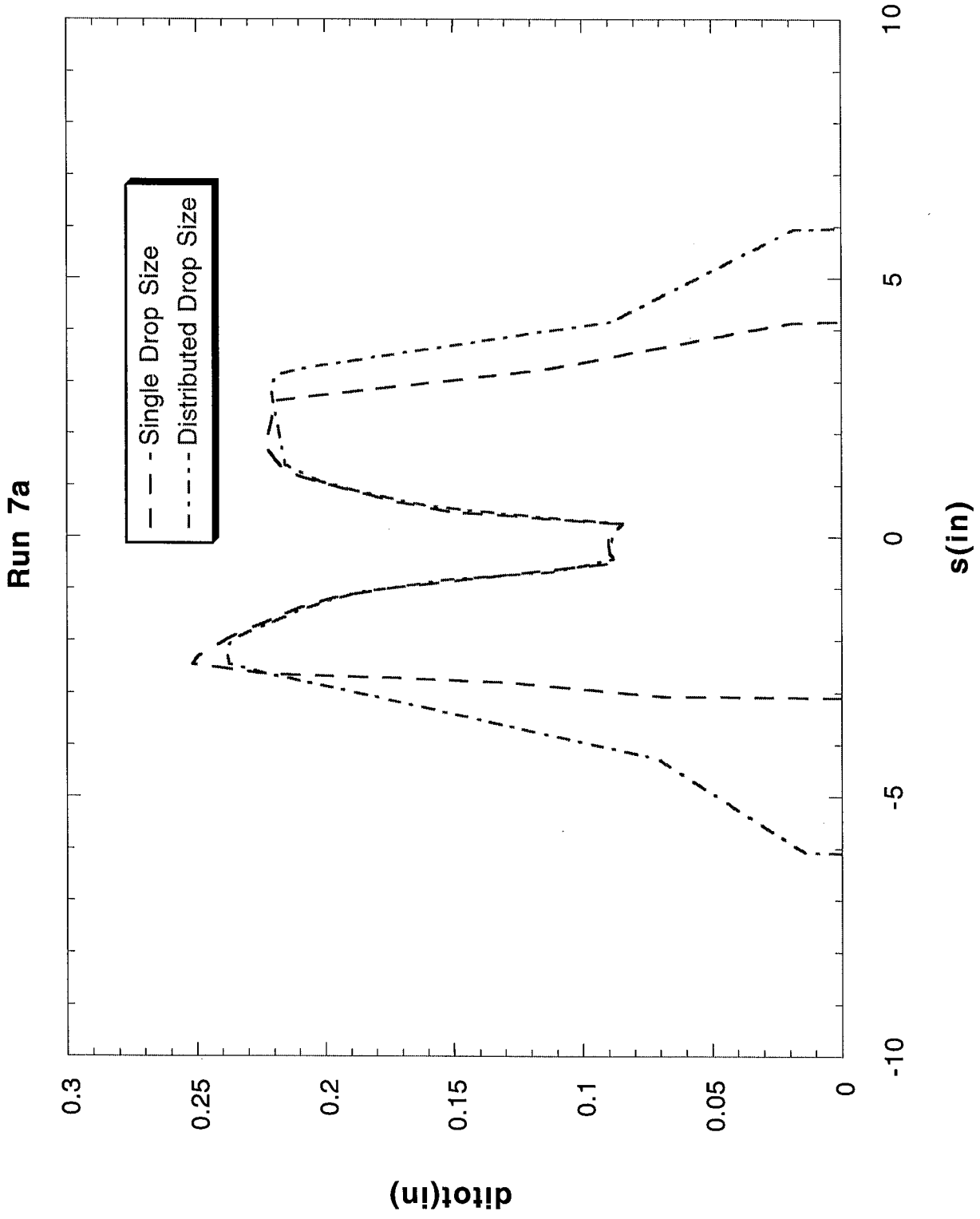
Run 7a
Single Drop Size
Distributed Drop Size
ditot(in)
0.3
0.25
0.2
0.15
0.1
0.05
0
s(in)
10
5
0
-5
-10

FIGURE 94

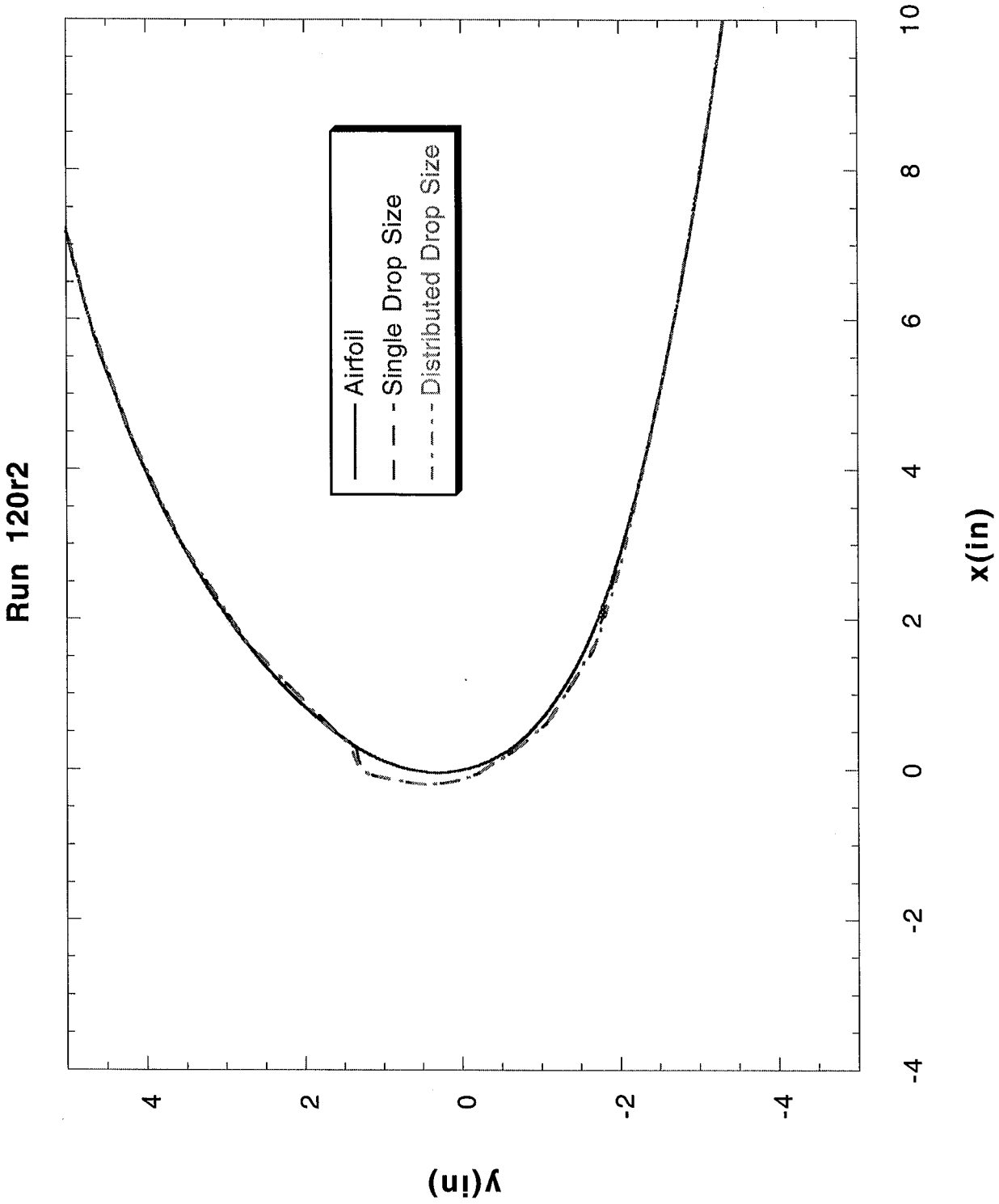
Run 120r2
Airfoil
Single Drop Size
Distributed Drop Size
y(in)
x(in)
4
2
0
-2
-4
10
8
6
4
2
0
-2
-4

FIGURE 95

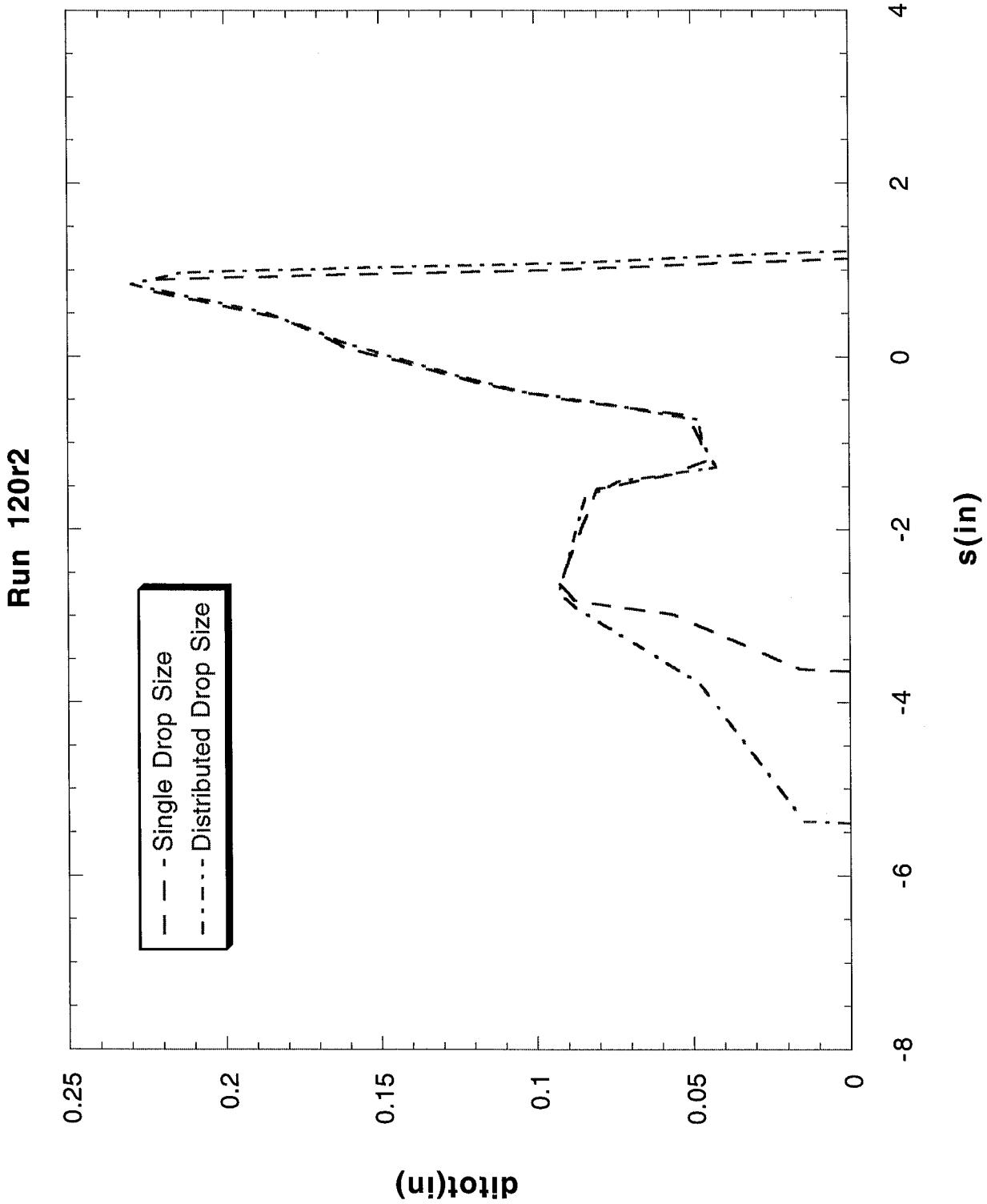
Run 120r2
Single Drop Size
Distributed Drop Size
ditot(in)
0.25
0.2
0.15
0.1
0.05
0
s(in)
4
2
0
-2
-4
-6
-8

FIGURE 96

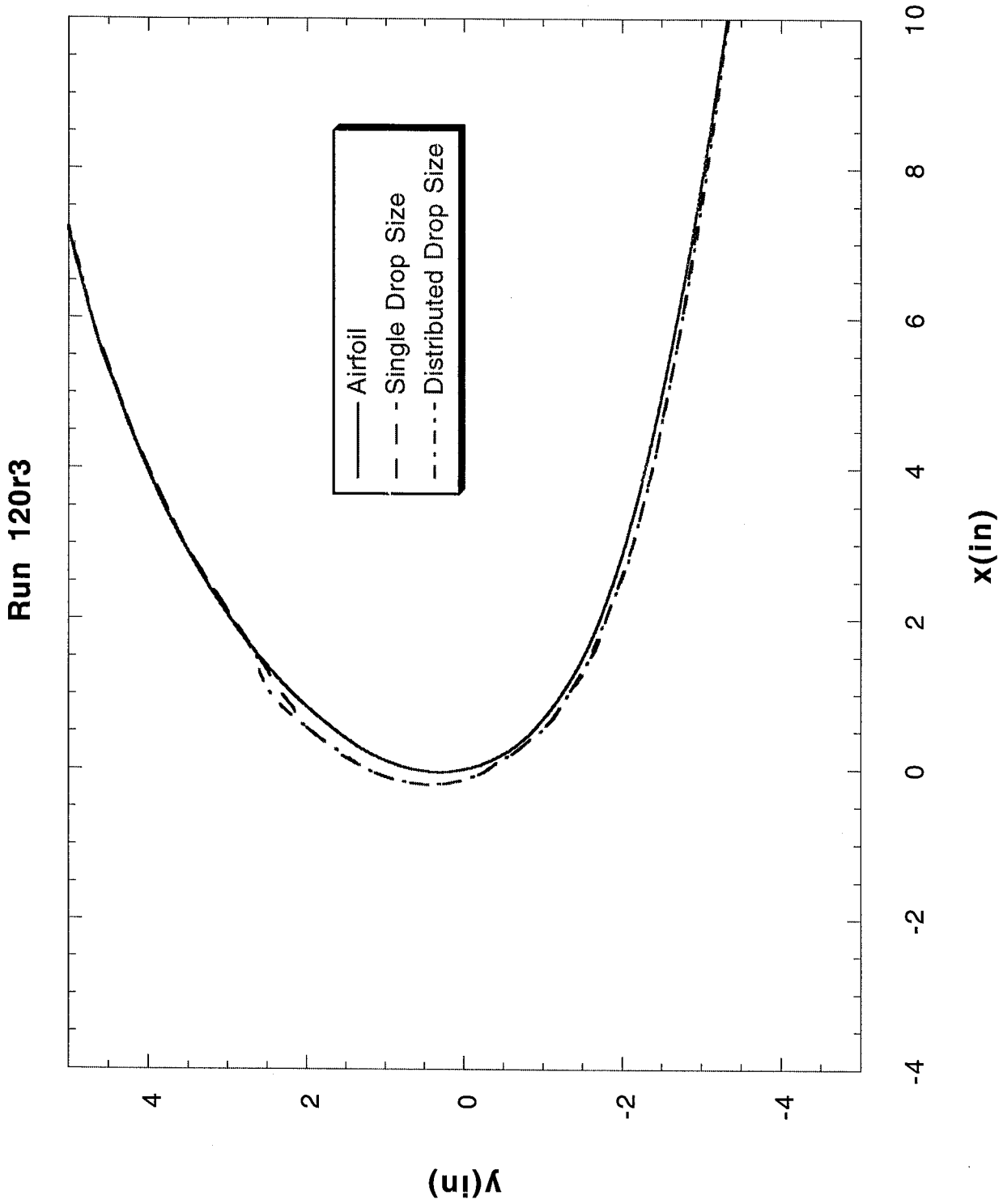
Run 120r3
Airfoil
Single Drop Size
Distributed Drop Size
y(in)
x(in)
4
2
0
-2
-4
10
8
6
4
2
0
-2
-4

FIGURE 97

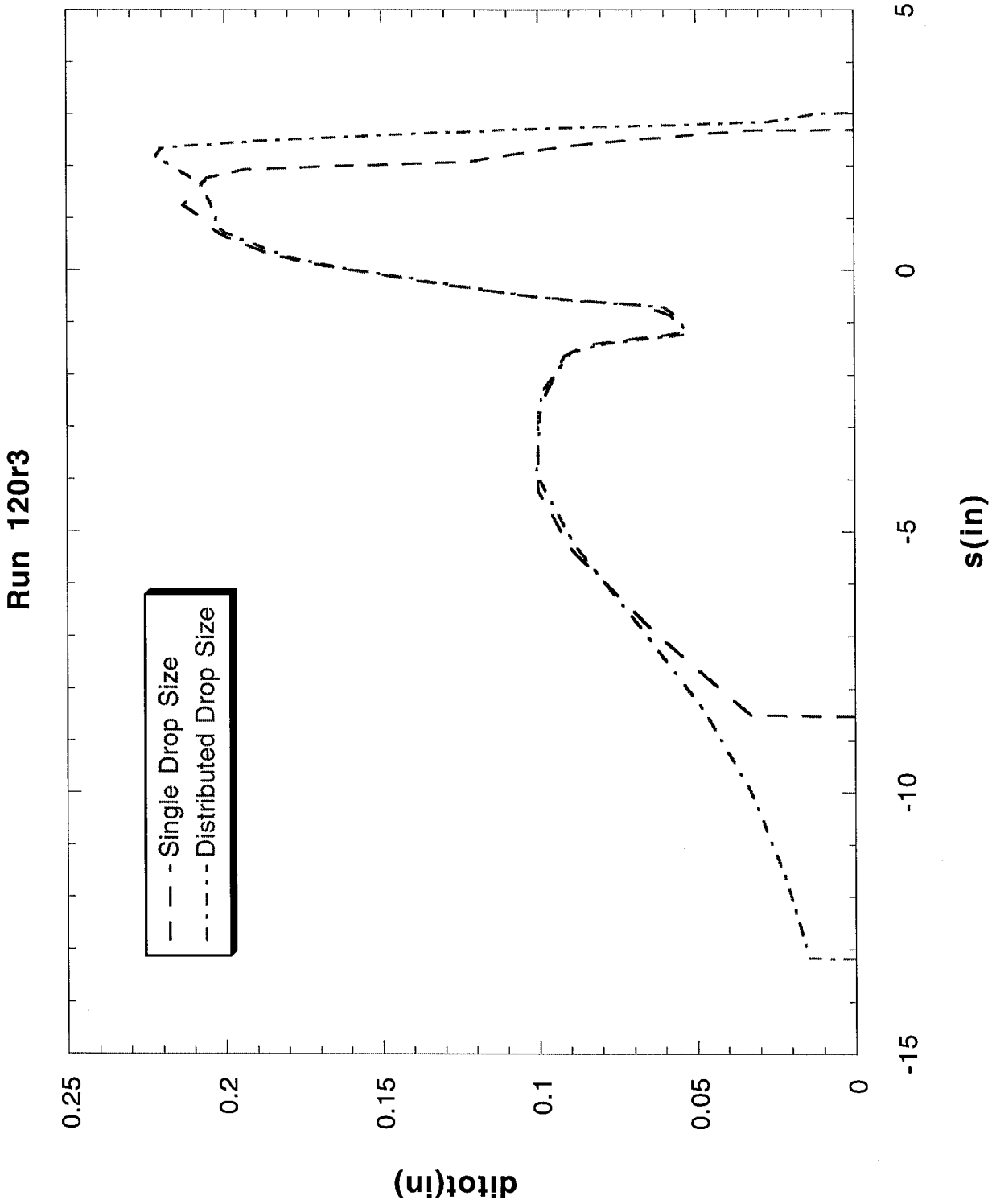
Run 120r3
Single Drop Size
Distributed Drop Size
dltot(in)
0.25
0.2
0.15
0.1
0.05
0
s(in)
5
0
-5
-10
-15

FIGURE 98

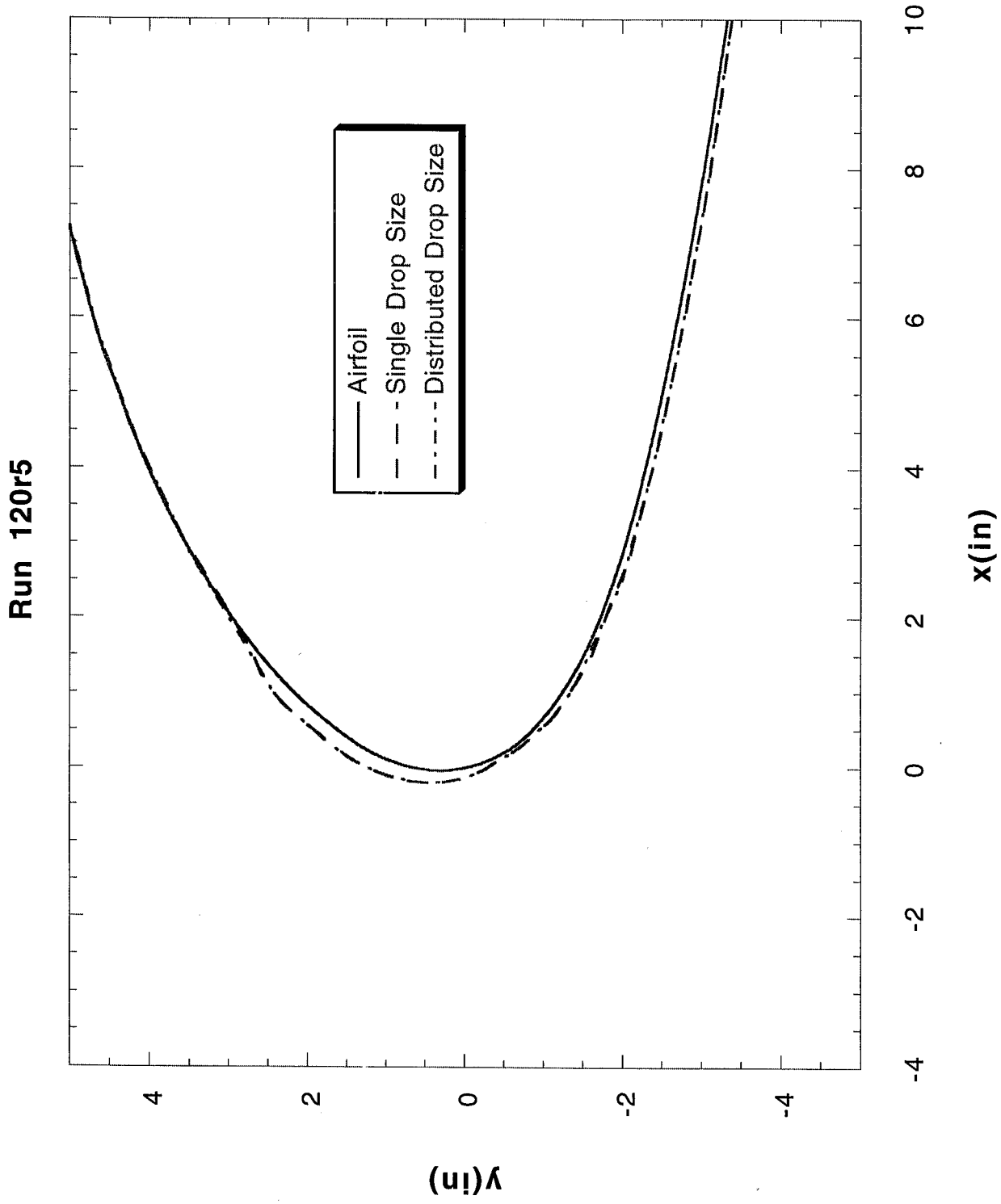
Run 120r5
Airfoil
Single Drop Size
Distributed Drop Size
y(in)
x(in)
4
2
0
-2
-4
10
8
6
4
2
0
-2
-4

FIGURE 99

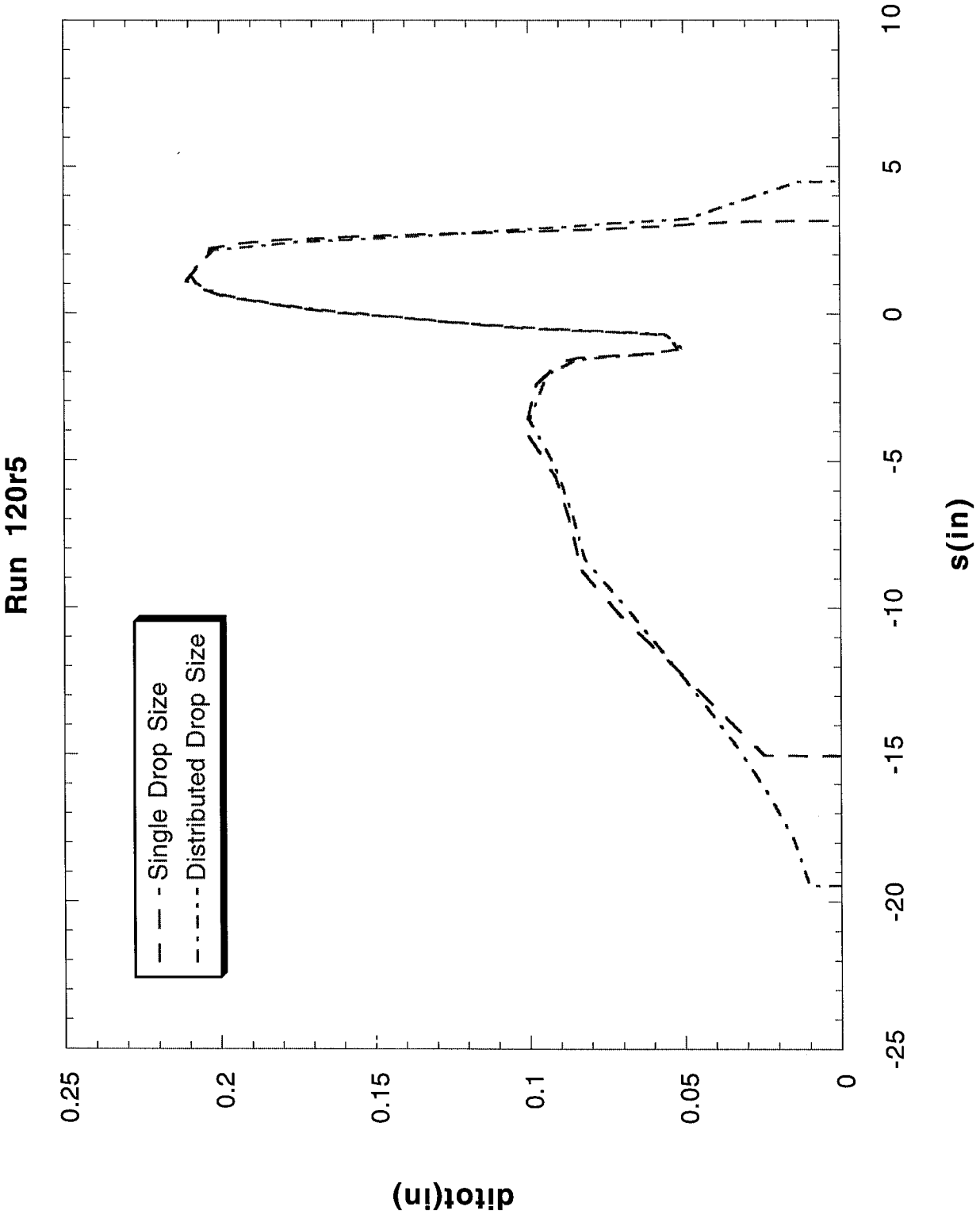
Run 120r5
- - - Single Drop Size
- . - . - Distributed Drop Size
dltot(in)
0.25
0.2
0.15
0.1
0.05
0
s(in)
10
5
0
-5
-10
-15
-20
-25

FIGURE 100

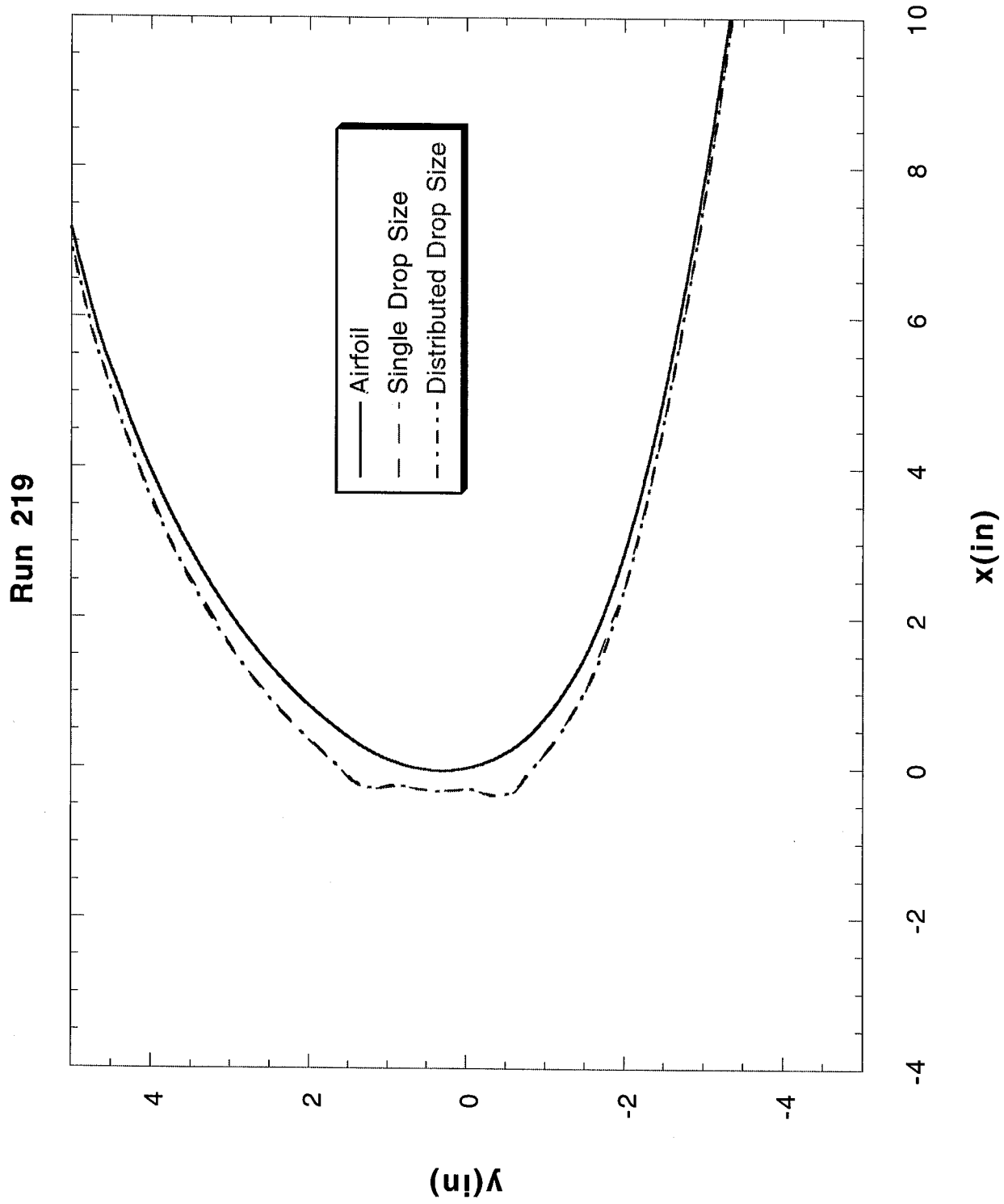
Run 219
Airfoil
Single Drop Size
Distributed Drop Size
y(in)
x(in)
4
2
0
-2
-4
10
8
6
4
2
0
-2
-4

FIGURE 101

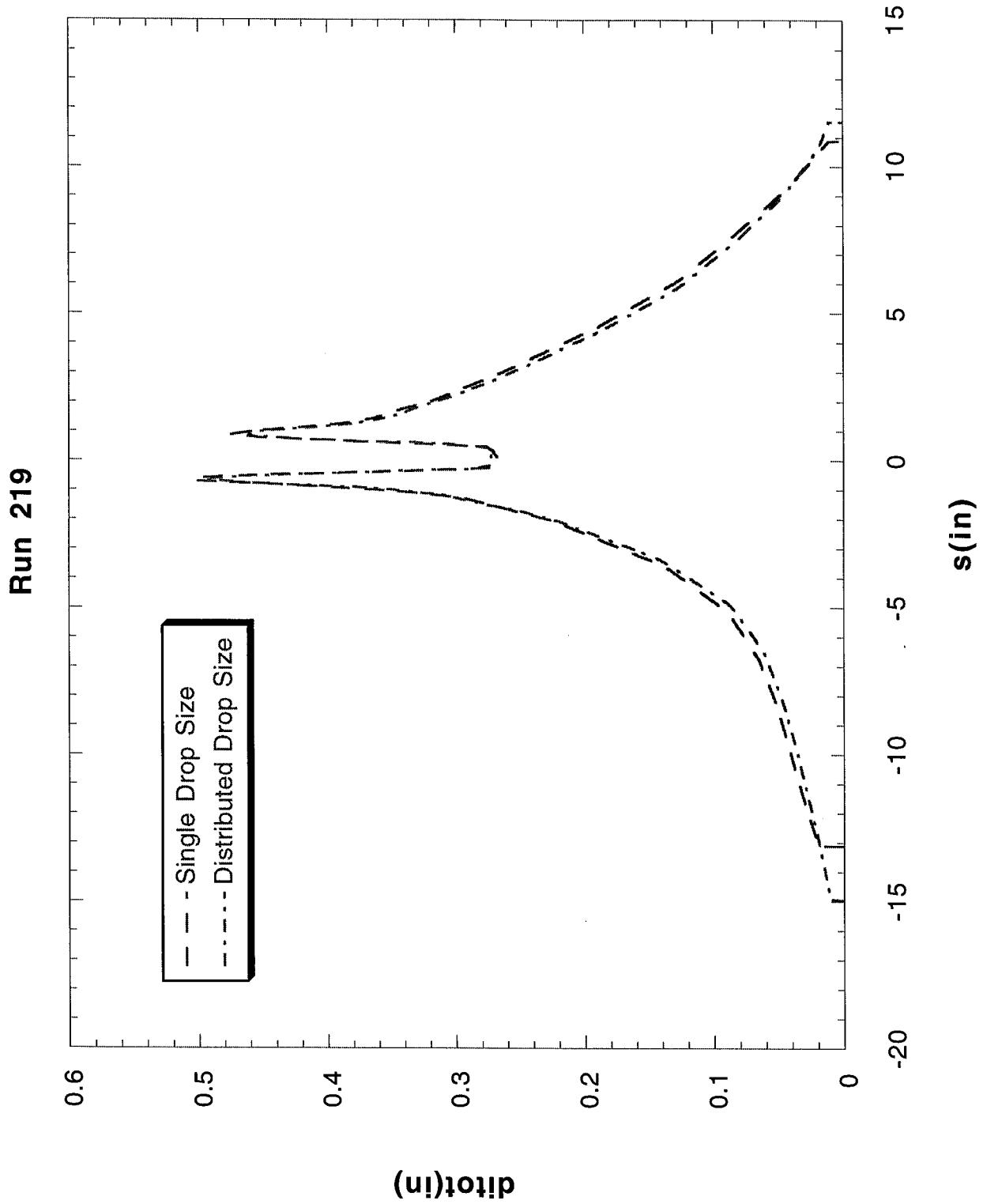
Run 219
dltot(in)
s(in)
0.6
0.5
0.4
0.3
0.2
0.1
0
15
10
5
0
-5
-10
-15
-20
Single Drop Size
Distributed Drop Size

Spacing Cases - Other

FIGURE 102

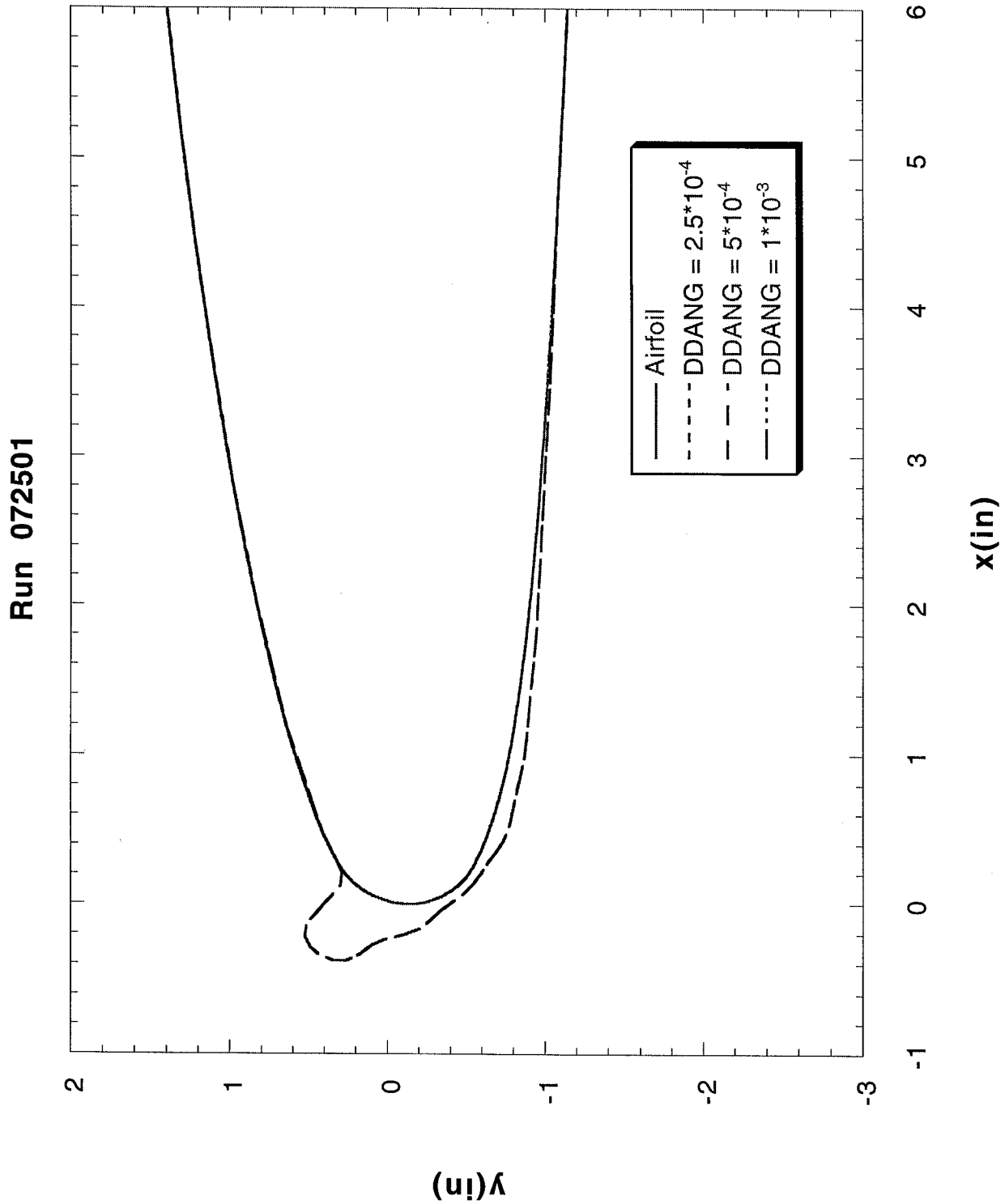
Run 072501
Airfoil
DDANG = 2.5*10^-4
DDANG = 5*10^-4
DDANG = 1*10^-3
y(in)
x(in)
2
1
0
-1
-2
-3
-1
0
1
2
3
4
5
6

FIGURE 103

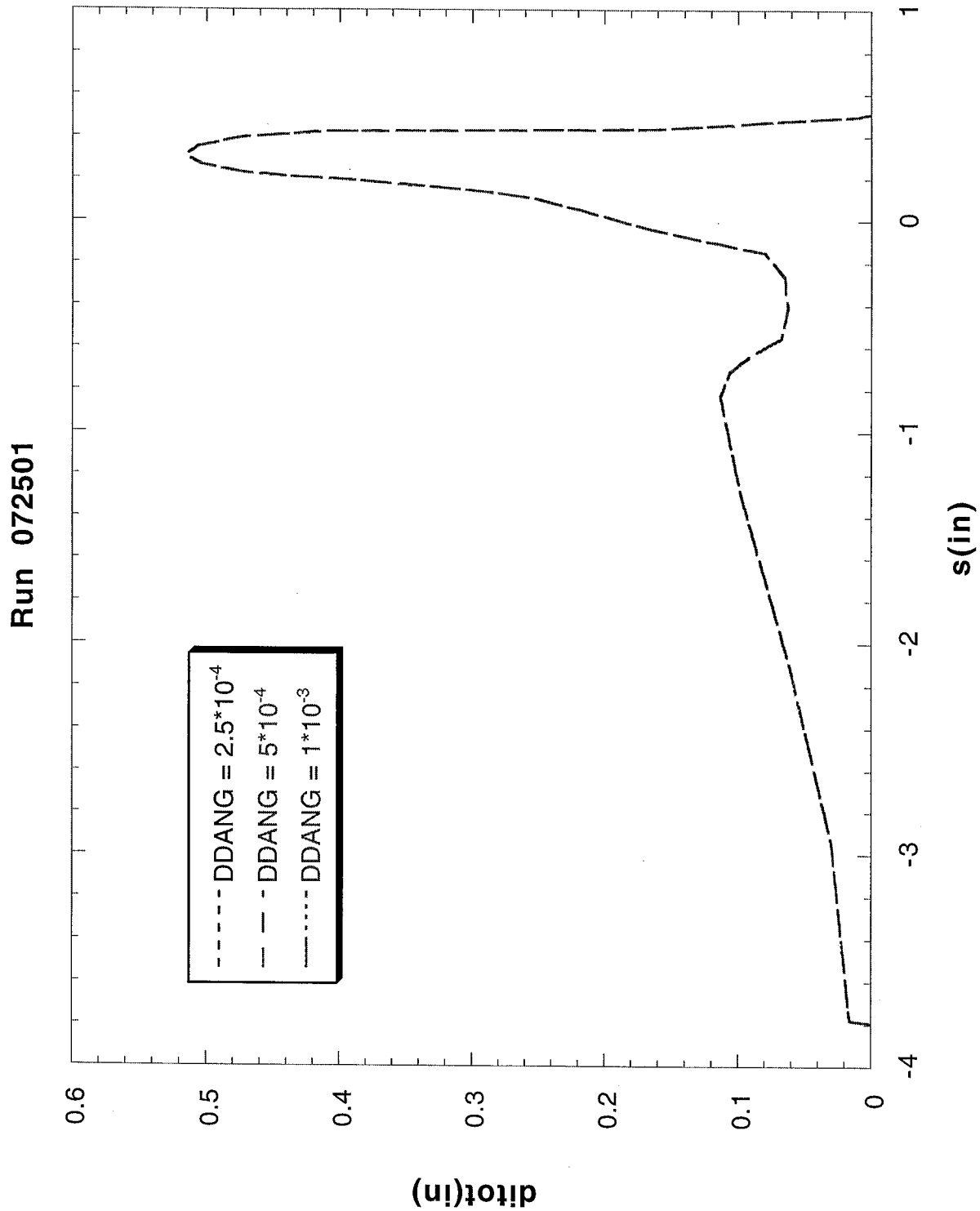
Run 072501
ditot(in)
s(in)
DDANG = 2.5*10^-4
DDANG = 5*10^-4
DDANG = 1*10^-3
0.6
0.5
0.4
0.3
0.2
0.1
0
-4
-3
-2
-1
0
1

FIGURE 104

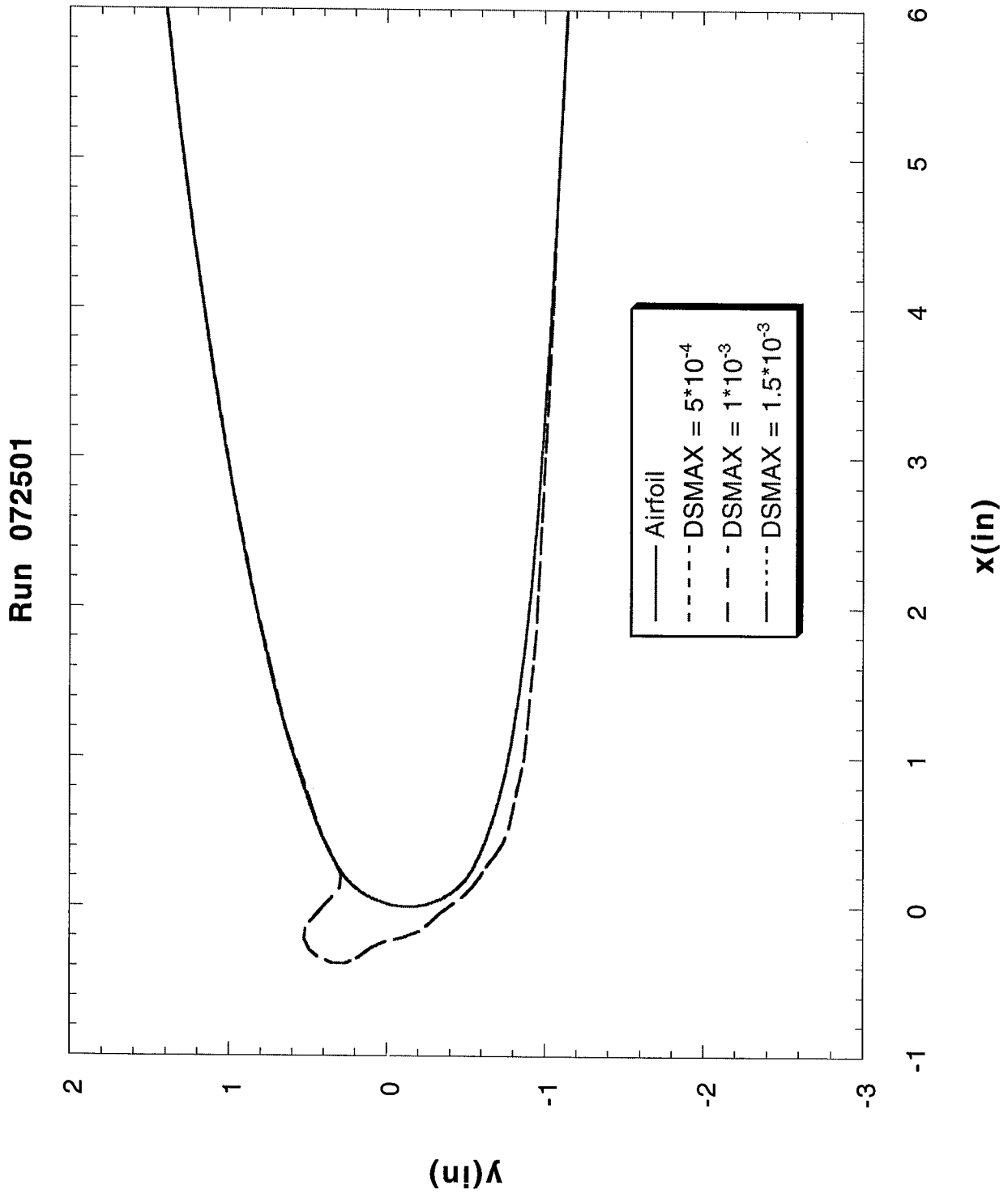
Run 072501
Airfoil
DSMAX = 5*10-4
DSMAX = 1*10-3
DSMAX = 1.5*10-3
y(in)
x(in)
2
1
0
-1
-2
-3
-1
0
1
2
3
4
5
6

FIGURE 105

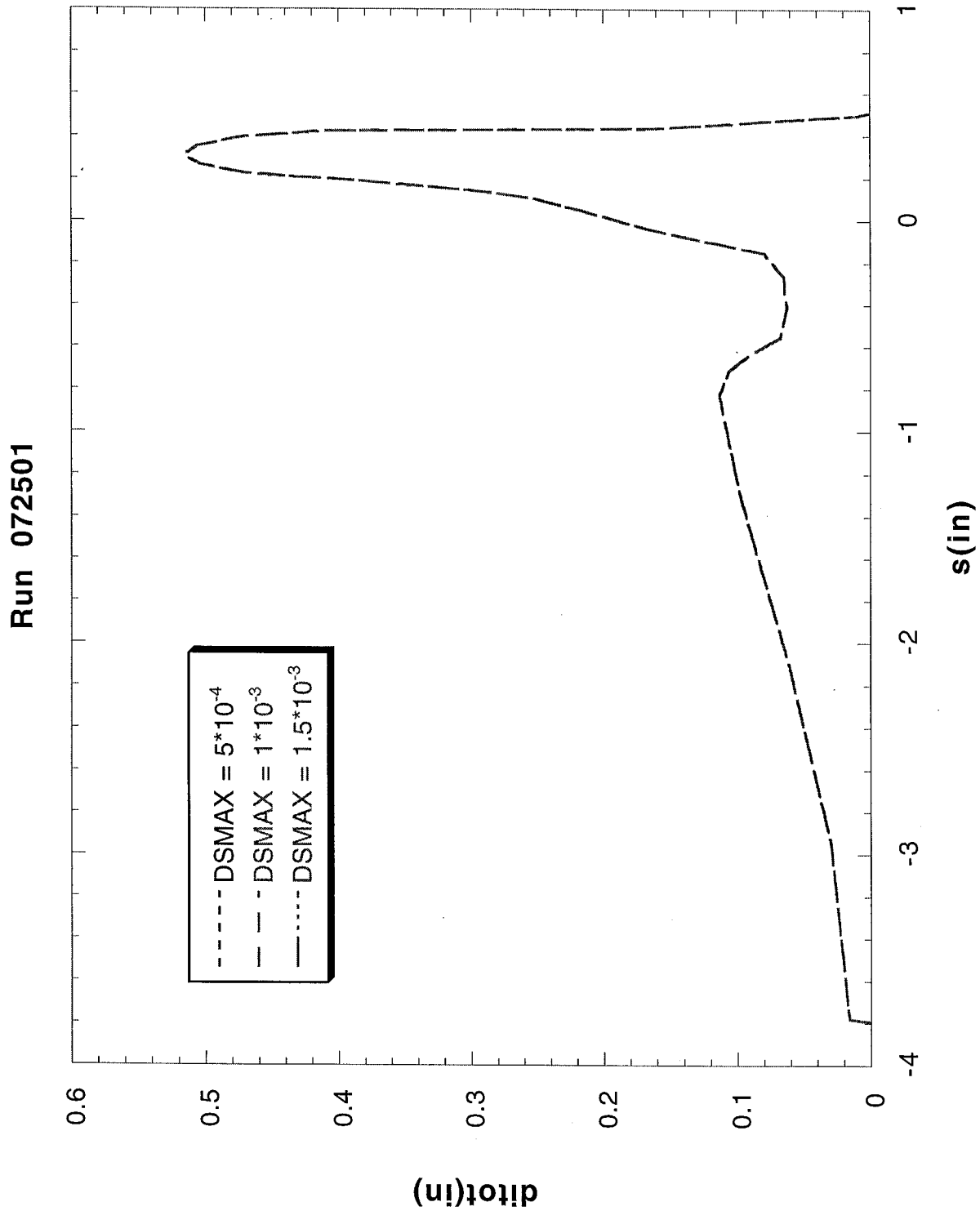
Run 072501
DSMAX = 5*10^-4
DSMAX = 1*10^-3
DSMAX = 1.5*10^-3
ditot(in)
s(in)
0.6
0.5
0.4
0.3
0.2
0.1
0
-4
-3
-2
-1
0
1

FIGURE 106

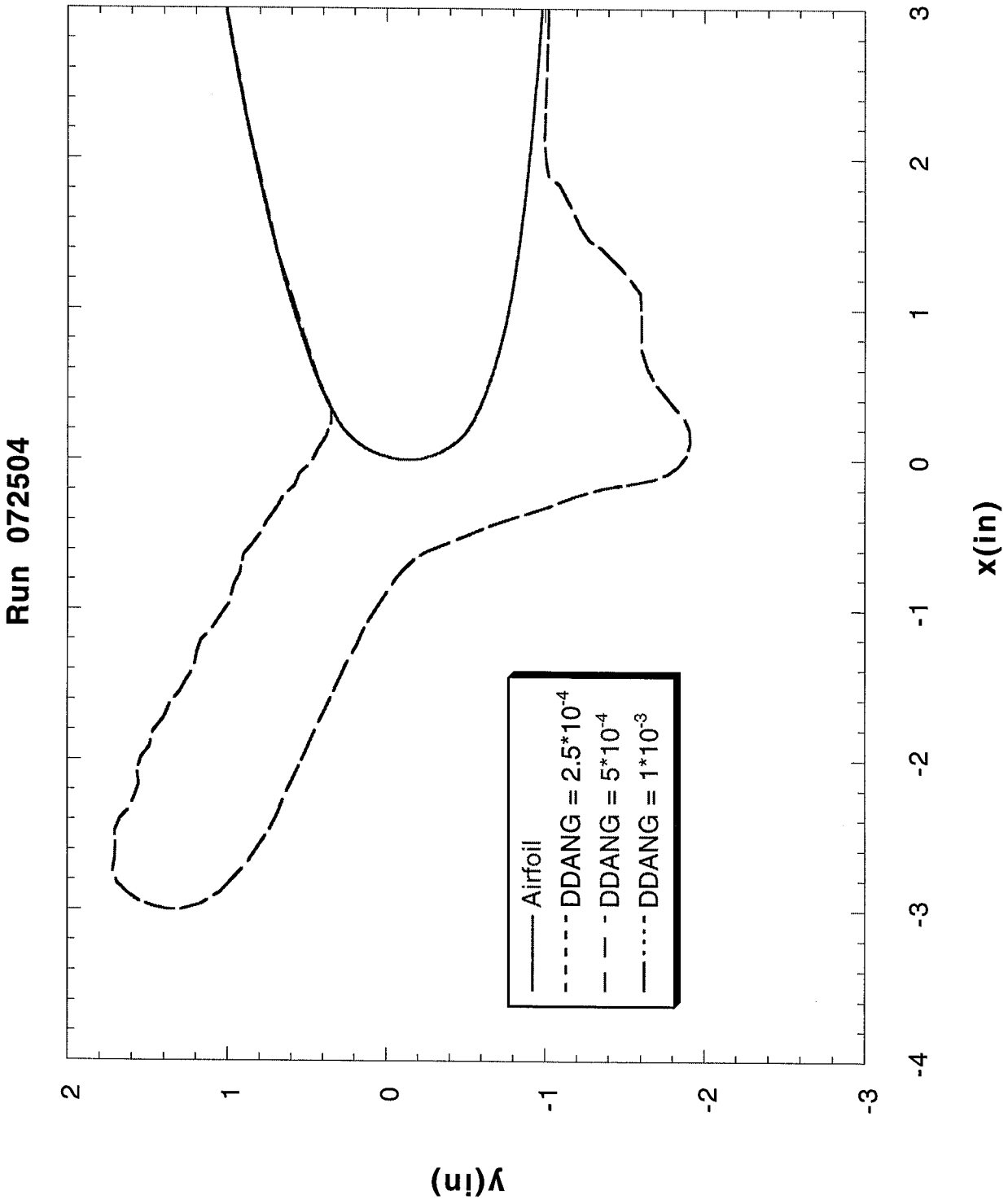
Run 072504
Airfoil
DDANG = 2.5*10^-4
DDANG = 5*10^-4
DDANG = 1*10^-3
y(in)
x(in)
2
1
0
-1
-2
-3
3
2
1
0
-1
-2
-3
-4

FIGURE 107

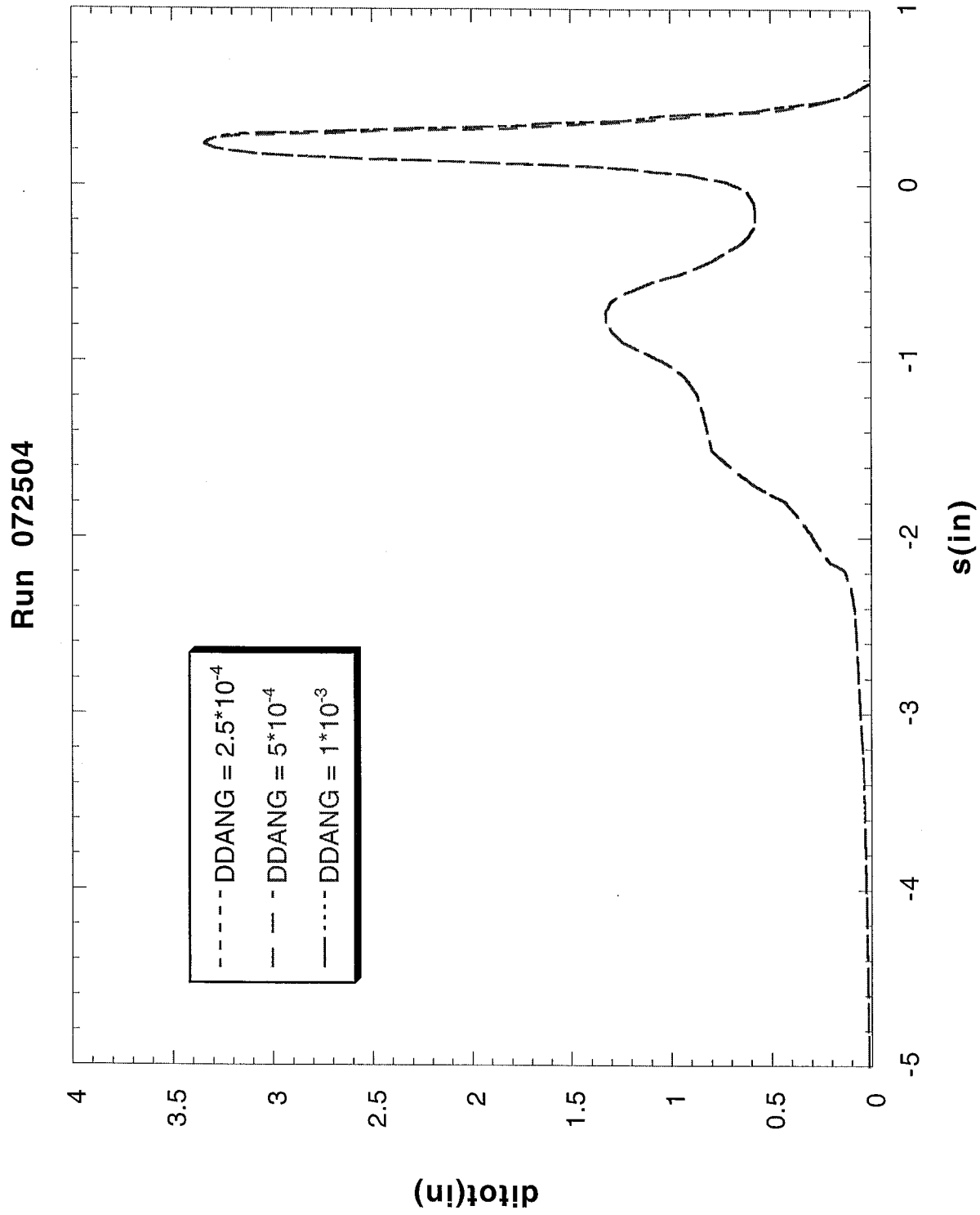
Run 072504
DDANG = 2.5*10^-4
DDANG = 5*10^-4
DDANG = 1*10^-3
ditot(in)
s(in)
4
3.5
3
2.5
2
1.5
1
0.5
0
1
0
-1
-2
-3
-4
-5

FIGURE 108

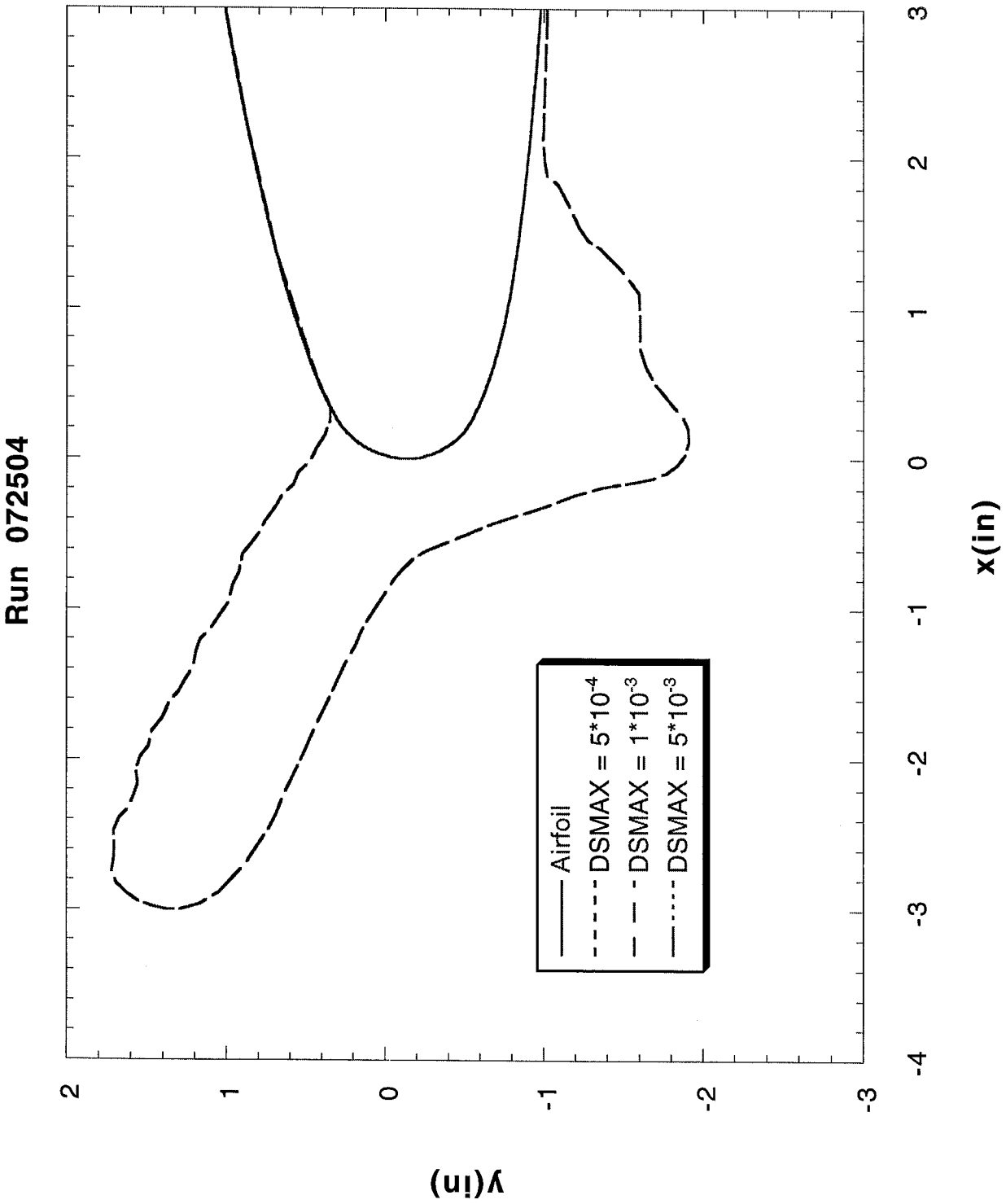
Run 072504
y(in)
x(in)
2
1
0
-1
-2
-3
3
2
1
0
-1
-2
-3
-4
Airfoil
DSMAX = 5*10-4
DSMAX = 1*10-3
DSMAX = 5*10-3

FIGURE 109

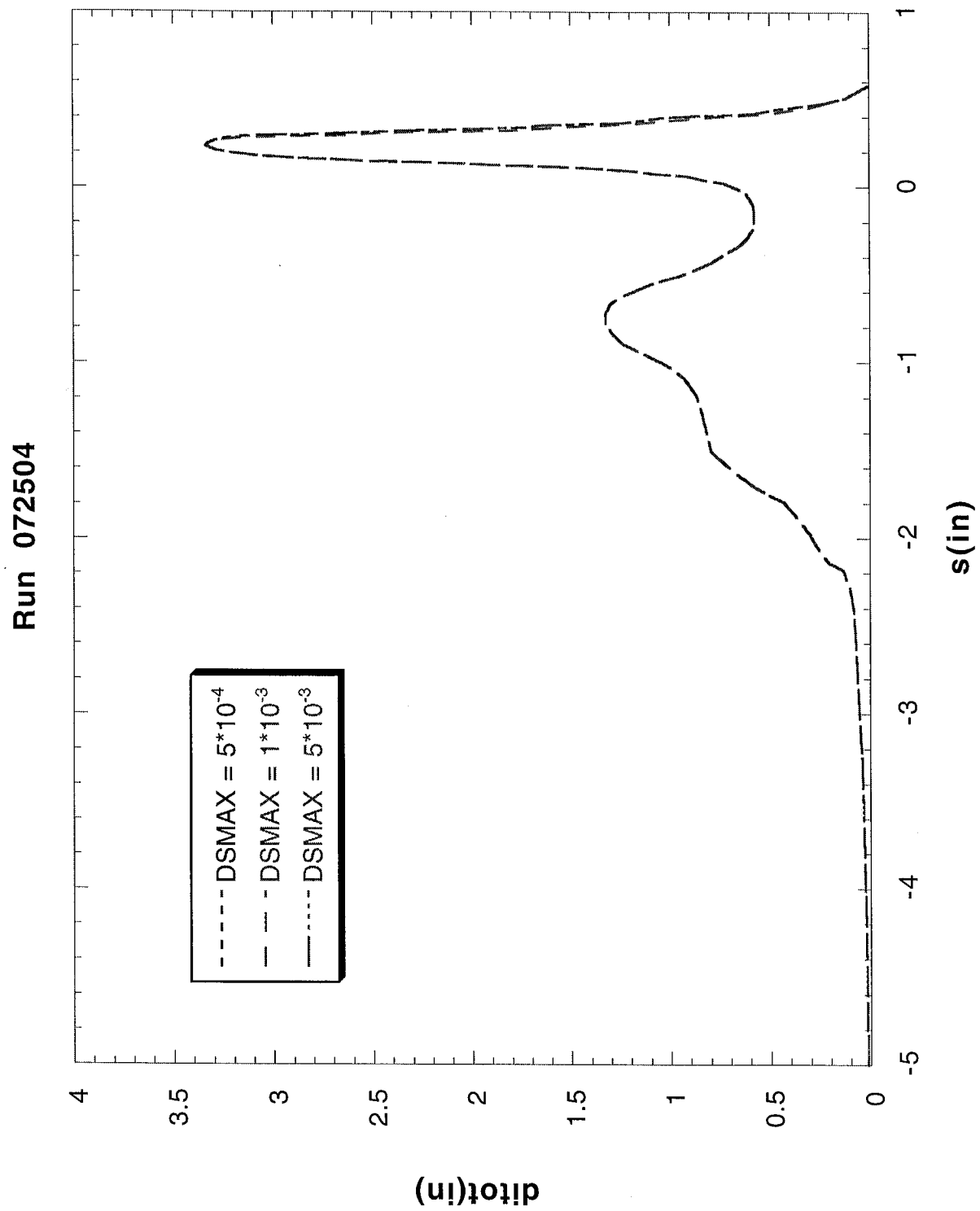
Run 072504
DSMAX = 5*10^-4
DSMAX = 1*10^-3
DSMAX = 5*10^-3
ditot(in)
s(in)
4
3.5
3
2.5
2
1.5
1
0.5
0
1
0
-1
-2
-3
-4
-5

Blanket Smoothing

FIGURE110

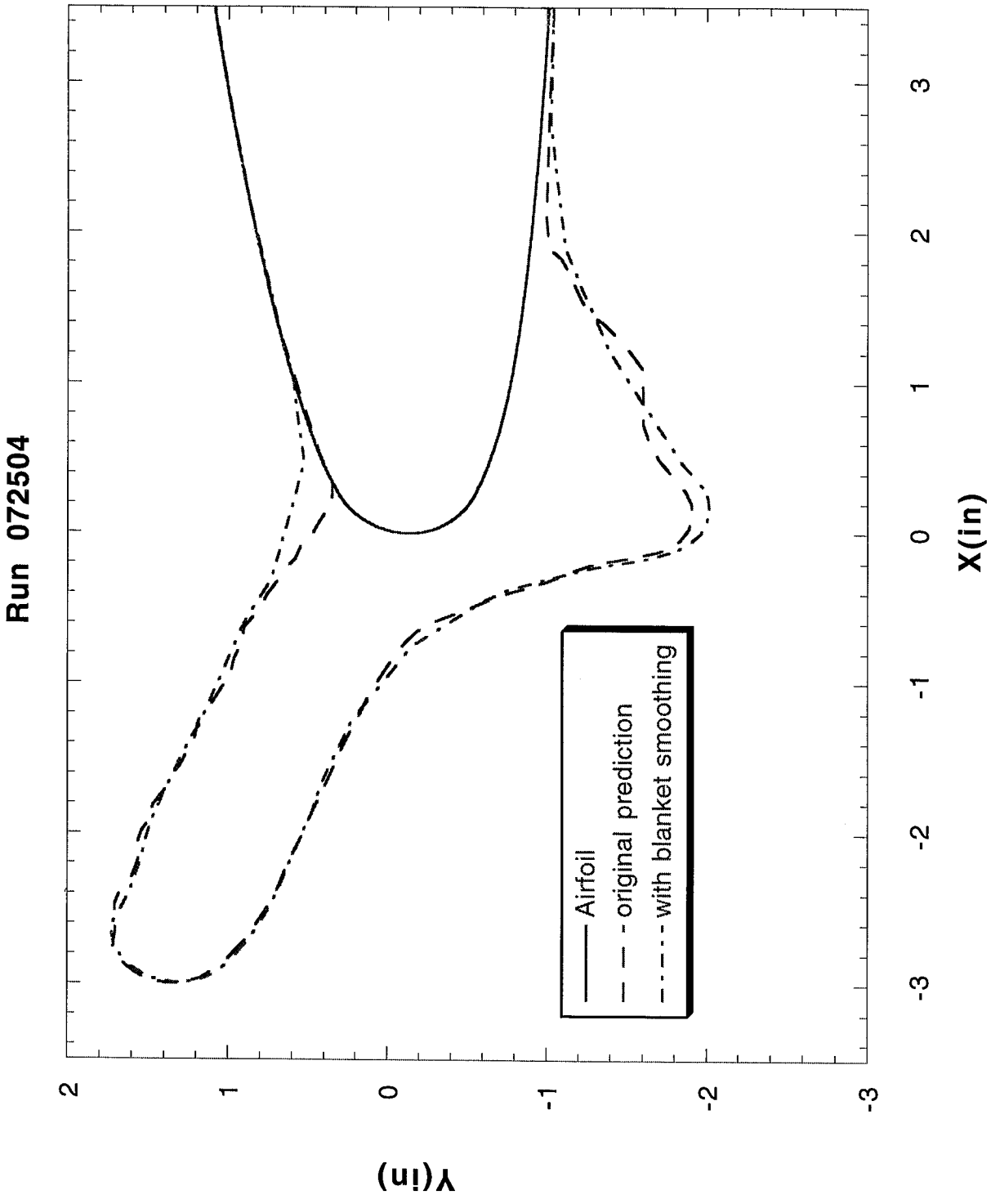
Run 072504
Y(in)
X(in)
2
1
0
-1
-2
-3
3
2
1
0
-1
-2
-3
Airfoil
original prediction
with blanket smoothing

FIGURE 111

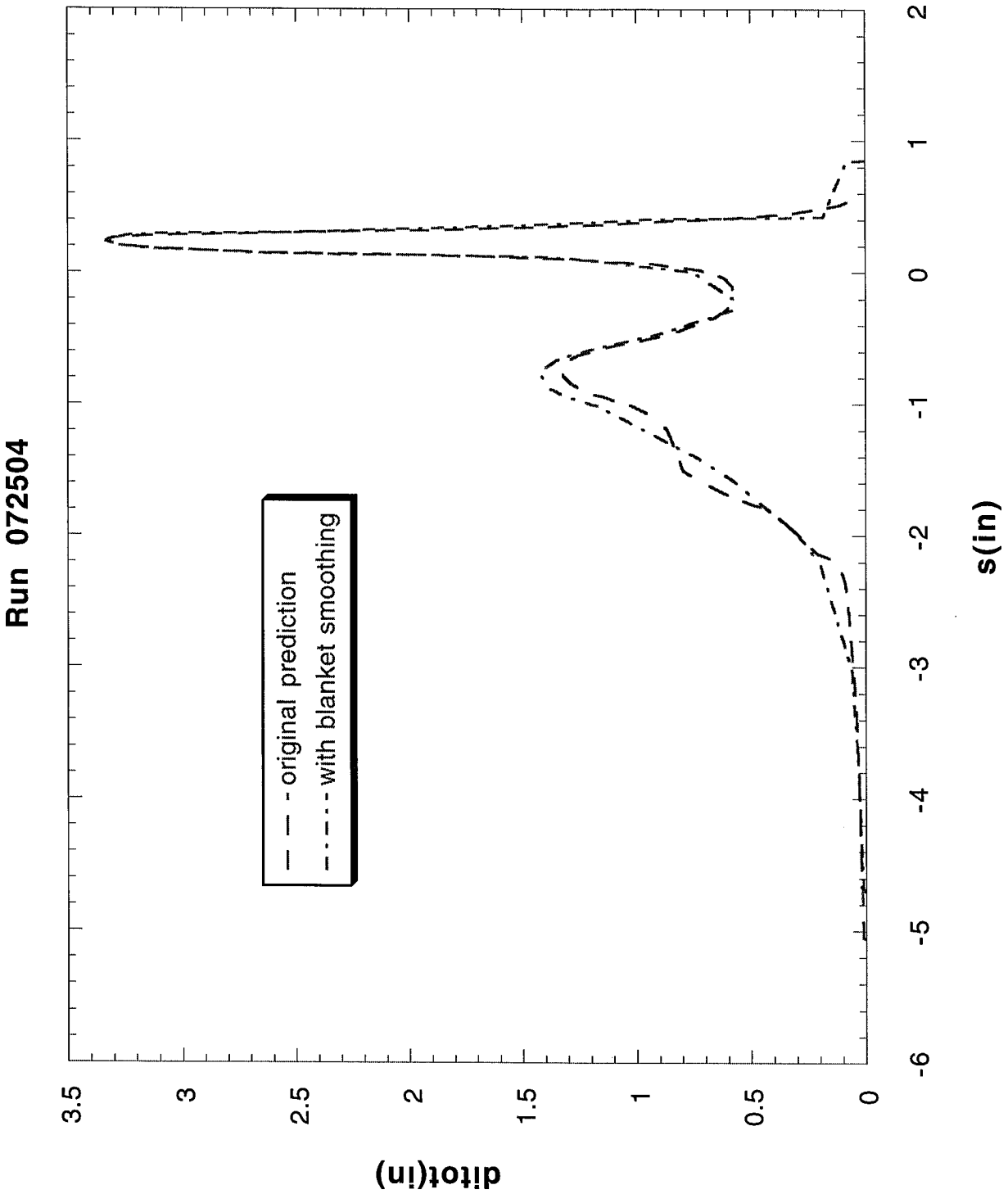
Run 072504
dltot(in)
s(in)
original prediction
with blanket smoothing
3.5
3
2.5
2
1.5
1
0.5
0
2
1
0
-1
-2
-3
-4
-5
-6

FIGURE112

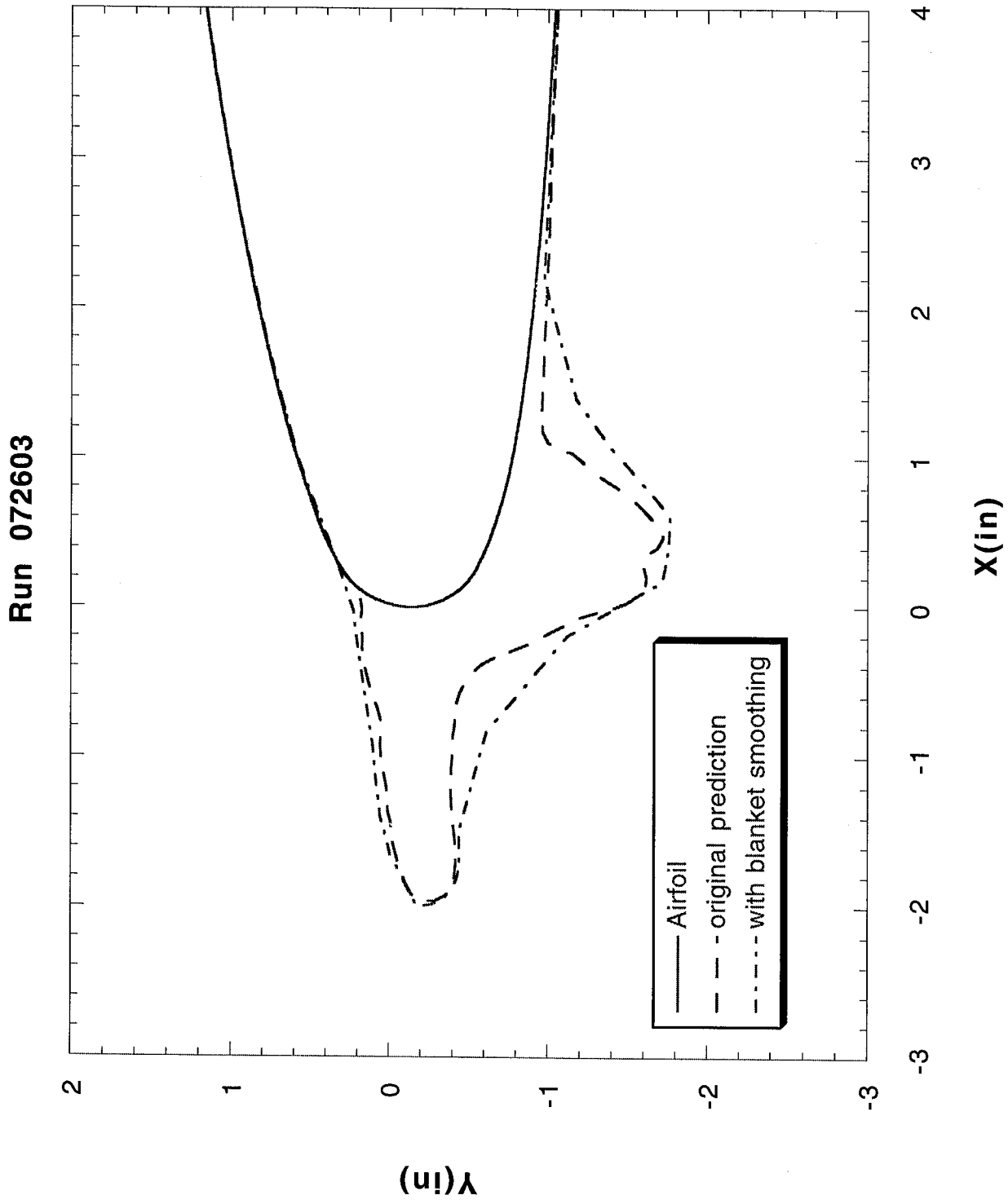
Run 072603
Y(in)
X(in)
2
1
0
-1
-2
-3
4
3
2
1
0
-1
-2
-3
Airfoil
original prediction
with blanket smoothing

FIGURE113

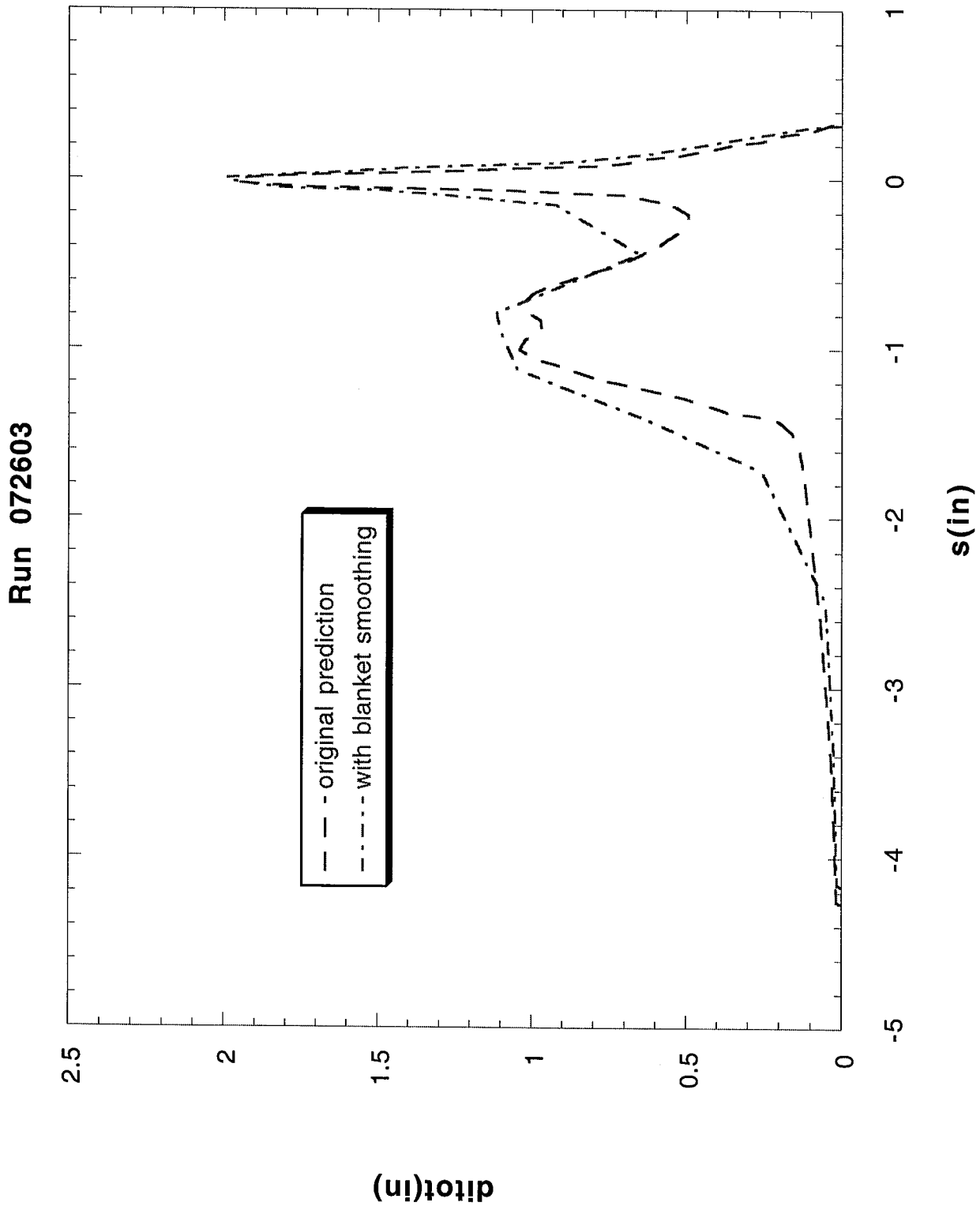
Run 072603
dtot(in)
s(in)
2.5
2
1.5
1
0.5
0
1
0
-1
-2
-3
-4
-5
original prediction
with blanket smoothing

FIGURE 114

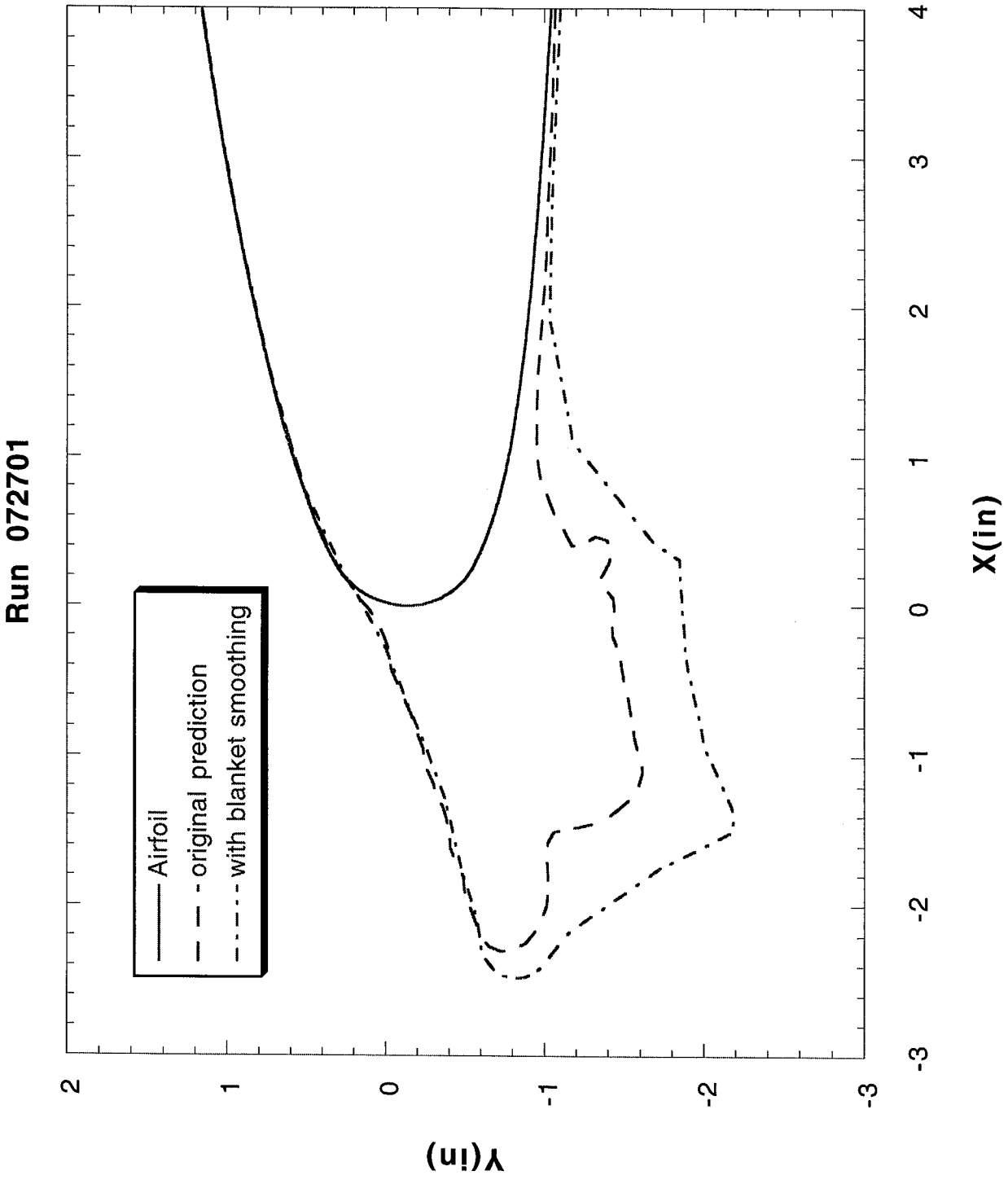
Run 072701
Airfoil
- original prediction
with blanket smoothing
Y(in)
X(in)
2
1
0
-1
-2
-3
4
3
2
1
0
-1
-2
-3

FIGURE115

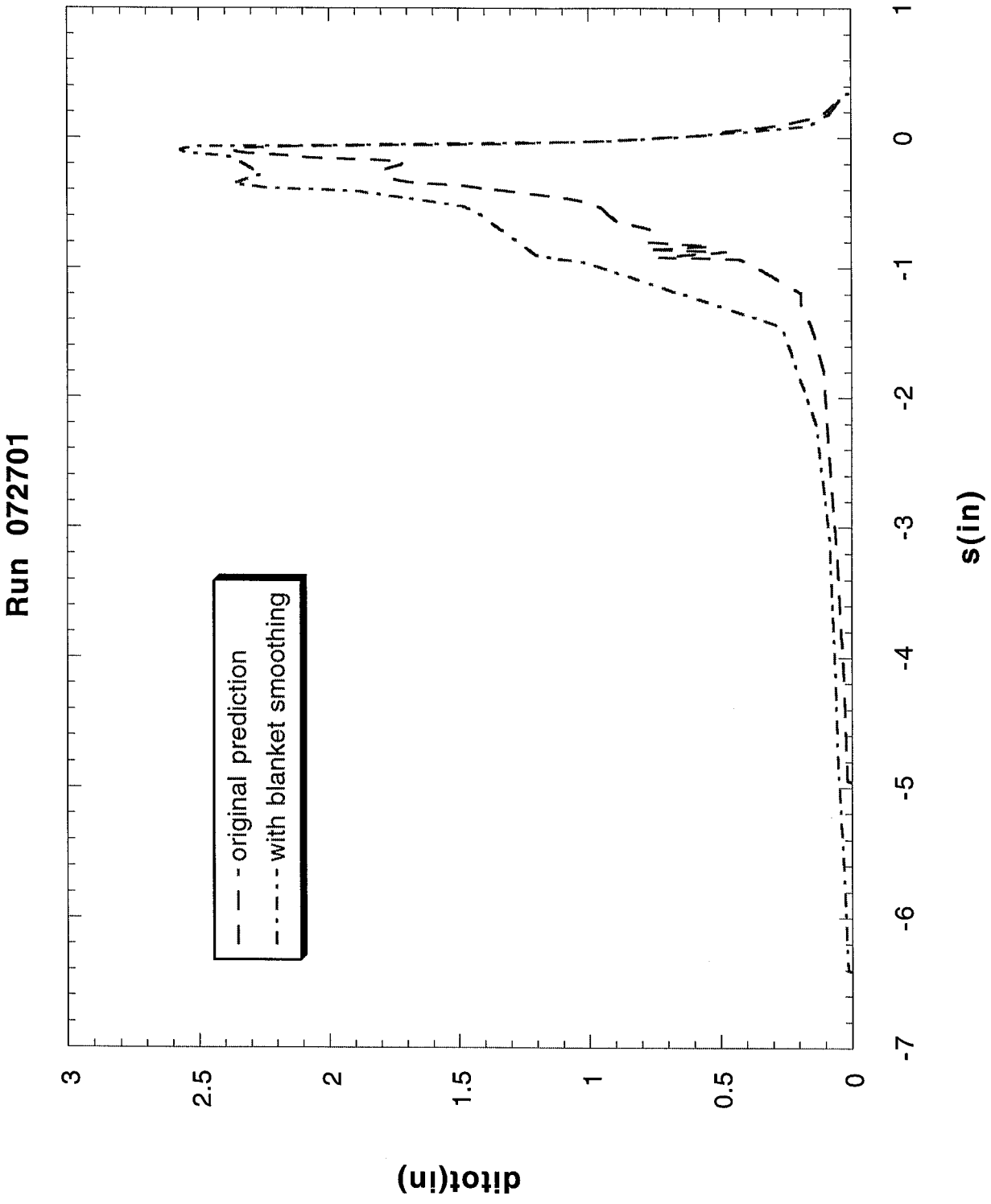
Run 072701
original prediction
with blanket smoothing
ditot(in)
s(in)
3
2.5
2
1.5
1
0.5
0
1
0
-1
-2
-3
-4
-5
-6
-7

FIGURE 116

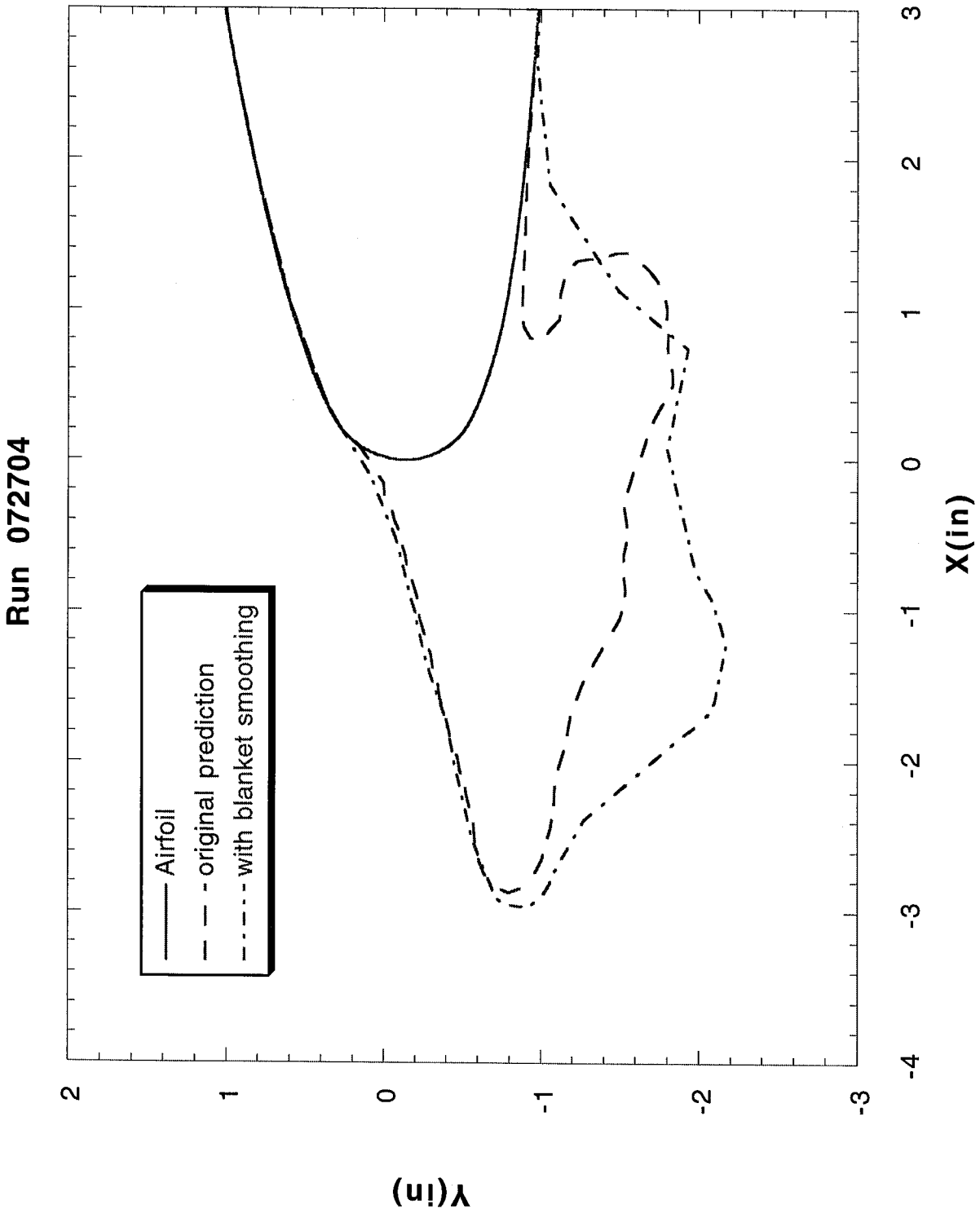
Run 072704
Airfoil
original prediction
with blanket smoothing
Y(in)
X(in)
2
1
0
-1
-2
-3
3
2
1
0
-1
-2
-3
-4

FIGURE 117

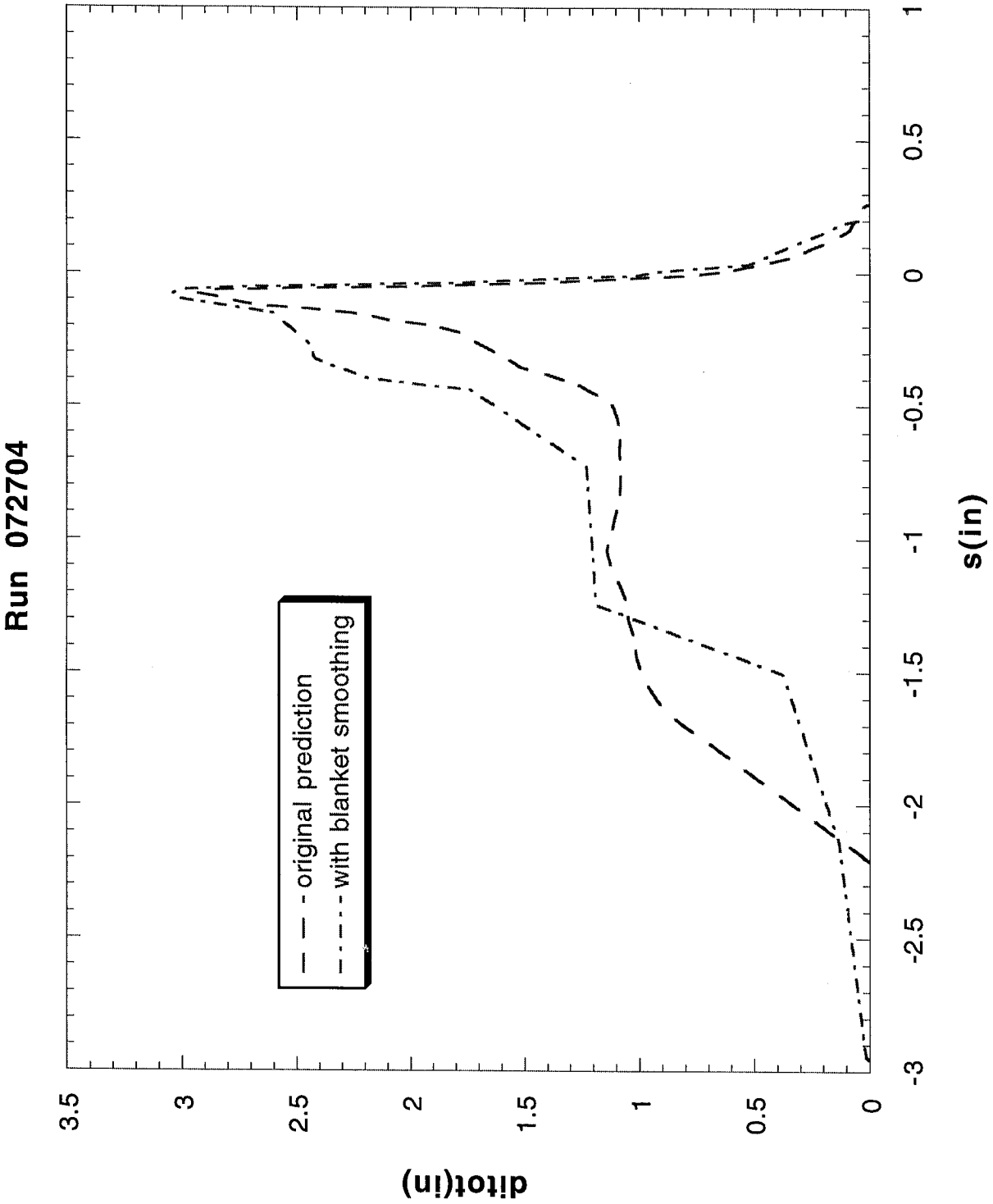
Run 072704
dltot(in)
s(in)
original prediction
with blanket smoothing
3.5
3
2.5
2
1.5
1
0.5
0
-3
-2.5
-2
-1.5
-1
-0.5
0
0.5
1

FIGURE 118

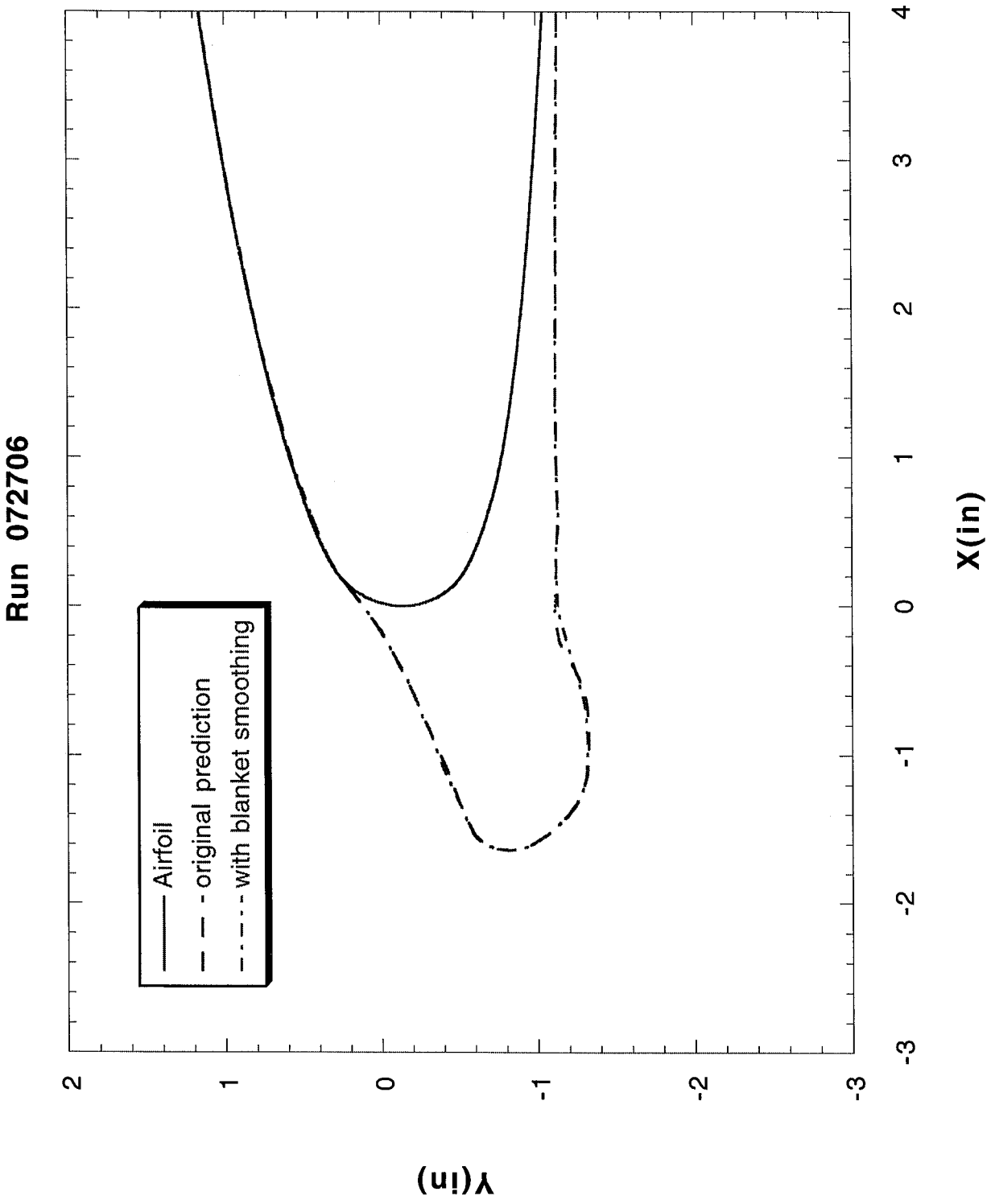
Run 072706
Airfoil
- original prediction
- with blanket smoothing
Y(in)
X(in)
2
1
0
-1
-2
-3
4
3
2
1
0
-1
-2
-3

FIGURE 119

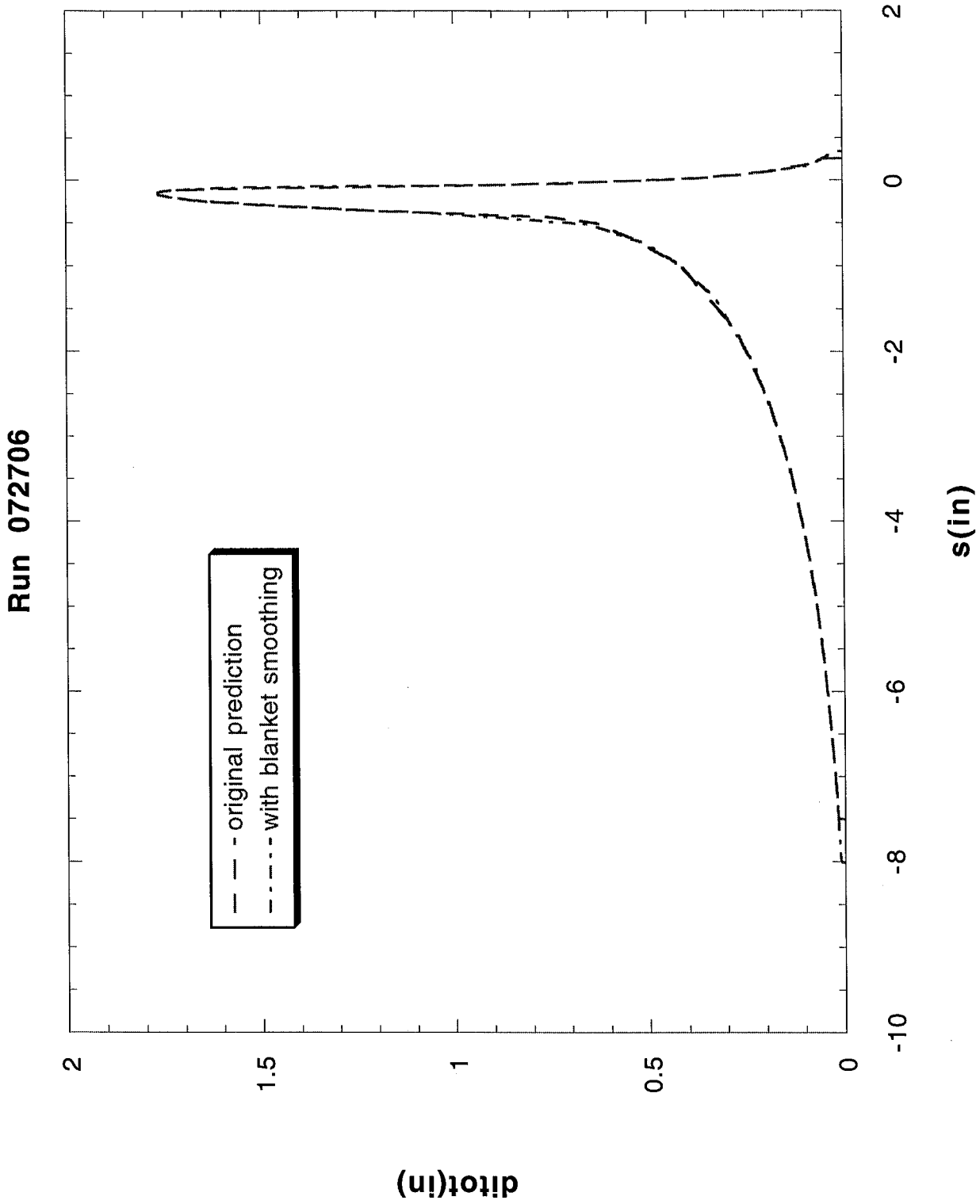
Run 072706
- - original prediction
- - - - with blanket smoothing
dltot(in)
2
1.5
1
0.5
0
s(in)
2
0
-2
-4
-6
-8
-10

FIGURE 120

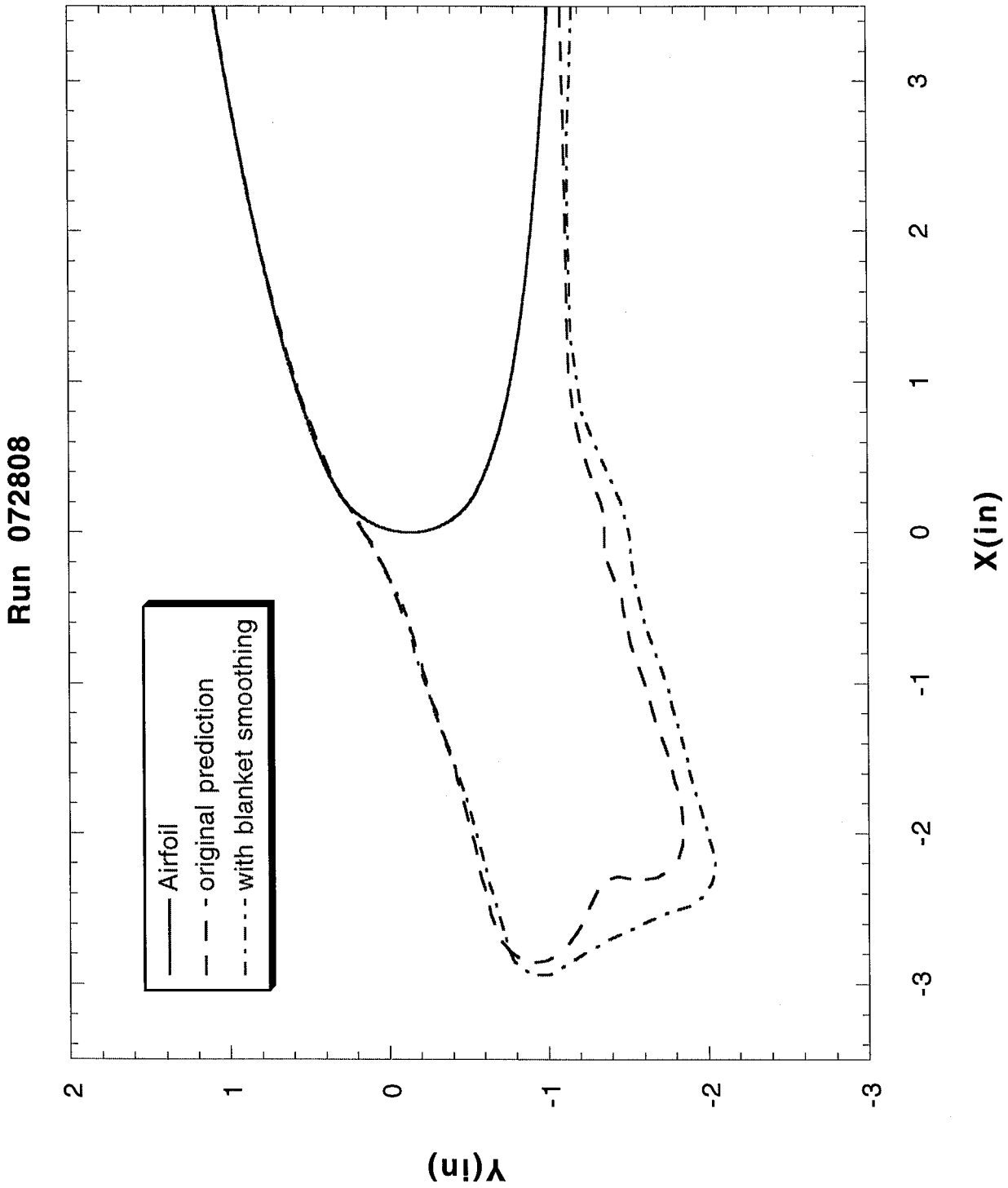
Run 072808
Airfoil
- original prediction
- with blanket smoothing
Y(in)
X(in)
2
1
0
-1
-2
-3
3
2
1
0
-1
-2
-3

FIGURE 121

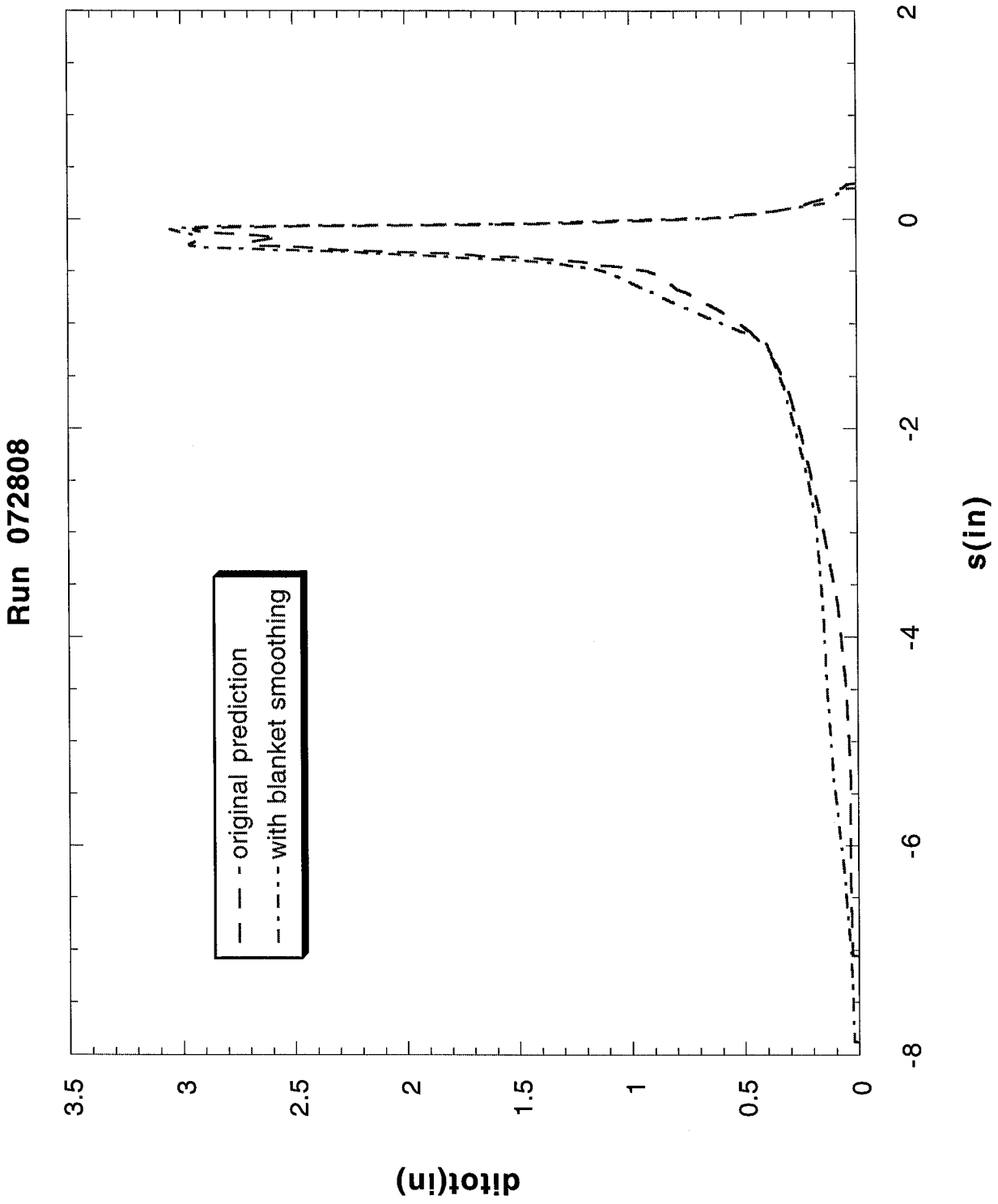
Run 072808
original prediction
with blanket smoothing
ditot(in)
s(in)
3.5
3
2.5
2
1.5
1
0.5
0
2
0
-2
-4
-6
-8

Case Study

FIGURE 122

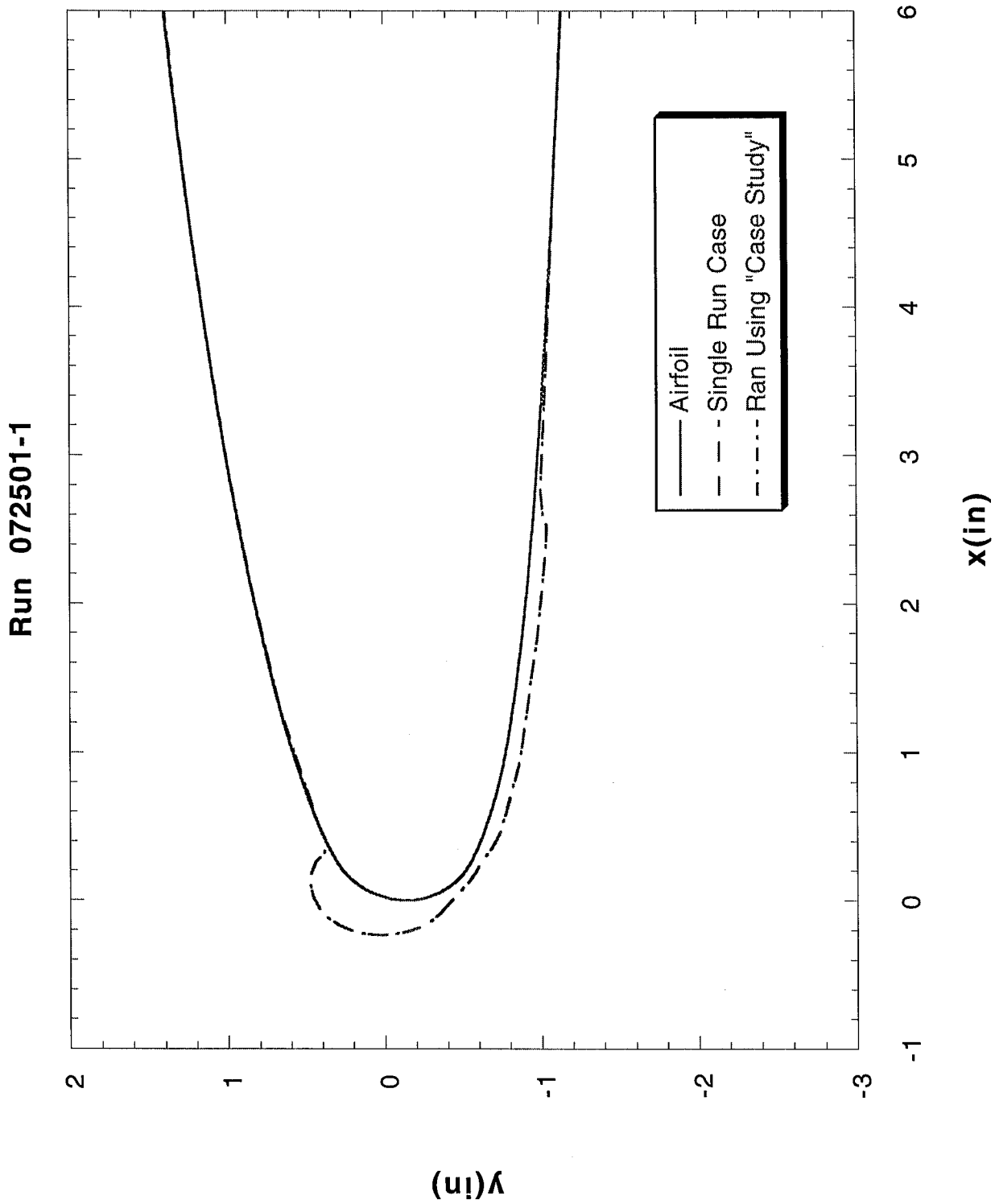
Run 072501-1
Airfoil
Single Run Case
Ran Using "Case Study"
y(in)
x(in)
2
1
0
-1
-2
-3
-1
0
1
2
3
4
5
6

FIGURE 123

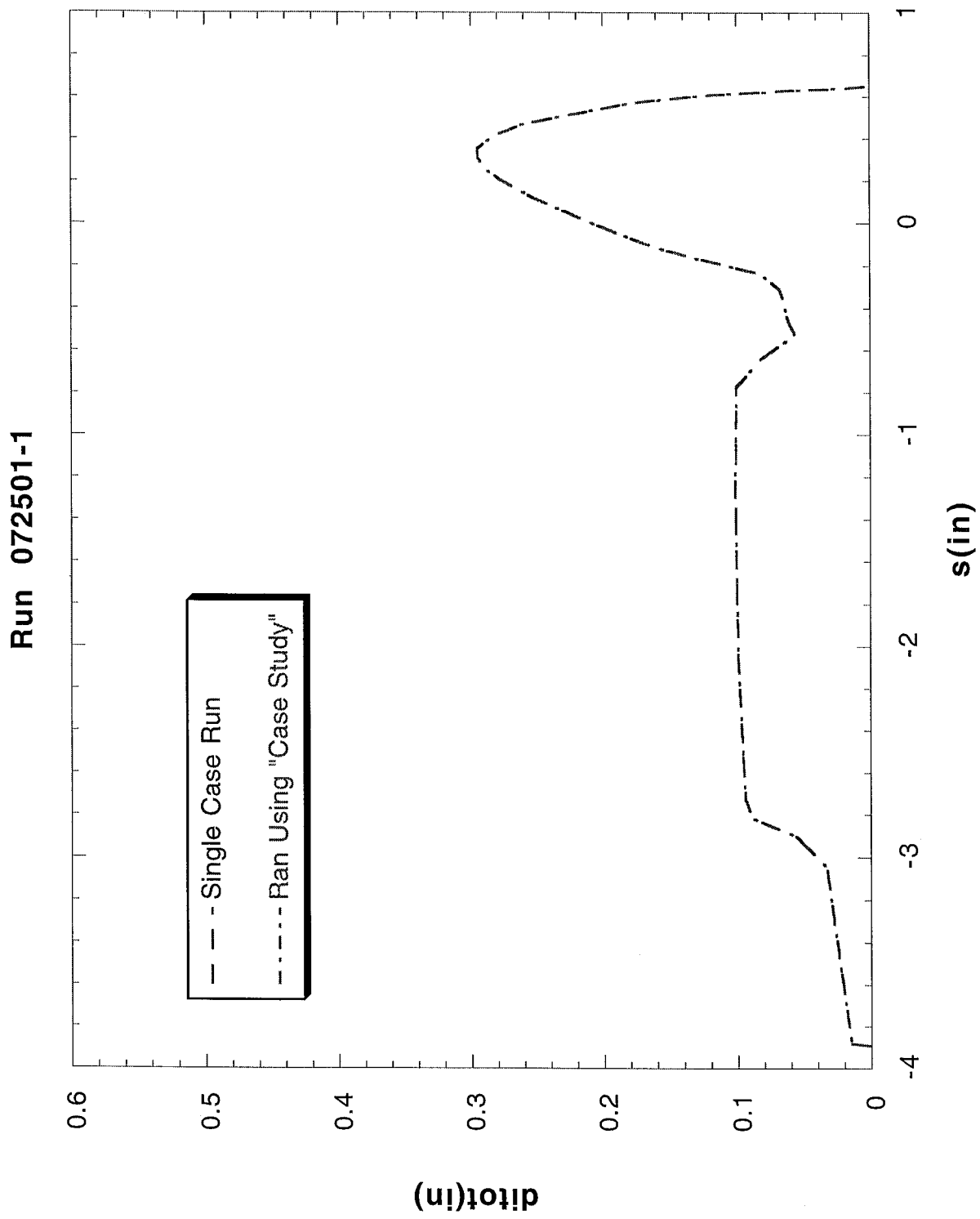
Run 072501-1
Single Case Run
Ran Using "Case Study"
dltot(in)
s(in)
0.6
0.5
0.4
0.3
0.2
0.1
0
-4
-3
-2
-1
0
1

FIGURE 124

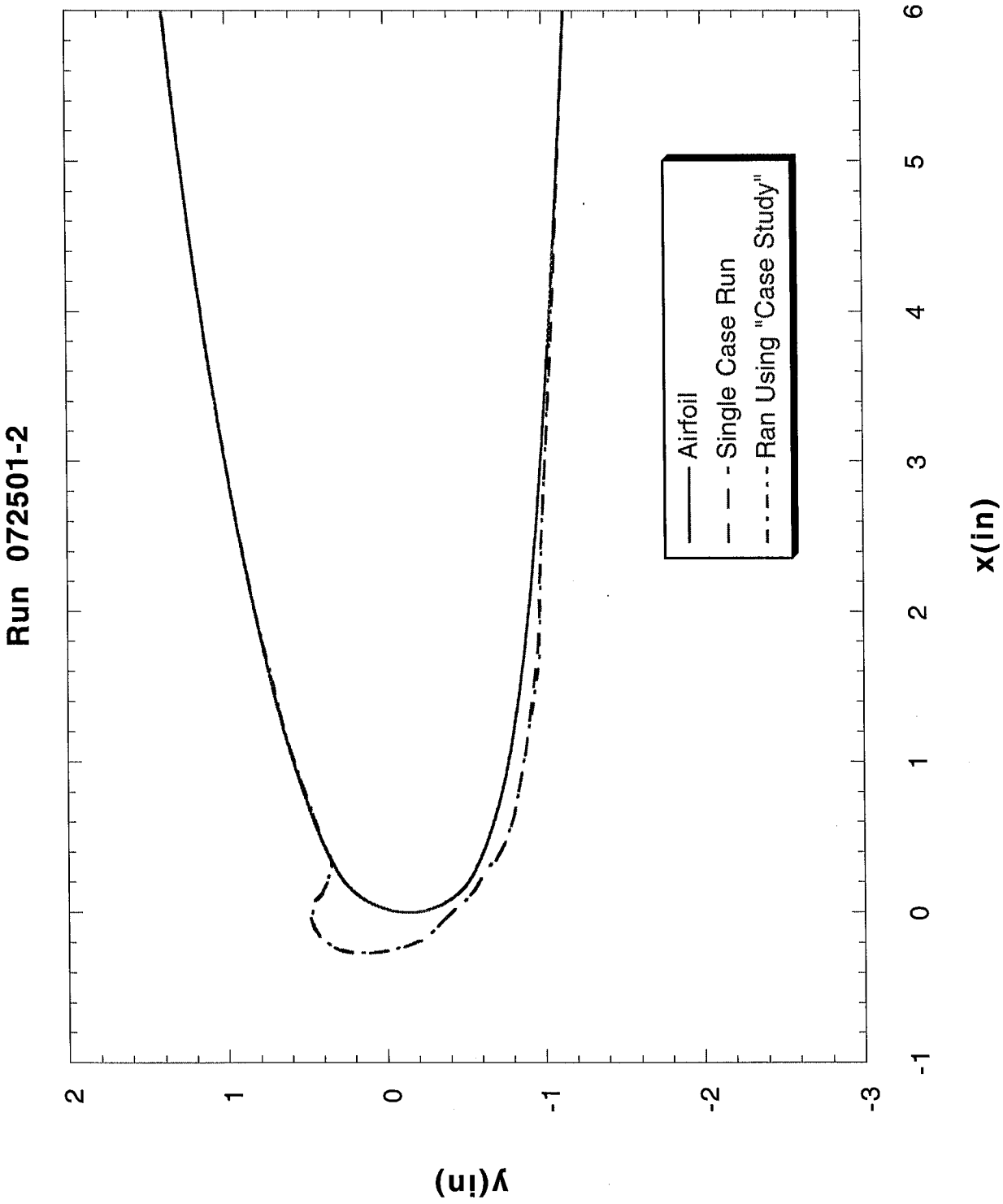
Run 072501-2
Airfoil
- Single Case Run
- Ran Using "Case Study"
y(in)
x(in)
2
1
0
-1
-2
-3
-1
0
1
2
3
4
5
6

FIGURE 125

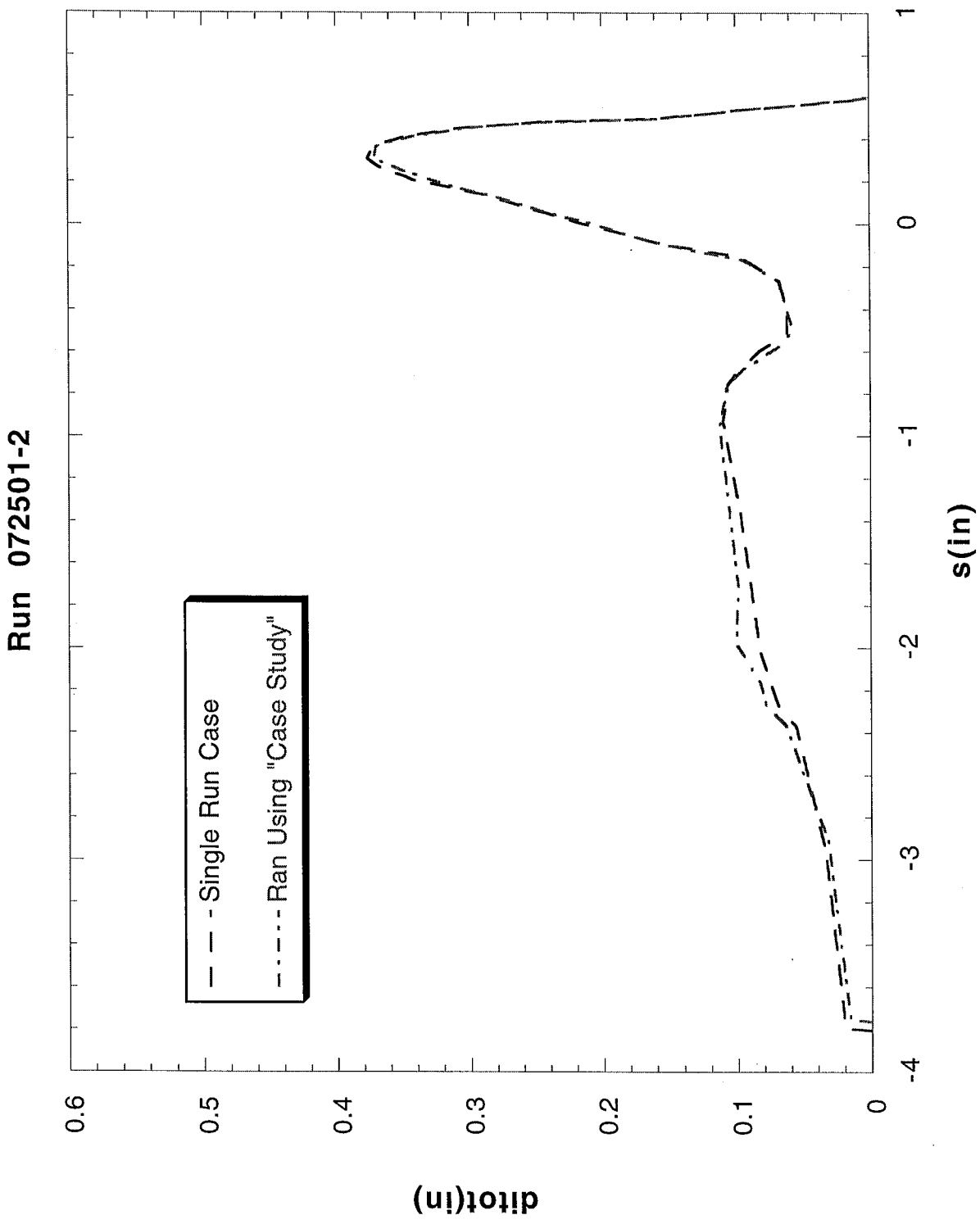
Run 072501-2
dltot(in)
s(in)
0.6
0.5
0.4
0.3
0.2
0.1
0
-4
-3
-2
-1
0
1
- - - Single Run Case
- - - - Ran Using "Case Study"

FIGURE 126

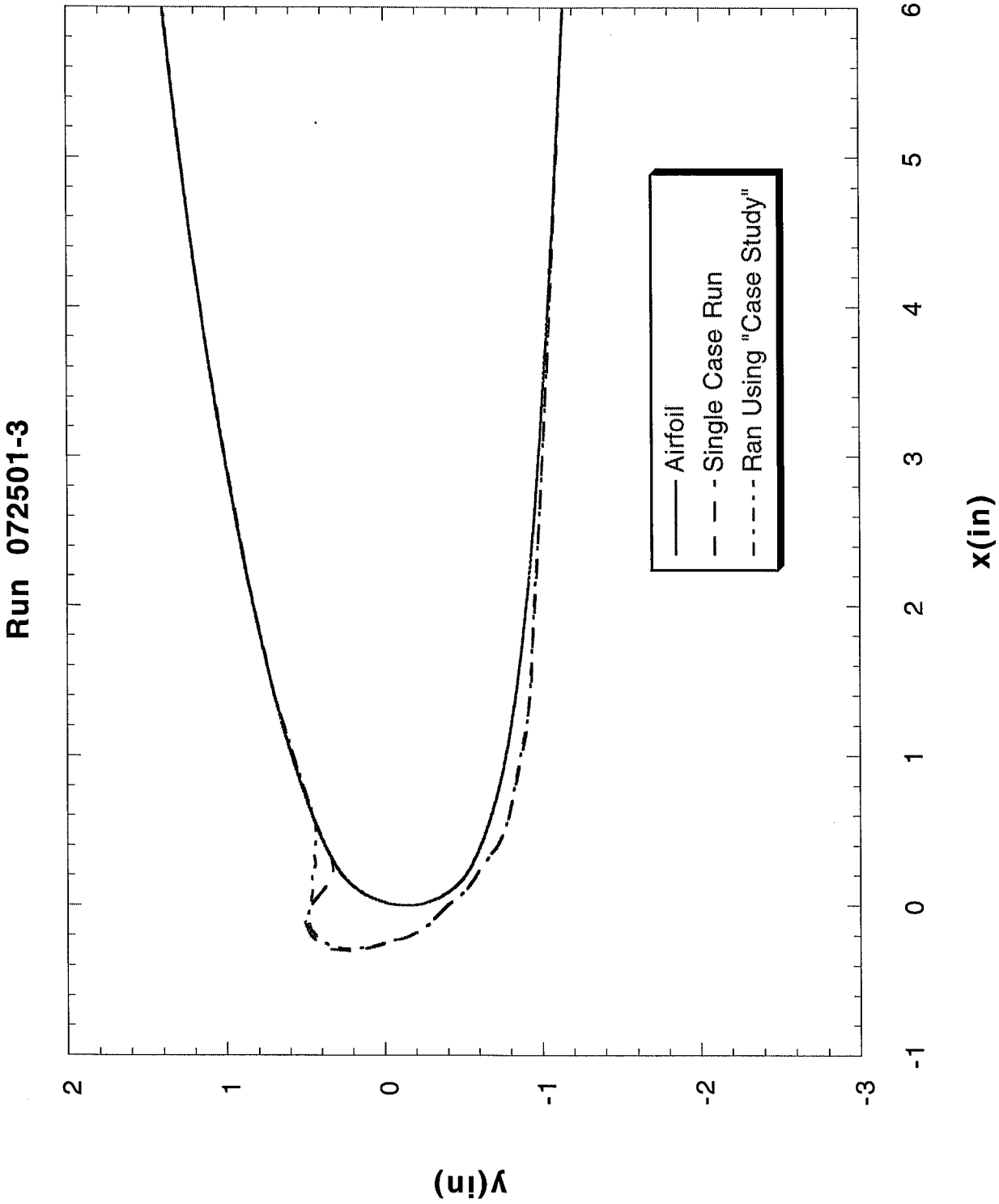
Run 072501-3
Airfoil
Single Case Run
Ran Using "Case Study"
y(in)
x(in)
2
1
0
-1
-2
-3
-1
0
1
2
3
4
5
6

FIGURE 127

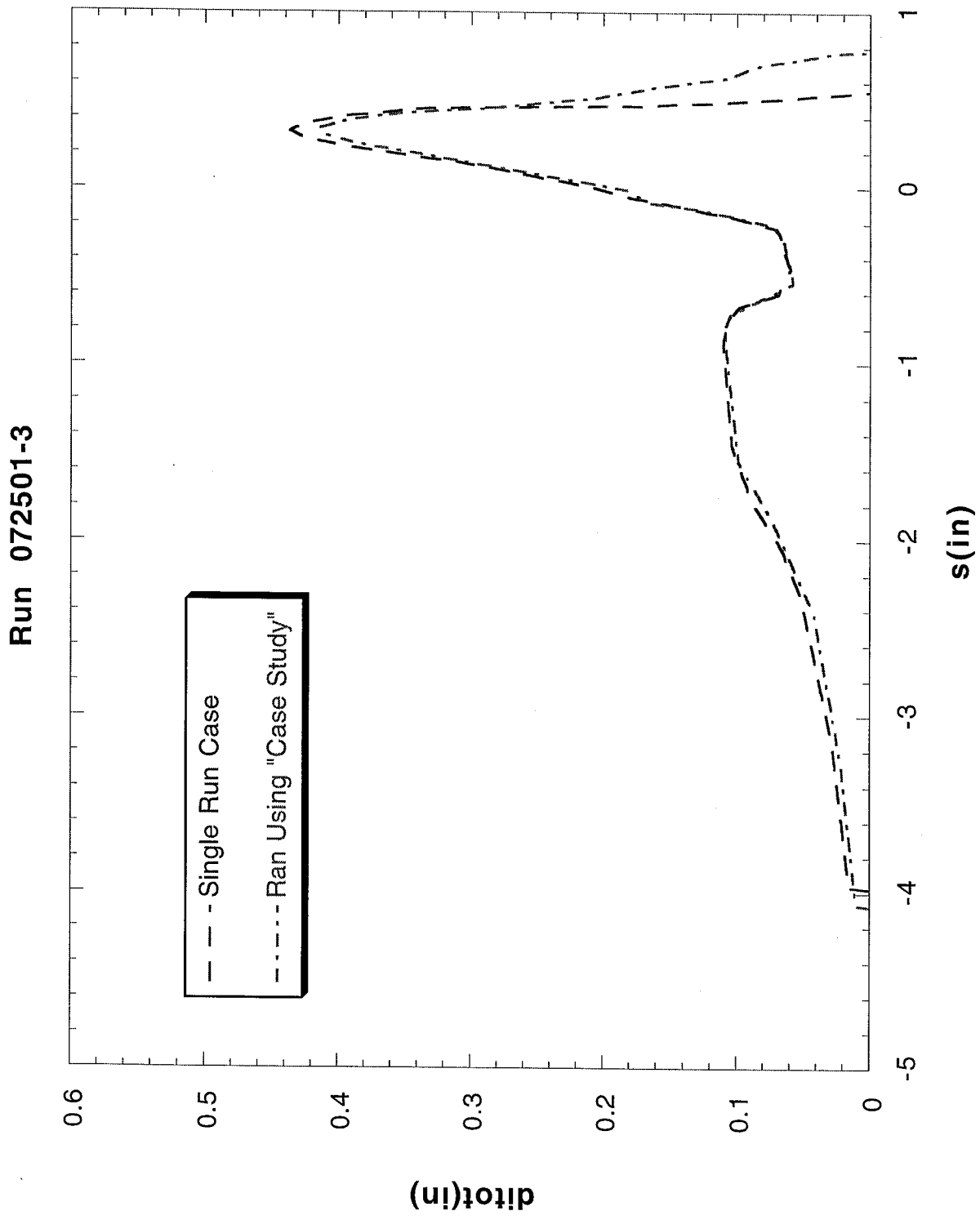
Run 072501-3
Single Run Case
Ran Using "Case Study"
ditot(in)
s(in)
0.6
0.5
0.4
0.3
0.2
0.1
0
1
0
-1
-2
-3
-4
-5

FIGURE 128

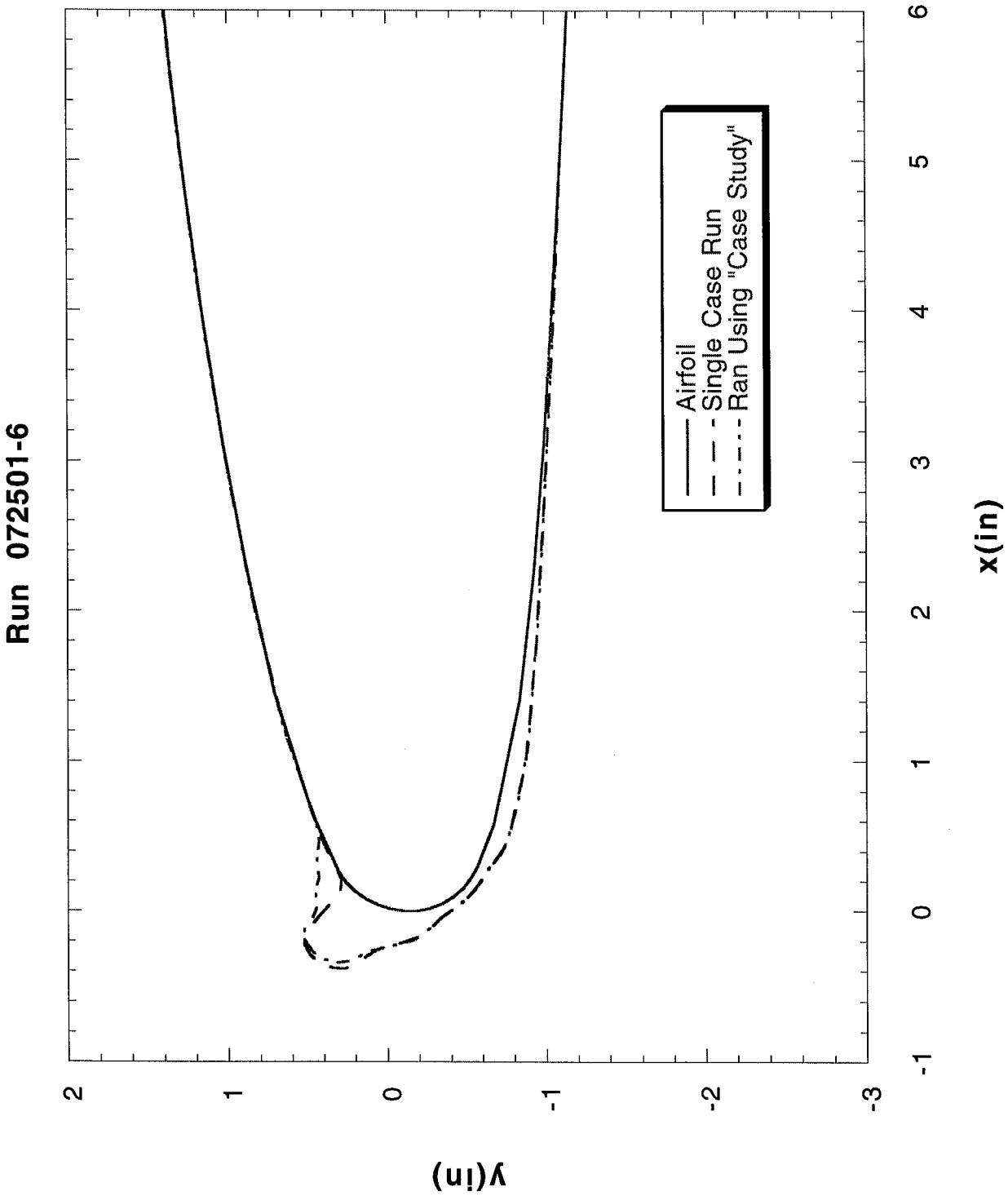
Run 072501-6
Airfoil
Single Case Run
Ran Using "Case Study"
y(in)
x(in)
2
1
0
-1
-2
-3
-1
0
1
2
3
4
5
6

FIGURE 129

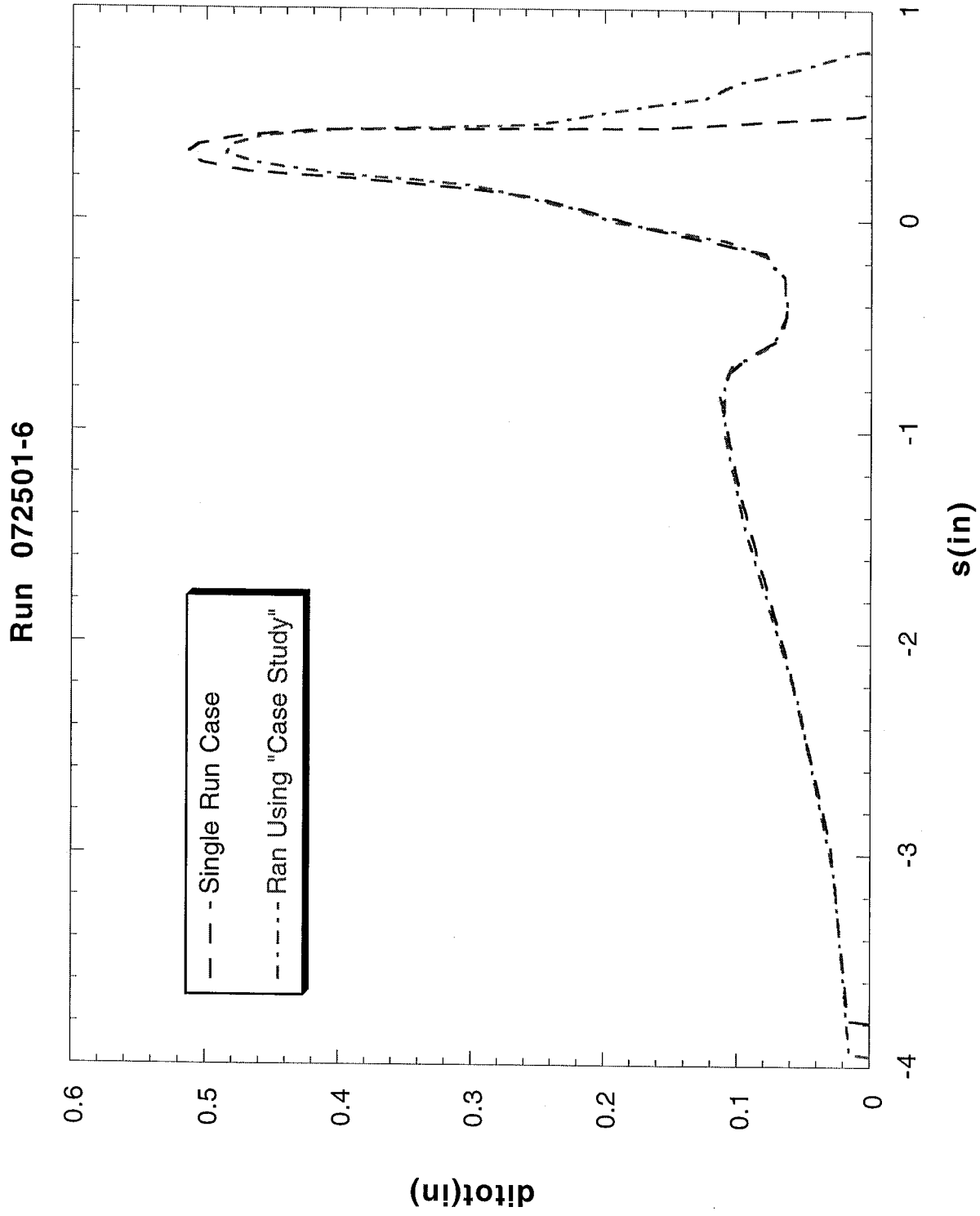
Run 072501-6
dltot(in)
s(in)
0.6
0.5
0.4
0.3
0.2
0.1
0
-4
-3
-2
-1
0
1
- - - Single Run Case
- · - · - Ran Using "Case Study"

Compiler Effects

FIGURE 130

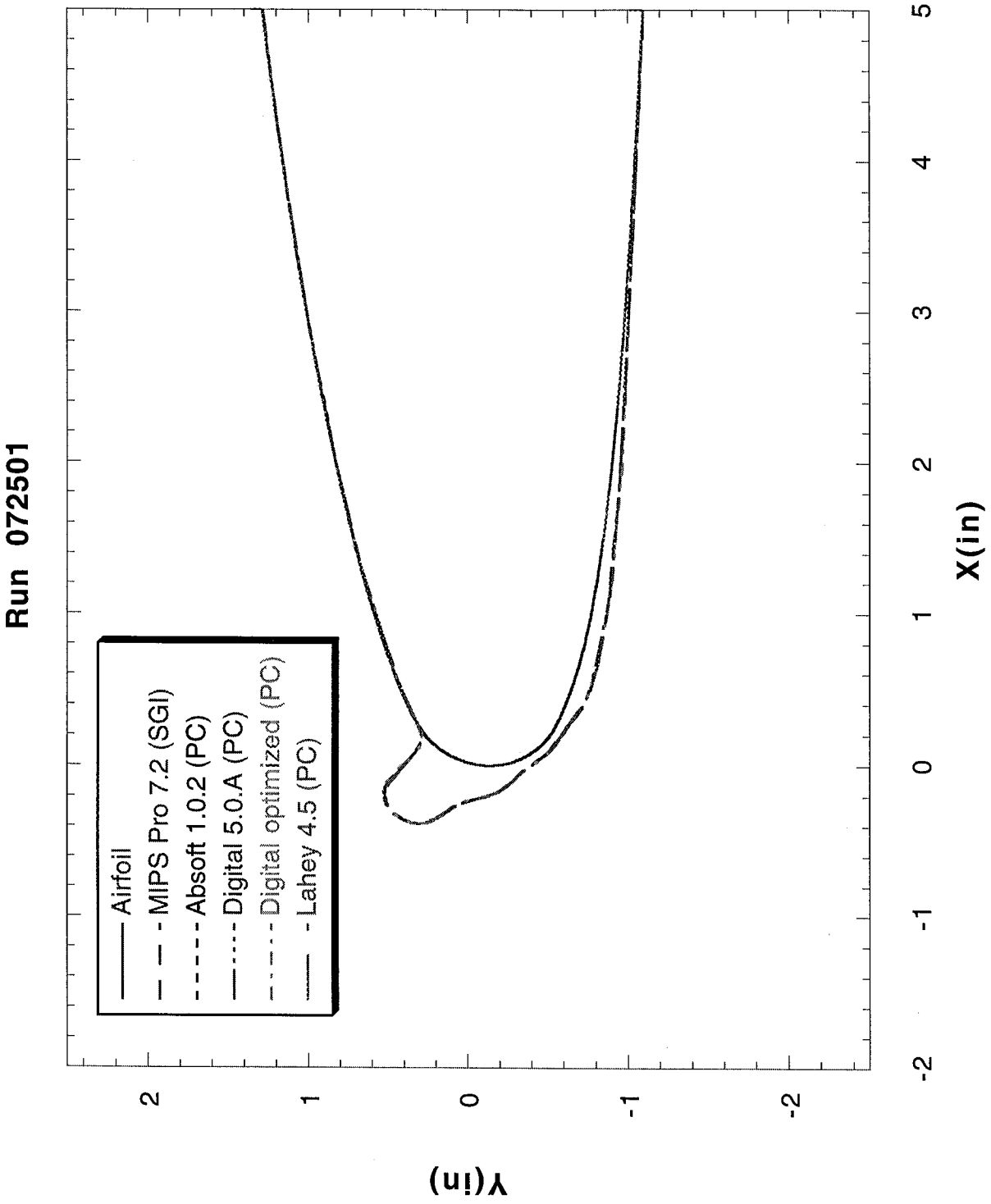
Run 072501
Airfoil
- MIPS Pro 7.2 (SGI)
- Absoft 1.0.2 (PC)
Digital 5.0.A (PC)
Digital optimized (PC)
- Lahey 4.5 (PC)
Y(in)
X(in)
2
1
0
-1
-2
5
4
3
2
1
0
-1
-2

FIGURE 131

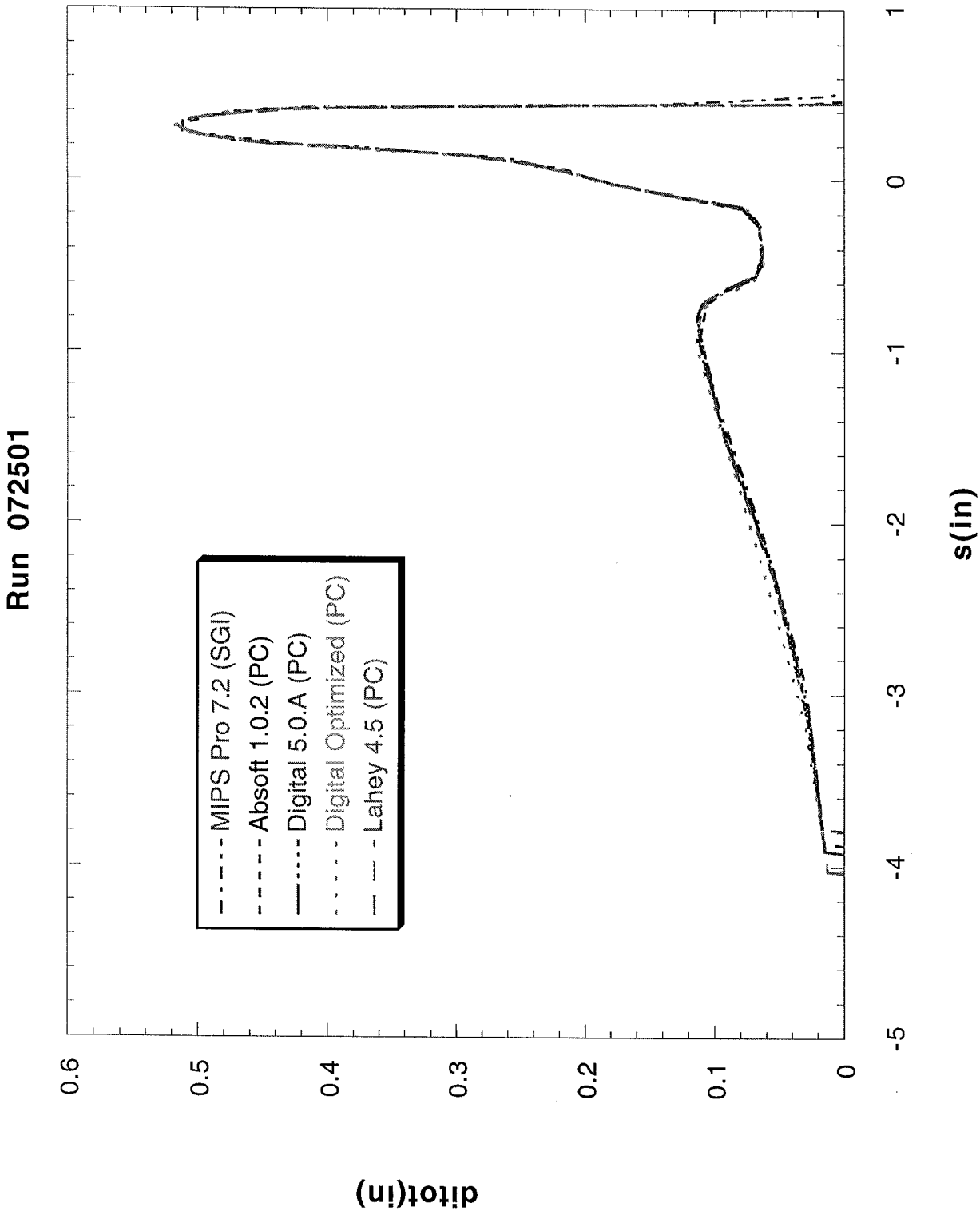
Run 072501
MIPS Pro 7.2 (SGI)
Absoft 1.0.2 (PC)
Digital 5.0.A (PC)
Digital Optimized (PC)
Lahey 4.5 (PC)
ditot(in)
0.6
0.5
0.4
0.3
0.2
0.1
0
s(in)
1
0
-1
-2
-3
-4
-5

FIGURE 132

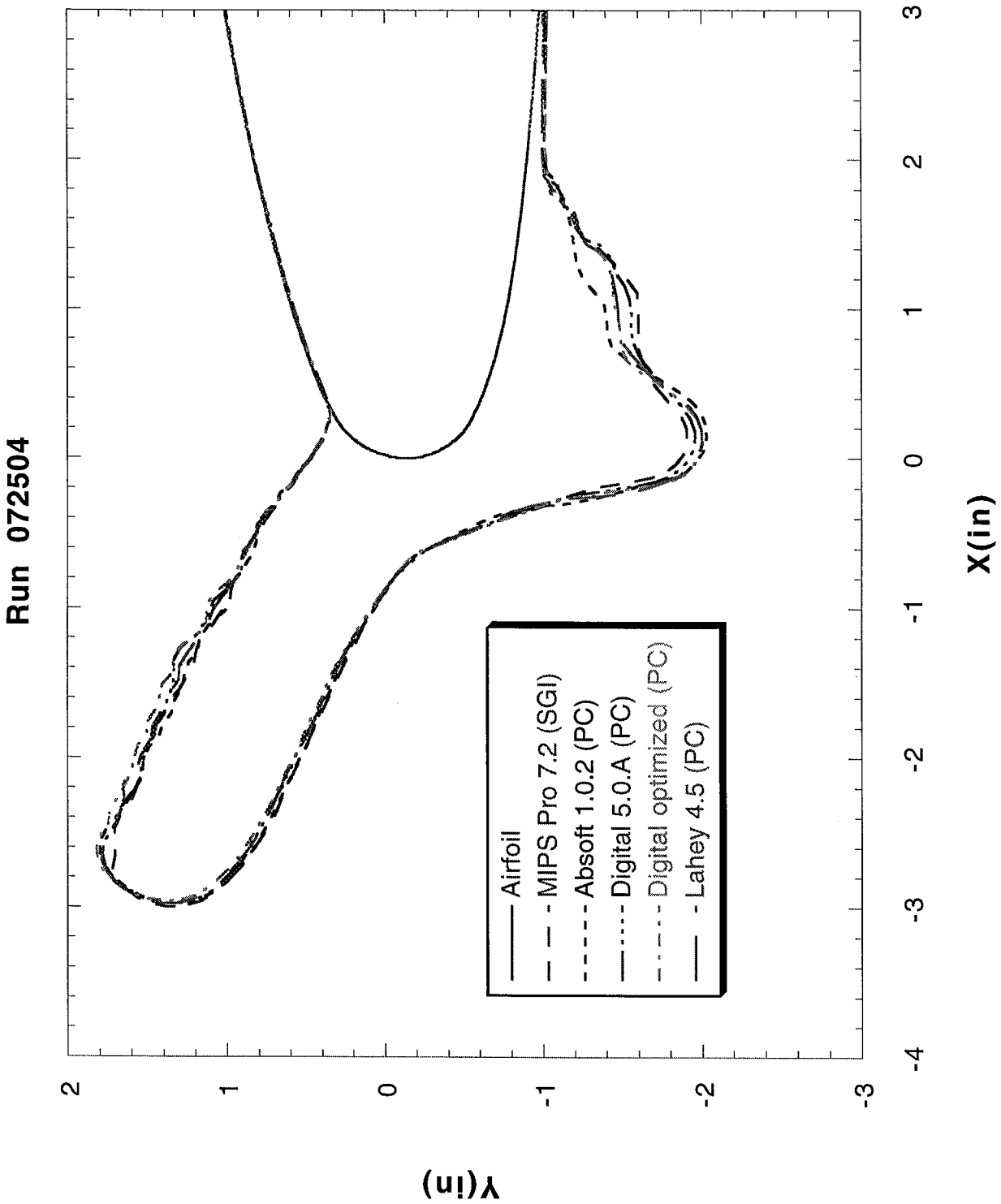
Run 072504
Y(in)
X(in)
2
1
0
-1
-2
-3
3
2
1
0
-1
-2
-3
-4
Airfoil
- MIPS Pro 7.2 (SGI)
- Absoft 1.0.2 (PC)
- Digital 5.0.A (PC)
- Digital optimized (PC)
- Lahey 4.5 (PC)

FIGURE 133

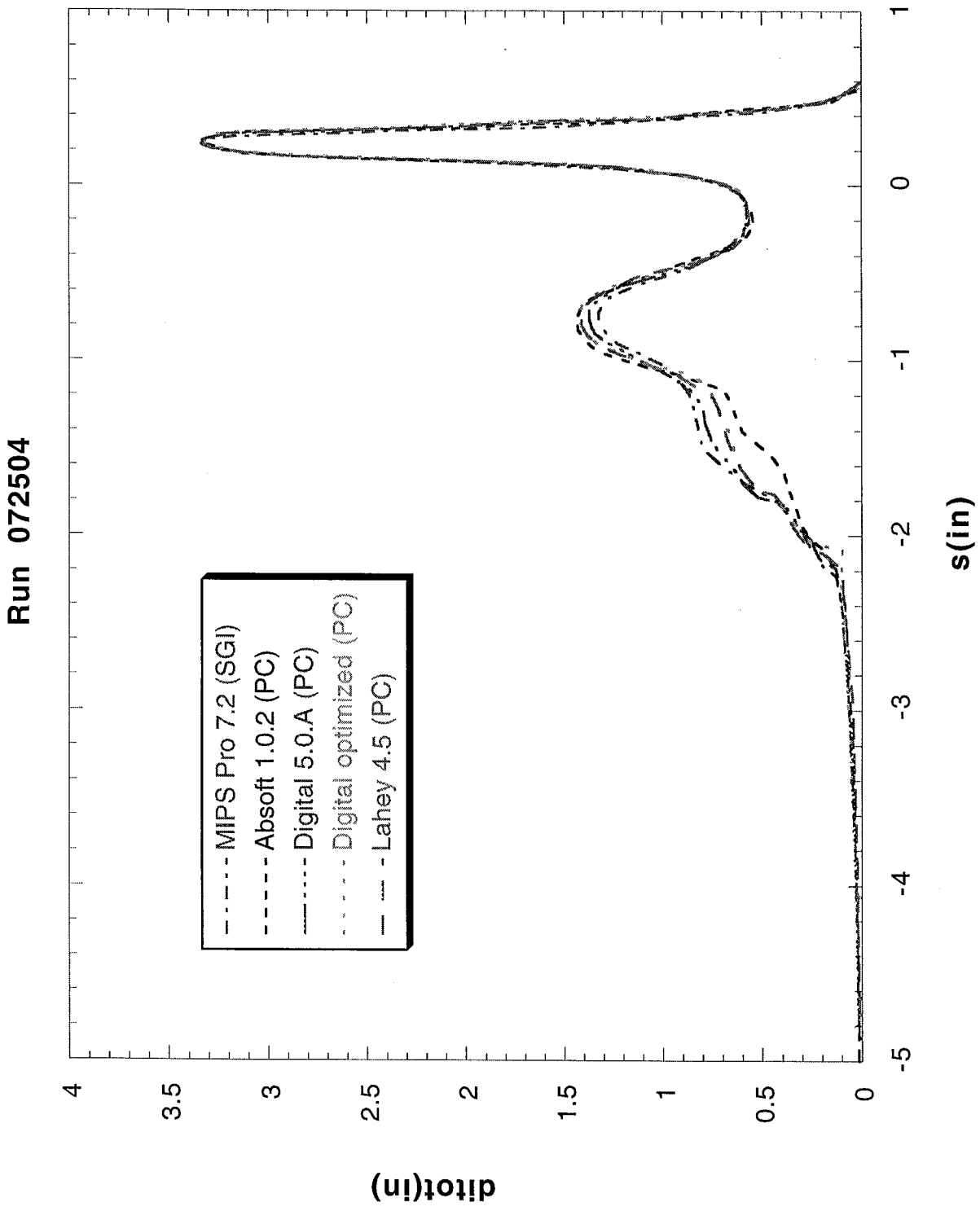
Run 072504
MIPS Pro 7.2 (SGI)
Absoft 1.0.2 (PC)
Digital 5.0.A (PC)
Digital optimized (PC)
Lahey 4.5 (PC)
ditot(in)
s(in)
4
3.5
3
2.5
2
1.5
1
0.5
0
1
0
-1
-2
-3
-4
-5

FIGURE 134

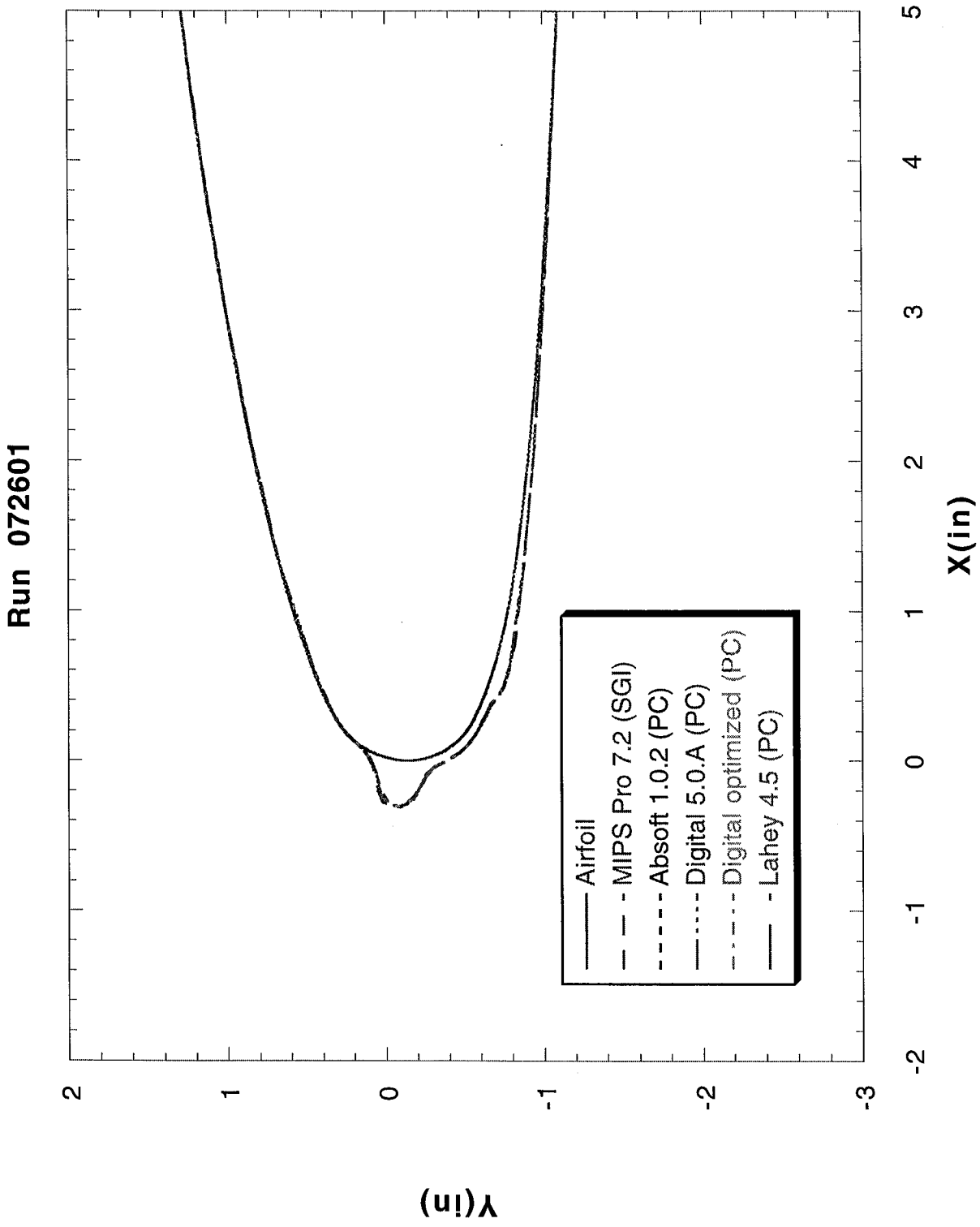
Run 072601
Y(in)
X(in)
2
1
0
-1
-2
-3
5
4
3
2
1
0
-1
-2
Airfoil
MIPS Pro 7.2 (SGI)
Absoft 1.0.2 (PC)
Digital 5.0.A (PC)
Digital optimized (PC)
Lahey 4.5 (PC)

FIGURE 135

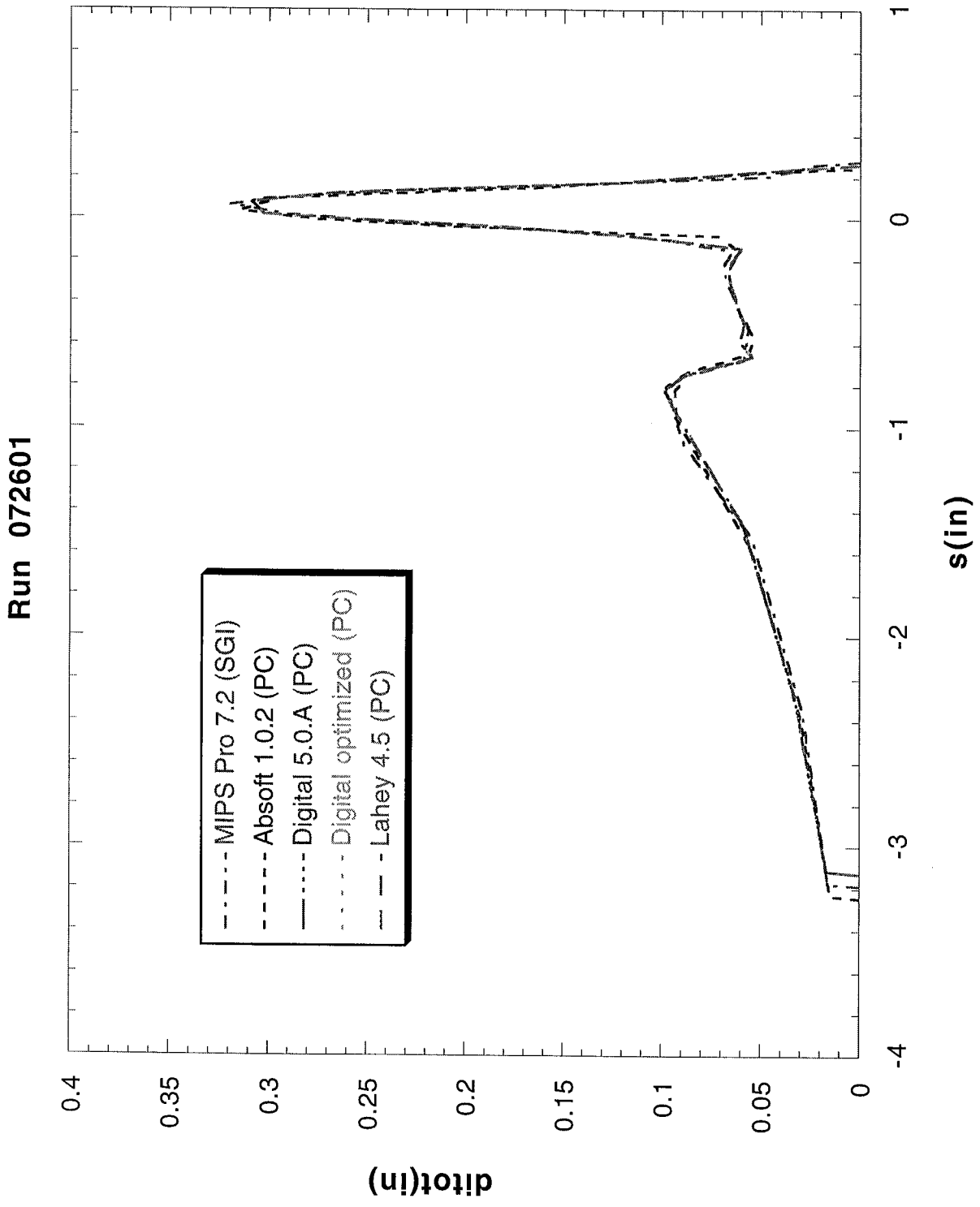
Run 072601
MIPS Pro 7.2 (SGI)
Absoft 1.0.2 (PC)
Digital 5.0.A (PC)
Digital optimized (PC)
Lahey 4.5 (PC)
ditot(in)
0.4
0.35
0.3
0.25
0.2
0.15
0.1
0.05
0
s(in)
1
0
-1
-2
-3
-4

FIGURE 136

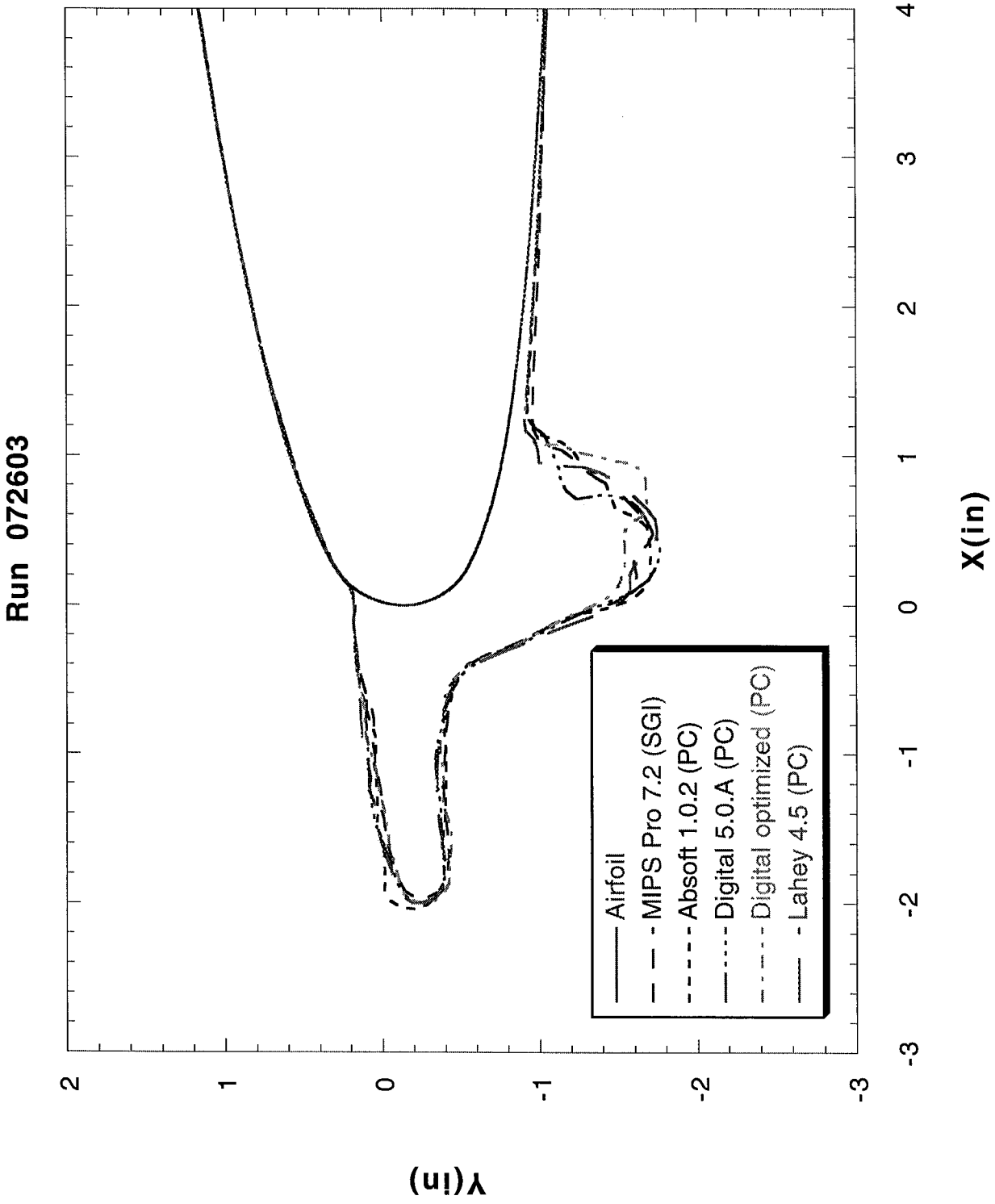
Run 072603
Y(in)
X(in)
2
1
0
-1
-2
-3
4
3
2
1
0
-1
-2
-3
Airfoil
- MIPS Pro 7.2 (SGI)
Absoft 1.0.2 (PC)
Digital 5.0.A (PC)
Digital optimized (PC)
- Lahey 4.5 (PC)

FIGURE 137

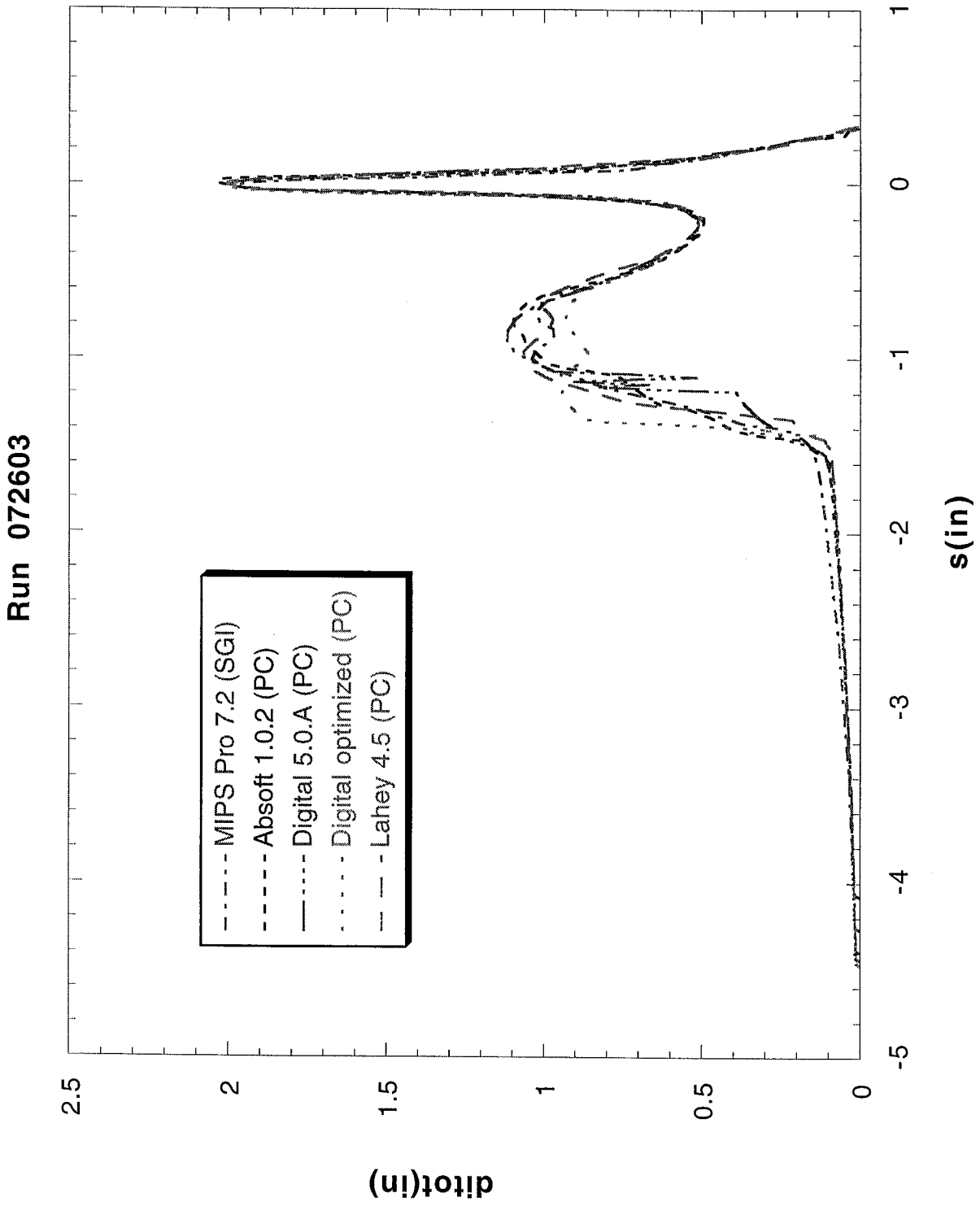
Run 072603
MIPS Pro 7.2 (SGI)
Absoft 1.0.2 (PC)
Digital 5.0.A (PC)
Digital optimized (PC)
Lahey 4.5 (PC)
ditot(in)
2.5
2
1.5
1
0.5
0
-5
-4
-3
-2
-1
0
1
s(in)

FIGURE 138

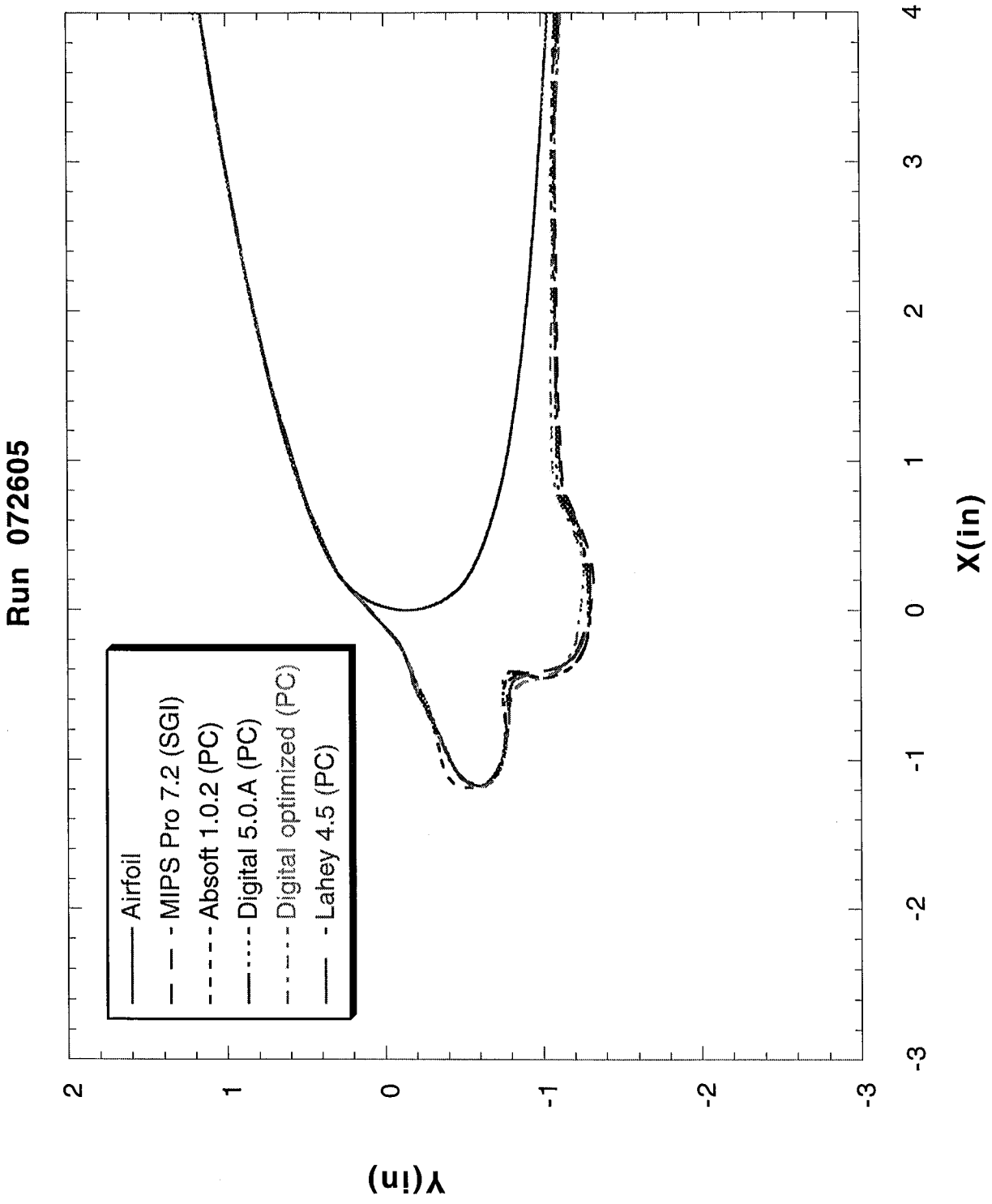
Run 072605
Airfoil
- MIPS Pro 7.2 (SGI)
- Absoft 1.0.2 (PC)
- Digital 5.0.A (PC)
- Digital optimized (PC)
- Lahey 4.5 (PC)
Y(in)
X(in)
2
1
0
-1
-2
-3
4
3
2
1
0
-1
-2
-3

FIGURE 139

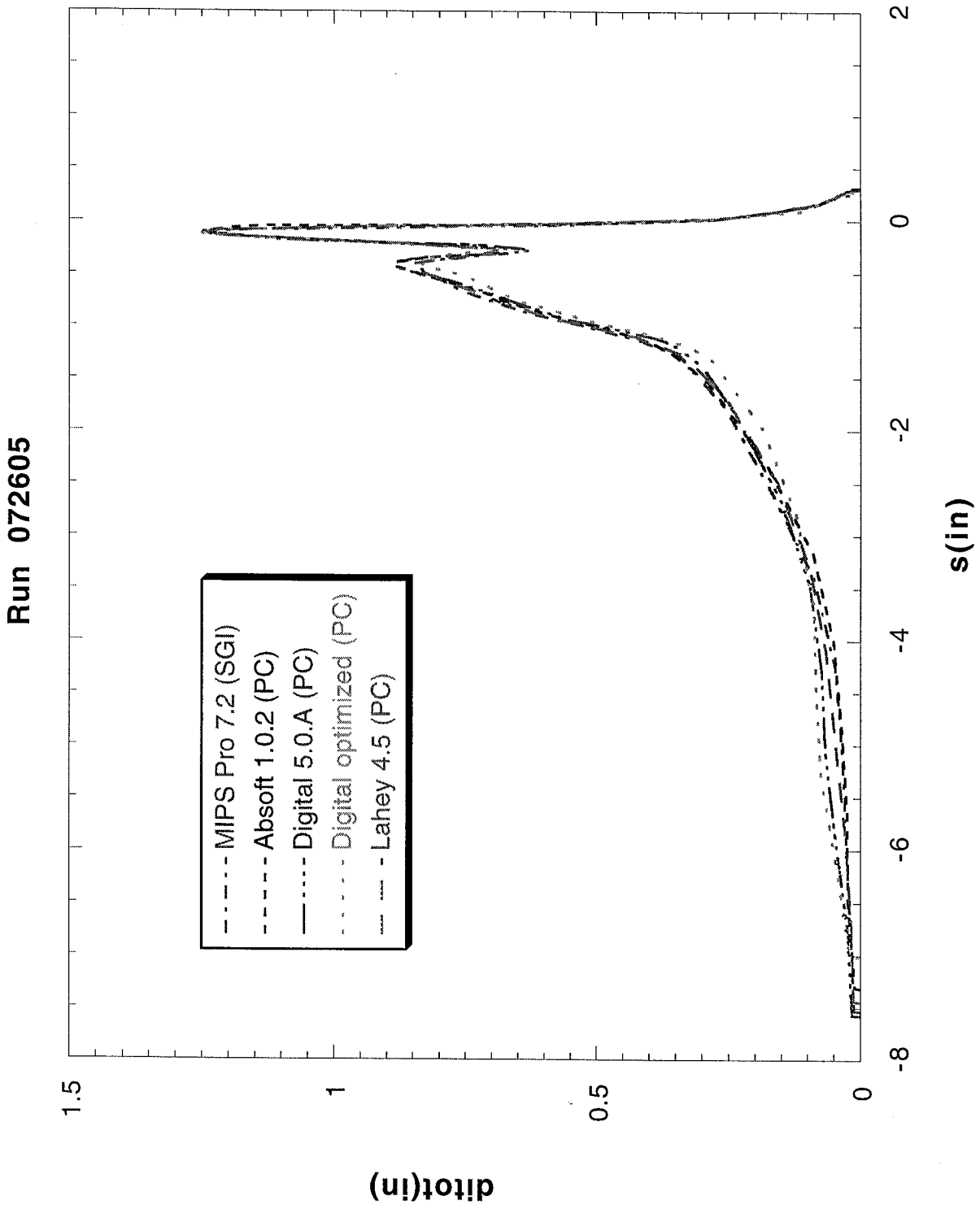
Run 072605
MIPS Pro 7.2 (SGI)
Absoft 1.0.2 (PC)
Digital 5.0.A (PC)
Digital optimized (PC)
Lahey 4.5 (PC)
ditot(in)
s(in)
1.5
1
0.5
0
2
0
-2
-4
-6
-8

FIGURE 140

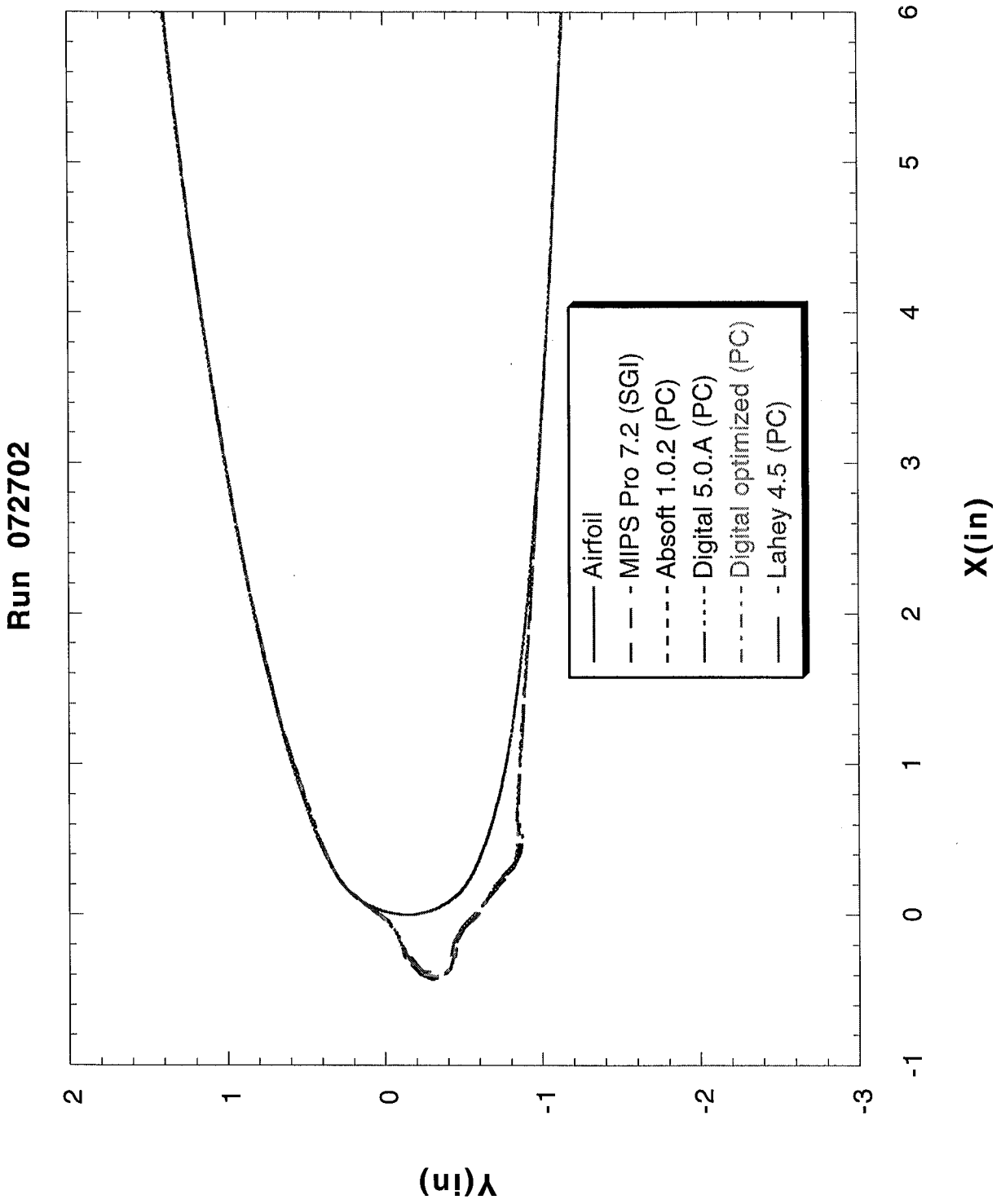
Run 072702
Airfoil
- MIPS Pro 7.2 (SGI)
Absoft 1.0.2 (PC)
Digital 5.0.A (PC)
Digital optimized (PC)
- Lahey 4.5 (PC)
Y(in)
X(in)
2
1
0
-1
-2
-3
-1
0
1
2
3
4
5
6

FIGURE 141

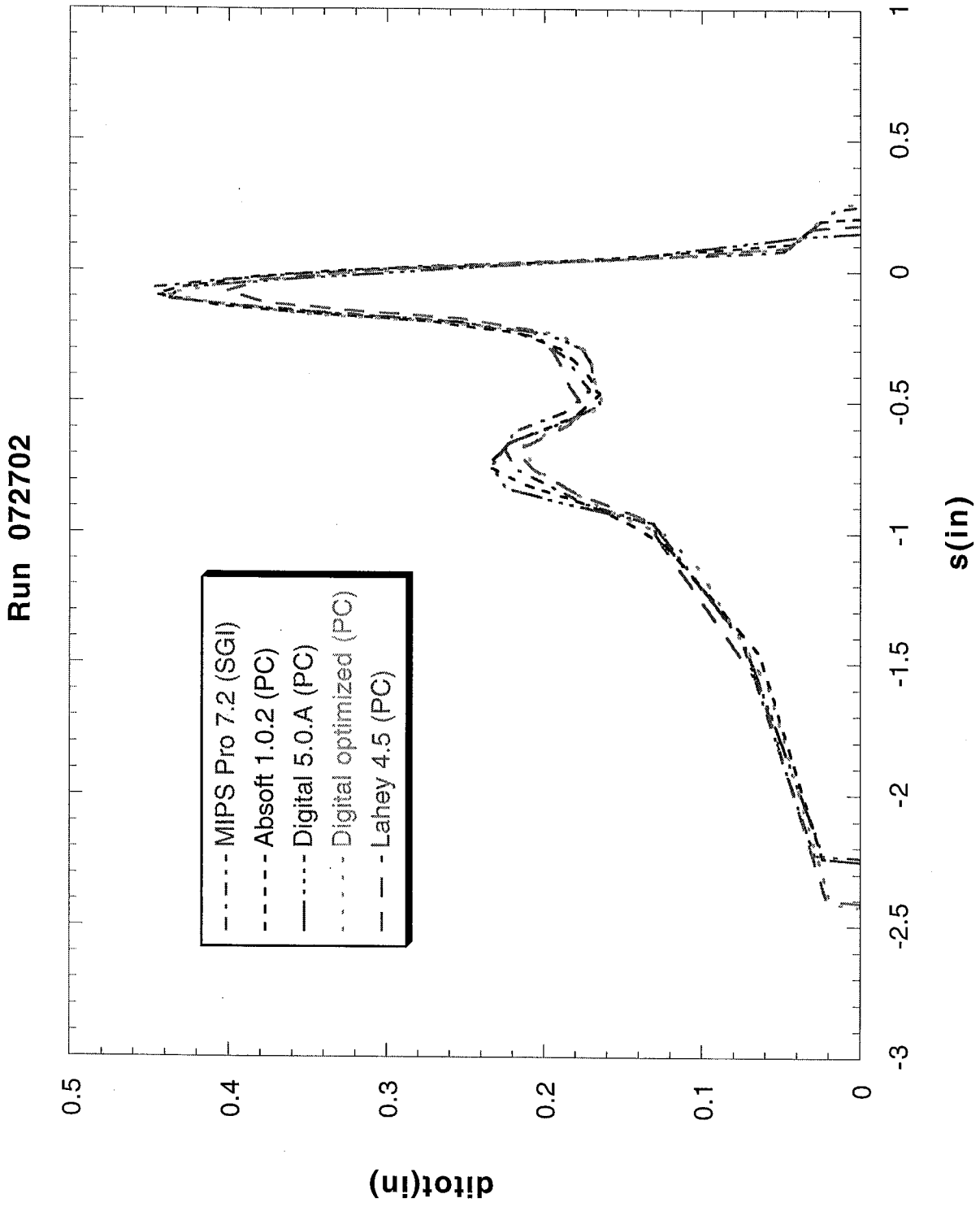
Run 072702
MIPS Pro 7.2 (SGI)
Absoft 1.0.2 (PC)
Digital 5.0.A (PC)
Digital optimized (PC)
Lahey 4.5 (PC)
ditot(in)
s(in)
0.5
0.4
0.3
0.2
0.1
0
-3
-2.5
-2
-1.5
-1
-0.5
0
0.5
1

FIGURE 142

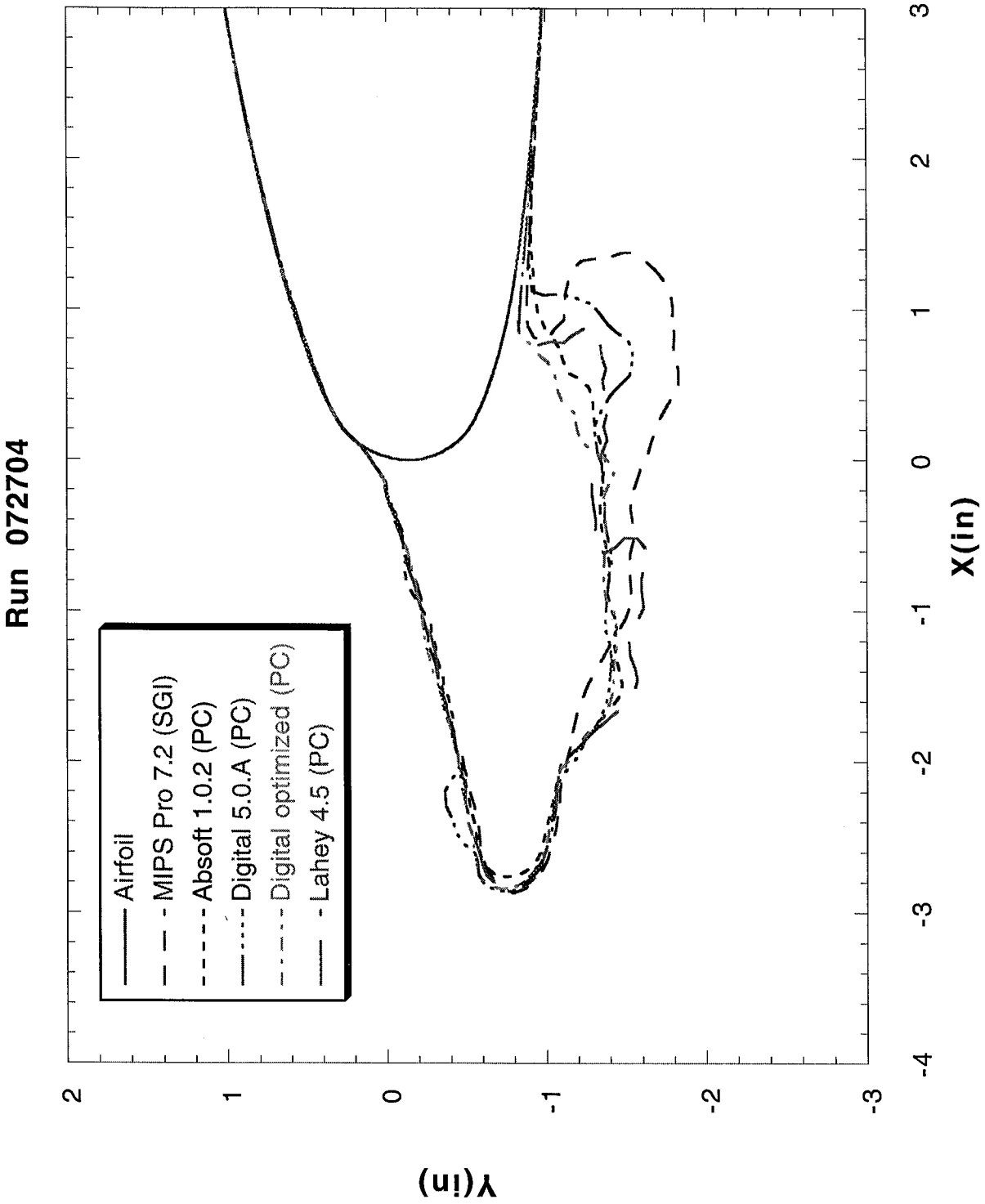
Run 072704
Airfoil
- MIPS Pro 7.2 (SGI)
- Absoft 1.0.2 (PC)
Digital 5.0.A (PC)
Digital optimized (PC)
- Lahey 4.5 (PC)
Y(in)
X(in)
2
1
0
-1
-2
-3
3
2
1
0
-1
-2
-3
-4

FIGURE 143

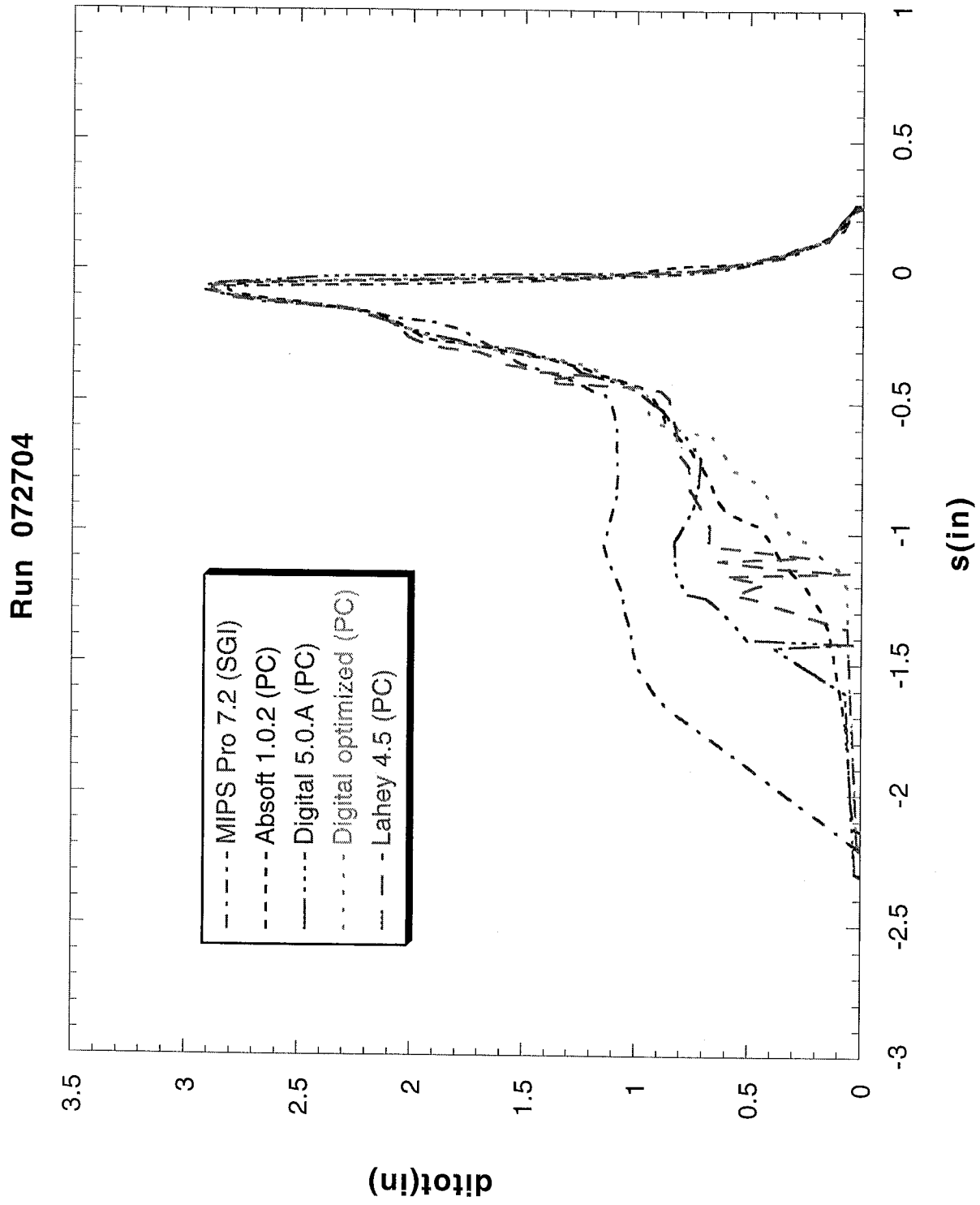
Run 072704
MIPS Pro 7.2 (SGI)
Absoft 1.0.2 (PC)
Digital 5.0.A (PC)
Digital optimized (PC)
Lahey 4.5 (PC)
ditot(in)
s(in)
3.5
3
2.5
2
1.5
1
0.5
0
-3
-2.5
-2
-1.5
-1
-0.5
0
0.5
1

FIGURE 144

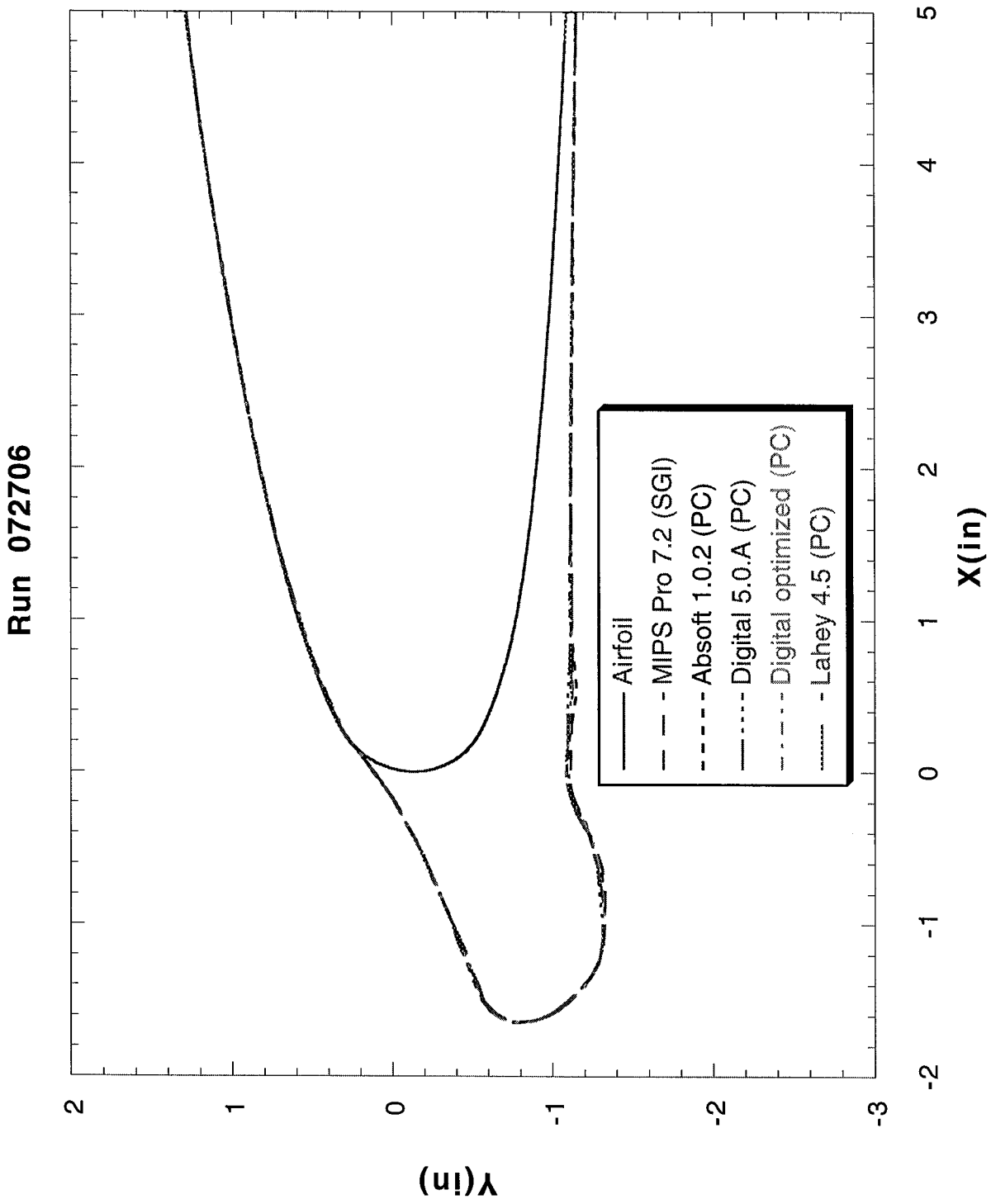
Run 072706
Y(in)
X(in)
2
1
0
-1
-2
-3
-2
-1
0
1
2
3
4
5
Airfoil
MIPS Pro 7.2 (SGI)
Absoft 1.0.2 (PC)
Digital 5.0.A (PC)
Digital optimized (PC)
Lahey 4.5 (PC)

FIGURE 145

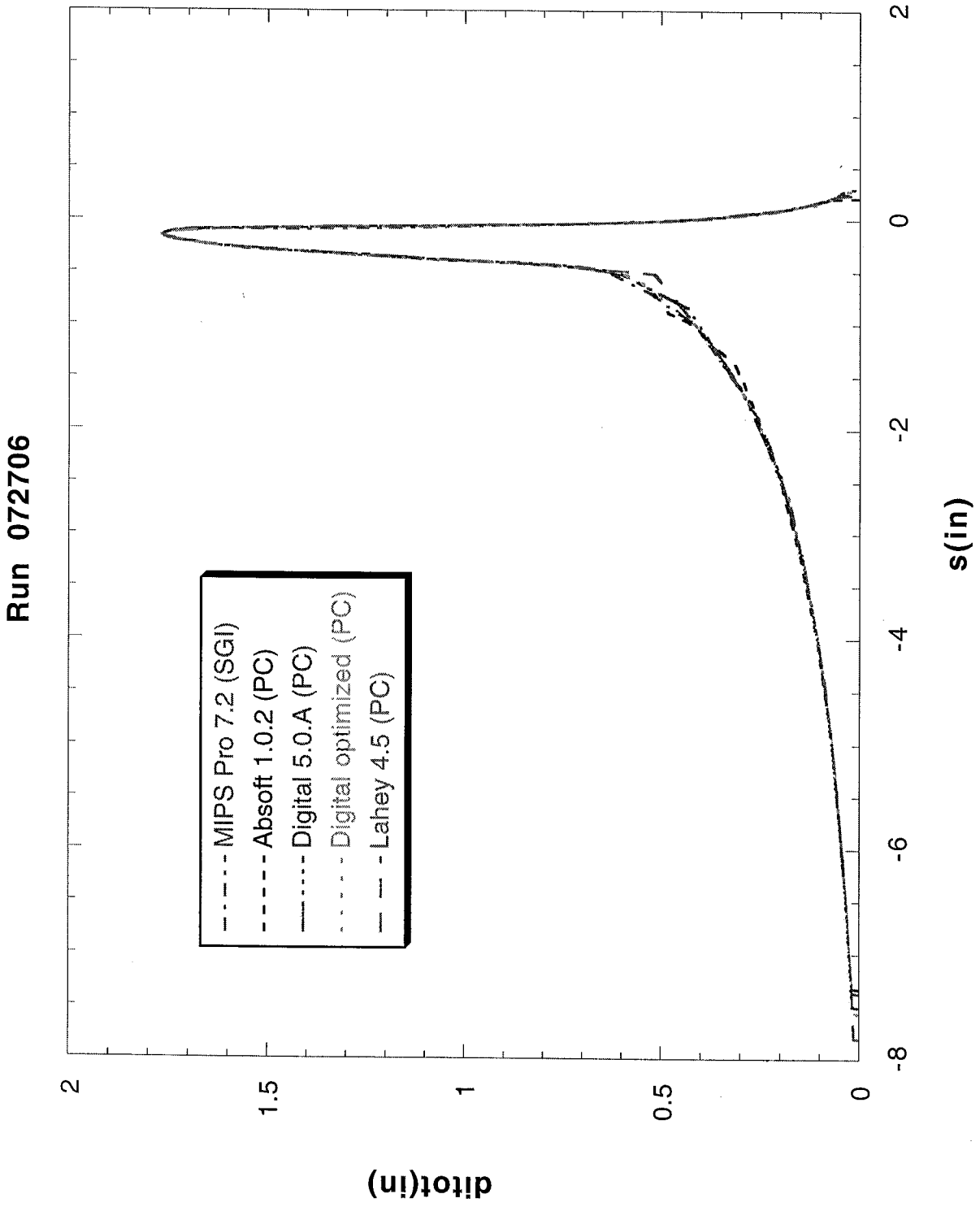
Run 072706
MIPS Pro 7.2 (SGI)
Absoft 1.0.2 (PC)
Digital 5.0.A (PC)
Digital optimized (PC)
Lahey 4.5 (PC)
ditot(in)
s(in)
2
1.5
1
0.5
0
-8
-6
-4
-2
0
2

FIGURE 146

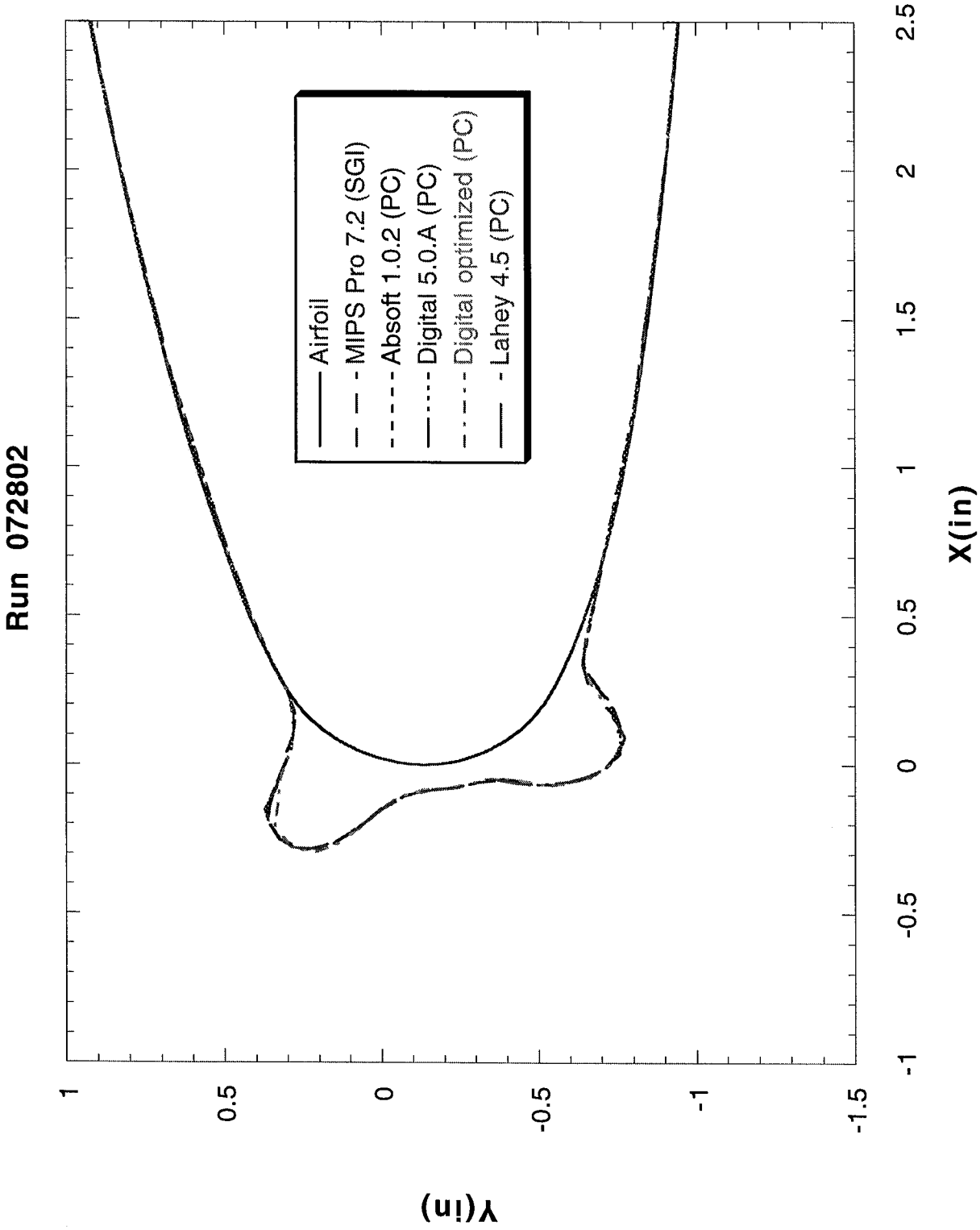
Run 072802
Airfoil
MIPS Pro 7.2 (SGI)
Absoft 1.0.2 (PC)
Digital 5.0.A (PC)
Digital optimized (PC)
Lahey 4.5 (PC)
Y(in)
X(in)
1
0.5
0
-0.5
-1
-1.5
2.5
2
1.5
1
0.5
0
-0.5
-1

FIGURE 147

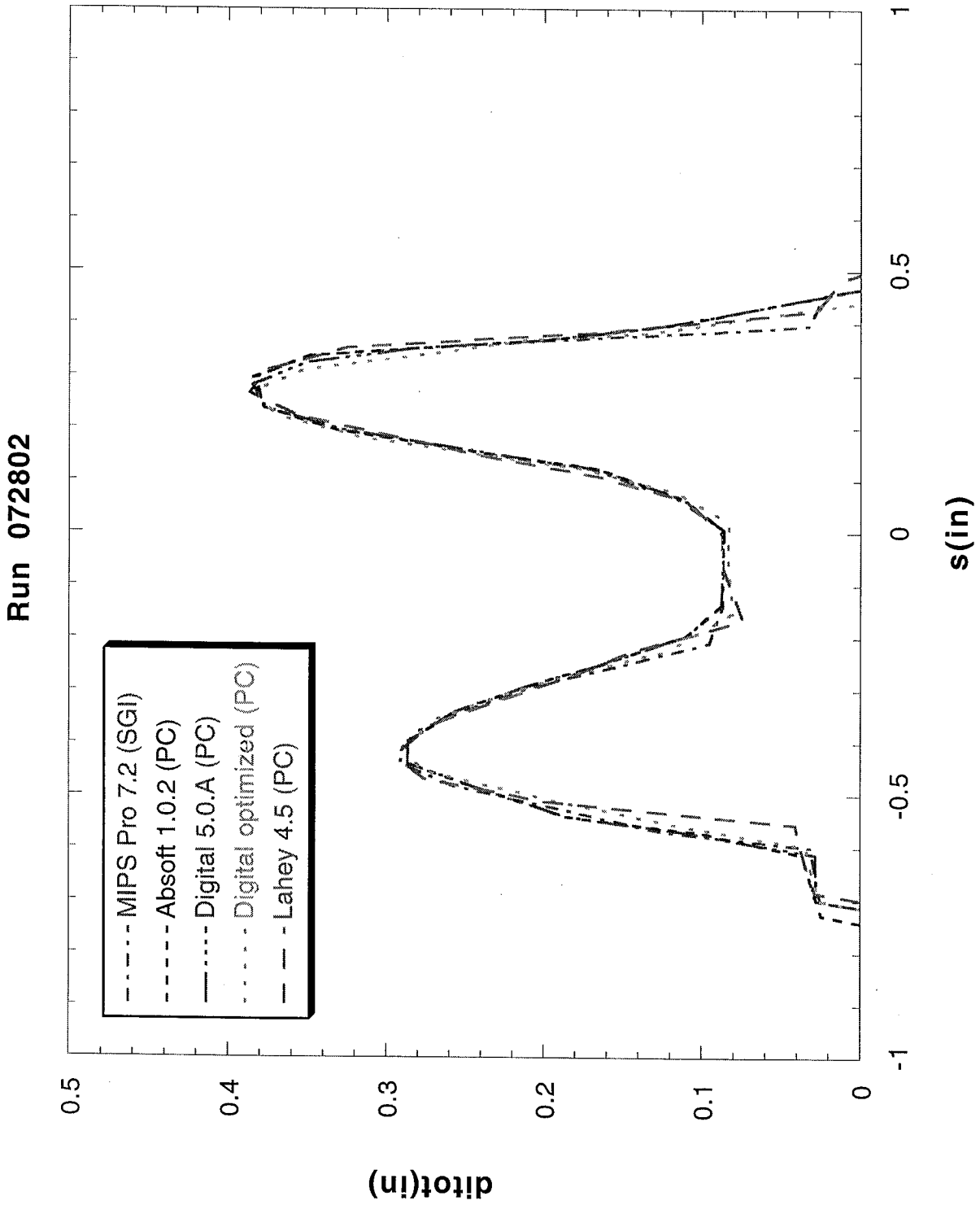
Run 072802
MIPS Pro 7.2 (SGI)
Absoft 1.0.2 (PC)
Digital 5.0.A (PC)
Digital optimized (PC)
Lahey 4.5 (PC)
ditot(in)
s(in)
0.5
0.4
0.3
0.2
0.1
0
-1
-0.5
0
0.5
1

FIGURE 148

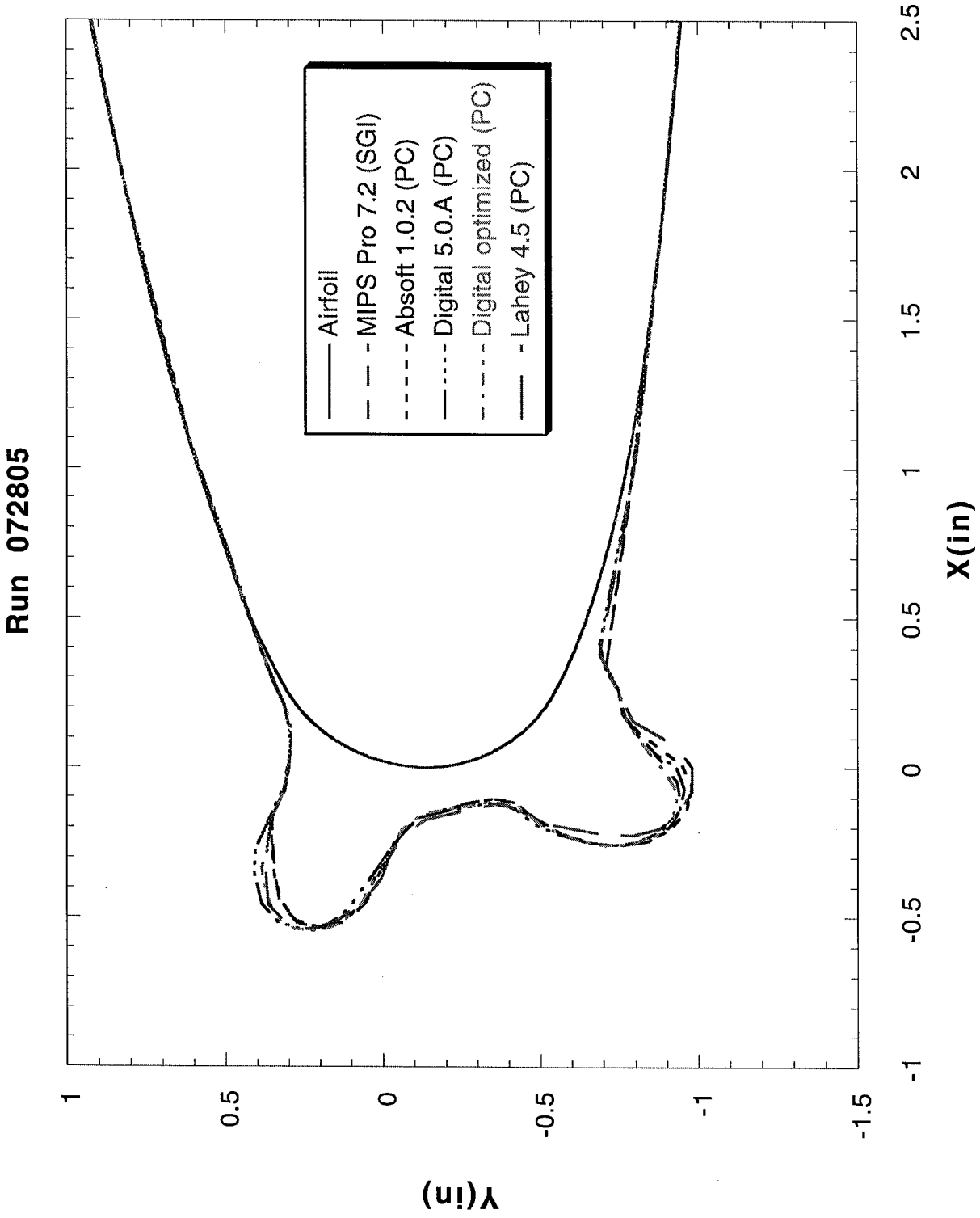
Run 072805
Airfoil
MIPS Pro 7.2 (SGI)
Absoft 1.0.2 (PC)
Digital 5.0.A (PC)
Digital optimized (PC)
Lahey 4.5 (PC)
Y(in)
X(in)
1
0.5
0
-0.5
-1
-1.5
2.5
2
1.5
1
0.5
0
-0.5
-1

FIGURE 149

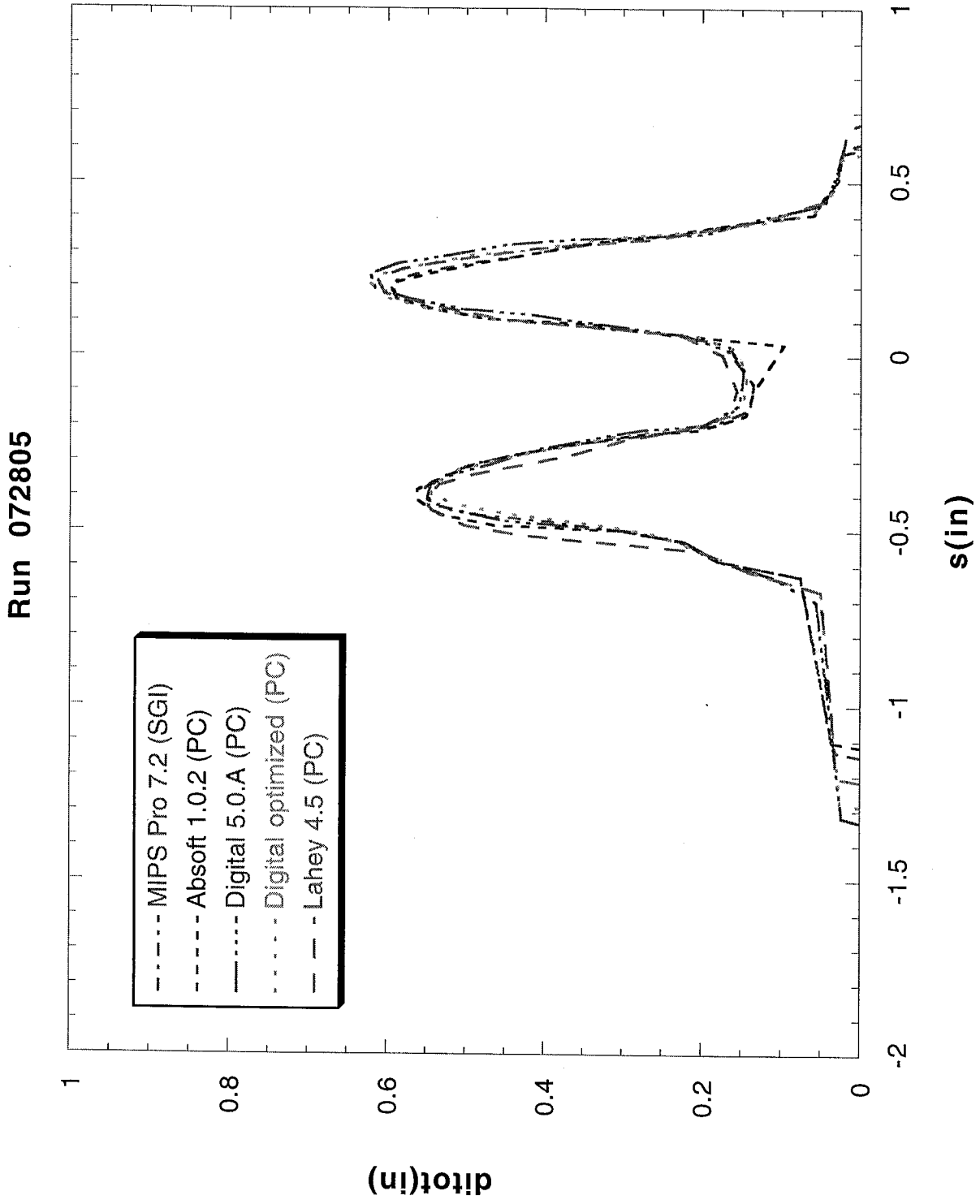
Run 072805
MIPS Pro 7.2 (SGI)
Absoft 1.0.2 (PC)
Digital 5.0.A (PC)
Digital optimized (PC)
Lahey 4.5 (PC)
ditot(in)
s(in)
1
0.8
0.6
0.4
0.2
0
-2
-1.5
-1
-0.5
0
0.5
1

FIGURE 150

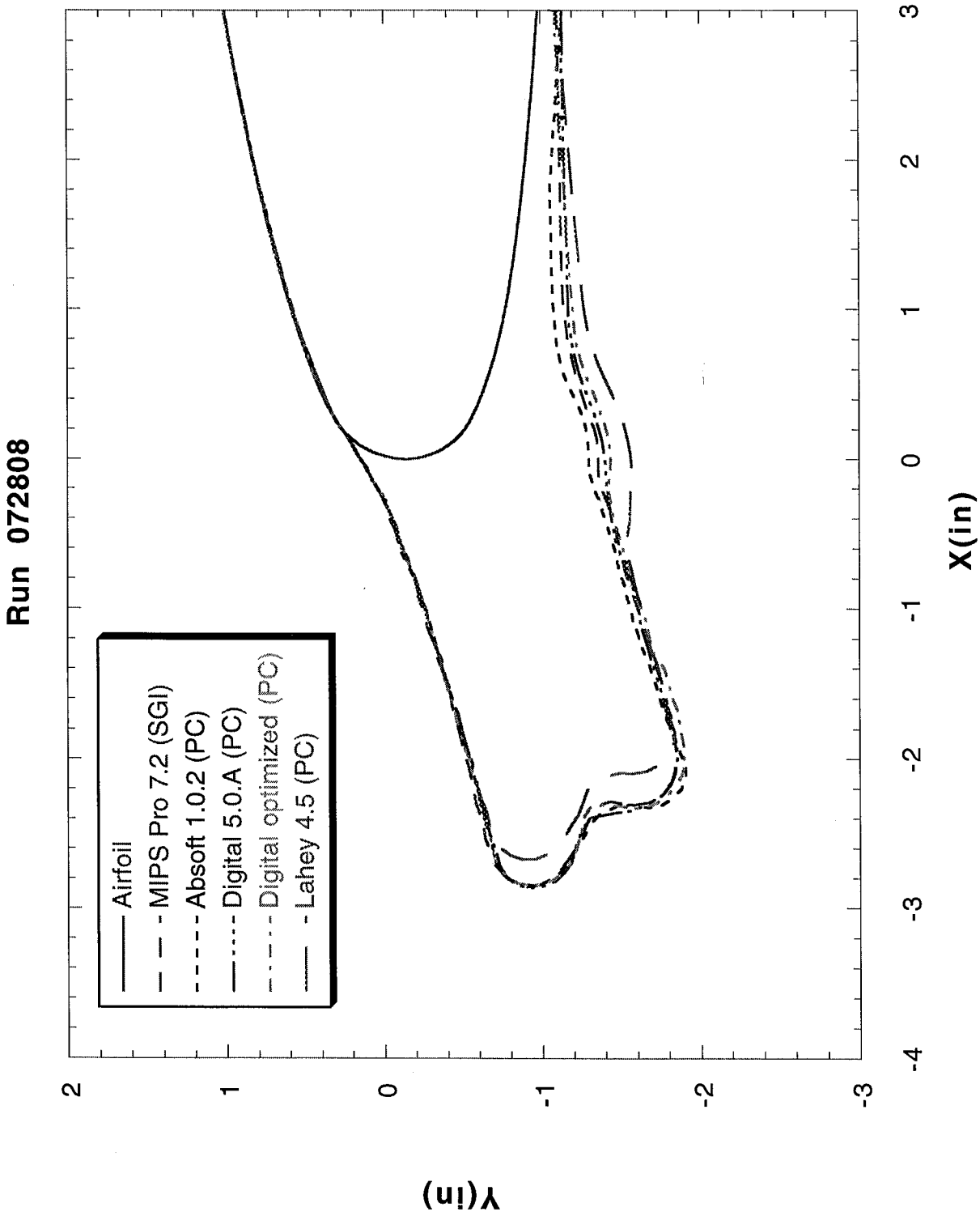
Run 072808
Airfoil
- MIPS Pro 7.2 (SGI)
- Absoft 1.0.2 (PC)
- Digital 5.0.A (PC)
- Digital optimized (PC)
- Lahey 4.5 (PC)
Y(in)
X(in)
2
1
0
-1
-2
-3
3
2
1
0
-1
-2
-3
-4

FIGURE 151

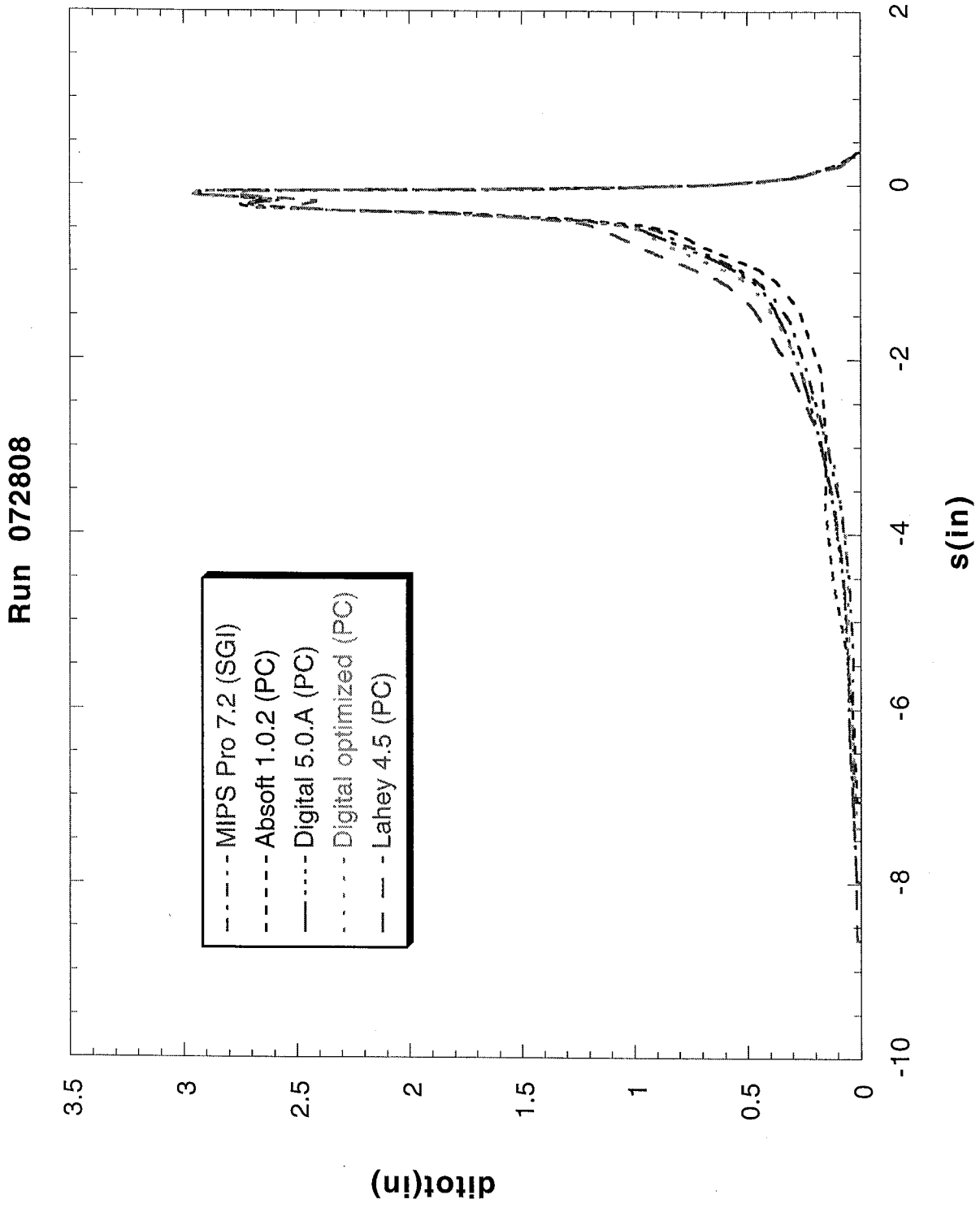
Run 072808
MIPS Pro 7.2 (SGI)
Absoft 1.0.2 (PC)
Digital 5.0.A (PC)
Digital optimized (PC)
Lahey 4.5 (PC)
ditot(in)
3.5
3
2.5
2
1.5
1
0.5
0
s(in)
2
0
-2
-4
-6
-8
-10

FIGURE 152

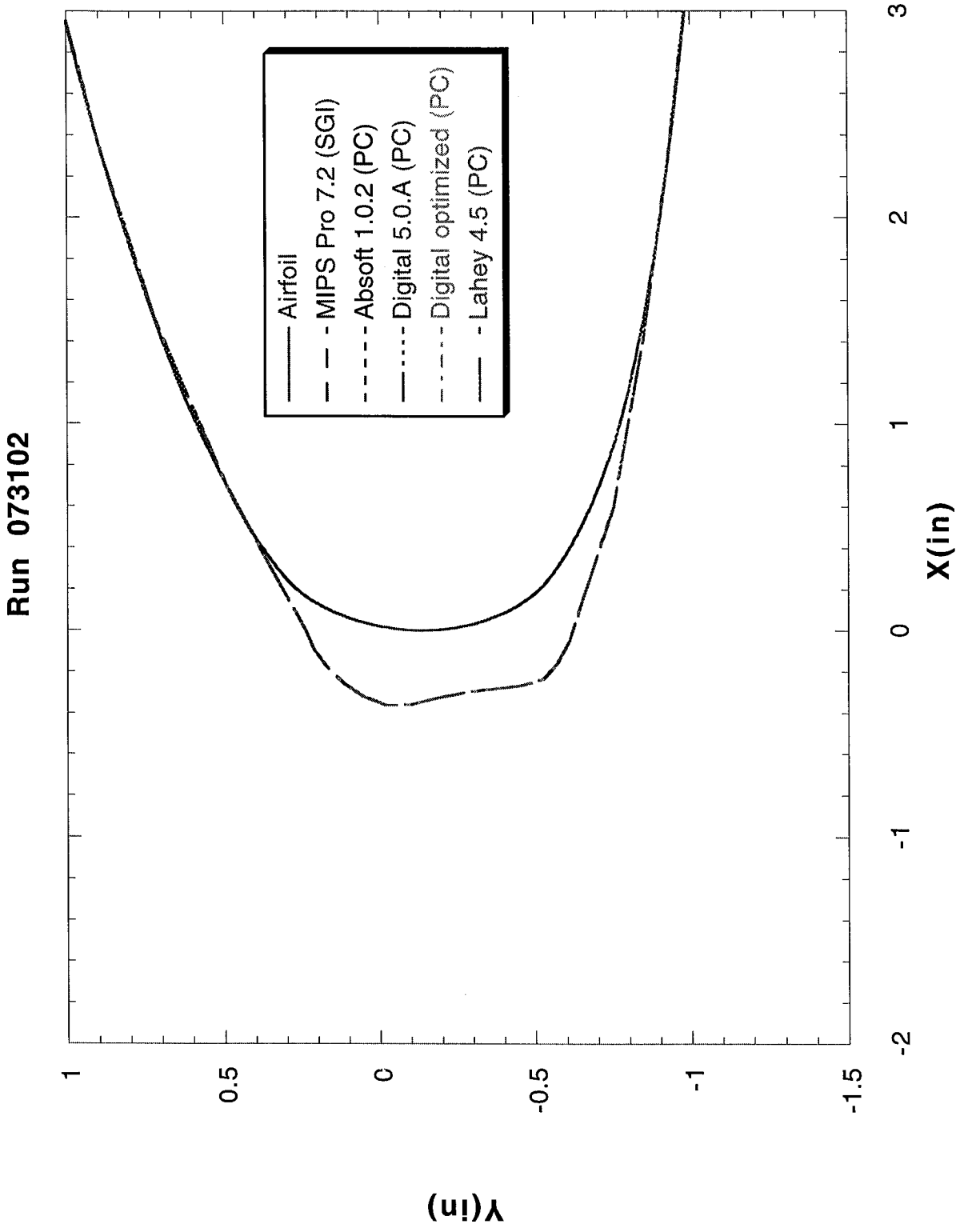
Run 073102
Airfoil
MIPS Pro 7.2 (SGI)
Absoft 1.0.2 (PC)
Digital 5.0.A (PC)
Digital optimized (PC)
Lahey 4.5 (PC)
Y(in)
X(in)
1
0.5
0
-0.5
-1
-1.5
3
2
1
0
-1
-2

FIGURE 153

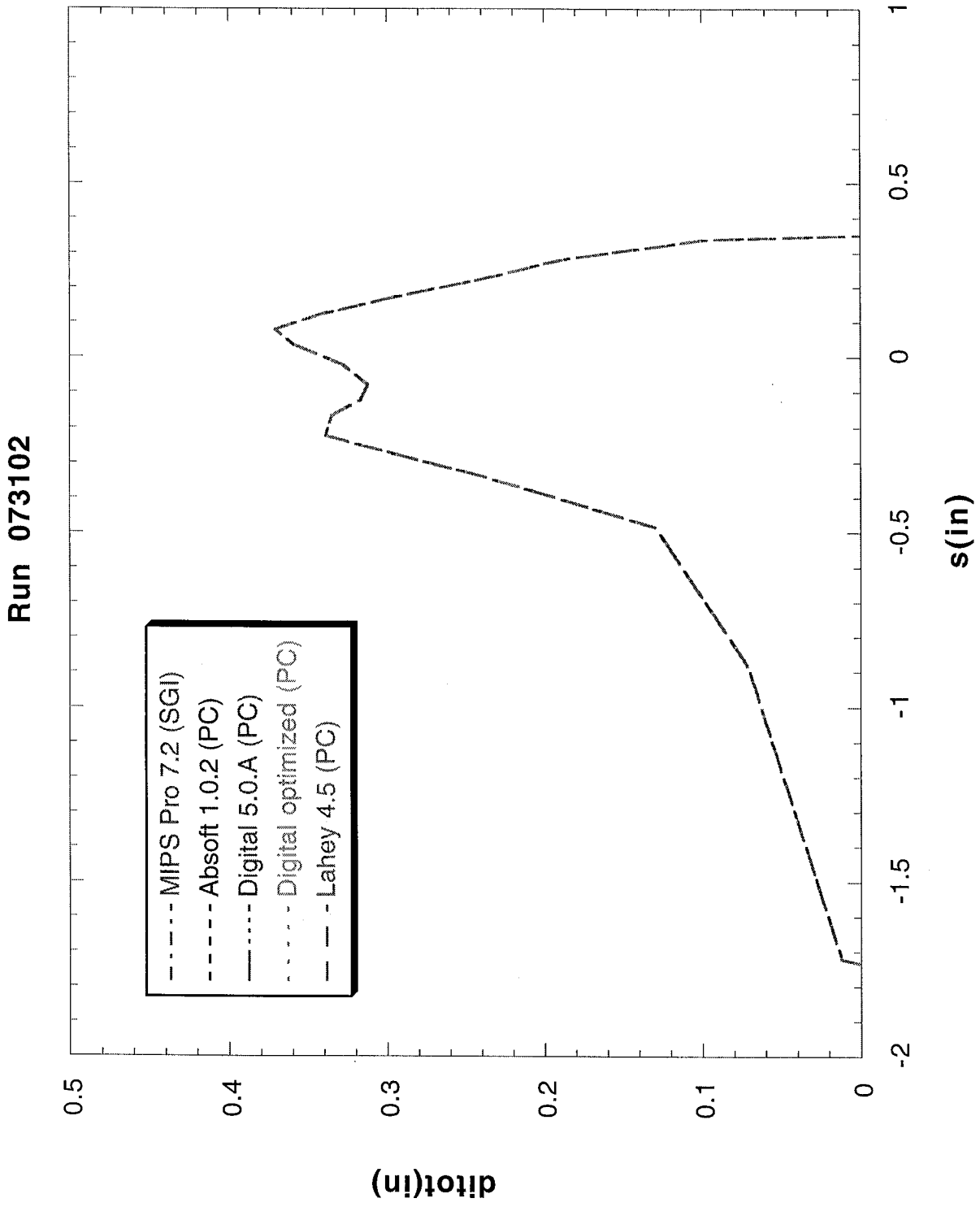
Run 073102
MIPS Pro 7.2 (SGI)
Absoft 1.0.2 (PC)
Digital 5.0.A (PC)
Digital optimized (PC)
Lahey 4.5 (PC)
ditot(in)
0.5
0.4
0.3
0.2
0.1
0
-2
-1.5
-1
-0.5
0
0.5
1
s(in)

FIGURE 154

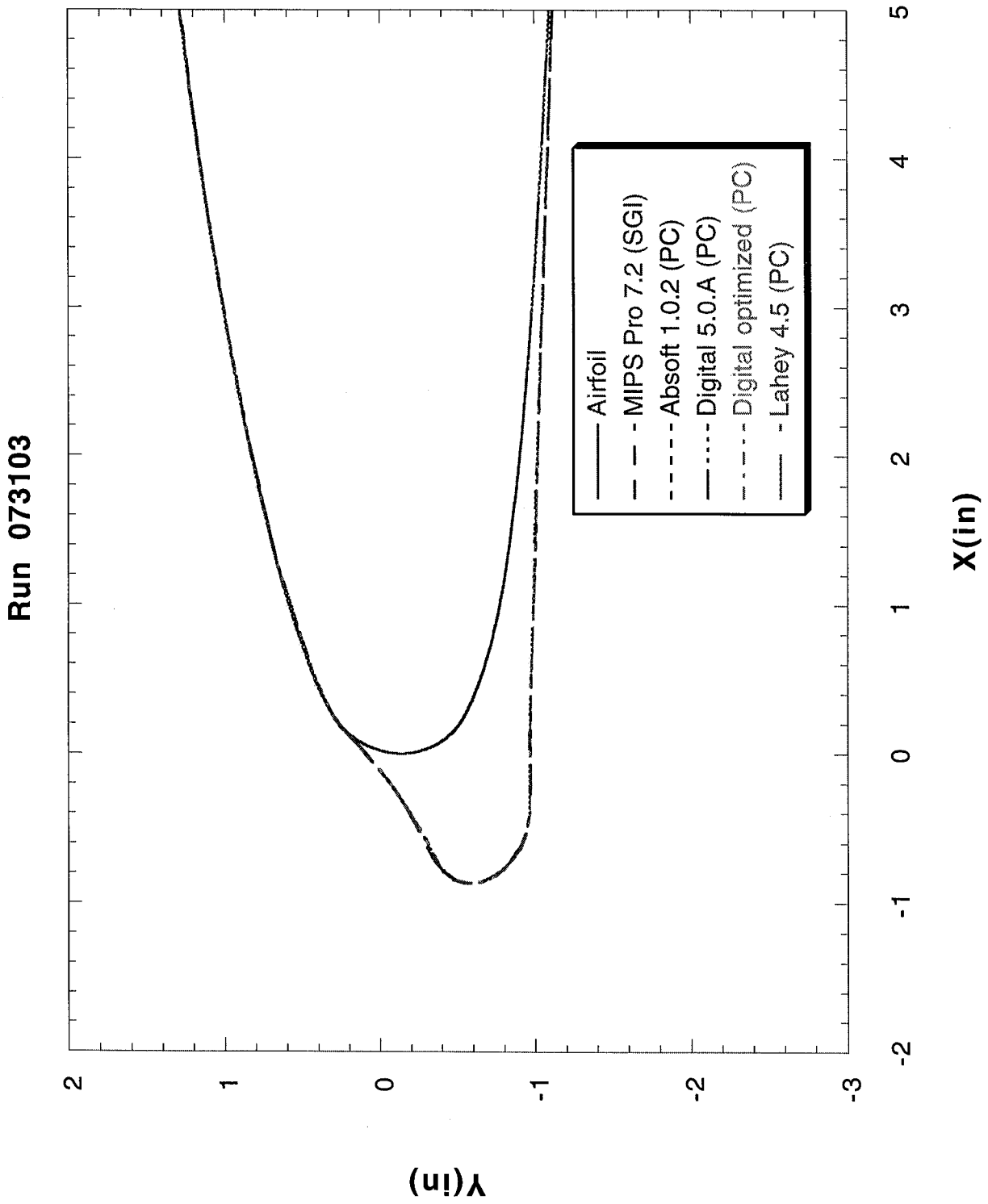
Run 073103
Airfoil
- MIPS Pro 7.2 (SGI)
- Absoft 1.0.2 (PC)
Digital 5.0.A (PC)
Digital optimized (PC)
- Lahey 4.5 (PC)
Y(in)
X(in)
2
1
0
-1
-2
-3
5
4
3
2
1
0
-1
-2

FIGURE 155

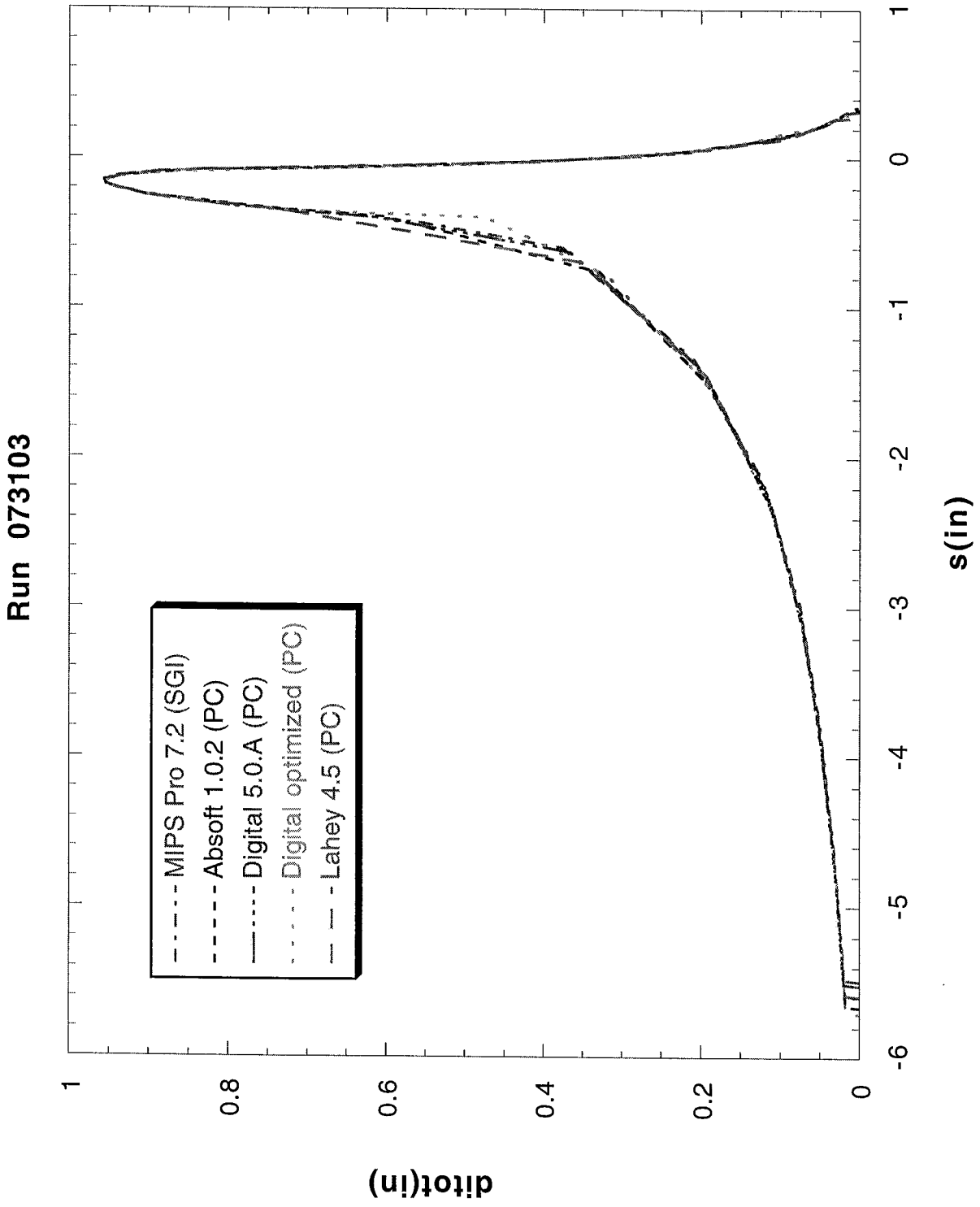
Run 073103
MIPS Pro 7.2 (SGI)
Absoft 1.0.2 (PC)
Digital 5.0.A (PC)
Digital optimized (PC)
Lahey 4.5 (PC)
ditot(in)
0
0.2
0.4
0.6
0.8
1
s(in)
1
0
-1
-2
-3
-4
-5
-6

FIGURE 156

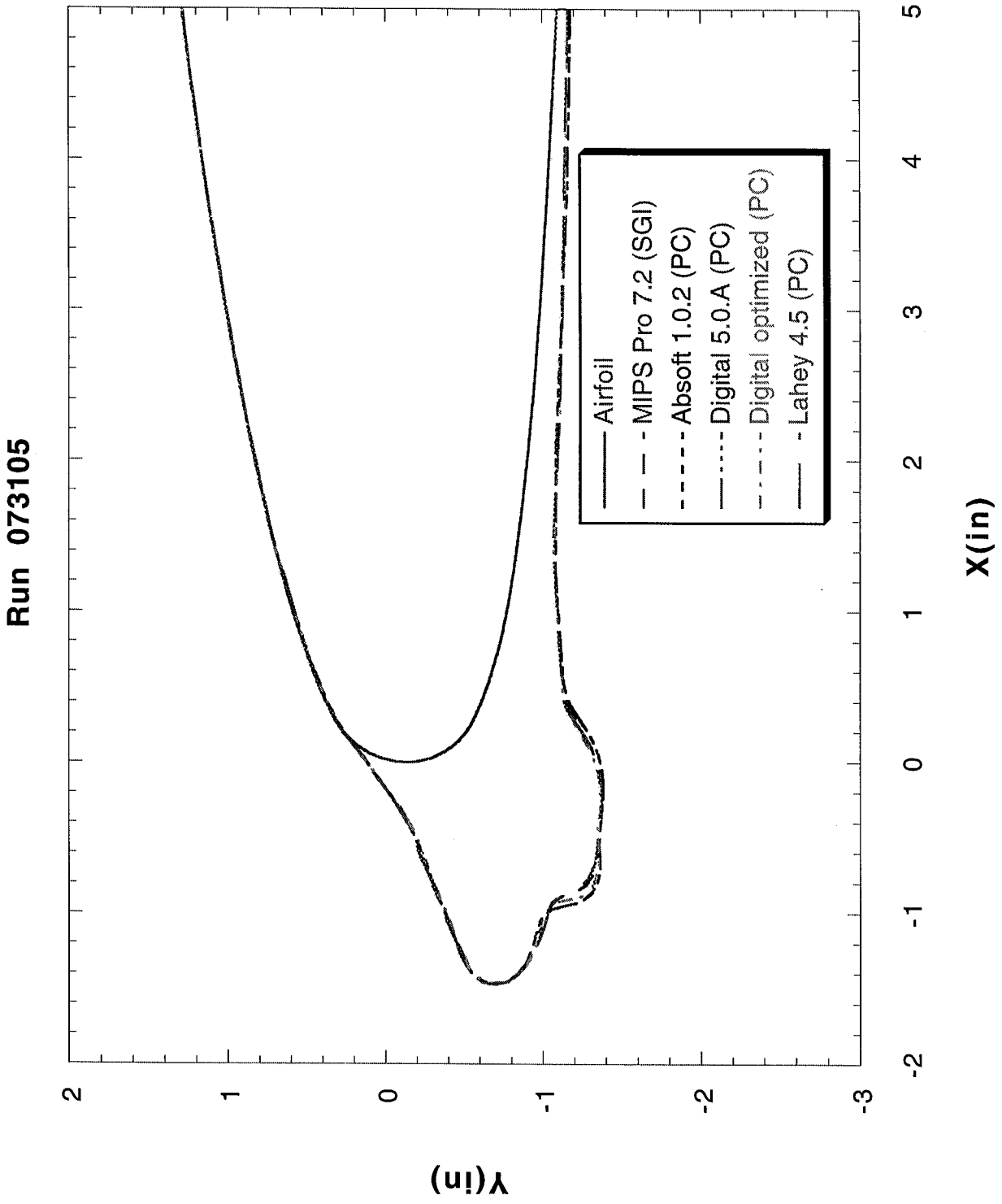
Run 073105
Airfoil
MIPS Pro 7.2 (SGI)
Absoft 1.0.2 (PC)
Digital 5.0.A (PC)
Digital optimized (PC)
Lahey 4.5 (PC)
Y(in)
X(in)
2
1
0
-1
-2
-3
5
4
3
2
1
0
-1
-2

FIGURE 157

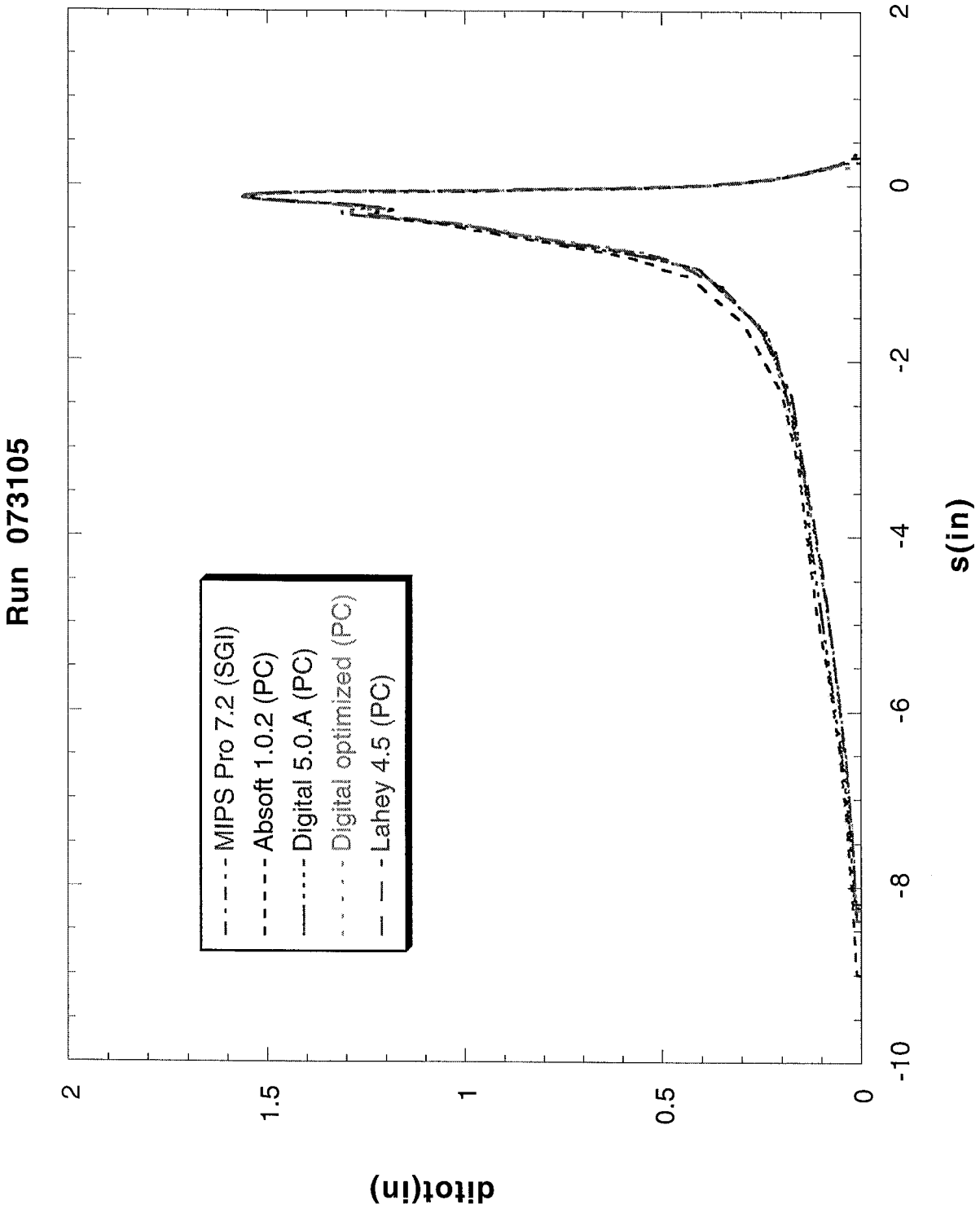
Run 073105
MIPS Pro 7.2 (SGI)
Absoft 1.0.2 (PC)
Digital 5.0.A (PC)
Digital optimized (PC)
Lahey 4.5 (PC)
ditot(in)
s(in)
2
1.5
1
0.5
0
-10
-8
-6
-4
-2
0
2

FIGURE 158

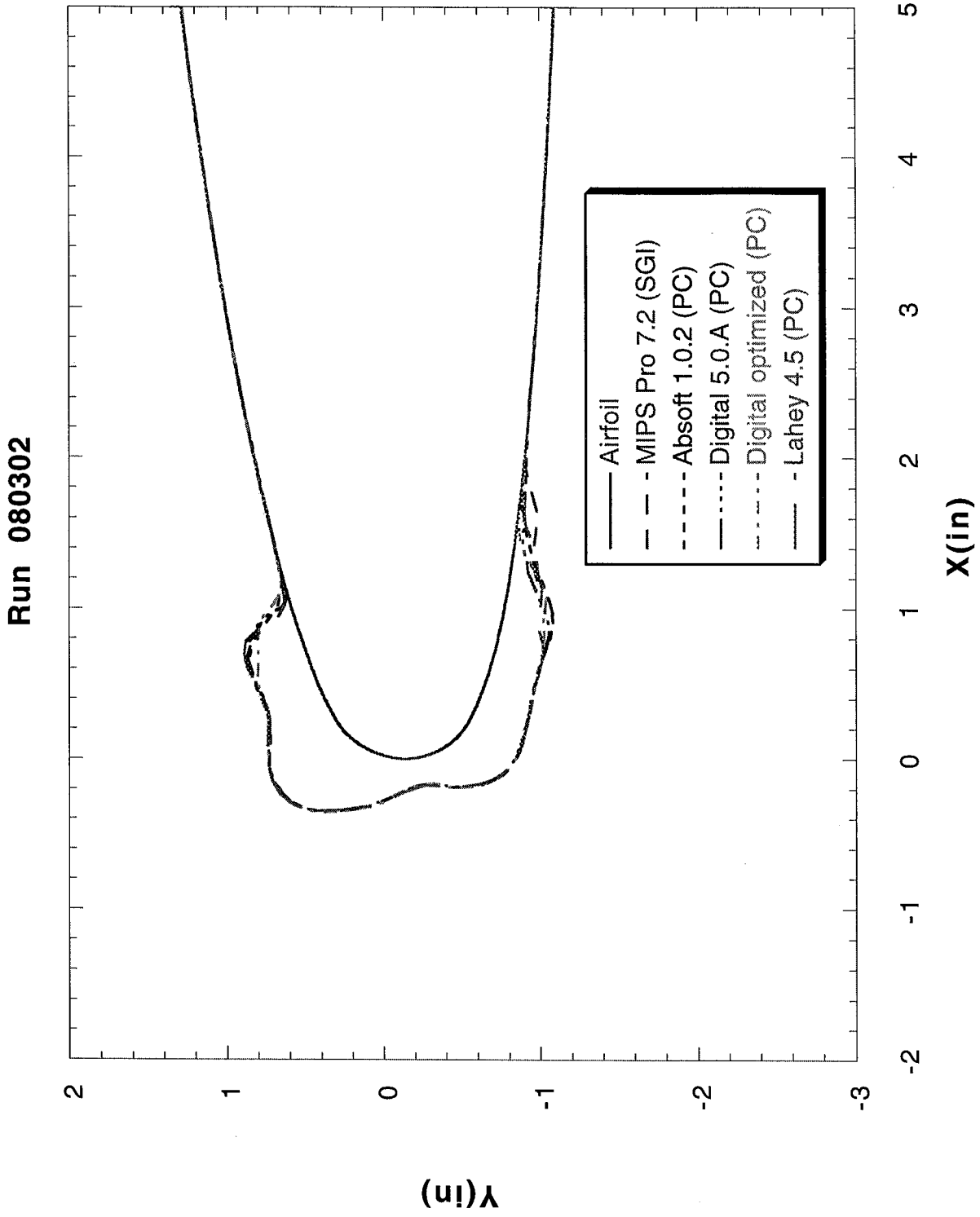
Run 080302
Airfoil
- MIPS Pro 7.2 (SGI)
Absoft 1.0.2 (PC)
Digital 5.0.A (PC)
Digital optimized (PC)
- Lahey 4.5 (PC)
X(in)
Y(in)
5
4
3
2
1
0
-1
-2
2
1
0
-1
-2
-3

FIGURE 159

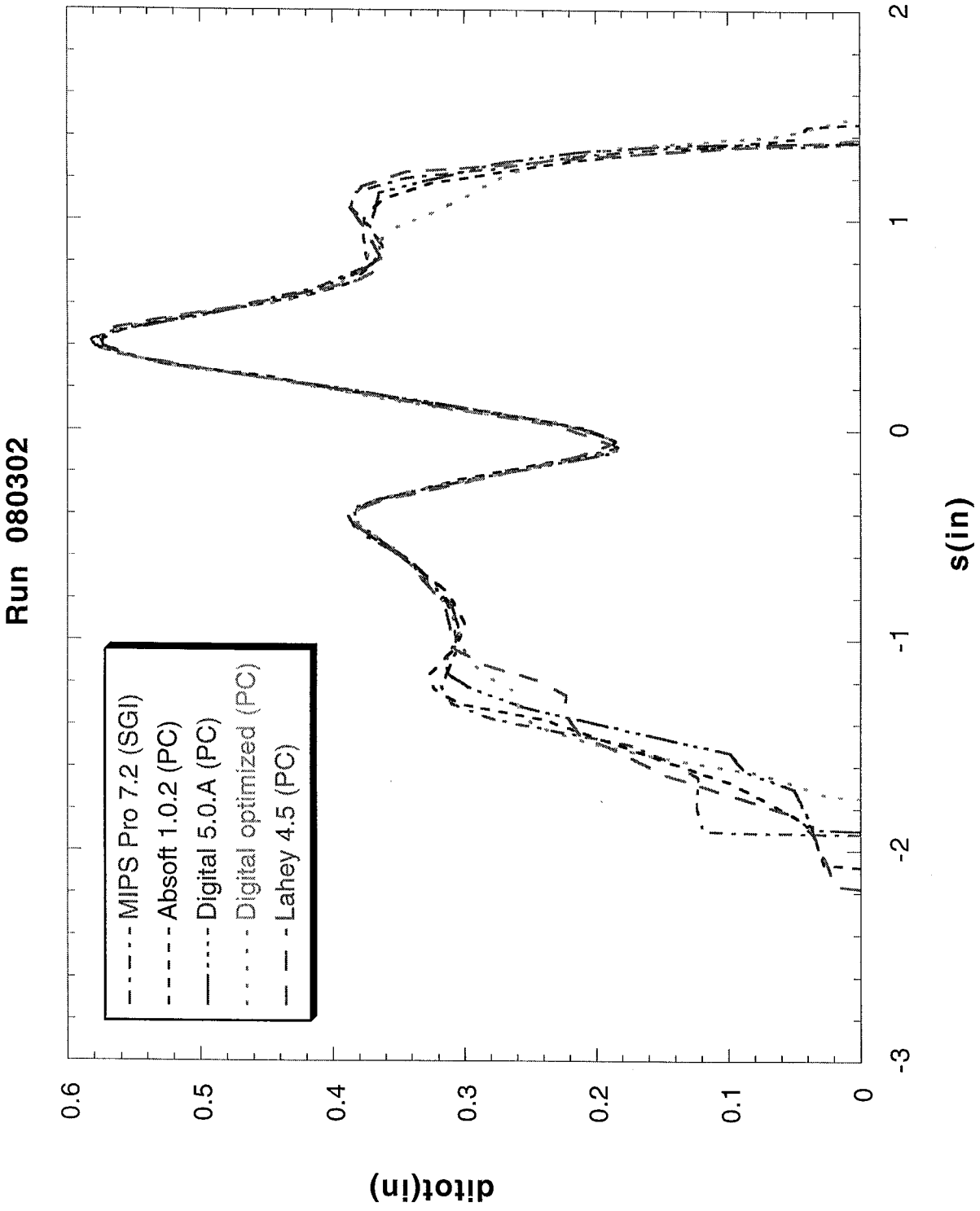
Run 080302
MIPS Pro 7.2 (SGI)
Absoft 1.0.2 (PC)
Digital 5.0.A (PC)
Digital optimized (PC)
Lahey 4.5 (PC)
ditot(in)
s(in)
0.6
0.5
0.4
0.3
0.2
0.1
0
-3
-2
-1
0
1
2

FIGURE 160

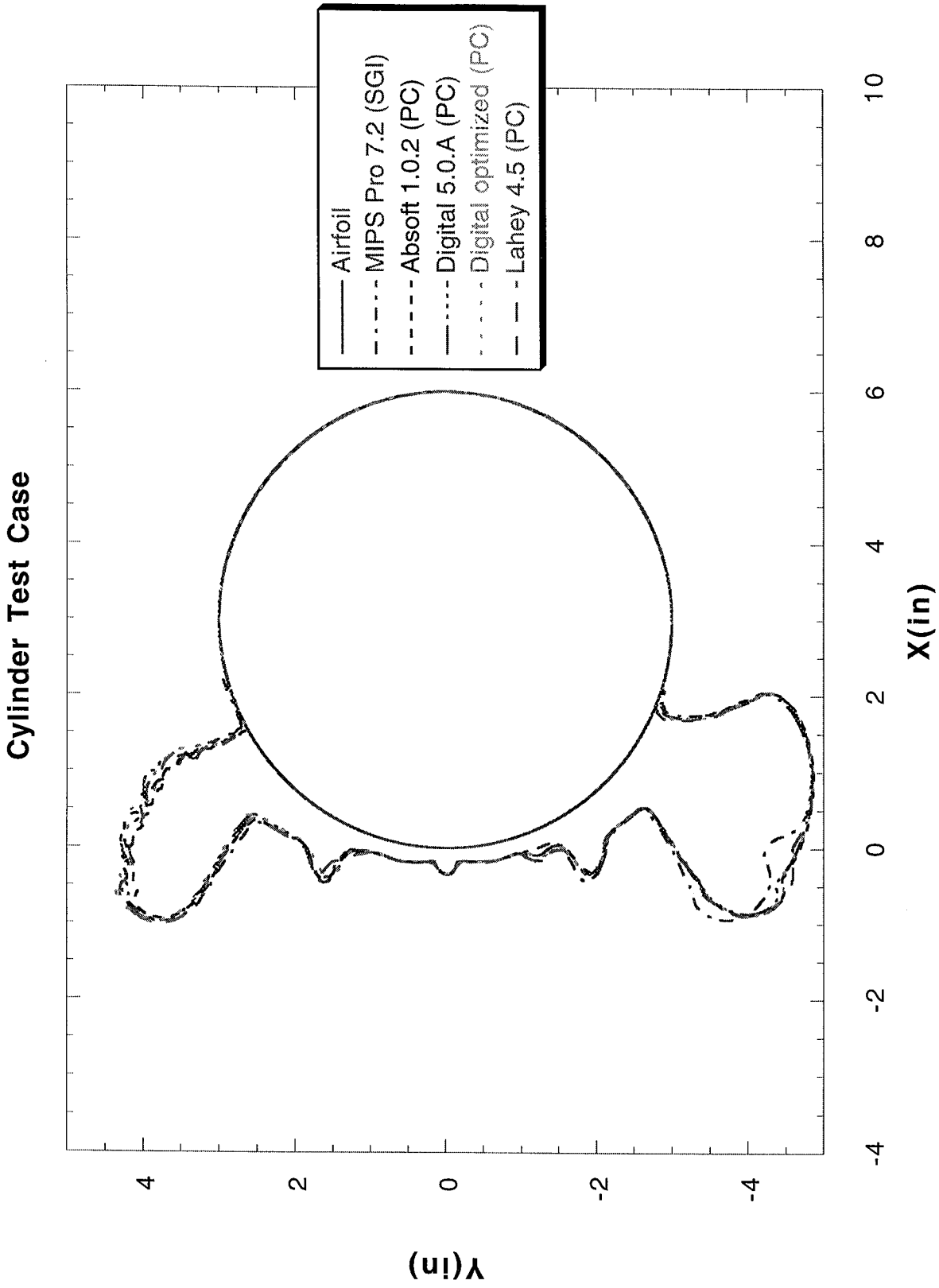
Cylinder Test Case
Airfoil
MIPS Pro 7.2 (SGI)
Absoft 1.0.2 (PC)
Digital 5.0.A (PC)
Digital optimized (PC)
Lahey 4.5 (PC)
Y(in)
X(in)
4
2
0
-2
-4
10
8
6
4
2
0
-2
-4

FIGURE 161

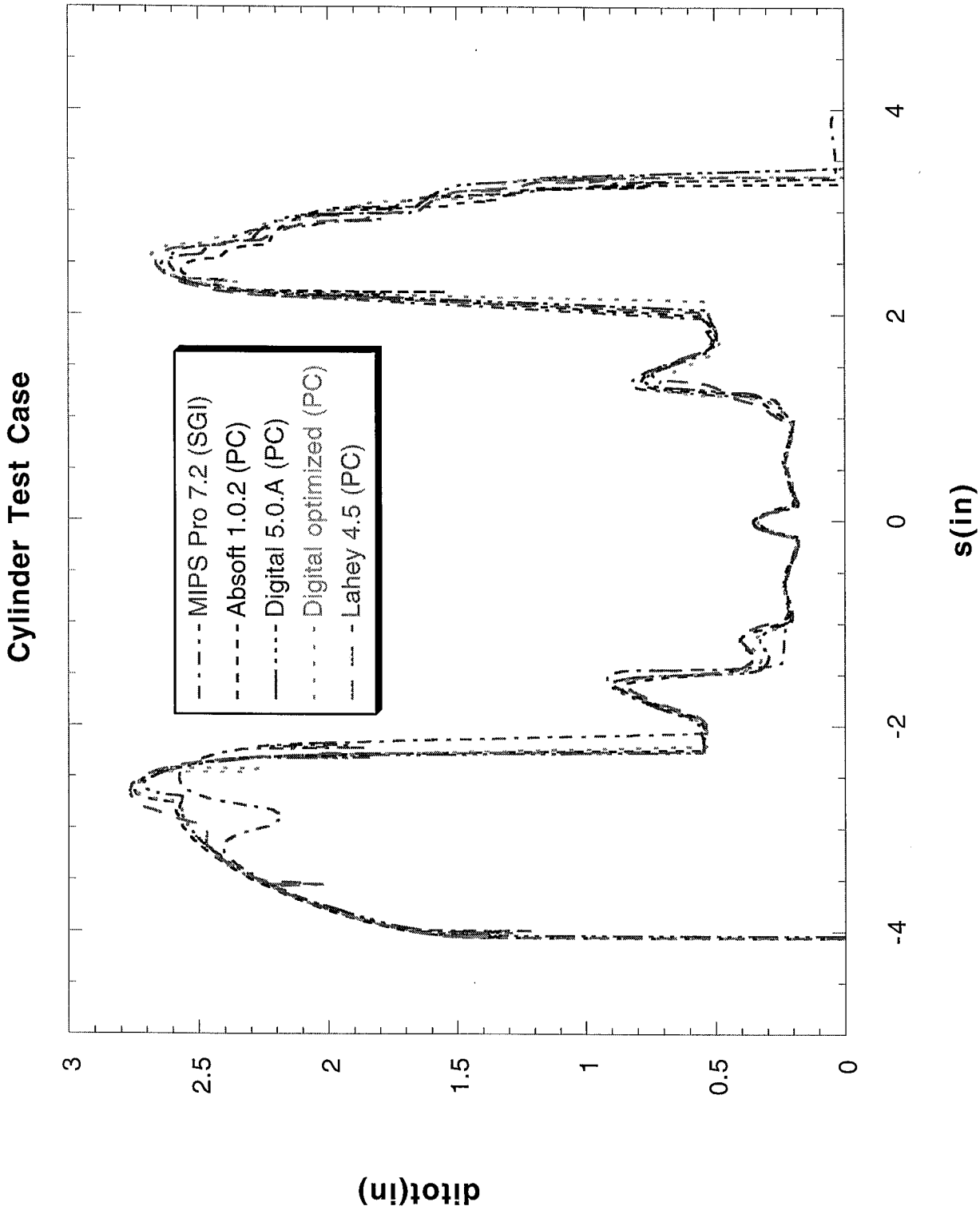
Cylinder Test Case
MIPS Pro 7.2 (SGI)
Absoft 1.0.2 (PC)
Digital 5.0.A (PC)
Digital optimized (PC)
Lahey 4.5 (PC)
ditot(in)
s(in)
3
2.5
2
1.5
1
0.5
0
-4
-2
0
2
4

NACA 23014 (mod)
Figures 162 – 241

NACA23014(mod) Test Conditions

Principal Investigator	Airfoil	Test Date	Chord (in)	Run Number	Previous Identical Run	Velocity (kts)	Velocity (m/s)	Tt (°F)	Static Temperature (K)	A.O.A.	Corrected A.O.A.	LWC (g/m^3)	MVD (microns)	Spray Time (min)	Digitized Tracing Locations
Miller/Addy	NACA23014(mod)	Nov. 1995	68.7"	219		169.5	87.2	0	251.30	0	0	0.82	160	3	30", 36" & 42"
Miller/Addy	NACA23014(mod)	Nov. 1995	68.7"	251		169.5	87.2	28	266.85	0	0	0.82	160	21.2	30", 36" & 42"
Addy	NACA23014(mod)	Feb. 1996	68.7"	412		169.5	87.2	32	269.08	0	0	0.82	160	18	30", 36" & 42"
Addy	NACA23014(mod)	Feb. 1996	68.7"	416		169.5	87.2	28	266.85	0	0	0.82	160	18	30", 36" & 42"
Reehorst	NACA23014(mod)	Jan. 1998	68.7"	1-20-run2		172.1	88.5	30	267.85	5	4.5	0.80	20	5	36"
Reehorst	NACA23014(mod)	Jan. 1998	68.7"	1-20-run3		172.1	88.5	30	267.85	5	4.5	0.80	40	5	36"
Reehorst	NACA23014(mod)	Jan. 1998	68.7"	1-20-run4		172.1	88.5	30	267.85	5	4.5	0.52	40	5	36"
Reehorst	NACA23014(mod)	Jan. 1998	68.7"	1-20-run5		172.1	88.5	30	267.85	5	4.5	0.58	70	5	36"
Reehorst	NACA23014(mod)	Jan. 1998	68.7"	1-21-run2		172.1	88.5	30	267.85	7	6.2	0.80	20	5	36"
Reehorst	NACA23014(mod)	Jan. 1998	68.7"	1-21-run3		172.1	88.5	30	267.85	7	6.2	0.80	40	5	36"
Reehorst	NACA23014(mod)	Jan. 1998	68.7"	1-21-run4		172.1	88.5	30	267.85	7	6.2	0.52	40	5	36"
Reehorst	NACA23014(mod)	Jan. 1998	68.7"	1-21-run5		172.1	88.5	30	267.85	7	6.2	0.58	70	5	36"
Reehorst	NACA23014(mod)	Jan. 1998	68.7"	1-21-run6		172.1	88.5	30	267.85	3	2.7	0.80	20	5	36"
Reehorst	NACA23014(mod)	Jan. 1998	68.7"	1-21-run7		172.1	88.5	30	267.85	3	2.7	0.80	40	5	36"
Reehorst	NACA23014(mod)	Jan. 1998	68.7"	1-21-run8		172.1	88.5	30	267.85	3	2.7	0.52	40	5	36"
Reehorst	NACA23014(mod)	Jan. 1998	68.7"	1-22-run3		172.1	88.5	30	267.85	3	2.7	0.58	70	5	36"
Reehorst	NACA23014(mod)	Jan. 1998	68.7"	1-22-run4		172.1	88.5	31	268.41	5	4.5	0.80	20	5	36"
Reehorst	NACA23014(mod)	Jan. 1998	68.7"	1-22-run5		172.1	88.5	31	268.41	5	4.5	0.80	40	5	36"
Reehorst	NACA23014(mod)	Jan. 1998	68.7"	1-22-run6		172.1	88.5	31	268.41	5	4.5	0.52	40	5	36"
Reehorst	NACA23014(mod)	Jan. 1998	68.7"	1-22-run7		172.1	88.5	31	268.41	5	4.5	0.58	70	5	36"
Reehorst	NACA23014(mod)	Jan. 1998	68.7"	1-22-run8		172.1	88.5	28	266.74	5	4.5	0.80	20	5	36"
Reehorst	NACA23014(mod)	Jan. 1998	68.7"	1-22-run9		172.1	88.5	28	266.74	5	4.5	0.80	40	5	36"
Reehorst	NACA23014(mod)	Jan. 1998	68.7"	1-23-run2		172.1	88.5	28	266.74	5	4.5	0.52	40	5	36"
Reehorst	NACA23014(mod)	Jan. 1998	68.7"	1-23-run3		172.1	88.5	28	266.74	5	4.5	0.58	70	5	36"
Reehorst	NACA23014(mod)	Jan. 1998	68.7"	1-23-run4		172.1	88.5	26	265.63	5	4.5	0.80	20	5	36"
Reehorst	NACA23014(mod)	Jan. 1998	68.7"	1-23-run5		172.1	88.5	26	265.63	5	4.5	0.80	40	5	36"
Reehorst	NACA23014(mod)	Jan. 1998	68.7"	1-23-run6		172.1	88.5	26	265.63	5	4.5	0.52	70	5	36"
Reehorst	NACA23014(mod)	Jan. 1998	68.7"	1-23-run7		172.1	88.5	26	265.63	5	4.5	0.58	70	5	36"
Reehorst	NACA23014(mod)	Jan. 1998	68.7"	1-23-run8		172.1	88.5	30	267.85	5	4.5	0.80	20	10	36"
Reehorst	NACA23014(mod)	Jan. 1998	68.7"	1-23-run9		172.1	88.5	30	267.85	5	4.5	0.80	40	10	36"
Reehorst	NACA23014(mod)	Jan. 1998	68.7"	1-23-run10		172.1	88.5	30	267.85	5	4.5	0.52	40	10	36"
Reehorst	NACA23014(mod)	Jan. 1998	68.7"	1-23-run11		172.1	88.5	30	267.85	5	4.5	0.58	70	10	36"
Reehorst	NACA23014(mod)	Jan. 1998	68.7"	1-26-run2R	1-20-run5	172.1	88.5	30	267.85	5	4.5	0.58	70	5	36"
Reehorst	NACA23014(mod)	Jan. 1998	68.7"	1-26-run3R	1-20-run5	172.1	88.5	30	267.85	5	4.5	0.58	70	5	36"
Reehorst	NACA23014(mod)	Jan. 1998	68.7"	1-26-run4R	1-20-run4	172.1	88.5	30	267.85	5	4.5	0.52	40	5	36"
Reehorst	NACA23014(mod)	Jan. 1998	68.7"	1-26-run5R	1-20-run4	172.1	88.5	30	267.85	5	4.5	0.52	40	5	36"
Reehorst	NACA23014(mod)	Jan. 1998	68.7"	1-26-run6R	1-20-run3	172.1	88.5	30	267.85	5	4.5	0.80	40	5	36"
Reehorst	NACA23014(mod)	Jan. 1998	68.7"	1-26-run7R	1-20-run3	172.1	88.5	30	267.85	5	4.5	0.80	40	5	36"
Reehorst	NACA23014(mod)	Jan. 1998	68.7"	1-26-run8R	1-20-run2	172.1	88.5	30	267.85	5	4.5	0.80	20	5	36"
Reehorst	NACA23014(mod)	Jan. 1998	68.7"	1-26-run9R	1-20-run2	172.1	88.5	30	267.85	5	4.5	0.80	20	5	36"
Reehorst	NACA23014(mod)	Jan. 1998	68.7"	1-27-run2		172.1	88.5	30	267.85	5	4.5	0.60	100	5	36"
Reehorst	NACA23014(mod)	Jan. 1998	68.7"	1-27-run3		172.1	88.5	30	267.85	5	4.5	0.60	120	5	36"
Reehorst	NACA23014(mod)	Jan. 1998	68.7"	1-27-run4		172.1	88.5	30	267.85	5	4.5	0.85	175	5	36"
Reehorst	NACA23014(mod)	Jan. 1998	68.7"	1-27-run5		172.1	88.5	30	267.85	5	4.5	0.85	270	5	36"
Reehorst	NACA23014(mod)	Jan. 1998	68.7"	1-27-run6R	1-23-run4	172.1	88.5	26	265.63	5	4.5	0.80	20	5	36"
Reehorst	NACA23014(mod)	Jan. 1998	68.7"	1-28-run2R	1-22-run8	172.1	88.5	28	266.74	5	4.5	0.80	20	5	36"
Reehorst	NACA23014(mod)	Jan. 1998	68.7"	1-28-run3R	1-22-run9	172.1	88.5	28	266.74	5	4.5	0.80	40	5	36"
Reehorst	NACA23014(mod)	Jan. 1998	68.7"	1-28-run4R	1-23-run2	172.1	88.5	28	266.74	5	4.5	0.52	40	5	36"

NACA23014(mod) Test Conditions

Principal Investigator	Airfoil	Test Date	Chord (in)	Run Number	Previous Identical Run	Velocity (kts)	Velocity (m/s)	Tt (°F)	Static Temperature (K)	A.O.A.	Corrected A.O.A.	LWC (g/m^3)	MVD (microns)	Spray Time (min)	Digitized Tracing Locations
Reehorst	NACA23014(mod)	Jan. 1998	68.7"	1-28-run5R	1-23-run3	172.1	88.5	28	266.74	5	4.5	0.58	70	5	36"
Reehorst	NACA23014(mod)	Jan. 1998	68.7"	1-28-run6		172.1	88.5	28	266.74	5	4.5	0.60	100	5	36"
Reehorst	NACA23014(mod)	Jan. 1998	68.7"	1-28-run7		172.1	88.5	26	265.63	5	4.5	0.52	40	5	36"
Reehorst	NACA23014(mod)	Jan. 1998	68.7"	1-28-run8R	1-23-run7	172.1	88.5	26	265.63	5	4.5	0.58	70	5	36"
Reehorst	NACA23014(mod)	Jan. 1998	68.7"	1-29-run2R	1-20-run2	172.1	88.5	30	267.85	5	4.5	0.80	20	5	36"
Reehorst	NACA23014(mod)	Jan. 1998	68.7"	1-29-run3R	1-21-run7	172.1	88.5	30	267.85	3	2.7	0.80	40	5	36"
Reehorst	NACA23014(mod)	Jan. 1998	68.7"	1-29-run4R	1-21-run8	172.1	88.5	30	267.85	3	2.7	0.52	40	5	36"
Reehorst	NACA23014(mod)	Jan. 1998	68.7"	1-29-run5R	1-22-run3	172.1	88.5	30	267.85	3	2.7	0.58	70	5	36"
Reehorst	NACA23014(mod)	Jan. 1998	68.7"	1-29-run6		172.1	88.5	30	267.85	3	2.7	0.60	100	5	36"
Reehorst	NACA23014(mod)	Jan. 1998	68.7"	1-29-run7R	1-21-run2	172.1	88.5	30	267.85	7	6.2	0.80	20	5	36"
Reehorst	NACA23014(mod)	Jan. 1998	68.7"	1-29-run8R	1-21-run3	172.1	88.5	30	267.85	7	6.2	0.80	40	5	36"
Reehorst	NACA23014(mod)	Jan. 1998	68.7"	1-30-run2R	1-21-run4	172.1	88.5	30	267.85	7	6.2	0.52	40	5	36"
Reehorst	NACA23014(mod)	Jan. 1998	68.7"	1-30-run3R	1-21-run5	172.1	88.5	30	267.85	7	6.2	0.58	70	5	36"
Reehorst	NACA23014(mod)	Jan. 1998	68.7"	1-30-run4		172.1	88.5	30	267.85	7	6.2	0.60	100	5	36"

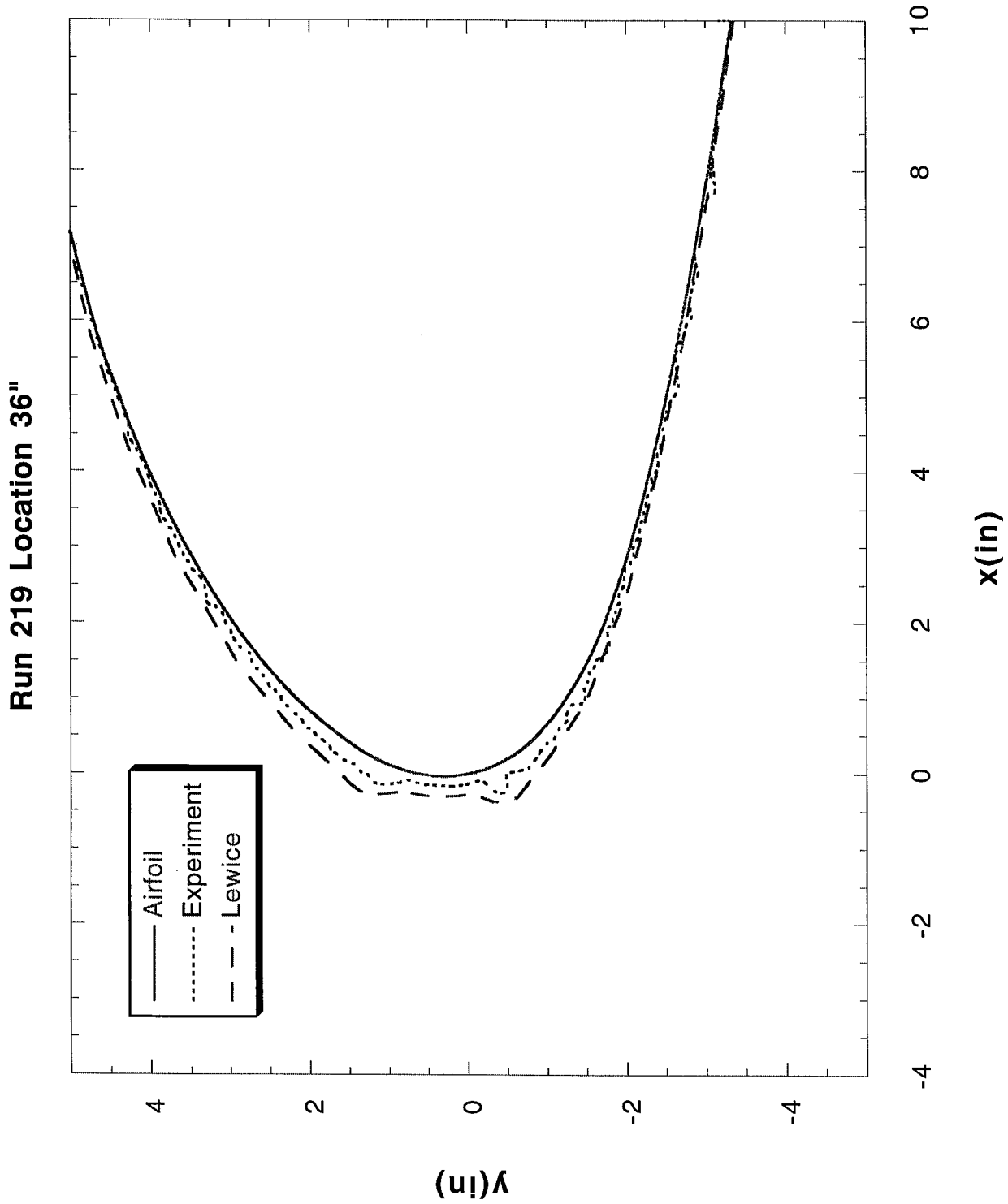
Run 219 Location 36"
Airfoil
Experiment
Lewice
y(in)
x(in)
4
2
0
-2
-4
-4
-2
0
2
4
6
8
10

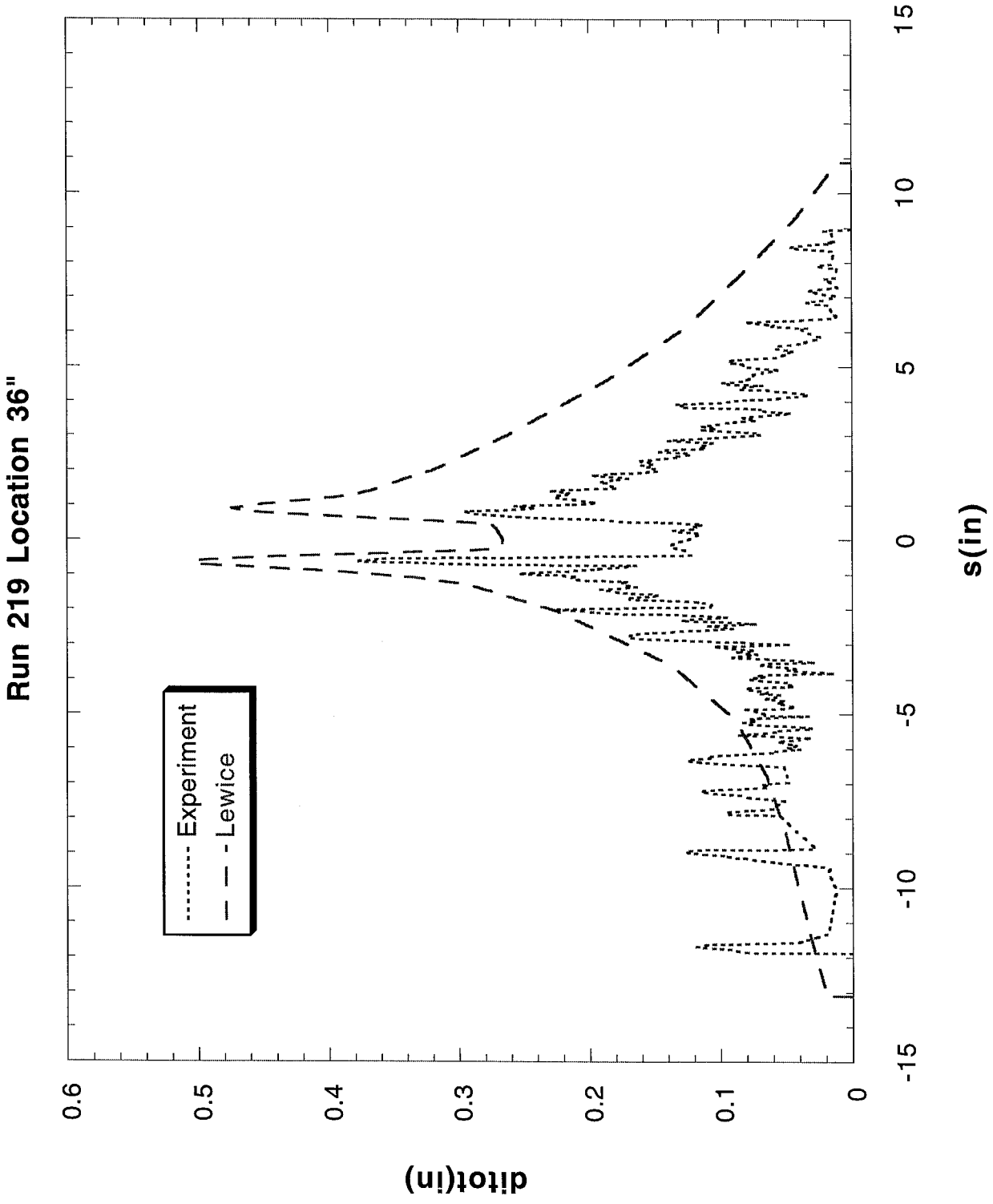
Run 219 Location 36"
Experiment
Lewice
ditot(in)
s(in)
0.6
0.5
0.4
0.3
0.2
0.1
0
-15
-10
-5
0
5
10
15

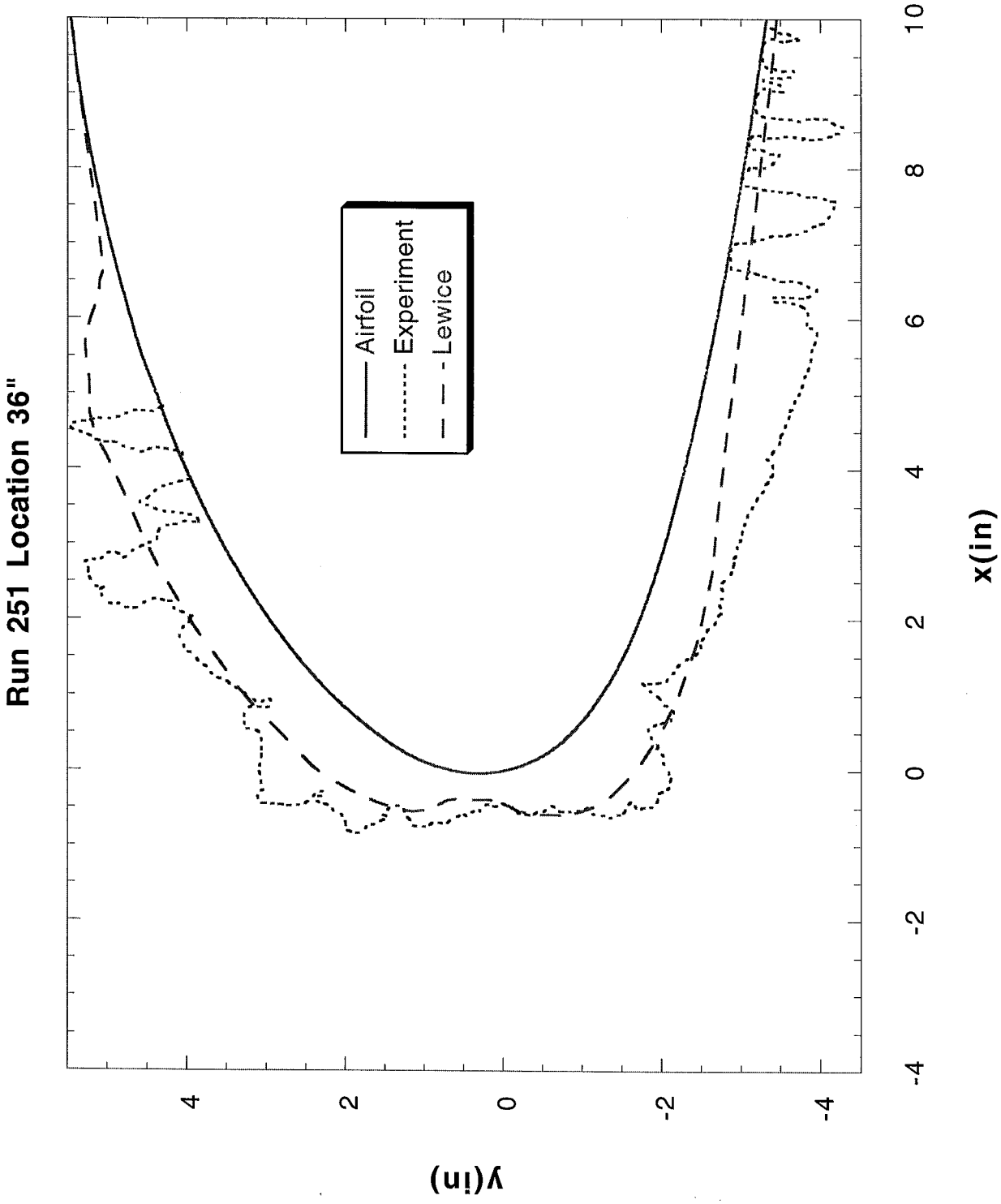
Run 251 Location 36"
Airfoil
Experiment
Lewice
y(in)
x(in)
4
2
0
-2
-4
-4
-2
0
2
4
6
8
10

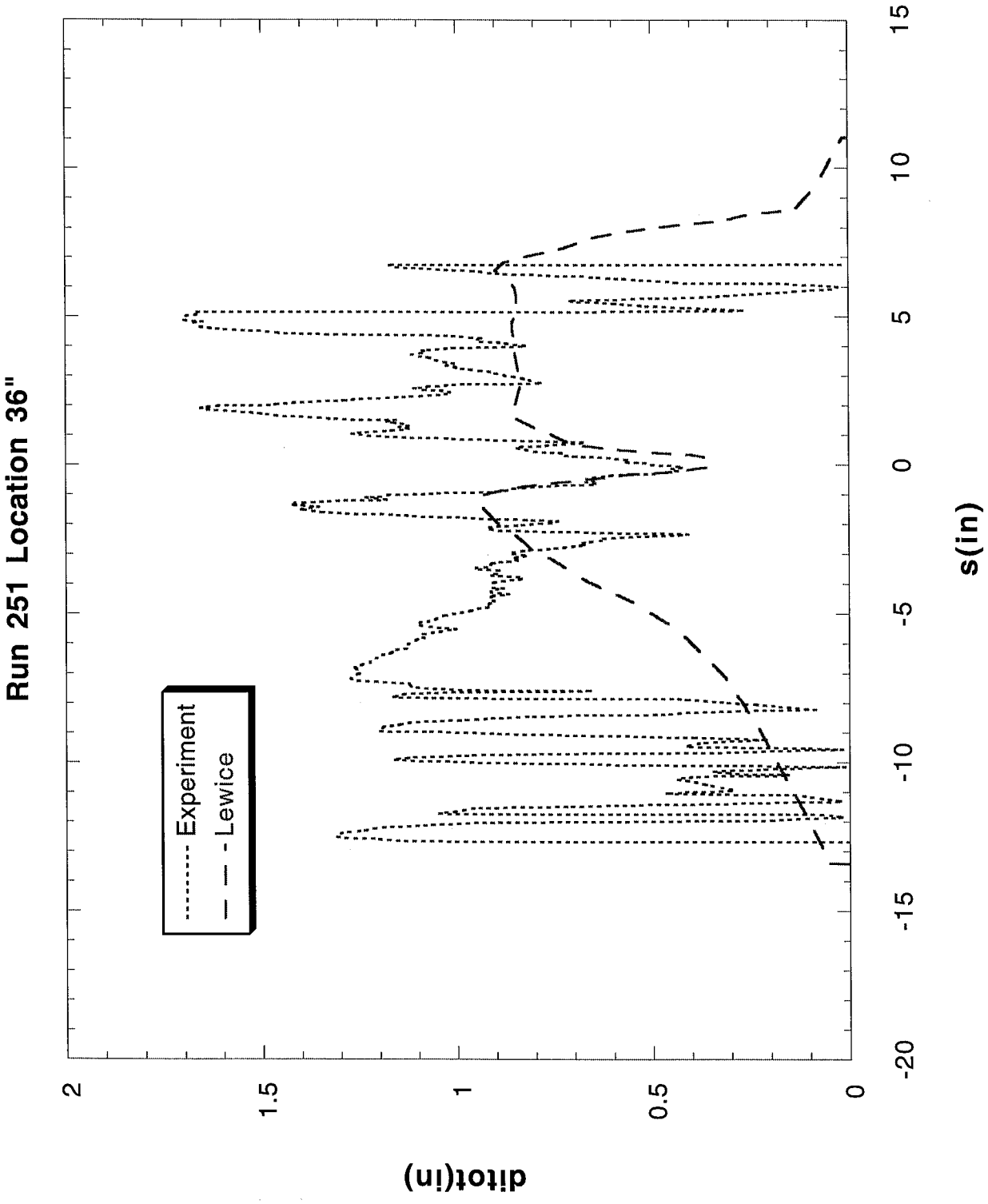
Run 251 Location 36"
Experiment
Lewice
dltot(in)
s(in)
2
1.5
1
0.5
0
-20
-15
-10
-5
0
5
10
15

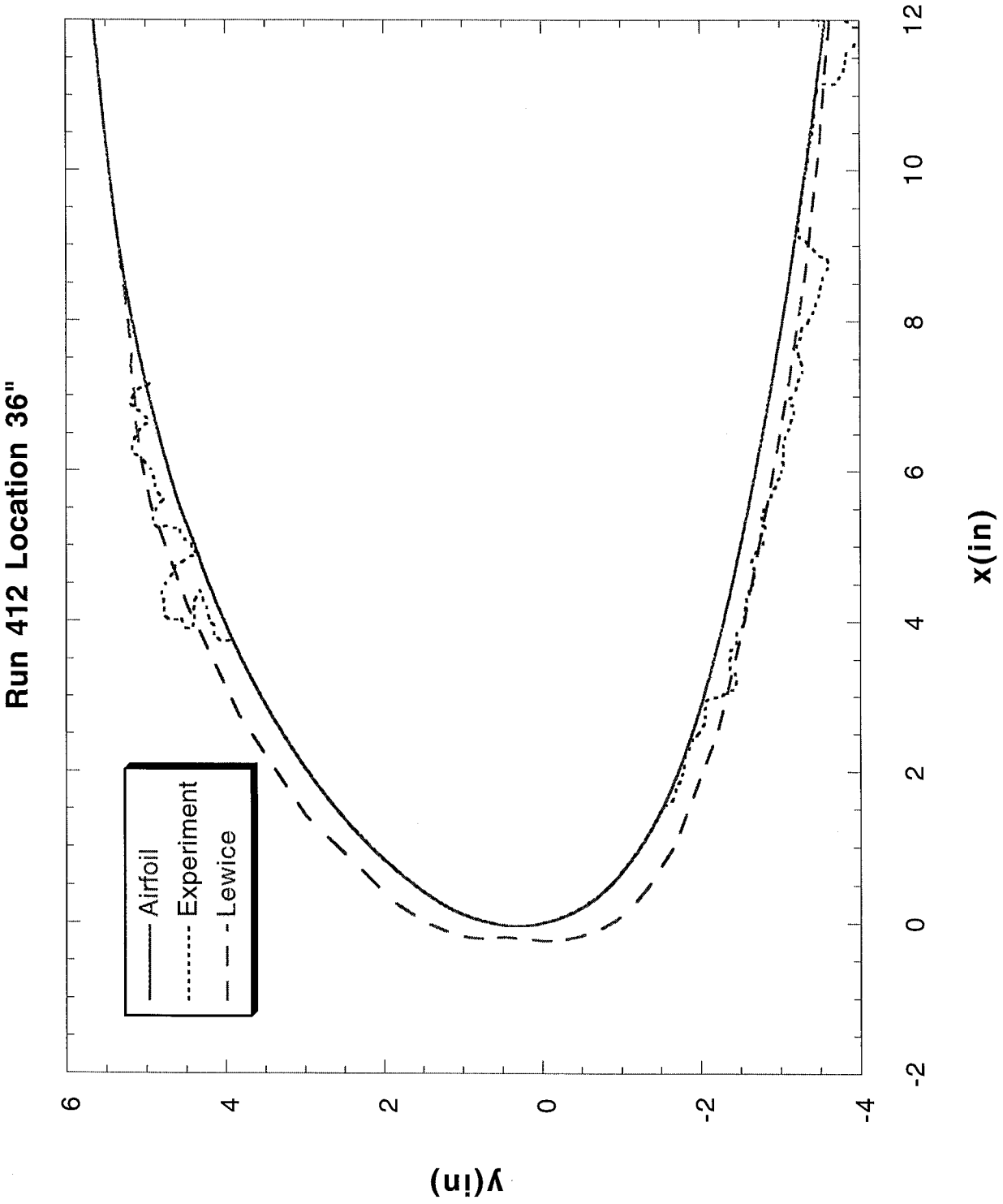
Run 412 Location 36"
Airfoil
Experiment
Lewice
y(in)
x(in)
6
4
2
0
-2
-4
-2
0
2
4
6
8
10
12

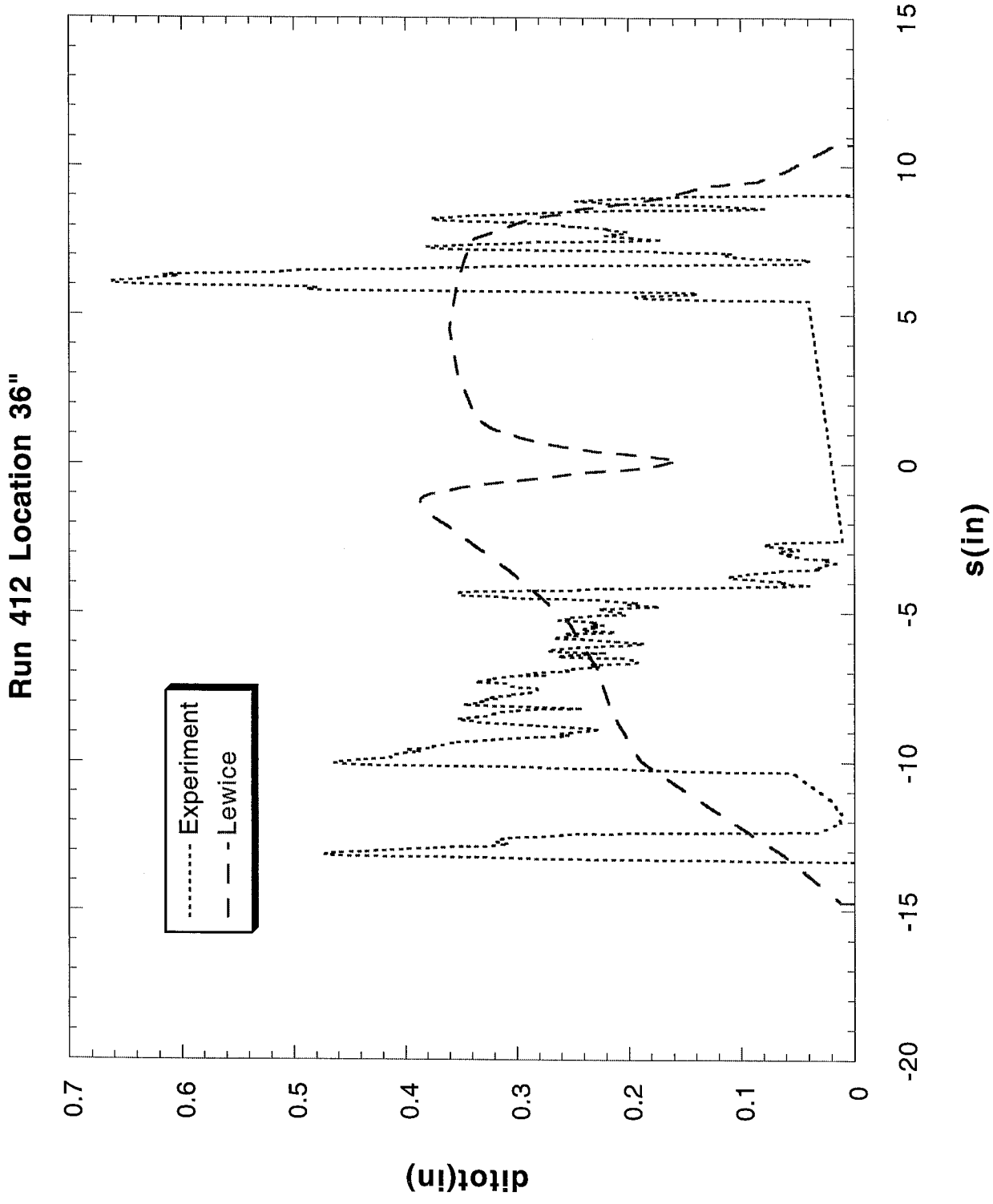
Run 412 Location 36"
Experiment
Lewice
dltot(in)
s(in)
0
0.1
0.2
0.3
0.4
0.5
0.6
0.7
-20
-15
-10
-5
0
5
10
15

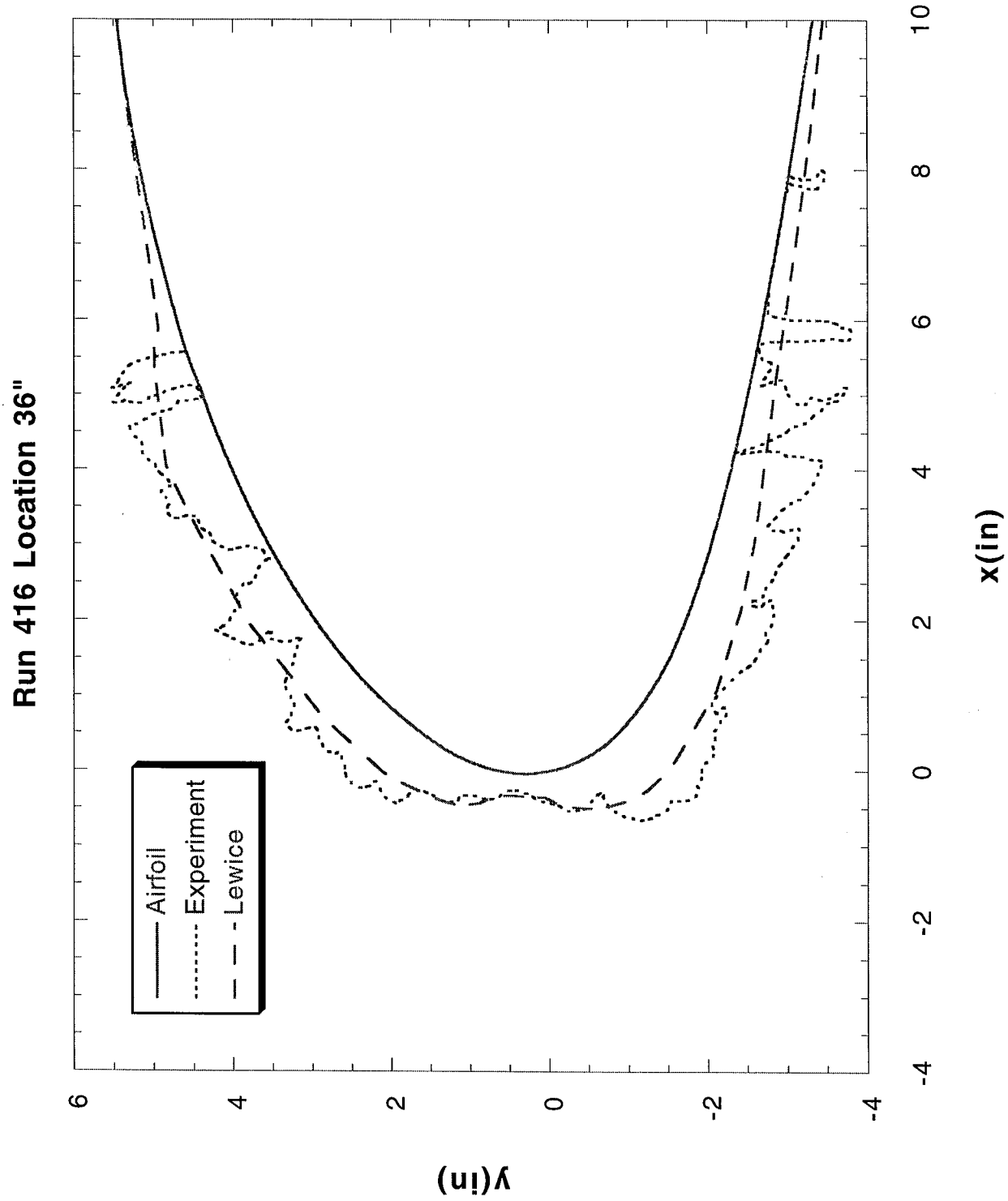
Run 416 Location 36"
Airfoil
Experiment
Lewice
y(in)
x(in)
6
4
2
0
-2
-4
-4
-2
0
2
4
6
8
10

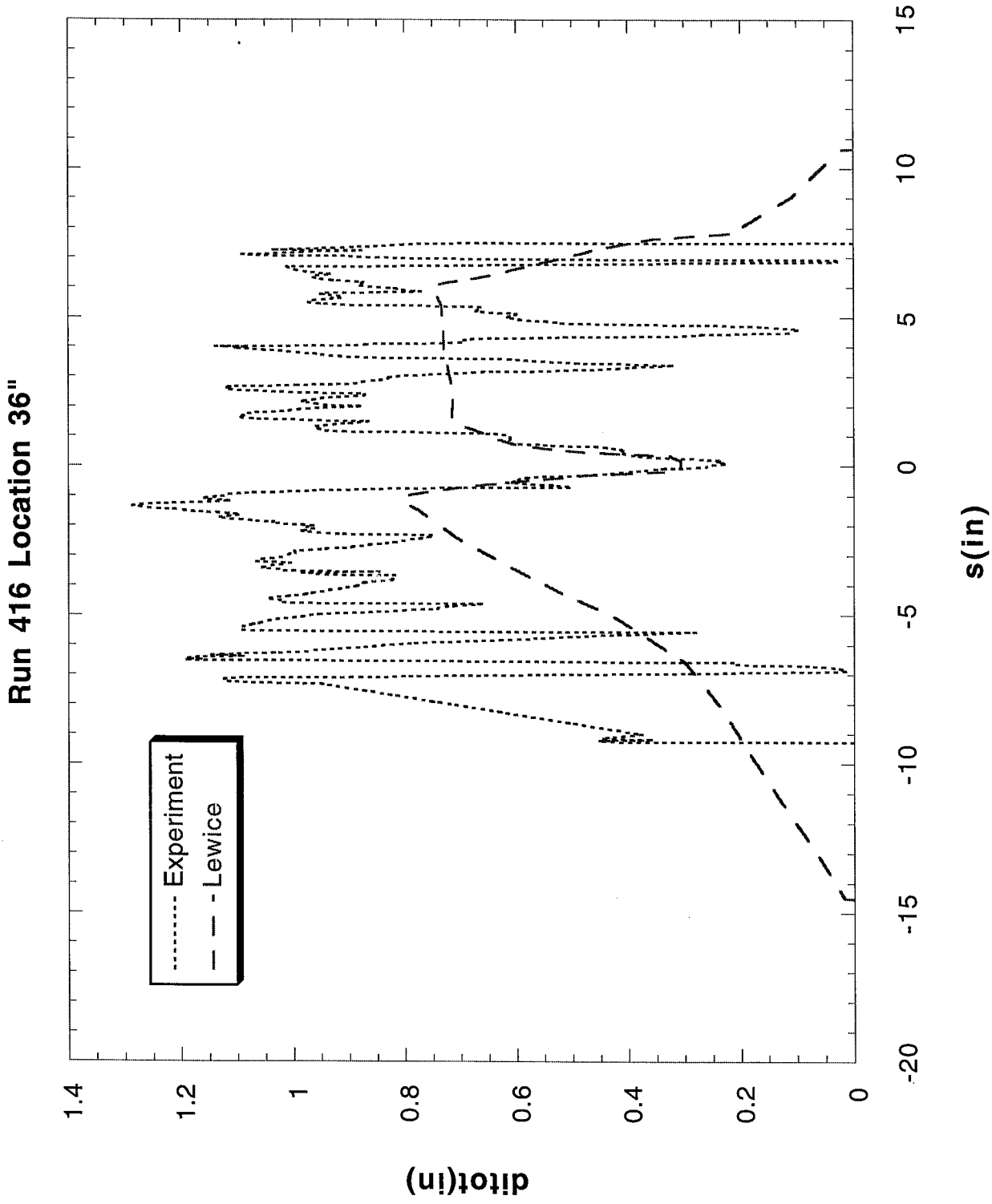
Run 416 Location 36"
Experiment
Lewice
ditot(in)
s(in)
1.4
1.2
1
0.8
0.6
0.4
0.2
0
-20
-15
-10
-5
0
5
10
15

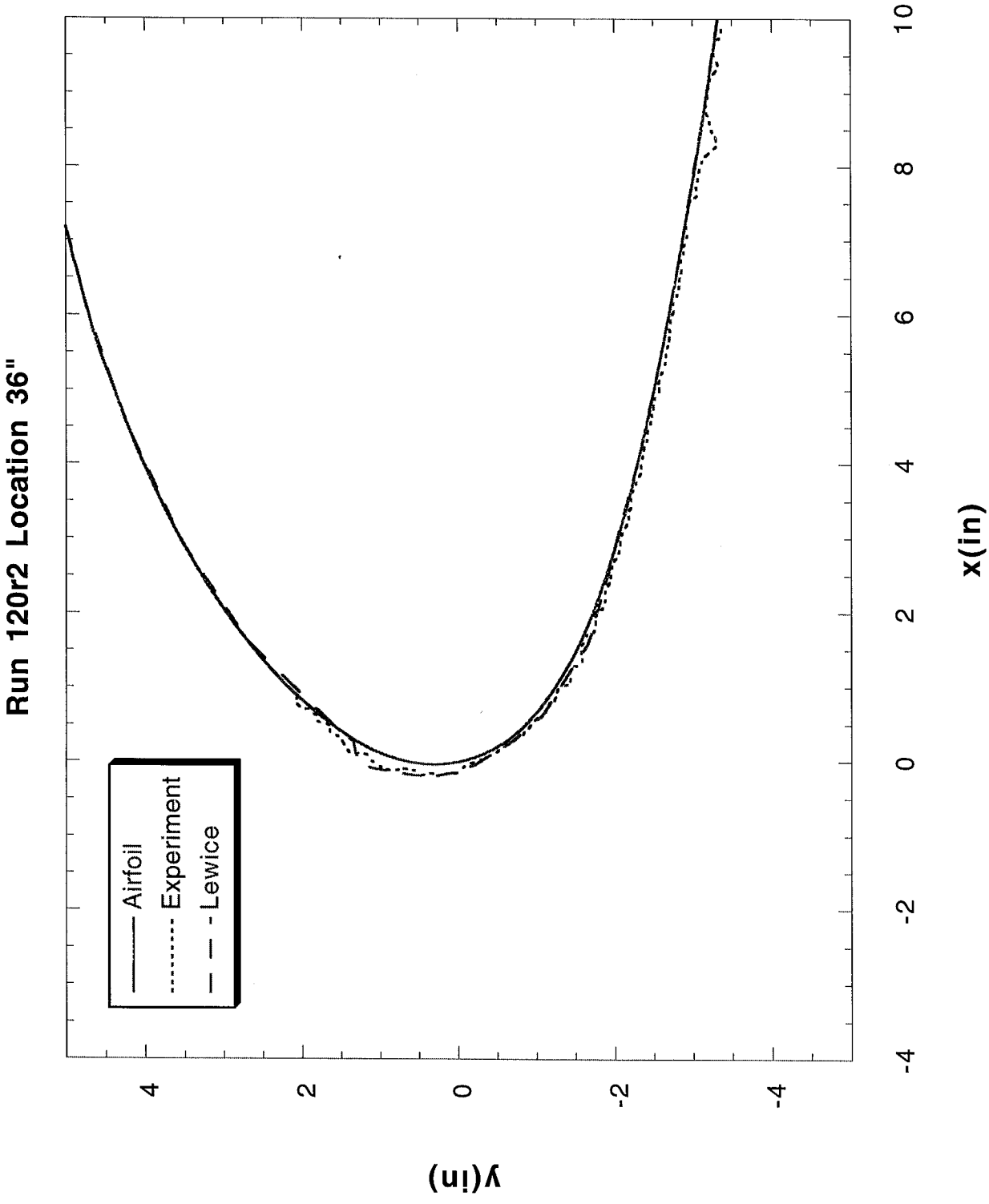
Run 120r2 Location 36"
Airfoil
Experiment
Lewice
y(in)
x(in)
4
2
0
-2
-4
-4
-2
0
2
4
6
8
10

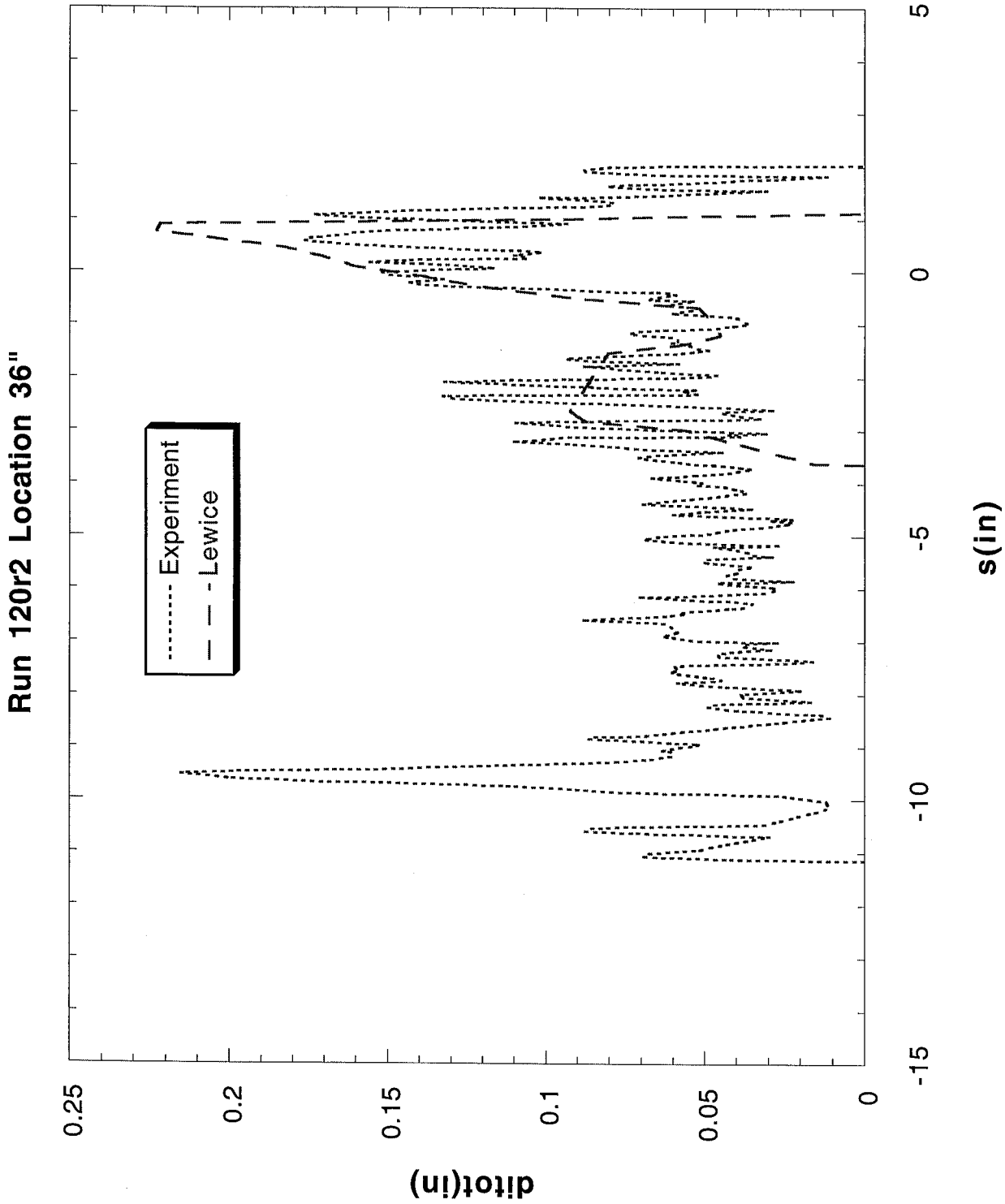
Run 120r2 Location 36"
Experiment
Lewice
dltot(in)
0.25
0.2
0.15
0.1
0.05
0
5
0
-5
-10
-15
s(in)

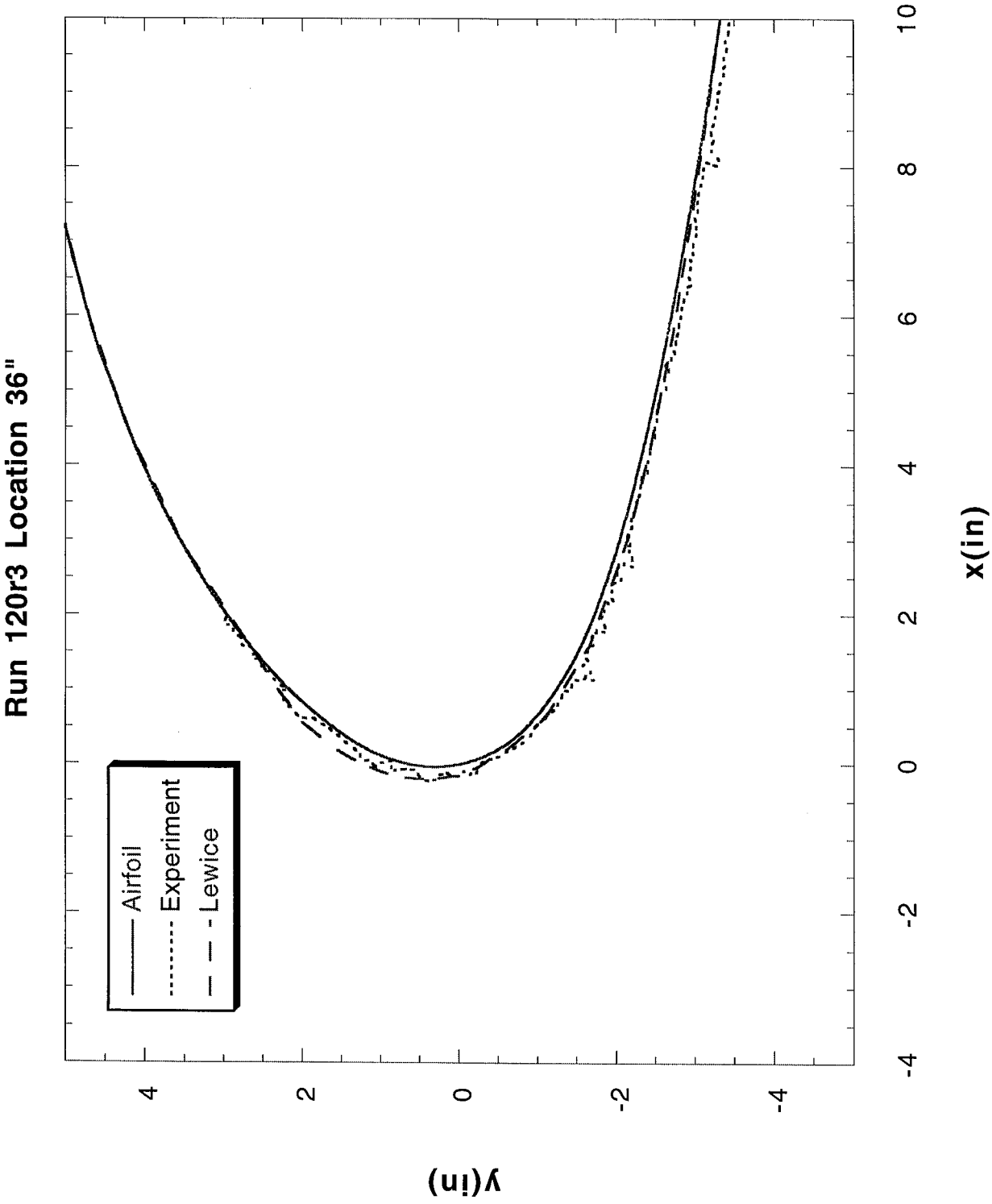
Run 120r3 Location 36"
Airfoil
Experiment
Lewice
y(in)
x(in)
4
2
0
-2
-4
-4
-2
0
2
4
6
8
10

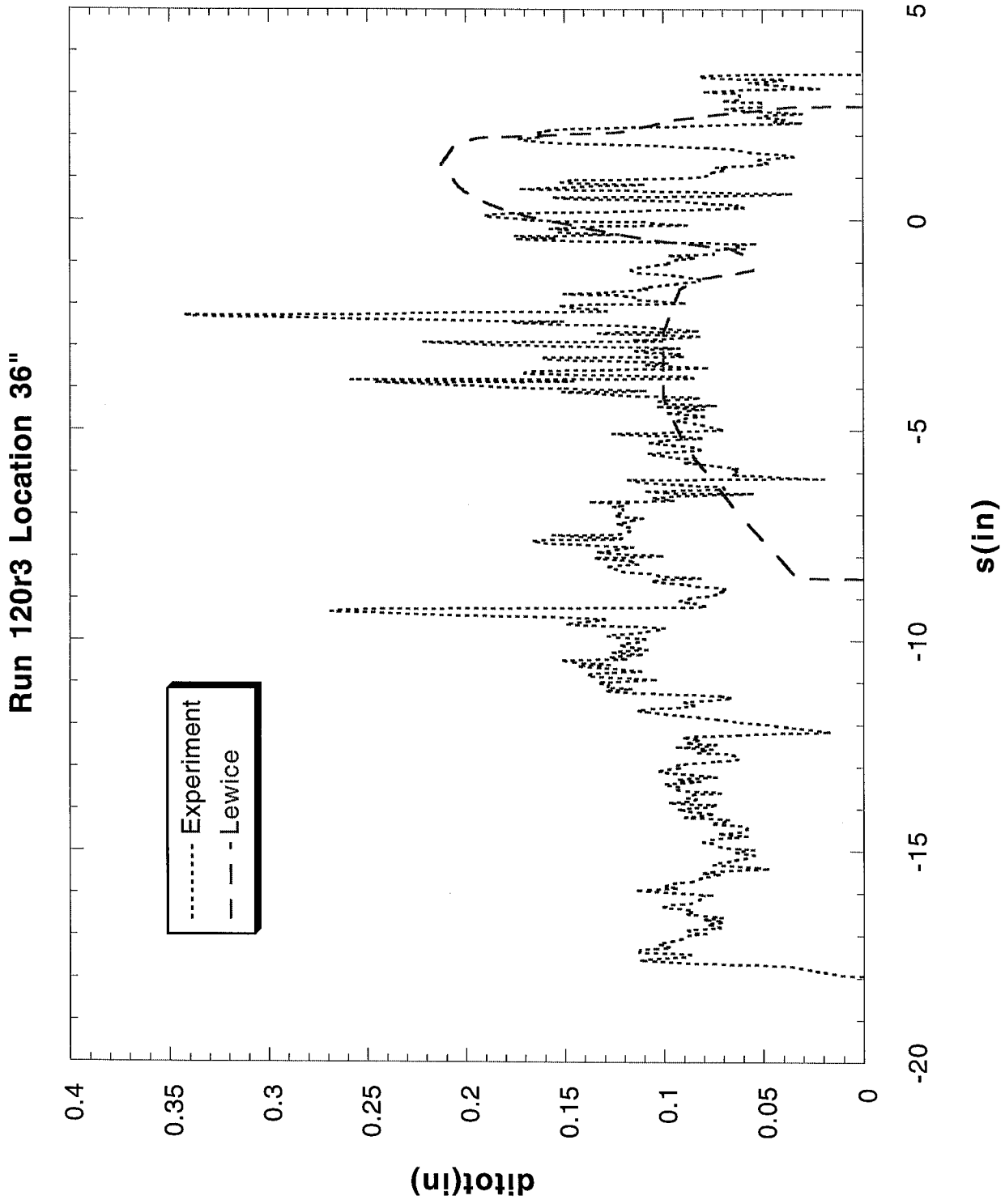
Run 120r3 Location 36"
Experiment
Lewice
dltot(in)
s(in)
0.4
0.35
0.3
0.25
0.2
0.15
0.1
0.05
0
5
0
-5
-10
-15
-20

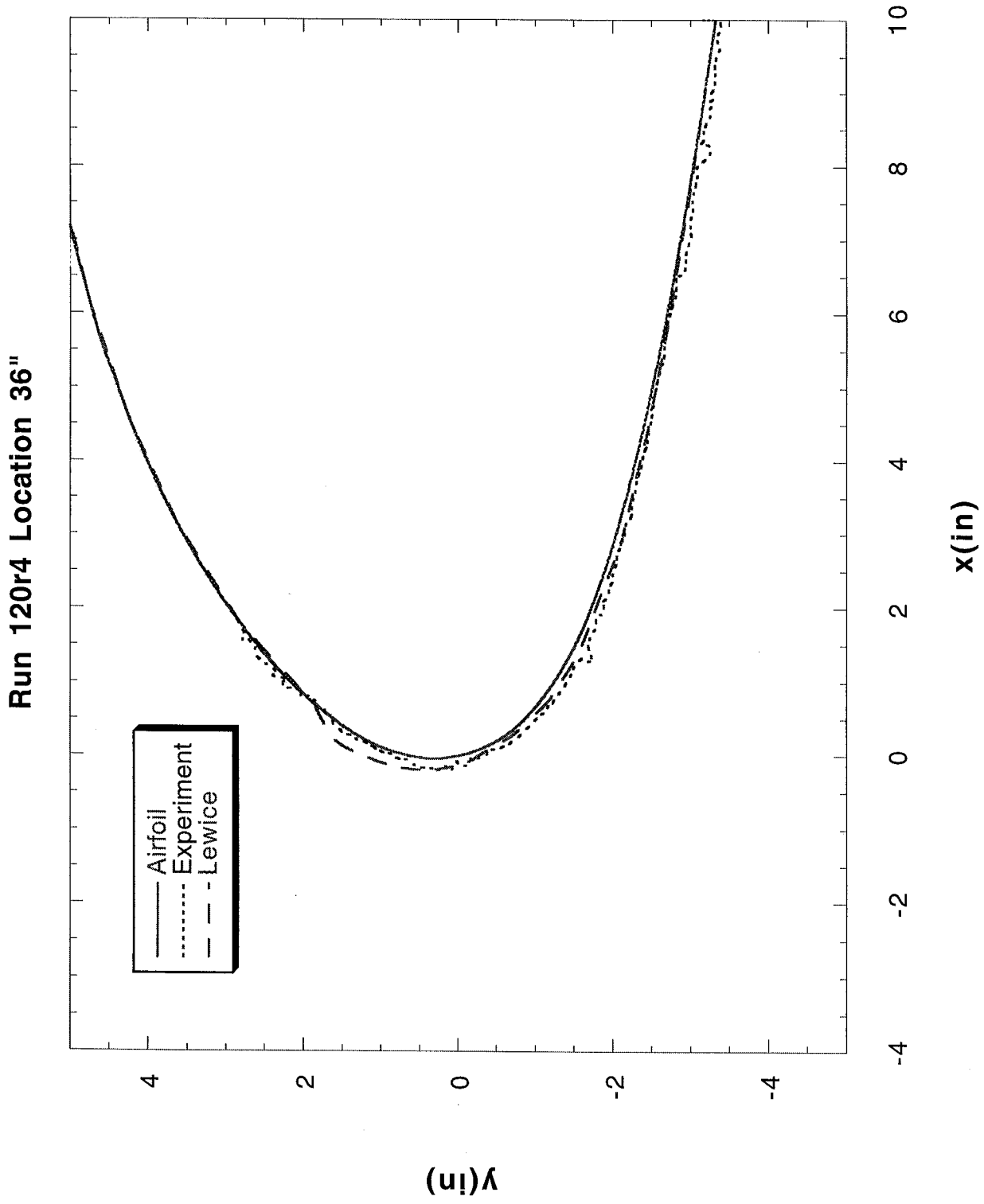
Run 120r4 Location 36"
Airfoil
Experiment
Lewice
y(in)
x(in)
4
2
0
-2
-4
-4
-2
0
2
4
6
8
10

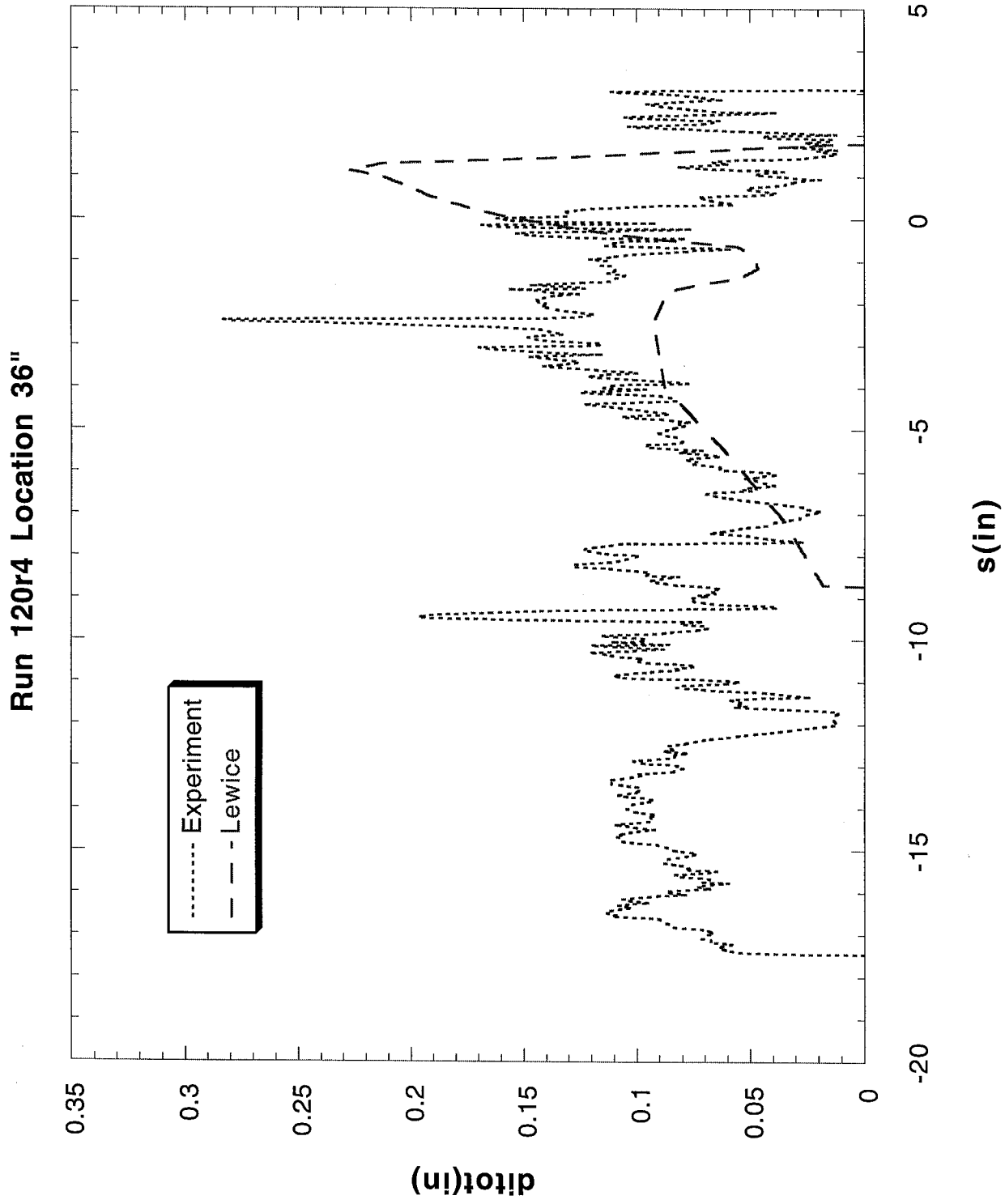
Run 120r4 Location 36"
Experiment
Lewice
dltot(in)
0.35
0.3
0.25
0.2
0.15
0.1
0.05
0
5
0
-5
-10
-15
-20
s(in)

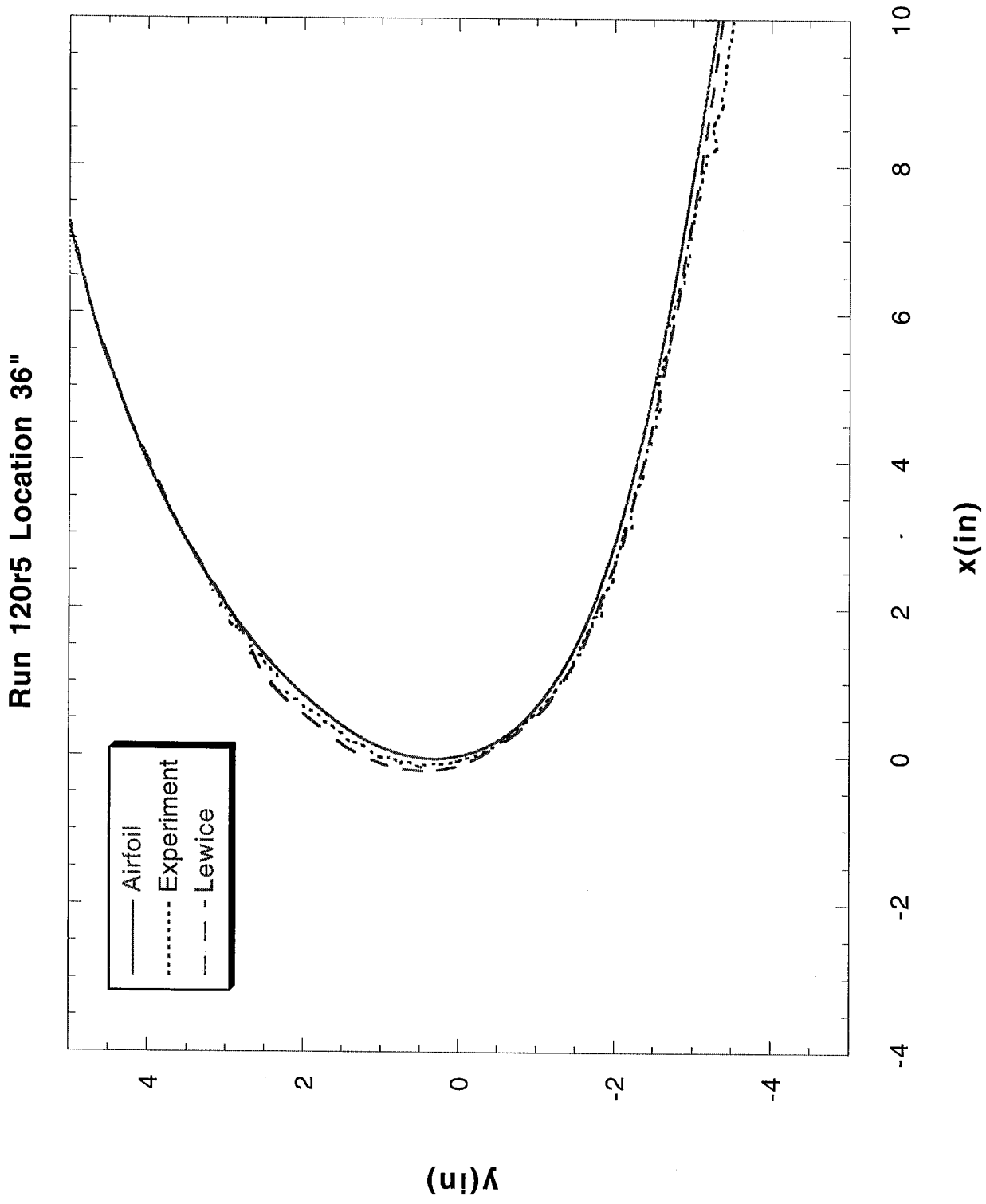
Run 120r5 Location 36"
Airfoil
Experiment
Lewice
y(in)
x(in)
4
2
0
-2
-4
-4
-2
0
2
4
6
8
10

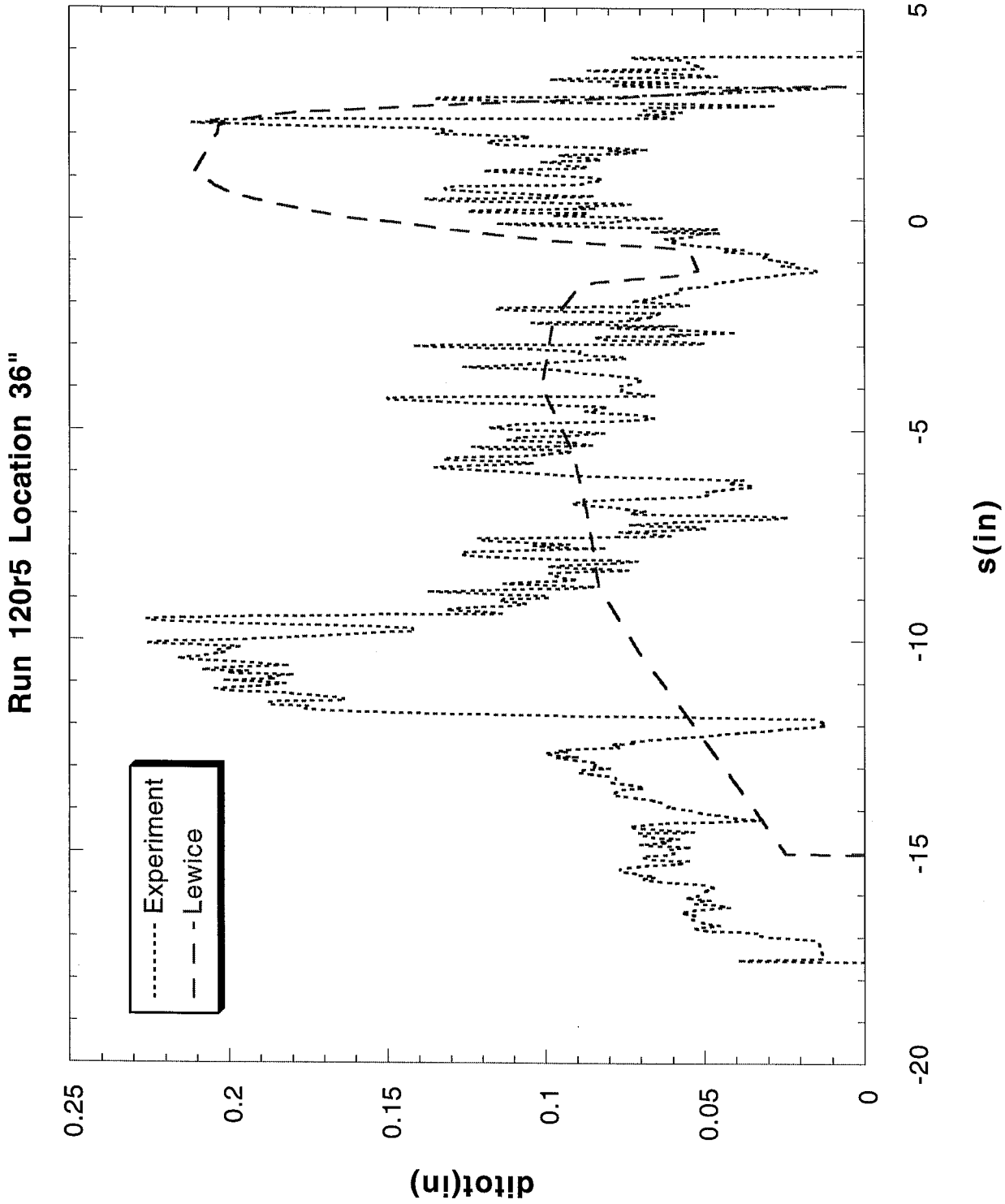
Run 120r5 Location 36"
Experiment
Lewice
dltot(in)
s(in)
0.25
0.2
0.15
0.1
0.05
0
5
0
-5
-10
-15
-20

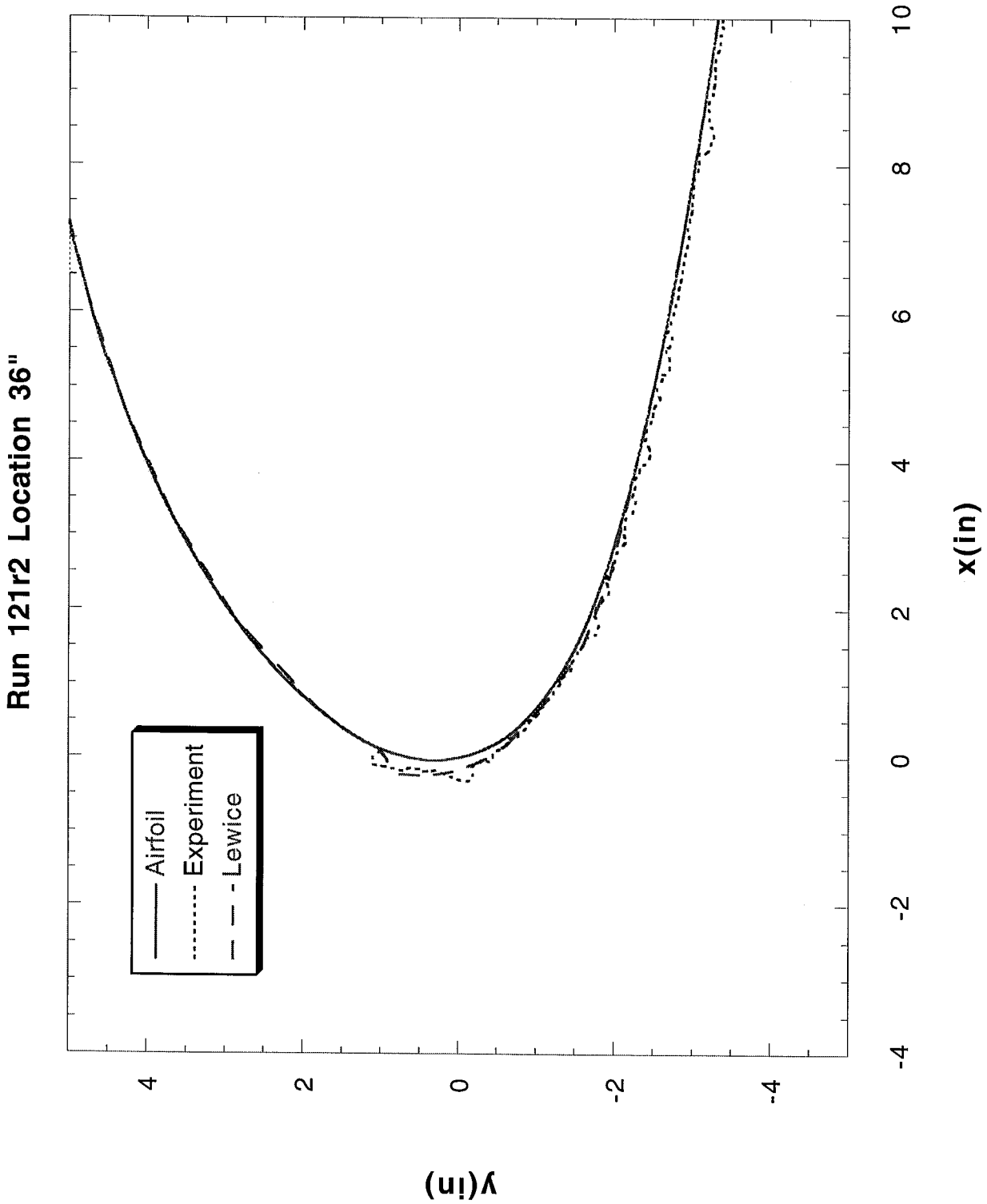
Run 121r2 Location 36"
Airfoil
Experiment
Lewice
y(in)
x(in)
4
2
0
-2
-4
-4
-2
0
2
4
6
8
10

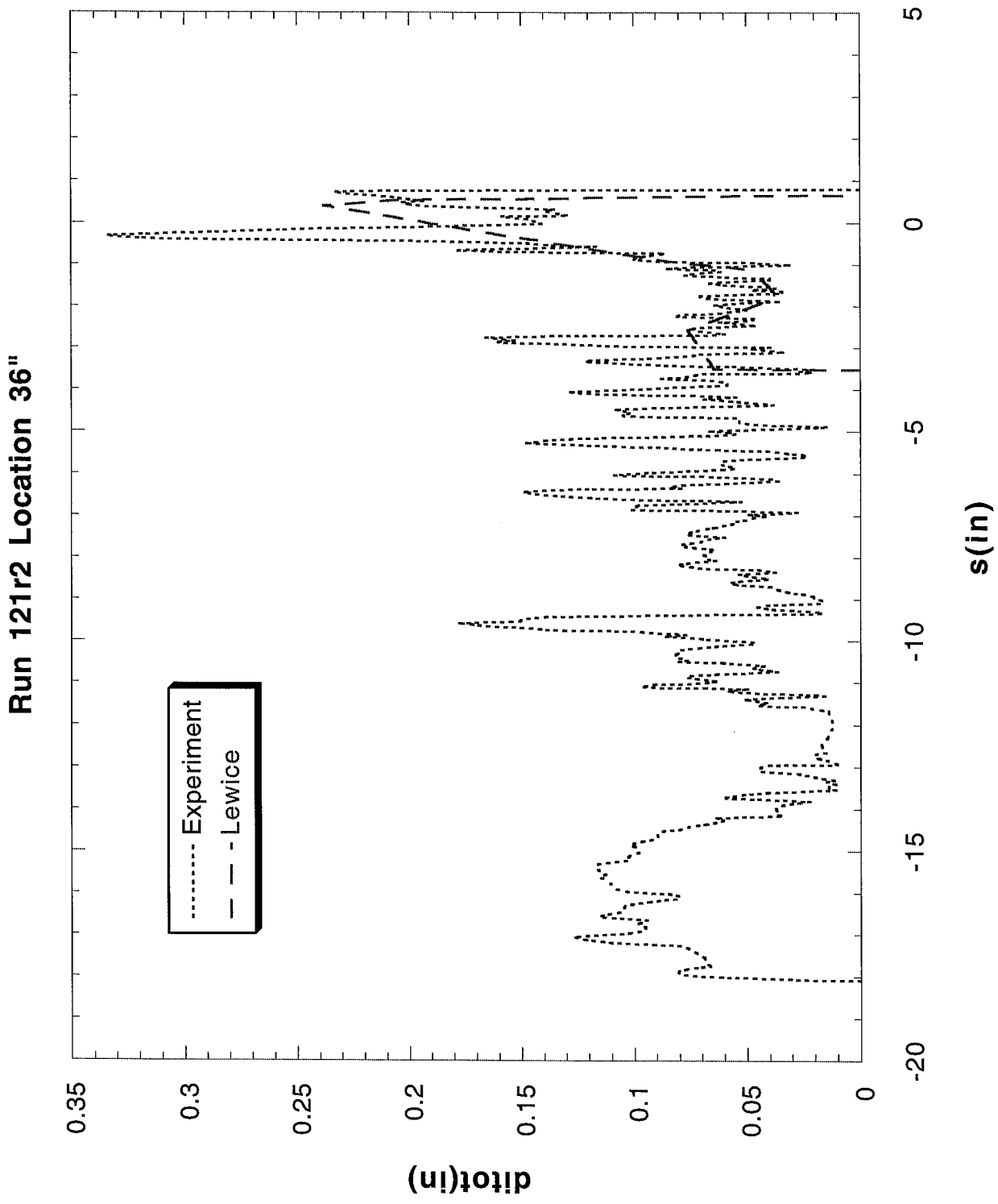
Run 121r2 Location 36"
Experiment
Lewice
dltot(in)
0.35
0.3
0.25
0.2
0.15
0.1
0.05
0
s(in)
5
0
-5
-10
-15
-20

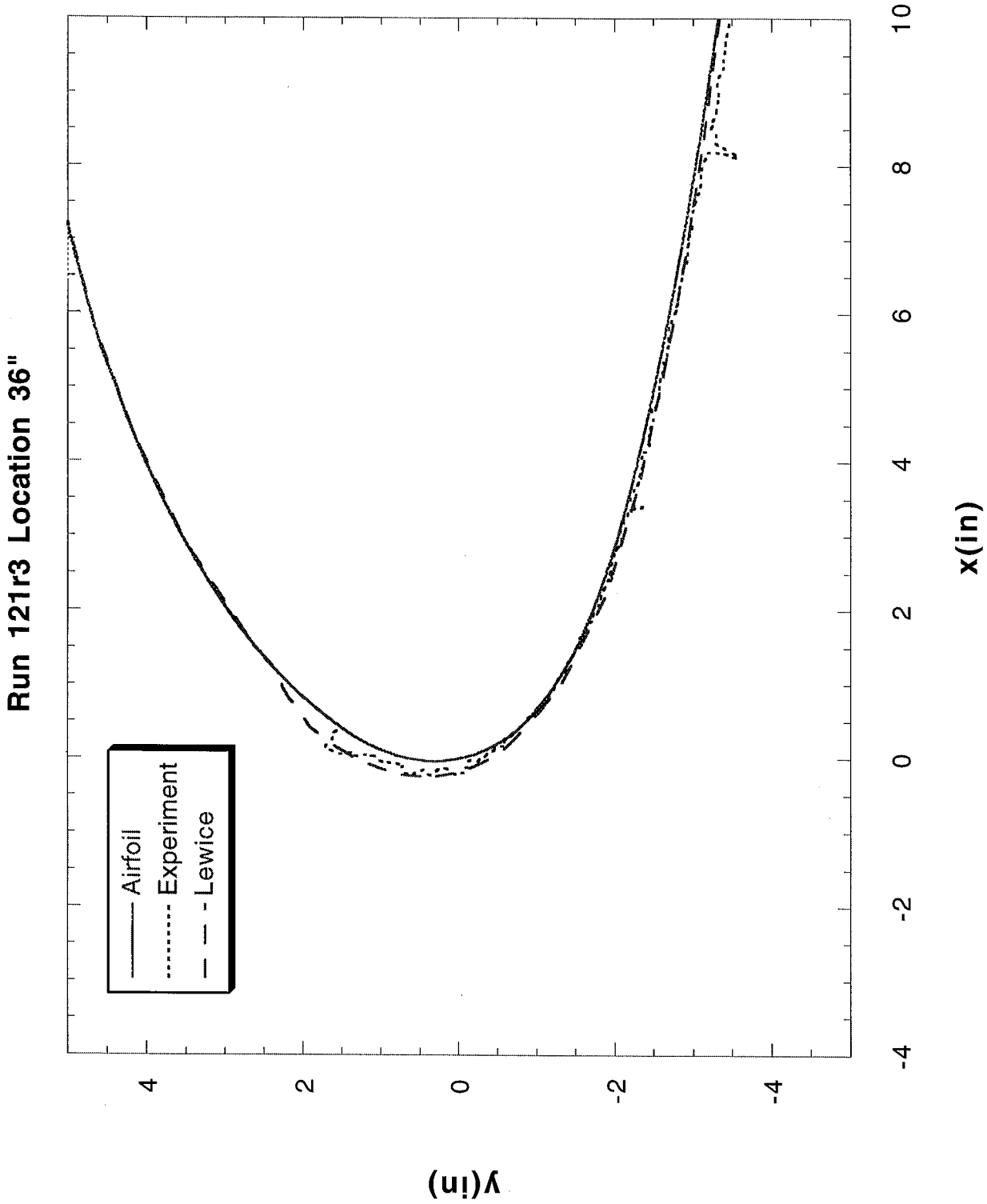
Run 121r3 Location 36"
Airfoil
Experiment
Lewice
y(in)
x(in)
4
2
0
-2
-4
-4
-2
0
2
4
6
8
10

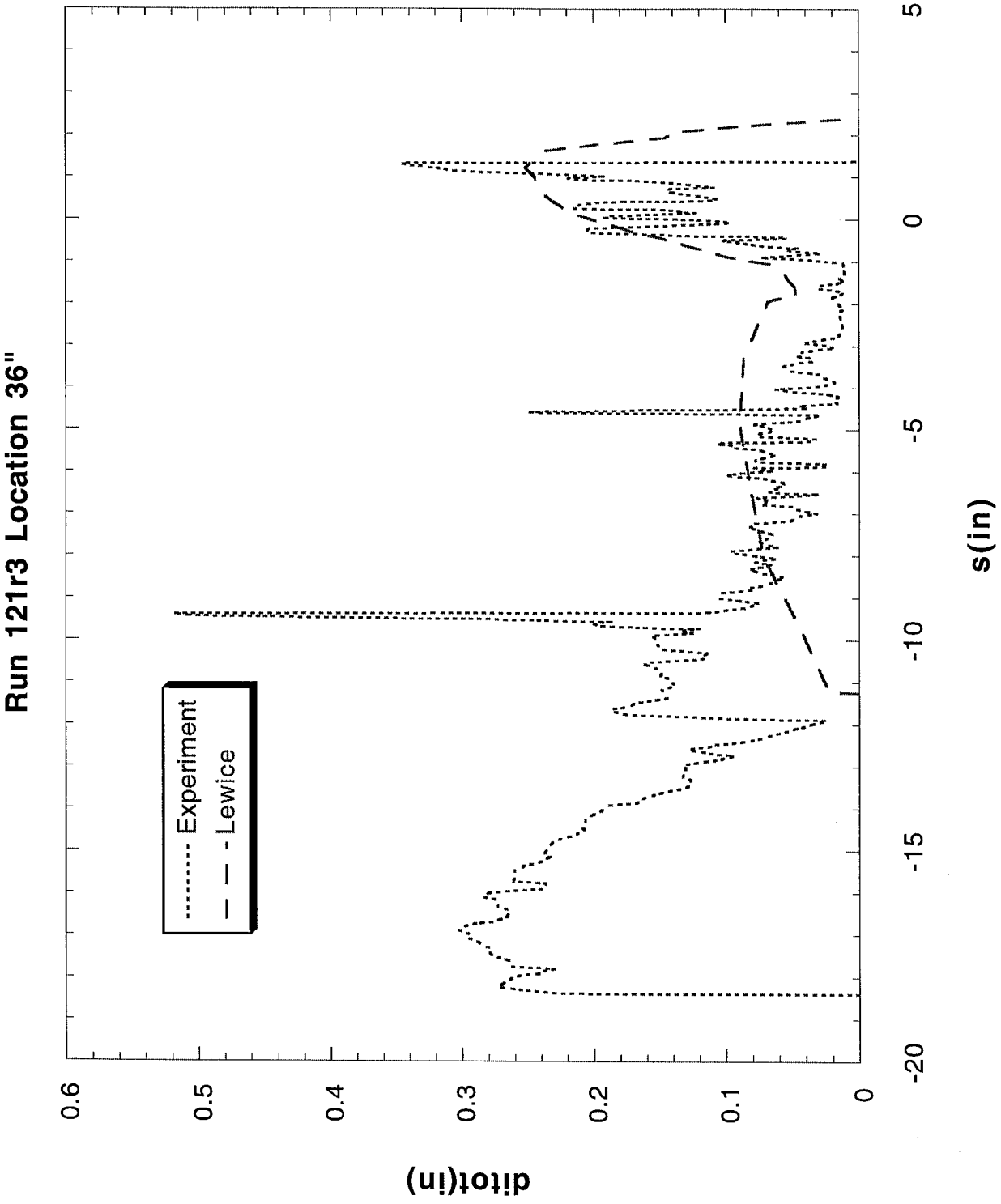
Run 121r3 Location 36"
Experiment
Lewice
dltot(in)
s(in)
0.6
0.5
0.4
0.3
0.2
0.1
0
-20
-15
-10
-5
0
5

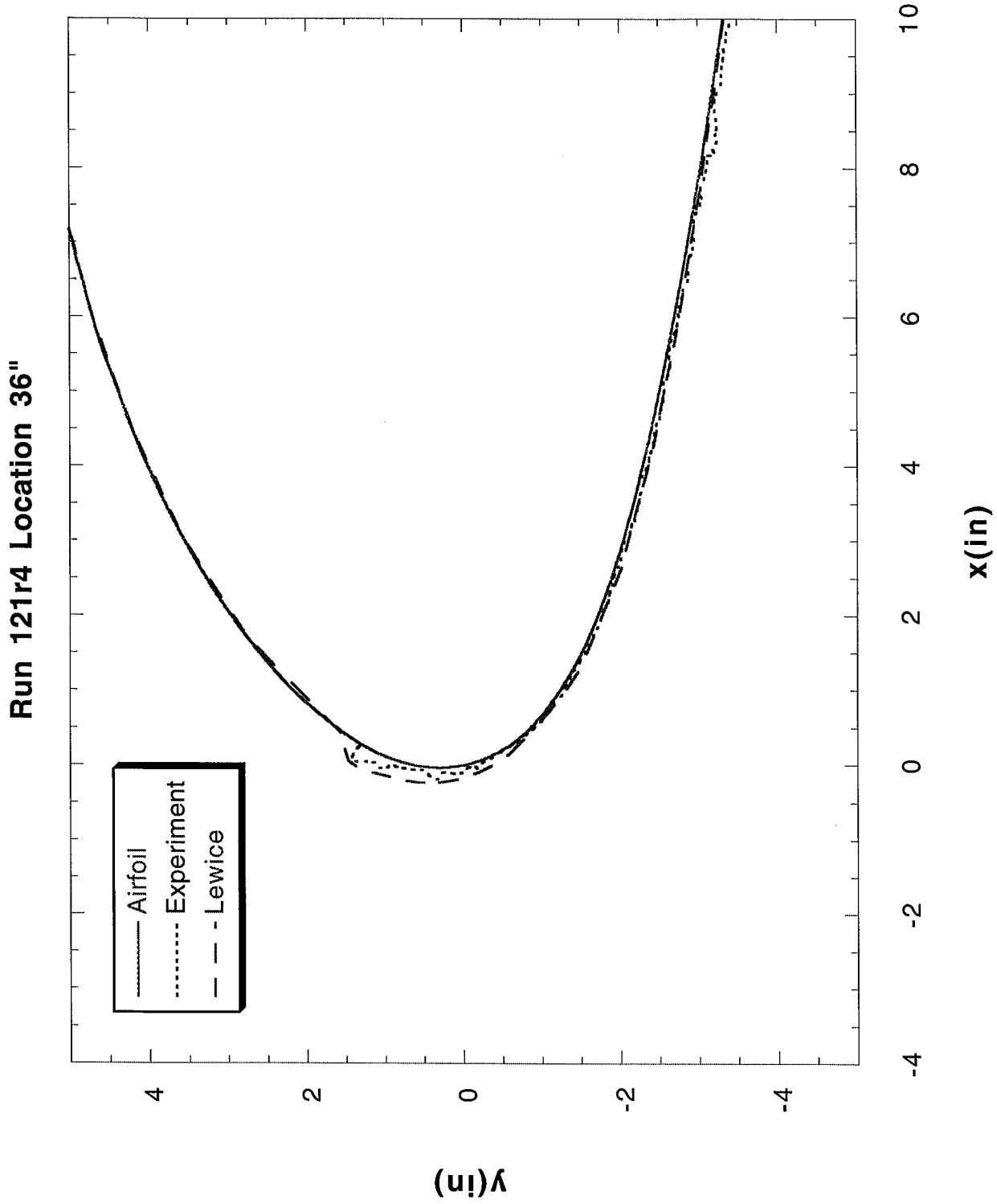
Run 121r4 Location 36"
Airfoil
Experiment
Lewice
y(in)
x(in)
4
2
0
-2
-4
-4
-2
0
2
4
6
8
10

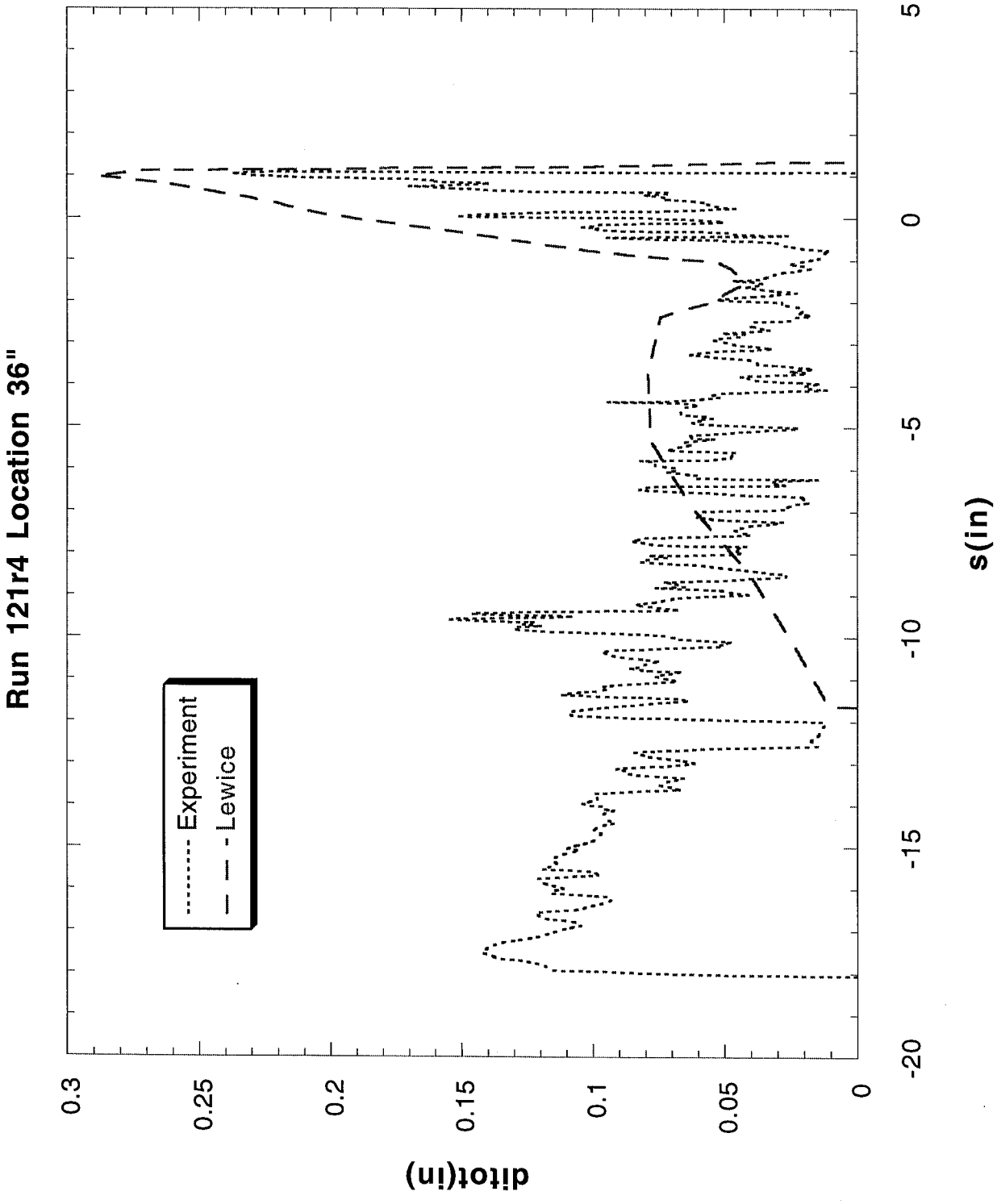
Run 121r4 Location 36"
Experiment
Lewice
dltot(in)
s(in)
0.3
0.25
0.2
0.15
0.1
0.05
0
5
0
-5
-10
-15
-20

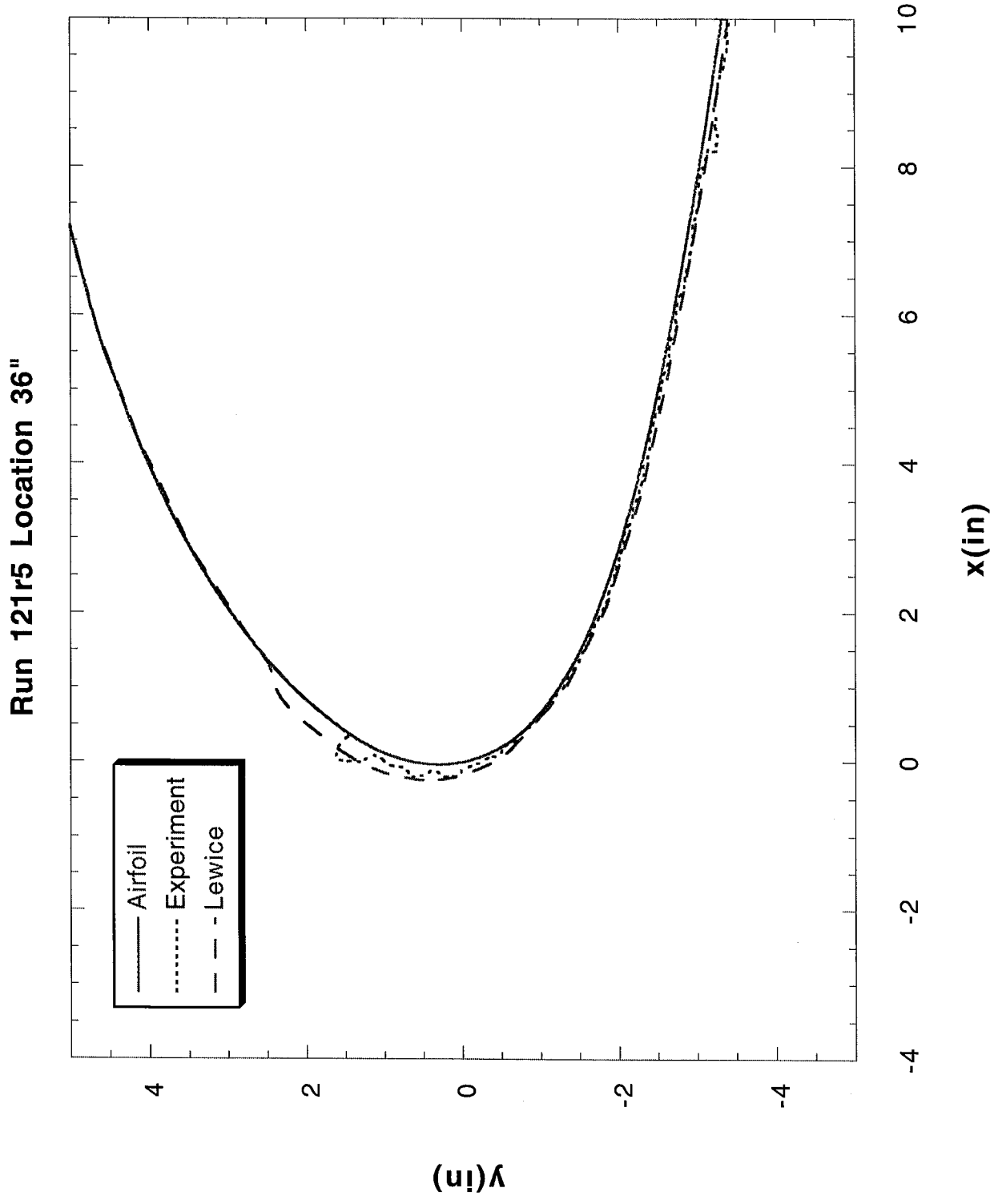
Run 121r5 Location 36"
Airfoil
Experiment
Lewice
y(in)
x(in)
4
2
0
-2
-4
-4
-2
0
2
4
6
8
10

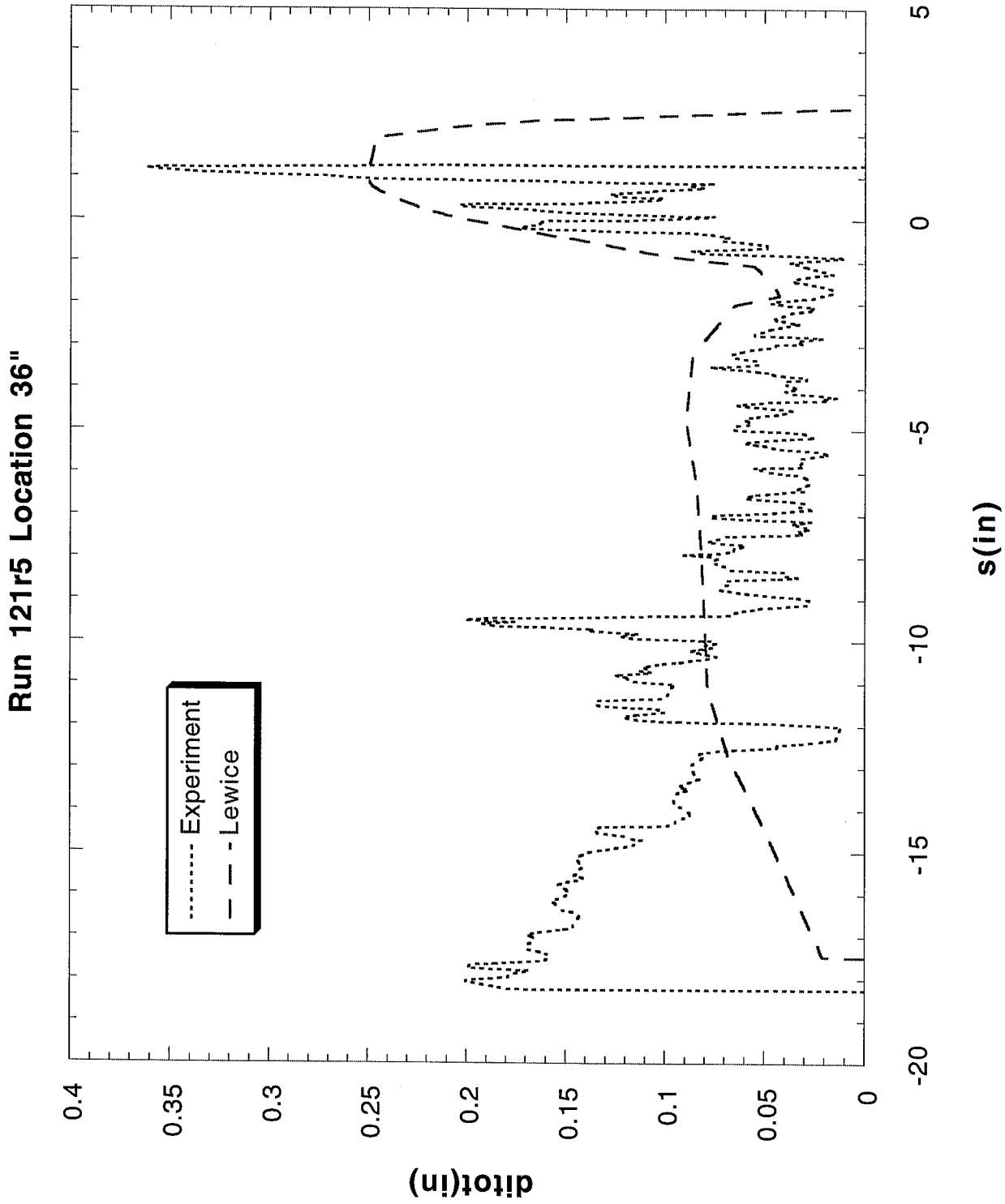
Run 121r5 Location 36"
Experiment
Lewice
ditot(in)
s(in)
0.4
0.35
0.3
0.25
0.2
0.15
0.1
0.05
0
5
0
-5
-10
-15
-20

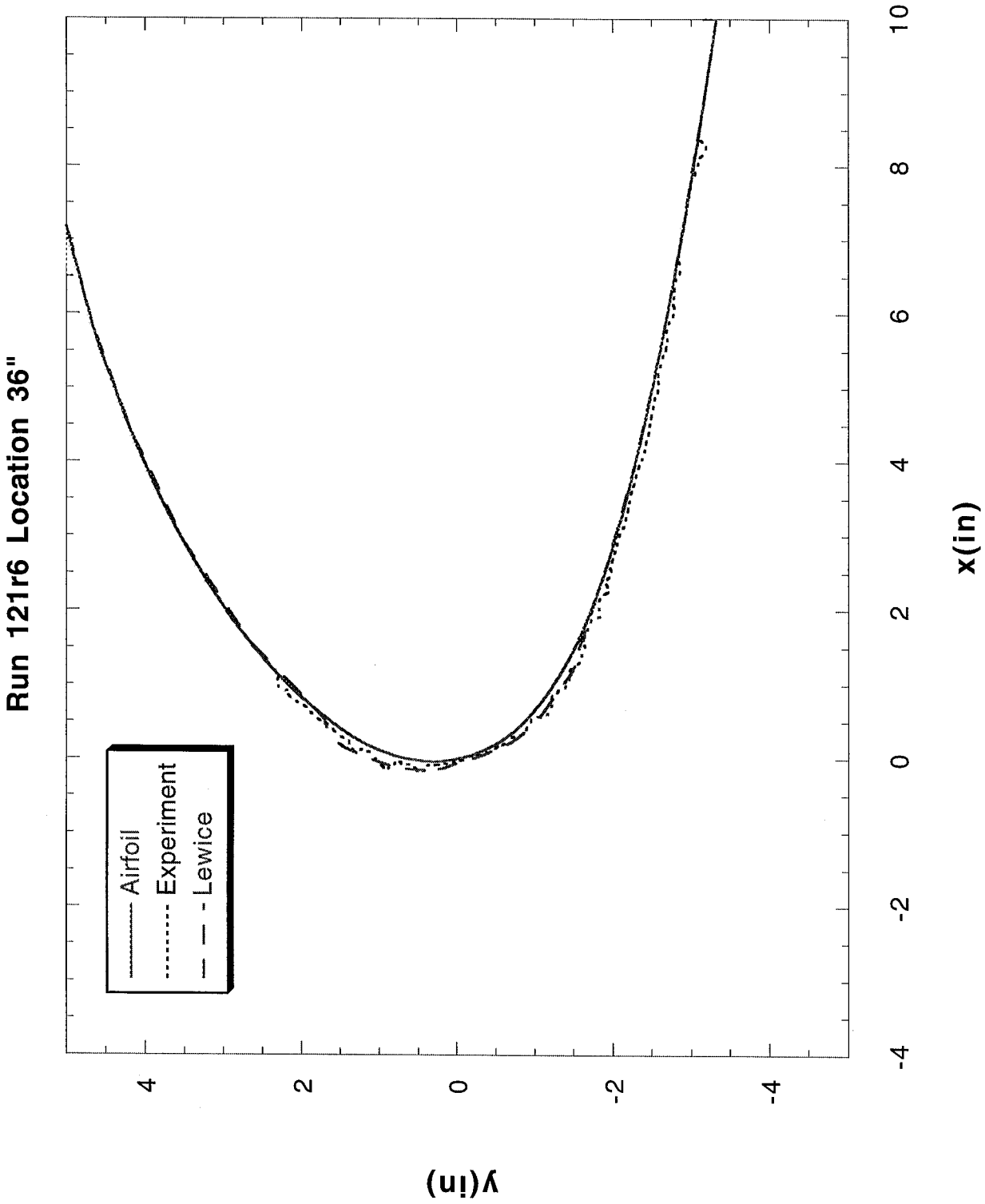
Run 121r6 Location 36"
Airfoil
Experiment
Lewice
y(in)
x(in)
4
2
0
-2
-4
-4
-2
0
2
4
6
8
10

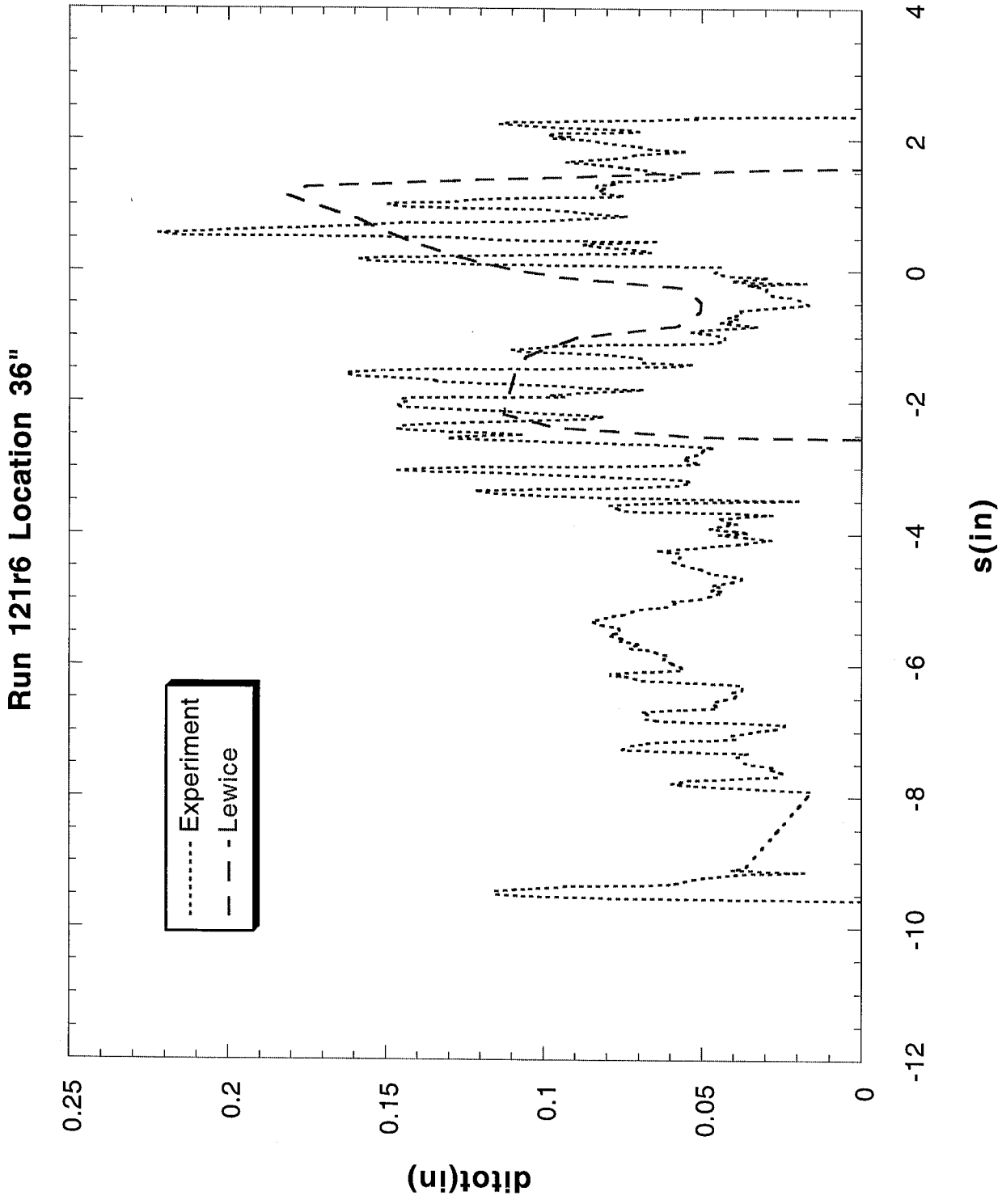
Run 121r6 Location 36"
Experiment
Lewice
ditot(in)
s(in)
0.25
0.2
0.15
0.1
0.05
0
4
2
0
-2
-4
-6
-8
-10
-12

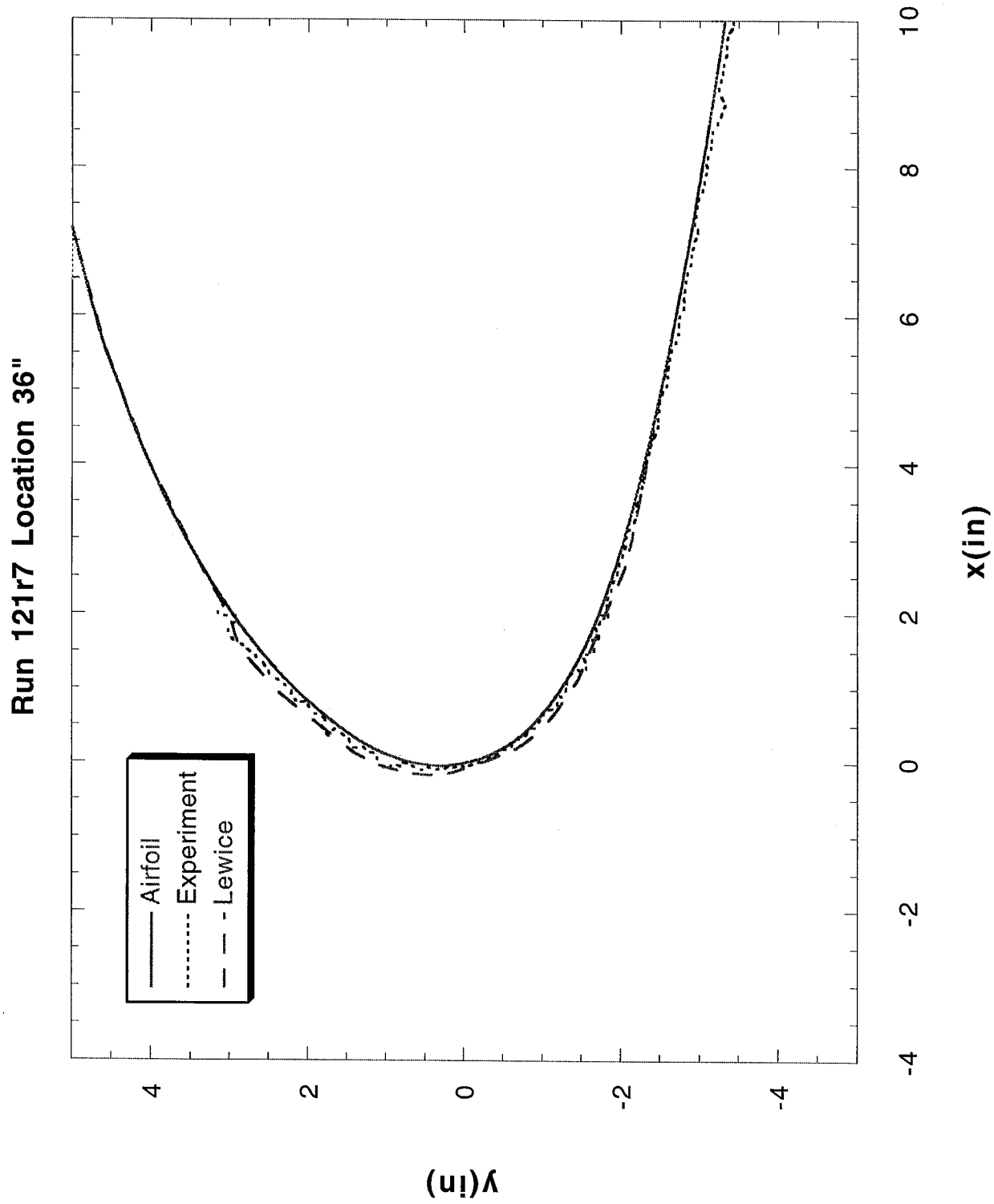
Run 121r7 Location 36"
Airfoil
Experiment
Lewice
y(in)
x(in)
4
2
0
-2
-4
-4
-2
0
2
4
6
8
10

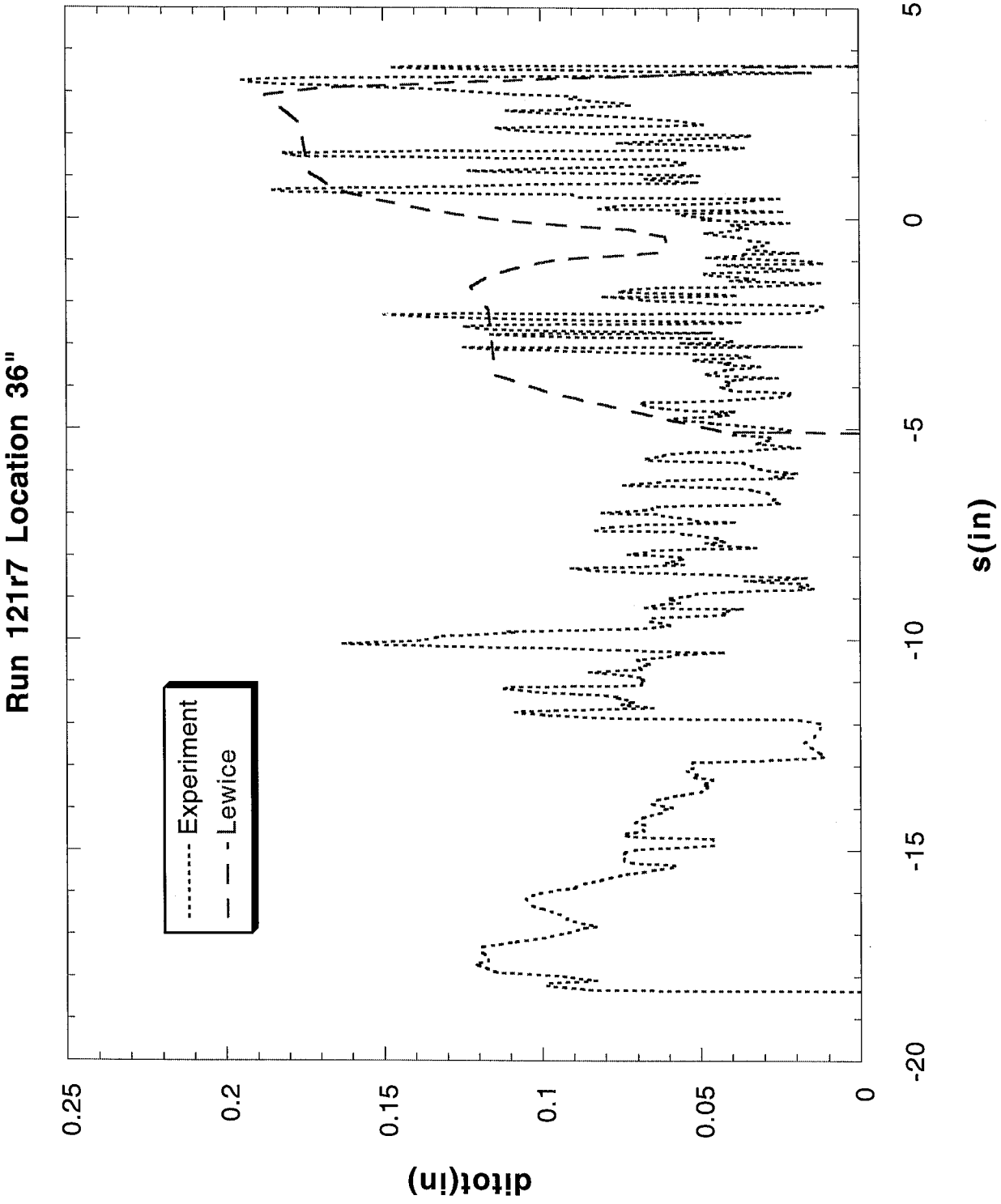
Run 121r7 Location 36"
Experiment
Lewice
dltot(in)
0.25
0.2
0.15
0.1
0.05
0
5
0
-5
-10
-15
-20
s(in)

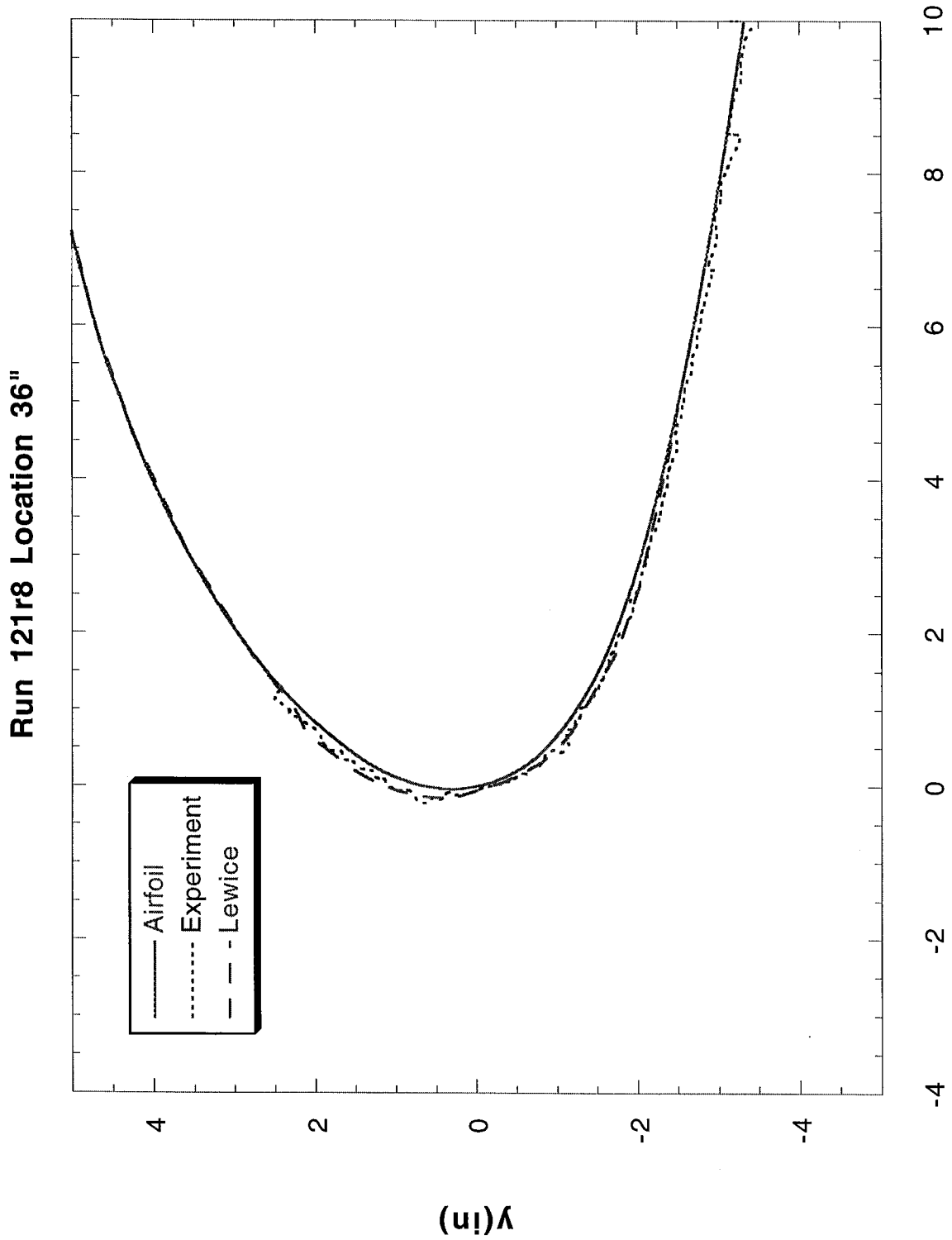
Run 121r8 Location 36"
Airfoil
Experiment
Lewice
y(in)
x(in)
4
2
0
-2
-4
-4
-2
0
2
4
6
8
10

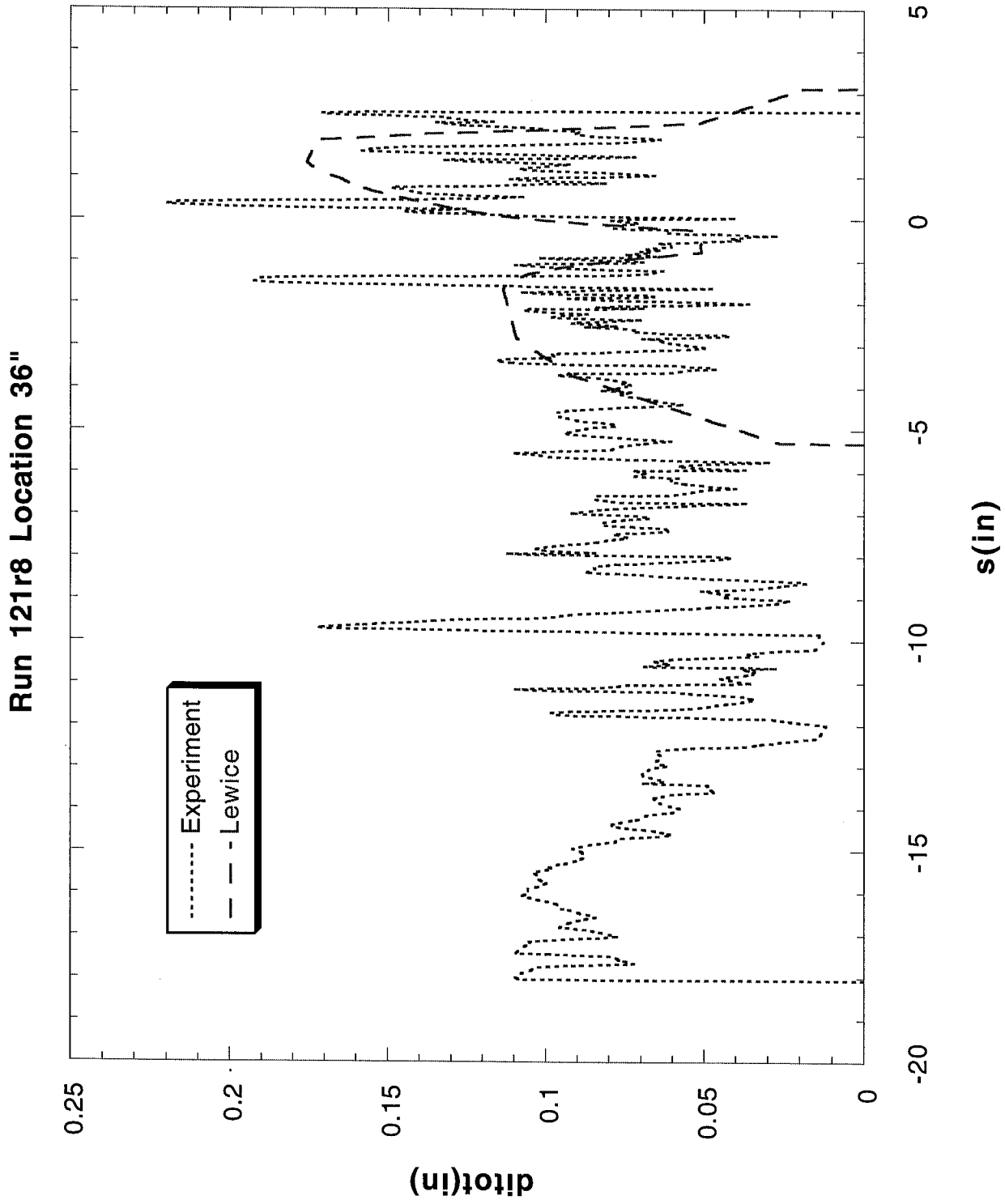
Run 121r8 Location 36"
Experiment
Lewice
dltot(in)
s(in)
0.25
0.2
0.15
0.1
0.05
0
5
0
-5
-10
-15
-20

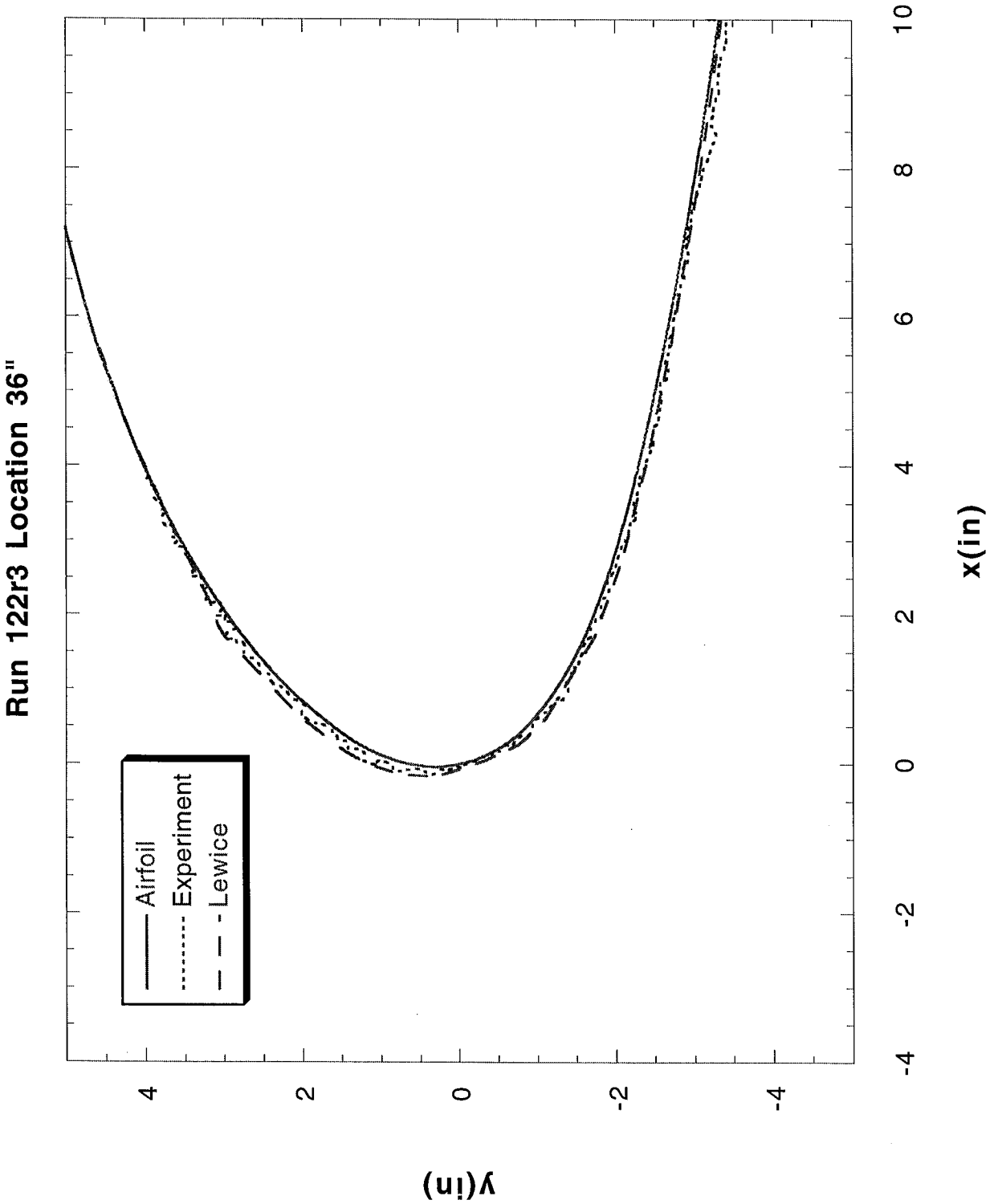
Run 122r3 Location 36"
Airfoil
Experiment
Lewice
y(in)
x(in)
4
2
0
-2
-4
-4
-2
0
2
4
6
8
10

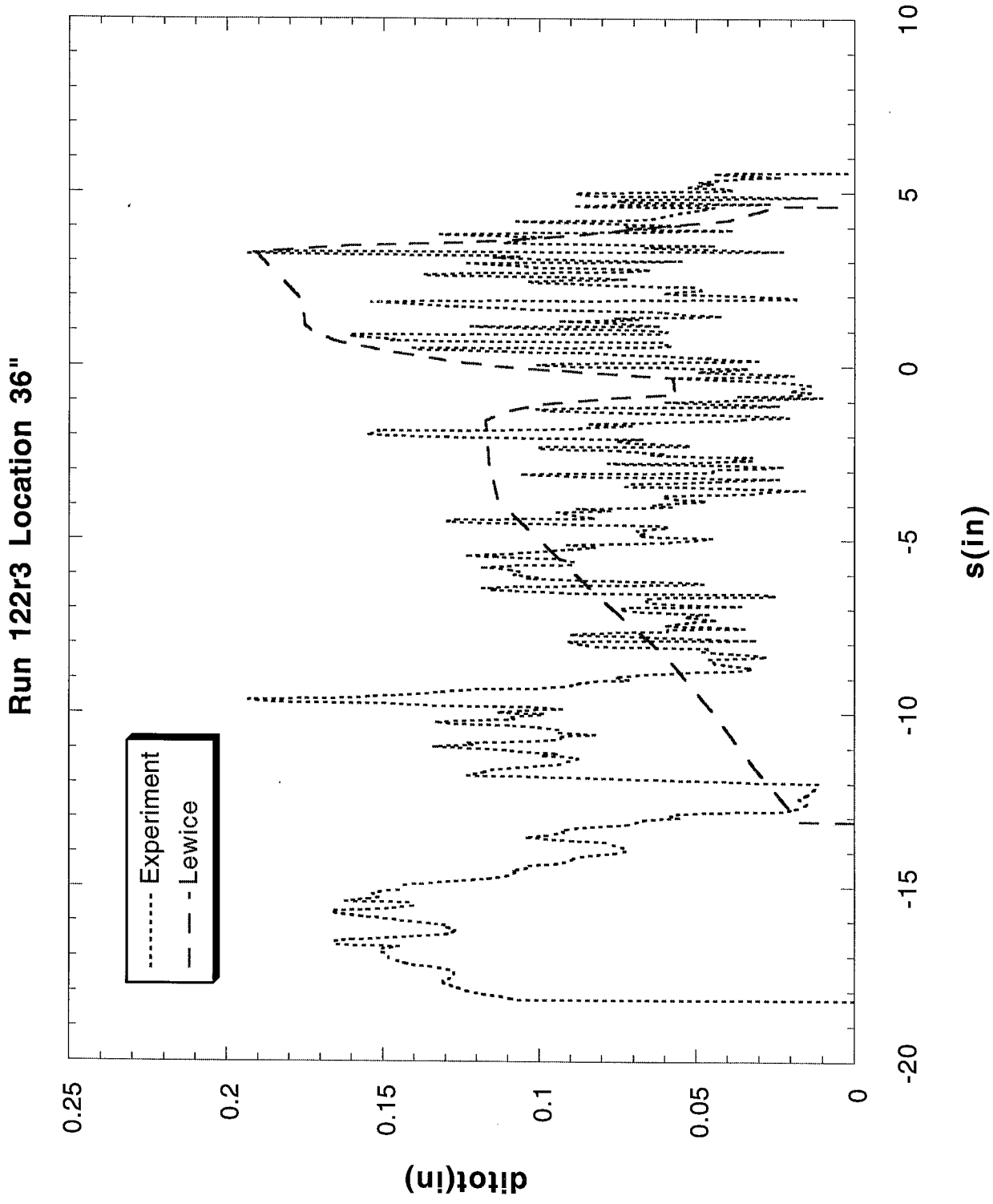
Run 122r3 Location 36"
Experiment
Lewice
dltot(in)
s(in)
0.25
0.2
0.15
0.1
0.05
0
10
5
0
-5
-10
-15
-20

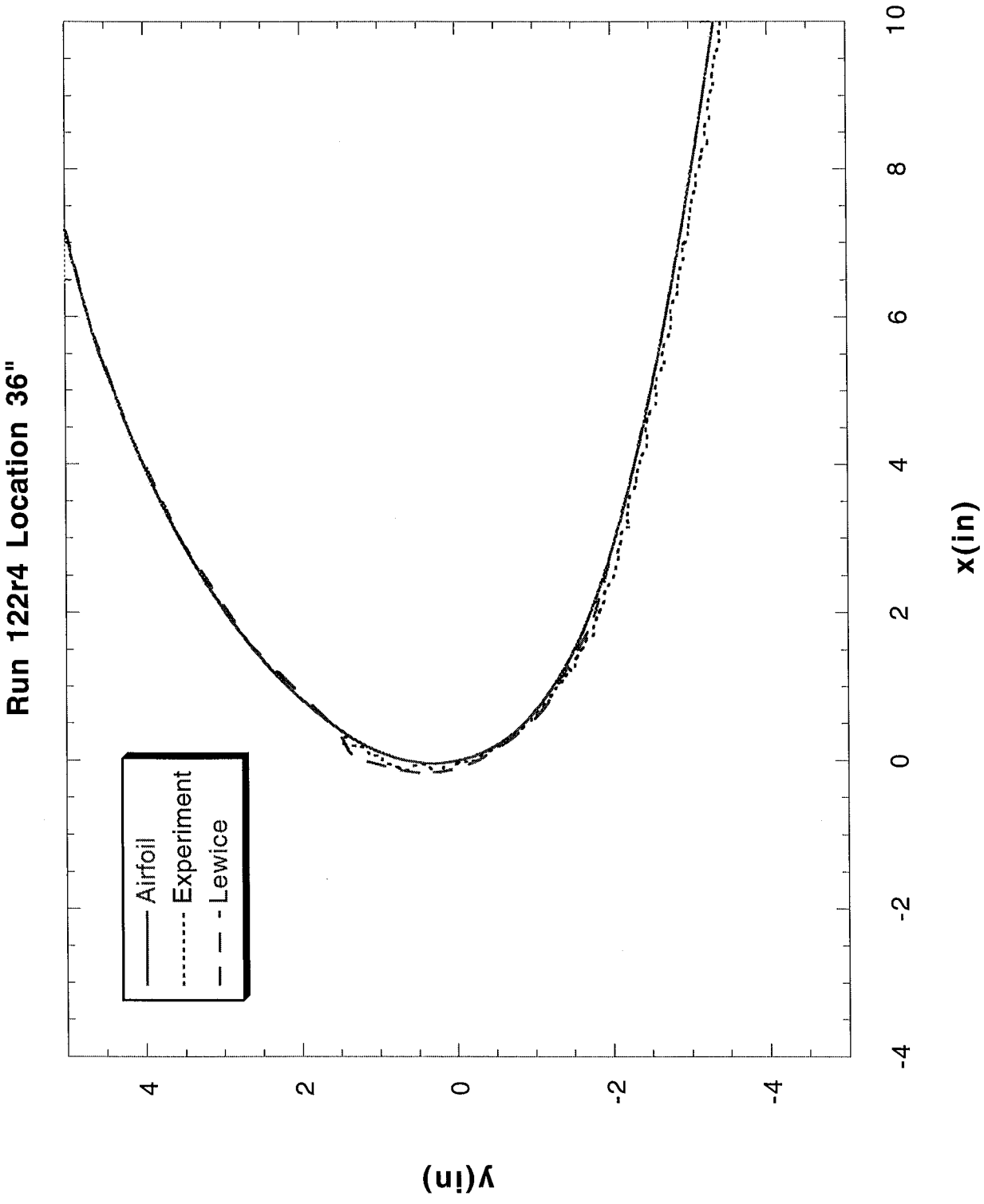
Run 122r4 Location 36"
Airfoil
Experiment
Lewice
y(in)
x(in)
4
2
0
-2
-4
-4
-2
0
2
4
6
8
10

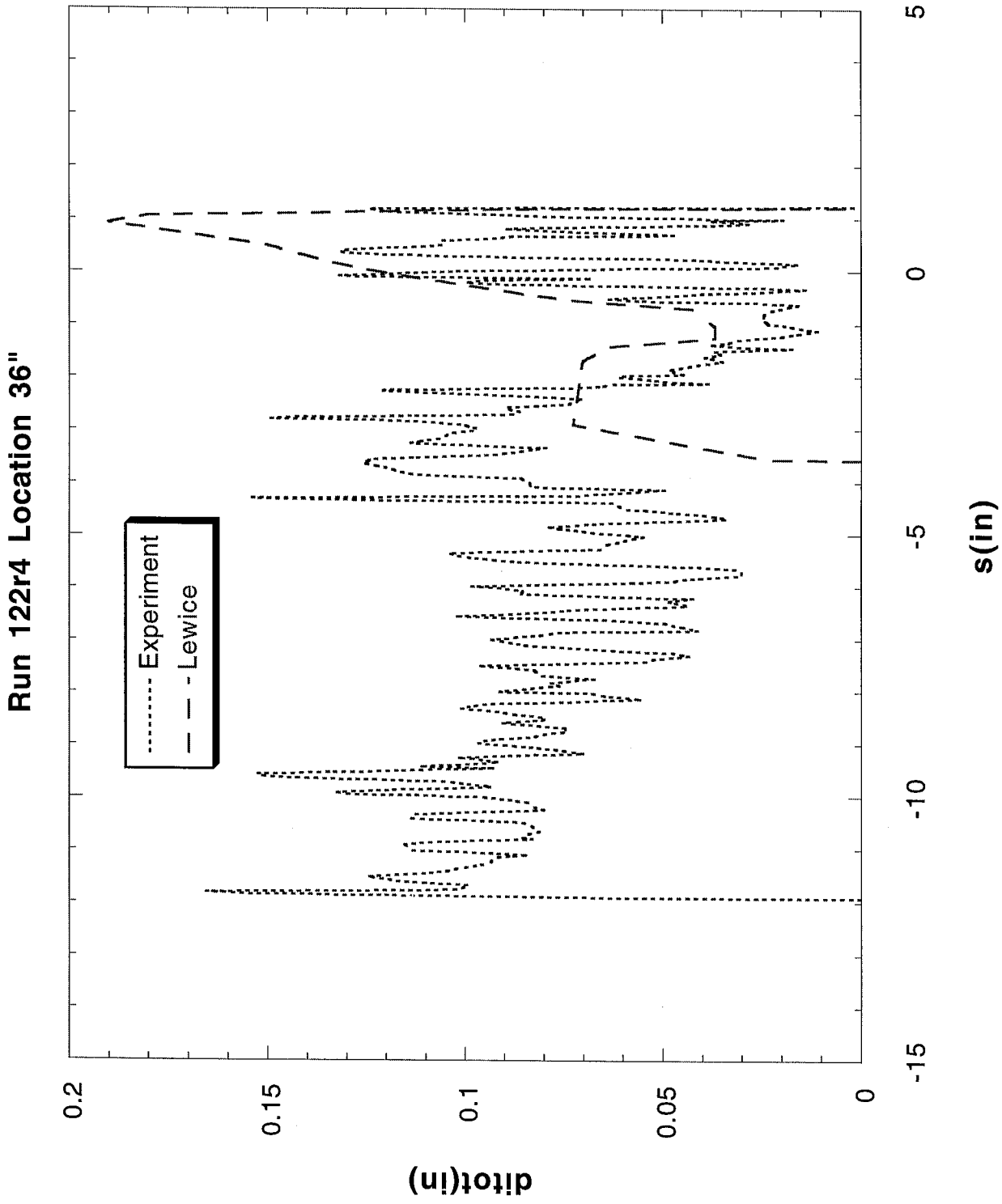
Run 122r4 Location 36"
Experiment
Lewice
dltot(in)
0.2
0.15
0.1
0.05
0
5
0
-5
-10
-15
s(in)

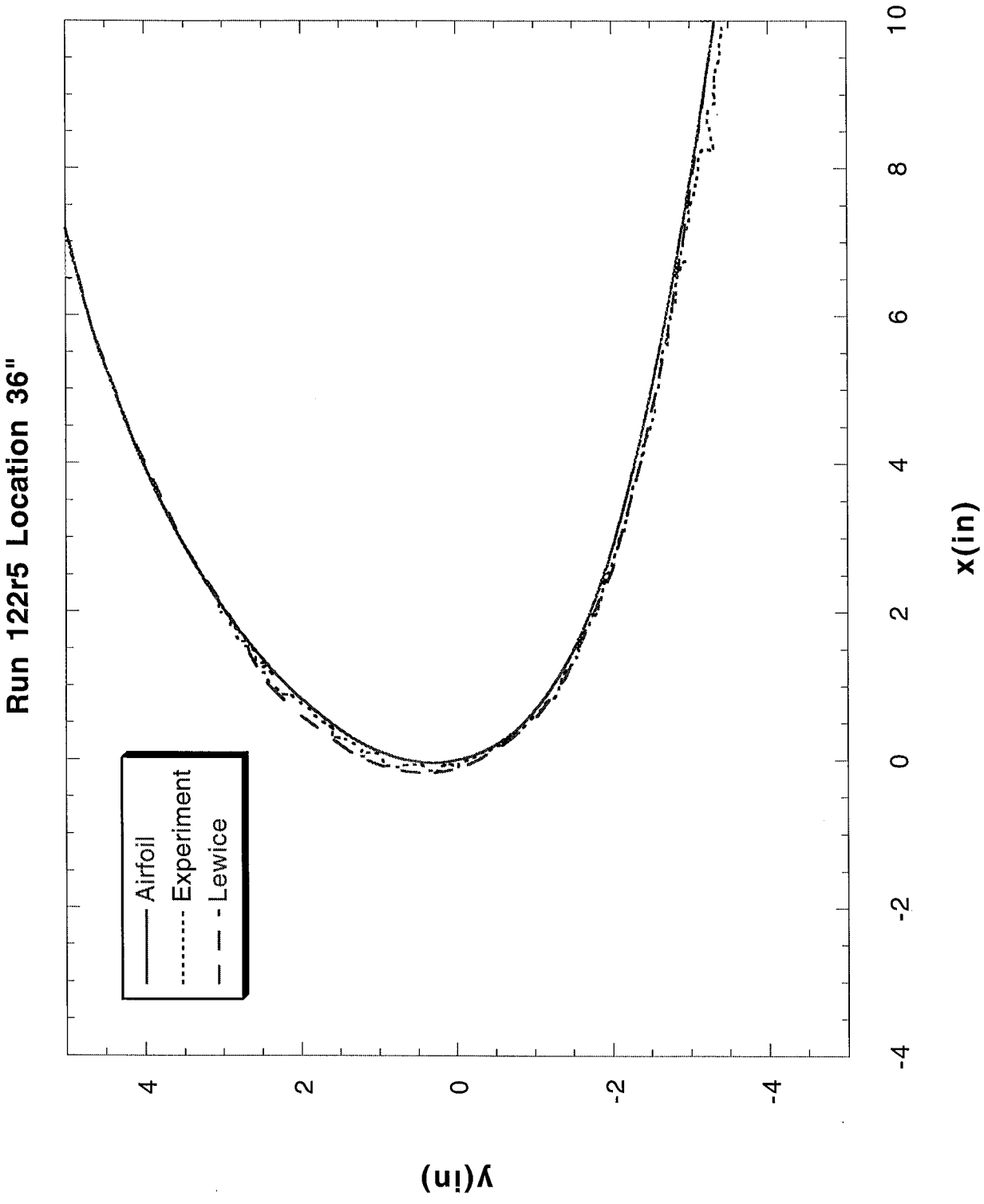
Run 122r5 Location 36"
Airfoil
Experiment
- Lewice
y(in)
x(in)
4
2
0
-2
-4
-4
-2
0
2
4
6
8
10

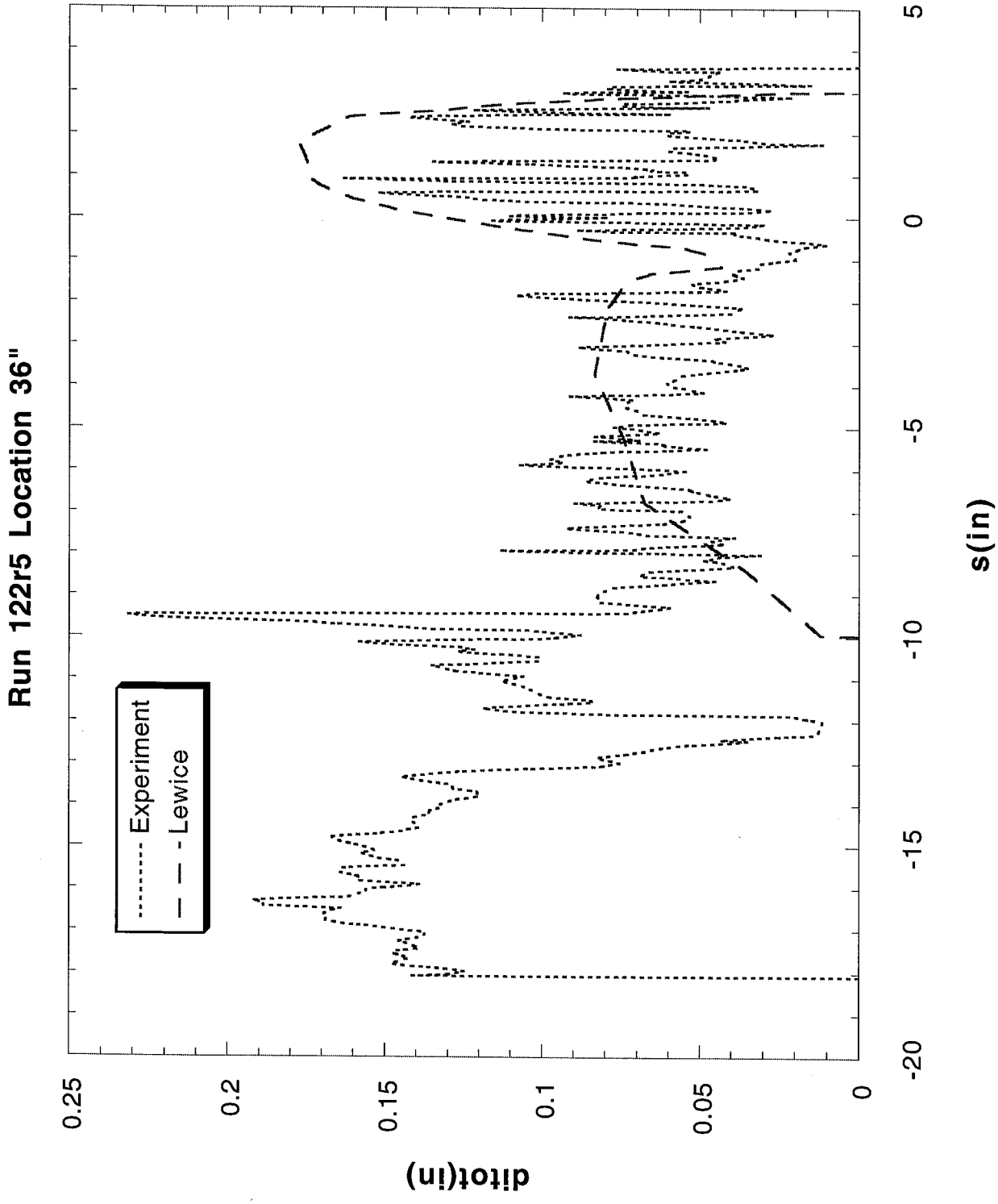
Run 122r5 Location 36"
Experiment
Lewice
dltot(in)
0.25
0.2
0.15
0.1
0.05
0
s(in)
5
0
-5
-10
-15
-20

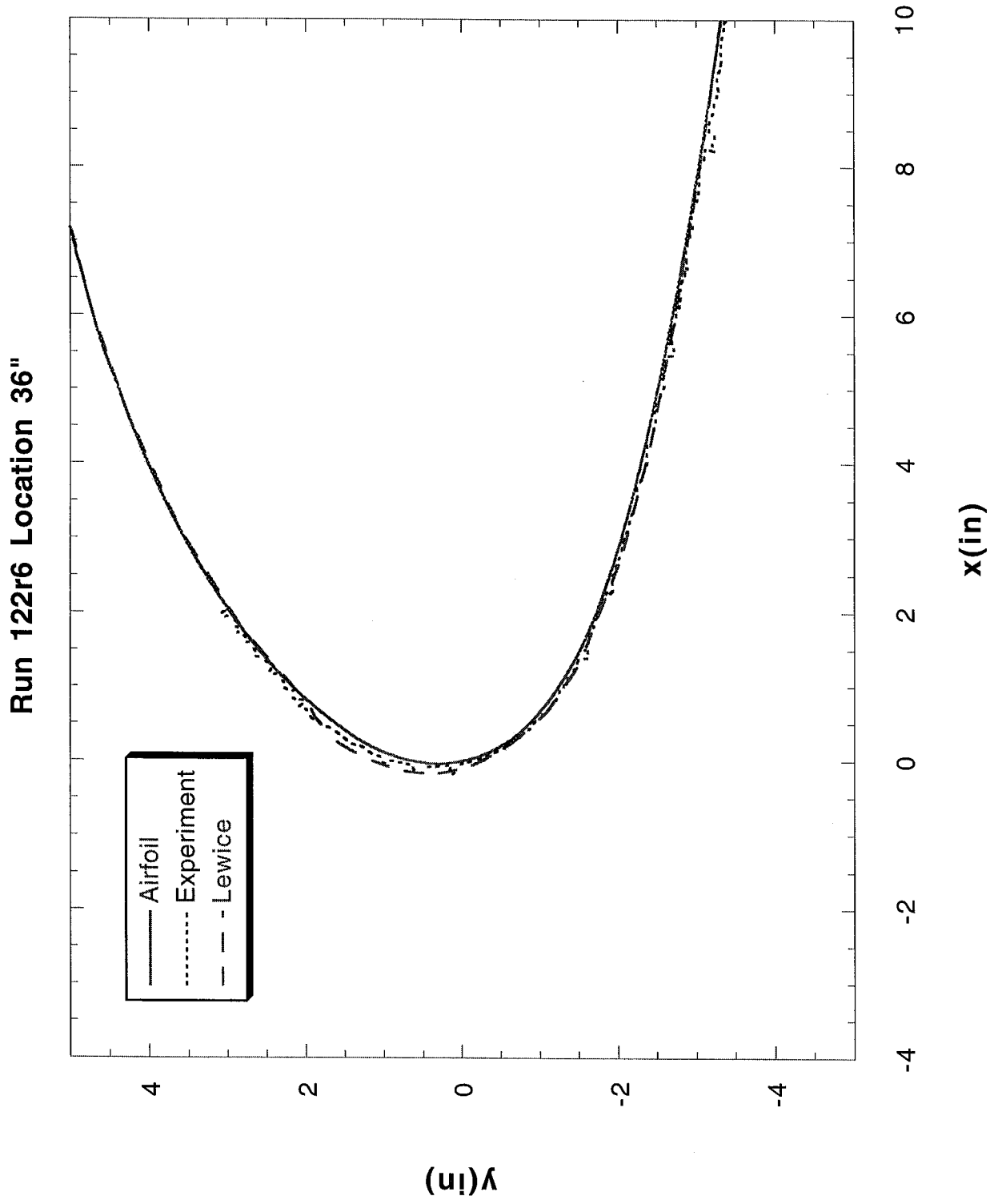
Run 122r6 Location 36"
Airfoil
Experiment
Lewice
y(in)
x(in)
4
2
0
-2
-4
-4
-2
0
2
4
6
8
10

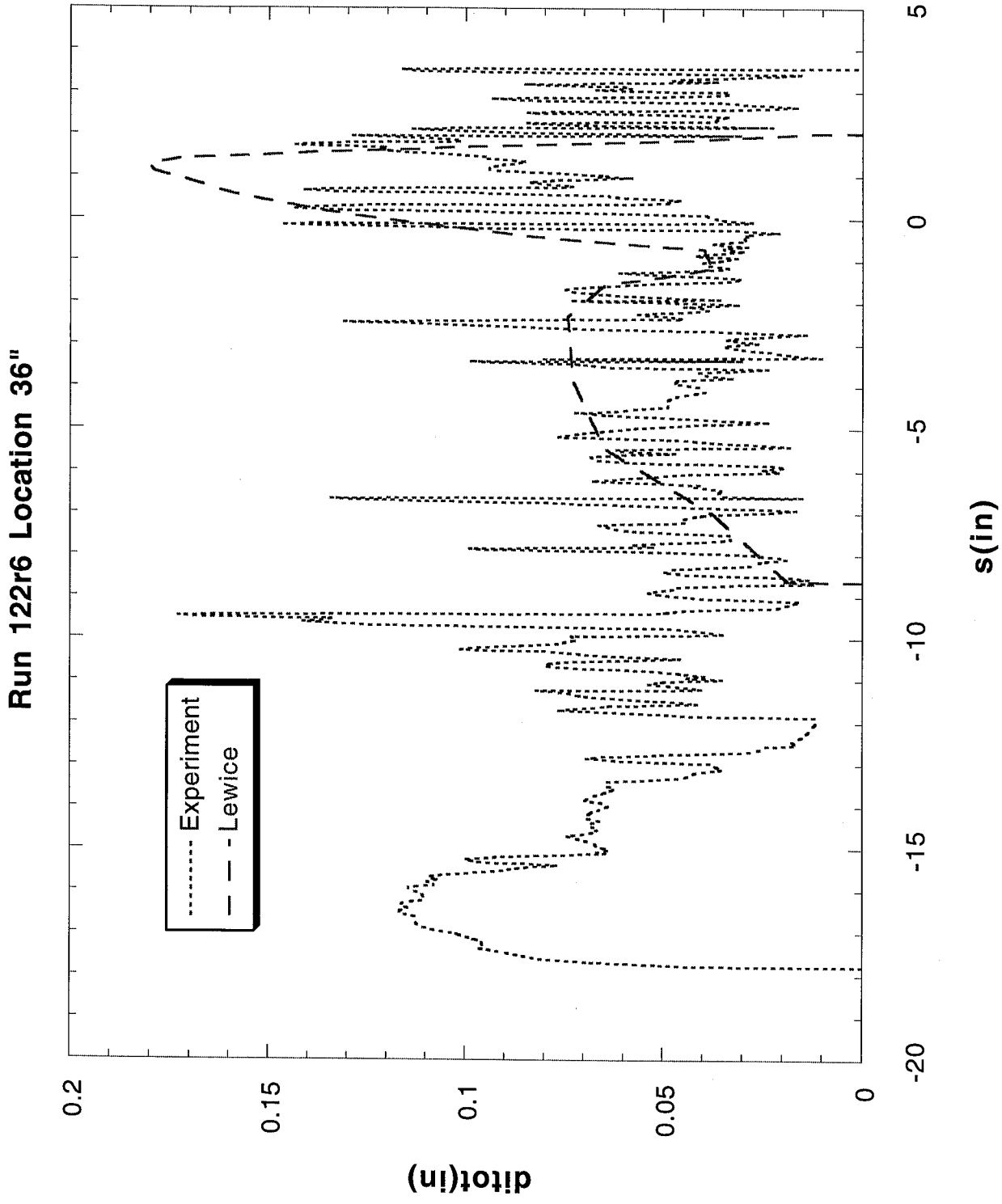
Run 122r6 Location 36"
Experiment
Lewice
ditot(in)
s(in)
0.2
0.15
0.1
0.05
0
5
0
-5
-10
-15
-20

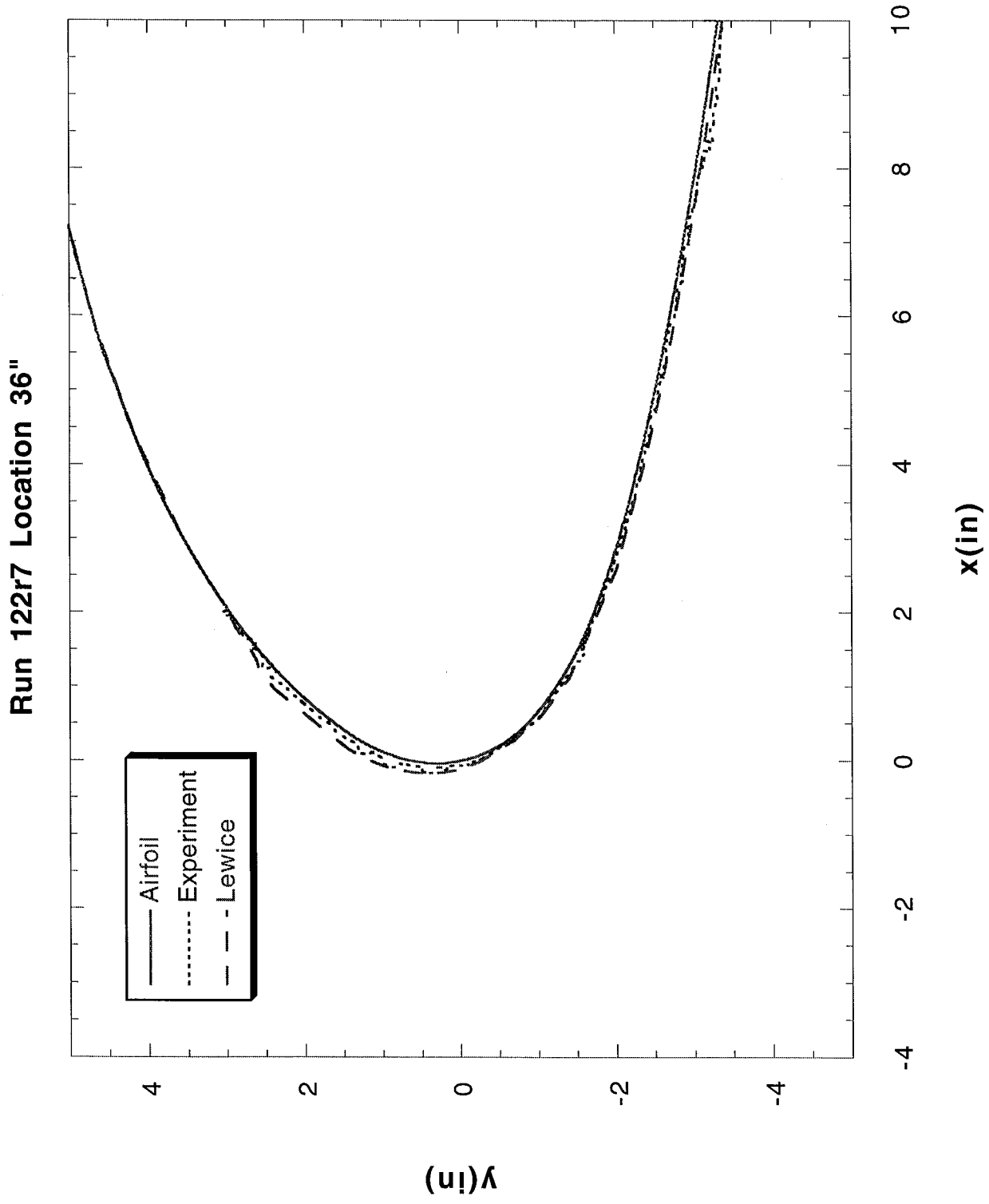
Run 122r7 Location 36"
Airfoil
Experiment
Lewice
y(in)
x(in)
4
2
0
-2
-4
-4
-2
0
2
4
6
8
10

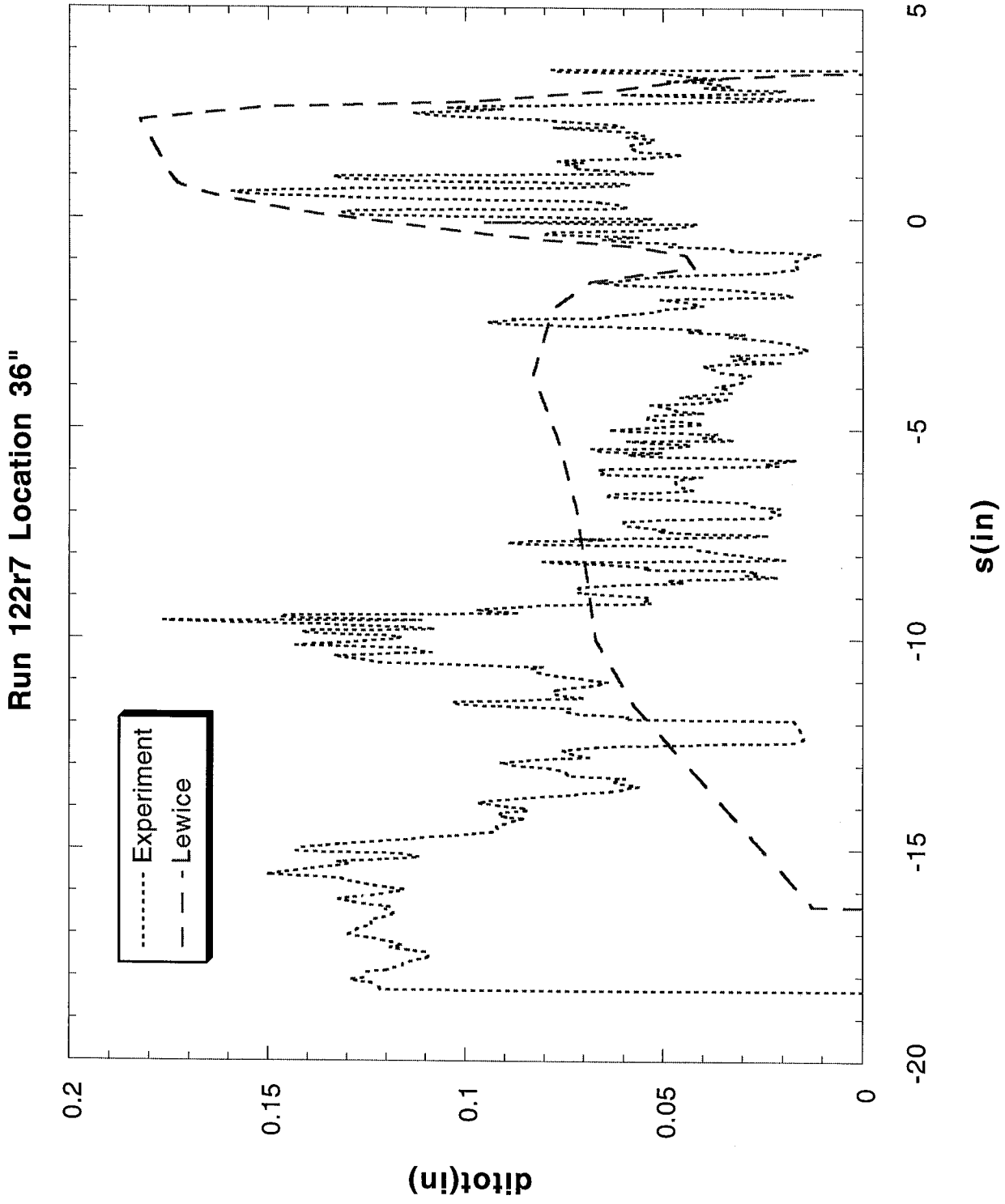
Run 122r7 Location 36"
Experiment
Lewice
dltot(in)
0.2
0.15
0.1
0.05
0
5
0
-5
-10
-15
-20
s(in)

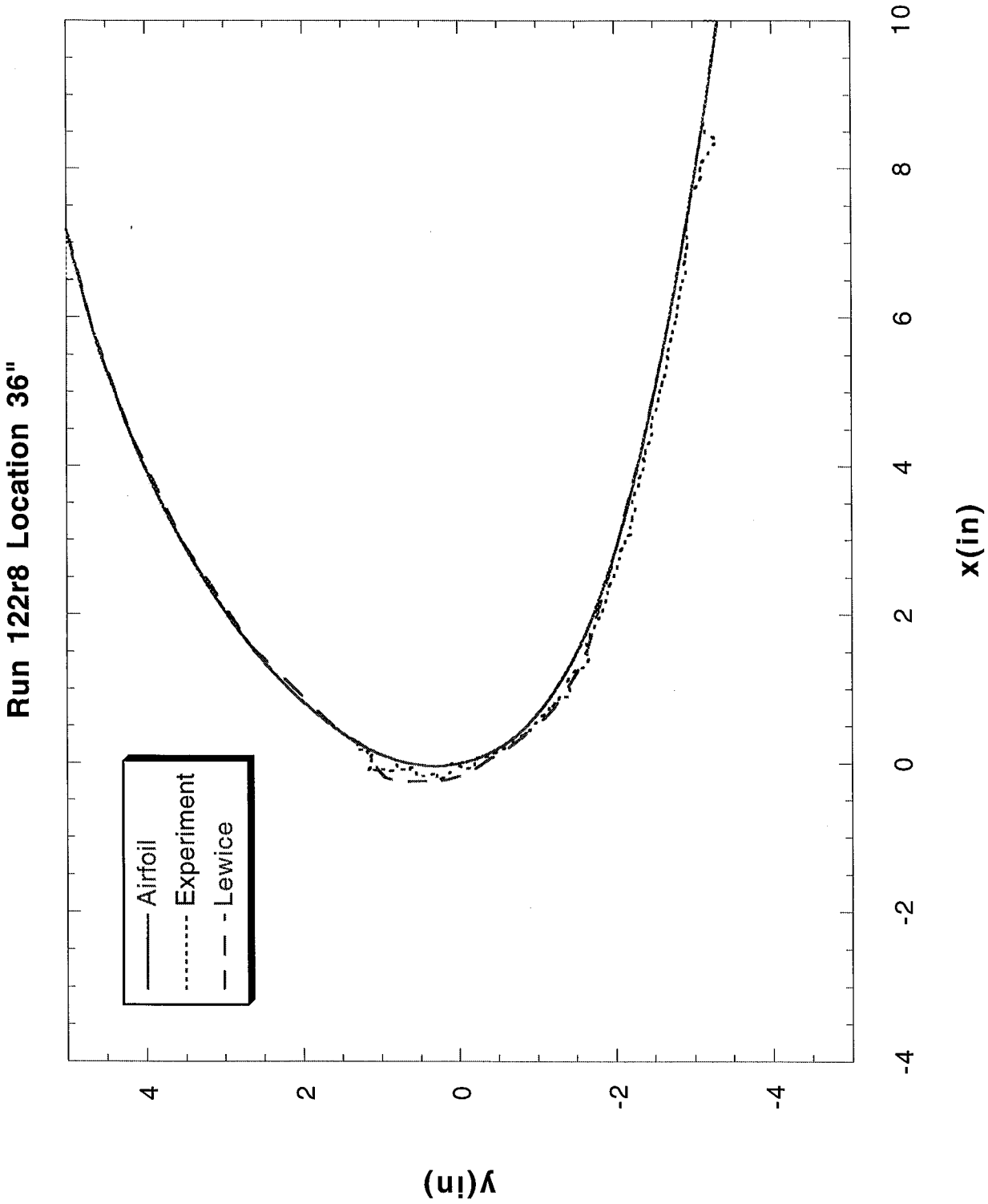
Run 122r8 Location 36"
Airfoil
Experiment
Lewice
y(in)
x(in)
4
2
0
-2
-4
-4
-2
0
2
4
6
8
10

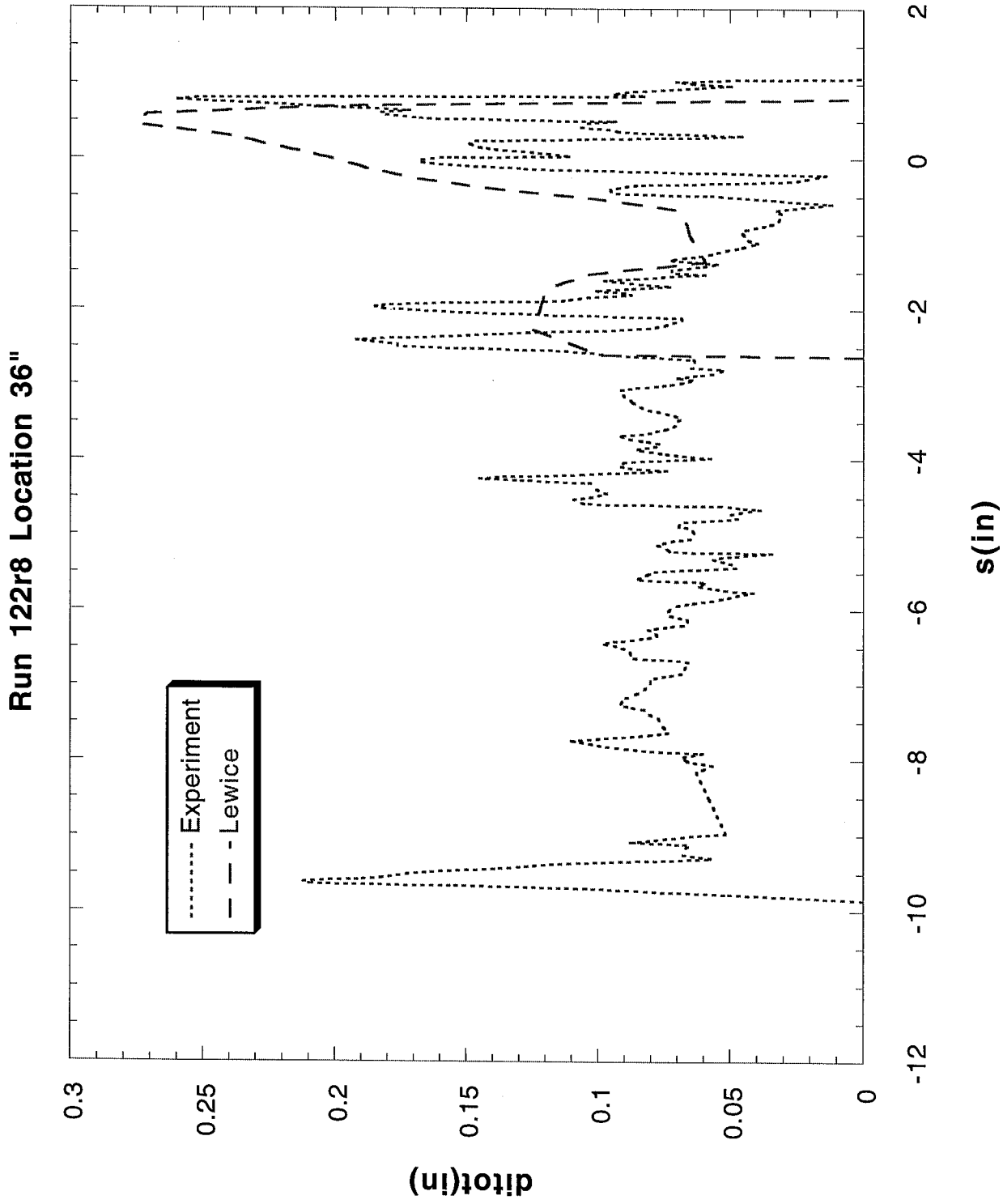
Run 122r8 Location 36"
Experiment
Lewice
ditot(in)
s(in)
0.3
0.25
0.2
0.15
0.1
0.05
0
2
0
-2
-4
-6
-8
-10
-12

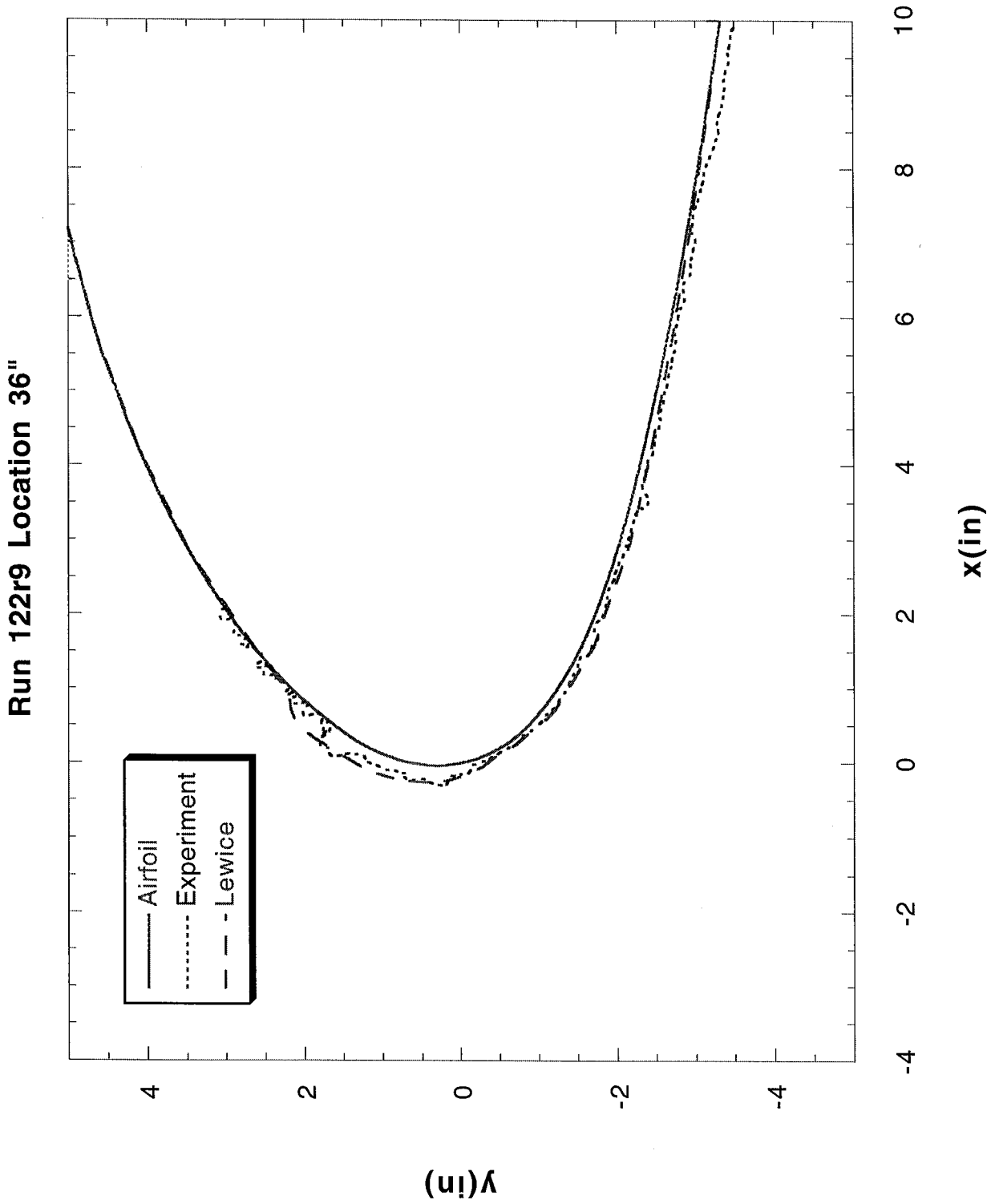
Run 122r9 Location 36"
Airfoil
Experiment
Lewice
y(in)
x(in)
4
2
0
-2
-4
-4
-2
0
2
4
6
8
10

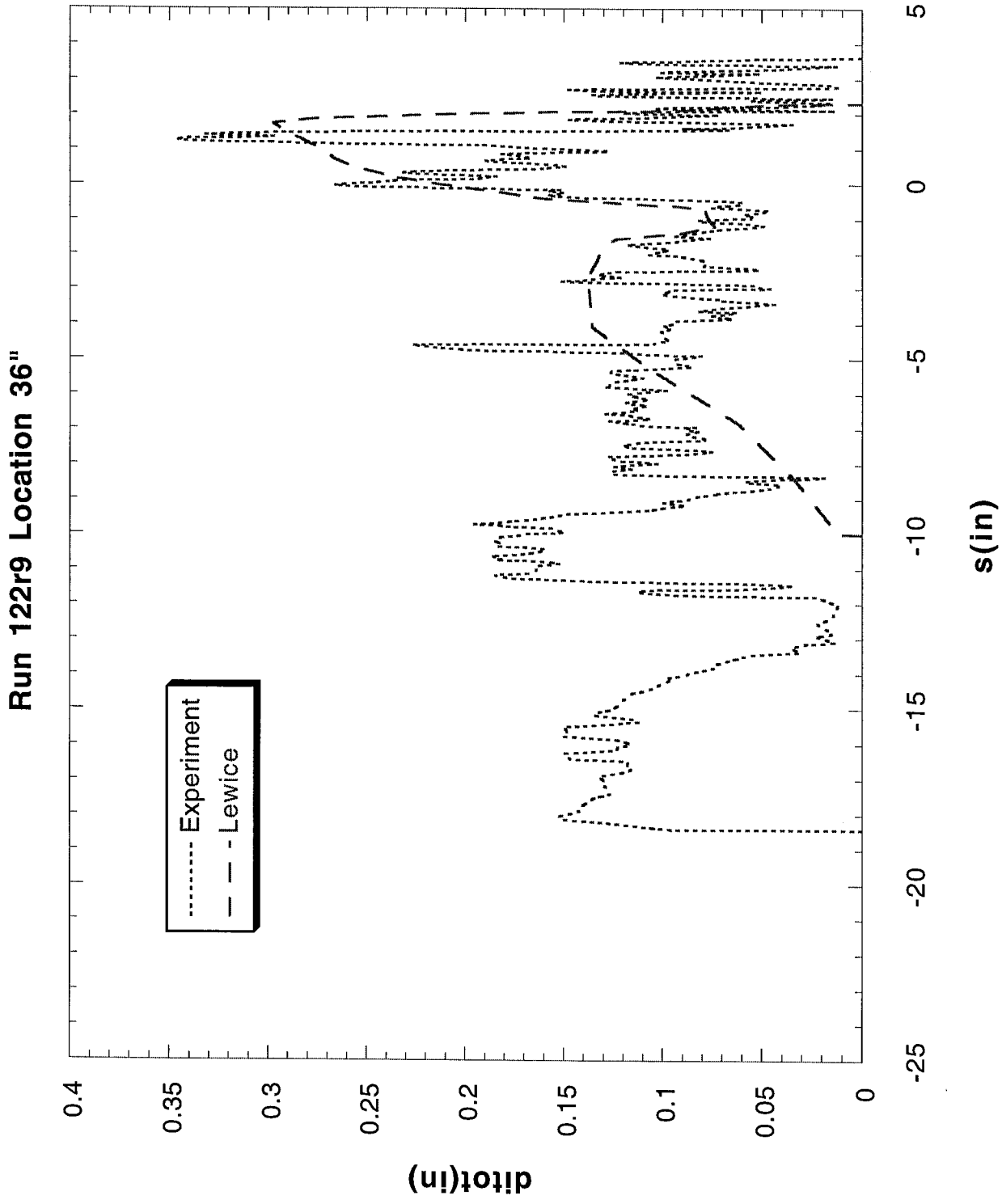
Run 122r9 Location 36"
Experiment
Lewice
dltot(in)
s(in)
0.4
0.35
0.3
0.25
0.2
0.15
0.1
0.05
0
5
0
-5
-10
-15
-20
-25

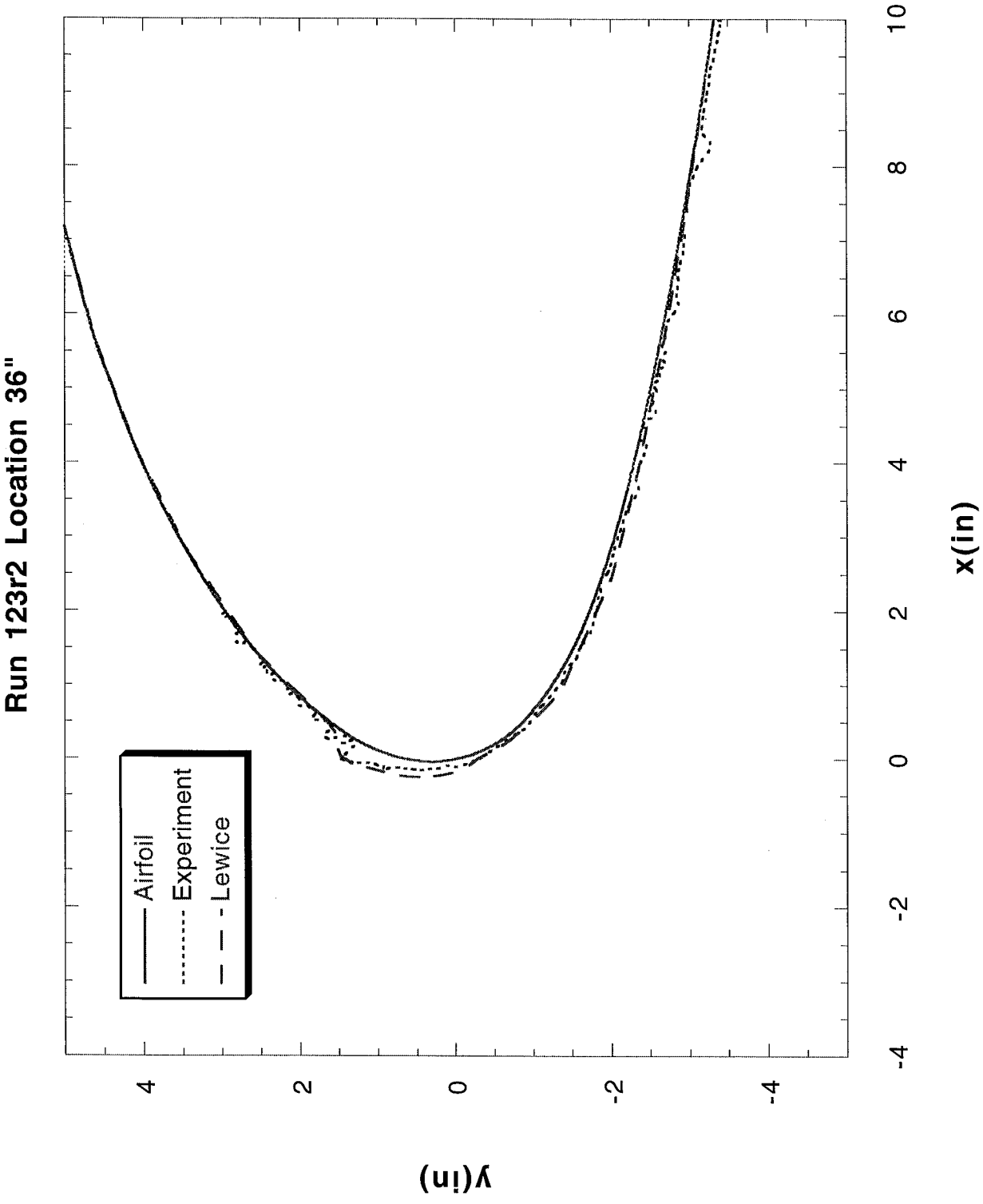
Run 123r2 Location 36"
Airfoil
Experiment
Lewice
y(in)
x(in)
4
2
0
-2
-4
-4
-2
0
2
4
6
8
10

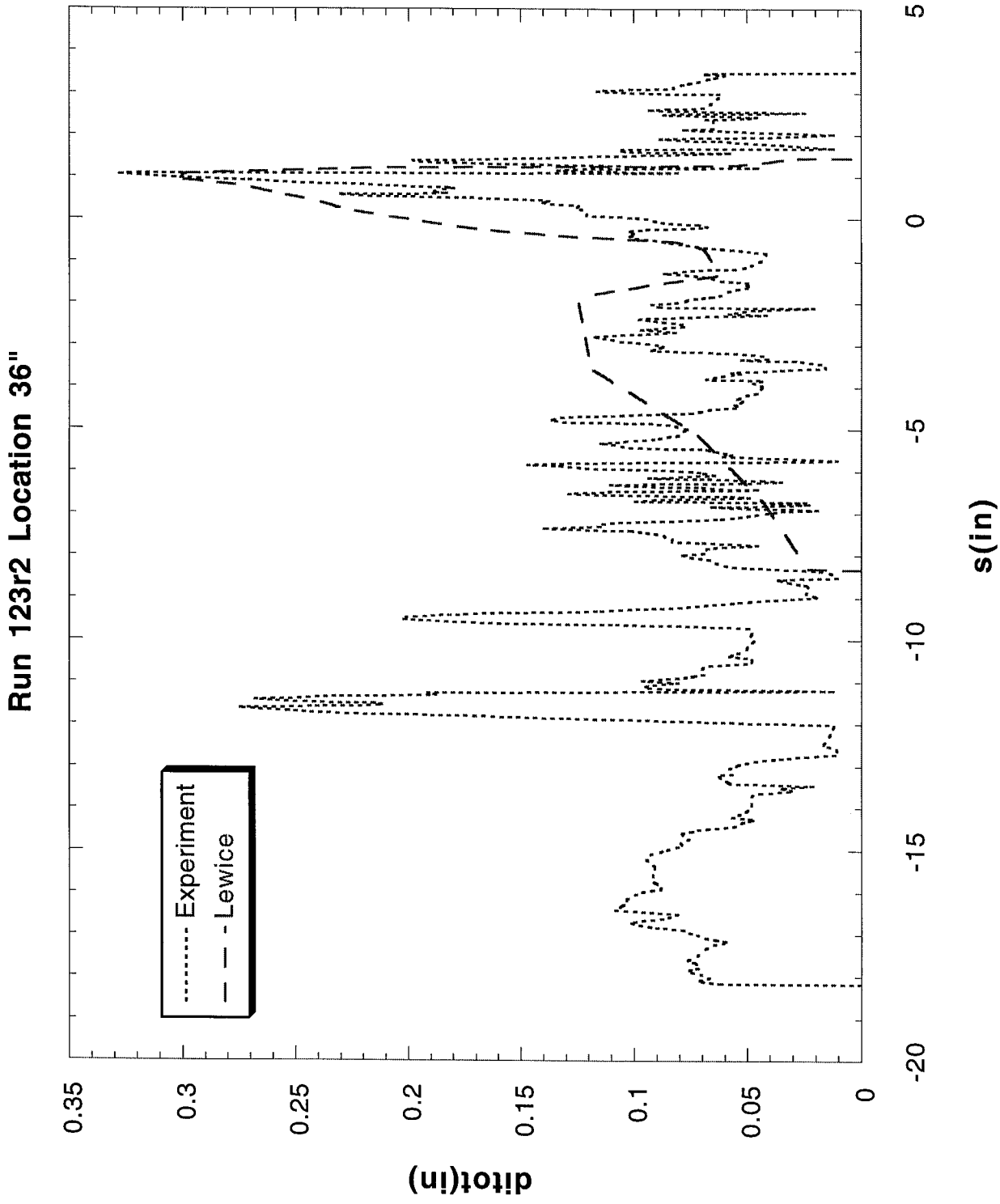
Run 123r2 Location 36"
Experiment
Lewice
dltot(in)
s(in)
0.35
0.3
0.25
0.2
0.15
0.1
0.05
0
5
0
-5
-10
-15
-20

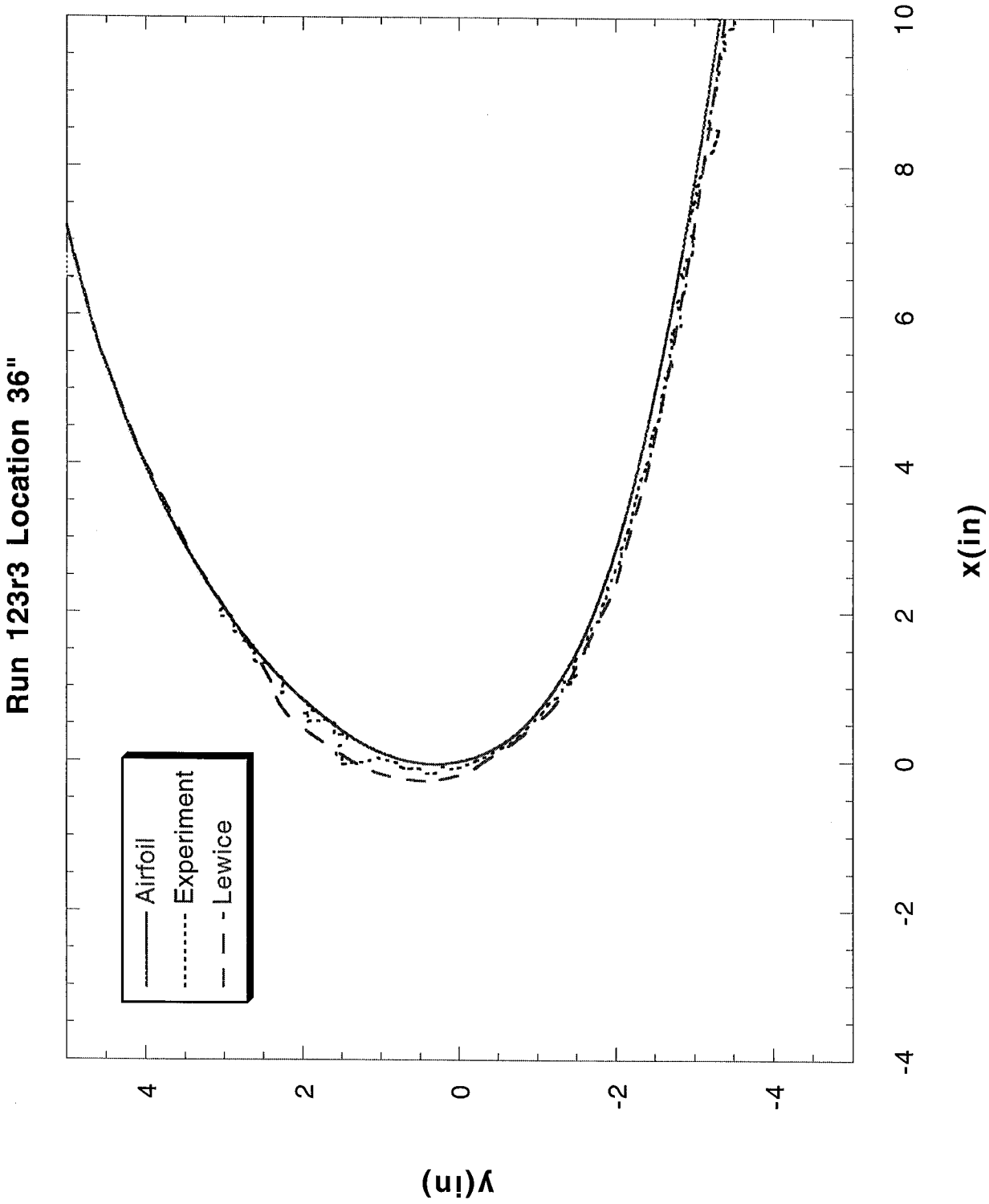
Run 123r3 Location 36"
Airfoil
Experiment
Lewice
y(in)
x(in)
4
2
0
-2
-4
-4
-2
0
2
4
6
8
10

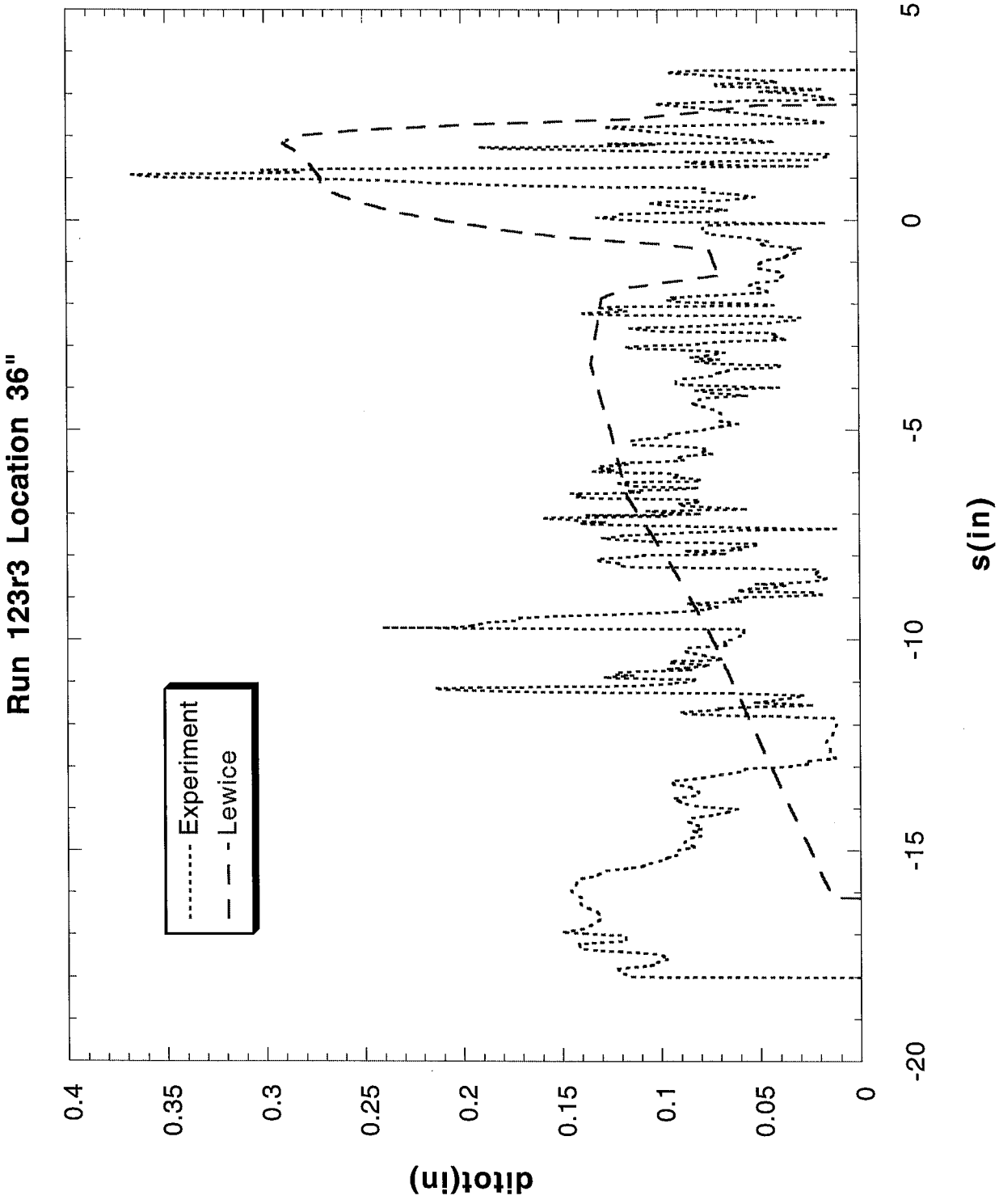
Run 123r3 Location 36"
Experiment
Lewice
dltot(in)
s(in)
0.4
0.35
0.3
0.25
0.2
0.15
0.1
0.05
0
5
0
-5
-10
-15
-20

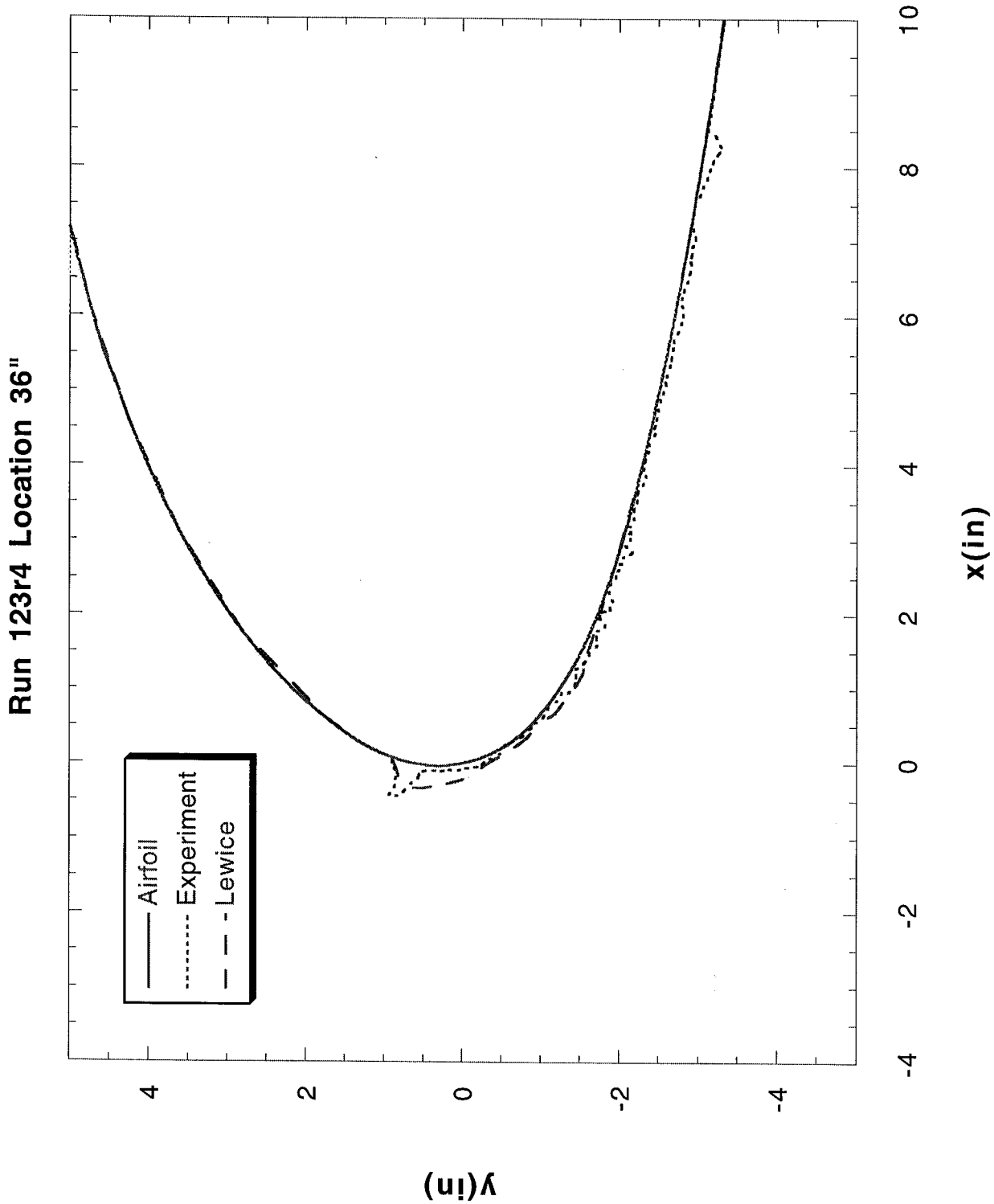
Run 123r4 Location 36"
Airfoil
Experiment
Lewice
y(in)
x(in)
4
2
0
-2
-4
-4
-2
0
2
4
6
8
10

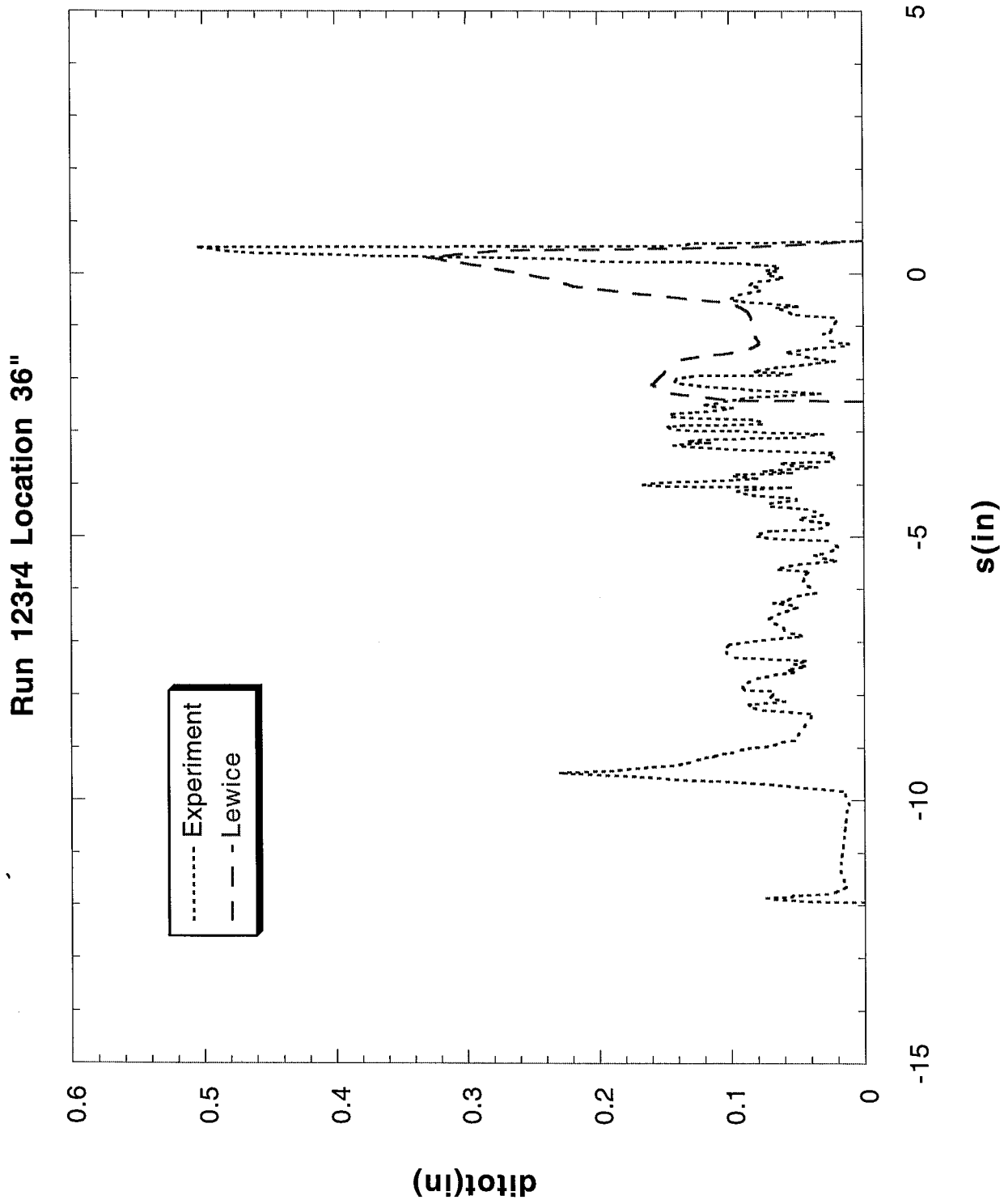
Run 123r4 Location 36"
Experiment
Lewice
dltot(in)
s(in)
0
0.1
0.2
0.3
0.4
0.5
0.6
-15
-10
-5
0
5

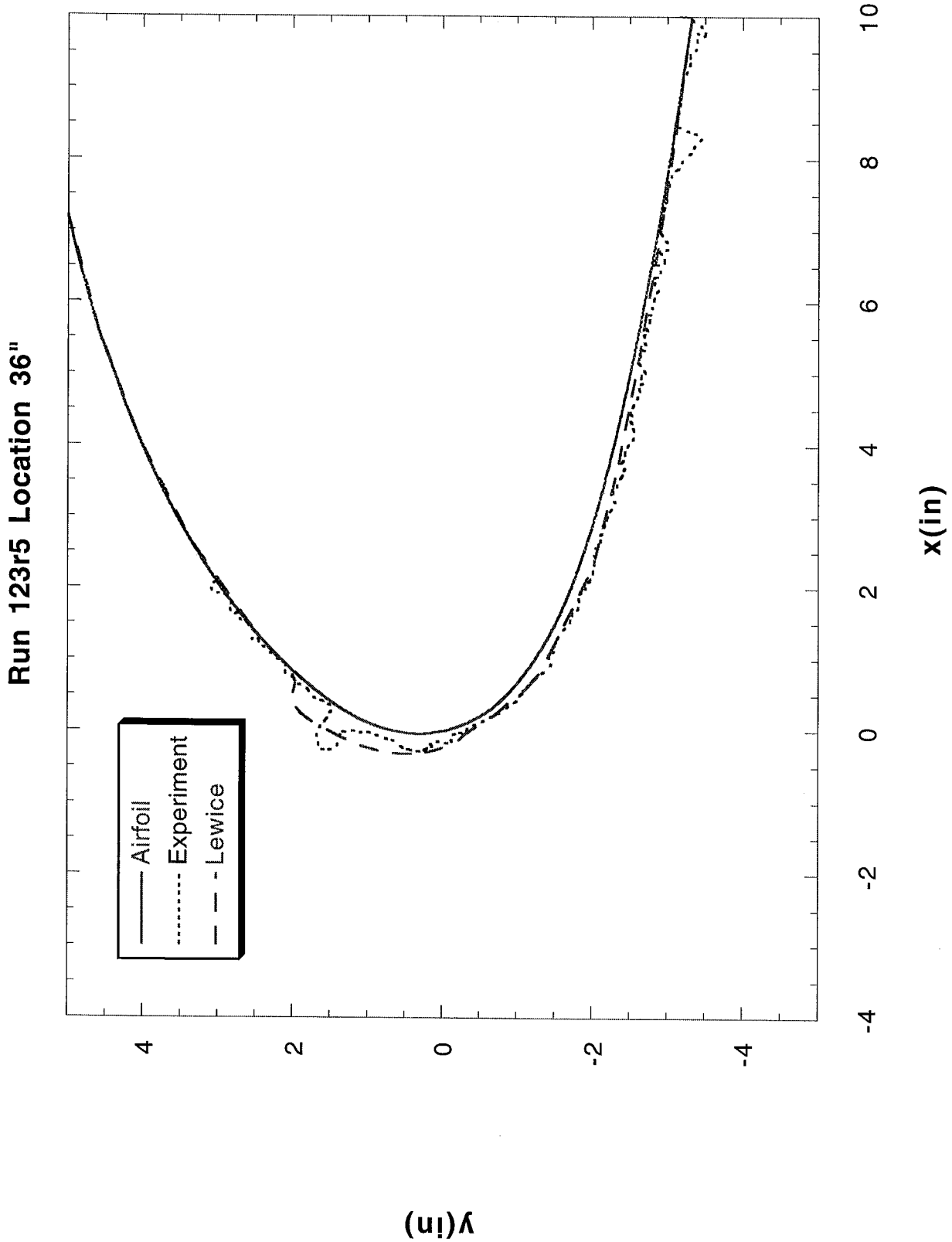
Run 123r5 Location 36"
Airfoil
Experiment
Lewice
y(in)
x(in)
4
2
0
-2
-4
-4
-2
0
2
4
6
8
10

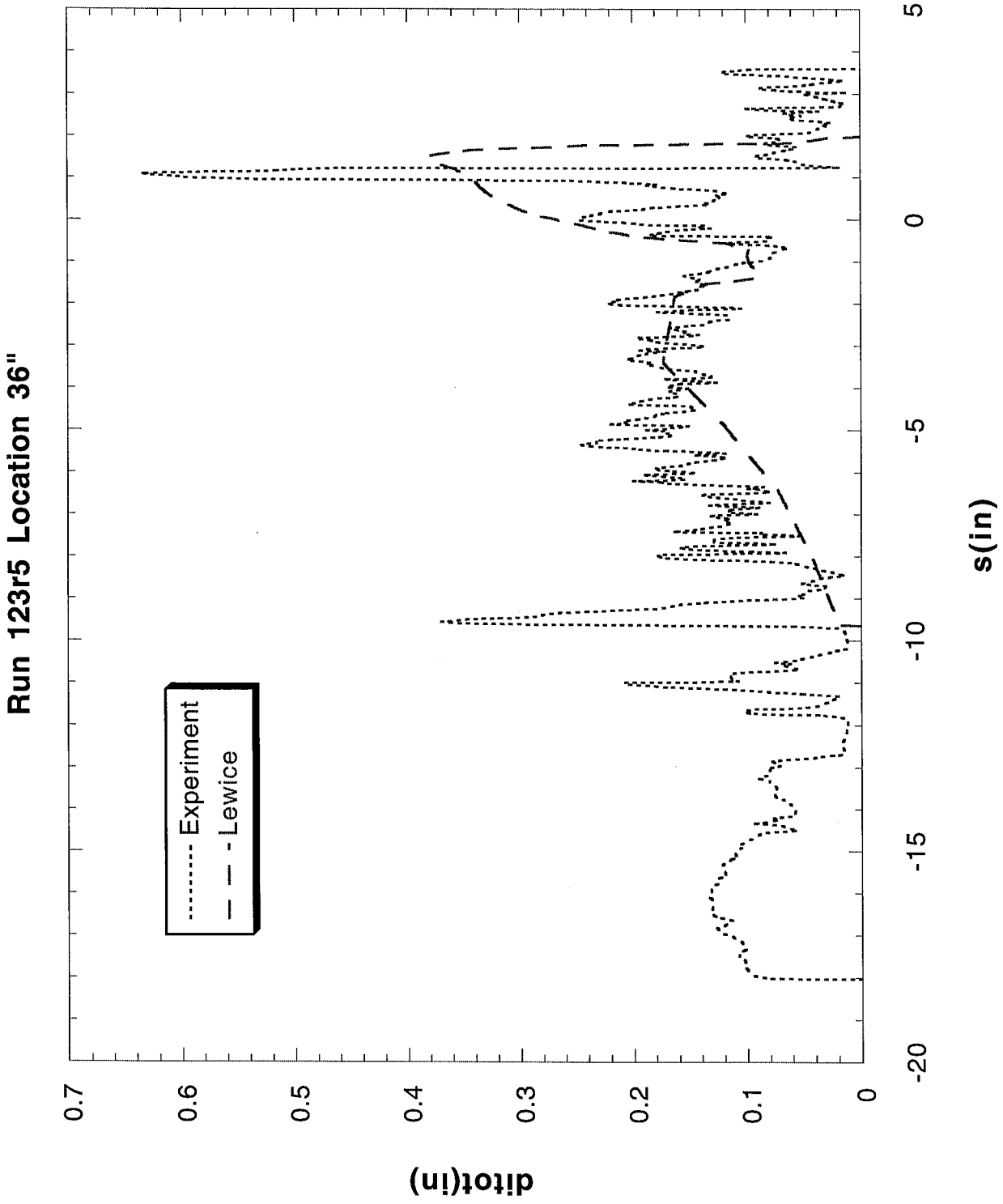
Run 123r5 Location 36"
Experiment
Lewice
dltot(in)
s(in)
0.7
0.6
0.5
0.4
0.3
0.2
0.1
0
-20
-15
-10
-5
0
5

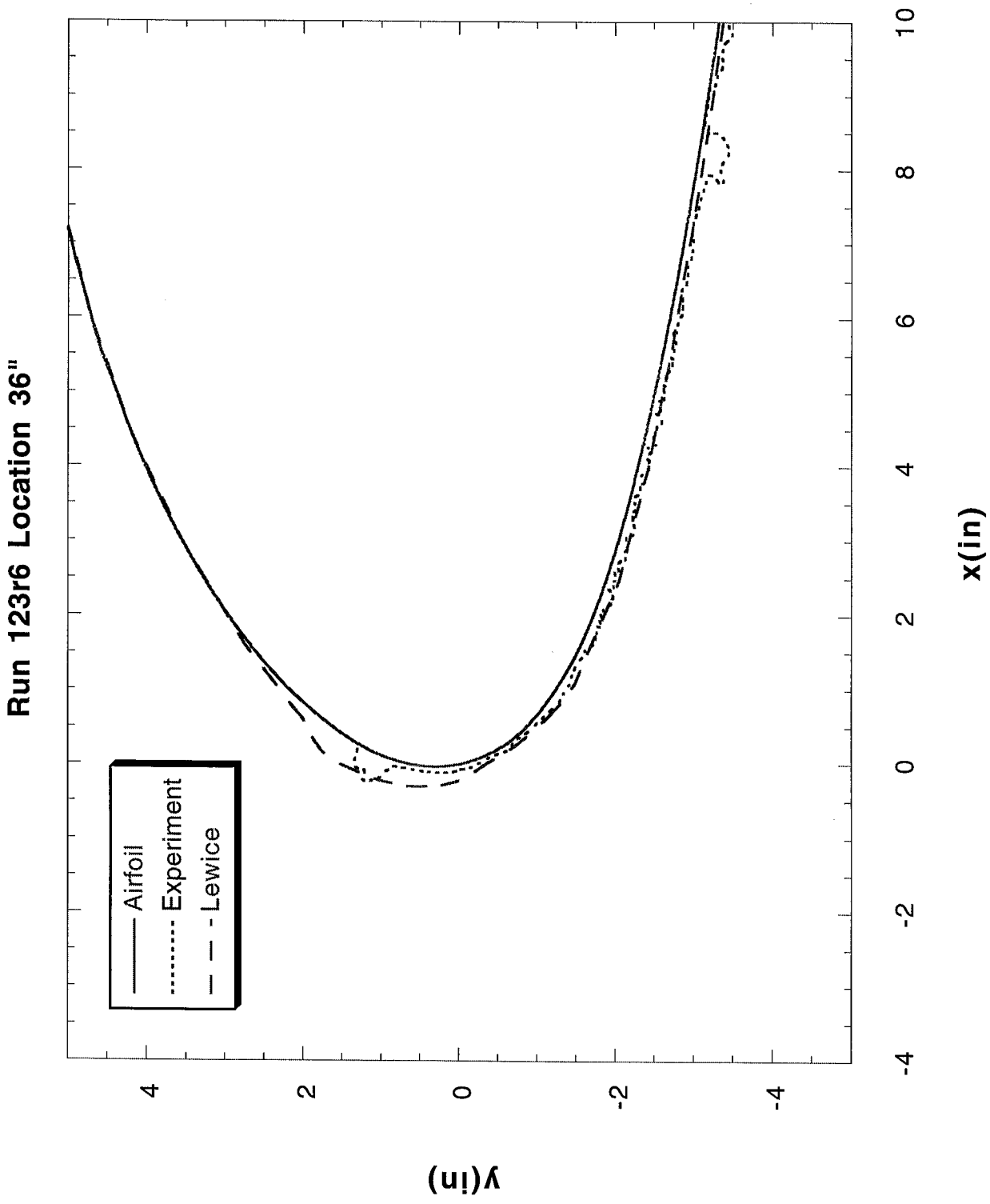
Run 123r6 Location 36"
Airfoil
Experiment
Lewice
y(in)
x(in)
4
2
0
-2
-4
-4
-2
0
2
4
6
8
10

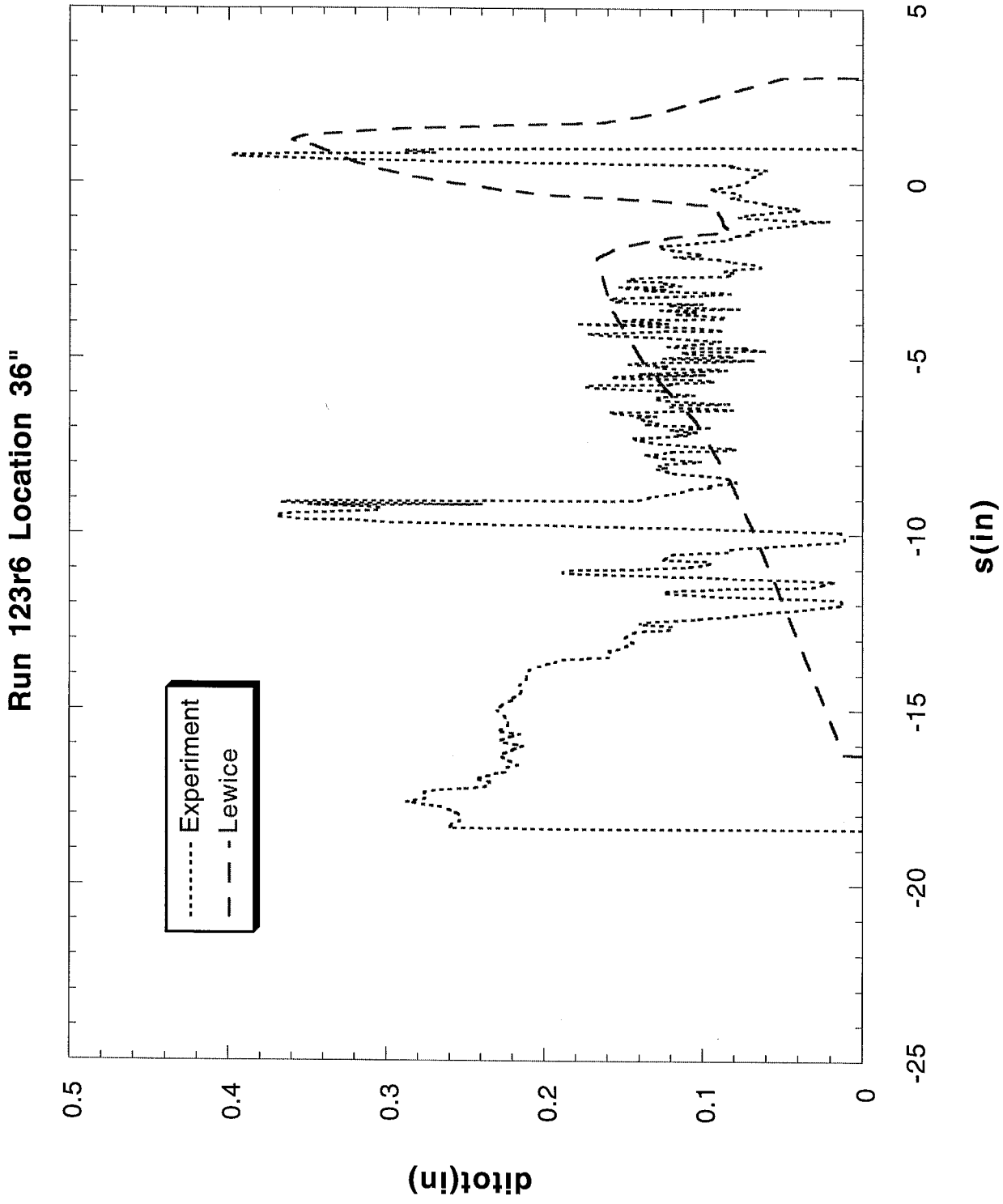
Run 123r6 Location 36"
Experiment
Lewice
ditot(in)
s(in)
0.5
0.4
0.3
0.2
0.1
0
5
0
-5
-10
-15
-20
-25

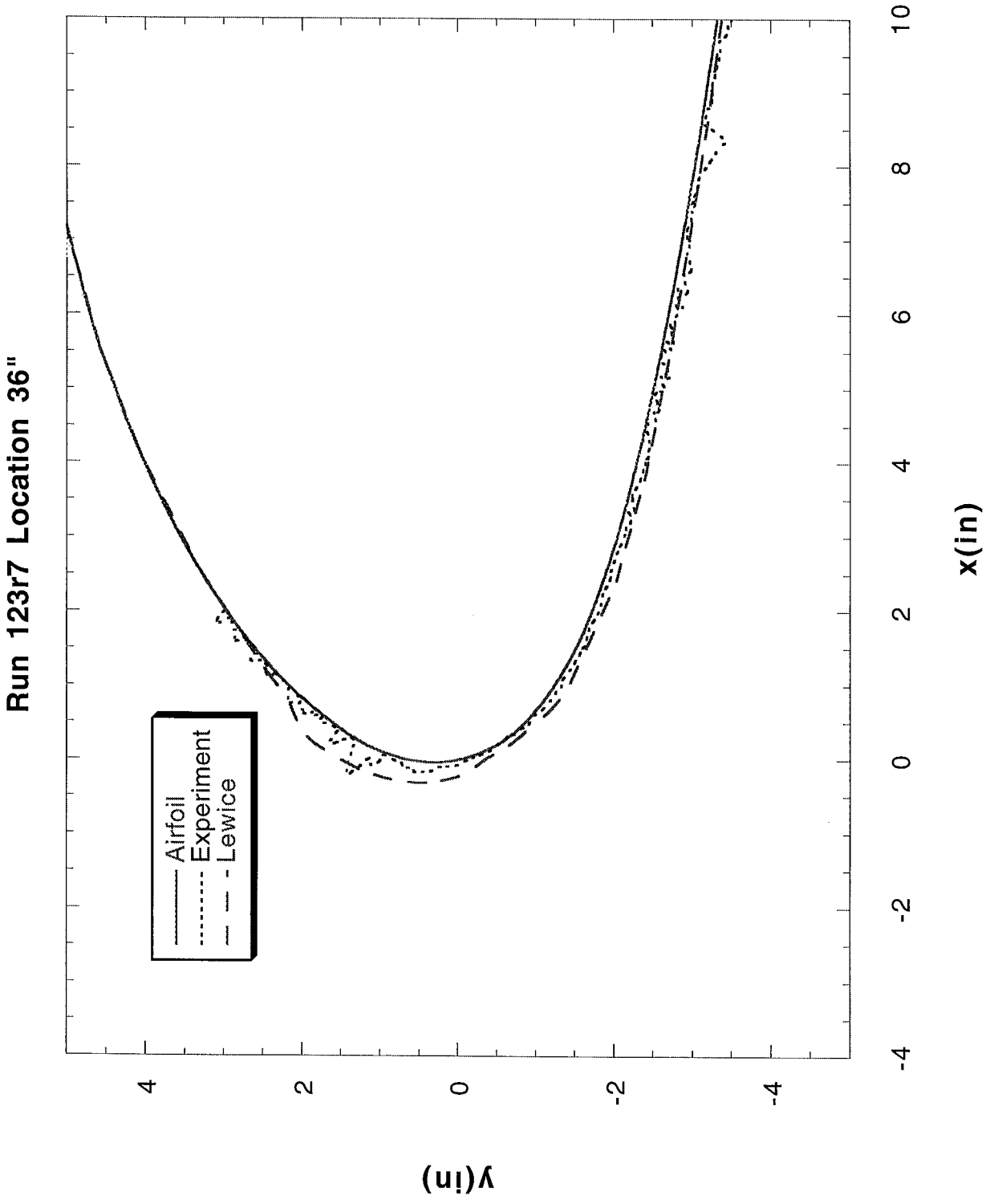
Run 123r7 Location 36"
Airfoil
Experiment
Lewice
y(in)
x(in)
4
2
0
-2
-4
-4
-2
0
2
4
6
8
10

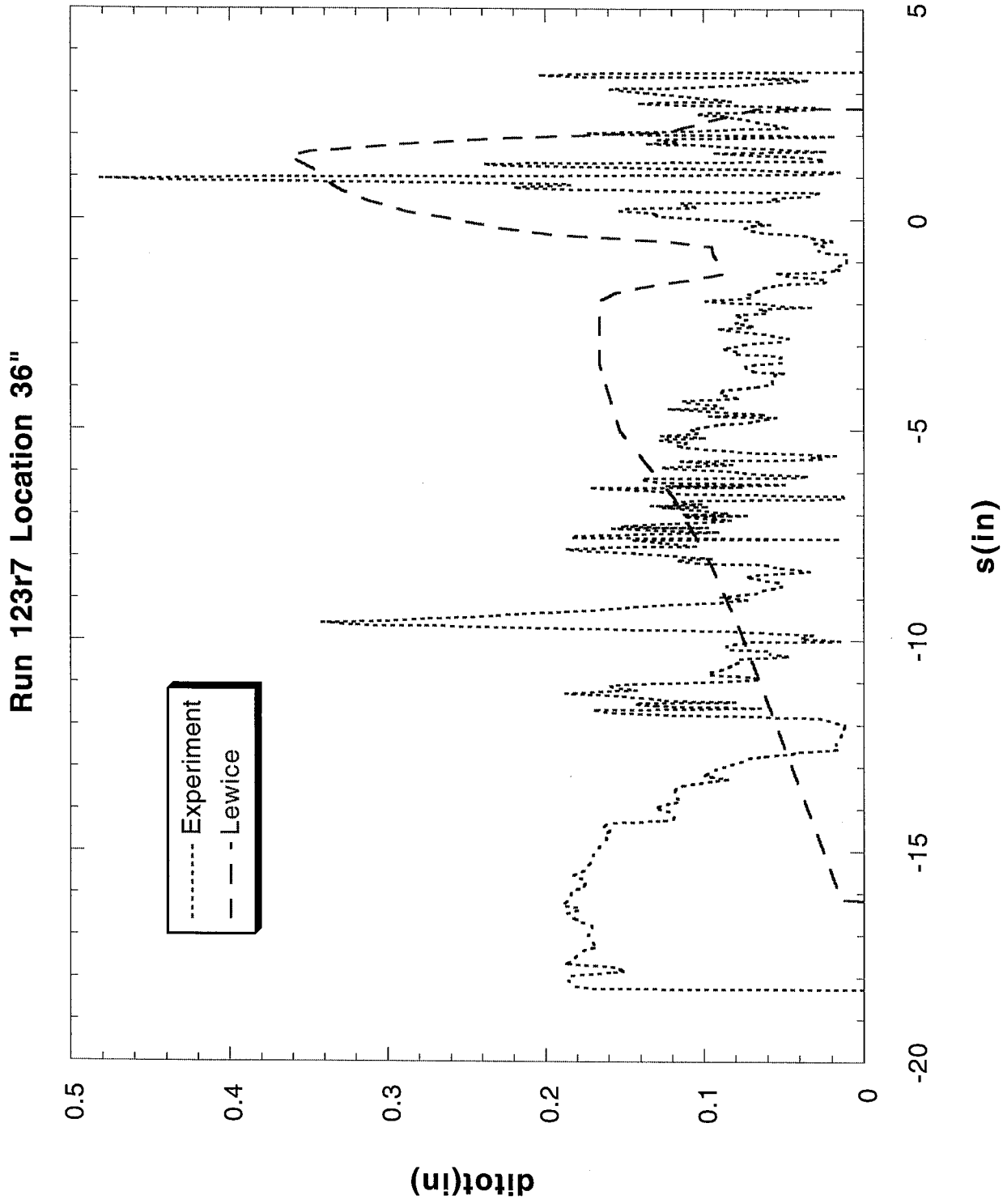
Run 123r7 Location 36"
Experiment
Lewice
dltot(in)
s(in)
0.5
0.4
0.3
0.2
0.1
0
5
0
-5
-10
-15
-20

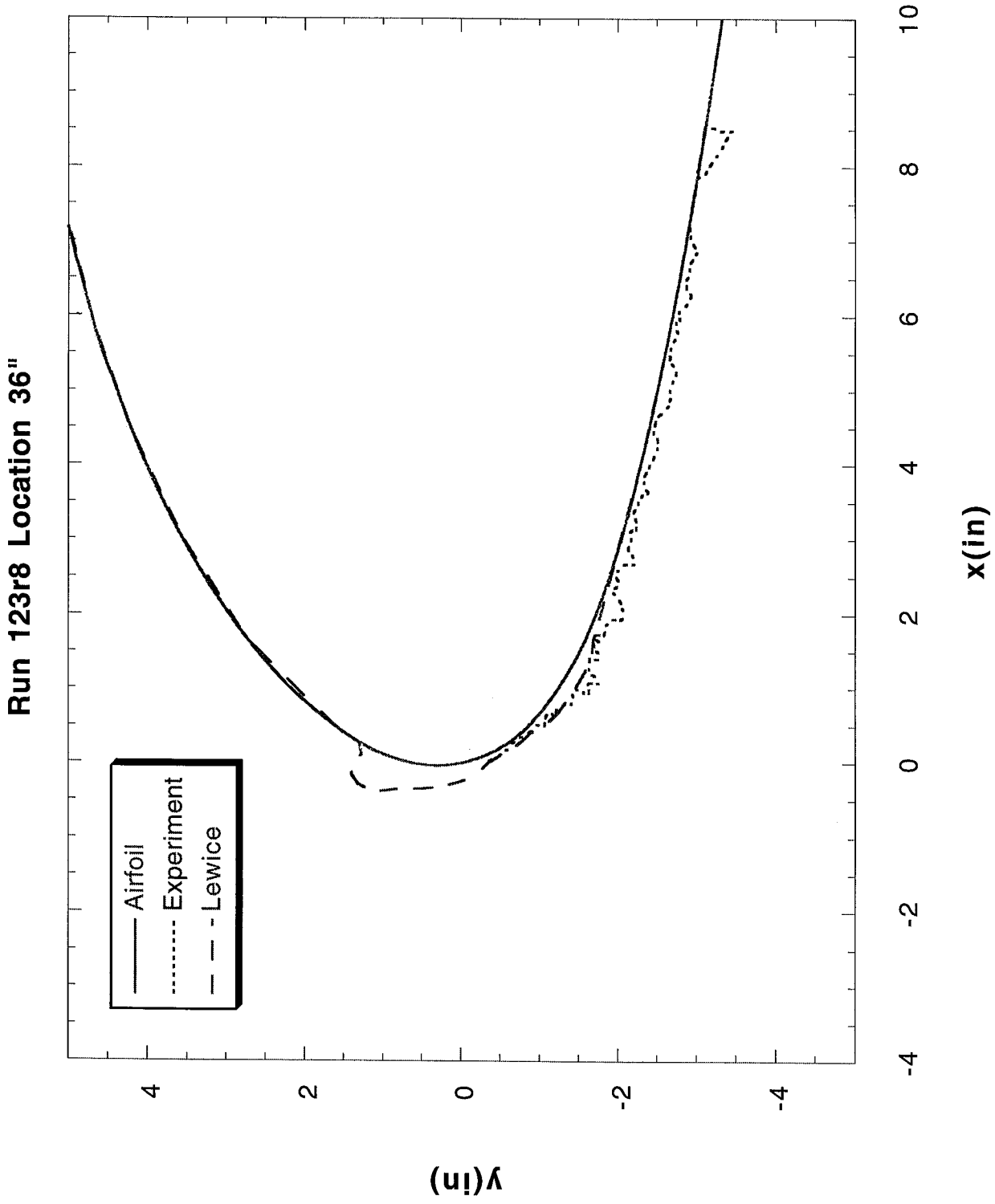
Run 123r8 Location 36"
Airfoil
Experiment
Lewice
y(in)
x(in)
4
2
0
-2
-4
-4
-2
0
2
4
6
8
10

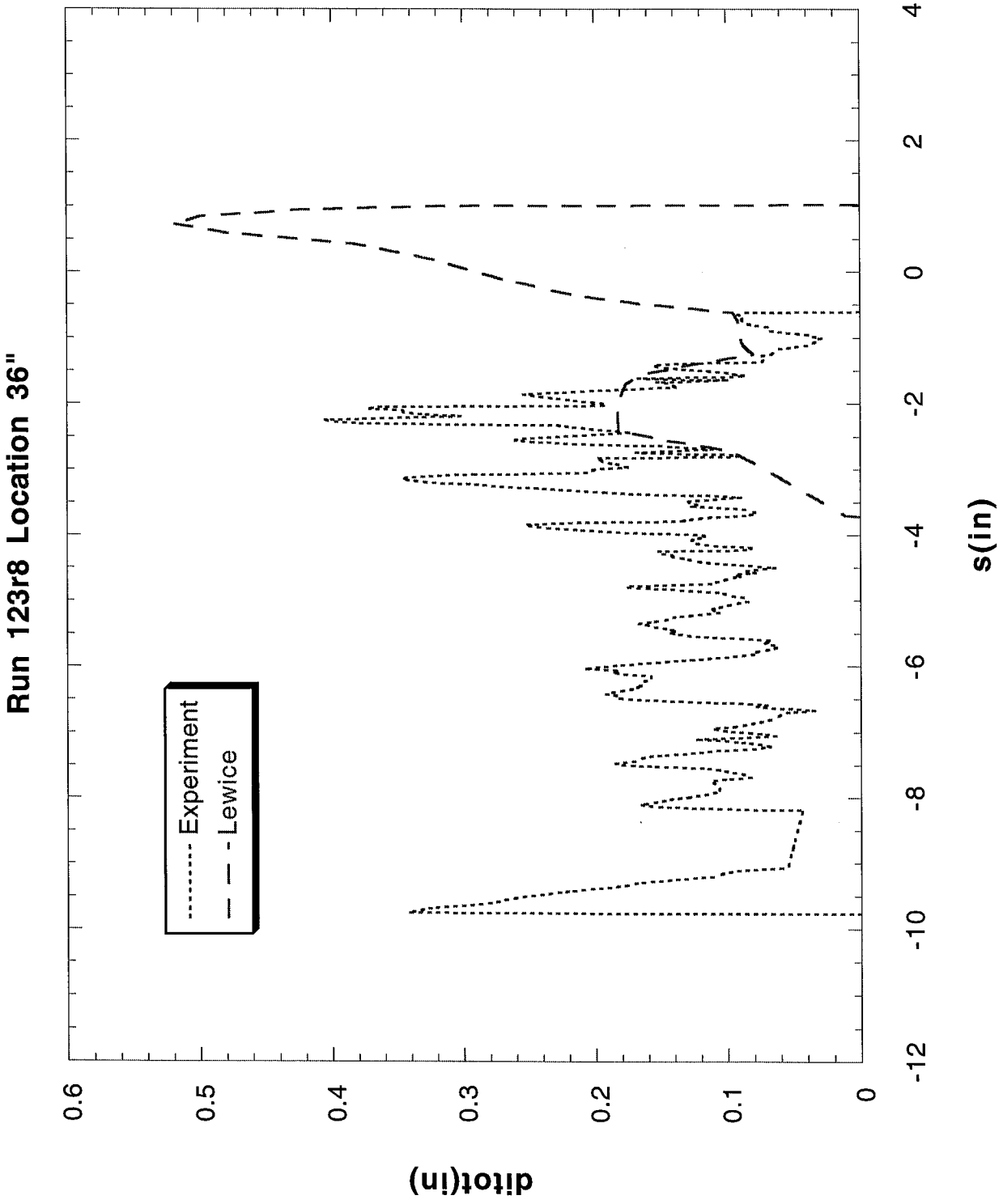
Run 123r8 Location 36"
Experiment
Lewice
dltot(in)
s(in)
0.6
0.5
0.4
0.3
0.2
0.1
0
-12
-10
-8
-6
-4
-2
0
2
4

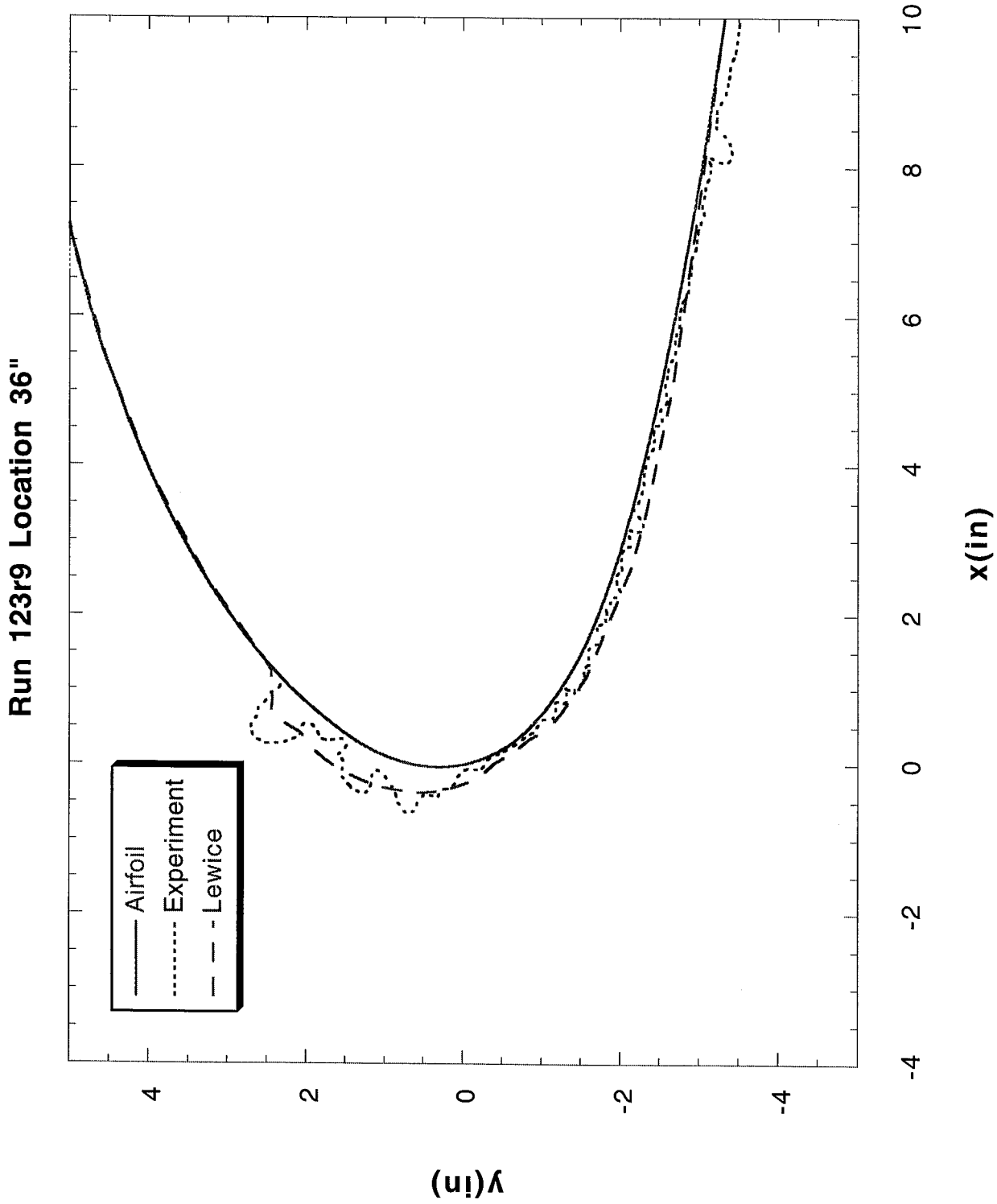
Run 123r9 Location 36"
Airfoil
Experiment
Lewice
y(in)
x(in)
4
2
0
-2
-4
-4
-2
0
2
4
6
8
10

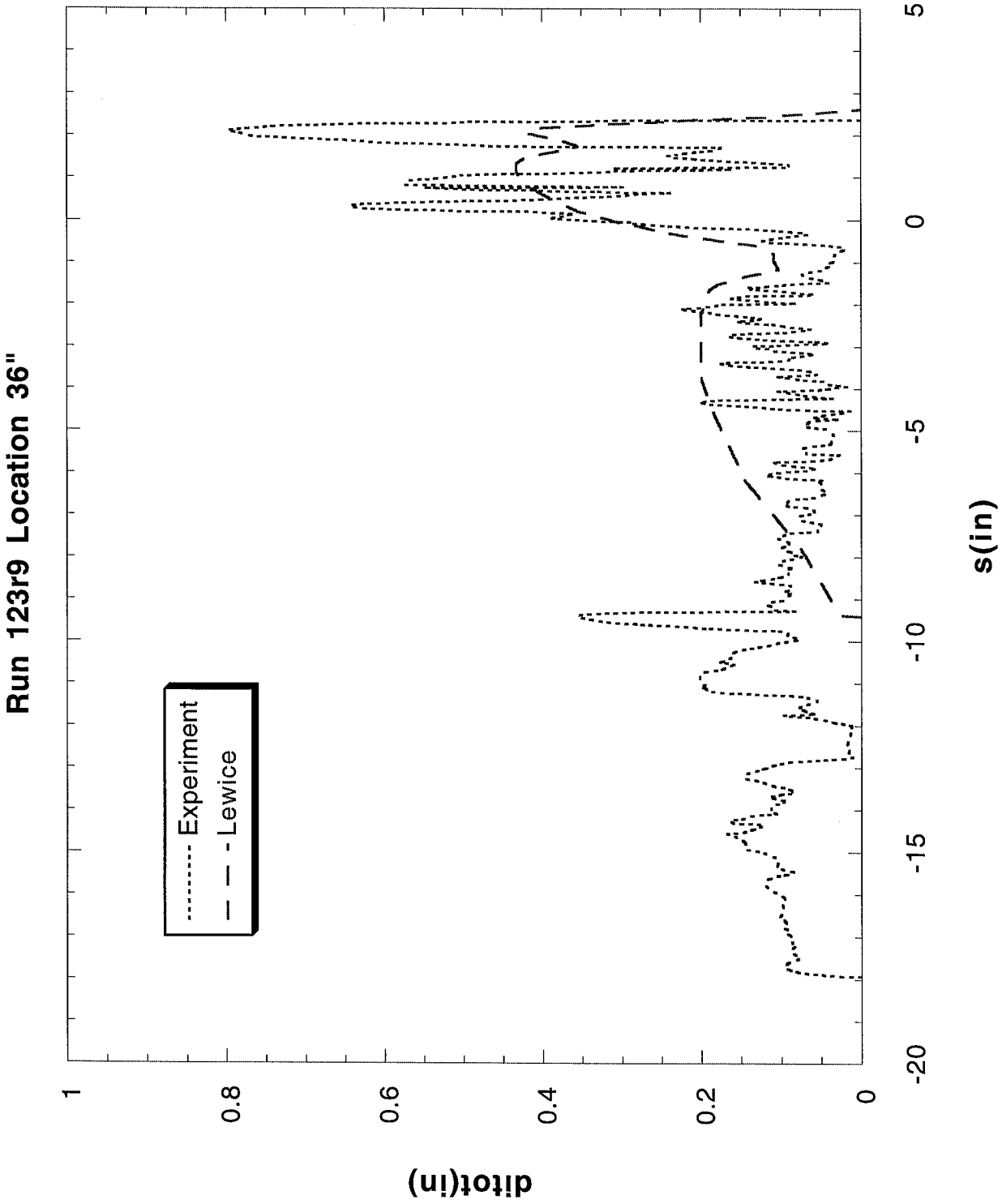
Run 123r9 Location 36"
Experiment
Lewice
dltot(in)
s(in)
1
0.8
0.6
0.4
0.2
0
5
0
-5
-10
-15
-20

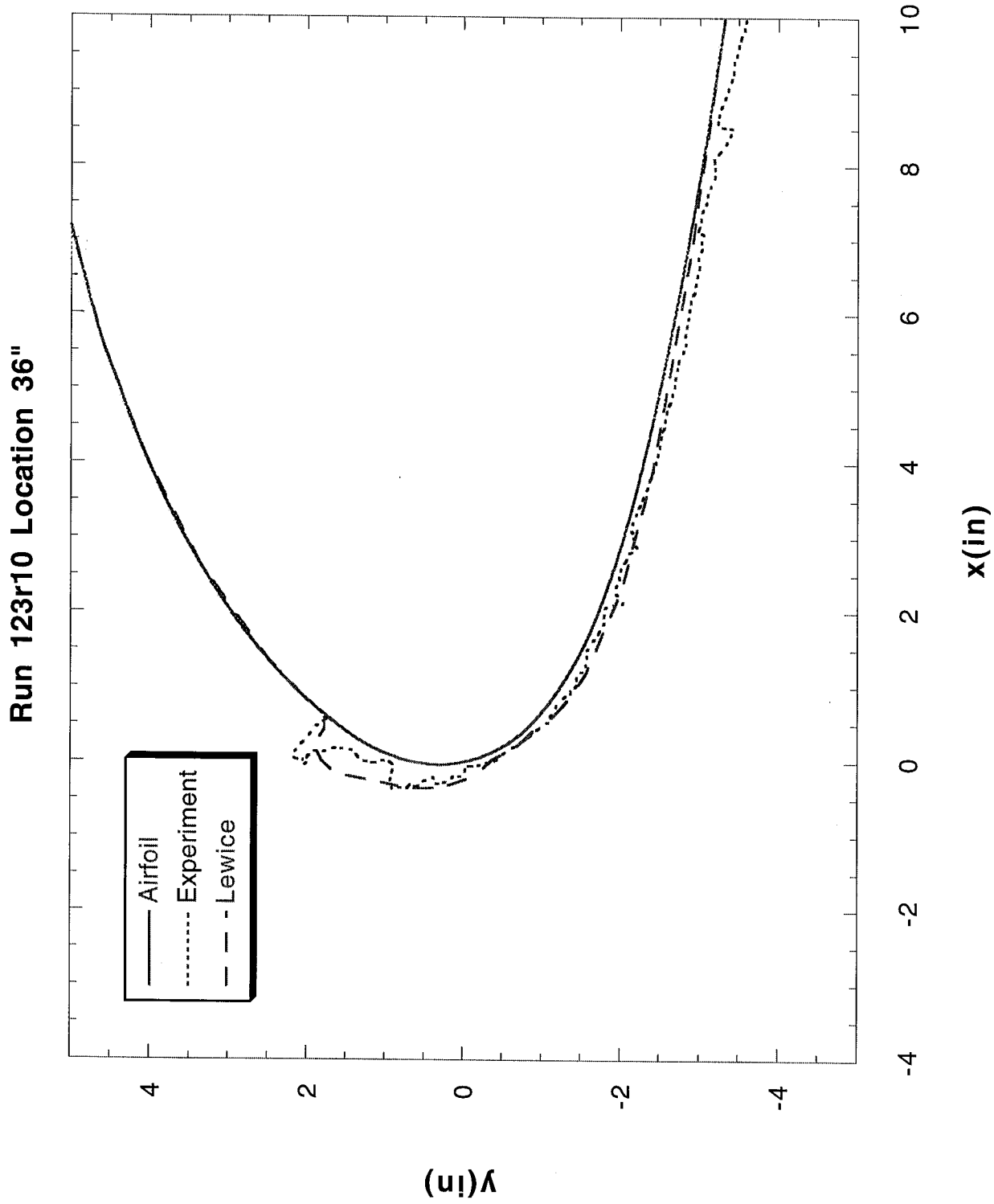
Run 123r10 Location 36"
Airfoil
Experiment
Lewice
y(in)
x(in)
4
2
0
-2
-4
-4
-2
0
2
4
6
8
10

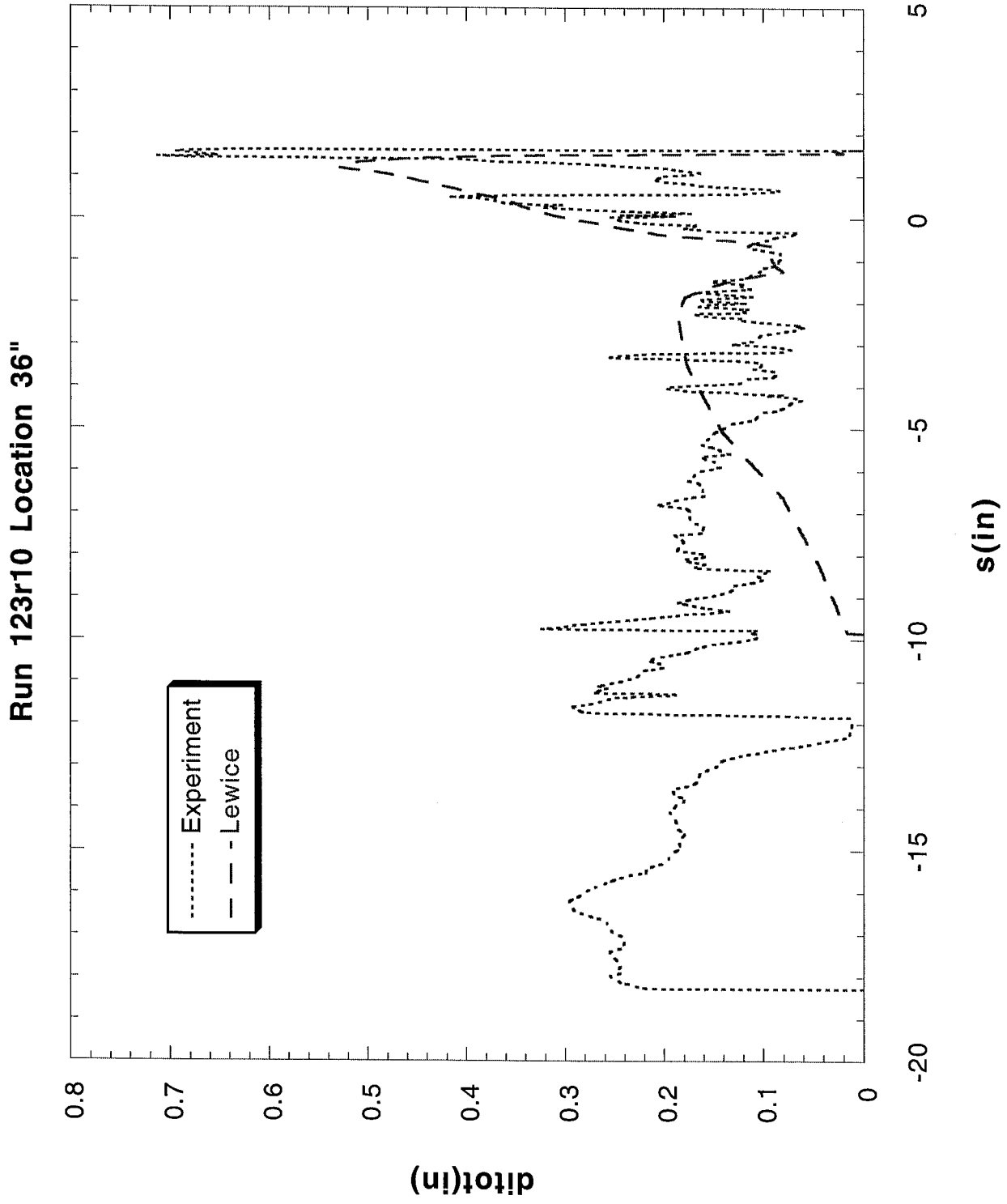
Run 123r10 Location 36"
Experiment
Lewice
dltot(in)
s(in)
0.8
0.7
0.6
0.5
0.4
0.3
0.2
0.1
0
5
0
-5
-10
-15
-20

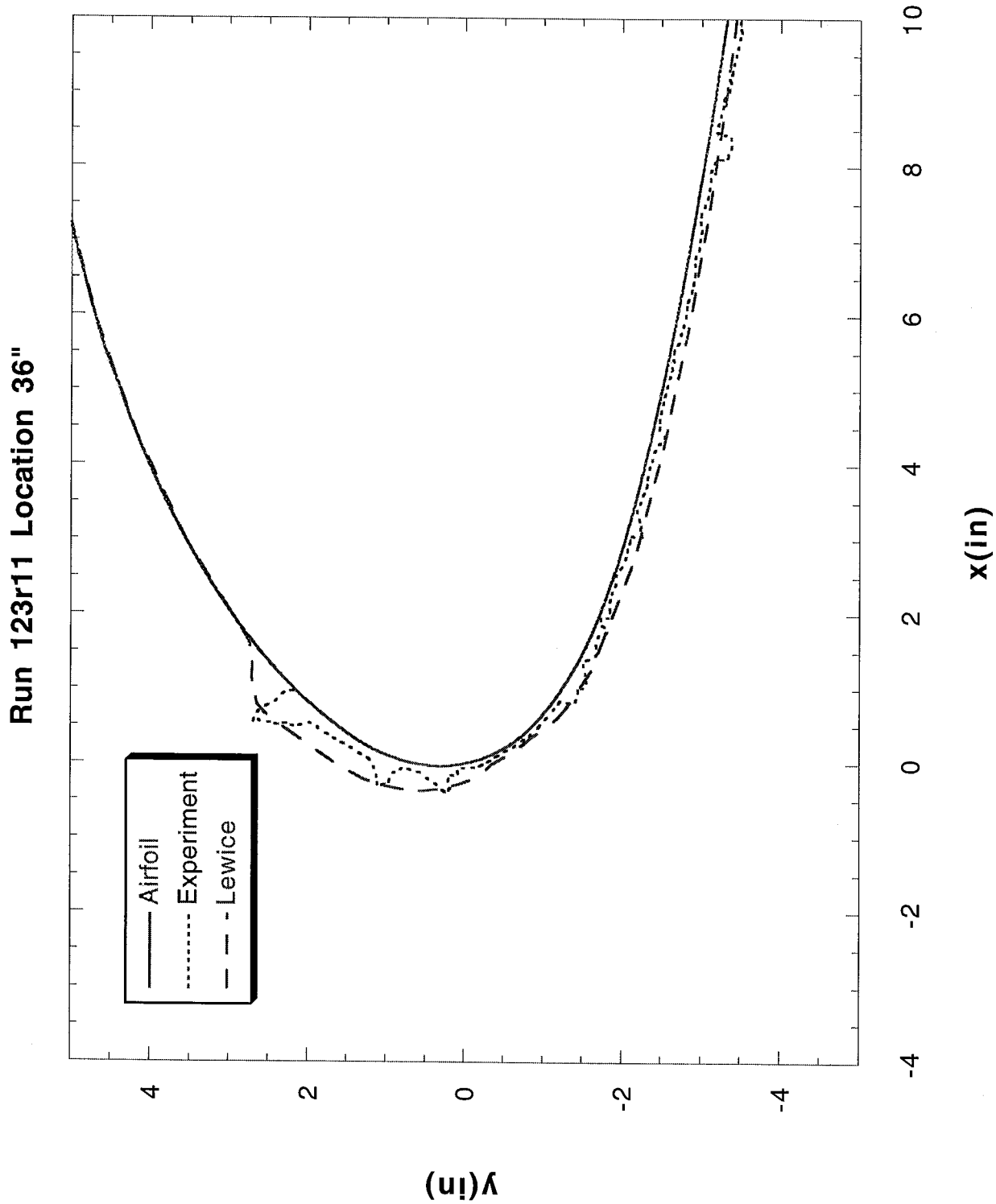
Run 123r11 Location 36"
Airfoil
Experiment
Lewice
y(in)
x(in)
4
2
0
-2
-4
-4
-2
0
2
4
6
8
10

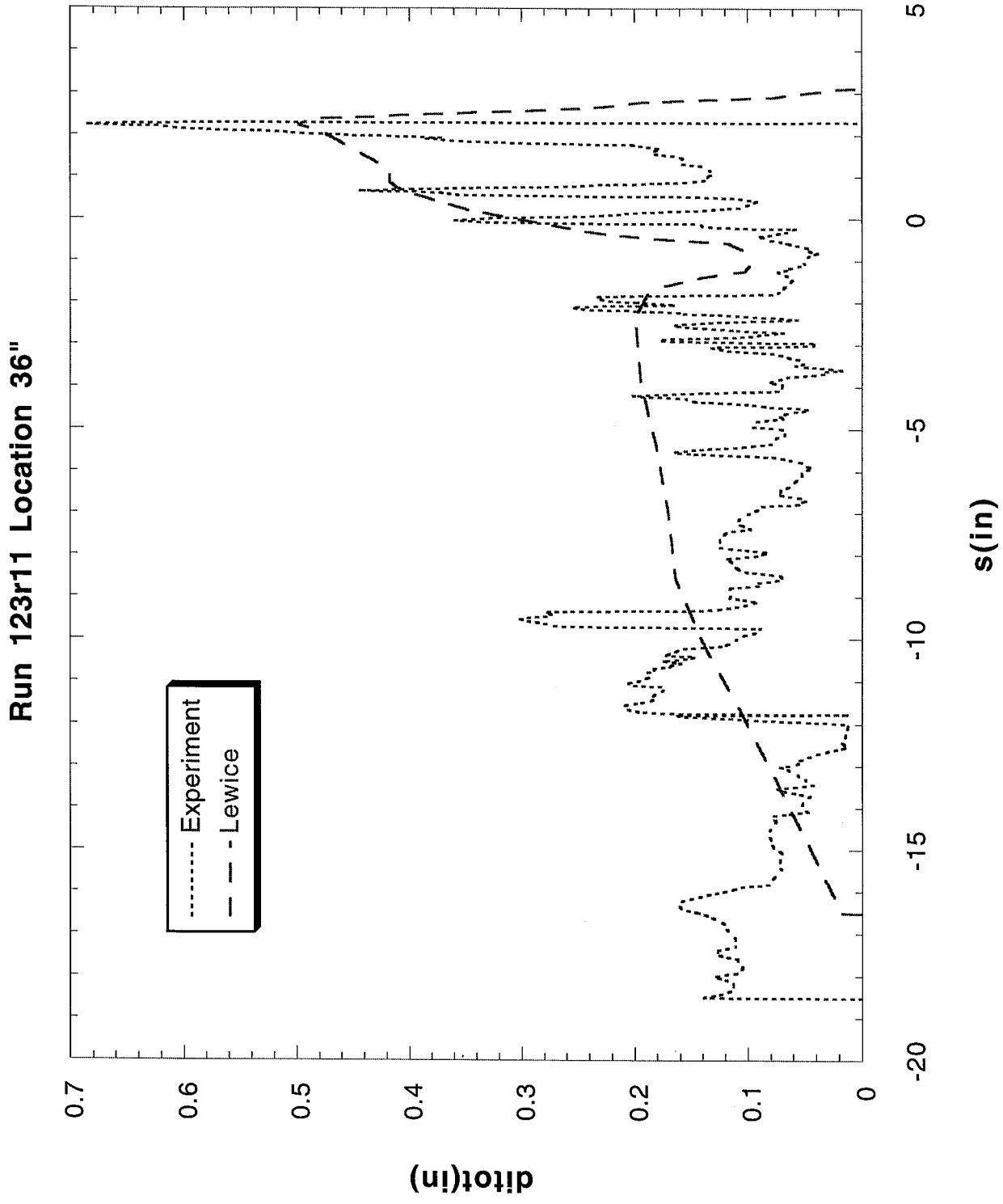
Run 123r11 Location 36"
Experiment
Lewice
dltot(in)
s(in)
0.7
0.6
0.5
0.4
0.3
0.2
0.1
0
5
0
-5
-10
-15
-20

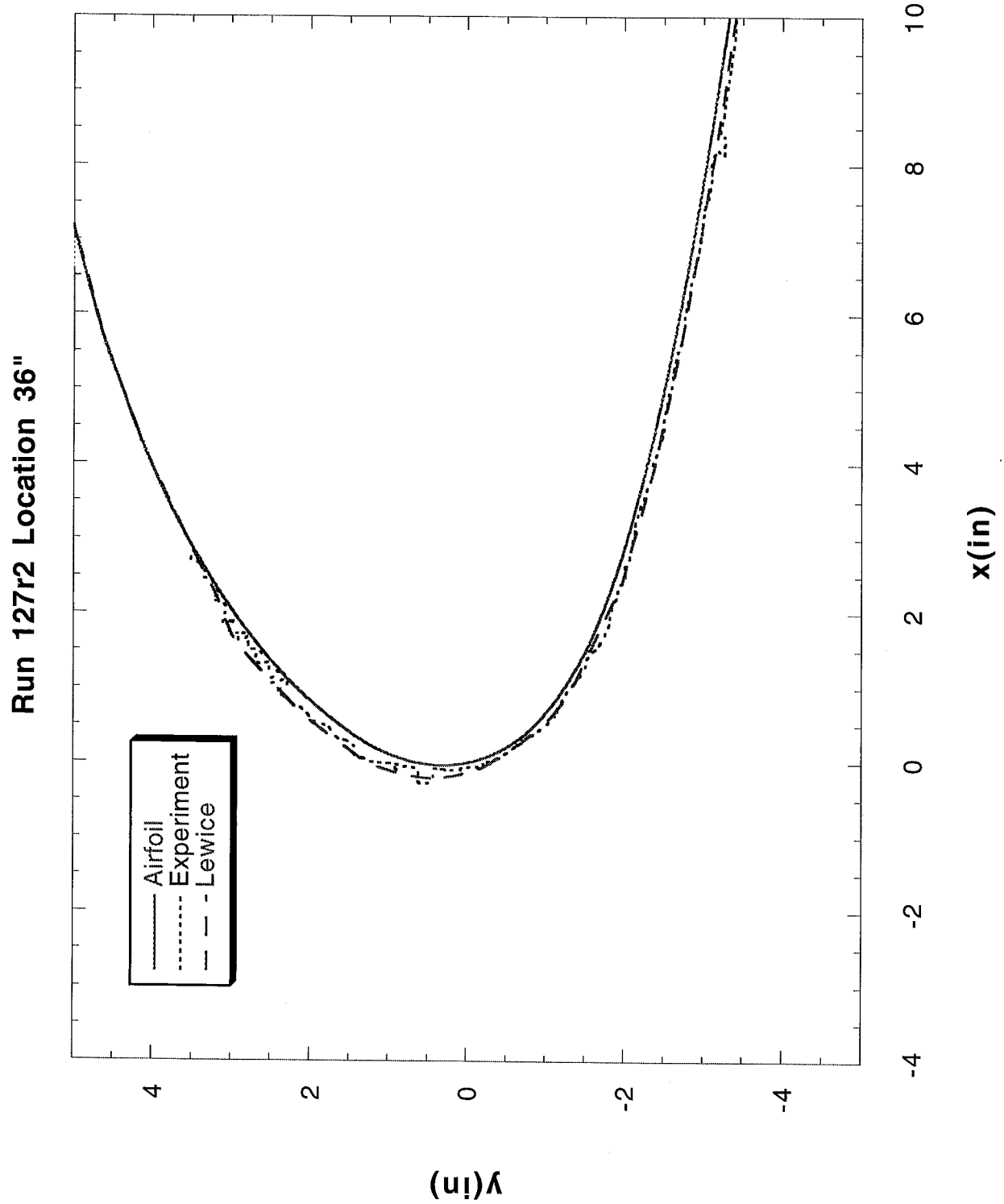
Run 127r2 Location 36"
Airfoil
Experiment
Lewice
y(in)
x(in)
4
2
0
-2
-4
-4
-2
0
2
4
6
8
10

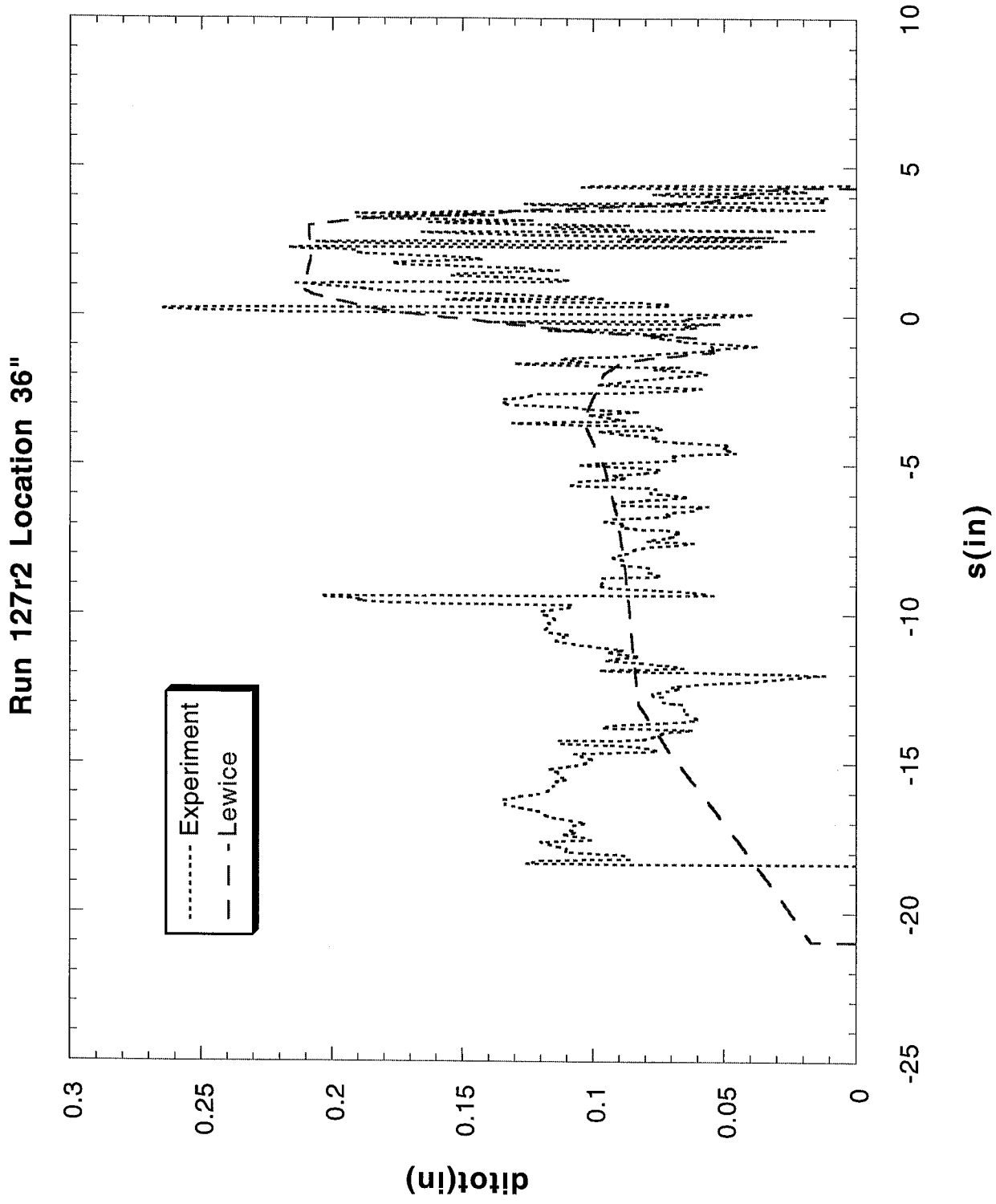
Run 127r2 Location 36"
Experiment
Lewice
dltot(in)
s(in)
0.3
0.25
0.2
0.15
0.1
0.05
0
10
5
0
-5
-10
-15
-20
-25

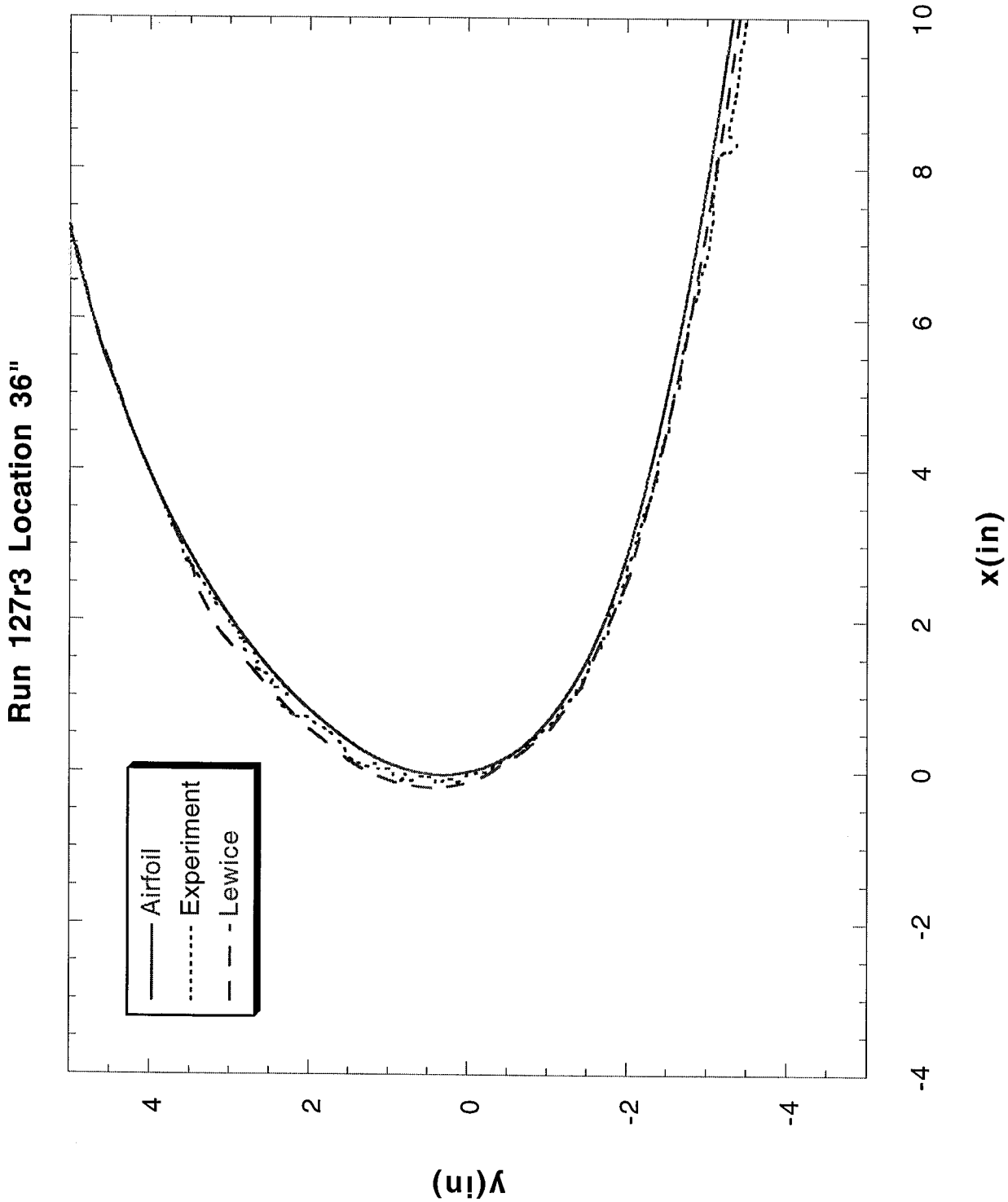
Run 127r3 Location 36"
Airfoil
Experiment
Lewice
y(in)
x(in)
4
2
0
-2
-4
-4
-2
0
2
4
6
8
10

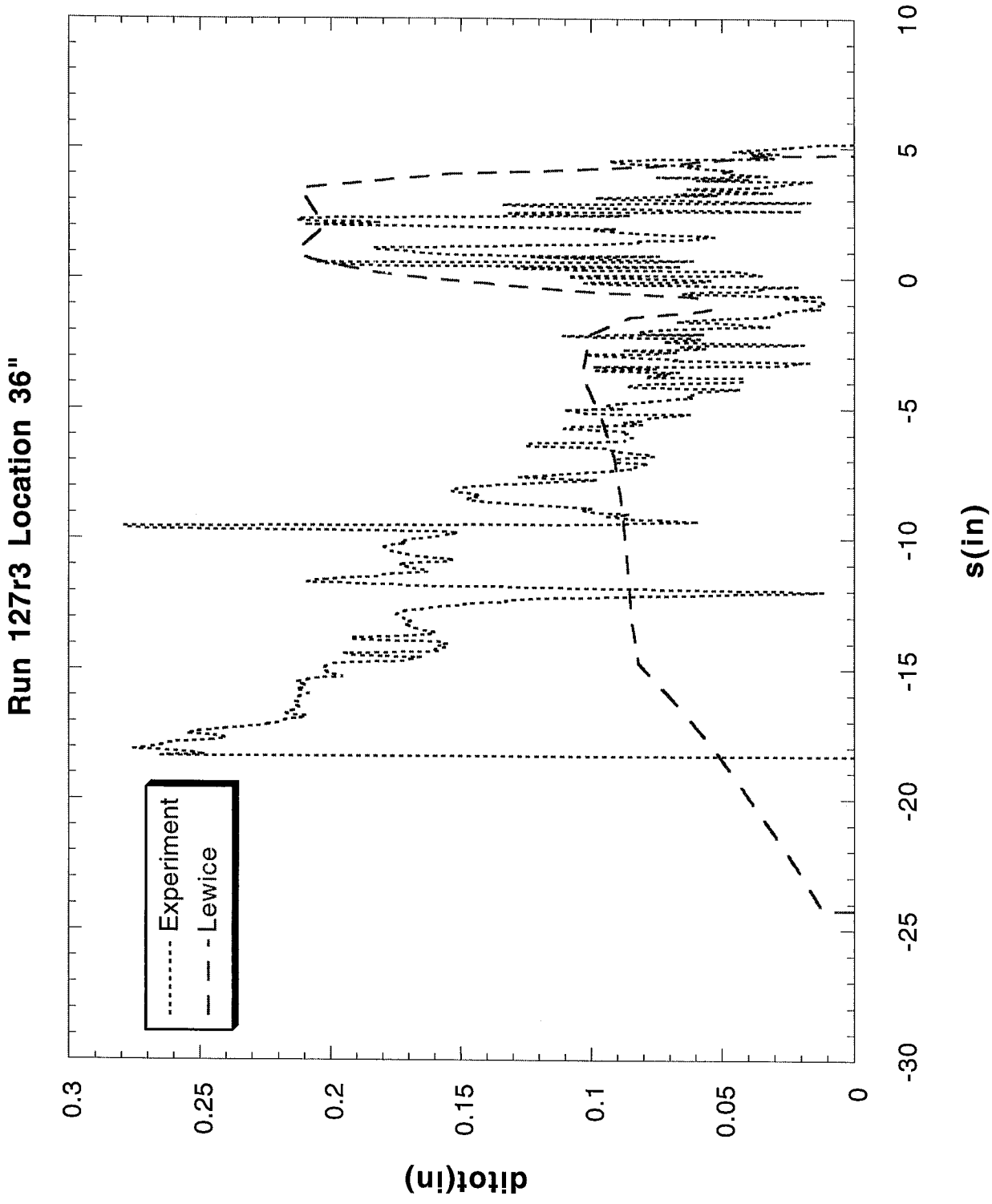
Run 127r3 Location 36"
Experiment
Lewice
dltot(in)
s(in)
0.3
0.25
0.2
0.15
0.1
0.05
0
10
5
0
-5
-10
-15
-20
-25
-30

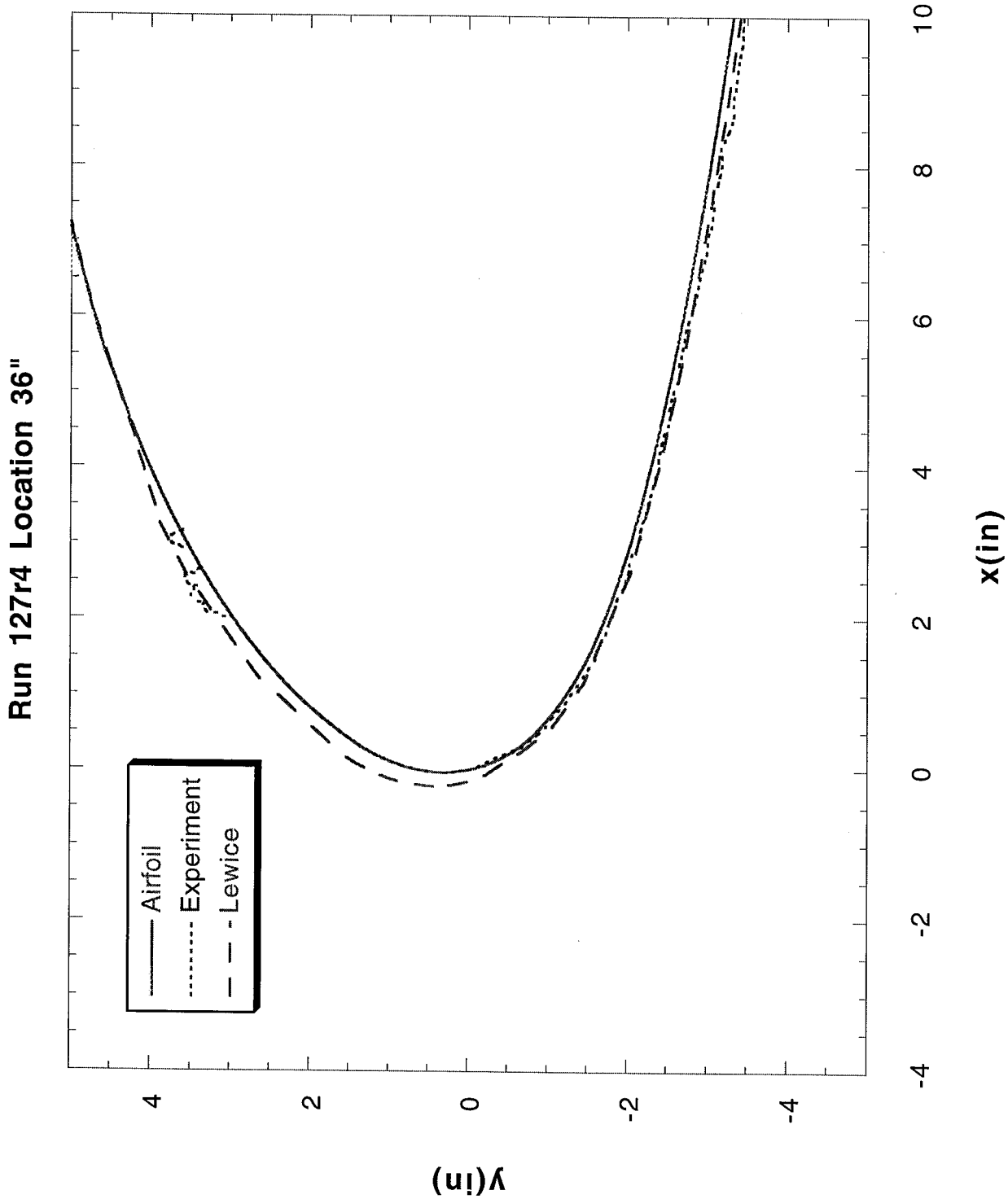
Run 127r4 Location 36"
Airfoil
Experiment
Lewice
y(in)
x(in)
4
2
0
-2
-4
-4
-2
0
2
4
6
8
10

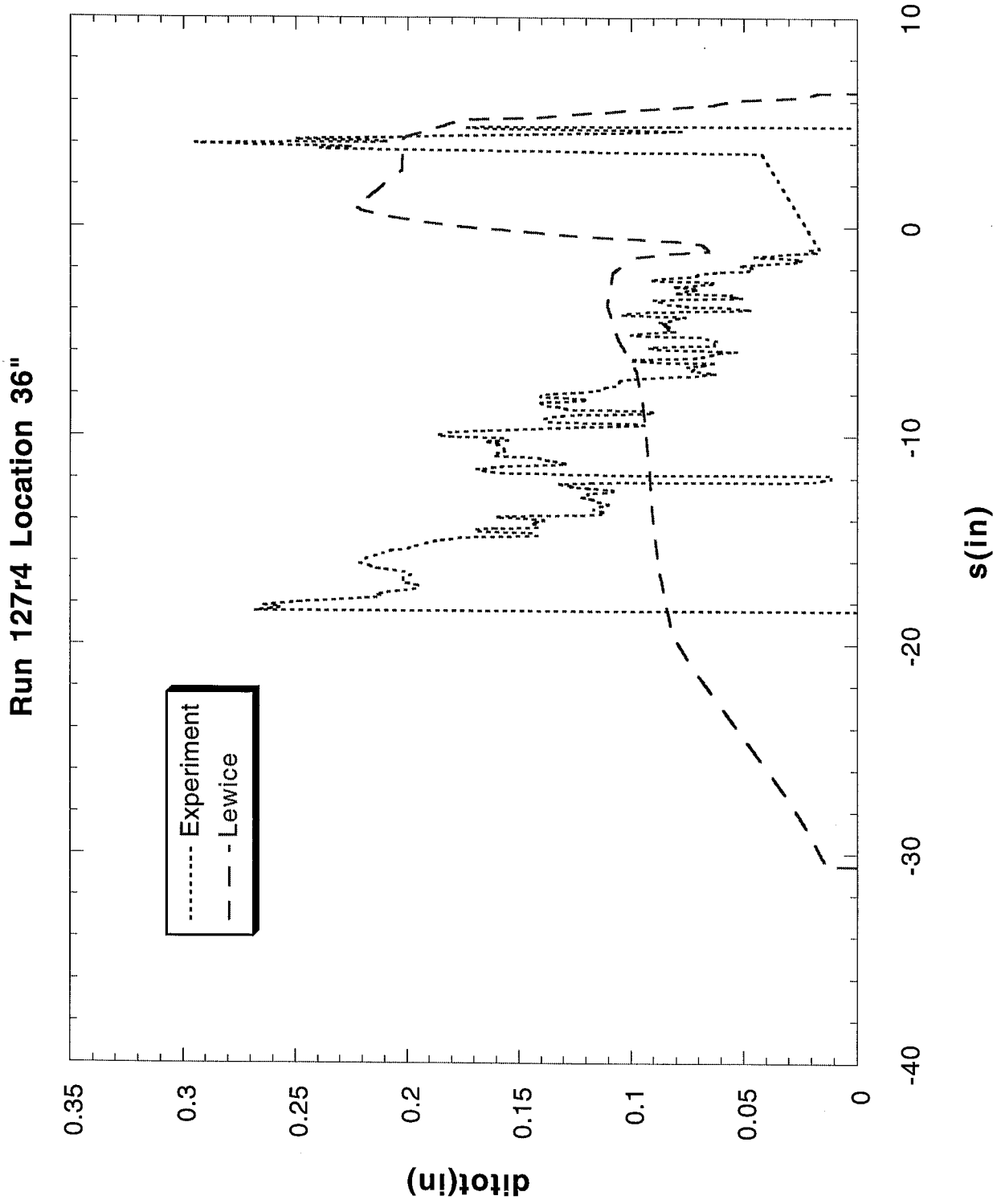
Run 127r4 Location 36"
Experiment
Lewice
dltot(in)
s(in)
0.35
0.3
0.25
0.2
0.15
0.1
0.05
0
10
0
-10
-20
-30
-40

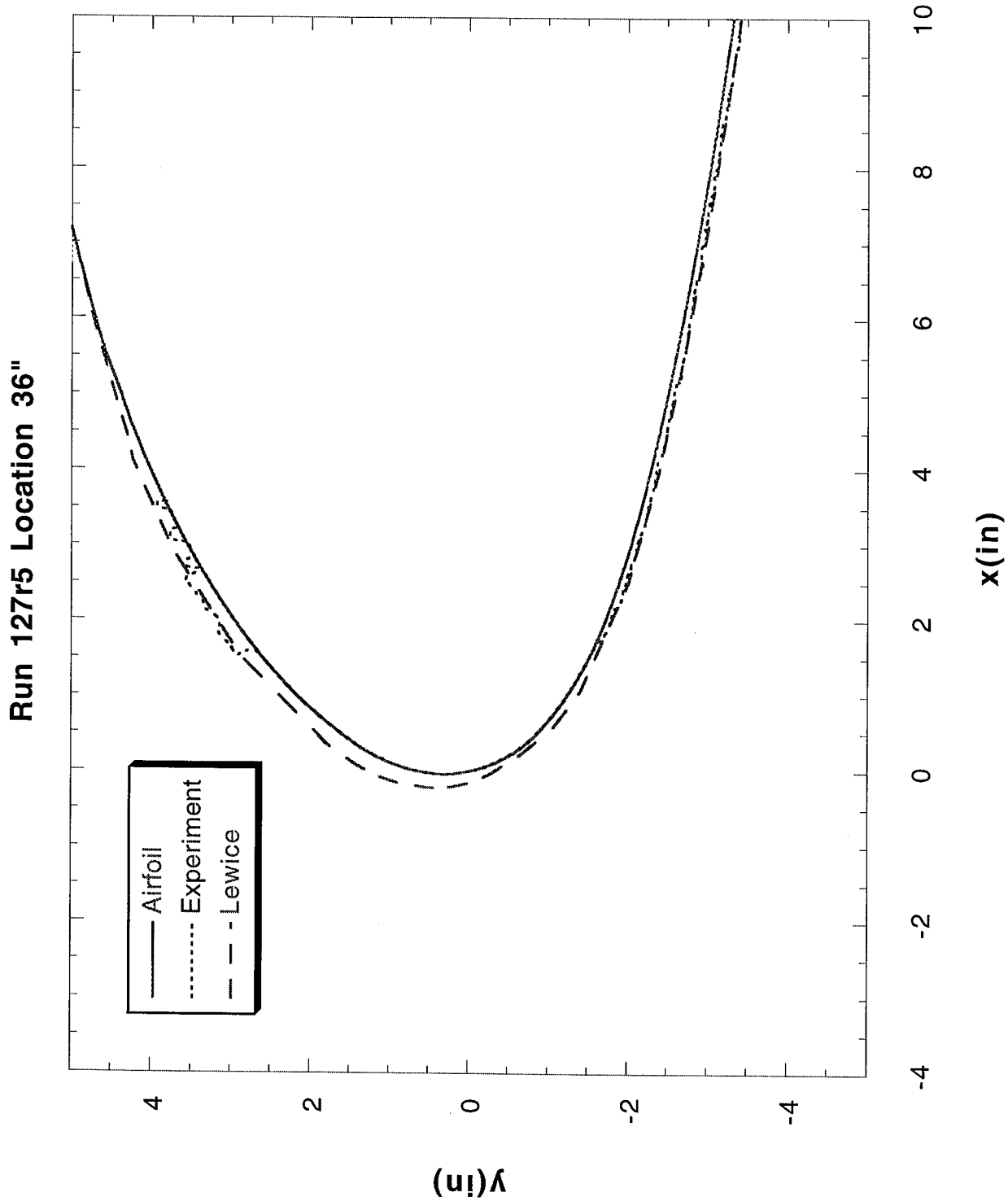
Run 127r5 Location 36"
Airfoil
Experiment
Lewice
y(in)
x(in)
4
2
0
-2
-4
-4
-2
0
2
4
6
8
10

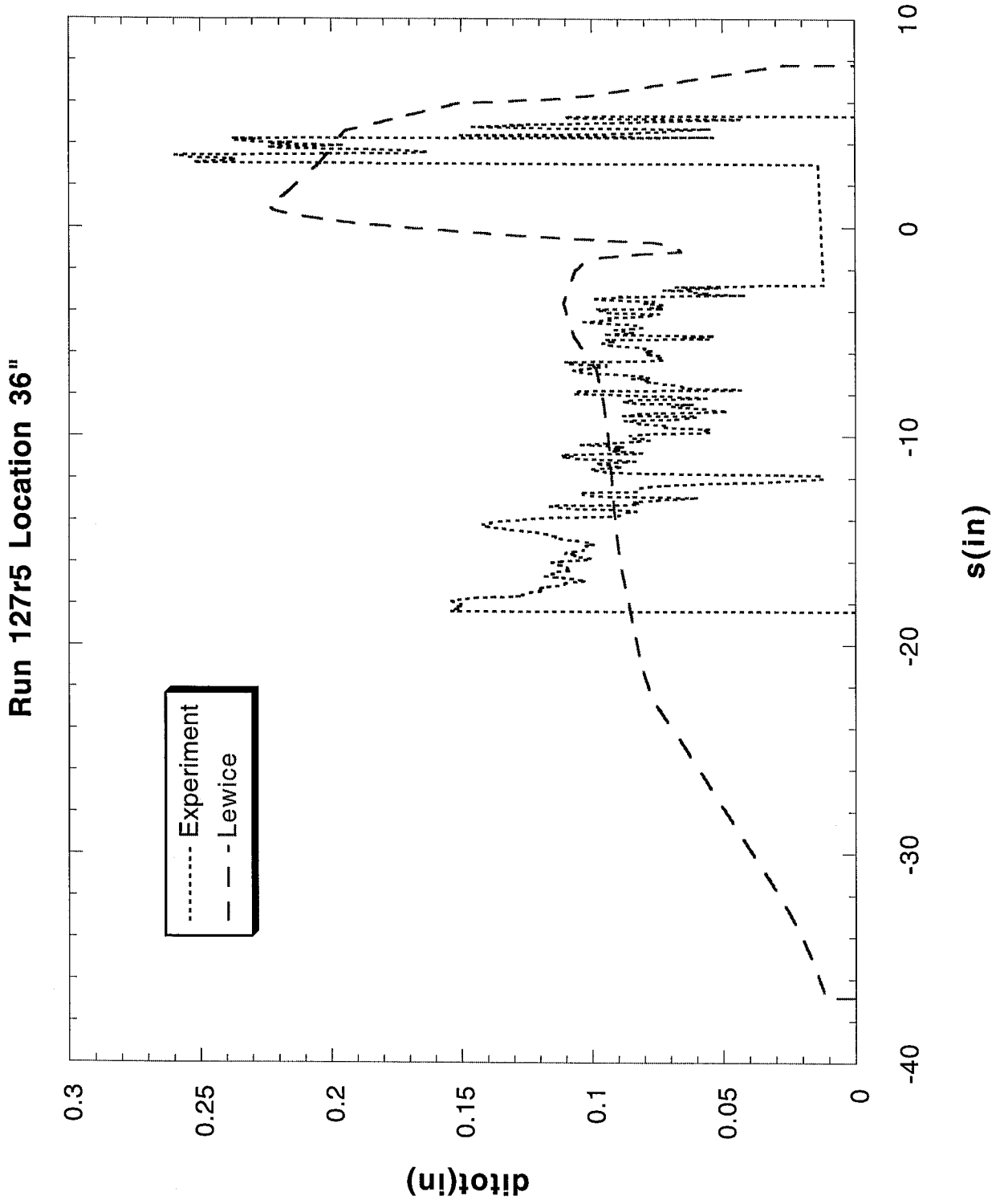
Run 127r5 Location 36"
Experiment
Lewice
dltot(in)
s(in)
0.3
0.25
0.2
0.15
0.1
0.05
0
10
0
-10
-20
-30
-40

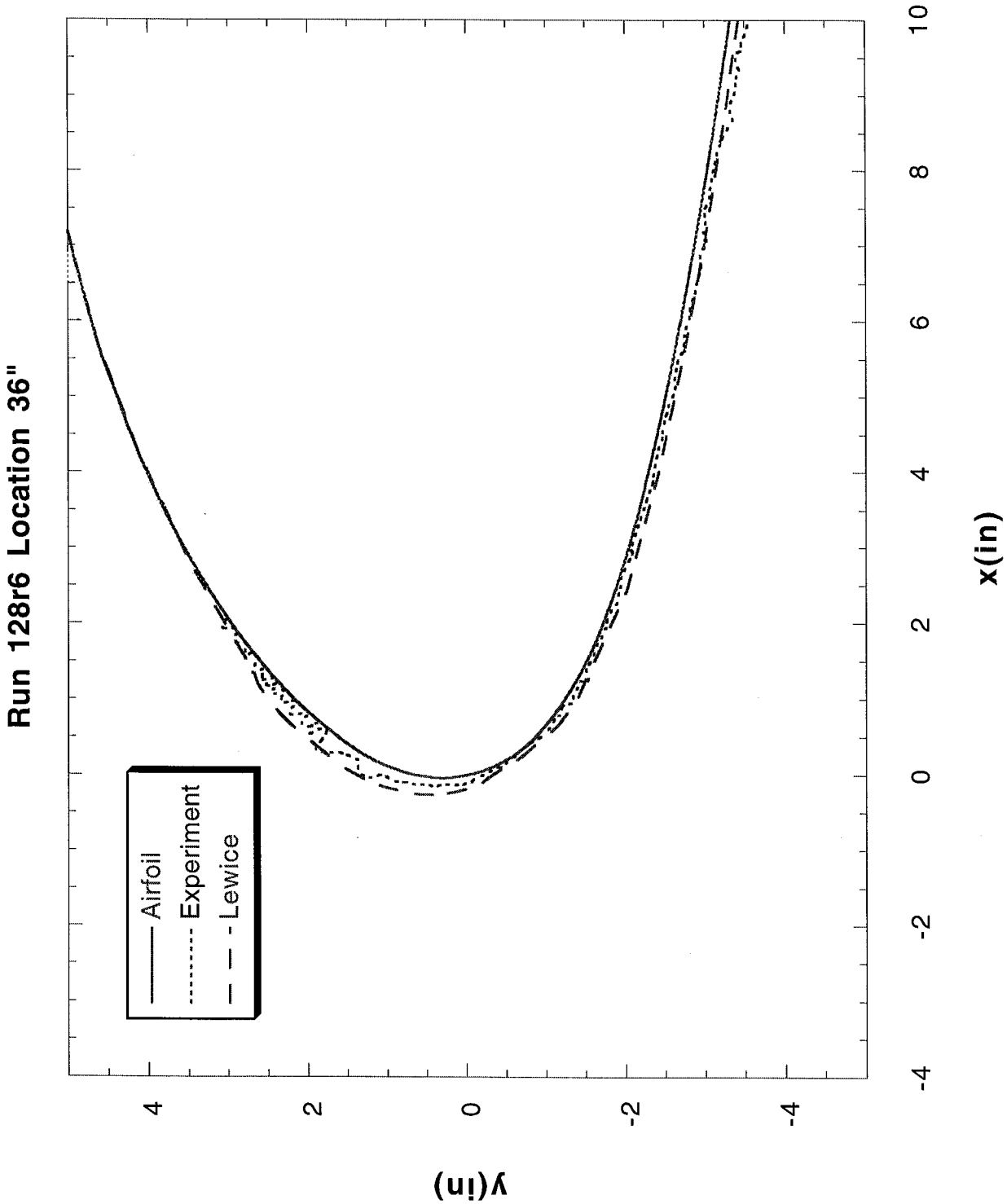
Run 128r6 Location 36"
Airfoil
Experiment
Lewice
y(in)
x(in)
4
2
0
-2
-4
-4
-2
0
2
4
6
8
10

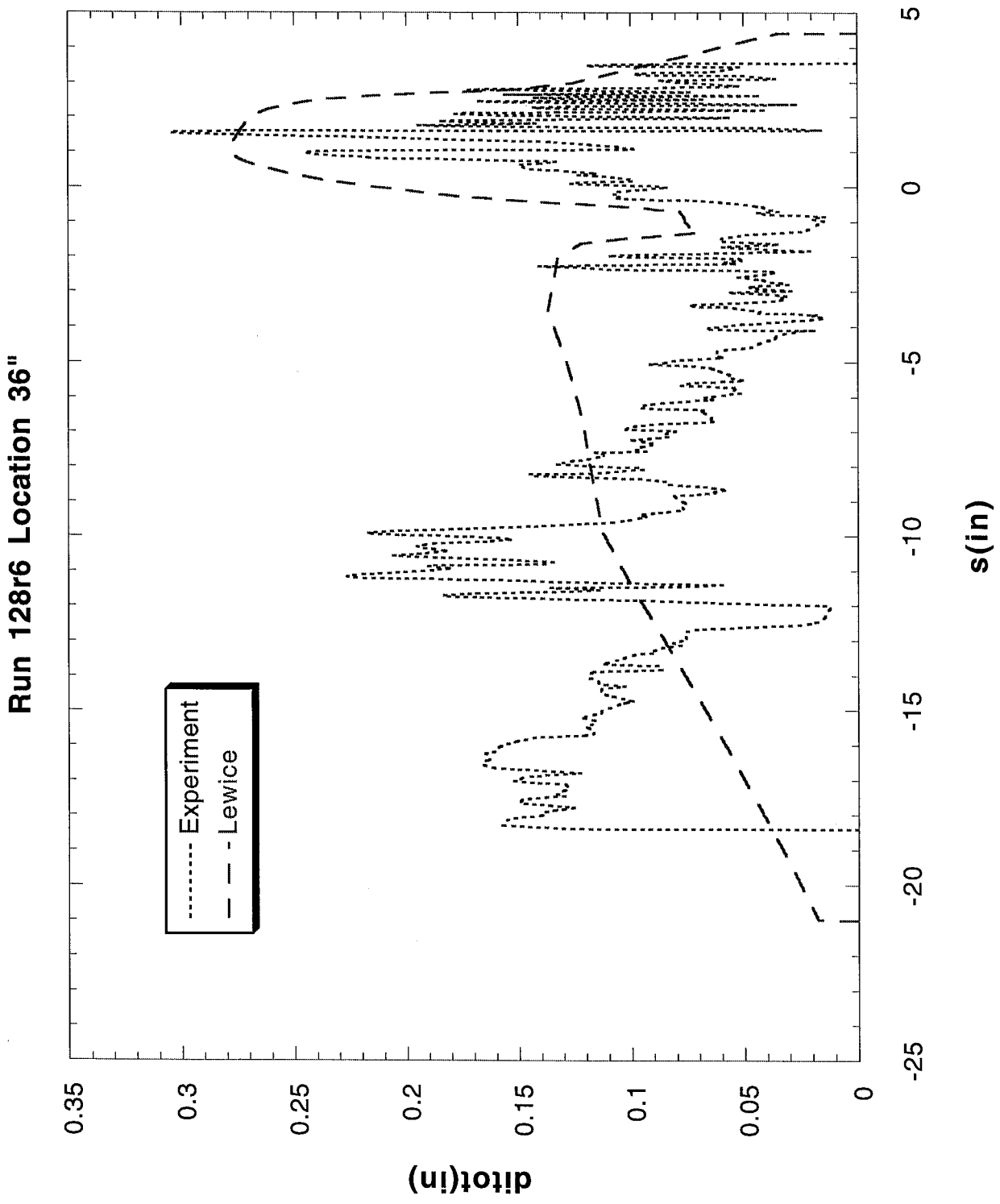
Run 128r6 Location 36"
Experiment
Lewice
ditot(in)
s(in)
0.35
0.3
0.25
0.2
0.15
0.1
0.05
0
5
0
-5
-10
-15
-20
-25

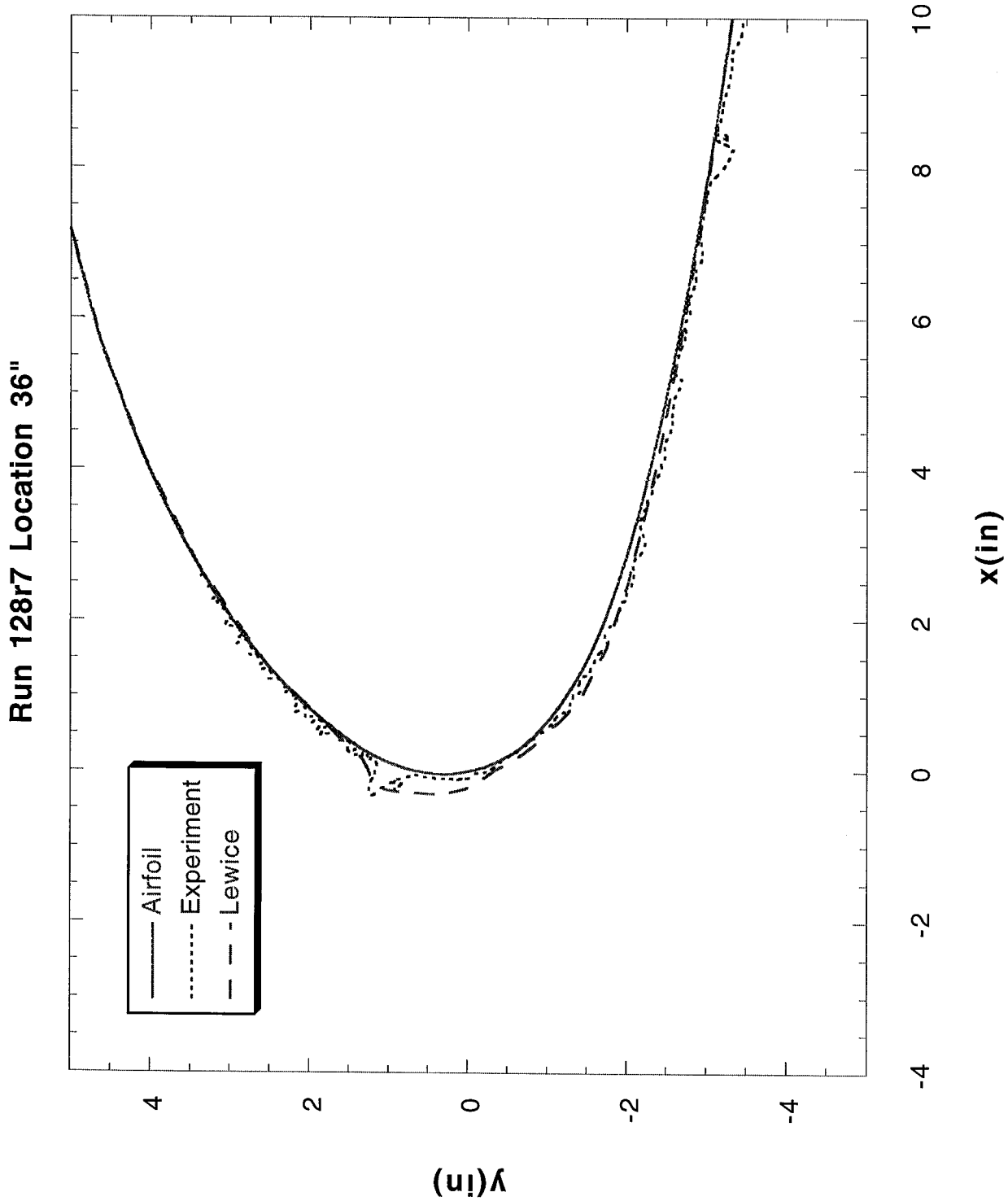
Run 128r7 Location 36"
Airfoil
Experiment
- Lewice
y(in)
x(in)
4
2
0
-2
-4
-4
-2
0
2
4
6
8
10

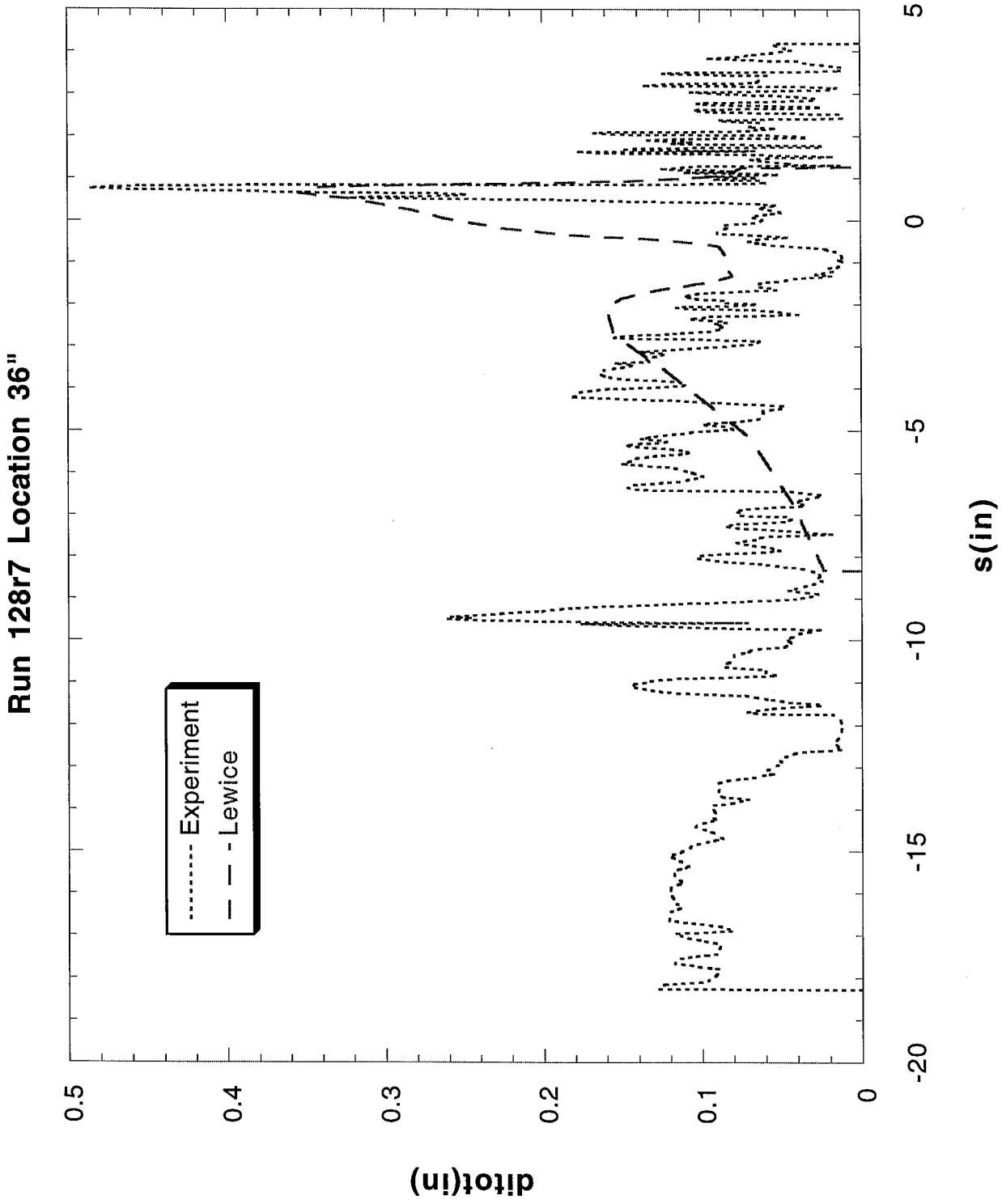
Run 128r7 Location 36"
Experiment
Lewice
dltot(in)
s(in)
0.5
0.4
0.3
0.2
0.1
0
5
0
-5
-10
-15
-20

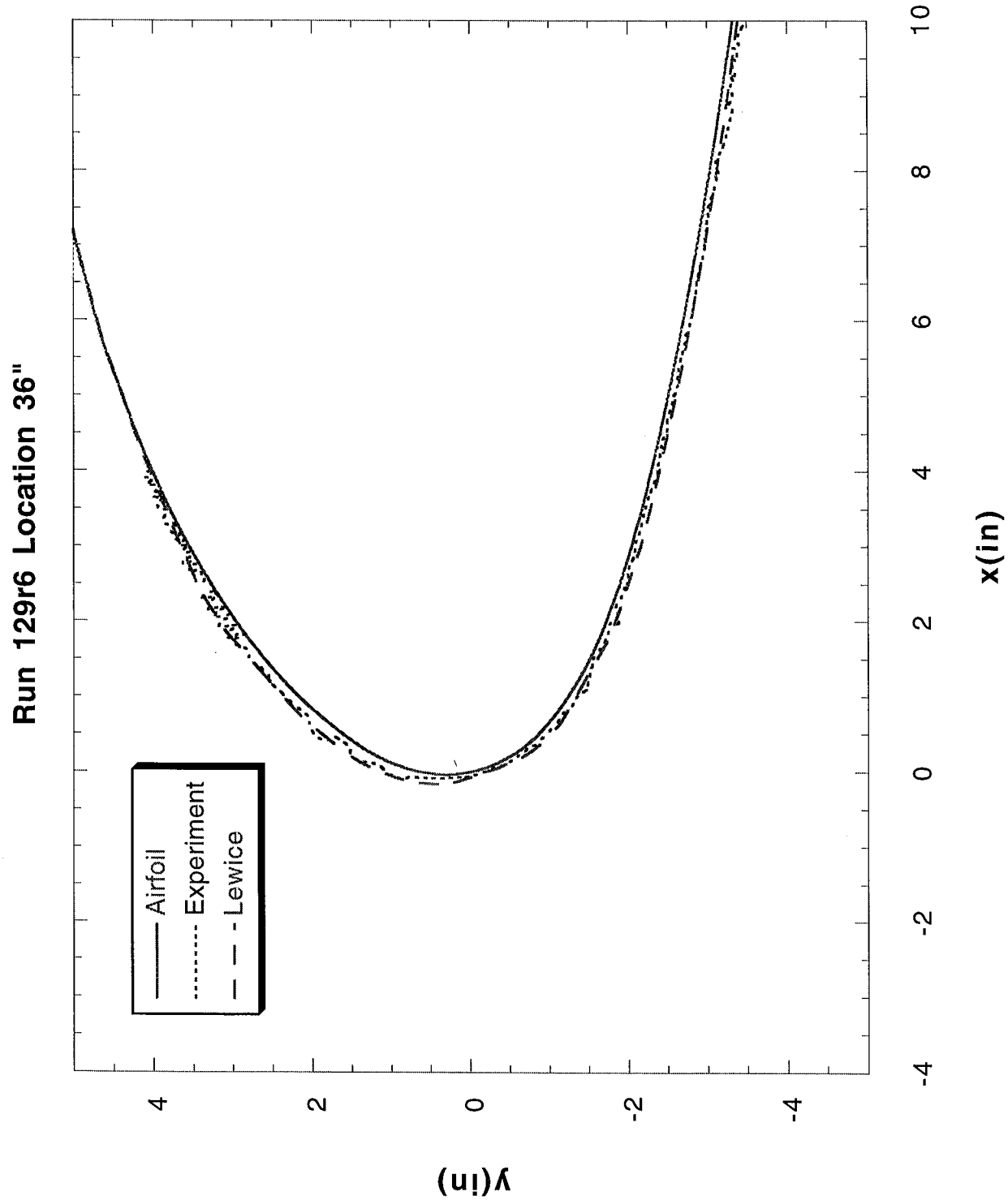
Run 129r6 Location 36"
Airfoil
Experiment
Lewice
y(in)
x(in)
4
2
0
-2
-4
-4
-2
0
2
4
6
8
10

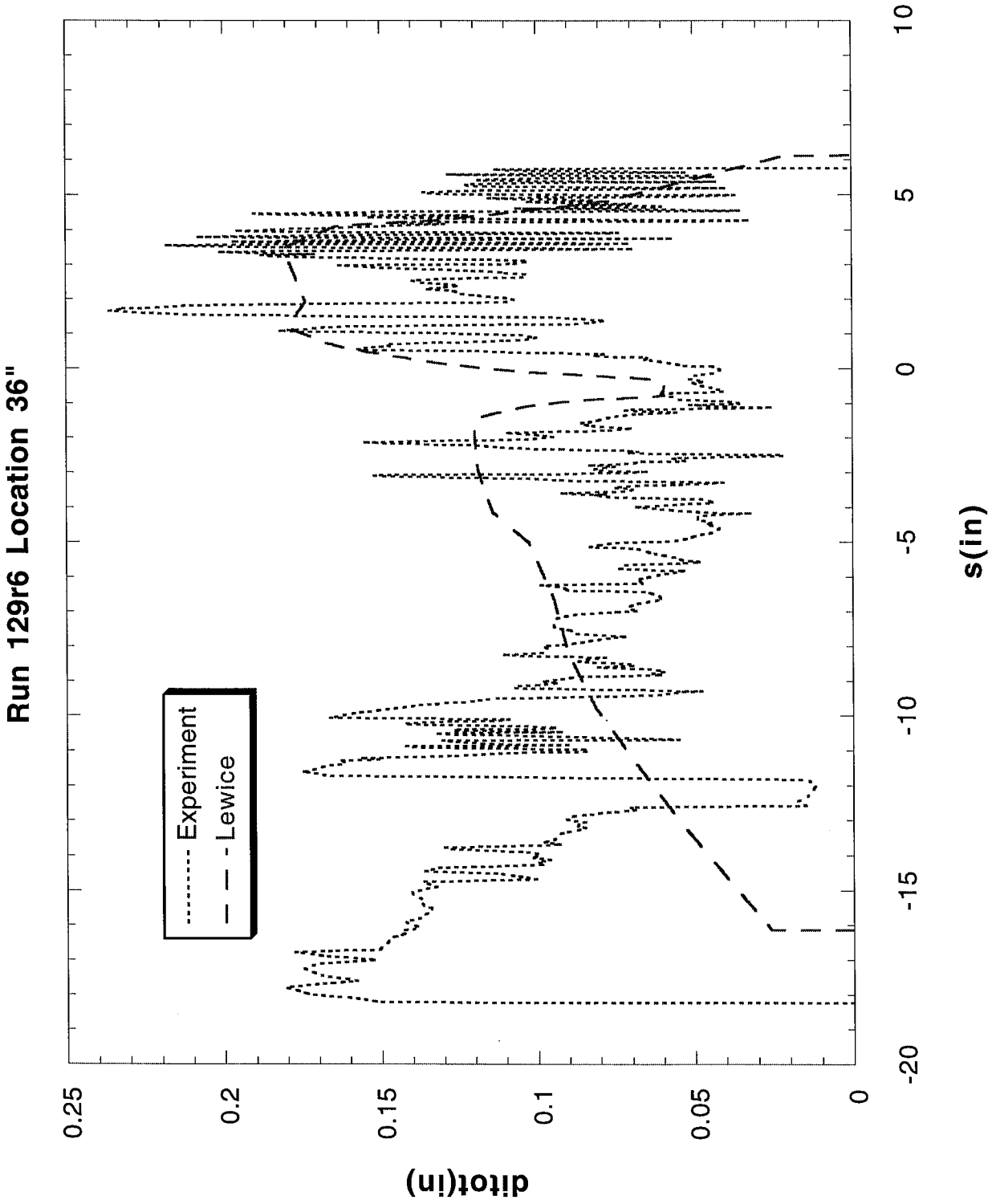
Run 129r6 Location 36"
Experiment
Lewice
dltot(in)
0.25
0.2
0.15
0.1
0.05
0
s(in)
10
5
0
-5
-10
-15
-20

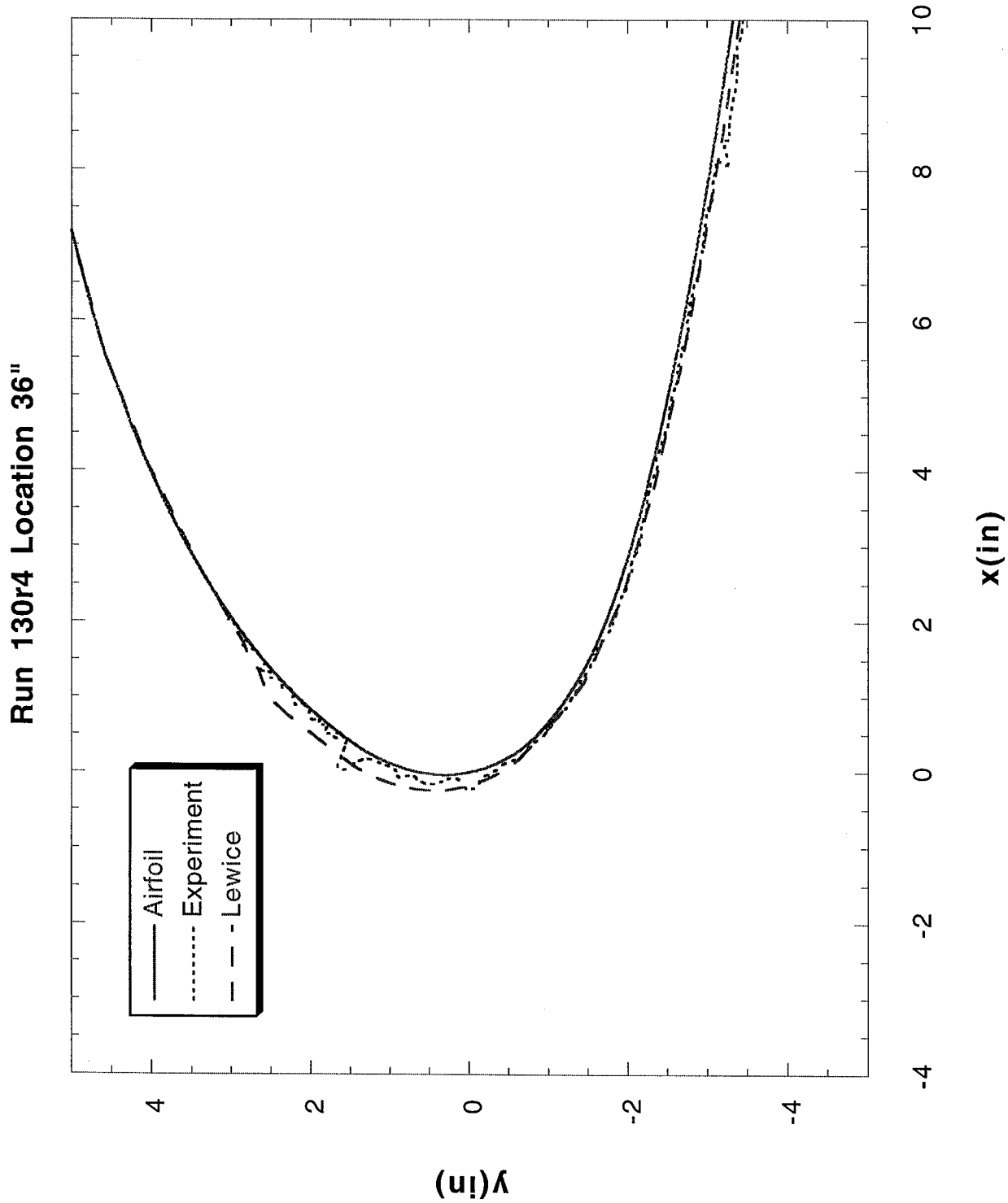
Run 130r4 Location 36"
Airfoil
Experiment
Lewice
y(in)
x(in)
4
2
0
-2
-4
-4
-2
0
2
4
6
8
10

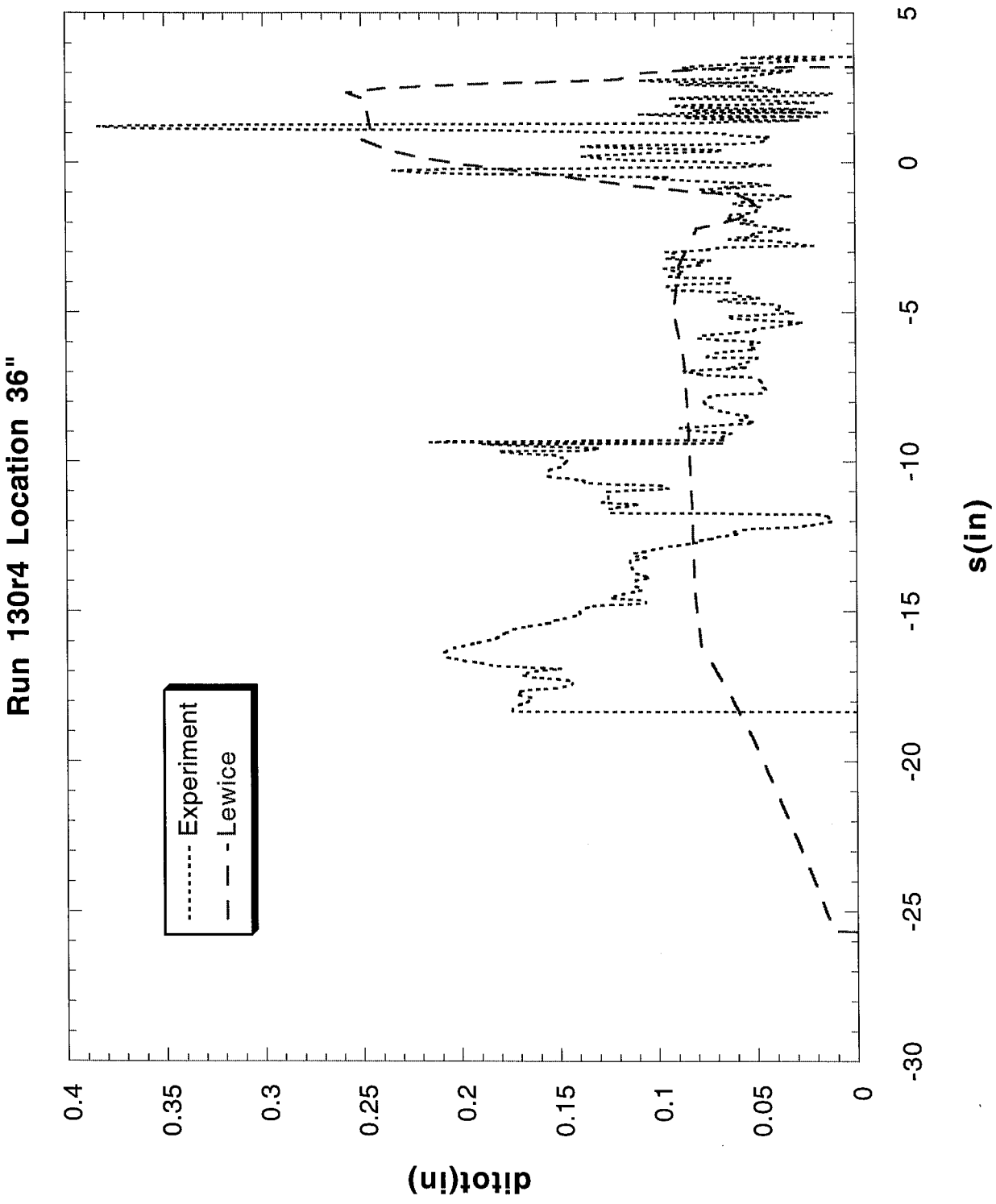
Run 130r4 Location 36"
Experiment
Lewice
ditot(in)
s(in)
0.4
0.35
0.3
0.25
0.2
0.15
0.1
0.05
0
5
0
-5
-10
-15
-20
-25
-30

LTHS
Figures 242 – 295

LTHS Test Conditions

Principal Investigator	Airfoil	Test Date	Chord (in)	Run Number	Previous Identical Run	Velocity (kts)	Velocity (m/s)	Tt (°F)	Static Temperature (K)	A.O.A.	Corrected A.O.A.	LWC (g/m^3)	MVD (microns)	Spray Time (min)	Digitized Tracing Locations
Addy	LTHS	Feb. 1996	36"	101		284	146.1	32	262.22	0	0	0.41	20	6	30", 36" & 42"
Addy	LTHS	Feb. 1996	36"	102		250	128.6	32	264.62	0	0	0.41	20	6	30", 36" & 42"
Addy	LTHS	Feb. 1996	36"	103		250	128.6	32	264.62	0	0	0.41	20	22.5	30", 36" & 42"
Addy	LTHS	Feb. 1996	36"	104		248	127.6	10.5	252.80	-1	-1	0.339	15	5.9	30", 36" & 42"
Addy	LTHS	Feb. 1996	36"	105		248	127.6	10.5	252.80	-1	-1	0.339	15	22	30", 36" & 42"
Addy	LTHS	Feb. 1996	36"	106		248	127.6	10.5	252.80	0	0	0.339	15	5.9	30", 36" & 42"
Addy	LTHS	Feb. 1996	36"	106r1	106	248	127.6	10.5	252.80	0	0	0.339	15	5.9	30", 36" & 42"
Addy	LTHS	Feb. 1996	36"	107		248	127.6	10.5	252.80	0	0	0.339	15	22	30", 36" & 42"
Addy	LTHS	Feb. 1996	36"	108		248	127.6	10.5	252.80	0	0	0.339	15	29.3	30", 36" & 42"
Addy	LTHS	Feb. 1996	36"	110		250	128.6	20	257.95	-1	-1	0.341	21	5.7	30", 36" & 42"
Addy	LTHS	Feb. 1996	36"	111		250	128.6	20	257.95	-1	-1	0.341	21	22.5	30", 36" & 42"
Addy	LTHS	Feb. 1996	36"	112		250	128.6	20	257.95	0	0	0.341	21	5.7	30", 36" & 42"
Addy	LTHS	Feb. 1996	36"	113		250	128.6	20	257.95	0	0	0.341	21	42.4	30", 36" & 42"
Addy	LTHS	Feb. 1996	36"	114		250	128.6	20	257.95	0	0	0.341	21	28.3	30", 36" & 42"
Addy	LTHS	Feb. 1996	36"	115		250	128.6	20	257.95	0	0	0.341	21	21.1	30"
Addy	LTHS	Feb. 1996	36"	122		253	130.1	29.5	263.03	-1	-1	0.563	21	4.9	30", 36" & 42"
Addy	LTHS	Feb. 1996	36"	123		253	130.1	29.5	263.03	-1	-1	0.563	21	18.5	30", 36" & 42"
Addy	LTHS	Feb. 1996	36"	124		253	130.1	29.5	263.03	0	0	0.563	21	4.9	30", 36" & 42"
Addy	LTHS	Feb. 1996	36"	125		253	130.1	29.5	263.03	0	0	0.563	21	36.9	30", 36" & 42"
Addy	LTHS	Feb. 1996	36"	126		253	130.1	29.5	263.03	0	0	0.563	21	24.6	30", 36" & 42"
Addy	LTHS	Feb. 1996	36"	127		253	130.1	29.5	263.03	0	0	0.563	21	18.5	30"
Addy	LTHS	Feb. 1996	36"	128		250	128.6	20	257.95	0	0	0.341	21	2	30", 36" & 42"
Addy	LTHS	Feb. 1996	36"	129		253	130.1	29.5	263.03	0	0	0.563	21	2	30", 36" & 42"
Addy	LTHS	Feb. 1996	36"	141		249	128.1	15	255.24	0	0	0.4	42	6.7	30", 36" & 42"
Addy	LTHS	Feb. 1996	36"	142		249	128.1	15	255.24	0	0	0.4	42	2	30", 36" & 42"
Addy	LTHS	Feb. 1996	36"	143		253	130.1	29	262.76	0	0	0.65	42	5.3	30", 36" & 42"
Addy	LTHS	Feb. 1996	36"	144		253	130.1	25.5	260.81	0	0	0.4	42	3	30", 36" & 42"
Addy	LTHS	Feb. 1996	36"	145		253	130.1	25.5	260.81	0	0	0.4	42	11.2	30", 36" & 42"

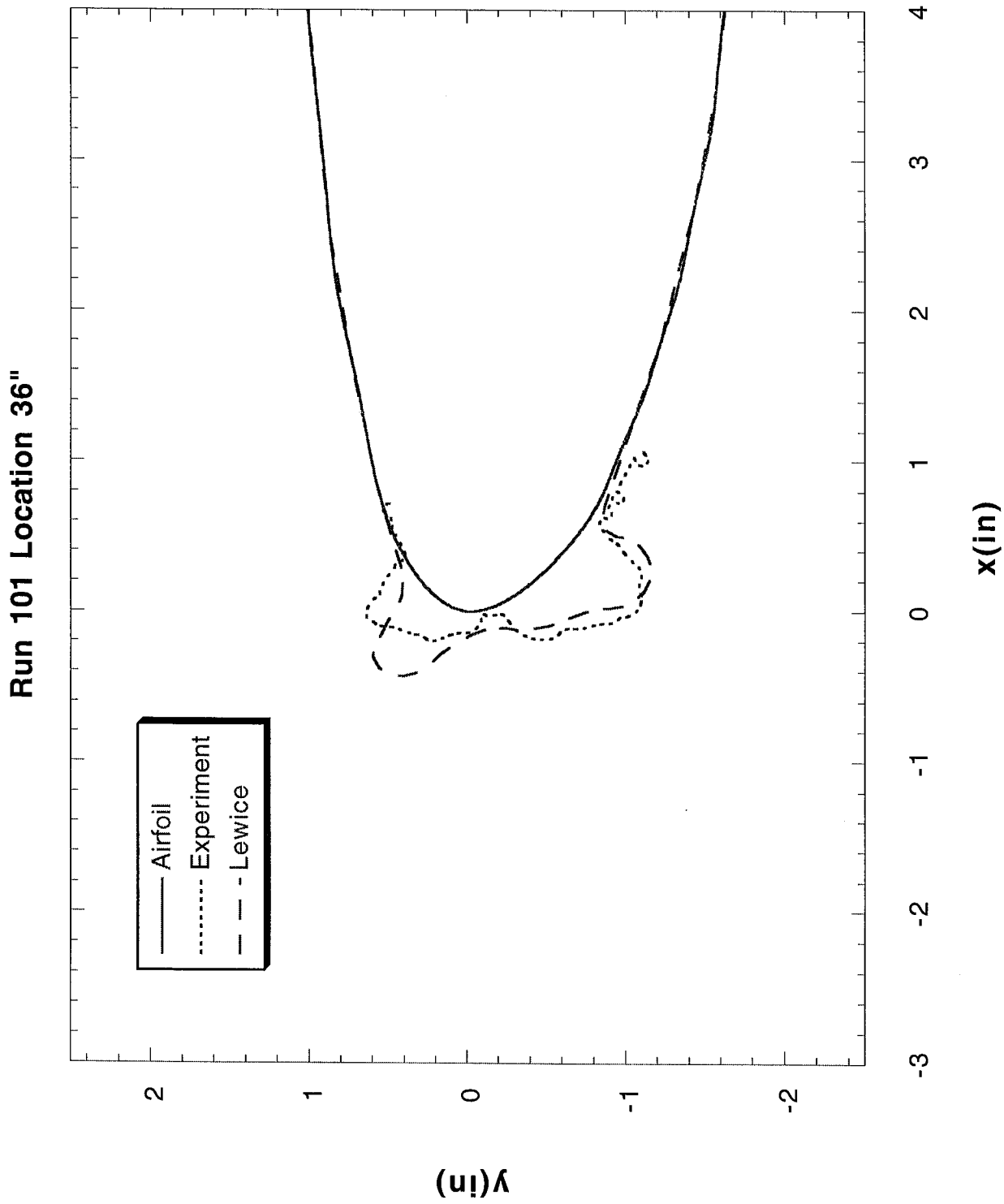
Run 101 Location 36"
Airfoil
Experiment
Lewice
y(in)
x(in)
2
1
0
-1
-2
-3
-2
-1
0
1
2
3
4

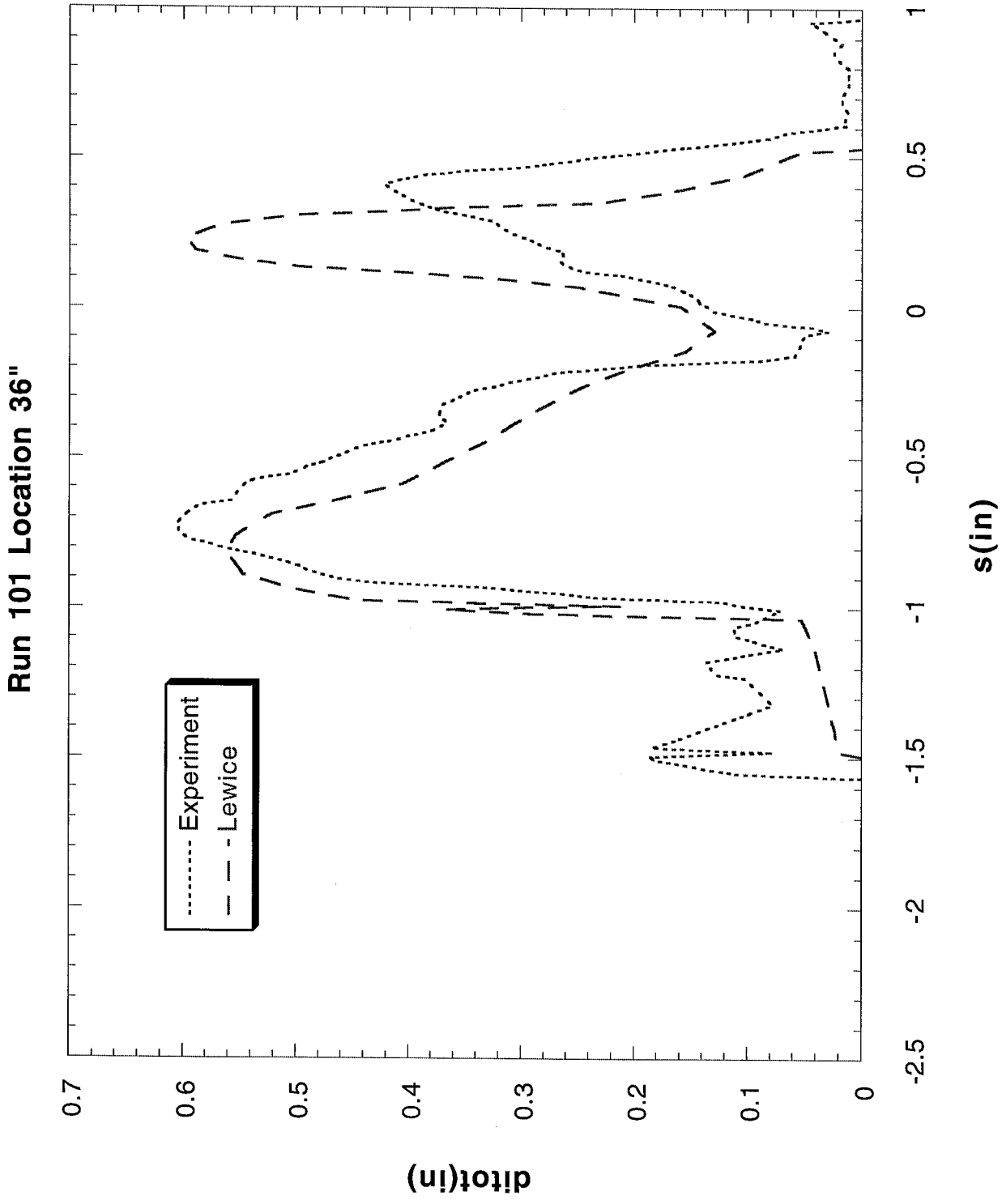
Run 101 Location 36"
Experiment
Lewice
dltot(in)
s(in)
0.7
0.6
0.5
0.4
0.3
0.2
0.1
0
-2.5
-2
-1.5
-1
-0.5
0
0.5
1

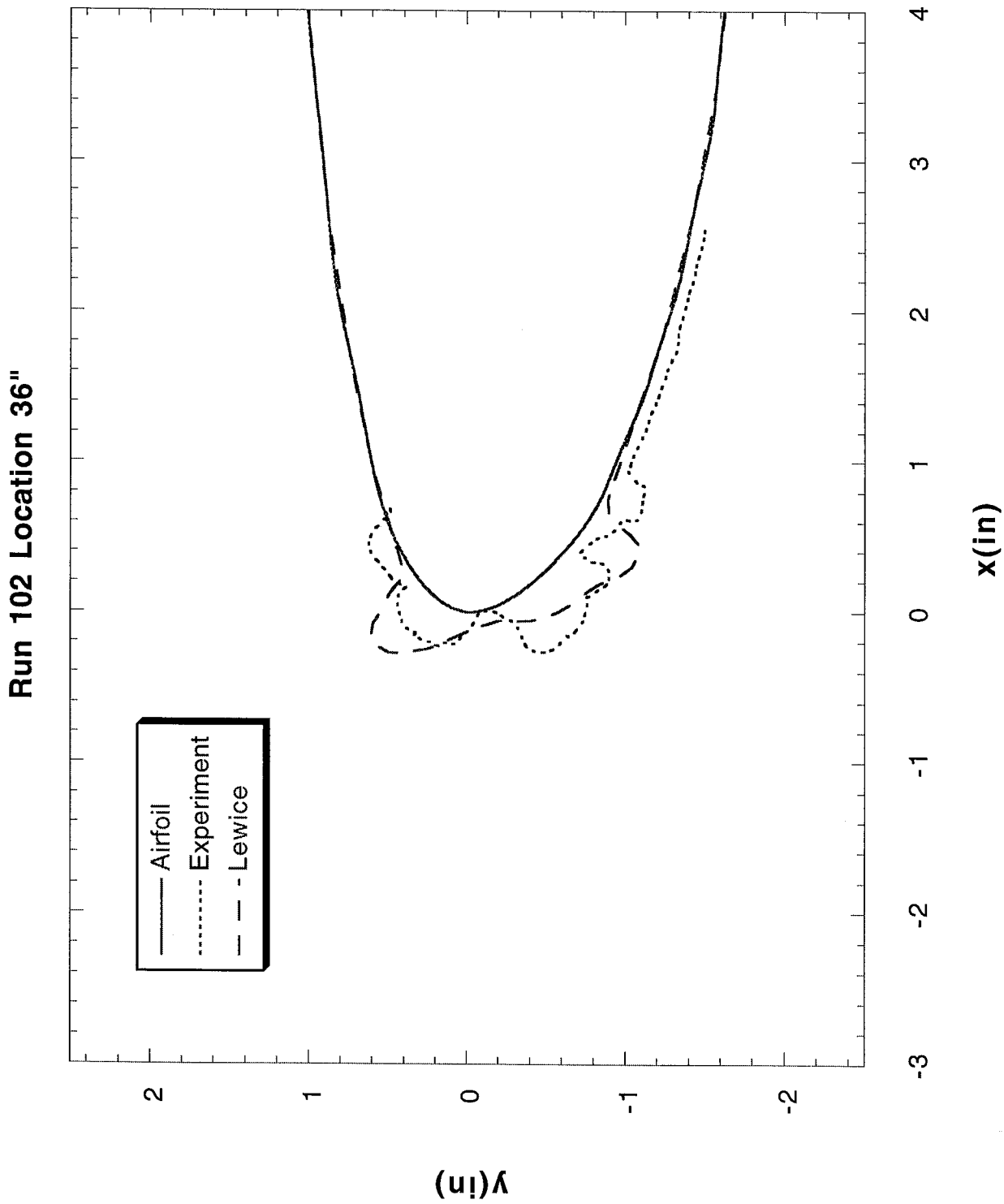
Run 102 Location 36"
Airfoil
Experiment
Lewice
y(in)
x(in)
2
1
0
-1
-2
-3
-2
-1
0
1
2
3
4

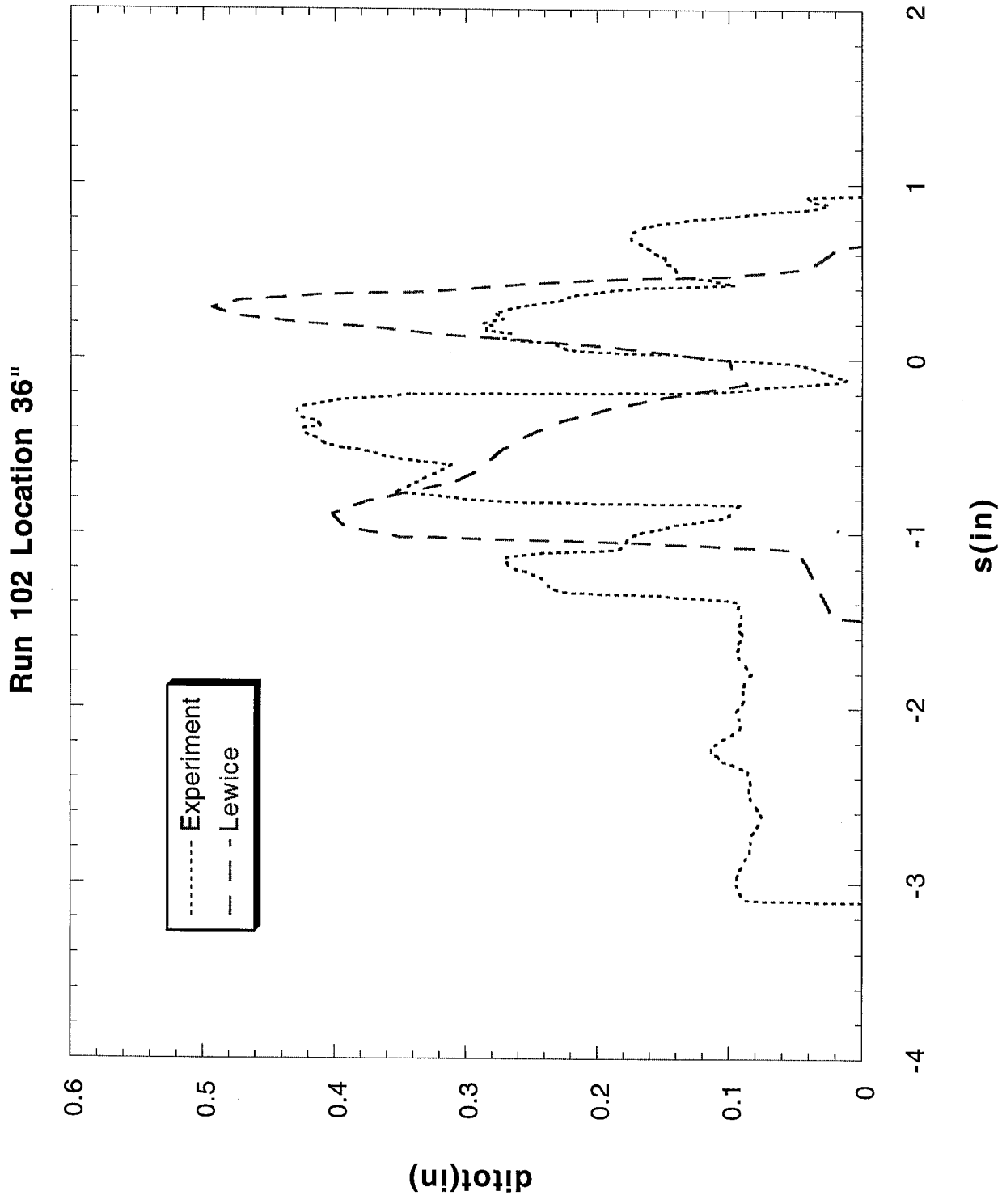
Run 102 Location 36"
Experiment
Lewice
ditot(in)
s(in)
0.6
0.5
0.4
0.3
0.2
0.1
0
-4
-3
-2
-1
0
1
2

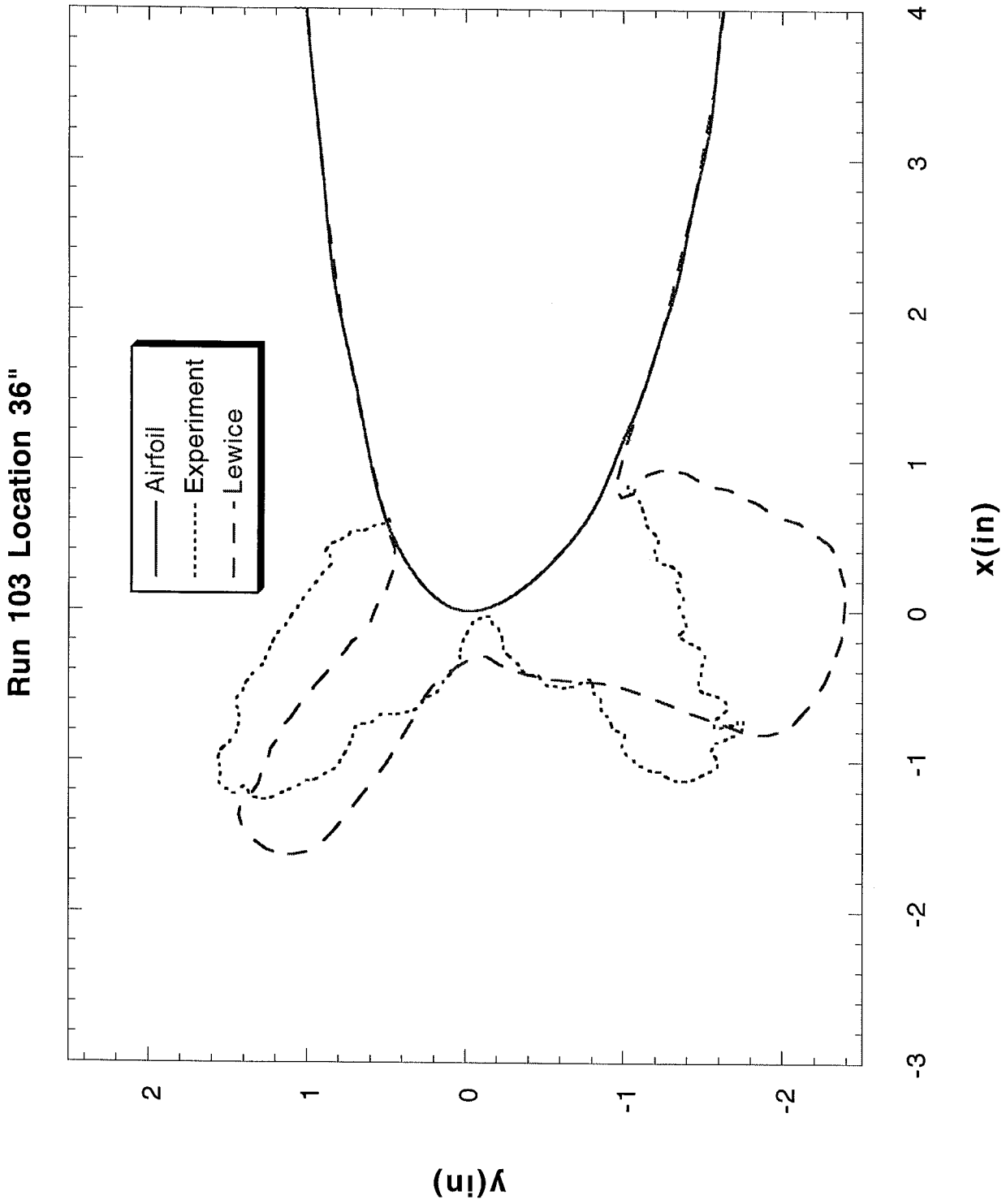
Run 103 Location 36"
Airfoil
Experiment
Lewice
y(in)
x(in)
2
1
0
-1
-2
-3
-2
-1
0
1
2
3
4

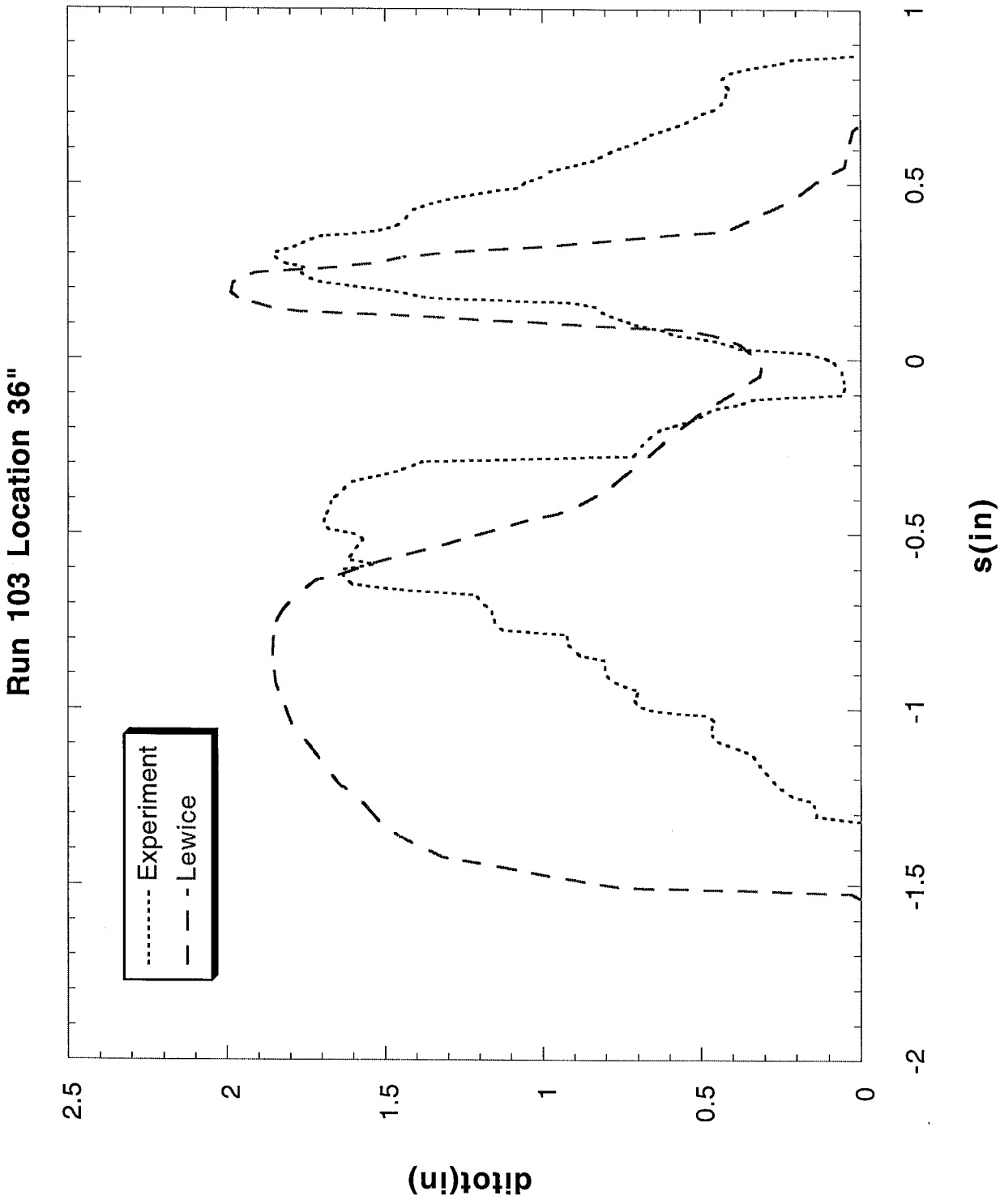
Run 103 Location 36"
Experiment
Lewice
ditot(in)
s(in)
2.5
2
1.5
1
0.5
0
-2
-1.5
-1
-0.5
0
0.5
1

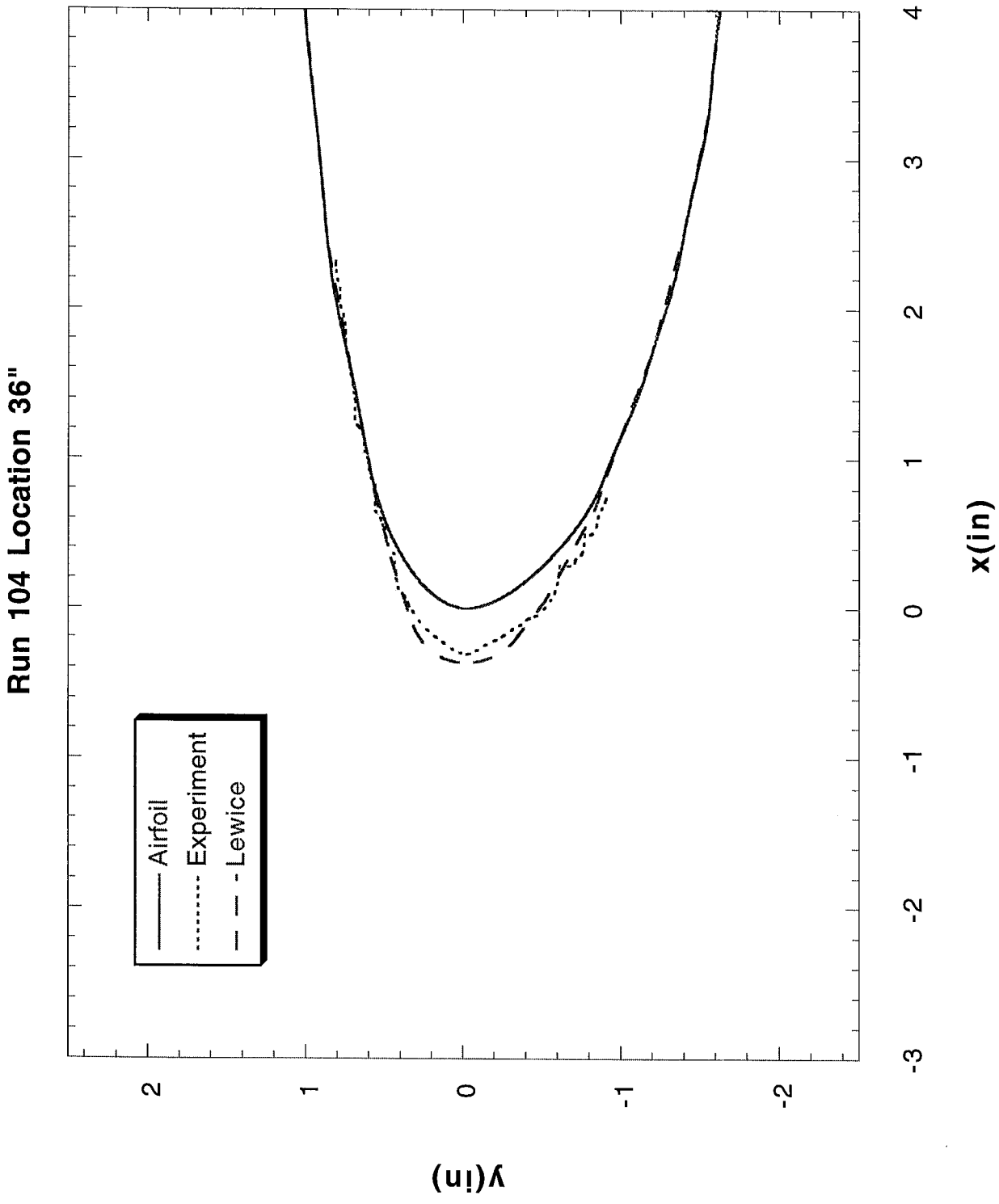
Run 104 Location 36"
Airfoil
Experiment
Lewice
y(in)
x(in)
2
1
0
-1
-2
-3
-2
-1
0
1
2
3
4

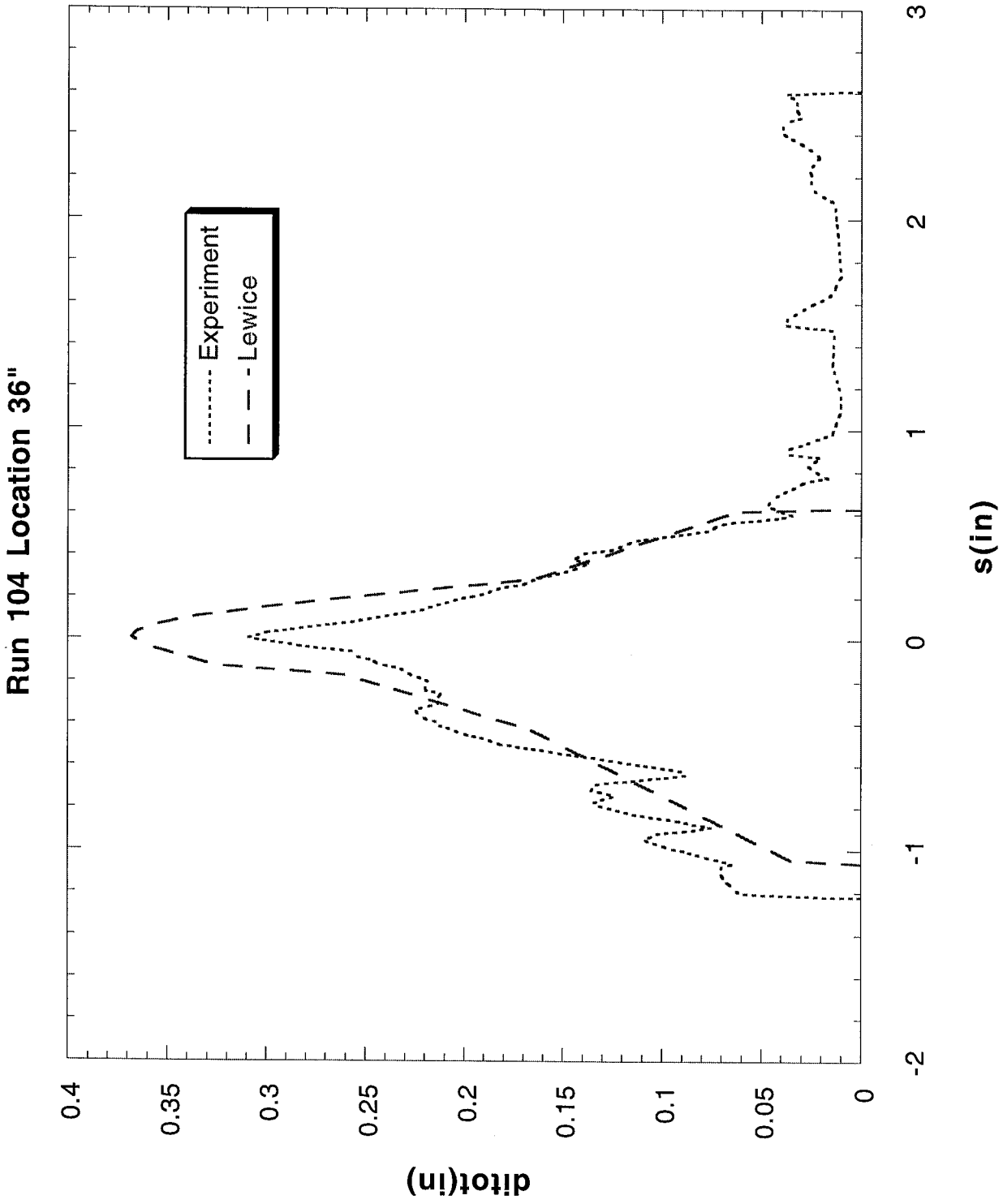
Run 104 Location 36"
Experiment
Lewice
dltot(in)
s(in)
0.4
0.35
0.3
0.25
0.2
0.15
0.1
0.05
0
-2
-1
0
1
2
3

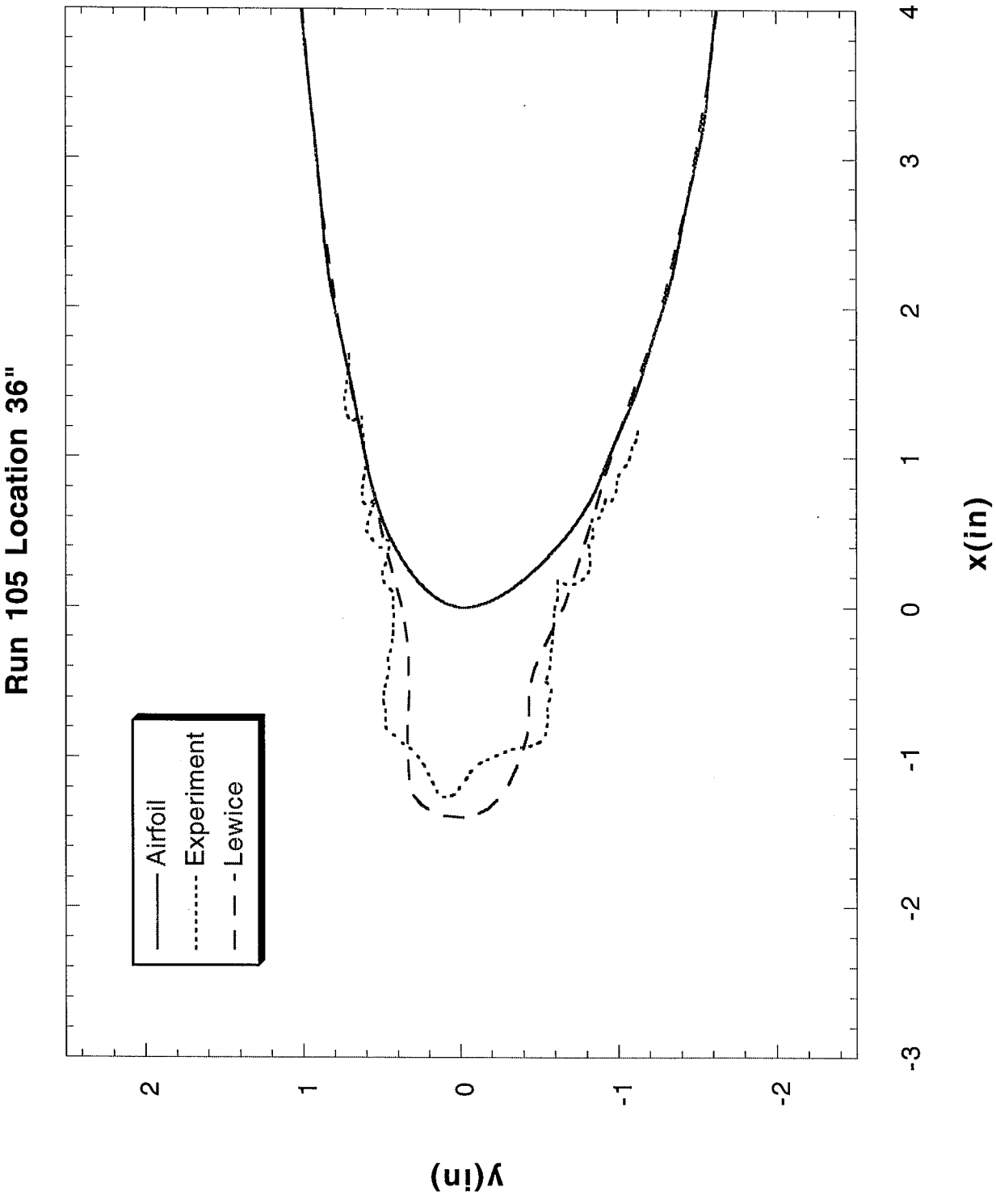
Run 105 Location 36"
Airfoil
Experiment
Lewice
y(in)
x(in)
2
1
0
-1
-2
-3
-2
-1
0
1
2
3
4

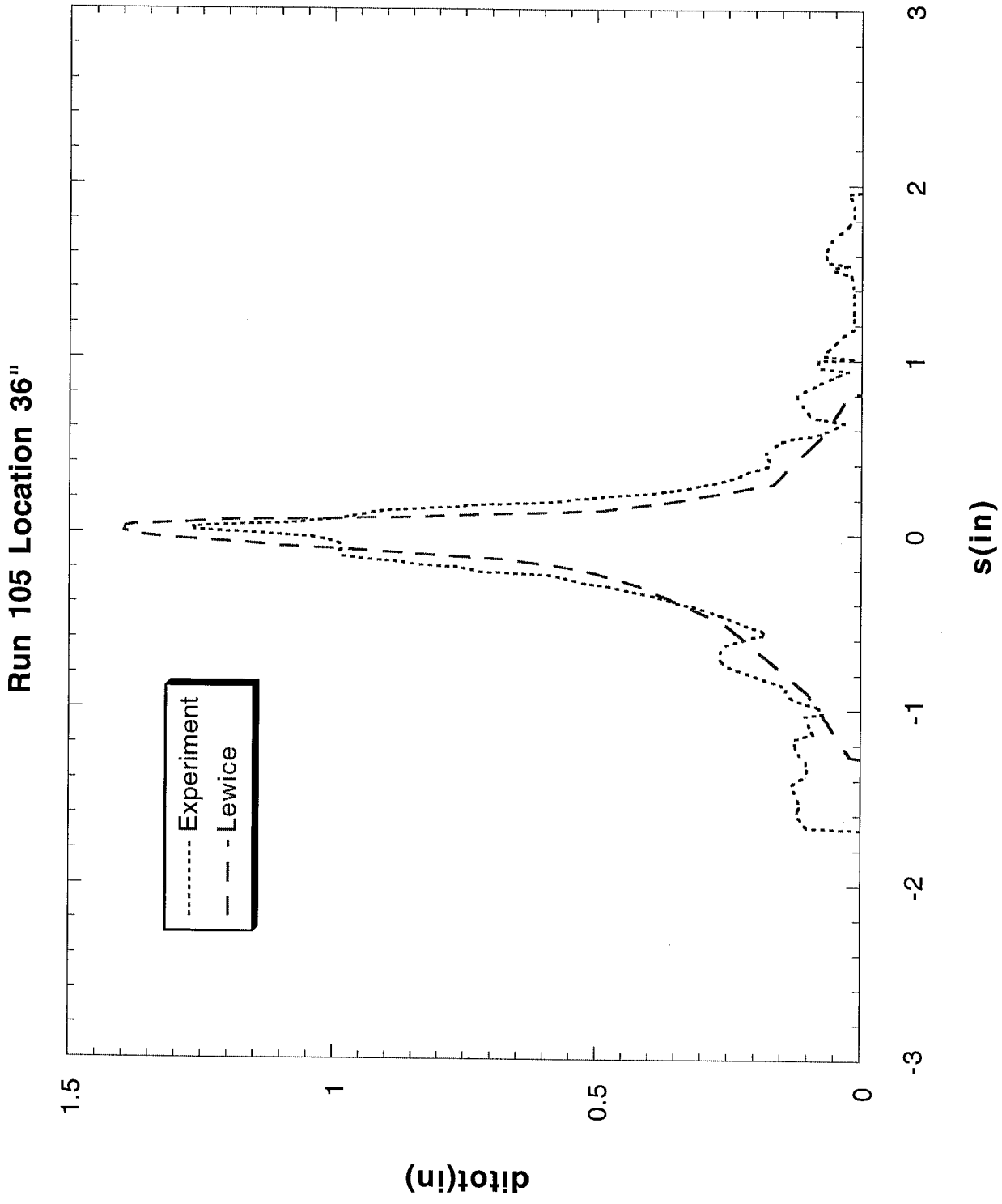
Run 105 Location 36"
Experiment
Lewice
dltot(in)
s(in)
1.5
1
0.5
0
-3
-2
-1
0
1
2
3

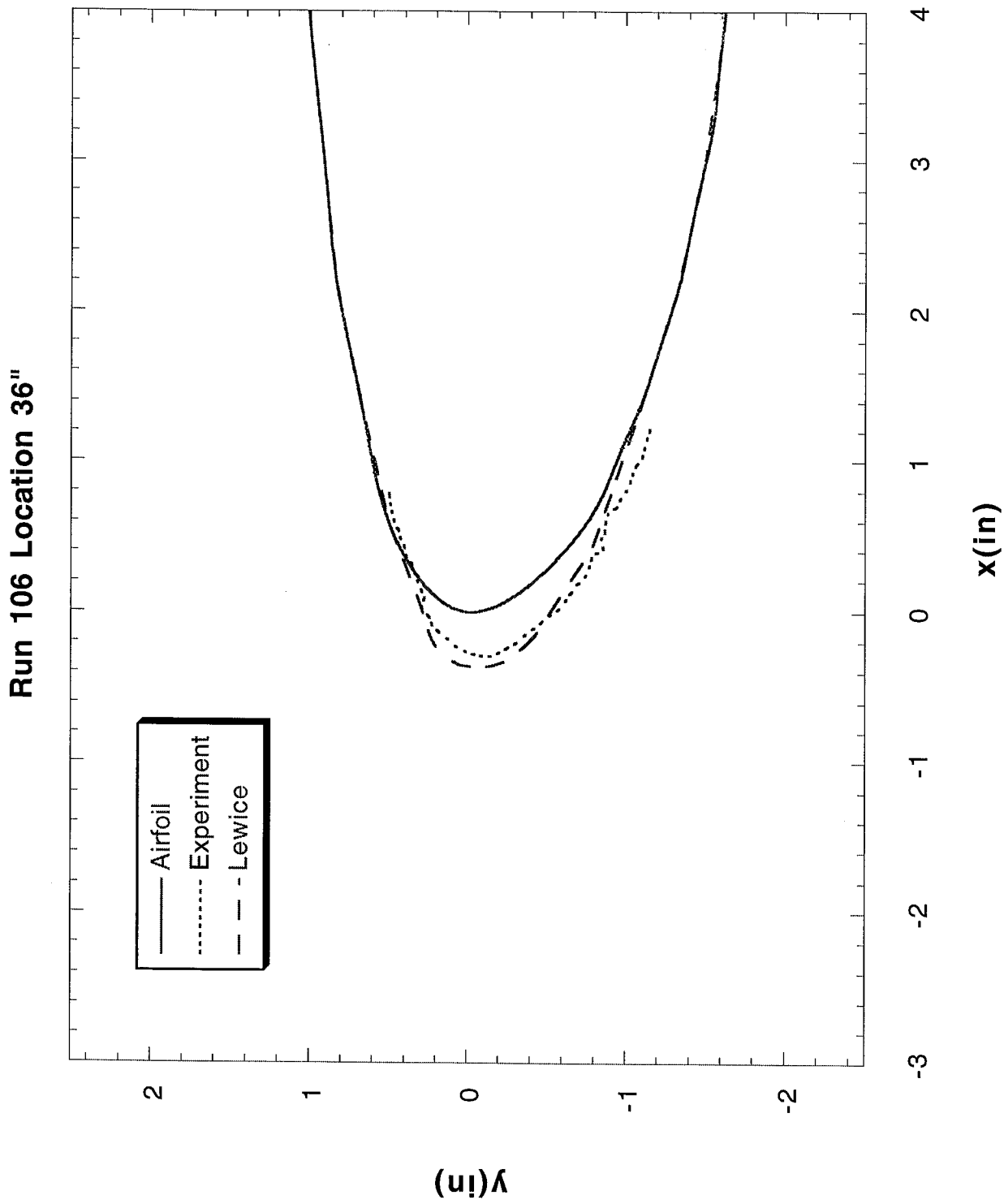
Run 106 Location 36"
Airfoil
Experiment
Lewice
y(in)
x(in)
2
1
0
-1
-2
-3
-2
-1
0
1
2
3
4

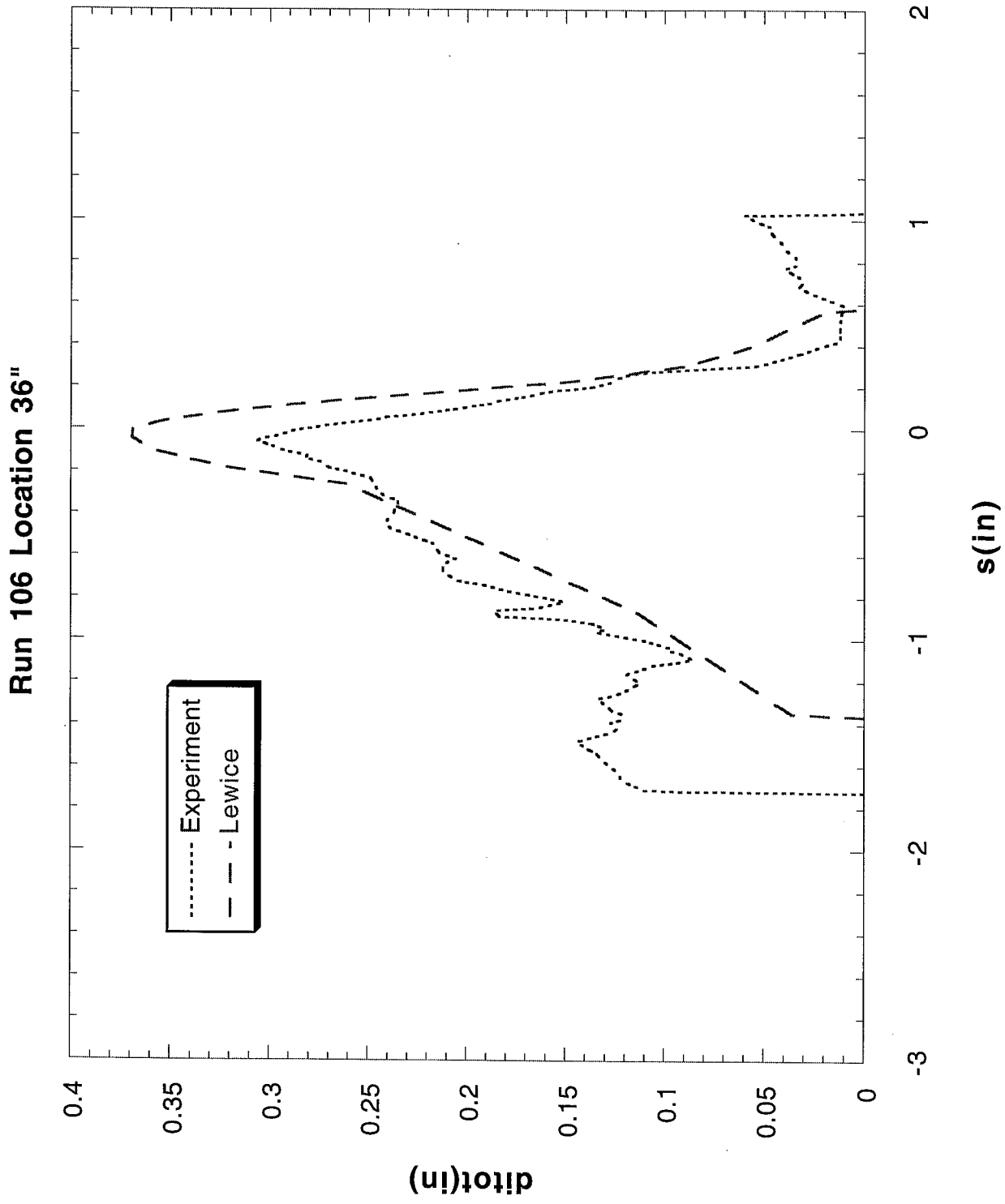
Run 106 Location 36"
Experiment
Lewice
dltot(in)
s(in)
0.4
0.35
0.3
0.25
0.2
0.15
0.1
0.05
0
-3
-2
-1
0
1
2

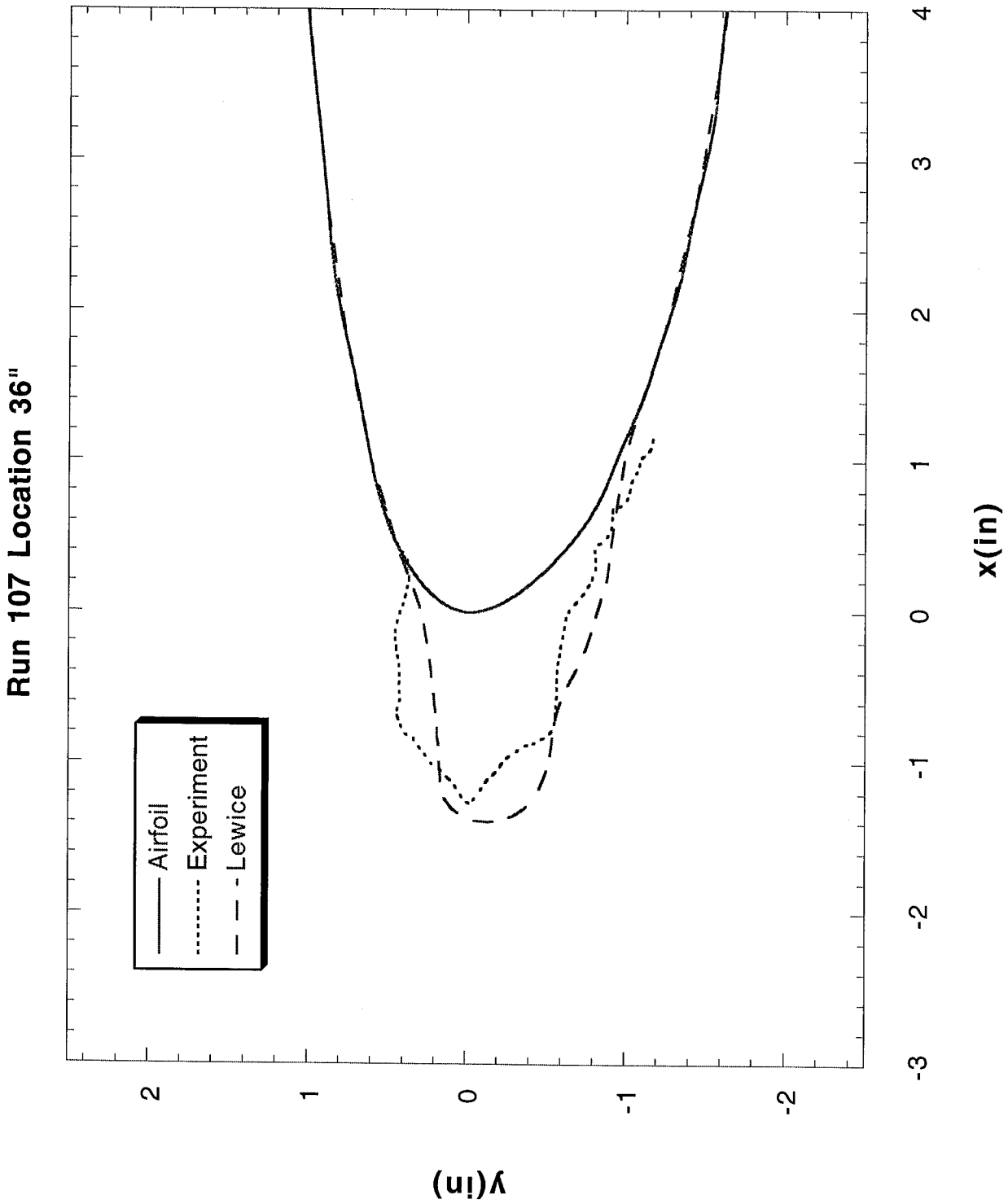
Run 107 Location 36"
Airfoil
Experiment
Lewice
y(in)
x(in)
2
1
0
-1
-2
-3
-2
-1
0
1
2
3
4

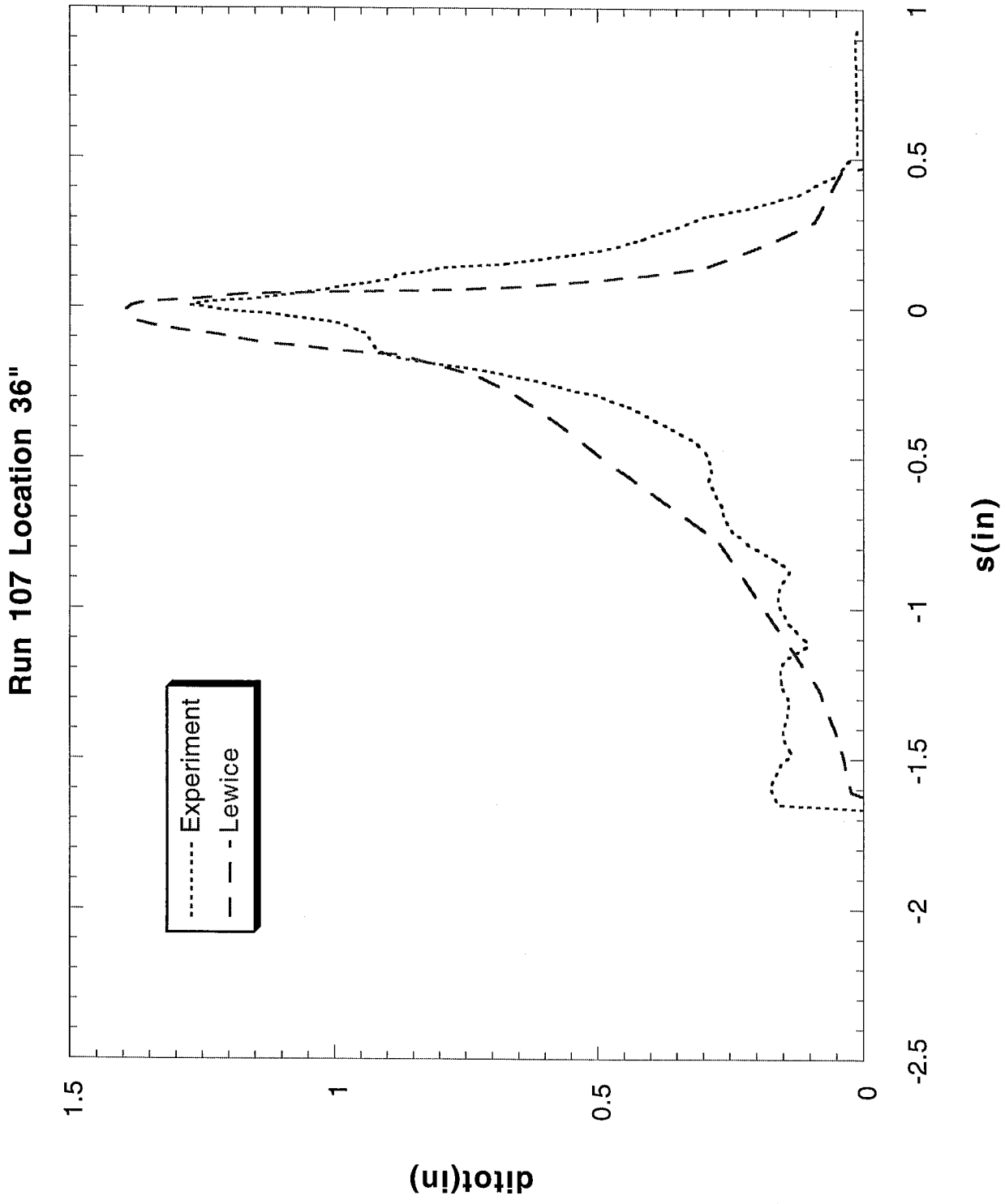
Run 107 Location 36"
Experiment
Lewice
ditot(in)
s(in)
1.5
1
0.5
0
-2.5
-2
-1.5
-1
-0.5
0
0.5
1

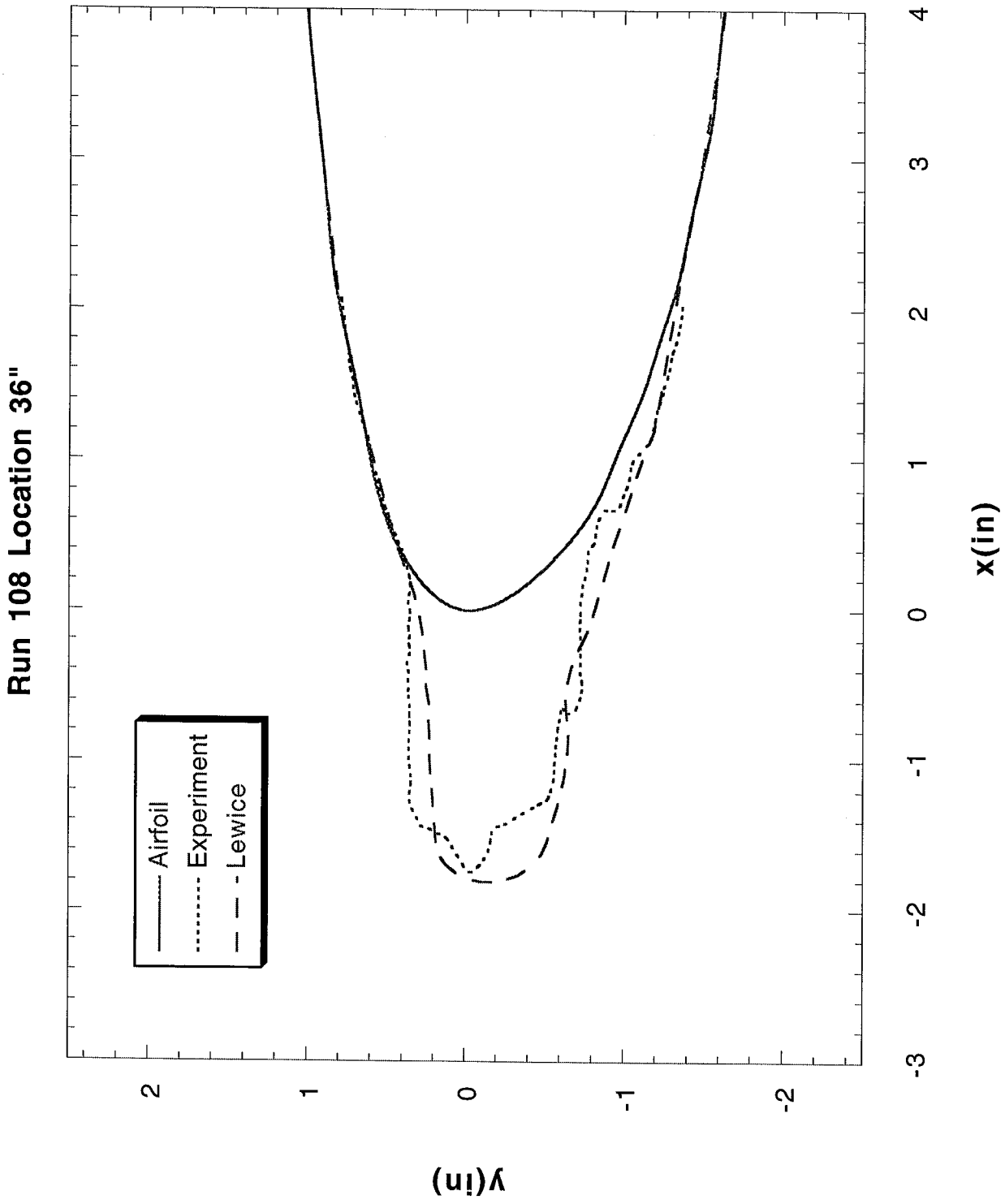
Run 108 Location 36"
Airfoil
Experiment
Lewice
y(in)
x(in)
2
1
0
-1
-2
-3
-2
-1
0
1
2
3
4

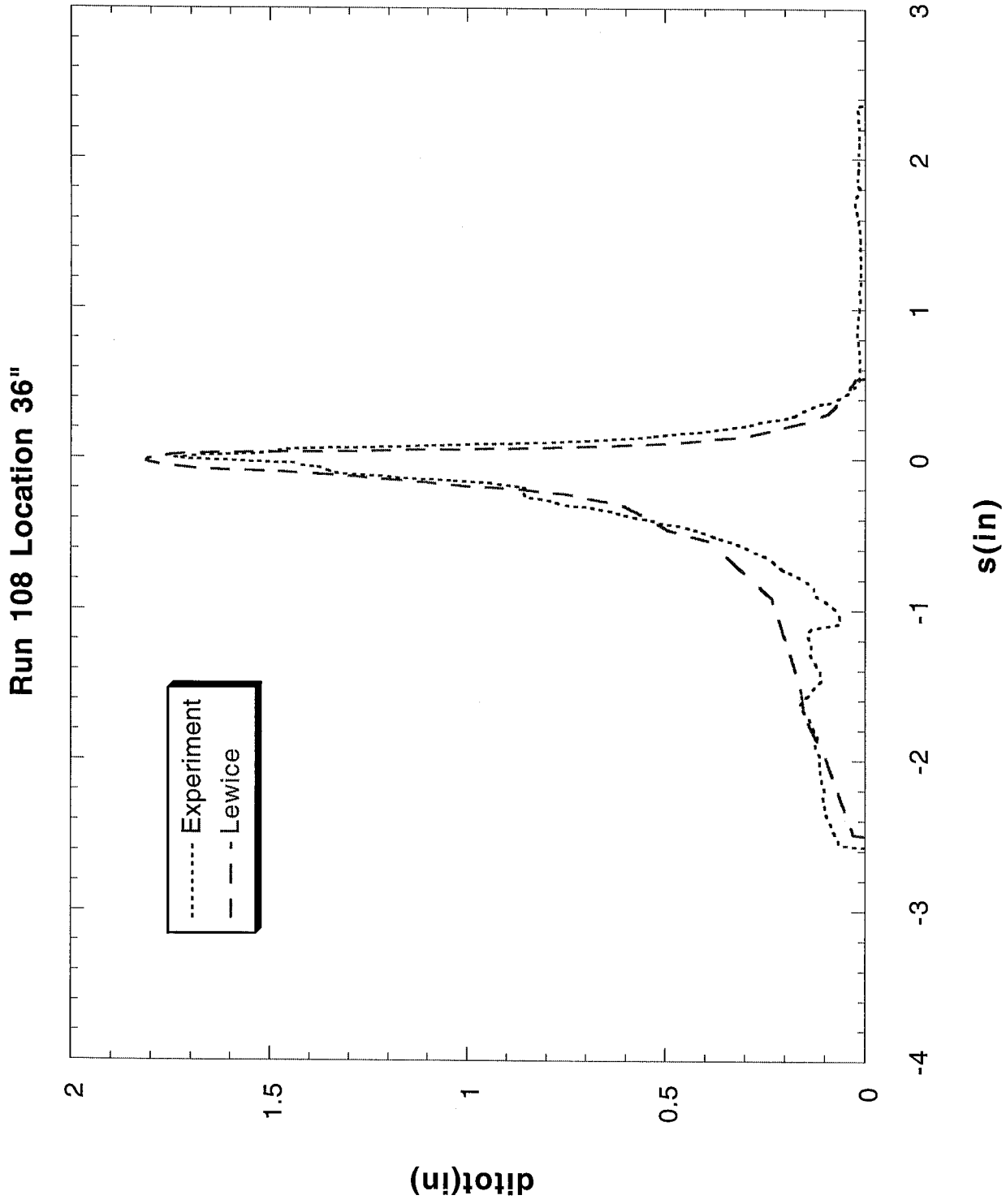
Run 108 Location 36"
Experiment
Lewice
dltot(in)
s(in)
2
1.5
1
0.5
0
-4
-3
-2
-1
0
1
2
3

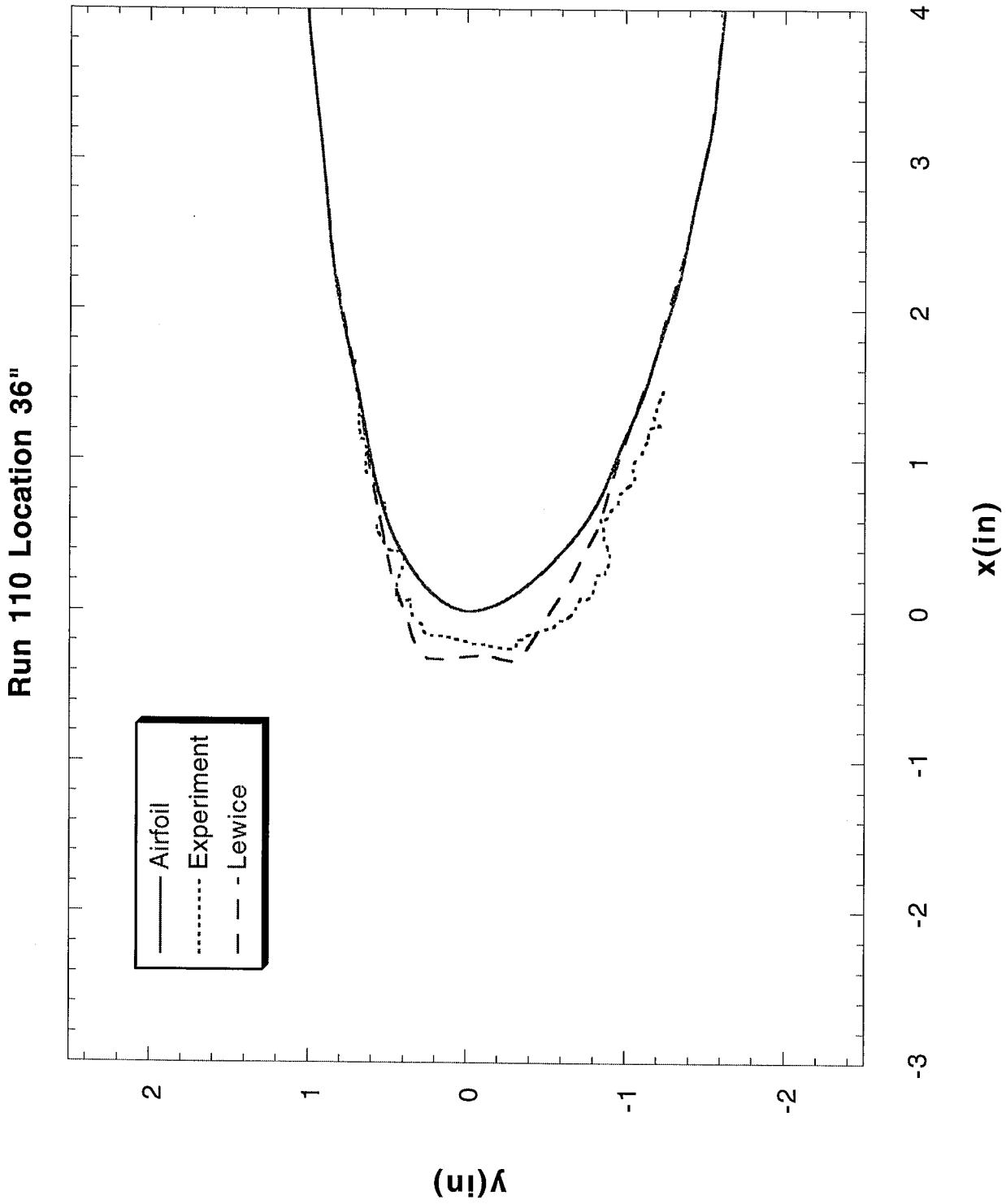
Run 110 Location 36"
Airfoil
Experiment
Lewice
y(in)
x(in)
2
1
0
-1
-2
-3
-2
-1
0
1
2
3
4

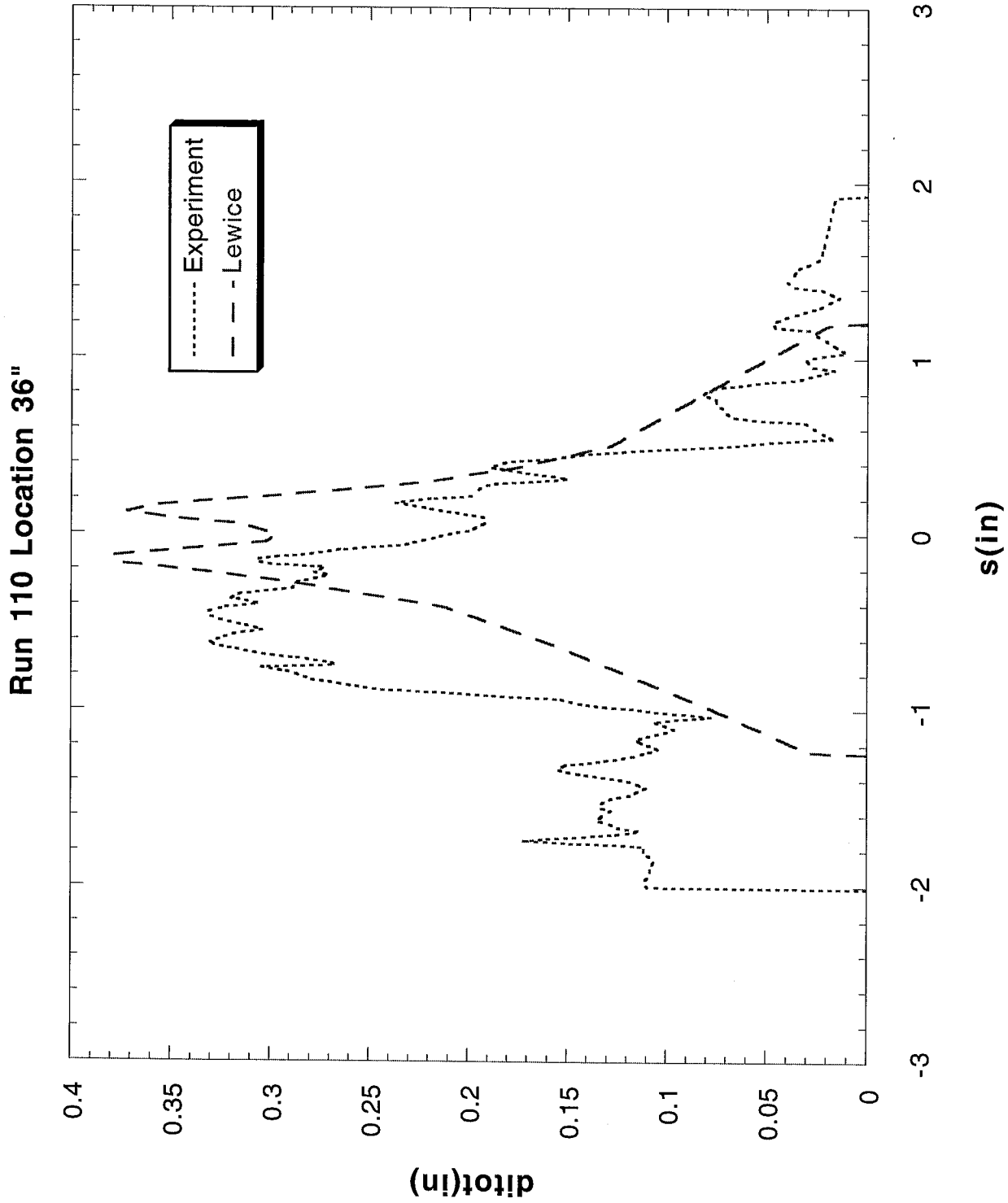
Run 110 Location 36"
Experiment
Lewice
dltot(in)
s(in)
0.4
0.35
0.3
0.25
0.2
0.15
0.1
0.05
0
-3
-2
-1
0
1
2
3

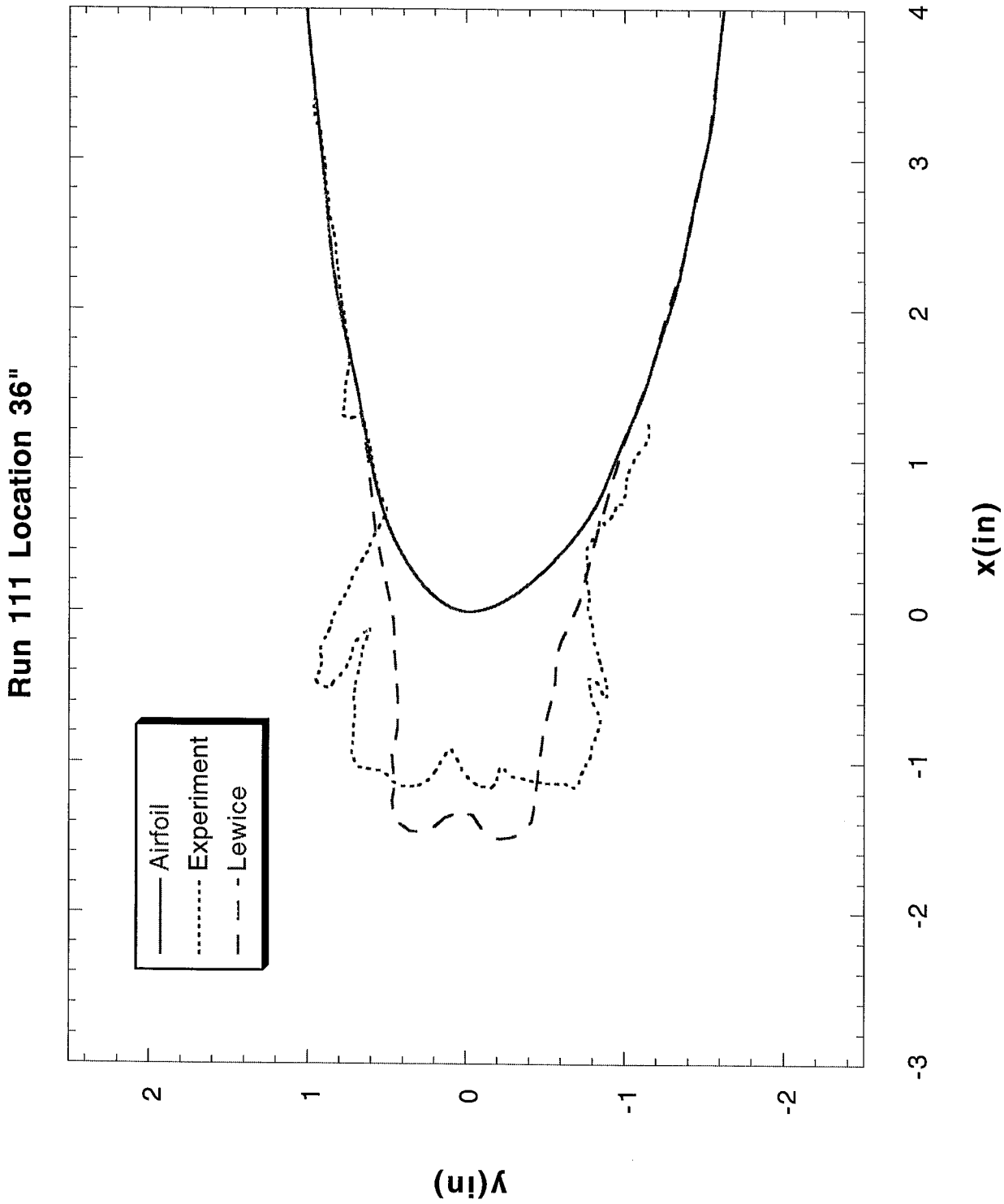
Run 111 Location 36"
Airfoil
Experiment
Lewice
y(in)
x(in)
2
1
0
-1
-2
-3
-2
-1
0
1
2
3
4

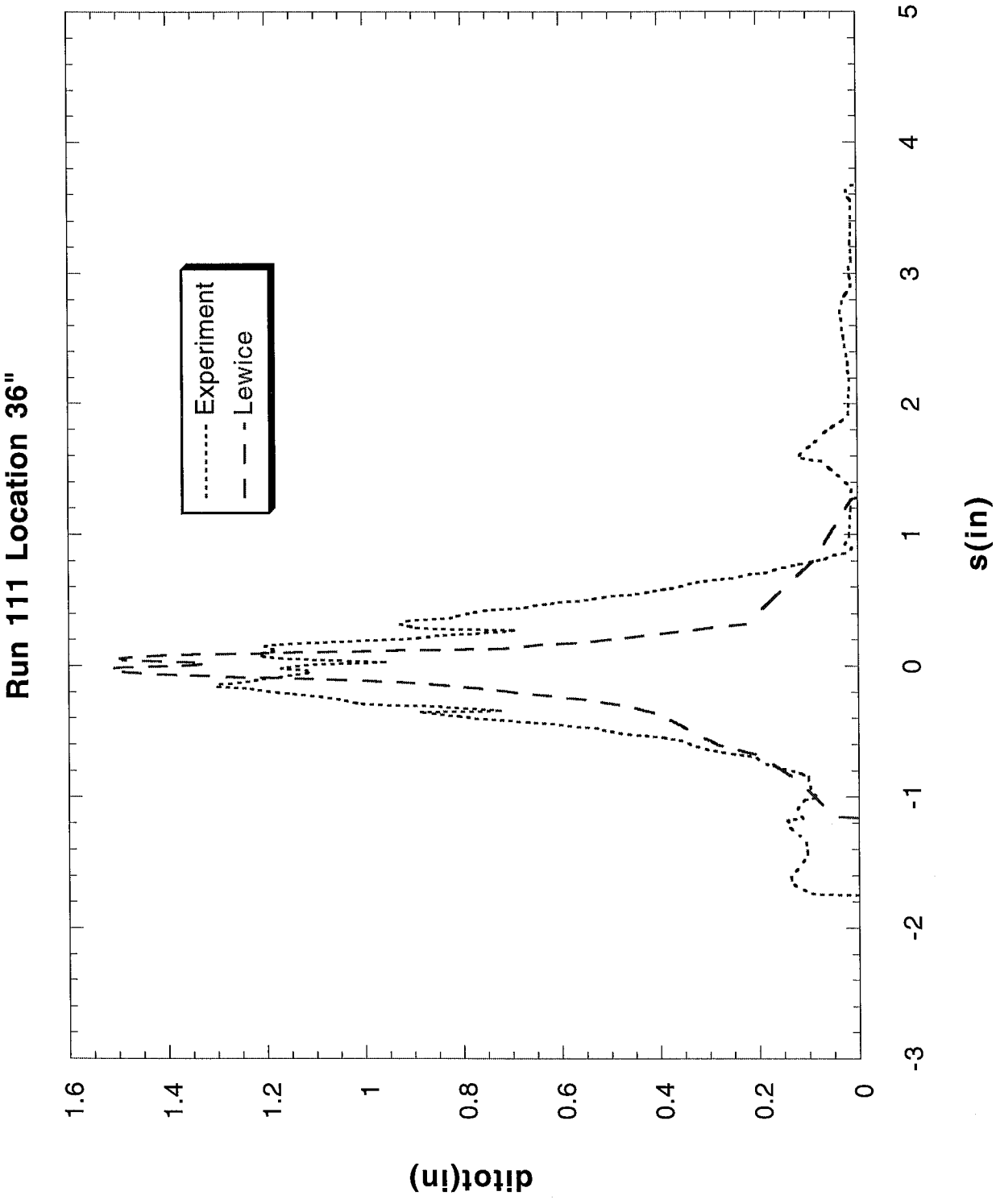
Run 111 Location 36"
Experiment
Lewice
dltot(in)
s(in)
1.6
1.4
1.2
1
0.8
0.6
0.4
0.2
0
-3
-2
-1
0
1
2
3
4
5

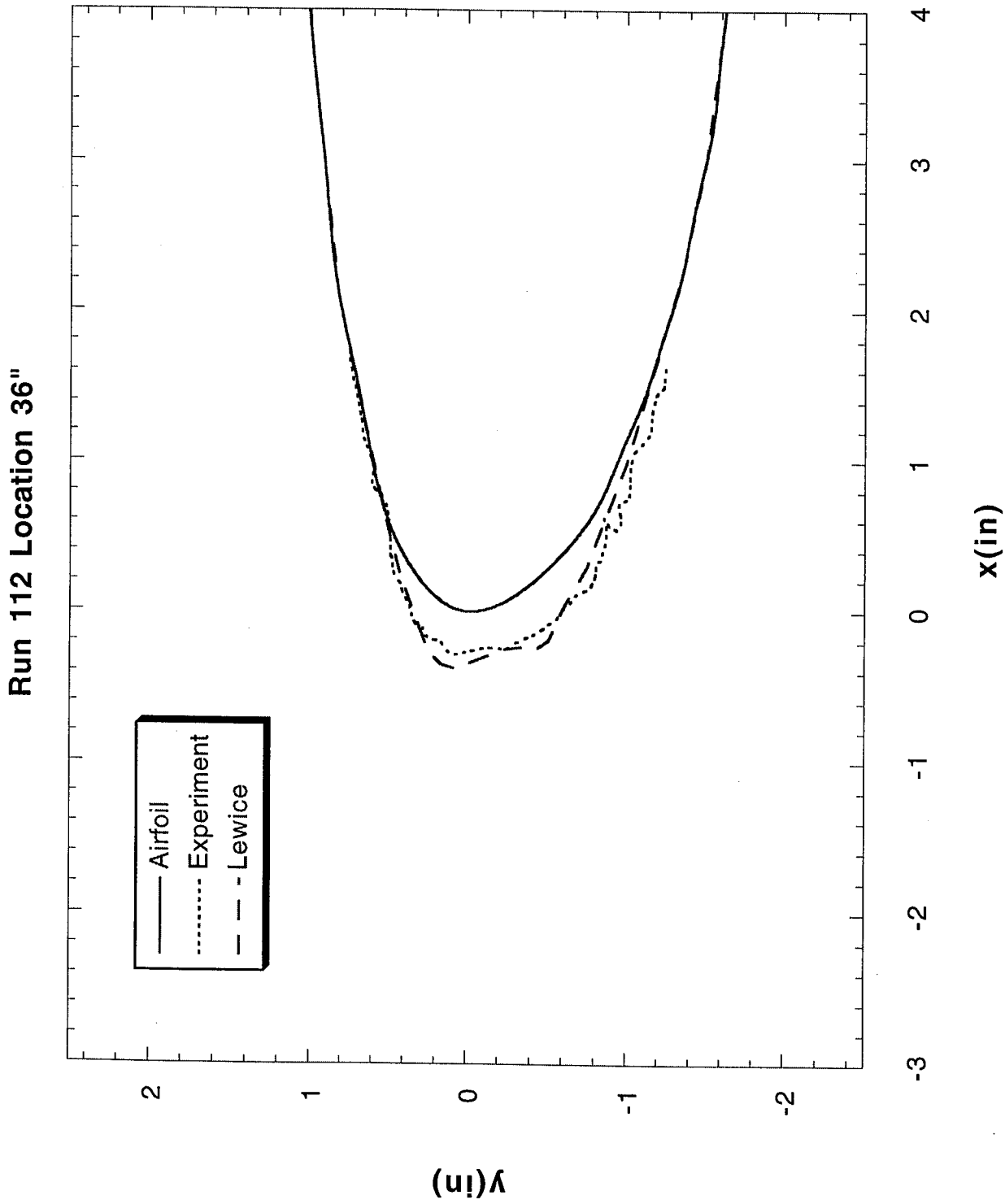
Run 112 Location 36"
Airfoil
Experiment
Lewice
y(in)
x(in)
2
1
0
-1
-2
-3
-2
-1
0
1
2
3
4

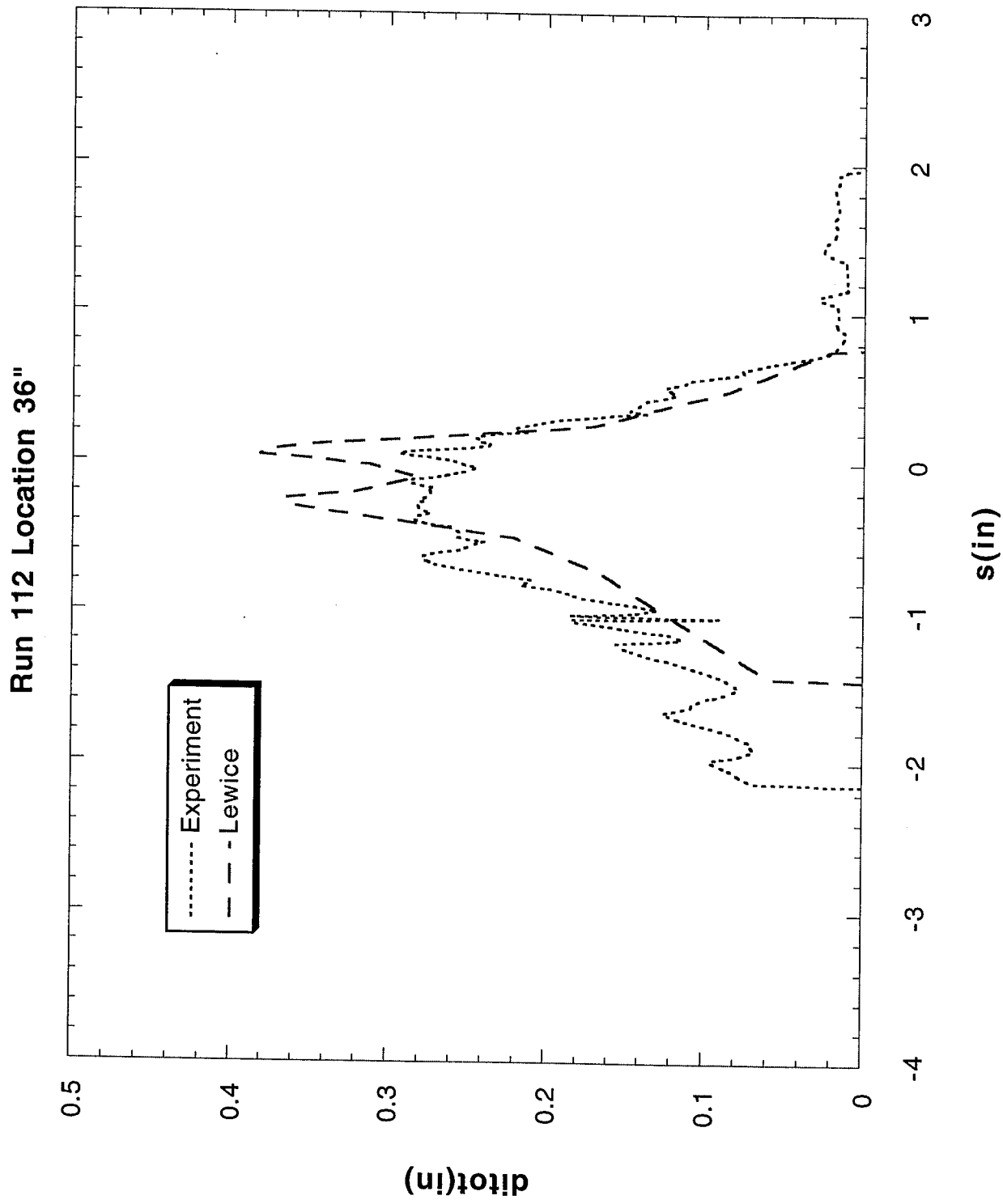
Run 112 Location 36"
Experiment
Lewice
dltot(in)
s(in)
0.5
0.4
0.3
0.2
0.1
0
-4
-3
-2
-1
0
1
2
3

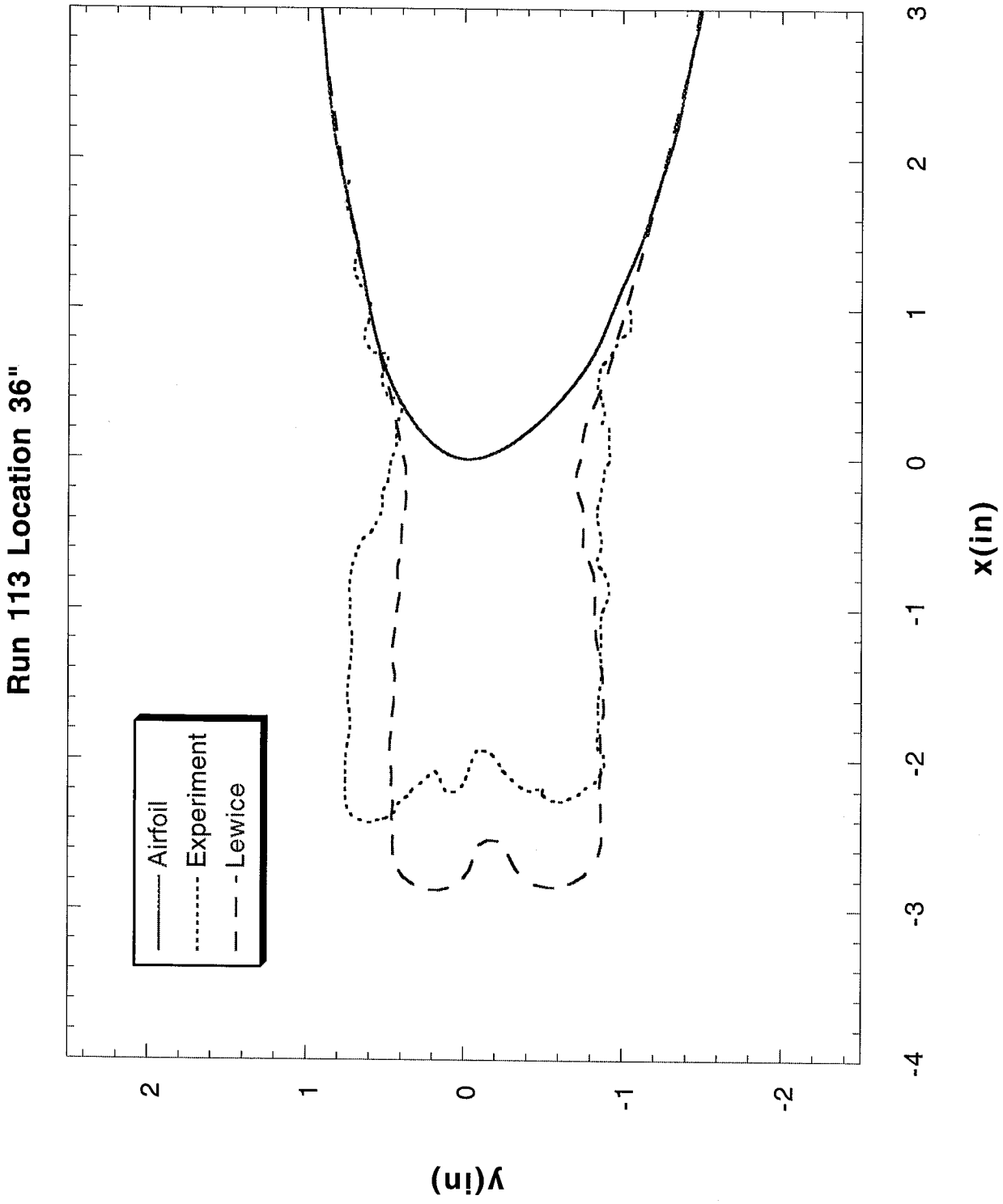
Run 113 Location 36"
Airfoil
Experiment
Lewice
y(in)
x(in)
2
1
0
-1
-2
-4
-3
-2
-1
0
1
2
3

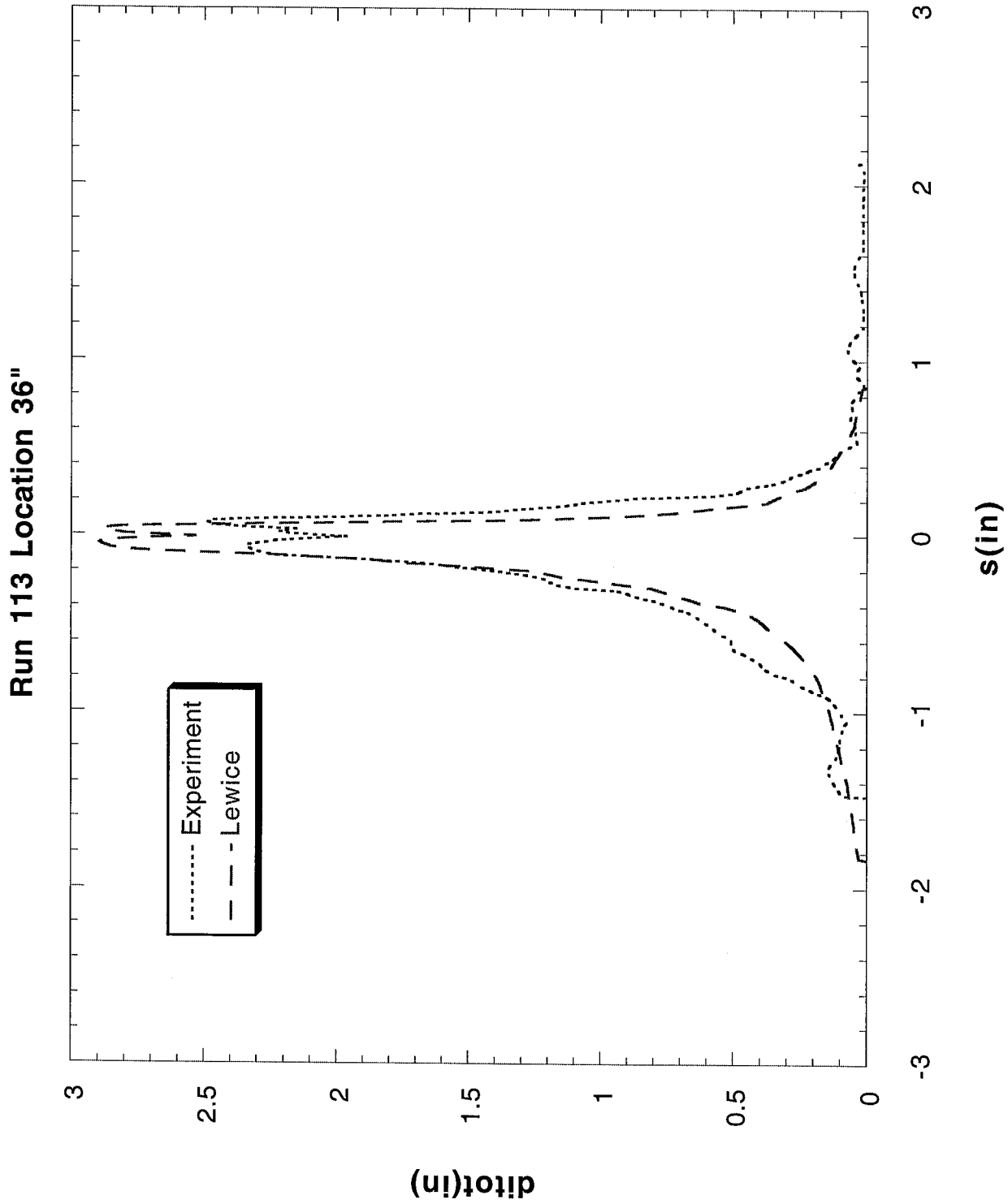
Run 113 Location 36"
Experiment
Lewice
dltot(in)
s(in)
3
2.5
2
1.5
1
0.5
0
-3
-2
-1
0
1
2
3

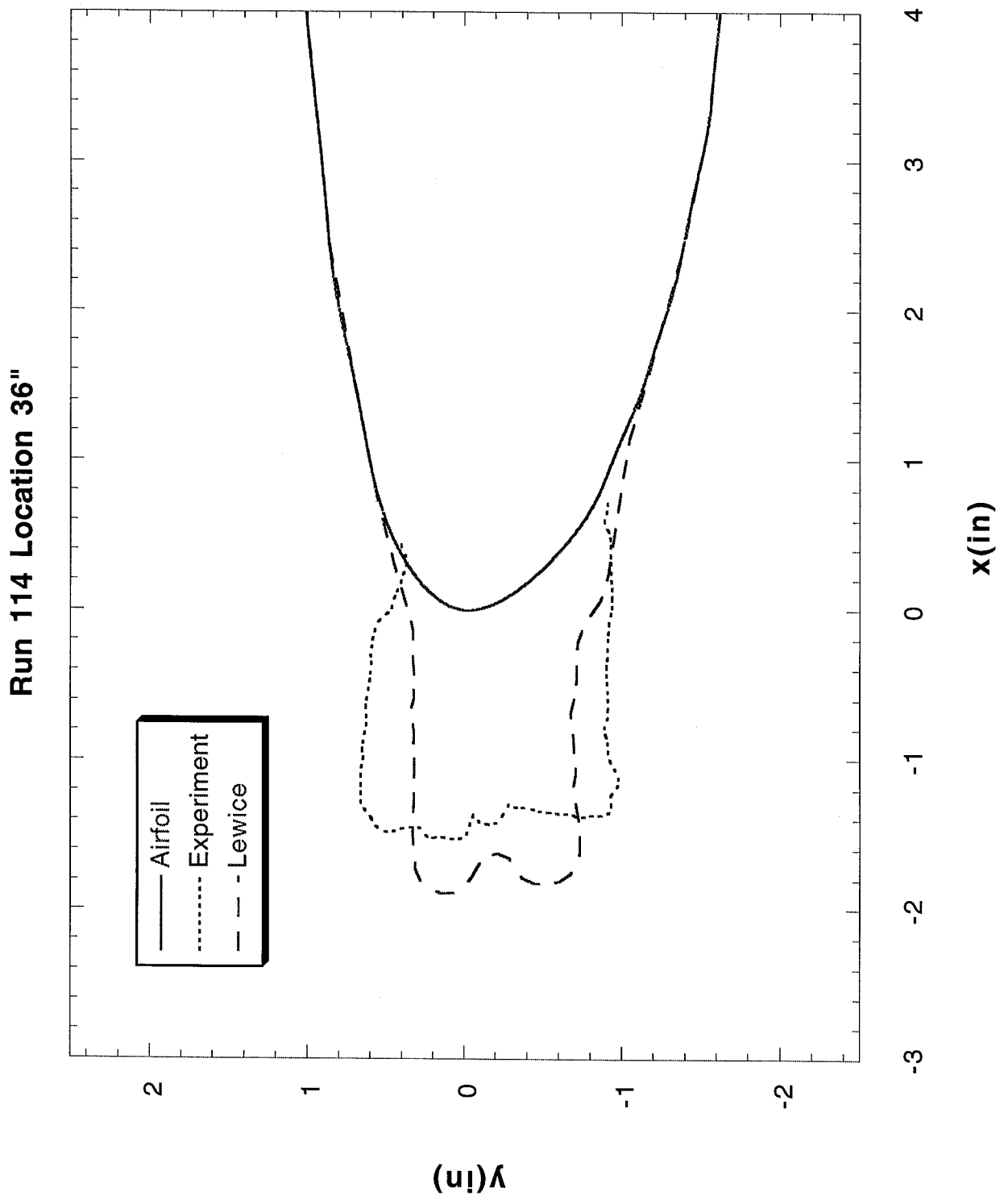
Run 114 Location 36"
Airfoil
Experiment
Lewice
y(in)
x(in)
2
1
0
-1
-2
-3
-2
-1
0
1
2
3
4

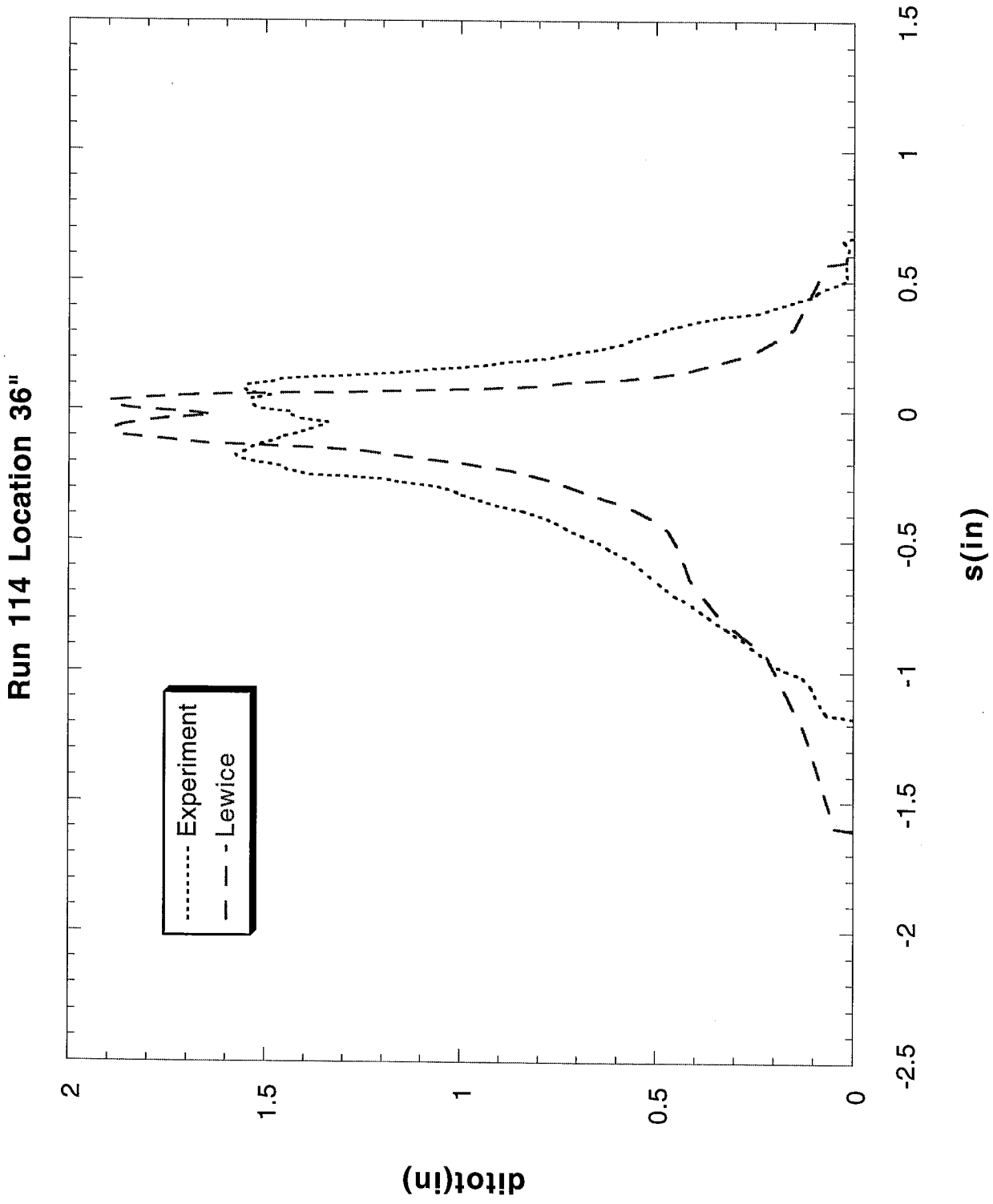
Run 114 Location 36"
Experiment
Lewice
ditot(in)
s(in)
2
1.5
1
0.5
0
-2.5
-2
-1.5
-1
-0.5
0
0.5
1
1.5

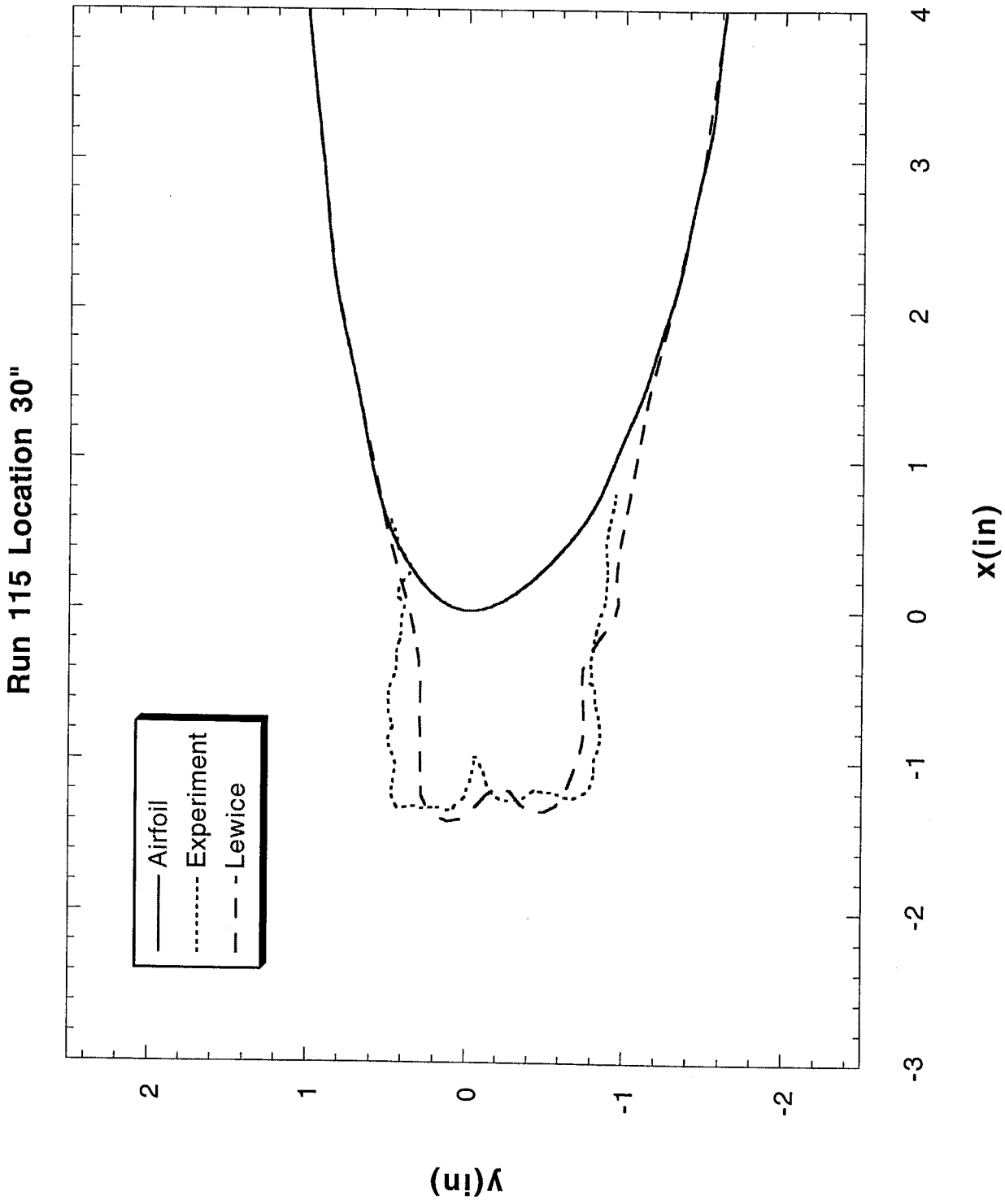
Run 115 Location 30"
Airfoil
Experiment
Lewice
y(in)
x(in)
2
1
0
-1
-2
-3
-2
-1
0
1
2
3
4

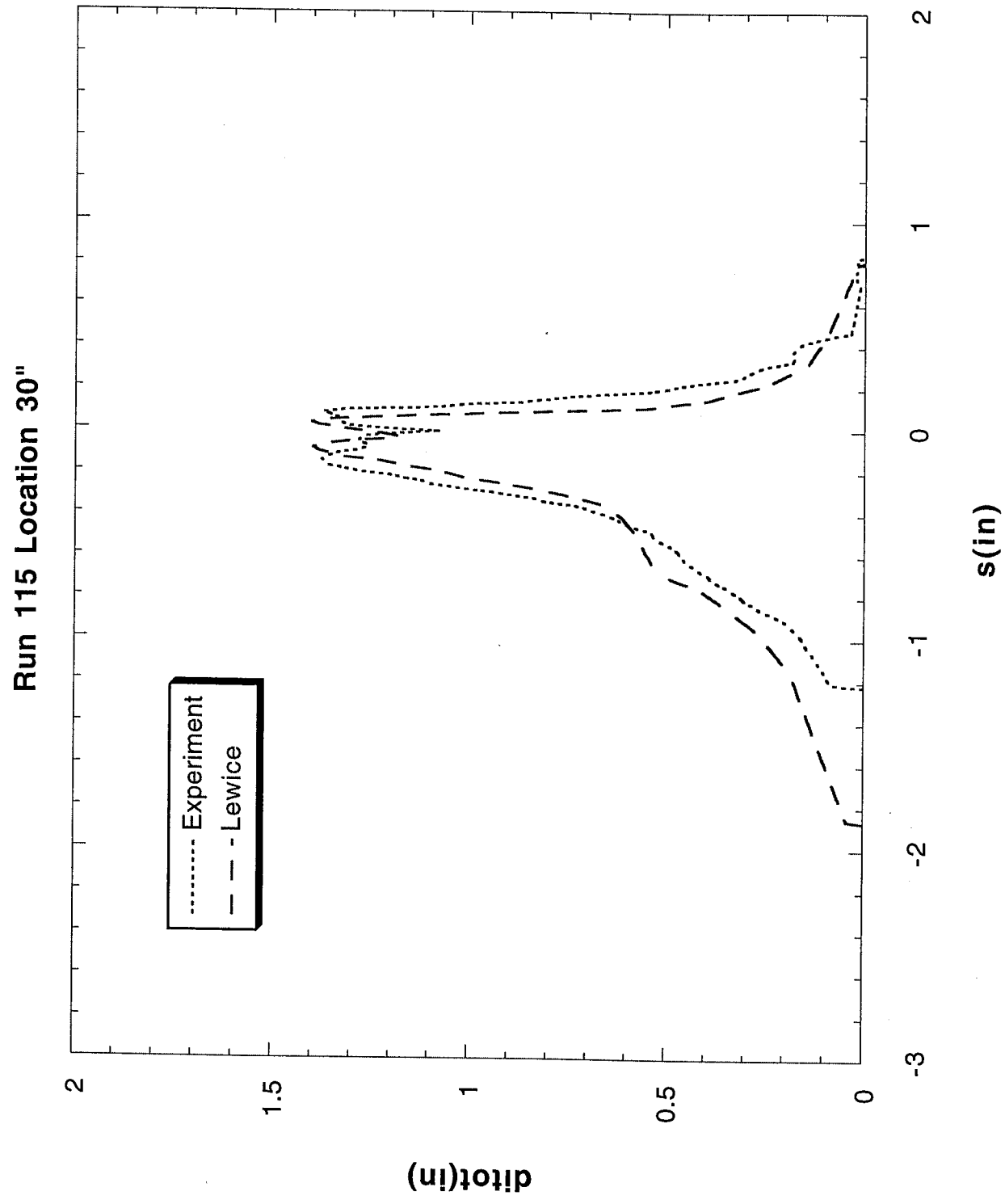
Run 115 Location 30"
Experiment
Lewice
ditot(in)
s(in)
2
1.5
1
0.5
0
-3
-2
-1
0
1
2

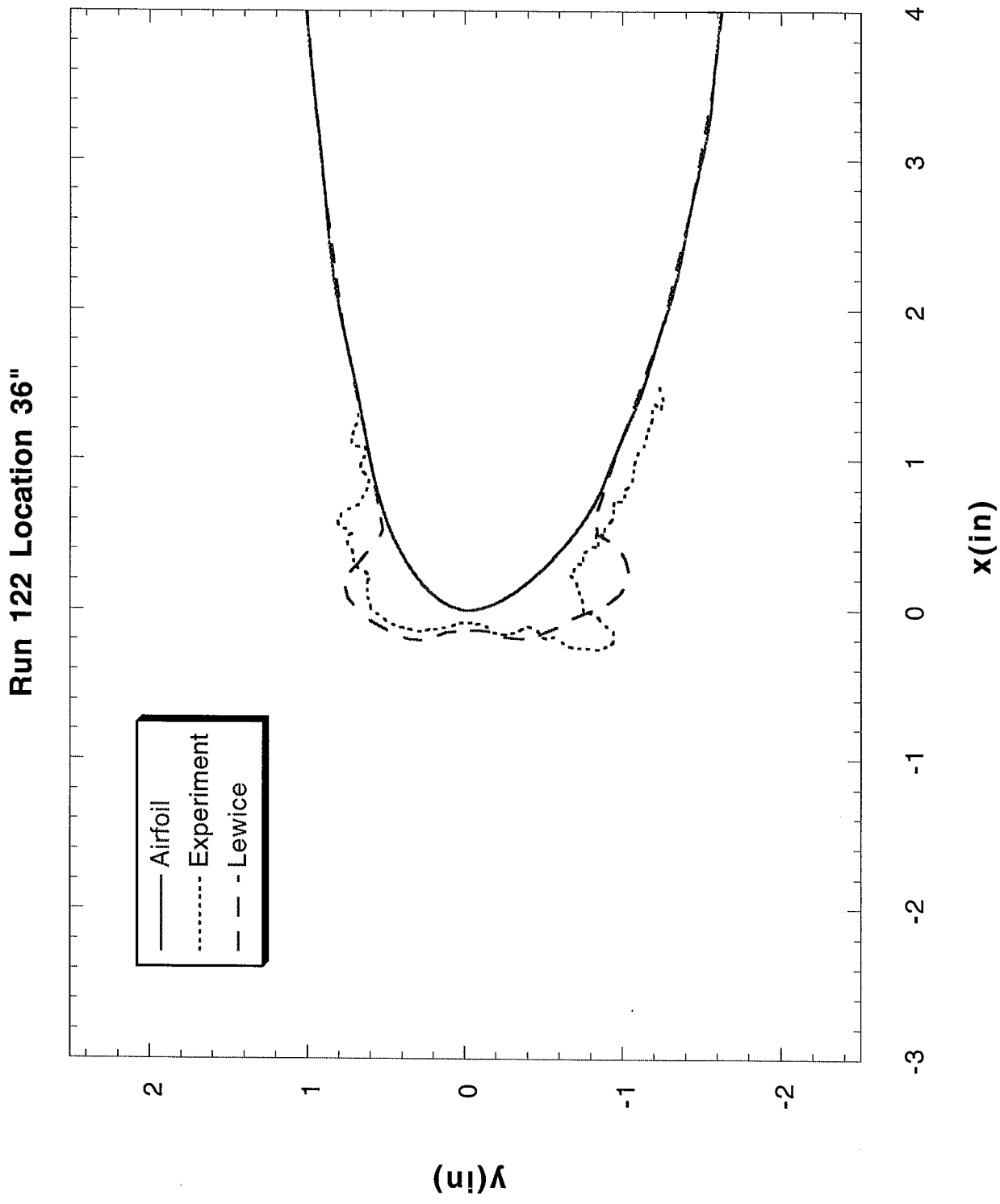
Run 122 Location 36"
Airfoil
Experiment
Lewice
y(in)
x(in)
2
1
0
-1
-2
-3
-2
-1
0
1
2
3
4

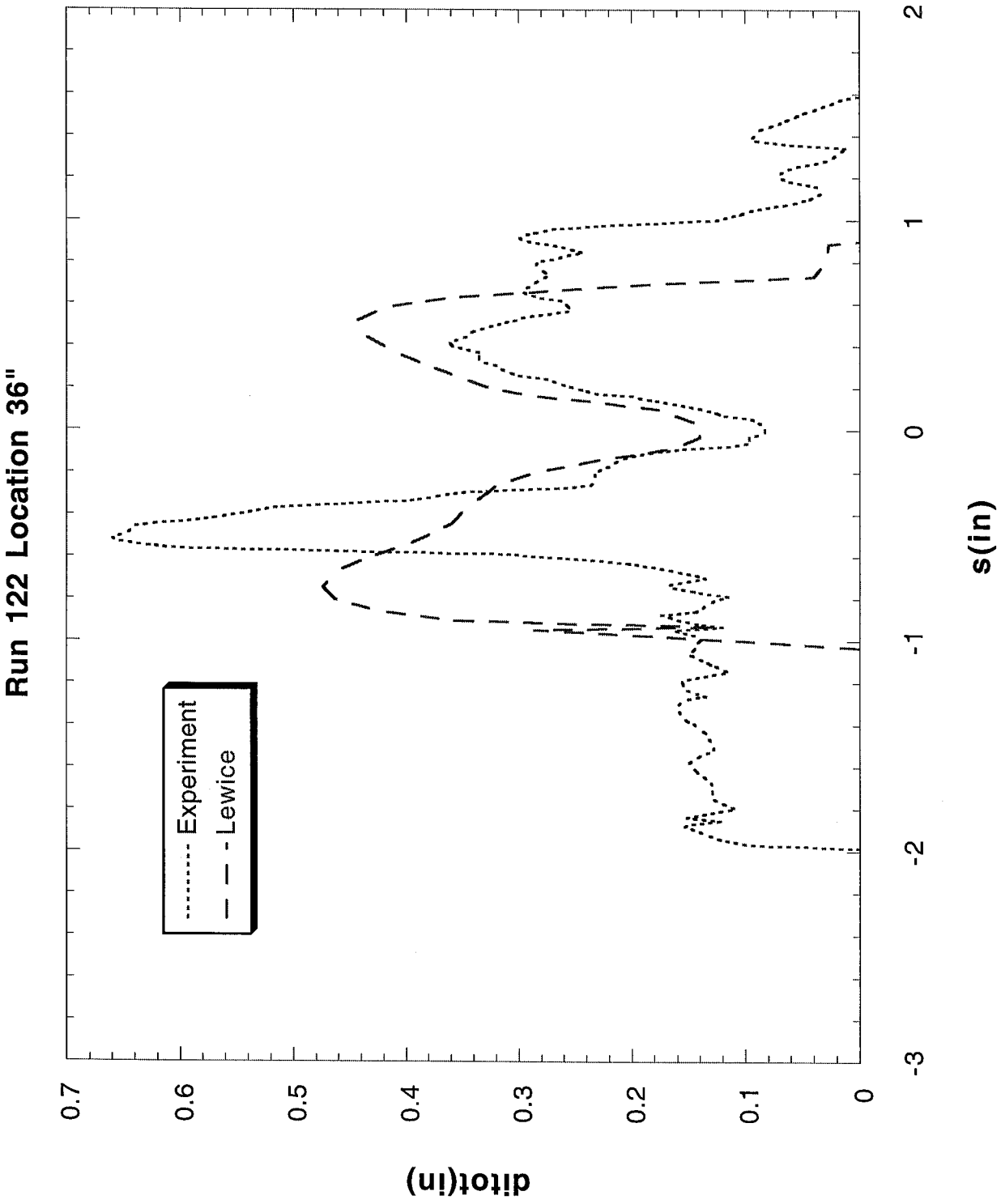
Run 122 Location 36"
Experiment
Lewice
dltot(in)
s(in)
0
0.1
0.2
0.3
0.4
0.5
0.6
0.7
-3
-2
-1
0
1
2

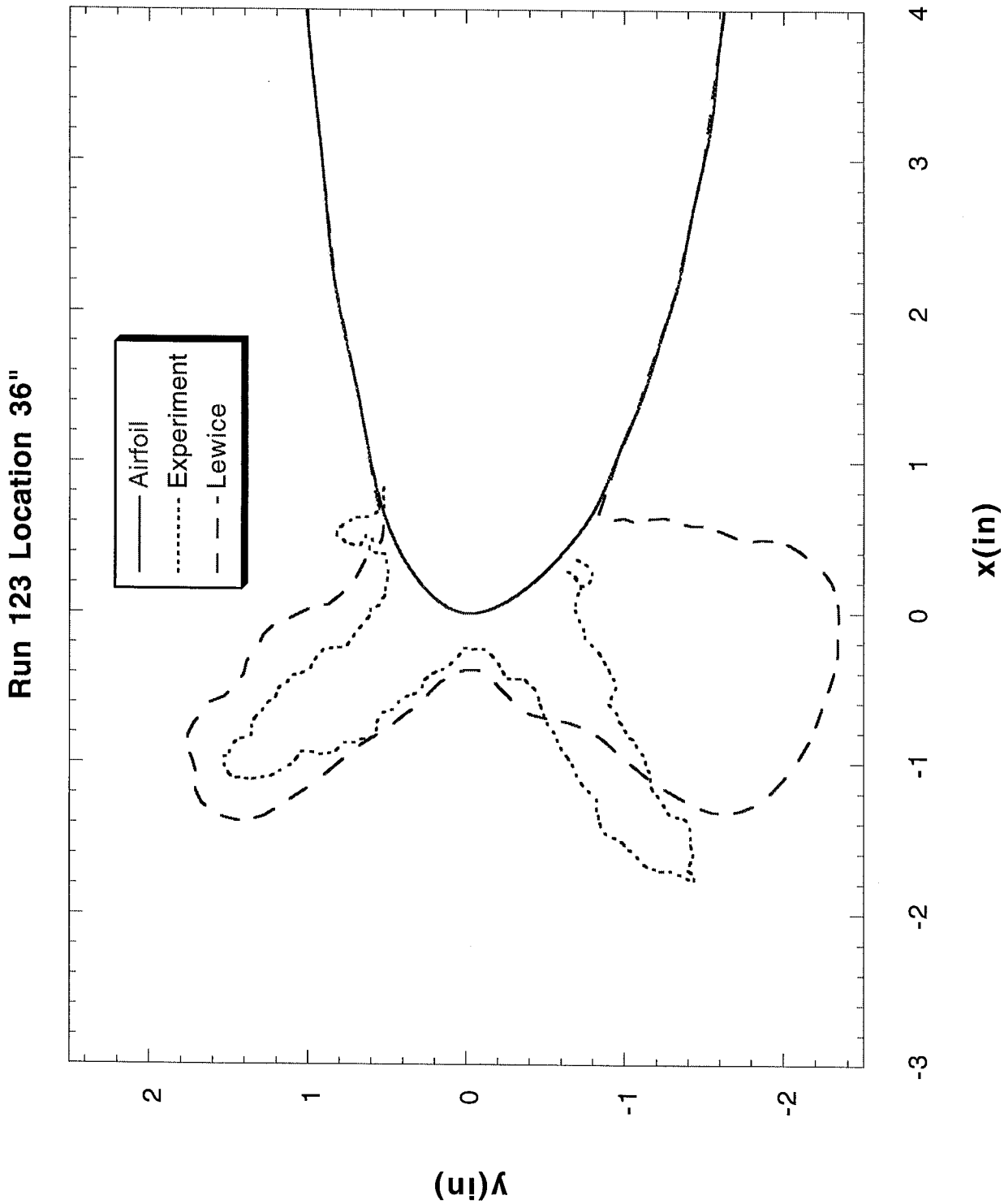
Run 123 Location 36"
Airfoil
Experiment
Lewice
y(in)
x(in)
2
1
0
-1
-2
-3
-2
-1
0
1
2
3
4

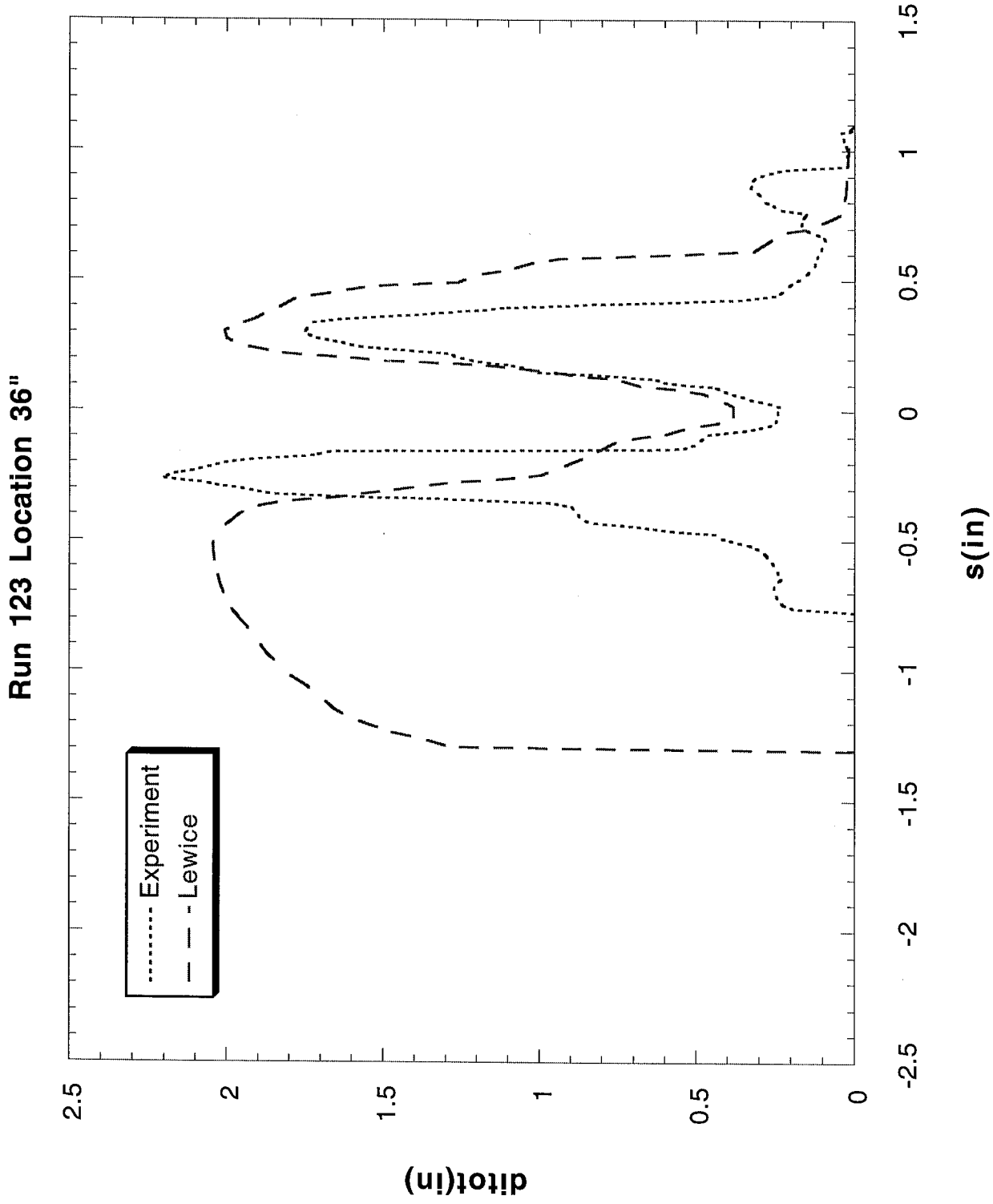
Run 123 Location 36"
Experiment
Lewice
dltot(in)
s(in)
2.5
2
1.5
1
0.5
0
-2.5
-2
-1.5
-1
-0.5
0
0.5
1
1.5

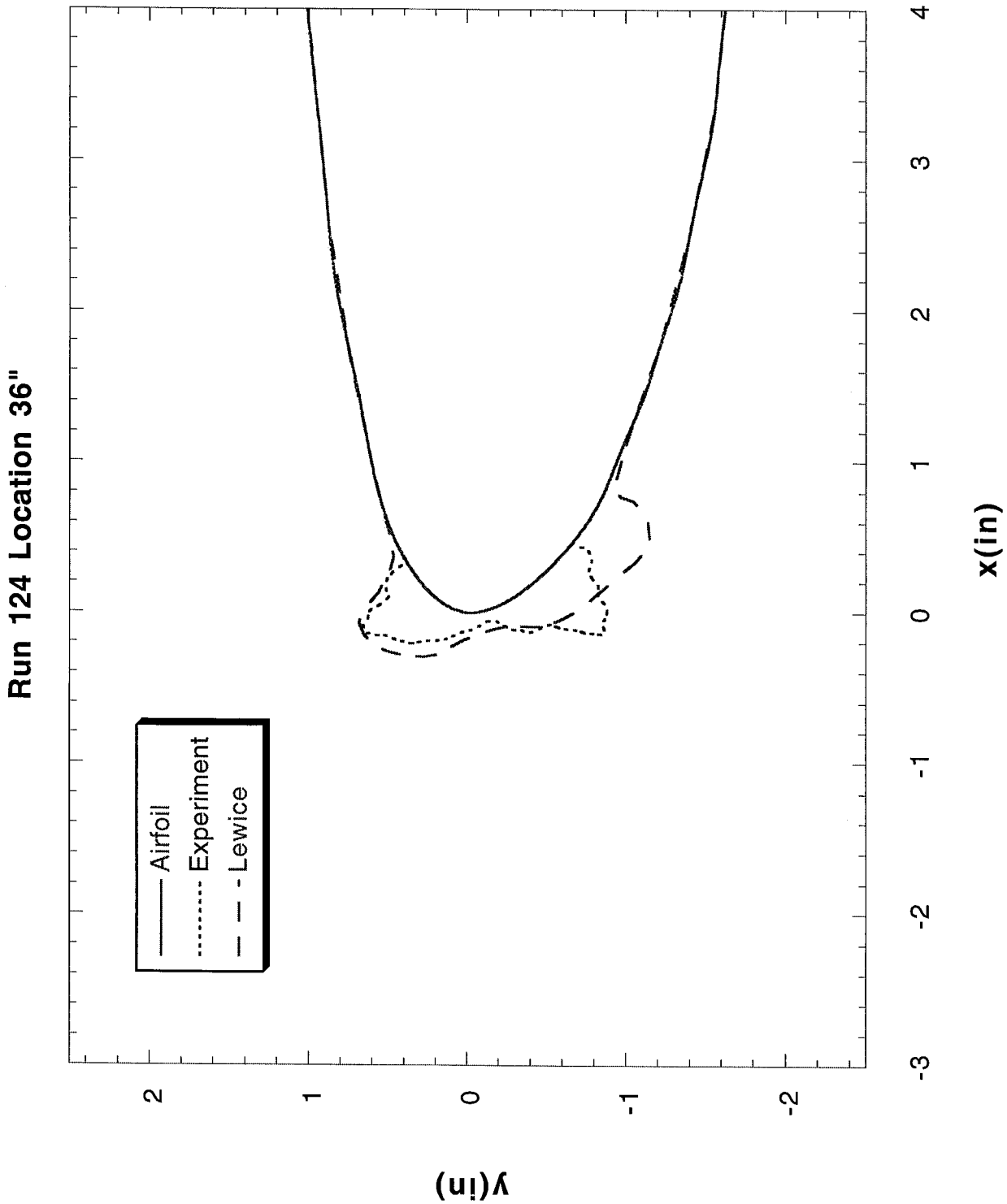
Run 124 Location 36"
Airfoil
Experiment
Lewice
y(in)
x(in)
2
1
0
-1
-2
-3
-2
-1
0
1
2
3
4

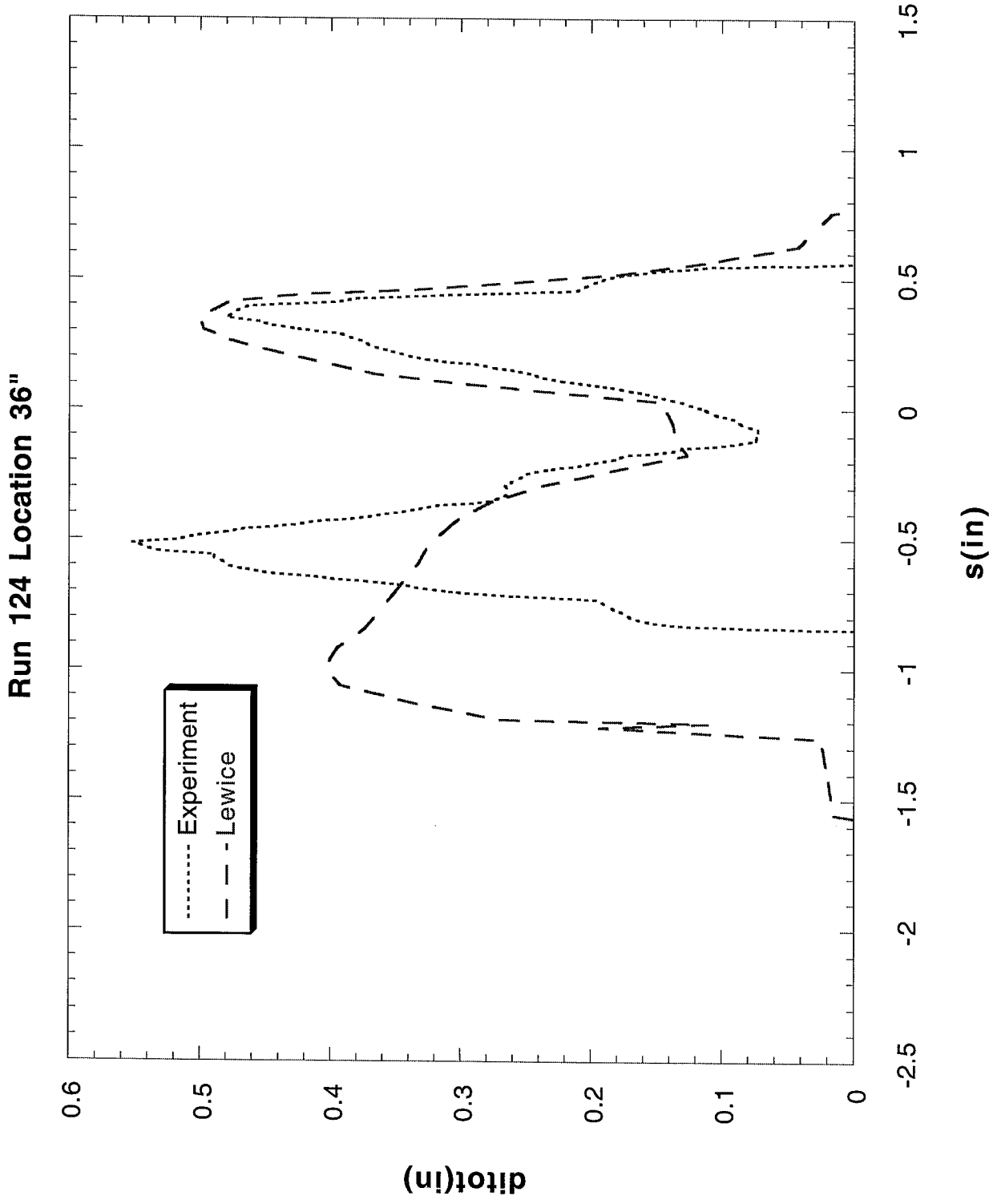
Run 124 Location 36"
Experiment
Lewice
ditot(in)
s(in)
0.6
0.5
0.4
0.3
0.2
0.1
0
-2.5
-2
-1.5
-1
-0.5
0
0.5
1
1.5

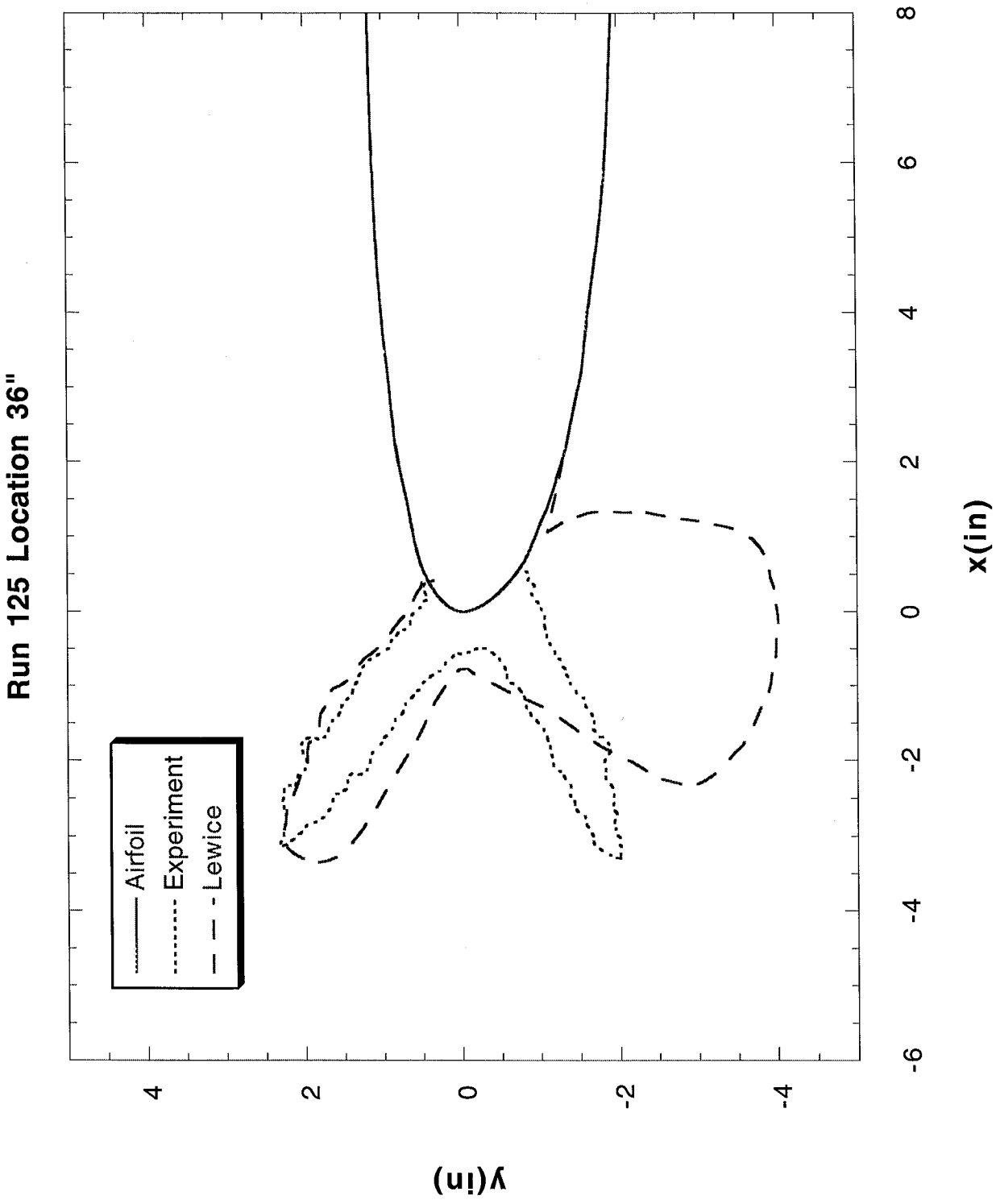
Run 125 Location 36"
Airfoil
Experiment
Lewice
y(in)
x(in)
4
2
0
-2
-4
8
6
4
2
0
-2
-4
-6

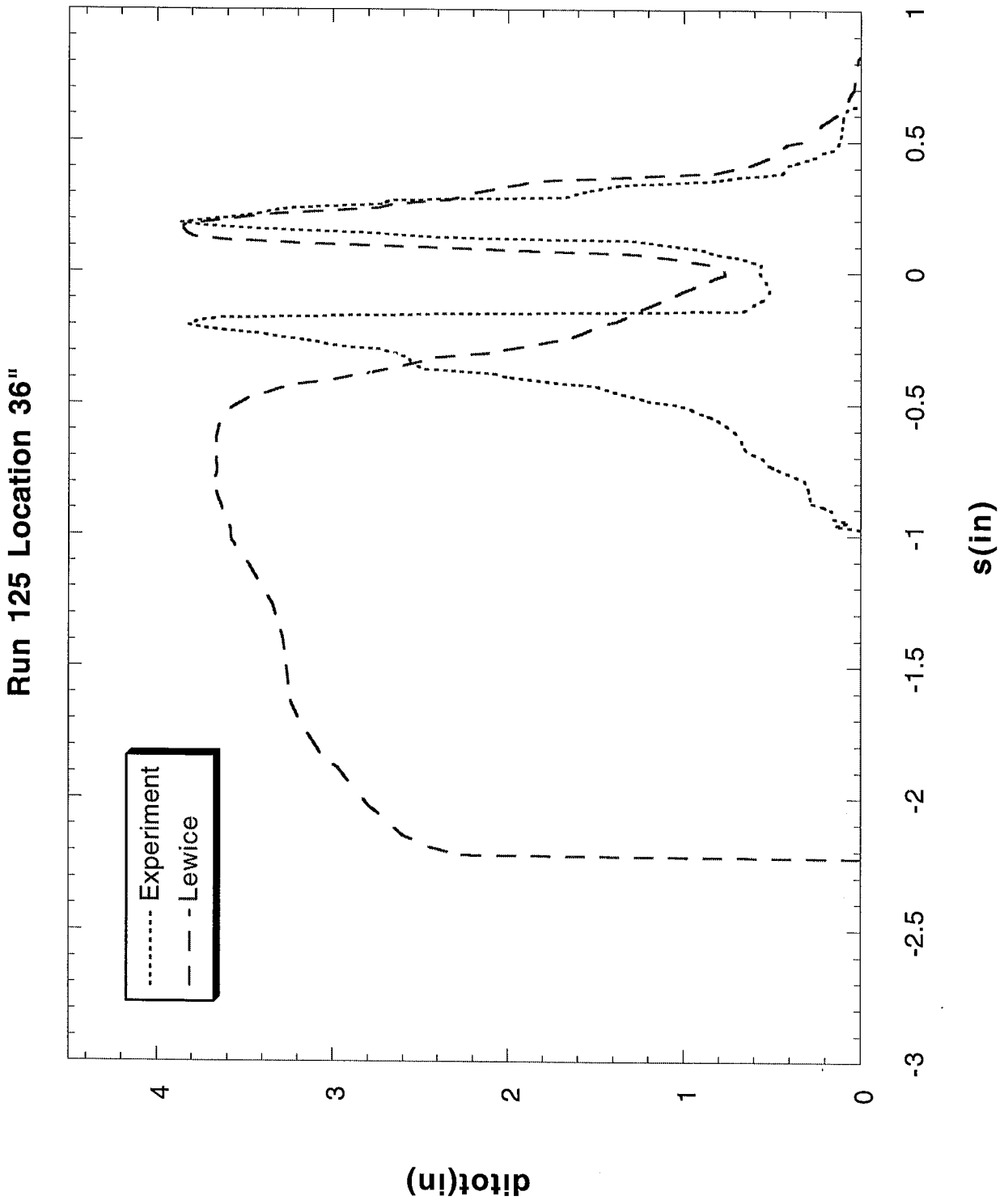
Run 125 Location 36"
Experiment
Lewice
dltot(in)
s(in)
0
1
2
3
4
-3
-2.5
-2
-1.5
-1
-0.5
0
0.5
1

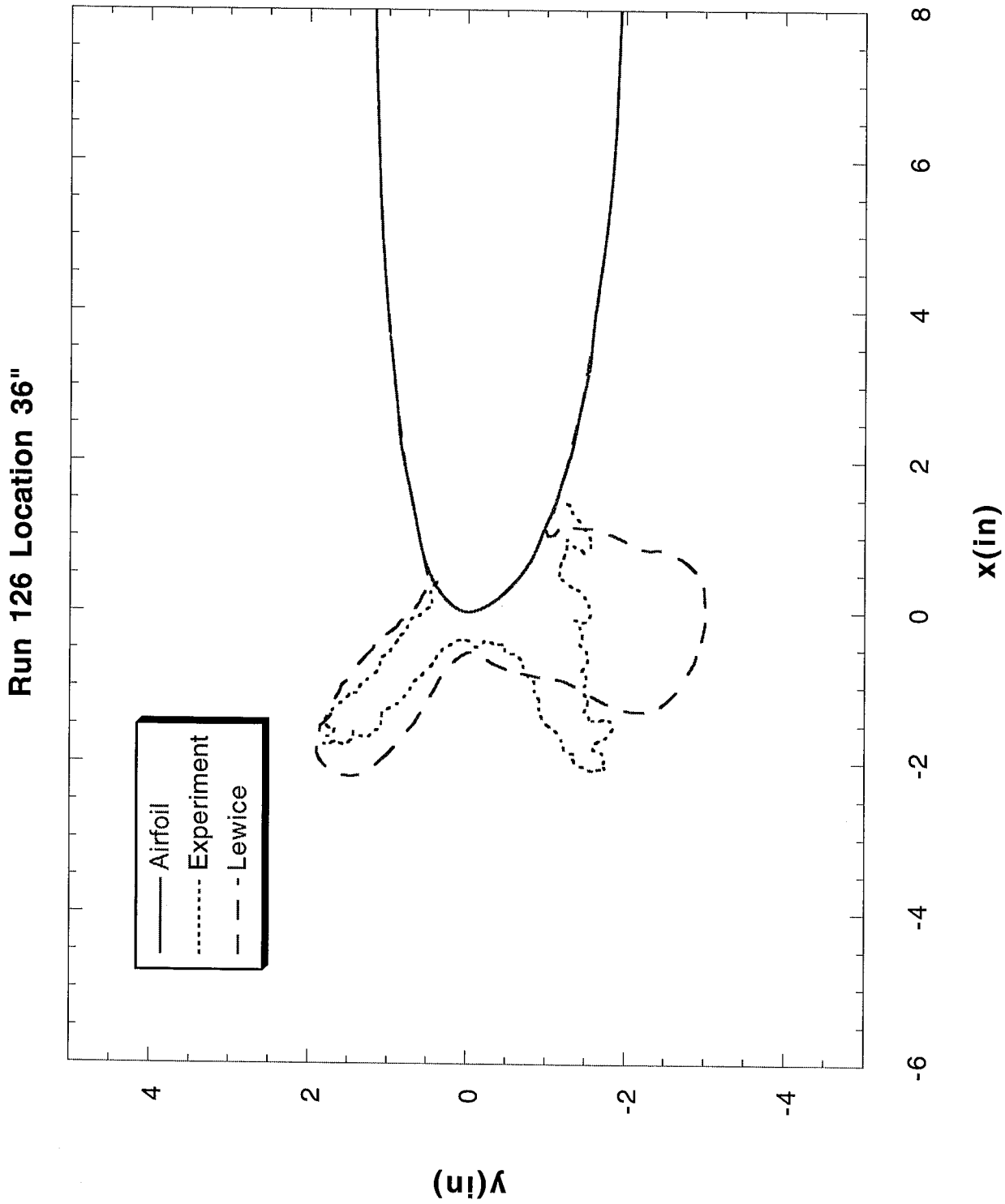
Run 126 Location 36"
Airfoil
Experiment
Lewice
y(in)
x(in)
4
2
0
-2
-4
-6
-4
-2
0
2
4
6
8

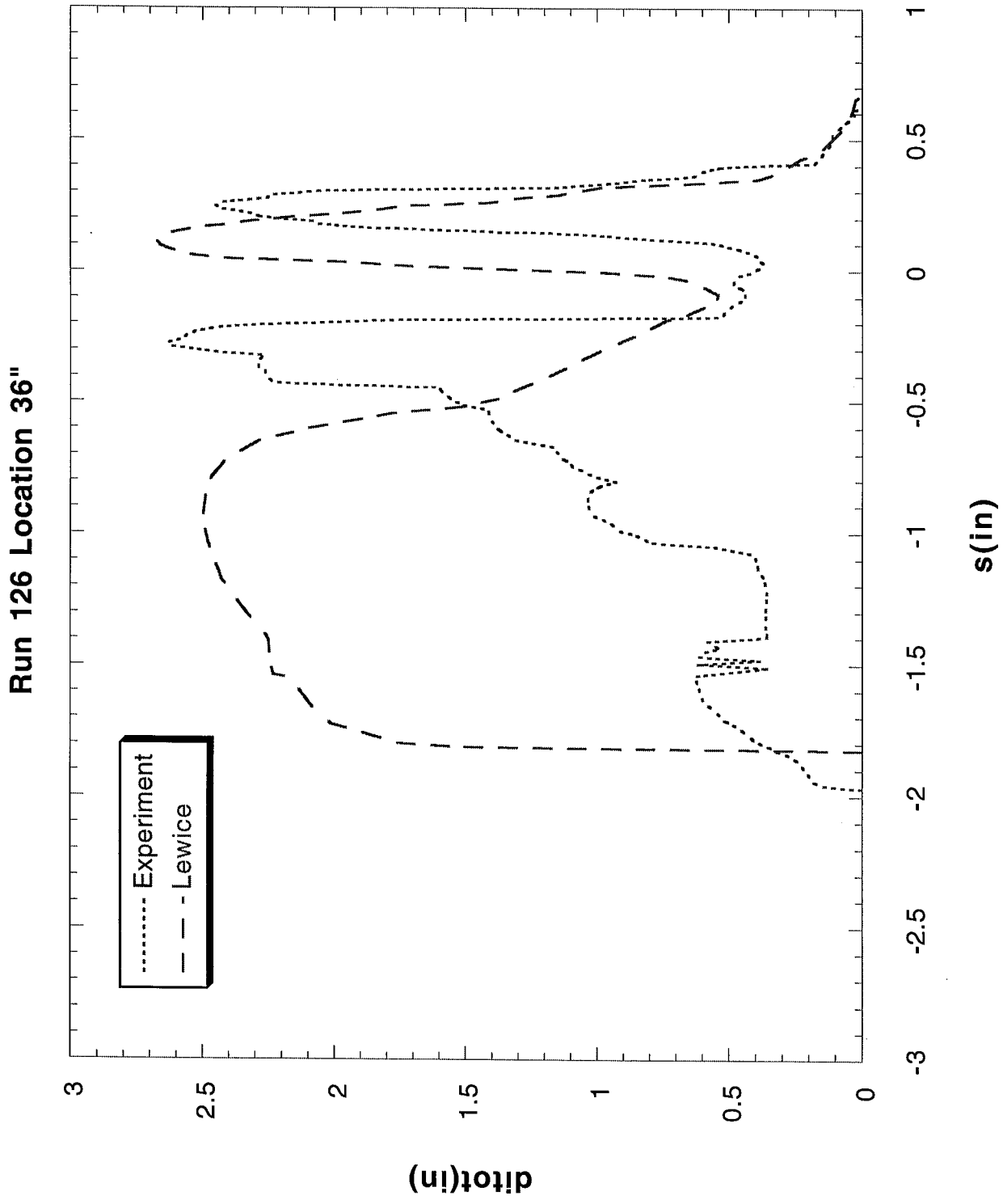
Run 126 Location 36"
Experiment
Lewice
dltot(in)
s(in)
3
2.5
2
1.5
1
0.5
0
-3
-2.5
-2
-1.5
-1
-0.5
0
0.5
1

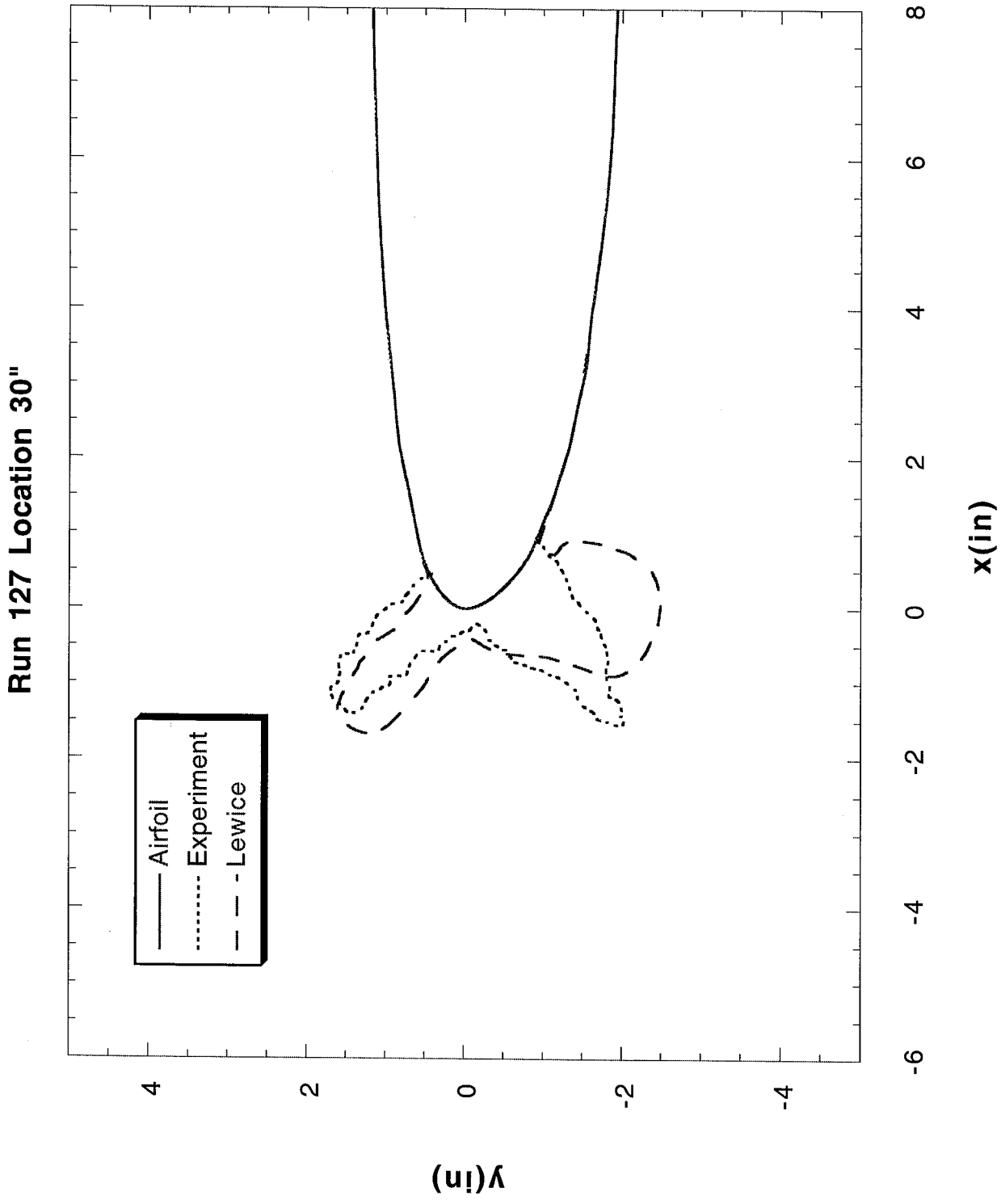
Run 127 Location 30"
Airfoil
Experiment
Lewice
y(in)
x(in)
4
2
0
-2
-4
-6
-4
-2
0
2
4
6
8

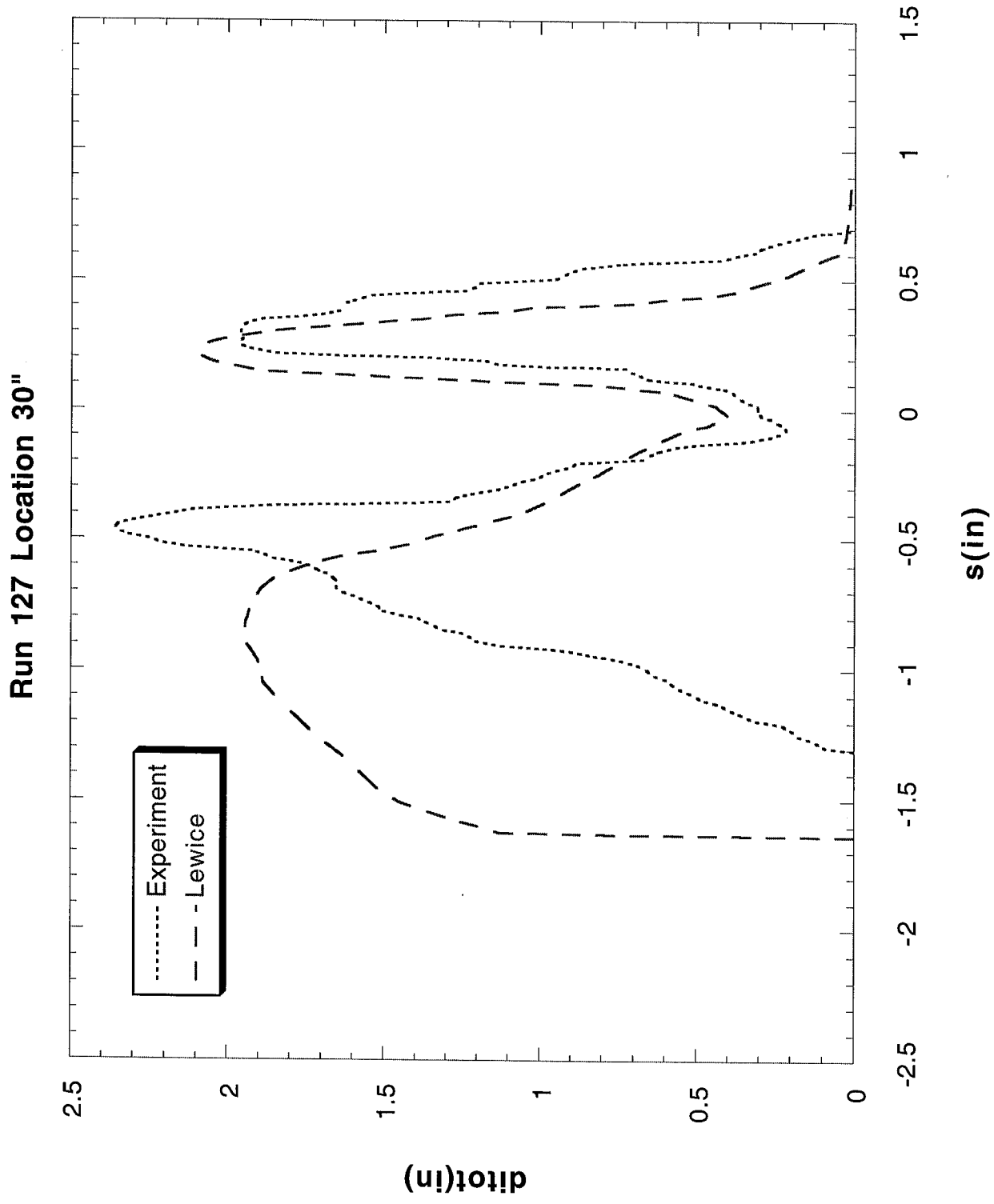
Run 127 Location 30"
Experiment
Lewice
dltot(in)
s(in)
2.5
2
1.5
1
0.5
0
-2.5
-2
-1.5
-1
-0.5
0
0.5
1
1.5

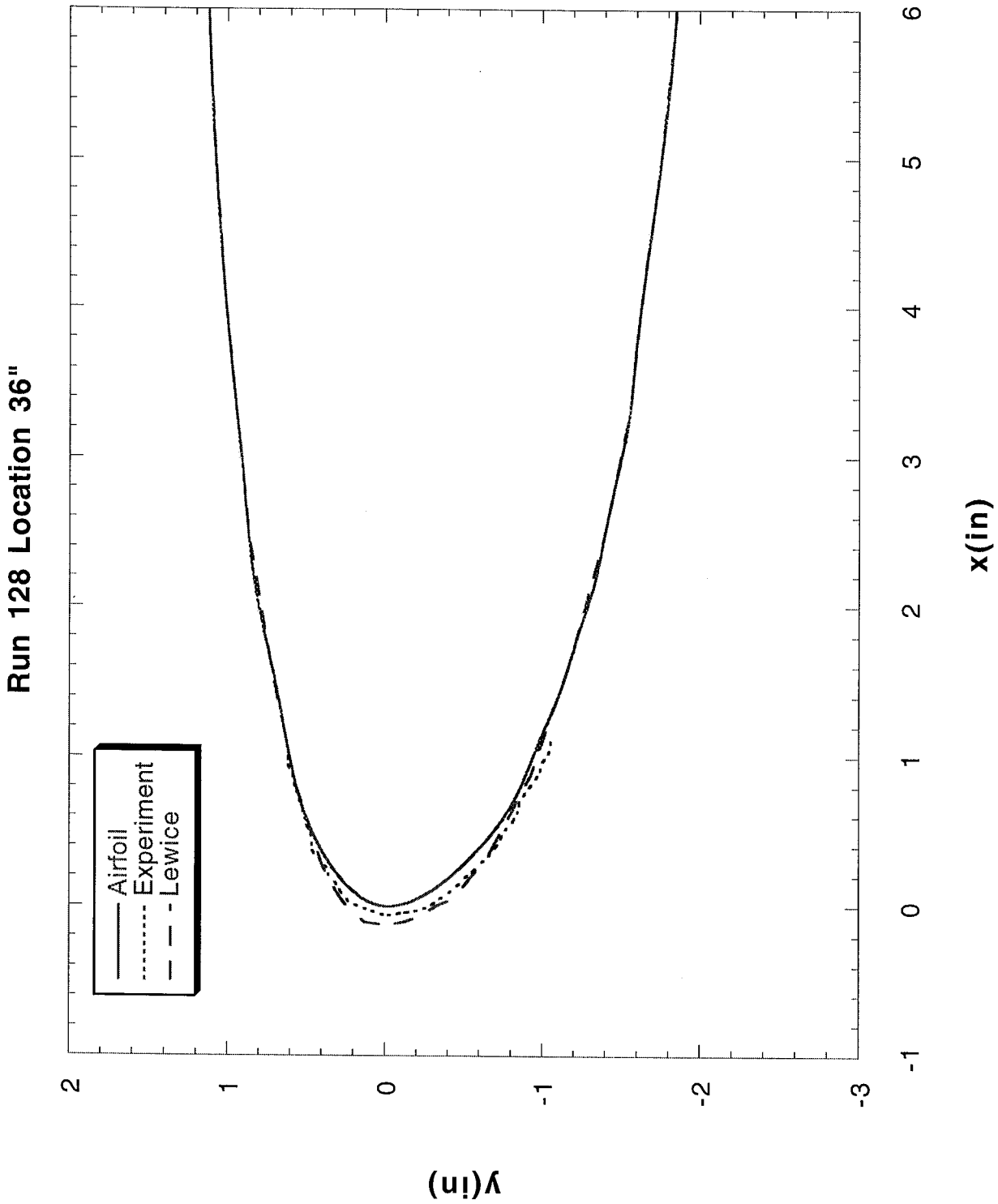
Run 128 Location 36"
Airfoil
Experiment
Lewice
y(in)
x(in)
2
1
0
-1
-2
-3
-1
0
1
2
3
4
5
6

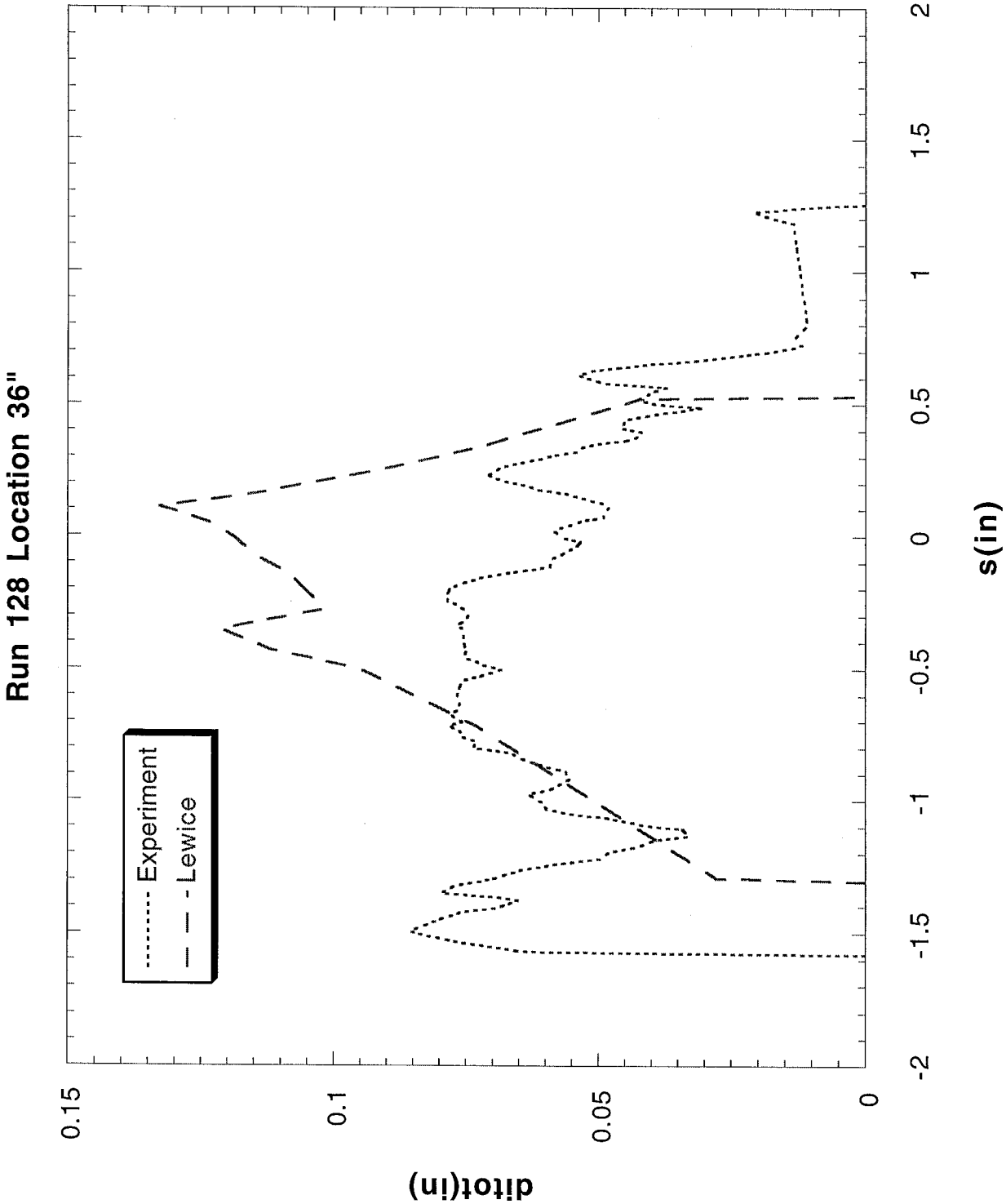
Run 128 Location 36"
Experiment
Lewice
dltot(in)
0.15
0.1
0.05
0
s(in)
-2
-1.5
-1
-0.5
0
0.5
1
1.5
2

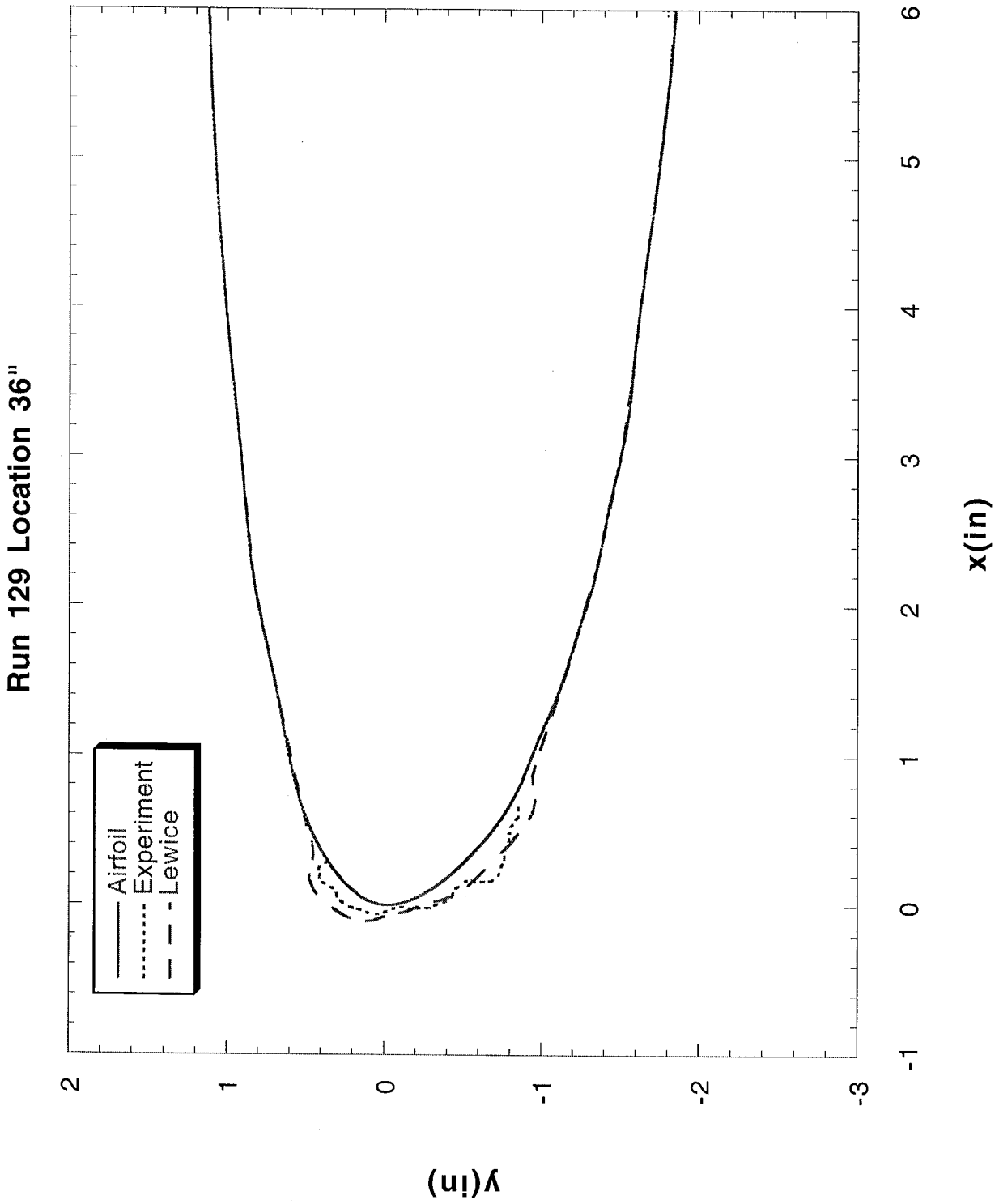
Run 129 Location 36"
Airfoil
Experiment
Lewice
y(in)
x(in)
2
1
0
-1
-2
-3
-1
0
1
2
3
4
5
6

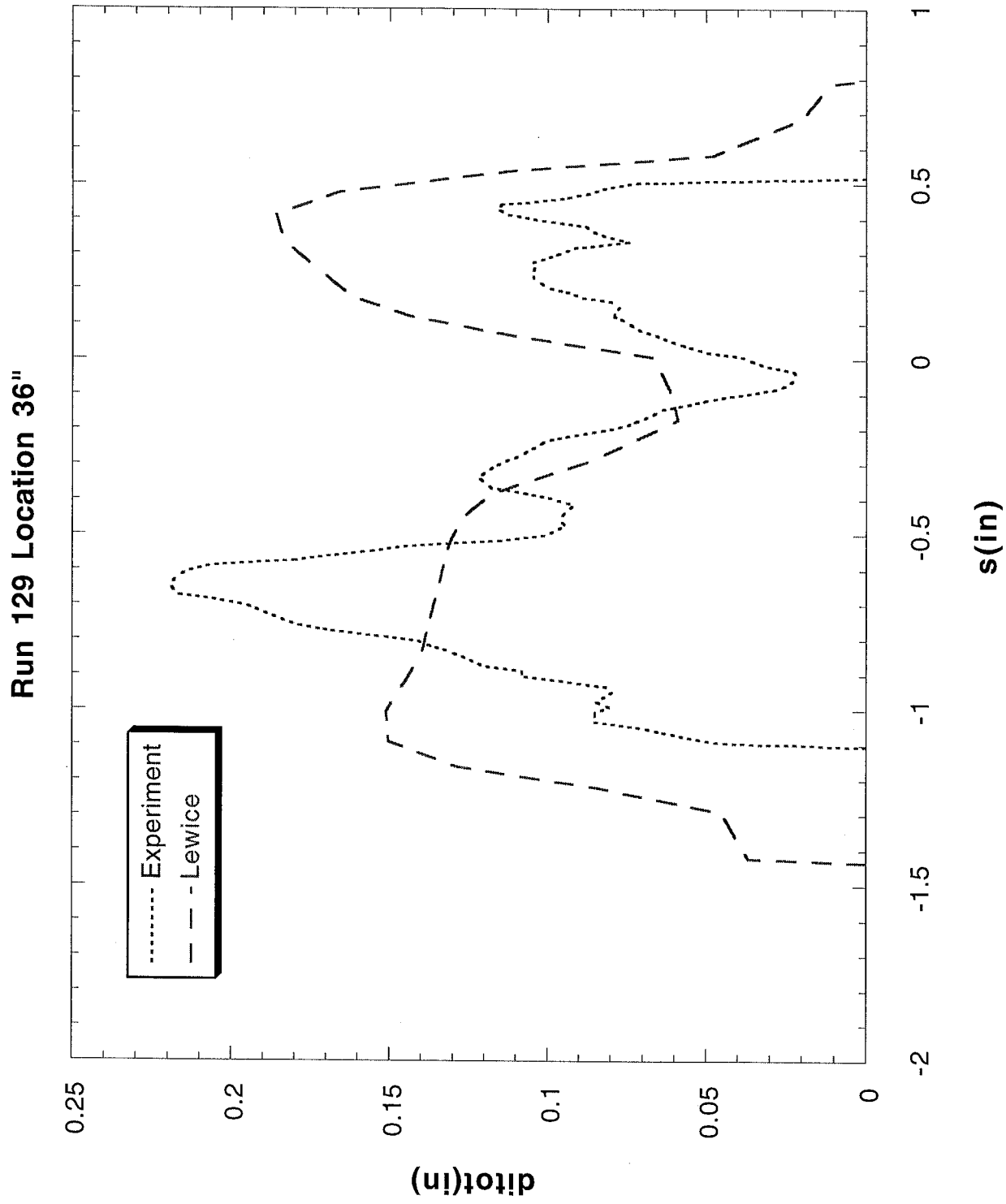
Run 129 Location 36"
Experiment
Lewice
dltot(in)
s(in)
0.25
0.2
0.15
0.1
0.05
0
-2
-1.5
-1
-0.5
0
0.5
1

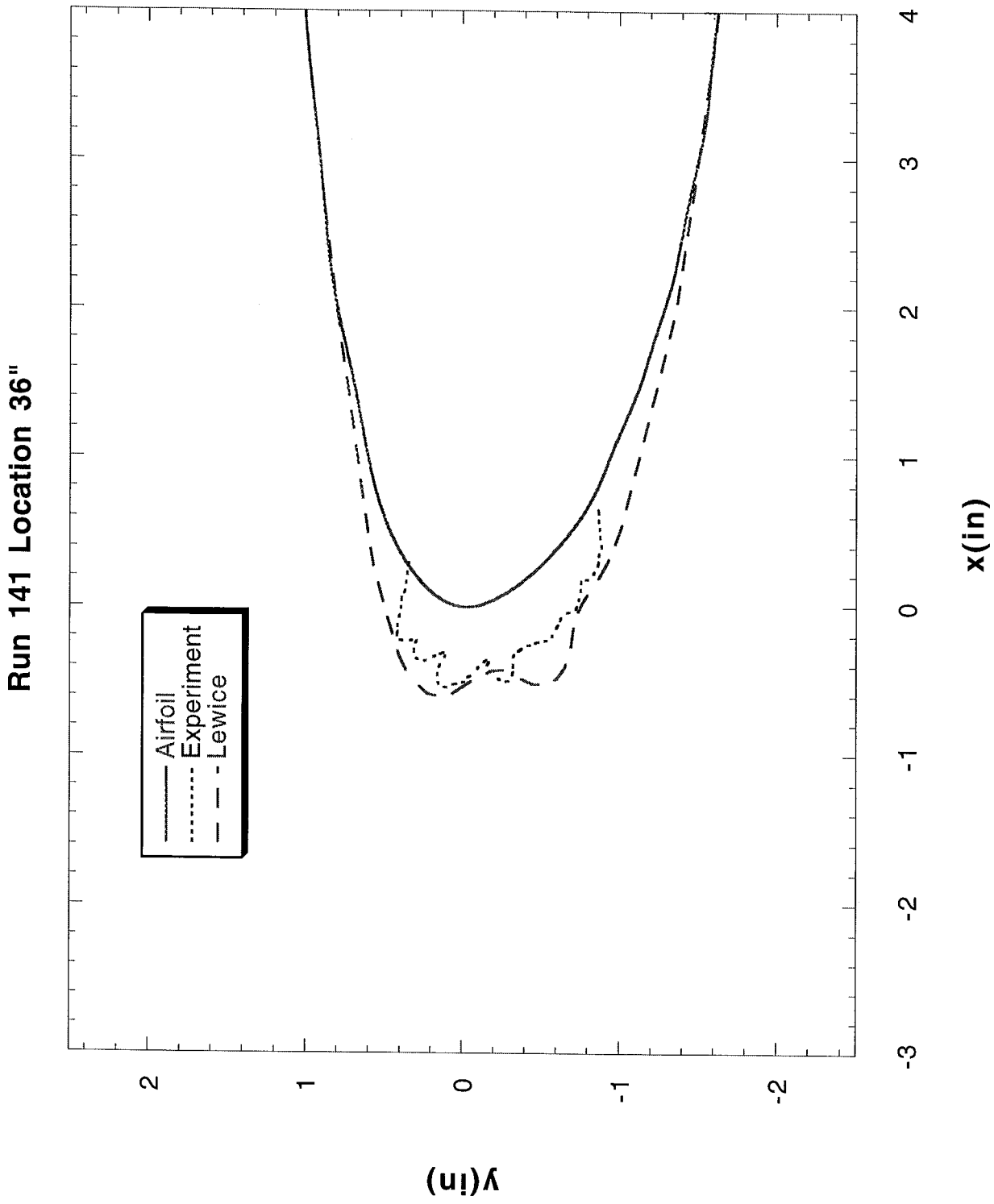
Run 141 Location 36"
Airfoil
Experiment
Lewice
y(in)
x(in)
2
1
0
-1
-2
-3
-2
-1
0
1
2
3
4

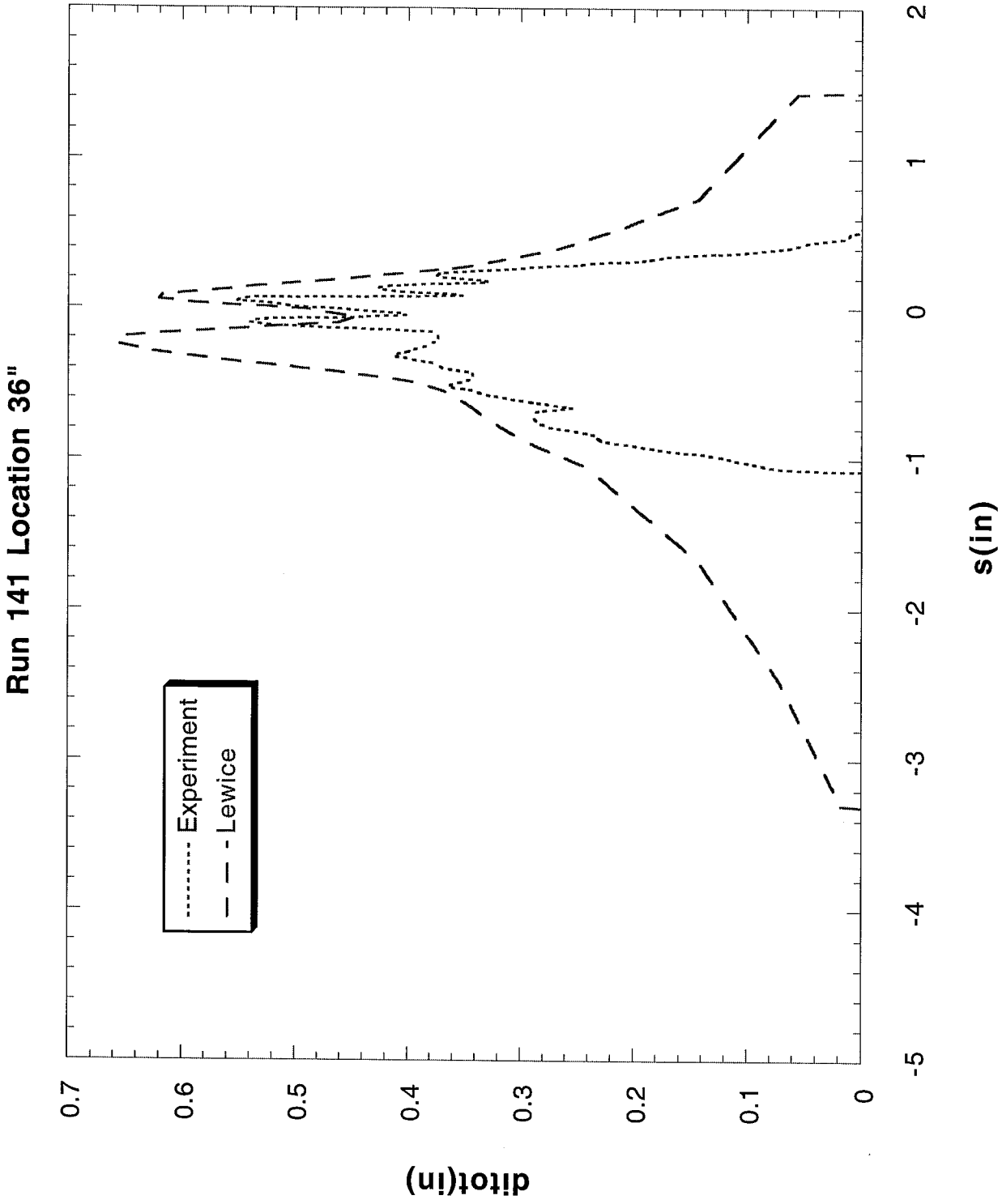
Run 141 Location 36"
Experiment
Lewice
dltot(in)
s(in)
0
0.1
0.2
0.3
0.4
0.5
0.6
0.7
-5
-4
-3
-2
-1
0
1
2

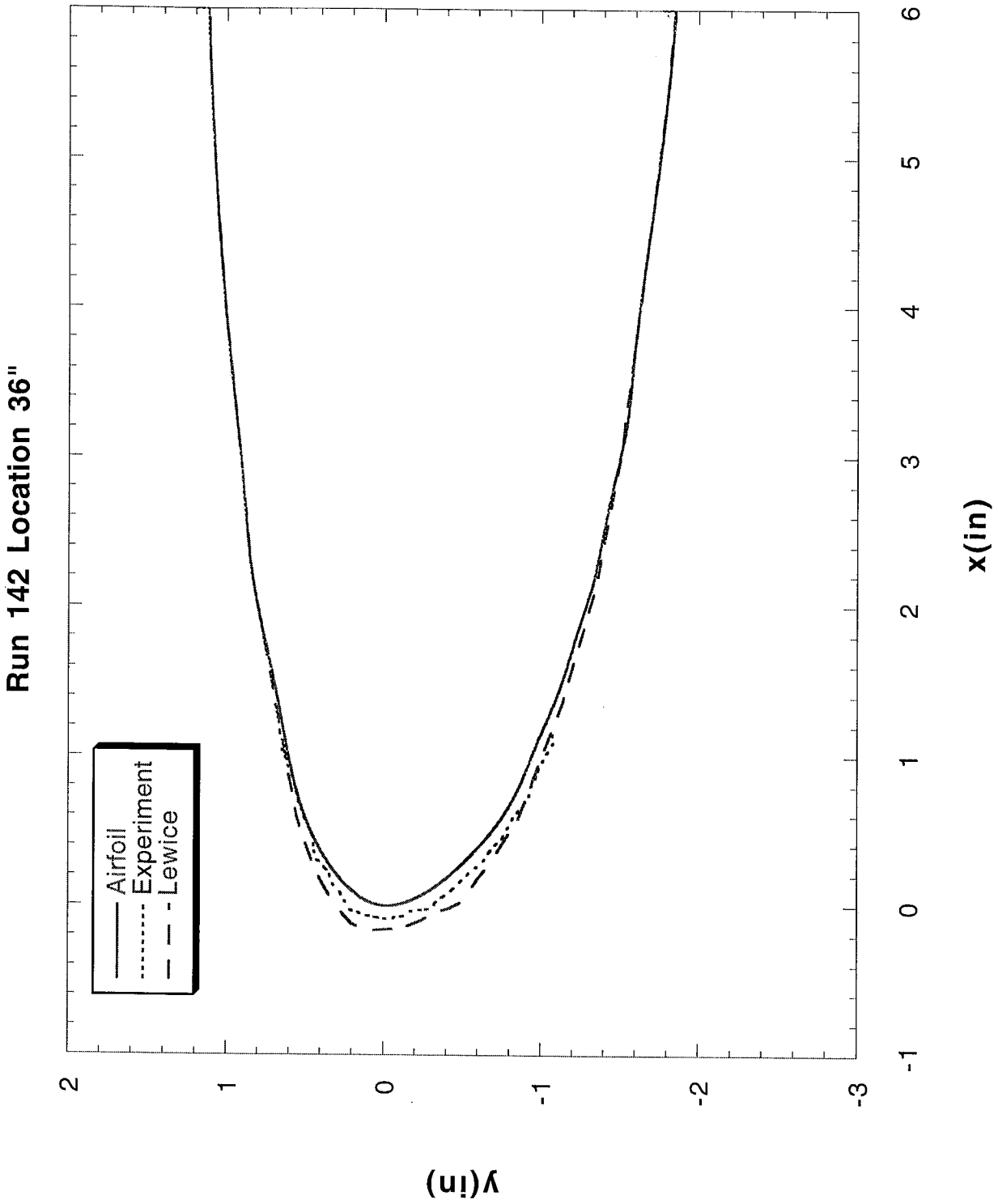
Run 142 Location 36"
Airfoil
Experiment
Lewice
y(in)
x(in)
2
1
0
-1
-2
-3
-1
0
1
2
3
4
5
6

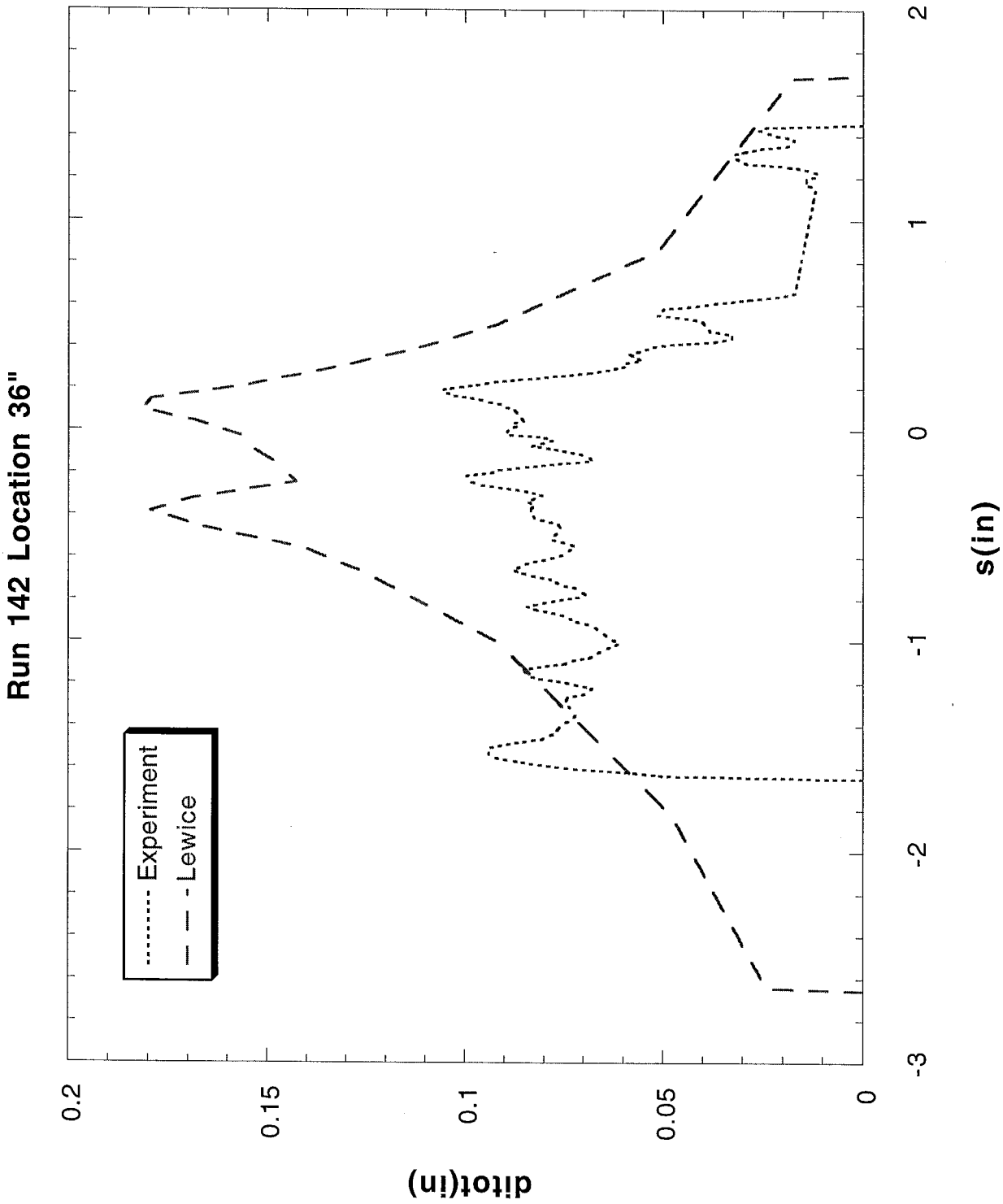
Run 142 Location 36"
Experiment
Lewice
dltot(in)
s(in)
0.2
0.15
0.1
0.05
0
-3
-2
-1
0
1
2

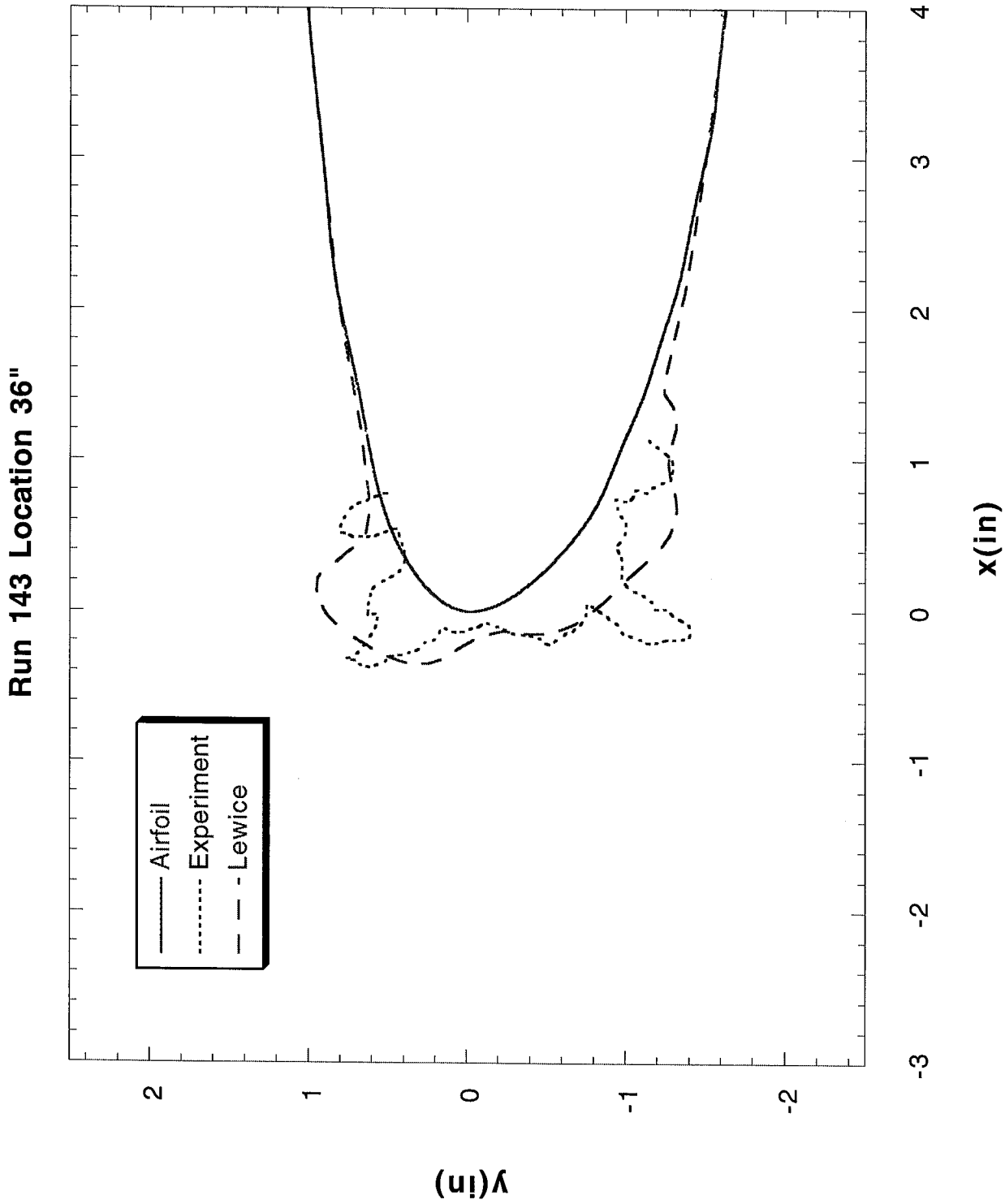
Run 143 Location 36"
Airfoil
Experiment
Lewice
y(in)
x(in)
2
1
0
-1
-2
-3
-2
-1
0
1
2
3
4

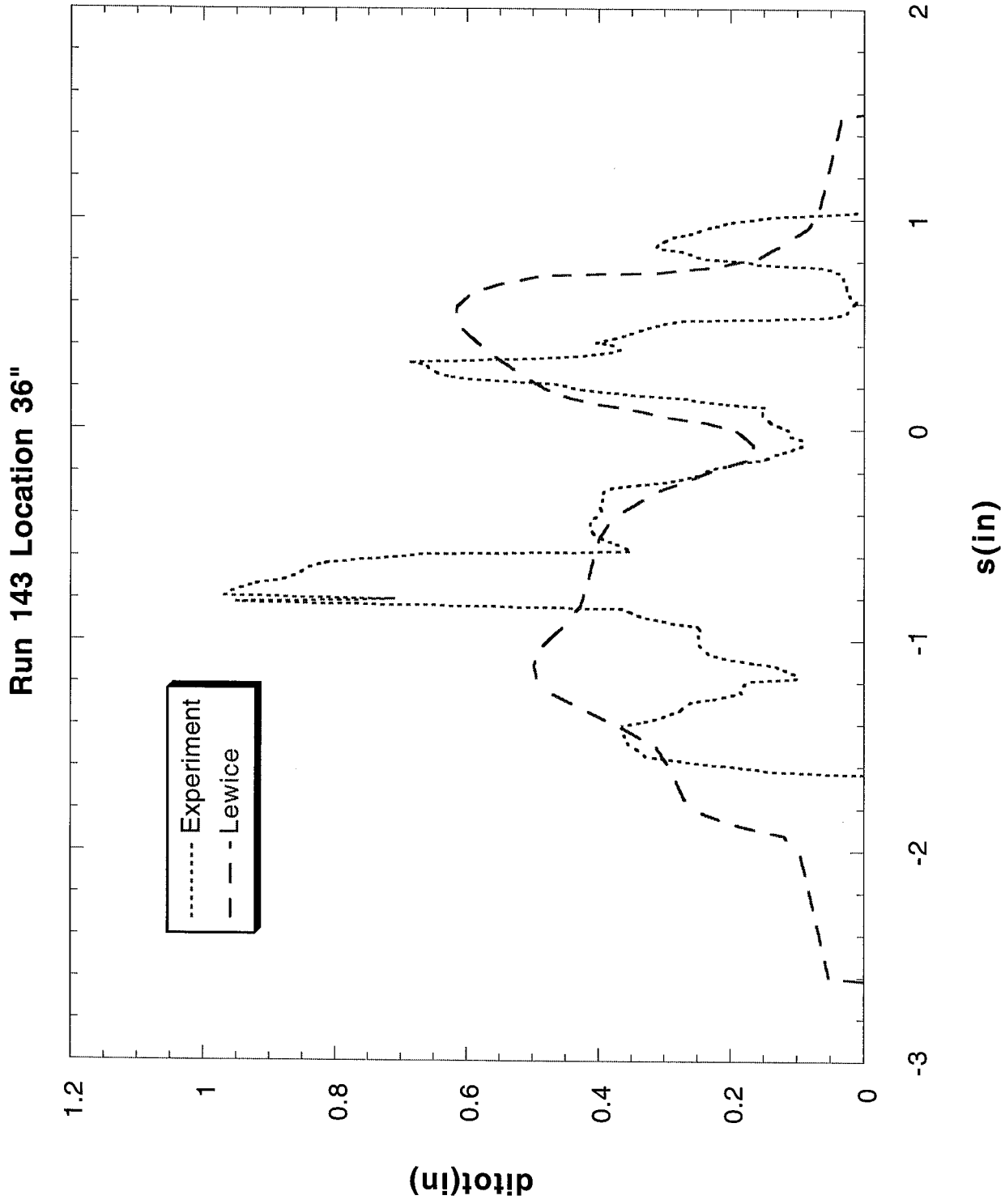
Run 143 Location 36"
Experiment
Lewice
ditot(in)
s(in)
1.2
1
0.8
0.6
0.4
0.2
0
-3
-2
-1
0
1
2

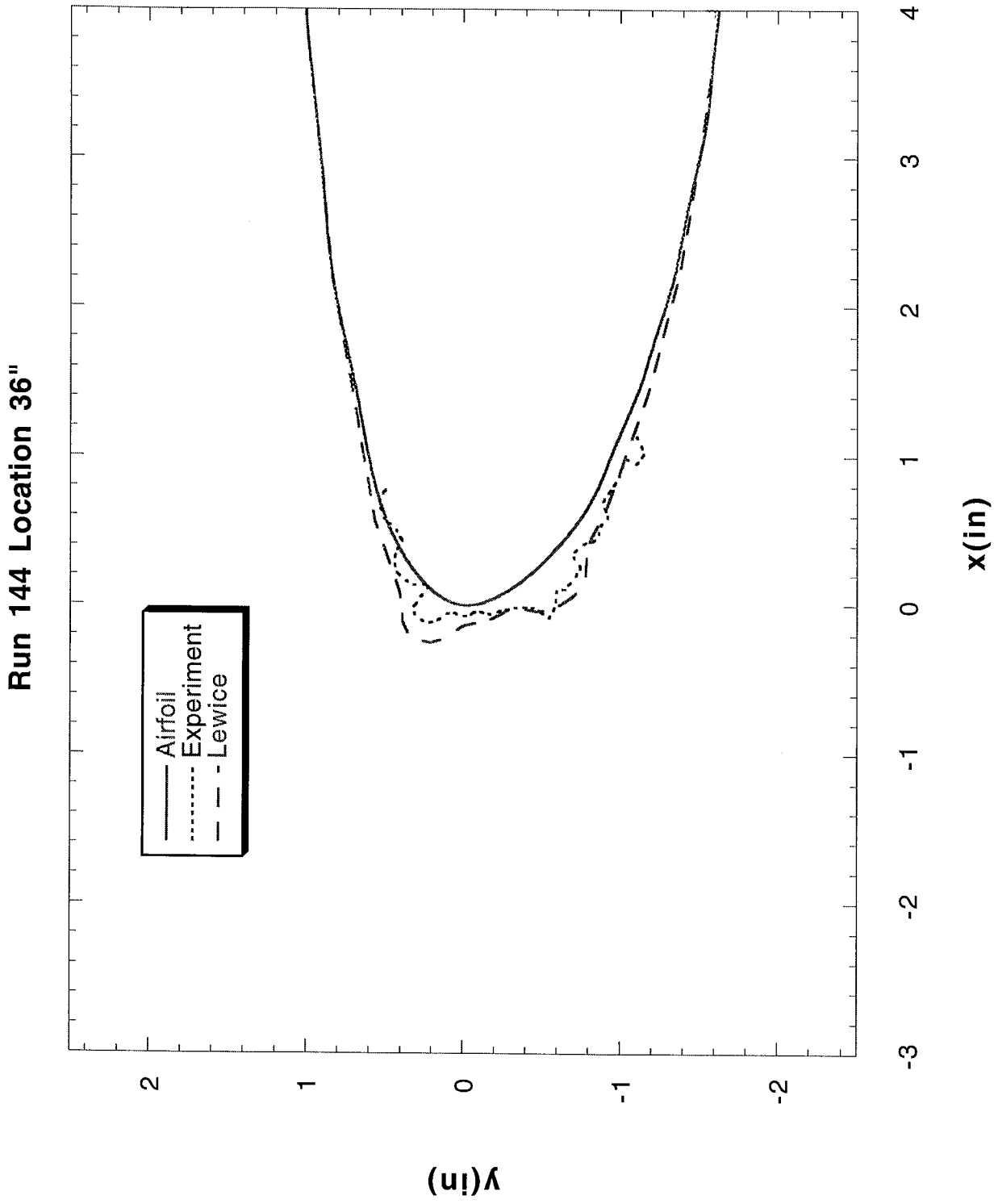
Run 144 Location 36"
Airfoil
Experiment
Lewice
y(in)
x(in)
2
1
0
-1
-2
-3
-2
-1
0
1
2
3
4

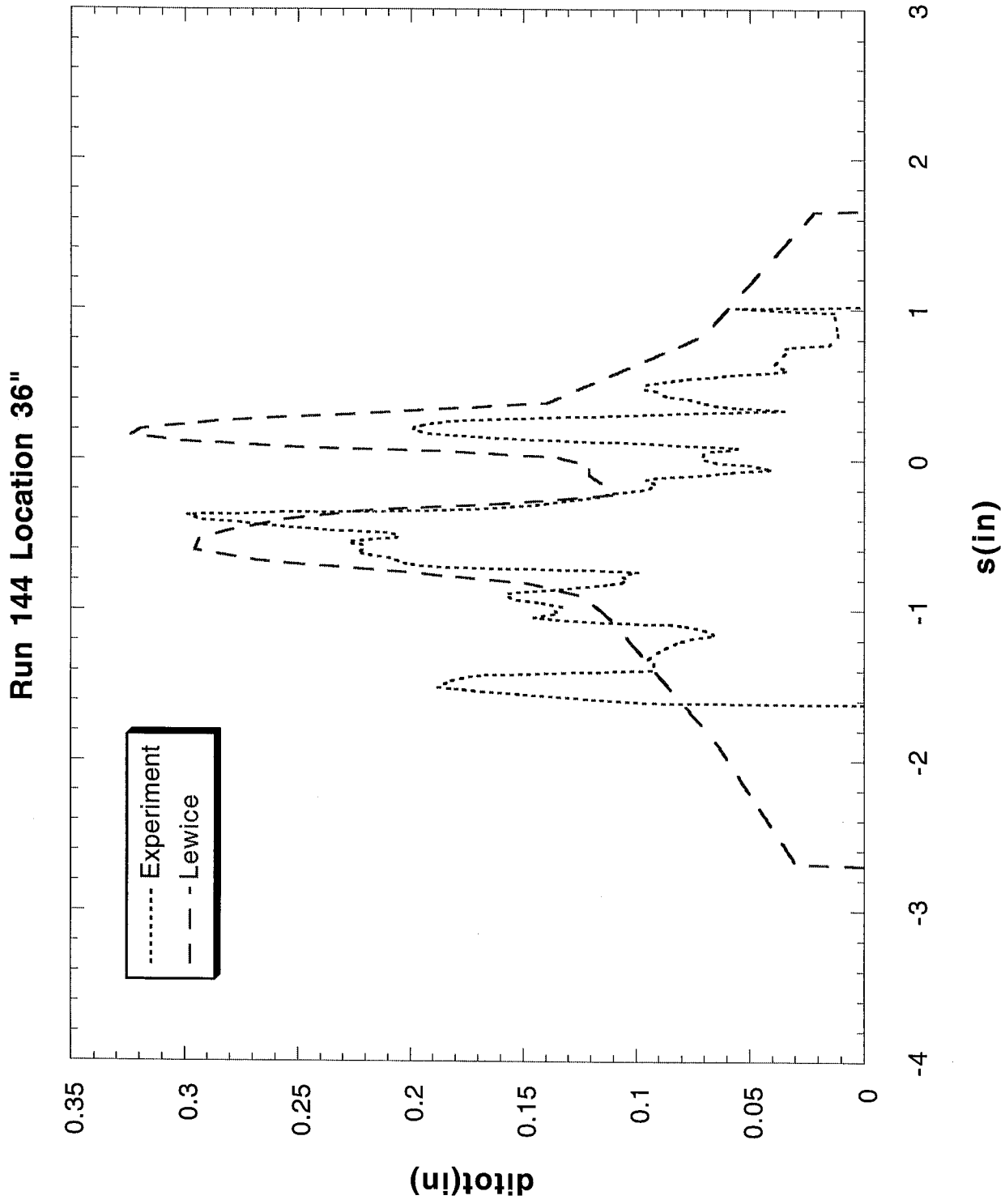
Run 144 Location 36"
Experiment
Lewice
dltot(in)
s(in)
0.35
0.3
0.25
0.2
0.15
0.1
0.05
0
-4
-3
-2
-1
0
1
2
3

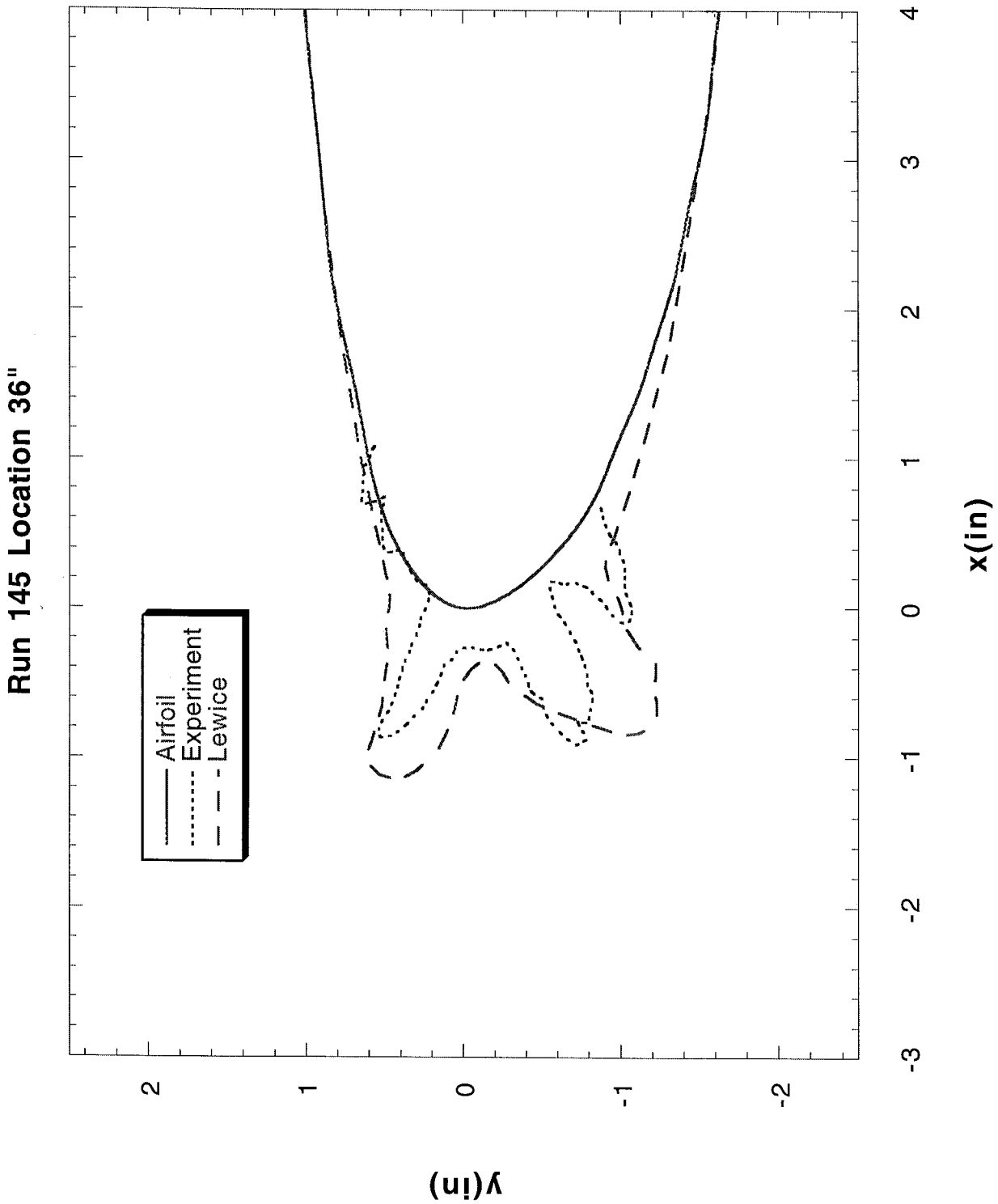
Run 145 Location 36"
Airfoil
Experiment
Lewice
y(in)
x(in)
2
1
0
-1
-2
-3
-2
-1
0
1
2
3
4

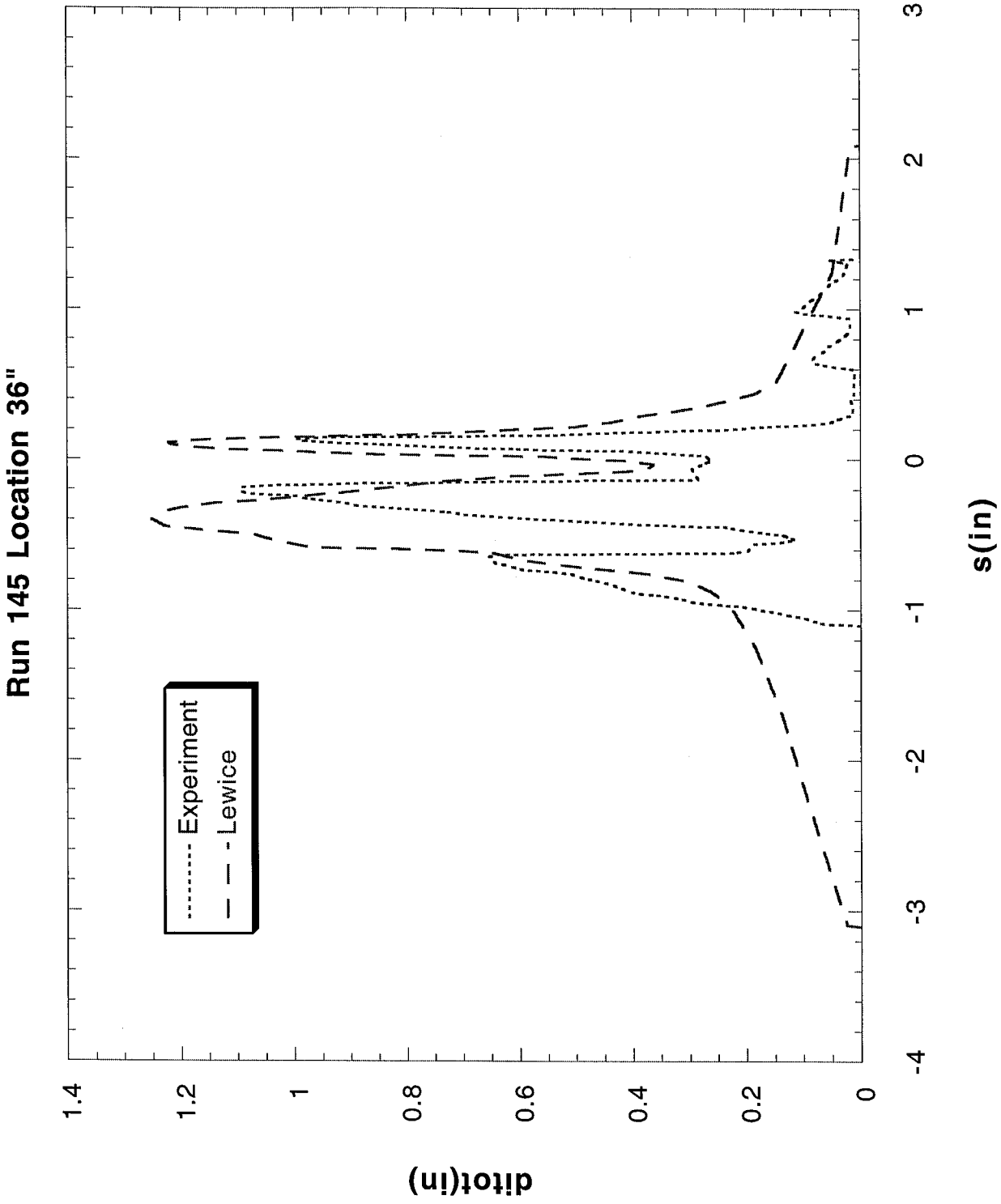
Run 145 Location 36"
Experiment
Lewice
ditot(in)
s(in)
1.4
1.2
1
0.8
0.6
0.4
0.2
0
-4
-3
-2
-1
0
1
2
3

GLC 305
Figures 296 – 447

GLC 305 Test Conditions

Principal Investigator	Airfoil	Test Date	Chord (in)	Run Number	Previous Identical Run	Velocity (kts)	Velocity (m/s)	Tt (°F)	Static Temperature (K)	A.O.A.	Corrected A.O.A.	LWC (g/m^3)	MVD (microns)	Spray Time (min)	Digitized Tracing Locations
Addy	GLC 305	Jul. 1995	36"	072595.01		175	90	30.56	268.30	6	4.5	0.54	20	6	36"
Addy	GLC 305	Jul. 1995	36"	072595.02R	072595.01	175	90	30.56	268.30	6	4.5	0.54	20	6	36"
Addy	GLC 305	Jul. 1995	36"	072595.03		175	90	30.56	268.30	6	4.5	0.54	20	22.5	36"
Addy	GLC 305	Jul. 1995	36"	072595.04		175	90	30.56	268.30	6	4.5	0.54	20	45	37"
Addy	GLC 305	Jul. 1995	36"	072695.01		175	90	28.76	267.30	6	4.5	0.405	20	4.4	36"
Addy	GLC 305	Jul. 1995	36"	072695.02		175	90	28.92	267.40	6	4.5	0.405	20	16.7	36"
Addy	GLC 305	Jul. 1995	36"	072695.03		175	90	28.92	267.40	6	4.5	0.405	20	33.3	36"
Addy	GLC 305	Jul. 1995	36"	072695.04		175	90	21.43	263.20	6	4.5	0.43	20	6	36"
Addy	GLC 305	Jul. 1995	36"	072695.05		175	90	21.43	263.20	6	4.5	0.43	20	22.5	36"
Addy	GLC 305	Jul. 1995	36"	072795.01		175	90	21.43	263.20	6	4.5	0.43	20	45	36"
Addy	GLC 305	Jul. 1995	36"	072795.02		175	90	21.43	263.20	6	4.5	0.60	15	6	36"
Addy	GLC 305	Jul. 1995	36"	072795.03		175	90	21.43	263.20	6	4.5	0.60	15	22.5	35"
Addy	GLC 305	Jul. 1995	36"	072795.04		175	90	21.2	263.10	6	4.5	0.60	15	45	36"
Addy	GLC 305	Jul. 1995	36"	072795.05		175	90	12.3	258.20	6	4.5	0.405	20	4.4	36"
Addy	GLC 305	Jul. 1995	36"	072795.06		175	90	12.3	258.20	6	4.5	0.405	20	33.3	36"
Addy	GLC 305	Jul. 1995	36"	072895.02		250	128.6	29.7	263.60	1.5	1.5	0.50	15	3.6	36" & 45"
Addy	GLC 305	Jul. 1995	36"	072895.03		250	128.6	29.7	263.60	1.5	1.5	0.50	15	7.2	36"
Addy	GLC 305	Jul. 1995	36"	072895.04		250	128.6	28.04	262.70	1.5	1.5	0.43	20	3	36"
Addy	GLC 305	Jul. 1995	36"	072895.05		250	128.6	28.04	262.70	1.5	1.5	0.43	20	6	36"
Addy	GLC 305	Jul. 1995	36"	072895.06		250	128.6	28.04	262.70	1.5	1.5	0.54	20	3	36"
Addy	GLC 305	Jul. 1995	36"	072895.07		250	128.6	28.04	262.70	1.5	1.5	0.54	20	6	36"
Addy	GLC 305	Jul. 1995	36"	072895.08		175	90	12.3	258.20	6	4.5	0.54	20	45	36"
Addy	GLC 305	Jul. 1995	36"	073195.01		250	128.6	18.86	257.60	1.5	1.5	0.31	20	2.9	36"
Addy	GLC 305	Jul. 1995	36"	073195.02		250	128.6	18.86	257.60	1.5	1.5	0.31	20	5.8	36"
Addy	GLC 305	Jul. 1995	36"	073195.03		175	90	12.3	258.20	6	4.5	0.405	20	16.7	36"
Addy	GLC 305	Jul. 1995	36"	073195.04		175	90	12.3	258.20	6	4.5	0.54	20	6	36"
Addy	GLC 305	Jul. 1995	36"	073195.05		175	90	12.3	258.20	6	4.5	0.54	20	22.5	36"
Addy	GLC 305	Jul. 1995	36"	080195.03		175	90	6.8	255.10	6	4.5	0.535	20	6	36"
Addy	GLC 305	Jul. 1995	36"	080195.04R	080195.03	175	90	6.8	255.10	6	4.5	0.535	20	6	36"
Addy	GLC 305	Jul. 1995	36"	080195.05		175	90	6.8	255.10	4	3.5	0.535	40	6	36"
Addy	GLC 305	Jul. 1995	36"	080195.06		212	109.1	6.8	253.20	4	3.5	0.535	40	6	36"
Addy	GLC 305	Jul. 1995	36"	080195.07		212	109.1	6.8	253.20	4	3.5	0.54	20	6	36"
Addy	GLC 305	Jul. 1995	36"	080195.08		175	90	6.8	255.10	6	4.5	0.535	40	6	36"
Addy	GLC 305	Jul. 1995	36"	080195.09		175	90	6.8	255.10	6	4.5	0.535	40	4.2	36"
Addy	GLC 305	Jul. 1995	36"	080295.01		175	90	30.56	268.30	6	4.5	0.54	20	12	36"
Addy	GLC 305	Jul. 1995	36"	080295.02		175	90	30.56	268.30	4	3.5	0.54	20	22.5	36"
Addy	GLC 305	Jul. 1995	36"	080295.04		175	90	30.56	268.30	4	3.5	0.54	20	6	36"
Addy	GLC 305	Jul. 1995	36"	080295.05		212	109.1	24.94	263.30	4	3.5	0.43	20	22.5	36"
Addy	GLC 305	Jul. 1995	36"	080295.06		175	90	30.56	268.30	4	3.5	0.54	20	22.5	36"
Addy	GLC 305	Jul. 1995	36"	080395.01		250	128.6	30.8	264.20	1.5	1.5	0.75	15	10	36"
Addy	GLC 305	Jul. 1995	36"	080395.02		250	128.6	30.8	264.20	1.5	1.5	1.25	20	5.4	26" & 45"
Addy	GLC 305	Jul. 1995	36"	080395.04		175	90	24.17	264.80	6	4.5	1.60	20	8.4	36"
Addy	GLC 305	Jul. 1995	36"	080395.05		250	128.6	18.77	257.50	1.5	1.5	0.75	15	10	36"
Addy	GLC 305	Jul. 1995	36"	080395.06		250	128.6	18.77	257.50	1.5	1.5	1.25	20	5.4	36"
Addy	GLC 305	Jul. 1995	36"	080395.07		175	90	12.3	258.20	6	4.5	1.60	20	8.4	36"
Addy	GLC 305	Jul. 1995	36"	080495.01		175	90	-0.5	241.30	6	4.5	0.83	160	6	36"
Addy	GLC 305	Jul. 1995	36"	080495.02		175	90	-0.5	241.30	4	3.5	0.83	160	6	36"
Addy	GLC 305	Jul. 1995	36"	080495.04		175	90	12.3	258.10	4	3.5	0.83	160	20	36"
Addy	GLC 305	Jul. 1995	36"	080495.05		175	90	30.56	268.30	6	4.5	0.83	160	20	36"
Addy	GLC 305	Jul. 1995	36"	080495.06		175	90	30.56	268.30	6	4.5	0.54	20	22.5	36"

GLC 305 Test Conditions

Addy	GLC 305	Mar. 1996	36"	201		175	90	30.6	268.05	6	4.5	0.405	20	4.4	30", 36" & 42"
Addy	GLC 305	Mar. 1996	36"	202		175	90	30.6	268.05	6	4.5	0.540	20	2	30", 36" & 42"
Addy	GLC 305	Mar. 1996	36"	202r	202	175	90	30.6	268.05	6	4.5	0.540	20	2	30", 36" & 42"
Addy	GLC 305	Mar. 1996	36"	202m	202	175	90	30.6	268.05	6	4.5	0.540	20	2	30"
Addy	GLC 305	Mar. 1996	36"	203		175	90	30.6	268.05	6	4.5	0.540	20	6	30", 36" & 42"
Addy	GLC 305	Mar. 1996	36"	204		175	90	30.6	268.05	6	4.5	0.540	20	22.5	30", 36" & 42"
Addy	GLC 305	Mar. 1996	36"	206		175	90	21.4	262.94	6	4.5	0.535	20	4.2	30", 36" & 42"
Addy	GLC 305	Mar. 1996	36"	207		175	90	21.4	262.94	6	4.5	0.430	20	2	30", 36" & 42"
Addy	GLC 305	Mar. 1996	36"	208		175	90	21.4	262.94	6	4.5	0.430	20	6	30", 36" & 42"
Addy	GLC 305	Mar. 1996	36"	209		175	90	21.4	262.94	6	4.5	0.430	20	22.5	30", 36" & 42"
Addy	GLC 305	Mar. 1996	36"	210		175	90	12.3	257.88	6	4.5	0.405	20	2	30", 36" & 42"
Addy	GLC 305	Mar. 1996	36"	211		175	90	12.3	257.88	6	4.5	0.405	20	4.4	30", 36" & 42"
Addy	GLC 305	Mar. 1996	36"	212		175	90	12.3	257.88	6	4.5	0.405	20	16.7	30"
Addy	GLC 305	Mar. 1996	36"	213		175	90	20.8	262.61	6	4.5	0.600	15	2	30", 36" & 42"
Addy	GLC 305	Mar. 1996	36"	214		175	90	20.8	262.61	6	4.5	0.600	15	6	30", 36" & 42"
Addy	GLC 305	Mar. 1996	36"	221		250	128.6	28.2	262.50	1.5	1.5	0.430	20	3	30", 36" & 42"
Addy	GLC 305	Mar. 1996	36"	222		250	128.6	28.2	262.50	1.5	1.5	0.430	20	6	30", 36" & 42"
Addy	GLC 305	Mar. 1996	36"	223		250	128.6	28.4	262.62	1.5	1.5	0.600	15	3.6	30", 36" & 42"
Addy	GLC 305	Mar. 1996	36"	224		250	128.6	28.4	262.62	1.5	1.5	0.600	15	7.2	30", 36" & 42"
Addy	GLC 305	Mar. 1996	36"	226		250	128.6	9.85	252.31	1.5	1.5	0.410	40	2	36"
Addy	GLC 305	Mar. 1996	36"	231		175	90	30	267.72	4	3.5	0.540	20	2	36"
Addy	GLC 305	Mar. 1996	36"	232		175	90	30	267.72	4	3.5	0.540	20	6	36"
Addy	GLC 305	Mar. 1996	36"	233		175	90	20.8	262.61	4	3.5	0.600	15	2	36"
Addy	GLC 305	Mar. 1996	36"	234		175	90	20.8	262.61	4	3.5	0.600	15	6	36"
Addy	GLC 305	Mar. 1996	36"	236		175	90	20.8	262.61	4	3.5	0.535	40	4.2	36"
Addy	GLC 305	Mar. 1996	36"	238		175	90	12.3	257.88	4	3.5	0.405	20	4.4	36"
Chen	GLC 305	Mar. 1998	24"	724.02		173.8	89.4	21.2	263.15	0	0	1.30	35	2	36"
Chen	GLC 305	Mar. 1998	24"	724.02D	724.02	173.8	89.4	21.2	263.15	0	0	1.30	35	2	36"
Chen	GLC 305	Mar. 1998	24"	724.03		173.8	89.4	21.2	263.15	0	0	1.30	35	4	36"
Chen	GLC 305	Mar. 1998	24"	724.03D	724.03	173.8	89.4	21.2	263.15	0	0	1.30	35	4	36"
Chen	GLC 305	Mar. 1998	24"	824.02		173.8	89.4	8.6	256.15	0	0	1.30	35	2	36"
Chen	GLC 305	Mar. 1998	24"	824.02D	824.02	173.8	89.4	8.6	256.15	0	0	1.30	35	2	36"
Chen	GLC 305	Mar. 1998	24"	824.03		173.8	89.4	8.6	256.15	0	0	1.30	35	4	36"
Chen	GLC 305	Mar. 1998	24"	824.03D	824.03	173.8	89.4	8.6	256.15	0	0	1.30	35	4	36"

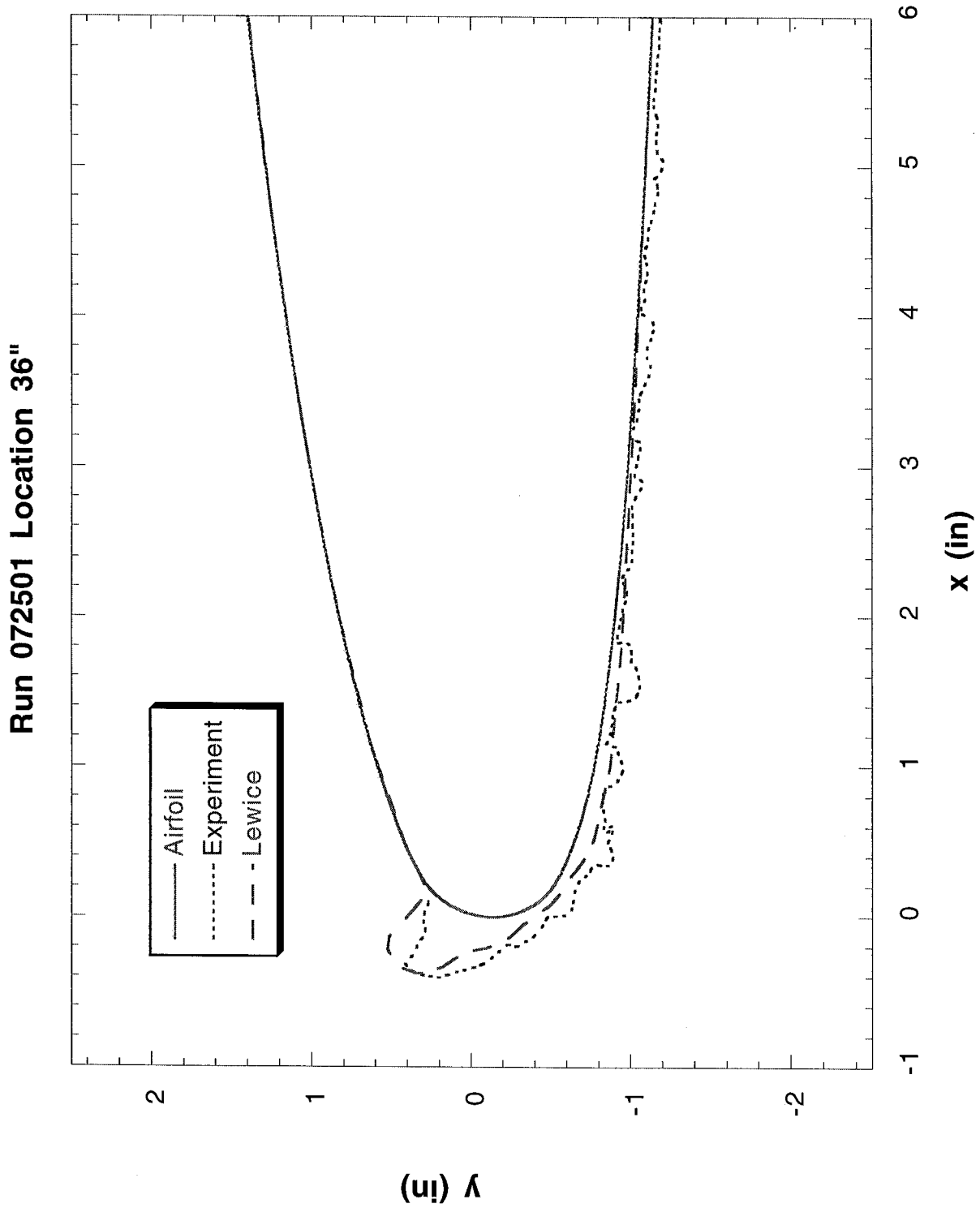
Run 072501 Location 36"
Airfoil
Experiment
Lewice
y (in)
x (in)
2
1
0
-1
-2
-1
0
1
2
3
4
5
6

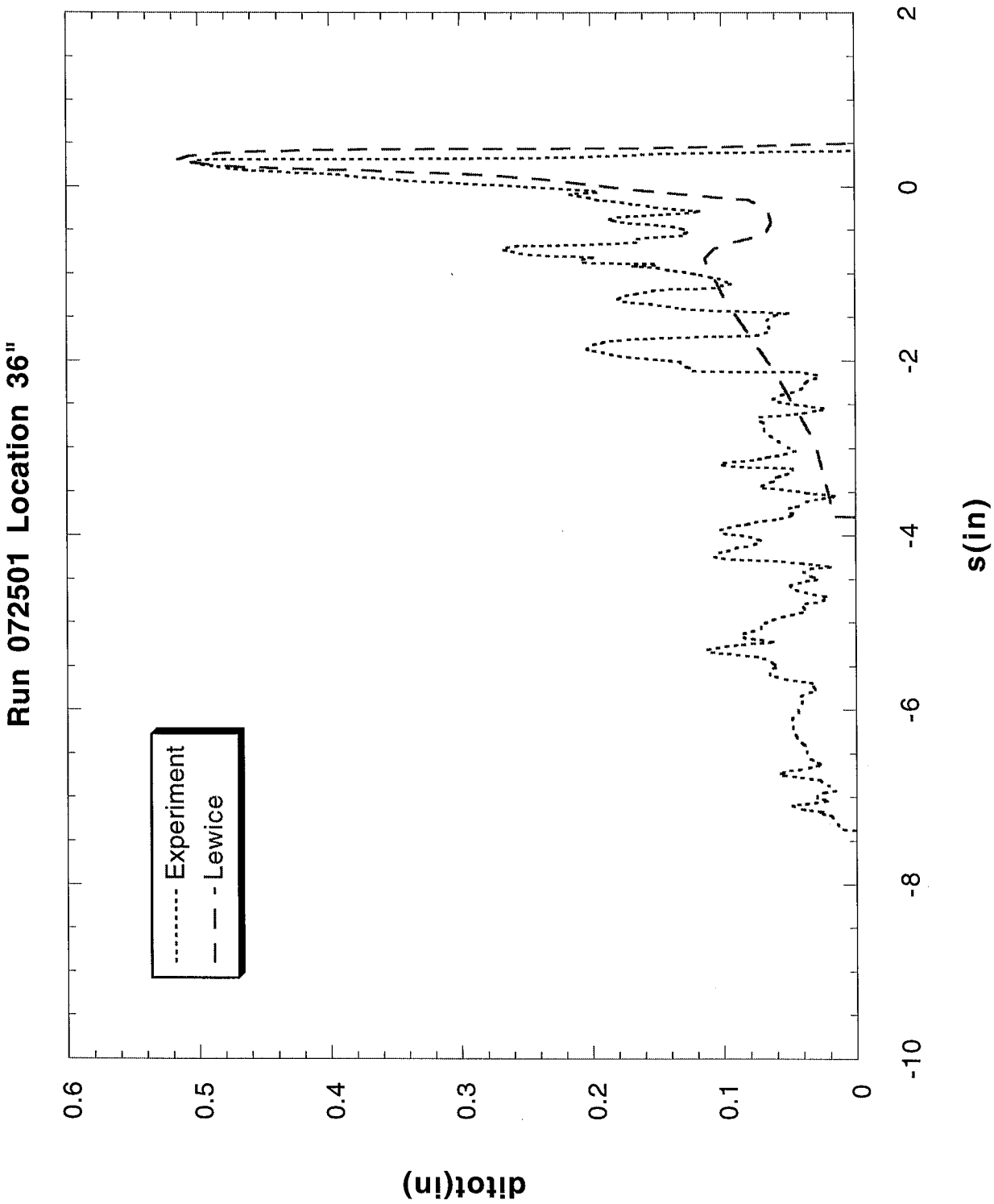
Run 072501 Location 36"
Experiment
Lewice
dltot(in)
s(in)
0.6
0.5
0.4
0.3
0.2
0.1
0
2
0
-2
-4
-6
-8
-10

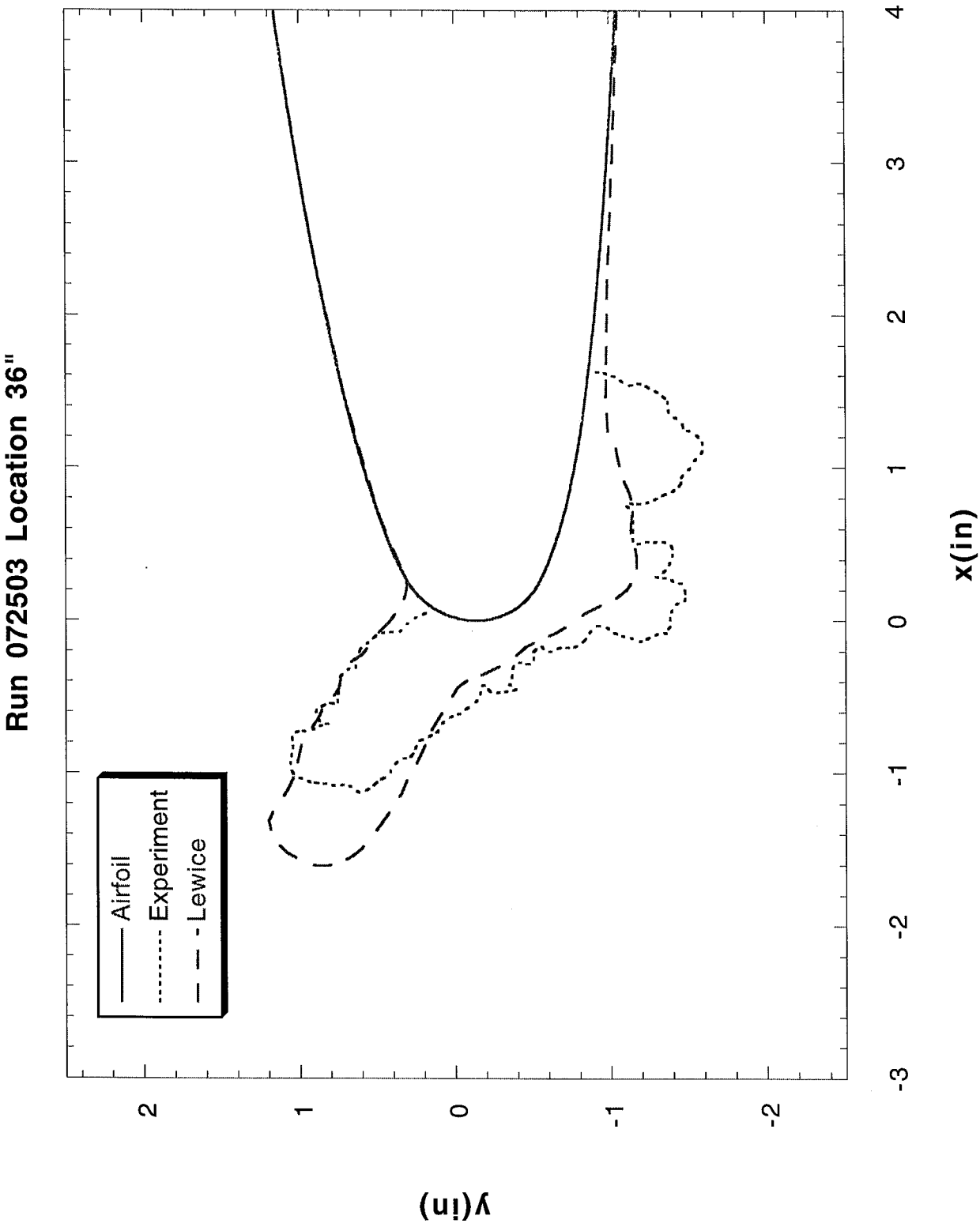
Run 072503 Location 36"
Airfoil
Experiment
Lewice
y(in)
x(in)
2
1
0
-1
-2
-3
-2
-1
0
1
2
3
4

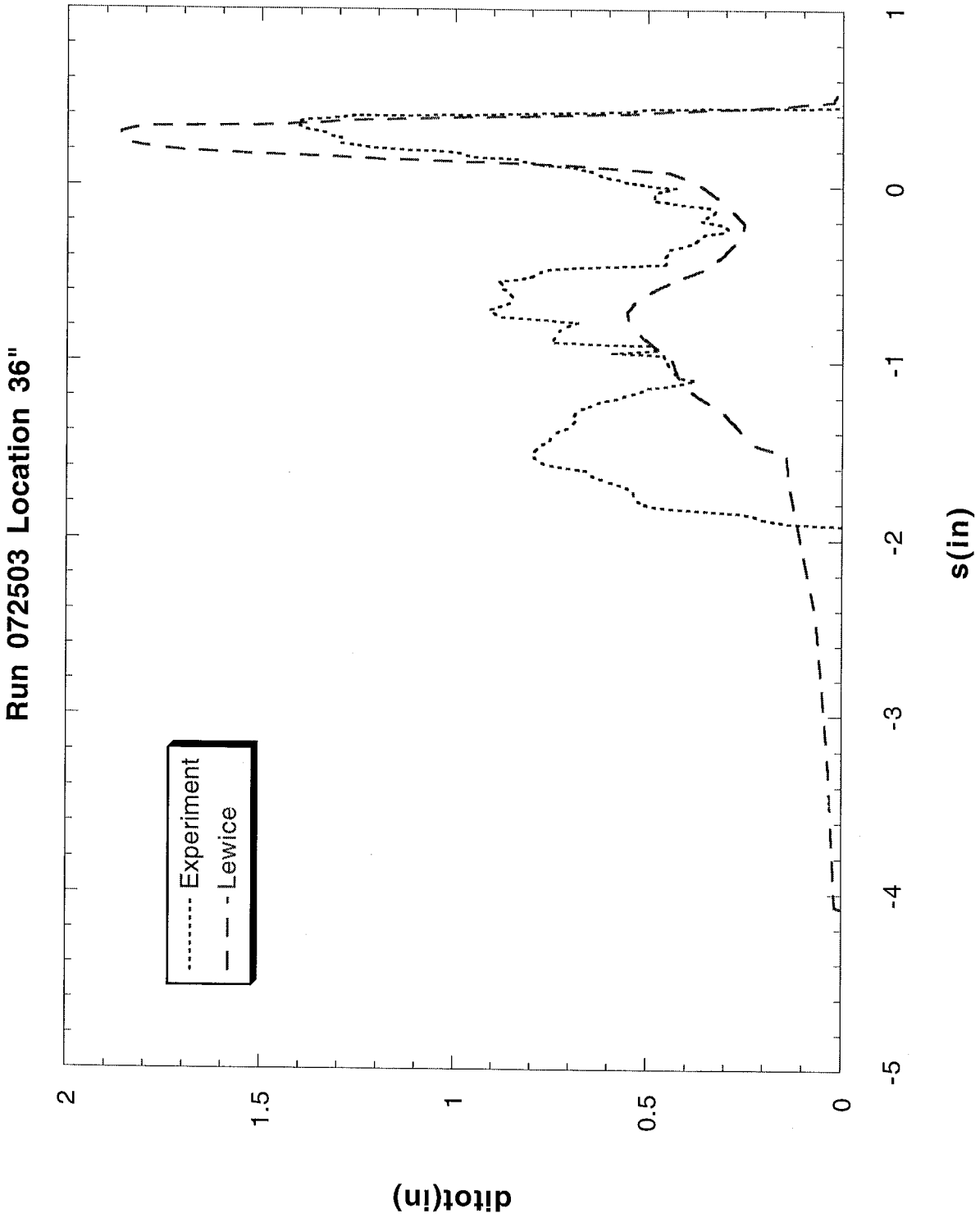
Run 072503 Location 36"
Experiment
Lewice
dltot(in)
s(in)
2
1.5
1
0.5
0
1
0
-1
-2
-3
-4
-5

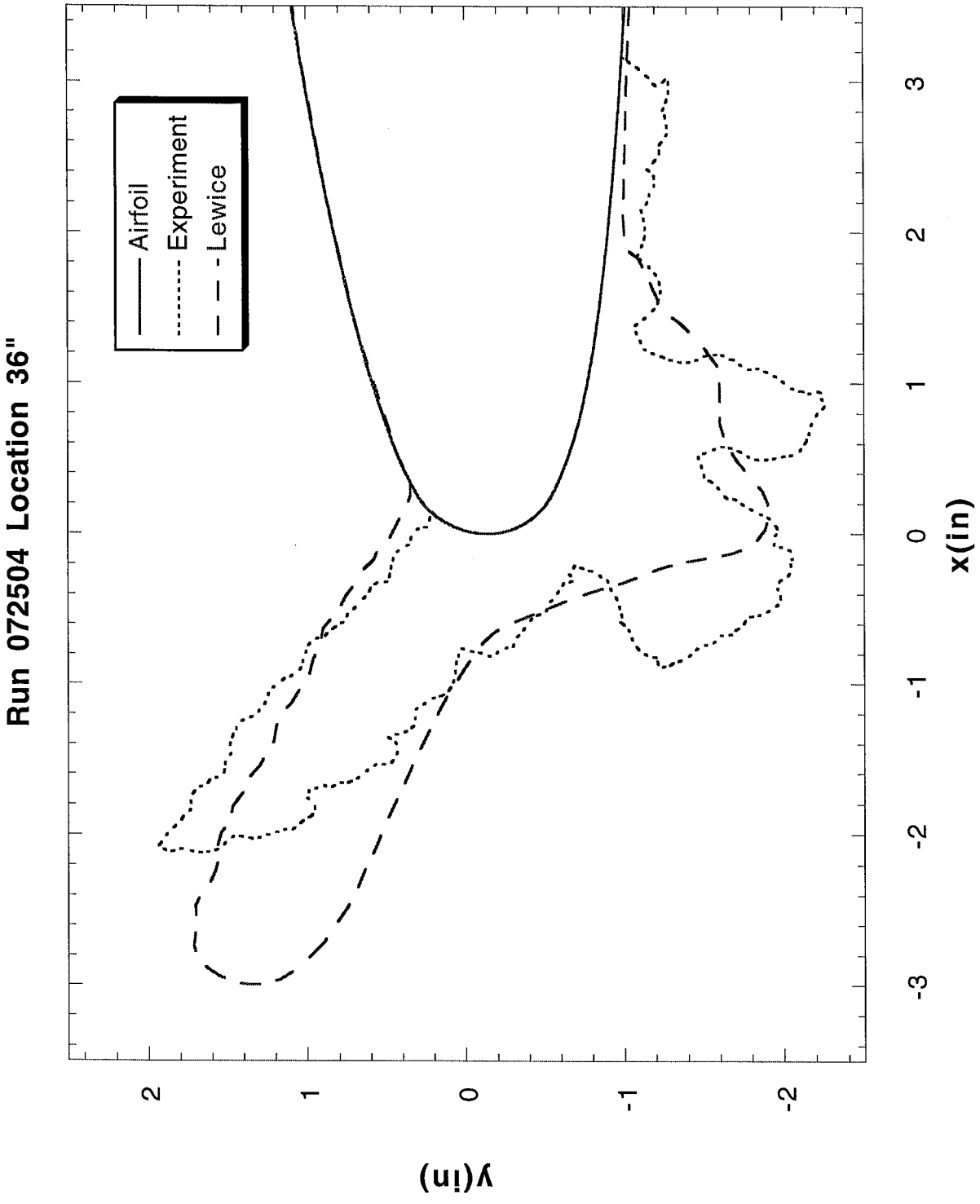
Run 072504 Location 36"
Airfoil
Experiment
Lewice
y(in)
x(in)
2
1
0
-1
-2
-3
-2
-1
0
1
2
3

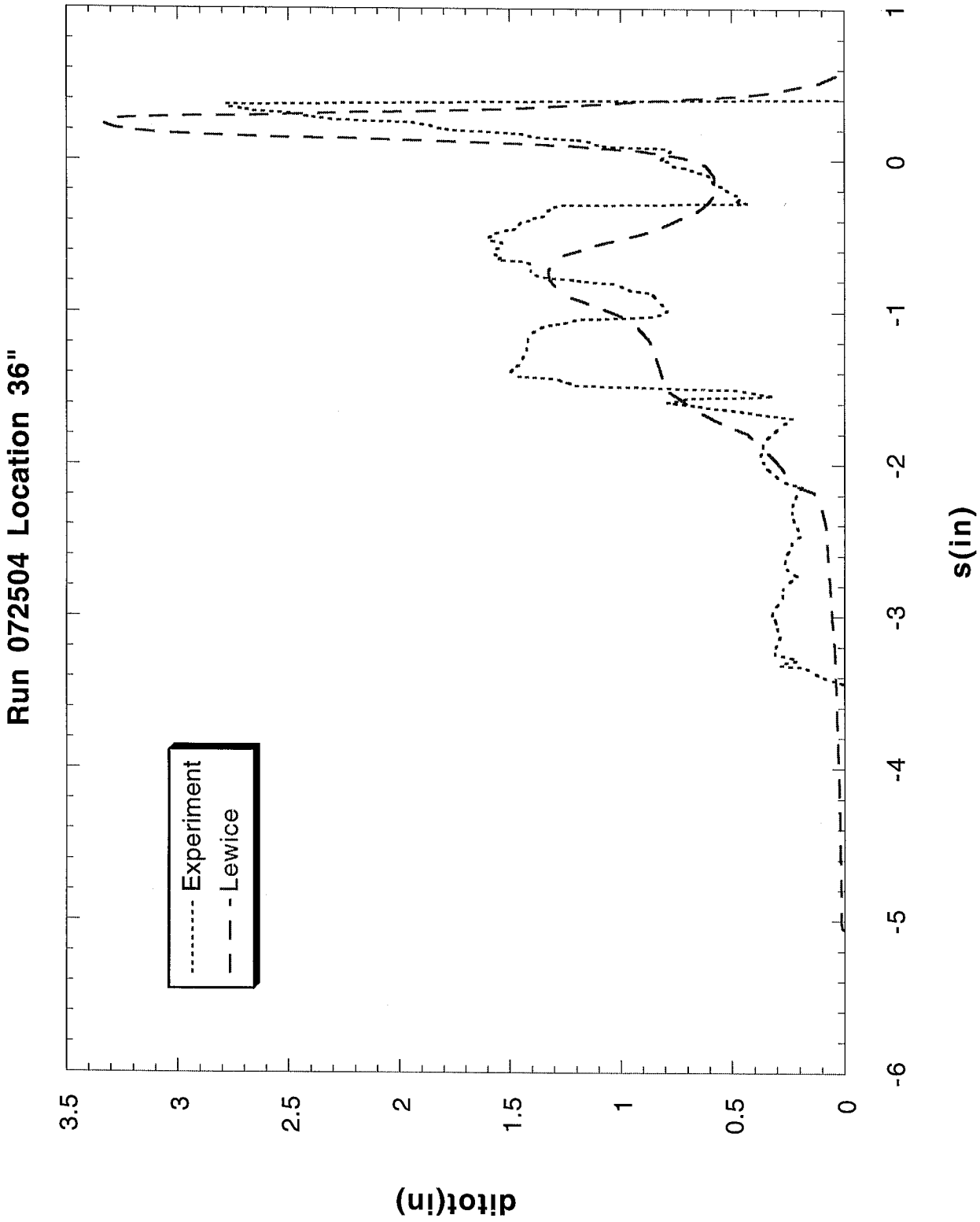
Run 072504 Location 36"
Experiment
Lewice
dltot(in)
s(in)
3.5
3
2.5
2
1.5
1
0.5
0
-6
-5
-4
-3
-2
-1
0
1

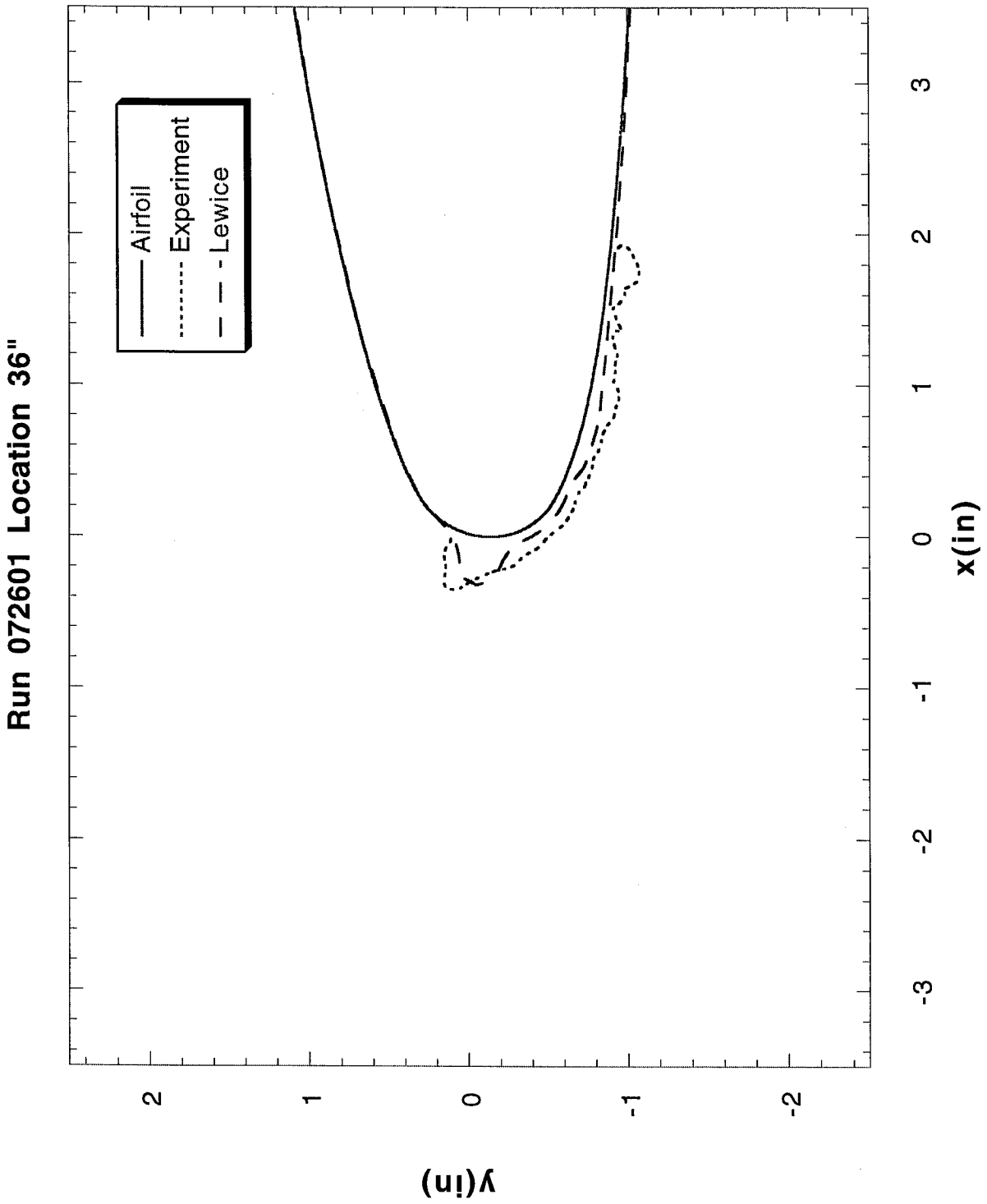
Run 072601 Location 36"
Airfoil
Experiment
Lewice
y(in)
x(in)
2
1
0
-1
-2
-3
-2
-1
0
1
2
3

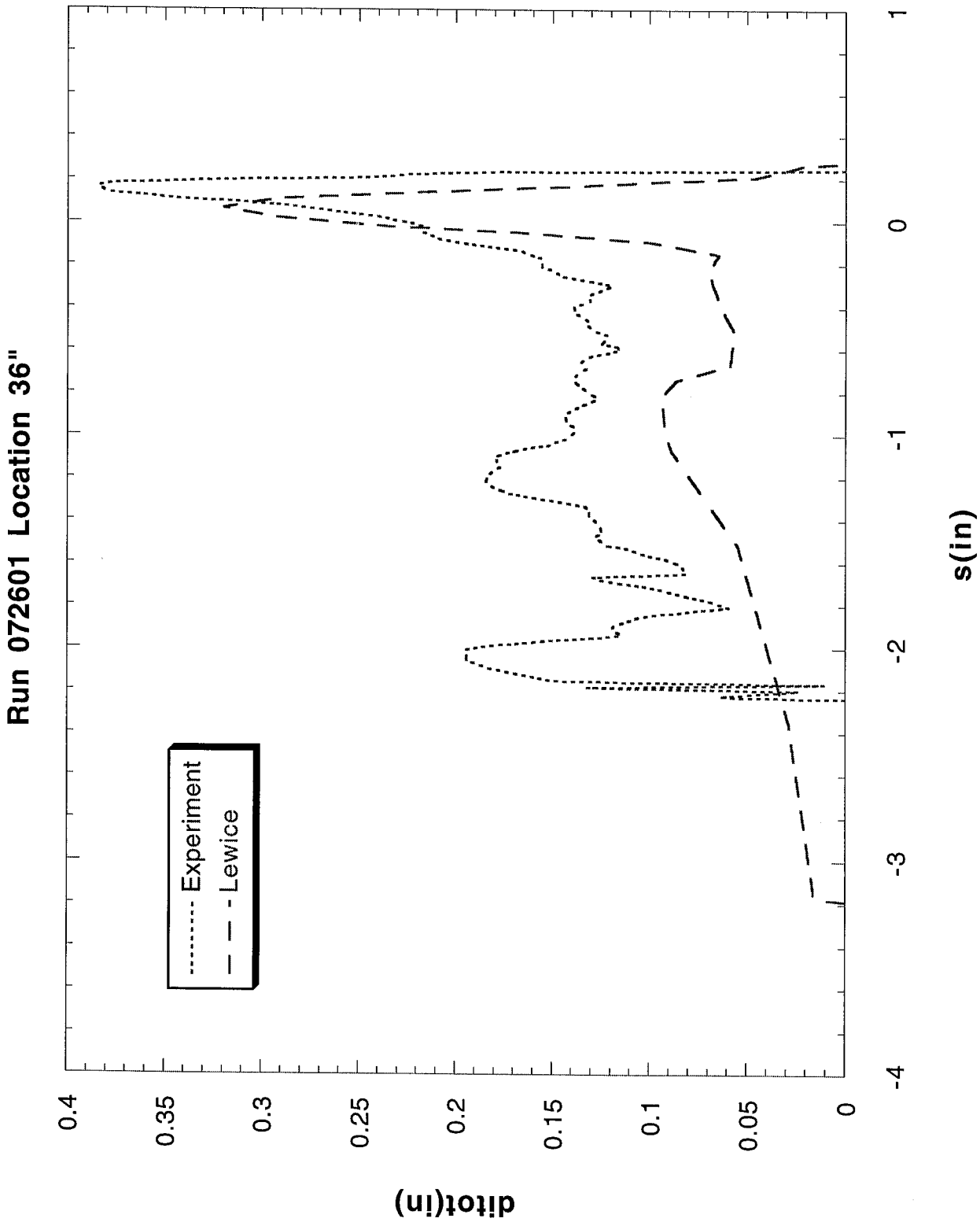
Run 072601 Location 36"
Experiment
Lewice
dltot(in)
s(in)
0.4
0.35
0.3
0.25
0.2
0.15
0.1
0.05
0
-4
-3
-2
-1
0
1

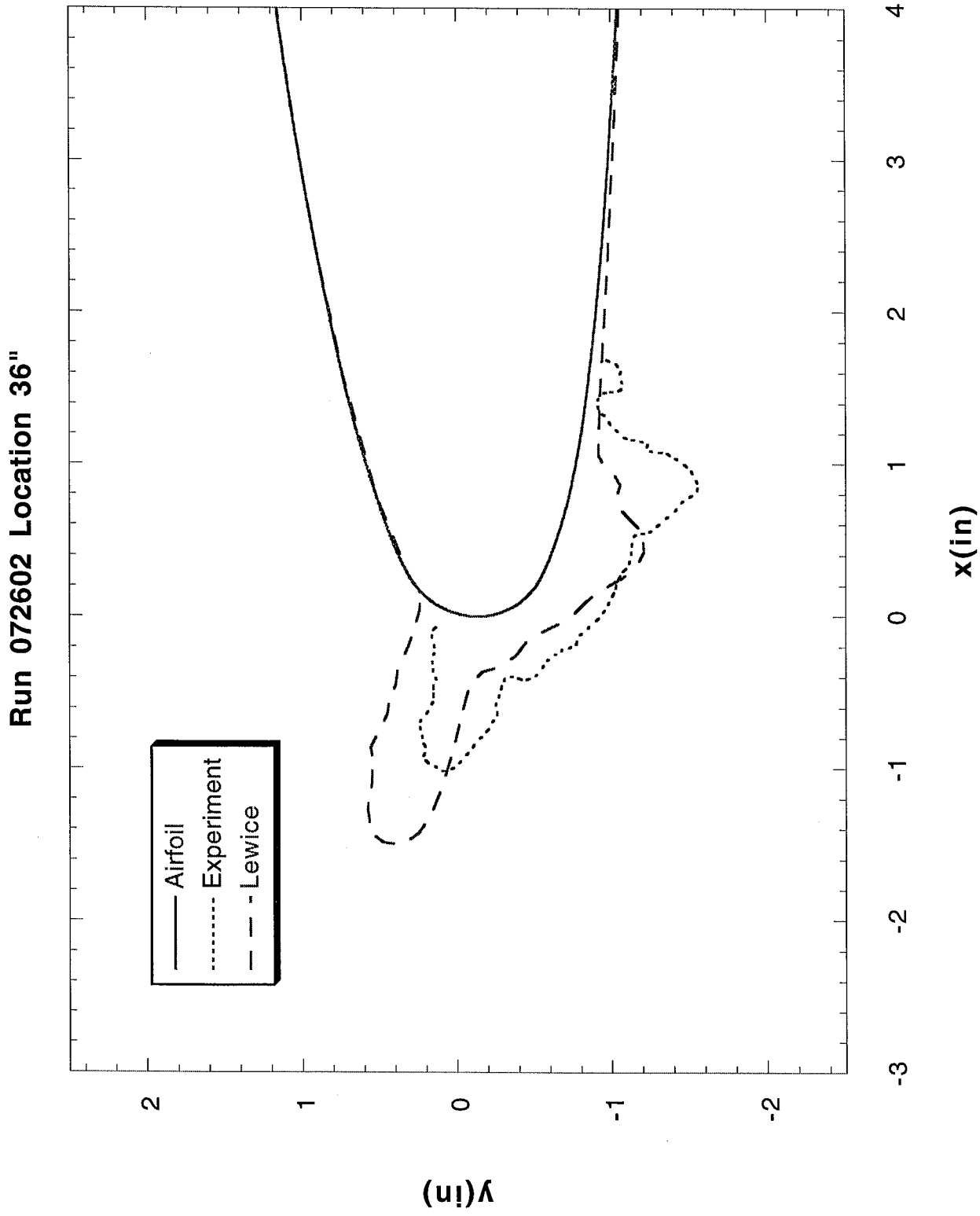
Run 072602 Location 36"
Airfoil
Experiment
Lewice
y(in)
x(in)
2
1
0
-1
-2
-3
-2
-1
0
1
2
3
4

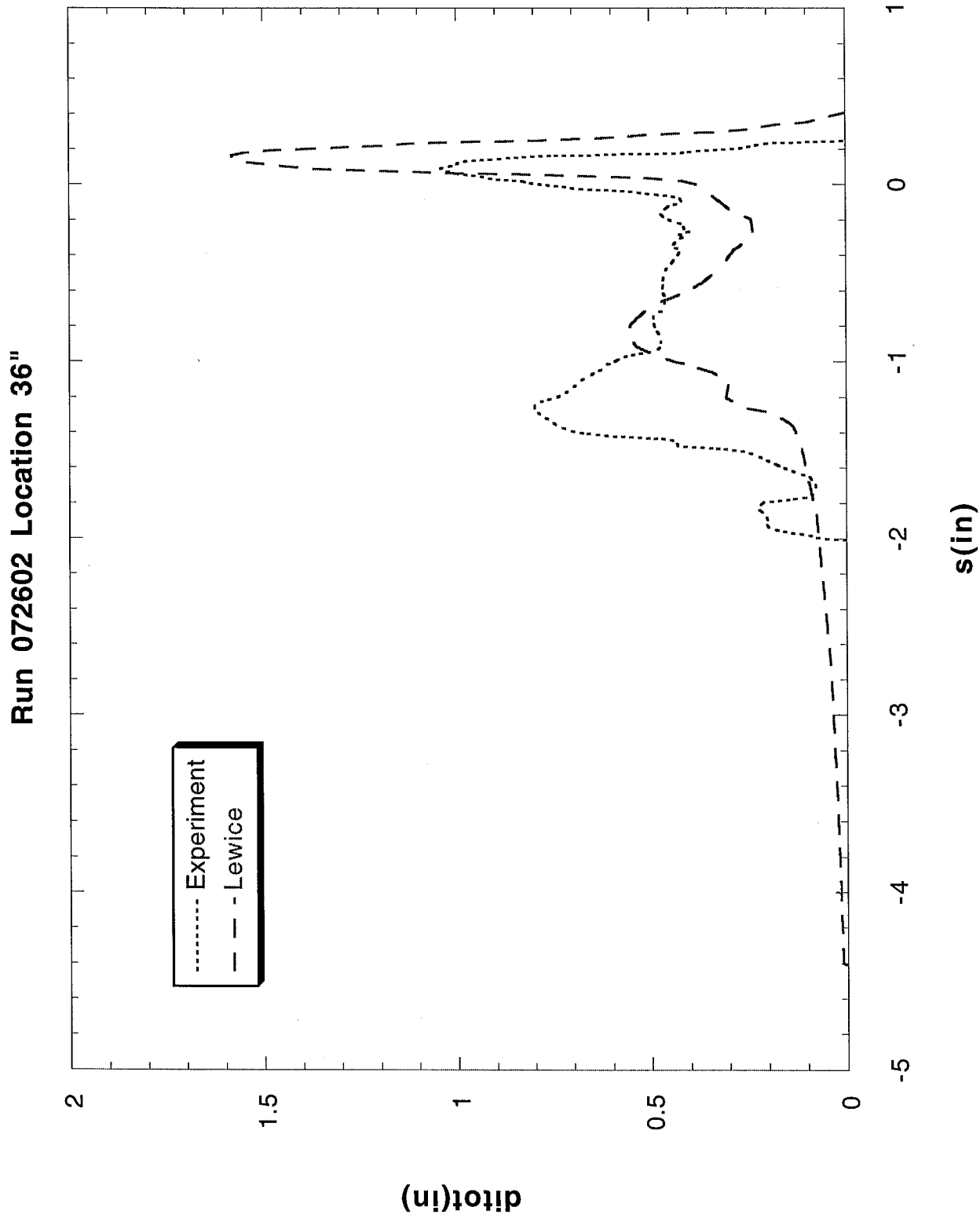
Run 072602 Location 36"
Experiment
Lewice
dltot(in)
s(in)
2
1.5
1
0.5
0
1
0
-1
-2
-3
-4
-5

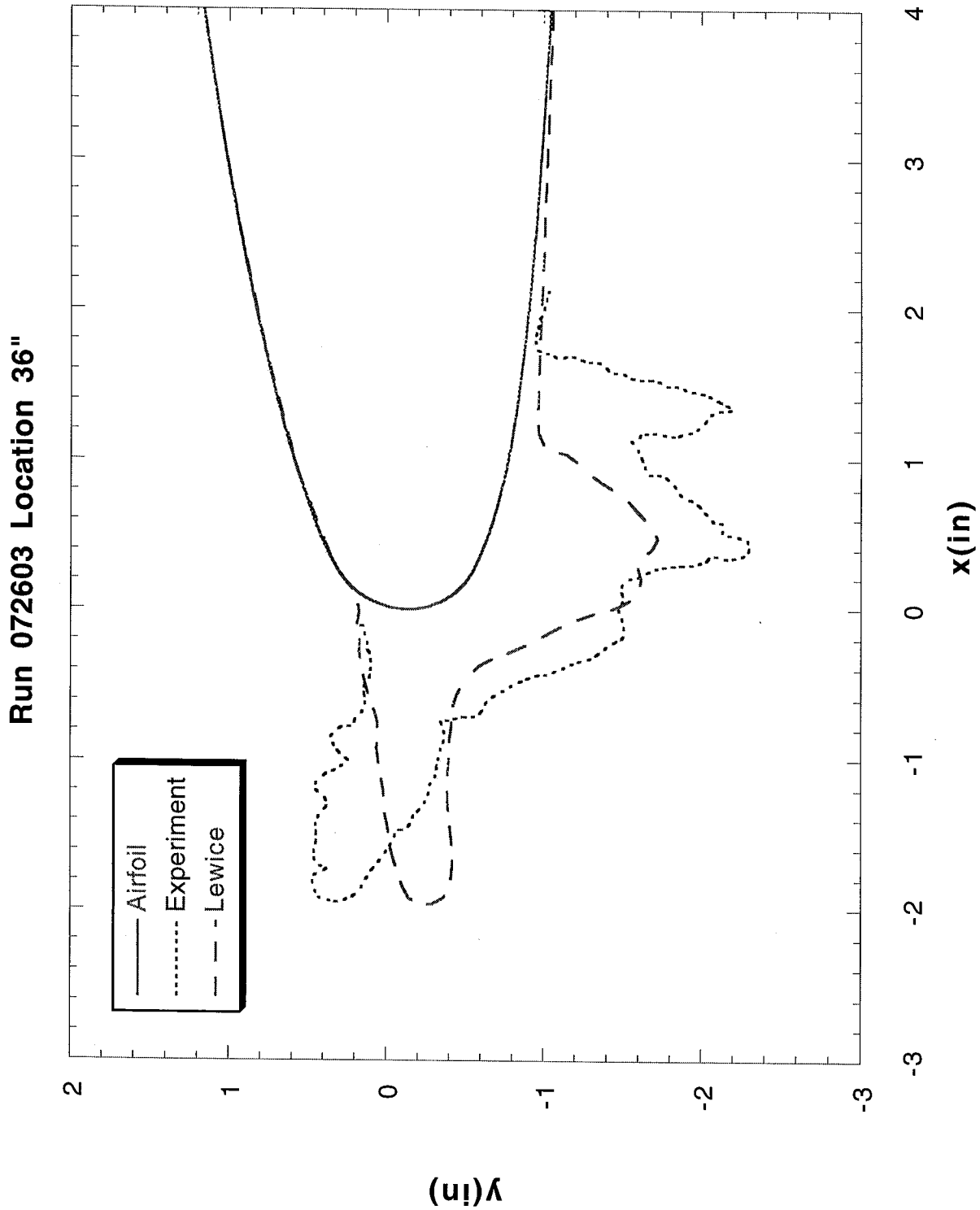
Run 072603 Location 36"
Airfoil
Experiment
- Lewice
y(in)
x(in)
2
1
0
-1
-2
-3
4
3
2
1
0
-1
-2
-3

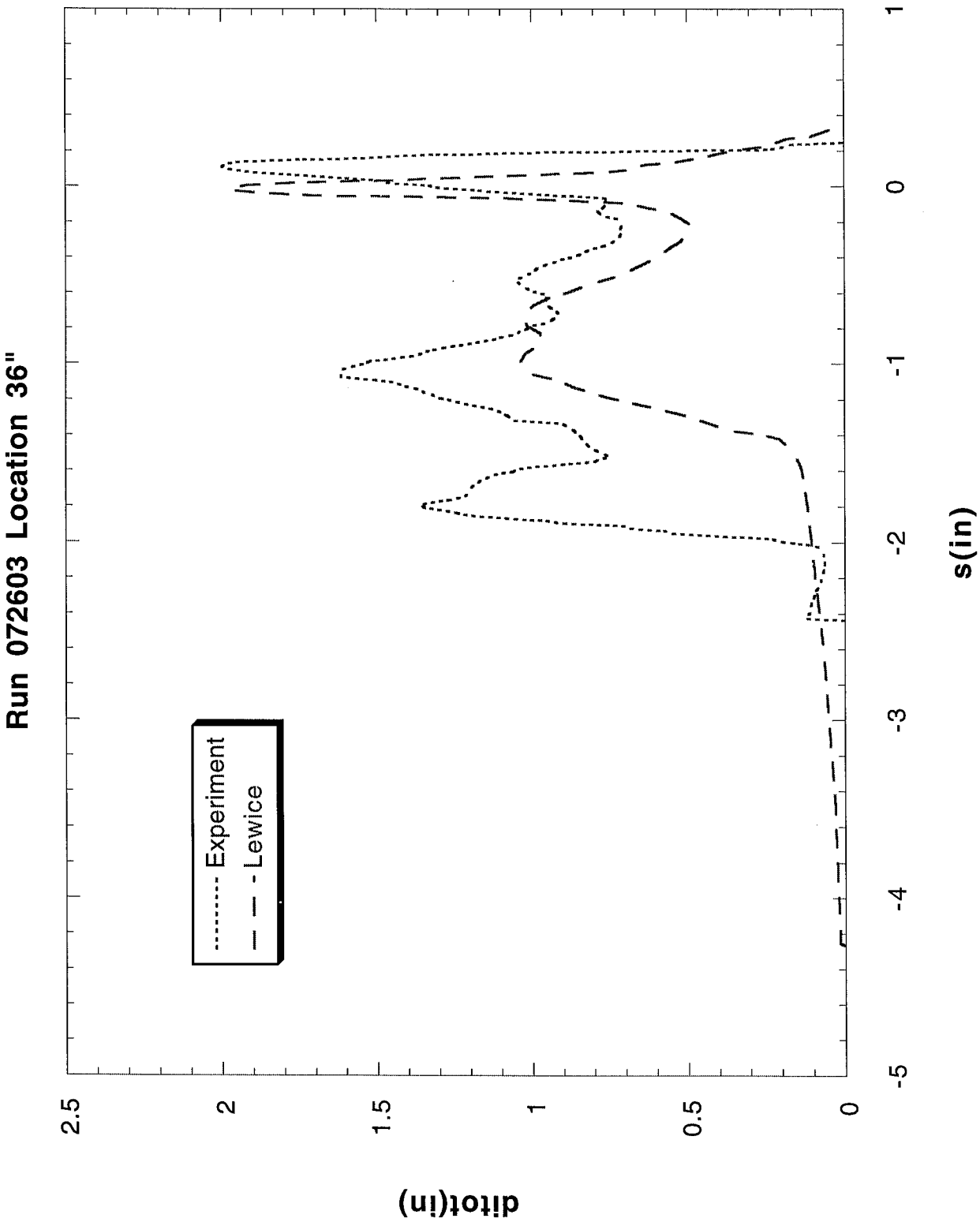
Run 072603 Location 36"
Experiment
Lewice
ditot(in)
s(in)
2.5
2
1.5
1
0.5
0
-5
-4
-3
-2
-1
0
1

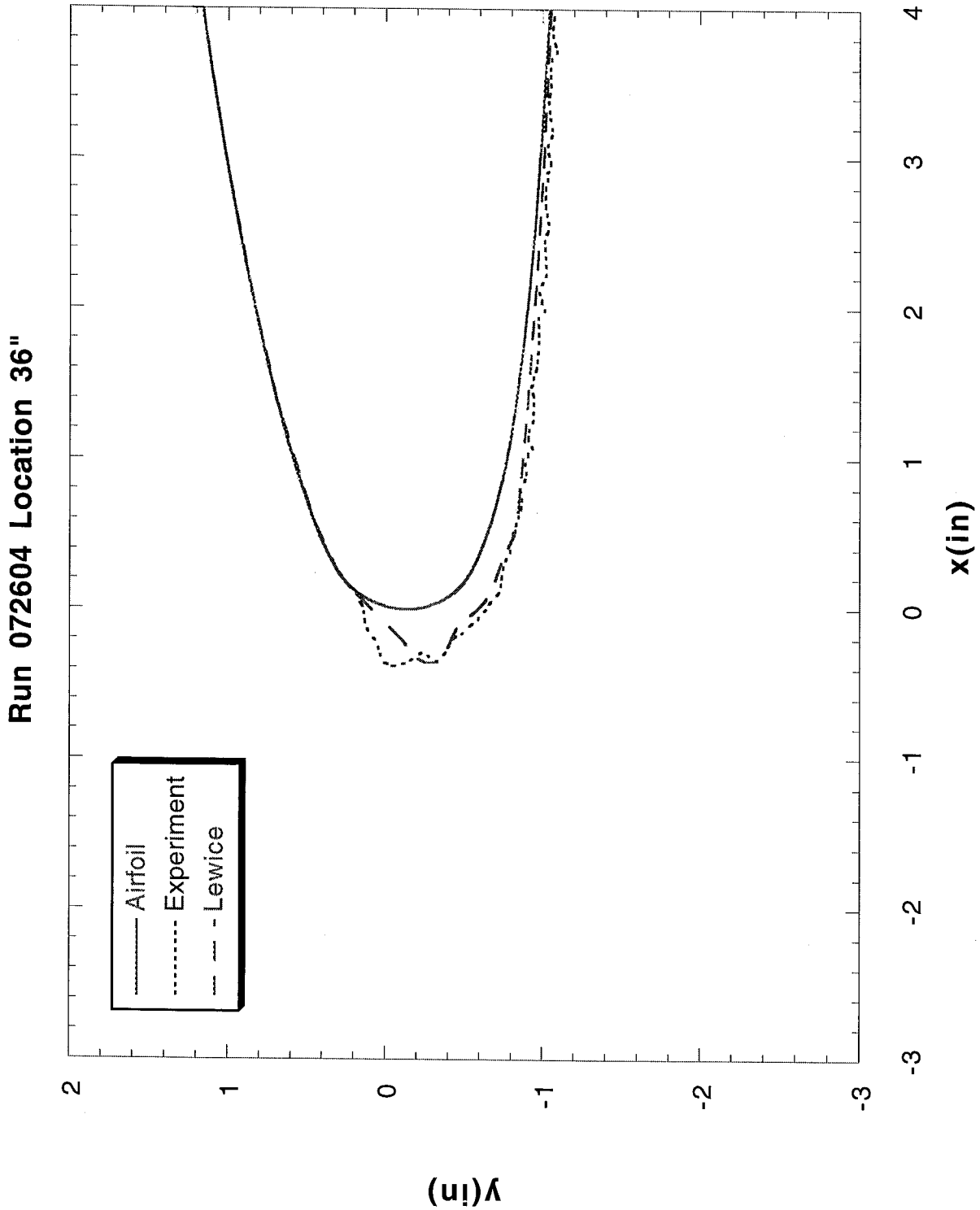
Run 072604 Location 36"
Airfoil
Experiment
Lewice
y(in)
x(in)
2
1
0
-1
-2
-3
4
3
2
1
0
-1
-2
-3

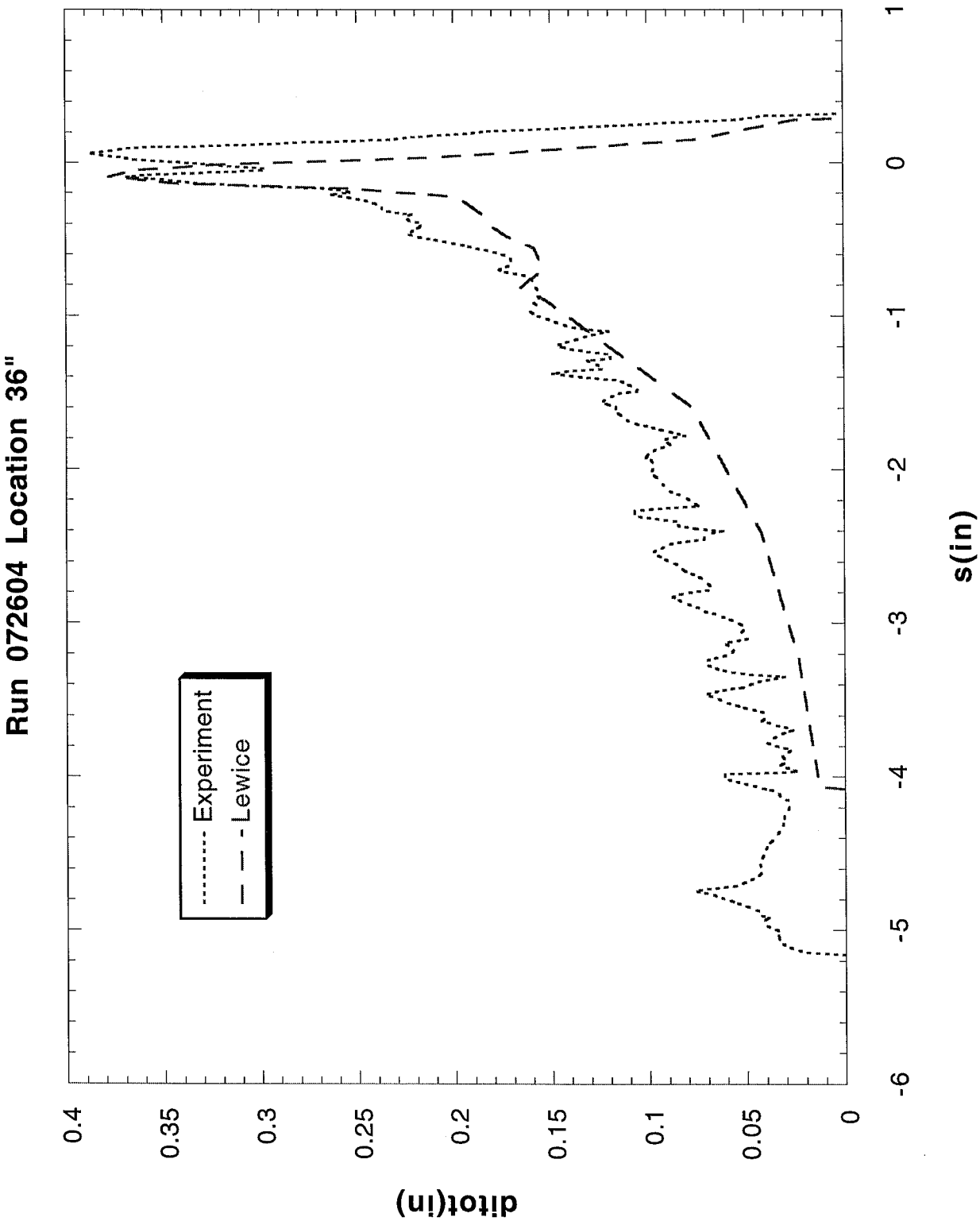
Run 072604 Location 36"
Experiment
Lewice
ditot(in)
s(in)
0.4
0.35
0.3
0.25
0.2
0.15
0.1
0.05
0
1
0
-1
-2
-3
-4
-5
-6

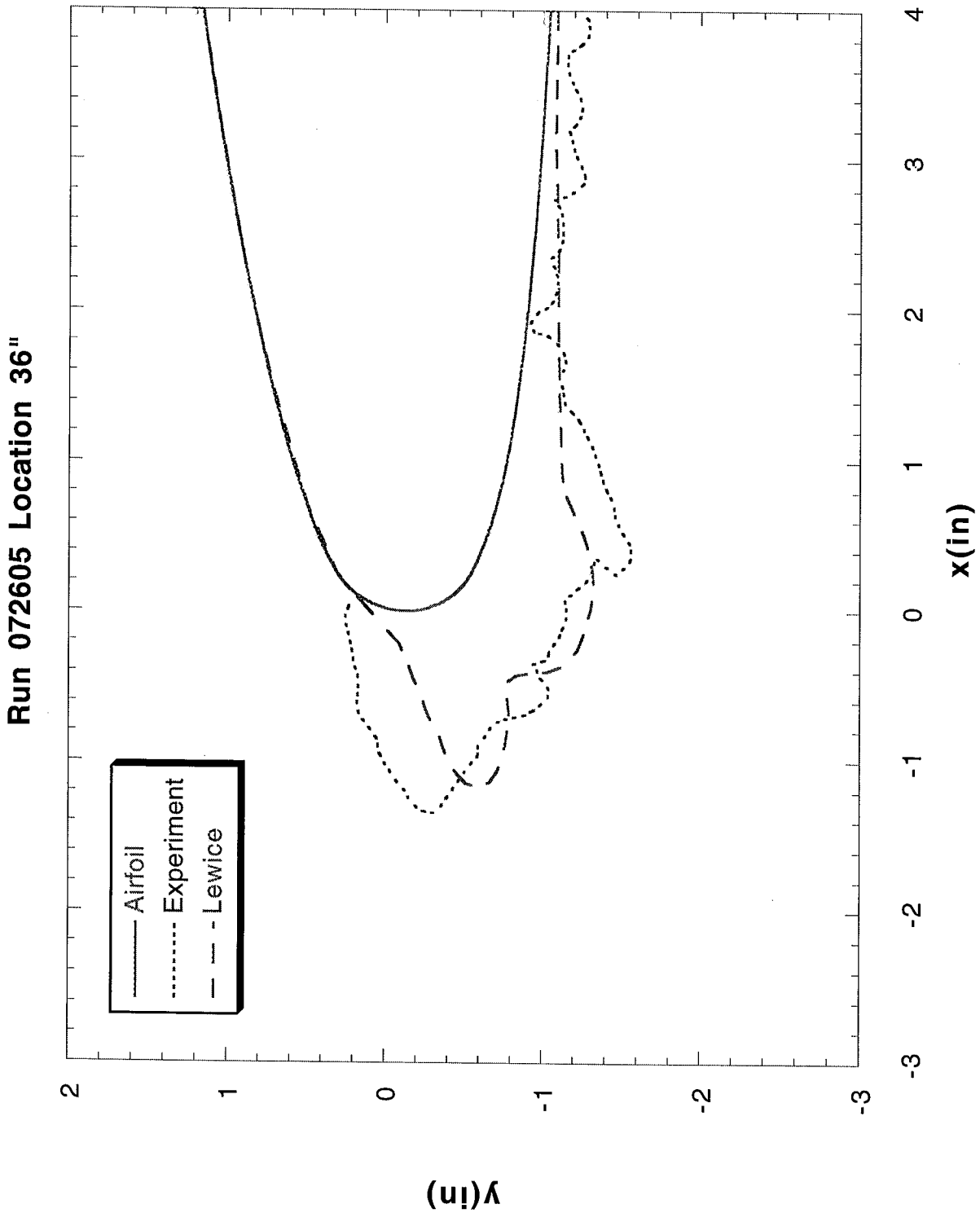
Run 072605 Location 36"
Airfoil
Experiment
Lewice
y(in)
x(in)
2
1
0
-1
-2
-3
-3
-2
-1
0
1
2
3
4

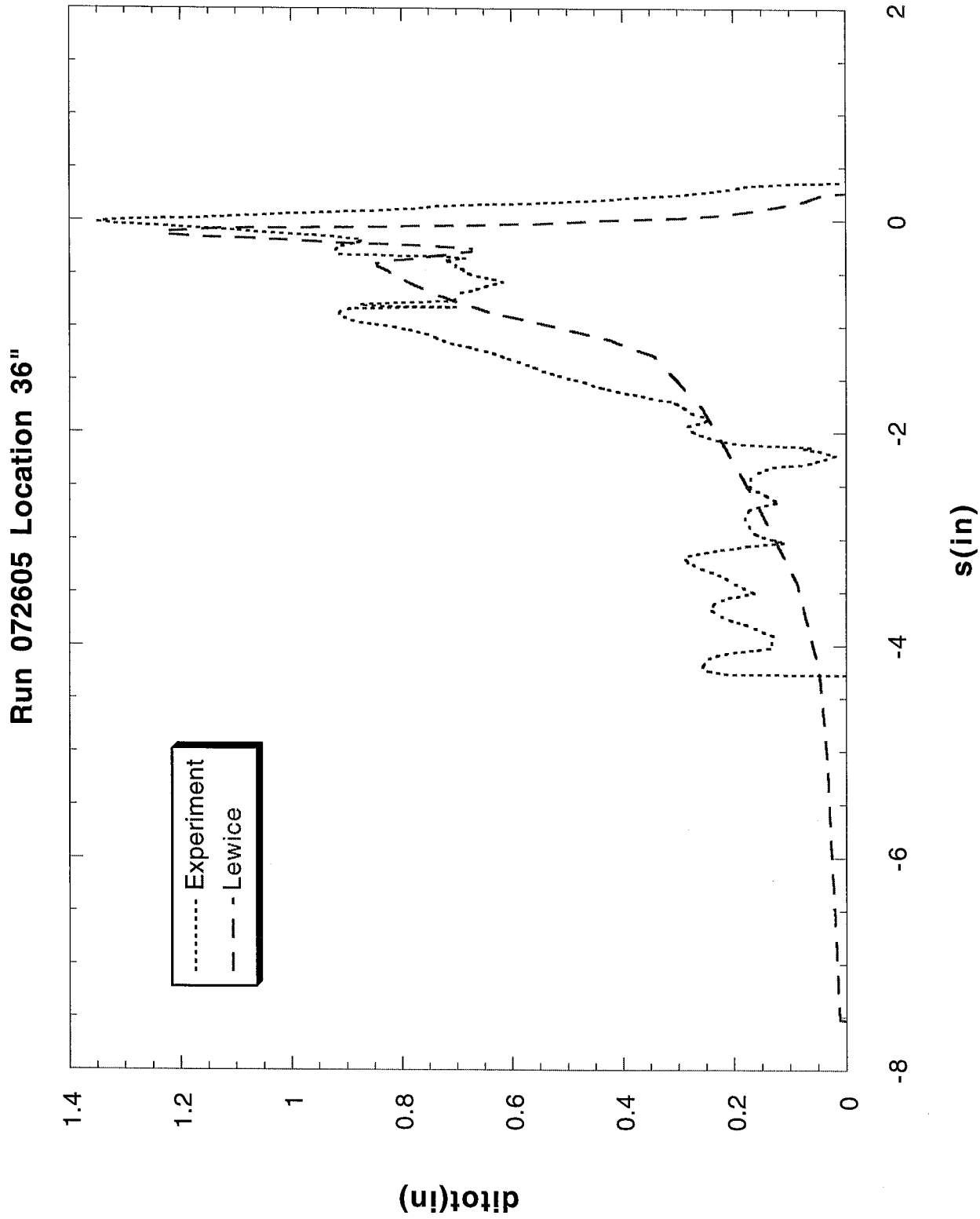
Run 072605 Location 36"
Experiment
Lewice
dltot(in)
s(in)
1.4
1.2
1
0.8
0.6
0.4
0.2
0
2
0
-2
-4
-6
-8

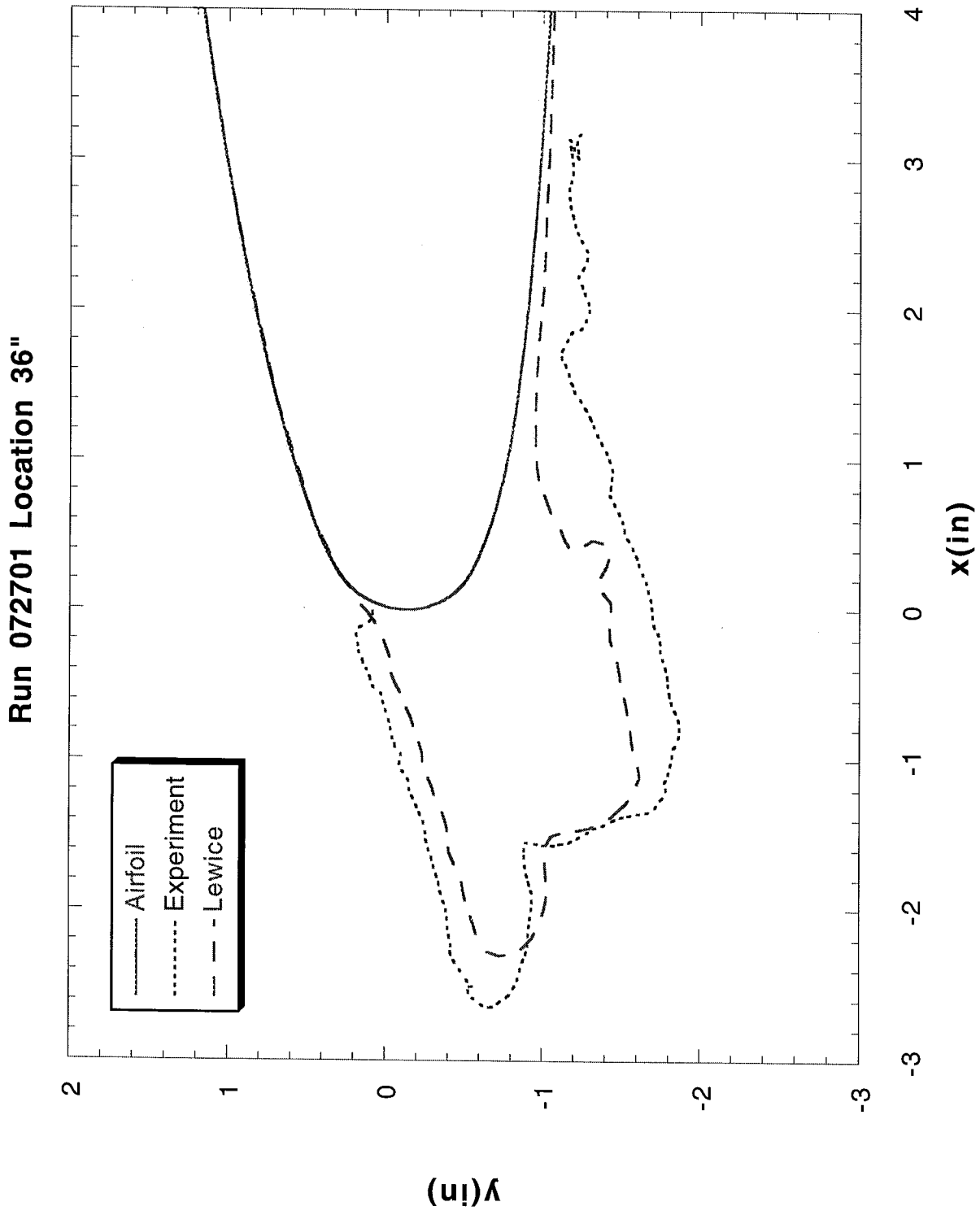
Run 072701 Location 36"
Airfoil
Experiment
- Lewice
y(in)
x(in)
2
1
0
-1
-2
-3
4
3
2
1
0
-1
-2
-3

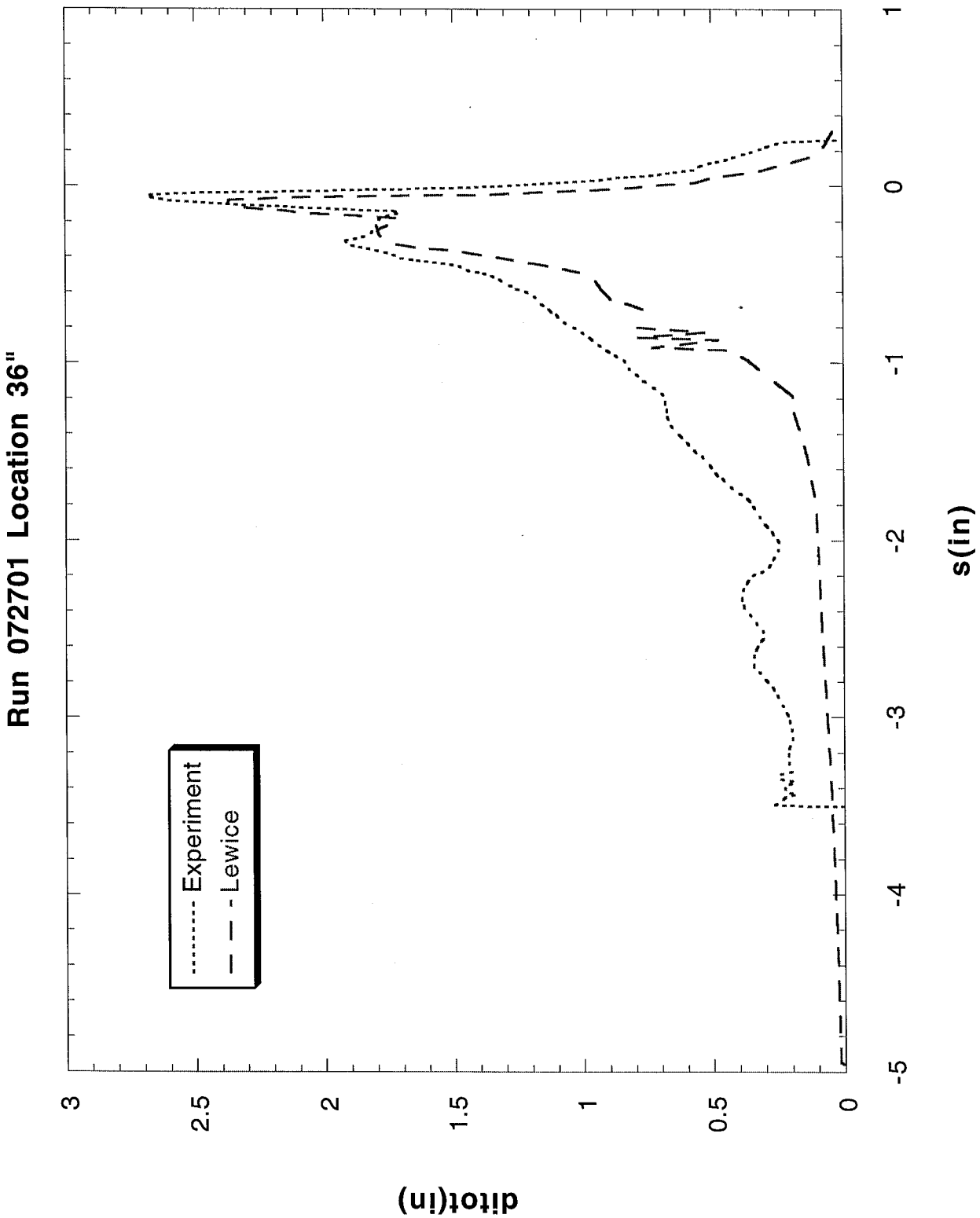
Run 072701 Location 36"
Experiment
Lewice
dltot(in)
s(in)
3
2.5
2
1.5
1
0.5
0
-5
-4
-3
-2
-1
0
1

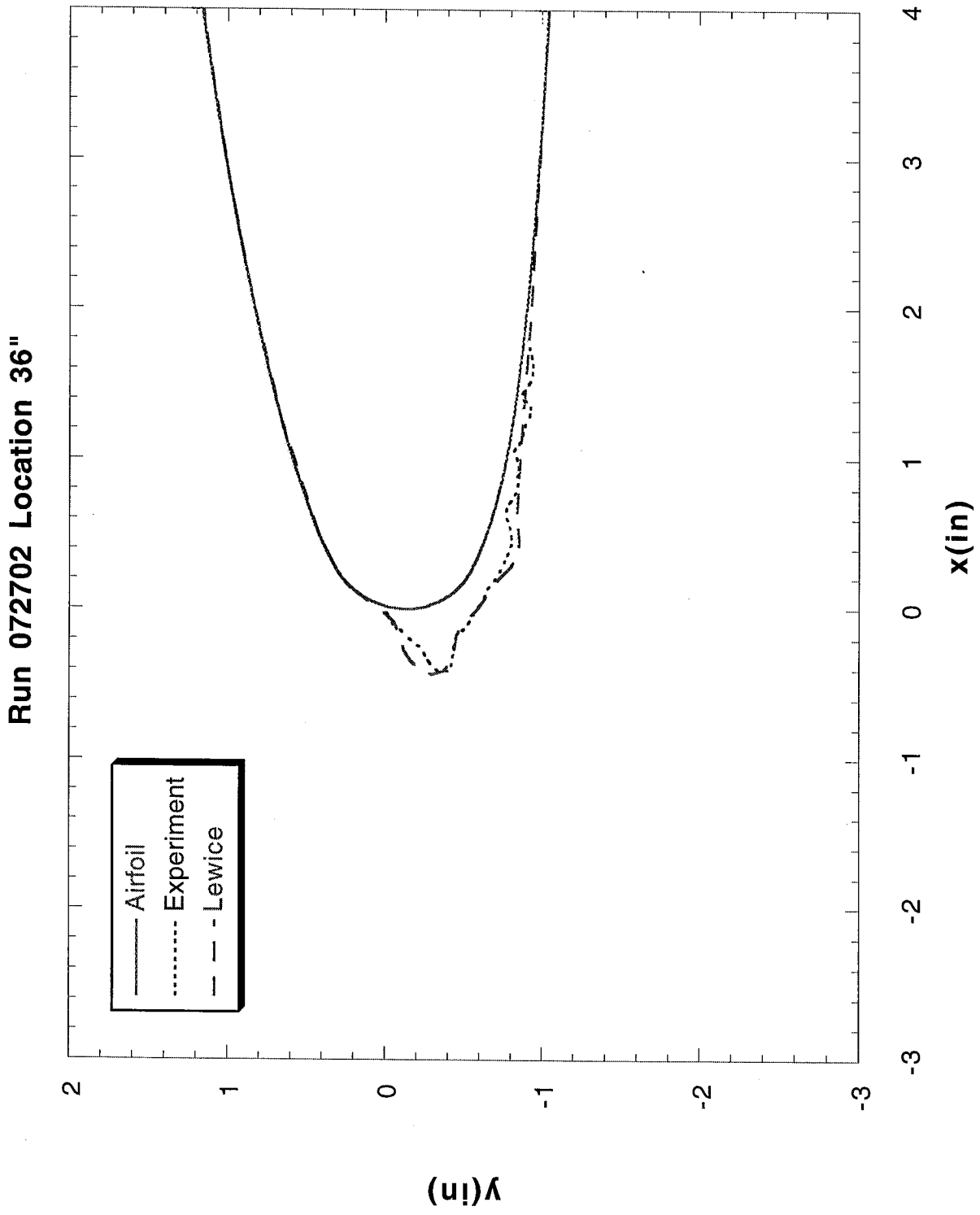
Run 072702 Location 36"
Airfoil
Experiment
Lewice
y(in)
x(in)
2
1
0
-1
-2
-3
4
3
2
1
0
-1
-2
-3

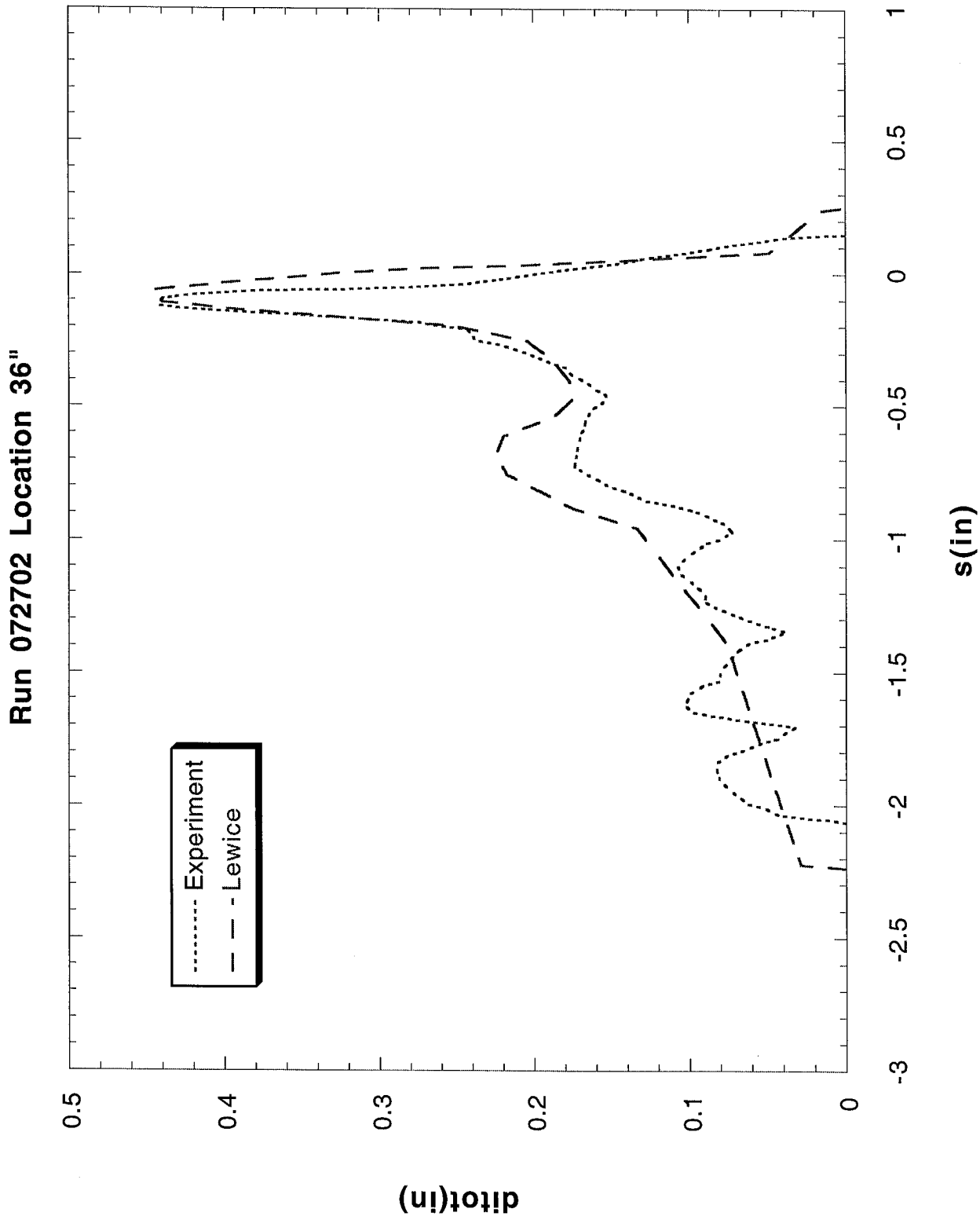
Run 072702 Location 36"
Experiment
Lewice
dltot(in)
s(in)
0.5
0.4
0.3
0.2
0.1
0
-3
-2.5
-2
-1.5
-1
-0.5
0
0.5
1

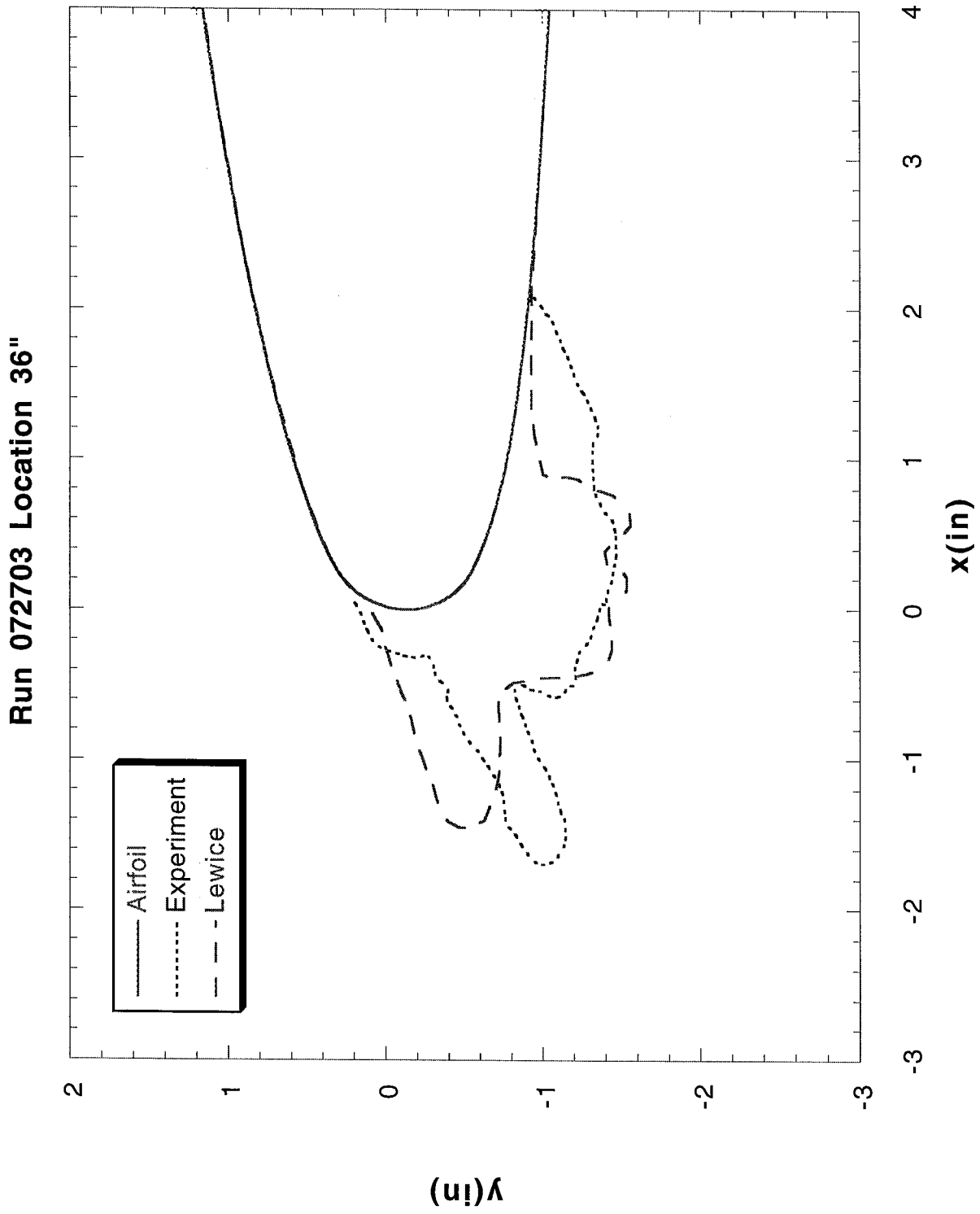
Run 072703 Location 36"
Airfoil
Experiment
Lewice
y(in)
x(in)
2
1
0
-1
-2
-3
-3
-2
-1
0
1
2
3
4

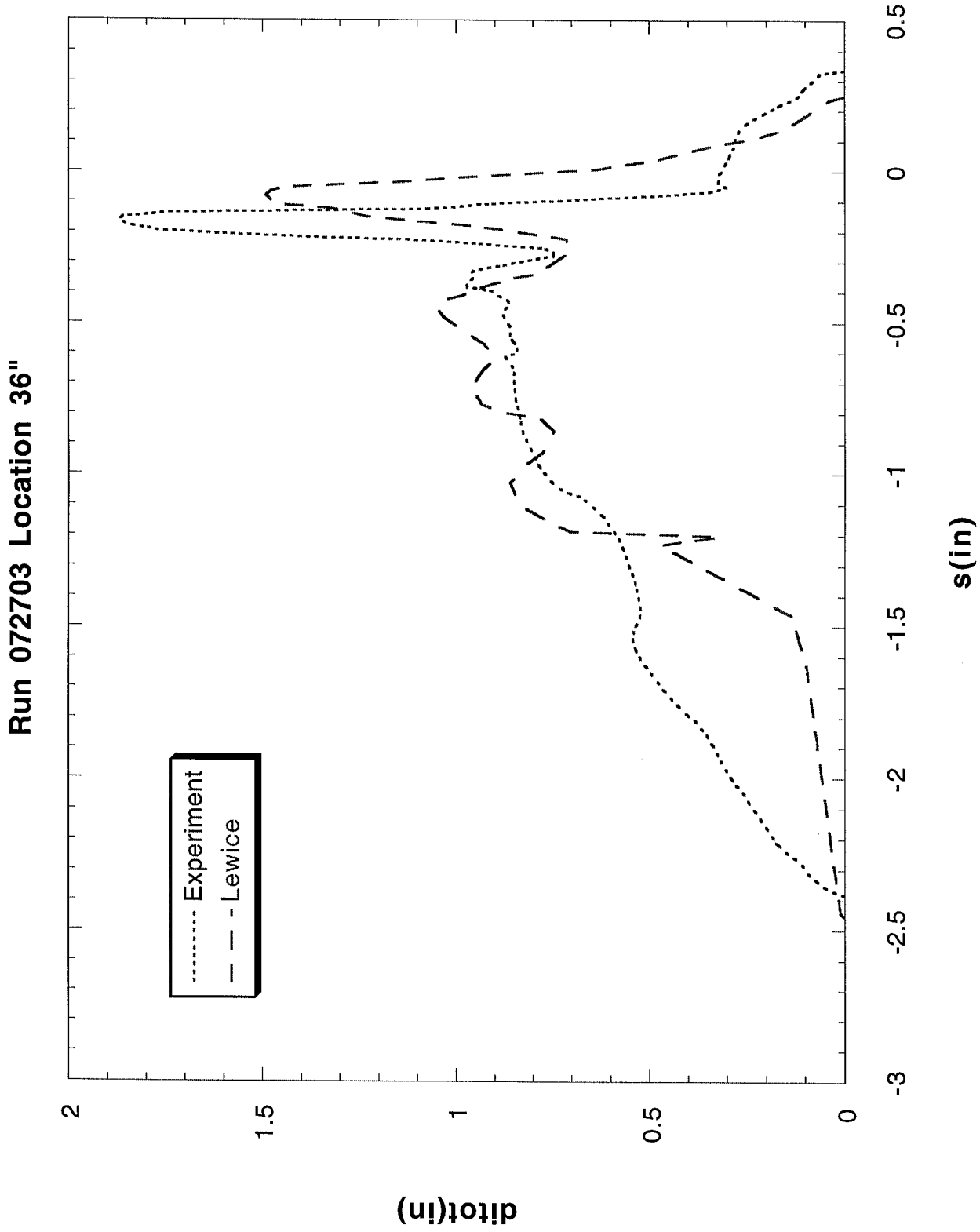
Run 072703 Location 36"
Experiment
Lewice
dltot(in)
s(in)
2
1.5
1
0.5
0
0.5
0
-0.5
-1
-1.5
-2
-2.5
-3

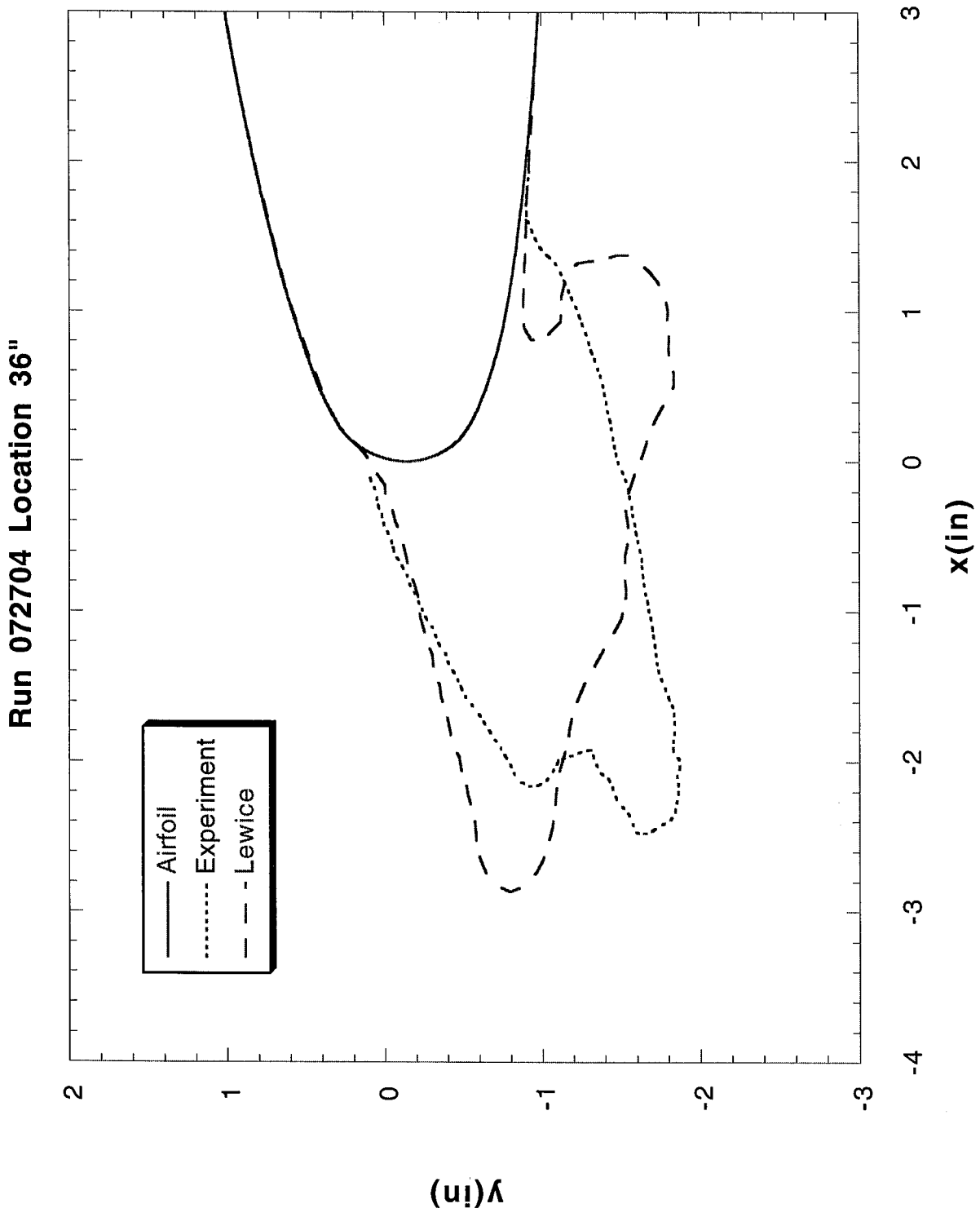
Run 072704 Location 36"
Airfoil
Experiment
Lewice
y(in)
x(in)
2
1
0
-1
-2
-3
3
2
1
0
-1
-2
-3
-4

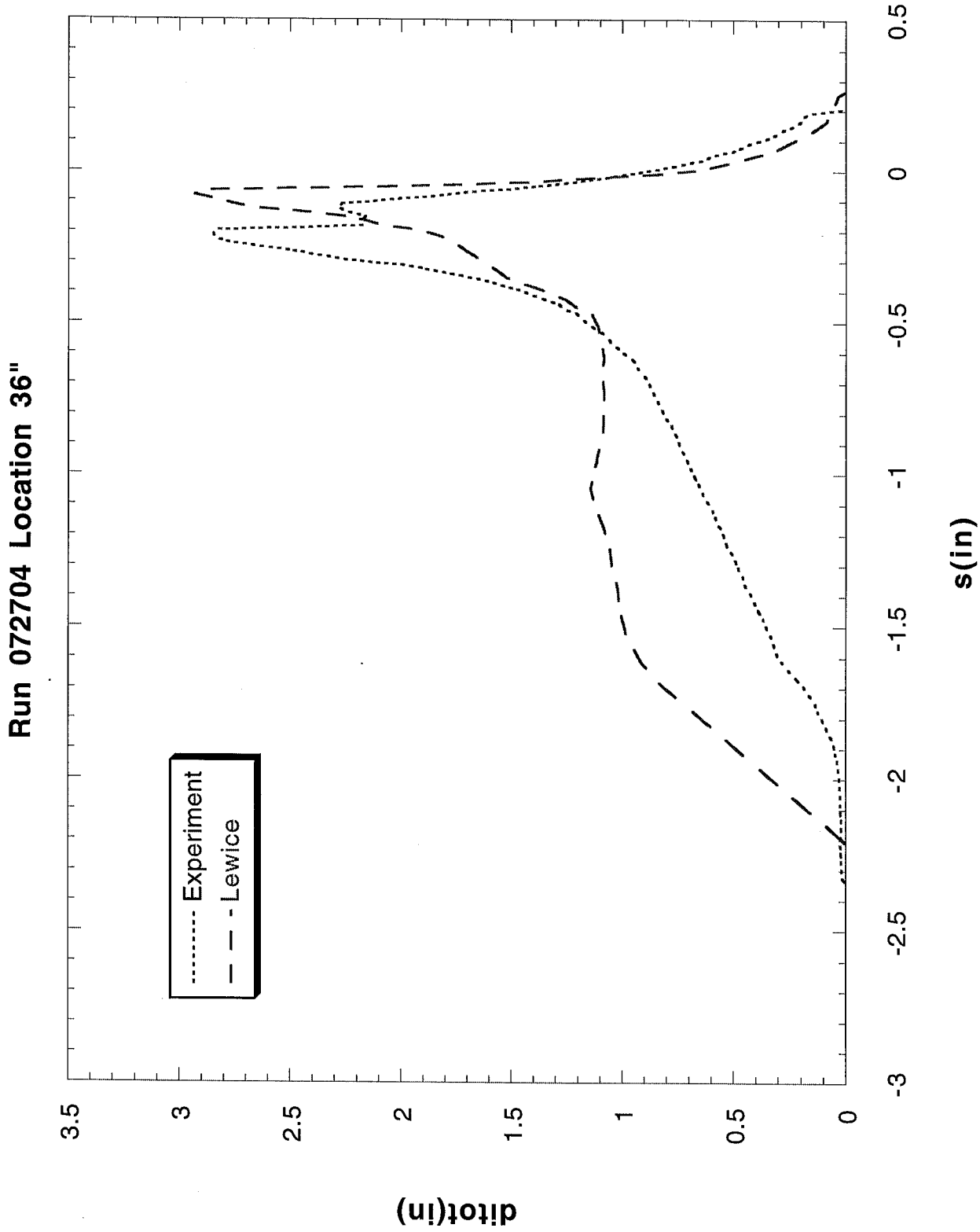
Run 072704 Location 36"
Experiment
Lewice
ditot(in)
s(in)
3.5
3
2.5
2
1.5
1
0.5
0
-3
-2.5
-2
-1.5
-1
-0.5
0
0.5

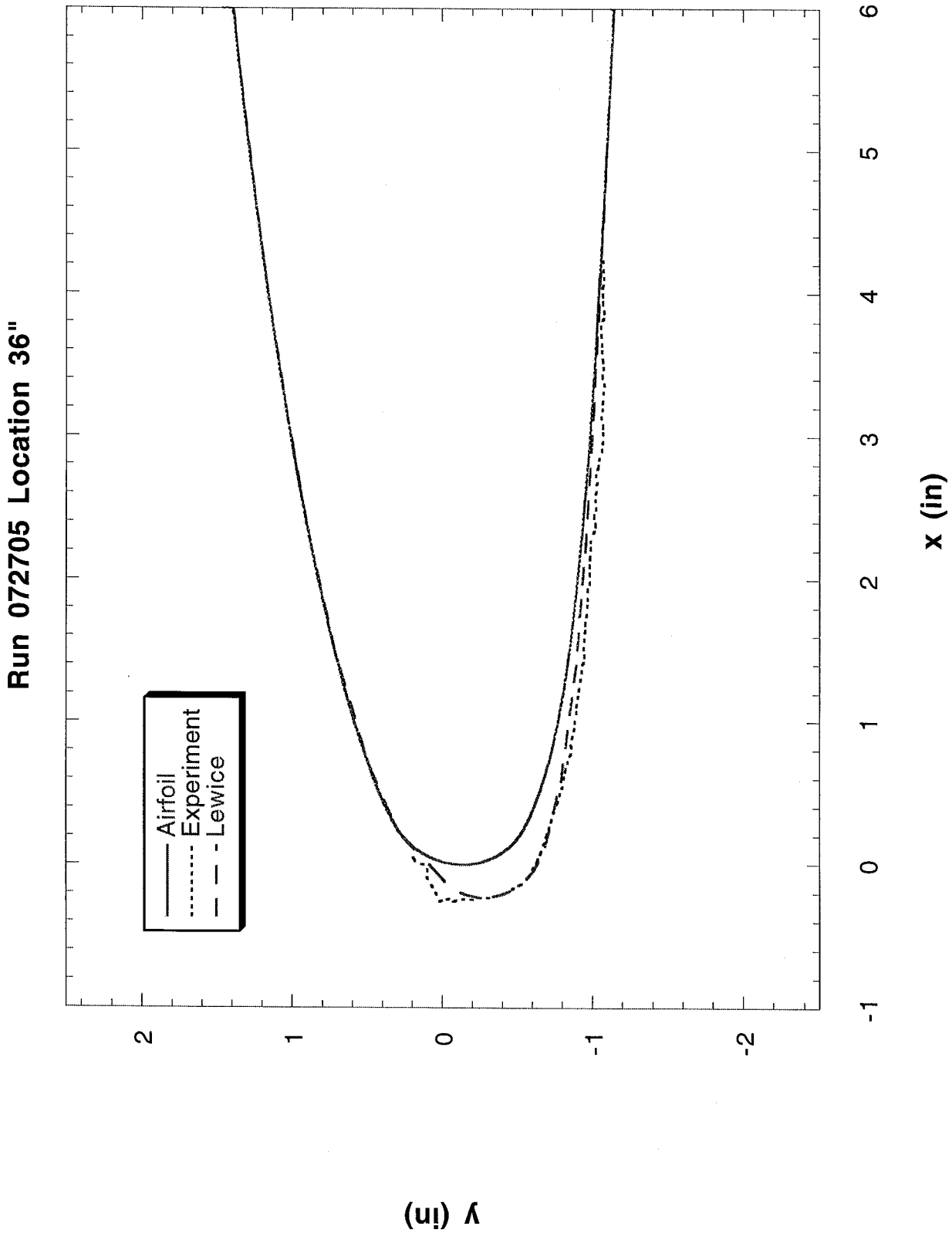
Run 072705 Location 36"
Airfoil
Experiment
Lewice
y (in)
x (in)
2
1
0
-1
-2
-1
0
1
2
3
4
5
6

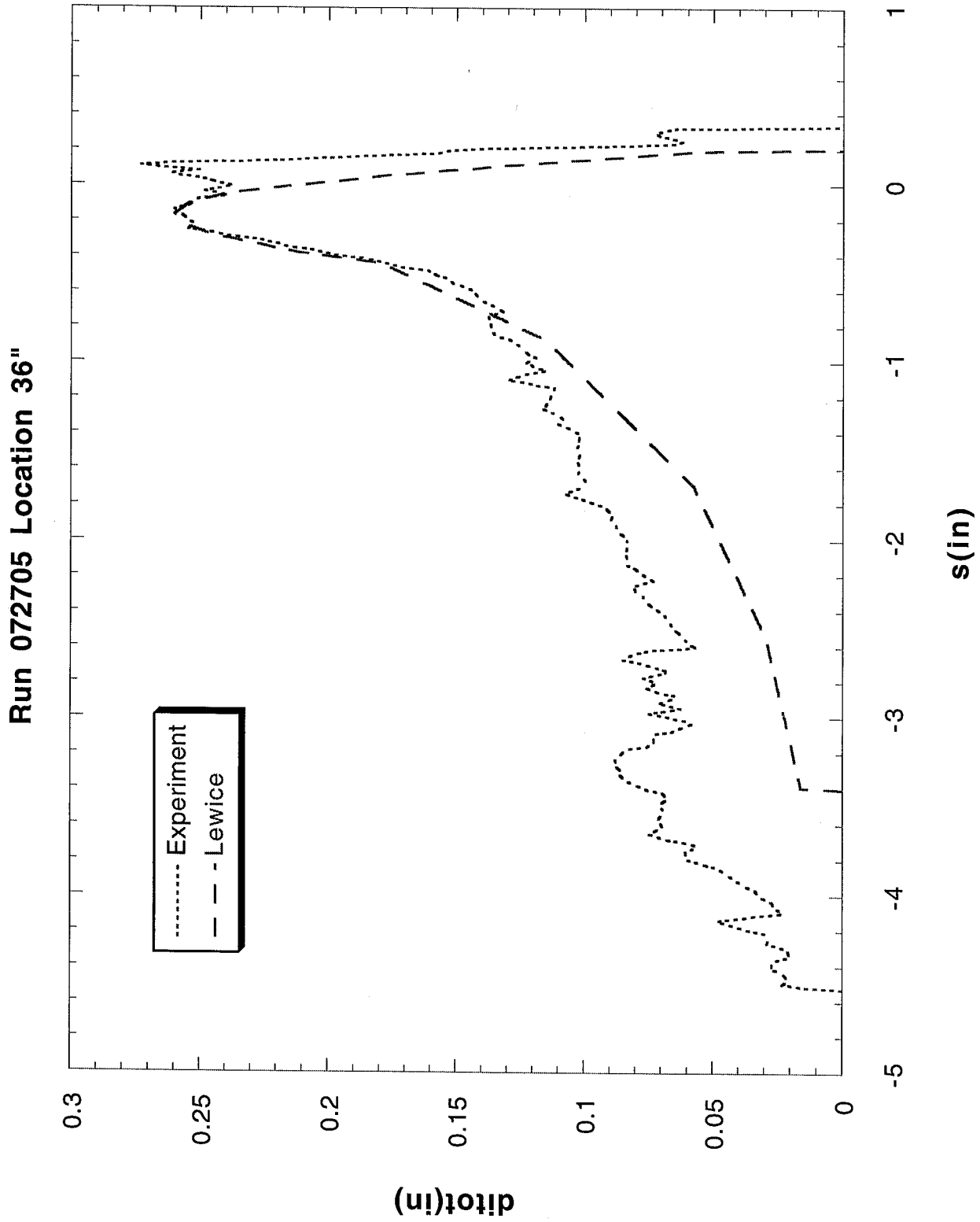
Run 072705 Location 36"
Experiment
Lewice
dltot(in)
s(in)
0.3
0.25
0.2
0.15
0.1
0.05
0
1
0
-1
-2
-3
-4
-5

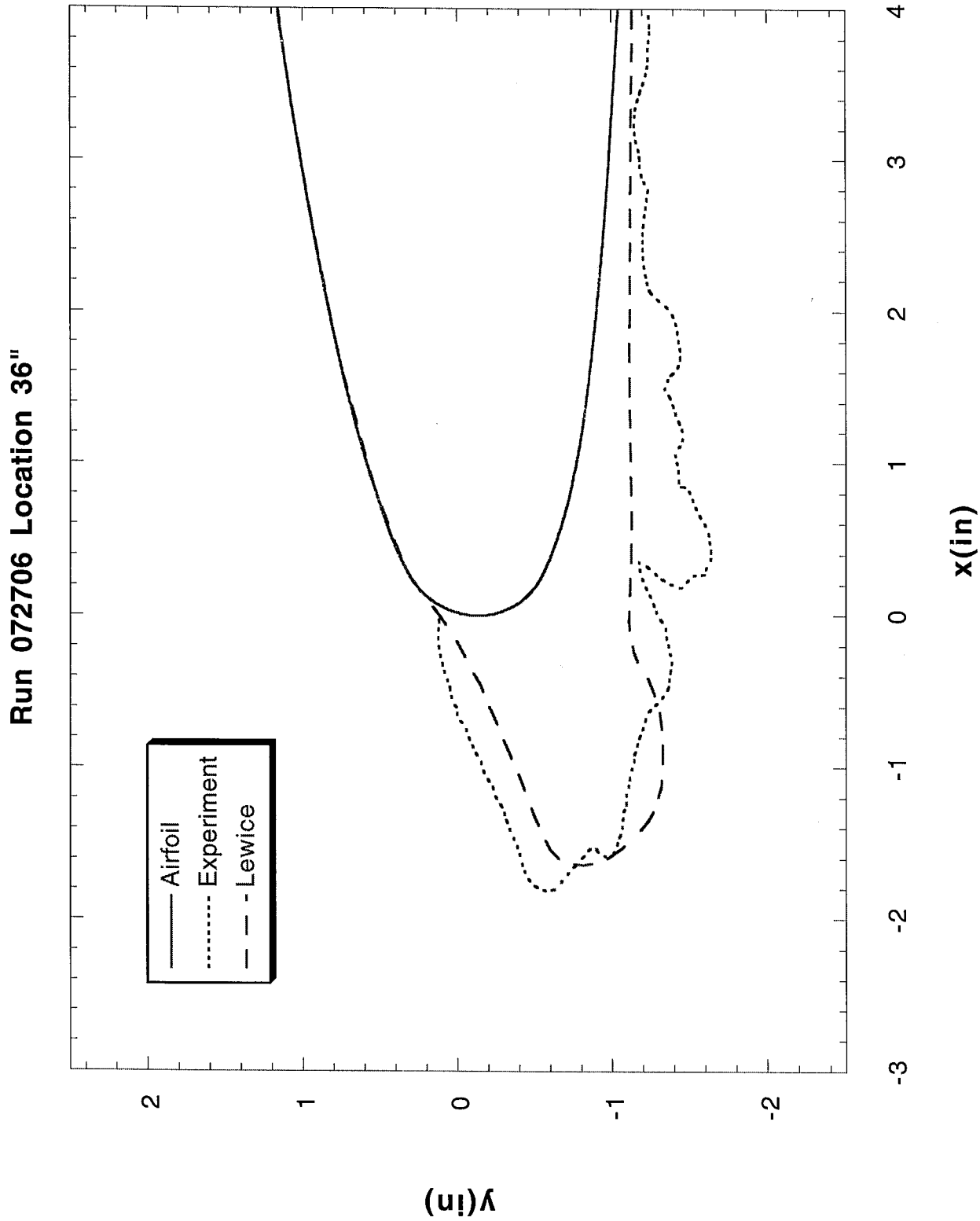
Run 072706 Location 36"
Airfoil
Experiment
Lewice
y(in)
x(in)
2
1
0
-1
-2
-3
-2
-1
0
1
2
3
4

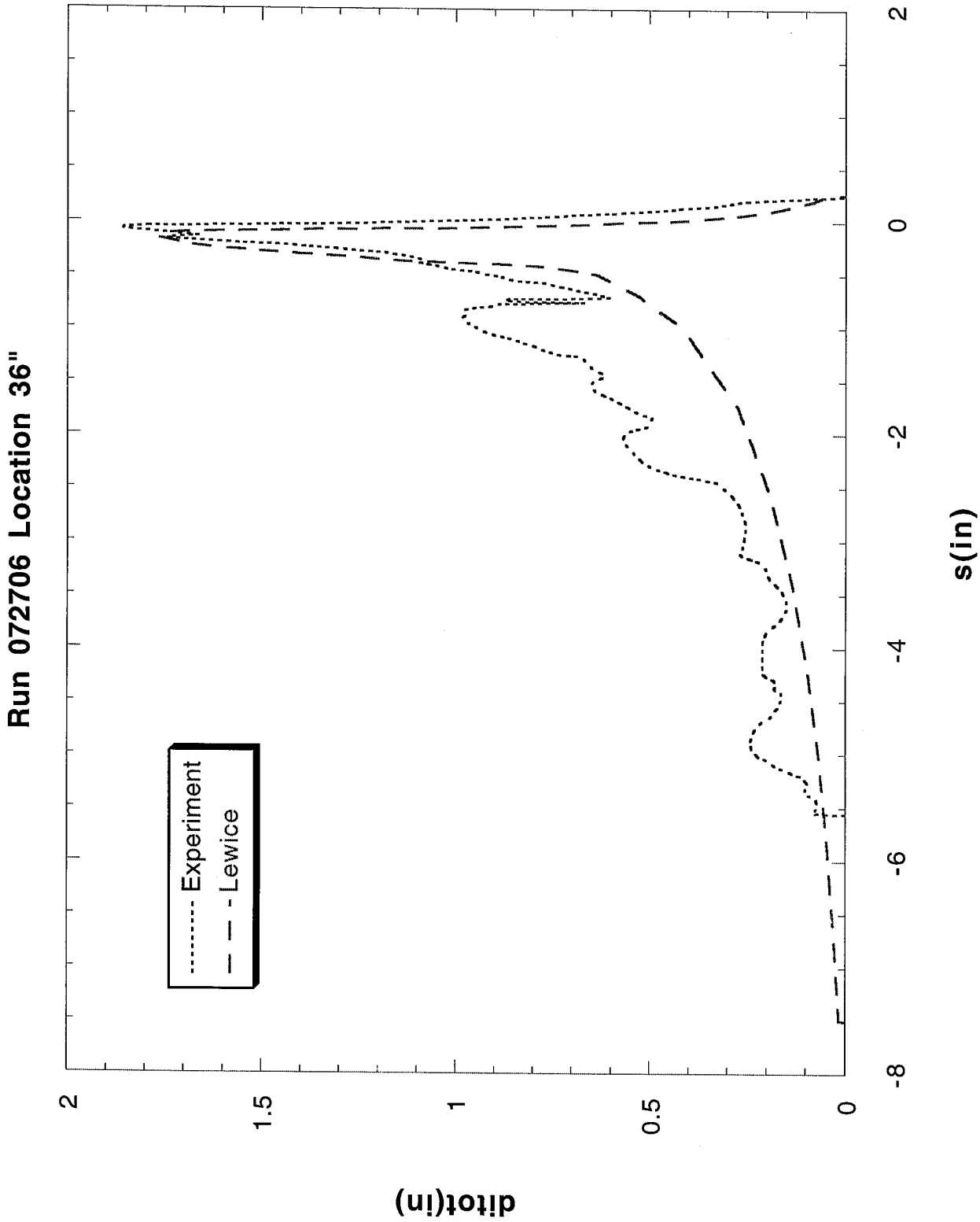
Run 072706 Location 36"
Experiment
Lewice
dltot(in)
s(in)
2
1.5
1
0.5
0
-8
-6
-4
-2
0
2

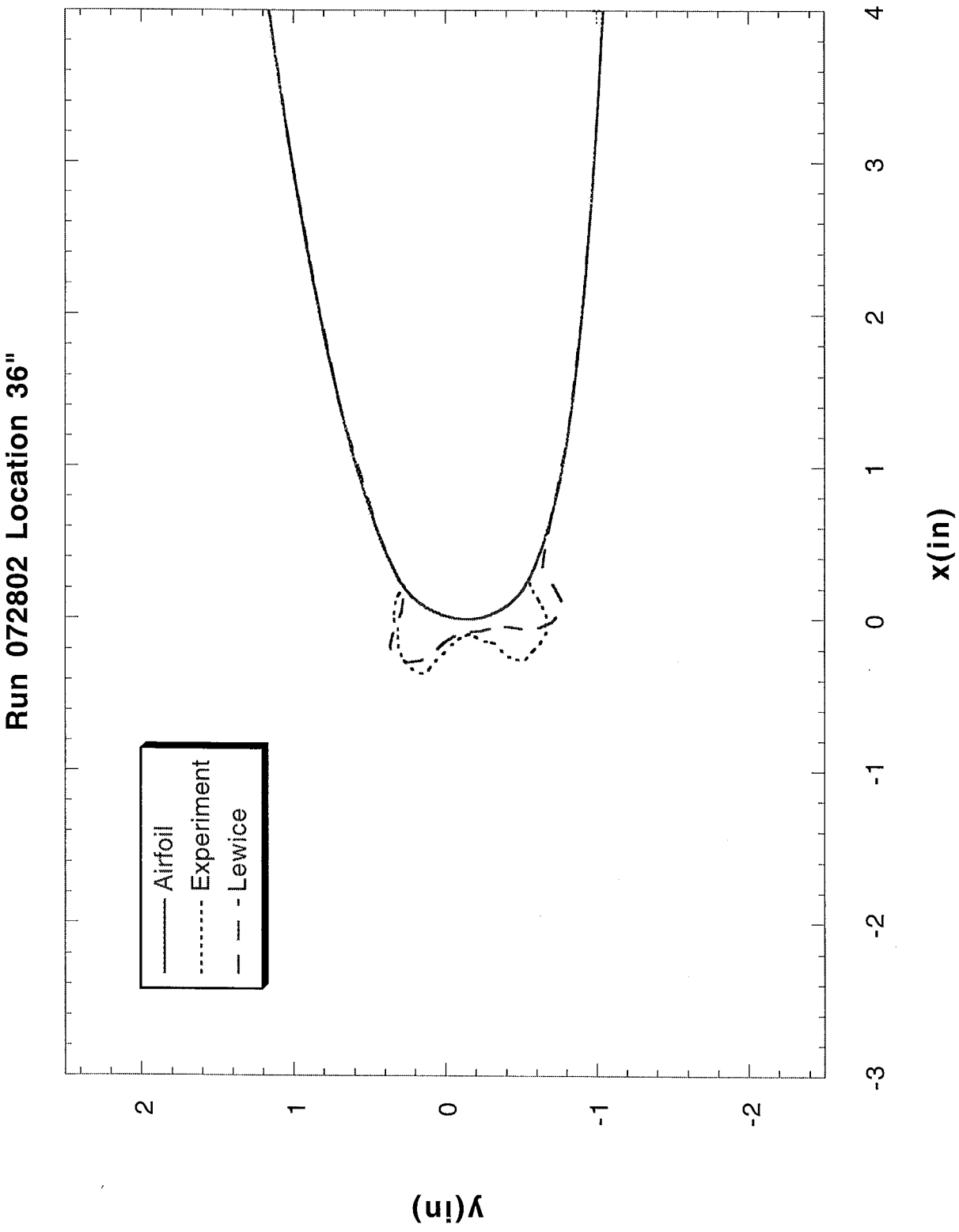
Run 072802 Location 36"
Airfoil
Experiment
- Lewice
y(in)
x(in)
2
1
0
-1
-2
-3
-2
-1
0
1
2
3
4

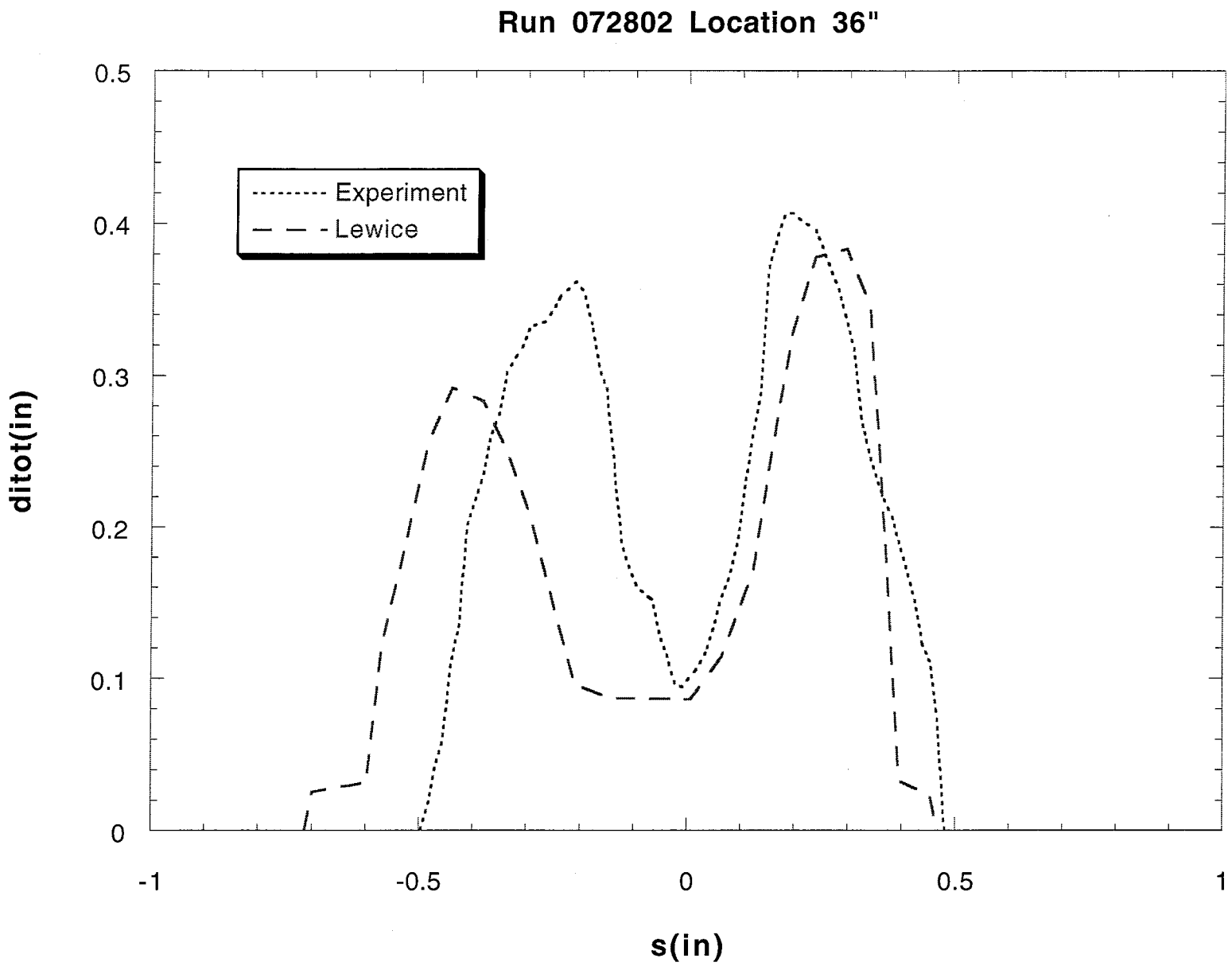
Run 072802 Location 36"
Experiment
Lewice
ditot(in)
s(in)
0.5
0.4
0.3
0.2
0.1
0
-1
-0.5
0
0.5
1

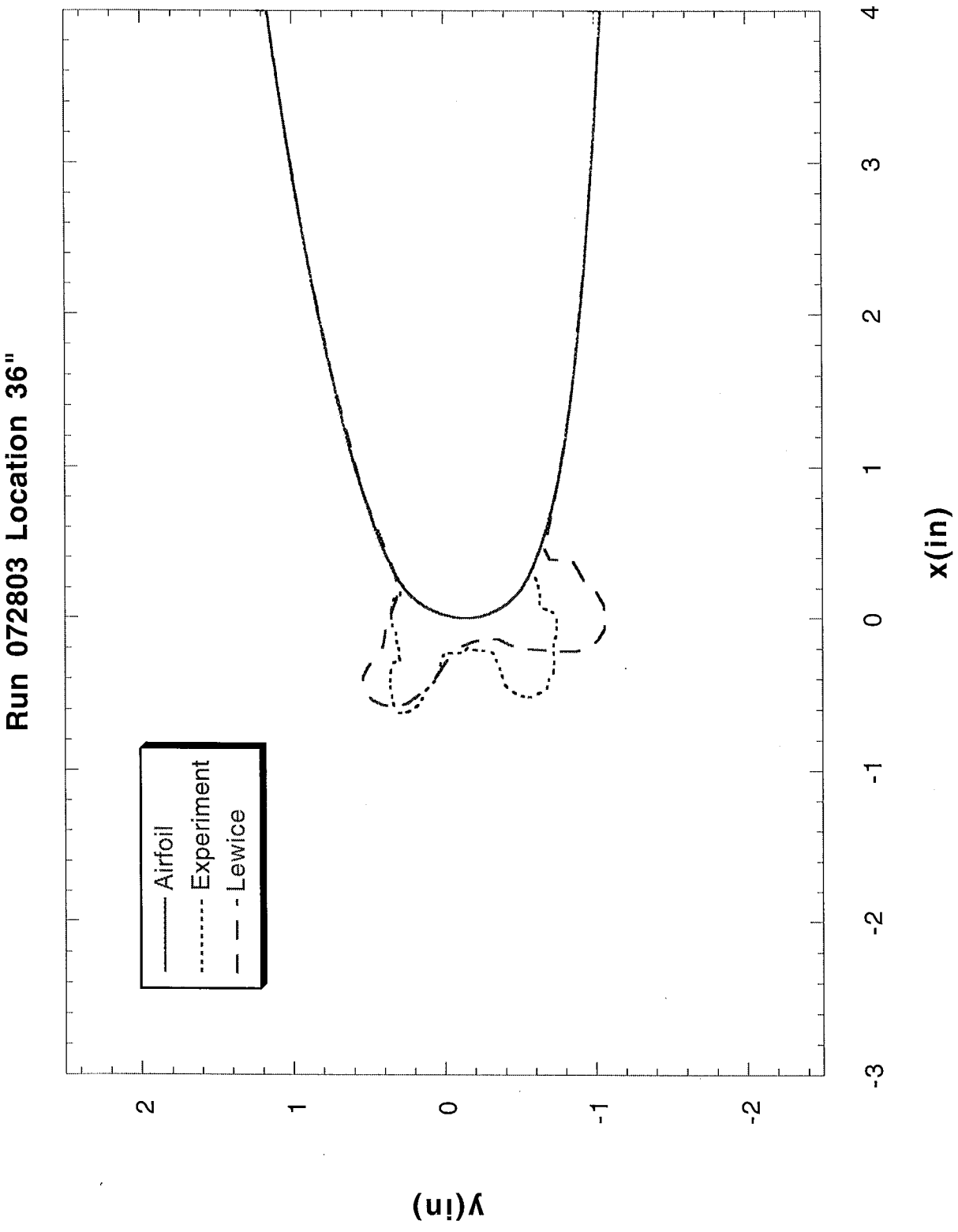
Run 072803 Location 36"
Airfoil
Experiment
Lewice
y(in)
x(in)
2
1
0
-1
-2
-3
-2
-1
0
1
2
3
4

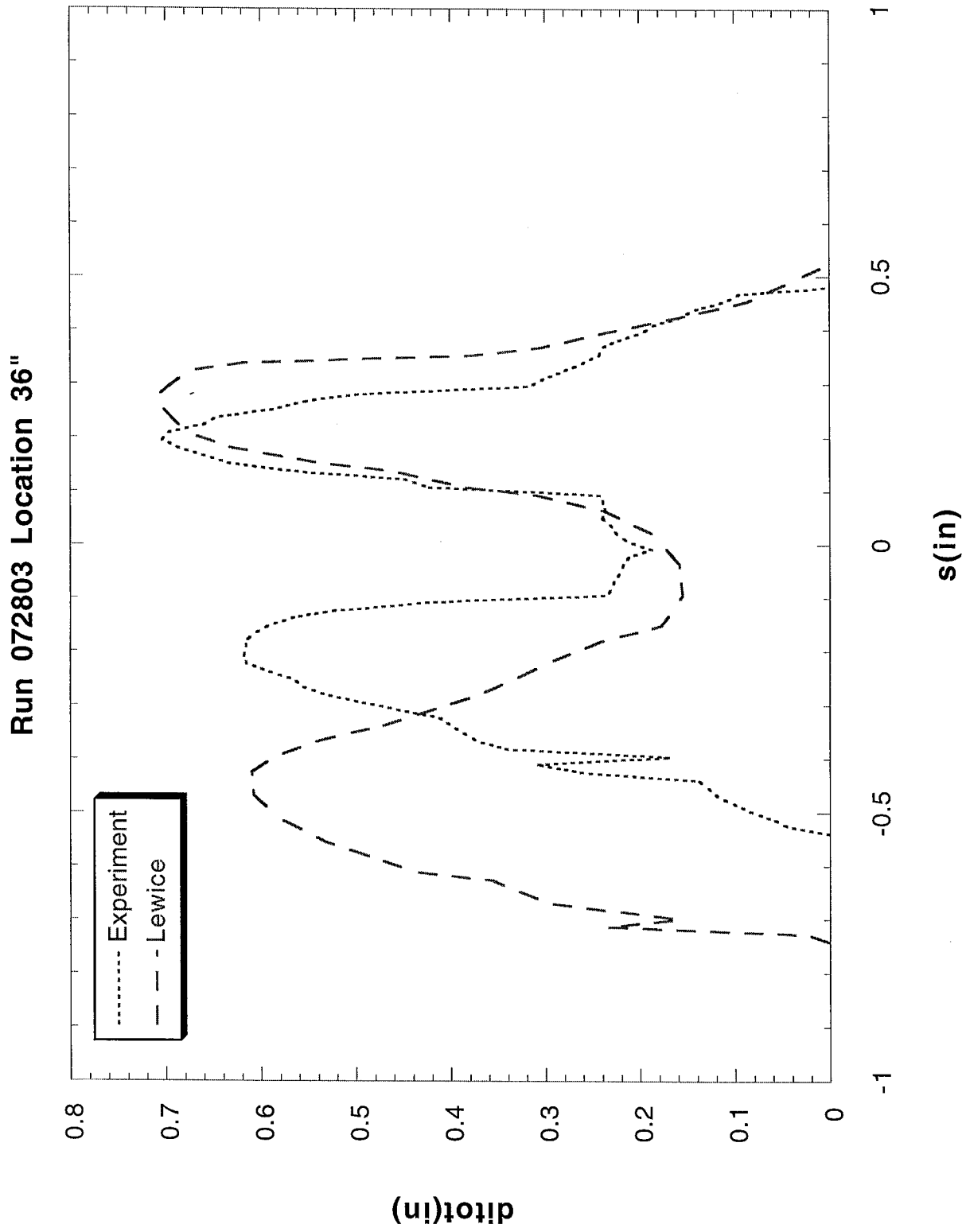
Run 072803 Location 36"
Experiment
Lewice
dltot(in)
s(in)
0.8
0.7
0.6
0.5
0.4
0.3
0.2
0.1
0
-1
-0.5
0
0.5
1

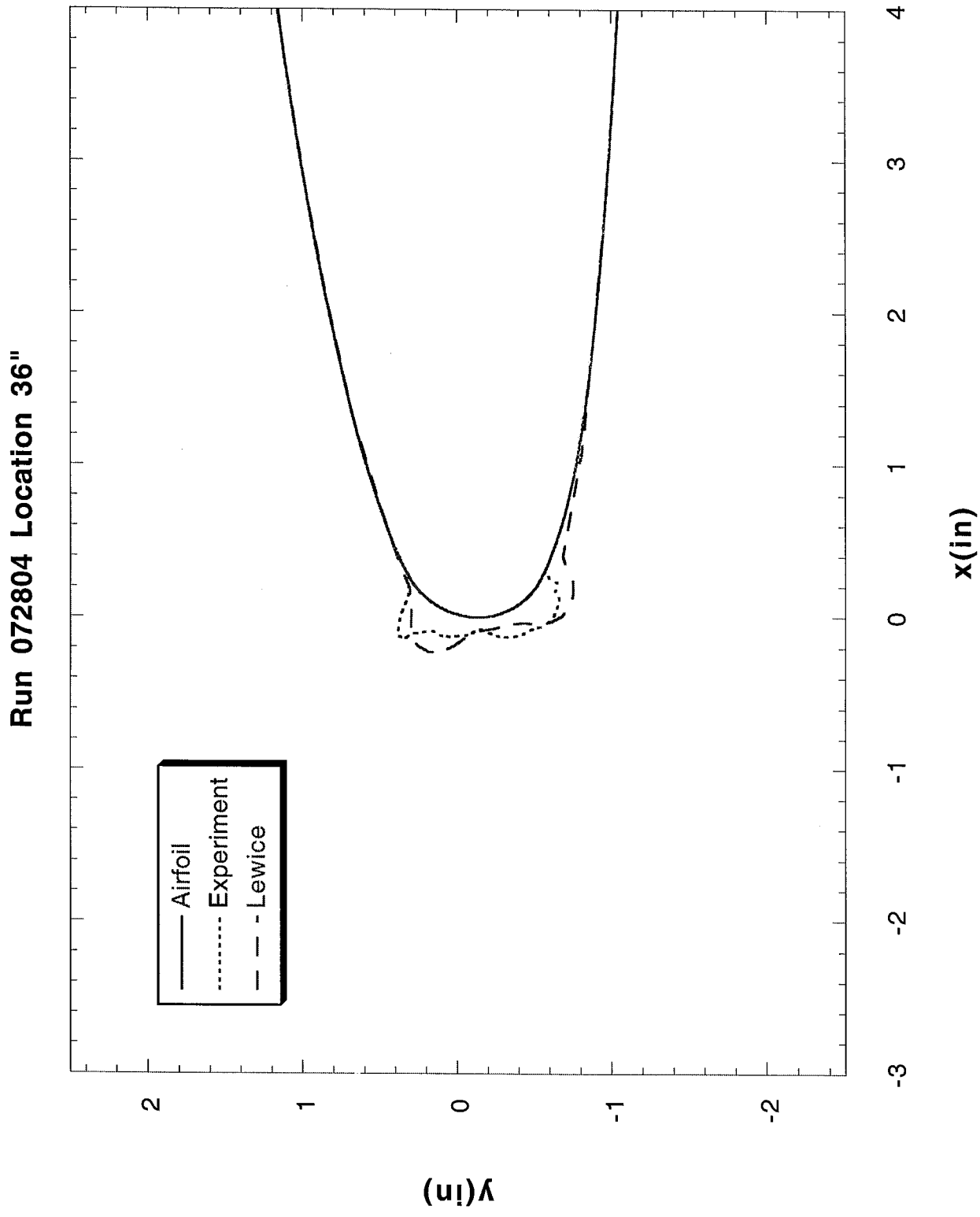
Run 072804 Location 36"
Airfoil
Experiment
Lewice
y(in)
x(in)
2
1
0
-1
-2
-3
-2
-1
0
1
2
3
4

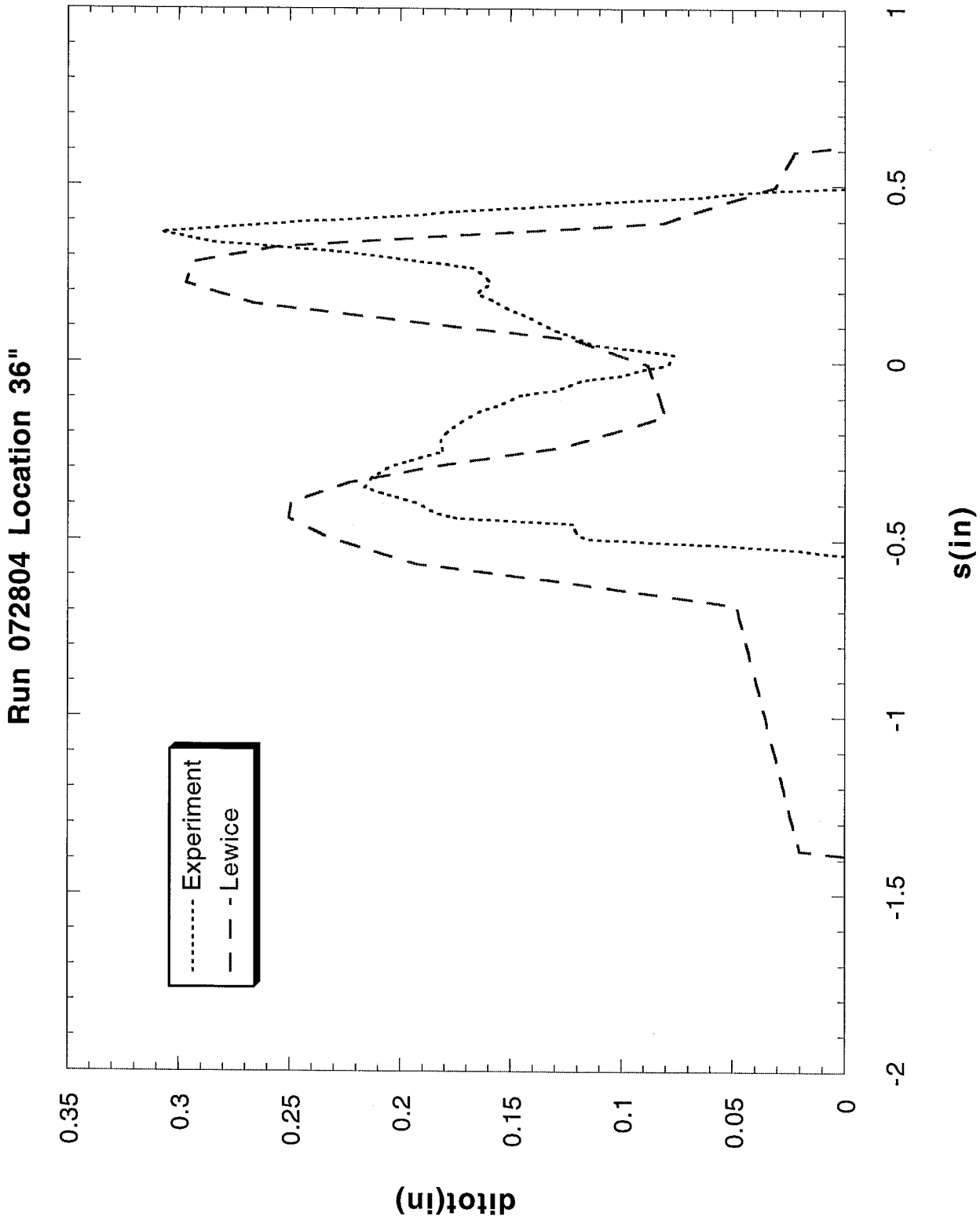
Run 072804 Location 36"
Experiment
Lewice
ditot(in)
s(in)
0.35
0.3
0.25
0.2
0.15
0.1
0.05
0
-2
-1.5
-1
-0.5
0
0.5
1

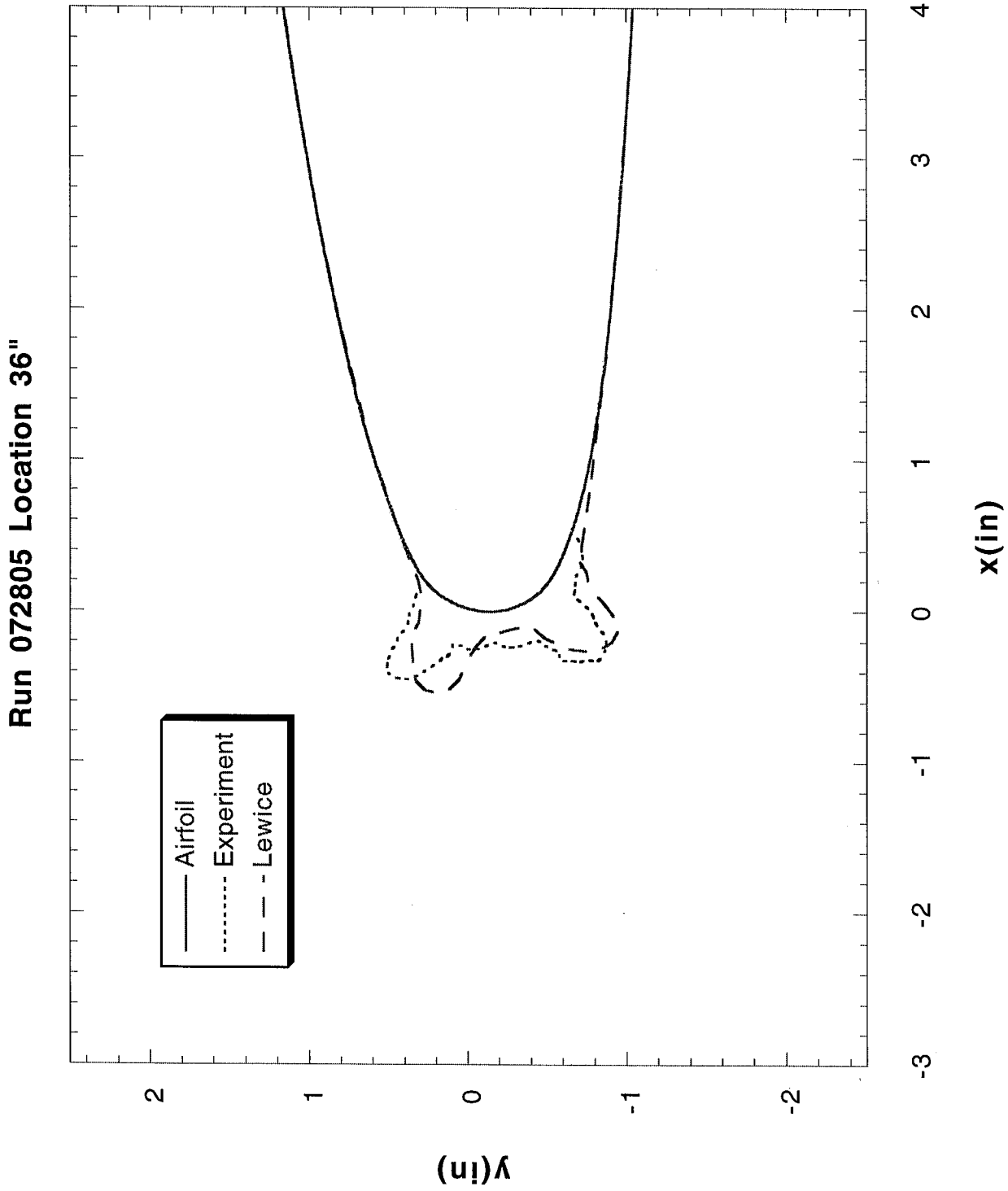
Run 072805 Location 36"
Airfoil
Experiment
Lewice
y(in)
x(in)
2
1
0
-1
-2
-3
-2
-1
0
1
2
3
4

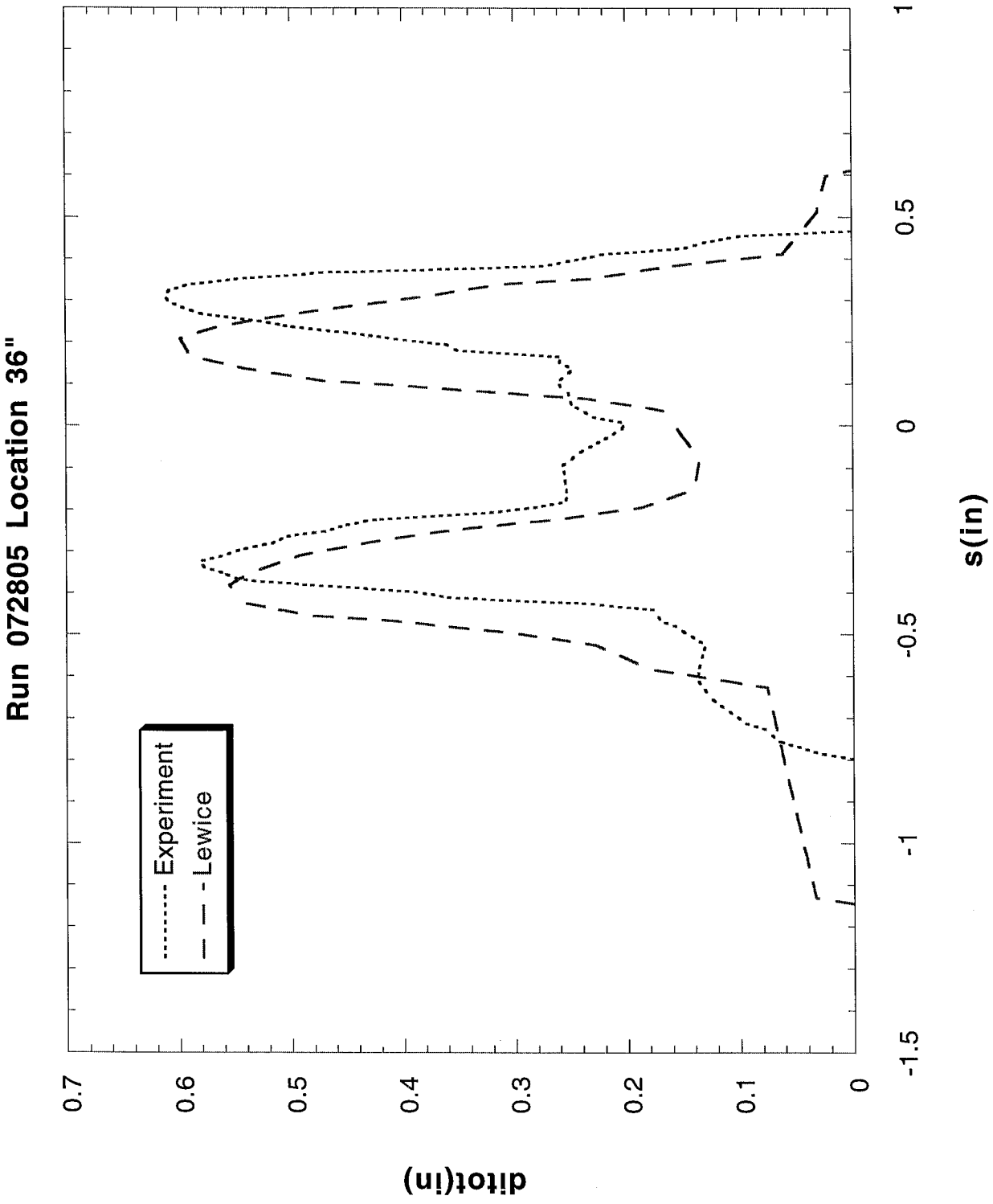
Run 072805 Location 36"
Experiment
Lewice
ditot(in)
s(in)
0
0.1
0.2
0.3
0.4
0.5
0.6
0.7
-1.5
-1
-0.5
0
0.5
1

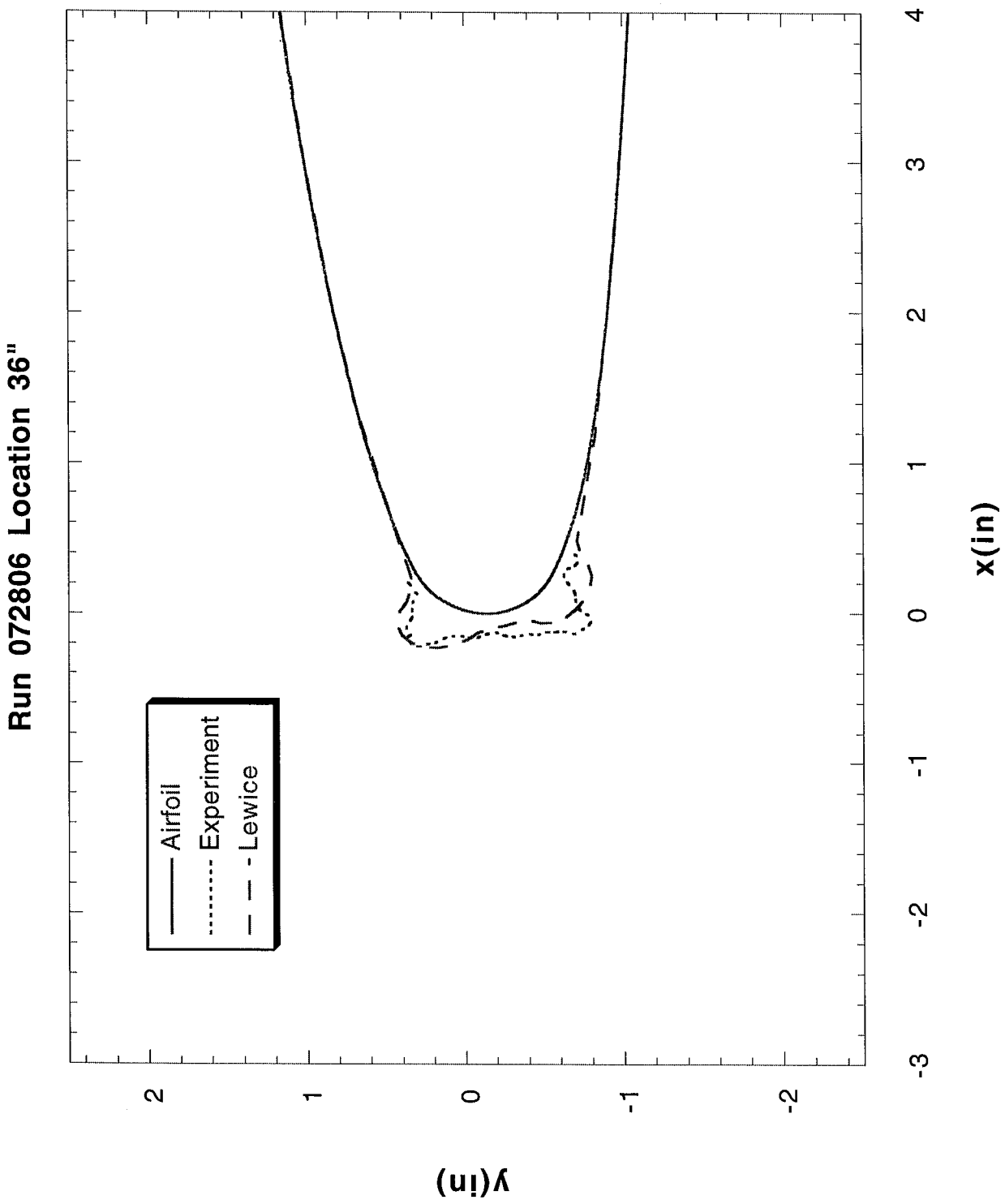
Run 072806 Location 36"
Airfoil
Experiment
Lewice
y(in)
x(in)
2
1
0
-1
-2
-3
-2
-1
0
1
2
3
4

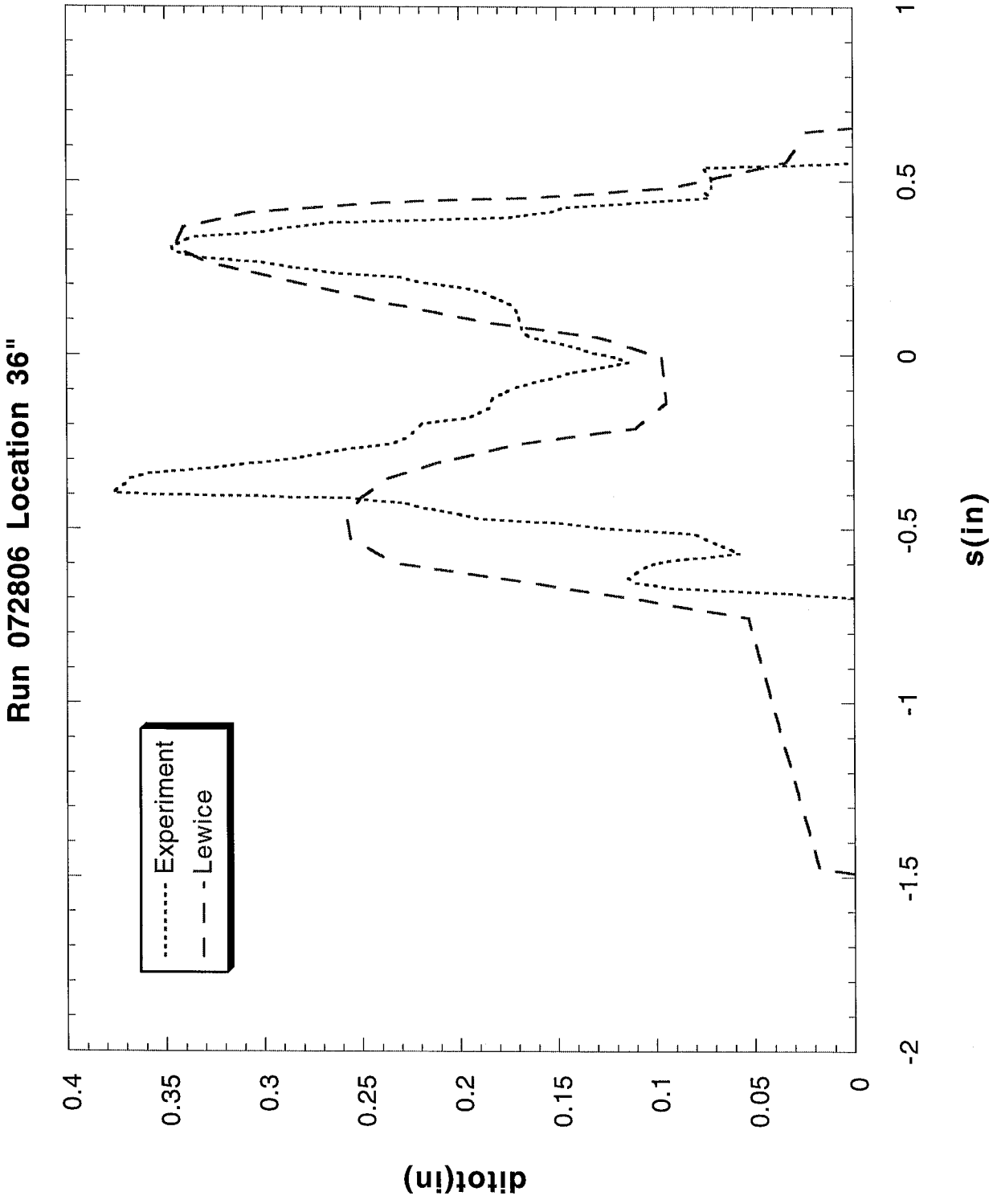
Run 072806 Location 36"
Experiment
Lewice
dltot(in)
s(in)
0.4
0.35
0.3
0.25
0.2
0.15
0.1
0.05
0
-2
-1.5
-1
-0.5
0
0.5
1

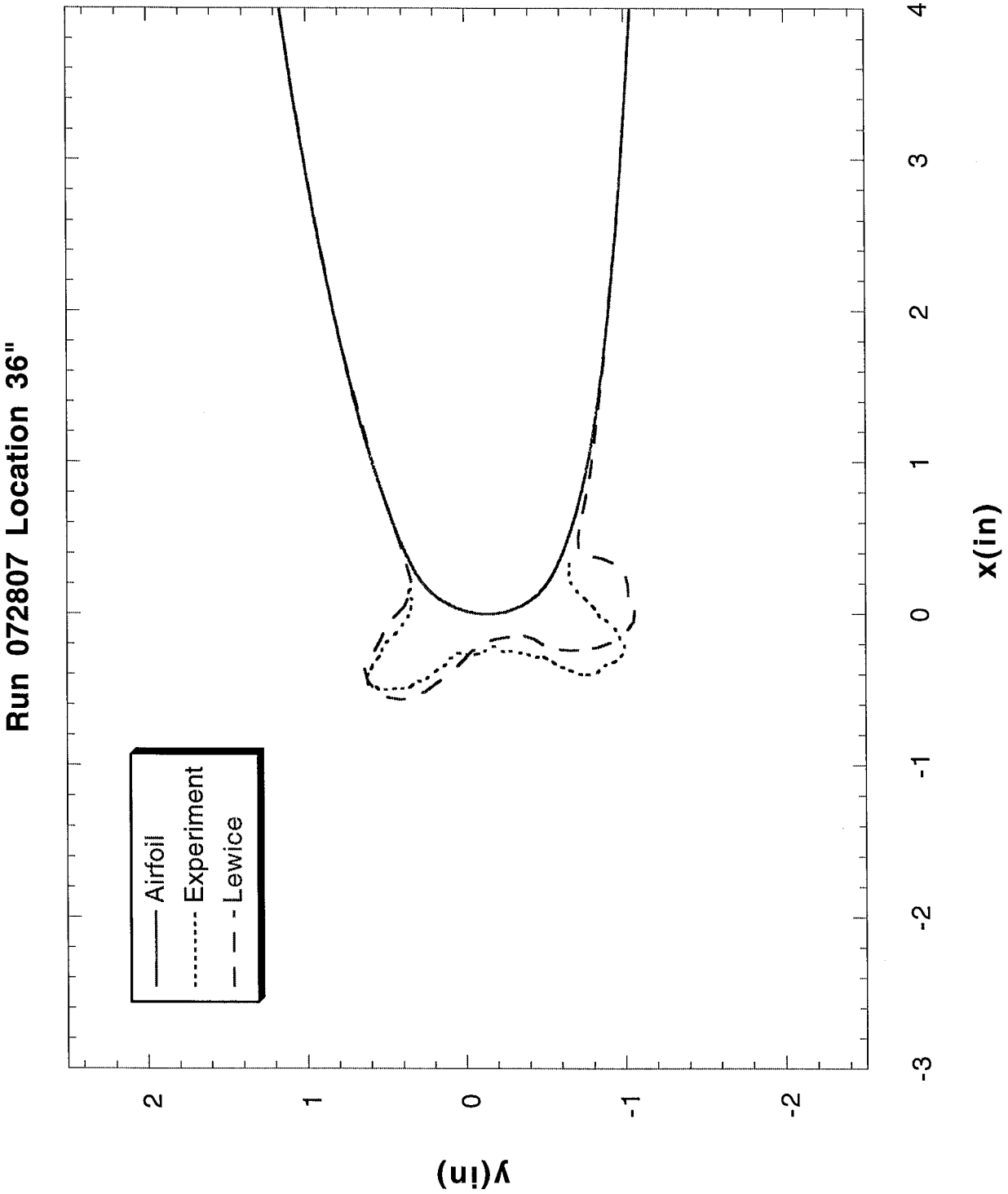
Run 072807 Location 36"
Airfoil
Experiment
Lewice
y(in)
x(in)
2
1
0
-1
-2
-3
-2
-1
0
1
2
3
4

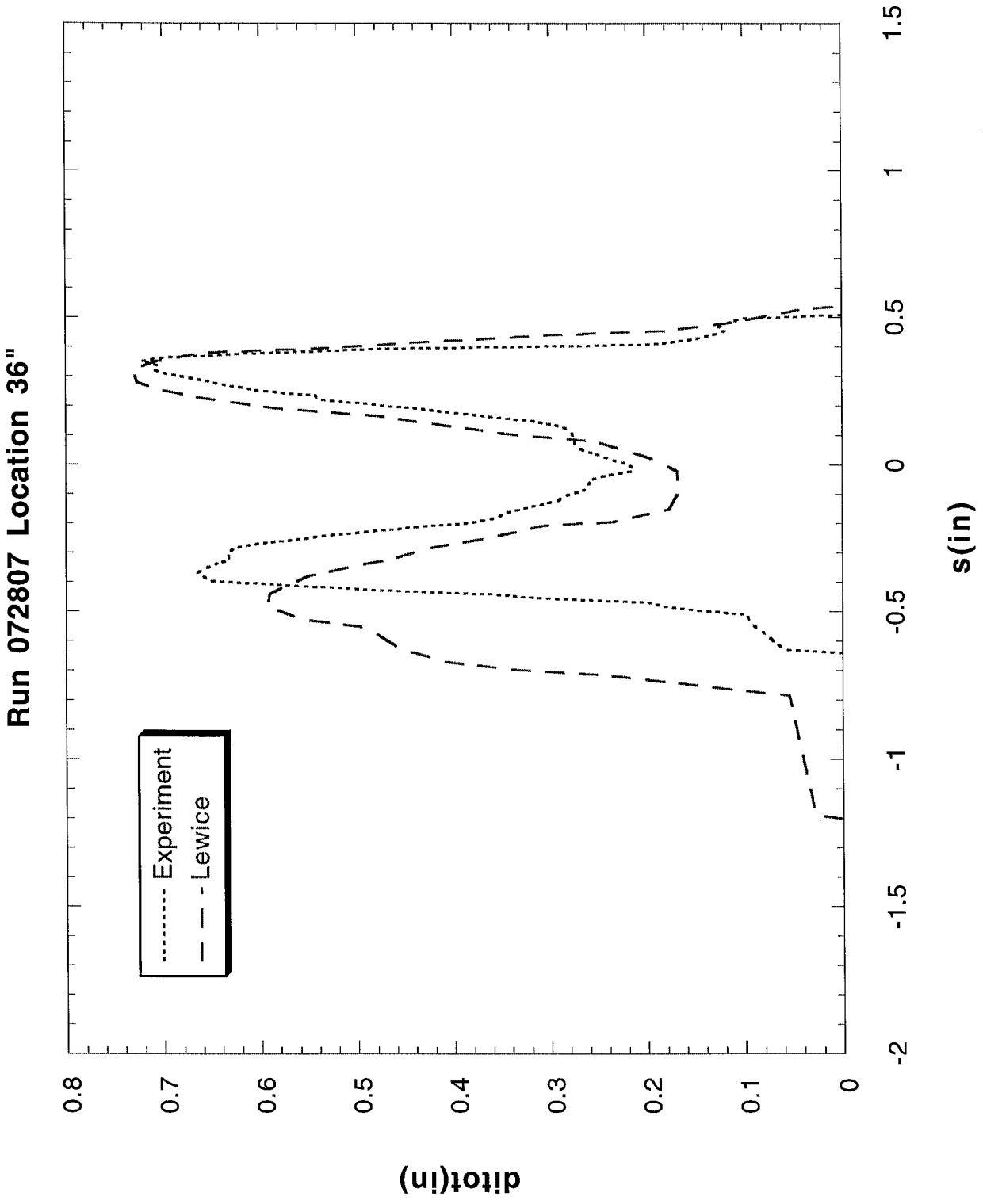
Run 072807 Location 36"
Experiment
Lewice
dltot(in)
s(in)
0
0.1
0.2
0.3
0.4
0.5
0.6
0.7
0.8
-2
-1.5
-1
-0.5
0
0.5
1
1.5

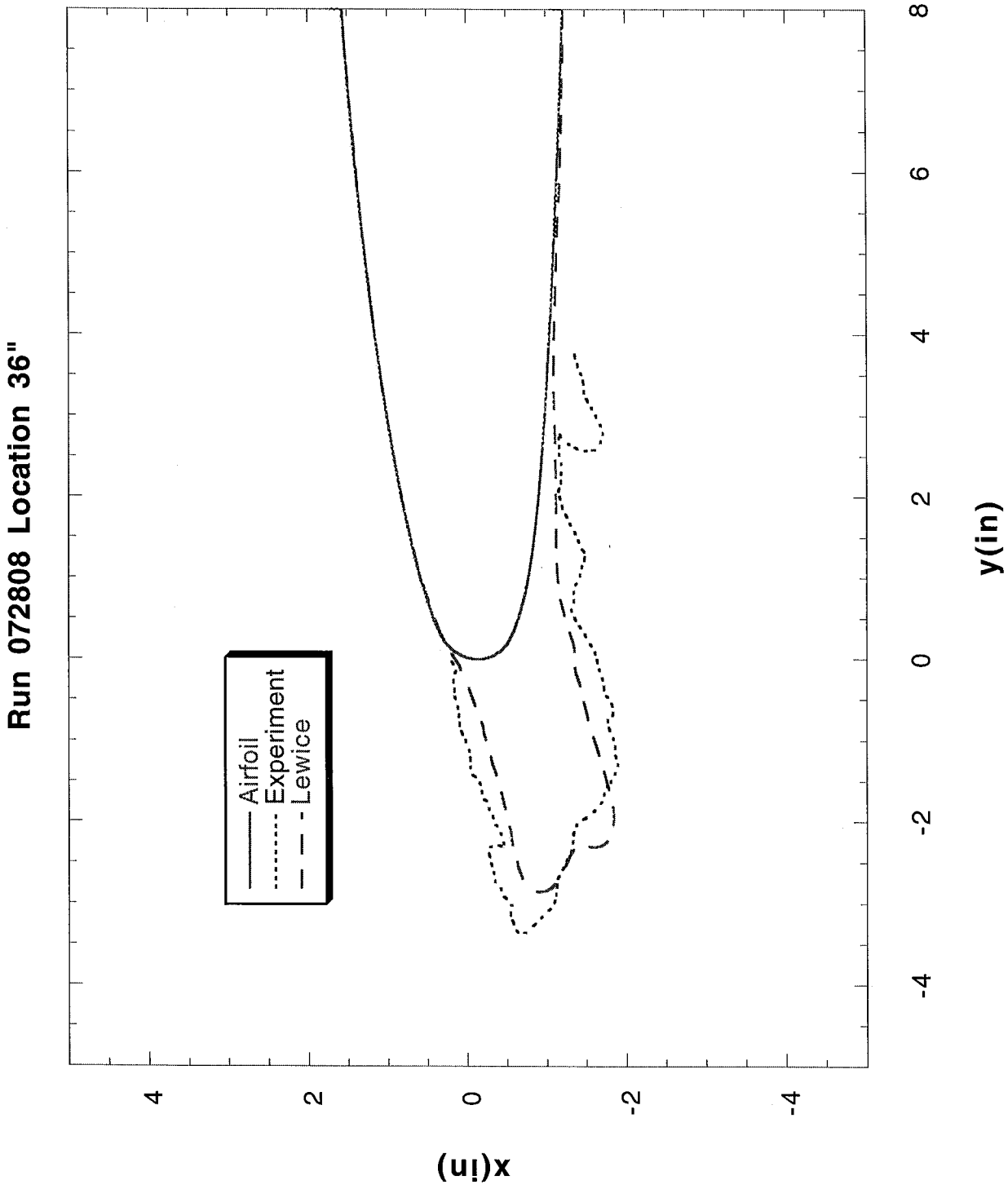
Run 072808 Location 36"
Airfoil
Experiment
Lewice
x(in)
y(in)
4
2
0
-2
-4
-4
-2
0
2
4
6
8

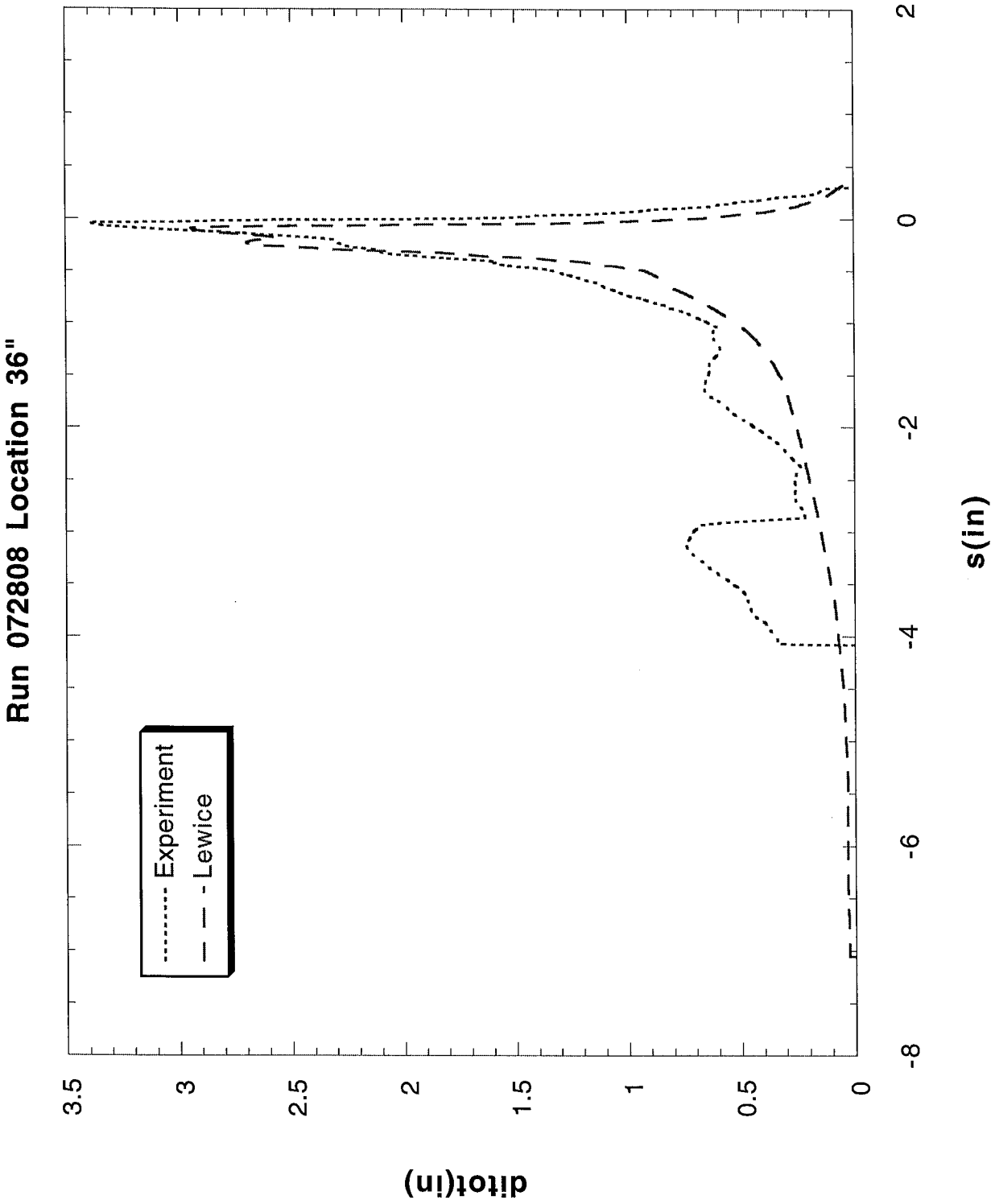
Run 072808 Location 36"
Experiment
Lewice
dltot(in)
s(in)
3.5
3
2.5
2
1.5
1
0.5
0
2
0
-2
-4
-6
-8

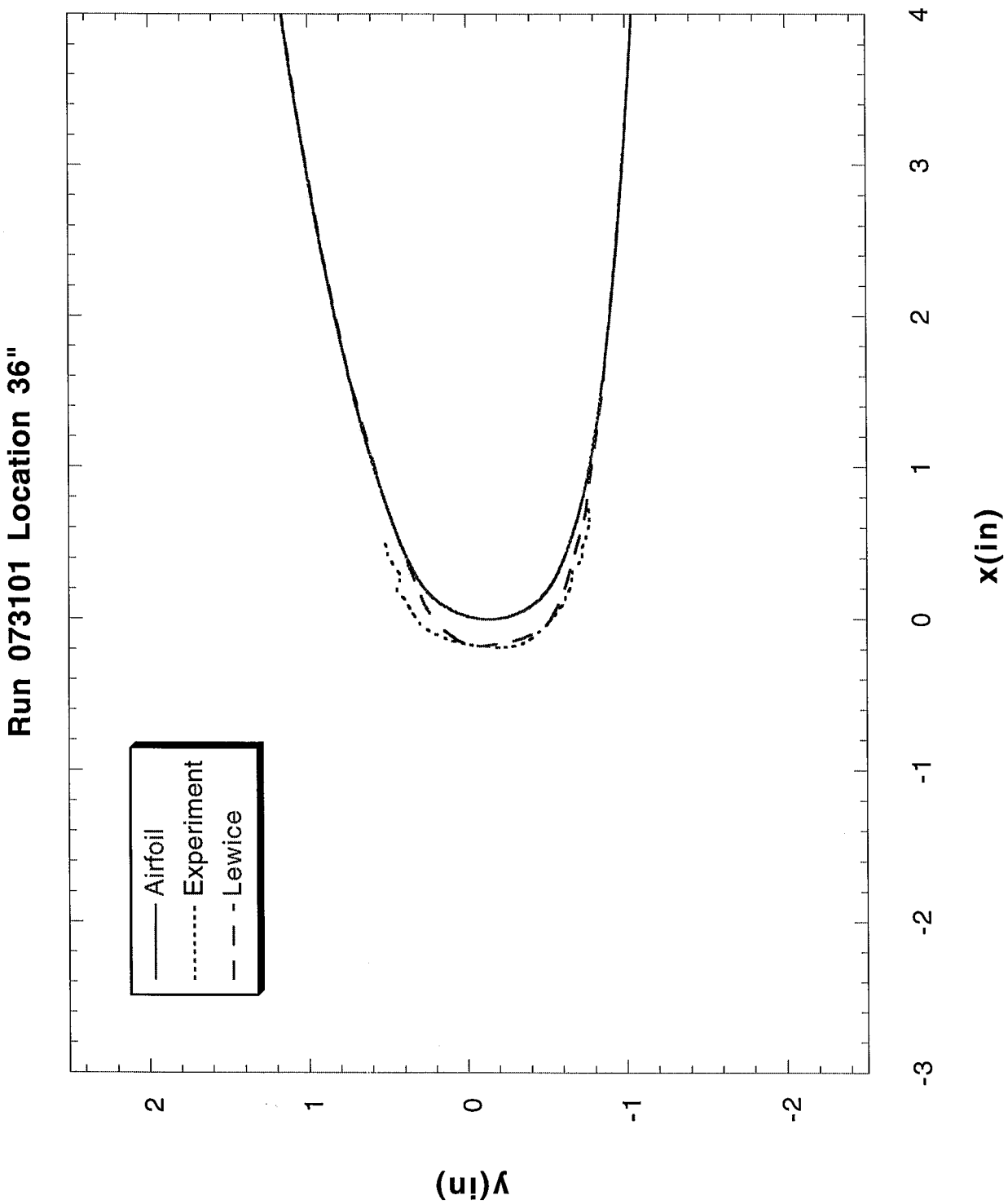
Run 073101 Location 36"
Airfoil
Experiment
Lewice
y(in)
x(in)
2
1
0
-1
-2
-3
-2
-1
0
1
2
3
4

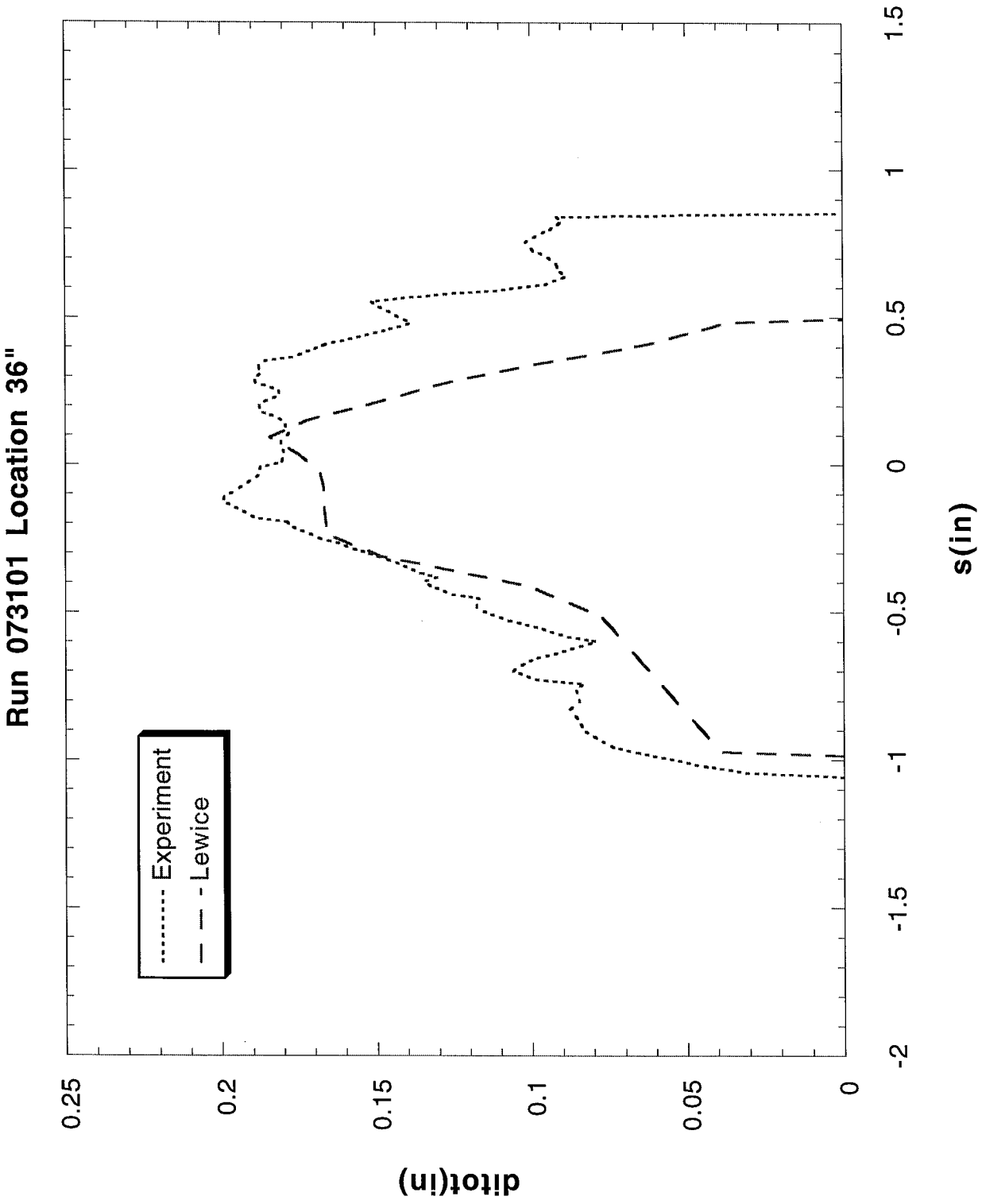
Run 073101 Location 36"
Experiment
Lewice
dltot(in)
s(in)
0.25
0.2
0.15
0.1
0.05
0
-2
-1.5
-1
-0.5
0
0.5
1
1.5

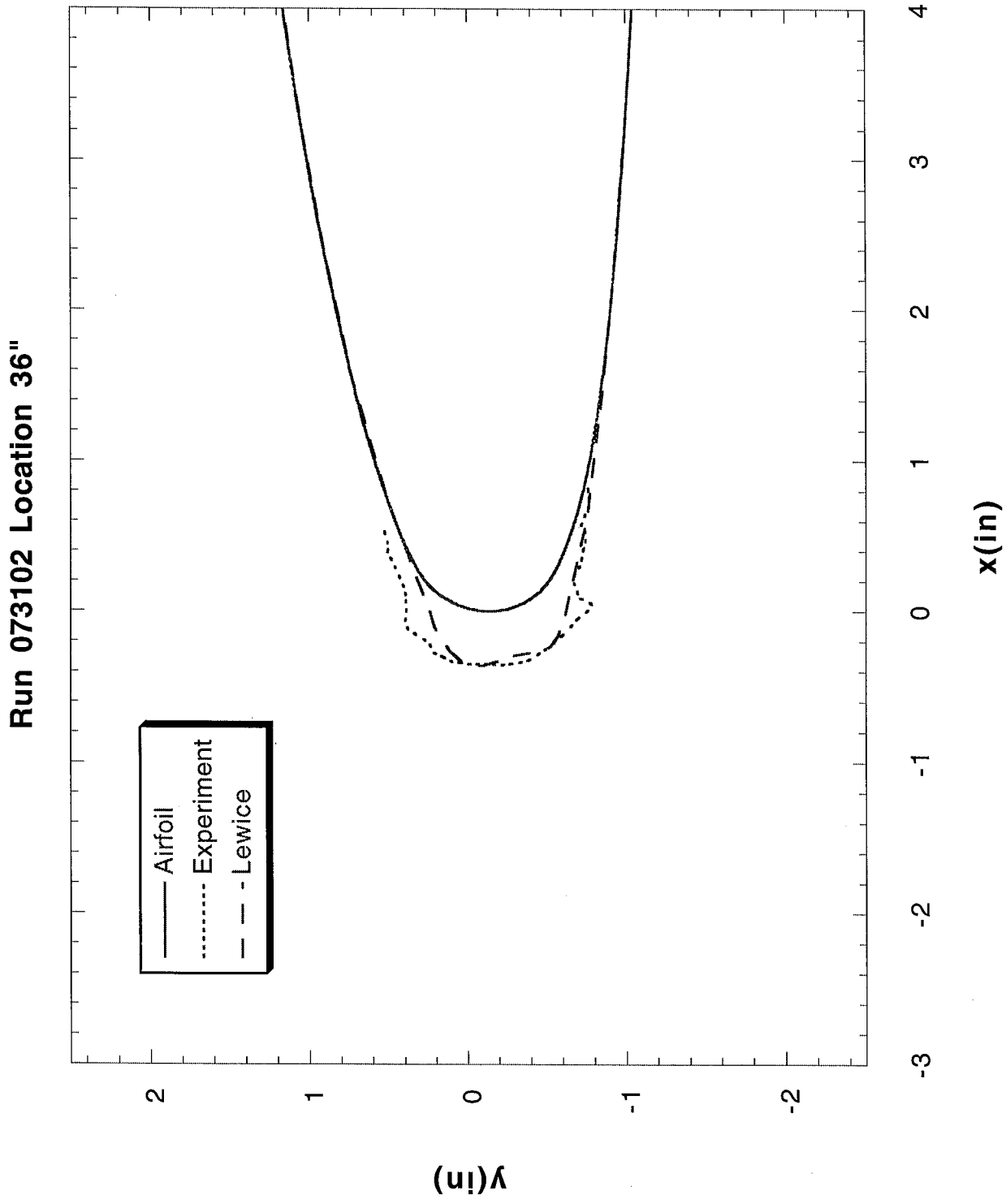
Run 073102 Location 36"
Airfoil
Experiment
Lewice
y(in)
x(in)
2
1
0
-1
-2
-3
-2
-1
0
1
2
3
4

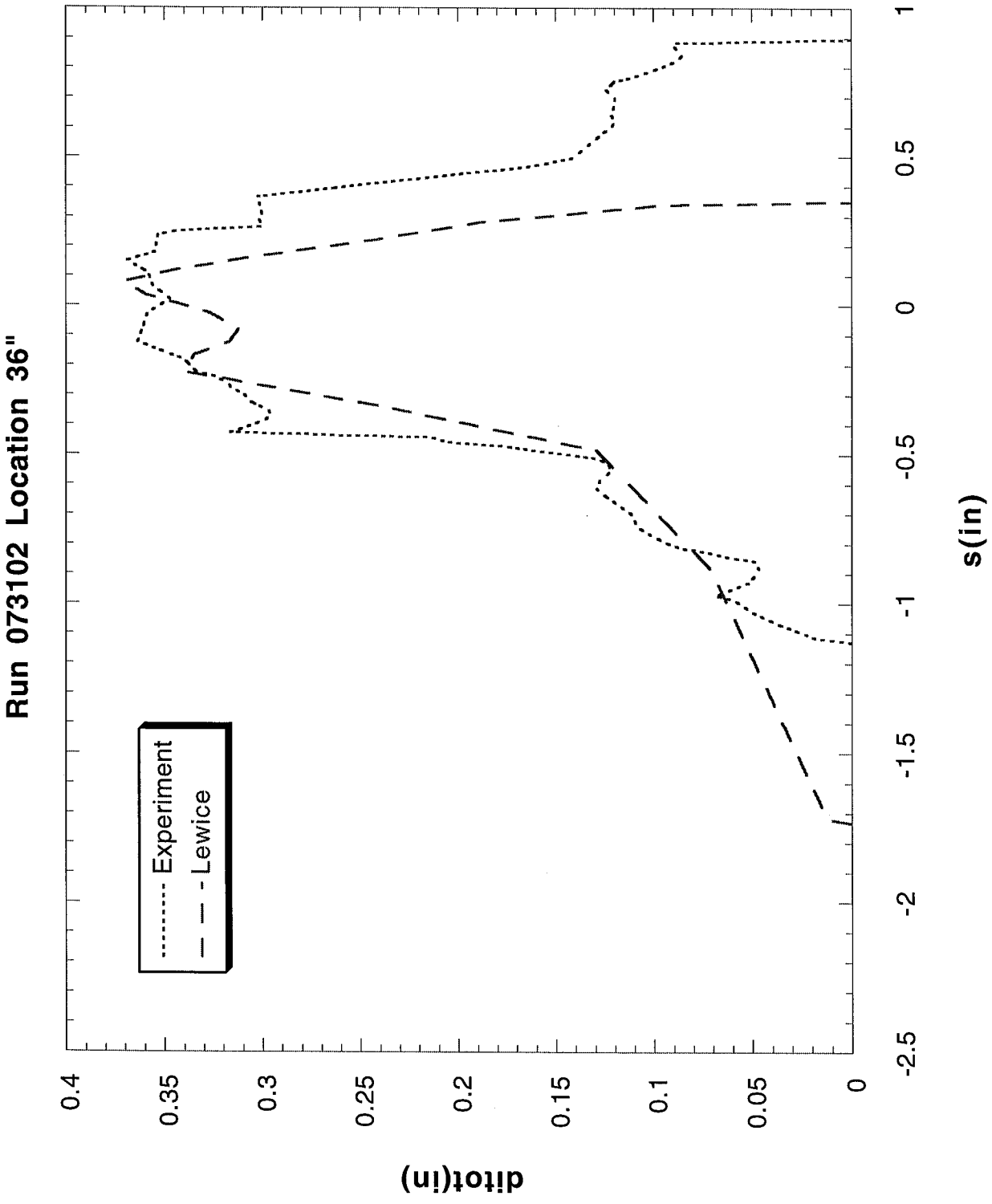
Run 073102 Location 36"
Experiment
Lewice
dltot(in)
s(in)
0.4
0.35
0.3
0.25
0.2
0.15
0.1
0.05
0
-2.5
-2
-1.5
-1
-0.5
0
0.5
1

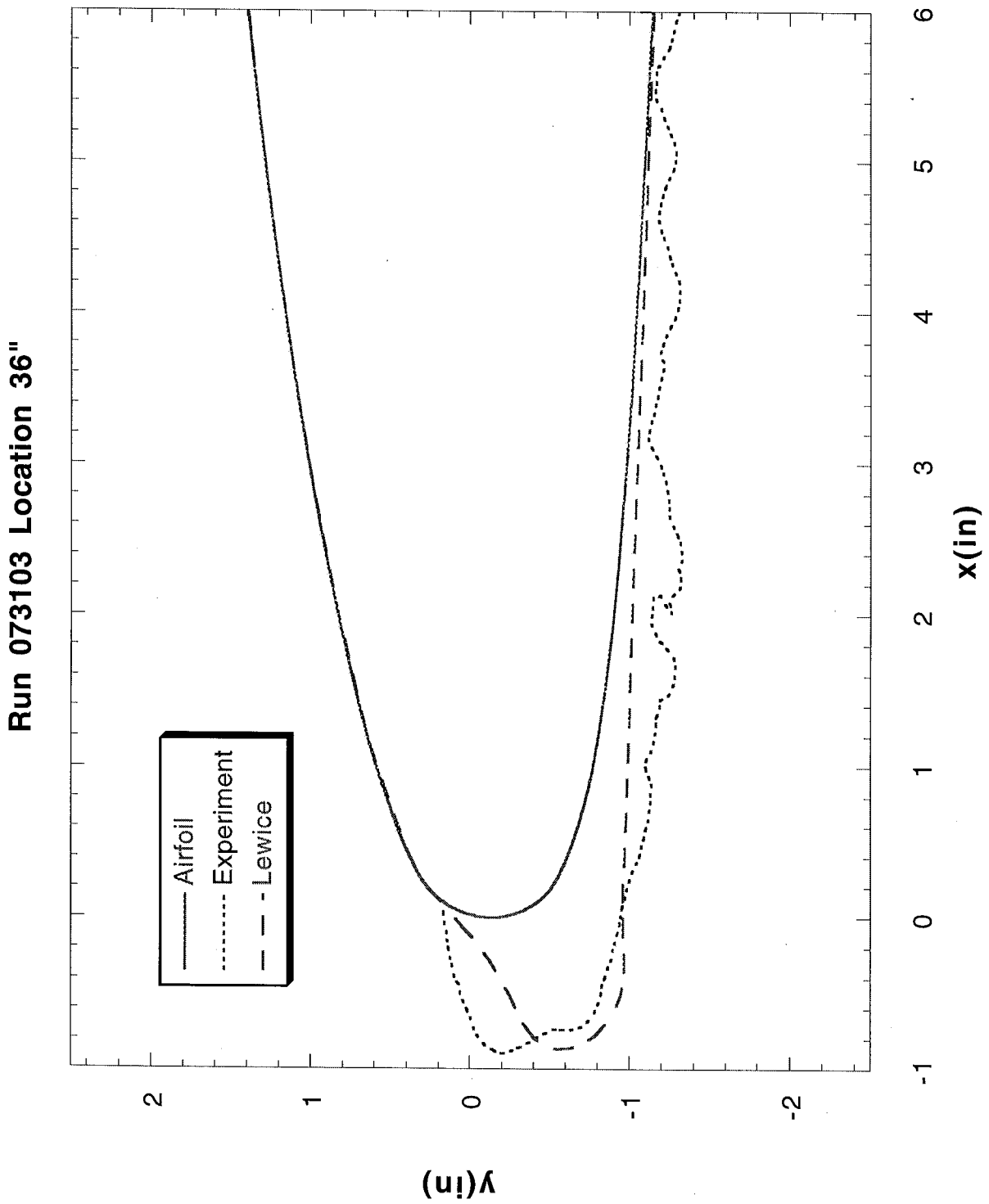
Run 073103 Location 36"
Airfoil
Experiment
Lewice
y(in)
x(in)
2
1
0
-1
-2
-1
0
1
2
3
4
5
6

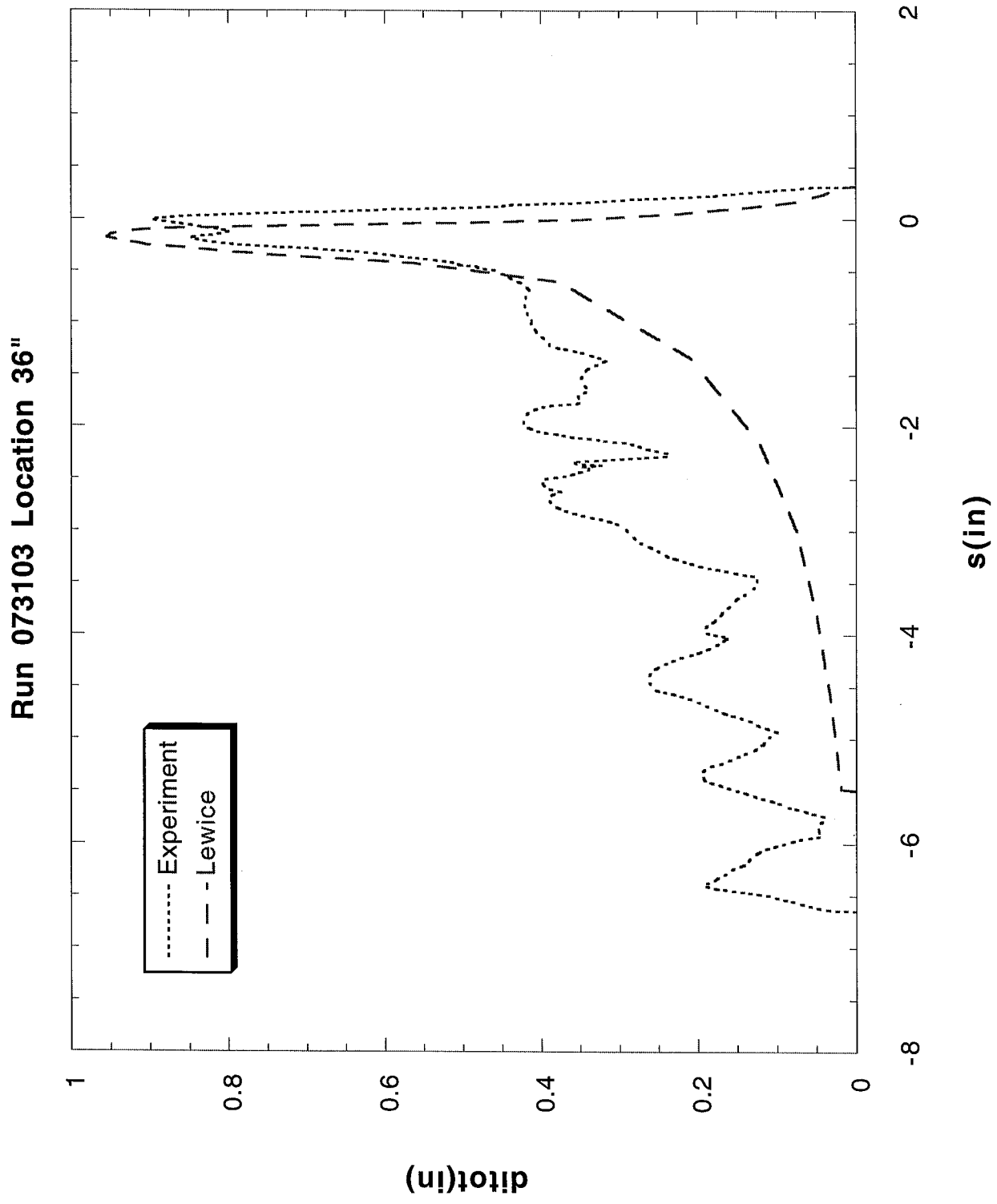
Run 073103 Location 36"
Experiment
Lewice
dltot(in)
s(in)
1
0.8
0.6
0.4
0.2
0
2
0
-2
-4
-6
-8

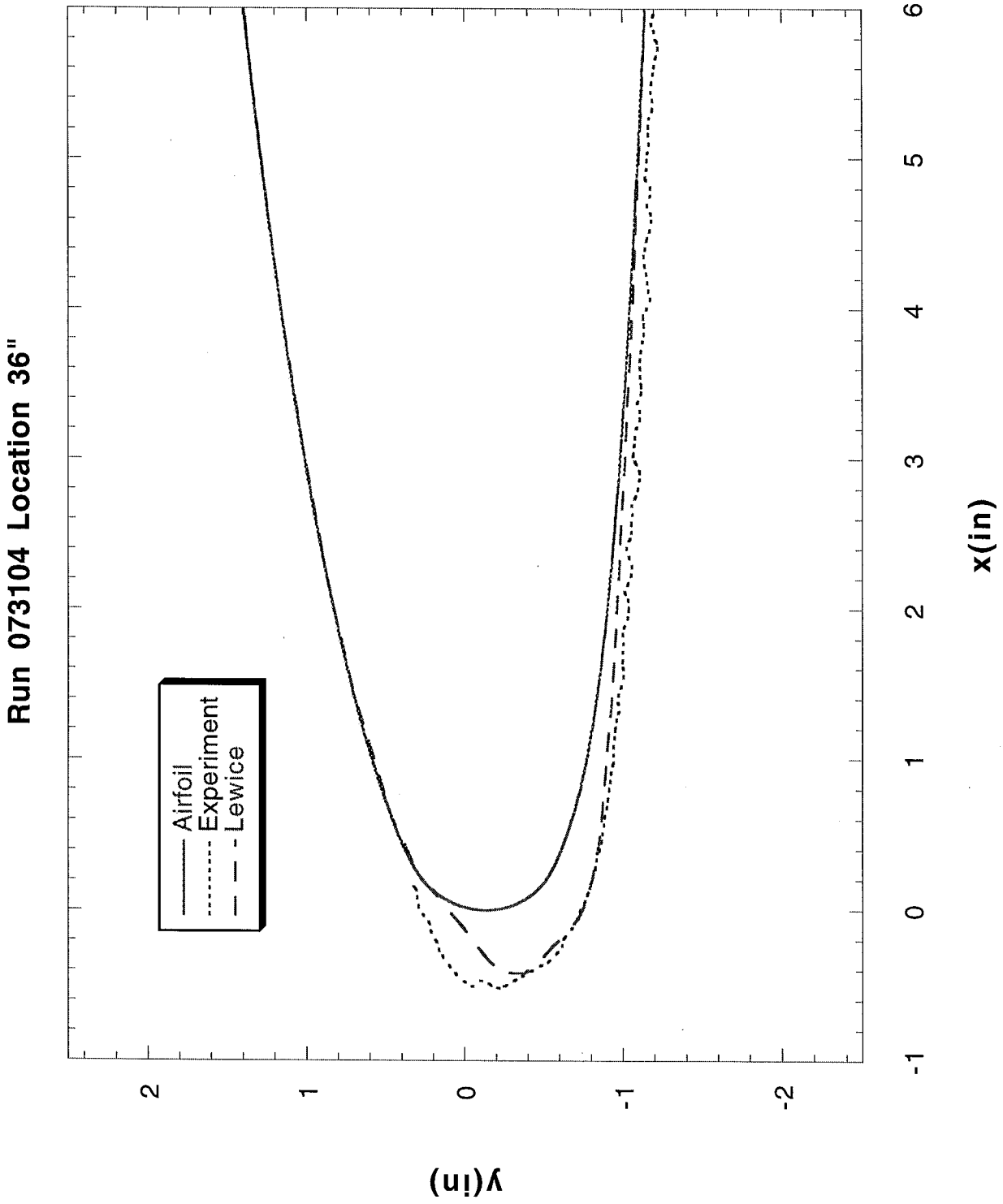
Run 073104 Location 36"
Airfoil
Experiment
Lewice
y(in)
x(in)
2
1
0
-1
-2
-1
0
1
2
3
4
5
6

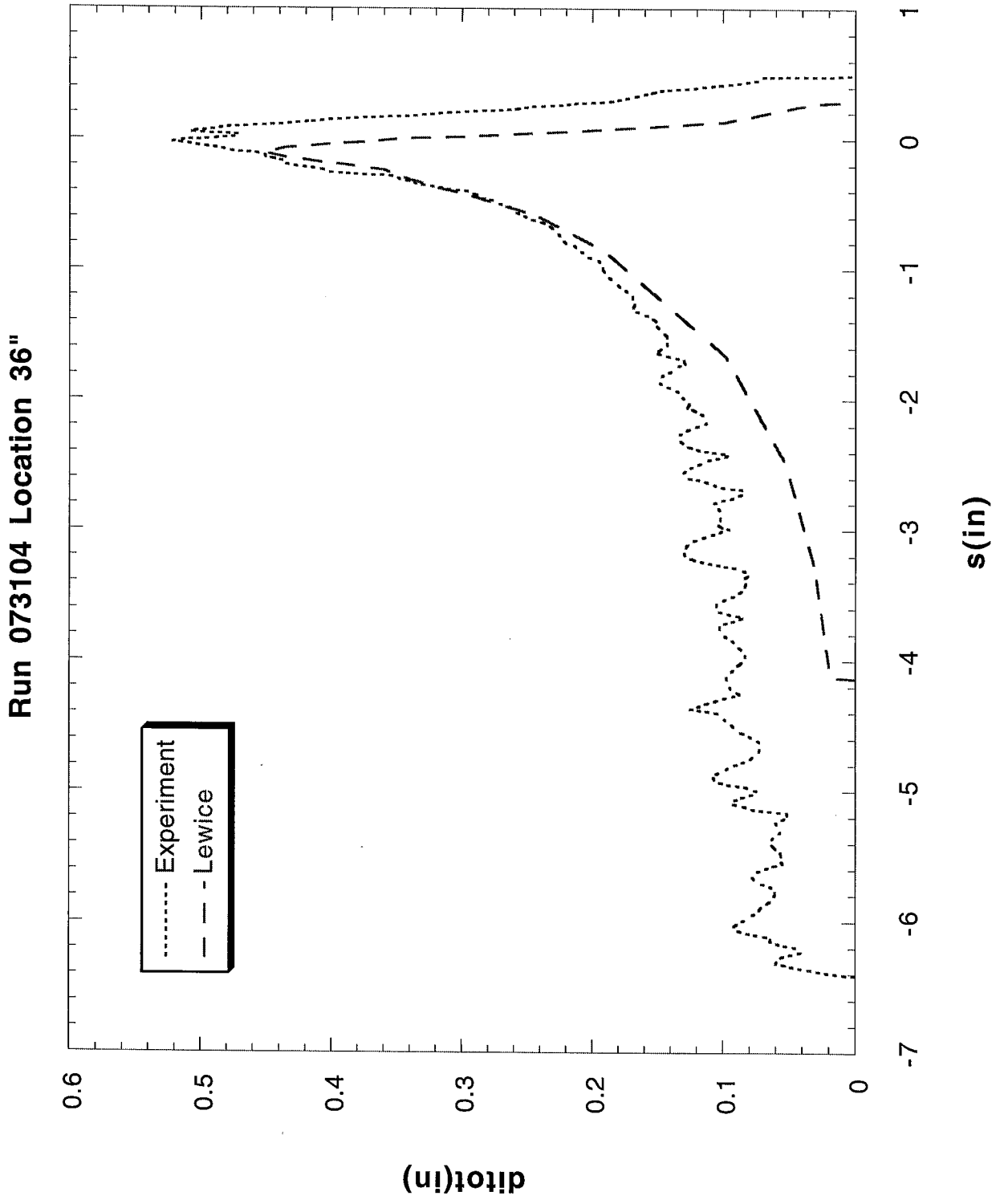
Run 073104 Location 36"
Experiment
Lewice
dltot(in)
s(in)
0.6
0.5
0.4
0.3
0.2
0.1
0
-7
-6
-5
-4
-3
-2
-1
0
1

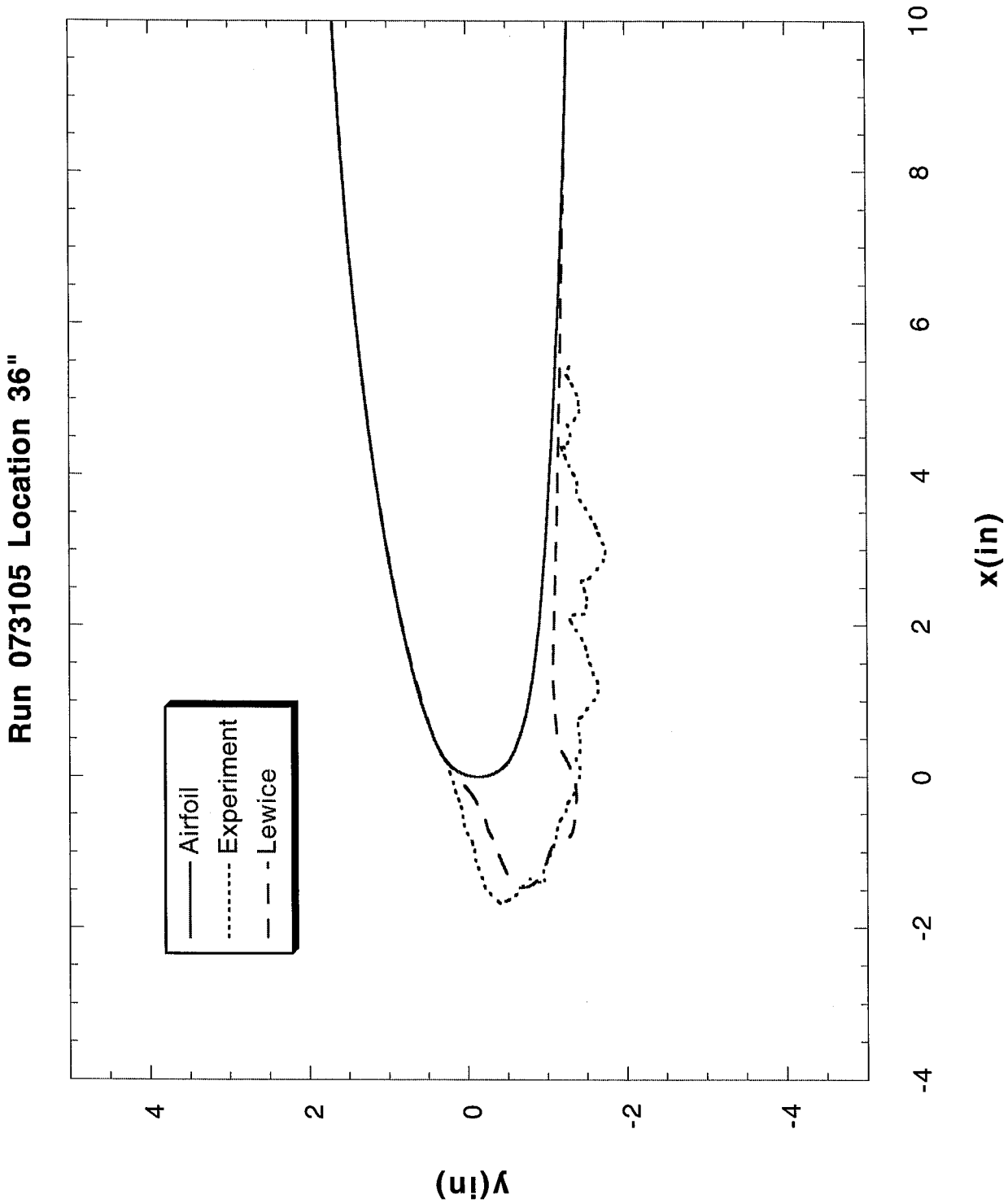
Run 073105 Location 36"
Airfoil
Experiment
Lewice
y(in)
x(in)
4
2
0
-2
-4
-4
-2
0
2
4
6
8
10

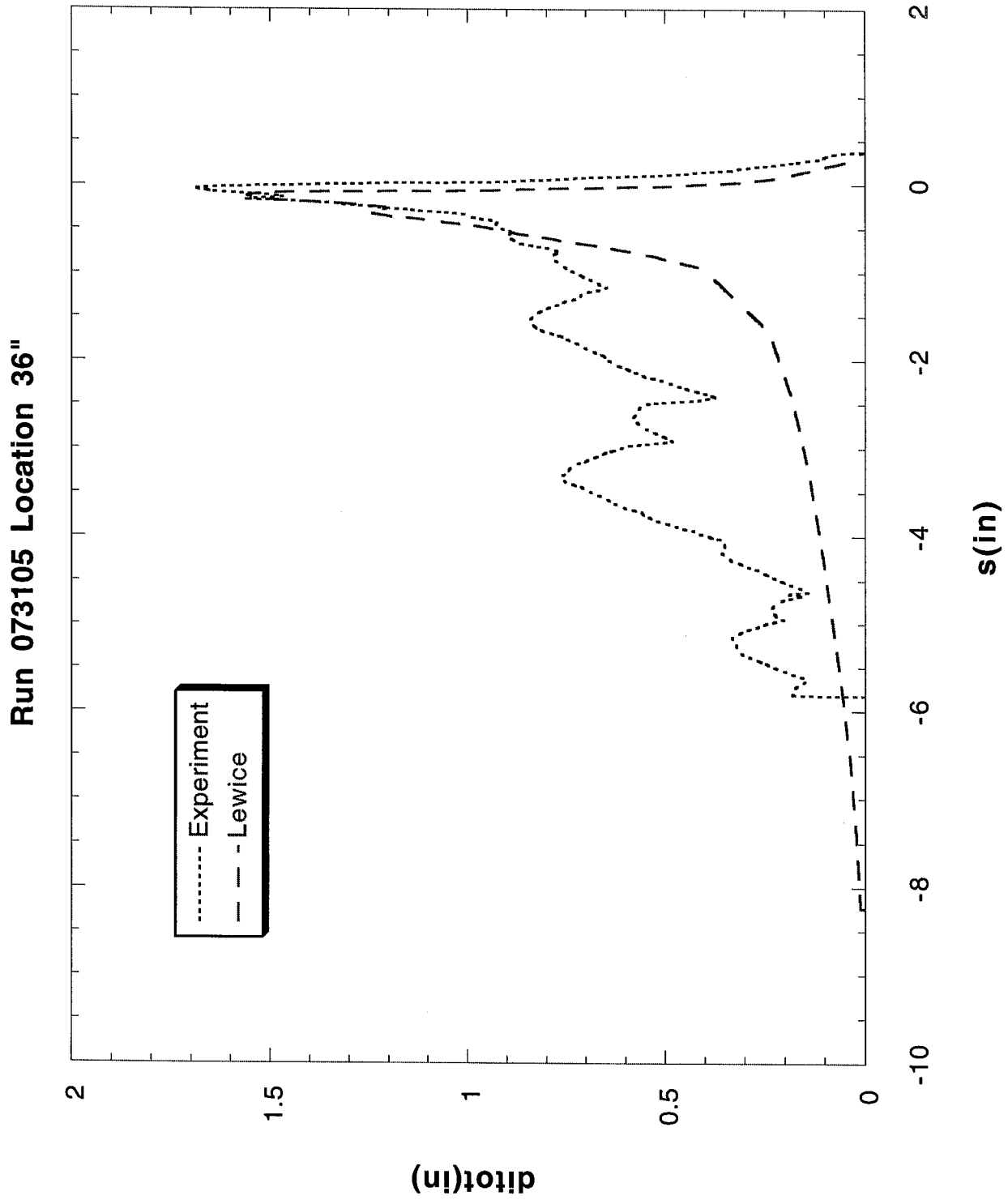
Run 073105 Location 36"
Experiment
Lewice
dltot(in)
s(in)
2
1.5
1
0.5
0
-10
-8
-6
-4
-2
0
2

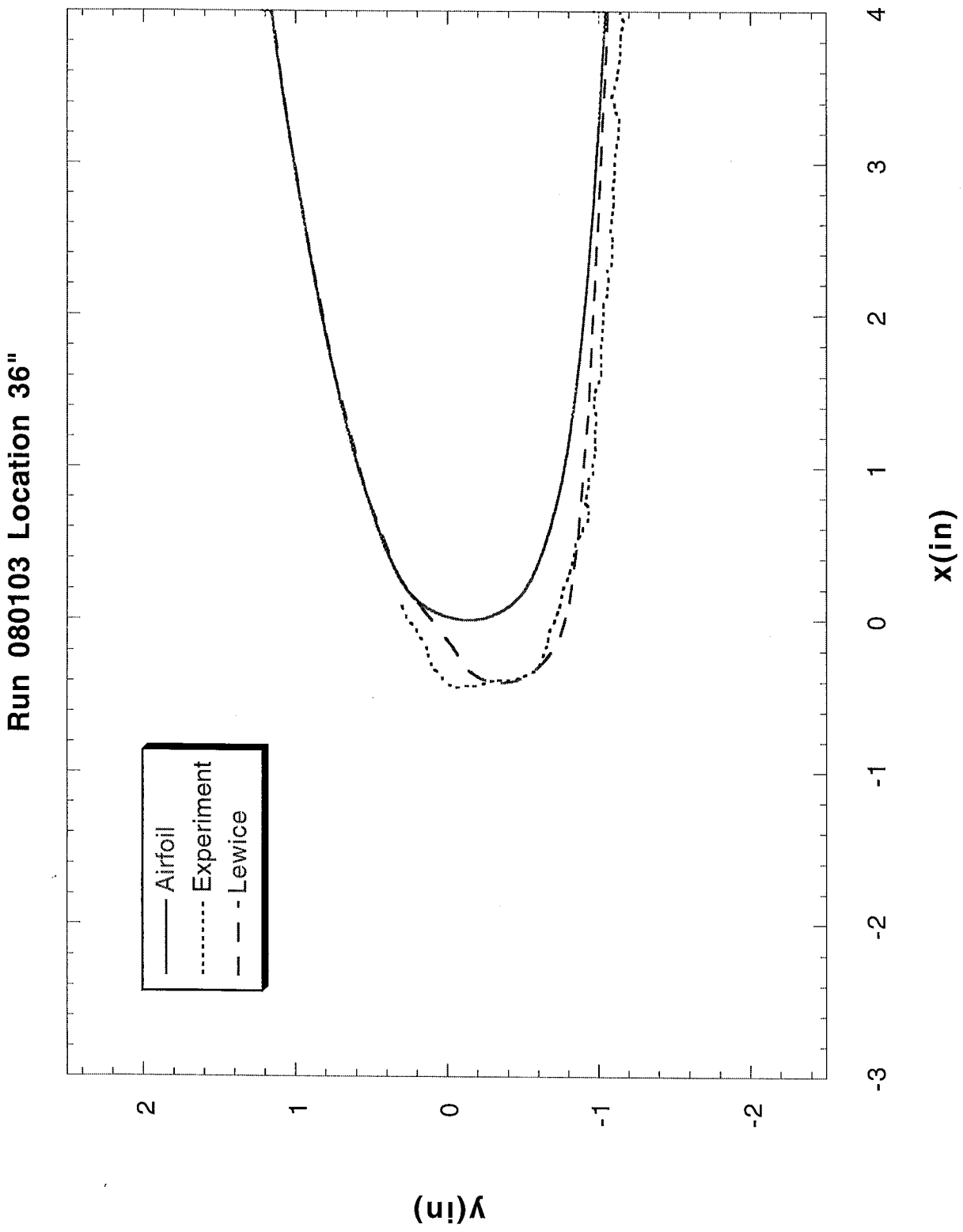
Run 080103 Location 36"
Airfoil
Experiment
Lewice
y(in)
x(in)
2
1
0
-1
-2
-3
-2
-1
0
1
2
3
4

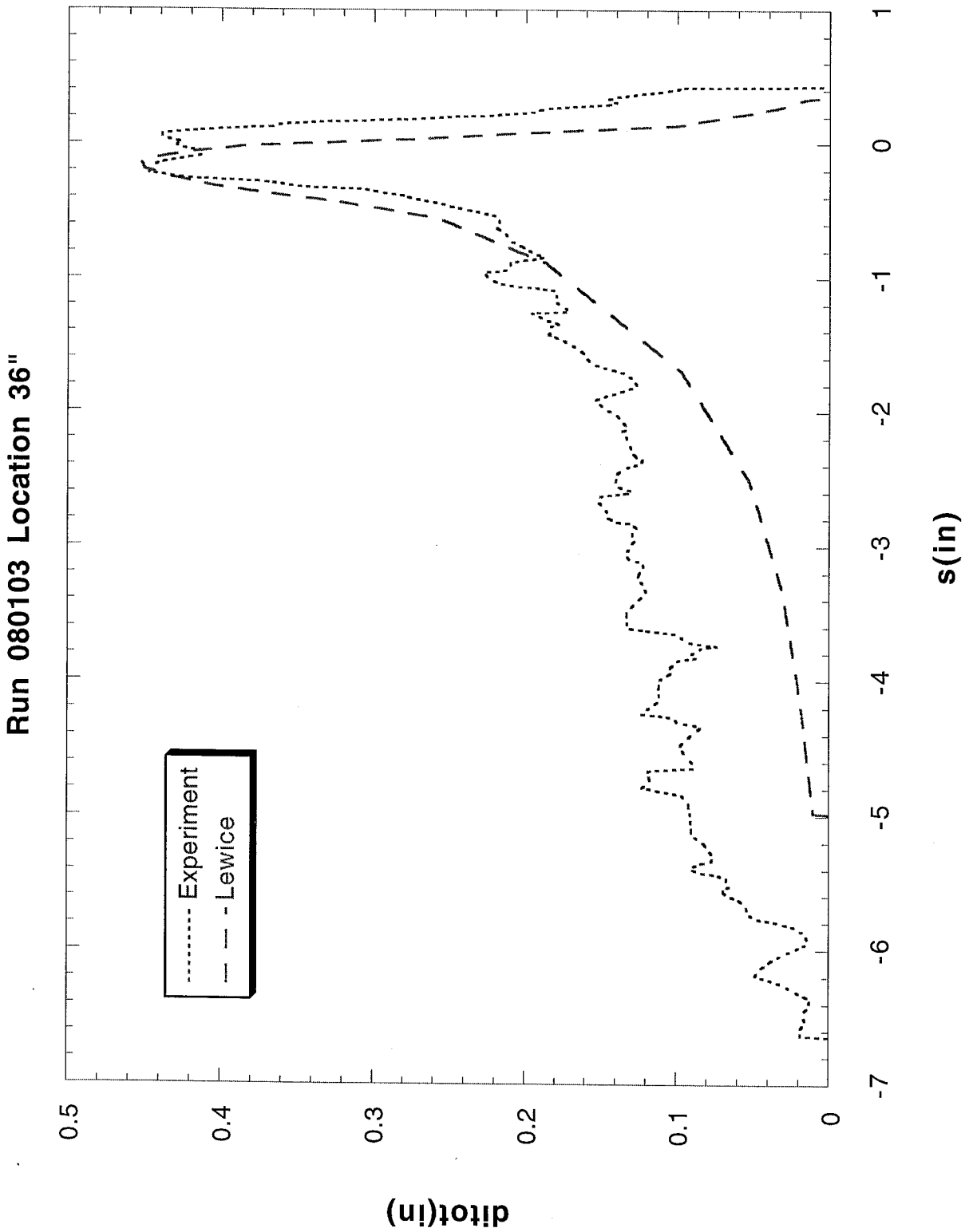
Run 080103 Location 36"
Experiment
- Lewice
dltot(in)
s(in)
0.5
0.4
0.3
0.2
0.1
0
-7
-6
-5
-4
-3
-2
-1
0
1

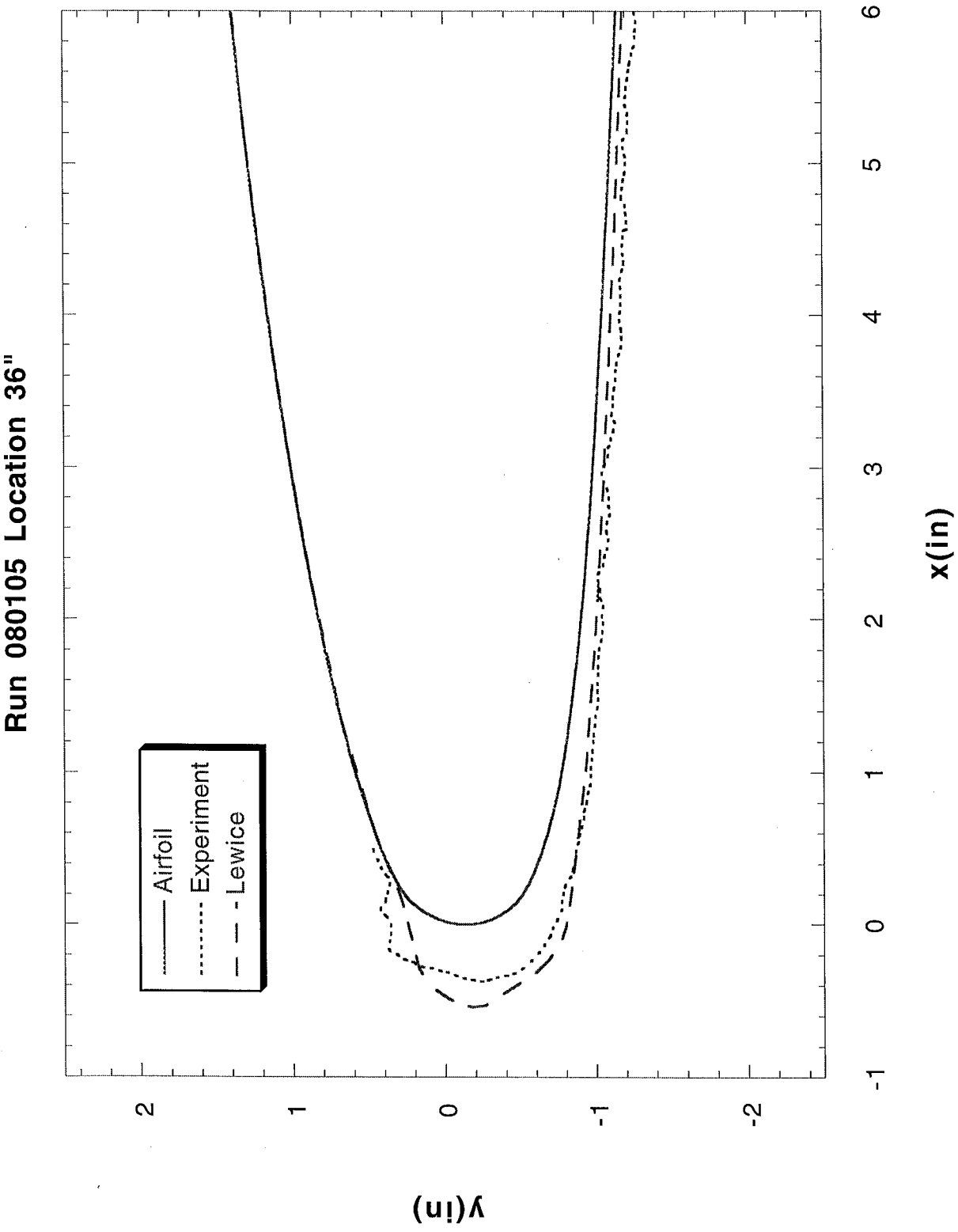
Run 080105 Location 36"
Airfoil
Experiment
Lewice
y(in)
x(in)
2
1
0
-1
-2
-1
0
1
2
3
4
5
6

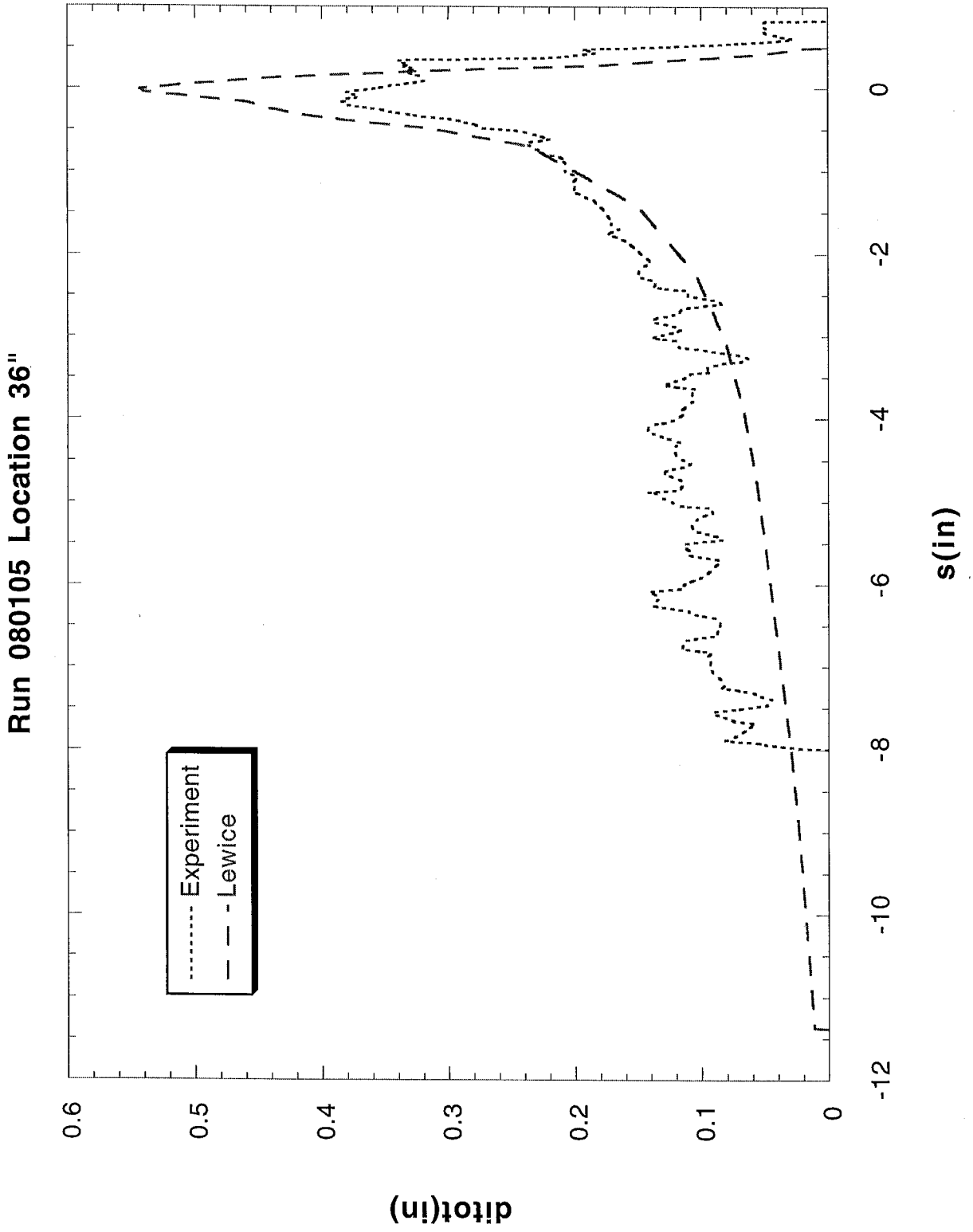
Run 080105 Location 36"
Experiment
Lewice
dltot(in)
s(in)
0.6
0.5
0.4
0.3
0.2
0.1
0
-12
-10
-8
-6
-4
-2
0

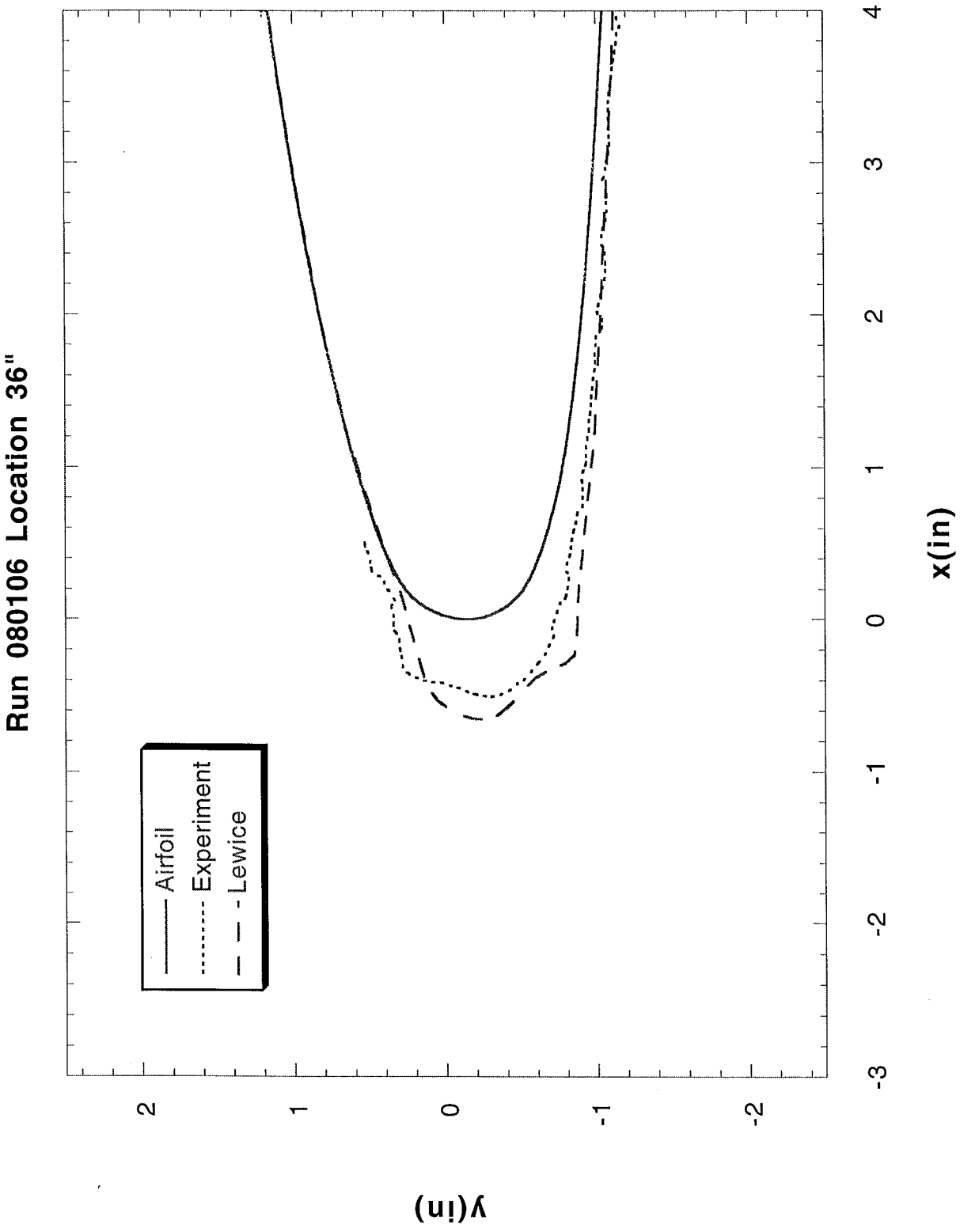
Run 080106 Location 36"
Airfoil
Experiment
Lewice
y(in)
x(in)
2
1
0
-1
-2
-3
-2
-1
0
1
2
3
4

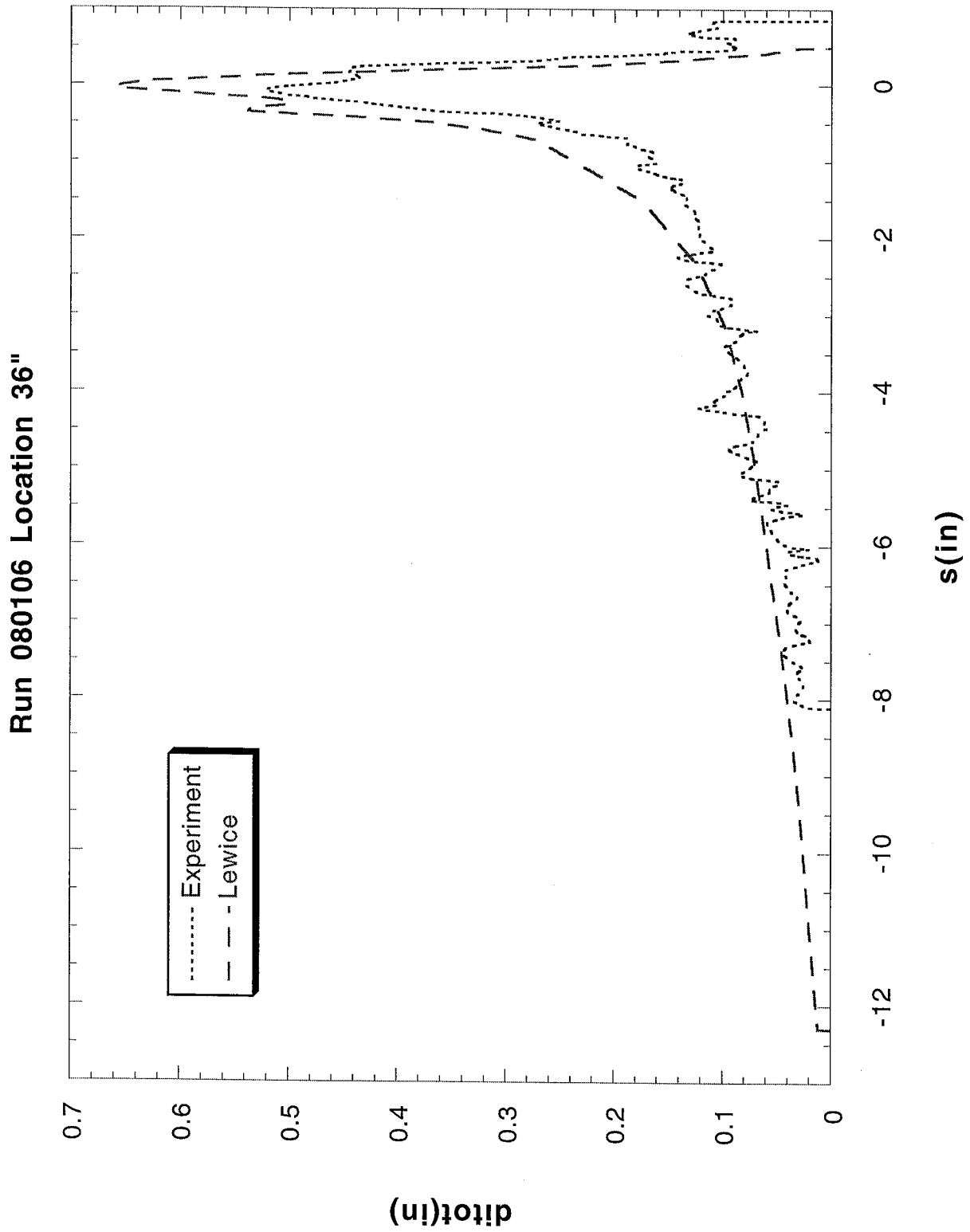
Run 080106 Location 36"
Experiment
Lewice
dltot(in)
0.7
0.6
0.5
0.4
0.3
0.2
0.1
0
s(in)
0
-2
-4
-6
-8
-10
-12

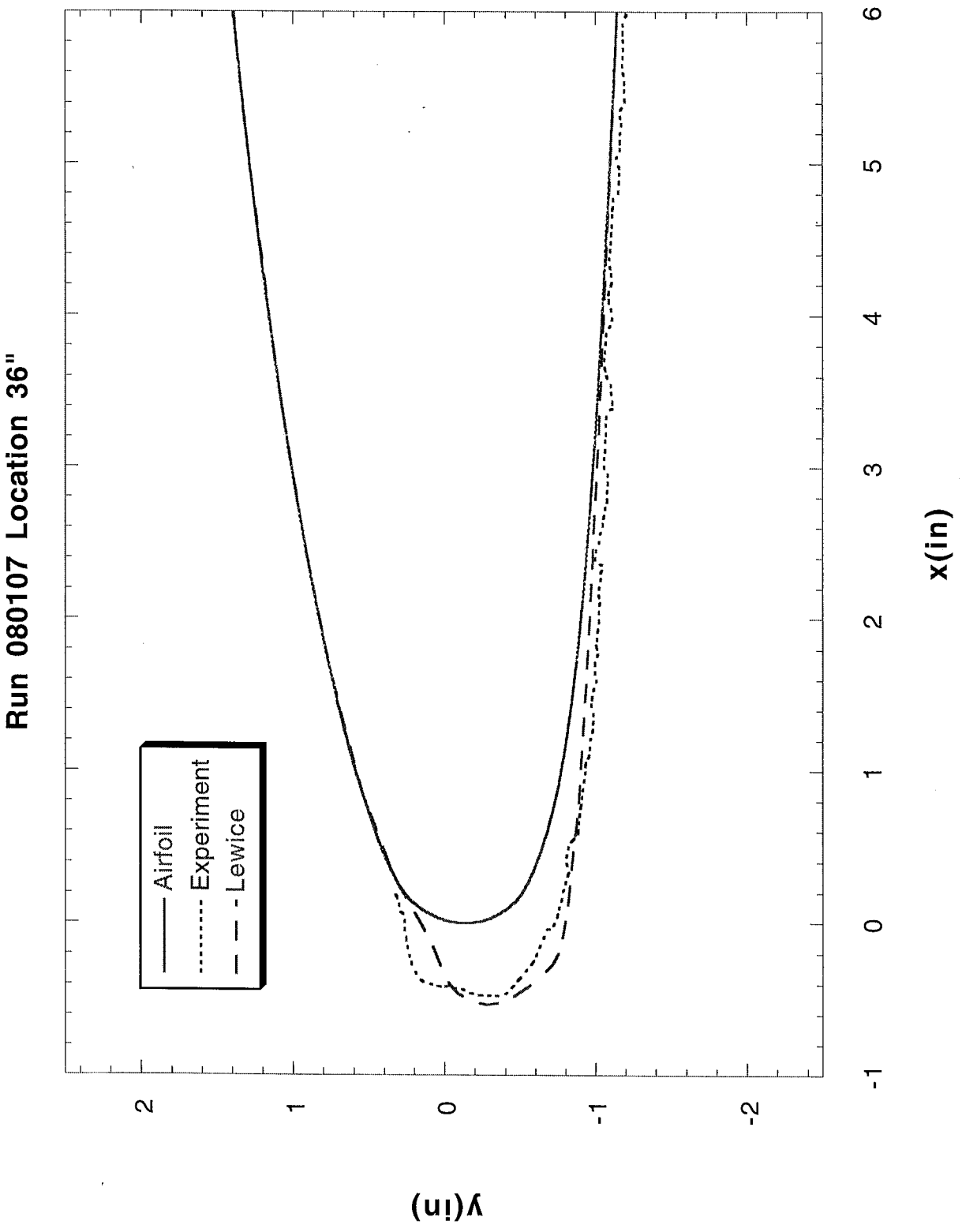
Run 080107 Location 36"
Airfoil
Experiment
Lewice
y(in)
x(in)
2
1
0
-1
-2
-1
0
1
2
3
4
5
6

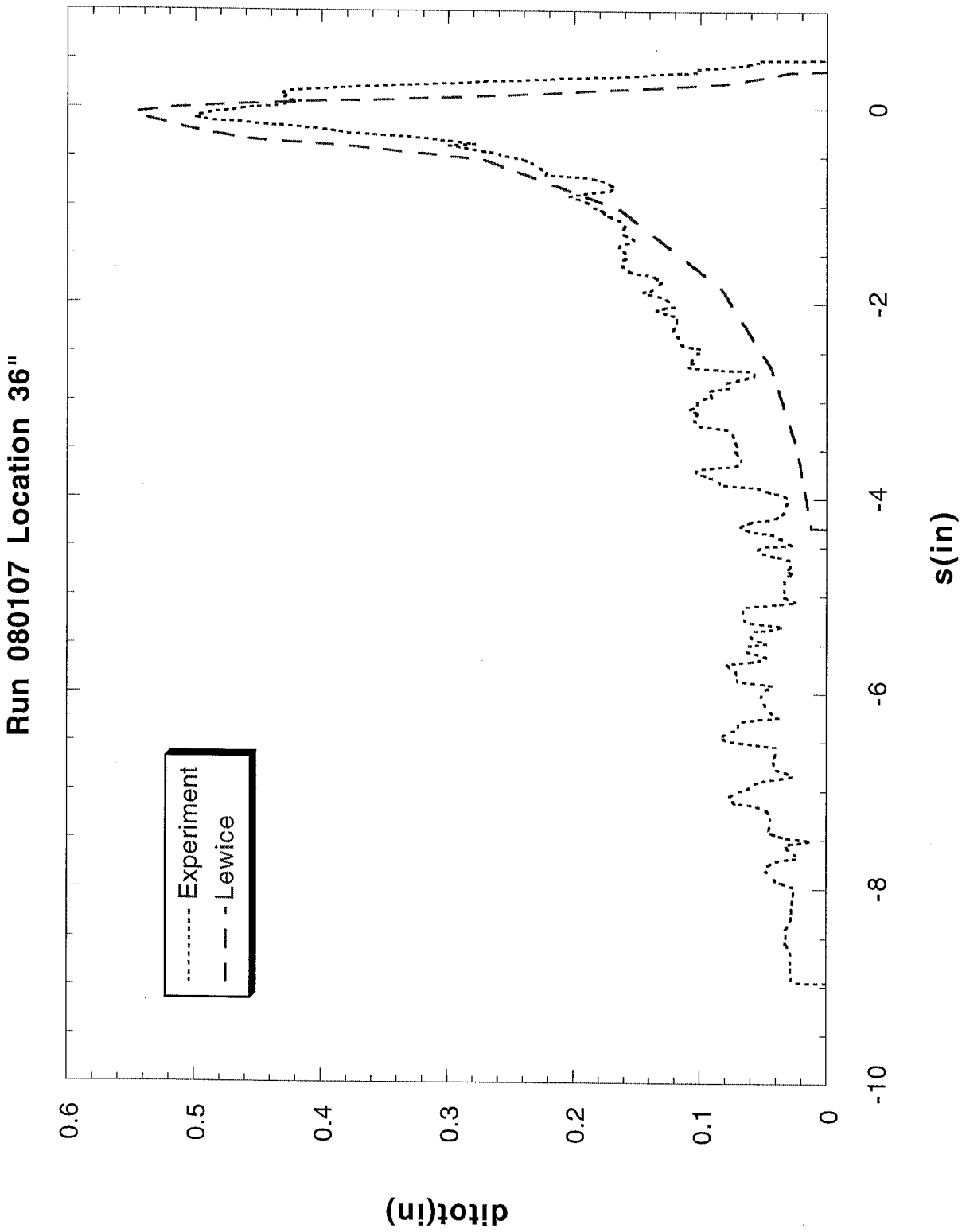
Run 080107 Location 36"
Experiment
Lewice
dltot(in)
s(in)
0.6
0.5
0.4
0.3
0.2
0.1
0
-10
-8
-6
-4
-2
0

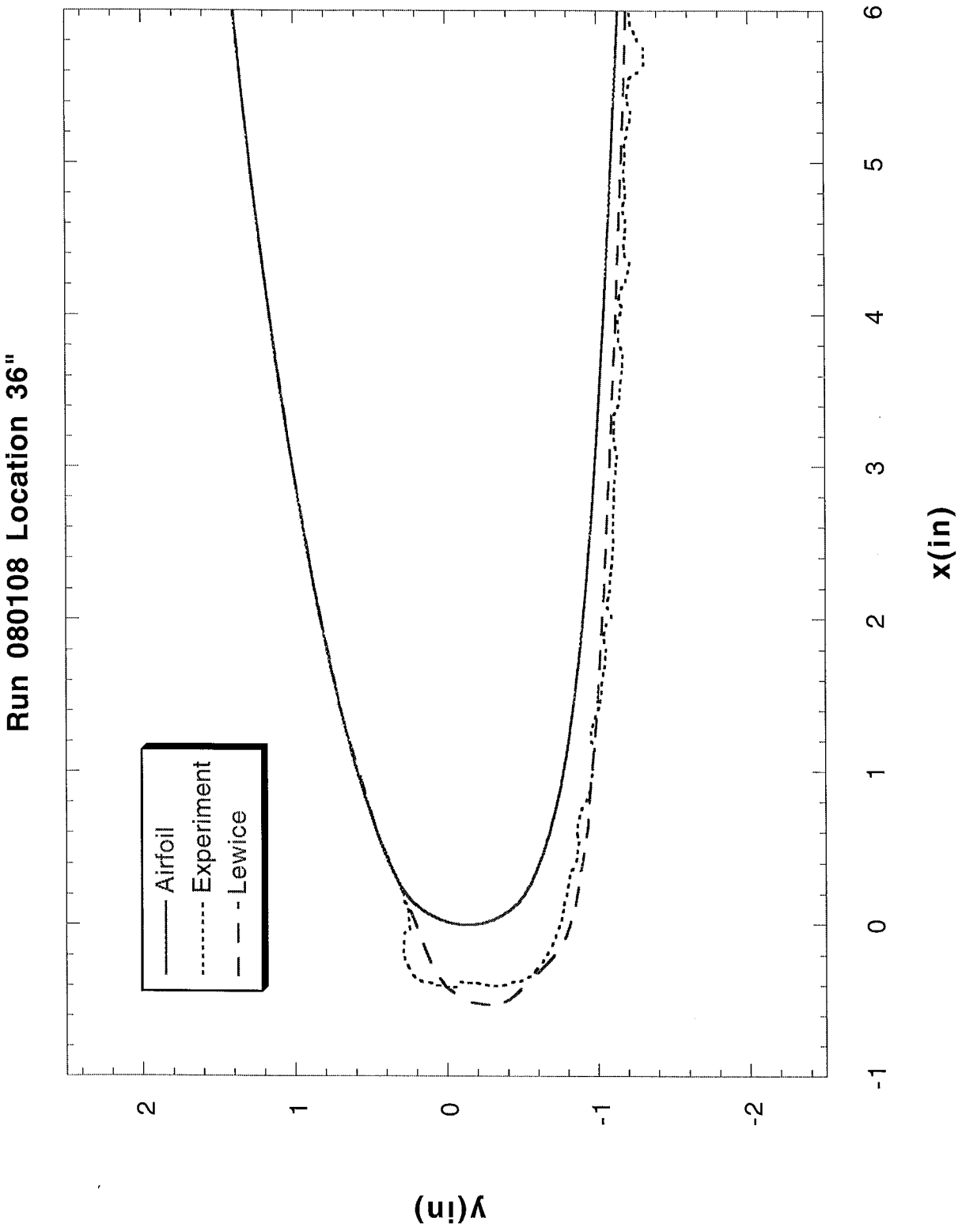
Run 080108 Location 36"
Airfoil
Experiment
Lewice
y(in)
x(in)
2
1
0
-1
-2
-1
0
1
2
3
4
5
6

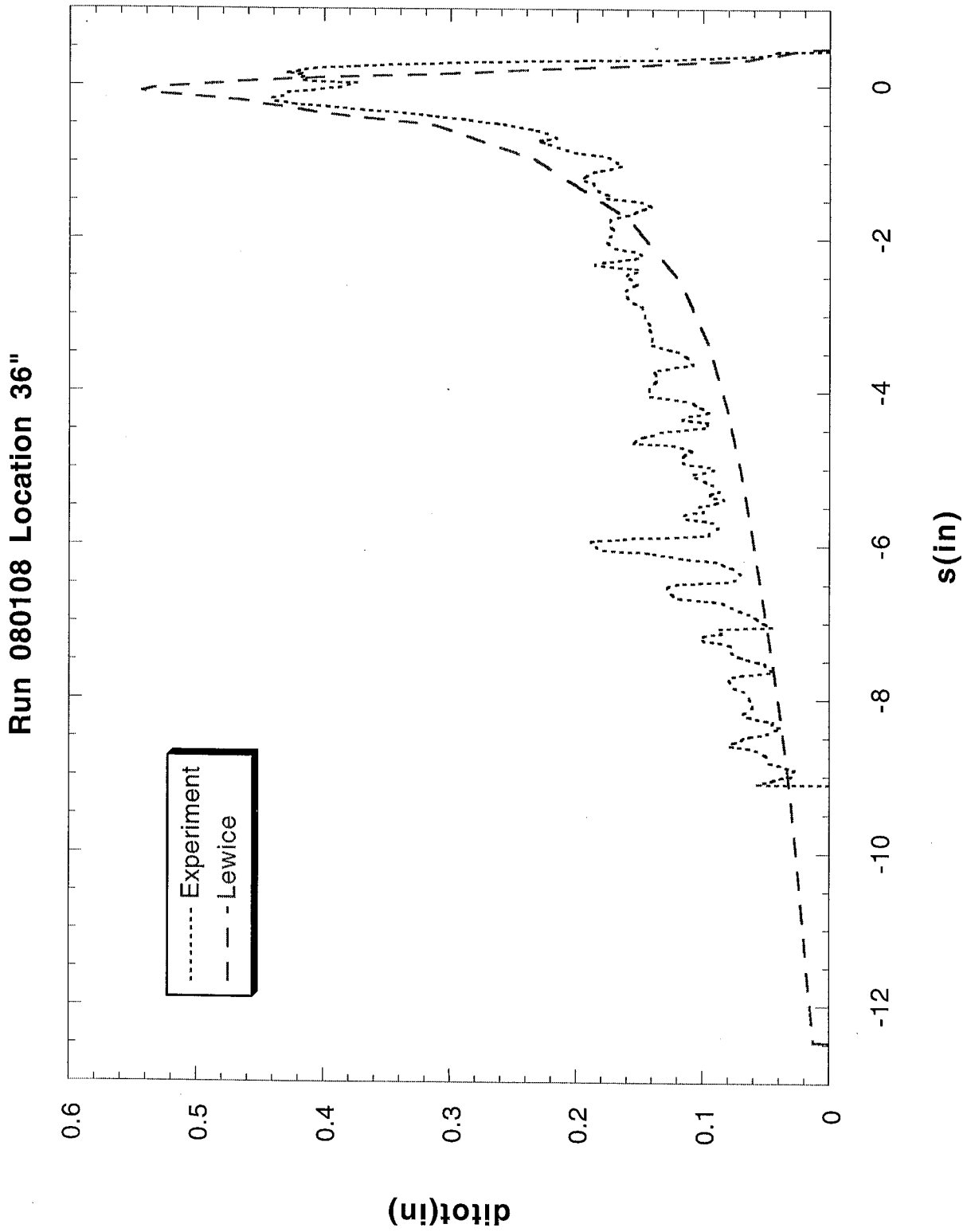
Run 080108 Location 36"
Experiment
Lewice
dltot(in)
s(in)
0.6
0.5
0.4
0.3
0.2
0.1
0
-12
-10
-8
-6
-4
-2
0

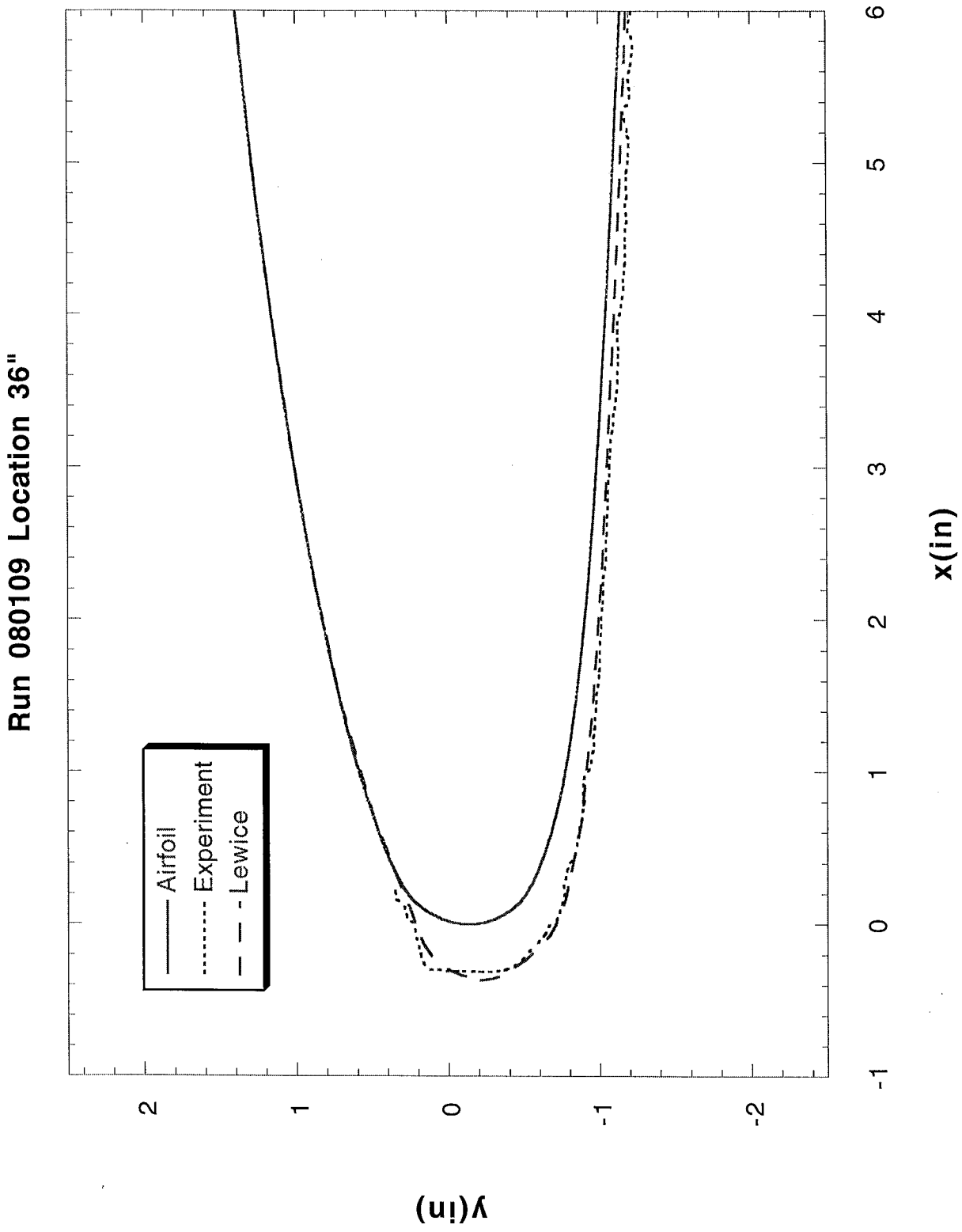
Run 080109 Location 36"
Airfoil
Experiment
Lewice
y(in)
x(in)
2
1
0
-1
-2
-1
0
1
2
3
4
5
6

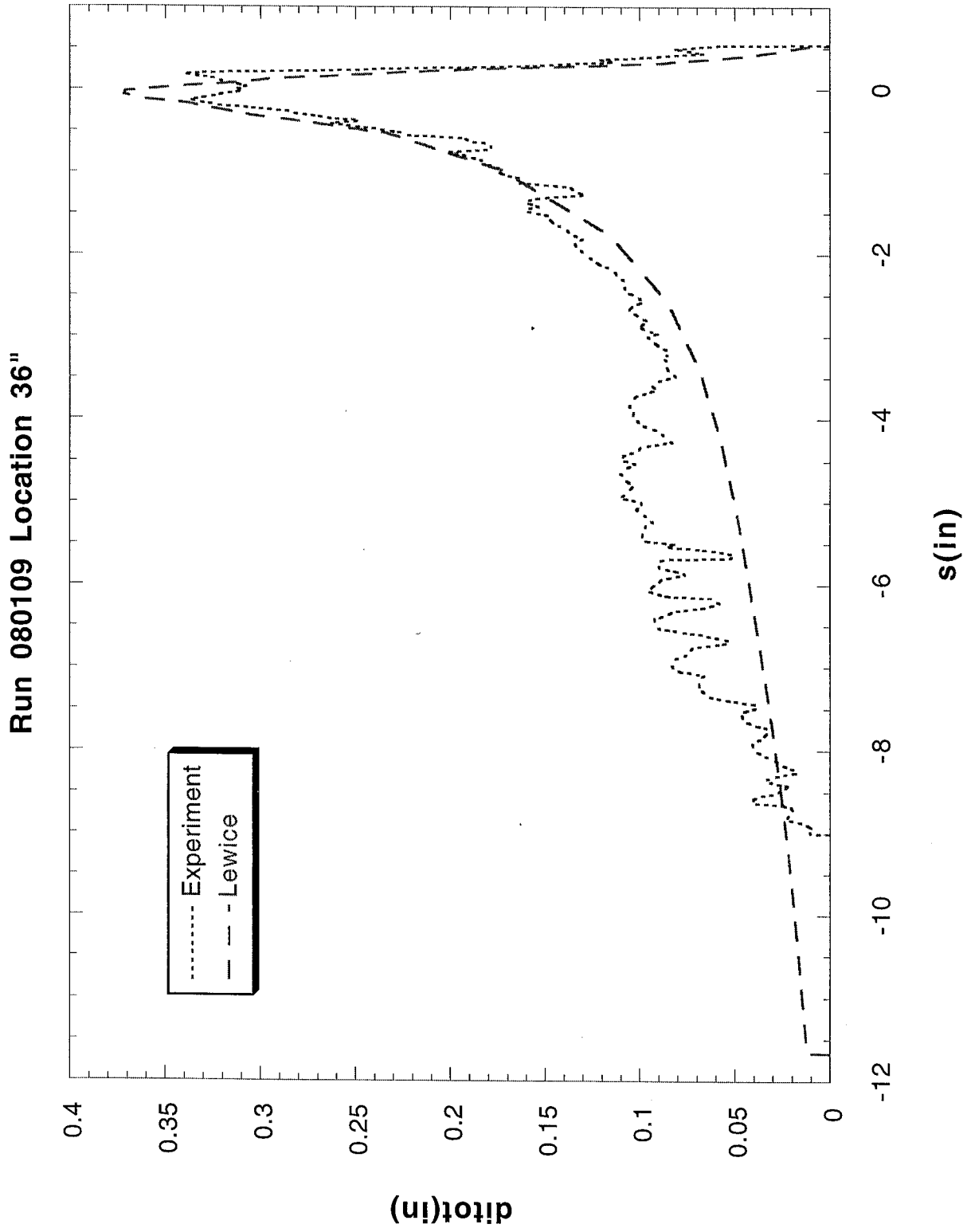
Run 080109 Location 36"
Experiment
Lewice
ditot(in)
s(in)
0.4
0.35
0.3
0.25
0.2
0.15
0.1
0.05
0
-12
-10
-8
-6
-4
-2
0

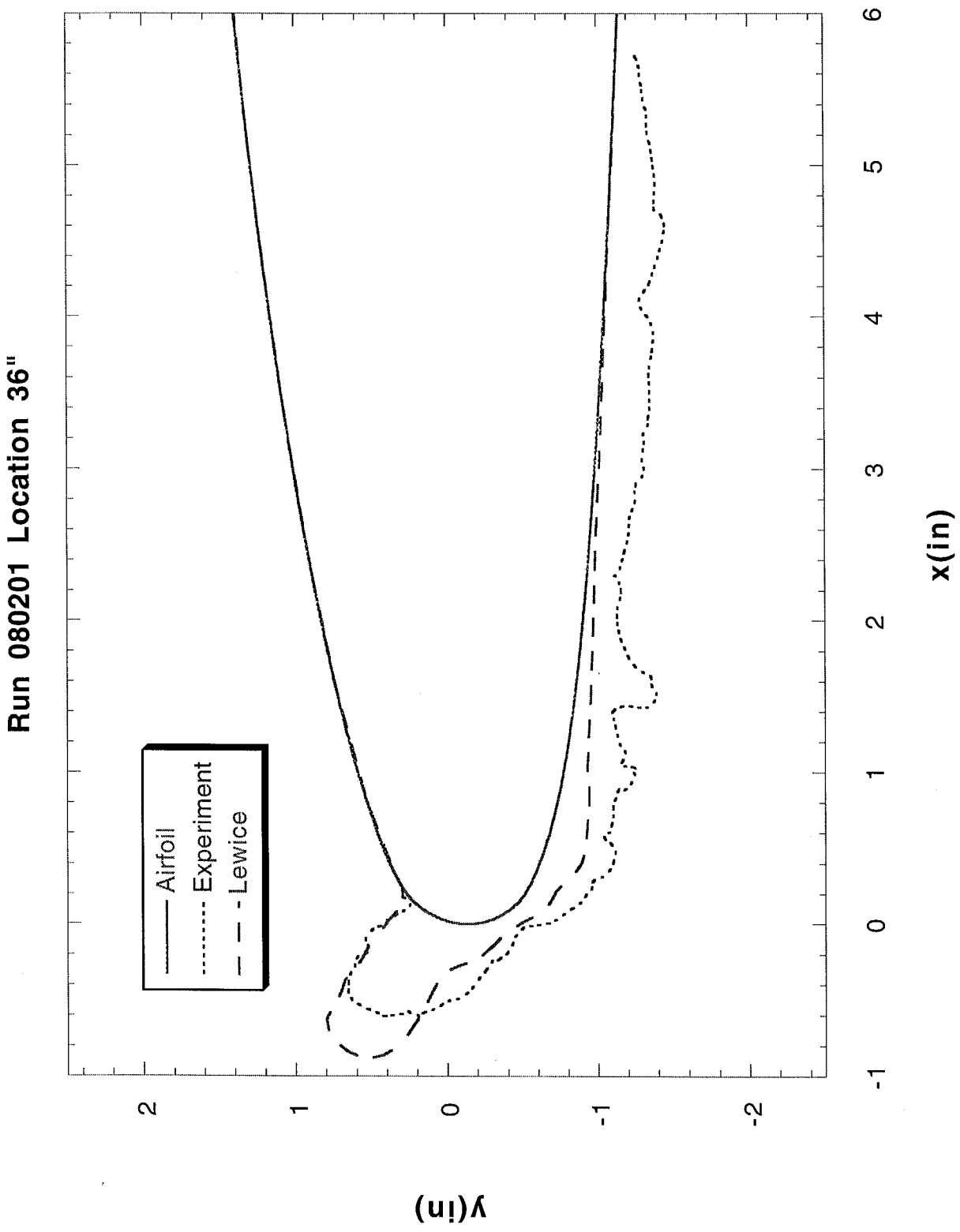
Run 080201 Location 36"
Airfoil
Experiment
Lewice
y(in)
x(in)
2
1
0
-1
-2
-1
0
1
2
3
4
5
6

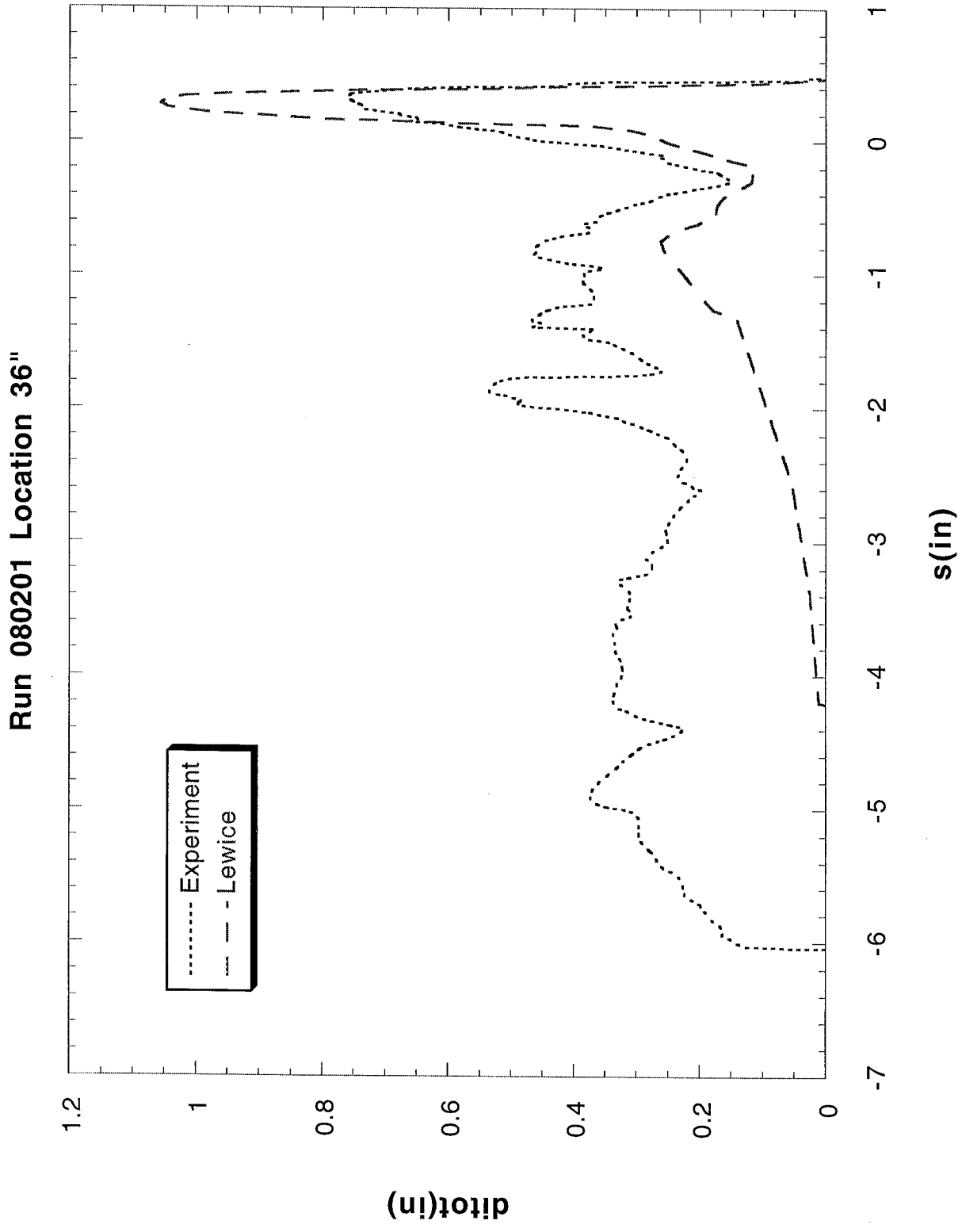
Run 080201 Location 36"
Experiment
Lewice
dltot(in)
s(in)
1.2
1
0.8
0.6
0.4
0.2
0
-7
-6
-5
-4
-3
-2
-1
0
1

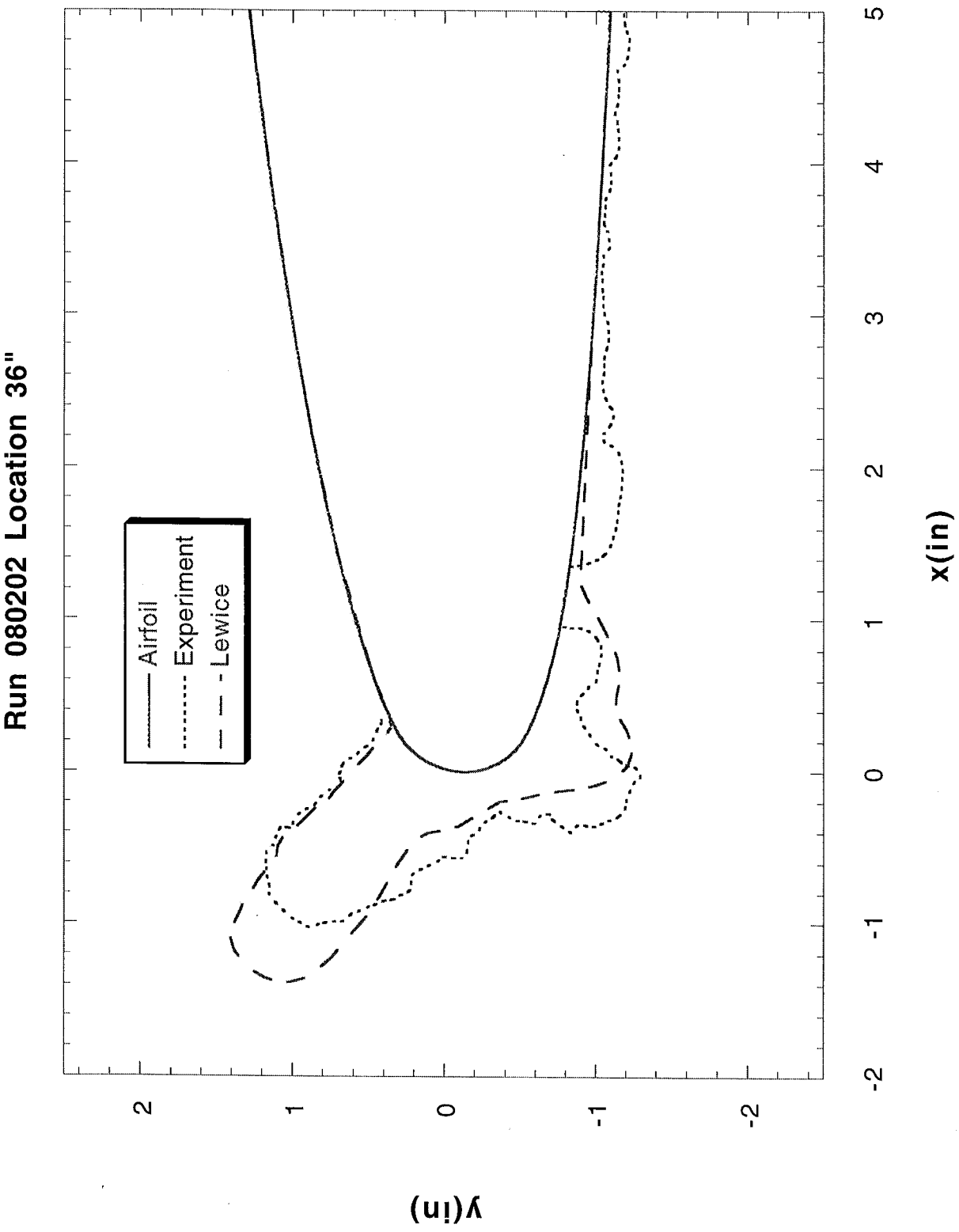
Run 080202 Location 36"
Airfoil
Experiment
Lewice
y(in)
x(in)
2
1
0
-1
-2
-2
-1
0
1
2
3
4
5

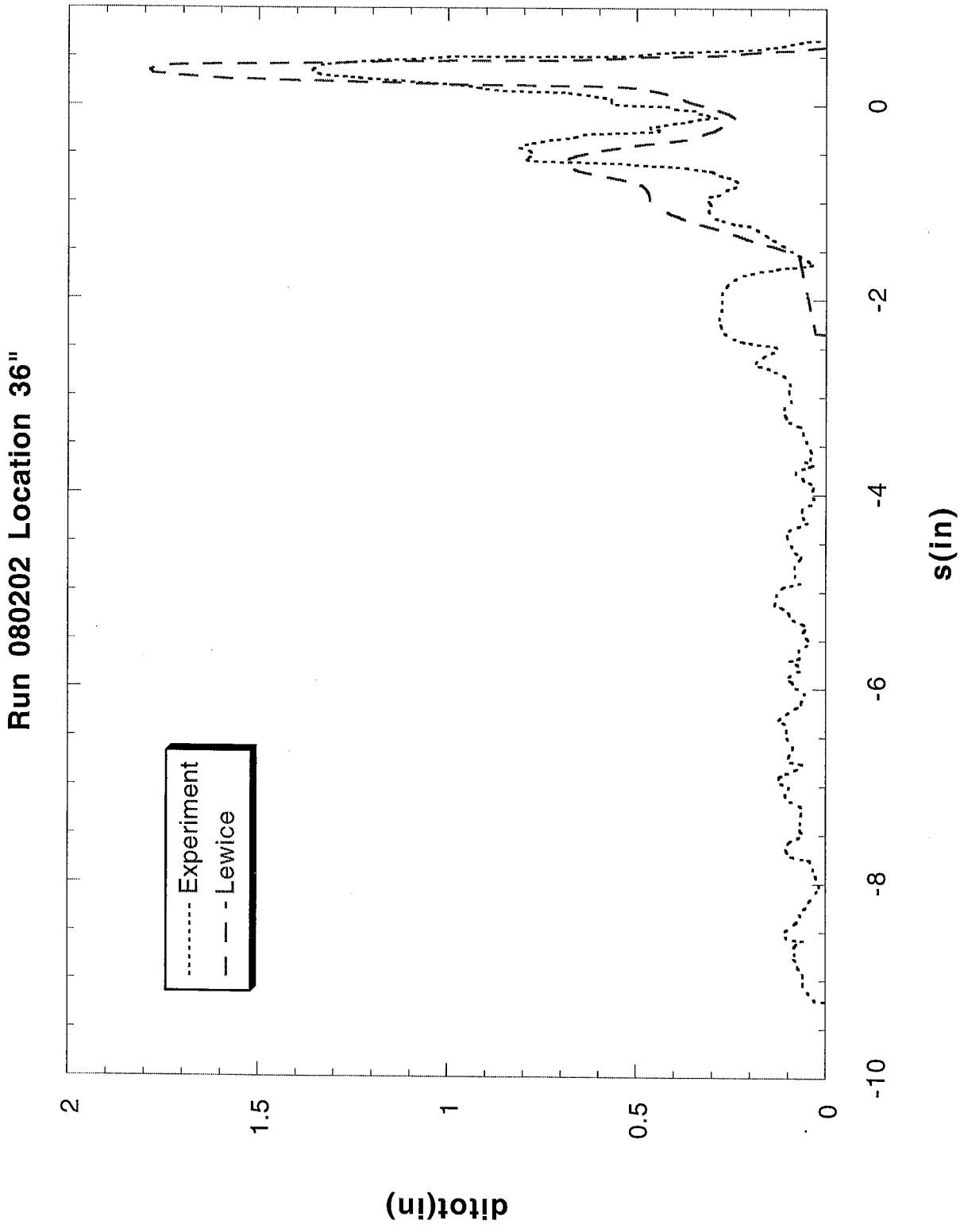
Run 080202 Location 36"
Experiment
Lewice
dltot(in)
s(in)
2
1.5
1
0.5
0
-10
-8
-6
-4
-2
0

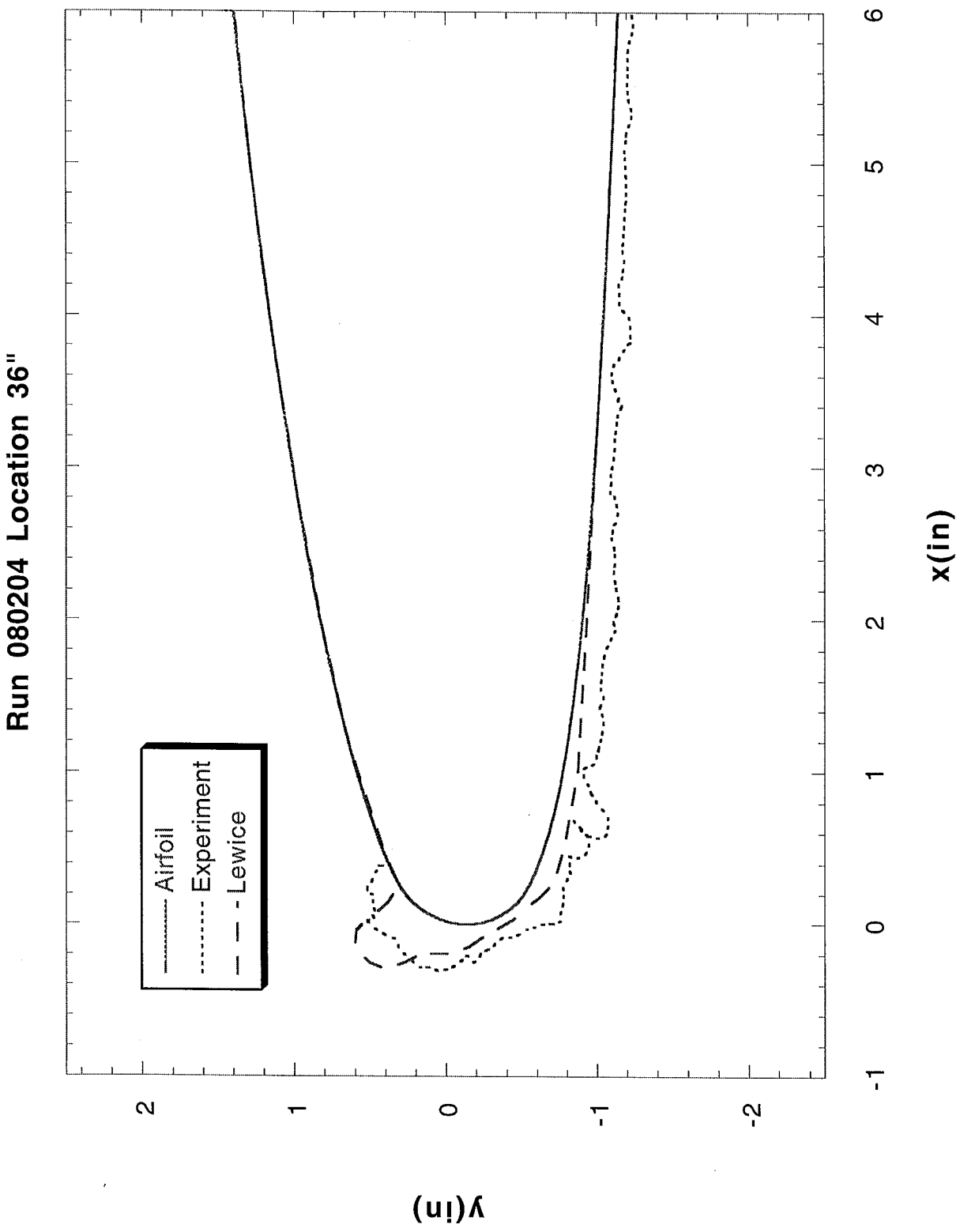
Run 080204 Location 36"
Airfoil
Experiment
Lewice
y(in)
x(in)
2
1
0
-1
-2
-1
0
1
2
3
4
5
6

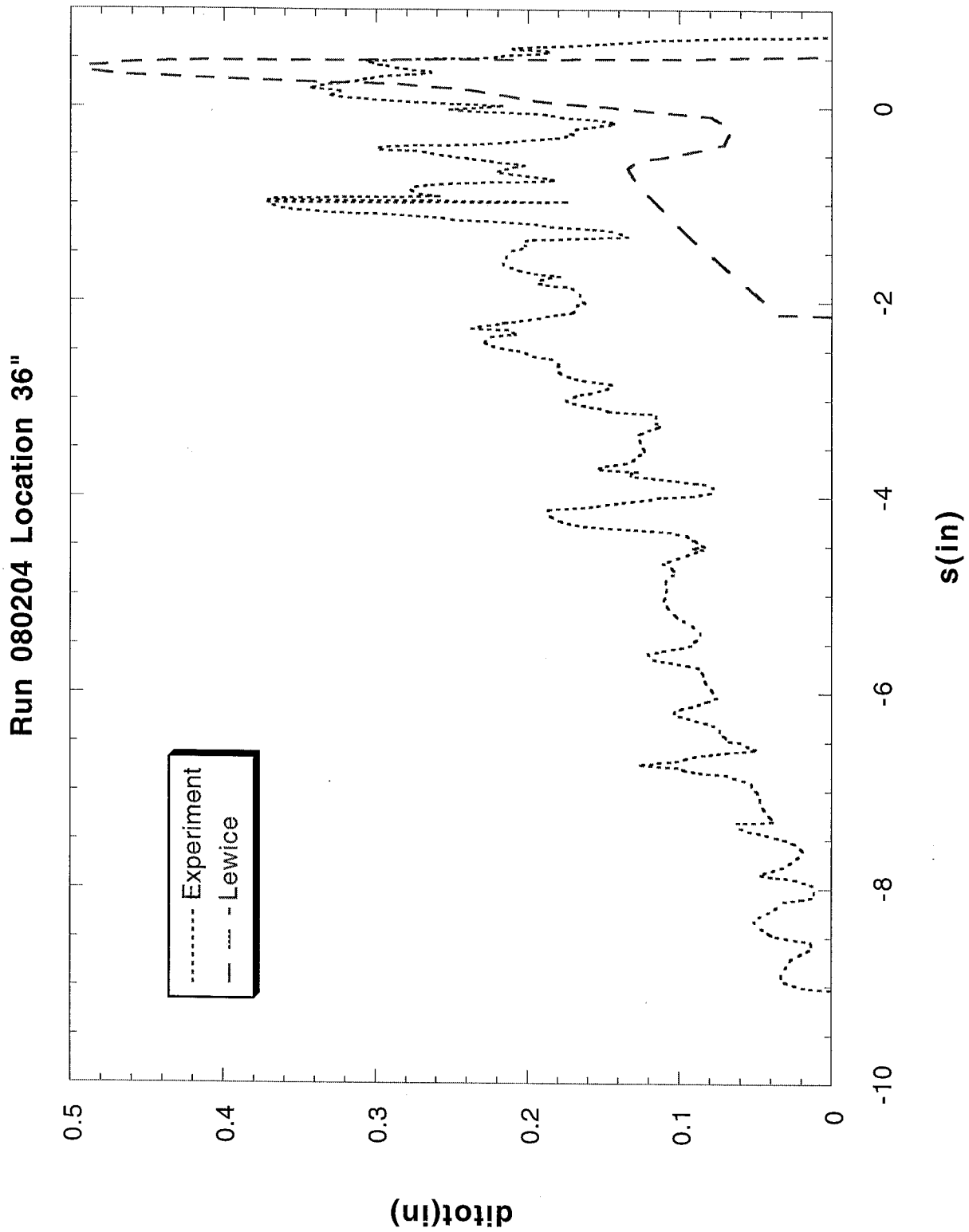
Run 080204 Location 36"
Experiment
Lewice
dltot(in)
s(in)
0.5
0.4
0.3
0.2
0.1
0
-10
-8
-6
-4
-2
0

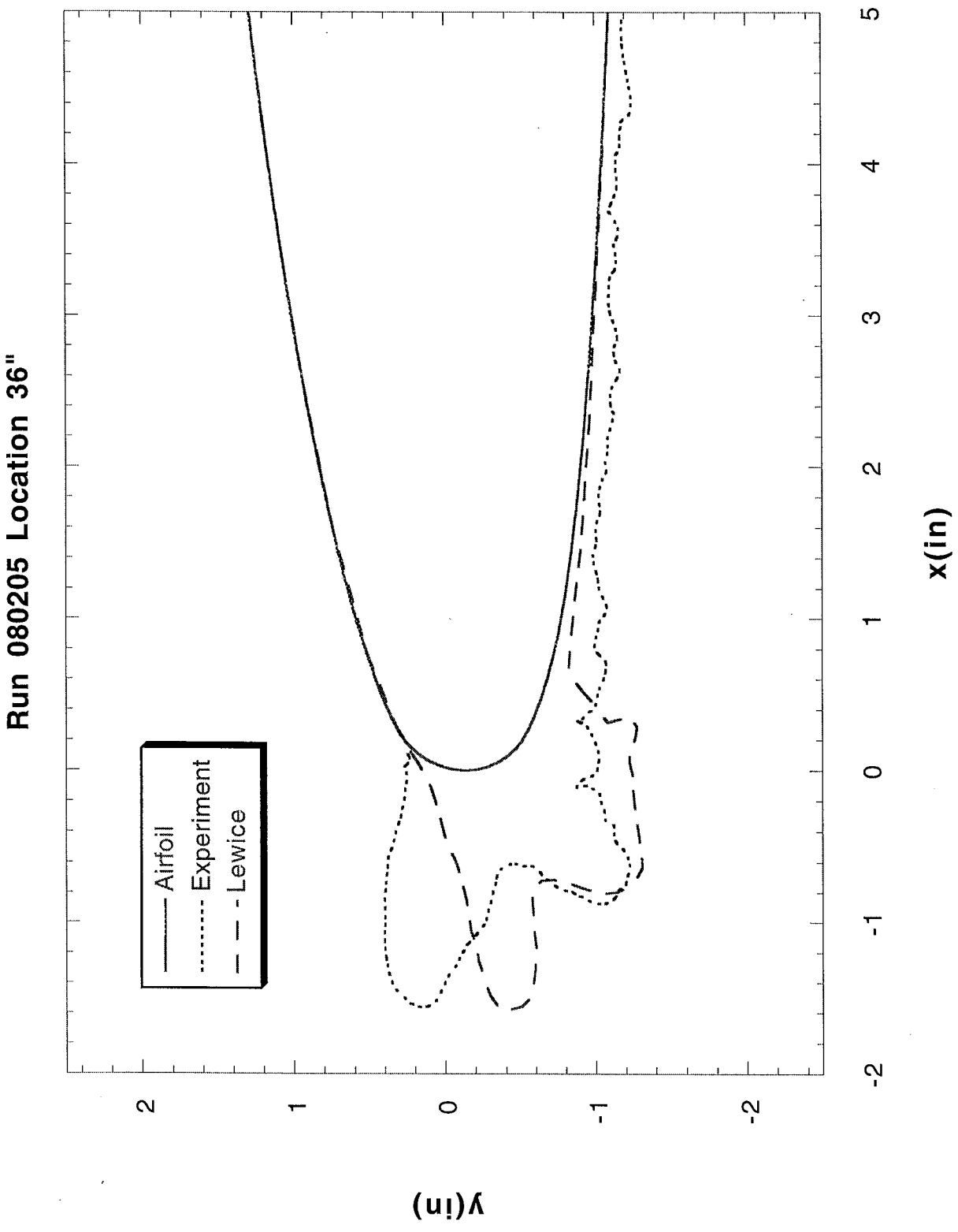
Run 080205 Location 36"
Airfoil
Experiment
Lewice
y(in)
x(in)
2
1
0
-1
-2
-2
-1
0
1
2
3
4
5

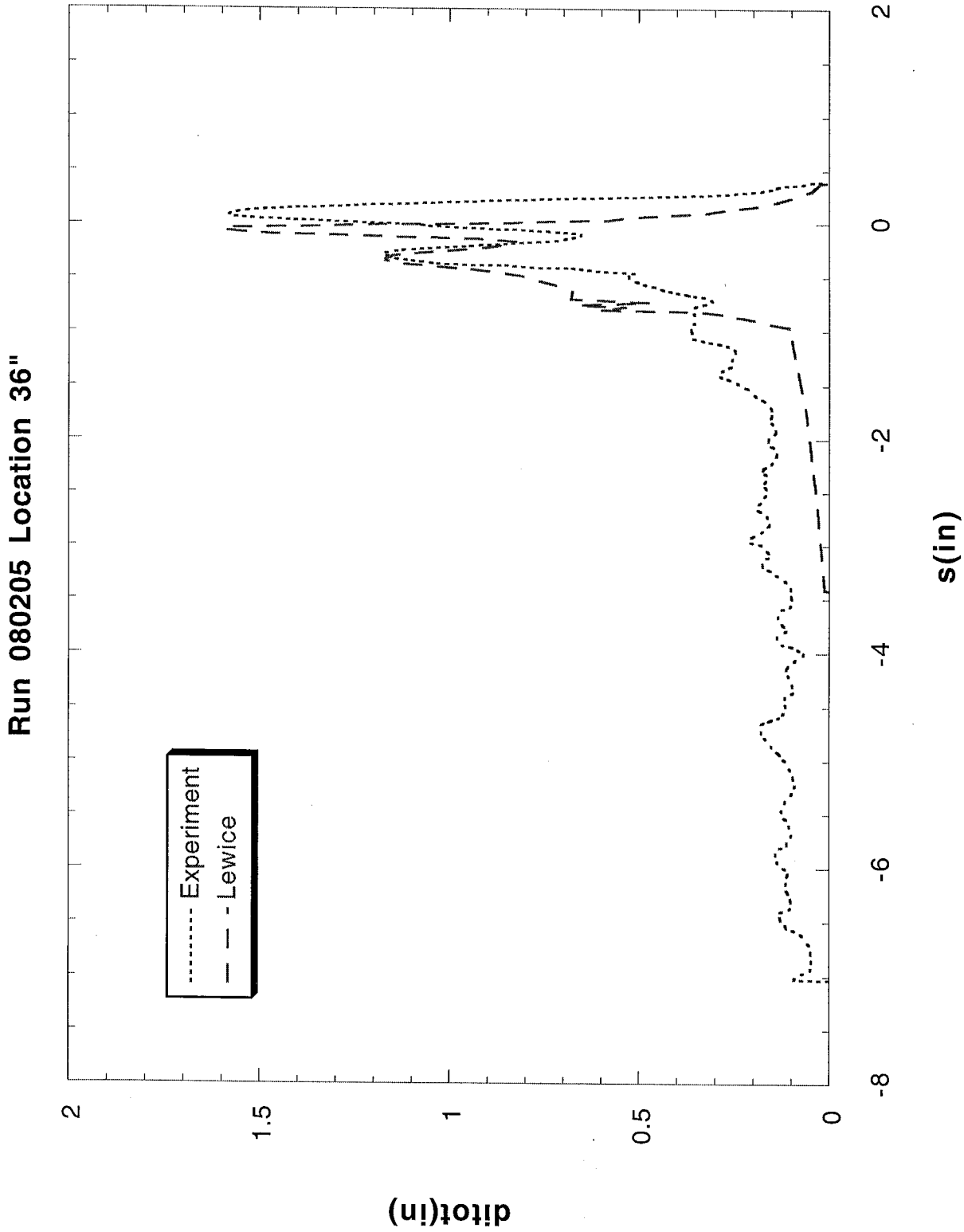
Run 080205 Location 36"
Experiment
Lewice
dltot(in)
s(in)
2
1.5
1
0.5
0
-8
-6
-4
-2
0
2

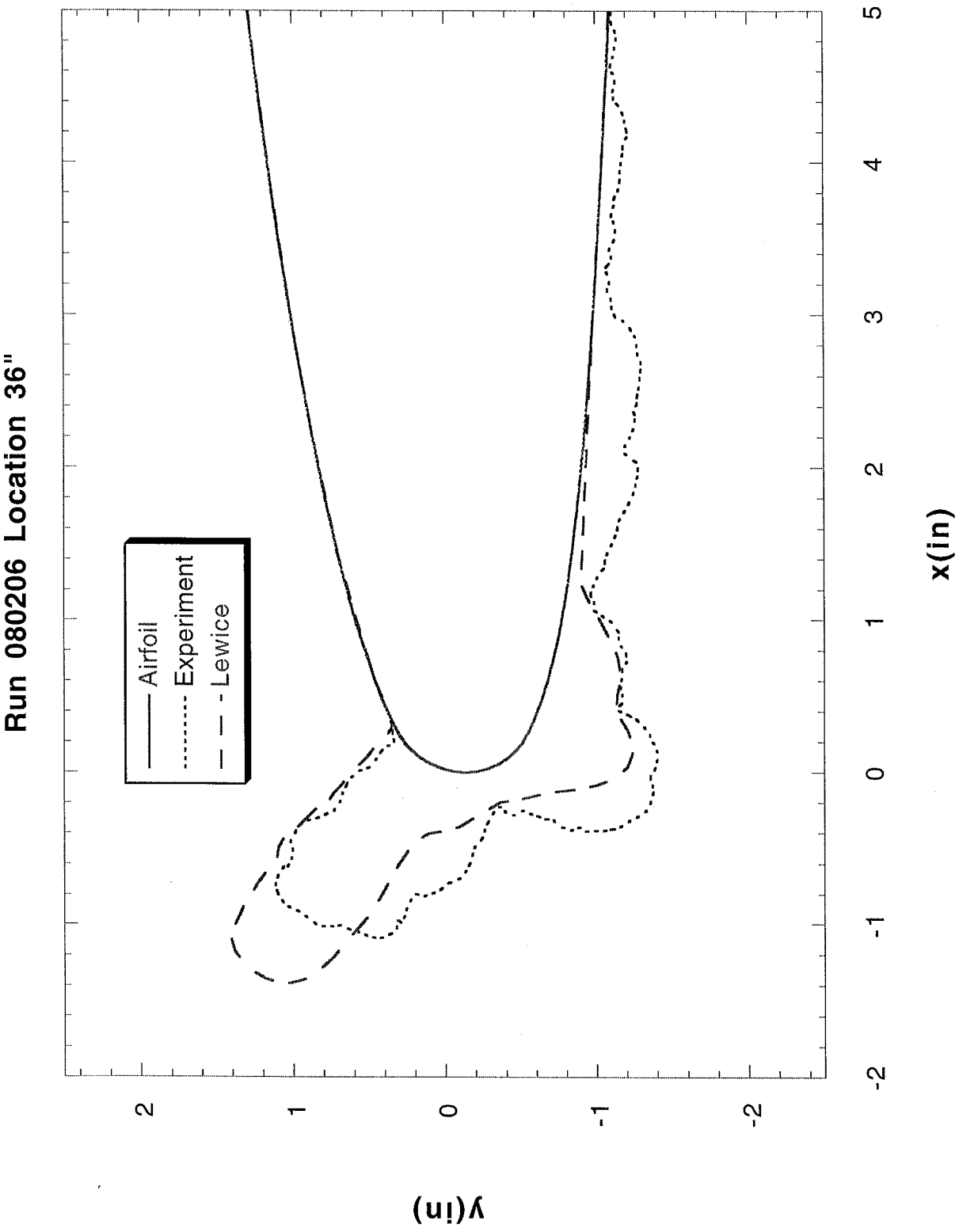
Run 080206 Location 36"
Airfoil
Experiment
Lewice
y(in)
x(in)
2
1
0
-1
-2
-2
-1
0
1
2
3
4
5

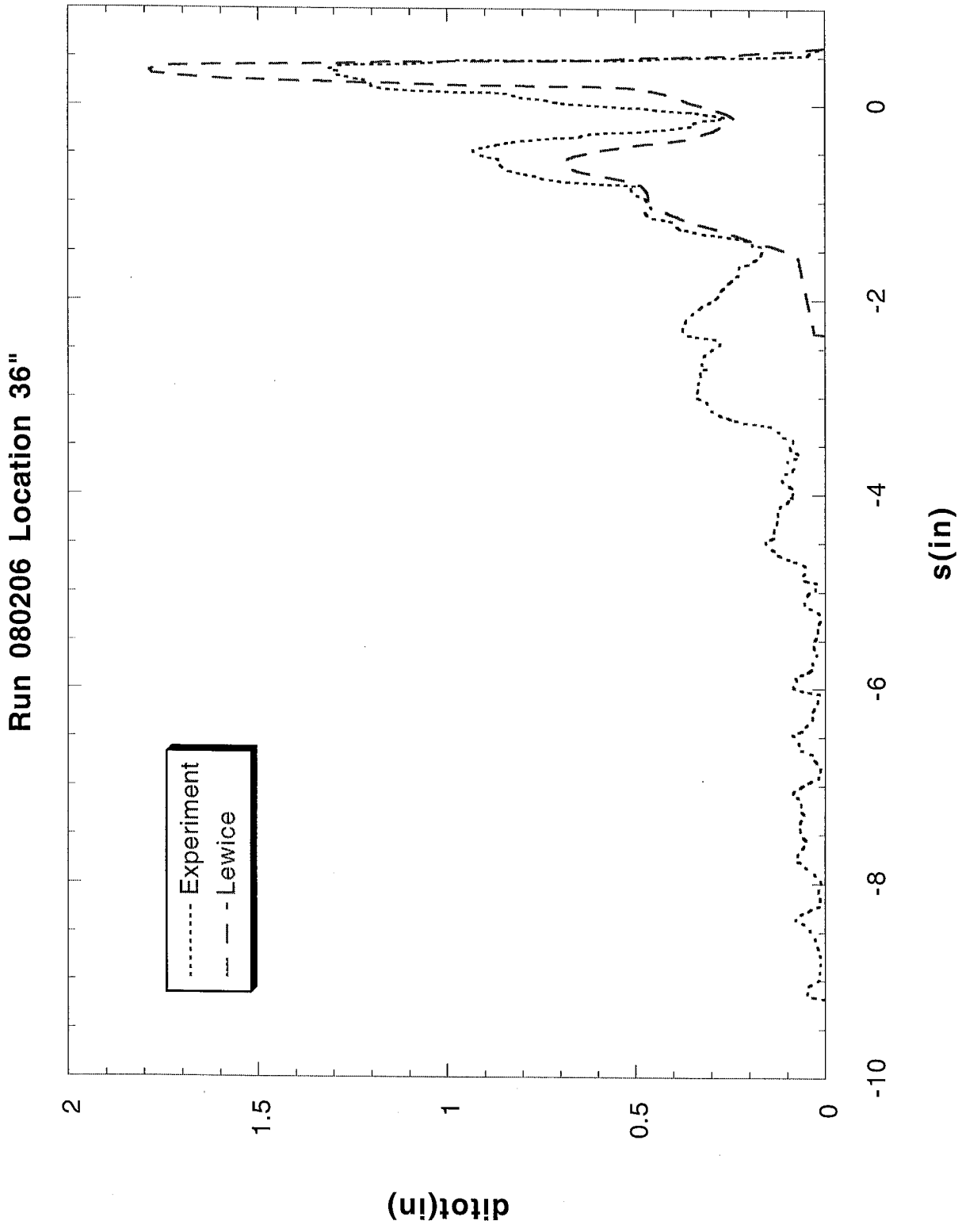
Run 080206 Location 36"
Experiment
Lewice
dltot(in)
s(in)
2
1.5
1
0.5
0
-10
-8
-6
-4
-2
0

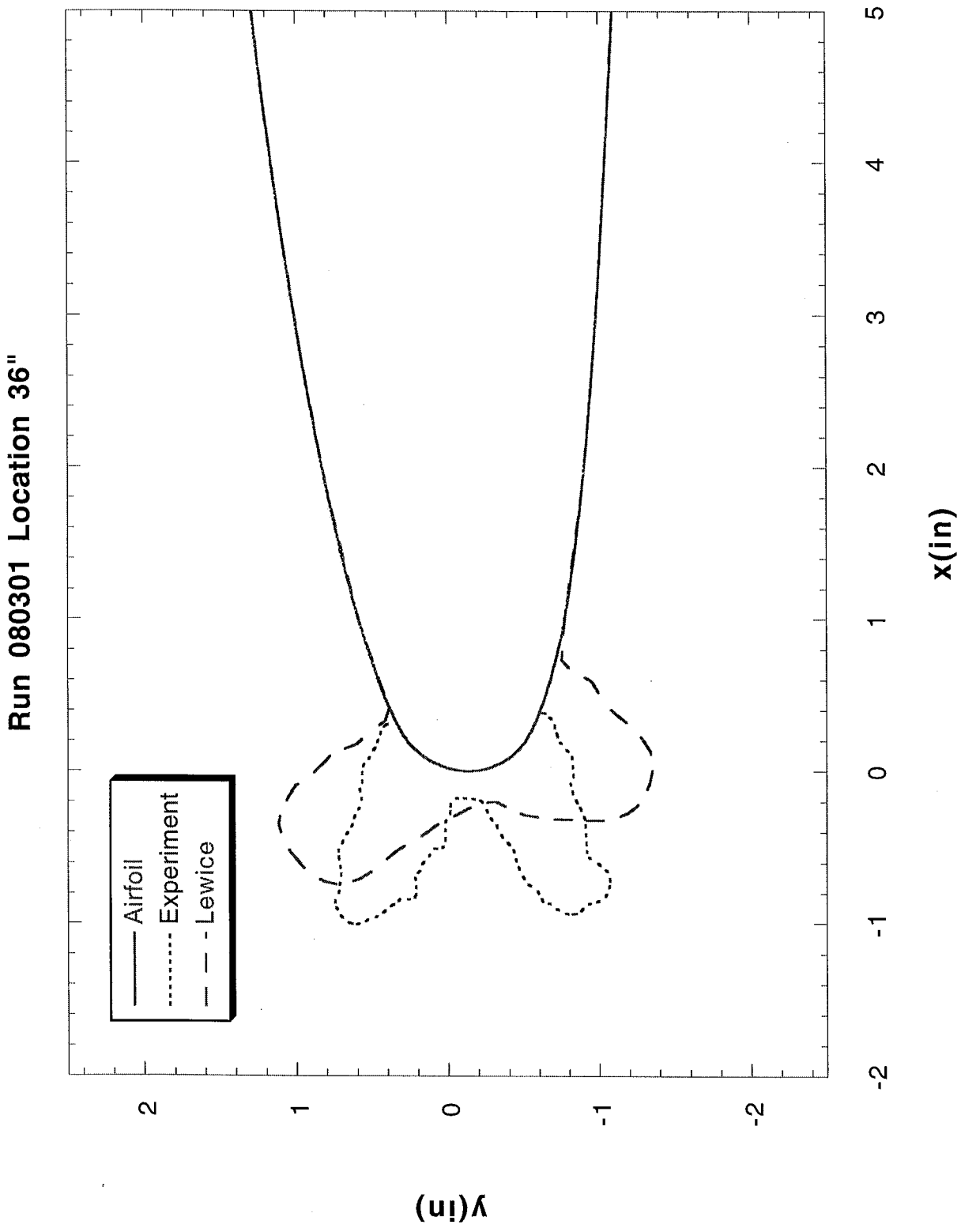
Run 080301 Location 36"
Airfoil
Experiment
Lewice
y(in)
x(in)
2
1
0
-1
-2
-2
-1
0
1
2
3
4
5

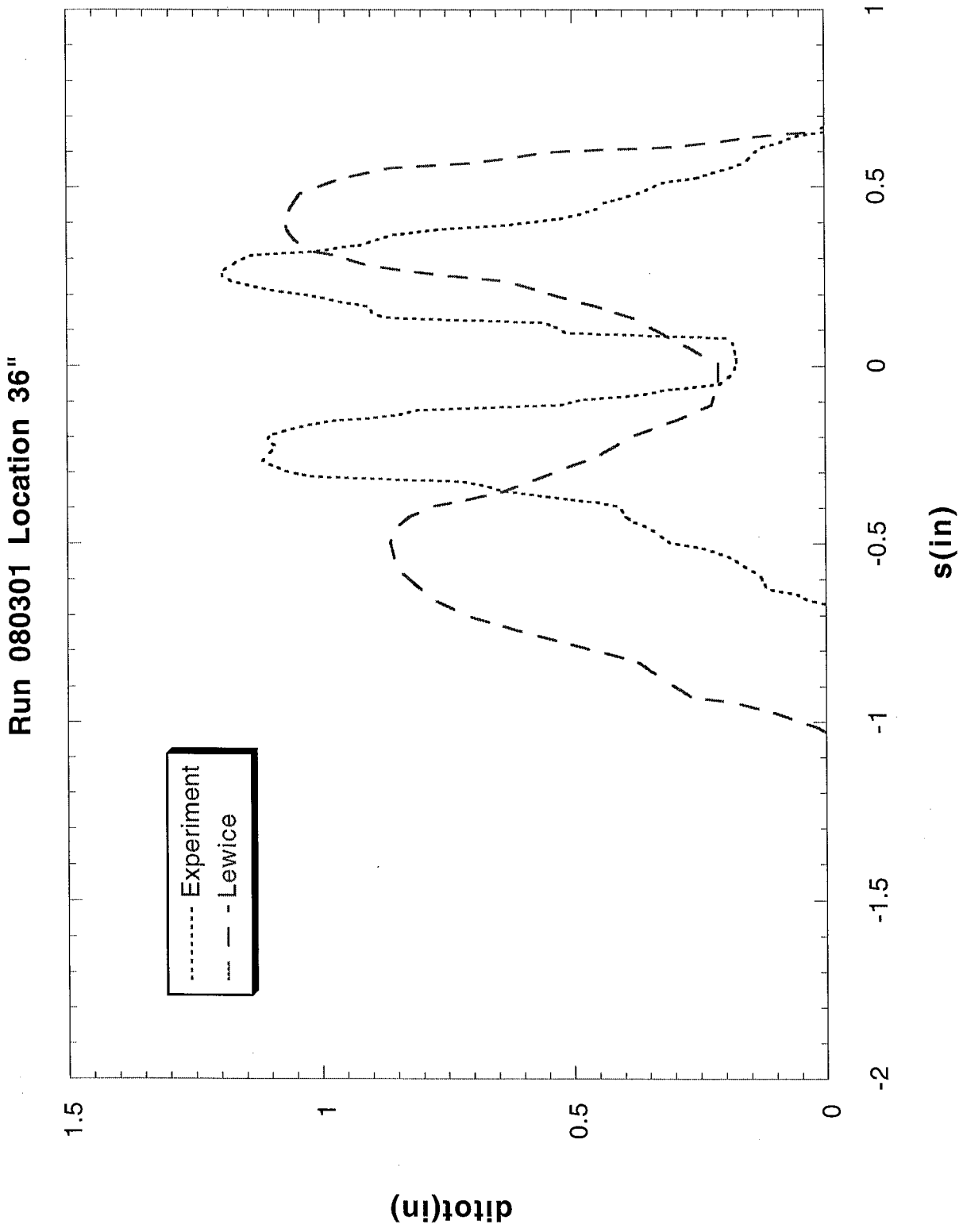
Run 080301 Location 36"
Experiment
Lewice
ditot(in)
s(in)
1.5
1
0.5
0
-2
-1.5
-1
-0.5
0
0.5
1

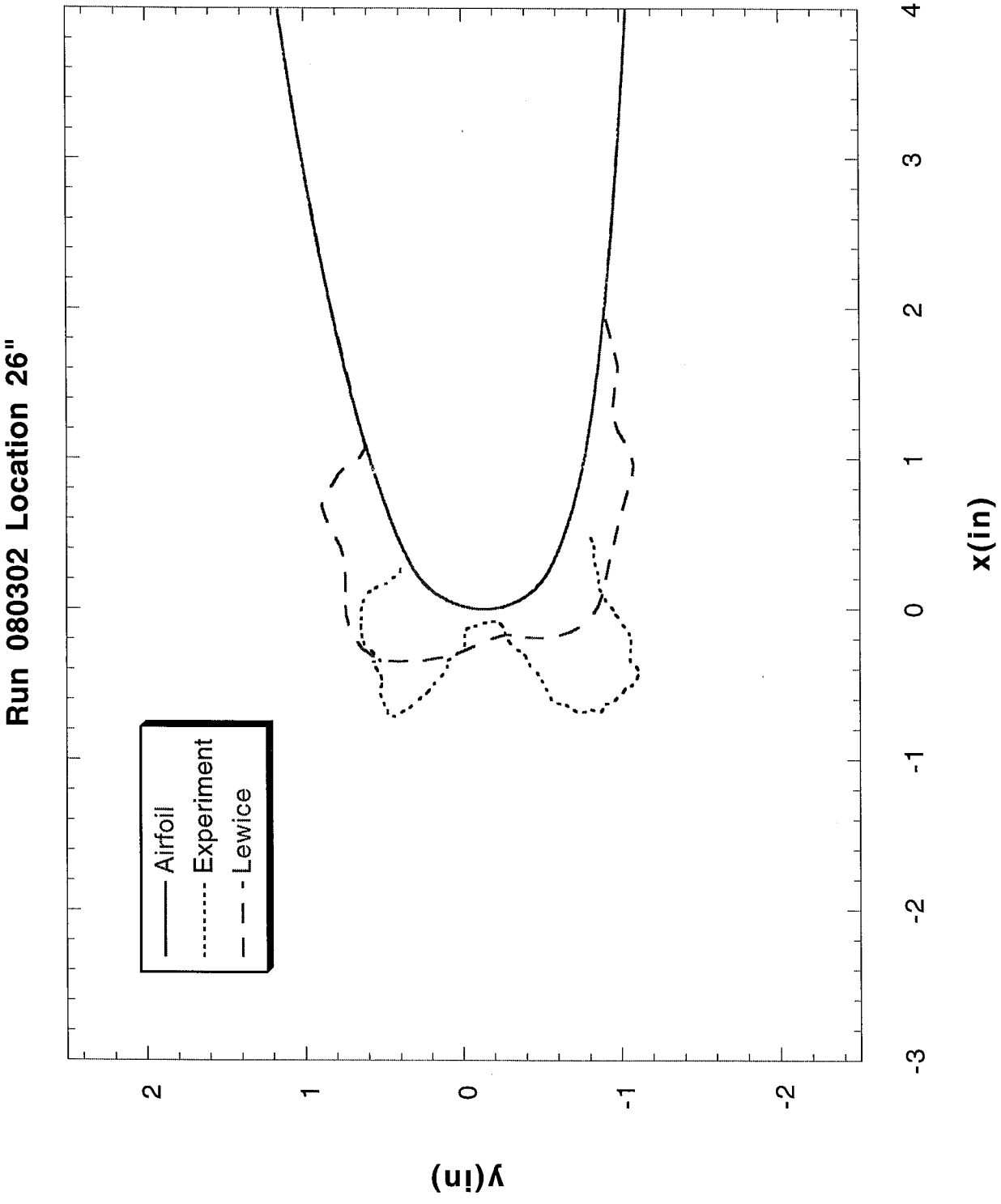
Run 080302 Location 26"
Airfoil
Experiment
Lewice
y(in)
x(in)
2
1
0
-1
-2
-3
-2
-1
0
1
2
3
4

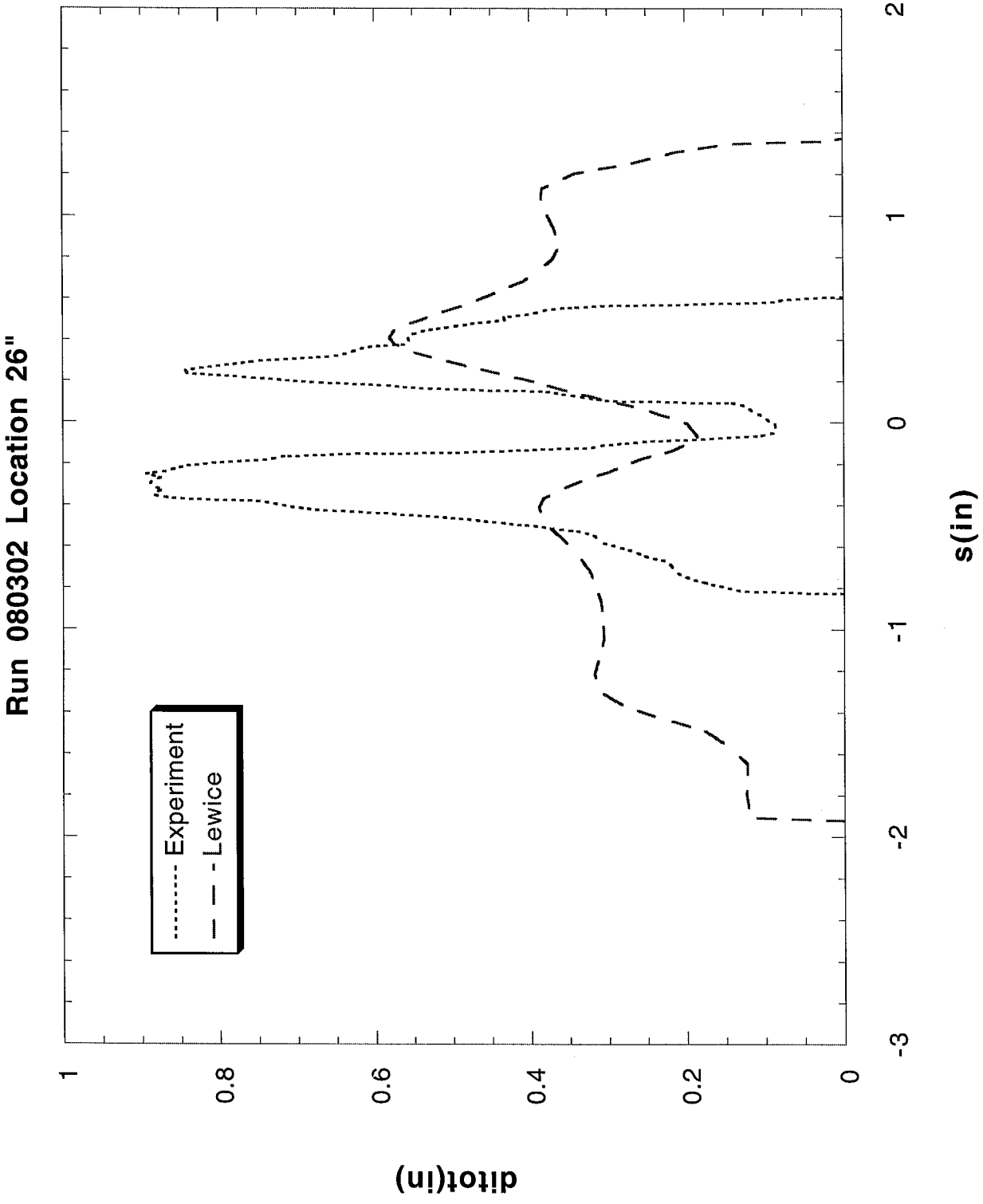
Run 080302 Location 26"
Experiment
Lewice
dltot(in)
s(in)
1
0.8
0.6
0.4
0.2
0
-3
-2
-1
0
1
2

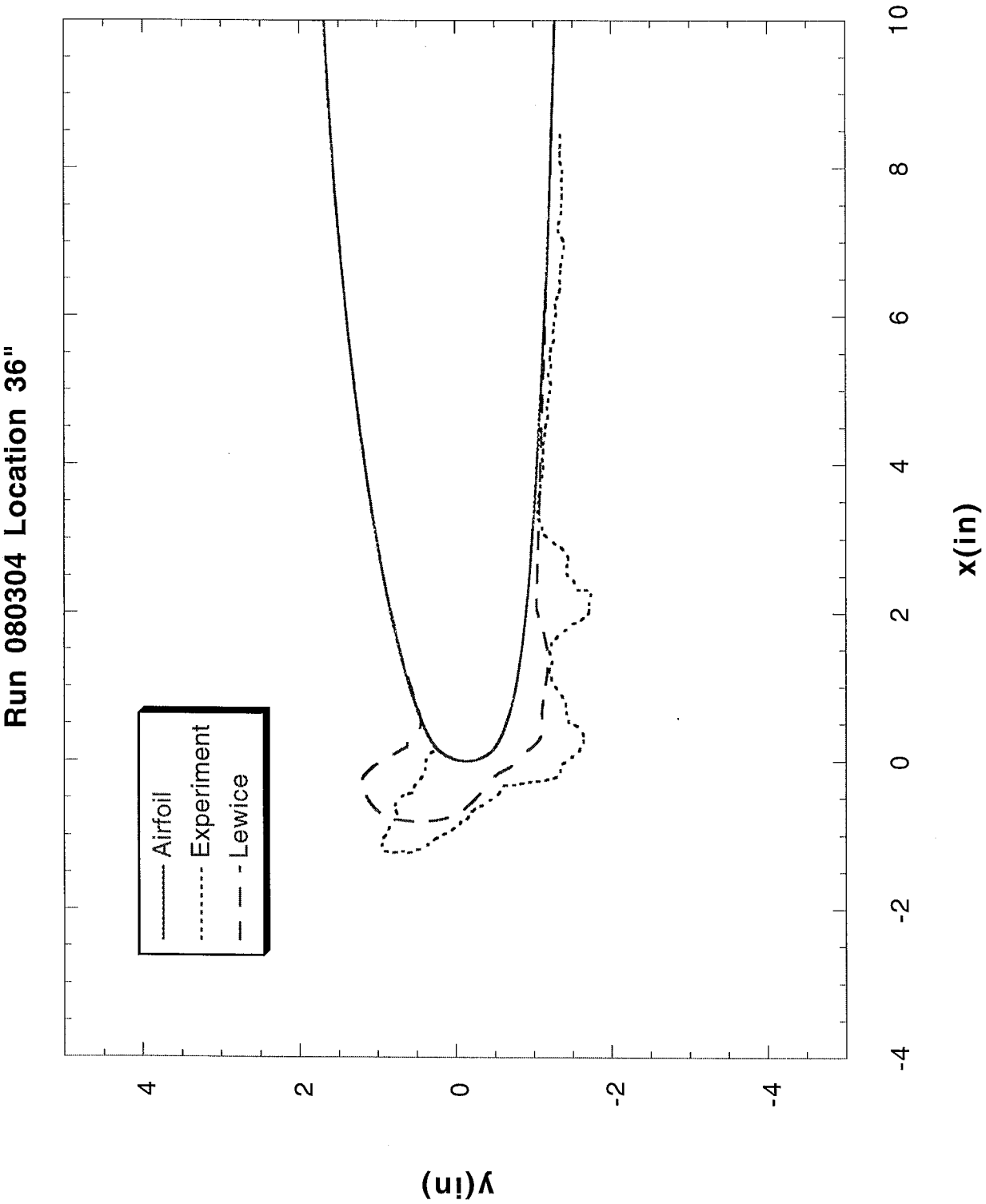
Run 080304 Location 36"
Airfoil
Experiment
Lewice
y(in)
x(in)
4
2
0
-2
-4
-4
-2
0
2
4
6
8
10

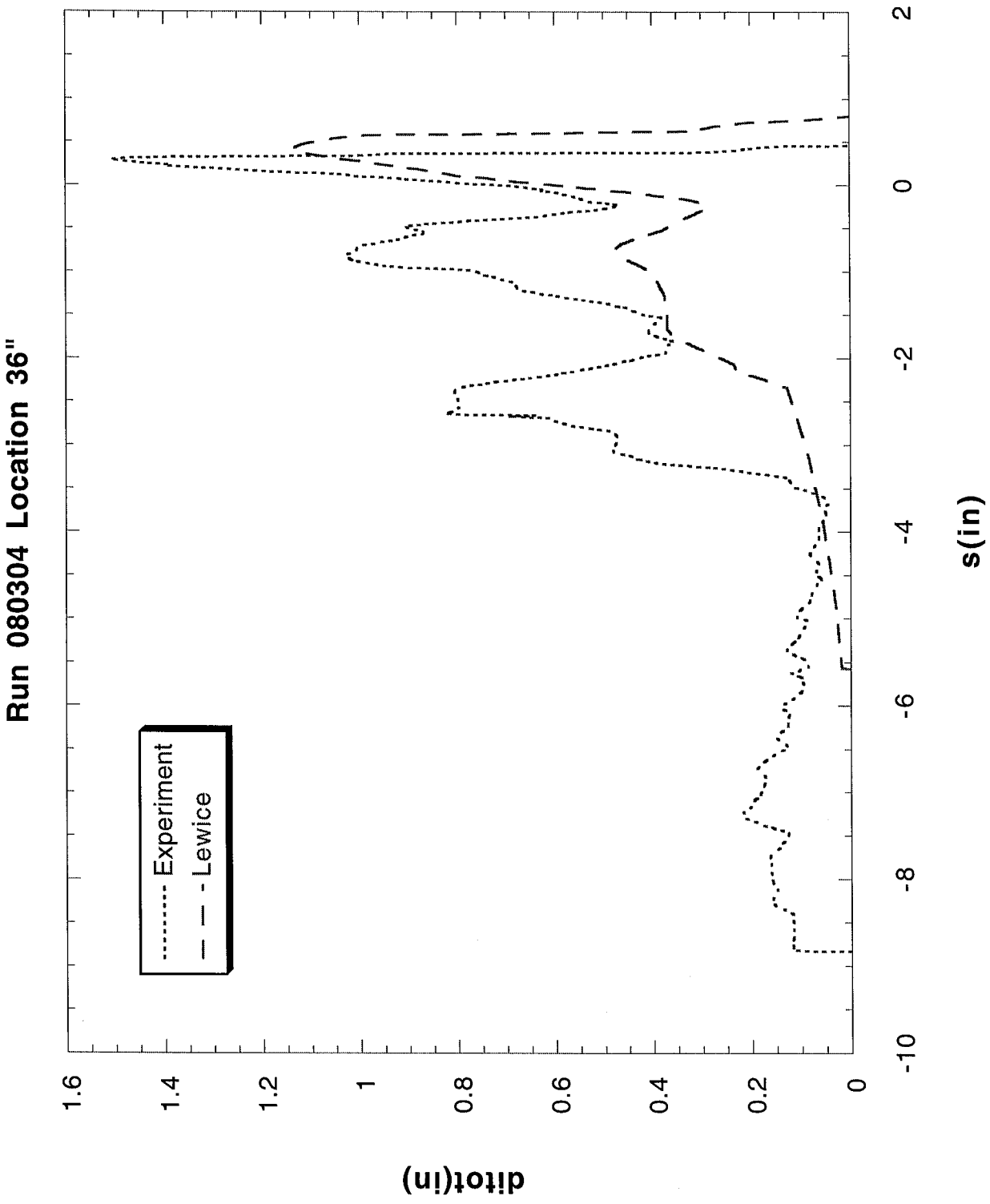
Run 080304 Location 36"
Experiment
Lewice
ditot(in)
s(in)
1.6
1.4
1.2
1
0.8
0.6
0.4
0.2
0
2
0
-2
-4
-6
-8
-10

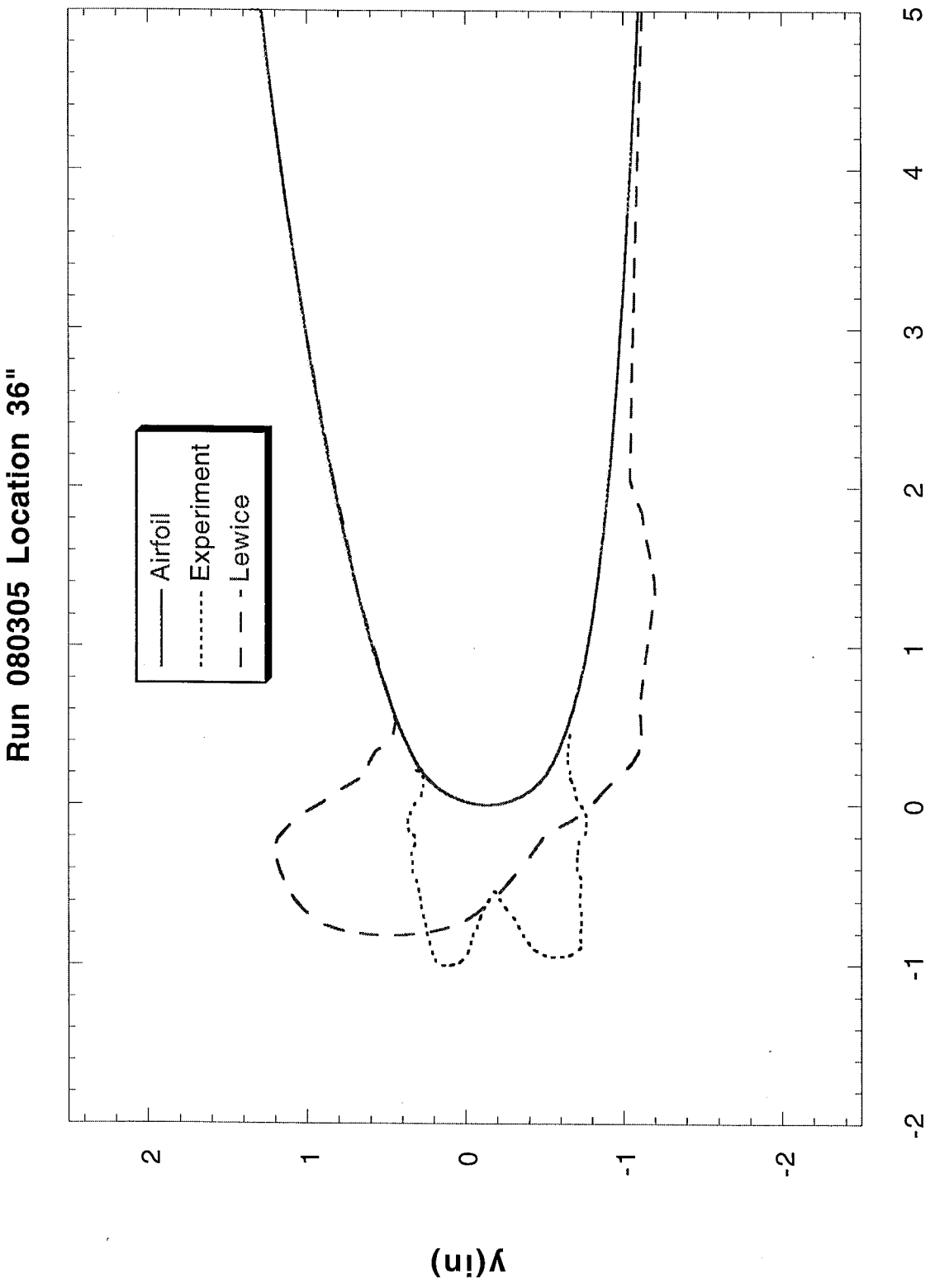
Run 080305 Location 36"
Airfoil
Experiment
Lewice
y(in)
x(in)
2
1
0
-1
-2
-2
-1
0
1
2
3
4
5

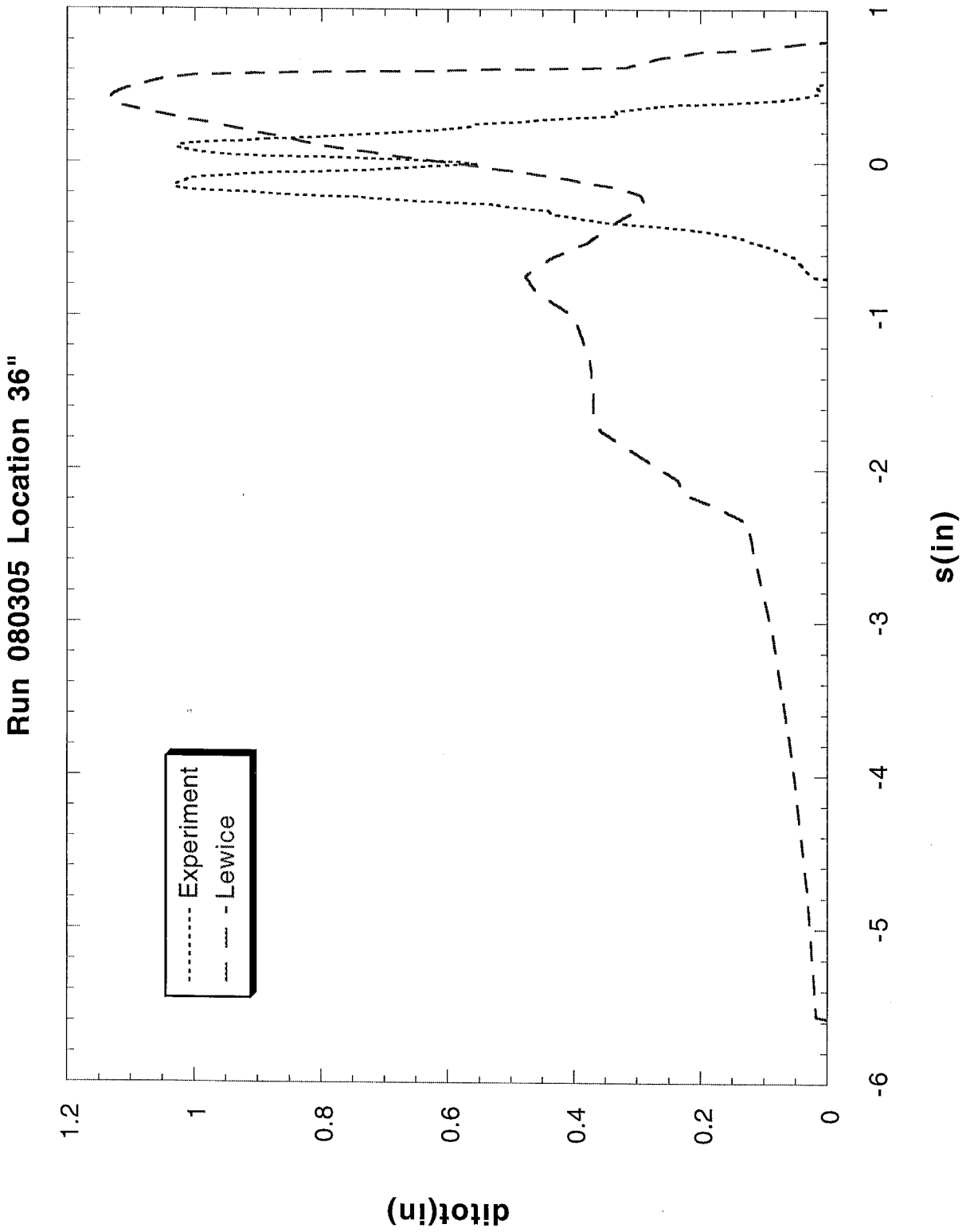
Run 080305 Location 36"
Experiment
Lewice
ditot(in)
s(in)
1.2
1
0.8
0.6
0.4
0.2
0
-6
-5
-4
-3
-2
-1
0
1

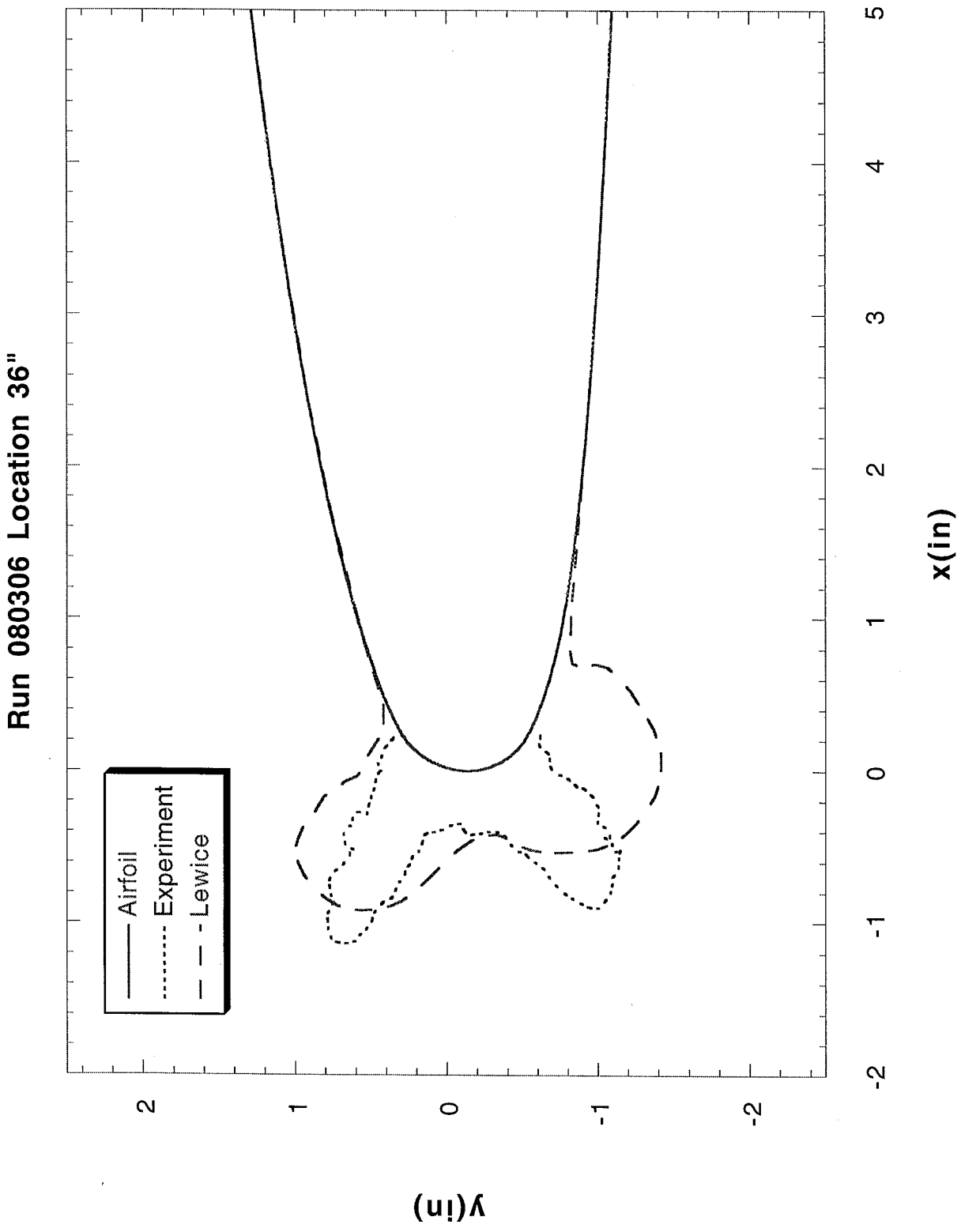
Run 080306 Location 36"
Airfoil
Experiment
Lewice
y(in)
x(in)
2
1
0
-1
-2
-2
-1
0
1
2
3
4
5

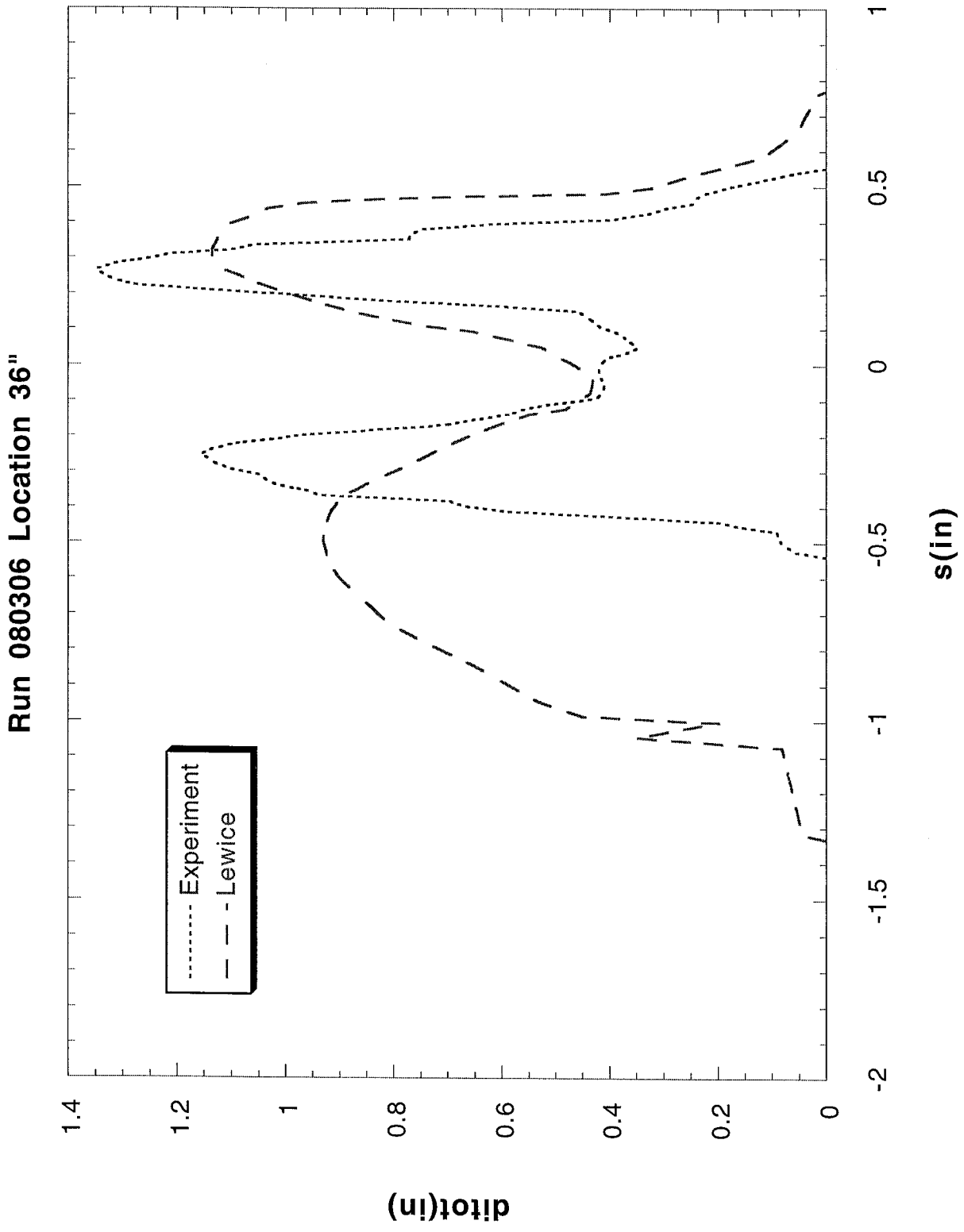
Run 080306 Location 36"
Experiment
Lewice
dltot(in)
s(in)
1.4
1.2
1
0.8
0.6
0.4
0.2
0
-2
-1.5
-1
-0.5
0
0.5
1

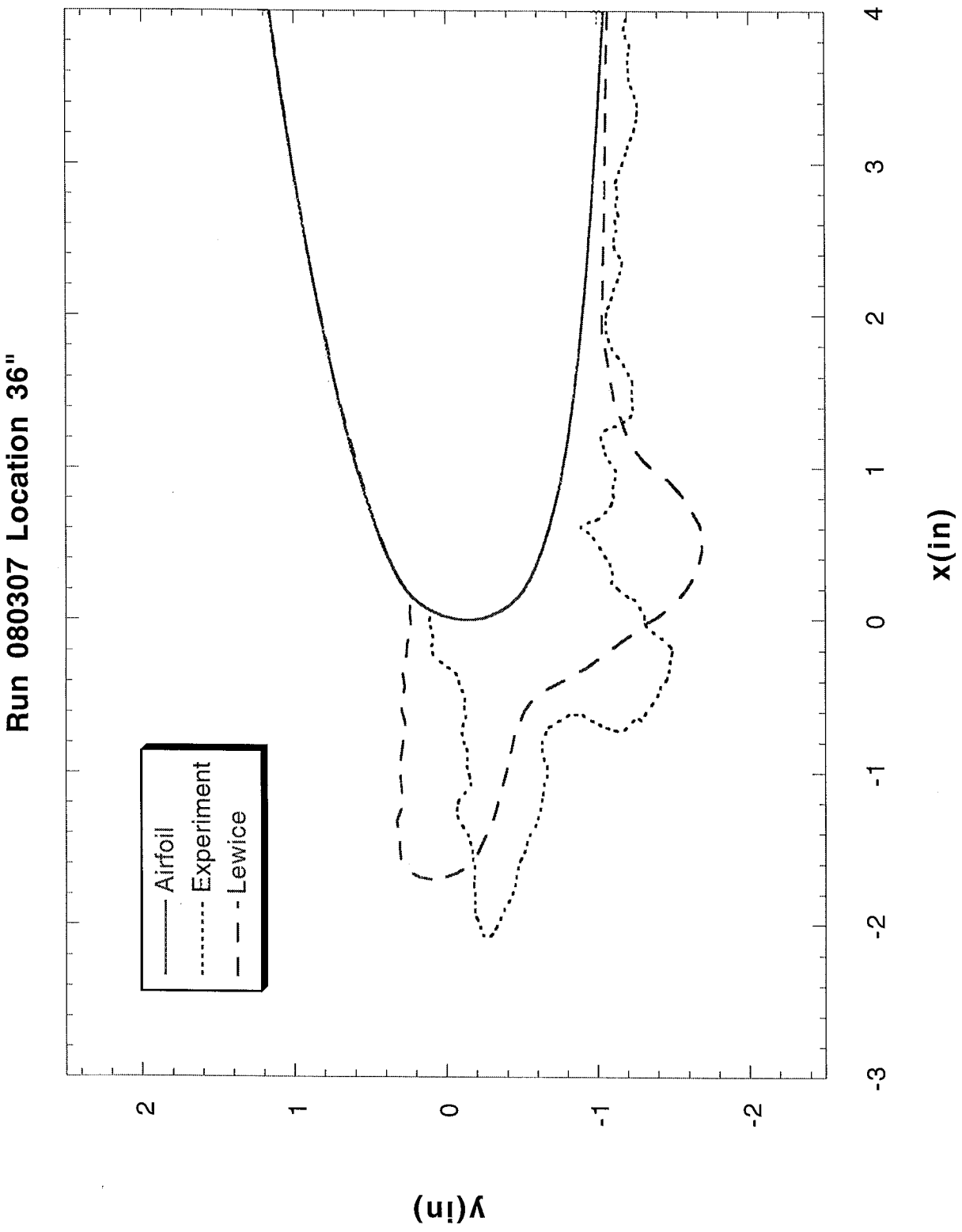
Run 080307 Location 36"
Airfoil
Experiment
Lewice
y(in)
x(in)
2
1
0
-1
-2
-3
-2
-1
0
1
2
3
4

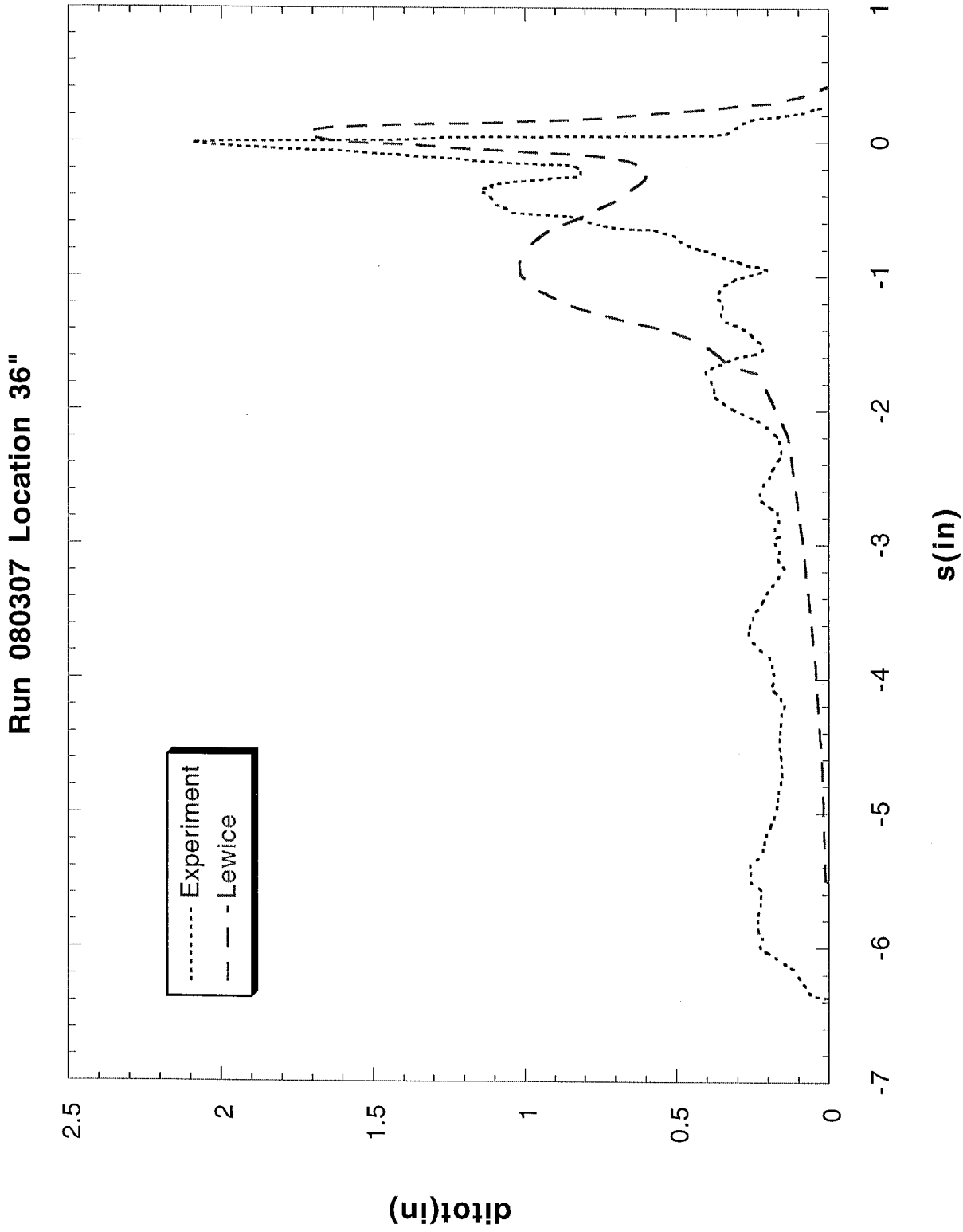
Run 080307 Location 36"
Experiment
Lewice
dltot(in)
s(in)
2.5
2
1.5
1
0.5
0
-7
-6
-5
-4
-3
-2
-1
0
1

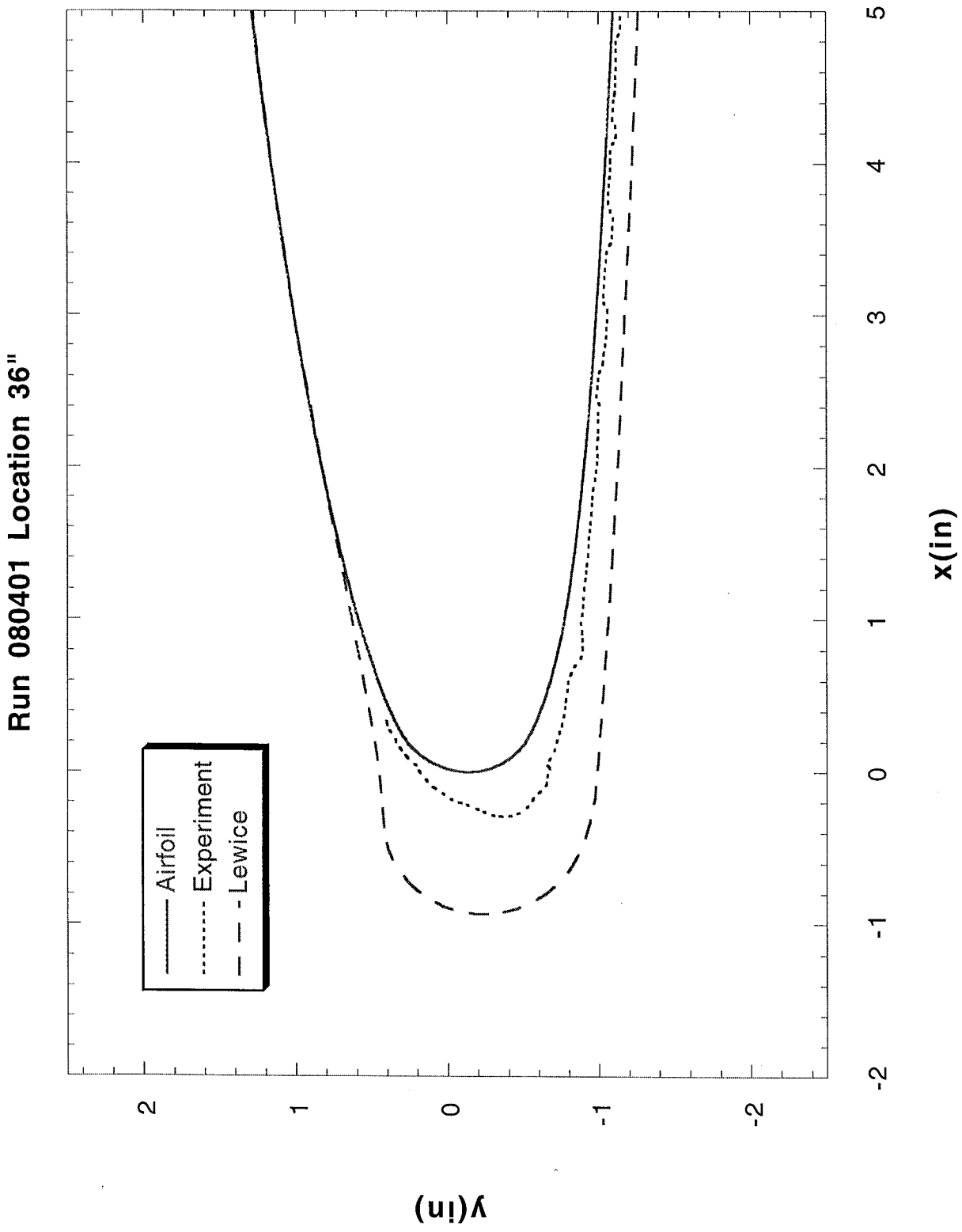
Run 080401 Location 36"
Airfoil
Experiment
Lewice
y(in)
x(in)
2
1
0
-1
-2
-2
-1
0
1
2
3
4
5

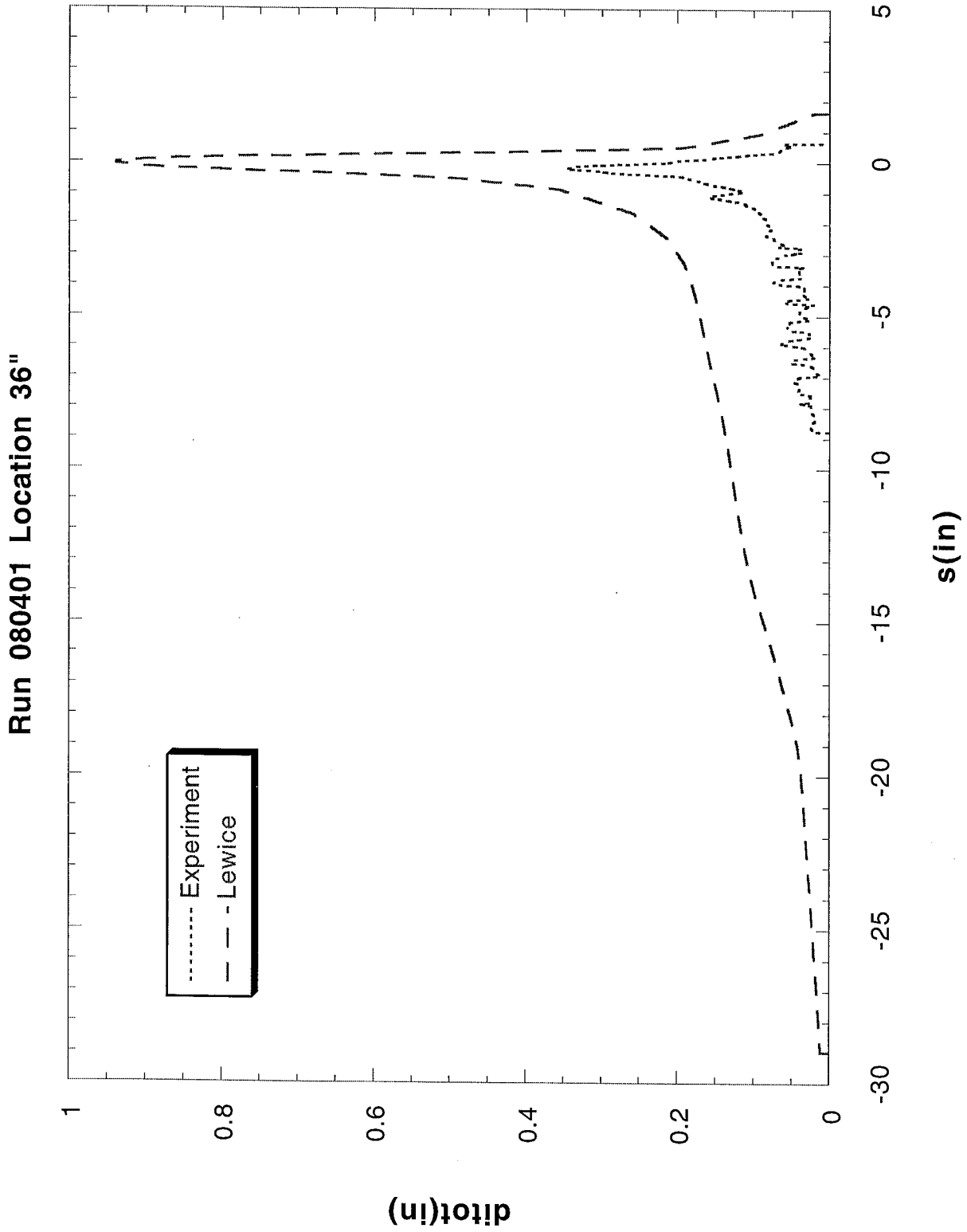
Run 080401 Location 36"
Experiment
Lewice
dltot(in)
s(in)
1
0.8
0.6
0.4
0.2
0
5
0
-5
-10
-15
-20
-25
-30

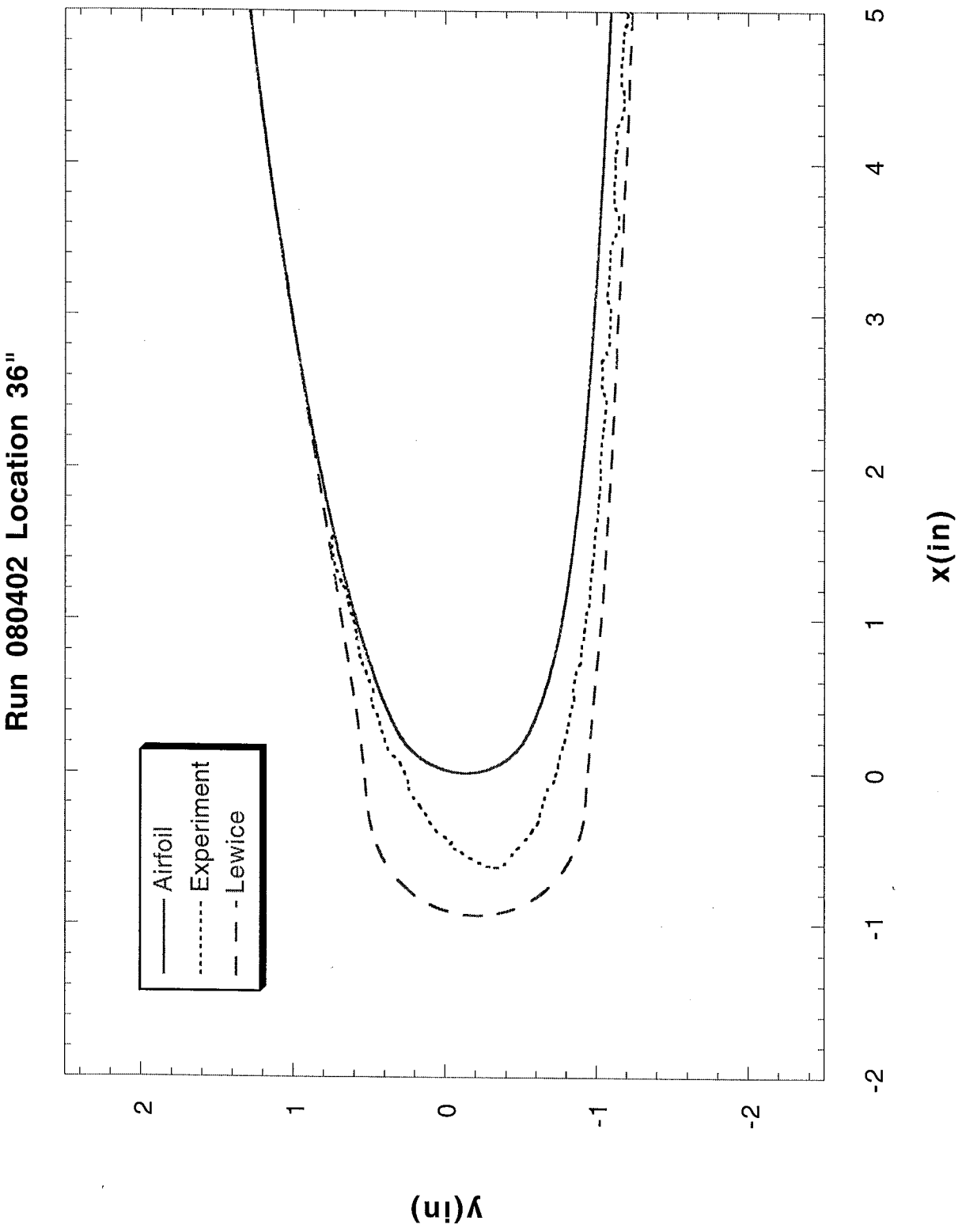
Run 080402 Location 36"
Airfoil
Experiment
Lewice
y(in)
x(in)
2
1
0
-1
-2
-2
-1
0
1
2
3
4
5

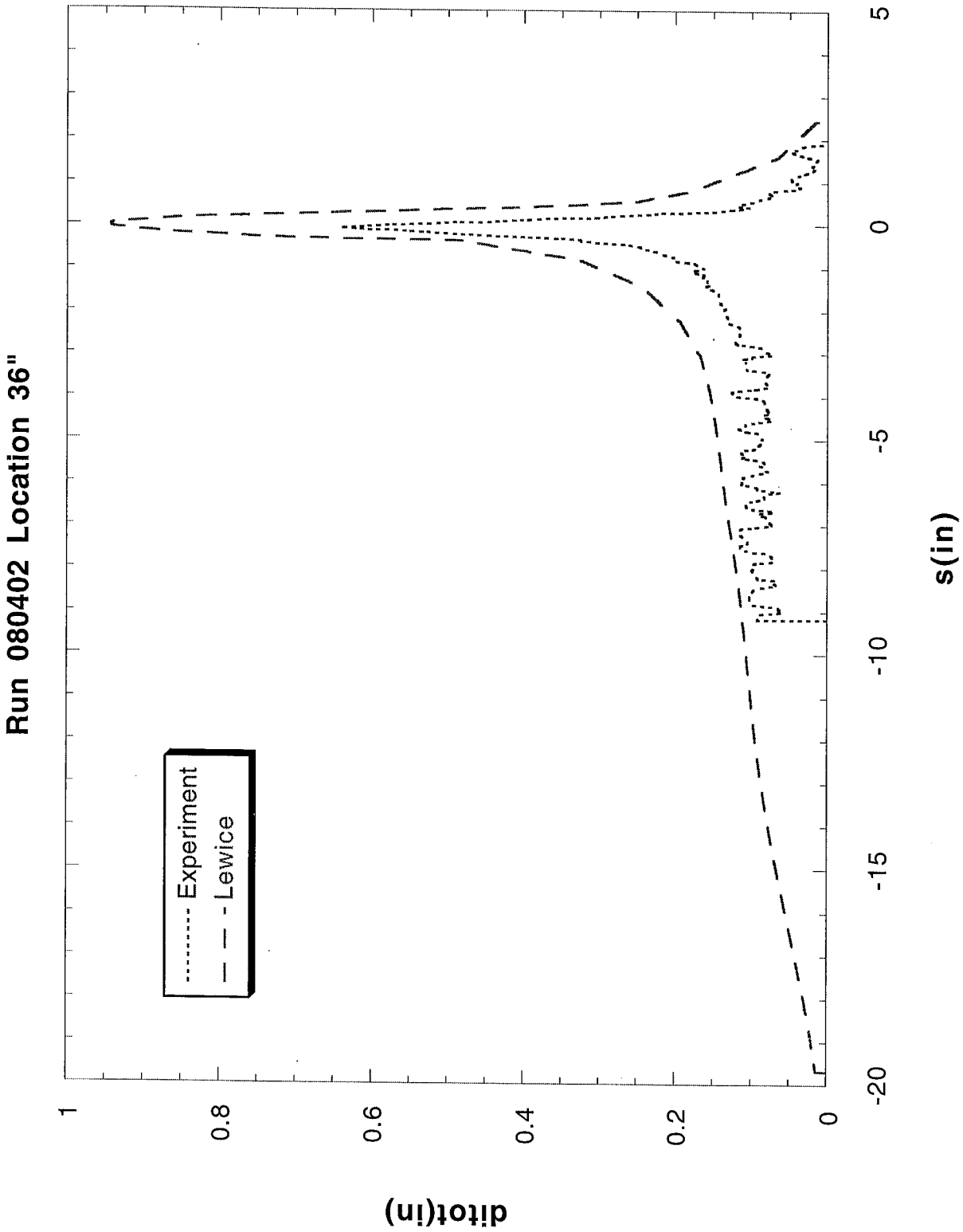
Run 080402 Location 36"
Experiment
Lewice
dltot(in)
s(in)
1
0.8
0.6
0.4
0.2
0
5
0
-5
-10
-15
-20

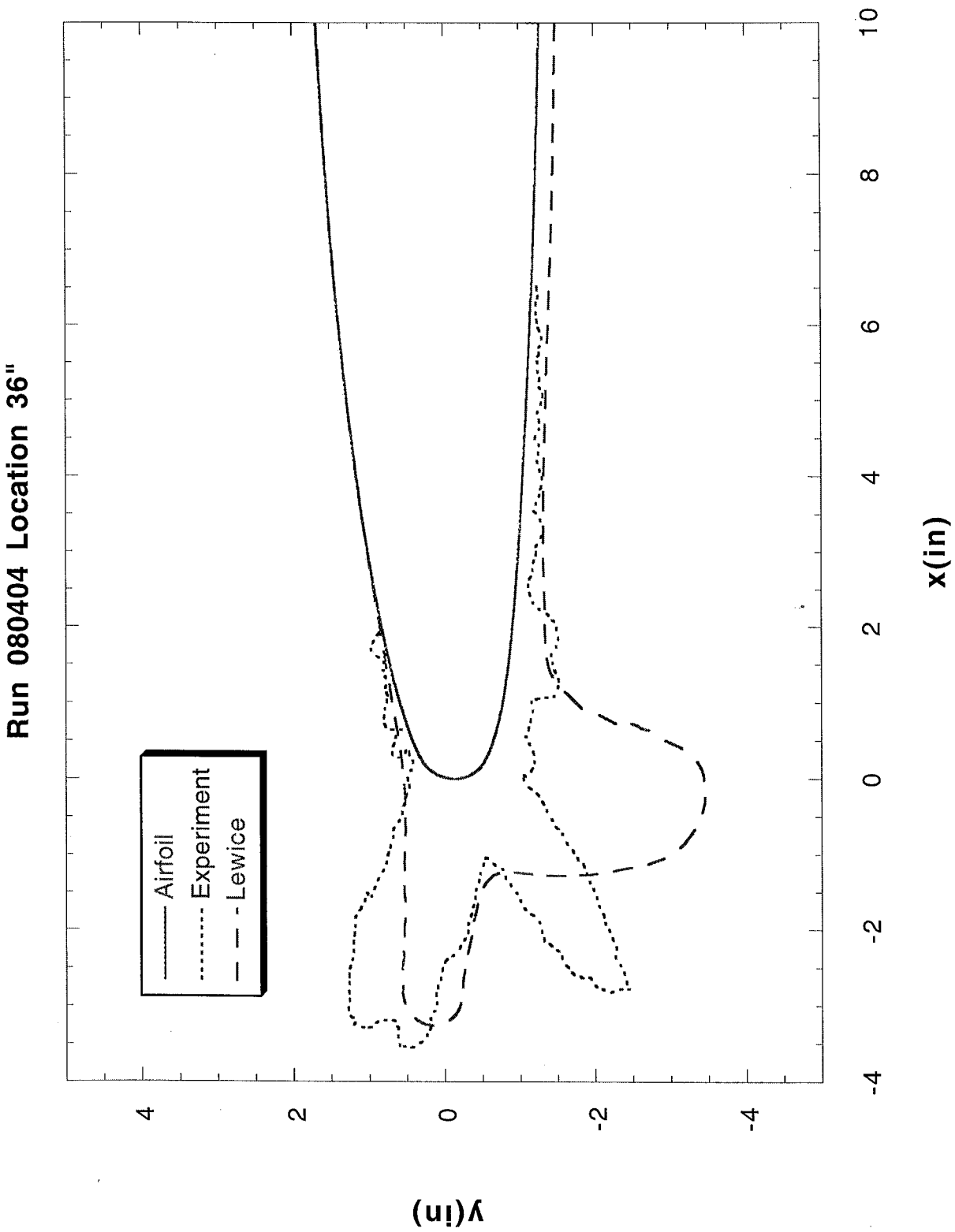
Run 080404 Location 36"
Airfoil
Experiment
Lewice
y(in)
x(in)
4
2
0
-2
-4
-4
-2
0
2
4
6
8
10

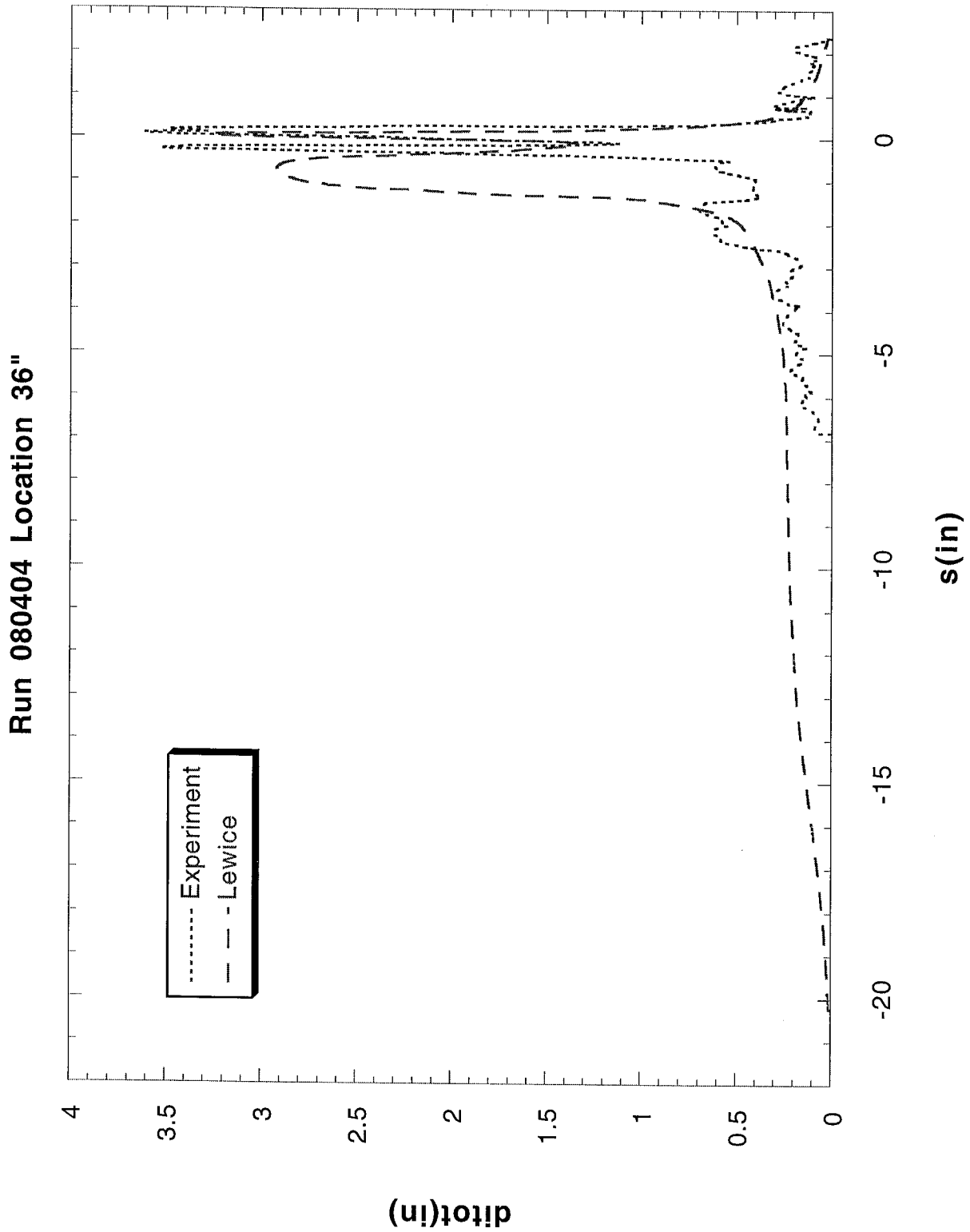
Run 080404 Location 36"
Experiment
Lewice
dltot(in)
s(in)
4
3.5
3
2.5
2
1.5
1
0.5
0
-20
-15
-10
-5
0

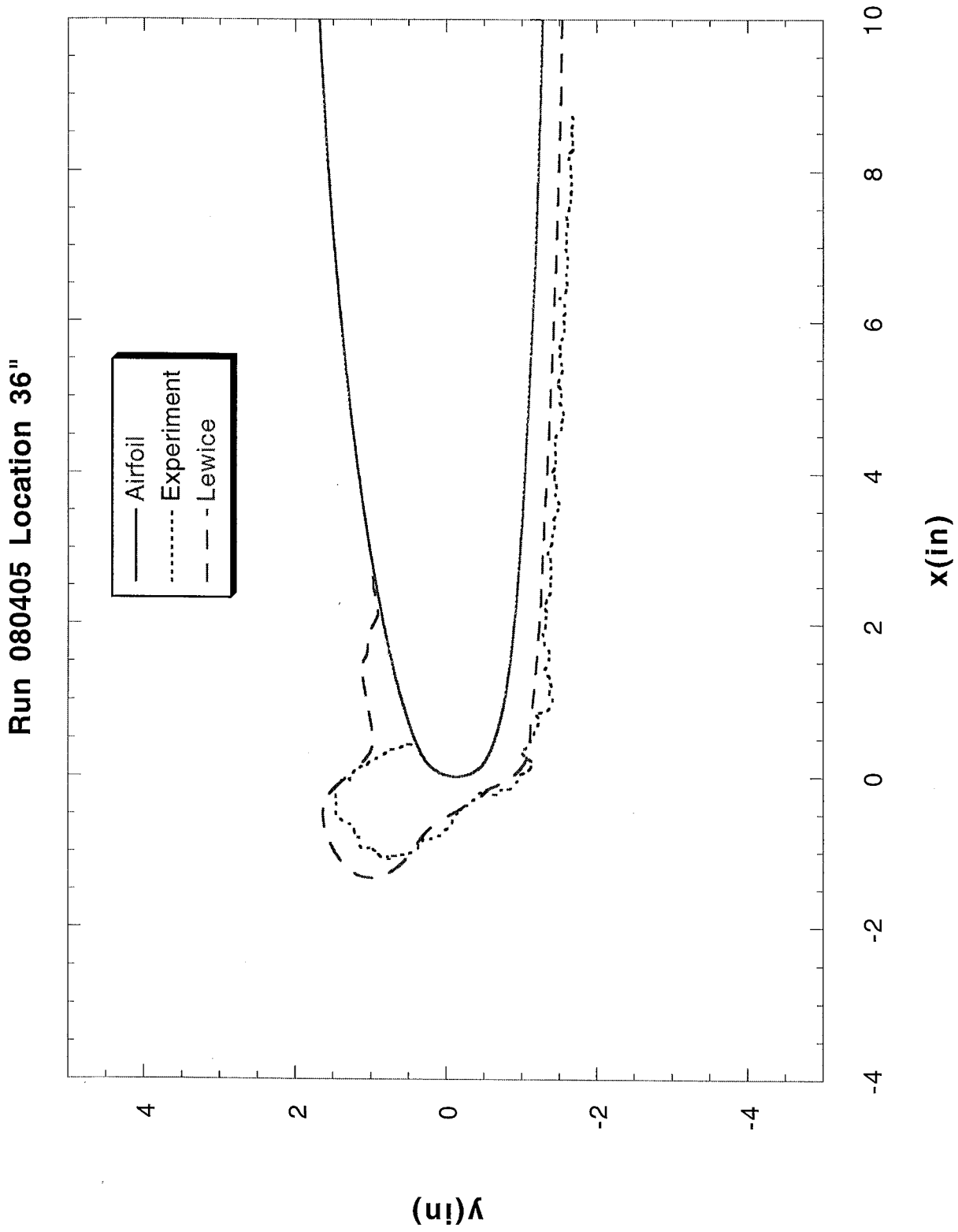
Run 080405 Location 36"
Airfoil
Experiment
Lewice
y(in)
x(in)
4
2
0
-2
-4
-4
-2
0
2
4
6
8
10

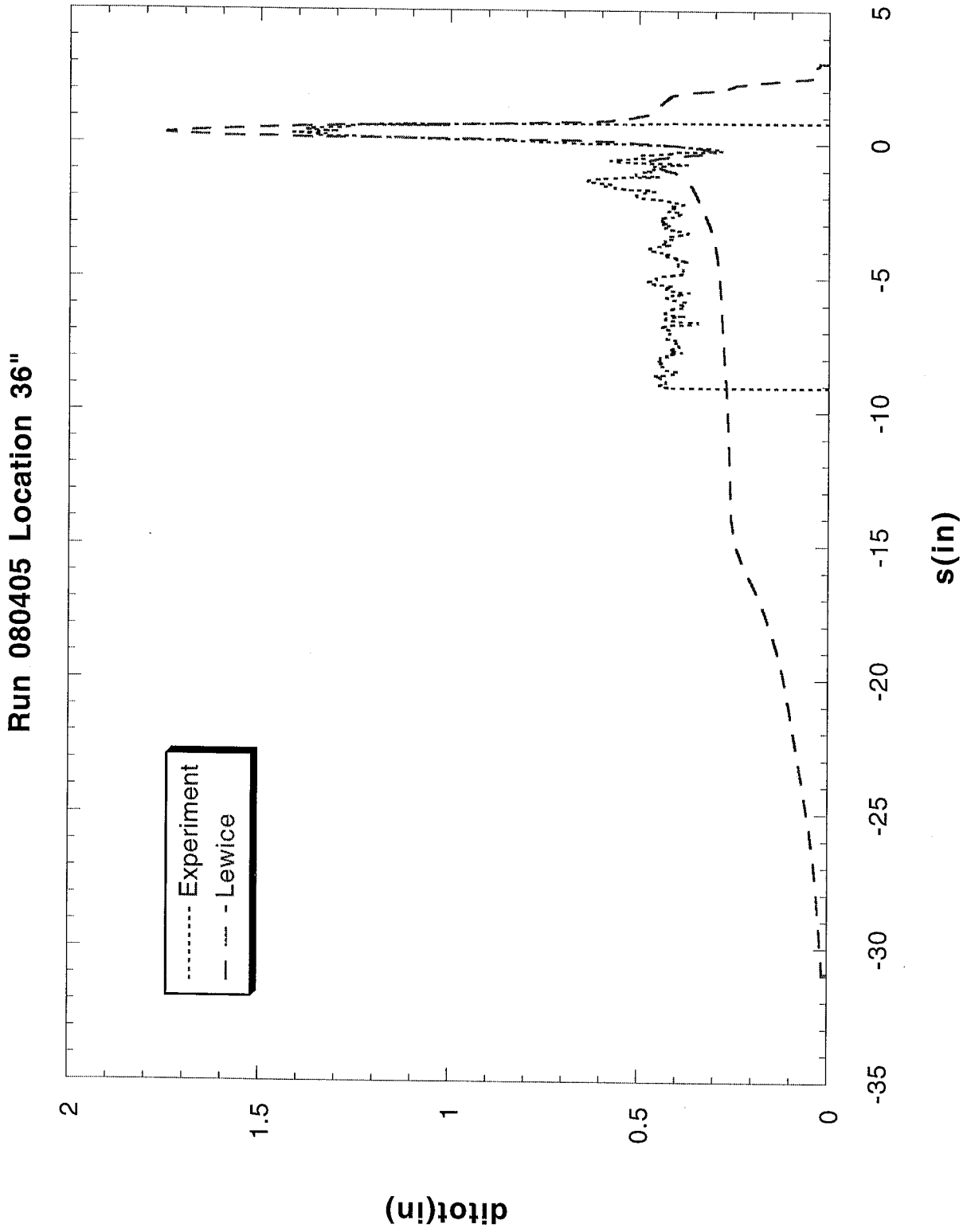
Run 080405 Location 36"
Experiment
Lewice
dltot(in)
s(in)
2
1.5
1
0.5
0
5
0
-5
-10
-15
-20
-25
-30
-35

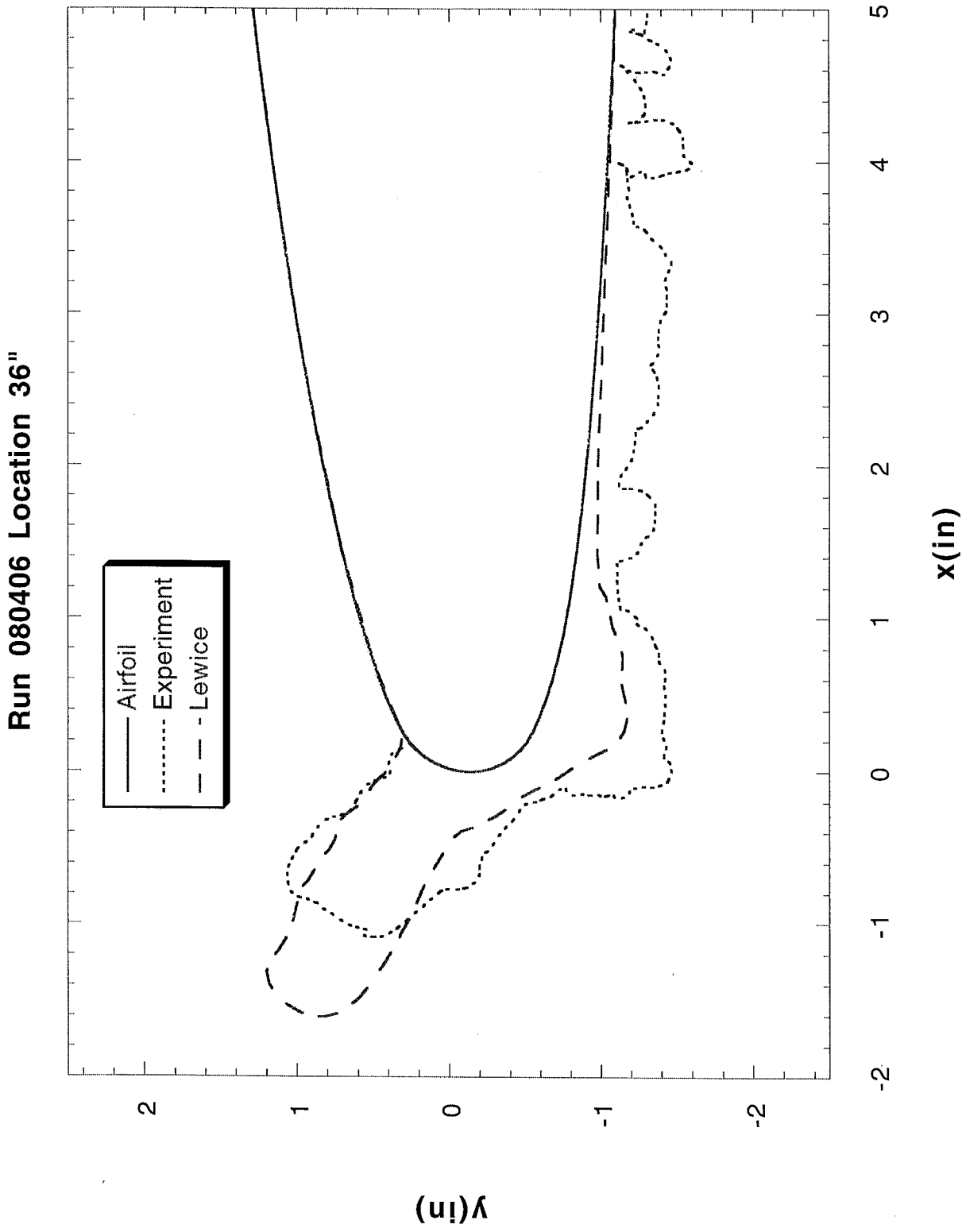
Run 080406 Location 36"
Airfoil
Experiment
Lewice
y(in)
x(in)
2
1
0
-1
-2
-2
-1
0
1
2
3
4
5

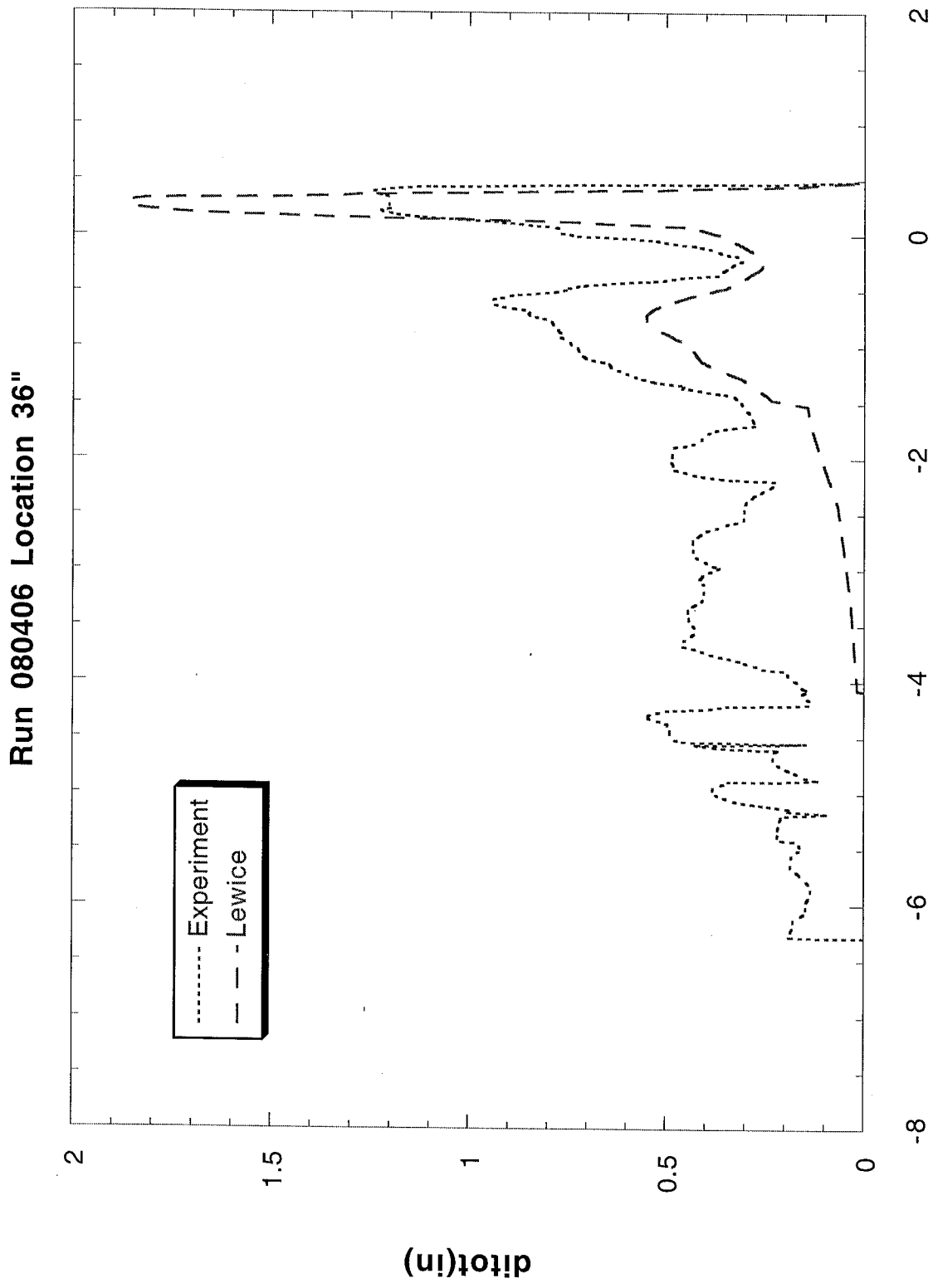
Run 080406 Location 36"
Experiment
Lewice
dltot(in)
s(in)
2
1.5
1
0.5
0
-8
-6
-4
-2
0
2

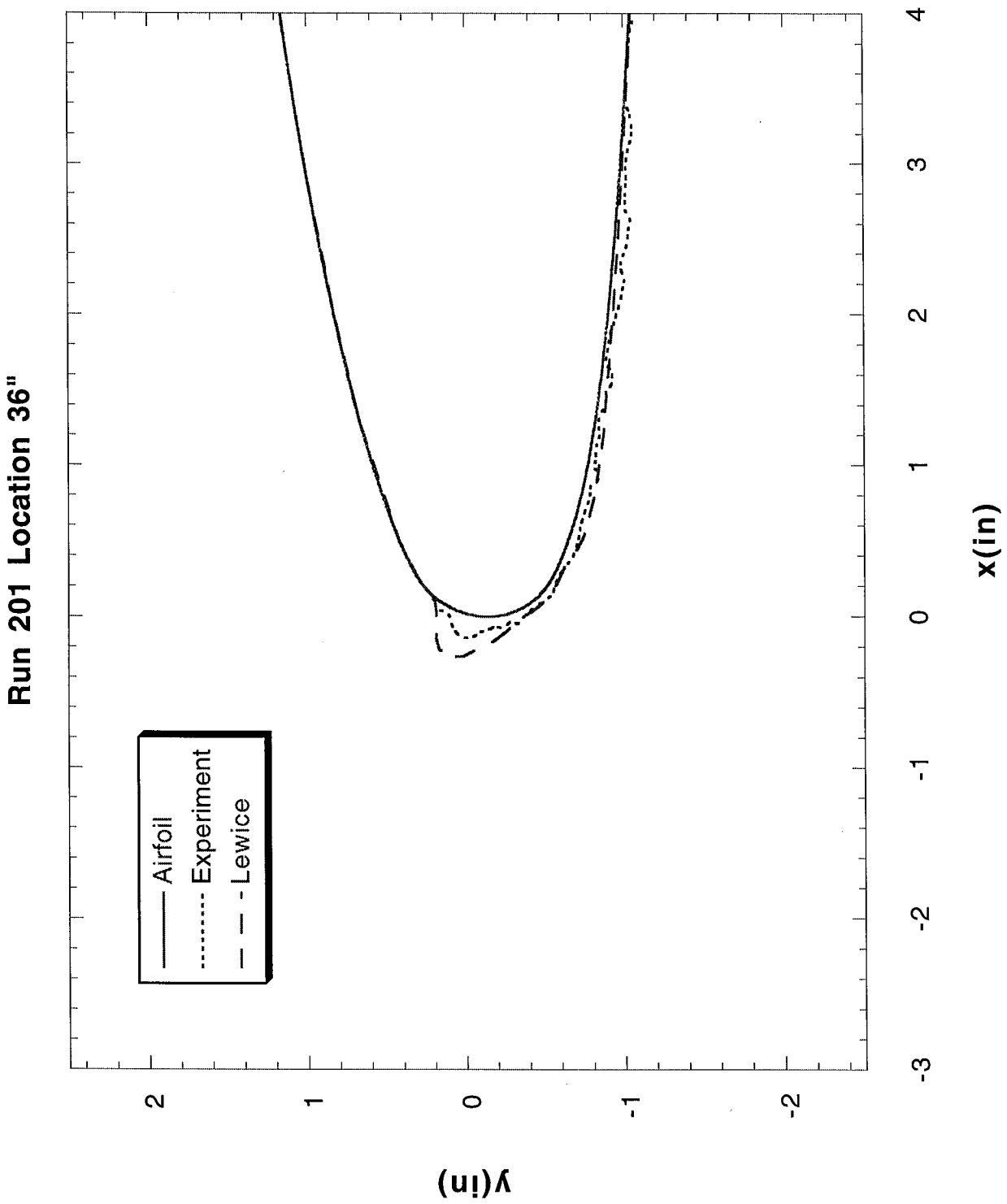
Run 201 Location 36"
Airfoil
Experiment
- Lewice
y(in)
x(in)
2
1
0
-1
-2
-3
-2
-1
0
1
2
3
4

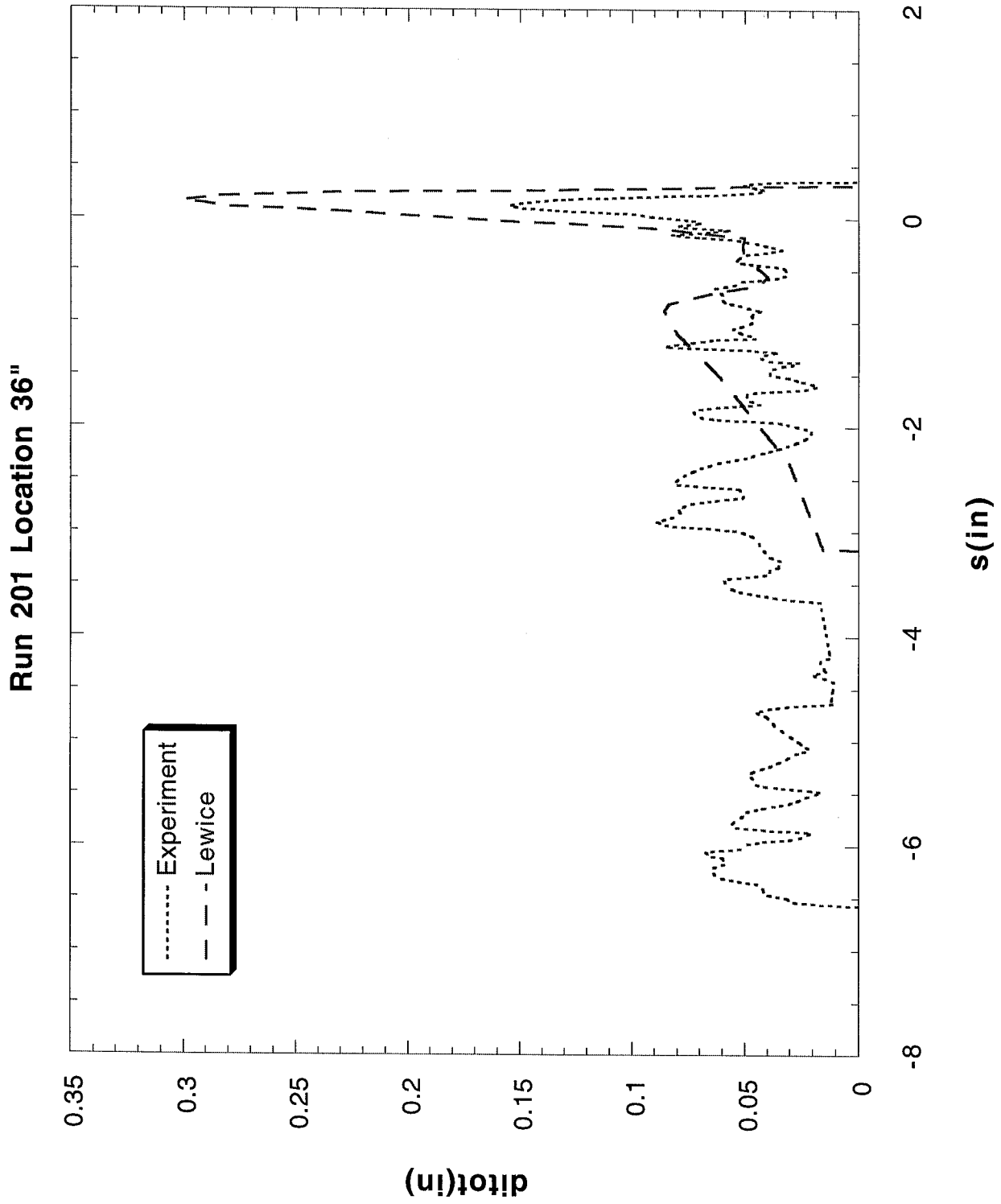
Run 201 Location 36"
Experiment
Lewice
dltot(in)
s(in)
0.35
0.3
0.25
0.2
0.15
0.1
0.05
0
2
0
-2
-4
-6
-8

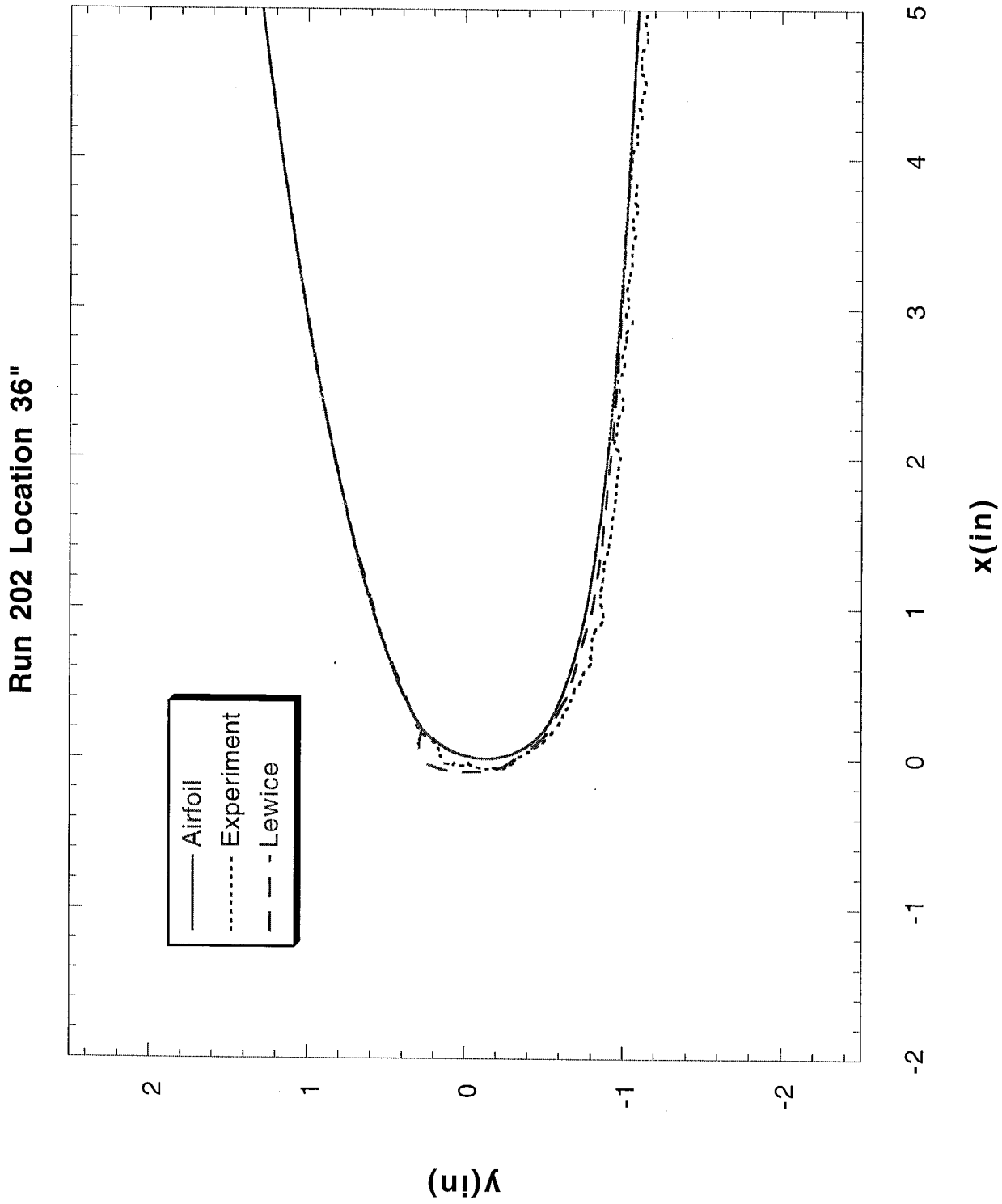
Run 202 Location 36"
Airfoil
Experiment
Lewice
y(in)
x(in)
2
1
0
-1
-2
-2
-1
0
1
2
3
4
5

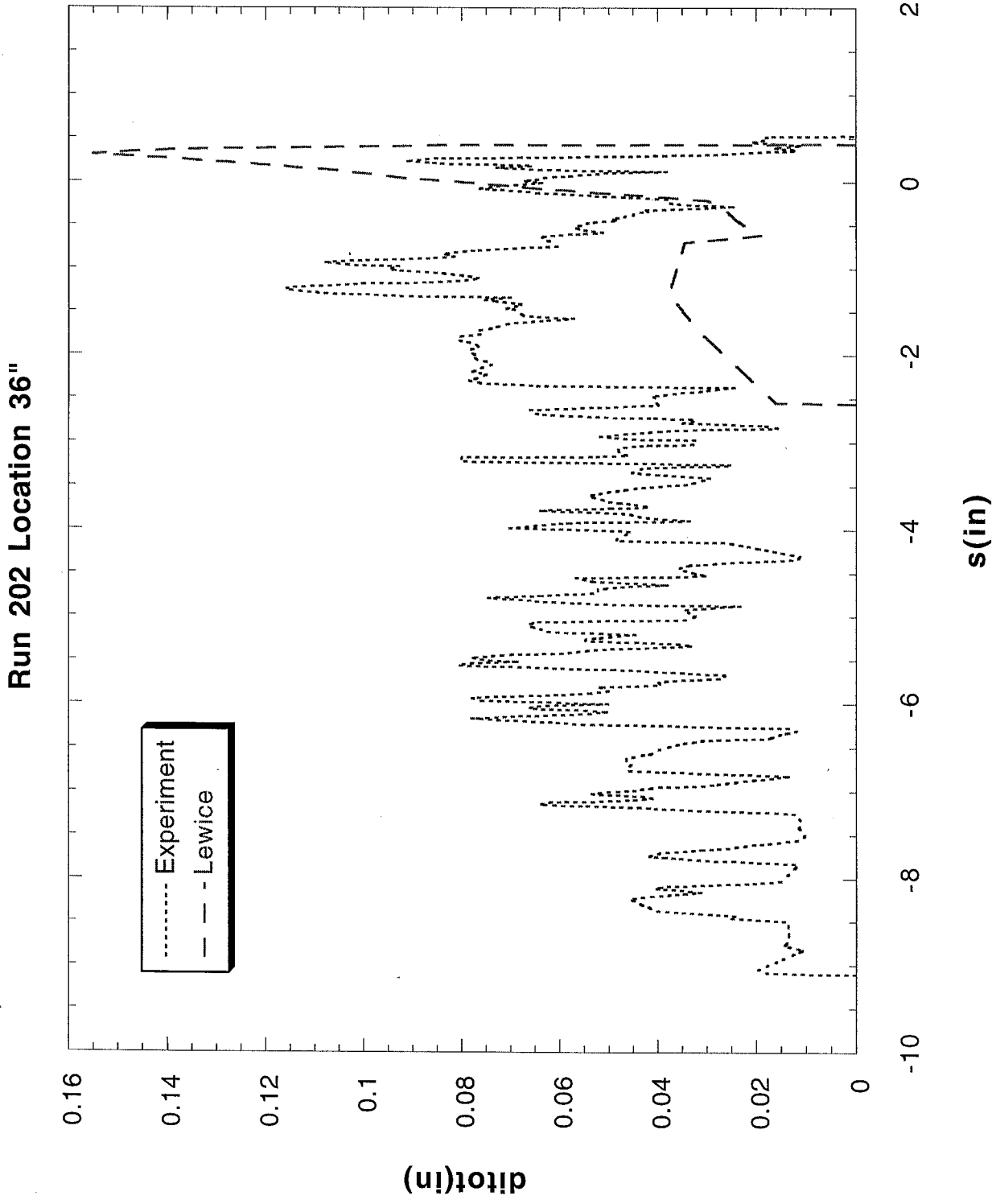
Run 202 Location 36"
Experiment
Lewice
dltot(in)
s(in)
0.16
0.14
0.12
0.1
0.08
0.06
0.04
0.02
0
2
0
-2
-4
-6
-8
-10

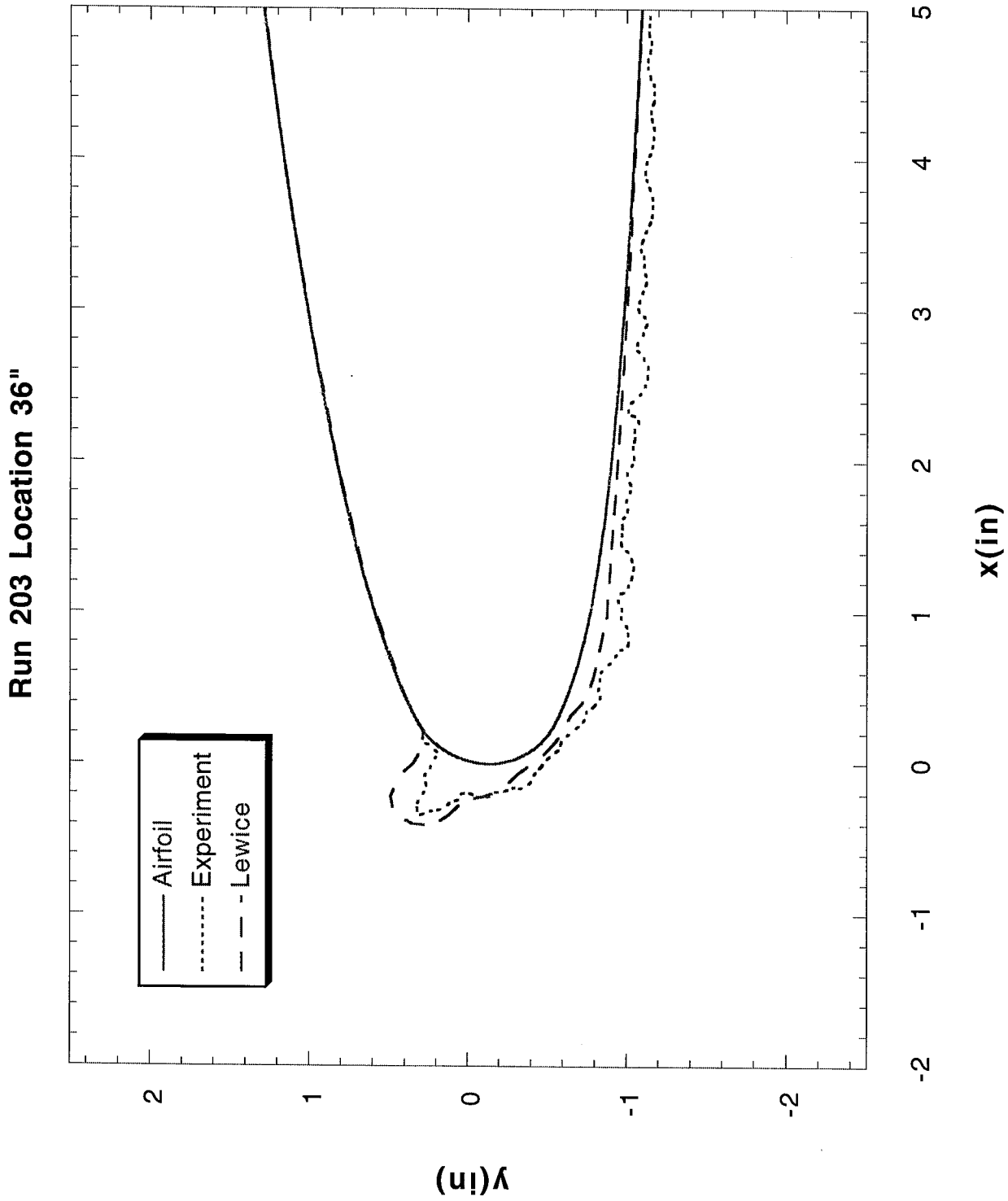
Run 203 Location 36"
Airfoil
Experiment
Lewice
y(in)
x(in)
2
1
0
-1
-2
-2
-1
0
1
2
3
4
5

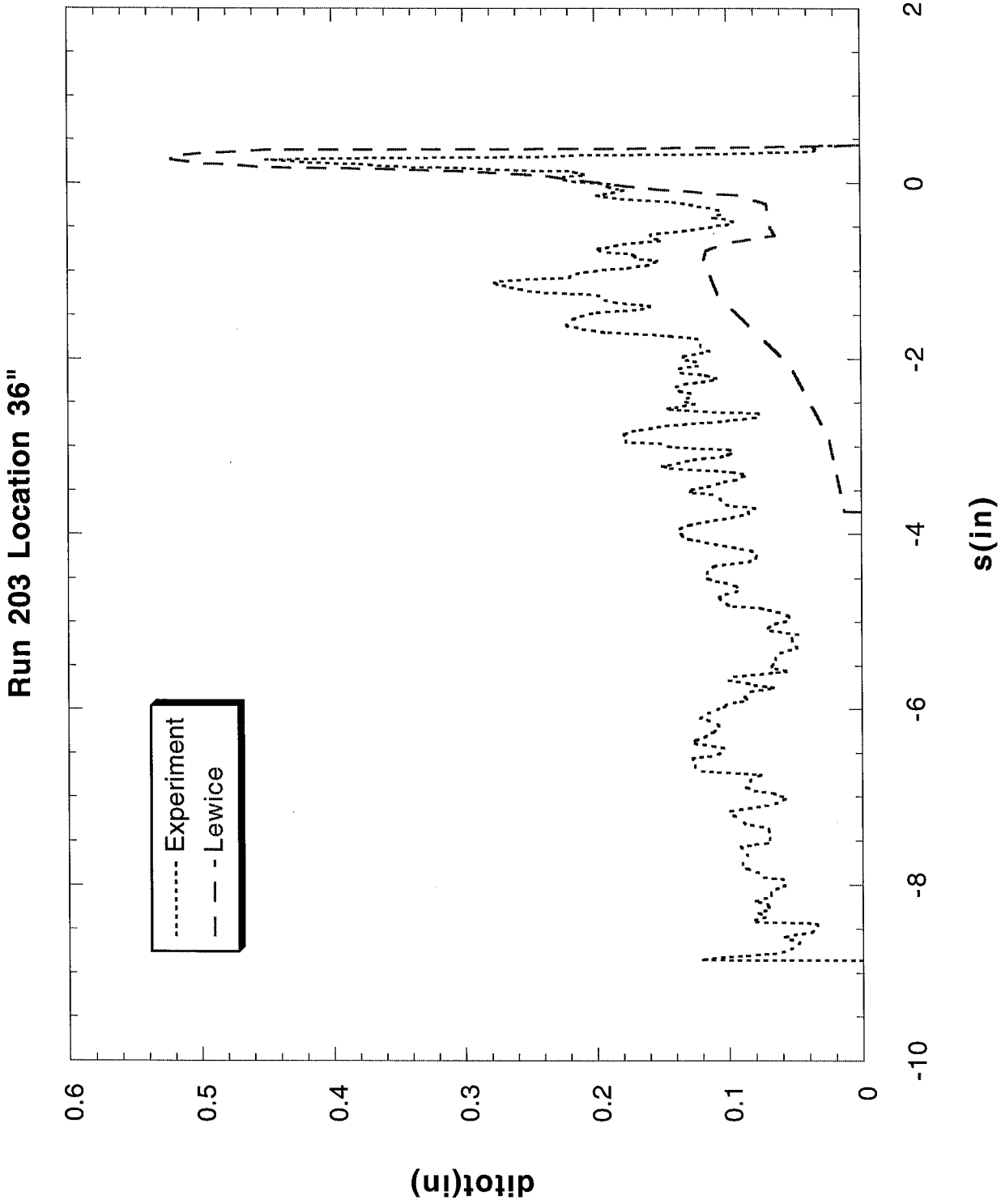
Run 203 Location 36"
Experiment
Lewice
dltot(in)
s(in)
0.6
0.5
0.4
0.3
0.2
0.1
0
2
0
-2
-4
-6
-8
-10

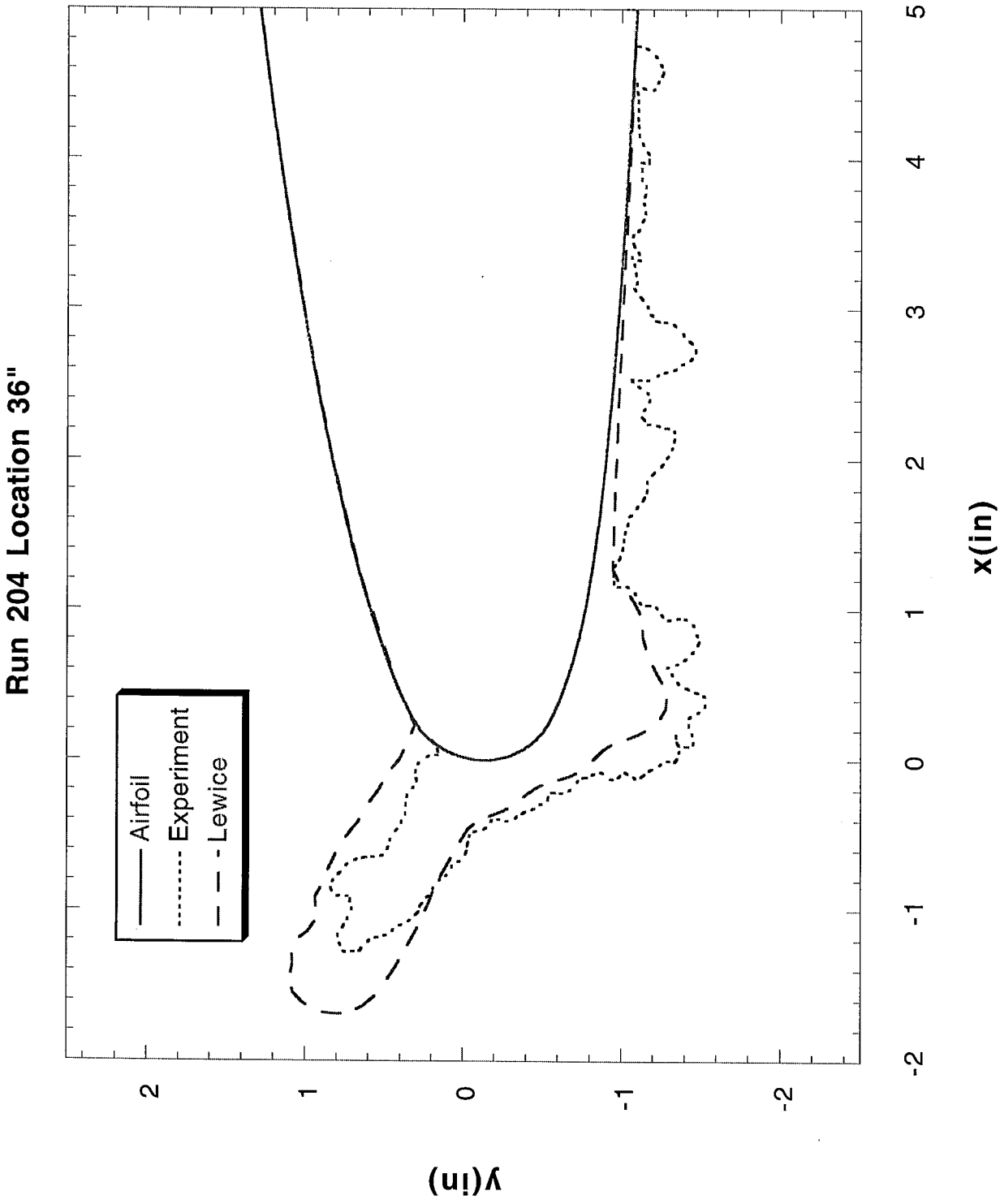
Run 204 Location 36"
Airfoil
Experiment
Lewice
y(in)
x(in)
2
1
0
-1
-2
5
4
3
2
1
0
-1
-2

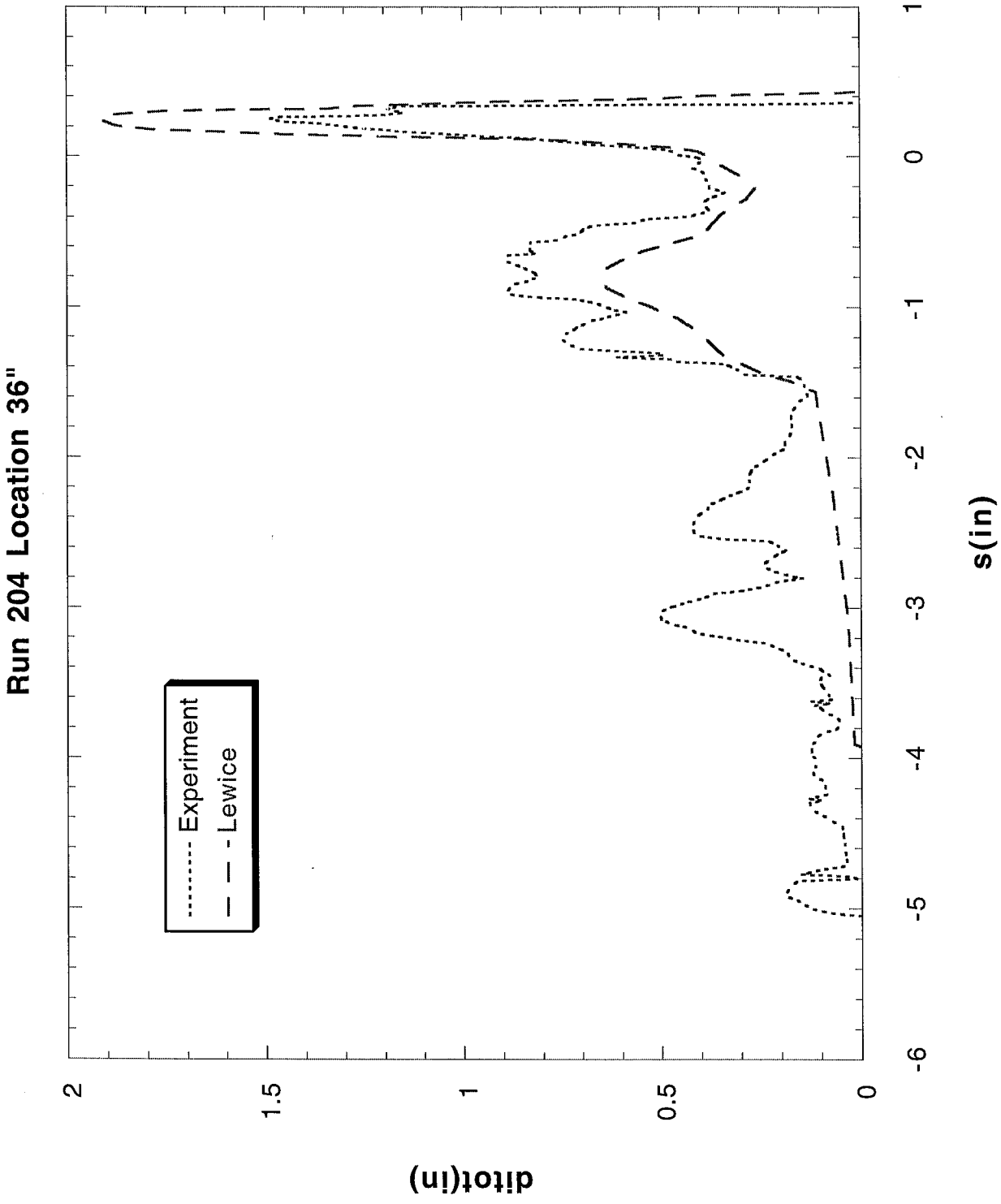
Run 204 Location 36"
Experiment
Lewice
ditot(in)
s(in)
2
1.5
1
0.5
0
1
0
-1
-2
-3
-4
-5
-6

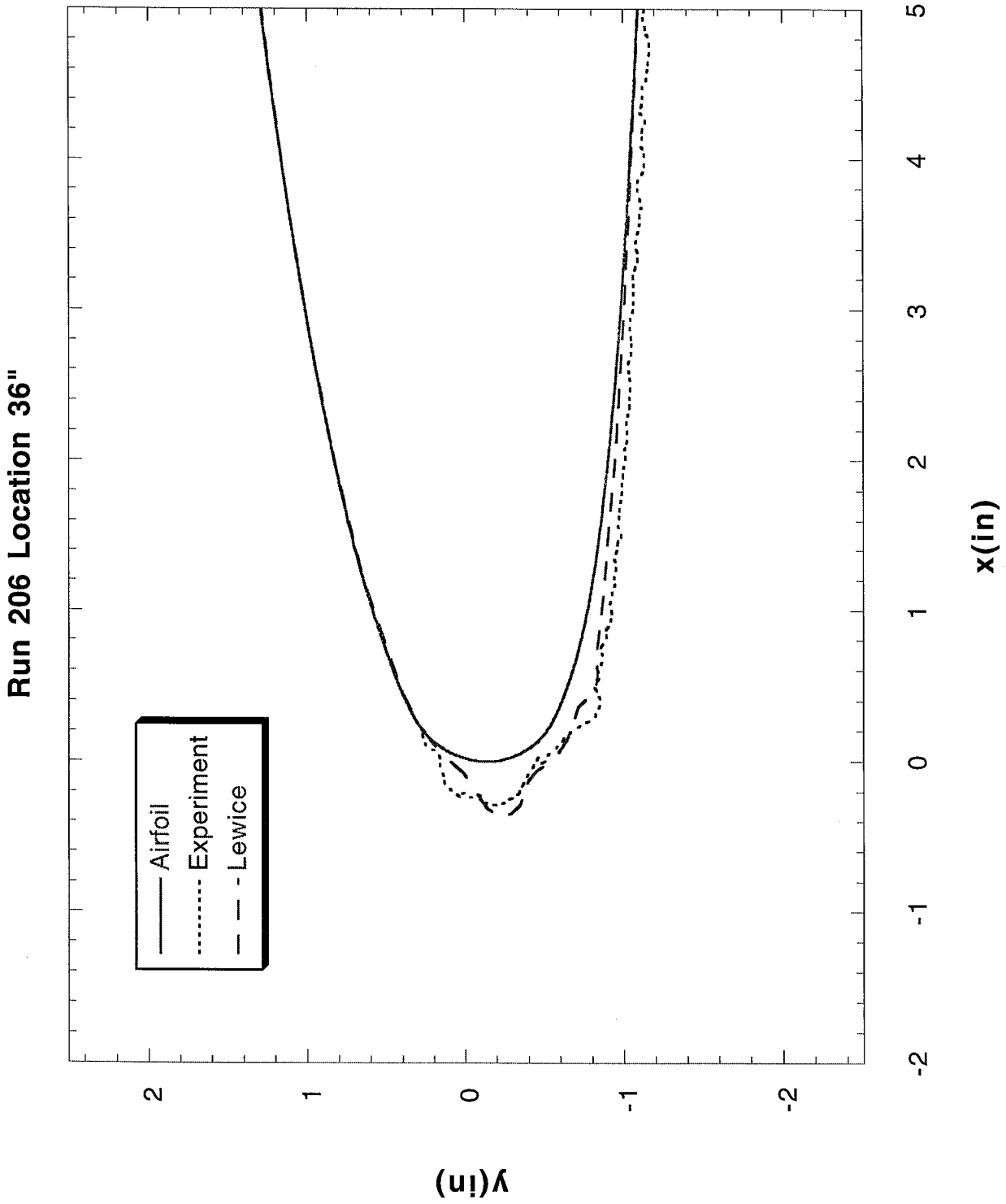
Run 206 Location 36"
Airfoil
Experiment
- Lewice
y(in)
x(in)
2
1
0
-1
-2
-2
-1
0
1
2
3
4
5

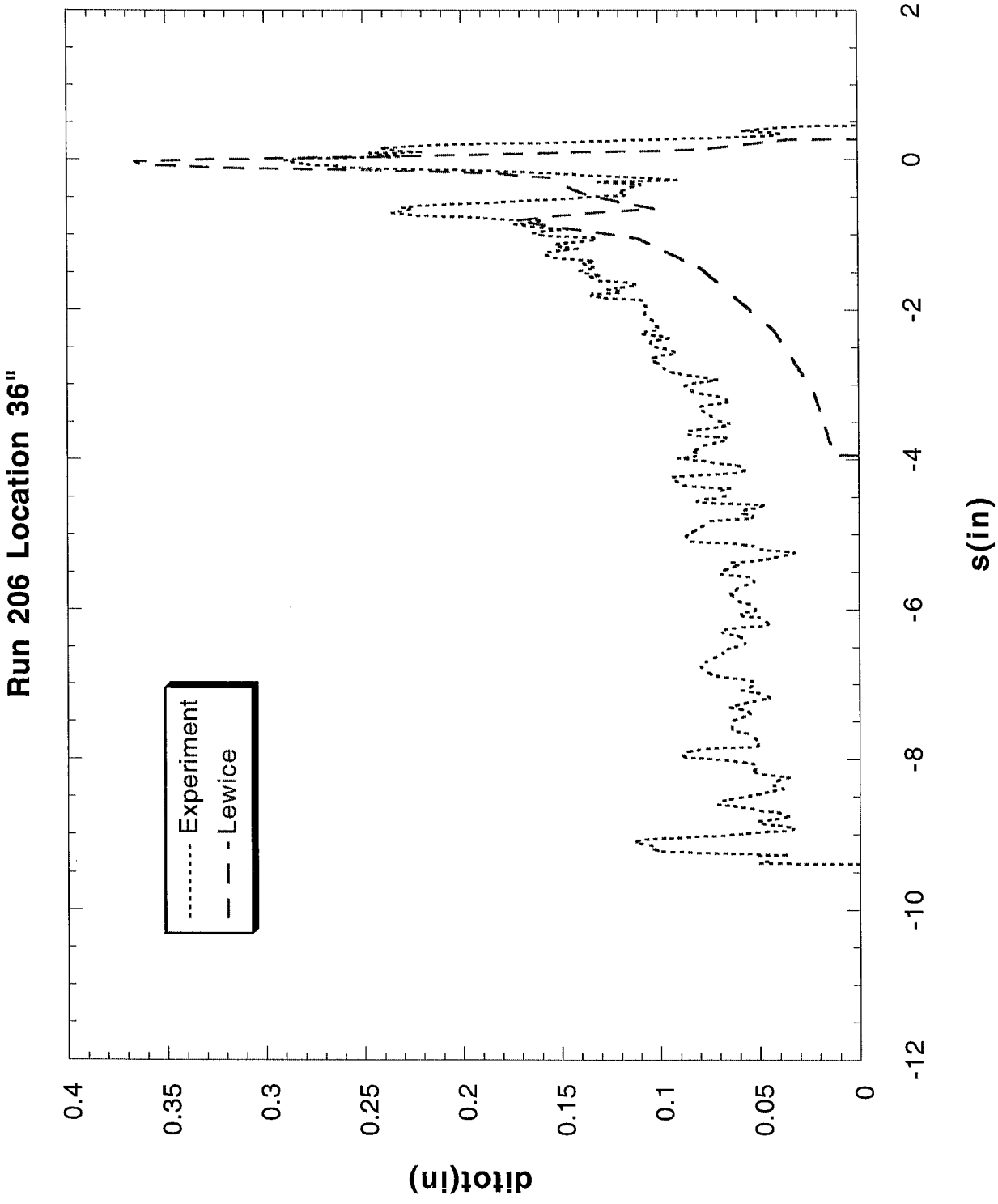
Run 206 Location 36"
Experiment
Lewice
ditot(in)
s(in)
0.4
0.35
0.3
0.25
0.2
0.15
0.1
0.05
0
2
0
-2
-4
-6
-8
-10
-12

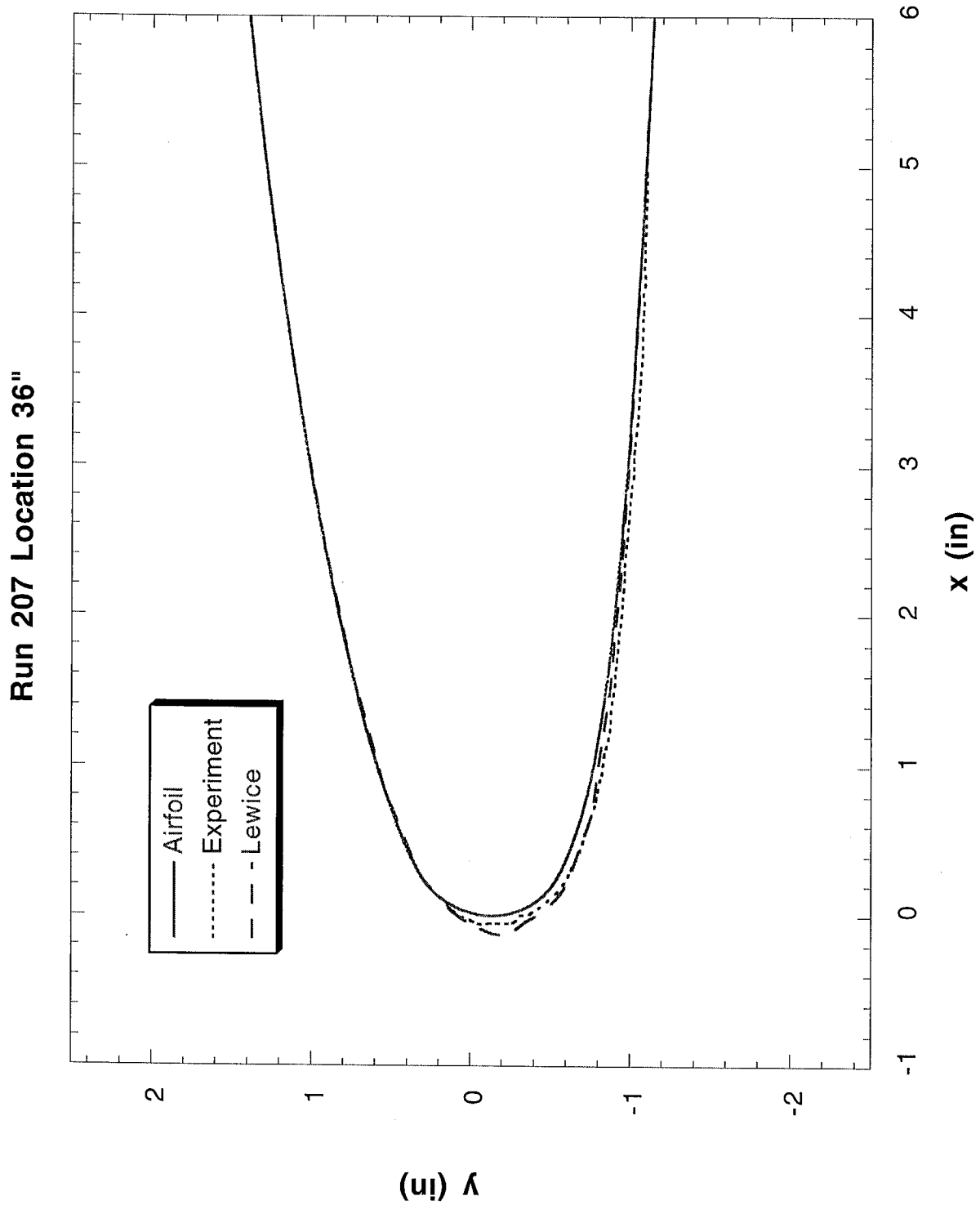
Run 207 Location 36"
Airfoil
Experiment
Lewice
y (in)
x (in)
2
1
0
-1
-2
-1
0
1
2
3
4
5
6

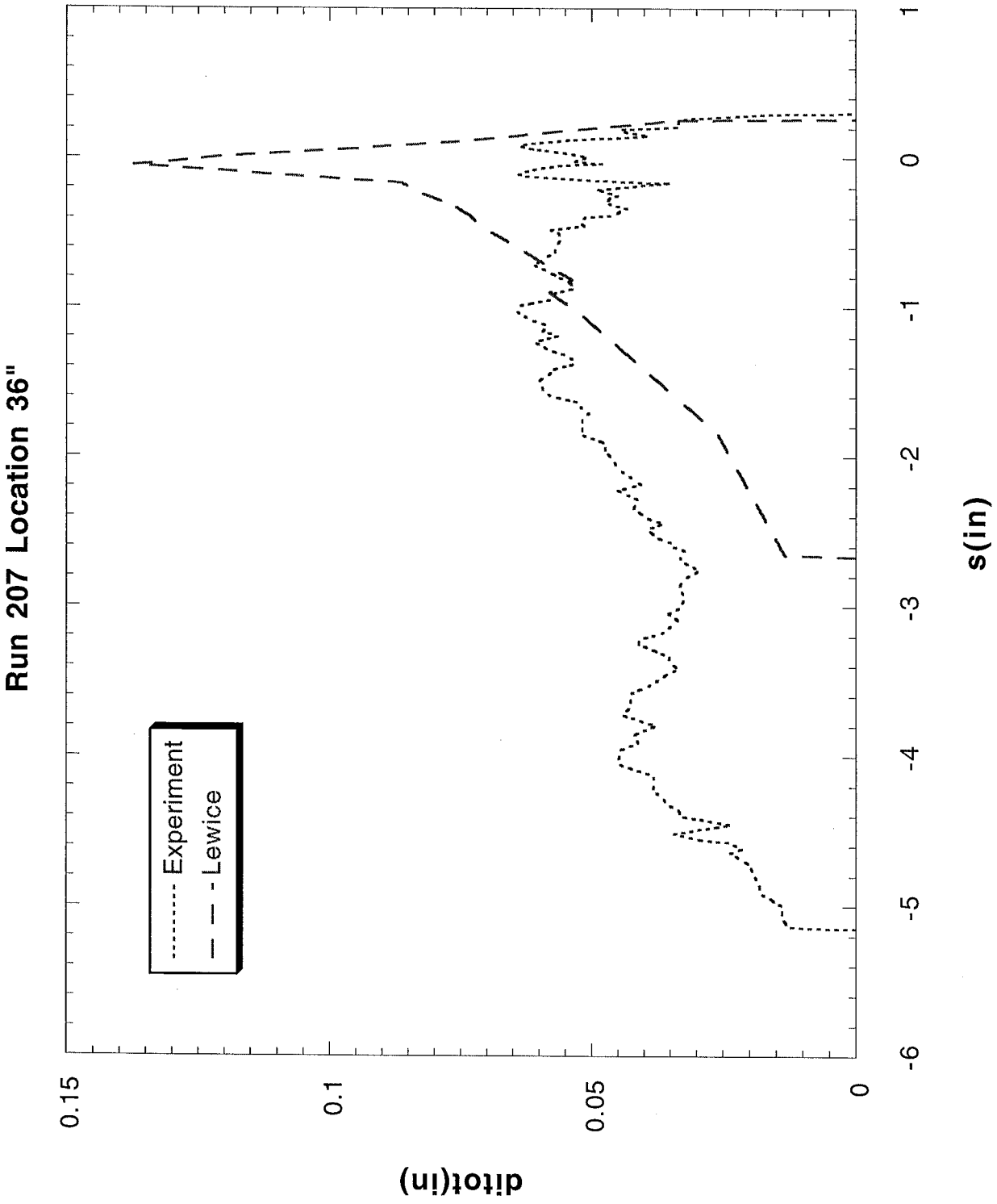
Run 207 Location 36"
Experiment
Lewice
dltot(in)
0.15
0.1
0.05
0
s(in)
1
0
-1
-2
-3
-4
-5
-6

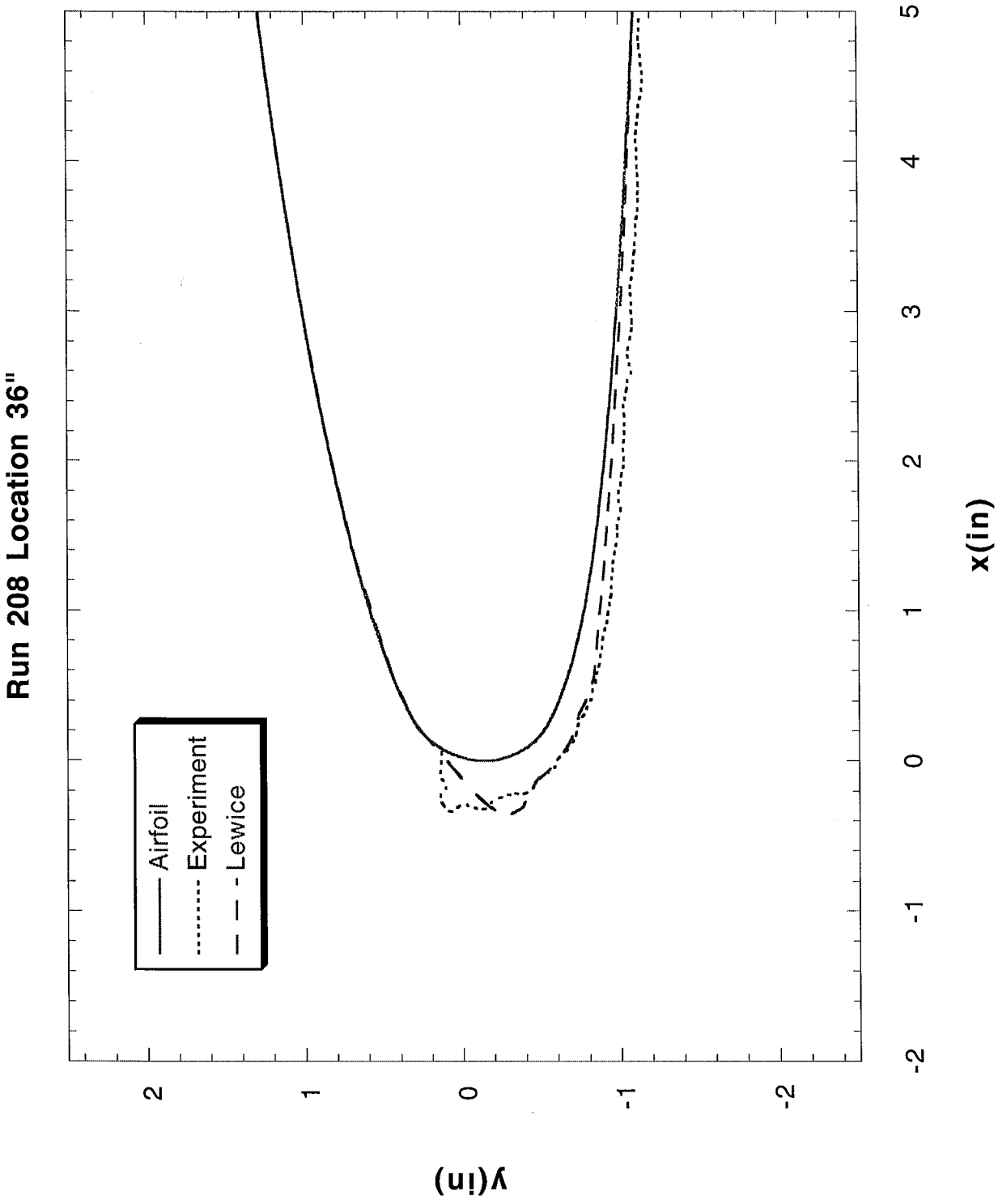
Run 208 Location 36"
Airfoil
Experiment
Lewice
y(in)
x(in)
2
1
0
-1
-2
-2
-1
0
1
2
3
4
5

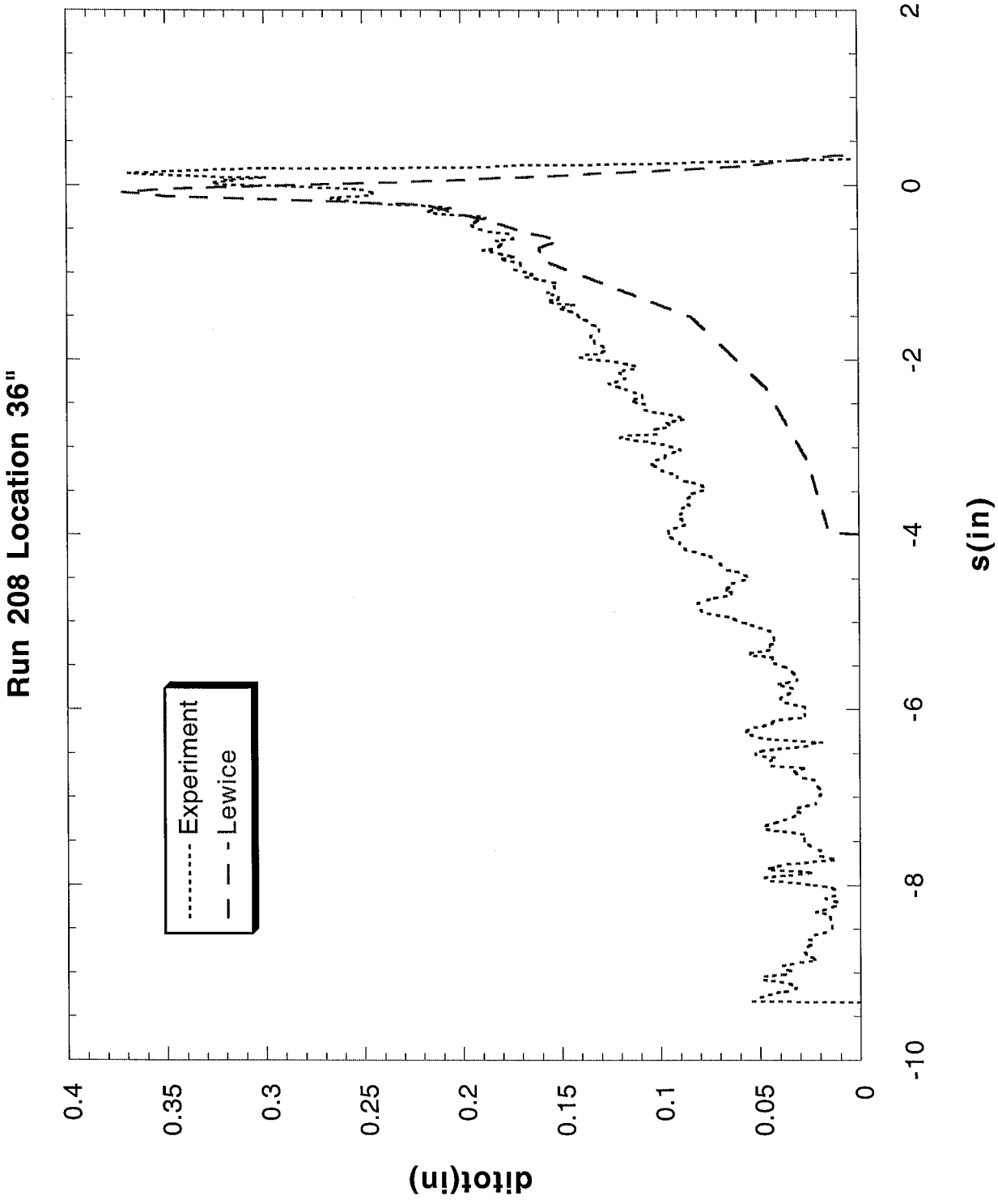
Run 208 Location 36"
Experiment
Lewice
ditot(in)
s(in)
0.4
0.35
0.3
0.25
0.2
0.15
0.1
0.05
0
2
0
-2
-4
-6
-8
-10

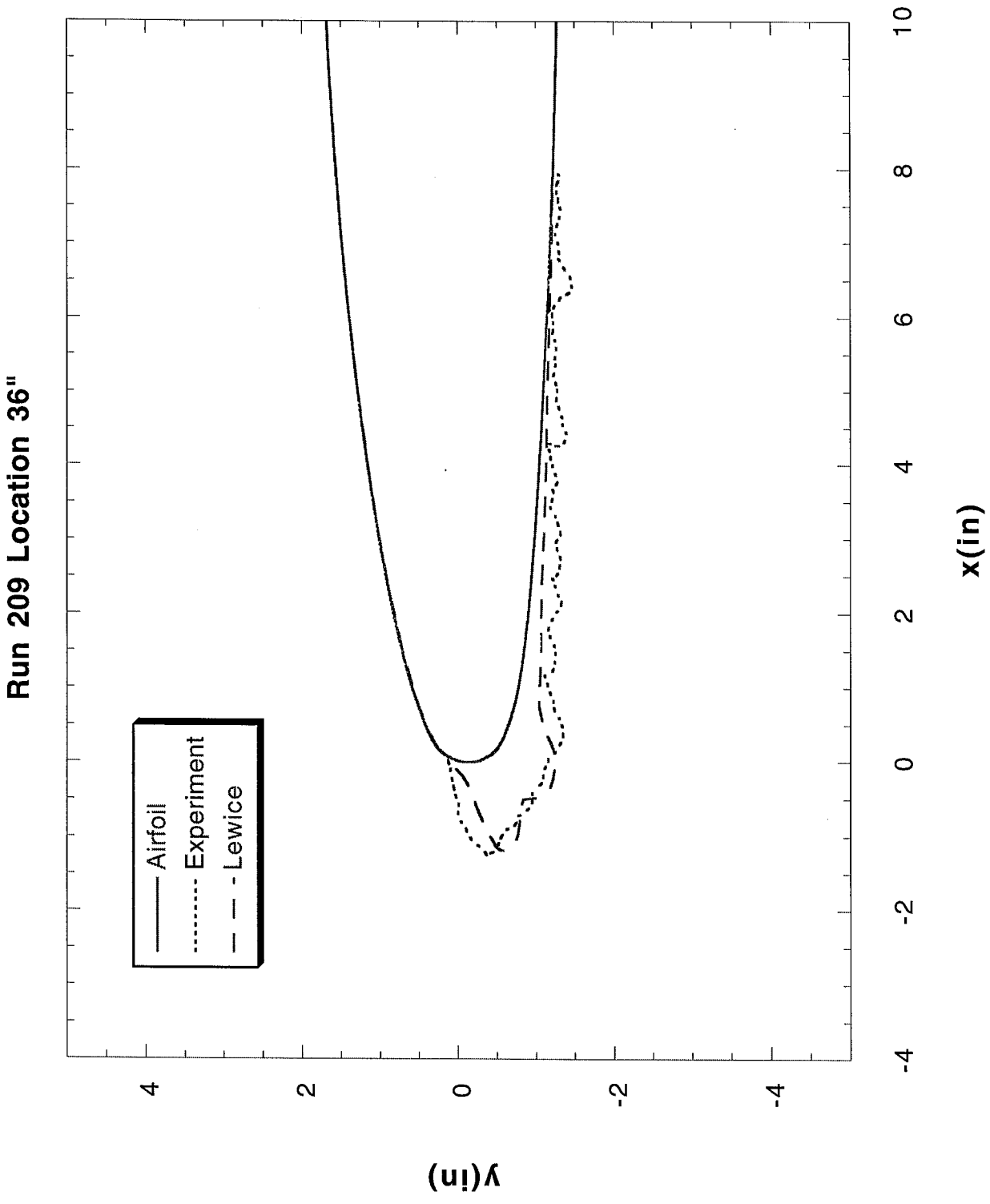
Run 209 Location 36"
Airfoil
Experiment
Lewice
y(in)
x(in)
4
2
0
-2
-4
-4
-2
0
2
4
6
8
10

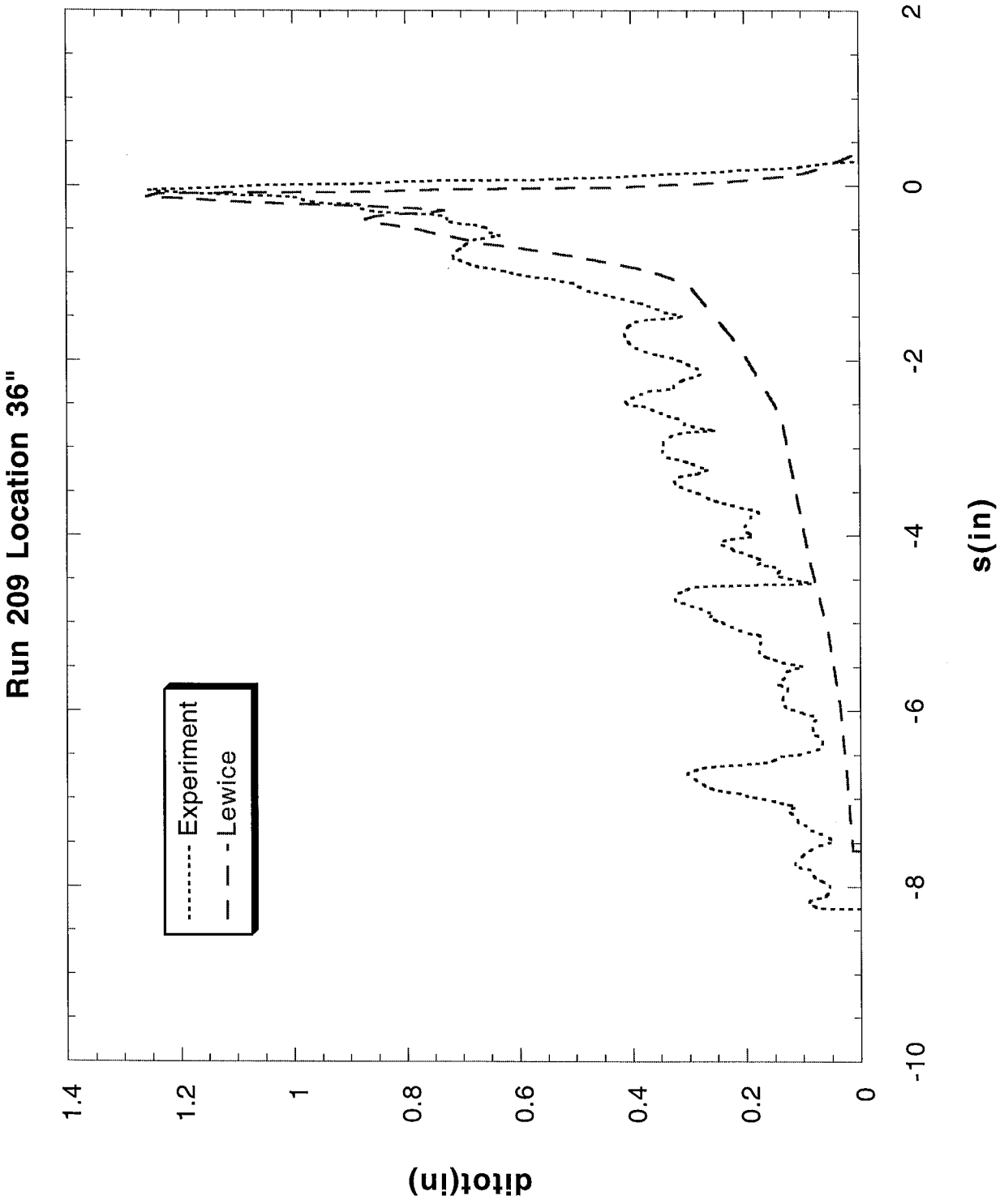
Run 209 Location 36"
Experiment
Lewice
dltot(in)
s(in)
1.4
1.2
1
0.8
0.6
0.4
0.2
0
2
0
-2
-4
-6
-8
-10

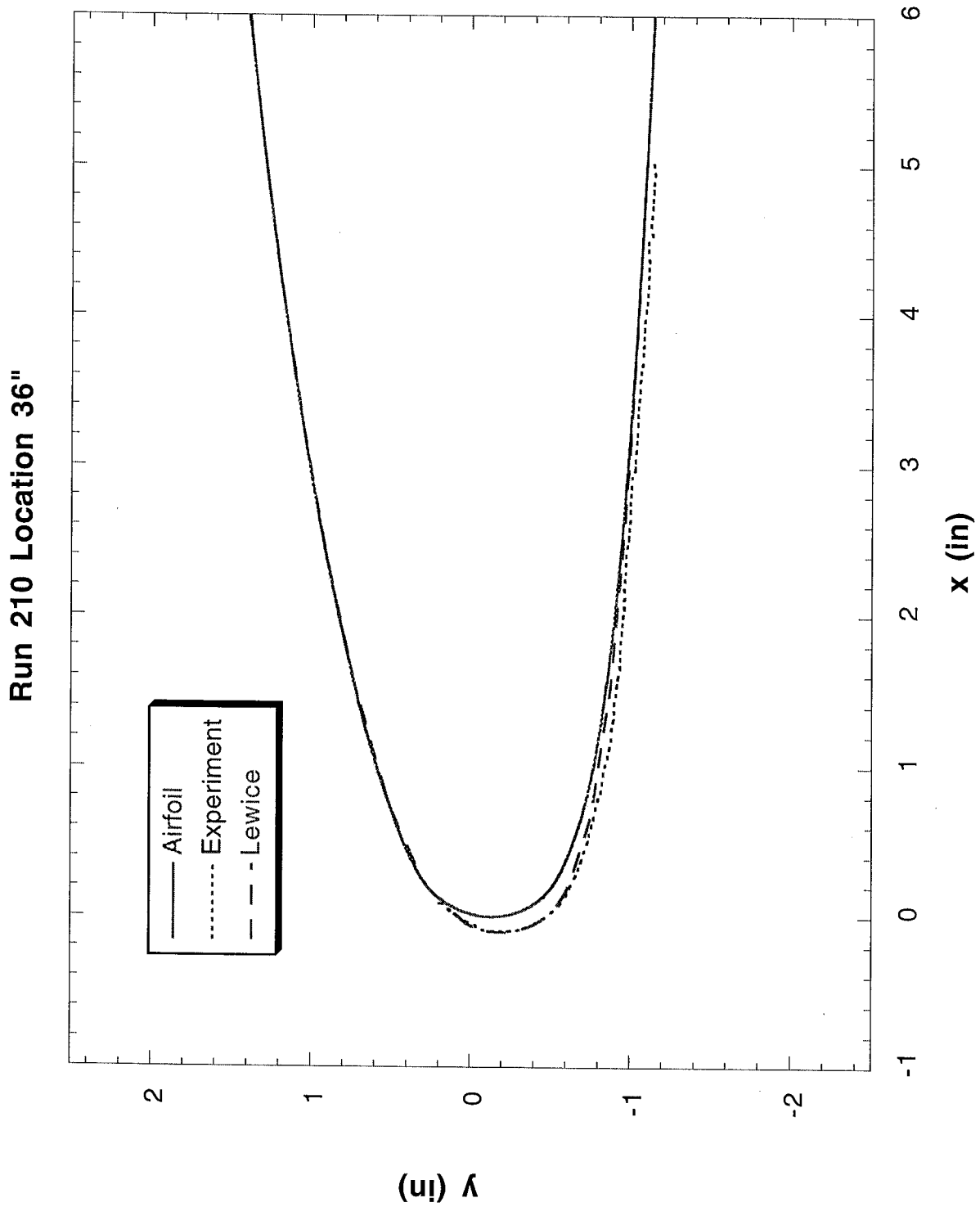
Run 210 Location 36"
Airfoil
Experiment
Lewice
y (in)
x (in)
2
1
0
-1
-2
-1
0
1
2
3
4
5
6

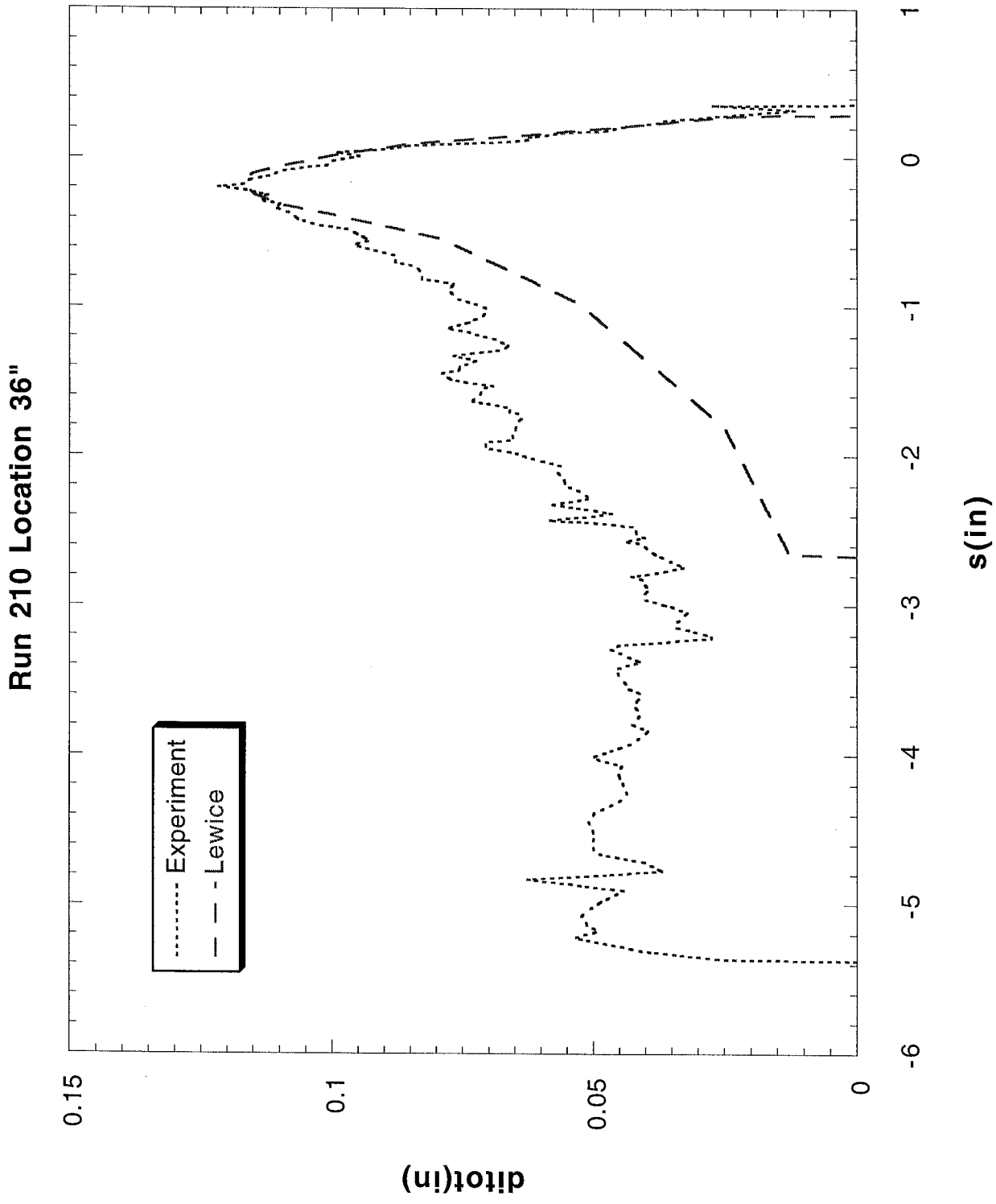
Run 210 Location 36"
Experiment
Lewice
dltot(in)
0.15
0.1
0.05
0
s(in)
1
0
-1
-2
-3
-4
-5
-6

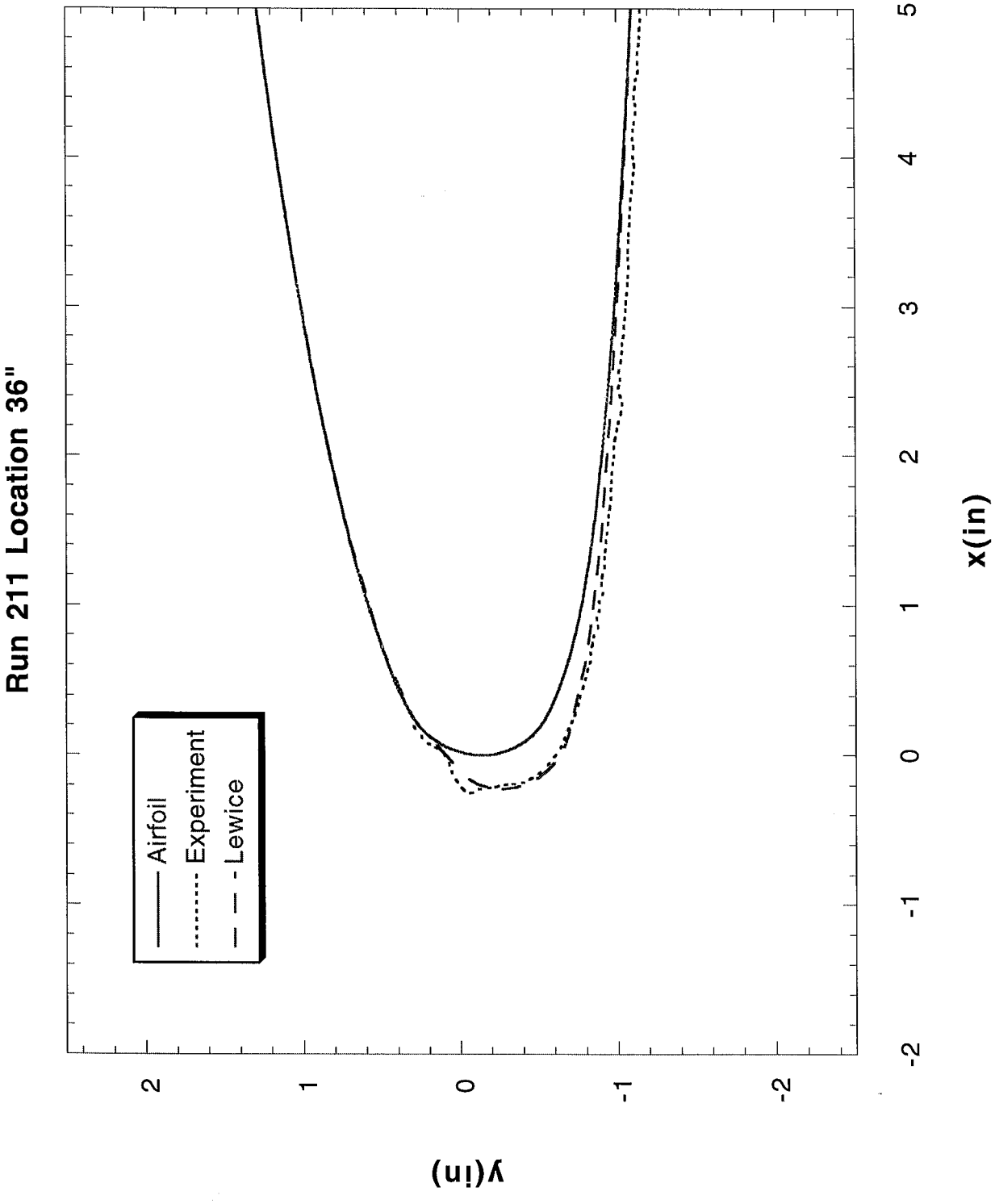
Run 211 Location 36"
Airfoil
Experiment
Lewice
y(in)
x(in)
2
1
0
-1
-2
-2
-1
0
1
2
3
4
5

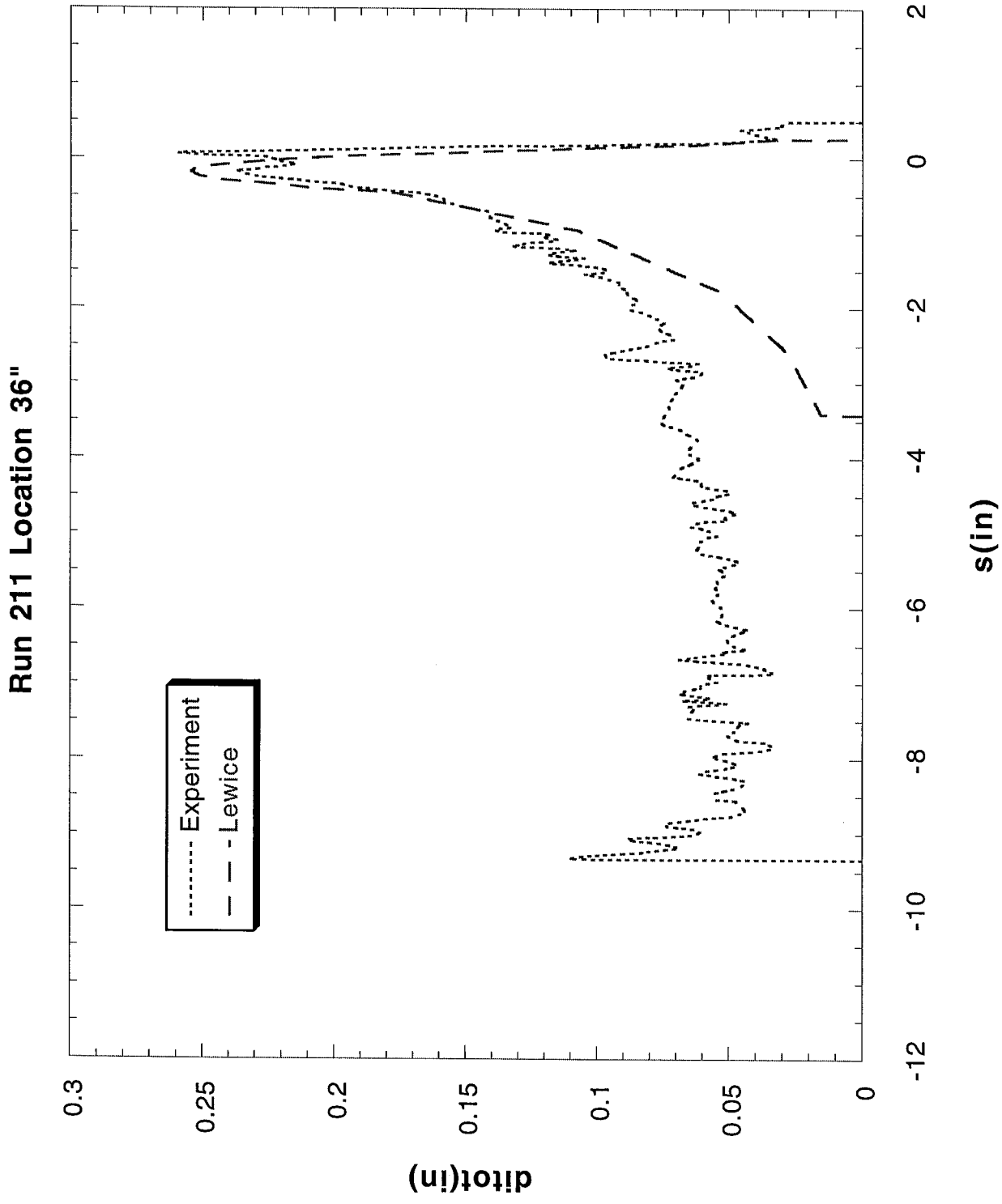
Run 211 Location 36"
Experiment
Lewice
dltot(in)
s(in)
0.3
0.25
0.2
0.15
0.1
0.05
0
2
0
-2
-4
-6
-8
-10
-12

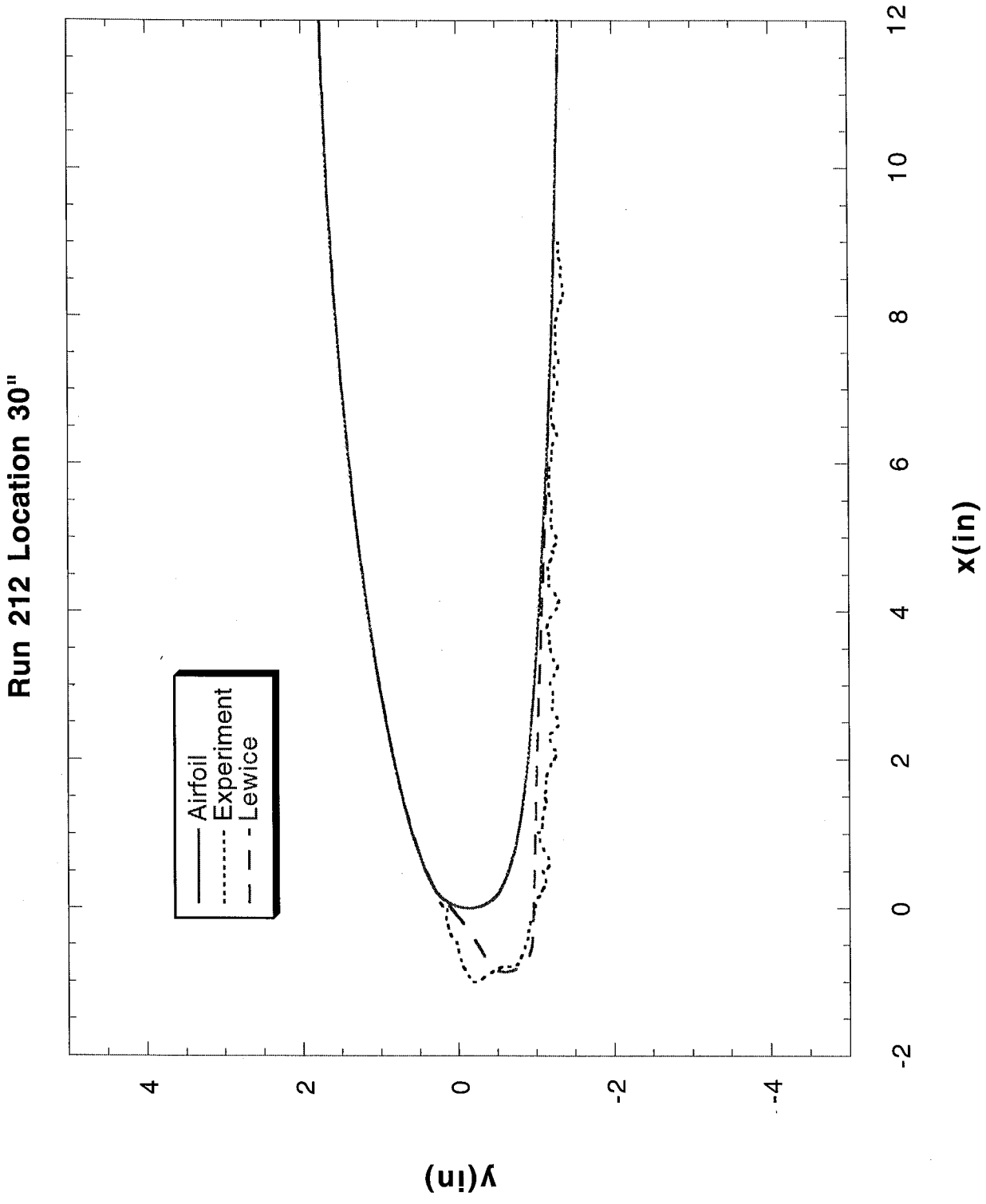
Run 212 Location 30"
Airfoil
Experiment
Lewice
y(in)
x(in)
4
2
0
-2
-4
-2
0
2
4
6
8
10
12

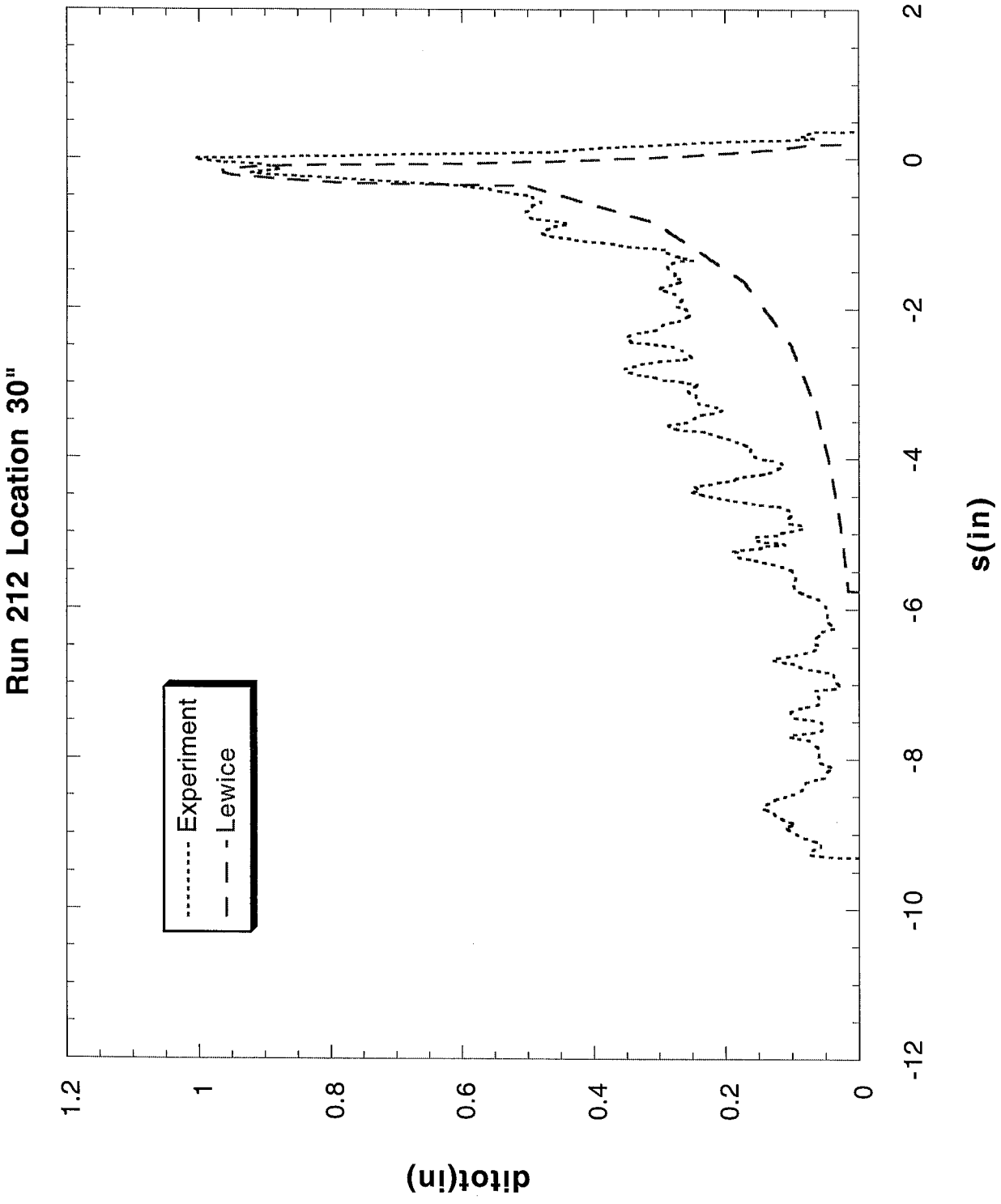
Run 212 Location 30"
Experiment
Lewice
dltot(in)
s(in)
1.2
1
0.8
0.6
0.4
0.2
0
2
0
-2
-4
-6
-8
-10
-12

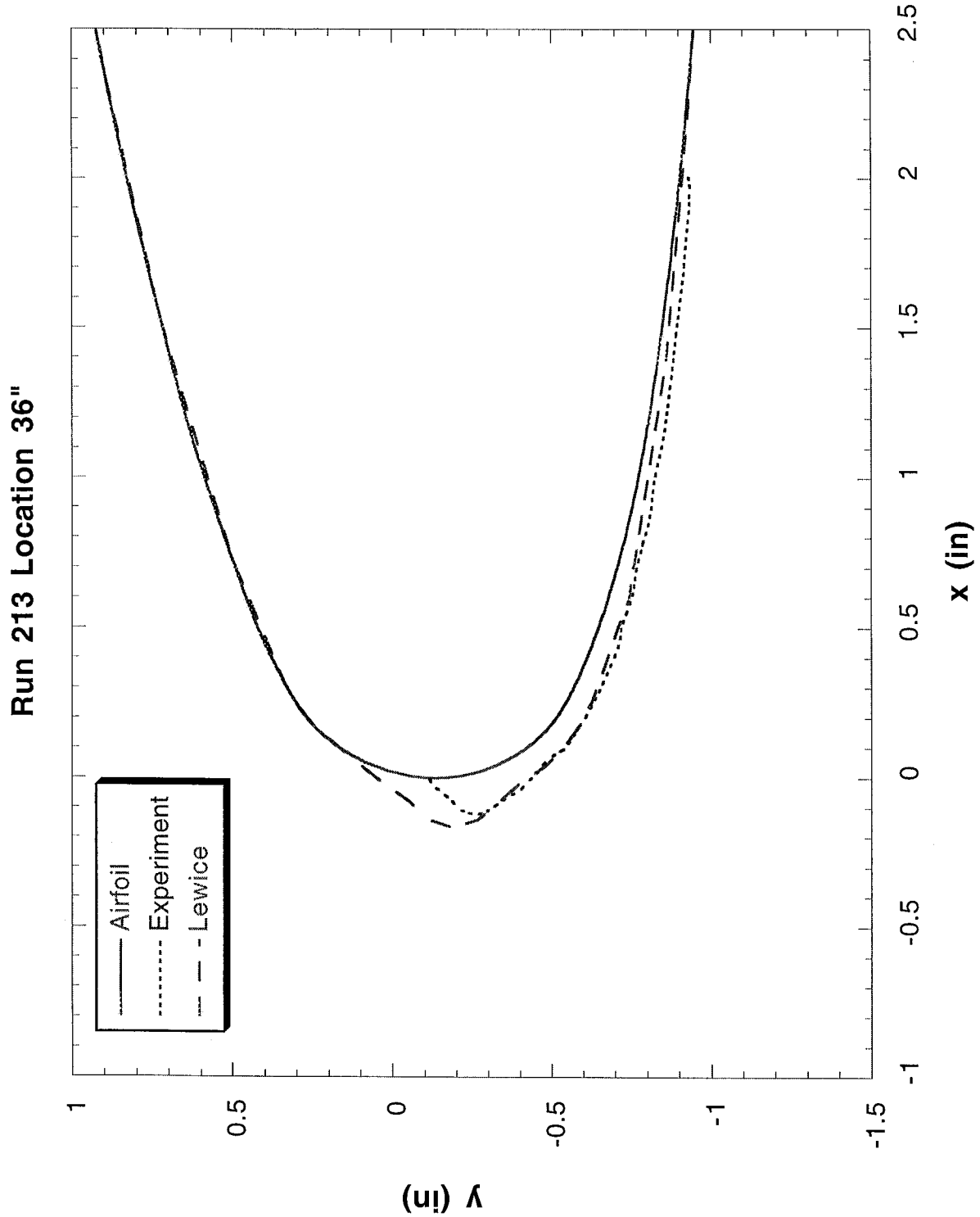
Run 213 Location 36"
Airfoil
Experiment
Lewice
y (in)
x (in)
1
0.5
0
-0.5
-1
-1.5
-1
-0.5
0
0.5
1
1.5
2
2.5

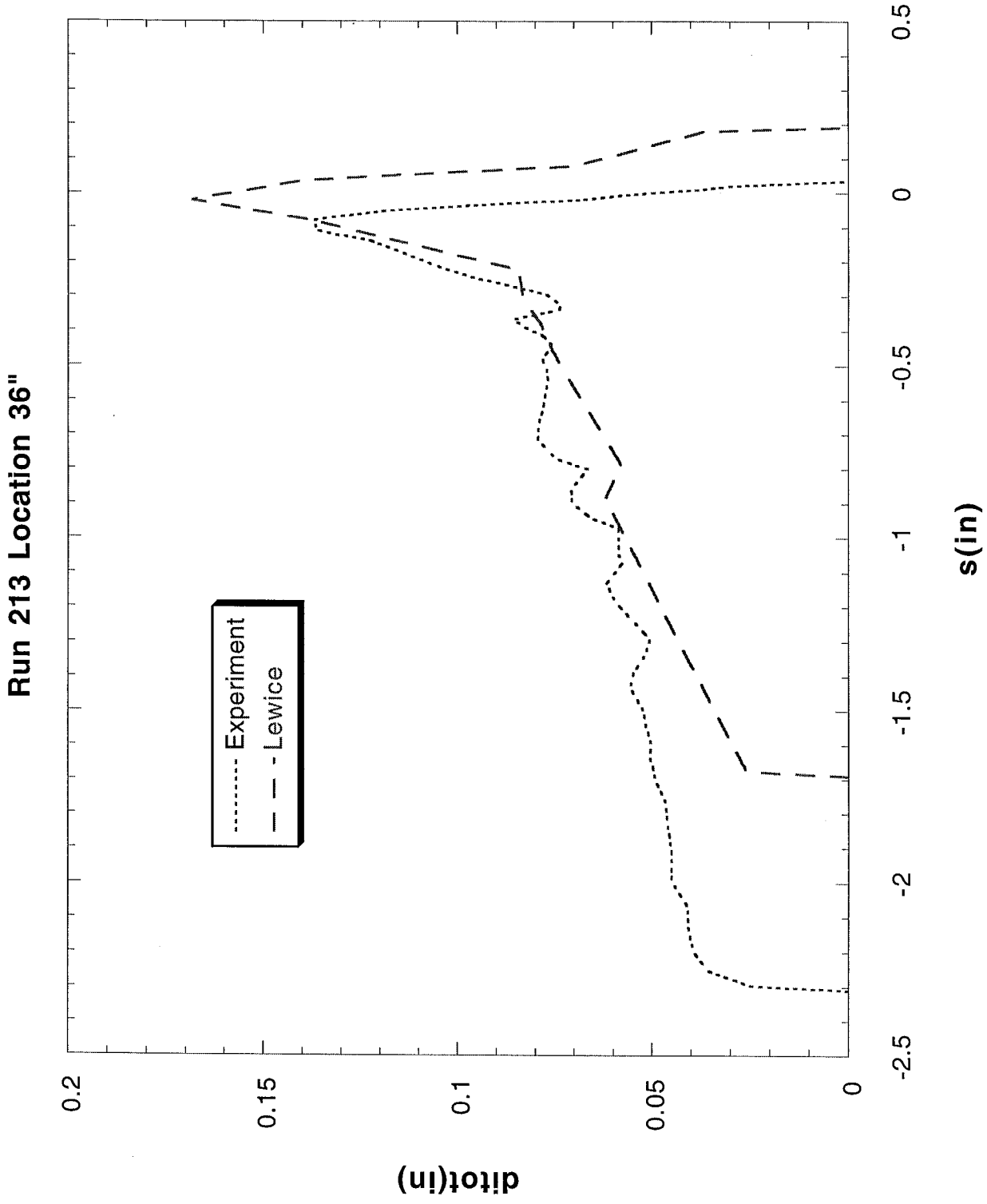
Run 213 Location 36"
Experiment
Lewice
dltot(in)
s(in)
0.2
0.15
0.1
0.05
0
-2.5
-2
-1.5
-1
-0.5
0
0.5

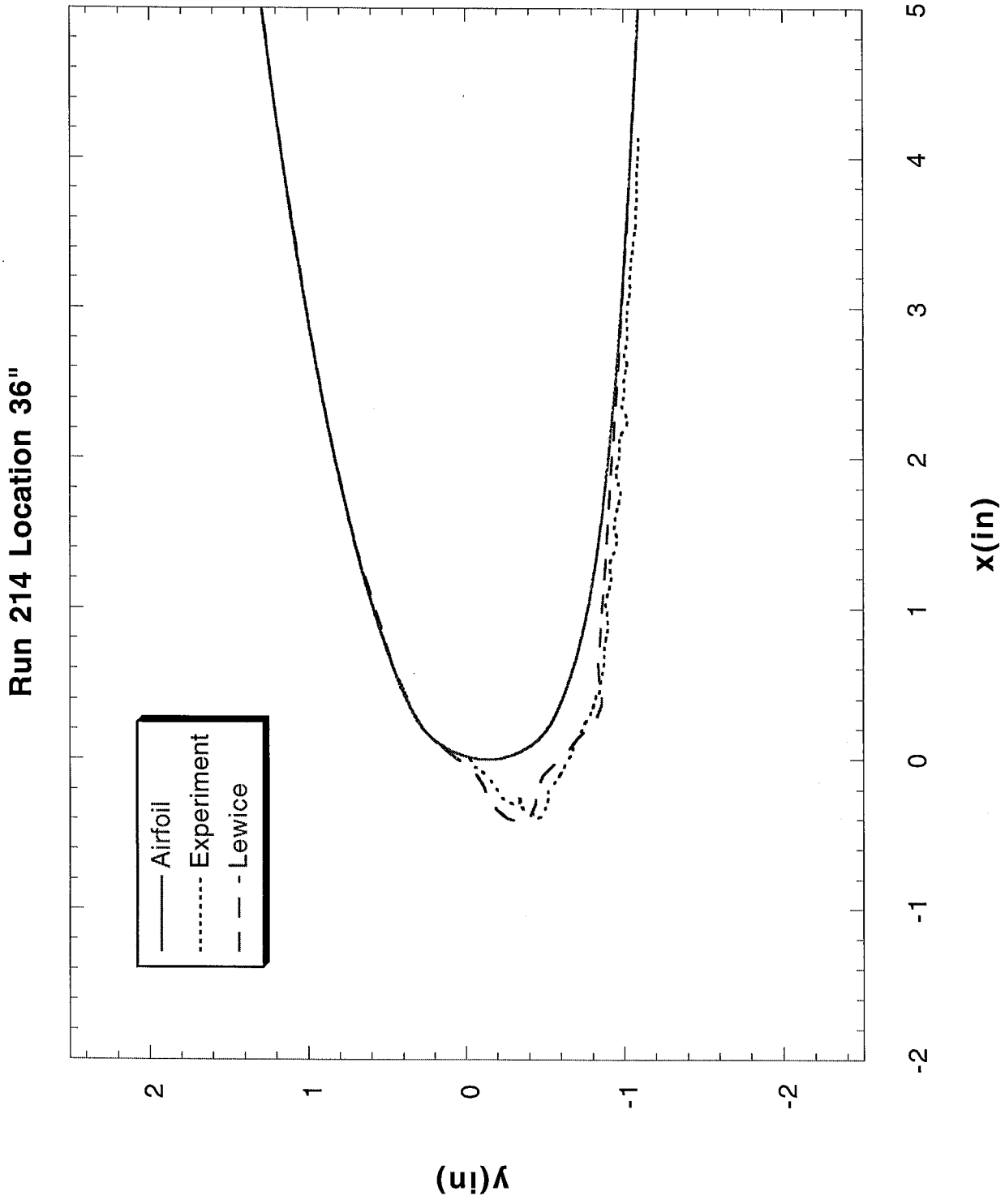
Run 214 Location 36"
Airfoil
Experiment
Lewice
y(in)
x(in)
2
1
0
-1
-2
-2
-1
0
1
2
3
4
5

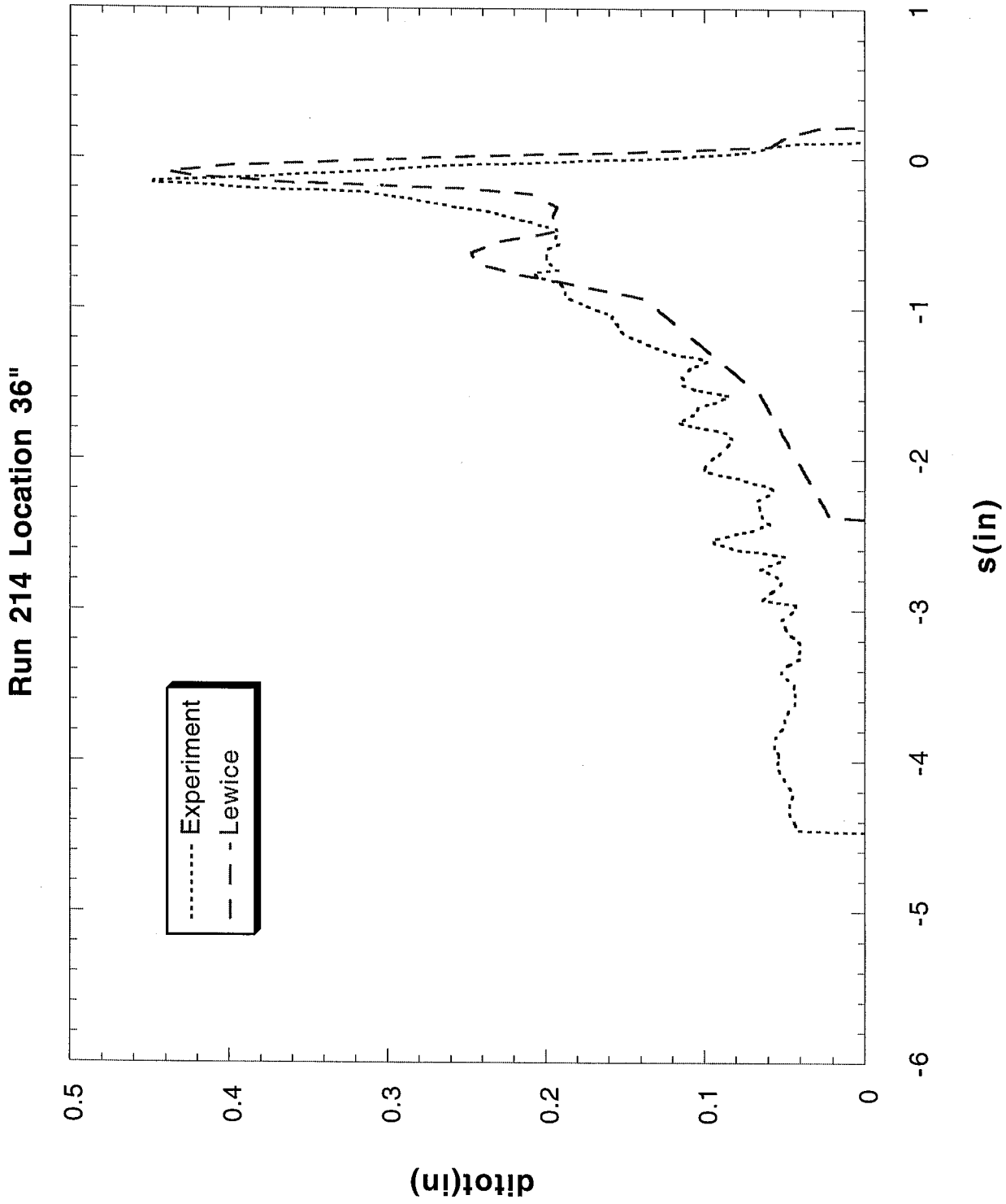
Run 214 Location 36"
Experiment
Lewice
dltot(in)
s(in)
0.5
0.4
0.3
0.2
0.1
0
-6
-5
-4
-3
-2
-1
0
1

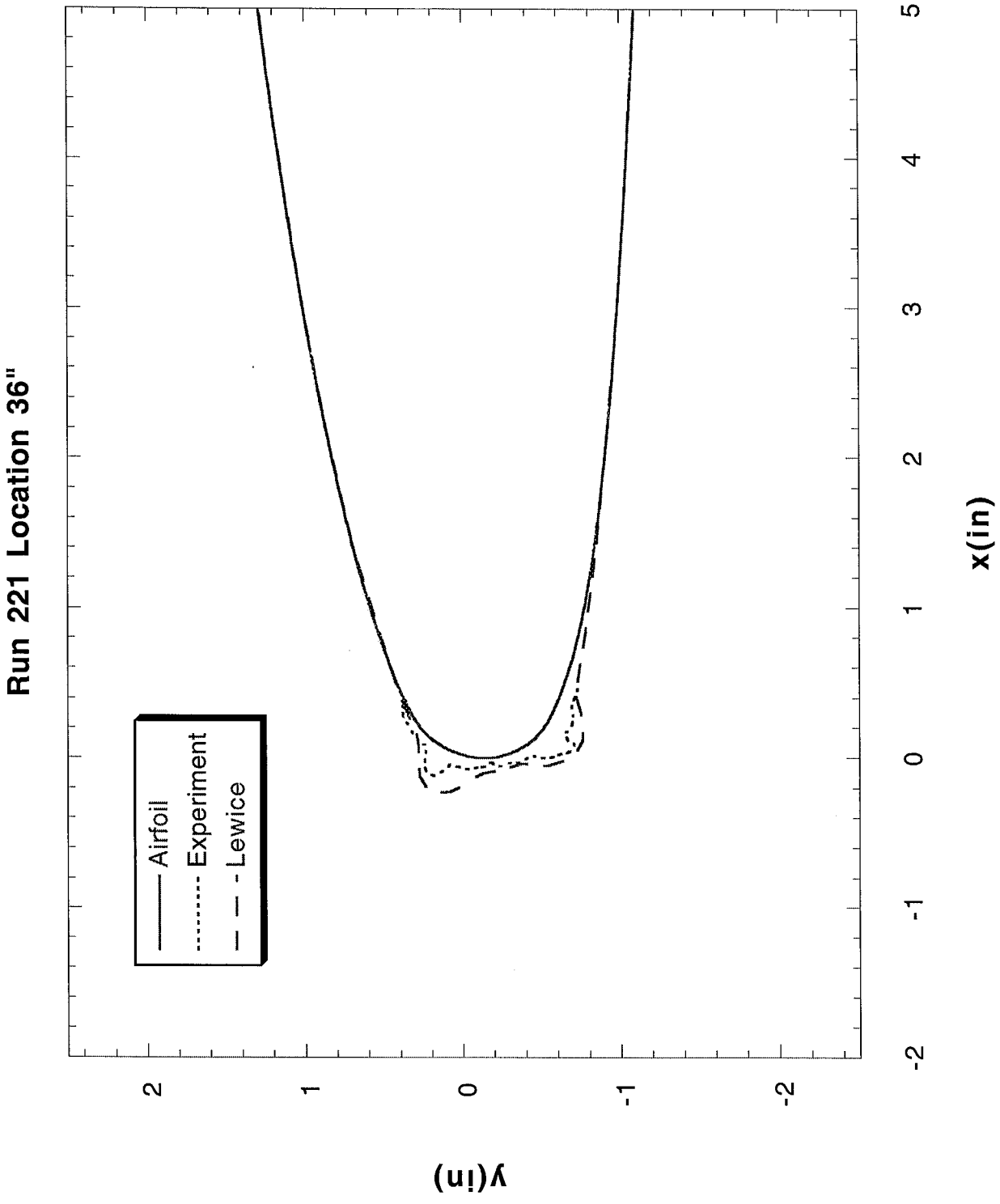
Run 221 Location 36"
Airfoil
Experiment
Lewice
y(in)
x(in)
2
1
0
-1
-2
-2
-1
0
1
2
3
4
5

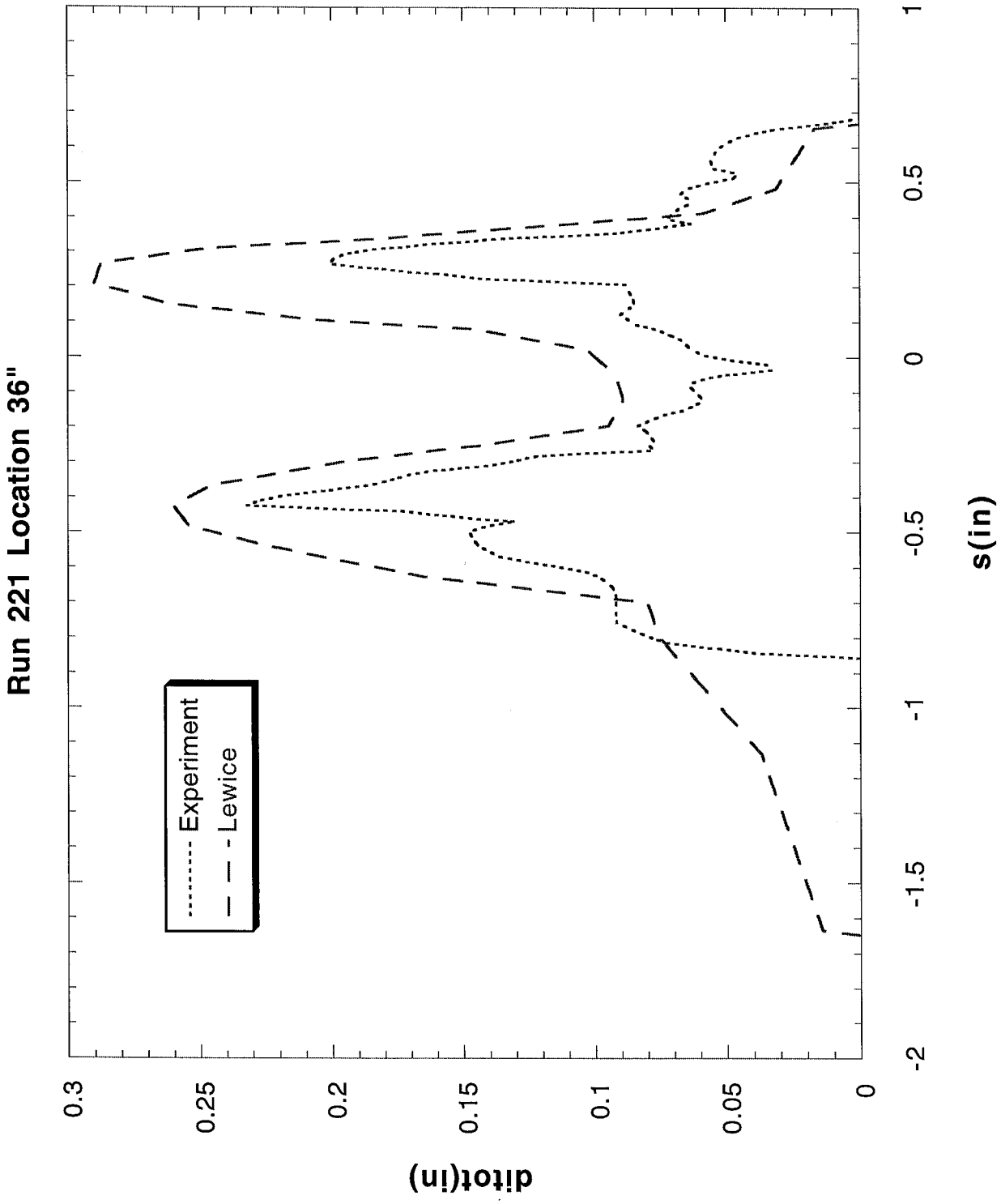
Run 221 Location 36"
Experiment
Lewice
dltot(in)
s(in)
0.3
0.25
0.2
0.15
0.1
0.05
0
-2
-1.5
-1
-0.5
0
0.5
1

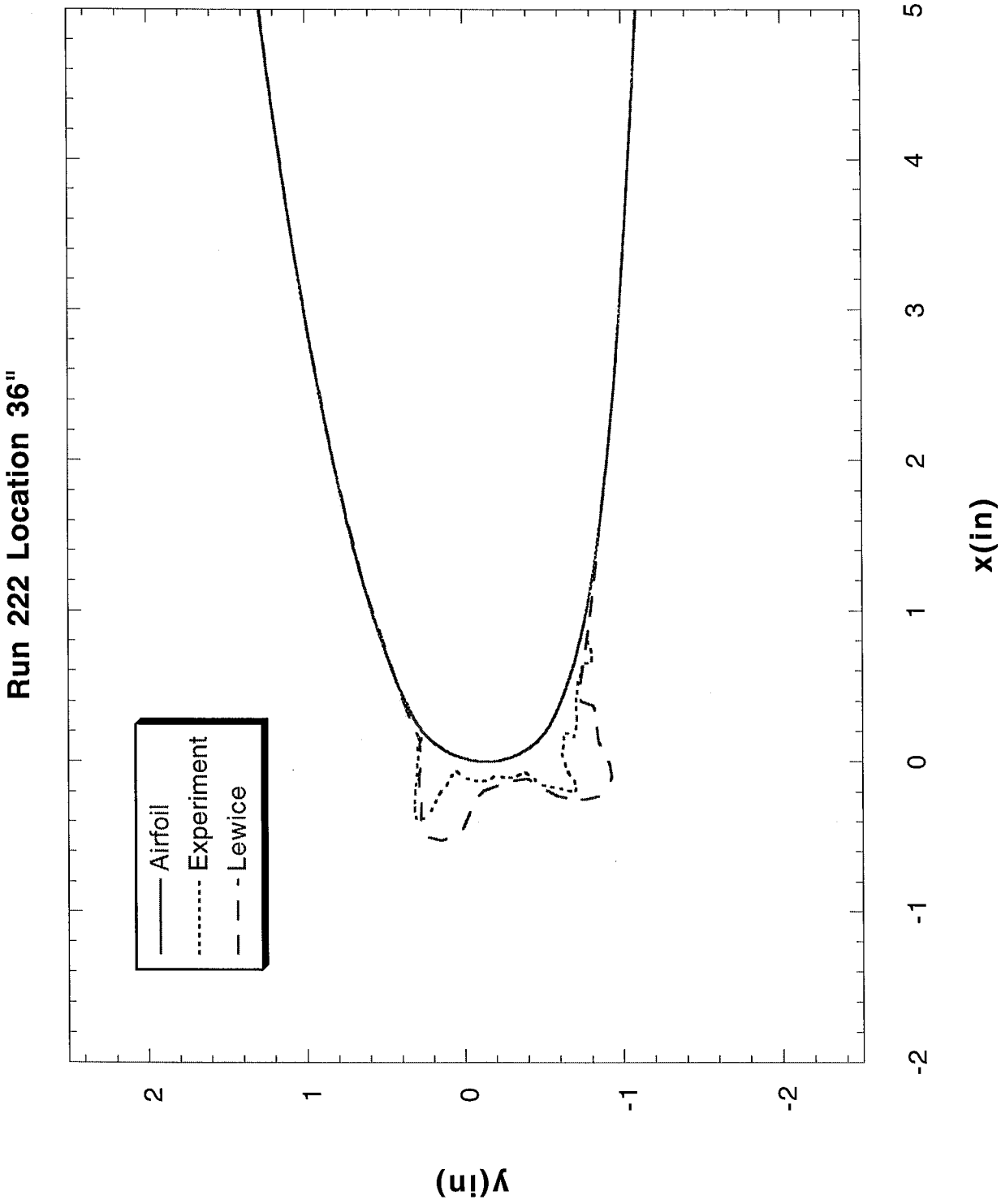
Run 222 Location 36"
Airfoil
Experiment
Lewice
y(in)
x(in)
2
1
0
-1
-2
-2
-1
0
1
2
3
4
5

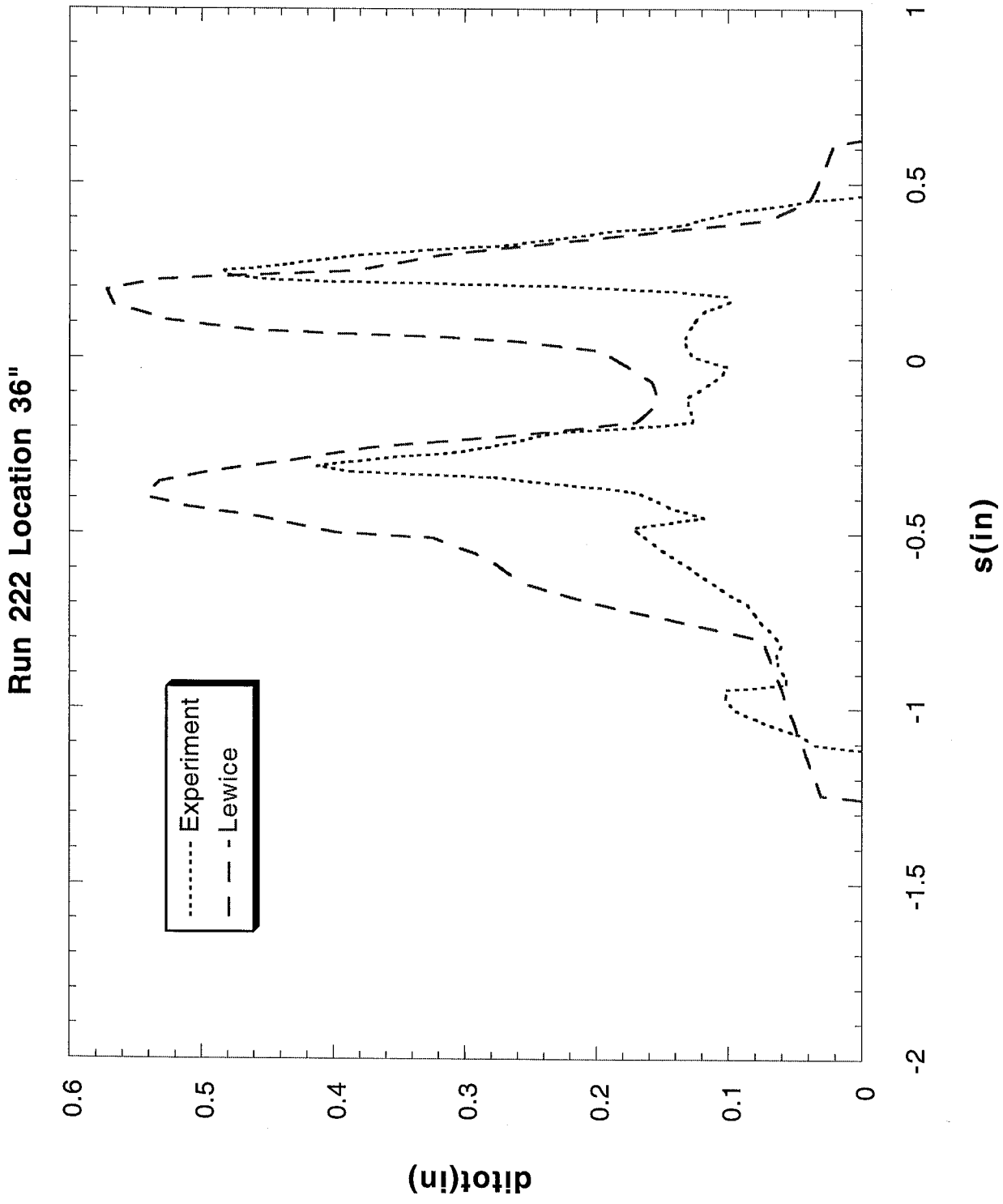
Run 222 Location 36"
Experiment
Lewice
dltot(in)
s(in)
0
0.1
0.2
0.3
0.4
0.5
0.6
-2
-1.5
-1
-0.5
0
0.5
1

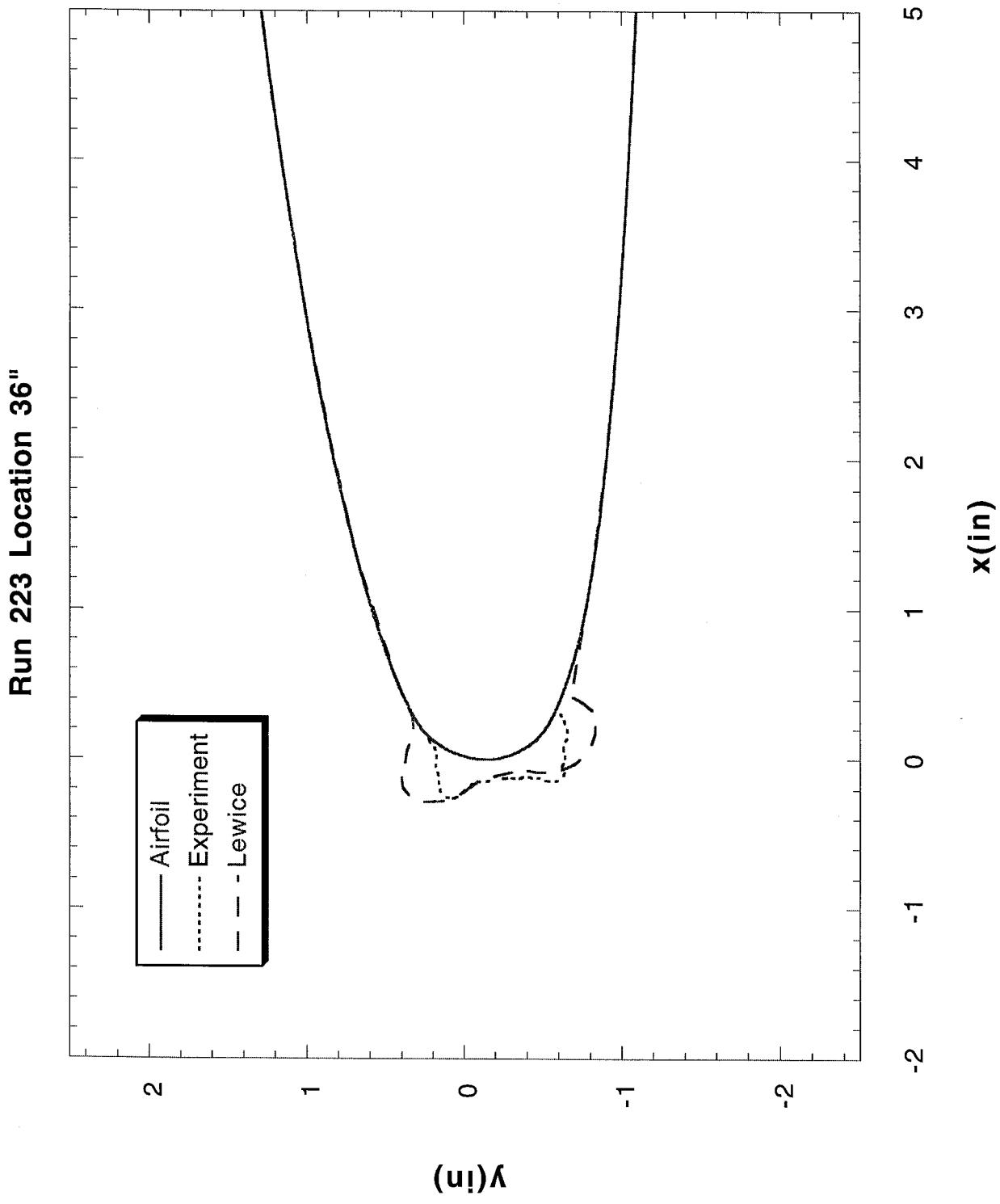
Run 223 Location 36"
Airfoil
Experiment
Lewice
y(in)
x(in)
2
1
0
-1
-2
-2
-1
0
1
2
3
4
5

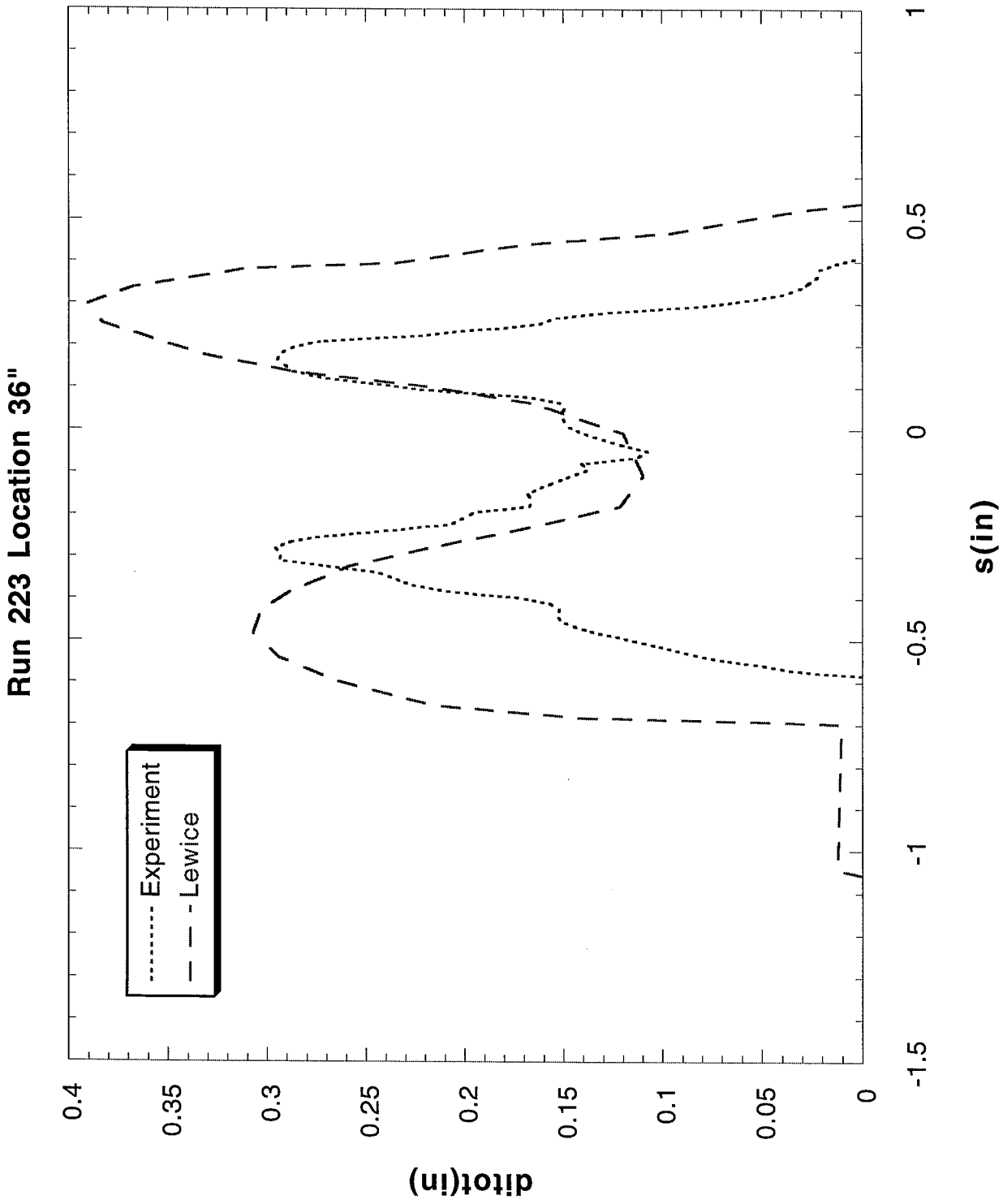
Run 223 Location 36"
Experiment
Lewice
dltot(in)
s(in)
0.4
0.35
0.3
0.25
0.2
0.15
0.1
0.05
0
-1.5
-1
-0.5
0
0.5
1

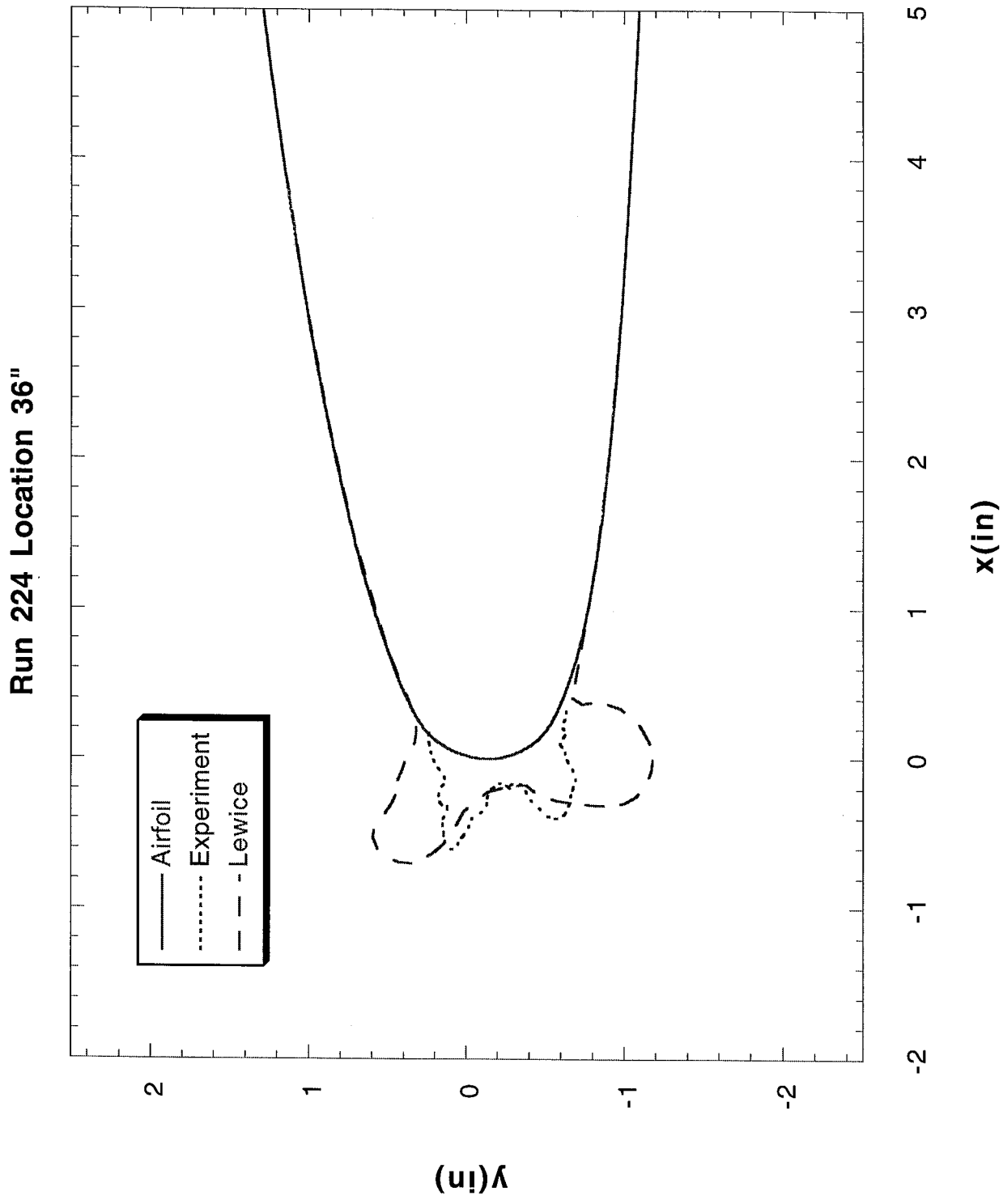
Run 224 Location 36"
Airfoil
Experiment
Lewice
y(in)
x(in)
2
1
0
-1
-2
-2
-1
0
1
2
3
4
5

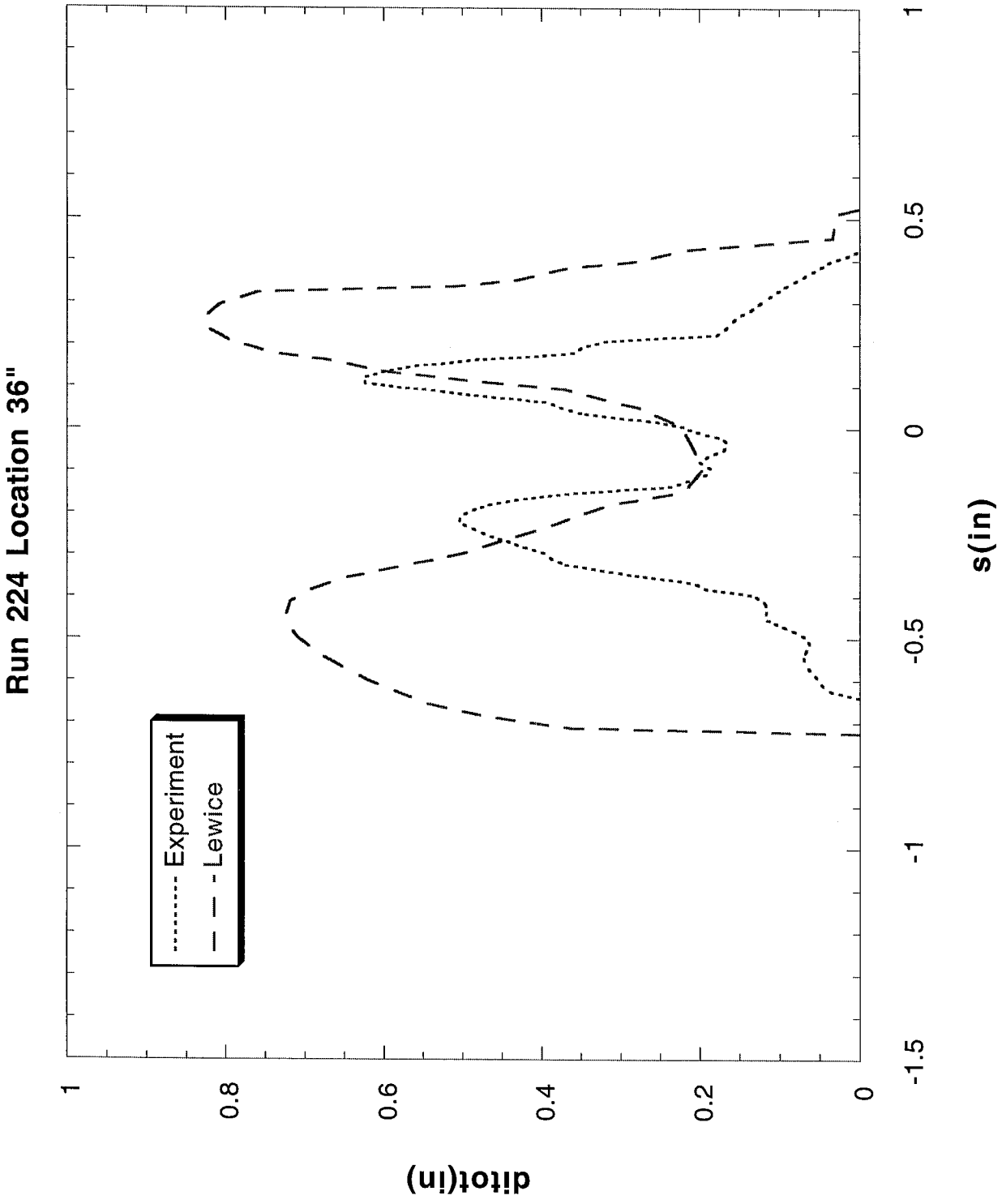
Run 224 Location 36"
Experiment
Lewice
dltot(in)
s(in)
1
0.8
0.6
0.4
0.2
0
-1.5
-1
-0.5
0
0.5
1

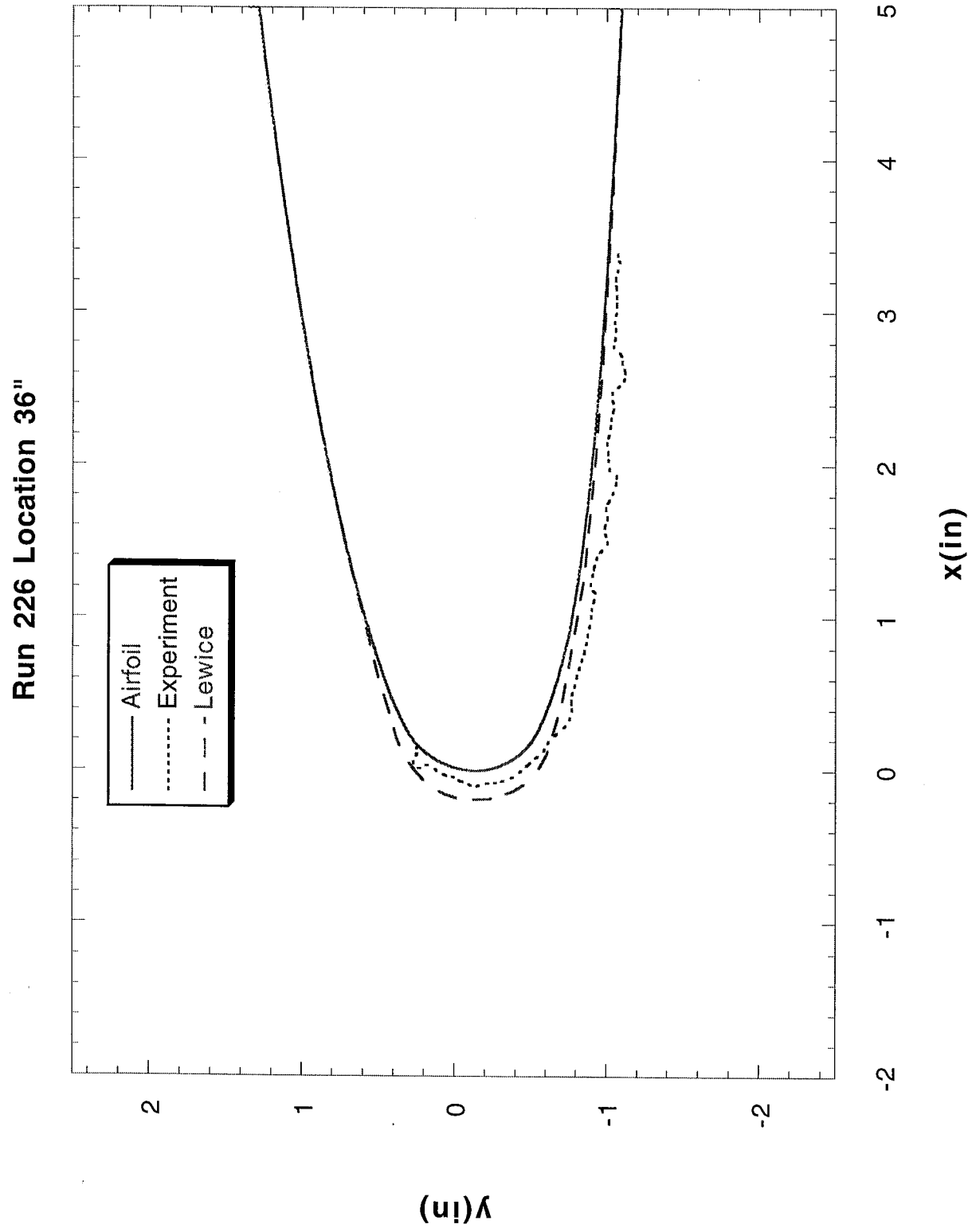
Run 226 Location 36"
Airfoil
Experiment
Lewice
y(in)
x(in)
2
1
0
-1
-2
-2
-1
0
1
2
3
4
5

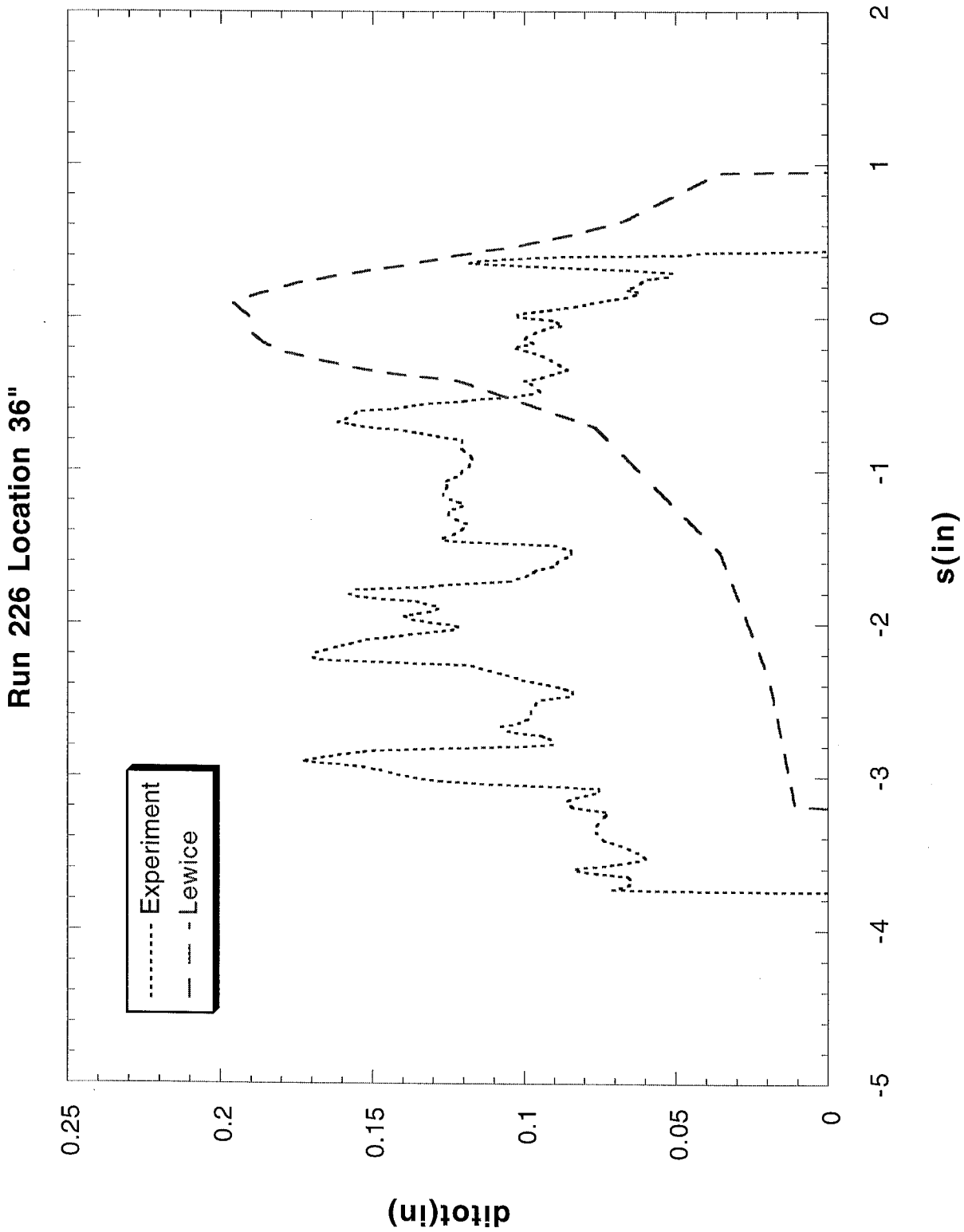
Run 226 Location 36"
Experiment
Lewice
dltot(in)
0.25
0.2
0.15
0.1
0.05
0
s(in)
2
1
0
-1
-2
-3
-4
-5

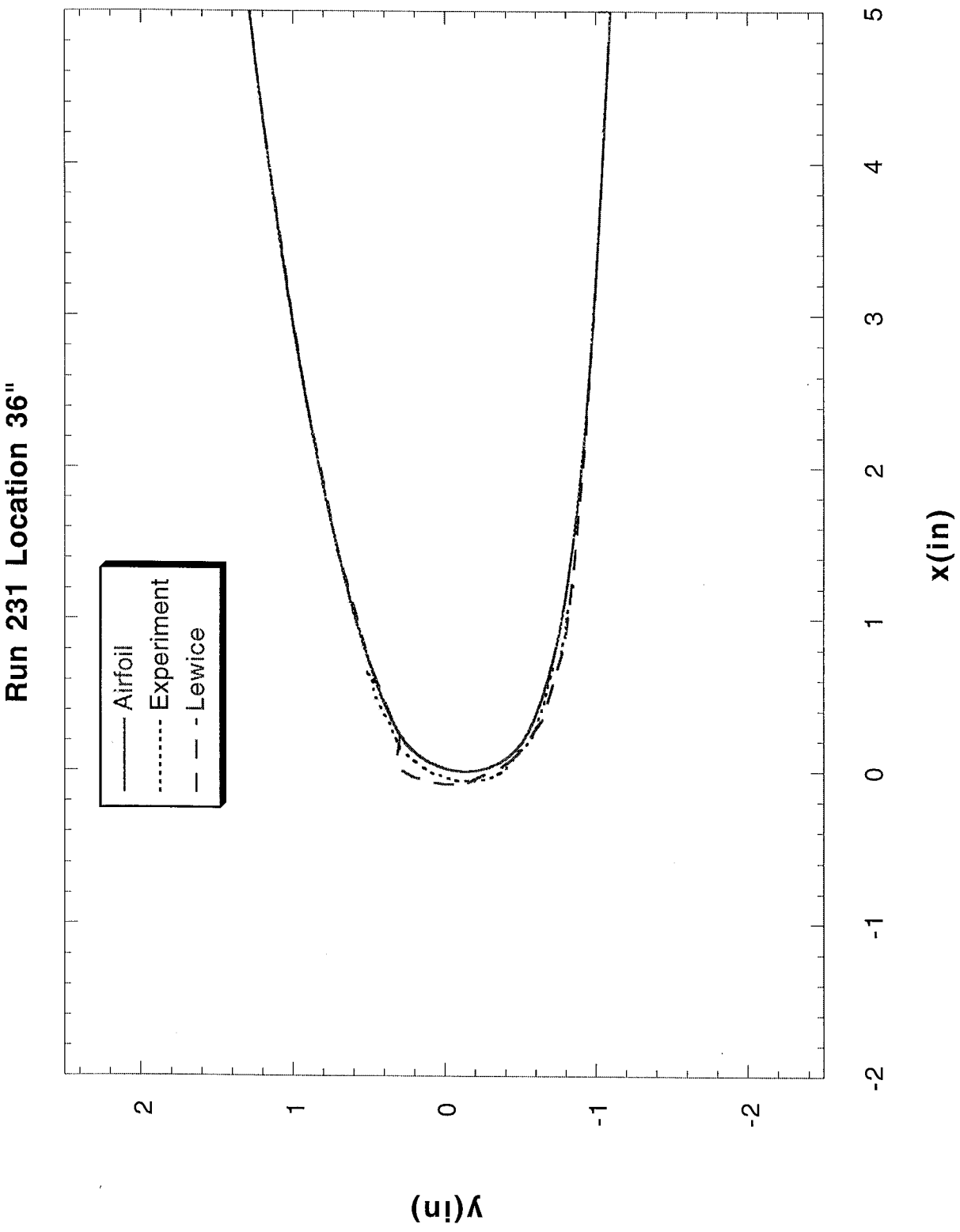
Run 231 Location 36"
Airfoil
Experiment
Lewice
y(in)
x(in)
2
1
0
-1
-2
-2
-1
0
1
2
3
4
5

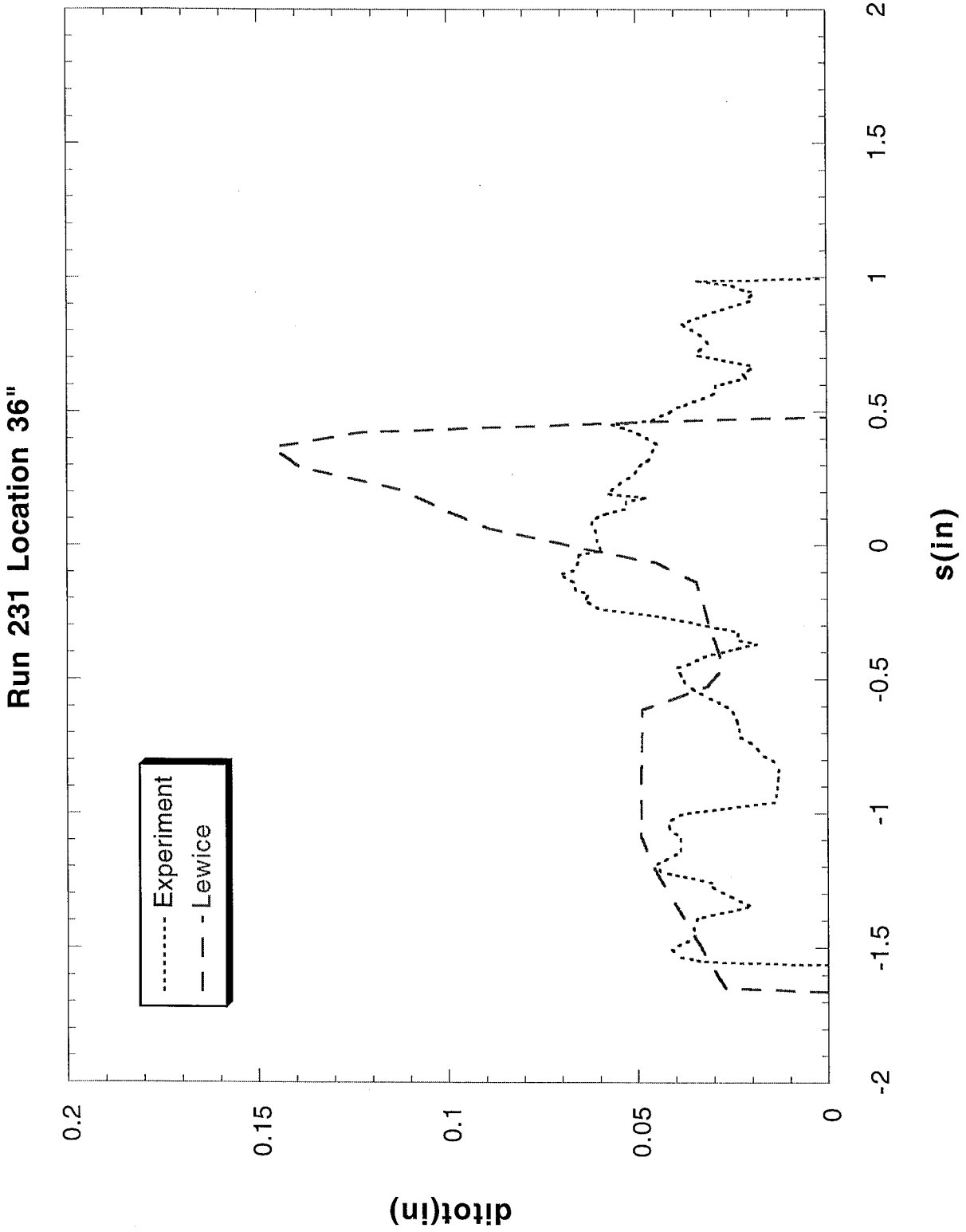
Run 231 Location 36"
Experiment
Lewice
dtot(in)
s(in)
0.2
0.15
0.1
0.05
0
-2
-1.5
-1
-0.5
0
0.5
1
1.5
2

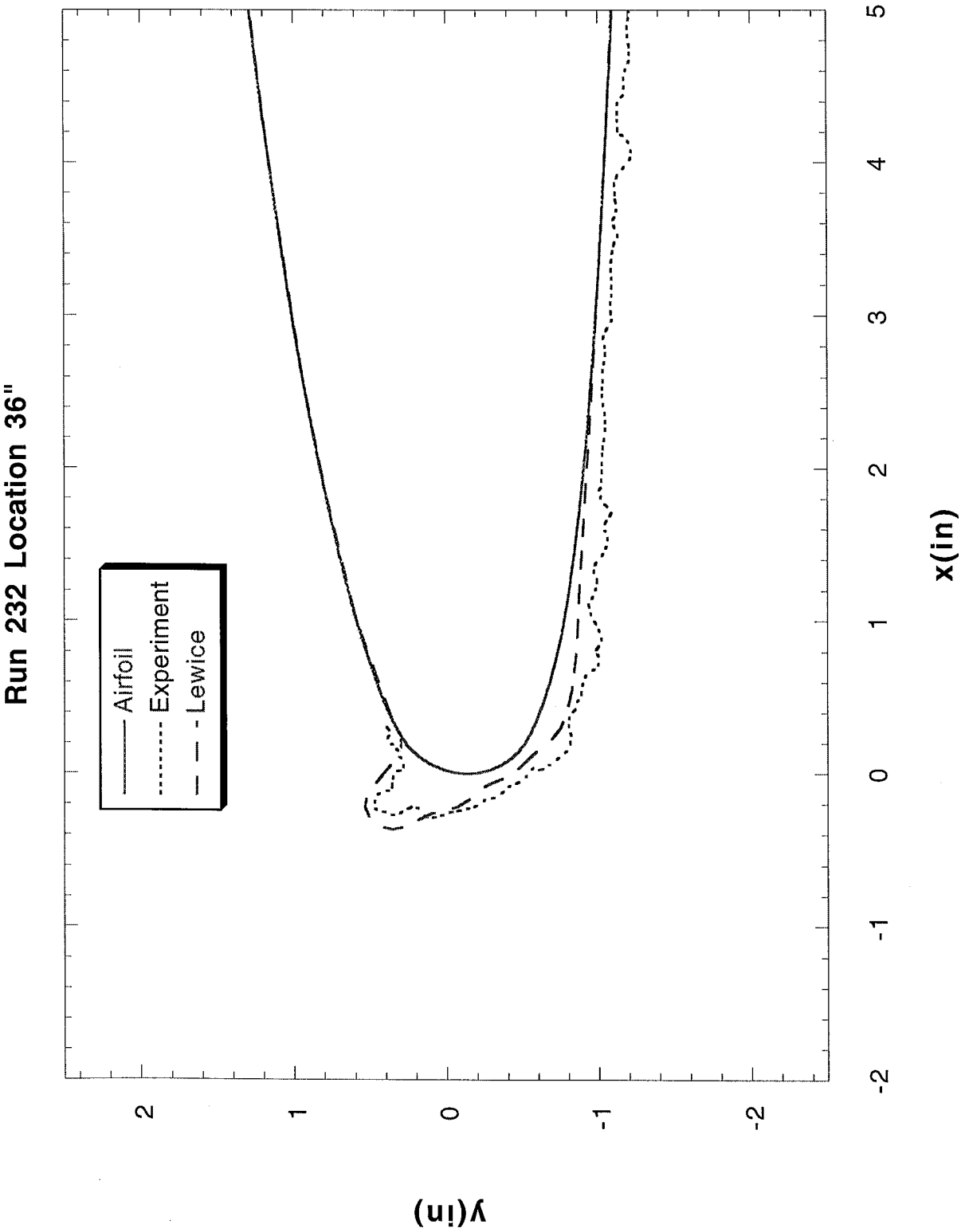
Run 232 Location 36"
Airfoil
Experiment
Lewice
y(in)
x(in)
2
1
0
-1
-2
-2
-1
0
1
2
3
4
5

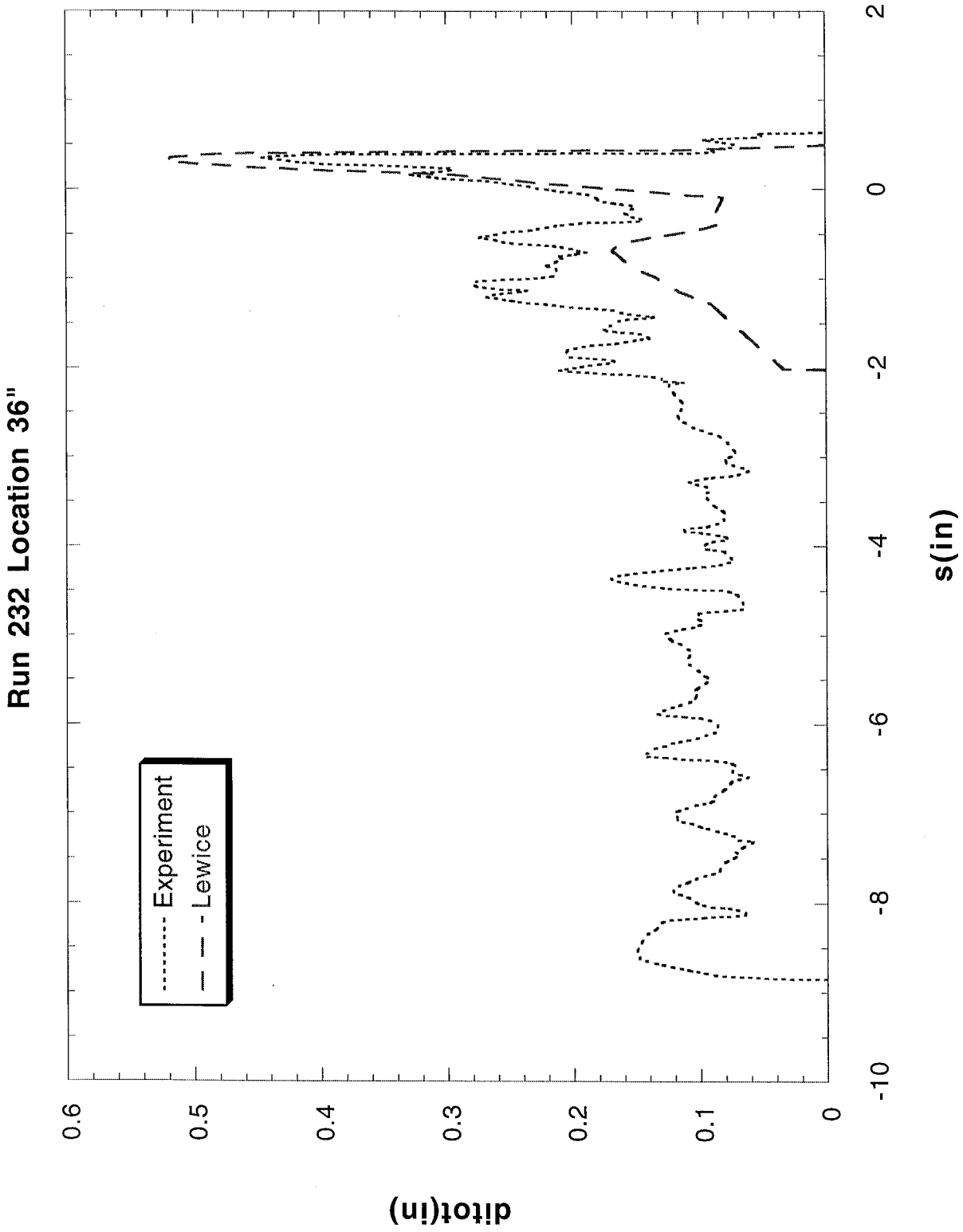
Run 232 Location 36"
Experiment
Lewice
dltot(in)
s(in)
0.6
0.5
0.4
0.3
0.2
0.1
0
-10
-8
-6
-4
-2
0
2

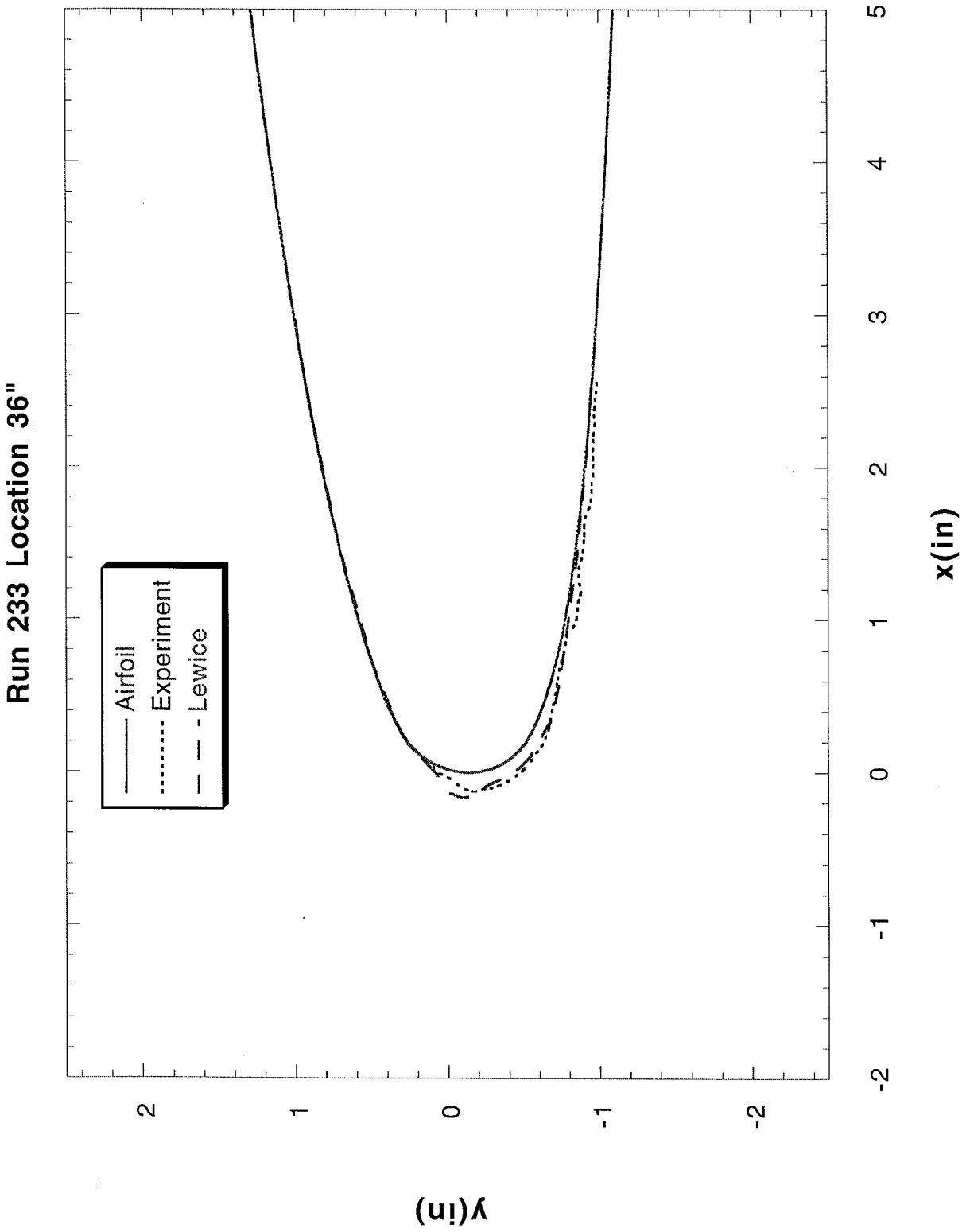
Run 233 Location 36"
Airfoil
Experiment
Lewice
y(in)
x(in)
2
1
0
-1
-2
-2
-1
0
1
2
3
4
5

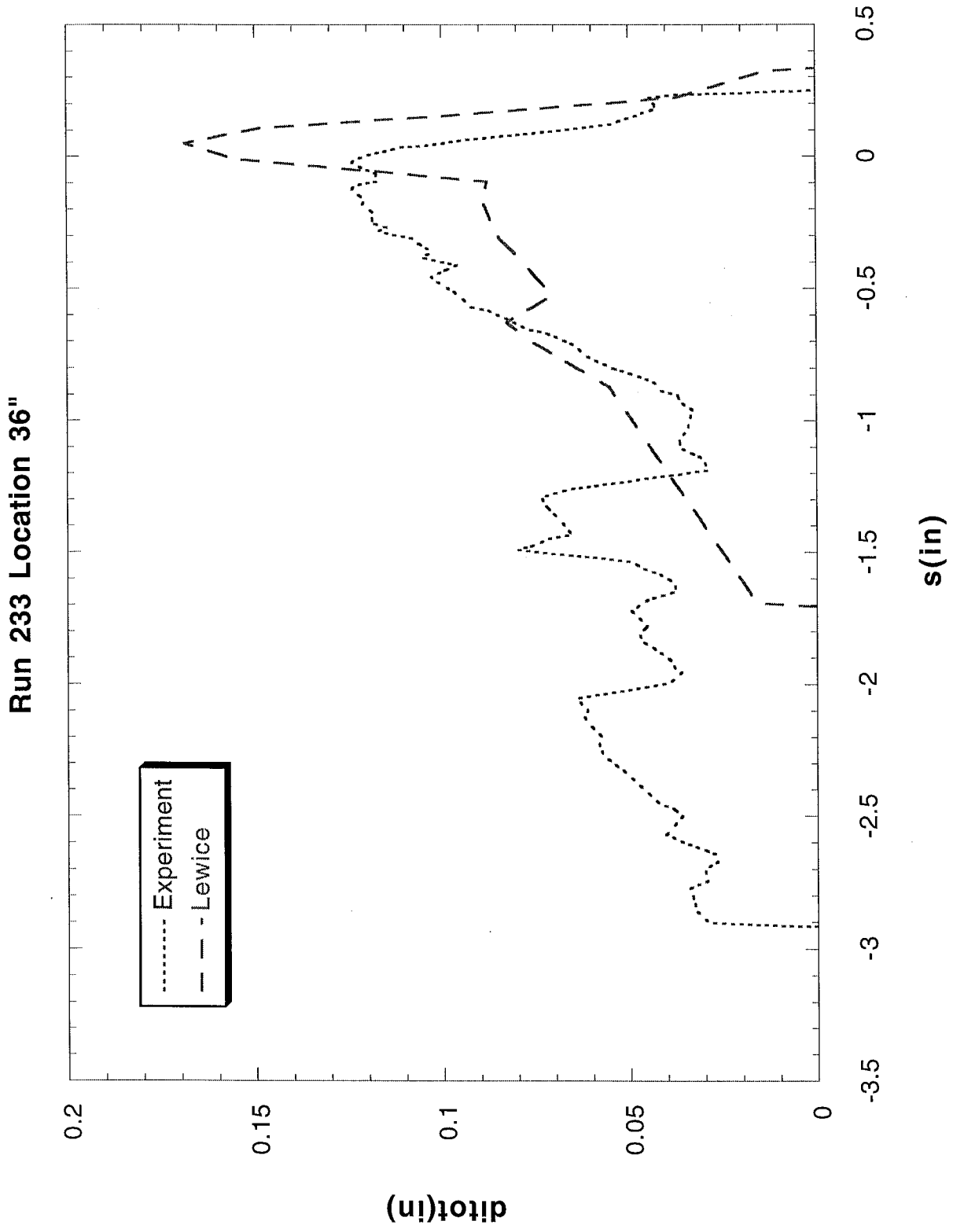
Run 233 Location 36"
Experiment
Lewice
dltot(in)
s(in)
0.2
0.15
0.1
0.05
0
-3.5
-3
-2.5
-2
-1.5
-1
-0.5
0
0.5

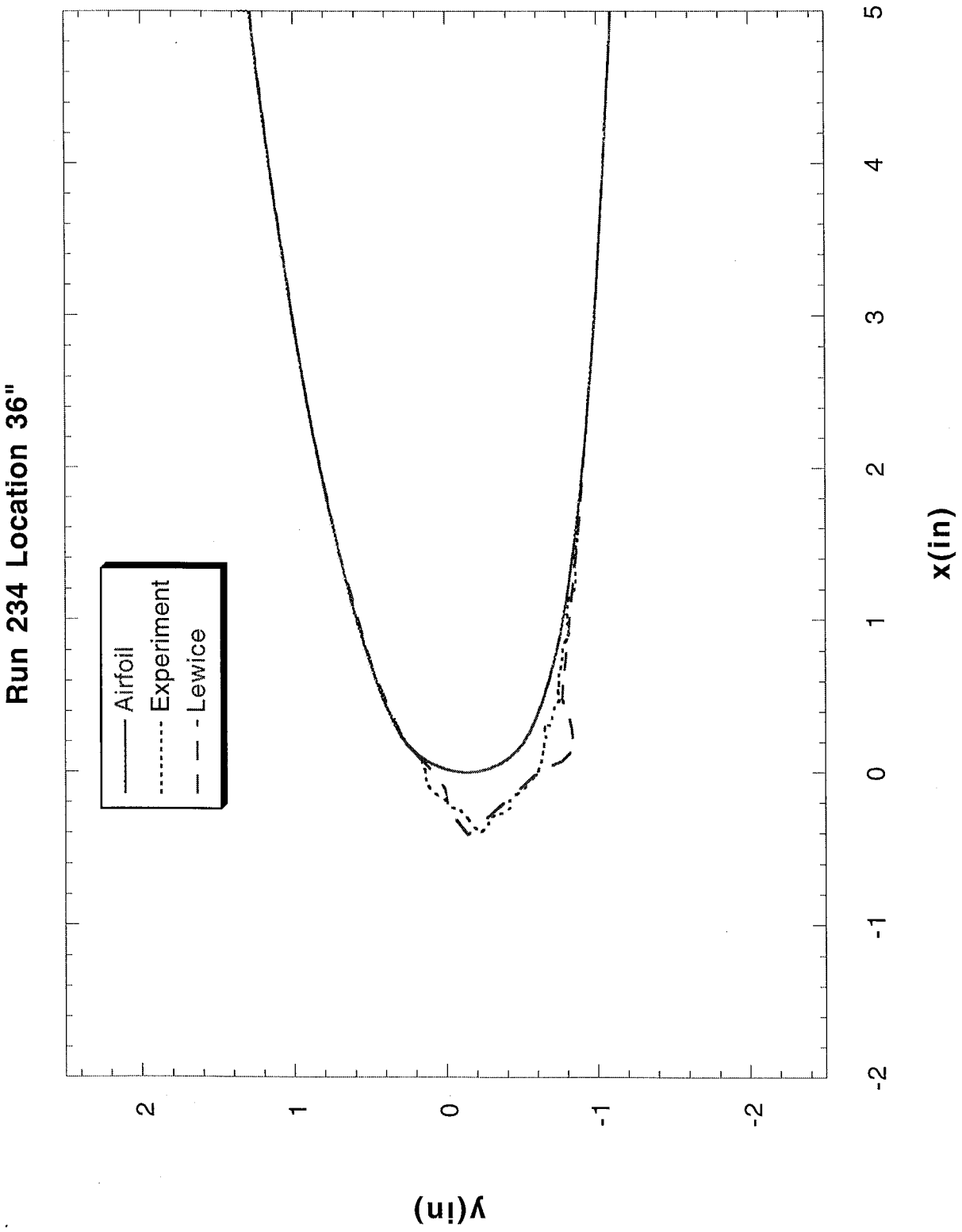
Run 234 Location 36"
Airfoil
Experiment
Lewice
y(in)
x(in)
2
1
0
-1
-2
-2
-1
0
1
2
3
4
5

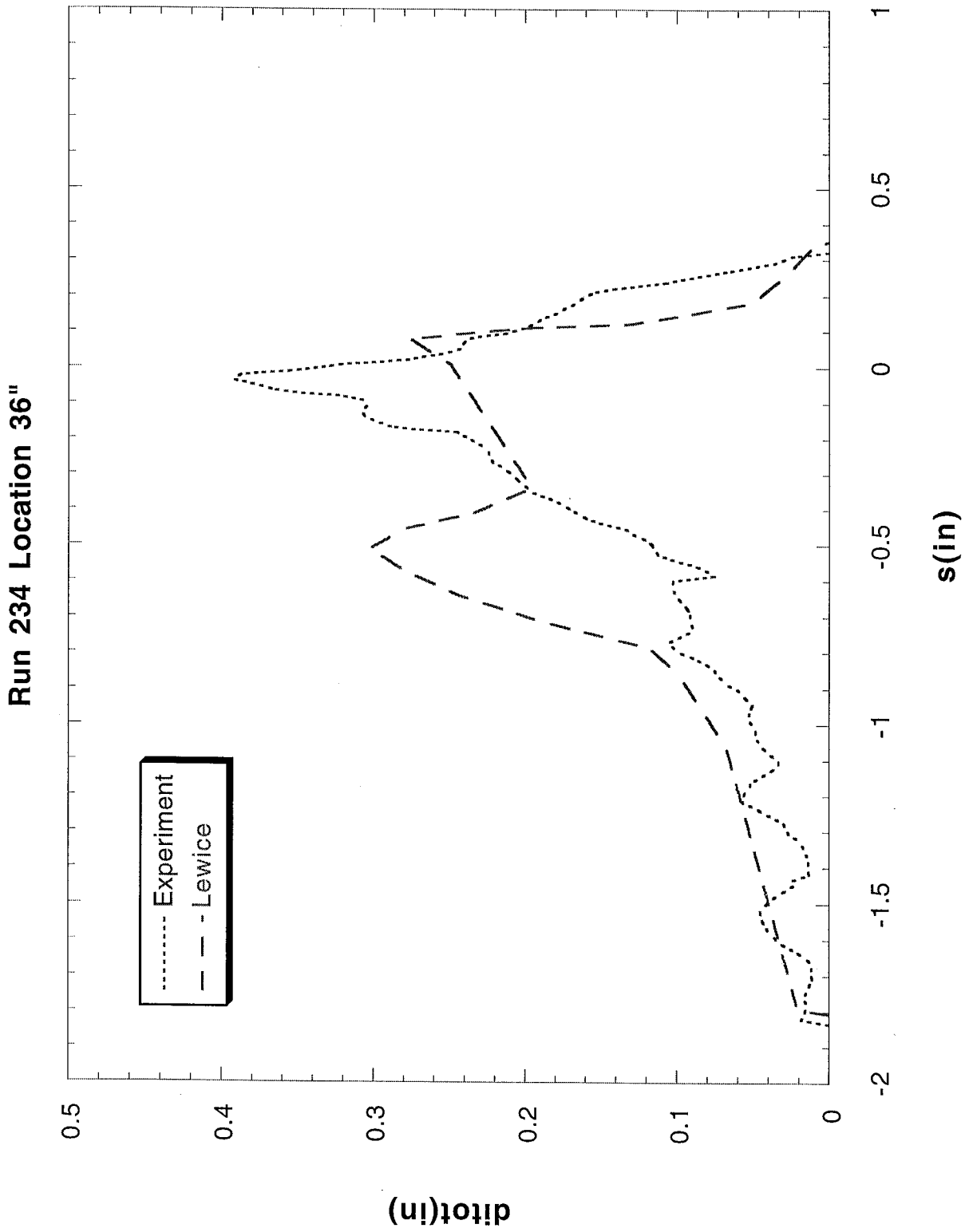
Run 234 Location 36"
Experiment
Lewice
dltot(in)
s(in)
0.5
0.4
0.3
0.2
0.1
0
-2
-1.5
-1
-0.5
0
0.5
1

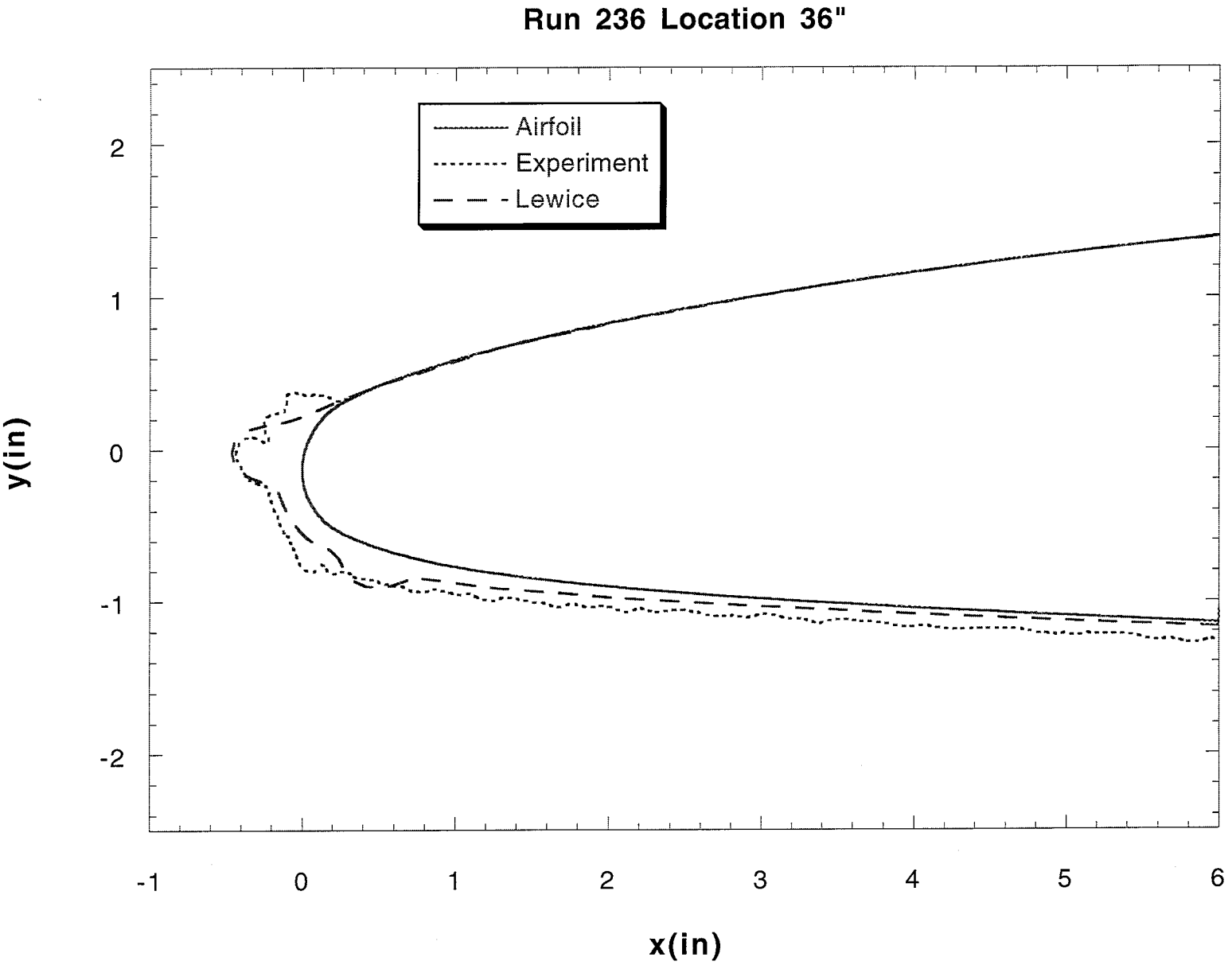
Run 236 Location 36"
Airfoil
Experiment
Lewice
y(in)
x(in)
2
1
0
-1
-2
-1
0
1
2
3
4
5
6

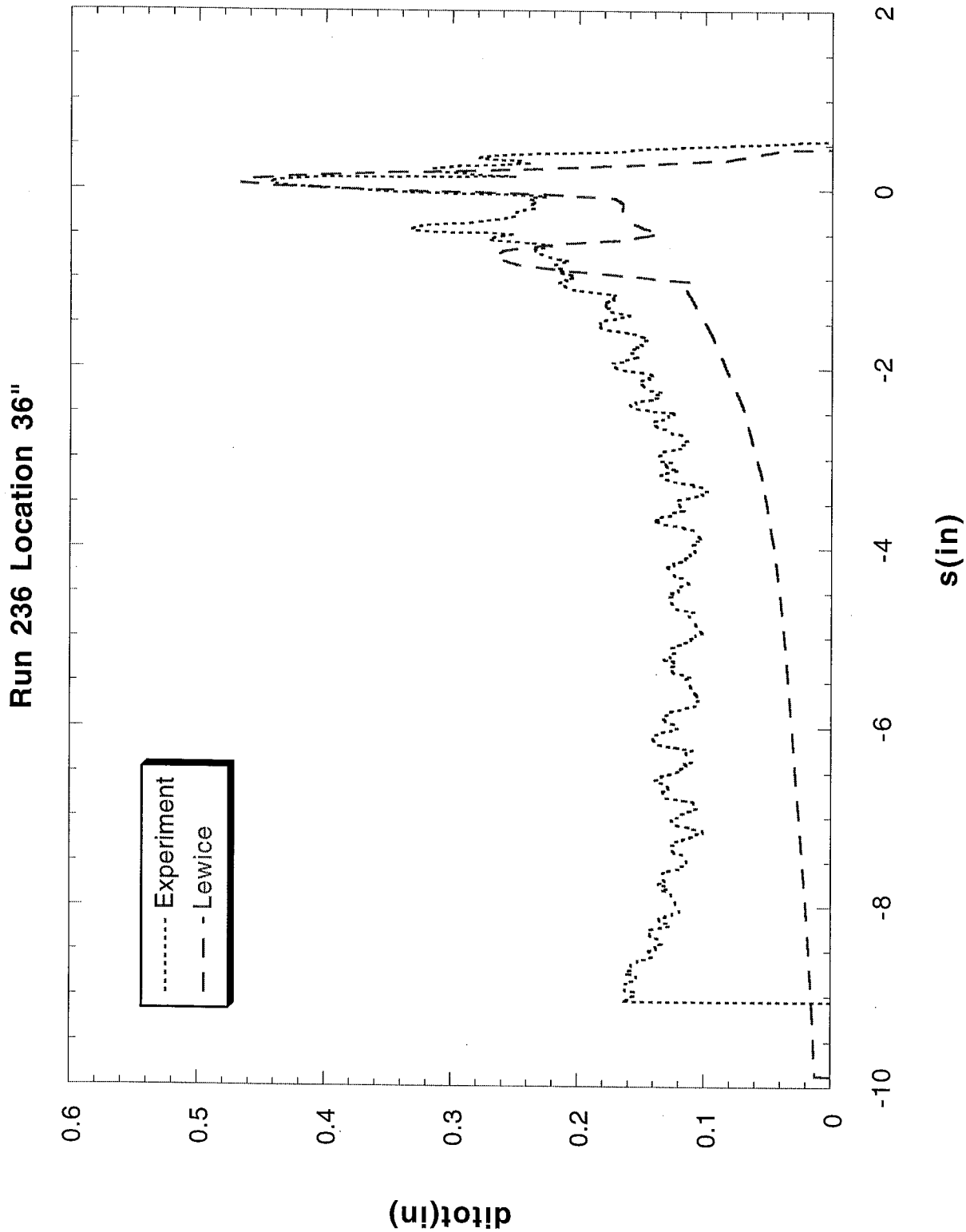
Run 236 Location 36"
Experiment
Lewice
dtot(in)
s(in)
0.6
0.5
0.4
0.3
0.2
0.1
0
-10
-8
-6
-4
-2
0
2

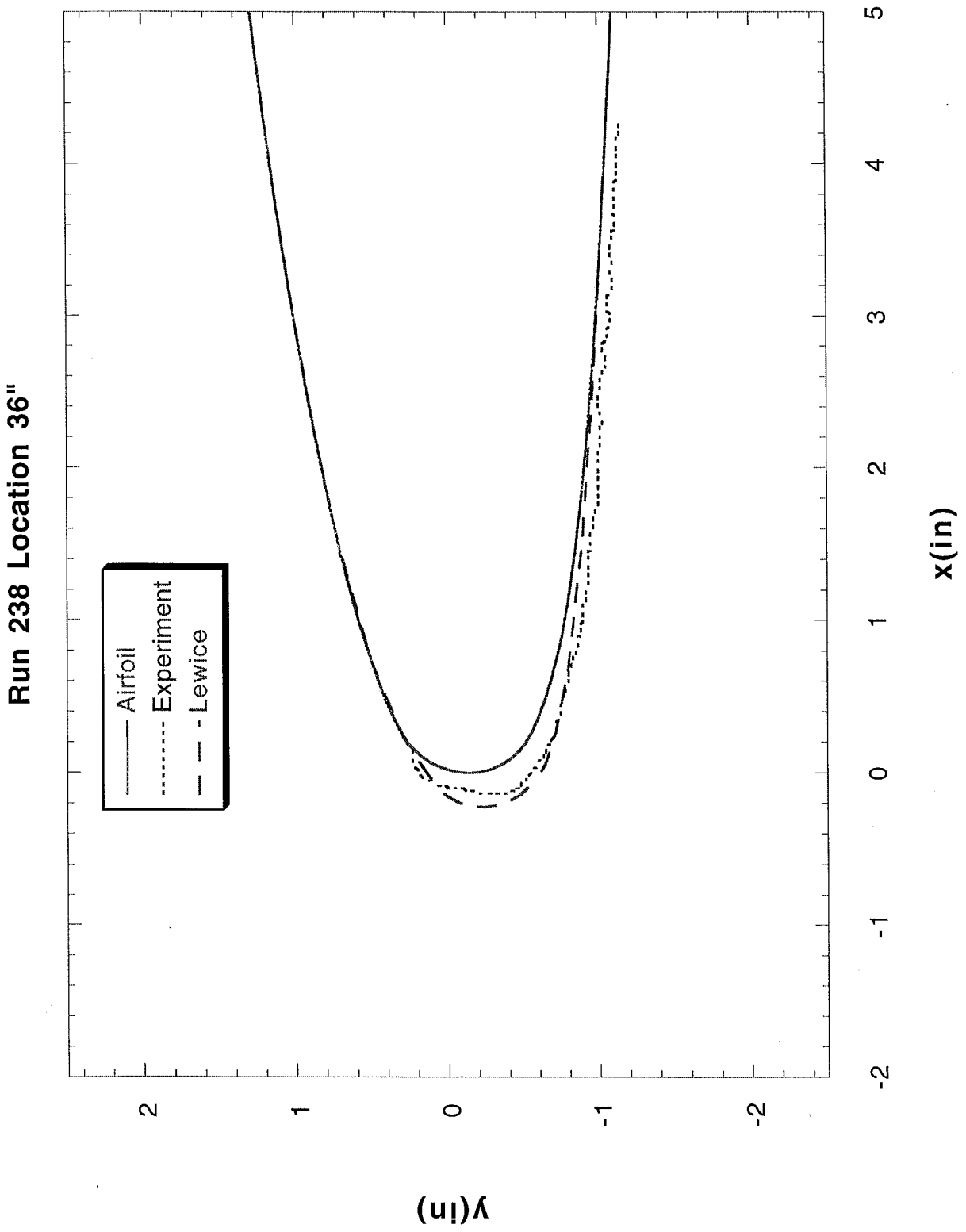
Run 238 Location 36"
Airfoil
Experiment
Lewice
y(in)
x(in)
2
1
0
-1
-2
-2
-1
0
1
2
3
4
5

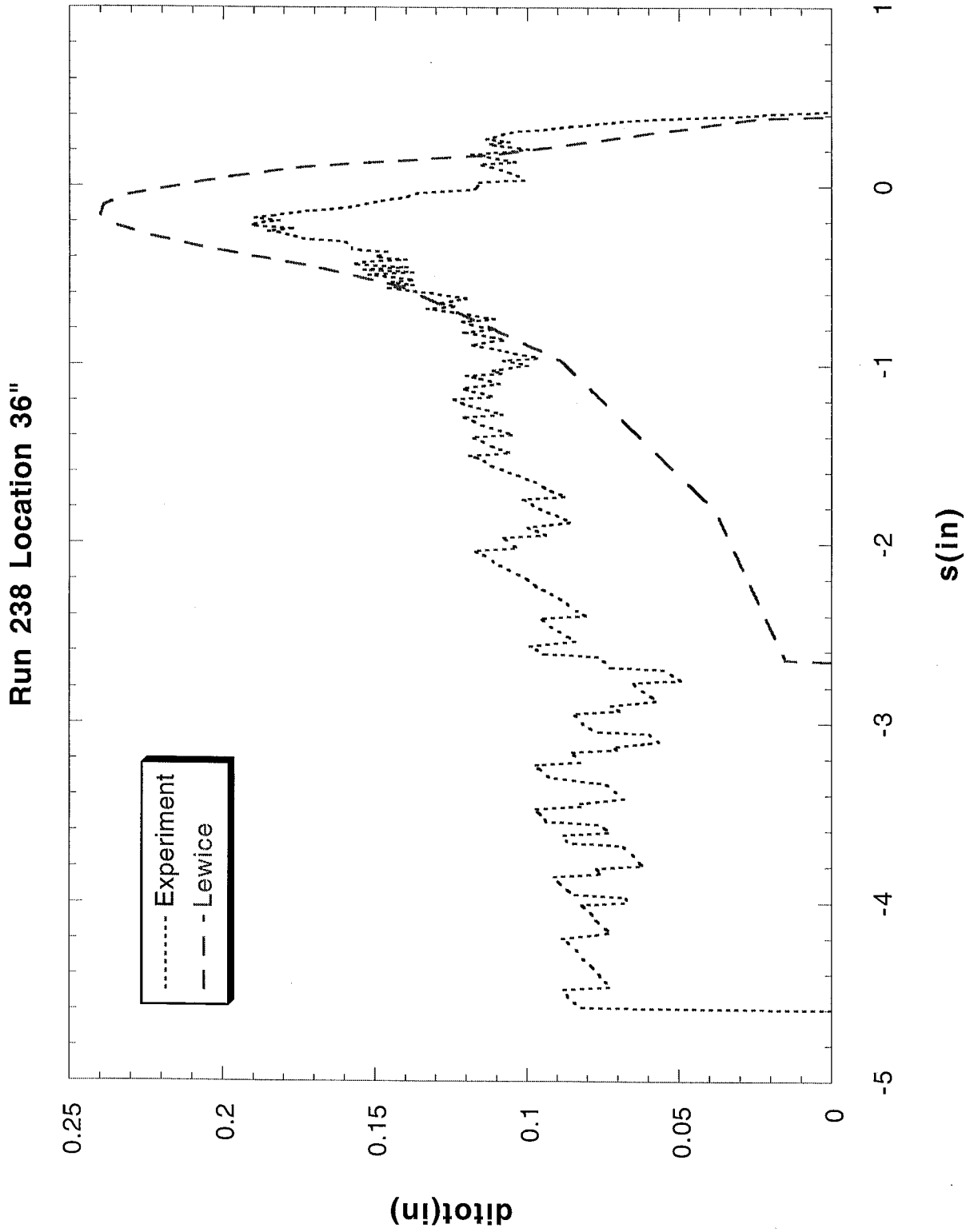
Run 238 Location 36"
Experiment
Lewice
dltot(in)
s(in)
0.25
0.2
0.15
0.1
0.05
0
-5
-4
-3
-2
-1
0
1

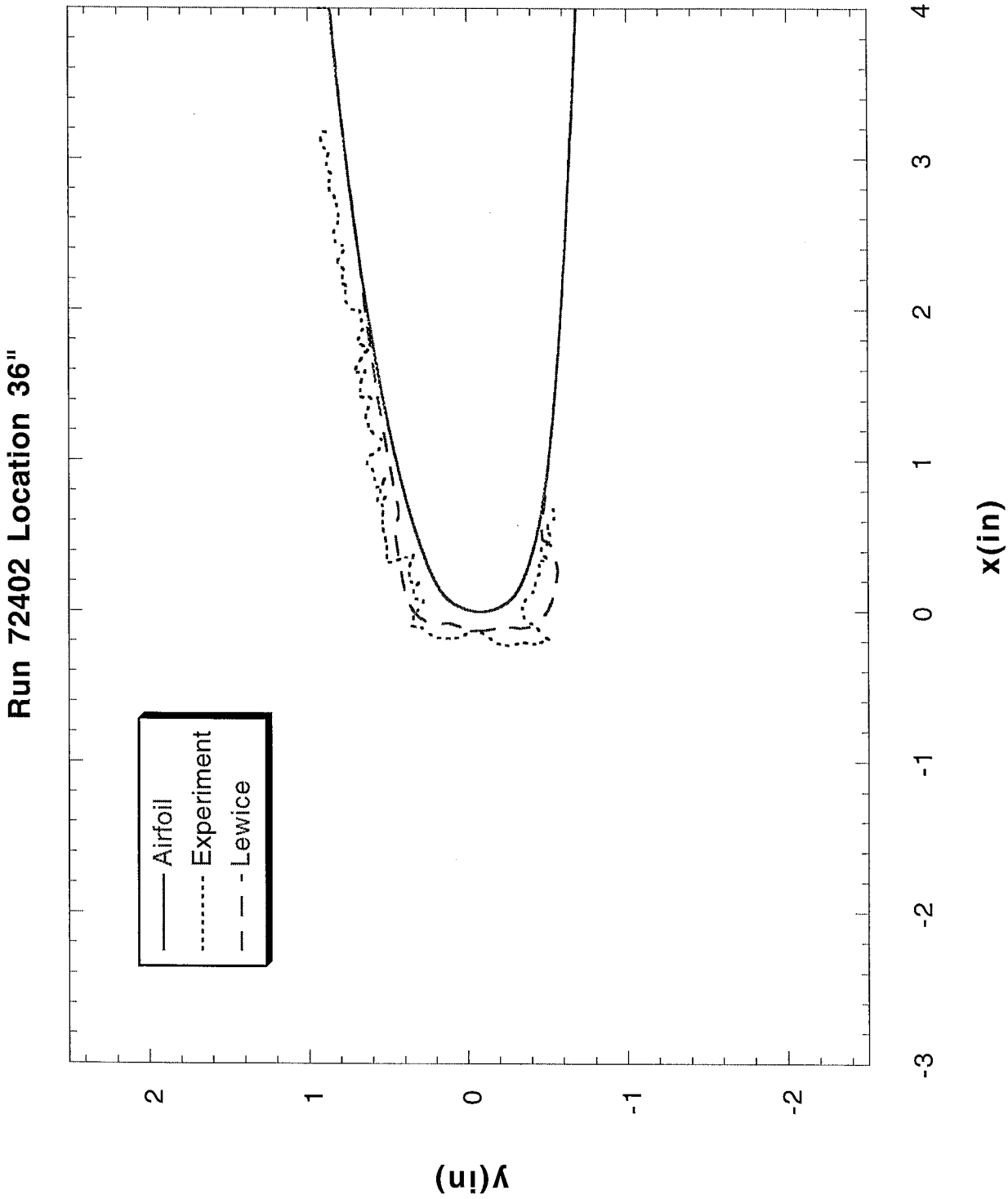
Run 72402 Location 36"
Airfoil
Experiment
Lewice
y(in)
x(in)
2
1
0
-1
-2
-3
-2
-1
0
1
2
3
4

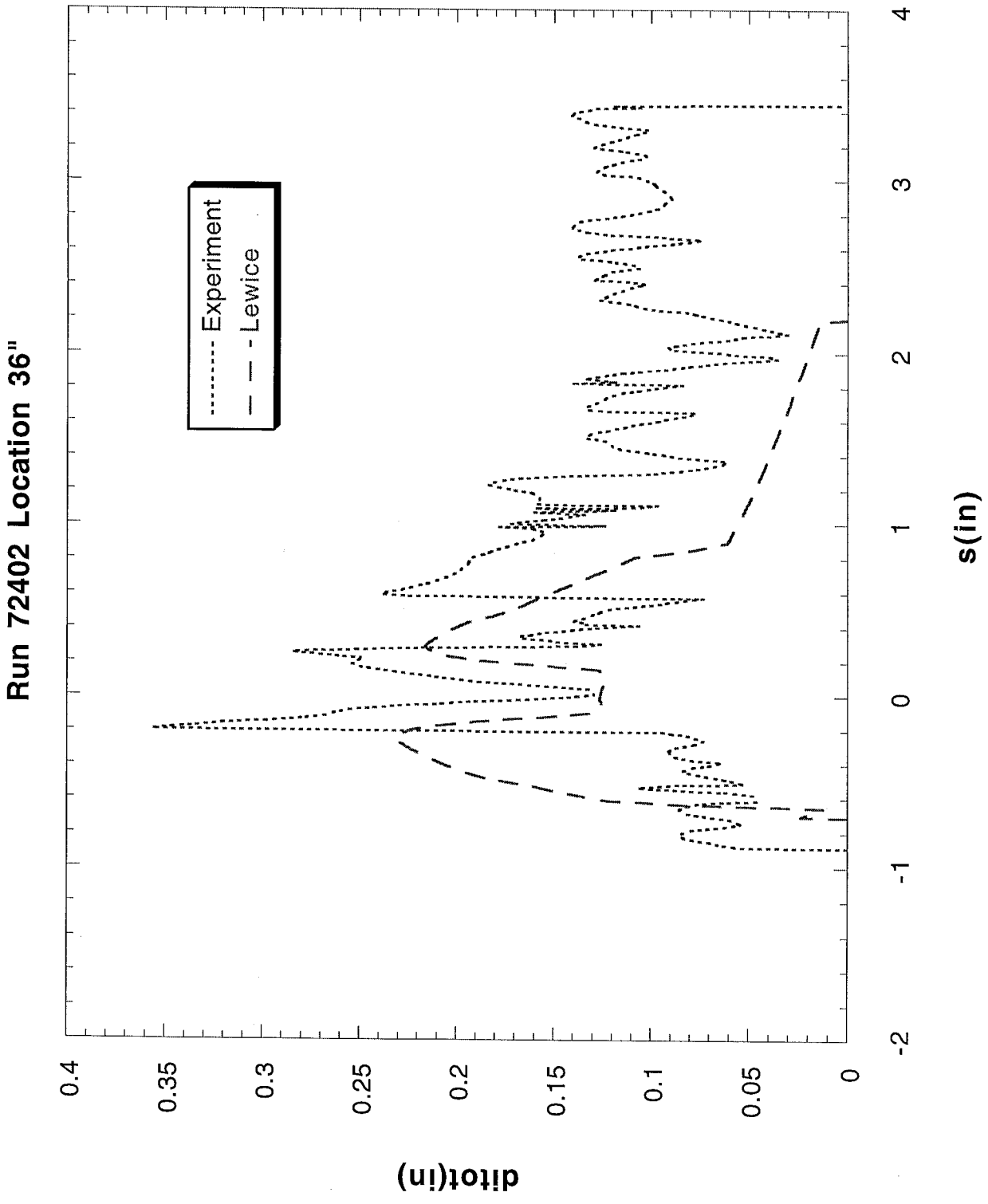
Run 72402 Location 36"
Experiment
Lewice
dltot(in)
s(in)
0.4
0.35
0.3
0.25
0.2
0.15
0.1
0.05
0
-2
-1
0
1
2
3
4

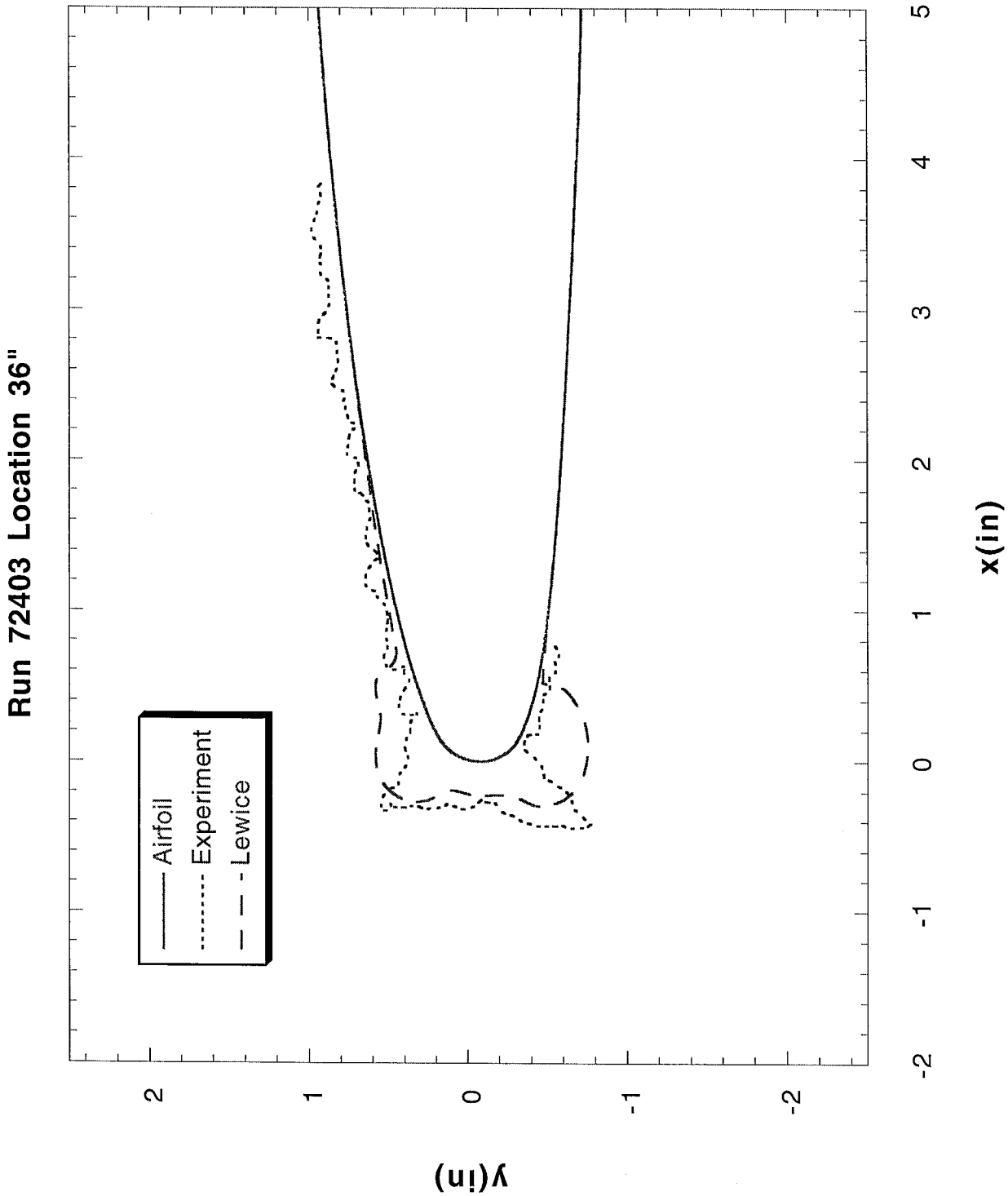
Run 72403 Location 36"
Airfoil
Experiment
Lewice
y(in)
x(in)
2
1
0
-1
-2
-2
-1
0
1
2
3
4
5

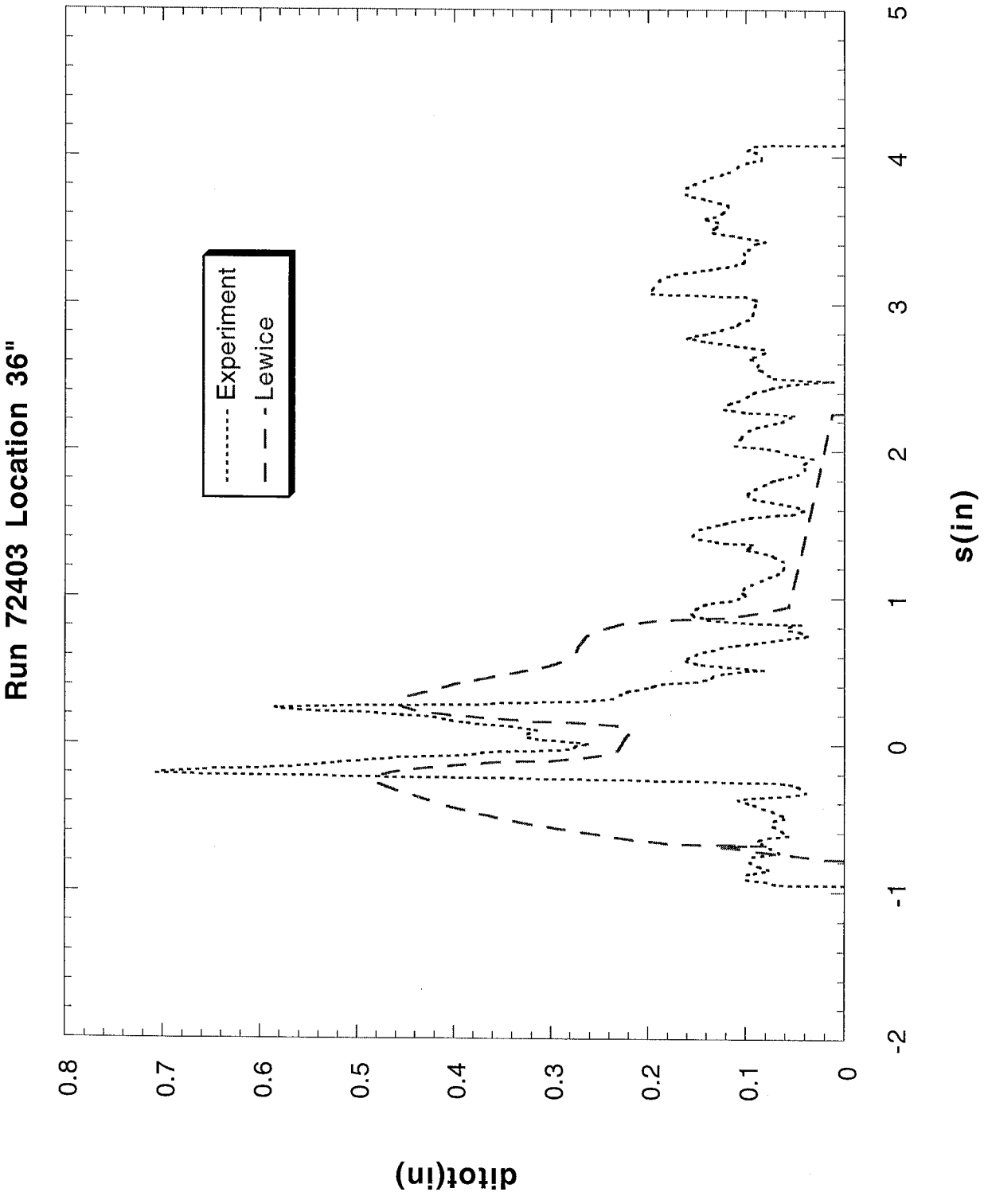
Run 72403 Location 36"
Experiment
Lewice
dltot(in)
s(in)
0
0.1
0.2
0.3
0.4
0.5
0.6
0.7
0.8
-2
-1
0
1
2
3
4
5

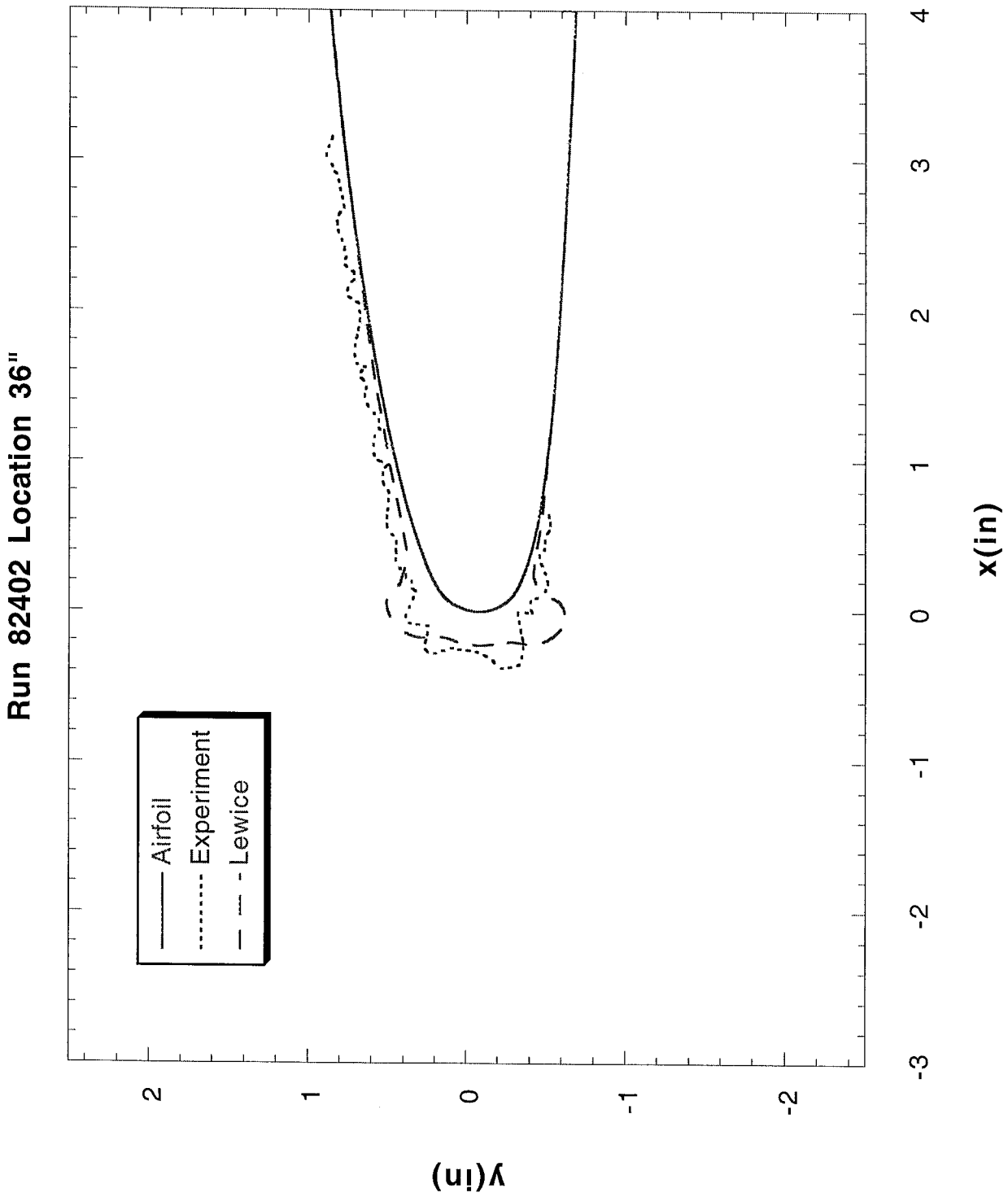
Run 82402 Location 36"
Airfoil
Experiment
Lewice
y(in)
x(in)
2
1
0
-1
-2
-3
-2
-1
0
1
2
3
4

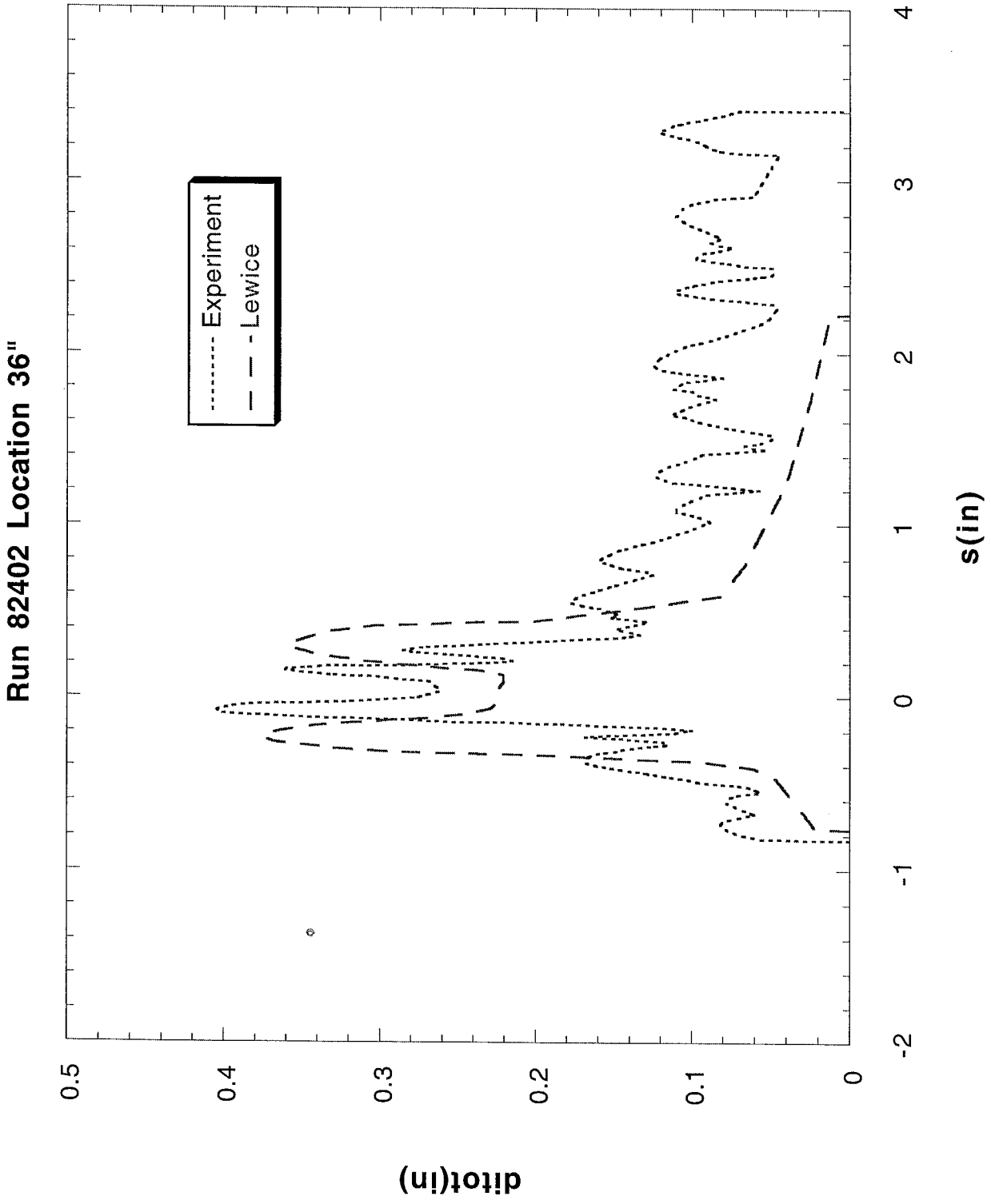
Run 82402 Location 36"
Experiment
Lewice
dltot(in)
s(in)
0.5
0.4
0.3
0.2
0.1
0
-2
-1
0
1
2
3
4

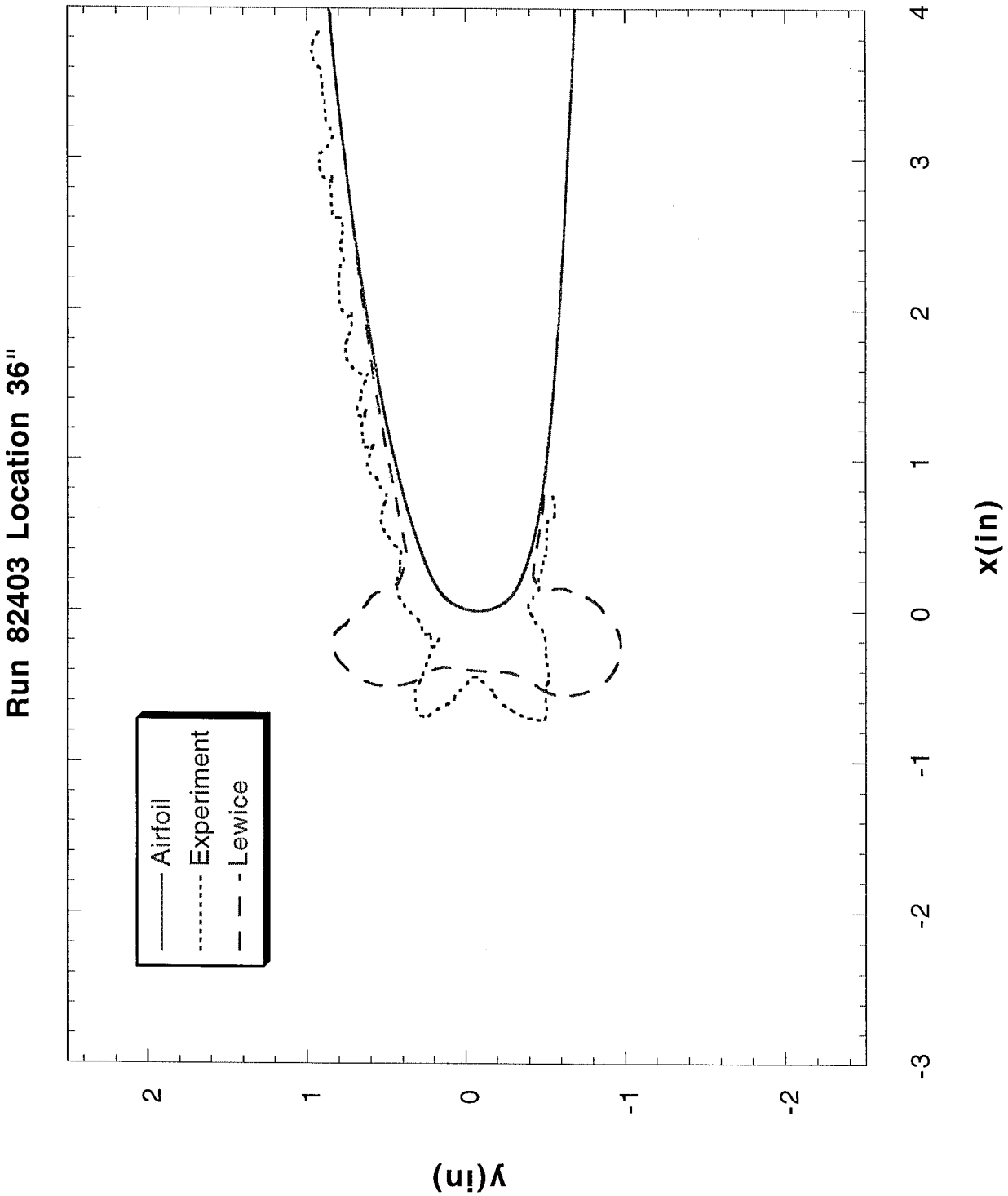
Run 82403 Location 36"
Airfoil
Experiment
Lewice
y(in)
x(in)
2
1
0
-1
-2
-3
-2
-1
0
1
2
3
4

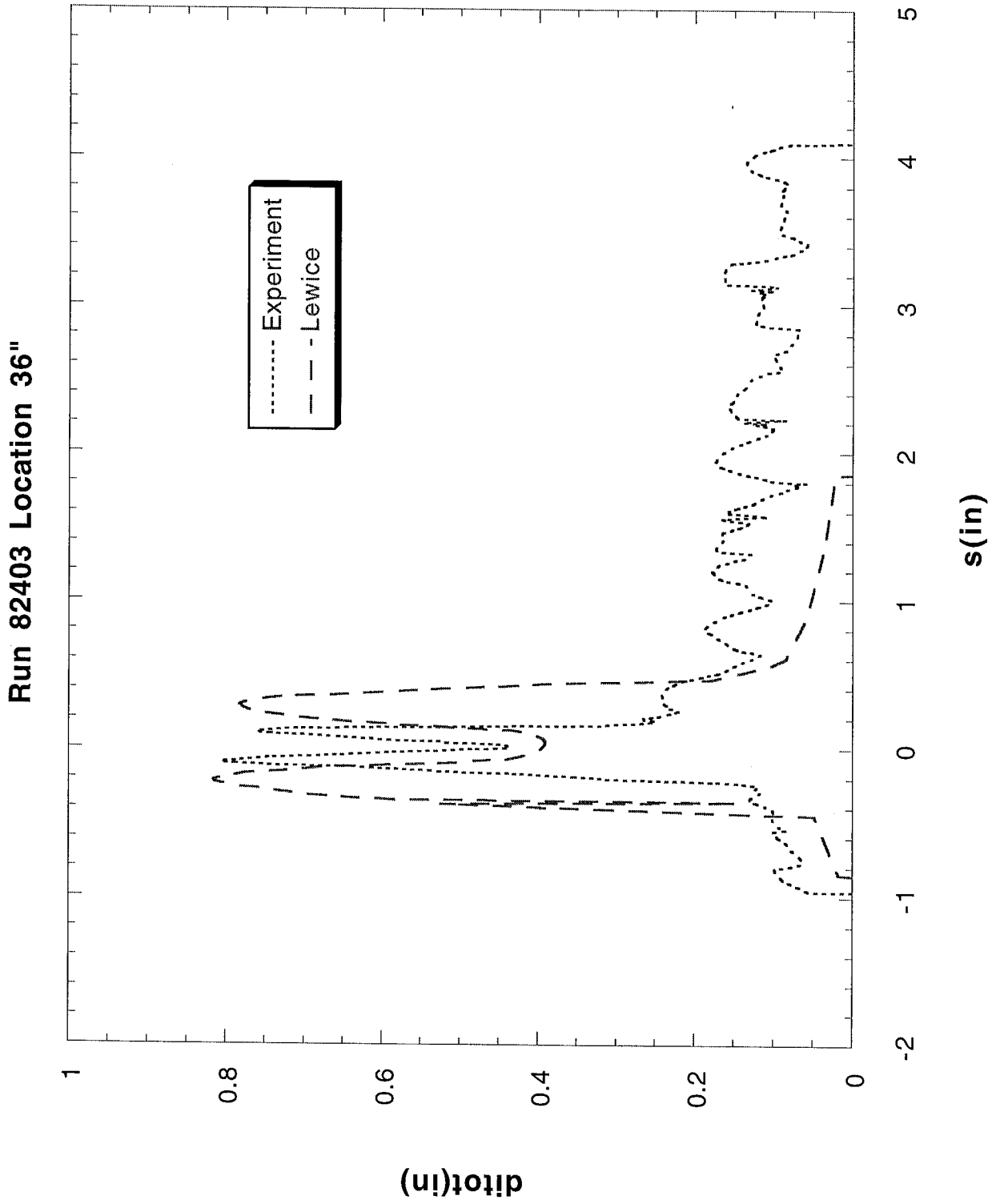
Run 82403 Location 36"
Experiment
Lewice
dltot(in)
s(in)
1
0.8
0.6
0.4
0.2
0
-2
-1
0
1
2
3
4
5

NACA 4415 (mod)
Figures 448 – 483

NACA 4415 (mod) Test Conditions

Principal Investigator	Airfoil	Test Date	Chord (in)	Run Number	Previous Identical Run	Velocity (kts)	Velocity (m/s)	Tt (°F)	Static Temperature (K)	A.O.A.	Corrected A.O.A.	LWC (g/m^3)	MVD (microns)	Spray Time (min)	Digitized Tracing Locations
Miller	NACA4415 (mod)	1995	78"	DC-1		169.5	87.2	30	267.96	0	0	0.83	160	15	40"
Miller	NACA4415 (mod)	1995	78"	DC-2		169.5	87.2	28	266.85	0	0	0.82	160	7	31", 36" & 40"
Miller	NACA4415 (mod)	1995	78"	DC-3		169.5	87.2	28	266.85	0	0	0.53	99	10.7	31", 36" & 40"
Miller	NACA4415 (mod)	1995	78"	DC-4R	DC-2	169.5	87.2	28	266.85	0	0	0.82	160	7	31", 36" & 40"
Miller	NACA4415 (mod)	1995	78"	DC-5R	DC-2	169.5	87.2	28	266.85	0	0	0.82	160	7	31", 36" & 40"
Miller	NACA4415 (mod)	1995	78"	DC-6R	DC-2	169.5	87.2	28	266.85	0	0	0.82	160	7	31", 36" & 40"
Miller	NACA4415 (mod)	1995	78"	DC-7R	DC-3	169.5	87.2	28	266.85	0	0	0.53	99	10.7	31", 36" & 40"
Miller	NACA4415 (mod)	1995	78"	DC-8R	DC-2	169.5	87.2	28	266.85	0	0	0.82	160	7	31", 36" & 40"
Miller	NACA4415 (mod)	1995	78"	DC-9R	DC-3	169.5	87.2	28	266.85	0	0	0.53	99	10.7	31", 36" & 40"
Miller	NACA4415 (mod)	1995	78"	DC-10		169.5	87.2	28	266.85	0	0	0.53	160	7	31", 36" & 40"
Miller	NACA4415 (mod)	1995	78"	DC-11		169.5	87.2	28	266.85	0	0	0.82	99	10.7	31", 36" & 40"
Miller	NACA4415 (mod)	1995	78"	DC-12R	DC-10	169.5	87.2	28	266.85	0	0	0.53	160	7	31", 36" & 40"
Miller	NACA4415 (mod)	1995	78"	DC-13R	DC-2	169.5	87.2	28	266.85	0	0	0.82	160	7	31", 36" & 40"
Miller	NACA4415 (mod)	1995	78"	DC-14R	DC-3	169.5	87.2	28	266.85	0	0	0.53	99	10.7	31", 36" & 40"
Miller	NACA4415 (mod)	1995	78"	DC-15R	DC-2	169.5	87.2	28	266.85	0	0	0.82	160	7	31", 36" & 40"
Miller	NACA4415 (mod)	1995	78"	DC-16R	DC-3	169.5	87.2	28	266.85	0	0	0.53	99	10.7	31", 36" & 40"
Miller	NACA4415 (mod)	1995	78"	7a		108.6	55.9	30	270.20	0	0	0.76	40	18	31", 36" & 40"
Miller	NACA4415 (mod)	1995	78"	15		108.6	55.9	0	253.53	-2	-2	1.36	160	3	31", 36" & 40"
Miller	NACA4415 (mod)	1995	78"	15a		108.6	55.9	0	253.53	-2	-2	0.96	40	4	31", 36" & 40"
Miller	NACA4415 (mod)	1995	78"	15b		108.6	55.9	0	253.53	-2	-2	0.85	99	3	31", 36" & 40"
Miller	NACA4415 (mod)	1995	78"	18		108.6	55.9	0	253.53	-2	-2	1.36	160	18	31 & 36"
Miller	NACA4415 (mod)	1995	78"	80a		169.5	87.2	33	269.63	0	0	0.82	160	18	36"
Miller	NACA4415 (mod)	1995	78"	81		169.5	87.2	32	269.08	0	0	0.82	160	18	36"
Miller	NACA4415 (mod)	1995	78"	81a		169.5	87.2	31	268.52	0	0	0.82	160	18	36"
Miller	NACA4415 (mod)	1995	78"	82		169.5	87.2	30	267.96	0	0	0.82	160	18	36"
Miller	NACA4415 (mod)	1995	78"	82a		125	55.9	30	270.20	0	0	1.36	160	18	36"
Miller	NACA4415 (mod)	1995	78"	83		195	87.2	28	266.85	0	0	0.82	160	18	36"
Miller	NACA4415 (mod)	1995	78"	83b		125	55.9	28	269.09	0	0	1.36	160	18	36"
Miller	NACA4415 (mod)	1995	78"	84		195	87.2	5	254.08	0	0	0.82	160	18	36"

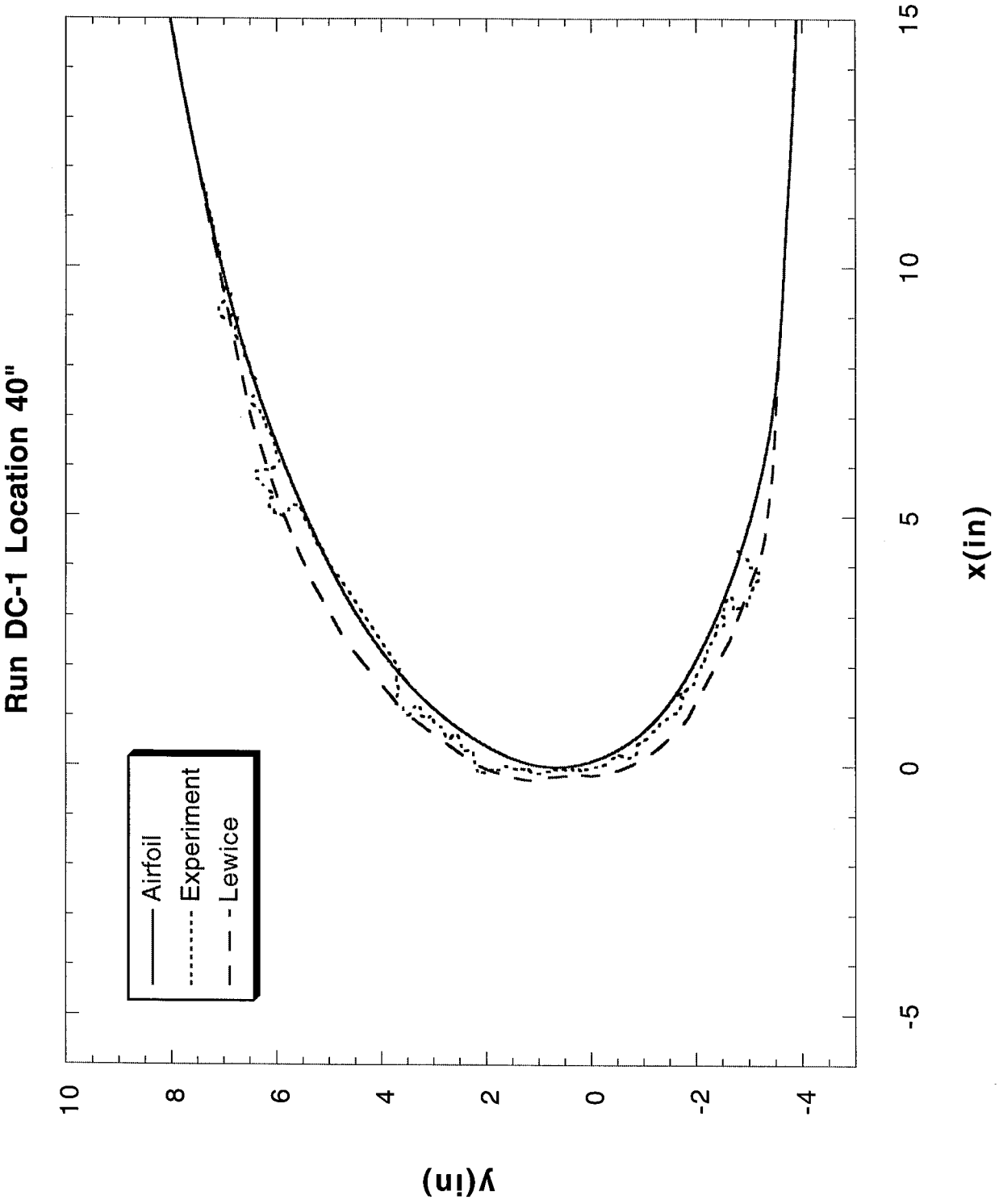
Run DC-1 Location 40"
Airfoil
Experiment
Lewice
y(in)
x(in)
10
8
6
4
2
0
-2
-4
-5
0
5
10
15

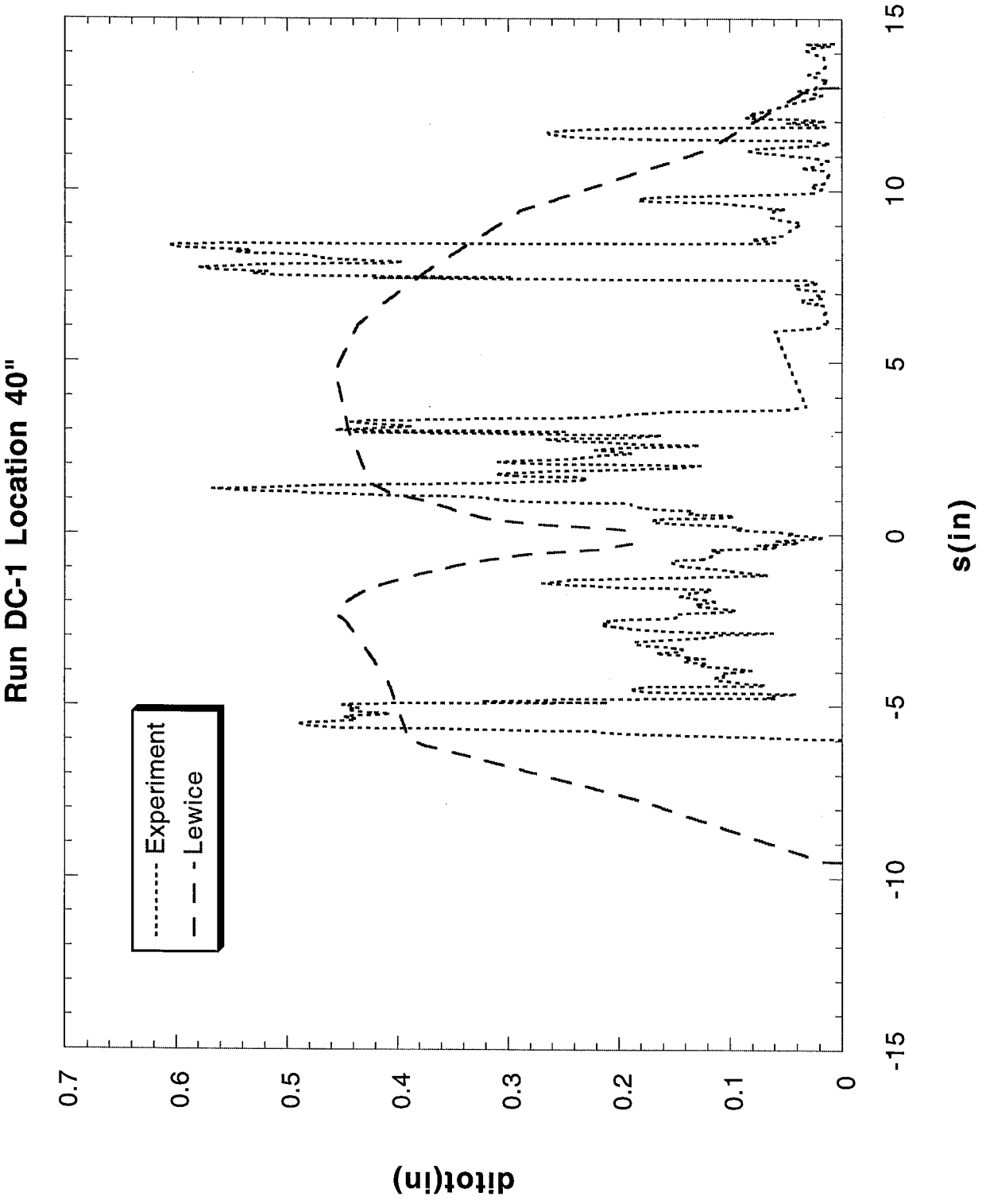
Run DC-1 Location 40"
Experiment
Lewice
dltot(in)
s(in)
0.7
0.6
0.5
0.4
0.3
0.2
0.1
0
-15
-10
-5
0
5
10
15

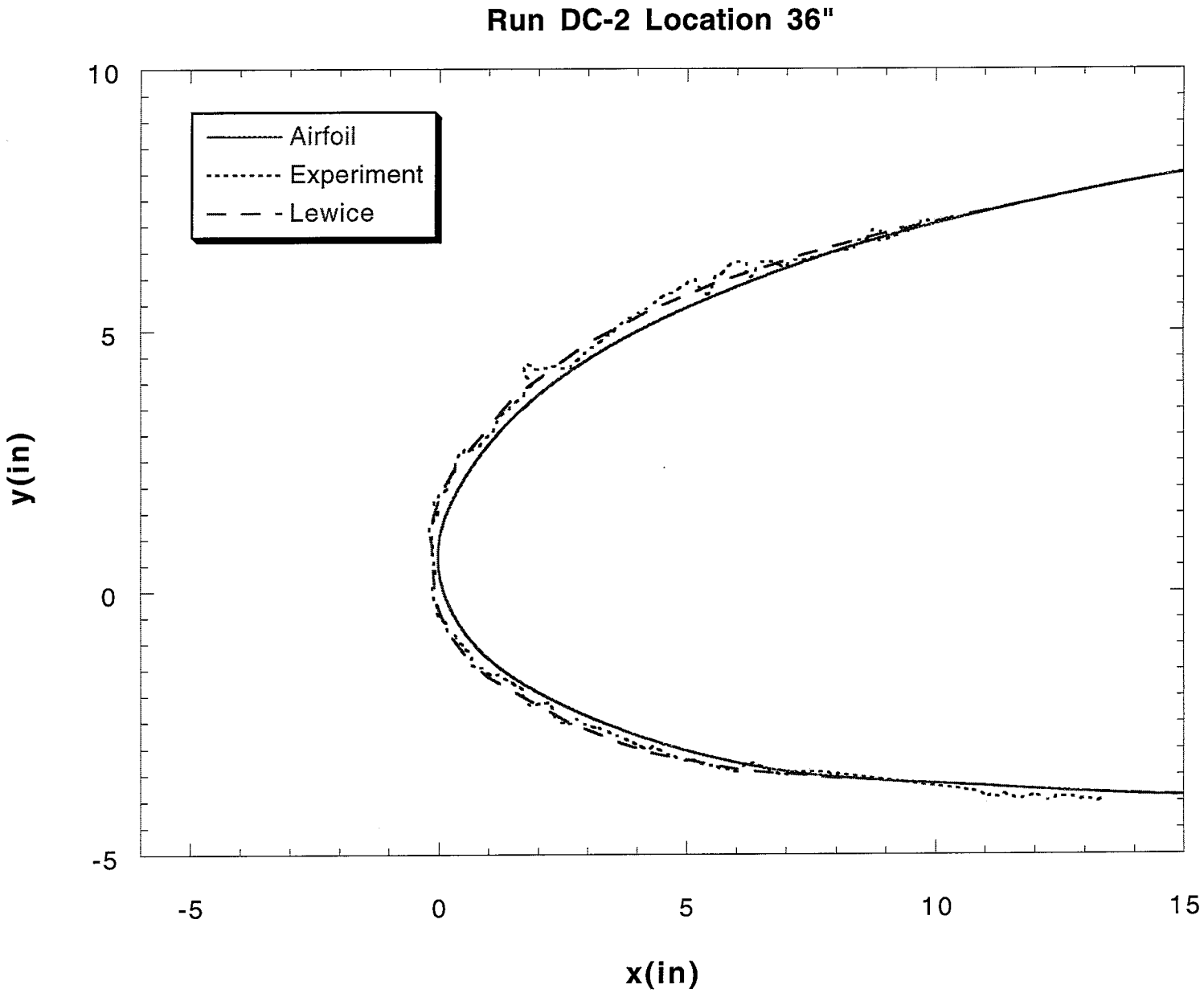
Run DC-2 Location 36"
Airfoil
Experiment
Lewice
y(in)
x(in)
10
5
0
-5
-5
0
5
10
15

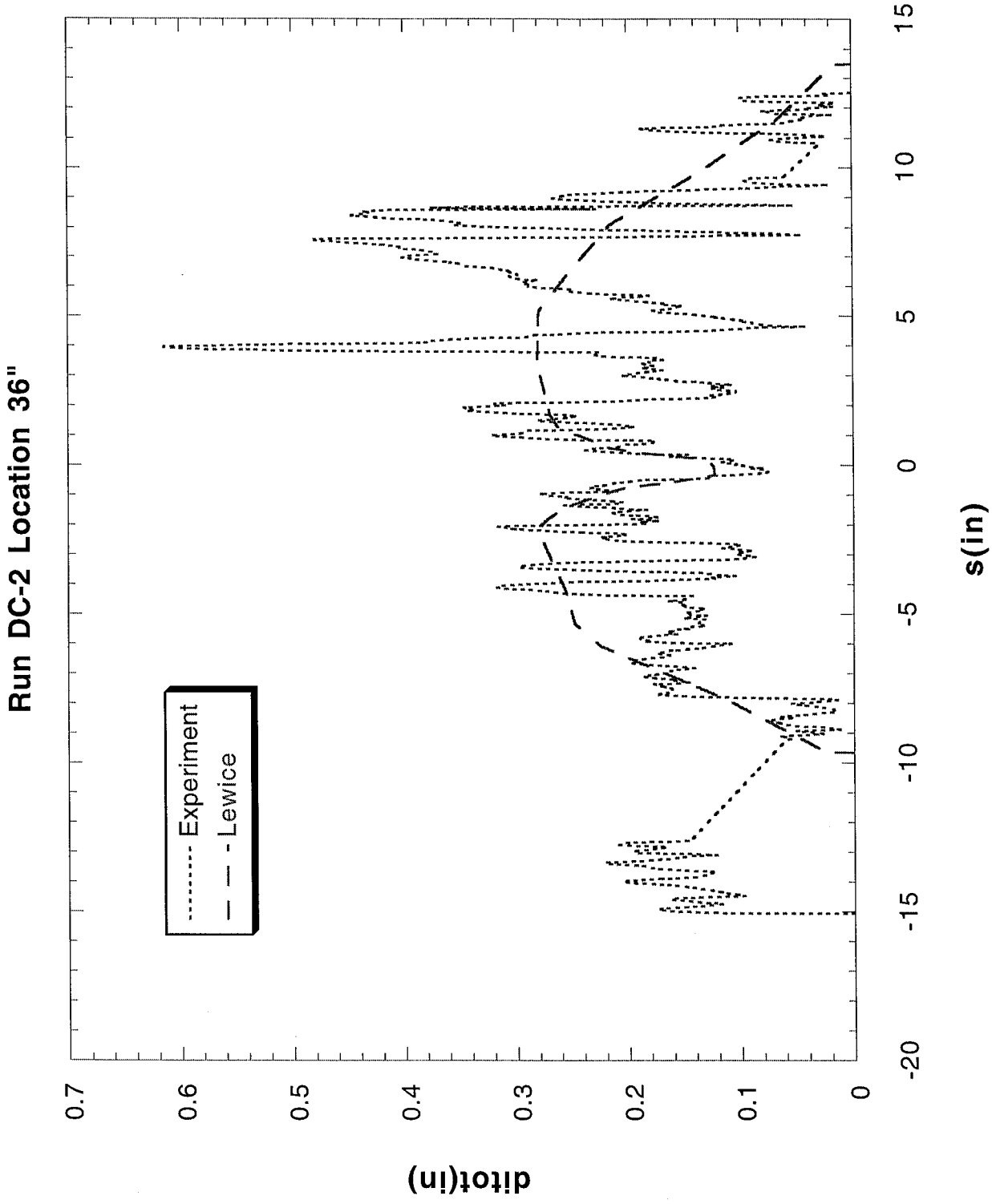
Run DC-2 Location 36"
Experiment
Lewice
ditot(in)
s(in)
0.7
0.6
0.5
0.4
0.3
0.2
0.1
0
-20
-15
-10
-5
0
5
10
15

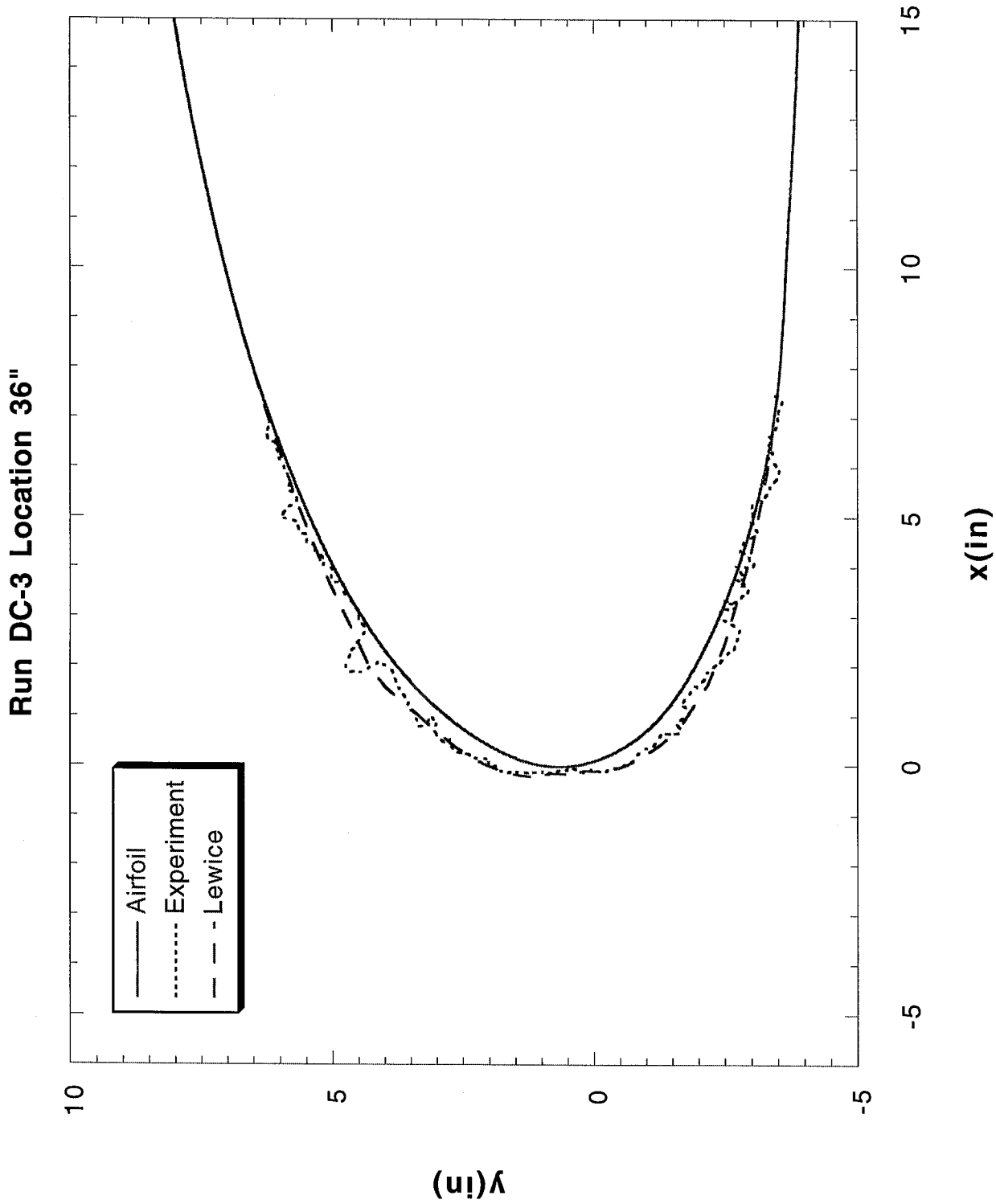
Run DC-3 Location 36"
Airfoil
Experiment
- Lewice
y(in)
x(in)
10
5
0
-5
-5
0
5
10
15

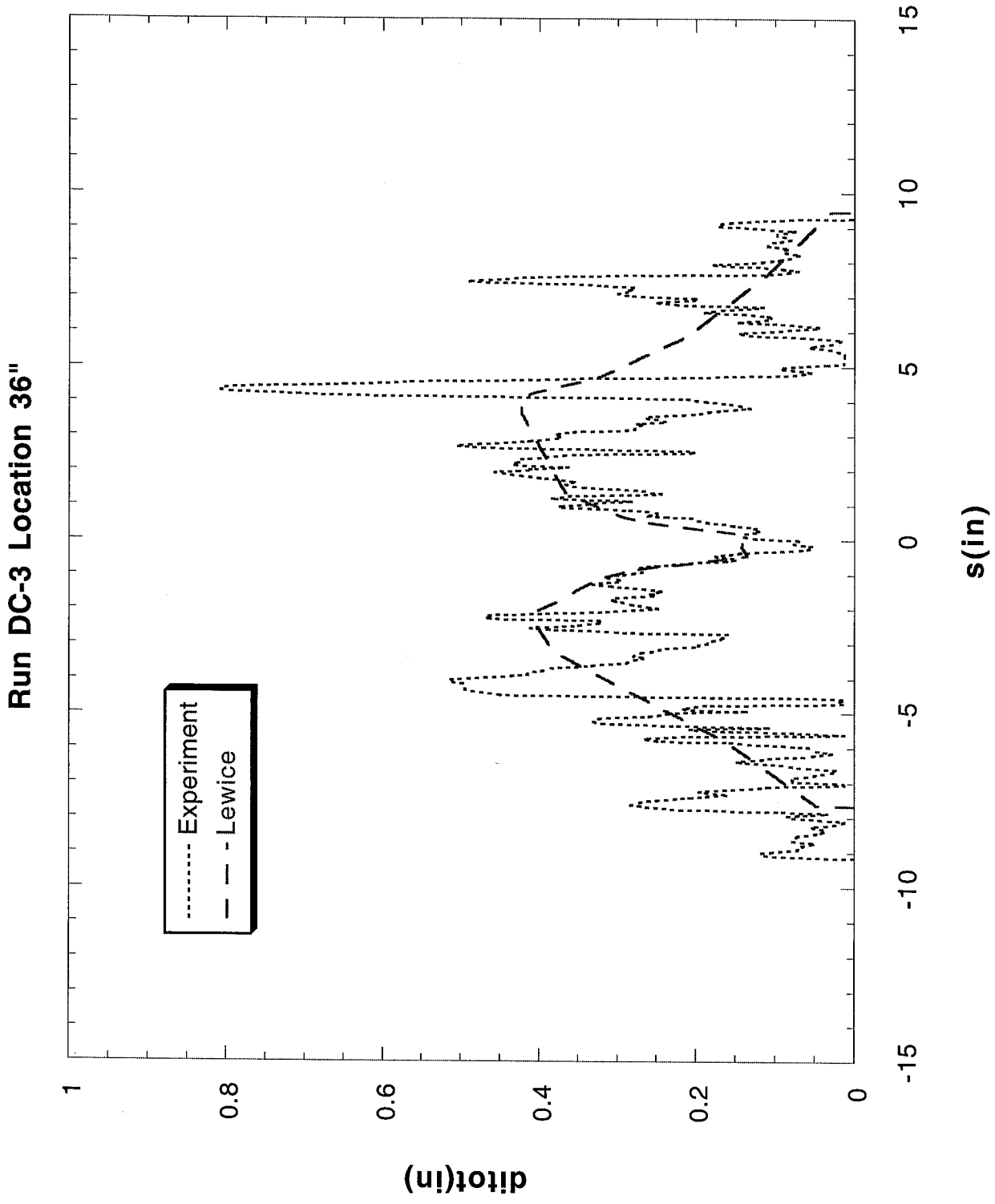
Run DC-3 Location 36"
Experiment
Lewice
dltot(in)
s(in)
1
0.8
0.6
0.4
0.2
0
15
10
5
0
-5
-10
-15

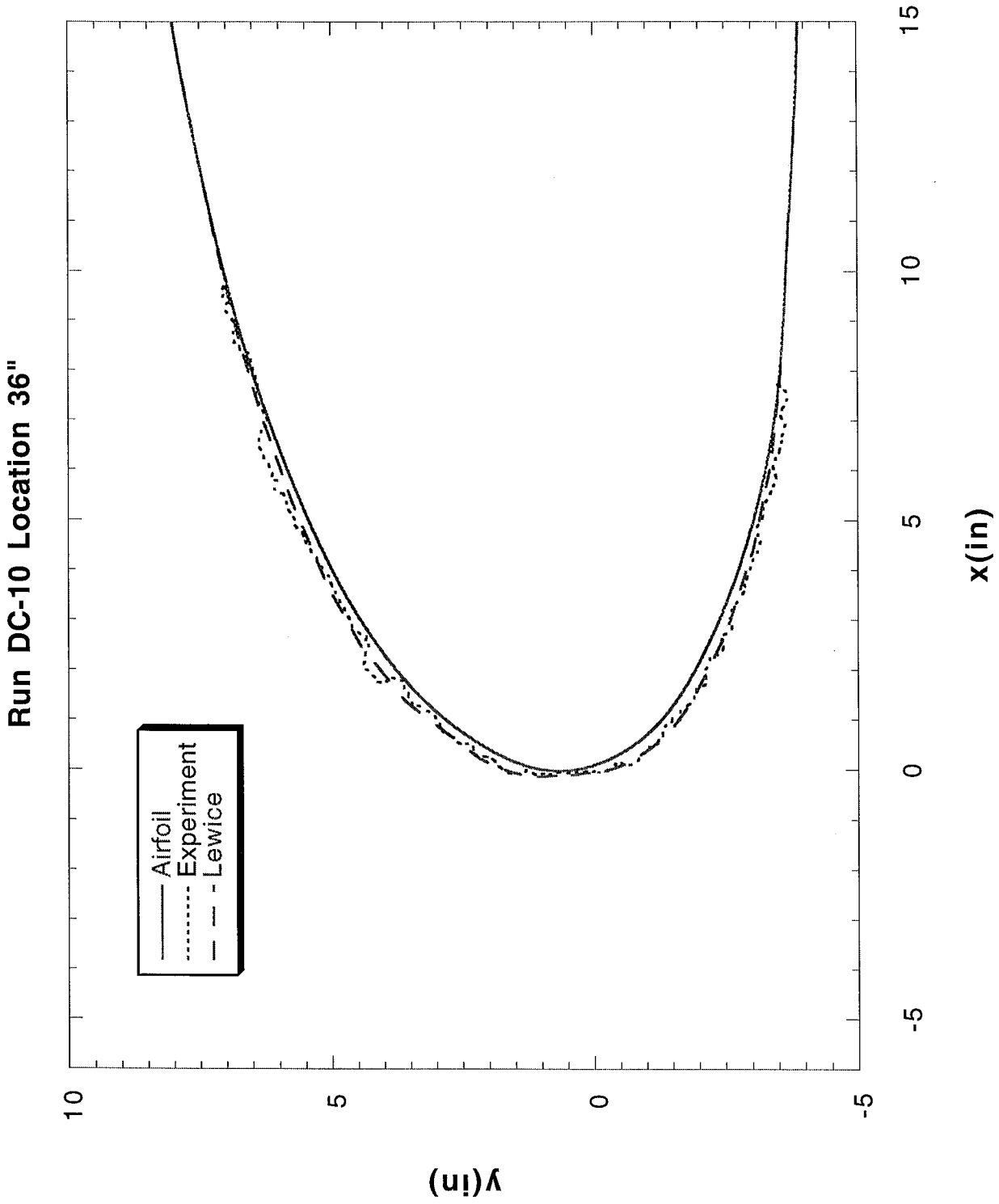
Run DC-10 Location 36"
Airfoil
Experiment
Lewice
y(in)
x(in)
10
5
0
-5
-5
0
5
10
15

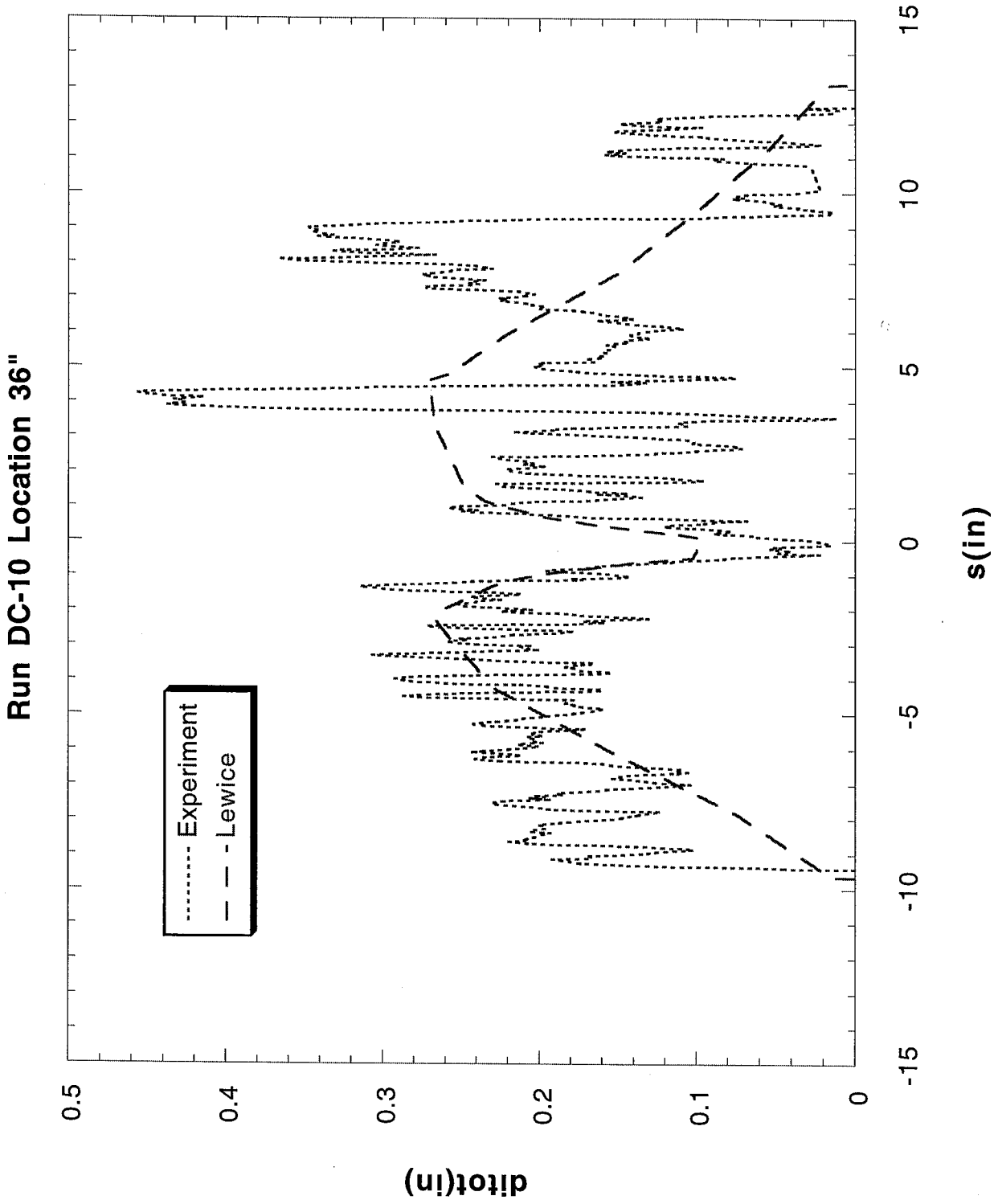
Run DC-10 Location 36"
Experiment
Lewice
dltot(in)
s(in)
0.5
0.4
0.3
0.2
0.1
0
15
10
5
0
-5
-10
-15

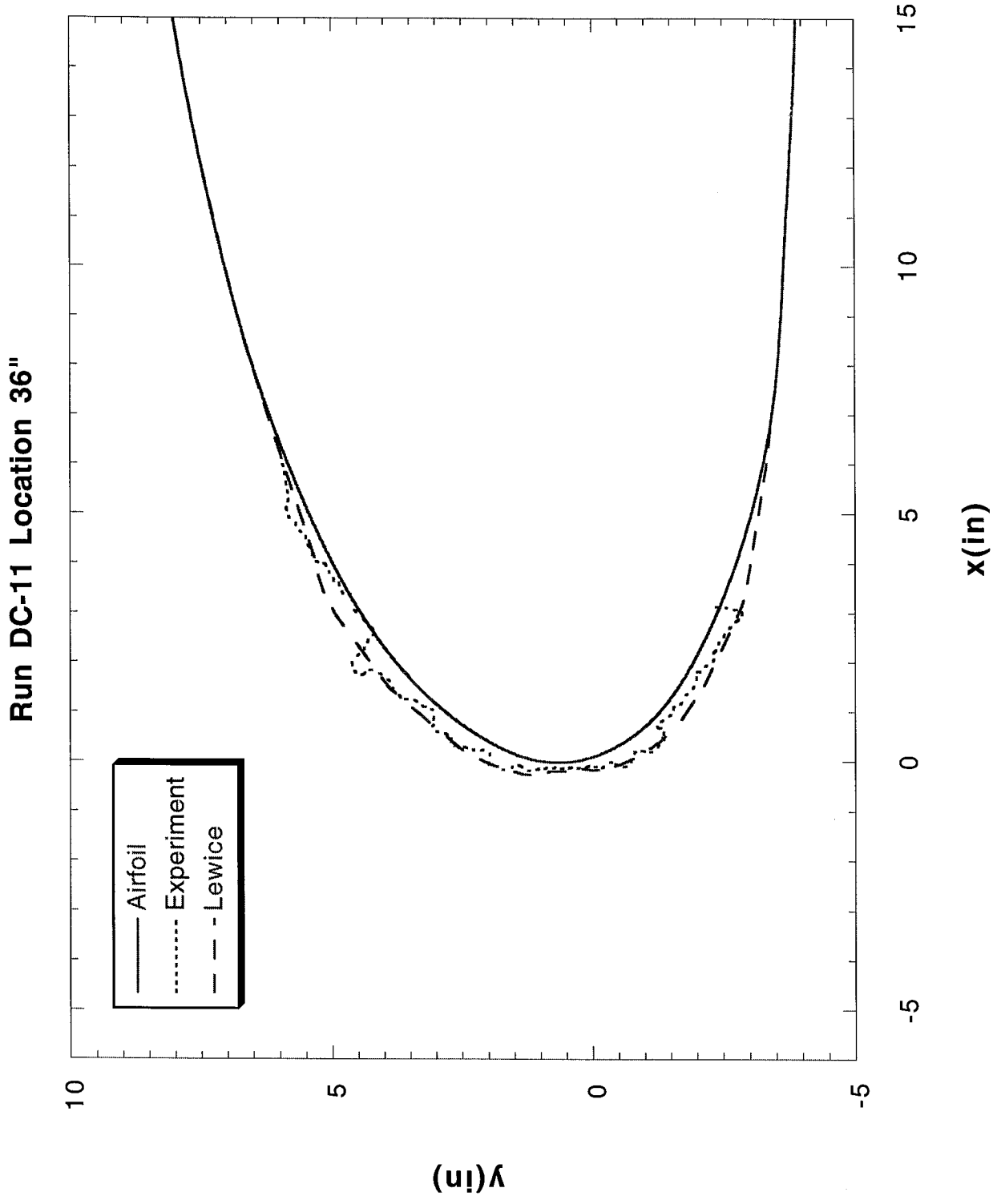
Run DC-11 Location 36"
Airfoil
Experiment
Lewice
y(in)
x(in)
10
5
0
-5
-5
0
5
10
15

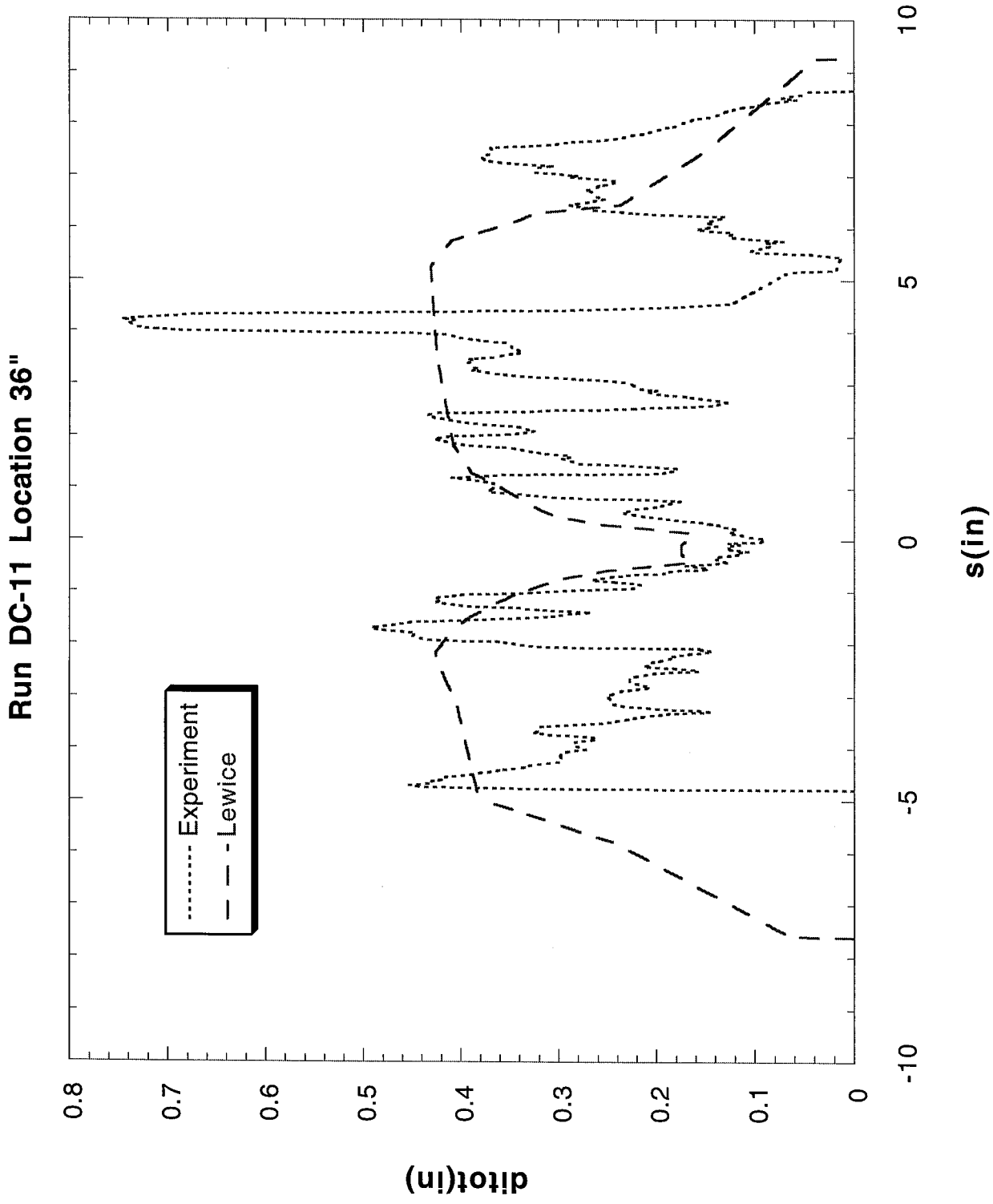
Run DC-11 Location 36"
Experiment
Lewice
dltot(in)
s(in)
0.8
0.7
0.6
0.5
0.4
0.3
0.2
0.1
0
-10
-5
0
5
10

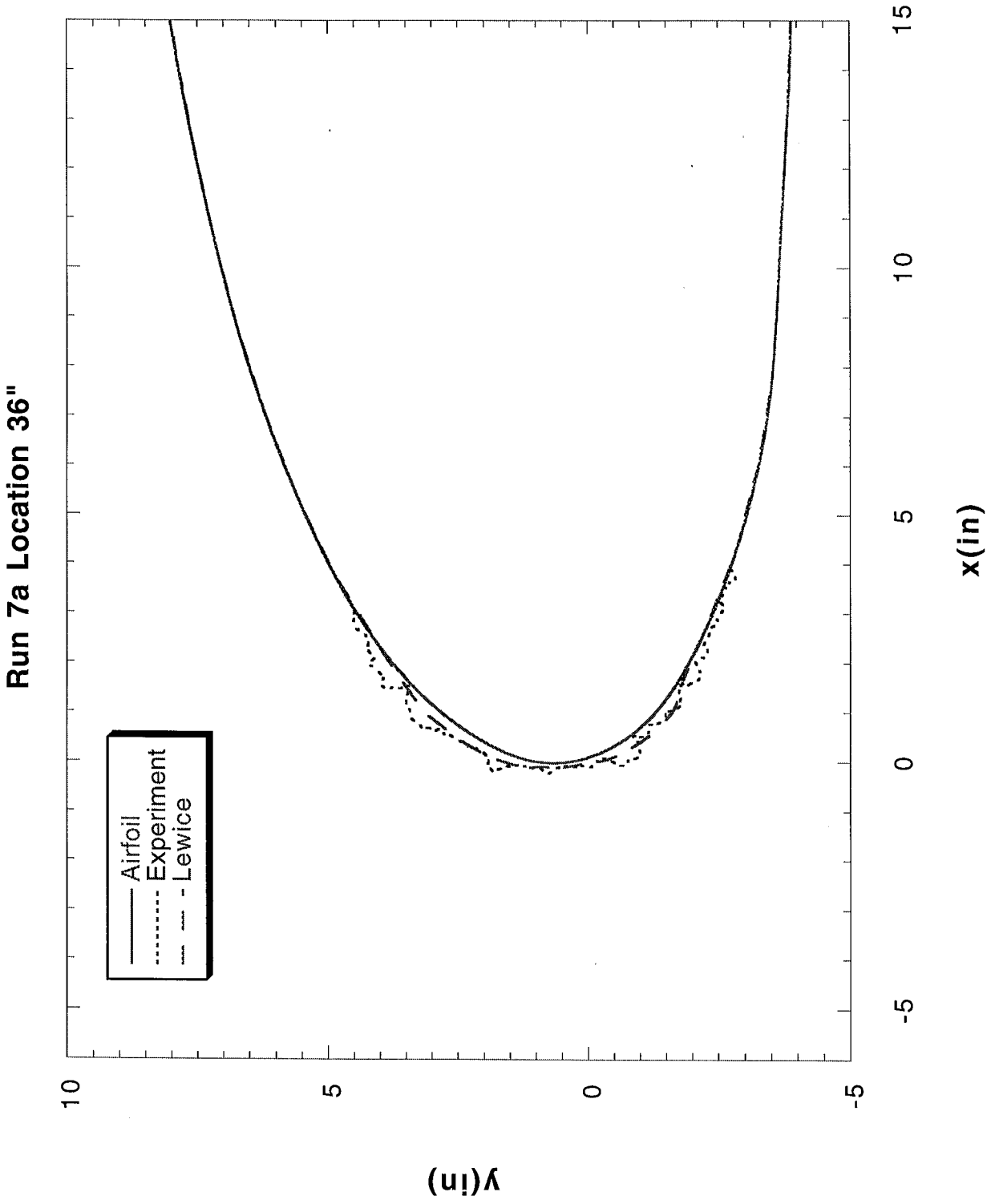
Run 7a Location 36"
Airfoil
Experiment
Lewice
y(in)
x(in)
10
5
0
-5
-5
0
5
10
15

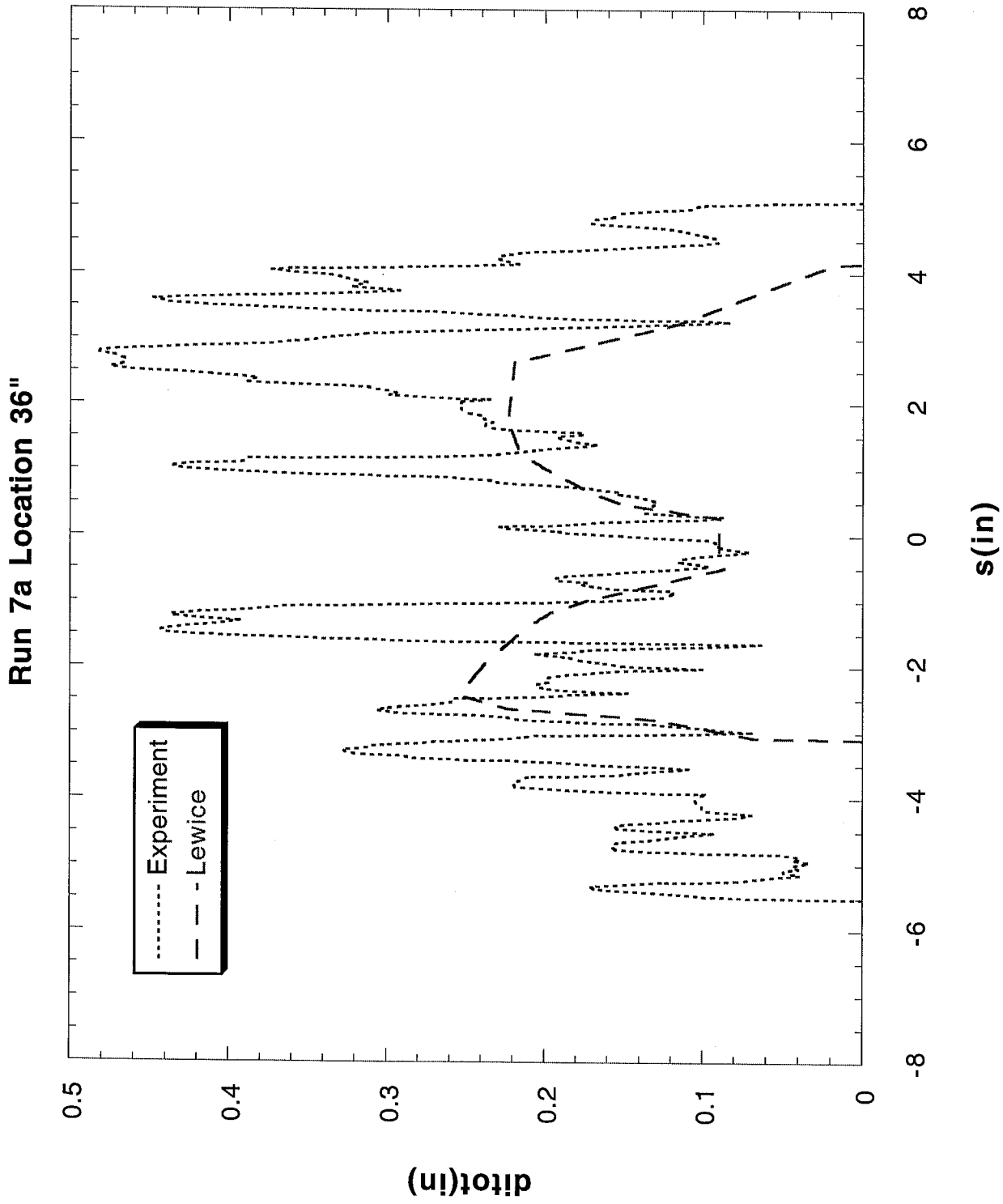
Run 7a Location 36"
Experiment
Lewice
dltot(in)
s(in)
0.5
0.4
0.3
0.2
0.1
0
8
6
4
2
0
-2
-4
-6
-8

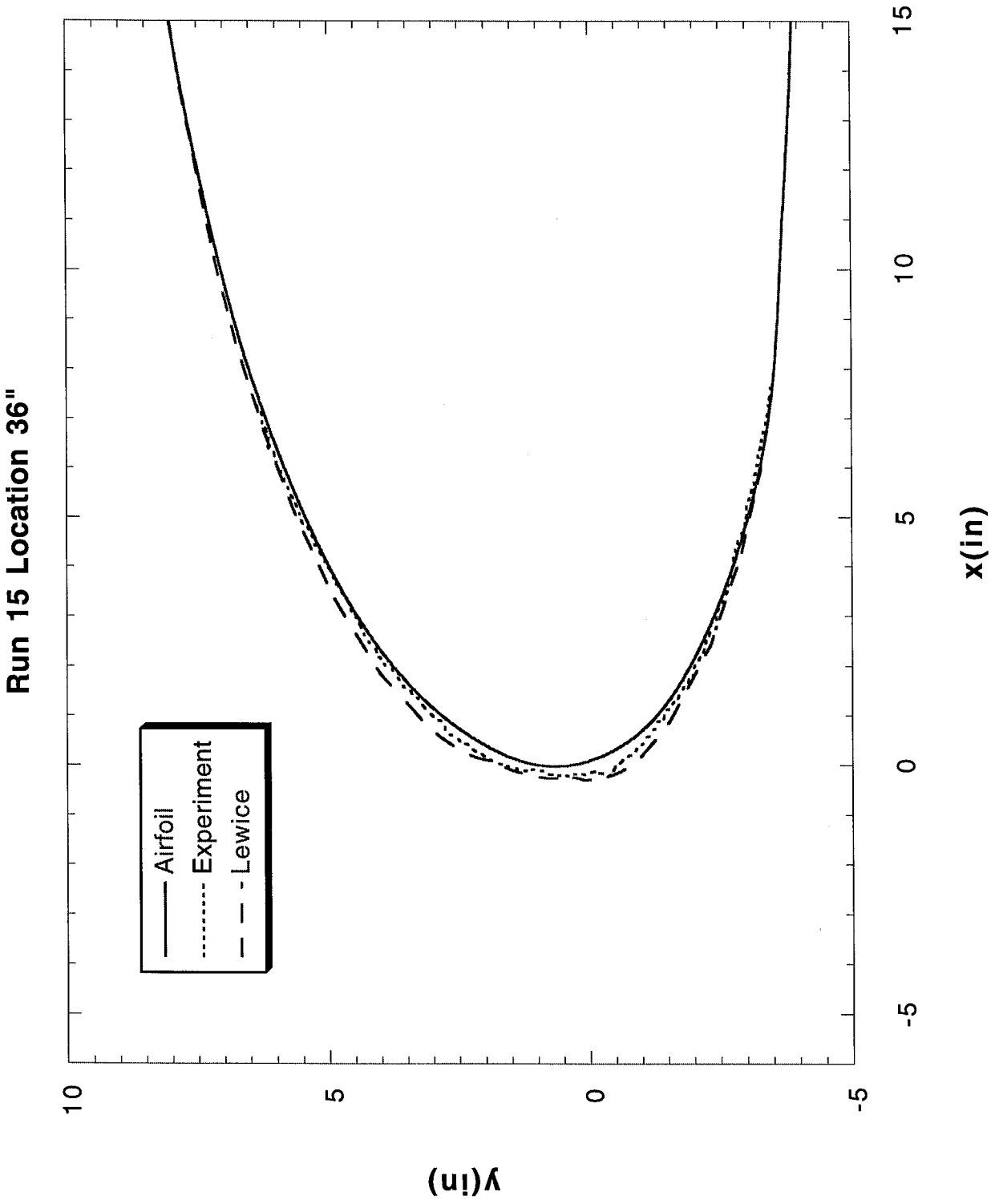
Run 15 Location 36"
Airfoil
Experiment
Lewice
y(in)
x(in)
10
5
0
-5
-5
0
5
10
15

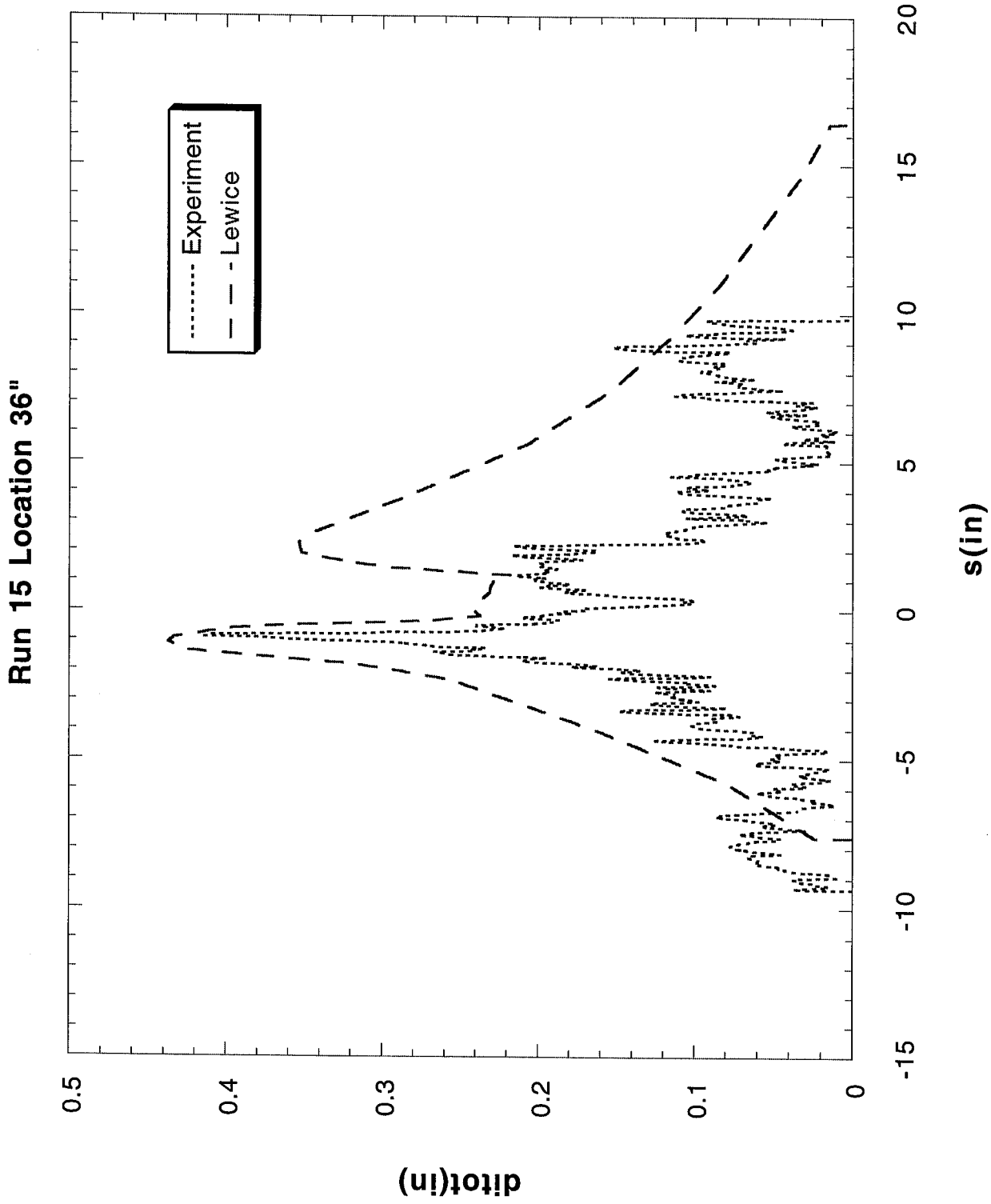
Run 15 Location 36"
Experiment
- Lewice
dltot(in)
s(in)
0.5
0.4
0.3
0.2
0.1
0
-15
-10
-5
0
5
10
15
20

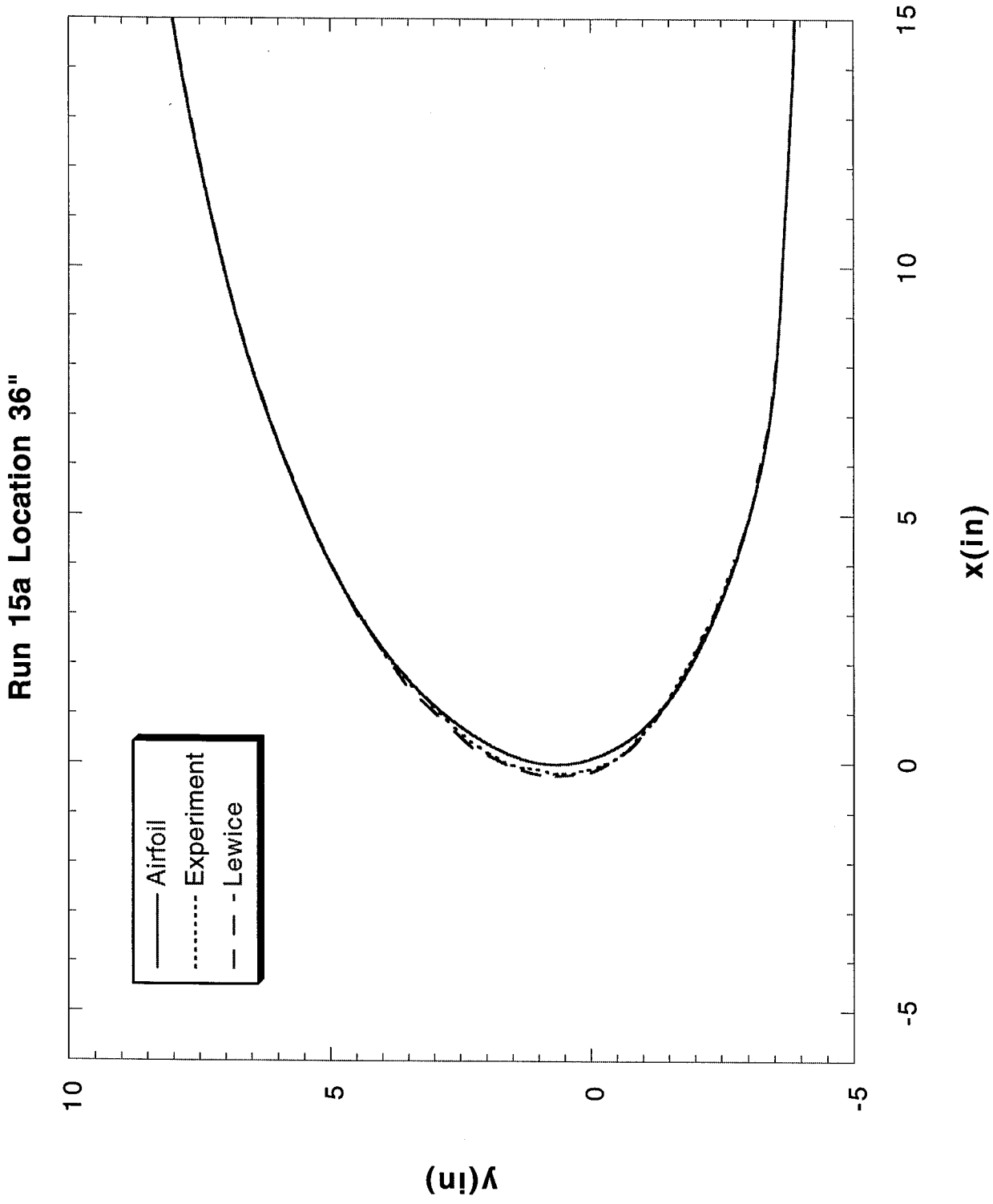
Run 15a Location 36"
Airfoil
Experiment
Lewice
y(in)
x(in)
10
5
0
-5
-5
0
5
10
15

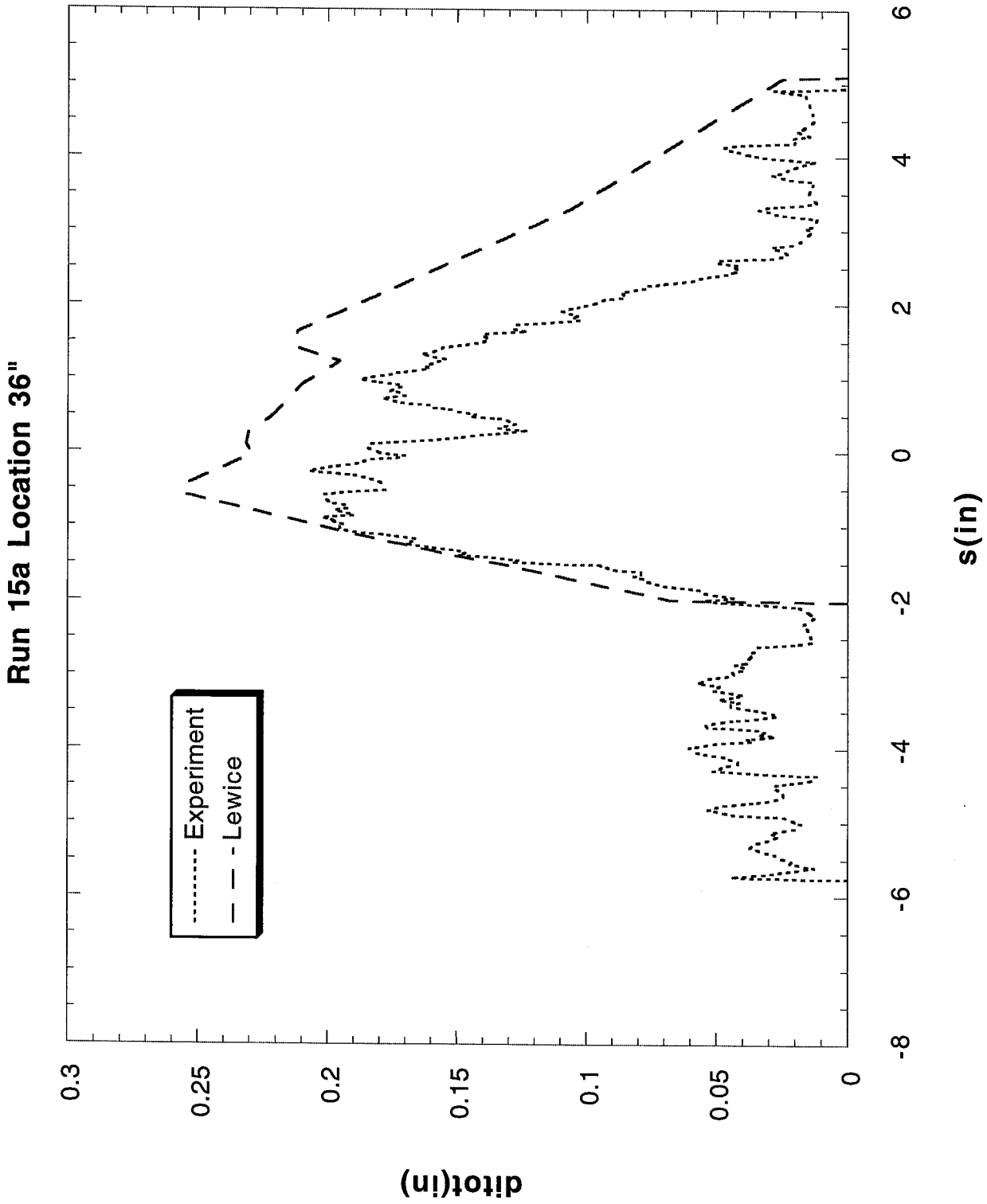
Run 15a Location 36"
Experiment
Lewice
dltot(in)
s(in)
0.3
0.25
0.2
0.15
0.1
0.05
0
-8
-6
-4
-2
0
2
4
6

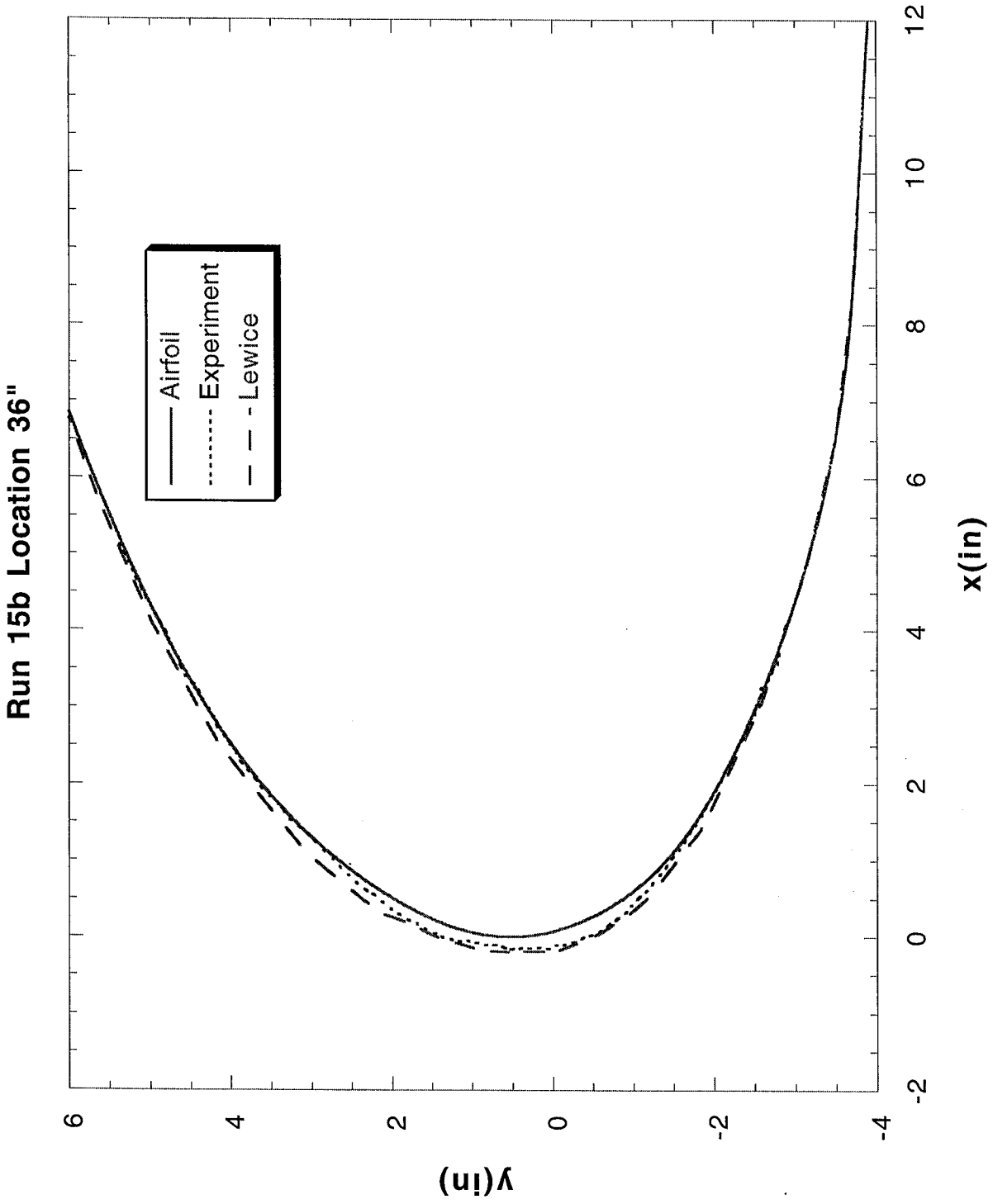
Run 15b Location 36"
Airfoil
Experiment
Lewice
y(in)
x(in)
6
4
2
0
-2
-4
-2
0
2
4
6
8
10
12

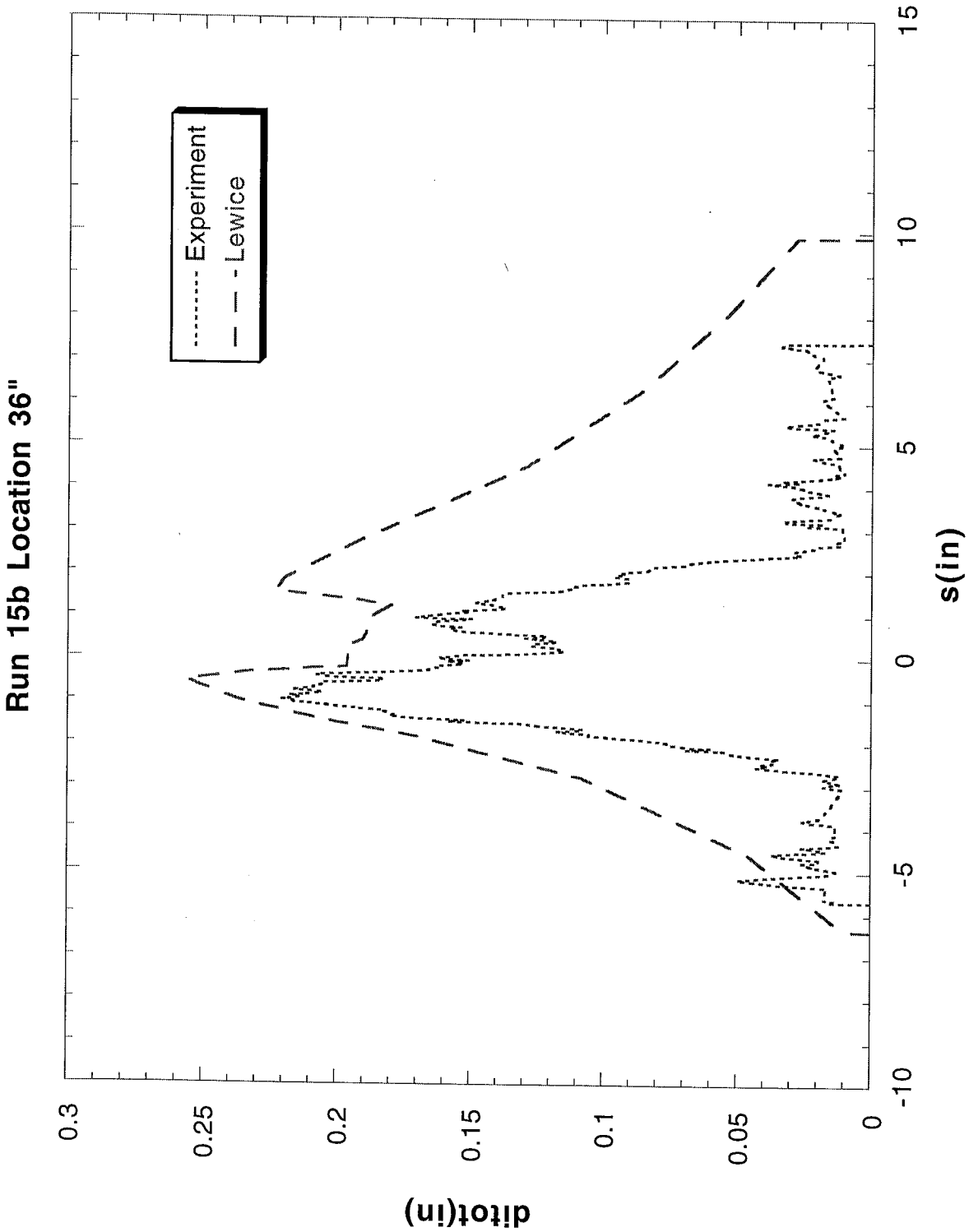
Run 15b Location 36"
Experiment
Lewice
dltot(in)
s(in)
0.3
0.25
0.2
0.15
0.1
0.05
0
-10
-5
0
5
10
15

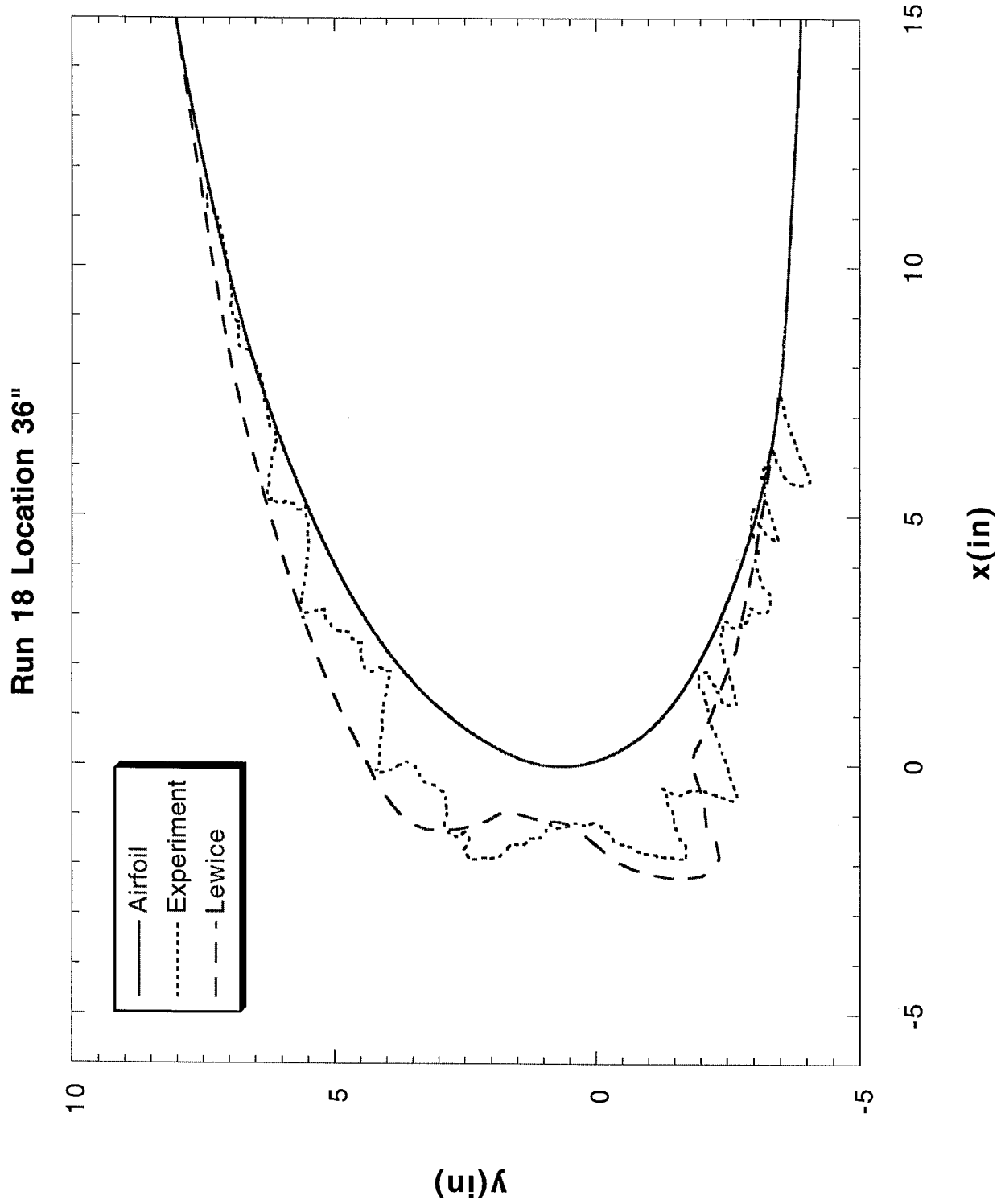
Run 18 Location 36"
Airfoil
Experiment
Lewice
y(in)
x(in)
10
5
0
-5
-5
0
5
10
15

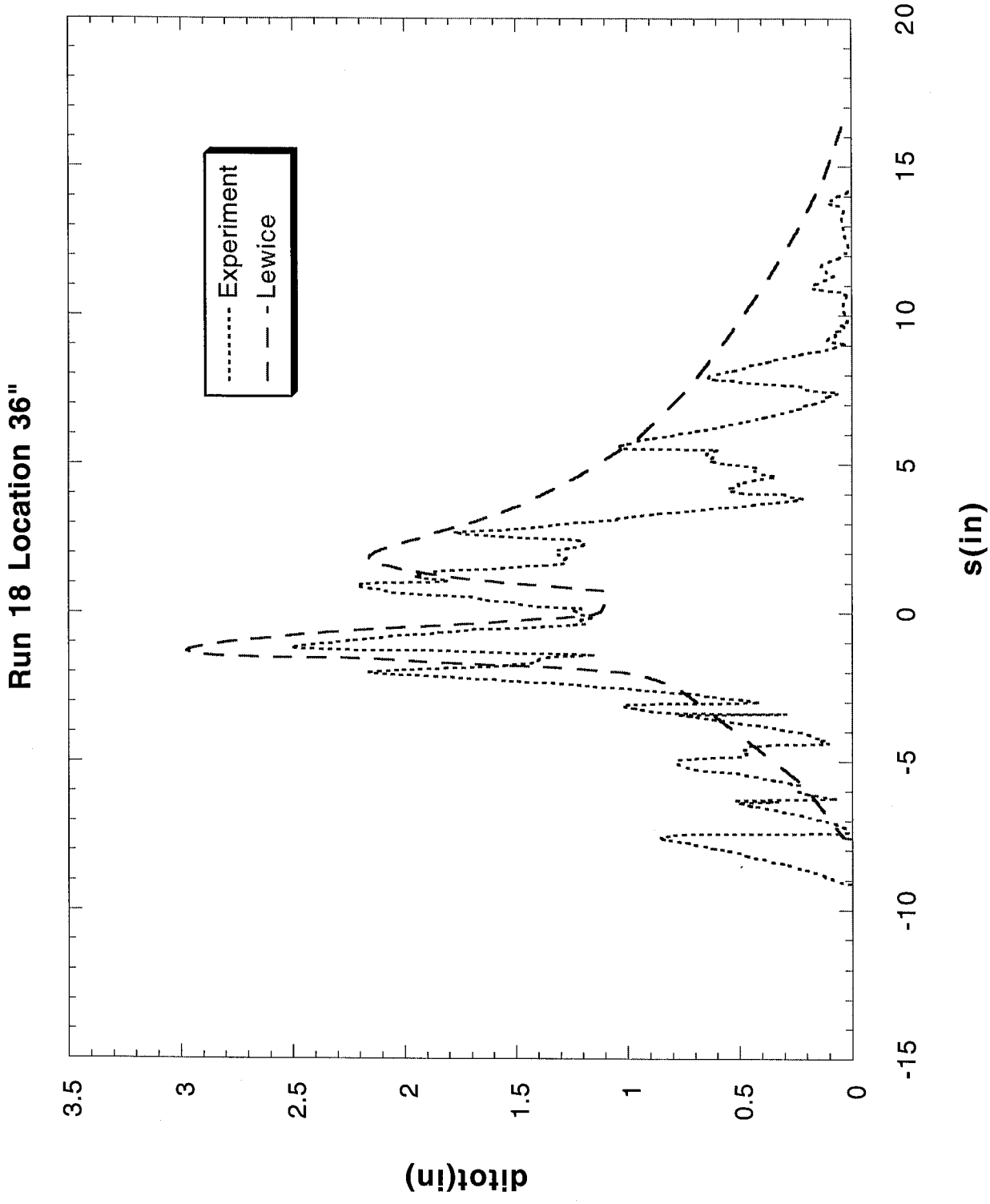
Run 18 Location 36"
Experiment
Lewice
dltot(in)
s(in)
3.5
3
2.5
2
1.5
1
0.5
0
-15
-10
-5
0
5
10
15
20

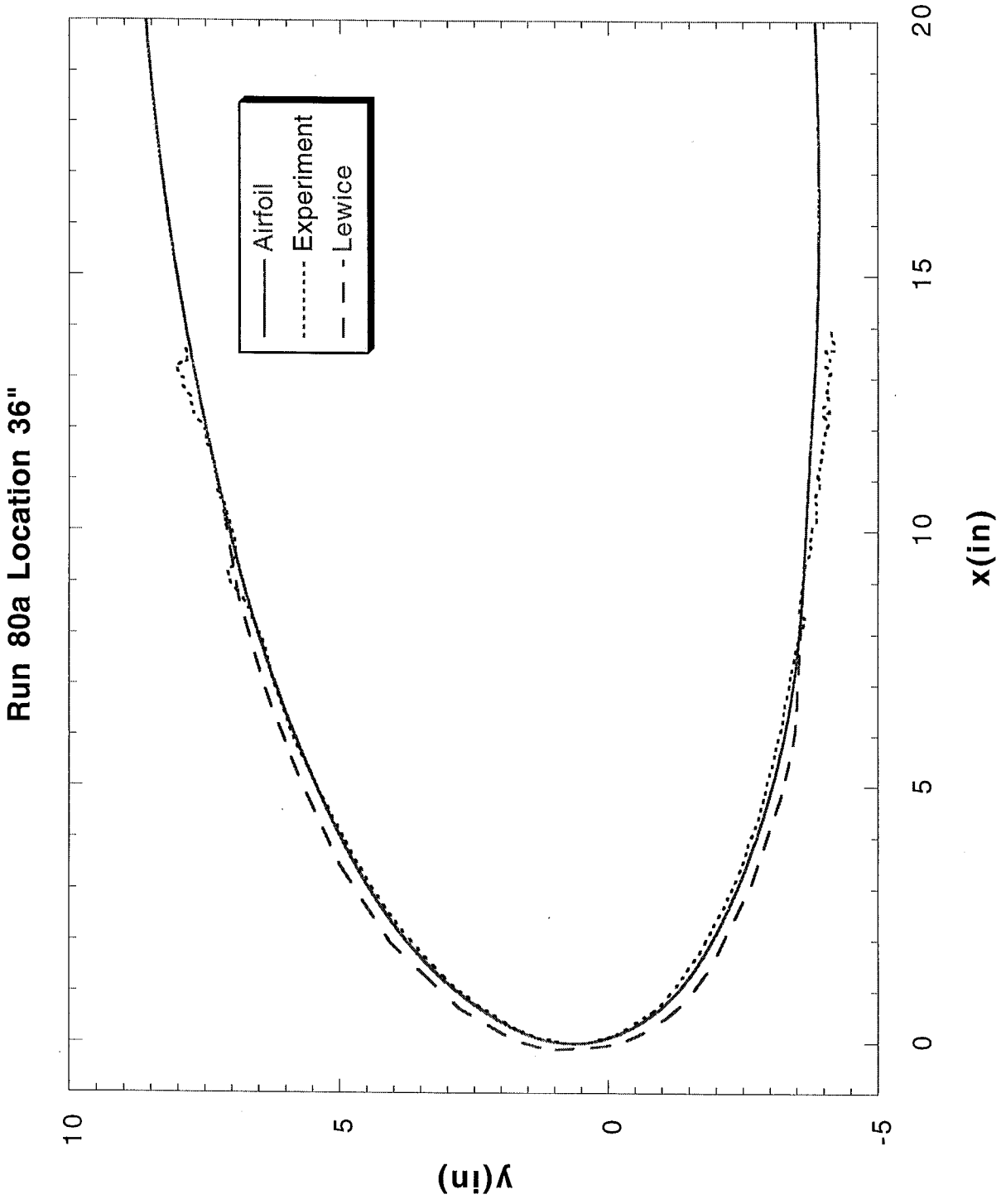
Run 80a Location 36"
Airfoil
Experiment
Lewice
y(in)
x(in)
10
5
0
-5
0
5
10
15
20

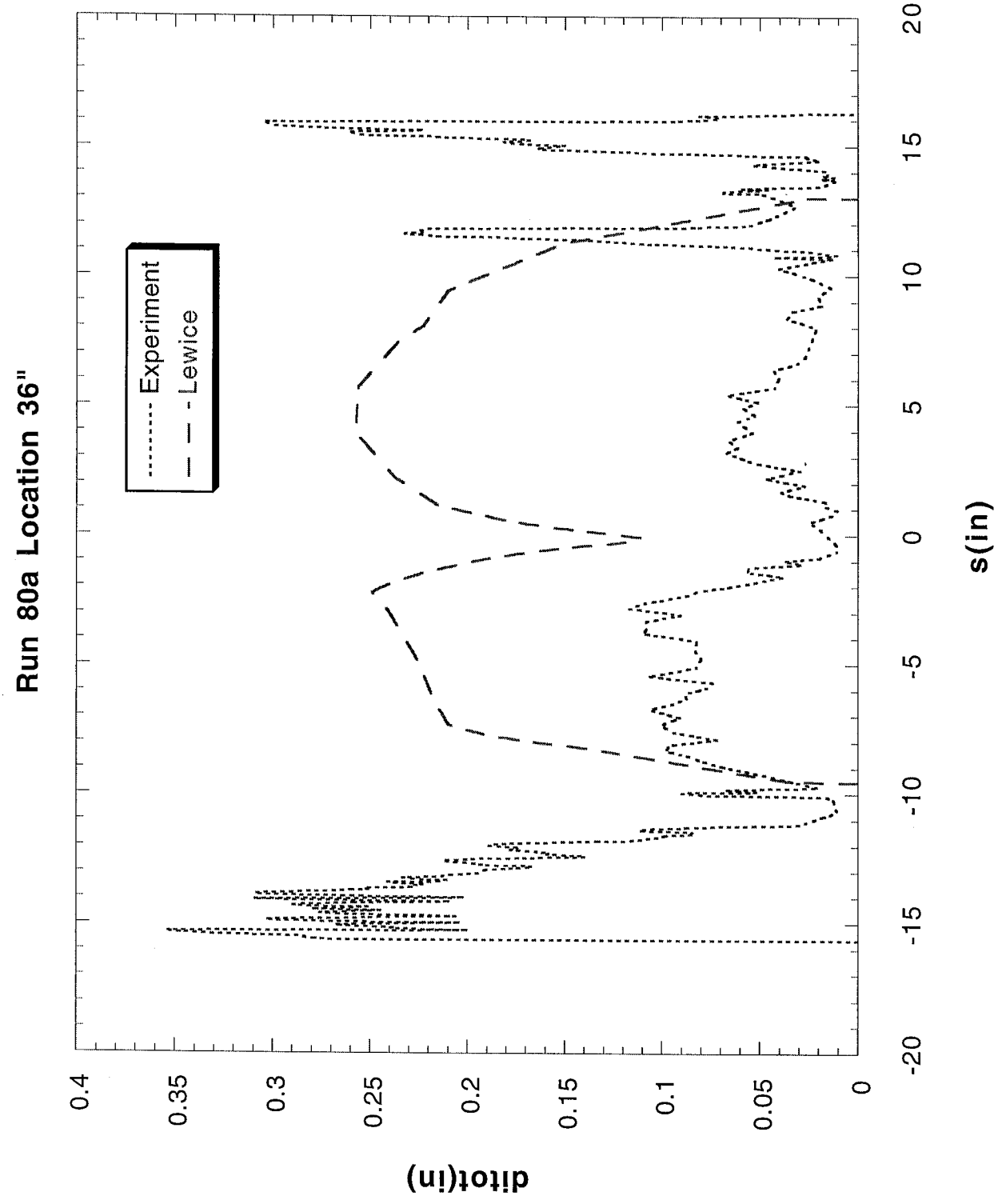
Run 80a Location 36"
Experiment
Lewice
dltot(in)
s(in)
0.4
0.35
0.3
0.25
0.2
0.15
0.1
0.05
0
-20
-15
-10
-5
0
5
10
15
20

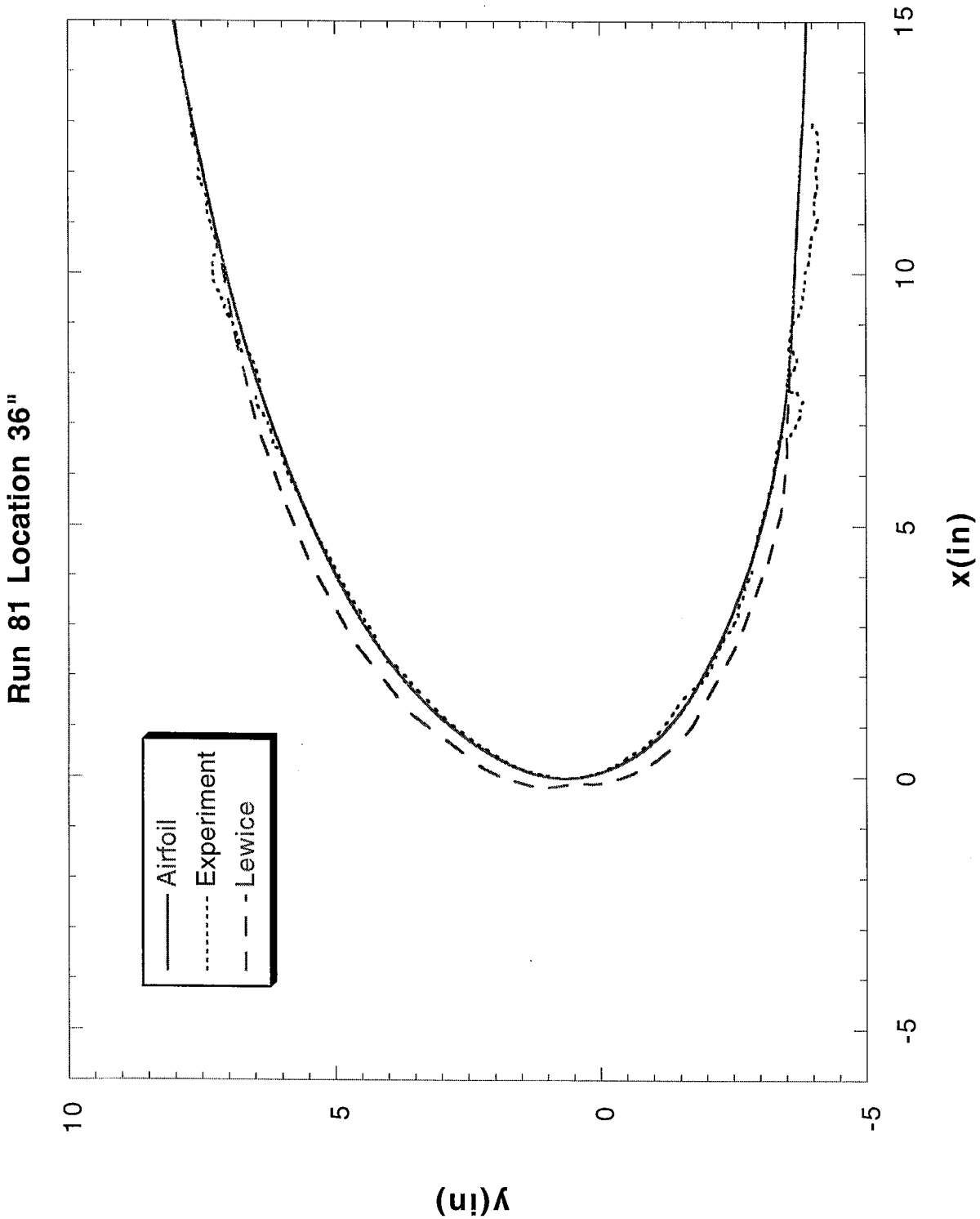
Run 81 Location 36"
Airfoil
Experiment
Lewice
y(in)
x(in)
10
5
0
-5
-5
0
5
10
15

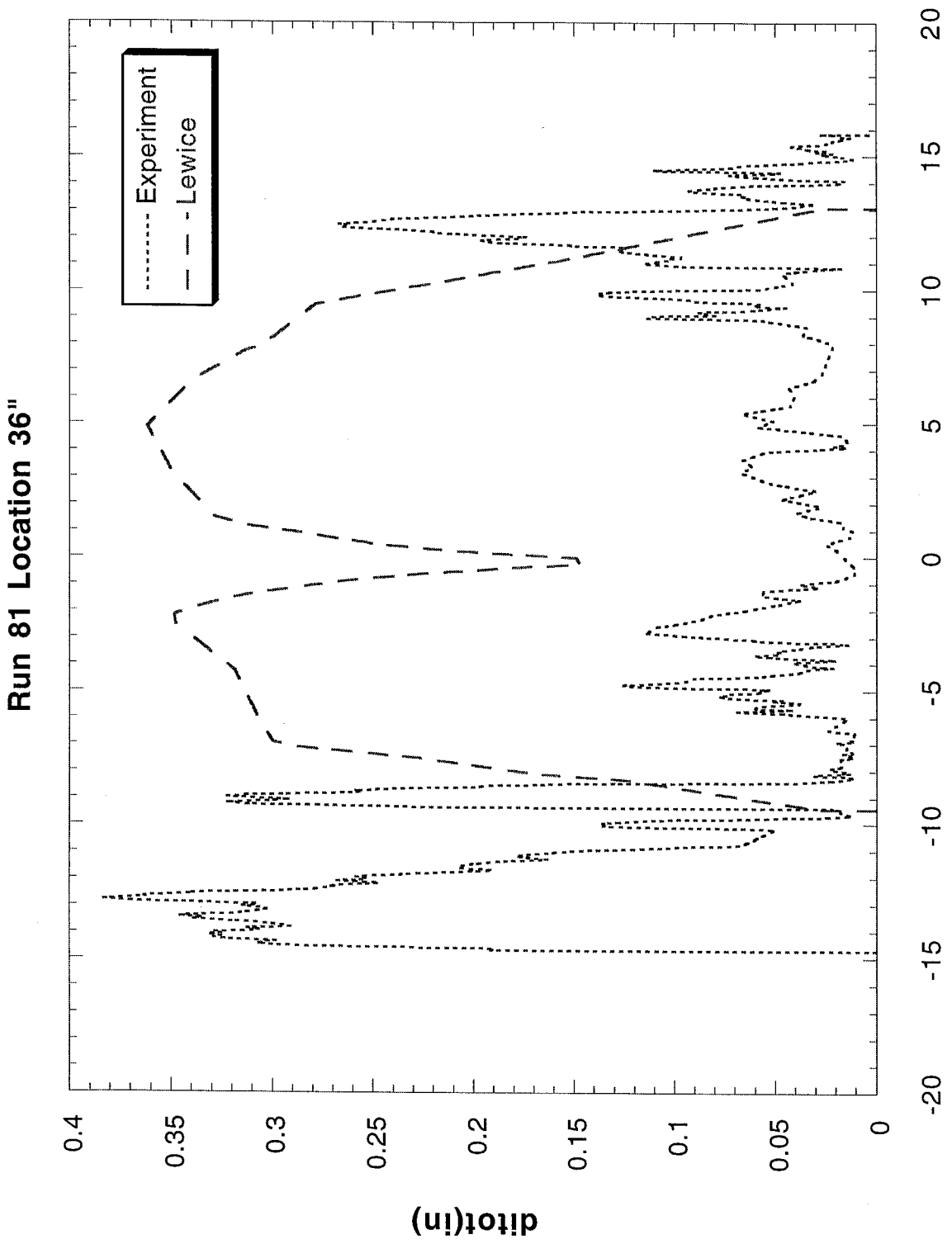
Run 81 Location 36"
Experiment
Lewice
dltot(in)
s(in)
0.4
0.35
0.3
0.25
0.2
0.15
0.1
0.05
0
-20
-15
-10
-5
0
5
10
15
20

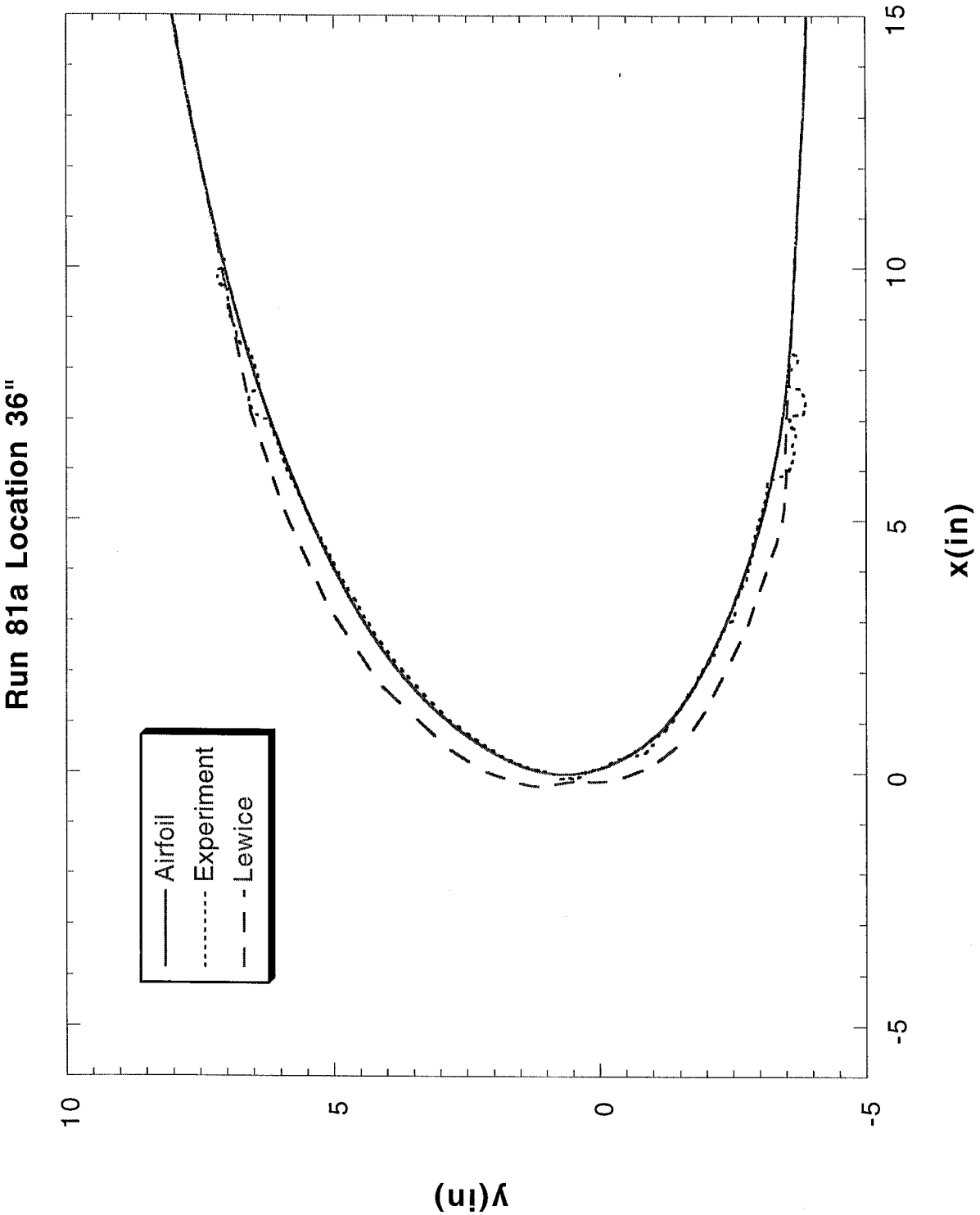
Run 81a Location 36"
Airfoil
Experiment
Lewice
y(in)
x(in)
10
5
0
-5
-5
0
5
10
15

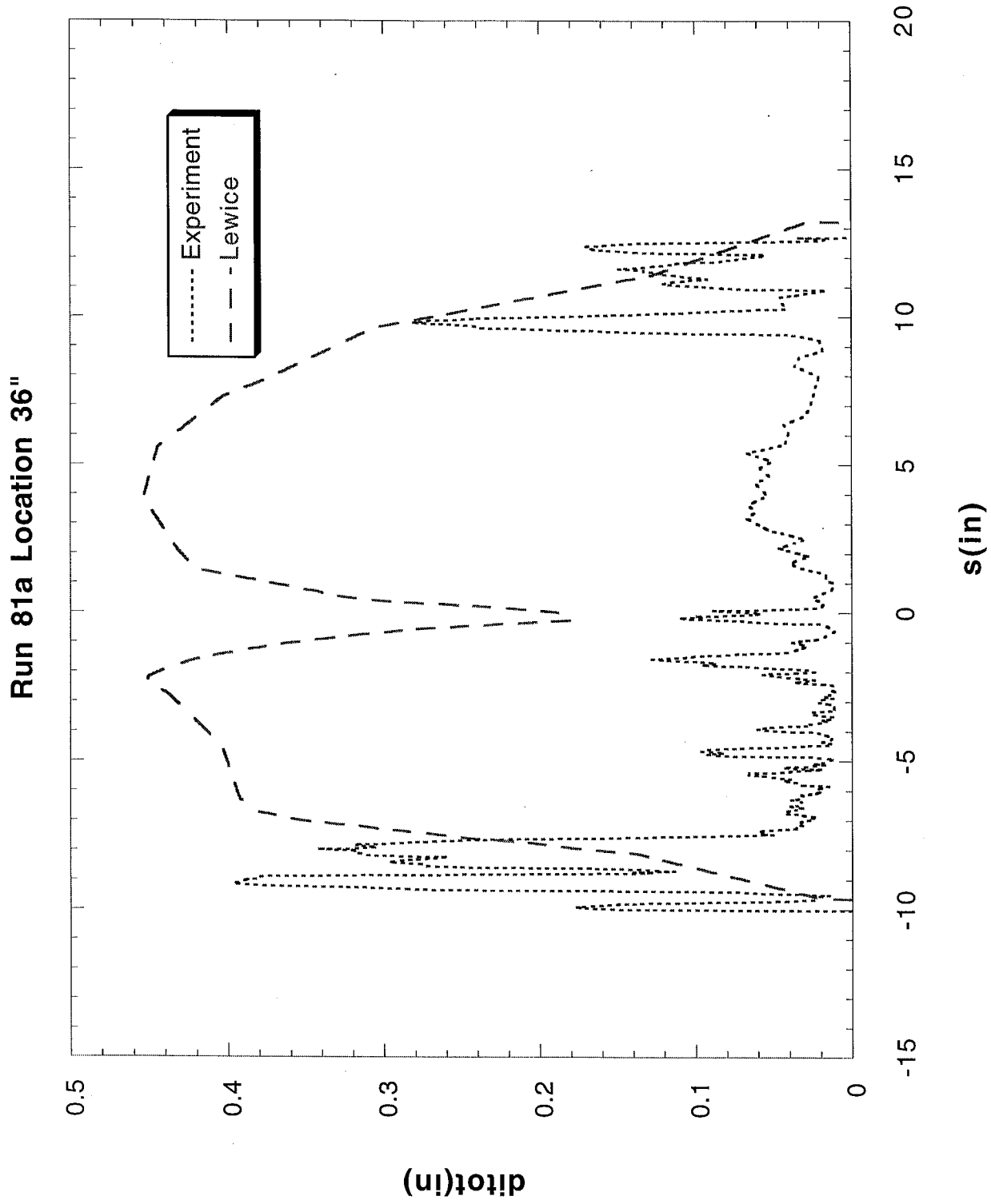
Run 81a Location 36"
Experiment
Lewice
dltot(in)
s(in)
0
0.1
0.2
0.3
0.4
0.5
-15
-10
-5
0
5
10
15
20

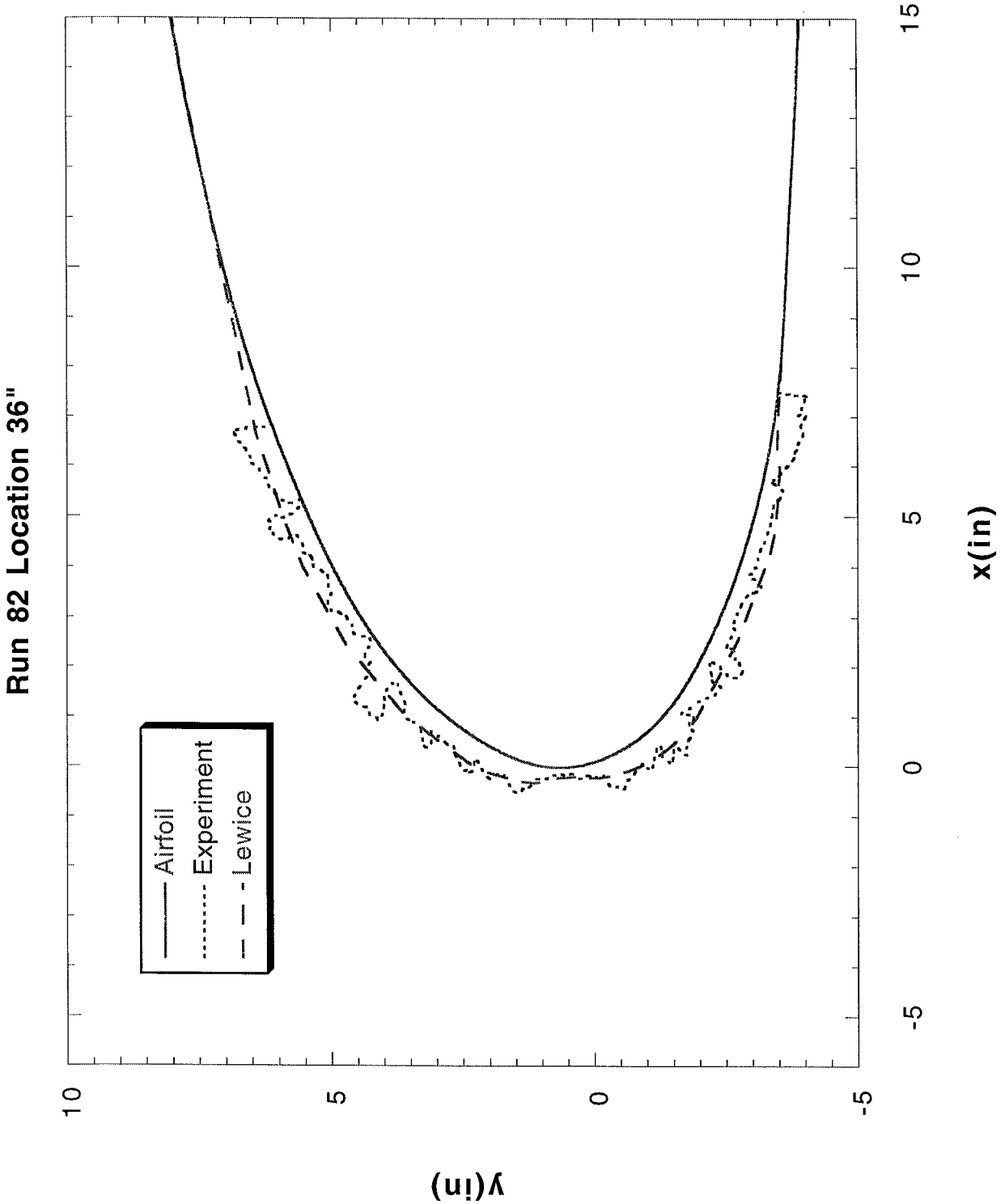
Run 82 Location 36"
Airfoil
Experiment
Lewice
y(in)
x(in)
10
5
0
-5
-5
0
5
10
15

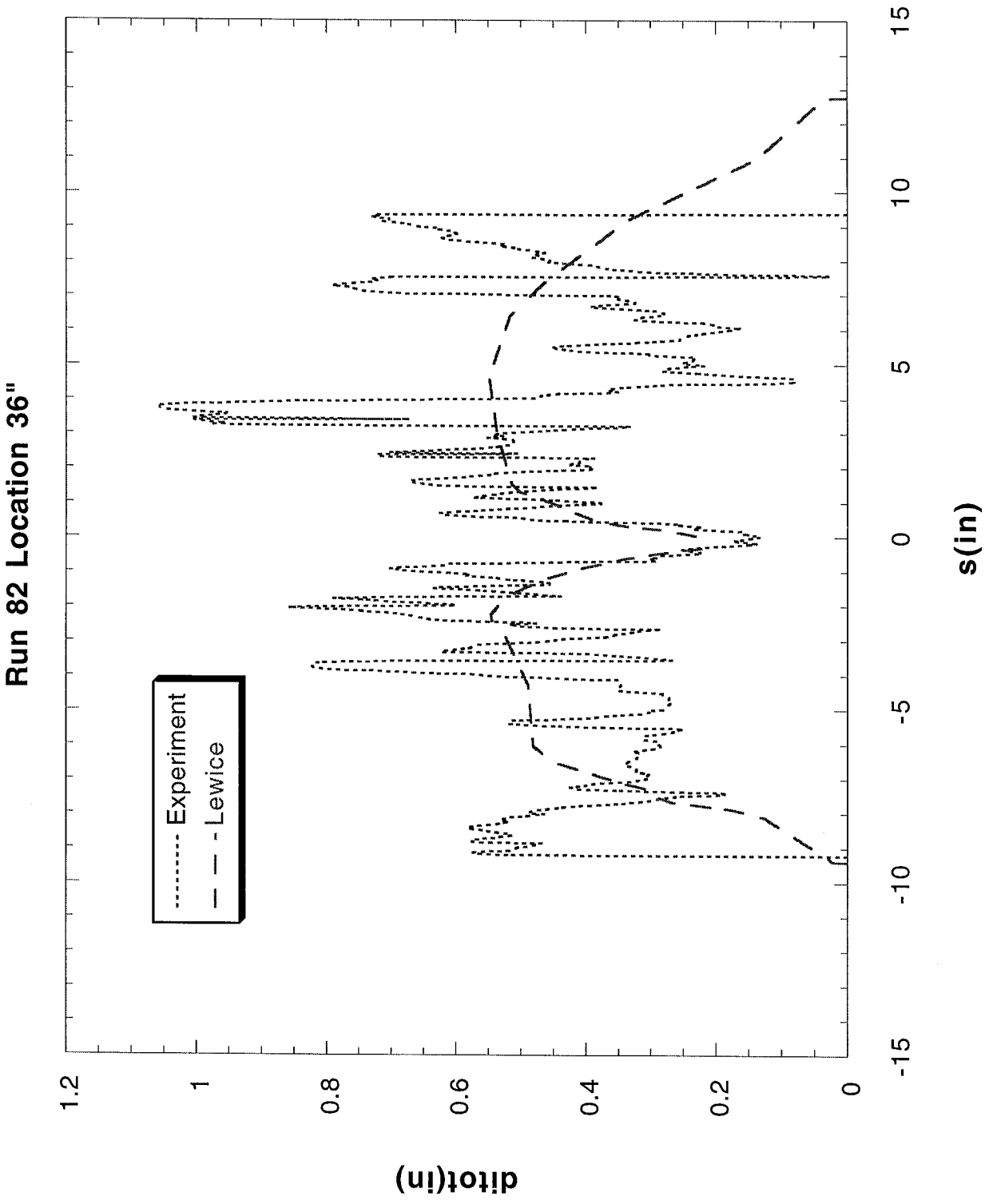
Run 82 Location 36"
Experiment
Lewice
ditot(in)
s(in)
1.2
1
0.8
0.6
0.4
0.2
0
-15
-10
-5
0
5
10
15

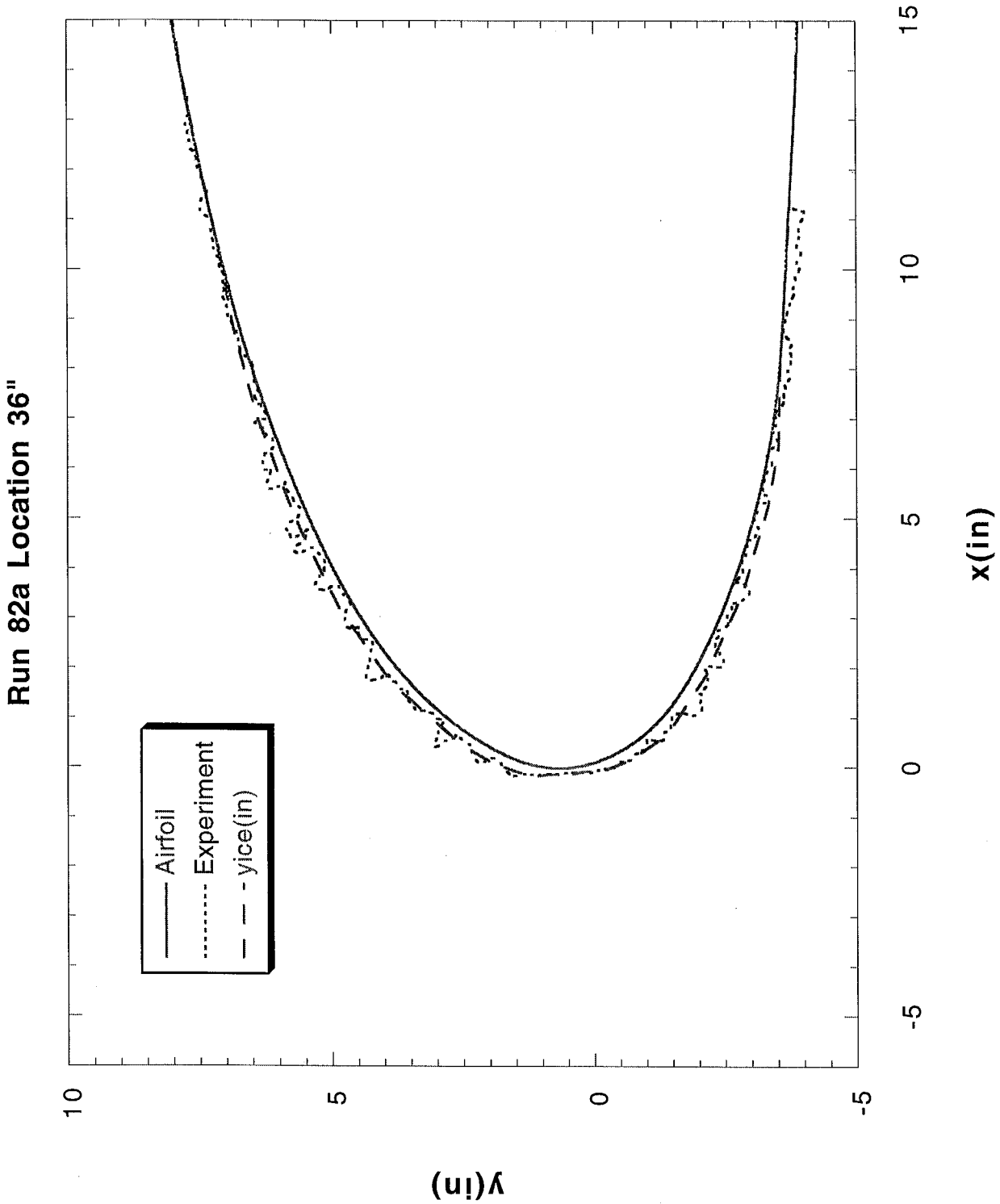
Run 82a Location 36"
Airfoil
Experiment
yice(in)
y(in)
x(in)
10
5
0
-5
-5
0
5
10
15

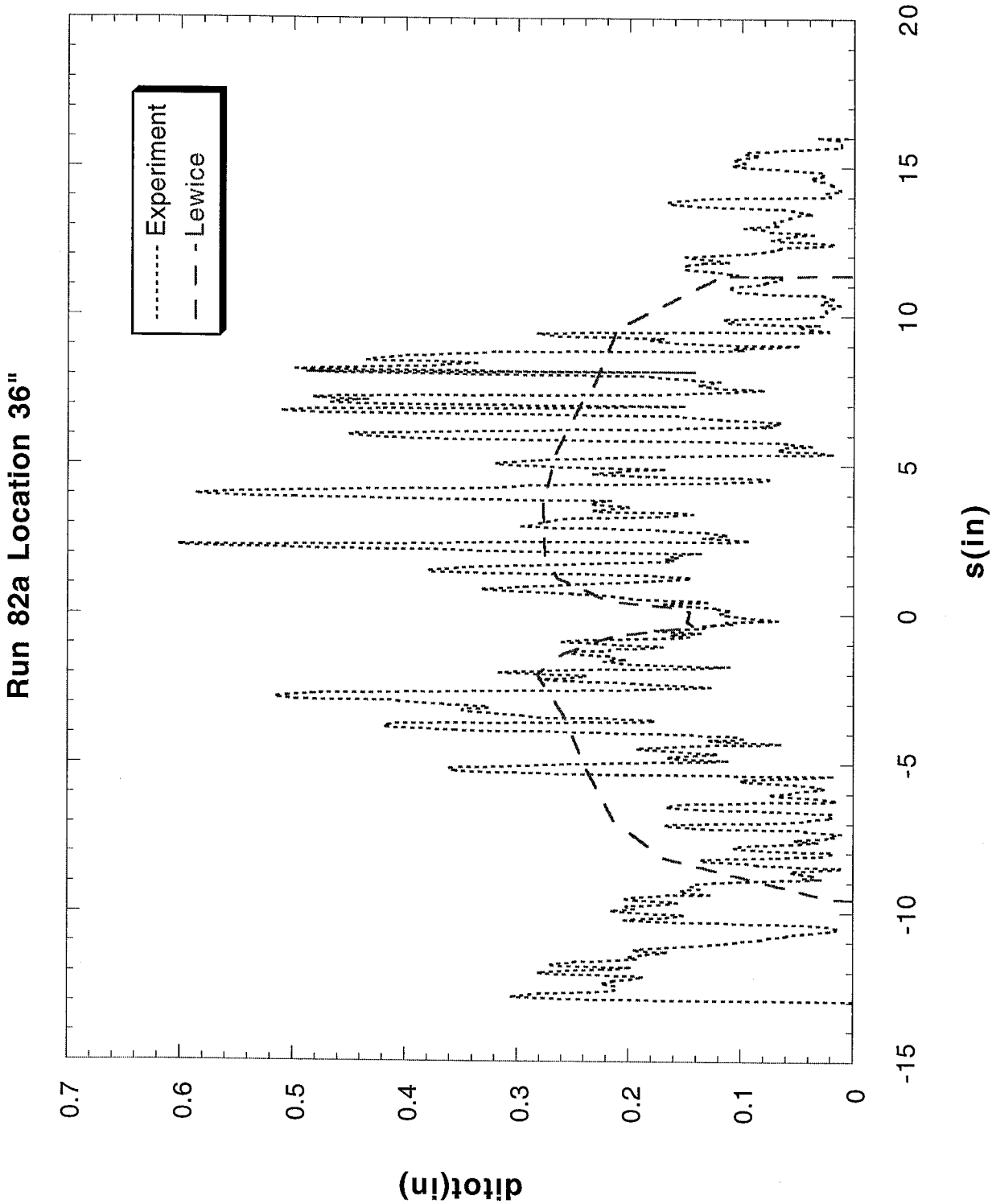
Run 82a Location 36"
Experiment
Lewice
dltot(in)
s(in)
0.7
0.6
0.5
0.4
0.3
0.2
0.1
0
-15
-10
-5
0
5
10
15
20

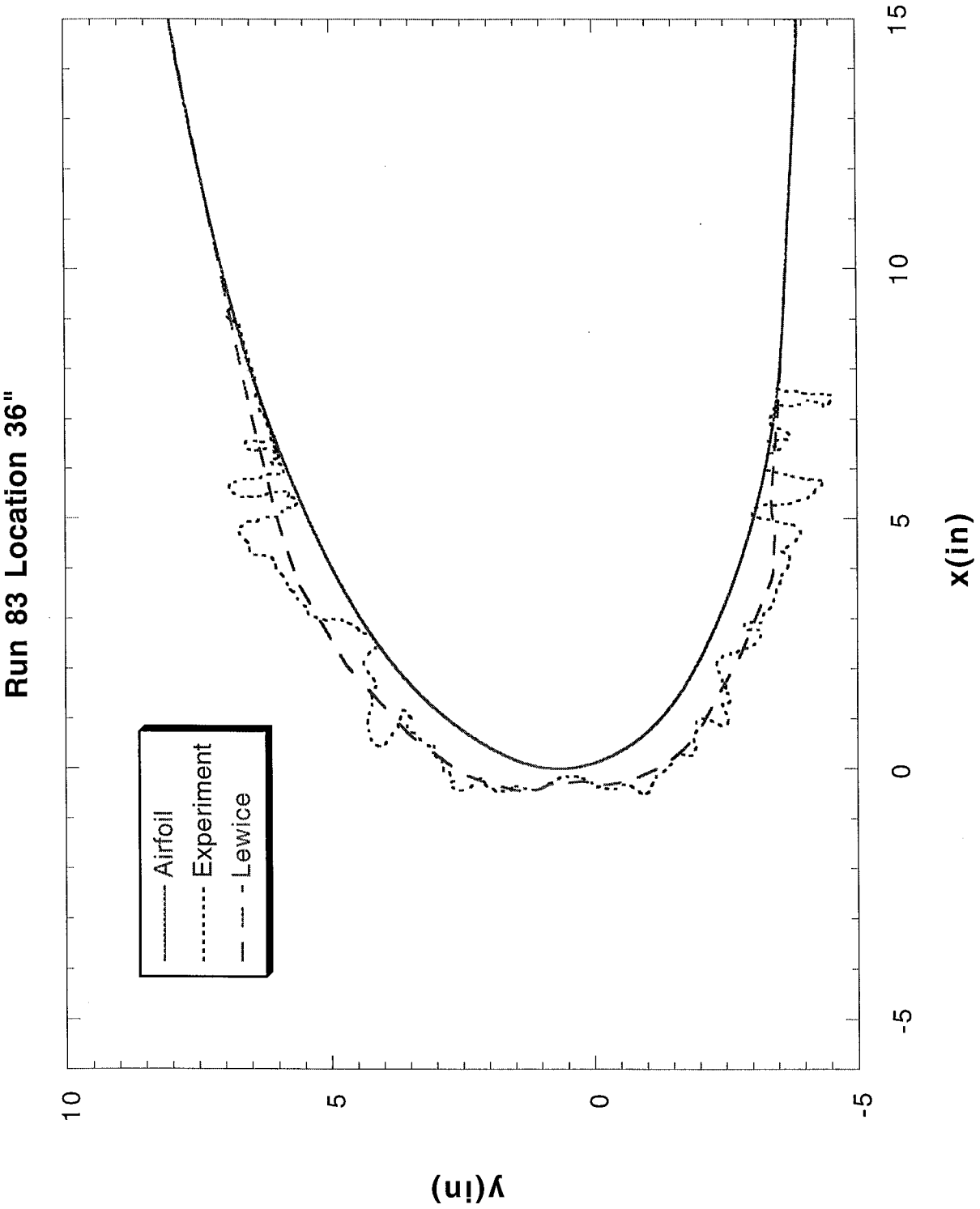
Run 83 Location 36"
Airfoil
Experiment
Lewice
y(in)
x(in)
10
5
0
-5
-5
0
5
10
15

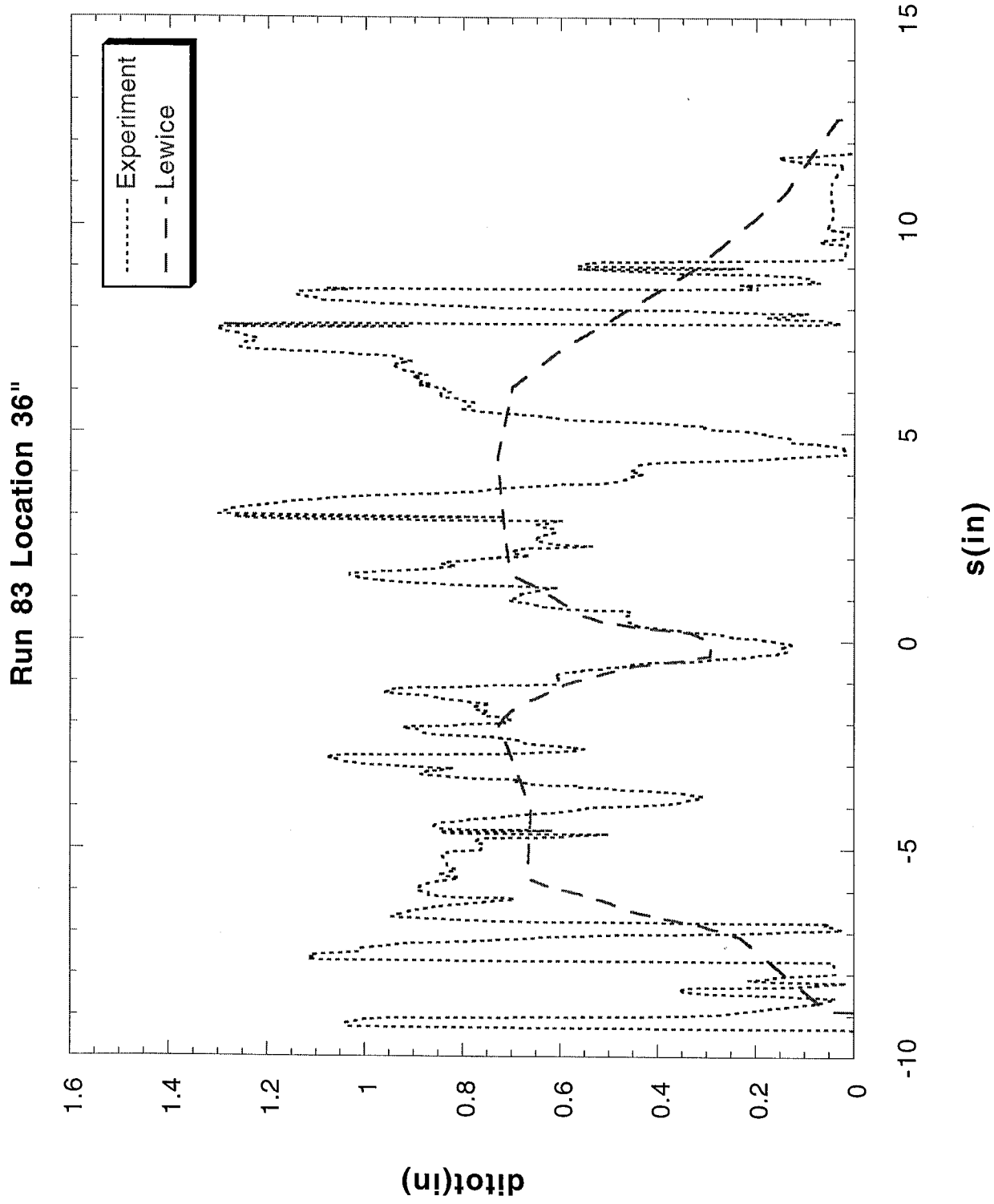
Run 83 Location 36"
Experiment
Lewice
dltot(in)
s(in)
1.6
1.4
1.2
1
0.8
0.6
0.4
0.2
0
-10
-5
0
5
10
15

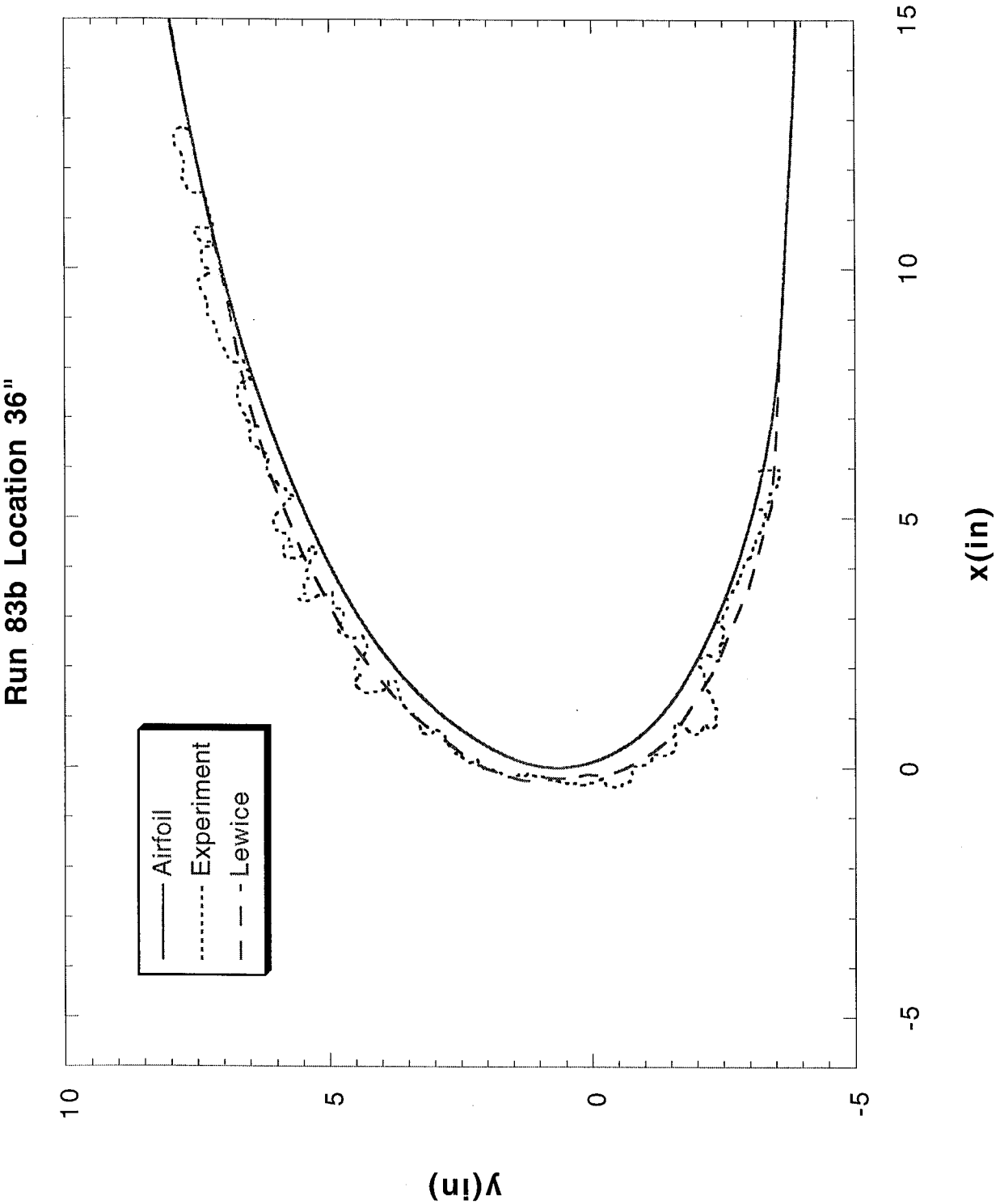
Run 83b Location 36"
Airfoil
Experiment
Lewice
y(in)
x(in)
10
5
0
-5
-5
0
5
10
15

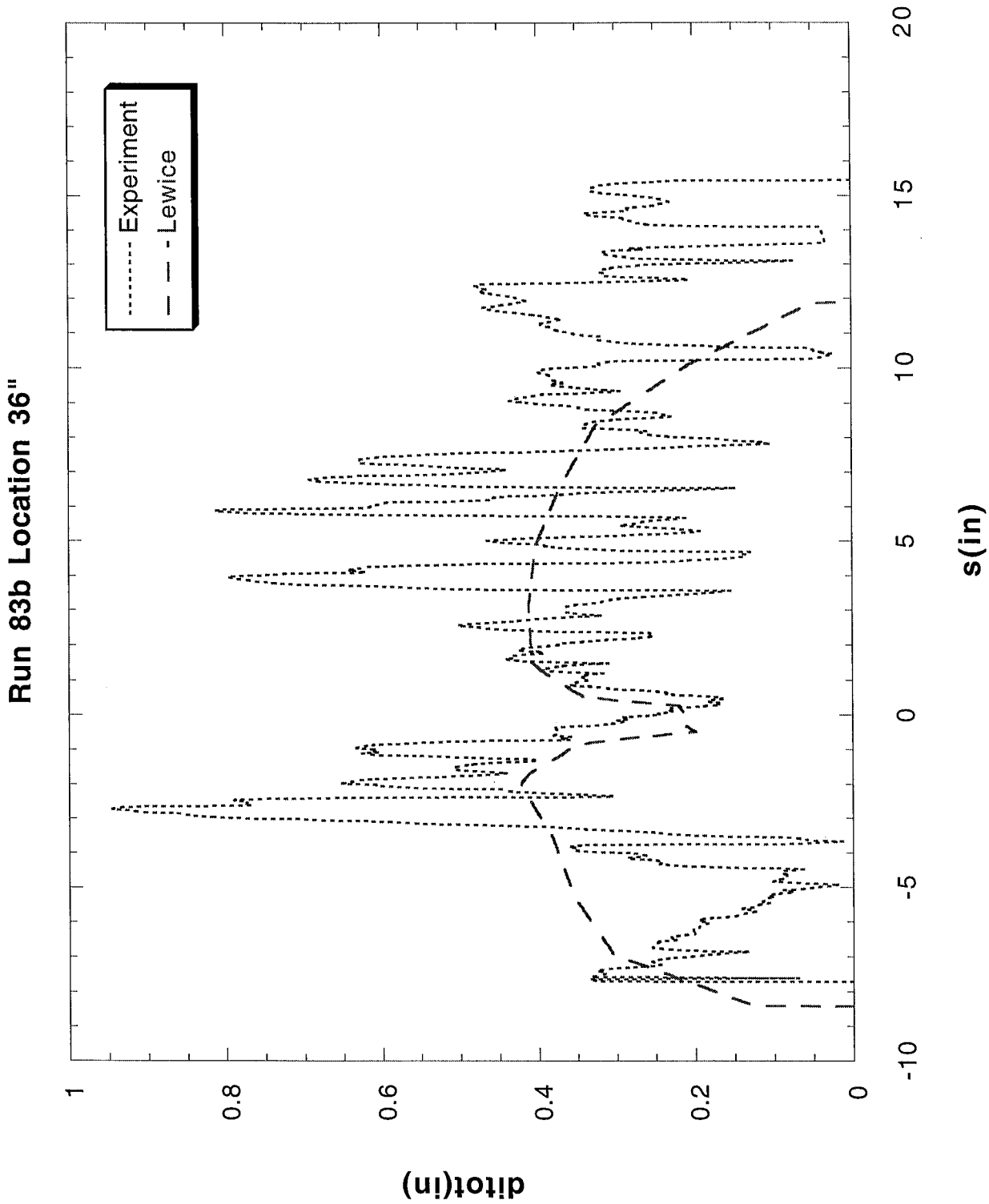
Run 83b Location 36"
Experiment
Lewice
dltot(in)
s(in)
1
0.8
0.6
0.4
0.2
0
-10
-5
0
5
10
15
20

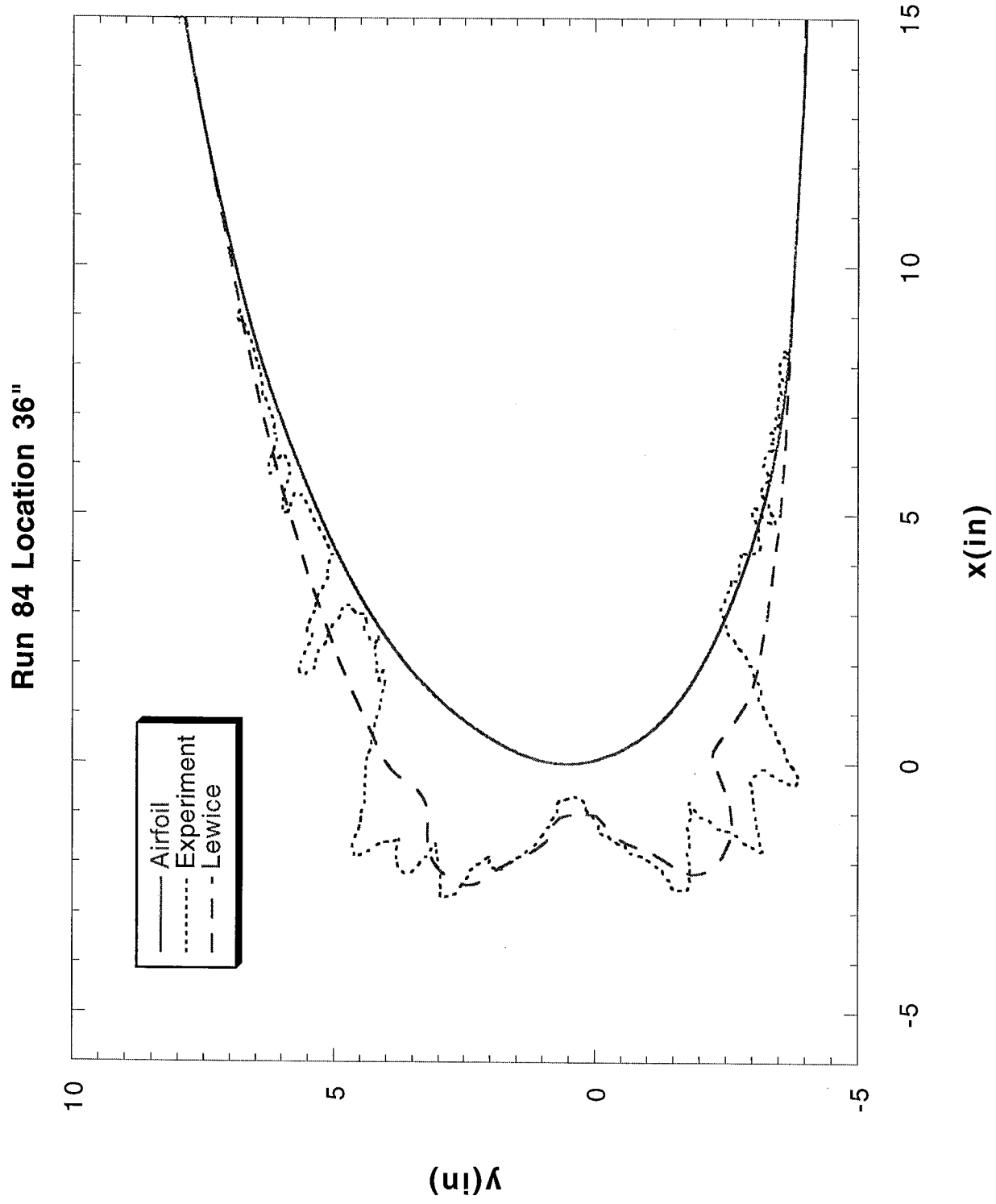
Run 84 Location 36"
Airfoil
Experiment
Lewice
y(in)
x(in)
10
5
0
-5
-5
0
5
10
15

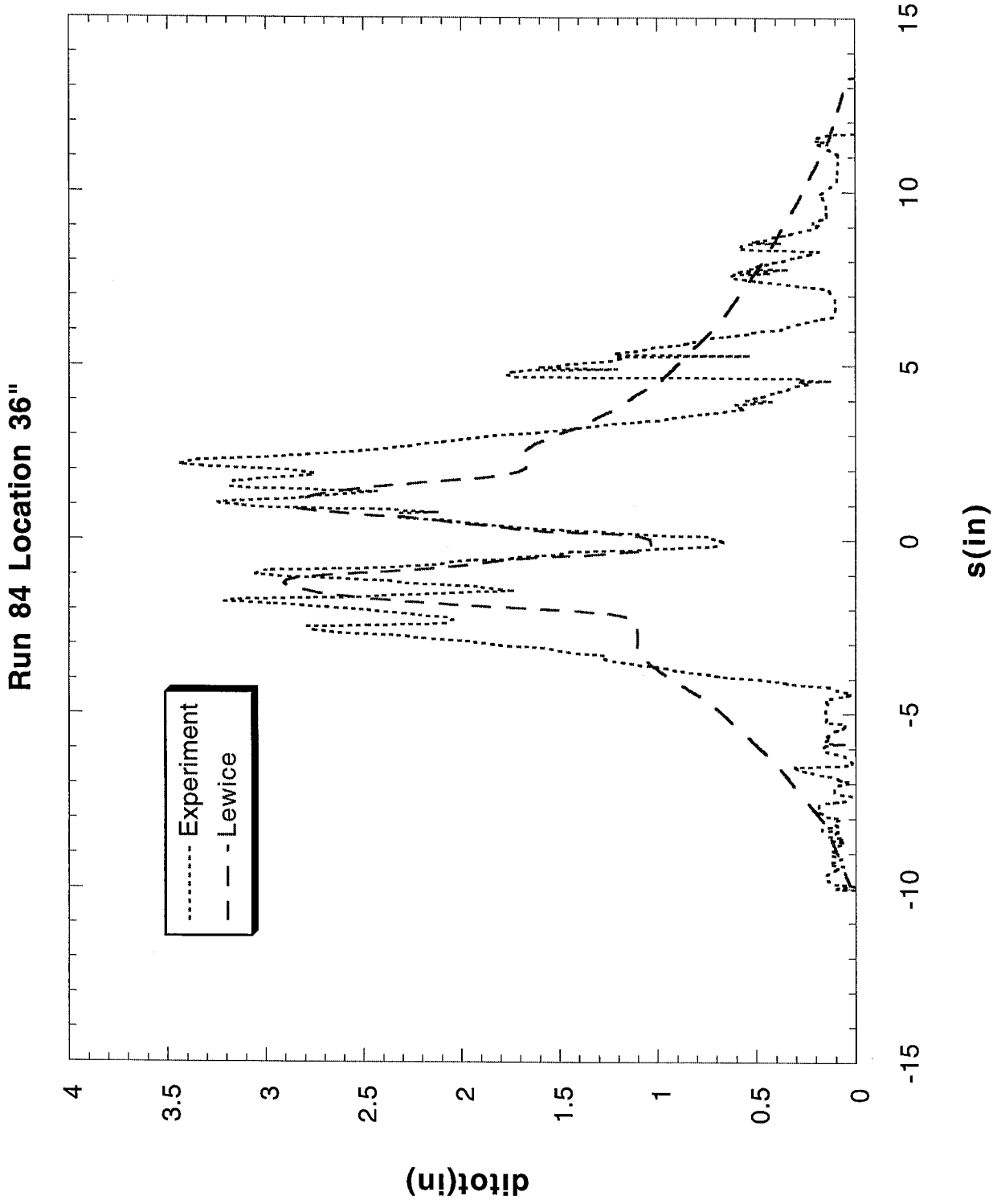
Run 84 Location 36"
Experiment
Lewice
ditot(in)
s(in)
4
3.5
3
2.5
2
1.5
1
0.5
0
15
10
5
0
-5
-10
-15

NLF 414
Figures 484 – 499

NLF 414 Test Conditions

Principal Investigator	Airfoil	Test Date	Chord (in)	Run Number	Previous Identical Run	Velocity (kts)	Velocity (m/s)	Tt (°F)	Static Temperature (K)	A.O.A.	Corrected A.O.A.	LWC (g/m^3)	MVD (microns)	Spray Time (min)	Digitized Tracing Locations
Addy	NLF 414	1998	36"	602		180	92.6	30	267.48	0	0	0.54	20	6	36"
Addy	NLF 414	1998	36"	607		180	92.6	21	262.48	0	0	0.43	20	6	36"
Addy	NLF 414	1998	36"	621		130	66.9	26	267.30	2	2	0.54	20	2	36"
Addy	NLF 414	1998	36"	622		130	66.9	26	267.30	2	2	0.54	20	6	36"
Addy	NLF 414	1998	36"	623		130	66.9	26	267.30	2	2	0.54	20	22.5	36"
Addy	NLF 414	1998	36"	627		130	66.9	17	262.30	2	2	0.44	20	5.9	36"
Addy	NLF 414	1998	36"	633		130	66.9	17	262.30	2	2	0.60	15	6	36"
Addy	NLF 414	1998	36"	645		130	66.9	17	262.30	4	3.5	0.44	20	5.9	36"

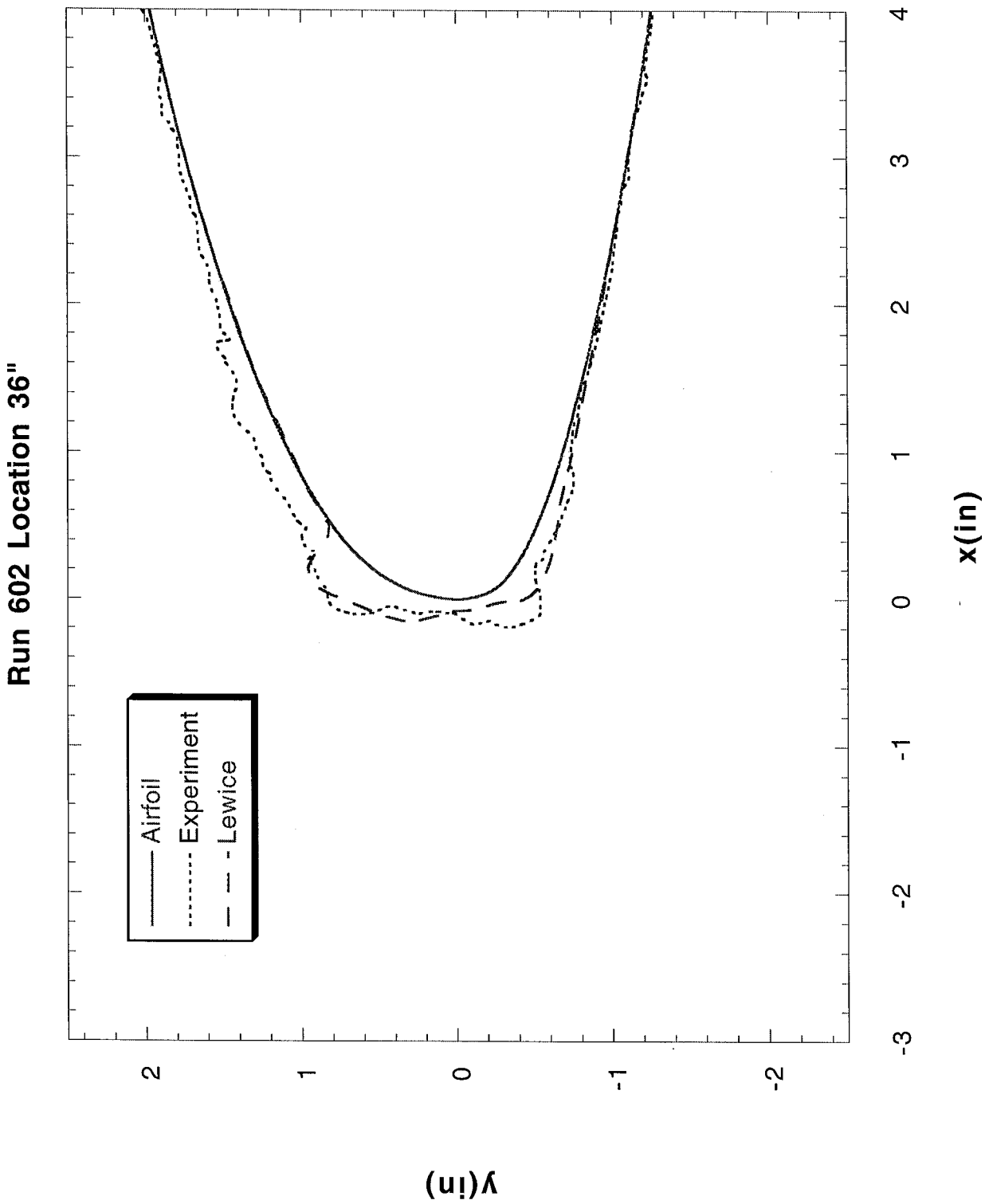
Run 602 Location 36"
Airfoil
Experiment
Lewice
y(in)
x(in)
2
1
0
-1
-2
-3
-2
-1
0
1
2
3
4

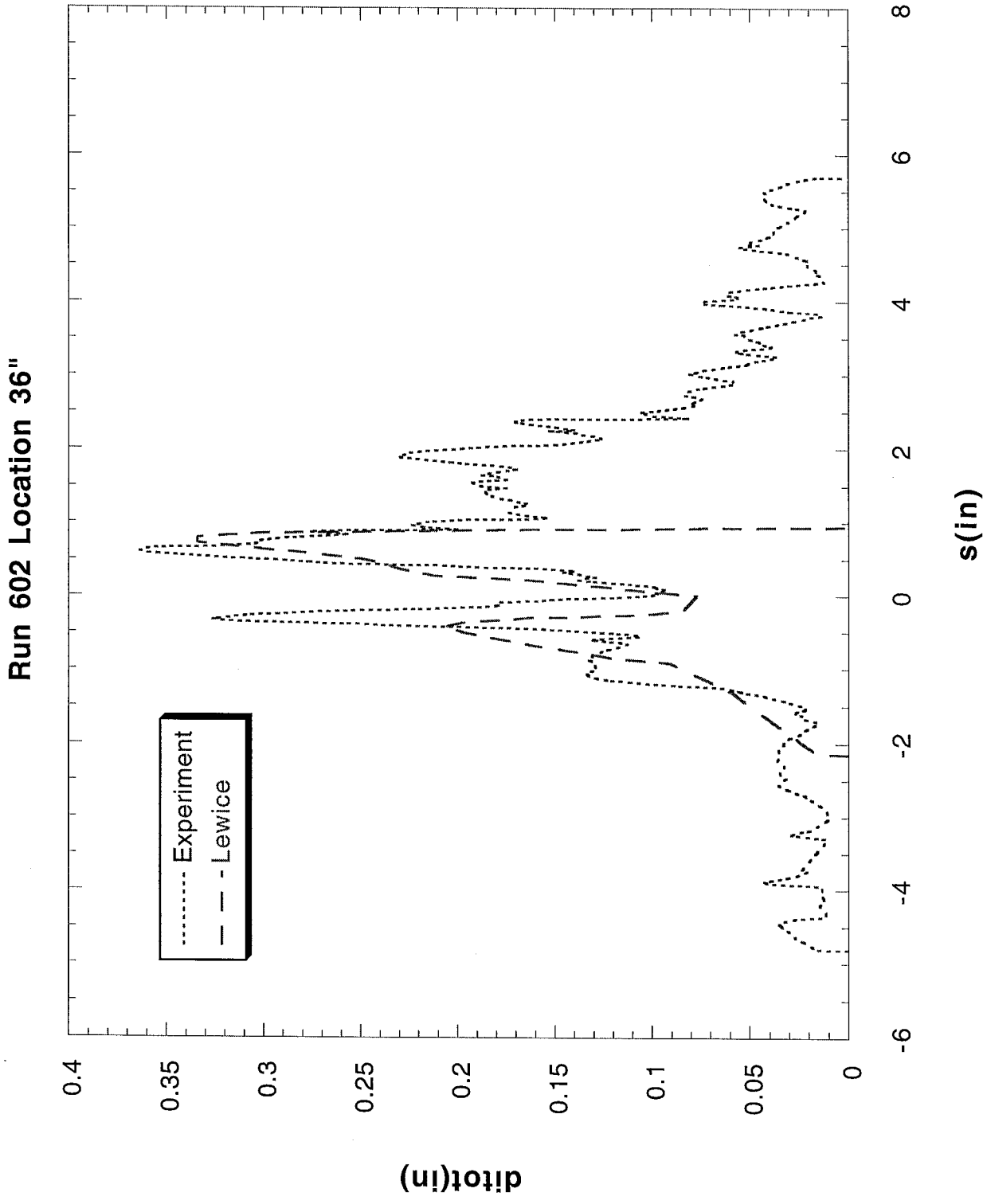
Run 602 Location 36"
Experiment
Lewice
dltot(in)
s(in)
0.4
0.35
0.3
0.25
0.2
0.15
0.1
0.05
0
-6
-4
-2
0
2
4
6
8

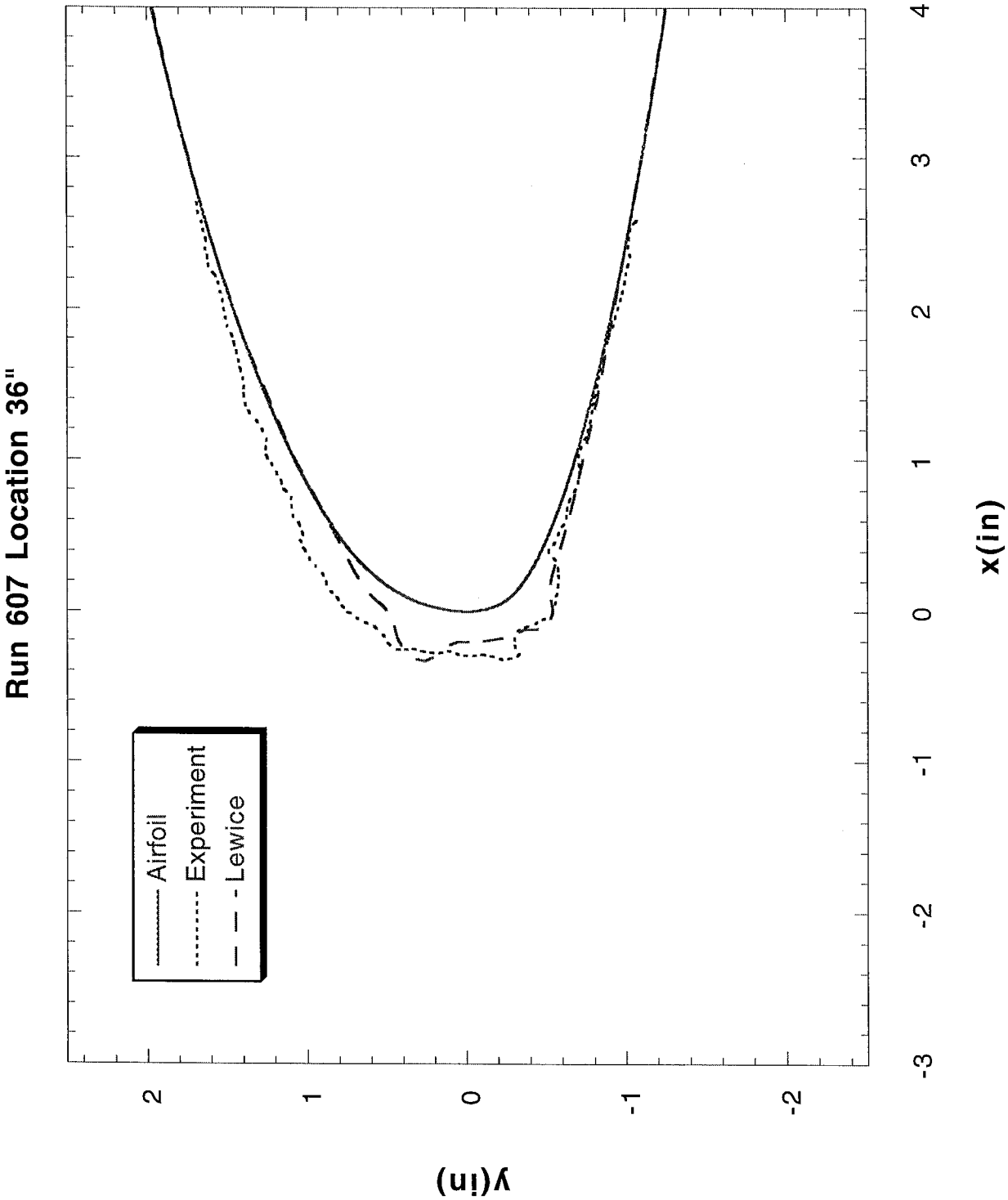
Run 607 Location 36"
Airfoil
Experiment
Lewice
y(in)
x(in)
2
1
0
-1
-2
-3
-2
-1
0
1
2
3
4

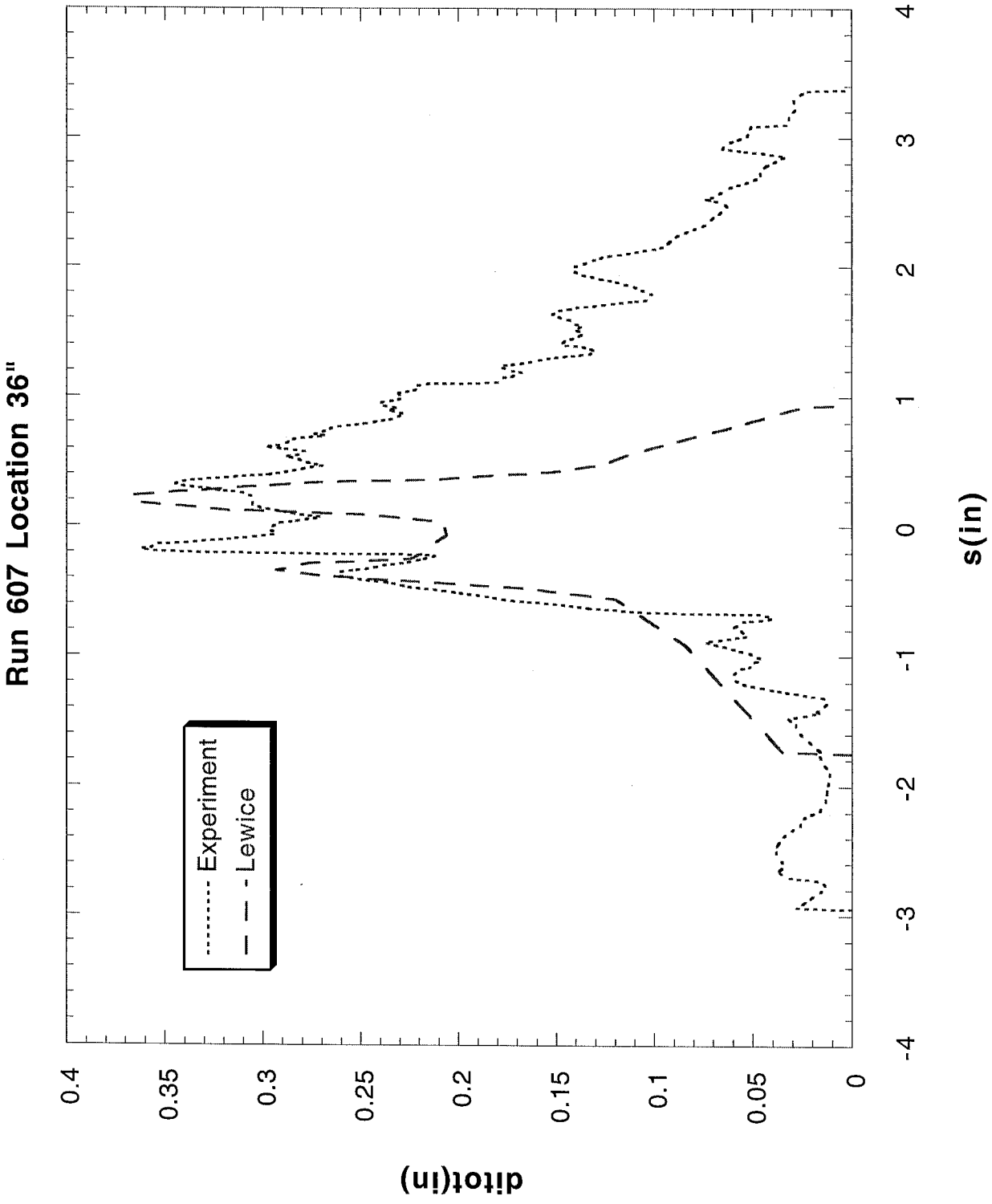
Run 607 Location 36"
Experiment
Lewice
dltot(in)
s(in)
0.4
0.35
0.3
0.25
0.2
0.15
0.1
0.05
0
-4
-3
-2
-1
0
1
2
3
4

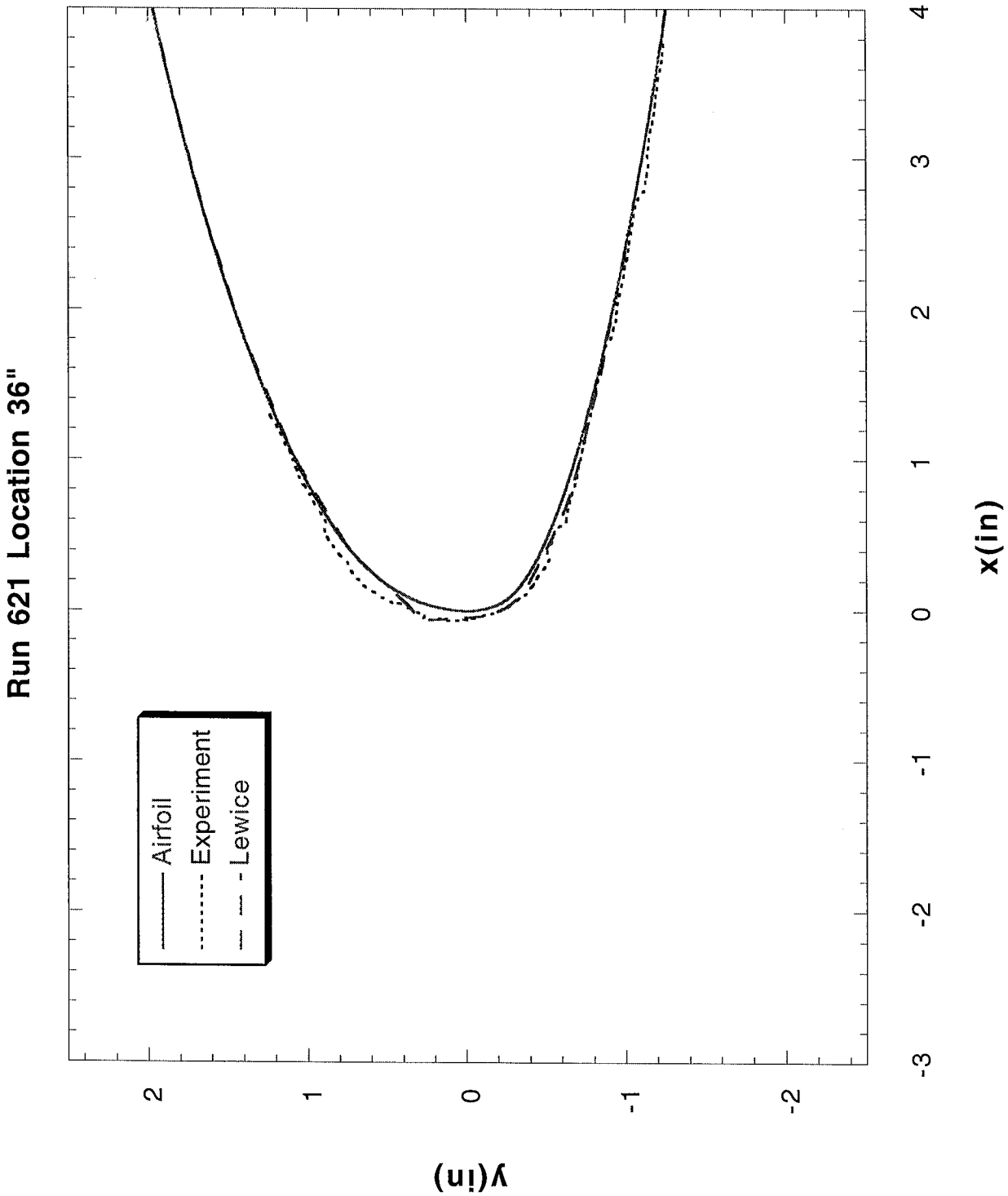
Run 621 Location 36"
Airfoil
Experiment
Lewice
y(in)
x(in)
2
1
0
-1
-2
-3
-2
-1
0
1
2
3
4

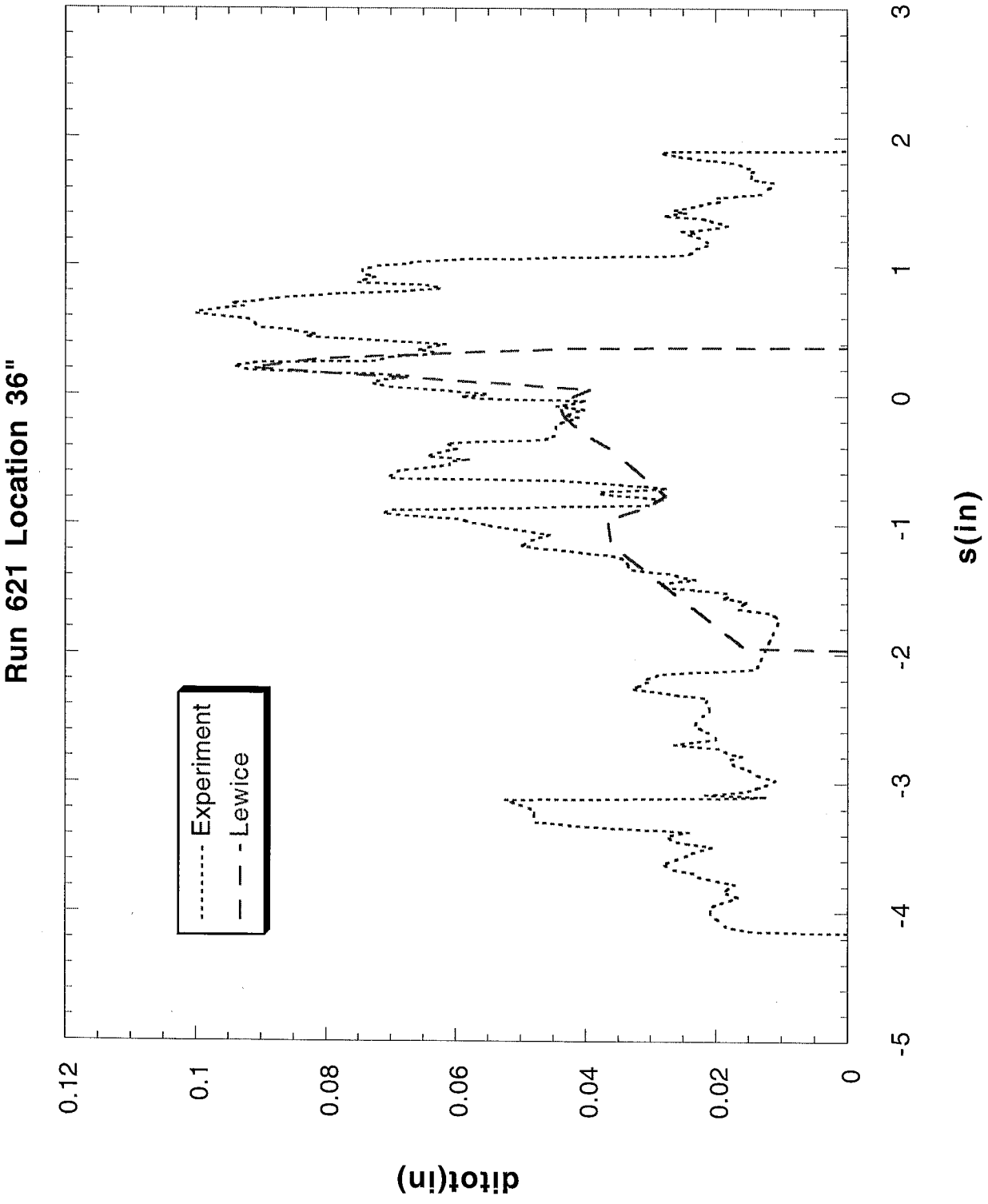
Run 621 Location 36"
Experiment
Lewice
dltot(in)
s(in)
0.12
0.1
0.08
0.06
0.04
0.02
0
-5
-4
-3
-2
-1
0
1
2
3

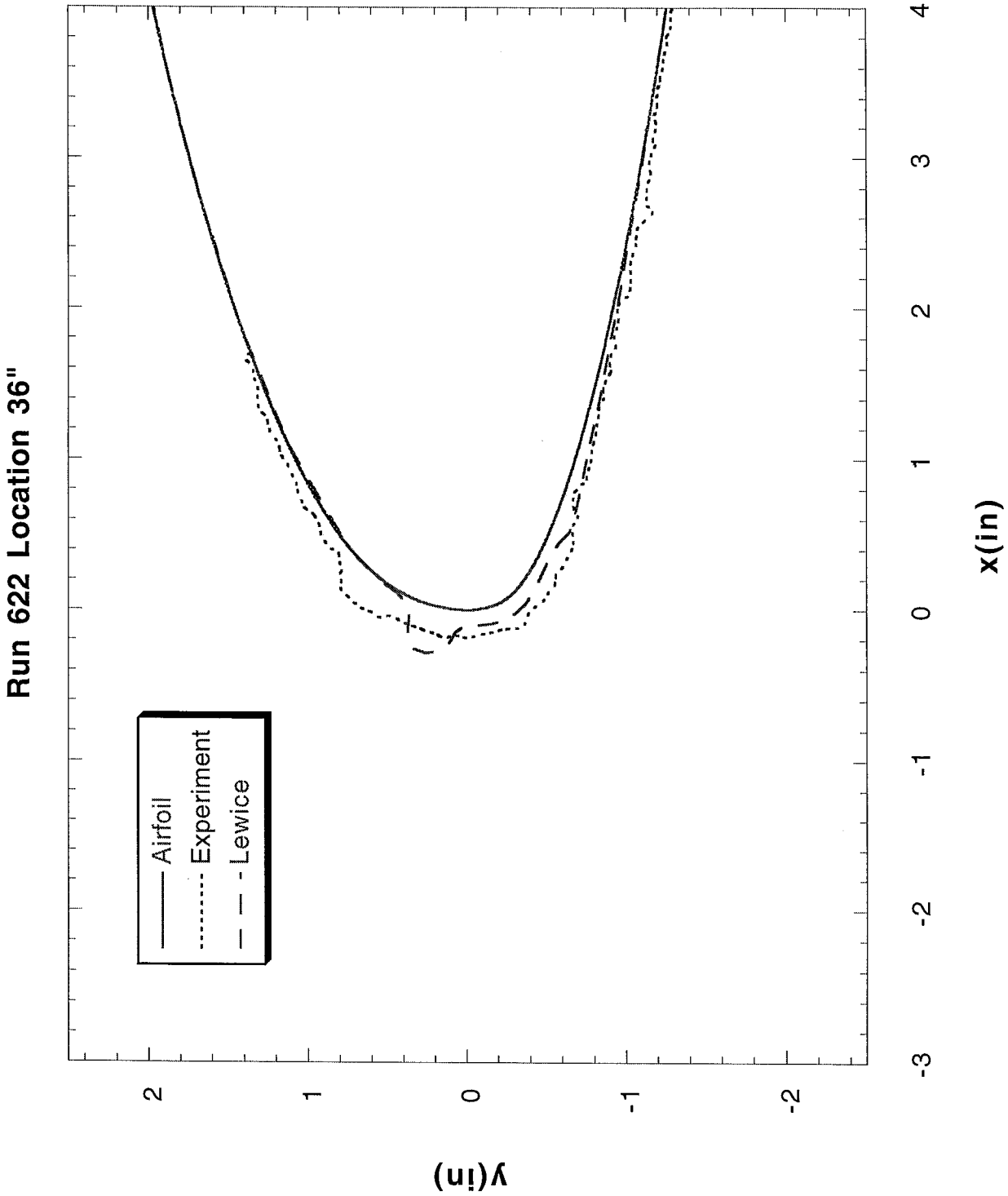
Run 622 Location 36"
Airfoil
Experiment
Lewice
y(in)
x(in)
2
1
0
-1
-2
-3
-2
-1
0
1
2
3
4

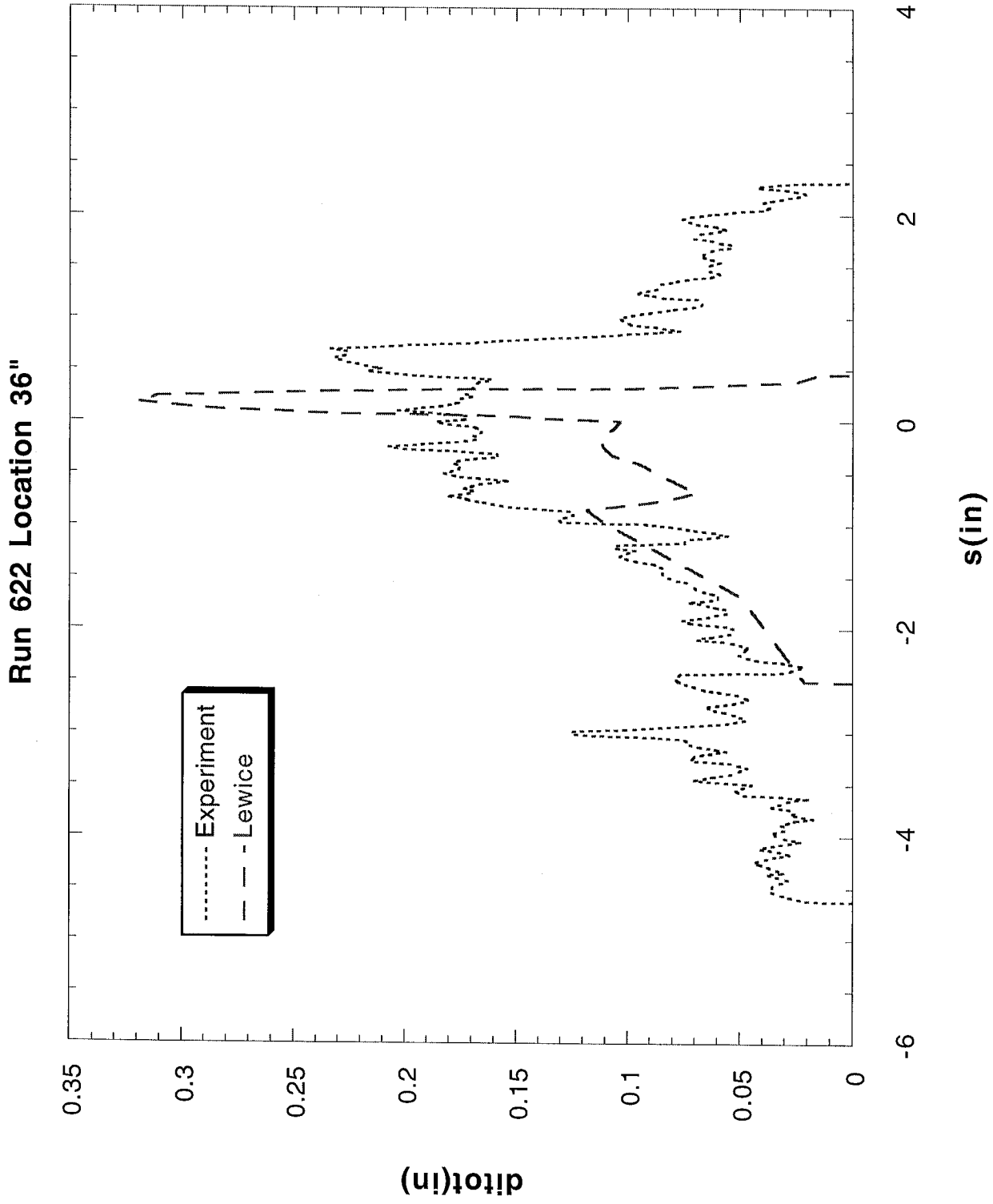
Run 622 Location 36"
Experiment
Lewice
dltot(in)
s(in)
0.35
0.3
0.25
0.2
0.15
0.1
0.05
0
4
2
0
-2
-4
-6

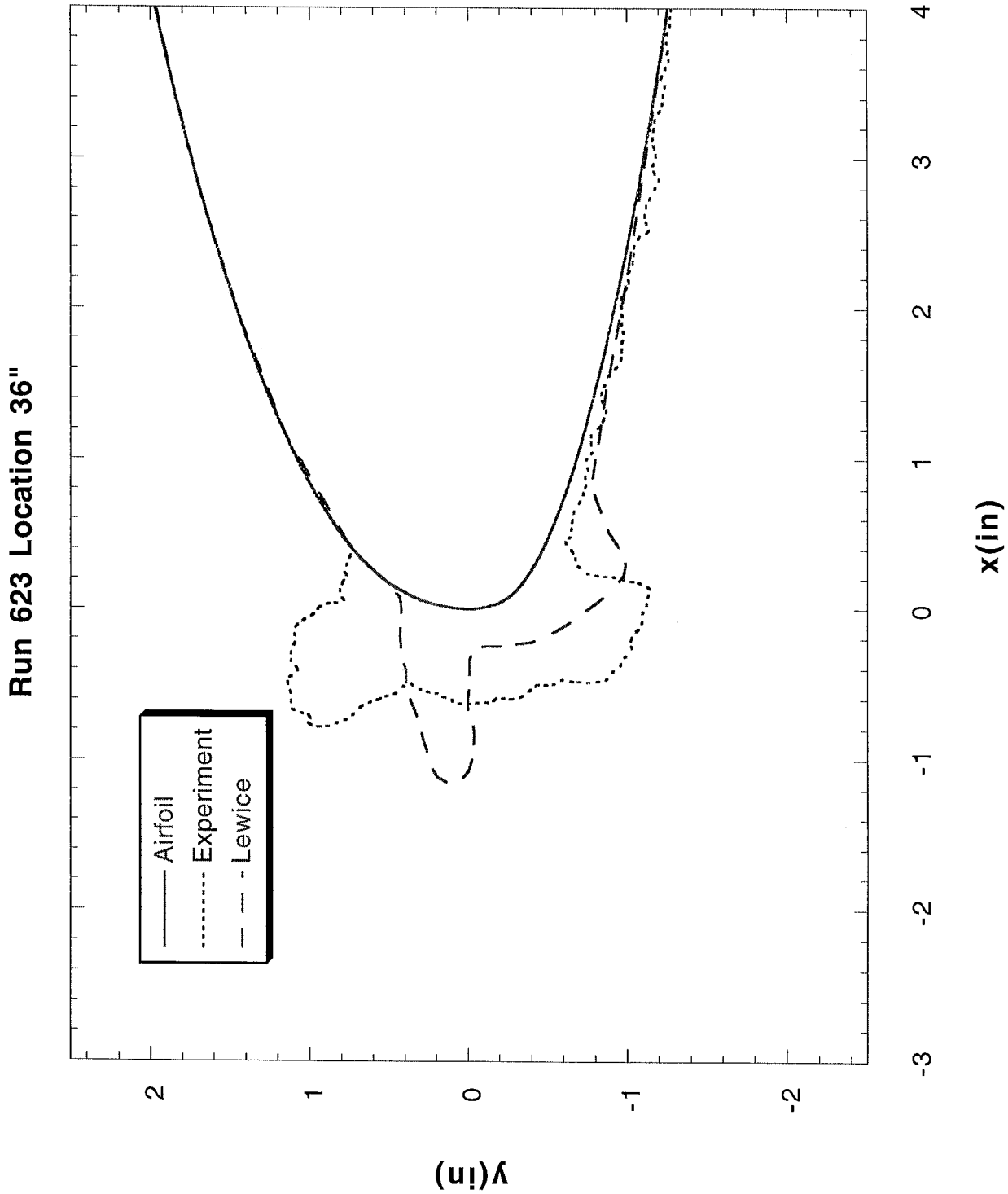
Run 623 Location 36"
Airfoil
Experiment
Lewice
y(in)
x(in)
2
1
0
-1
-2
-3
-2
-1
0
1
2
3
4

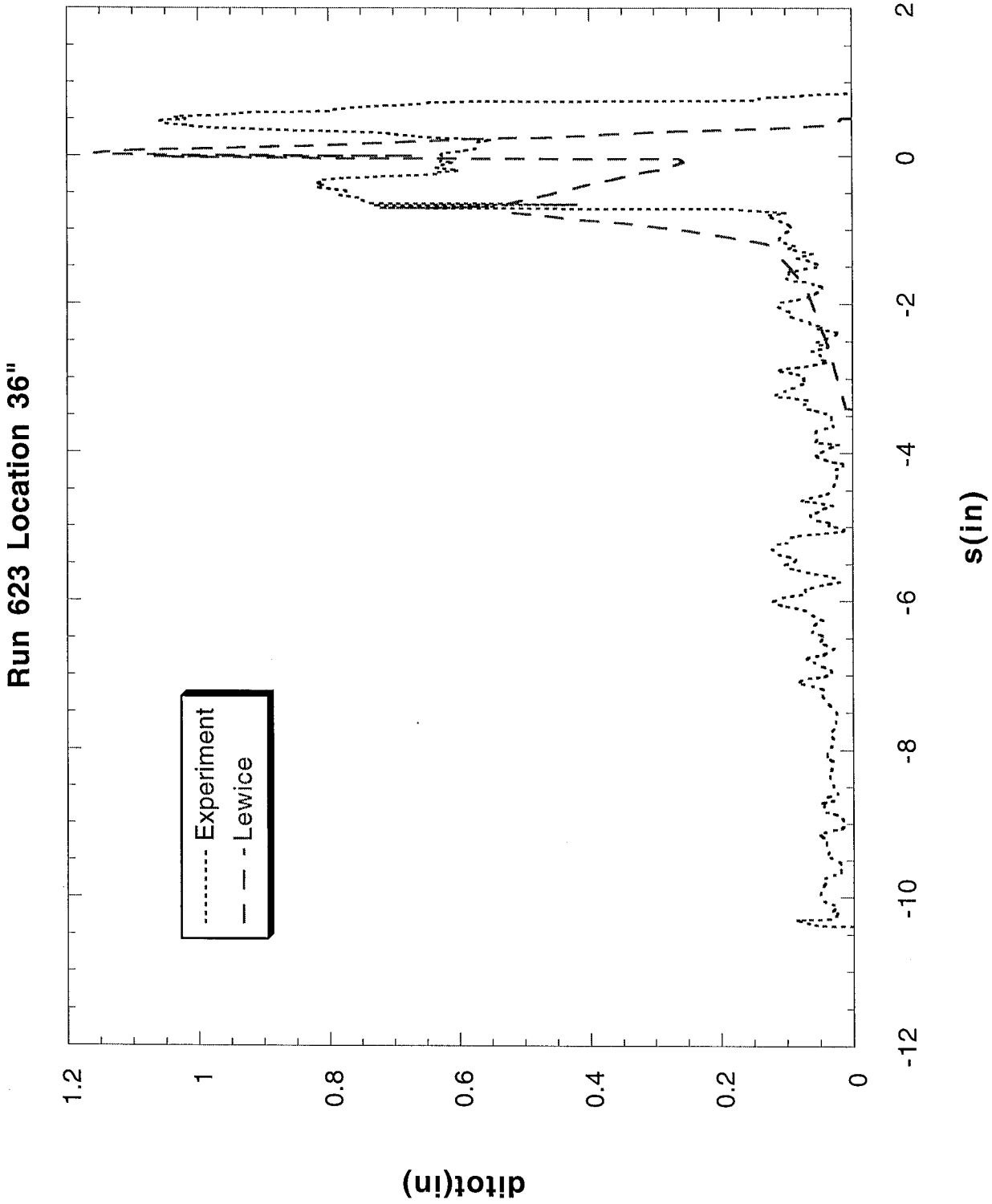
Run 623 Location 36"
Experiment
Lewice
ditot(in)
s(in)
1.2
1
0.8
0.6
0.4
0.2
0
2
0
-2
-4
-6
-8
-10
-12

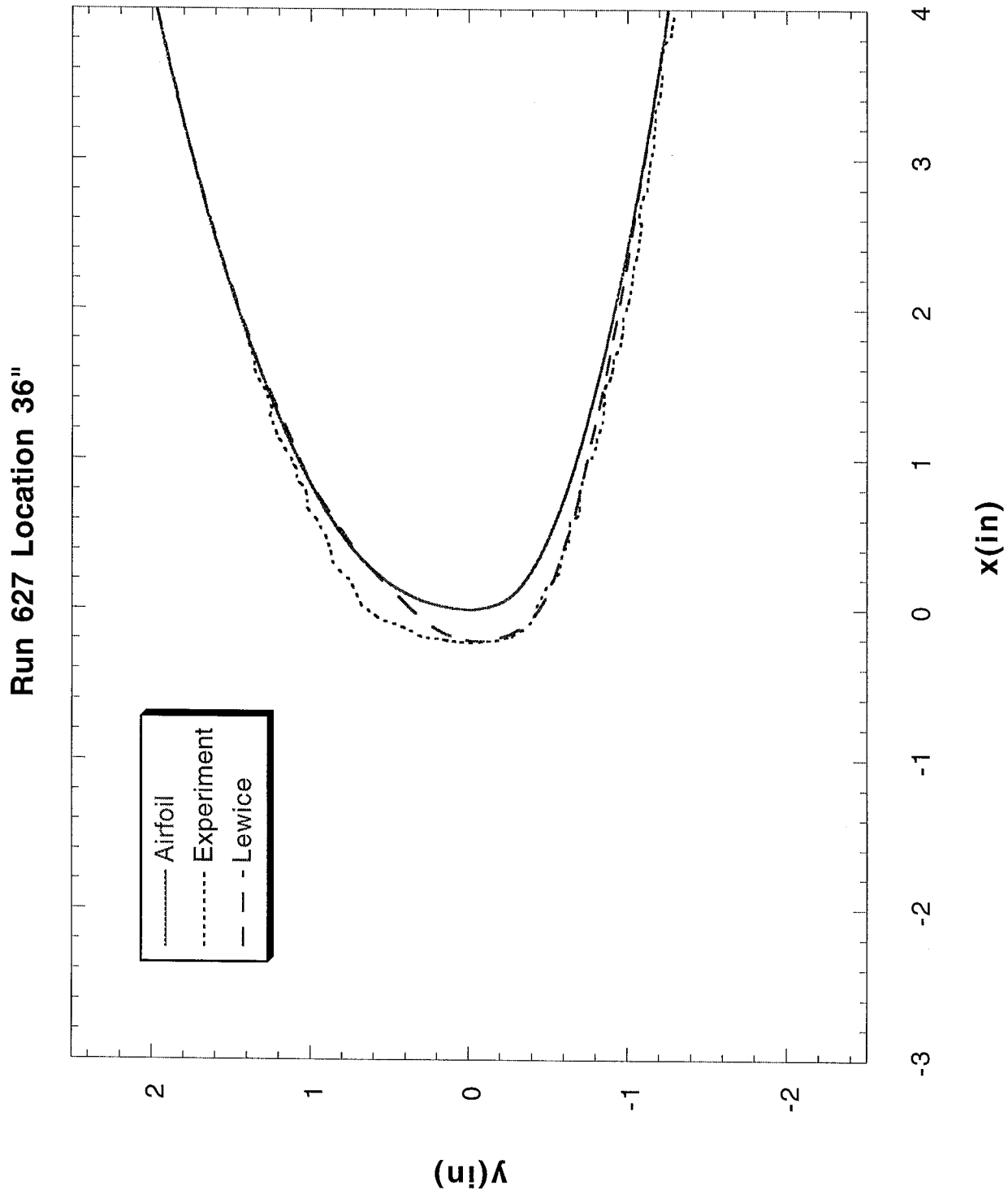
Run 627 Location 36"
Airfoil
Experiment
Lewice
y(in)
x(in)
2
1
0
-1
-2
-3
-2
-1
0
1
2
3
4

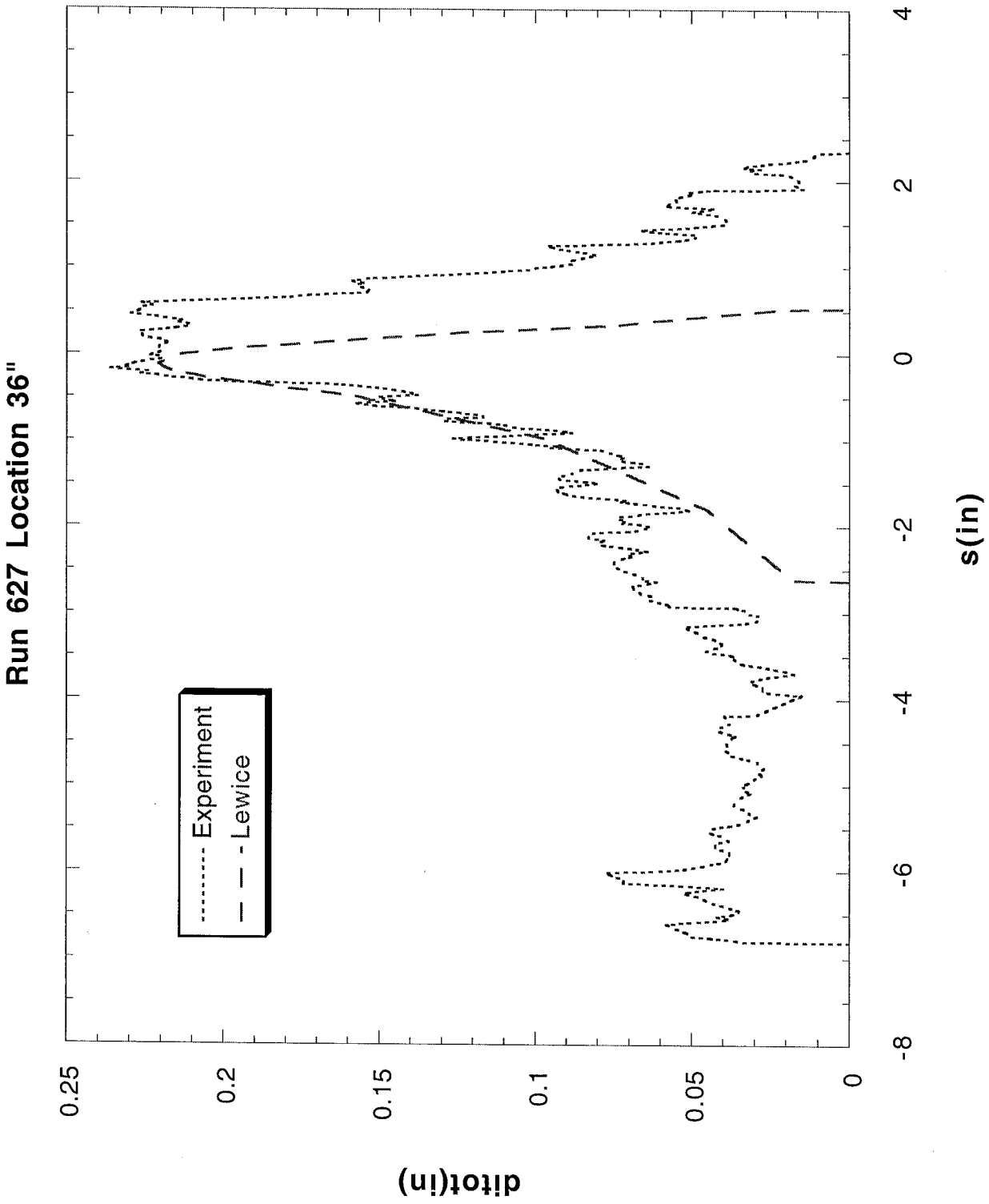
Run 627 Location 36"
Experiment
Lewice
dltot(in)
s(in)
0.25
0.2
0.15
0.1
0.05
0
-8
-6
-4
-2
0
2
4

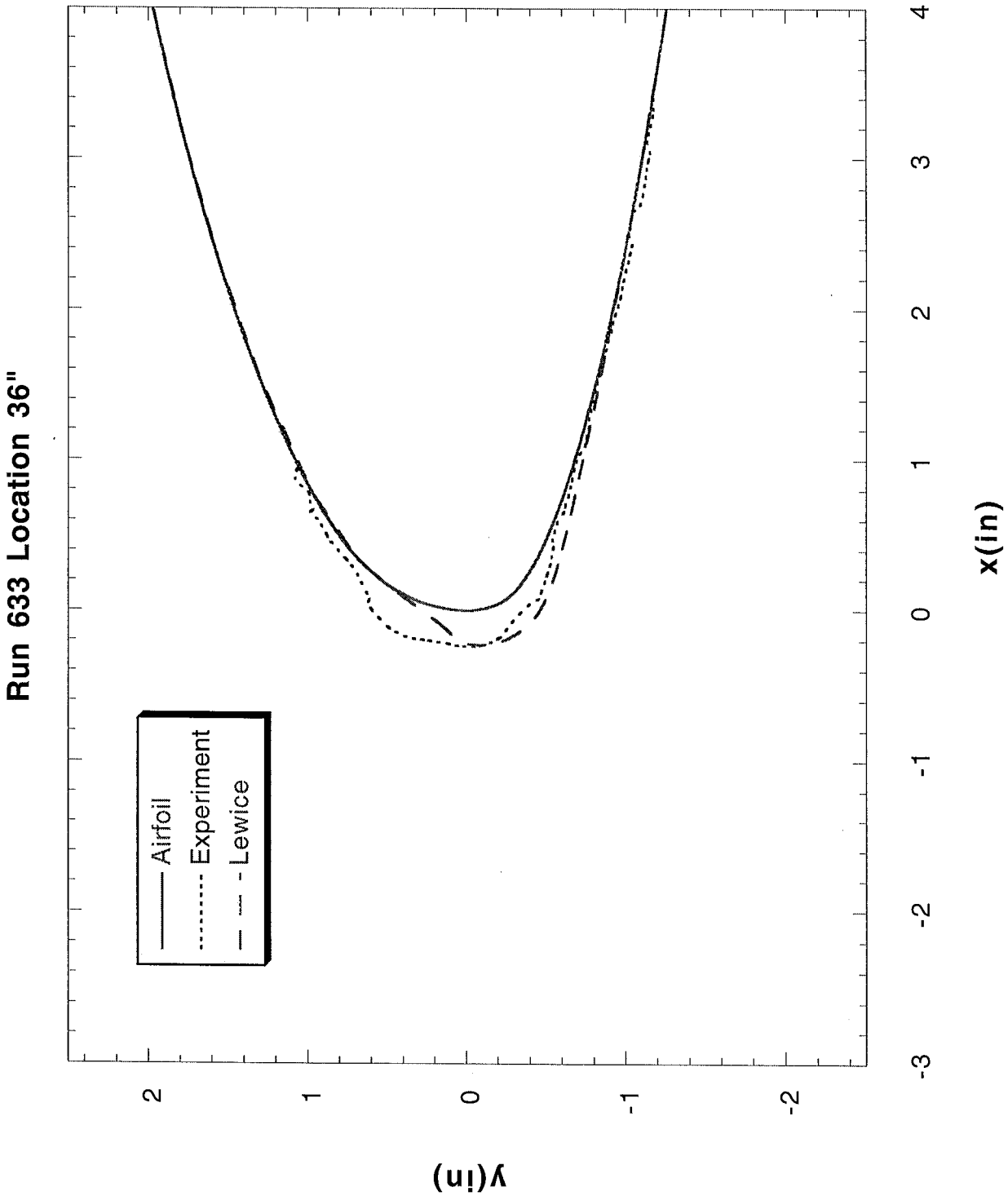
Run 633 Location 36"
Airfoil
Experiment
Lewice
y(in)
x(in)
2
1
0
-1
-2
-3
-2
-1
0
1
2
3
4

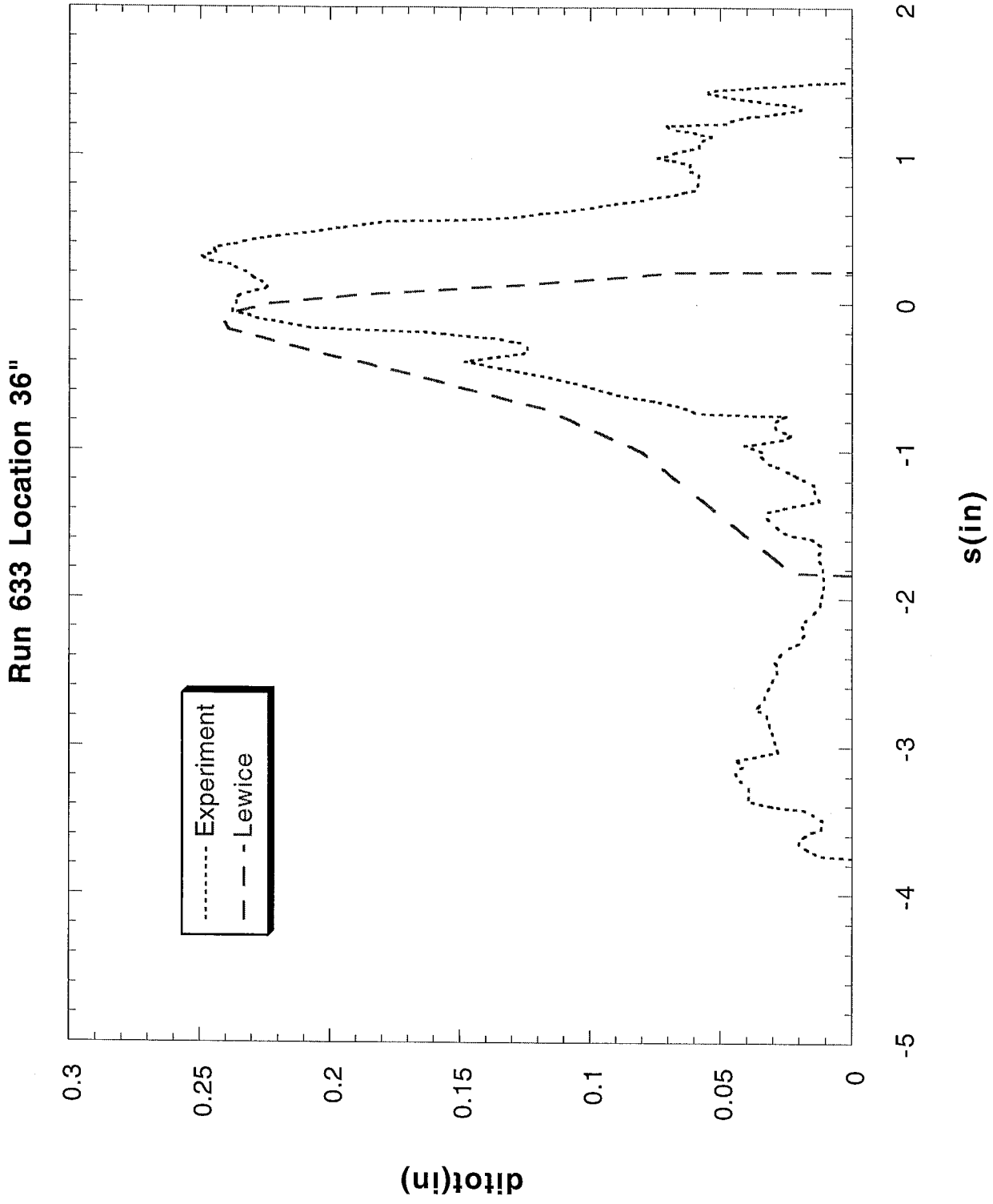
Run 633 Location 36"
Experiment
Lewice
dltot(in)
s(in)
0.3
0.25
0.2
0.15
0.1
0.05
0
-5
-4
-3
-2
-1
0
1
2

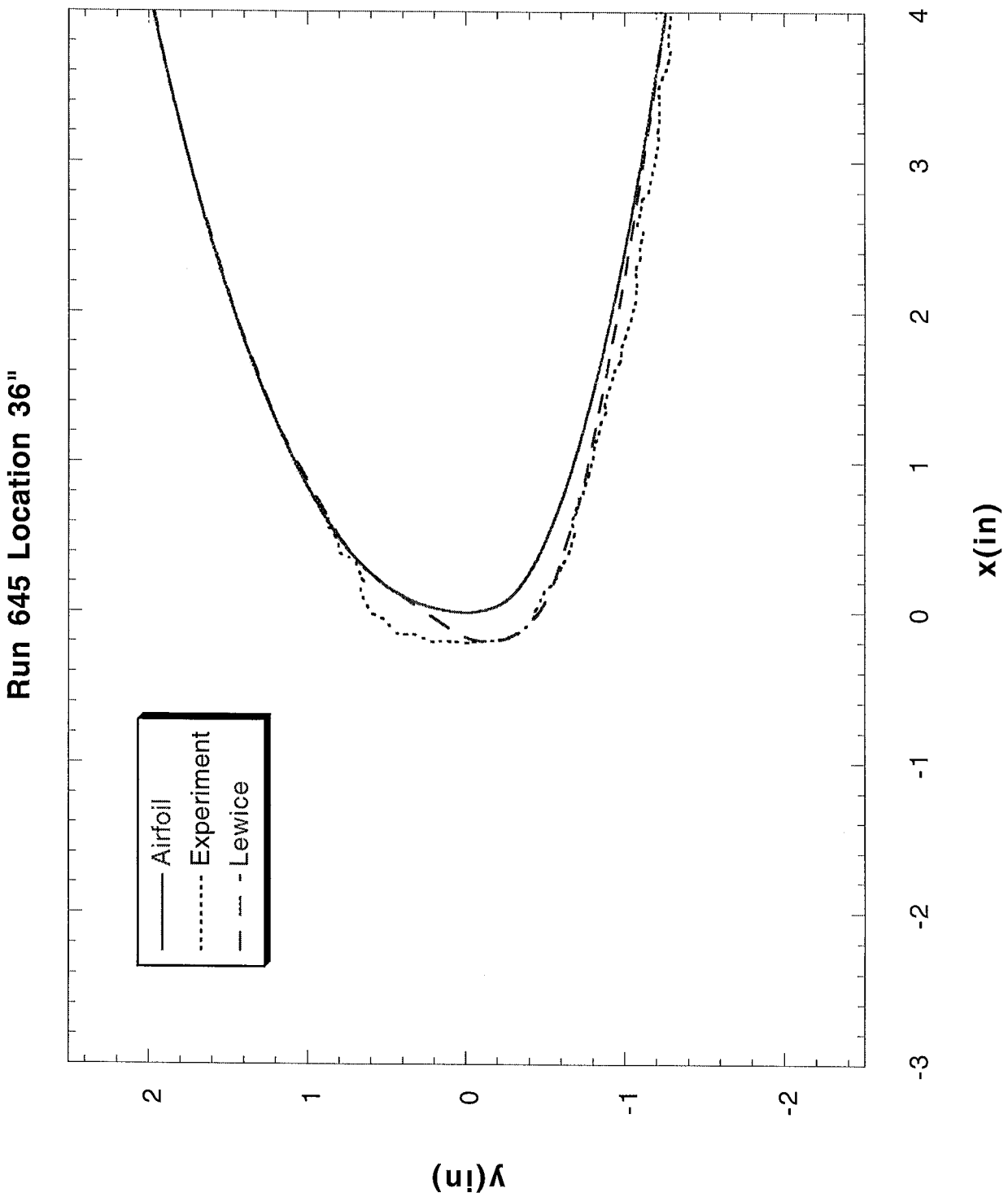
Run 645 Location 36"
Airfoil
Experiment
Lewice
y(in)
x(in)
2
1
0
-1
-2
-3
-2
-1
0
1
2
3
4

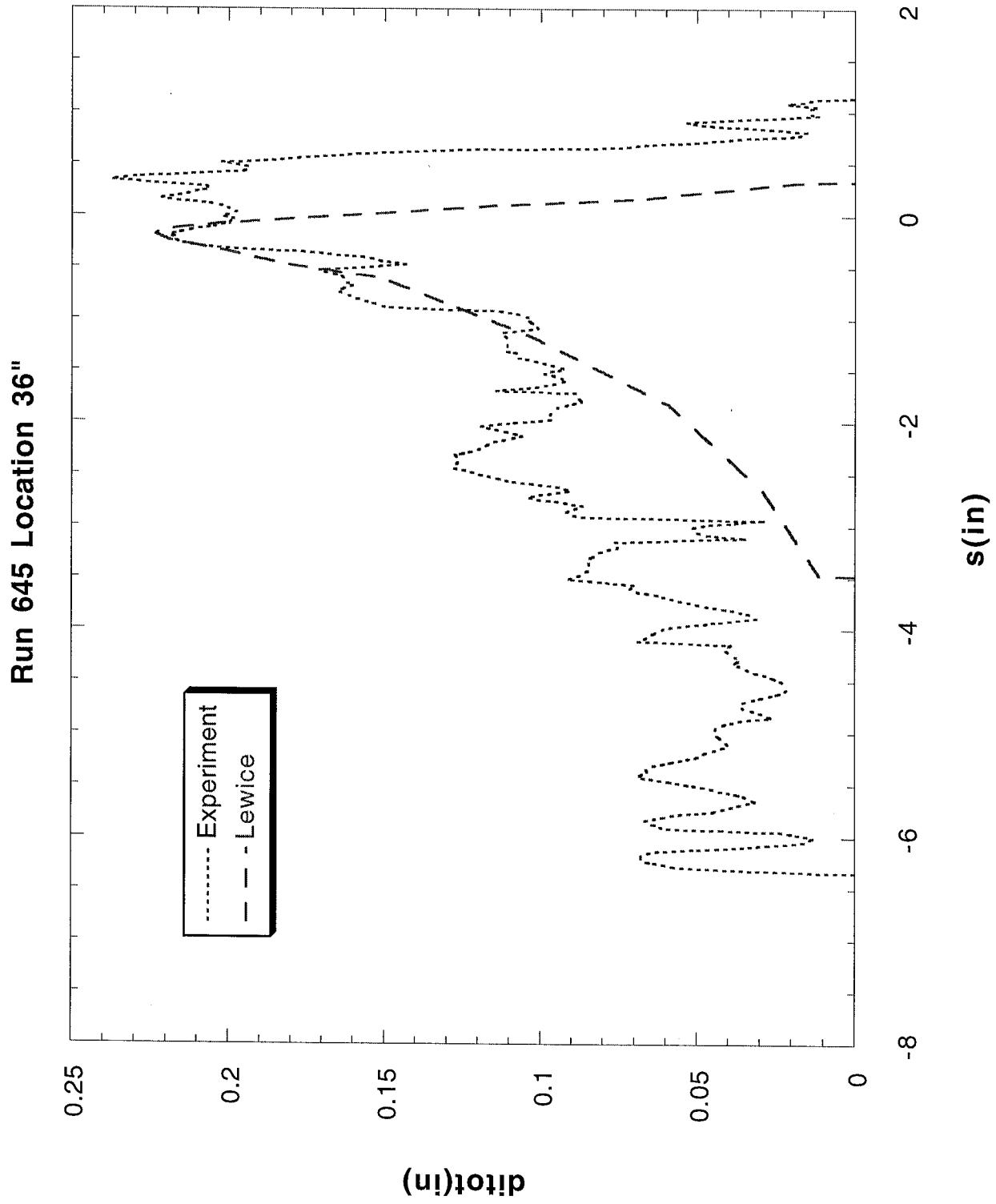
Run 645 Location 36"
Experiment
Lewice
dltot(in)
s(in)
0.25
0.2
0.15
0.1
0.05
0
2
0
-2
-4
-6
-8

NACA 0015
Figures 500 – 509

NACA 0015 Test Conditions

Principal Investigator	Airfoil	Test Date	Chord (in)	Run Number	Previous Identical Run	Velocity (kts)	Velocity (m/s)	Tt (°F)	Static Temperature (K)	A.O.A.	Corrected A.O.A.	LWC (g/m^3)	MVD (microns)	Spray Time (min)	Digitized Tracing Locations
Anderson	NACA0015	June 1996	13.9"	0624961		185.1	95.21544	31.1	267.85	0	0	0.75	19	10	36"
Anderson	NACA0015	June 1996	13.9"	0624962		166	85.3904	29.9	268.07	0	0	0.68	23.4	12.2	36"
Anderson	NACA0015	June 1996	13.9"	0624963		185.1	95.21544	22.1	262.85	0	0	0.75	19	10	36"
Anderson	NACA0015	June 1996	13.9"	0624964R	0624963	185.1	95.21544	22.1	262.85	0	0	0.75	19	10	36"
Anderson	NACA0015	June 1996	13.9"	0624965		185.1	95.21544	22.1	262.85	0	0	0.50	25	10	36"
Anderson	NACA0015	June 1996	13.9"	0624966		166	85.3904	20.9	263.07	0	0	0.77	23.4	10.8	36"

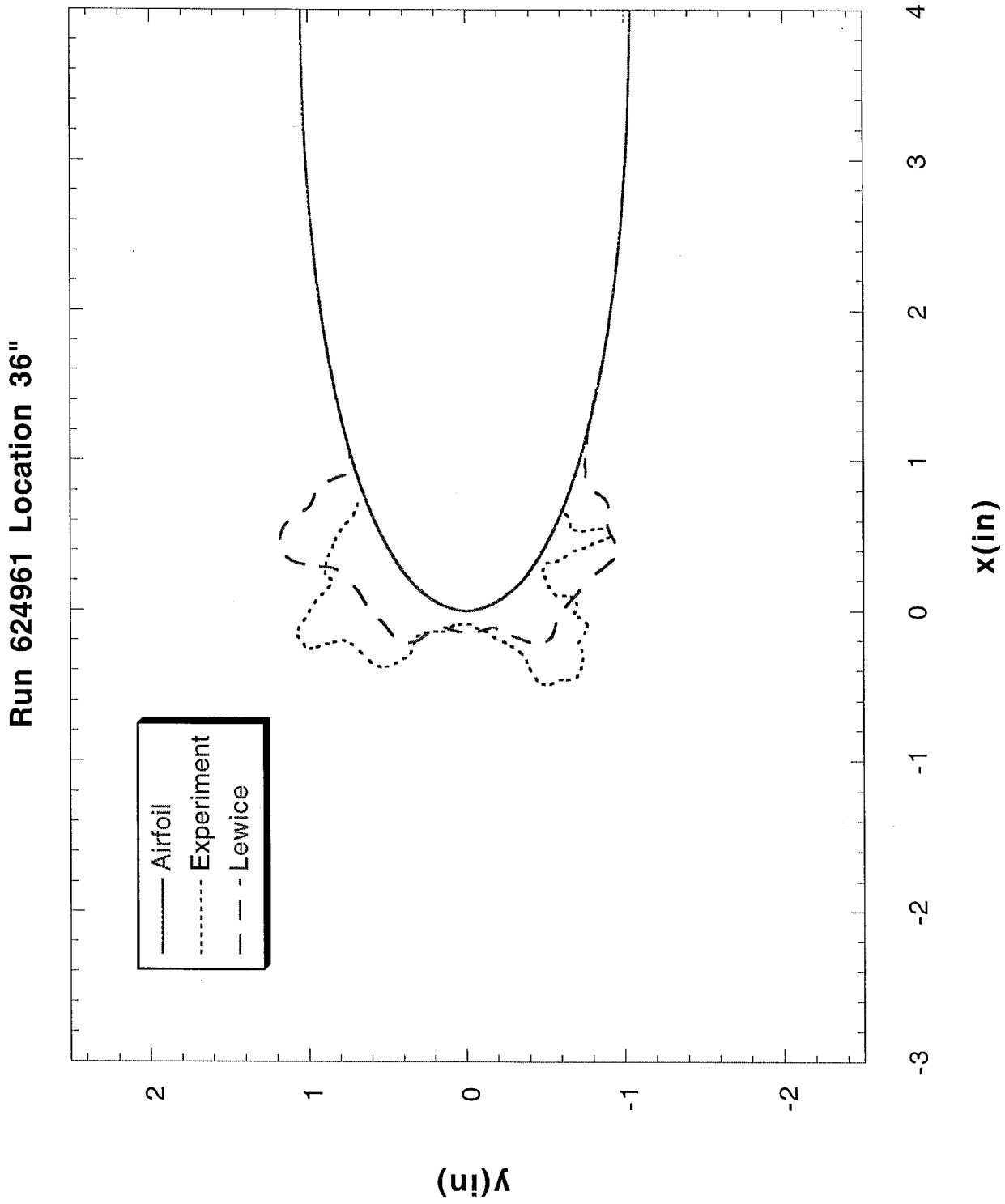
Run 624961 Location 36"
Airfoil
Experiment
Lewice
y(in)
x(in)
2
1
0
-1
-2
-3
-2
-1
0
1
2
3
4

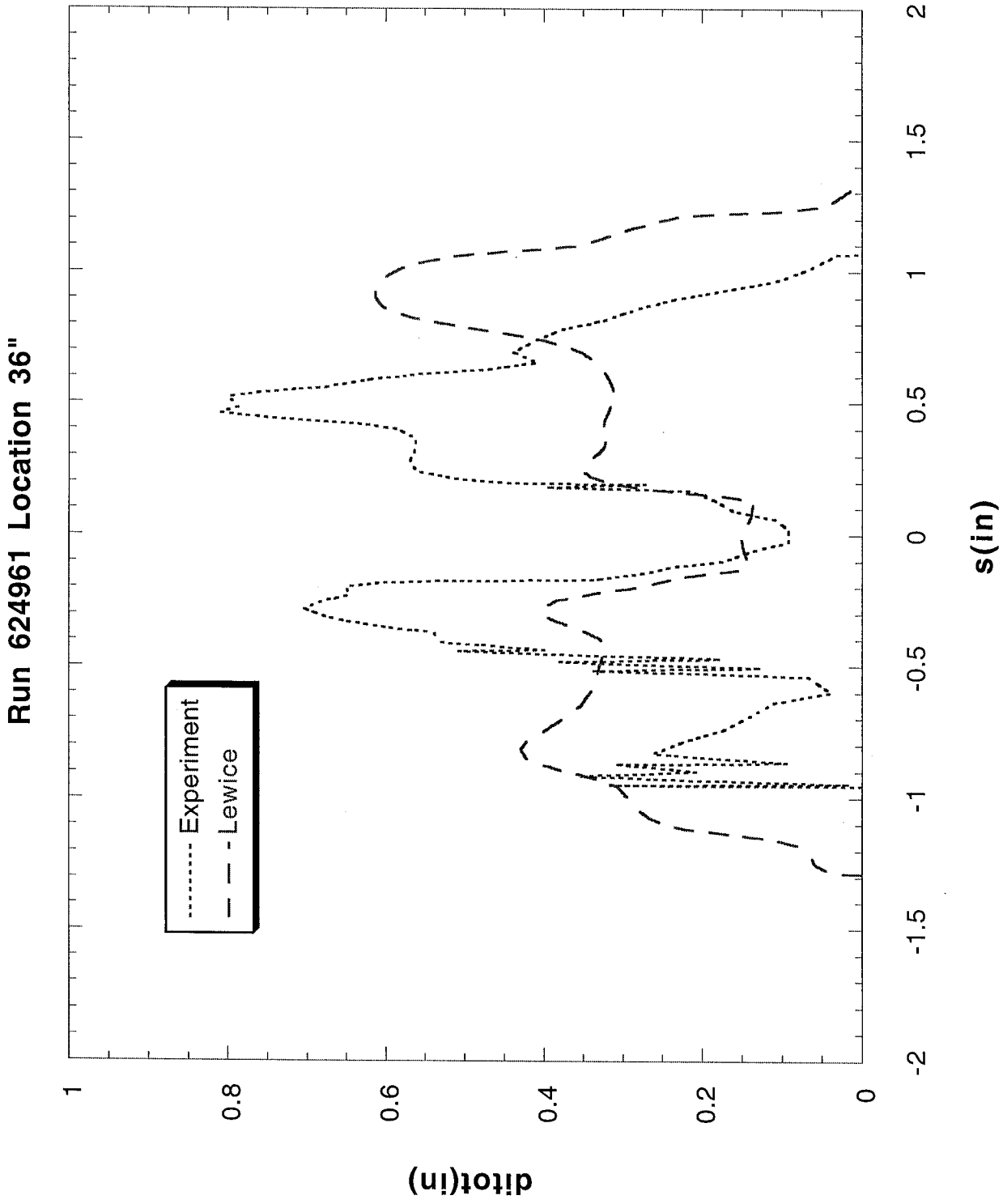
Run 624961 Location 36"
Experiment
Lewice
dltot(in)
s(in)
1
0.8
0.6
0.4
0.2
0
-2
-1.5
-1
-0.5
0
0.5
1
1.5
2

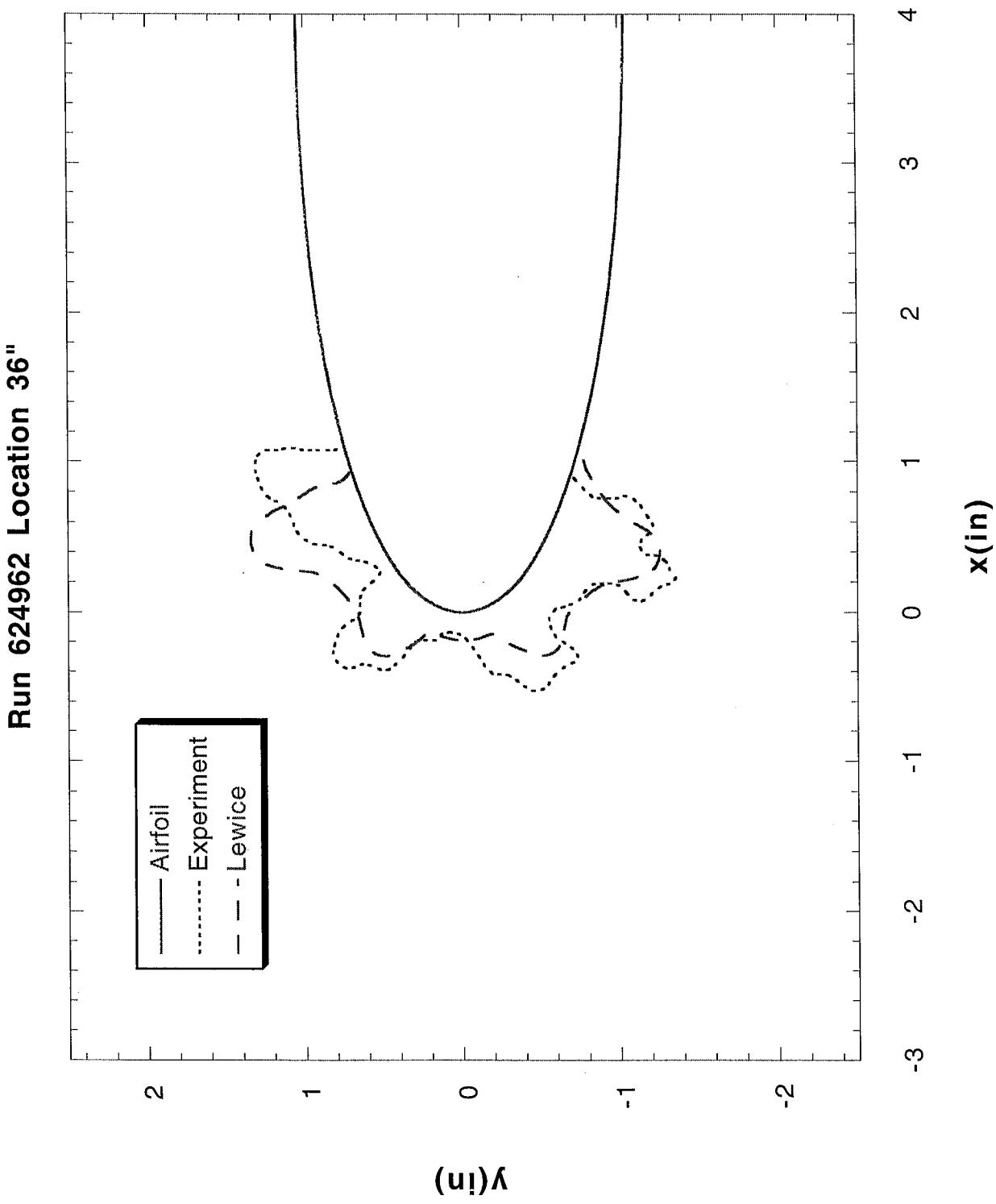
Run 624962 Location 36"
Airfoil
Experiment
Lewice
y(in)
x(in)
2
1
0
-1
-2
-3
-2
-1
0
1
2
3
4

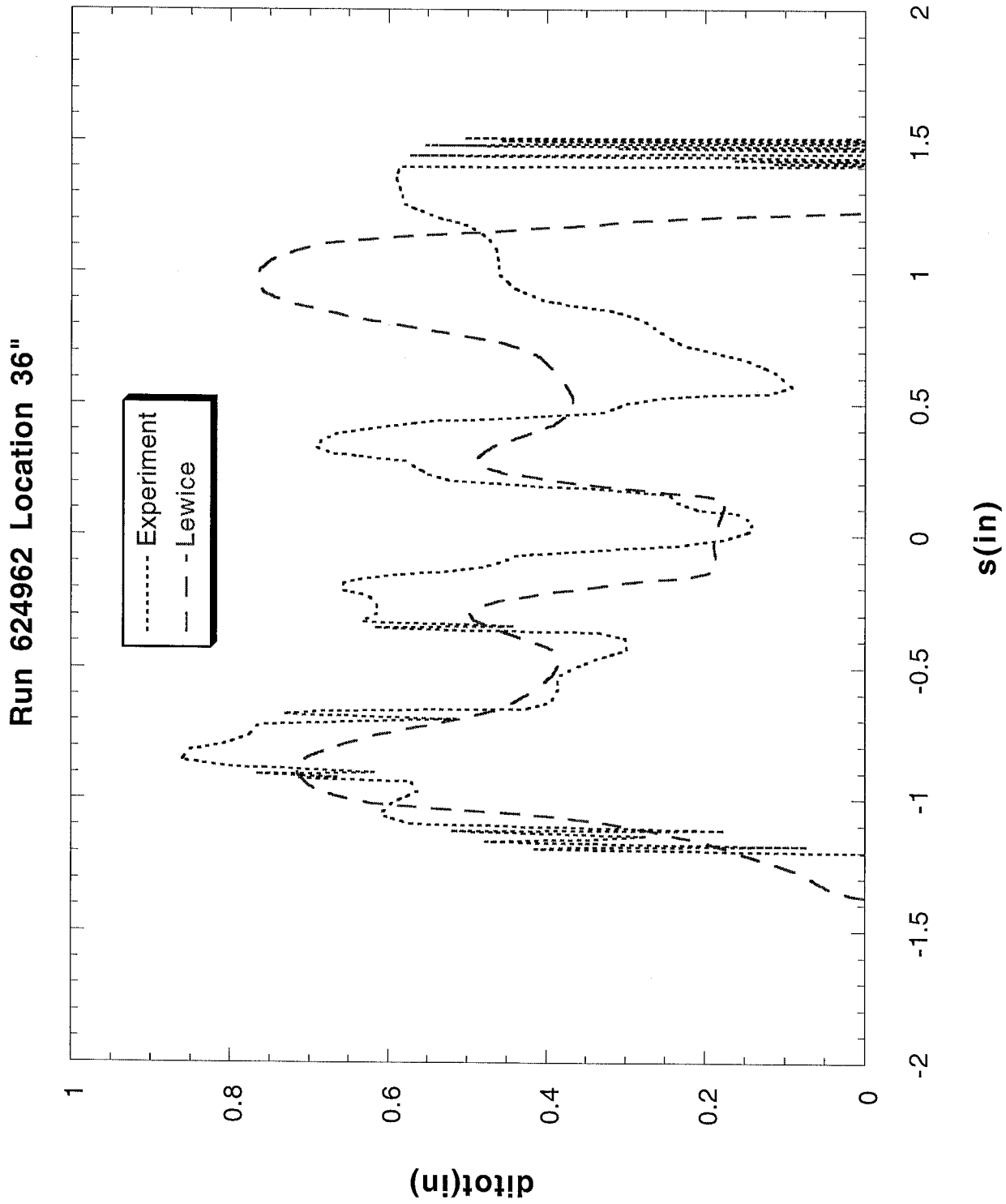
Run 624962 Location 36"
Experiment
- Lewice
ditot(in)
s(in)
1
0.8
0.6
0.4
0.2
0
-2
-1.5
-1
-0.5
0
0.5
1
1.5
2

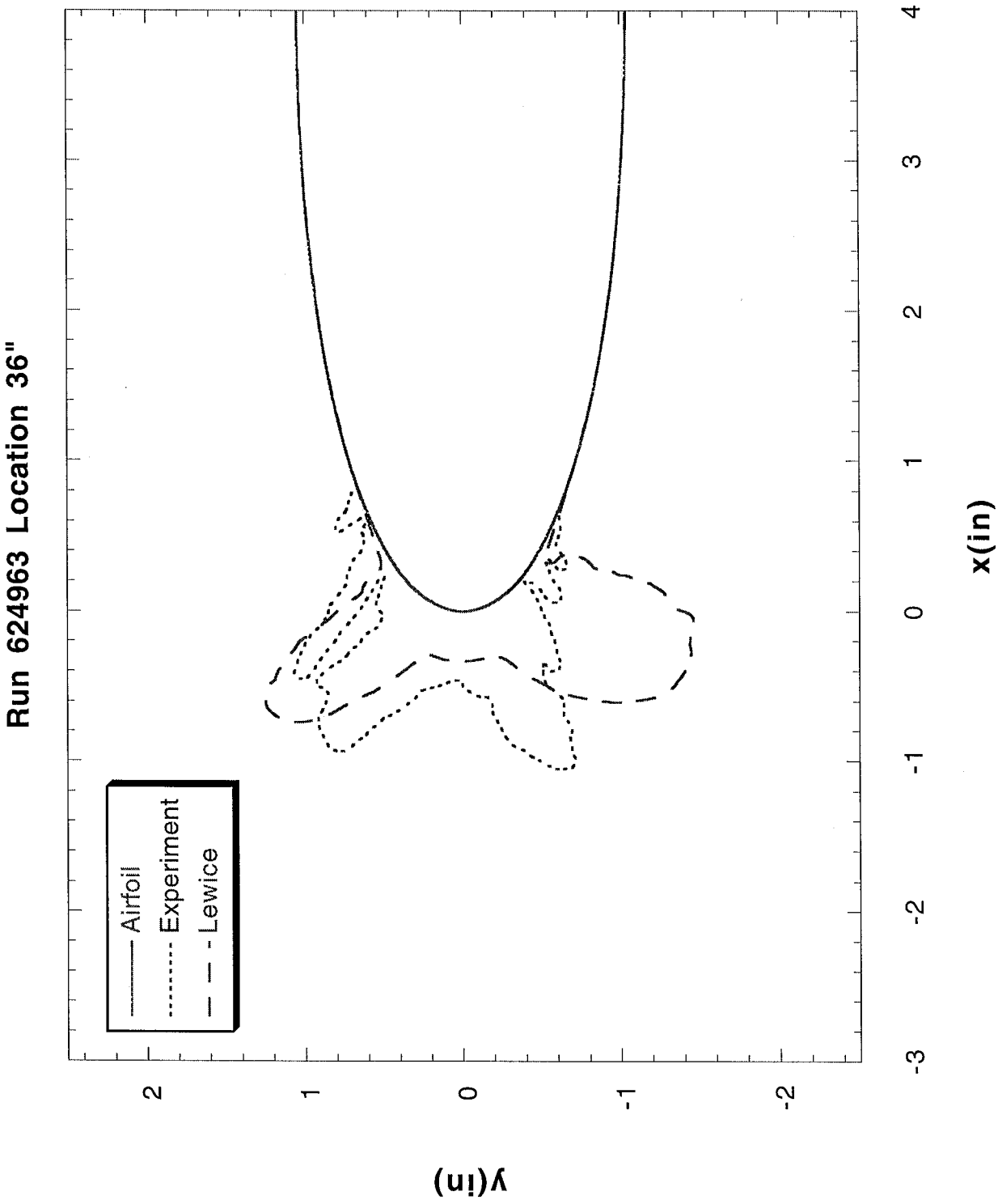
Run 624963 Location 36"
Airfoil
Experiment
Lewice
y(in)
x(in)
2
1
0
-1
-2
-3
-2
-1
0
1
2
3
4

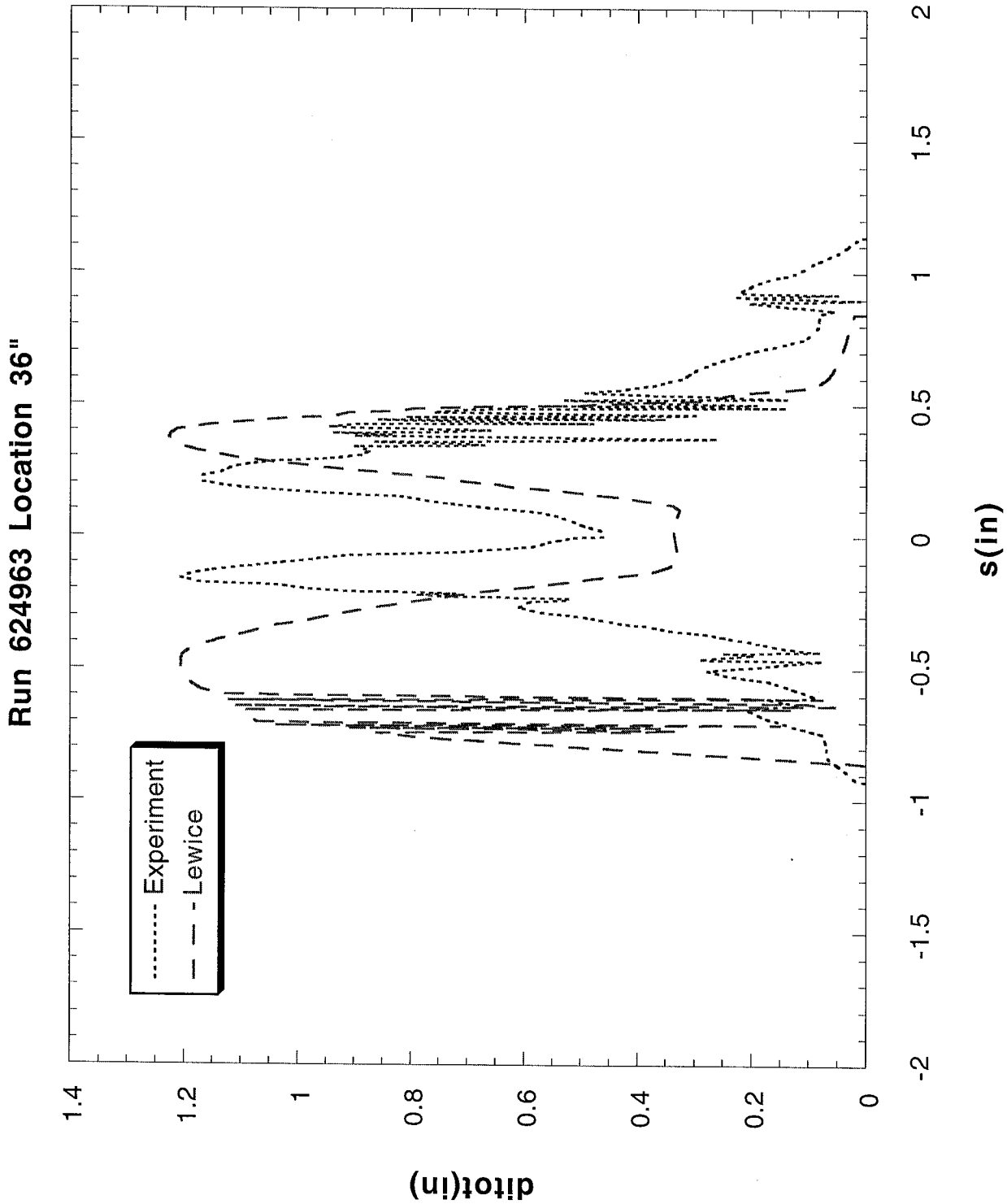
Run 624963 Location 36"
Experiment
Lewice
dltot(in)
s(in)
1.4
1.2
1
0.8
0.6
0.4
0.2
0
-2
-1.5
-1
-0.5
0
0.5
1
1.5
2

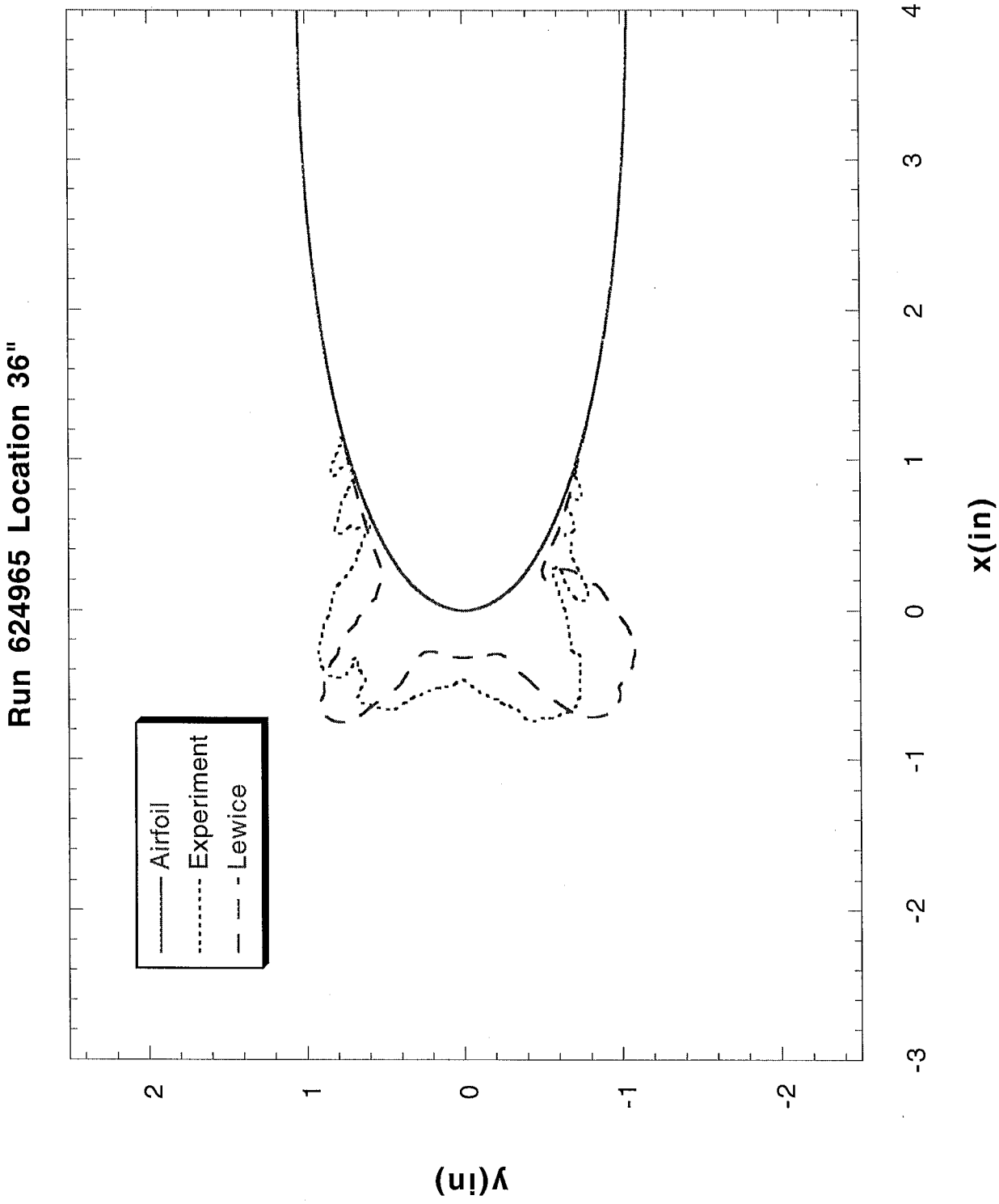
Run 624965 Location 36"
Airfoil
Experiment
Lewice
y(in)
x(in)
2
1
0
-1
-2
-3
-2
-1
0
1
2
3
4

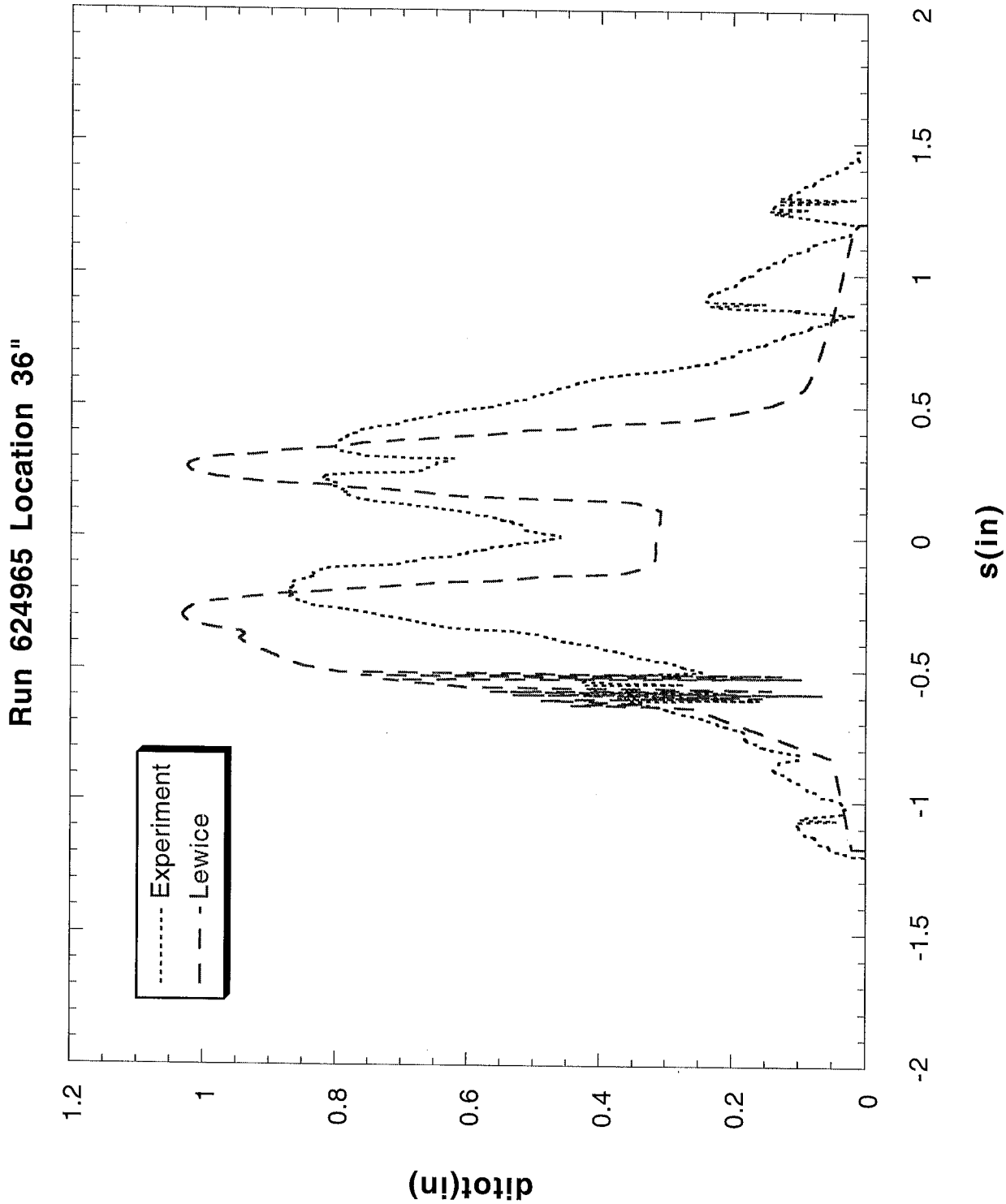
Run 624965 Location 36"
Experiment
Lewice
dltot(in)
s(in)
1.2
1
0.8
0.6
0.4
0.2
0
-2
-1.5
-1
-0.5
0
0.5
1
1.5
2

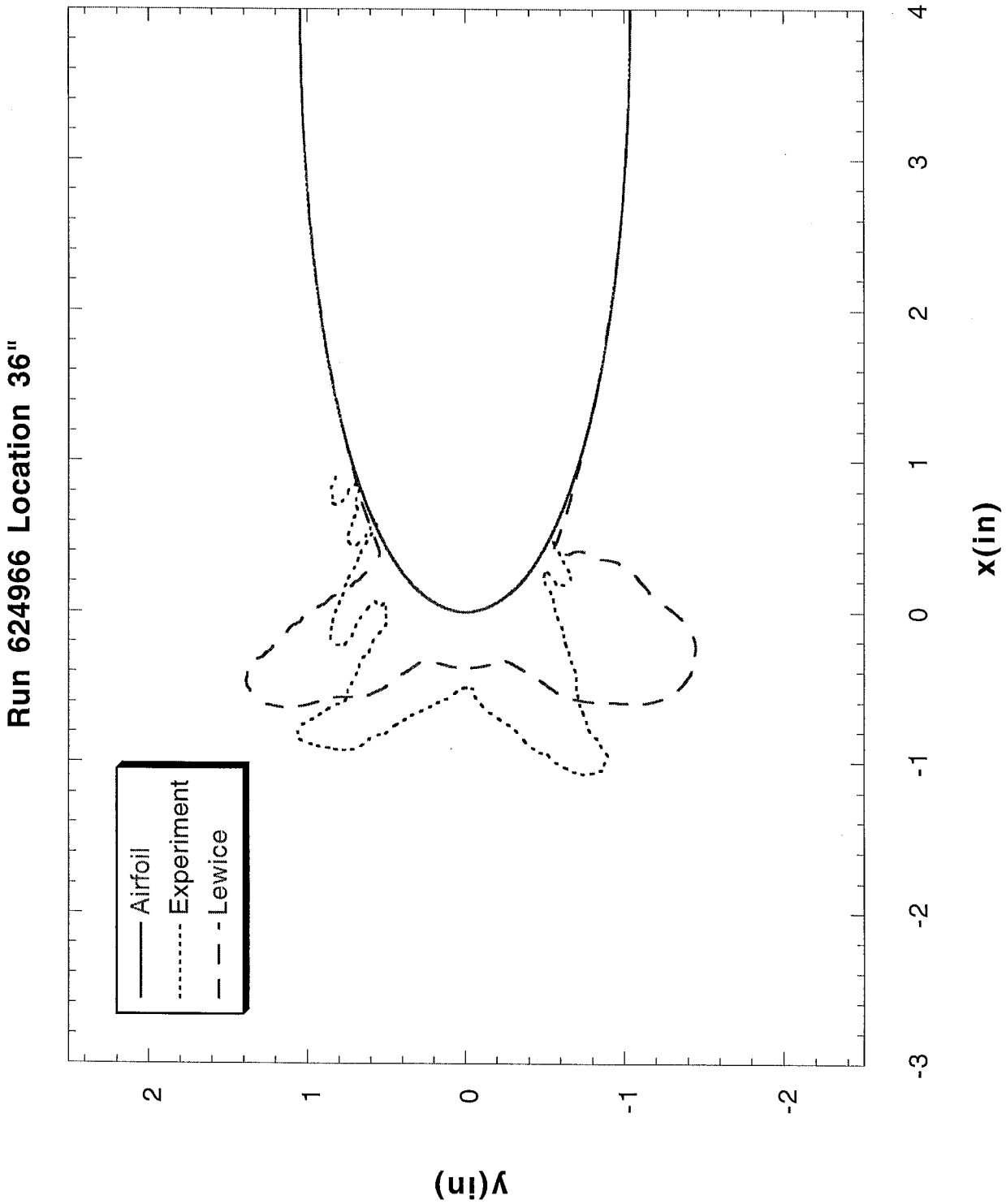
Run 624966 Location 36"
Airfoil
Experiment
Lewice
y(in)
x(in)
2
1
0
-1
-2
-3
-2
-1
0
1
2
3
4

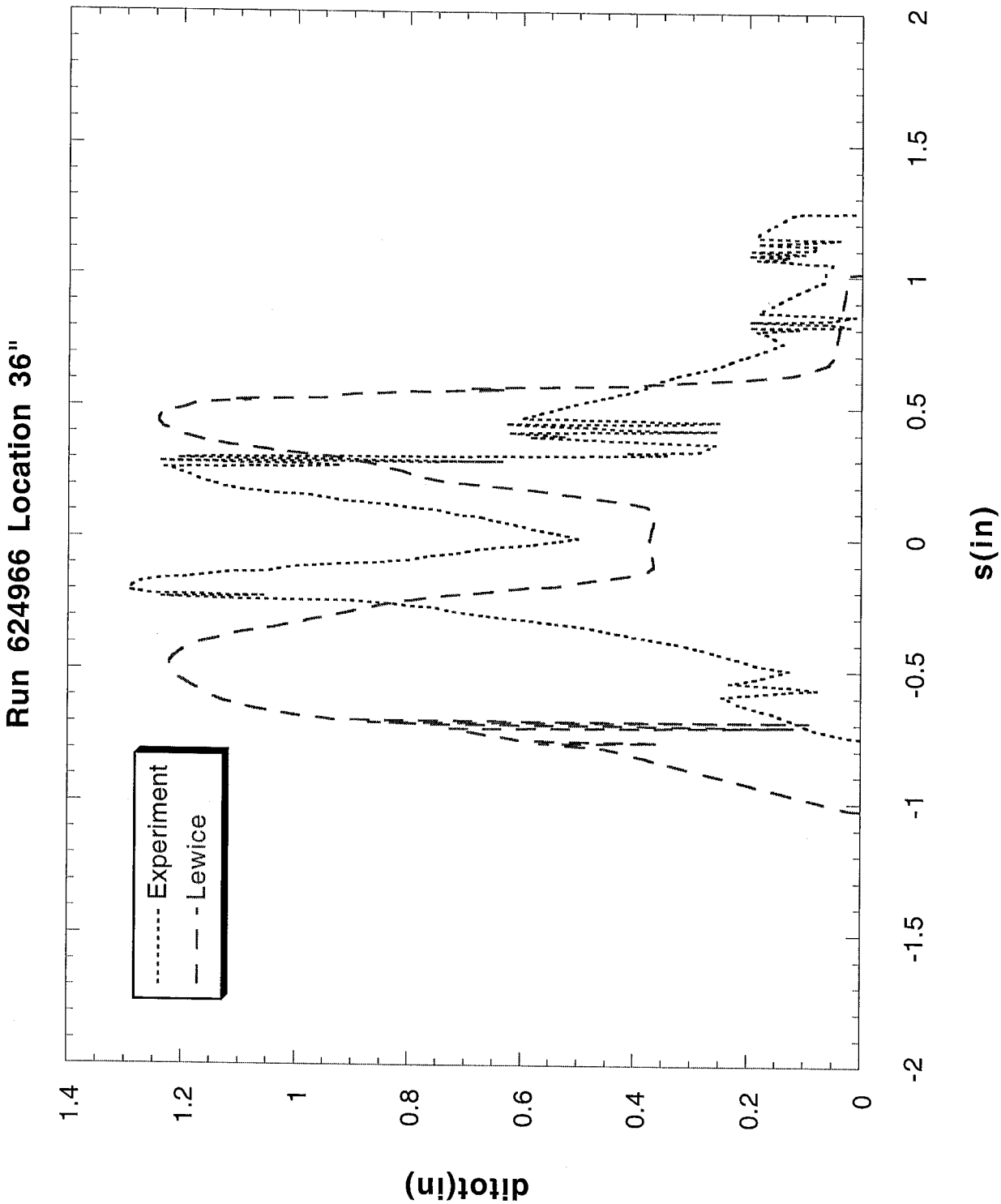
Run 624966 Location 36"
Experiment
Lewice
dltot(in)
s(in)
1.4
1.2
1
0.8
0.6
0.4
0.2
0
-2
-1.5
-1
-0.5
0
0.5
1
1.5
2

NACA 0012
Figures 510 – 623

NACA 0012 Test Conditions

Principal Investigator	Airfoil	Test Date	Chord (in)	Run Number	Previous Identical Run	Velocity (kts)	Velocity (m/s)	Tt (°F)	Static Tempurature (K)	A.O.A.	Corrected A.O.A.	LWC (g/m³)	MVD (microns)	Spray Time (min)	Digitized Tracing Locations
Bidwell/VanZante	NACA0012	Jan. 1998	21"	401		200	102.8	28	265.37	4	3.5	0.55	20	7	24", 36" & 48"
Bidwell/VanZante	NACA0012	Jan. 1998	21"	401r1	401	200	102.8	28	265.37	4	3.5	0.55	20	7	36"
Bidwell/VanZante	NACA0012	Jan. 1998	21"	401r2	401	200	102.8	28	265.37	4	3.5	0.55	20	7	24"
Bidwell/VanZante	NACA0012	Jan. 1998	21"	401r3	401	200	102.8	28	265.37	4	3.5	0.55	20	7	36"
Bidwell/VanZante	NACA0012	Jan. 1998	21"	401r4	401	200	102.8	28	265.37	4	3.5	0.55	20	7	36"
Bidwell/VanZante	NACA0012	Jan. 1998	21"	402		200	102.8	25	263.71	4	3.5	0.55	20	7	36"
Bidwell	NACA0012	Jan. 1998	21"	402r2B	402	200	102.8	25	263.71	4	3.5	0.55	20	7	24", 36" & 48"
VanZante	NACA0012	Jan. 1998	21"	402r2V	402	200	102.8	25	263.71	4	3.5	0.55	20	7	24", 36" & 48"
Bidwell/VanZante	NACA0012	Jan. 1998	21"	403		200	102.8	22	262.04	4	3.5	0.55	20	7	36"
Bidwell/VanZante	NACA0012	Jan. 1998	21"	403r1	403	200	102.8	22	262.04	4	3.5	0.55	20	7	36"
Bidwell/VanZante	NACA0012	Jan. 1998	21"	403r2	403	200	102.8	22	262.04	4	3.5	0.55	20	7	36"
Bidwell/VanZante	NACA0012	Jan. 1998	21"	404		200	102.8	12	256.49	4	3.5	0.55	20	7	36"
Bidwell/VanZante	NACA0012	Jan. 1998	21"	405		200	102.8	1	250.37	4	3.5	0.55	20	7	36"
Bidwell/VanZante	NACA0012	Jan. 1998	21"	406		200	102.8	26.2	264.37	4	3.5	0.40	20	9.8	36"
Bidwell/VanZante	NACA0012	Jan. 1998	21"	407		200	102.8	11.7	256.32	4	3.5	0.40	20	9.8	36"
Bidwell/VanZante	NACA0012	Jan. 1998	21"	408		200	102.8	22	262.04	4	3.5	0.86	20	4.5	36"
Bidwell/VanZante	NACA0012	Jan. 1998	21"	409		130.3	67.1	22	265.07	4	3.5	1.30	30	6	36"
Bidwell/VanZante	NACA0012	Jan. 1998	21"	410		200	102.8	22	262.04	4	3.5	0.55	20	3.5	36"
Bidwell/VanZante	NACA0012	Jan. 1998	21"	411		200	102.8	22	262.04	4	3.5	0.55	20	14	36"
Bidwell/VanZante	NACA0012	Jan. 1998	21"	412		200	102.8	21.1	261.54	4	3.5	0.47	30	8.2	36"
Bidwell/VanZante	NACA0012	Jan. 1998	21"	413		200	102.8	21.4	261.71	4	3.5	0.50	40	7.7	36"
Bidwell/VanZante	NACA0012	Jan. 1998	21"	414		200	102.8	22	262.04	4	3.5	0.55	25	7	36"
Bidwell/VanZante	NACA0012	Jan. 1998	21"	414r1	414	200	102.8	22	262.04	4	3.5	1.00	25	7	36"
Bidwell/VanZante	NACA0012	Jan. 1998	21"	415		200	102.8	22	262.04	4	3.5	0.60	15	6.4	36"
Bidwell/VanZante	NACA0012	Jan. 1998	21"	421		130.3	67.1	28	268.40	4	3.5	1.00	20	6	36"
Bidwell/VanZante	NACA0012	Jan. 1998	21"	421r1	421	130.3	67.1	28	268.40	4	3.5	1.00	20	6	18", 36" & 54"
Bidwell/VanZante	NACA0012	Jan. 1998	21"	421r2	421	130.3	67.1	28	268.40	4	3.5	1.00	20	6	36"
Bidwell/VanZante	NACA0012	Jan. 1998	21"	422		130.3	67.1	25	266.74	4	3.5	1.00	20	6	36"
Bidwell/VanZante	NACA0012	Jan. 1998	21"	422r1	422	130.3	67.1	25	266.74	4	3.5	1.00	20	6	36" & 54"
Bidwell/VanZante	NACA0012	Jan. 1998	21"	423		130.3	67.1	22	265.07	4	3.5	1.00	20	6	36"
Bidwell/VanZante	NACA0012	Jan. 1998	21"	423r1	423	130.3	67.1	22	265.07	4	3.5	1.00	20	6	36"
Bidwell/VanZante	NACA0012	Jan. 1998	21"	424		130.3	67.1	12	259.51	4	3.5	1.00	20	6	36"
Bidwell/VanZante	NACA0012	Jan. 1998	21"	425		130.3	67.1	-15	244.51	4	3.5	1.00	20	6	36"
Bidwell/VanZante	NACA0012	Jan. 1998	21"	426		130.3	67.1	22	265.07	4	3.5	1.06	30	6	36"
Bidwell/VanZante	NACA0012	Jan. 1998	21"	427		130.3	67.1	22	265.07	4	3.5	1.30	30	6	36"
Bidwell/VanZante	NACA0012	Jan. 1998	21"	427r1	427	130.3	67.1	22	265.07	4	3.5	1.30	30	6	36"
Bidwell/VanZante	NACA0012	Jan. 1998	21"	428		130.3	67.1	22	265.07	4	3.5	1.60	30	6	36"
Bidwell/VanZante	NACA0012	Jan. 1998	21"	429		200	102.8	22	262.04	4	3.5	0.86	40	4.5	36"
Addy	NACA0012	Apr. 1997	21"	301R	401	200	102.8	28	265.37	4	3.5	0.550	20	7	24", 36" & 48"
Addy	NACA0012	Apr. 1997	21"	301r1	401	200	102.8	28	265.37	4	3.5	0.550	20	7	24", 36" & 48"
Addy	NACA0012	Apr. 1997	21"	301r2	401	200	102.8	28	265.37	4	3.5	0.550	20	7	36"
Addy	NACA0012	Apr. 1997	21"	302R	402	200	102.8	25	263.71	4	3.5	0.550	20	7	36"
Addy	NACA0012	Apr. 1997	21"	302r1	402	200	102.8	25	263.71	4	3.5	0.550	20	7	36"
Addy	NACA0012	Apr. 1997	21"	303R	403	200	102.8	22	262.04	4	3.5	0.550	20	7	36"
Addy	NACA0012	Apr. 1997	21"	303r1	403	200	102.8	22	262.04	4	3.5	0.550	20	7	24", 28", 36", 48" & 55"
Addy	NACA0012	Apr. 1997	21"	304R	404	200	102.8	12	256.49	4	3.5	0.550	20	7	36"
Addy	NACA0012	Apr. 1997	21"	305R	405	200	102.8	1	250.37	4	3.5	0.550	20	7	36"
Addy	NACA0012	Apr. 1997	21"	306R	406	200	102.8	26.2	264.37	4	3.5	0.400	20	9.8	36"
Addy	NACA0012	Apr. 1997	21"	307R	407	200	102.8	11.7	256.32	4	3.5	0.400	20	9.8	36"

NACA 0012 Test Conditions

Principal Investigator	Airfoil	Test Date	Chord (in)	Run Number	Previous Identical Run	Velocity (kts)	Velocity (m/s)	Tt (°F)	Static Tempurature (K)	A.O.A.	Corrected A.O.A.	LWC (g/m^3)	MVD (microns)	Spray Time (min)	Digitized Tracing Locations
Addy	NACA0012	Apr. 1997	21"	308		200	102.8	22	262.04	4	3.5	1.000	20	3.85	36"
Addy	NACA0012	Apr. 1997	21"	309R	409	130.3	102.8	22	262.04	4	3.5	1.300	30	6	36"
Addy	NACA0012	Apr. 1997	21"	310R	410	200	102.8	22	262.04	4	3.5	0.550	20	3.5	36"
Addy	NACA0012	Apr. 1997	21"	311R	411	200	102.8	22	262.04	4	3.5	0.550	20	14	36"
Addy	NACA0012	Apr. 1997	21"	312R	412	200	102.8	21.1	261.54	4	3.5	0.470	30	8.2	35" & 36"
Addy	NACA0012	Apr. 1997	21"	313R	413	200	102.8	21.4	261.71	4	3.5	0.500	40	7.7	35" & 36"
Addy	NACA0012	Apr. 1997	21"	314		200	102.8	22	262.04	4	3.5	0.600	15	6.4	36"
Addy	NACA0012	Apr. 1997	21"	315R	314	200	102.8	22	262.04	4	3.5	0.600	15	6.4	36"
Addy	NACA0012	Apr. 1997	21"	316		200	102.8	22	262.04	4	3.5	0.550	20	3.22	36"
Addy	NACA0012	Apr. 1997	21"	321R	421	130.3	102.8	28	265.37	4	3.5	1.000	20	6	18", 36" & 54"
Addy	NACA0012	Apr. 1997	21"	321r1	421	130.3	102.8	28	265.37	4	3.5	1.000	20	6	36"
Addy	NACA0012	Apr. 1997	21"	321r2	421	130.3	102.8	28	265.37	4	3.5	1.000	20	6	36"
Addy	NACA0012	Apr. 1997	21"	322R	422	130.3	102.8	25	263.71	4	3.5	1.000	20	6	36"
Addy	NACA0012	Apr. 1997	21"	324R	424	130.3	102.8	12	256.49	4	3.5	1.000	20	6	36"
Addy	NACA0012	Apr. 1997	21"	325R	425	130.3	102.8	-15	241.49	4	3.5	1.000	20	6	36"
Addy	NACA0012	Apr. 1997	21"	326R	426	130.3	102.8	22	262.04	4	3.5	1.060	30	6	36"
Addy	NACA0012	Apr. 1997	21"	327R	427	130.3	102.8	22	262.04	4	3.5	1.300	30	6	35" & 36"
Addy	NACA0012	Apr. 1997	21"	328R	428	130.3	102.8	22	262.04	4	3.5	1.600	30	6	36"
Addy	NACA0012	Apr. 1997	21"	329R	429	200	102.8	22	262.04	4	3.5	0.860	40	4.5	36"
Addy	NACA0012	Jul. 1996	21"	201	401	200	102.8	28	265.37	4	3.5	0.55	20	7	36" & 48"
Addy	NACA0012	Jul. 1996	21"	201r2	401	200	102.8	28	265.37	4	3.5	0.55	20	7	24", 36", & 48"
Addy	NACA0012	Jul. 1996	21"	202	402	200	102.8	25	263.71	4	3.5	0.55	20	7	24", 36", & 48"
Addy	NACA0012	Jul. 1996	21"	202r1	402	200	102.8	25	263.71	4	3.5	0.55	20	7	24", 36", & 48"
Addy	NACA0012	Jul. 1996	21"	203	403	200	102.8	22	262.04	4	3.5	0.55	20	7	24", 36", & 48"
Addy	NACA0012	Jul. 1996	21"	203r1	403	200	102.8	22	262.04	4	3.5	0.55	20	7	24", 36", & 48"
Addy	NACA0012	Jul. 1996	21"	204	404	200	102.8	12	256.49	4	3.5	0.55	20	7	24", 36", & 48"
Addy	NACA0012	Jul. 1996	21"	205	405	200	102.8	1	250.37	4	3.5	0.55	20	7	24", 36", & 48"
Addy	NACA0012	Jul. 1996	21"	206		200	102.8	28	265.37	4	3.5	0.34	20	11.5	36"
Addy	NACA0012	Jul. 1996	21"	207		200	102.8	12	256.49	4	3.5	0.34	20	11.5	36"
Addy	NACA0012	Jul. 1996	21"	208	308	200	102.8	22	262.04	4	3.5	1.00	20	3.85	36"
Addy	NACA0012	Jul. 1996	21"	209	409	130.3	67.1	22	265.07	4	3.5	1.30	30	6	36"
Addy	NACA0012	Jul. 1996	21"	210	410	200	102.8	22	262.04	4	3.5	0.55	20	3.5	36"
Addy	NACA0012	Jul. 1996	21"	211	411	200	102.8	22	262.04	4	3.5	0.55	20	14	36"
Addy	NACA0012	Jul. 1996	21"	212		200	102.8	22	262.04	4	3.5	0.44	30	8.75	36"
Addy	NACA0012	Jul. 1996	21"	213		200	102.8	22	262.04	4	3.5	0.48	40	8	36"
Addy	NACA0012	Jul. 1996	21"	214	415	200	102.8	22	262.04	4	3.5	0.60	15	6.4	36"
Addy	NACA0012	Jul. 1996	21"	215	415	200	102.8	22	262.04	4	3.5	0.60	15	6.4	36"
Addy	NACA0012	Jul. 1996	21"	221	421	130.3	67.1	28	268.40	4	3.5	1.00	20	6	18", 36" & 54"
Addy	NACA0012	Jul. 1996	21"	221r1	421	130.3	67.1	28	268.40	4	3.5	1.00	20	6	18", 36" & 54"
Addy	NACA0012	Jul. 1996	21"	222	422	130.3	67.1	25	266.74	4	3.5	1.00	20	6	18", 36" & 54"
Addy	NACA0012	Jul. 1996	21"	223	423	130.3	67.1	22	265.07	4	3.5	1.00	20	6	18", 36" & 54"
Addy	NACA0012	Jul. 1996	21"	224	424	130.3	67.1	12	259.51	4	3.5	1.00	20	6	18", 36" & 54"
Addy	NACA0012	Jul. 1996	21"	225	325	130.3	67.1	-15	244.51	4	3.5	1.00	20	6	18", 36" & 54"
Addy	NACA0012	Jul. 1996	21"	226	326	130.3	67.1	22	265.07	4	3.5	1.06	30	6	18", 36" & 54"
Addy	NACA0012	Jul. 1996	21"	227	427	130.3	67.1	22	265.07	4	3.5	1.30	30	6	18", 36" & 54"
Addy	NACA0012	Jul. 1996	21"	228	428	130.3	67.1	22	265.07	4	3.5	1.60	30	6	18", 36" & 54"
Addy	NACA0012	Jul. 1996	21"	229	429	200	102.8	22	262.04	4	3.5	0.86	40	4.5	36"
Shin/Bond	NACA0012	Jun. 1991	21"	062091.001R	423	130.3	67.1	22	265.07	4	3.5	1.00	20	6	18.5", 36" & 52"

NACA 0012 Test Conditions

Principal Investigator	Airfoil	Test Date	Chord (in)	Run Number	Previous Identical Run	Velocity (kts)	Velocity (m/s)	Tt (°F)	Static Tempurature (K)	A.O.A.	Corrected A.O.A.	LWC (g/m^3)	MVD (microns)	Spray Time (min)	Digitized Tracing Locations
Shin/Bond	NACA0012	Jun. 1991	21"	062491.001R	423	130.3	67.1	22	265.07	4	3.5	1.00	20	6	18.5", 36" & 53.5"
Shin/Bond	NACA0012	Jun. 1991	21"	062491.002		130.3	67.1	22	265.07	-4	-3.3	1.00	20	12	18.5", 36" & 53.5"
Shin/Bond	NACA0012	Jun. 1991	21"	062491.004		130.3	67.1	18	262.85	4	3.5	1.00	20	6	18.5", 36" & 53.5"
Shin/Bond	NACA0012	Jun. 1991	21"	062491.005		130.3	67.1	18	262.85	4	3.5	1.00	20	12	18.5", 36" & 53.5"
Shin/Bond	NACA0012	Jun. 1991	21"	062591.001R	421	130.3	67.1	28	268.40	4	3.5	1.00	20	6	18.5", 36" & 53.5"
Shin/Bond	NACA0012	Jun. 1991	21"	062591.002		130.3	67.1	28	268.40	4	3.5	1.00	20	12	18.5", 36" & 53.5"
Shin/Bond	NACA0012	Jun. 1991	21"	062591.003R	422	130.3	67.1	25	266.74	4	3.5	1.00	20	6	18.5", 36" & 53.5"
Shin/Bond	NACA0012	Jun. 1991	21"	062591.004		130.3	67.1	25	266.74	4	3.5	1.00	20	12	18.5", 36" & 53.5"
Shin/Bond	NACA0012	Jun. 1991	21"	062591.005		130.3	67.1	22	265.07	4	3.5	1.00	20	12	18.5", 36" & 51"
Shin/Bond	NACA0012	Jun. 1991	21"	062591.006R	424	130.3	67.1	12	259.51	4	3.5	1.00	20	6	18.5", 36" & 53.5"
Shin/Bond	NACA0012	Jun. 1991	21"	062591.007		130.3	67.1	12	259.51	4	3.5	1.00	20	12	18.5", 36" & 53.5"
Shin/Bond	NACA0012	Jun. 1991	21"	062591.008		130.3	67.1	1	253.40	4	3.5	1.00	20	6	18.5", 36" & 53.5"
Shin/Bond	NACA0012	Jun. 1991	21"	062591.009R	325	130.3	67.1	-15	244.51	4	3.5	1.00	20	6	18.5", 30", 36" & 53.5"
Shin/Bond	NACA0012	Jun. 1991	21"	062791.001		113	58.1	23	266.19	4	3.5	1.30	20	8	18.5", 24", 36" & 53.5"
Shin/Bond	NACA0012	Jun. 1991	21"	062791.002		113	58.1	28.4	269.19	4	3.5	1.30	20	8	24", 36" & 53.5"
Shin/Bond	NACA0012	Jun. 1991	21"	062791.003		113	58.1	30.2	270.19	4	3.5	1.30	20	8	24", 36" & 52"
Shin/Bond	NACA0012	Jun. 1991	21"	062791.004		113	58.1	17.6	263.19	4	3.5	1.30	20	8	24", 36" & 53.5"
Shin/Bond	NACA0012	Jun. 1991	21"	062791.005		113	58.1	10.4	259.19	4	3.5	1.30	20	8	24", 36" & 53.5"
Shin/Bond	NACA0012	Jun. 1991	21"	062791.006		113	58.1	5	256.19	4	3.5	1.30	20	8	24", 36" & 53.5"
Shin/Bond	NACA0012	Jun. 1991	21"	062791.007		113	58.1	-0.4	253.19	4	3.5	1.30	20	8	24", 36" & 53.5"
Shin/Bond	NACA0012	Jun. 1991	21"	062791.008		113	58.1	-4	251.19	4	3.5	1.30	20	8	36" & 53.5"
Shin/Bond	NACA0012	Jun. 1991	21"	062791.009		113	58.1	-14.8	245.19	4	3.5	1.30	20	8	24", 36" & 53.5"
Shin/Bond	NACA0012	Jun. 1991	21"	062891.001R	423	130.3	67.1	22	265.07	4	3.5	1.00	20	6	18.5", 24", 36" & 53.5"
Shin/Bond	NACA0012	Jun. 1991	21"	062891.002R	062591.005	130.3	67.1	22	265.07	4	3.5	1.00	20	12	18.5", 24" & 36"
Shin/Bond	NACA0012	Jun. 1991	21"	062891.003		130.3	67.1	22	265.07	4	3.5	1.00	20	3	24", 36" & 53.5"
Shin/Bond	NACA0012	Jun. 1991	21"	062891.005R	062591.001	130.3	67.1	28	268.40	4	3.5	1.00	20	6	18.5", 24", 36" & 53.5"
Shin/Bond	NACA0012	Jun. 1991	21"	062891.006R	062591.002	130.3	67.1	28	268.40	4	3.5	1.00	20	12	18.5", 24", 36" & 53.5"
Shin/Bond	NACA0012	Jun. 1991	21"	062891.007		130.3	67.1	25	266.74	4	3.5	1.00	20	3	24", 36" & 53.5"
Shin/Bond	NACA0012	Jun. 1991	21"	062891.008R	062591.003	130.3	67.1	25	266.74	4	3.5	1.00	20	6	18.5", 24", 36" & 53.5"
Shin/Bond	NACA0012	Jun. 1991	21"	062891.009R	062591.004	130.3	67.1	25	266.74	4	3.5	1.00	20	12	18.5", 24", 36" & 53.5"
Shin/Bond	NACA0012	Jun. 1991	21"	062891.010R	062491.004	130.3	67.1	18	262.85	4	3.5	1.00	20	6	18", 24", 36" & 53"
Shin/Bond	NACA0012	Jun. 1991	21"	062891.011R	062491.005	130.3	67.1	18	262.85	4	3.5	1.00	20	12	18", 36" & 53"
Shin/Bond	NACA0012	Jun. 1991	21"	062991.003		200	102.8	22	262.04	4	3.5	1.00	30	6	18", 24" & 54"
Shin/Bond	NACA0012	Jun. 1991	21"	062991.004R	062591.007	130.3	67.1	12	259.51	4	3.5	1.00	20	12	18", 24" & 54"
Shin/Bond	NACA0012	Jul. 1991	21"	072291.001R	062091.001	130.3	67.1	22	265.07	4	3.5	1.00	20	6	18.5", 24", 36" & 53.5"
Shin/Bond	NACA0012	Jul. 1991	21"	072291.002R	062091.001	130.3	67.1	22	265.07	4	3.5	1.00	20	6	18.5", 24", 36" & 53.5"
Shin/Bond	NACA0012	Jul. 1991	21"	072291.003R	062091.001	130.3	67.1	22	265.07	4	3.5	1.00	20	6	18.5", 24", 36" & 53.5"
Shin/Bond	NACA0012	Jul. 1991	21"	072291.004R	062791.001	113	58.1	23	266.19	4	3.5	1.30	20	8	18.5", 24", 36" & 53.5"
Shin/Bond	NACA0012	Jul. 1991	21"	072391.001R	062791.003	113	58.1	30.2	270.19	4	3.5	1.30	20	8	18.5", 24", 36" & 53.5"
Shin/Bond	NACA0012	Jul. 1991	21"	072391.002R	062791.002	113	58.1	28.4	269.19	4	3.5	1.30	20	8	18.5", 24", 36" & 53.5"
Shin/Bond	NACA0012	Jul. 1991	21"	072391.003R	062791.004	113	58.1	17.6	263.19	4	3.5	1.30	20	8	18.5", 24", 36" & 53.5"
Shin/Bond	NACA0012	Jul. 1991	21"	072391.004R	062591.006	130.3	67.1	12	259.51	4	3.5	1.00	20	6	18.5", 36" & 53.5"
Shin/Bond	NACA0012	Jul. 1991	21"	072391.005R	062591.007	130.3	67.1	12	259.51	4	3.5	1.00	20	12	18.5", 24", 36" & 53.5"
Shin/Bond	NACA0012	Jul. 1991	21"	072391.006R	062791.005	113	58.1	10.4	259.19	4	3.5	1.30	20	8	18.5", 24", 36" & 53.5"
Shin/Bond	NACA0012	Jul. 1991	21"	072491.001R	062791.006	113	58.1	5	256.19	4	3.5	1.30	20	8	18.5", 24", 36" & 53.5"
Shin/Bond	NACA0012	Jul. 1991	21"	072491.002R	062791.007	113	58.1	-0.4	253.19	4	3.5	1.30	20	8	18.5", 24", 36" & 53.5"
Shin/Bond	NACA0012	Jul. 1991	21"	072491.003R	062791.008	113	58.1	-4	251.19	4	3.5	1.30	20	8	18.5", 24", 36" & 53.5"
Shin/Bond	NACA0012	Jul. 1991	21"	072491.004R	062591.008	130.3	67.1	1	253.40	4	3.5	1.00	20	6	18.5", 24", 36" & 53.5"
Shin/Bond	NACA0012	Jul. 1991	21"	072491.005R	062791.009	113	58.1	-14.8	245.19	4	3.5	1.30	20	8	18.5", 24", 36" & 53.5"
Shin/Bond	NACA0012	Jul. 1991	21"	072591.001R	062991.003	200	102.8	22	262.04	4	3.5	1.00	30	6	18.5", 24", 36" & 53.5"

NACA 0012 Test Conditions

Principal Investigator	Airfoil	Test Date	Chord (in)	Run Number	Previous Identical Run	Velocity (kts)	Velocity (m/s)	Tt (°F)	Static Tempurature (K)	A.O.A.	Corrected A.O.A.	LWC (g/m^3)	MVD (microns)	Spray Time (min)	Digitized Tracing Locations
Shin/Bond	NACA0012	Jul. 1991	21"	072591.002		200	102.8	22	262.04	4	3.5	1.30	30	6	18.5", 27", 36" & 53.5"
Shin/Bond	NACA0012	Jul. 1991	21"	072591.003		200	102.8	22	262.04	4	3.5	1.60	30	6	18.5", 24", 36" & 53.5"
Shin/Bond	NACA0012	Jul. 1991	21"	072591.004		200	102.8	22	262.04	4	3.5	1.80	30	6	18.5", 24", 36" & 53.5"
Shin/Bond	NACA0012	Jul. 1991	21"	072591.005R	062591.003	130.3	67.1	-15	244.51	4	3.5	1.00	20	6	18.5", 24", 36" & 53.5"
Shin/Bond	NACA0012	Jul. 1991	21"	072991.001R	325	130.3	67.1	25	266.74	4	3.5	1.00	20	6	18.5", 24", 36" & 53.5"
Shin/Bond	NACA0012	Jul. 1991	21"	072991.002R	423	130.3	67.1	22	265.07	4	3.5	1.00	20	6	18.5", 24", 36" & 53.5"
Shin/Bond	NACA0012	Jul. 1991	21"	073091.001R	062591.008	130.3	67.1	1	253.40	4	3.5	1.00	20	6	18.5", 24", 36" & 53.5"
Shin/Bond	NACA0012	Jul. 1991	21"	073091.002R	325	130.3	67.1	-15	244.51	4	3.5	1.00	20	6	18.5", 24", 36" & 53.5"
Shin/Bond	NACA0012	Jul. 1991	21"	073091.003R	325	130.3	67.1	-15	244.51	4	3.5	1.00	20	6	18.5", 24", 36" & 53.5"
Shin/Bond	NACA0012	Jul. 1991	21"	073091.005R	062991.003	200	102.8	22	262.04	4	3.5	1.00	30	6	24", 36", 48" & 53.5"
Shin/Bond	NACA0012	Jul. 1991	21"	073091.006R	072591.002	200	102.8	22	262.04	4	3.5	1.30	30	6	24", 36", 48" & 53.5"
Shin/Bond	NACA0012	Jul. 1991	21"	073191.001R	072591.004	200	102.8	22	262.04	4	3.5	1.80	30	6	24", 36", 48" & 53.5"
Shin/Bond	NACA0012	Jul. 1991	21"	073191.002R	072591.003	200	102.8	22	262.04	4	3.5	1.60	30	6	24", 36", 48" & 53.5"
Shin/Bond	NACA0012	Jul. 1991	21"	073191.003R	072591.002	200	102.8	22	262.04	4	3.5	1.30	30	6	24", 36", 48" & 53.5"
Shin/Bond	NACA0012	Jul. 1991	21"	073191.004R	421	130.3	67.1	28	268.40	4	3.5	1.00	20	6	18.5", 24", 36" & 53.5"
Shin/Bond	NACA0012	Aug. 1991	21"	080191.003		200	102.8	18	259.82	4	3.5	0.55	20	7	24", 36" & 48"
Shin/Bond	NACA0012	Aug. 1991	21"	080191.004R	404	200	102.8	12	256.49	4	3.5	0.55	20	7	24", 36", 48" & 53.5"
Shin/Bond	NACA0012	Aug. 1991	21"	080191.005R	403	200	102.8	22	262.04	4	3.5	0.55	20	7	24", 30", 36" & 48"
Shin/Bond	NACA0012	Aug. 1991	21"	080291.001R	401	200	102.8	28	265.37	4	3.5	0.55	20	7	24", 36" & 48"
Shin/Bond	NACA0012	Aug. 1991	21"	080291.002R	402	200	102.8	25	263.71	4	3.5	0.55	20	7	24", 36" & 48"
Shin/Bond	NACA0012	Aug. 1991	21"	080291.003		200	102.8	21	261.49	4	3.5	0.55	20	7	24", 36" & 48"
Shin/Bond	NACA0012	Aug. 1991	21"	080291.004R	080191.003	200	102.8	18	259.82	4	3.5	0.55	20	7	24", 36" & 48"
Shin/Bond	NACA0012	Aug. 1991	21"	080291.005R	062991.003	200	102.8	22	262.04	4	3.5	1.00	30	6	24", 36" & 48"
Shin/Bond	NACA0012	Aug. 1991	21"	080291.006R	404	200	102.8	12	256.49	4	3.5	0.55	20	7	24", 36" & 48"
Shin/Bond	NACA0012	Aug. 1991	21"	080291.007R	405	200	102.8	1	250.37	4	3.5	0.55	20	7	24", 36" & 48"
Shin/Bond	NACA0012	Aug. 1991	21"	080291.008R	405	200	102.8	1	250.37	4	3.5	0.55	20	7	24", 36" & 48"
Shin/Bond	NACA0012	Aug. 1991	21"	080291.009		200	102.8	-15	241.49	4	3.5	0.55	20	7	24", 36" & 48"
Shin/Bond	NACA0012	Aug. 1991	21"	080391.001R	401	200	102.8	28	265.37	4	3.5	0.55	20	7	24", 36" & 48"
Shin/Bond	NACA0012	Aug. 1991	21"	080391.002R	402	200	102.8	25	263.71	4	3.5	0.55	20	7	24", 36" & 48"
Shin/Bond	NACA0012	Aug. 1991	21"	080391.003R	403	200	102.8	22	262.04	4	3.5	0.55	20	7	24", 36" & 48"
Shin/Bond	NACA0012	Aug. 1991	21"	080391.004R	403	200	102.8	22	262.04	4	3.5	0.55	20	7	24", 36" & 48"
Shin/Bond	NACA0012	Aug. 1991	21"	080391.005R	403	200	102.8	22	262.04	4	3.5	0.55	20	7	24", 36" & 48"
Shin/Bond	NACA0012	Aug. 1991	21"	080391.006R	62991.003	200	102.8	22	262.04	4	3.5	1.00	30	6	24", 36", 48" & 53.5"
Shin/Bond	NACA0012	Aug. 1991	21"	080391.007R	404	200	102.8	12	256.49	4	3.5	0.55	20	7	24", 36" & 48"
Shin/Bond	NACA0012	Aug. 1991	21"	080391.008R	080291.009	200	102.8	-15	241.49	4	3.5	0.55	20	7	24", 36" & 48"
Shin/Bond	NACA0012	Aug. 1991	21"	080391.009R	080291.009	200	102.8	-15	241.49	4	3.5	0.55	20	7	24", 36" & 48"

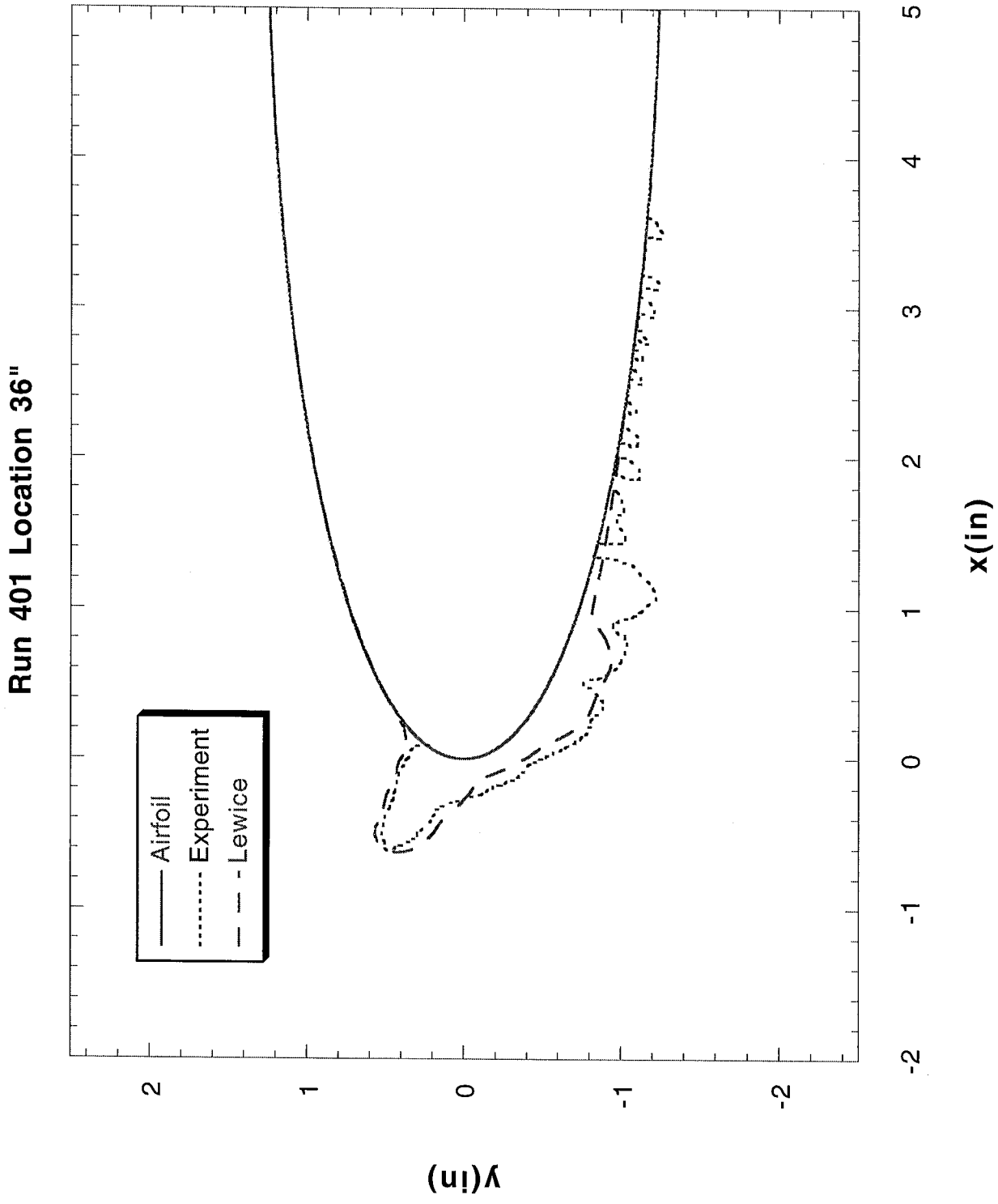
Run 401 Location 36"
Airfoil
Experiment
Lewice
y(in)
x(in)
2
1
0
-1
-2
-2
-1
0
1
2
3
4
5

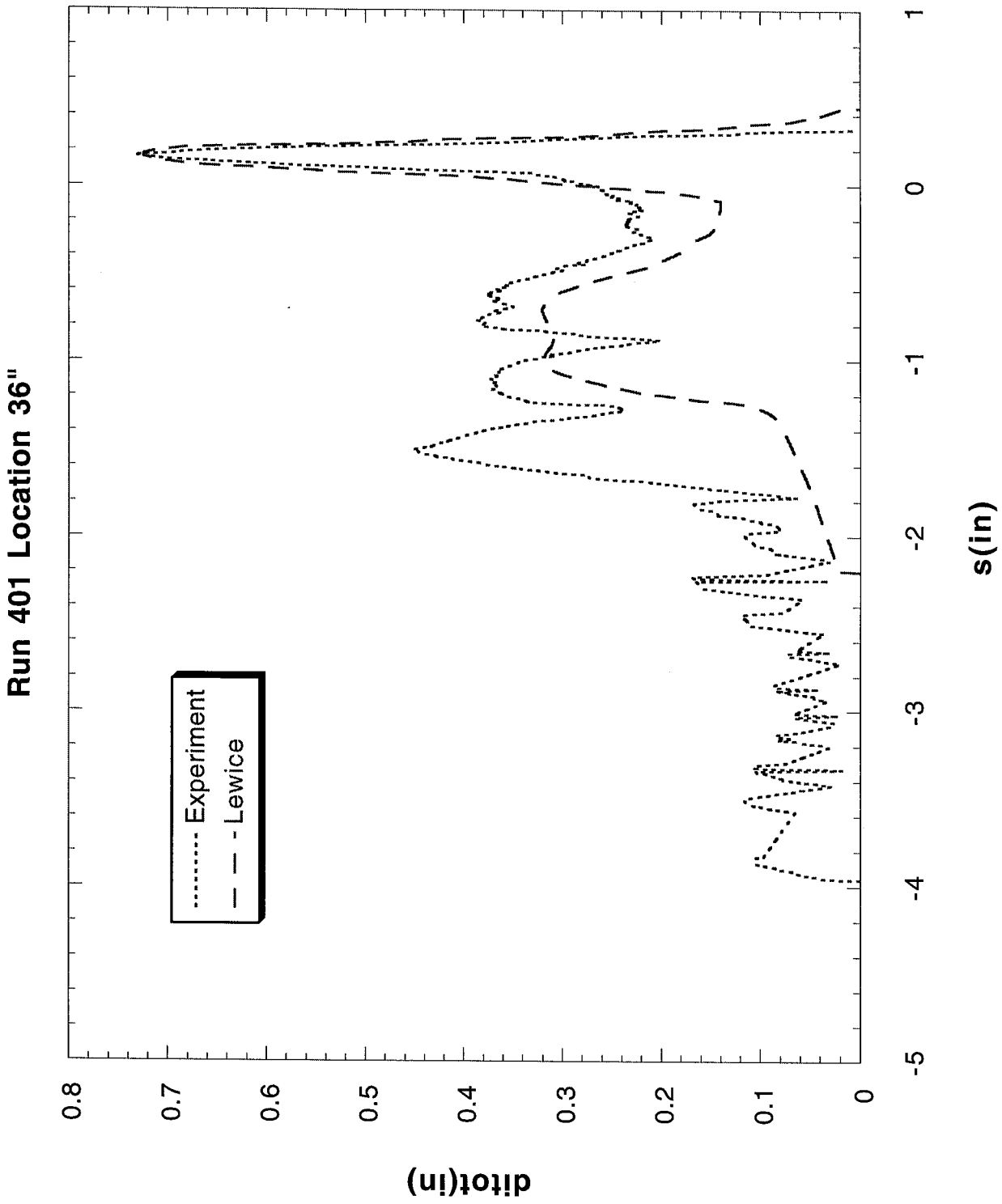
Run 401 Location 36"
Experiment
Lewice
dltot(in)
s(in)
0.8
0.7
0.6
0.5
0.4
0.3
0.2
0.1
0
-5
-4
-3
-2
-1
0
1

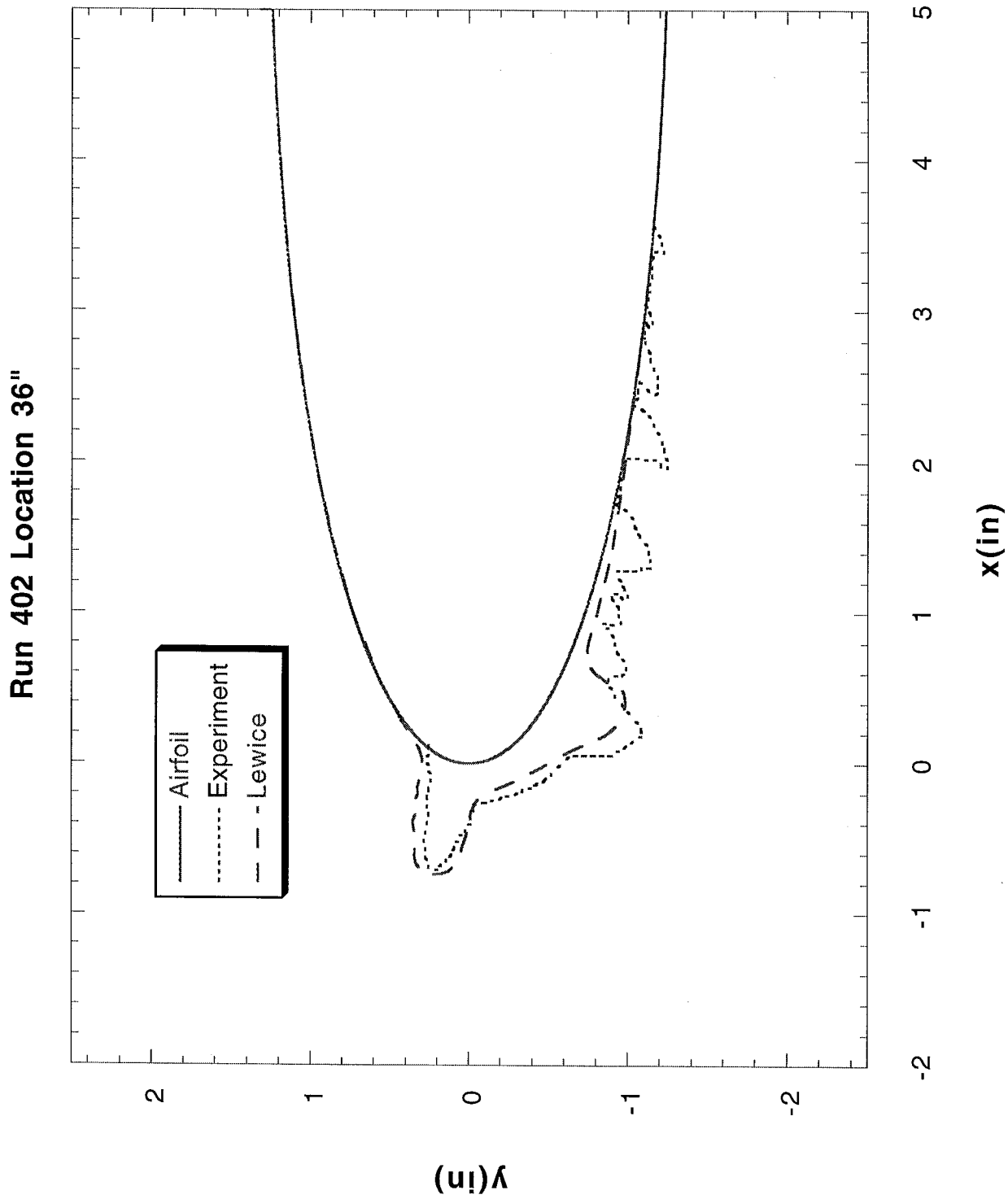
Run 402 Location 36"
Airfoil
Experiment
Lewice
y(in)
x(in)
2
1
0
-1
-2
-2
-1
0
1
2
3
4
5

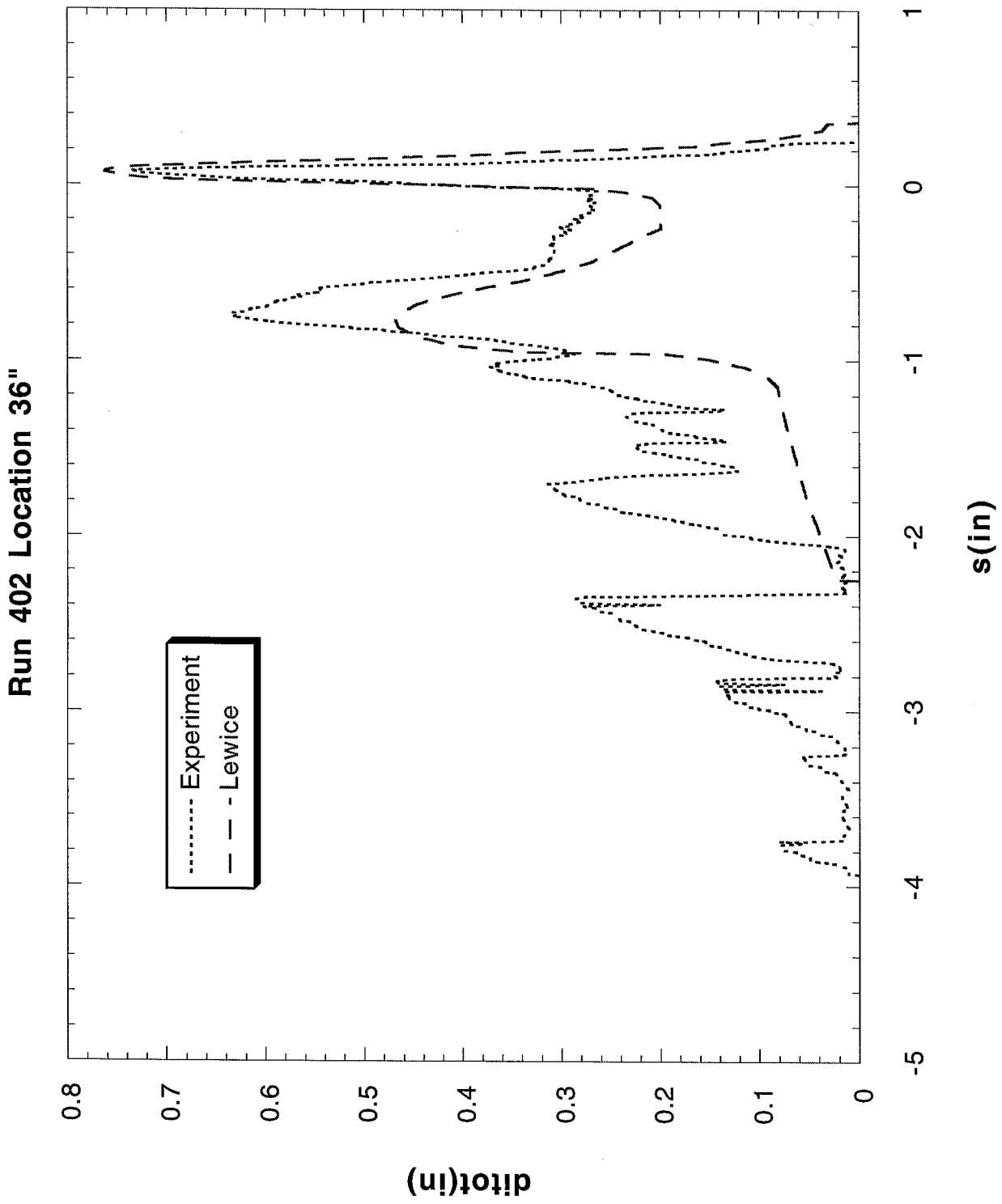
Run 402 Location 36"
Experiment
Lewice
dltot(in)
s(in)
0.8
0.7
0.6
0.5
0.4
0.3
0.2
0.1
0
-5
-4
-3
-2
-1
0
1

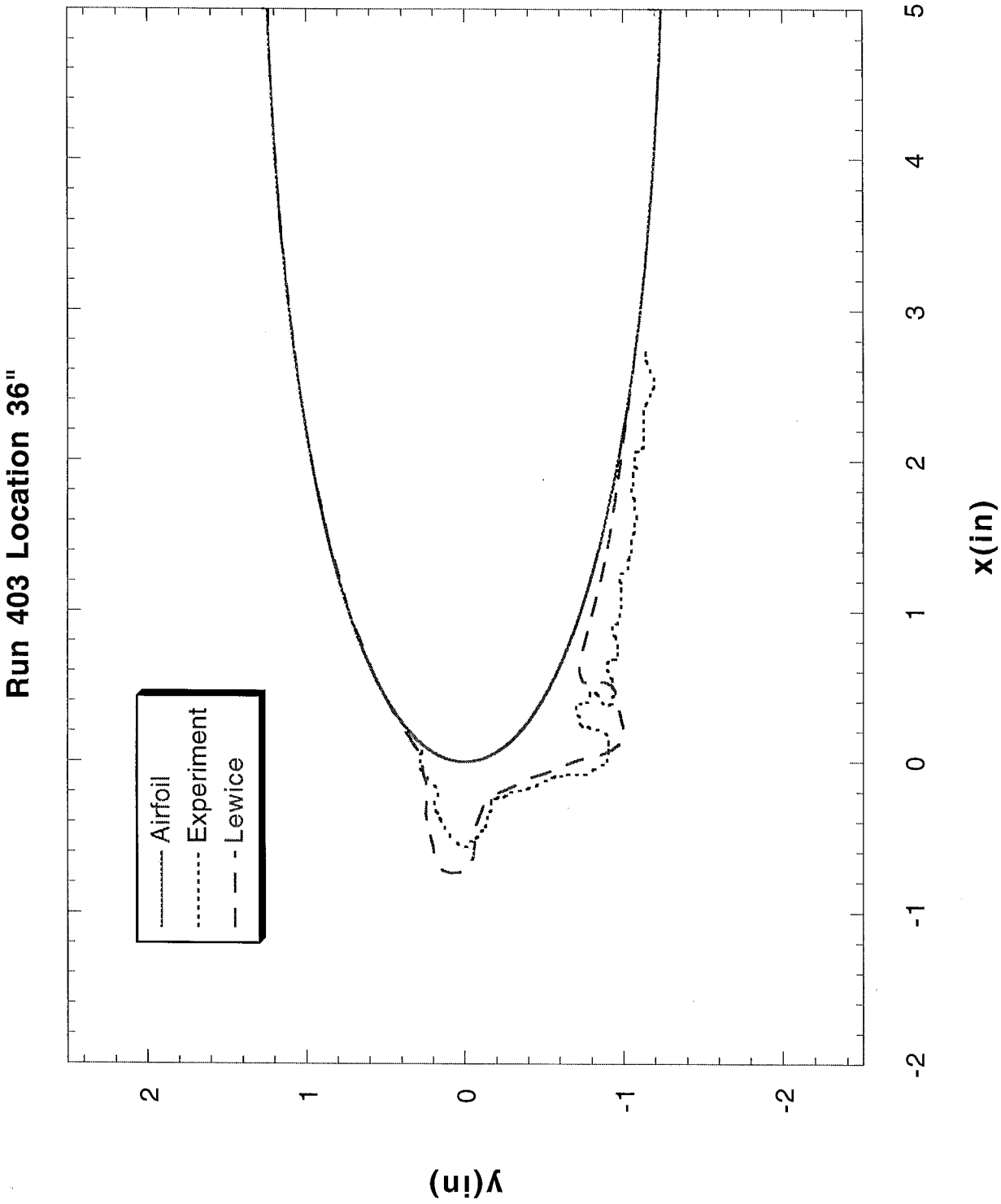
Run 403 Location 36"
Airfoil
Experiment
Lewice
y(in)
x(in)
2
1
0
-1
-2
-2
-1
0
1
2
3
4
5

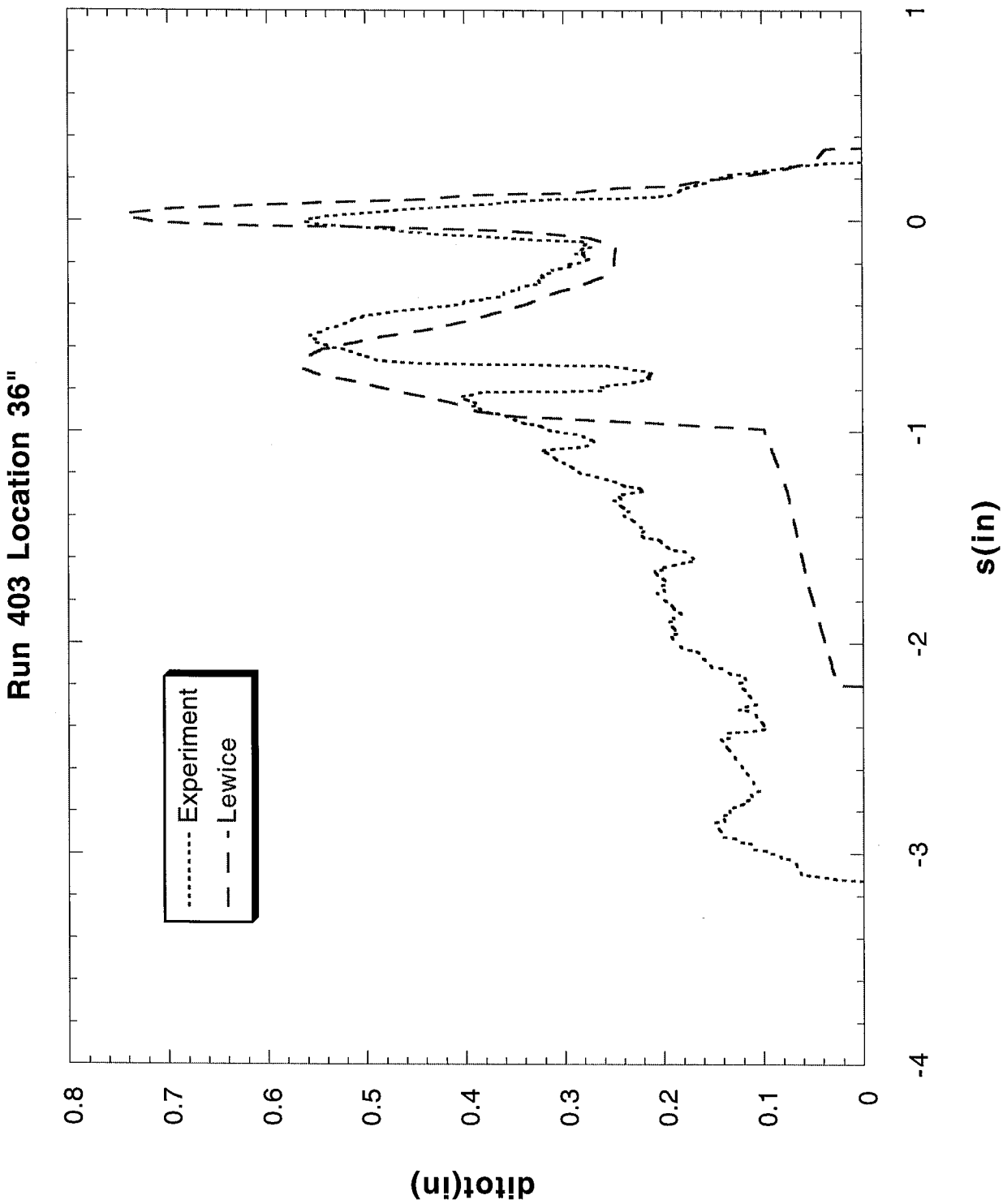
Run 403 Location 36"
Experiment
Lewice
dltot(in)
s(in)
0.8
0.7
0.6
0.5
0.4
0.3
0.2
0.1
0
-4
-3
-2
-1
0
1

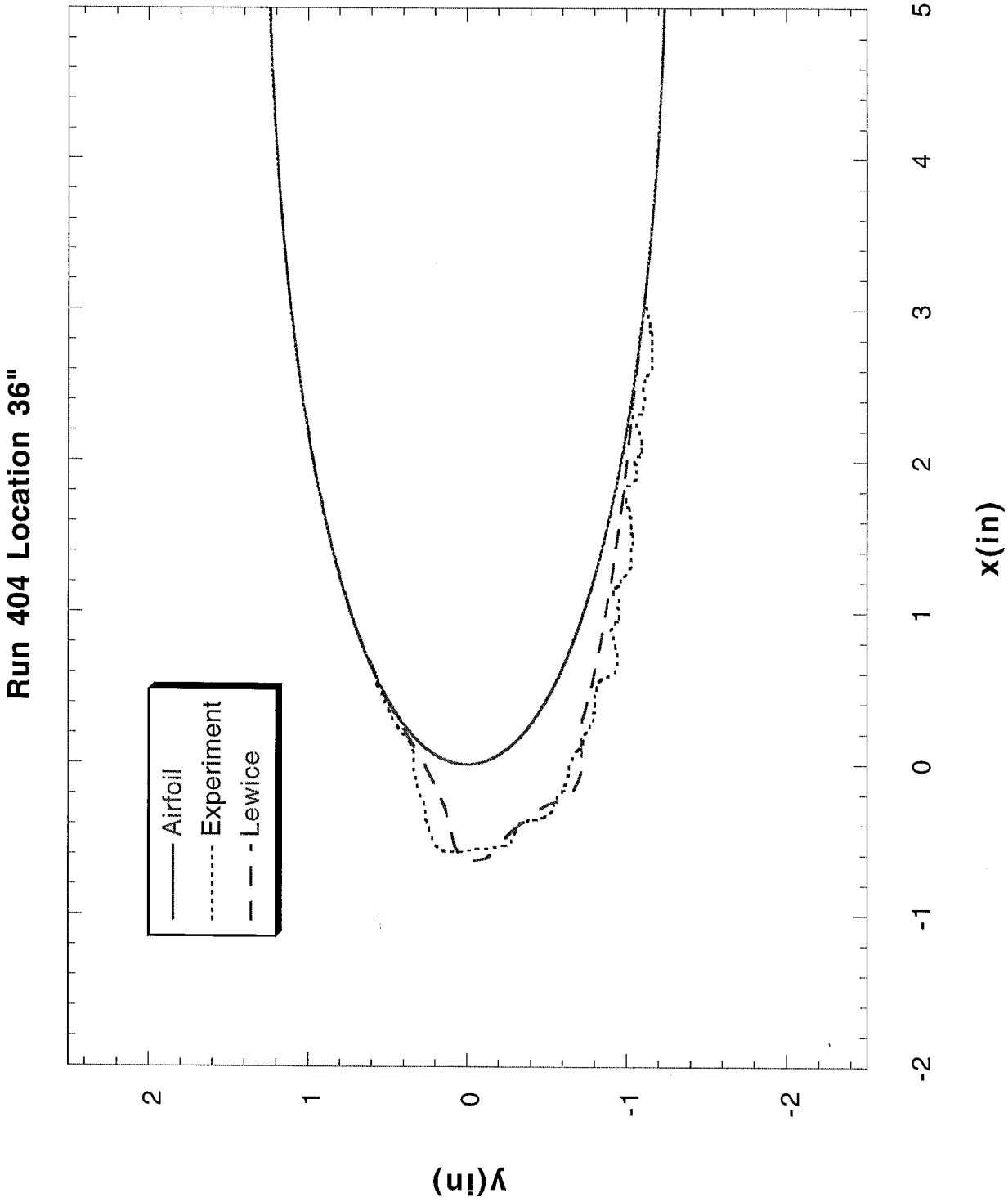
Run 404 Location 36"
Airfoil
Experiment
Lewice
y(in)
x(in)
2
1
0
-1
-2
-2
-1
0
1
2
3
4
5

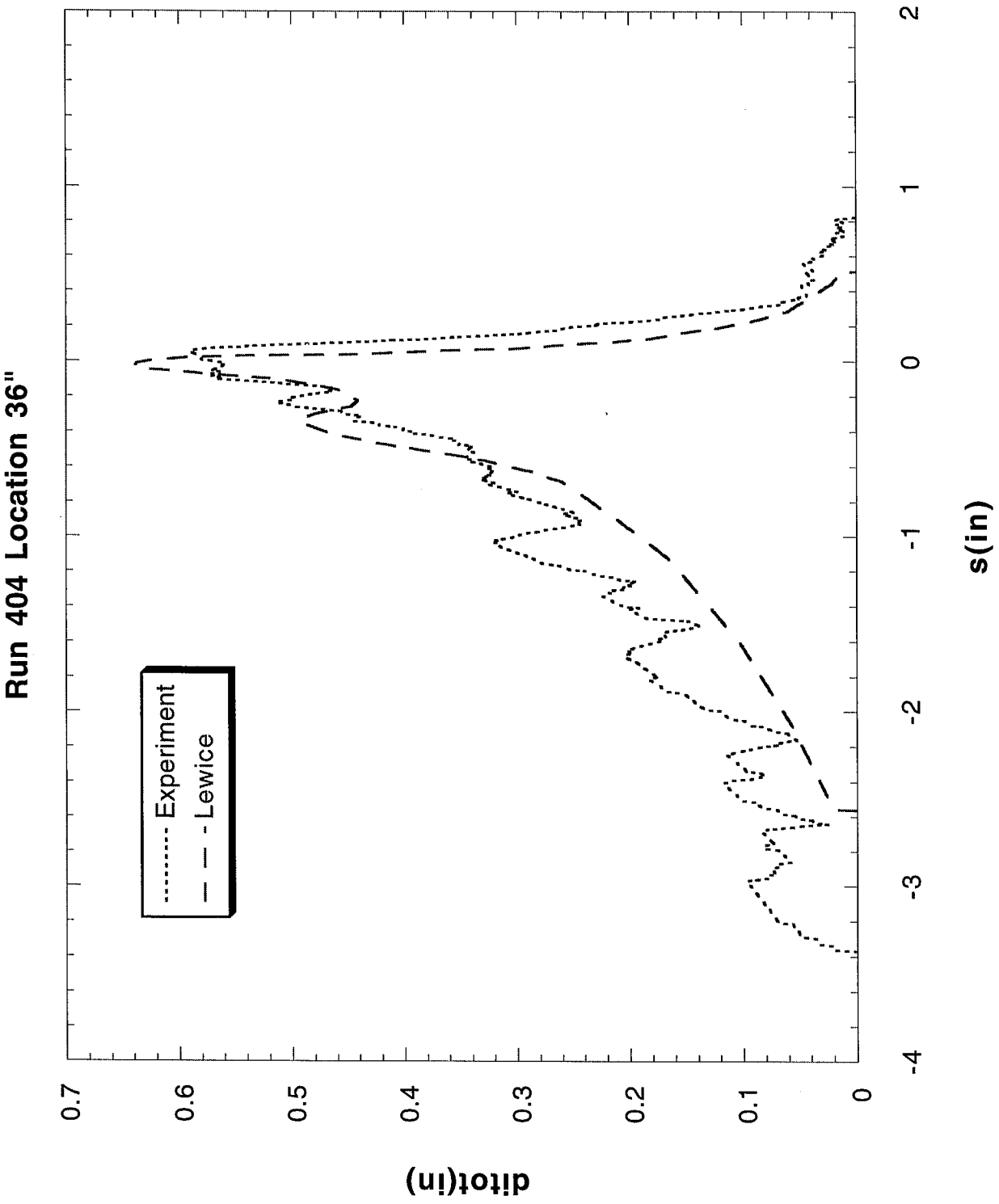
Run 404 Location 36"
Experiment
Lewice
ditot(in)
0.7
0.6
0.5
0.4
0.3
0.2
0.1
0
s(in)
-4
-3
-2
-1
0
1
2

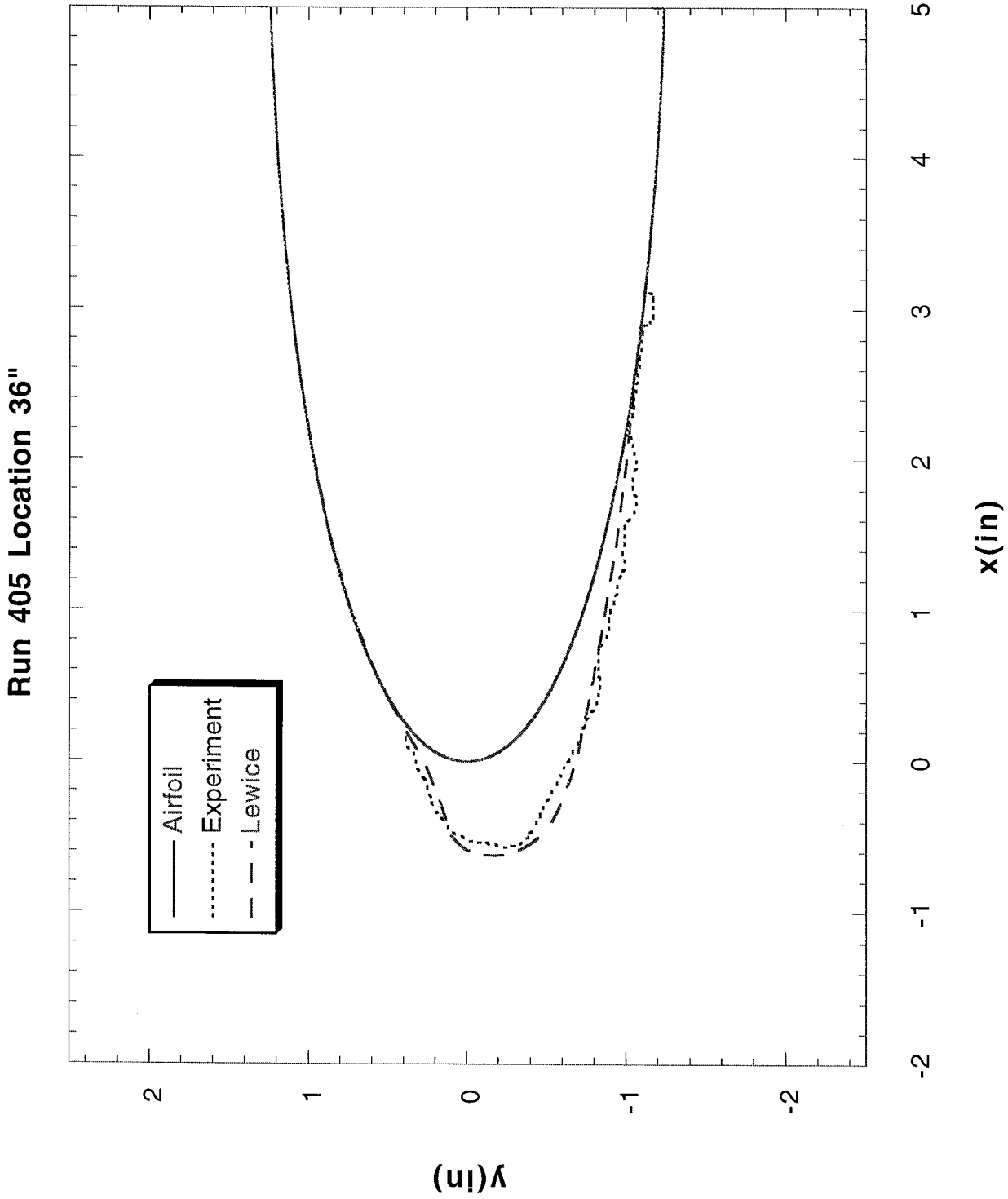
Run 405 Location 36"
Airfoil
Experiment
- - Lewice
y(in)
x(in)
2
1
0
-1
-2
-2
-1
0
1
2
3
4
5

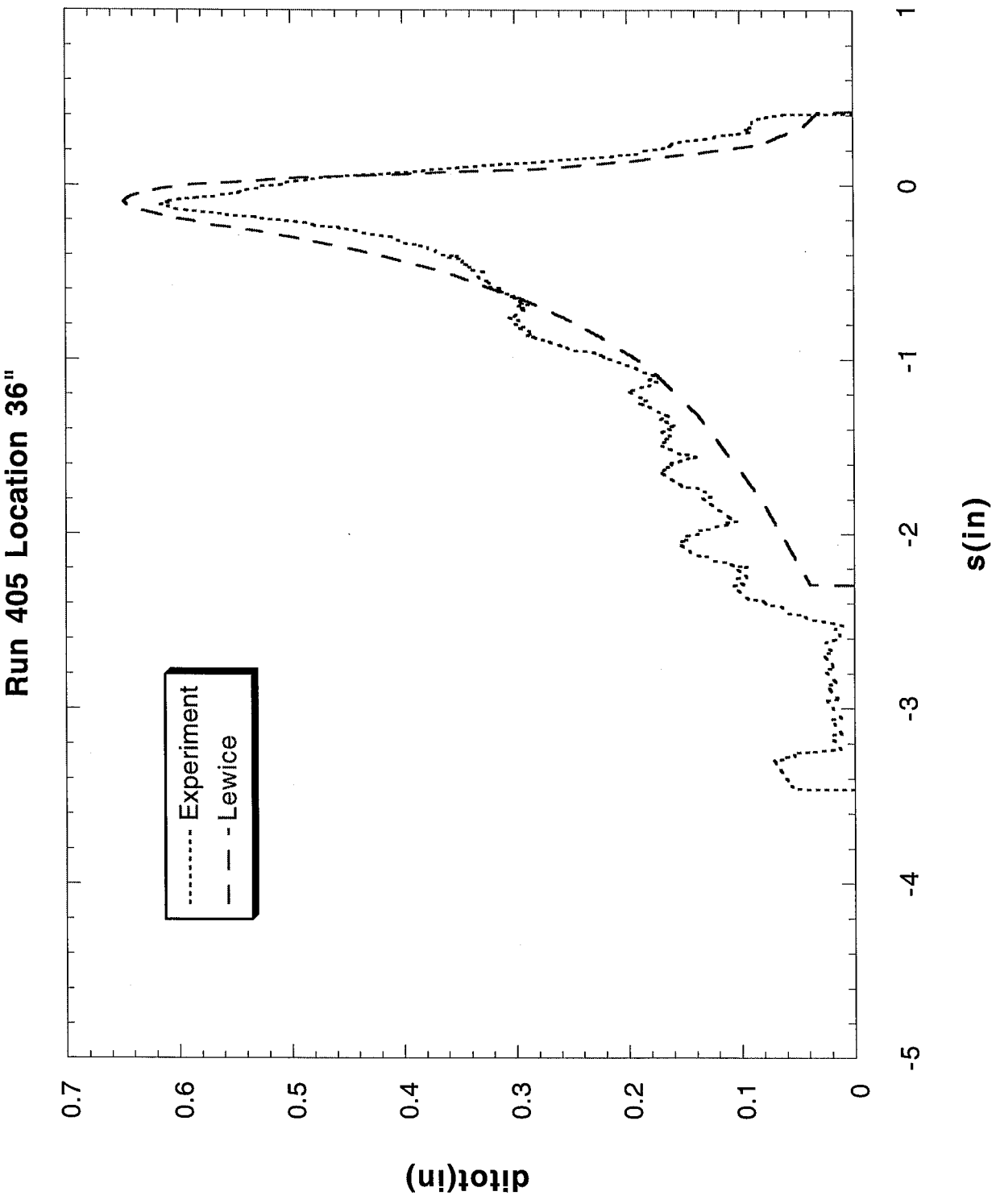
Run 405 Location 36"
Experiment
Lewice
dltot(in)
s(in)
0.7
0.6
0.5
0.4
0.3
0.2
0.1
0
-5
-4
-3
-2
-1
0
1

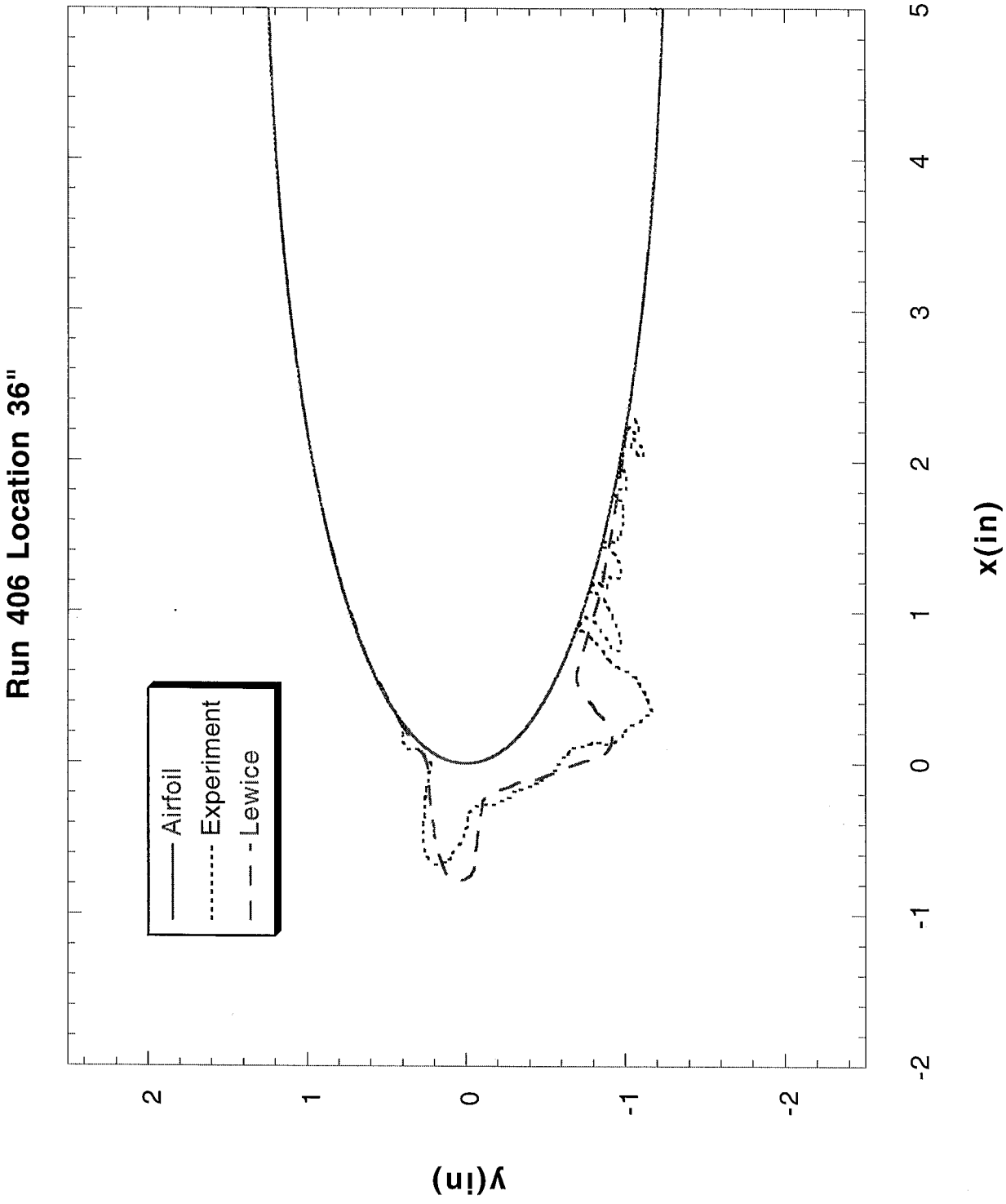
Run 406 Location 36"
Airfoil
Experiment
Lewice
y(in)
x(in)
2
1
0
-1
-2
-2
-1
0
1
2
3
4
5

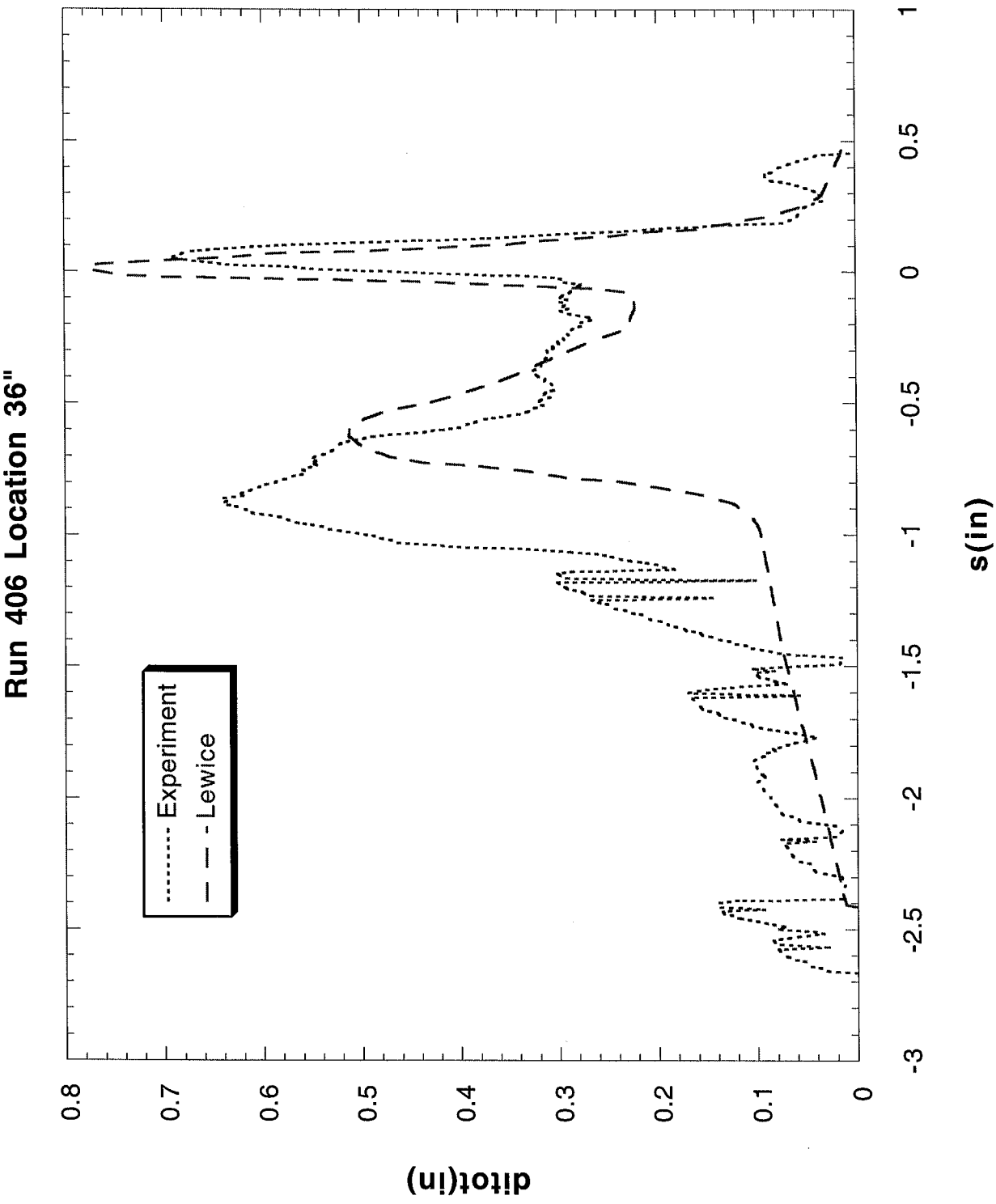
Run 406 Location 36"
Experiment
Lewice
dltot(in)
s(in)
0.8
0.7
0.6
0.5
0.4
0.3
0.2
0.1
0
-3
-2.5
-2
-1.5
-1
-0.5
0
0.5
1

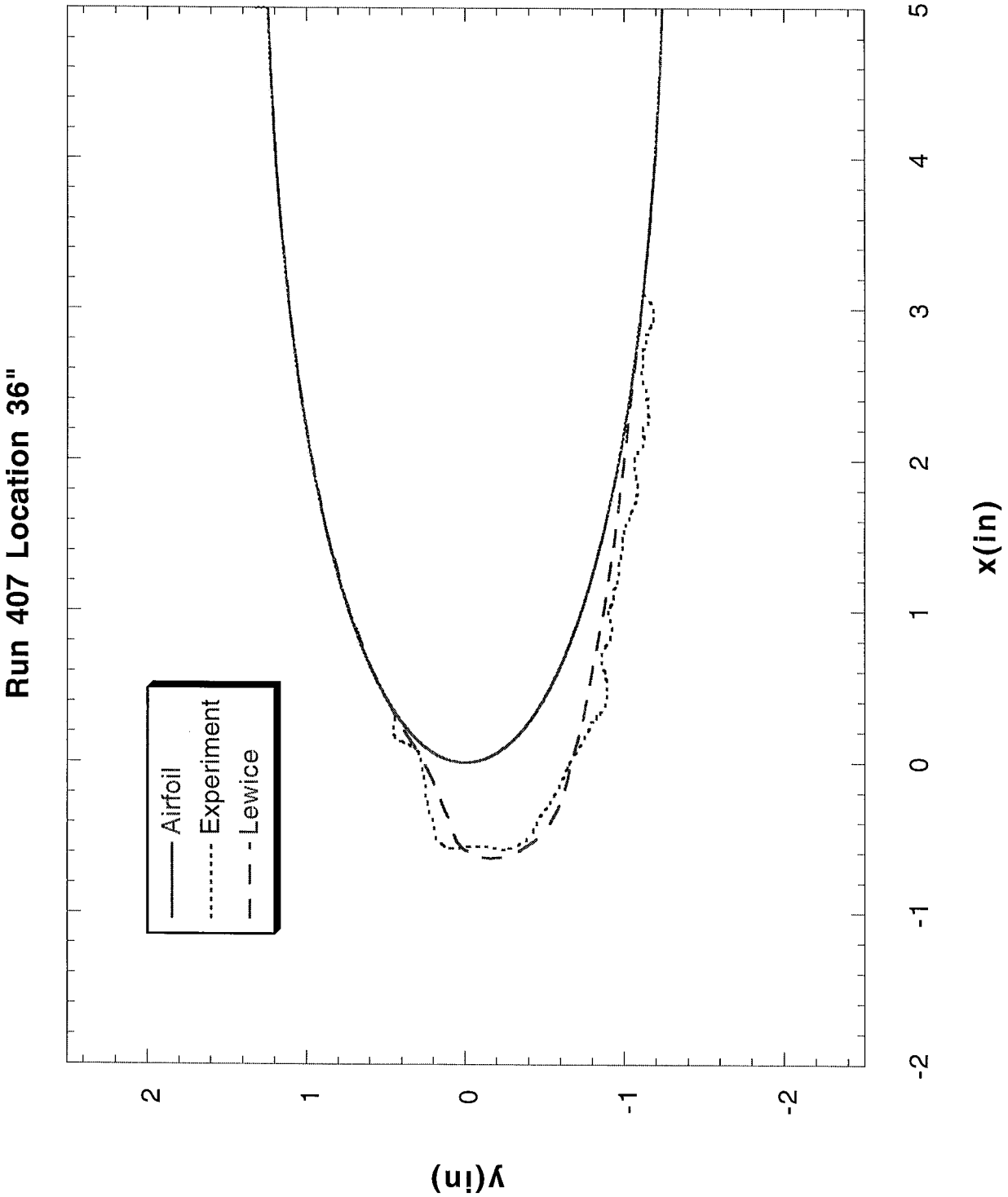
Run 407 Location 36"
Airfoil
Experiment
- Lewice
y(in)
x(in)
2
1
0
-1
-2
-2
-1
0
1
2
3
4
5

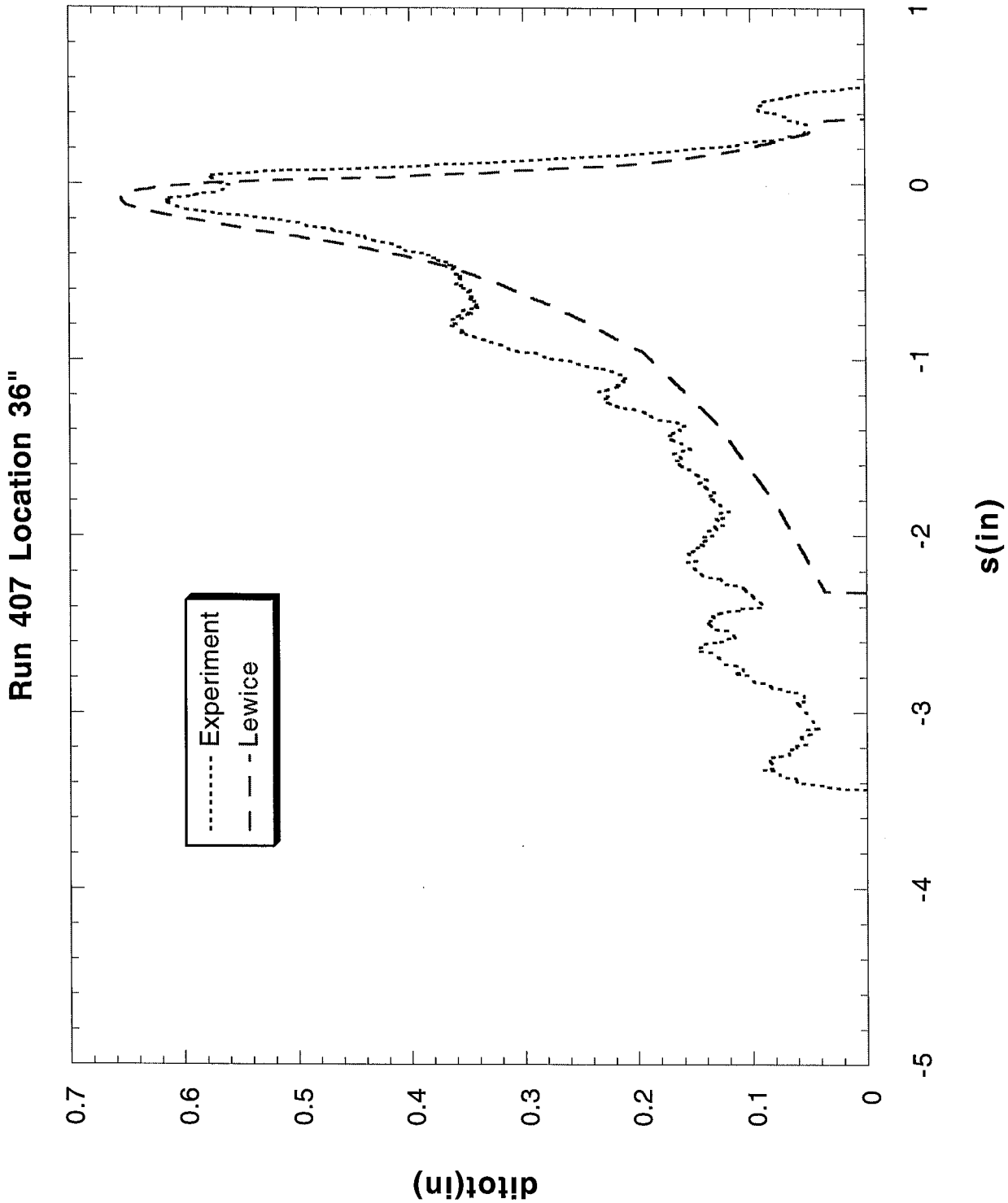
Run 407 Location 36"
Experiment
Lewice
dltot(in)
s(in)
0.7
0.6
0.5
0.4
0.3
0.2
0.1
0
-5
-4
-3
-2
-1
0
1

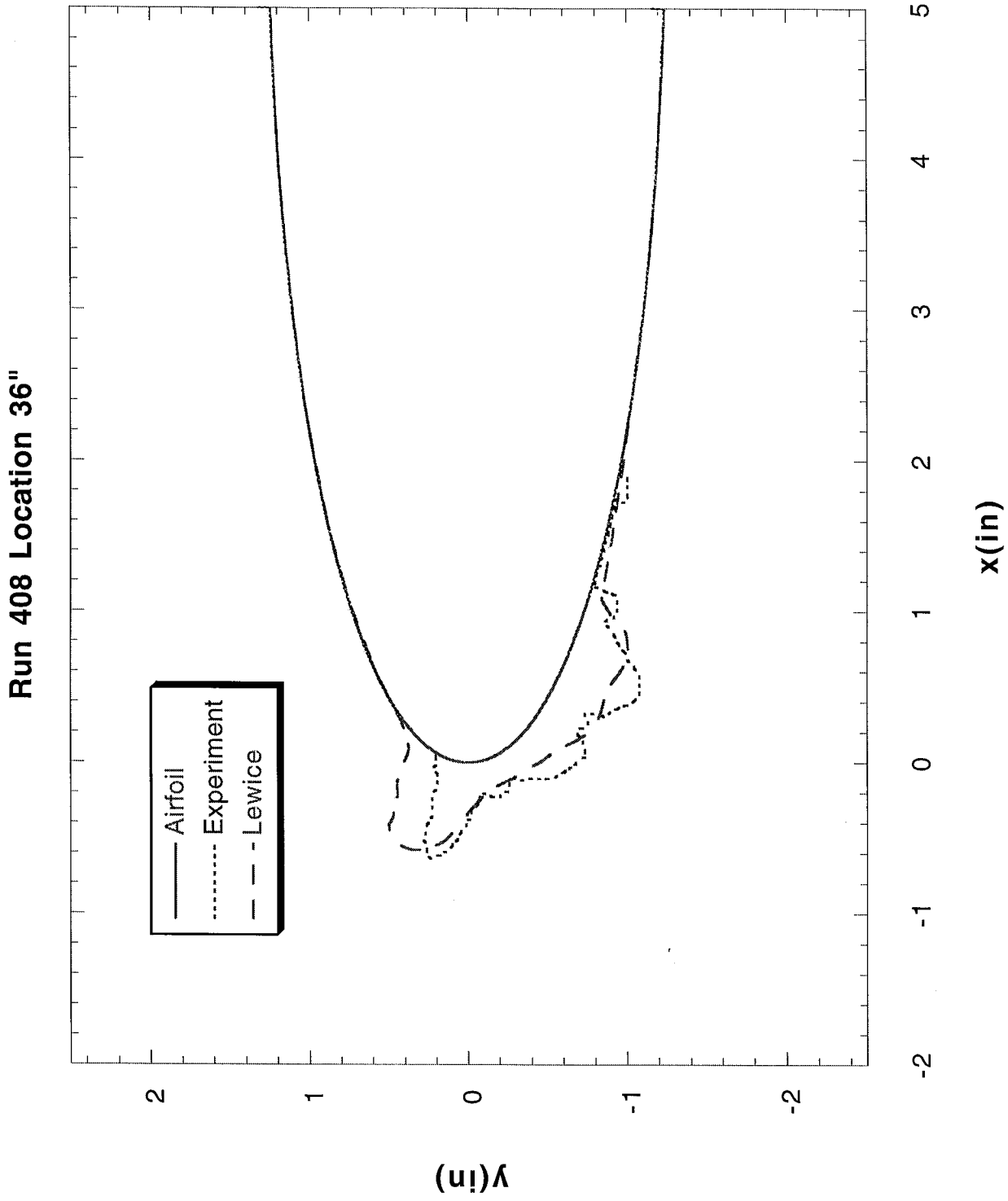
Run 408 Location 36"
Airfoil
Experiment
Lewice
y(in)
x(in)
2
1
0
-1
-2
-2
-1
0
1
2
3
4
5

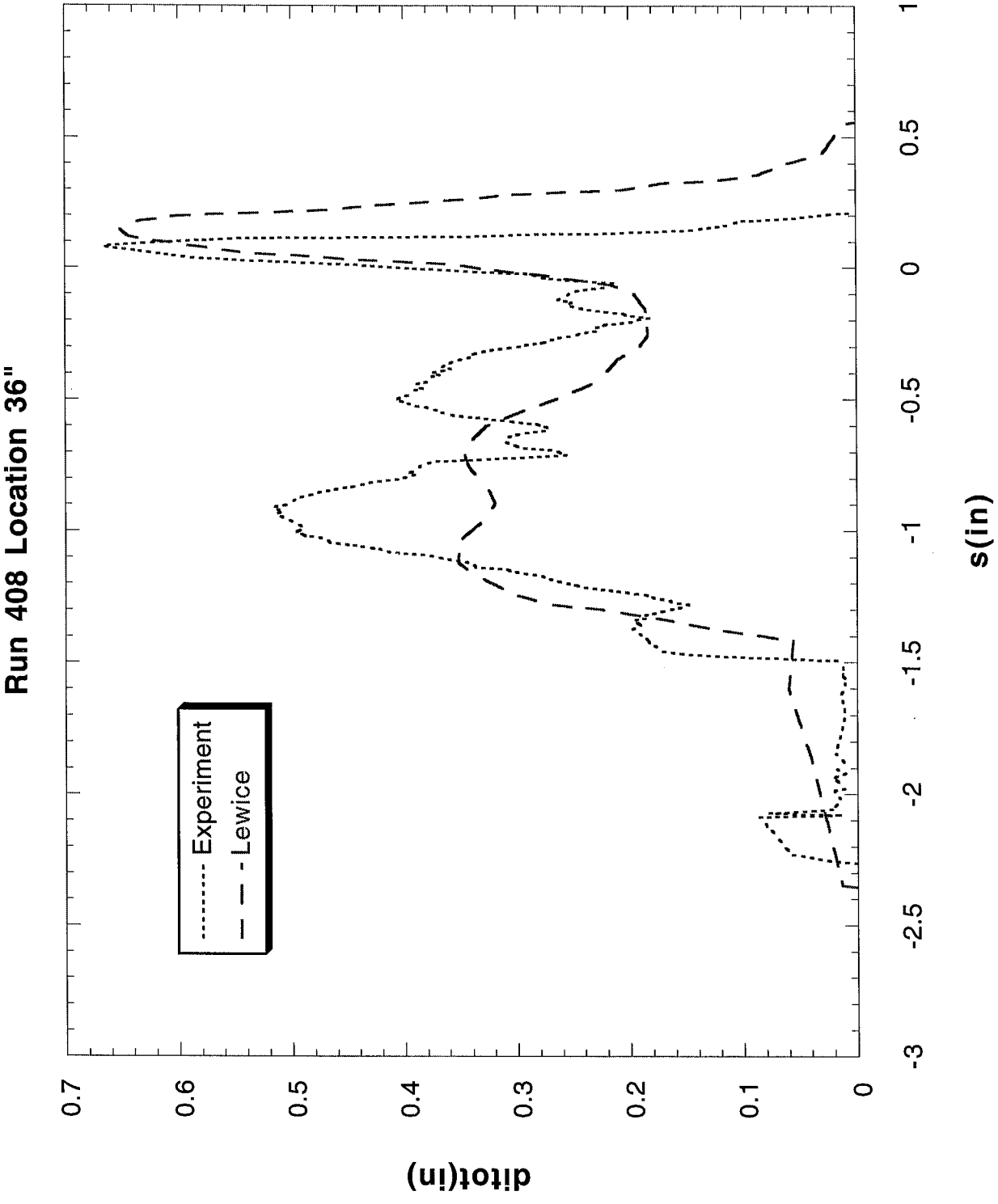
Run 408 Location 36"
Experiment
Lewice
dltot(in)
s(in)
0
0.1
0.2
0.3
0.4
0.5
0.6
0.7
-3
-2.5
-2
-1.5
-1
-0.5
0
0.5
1

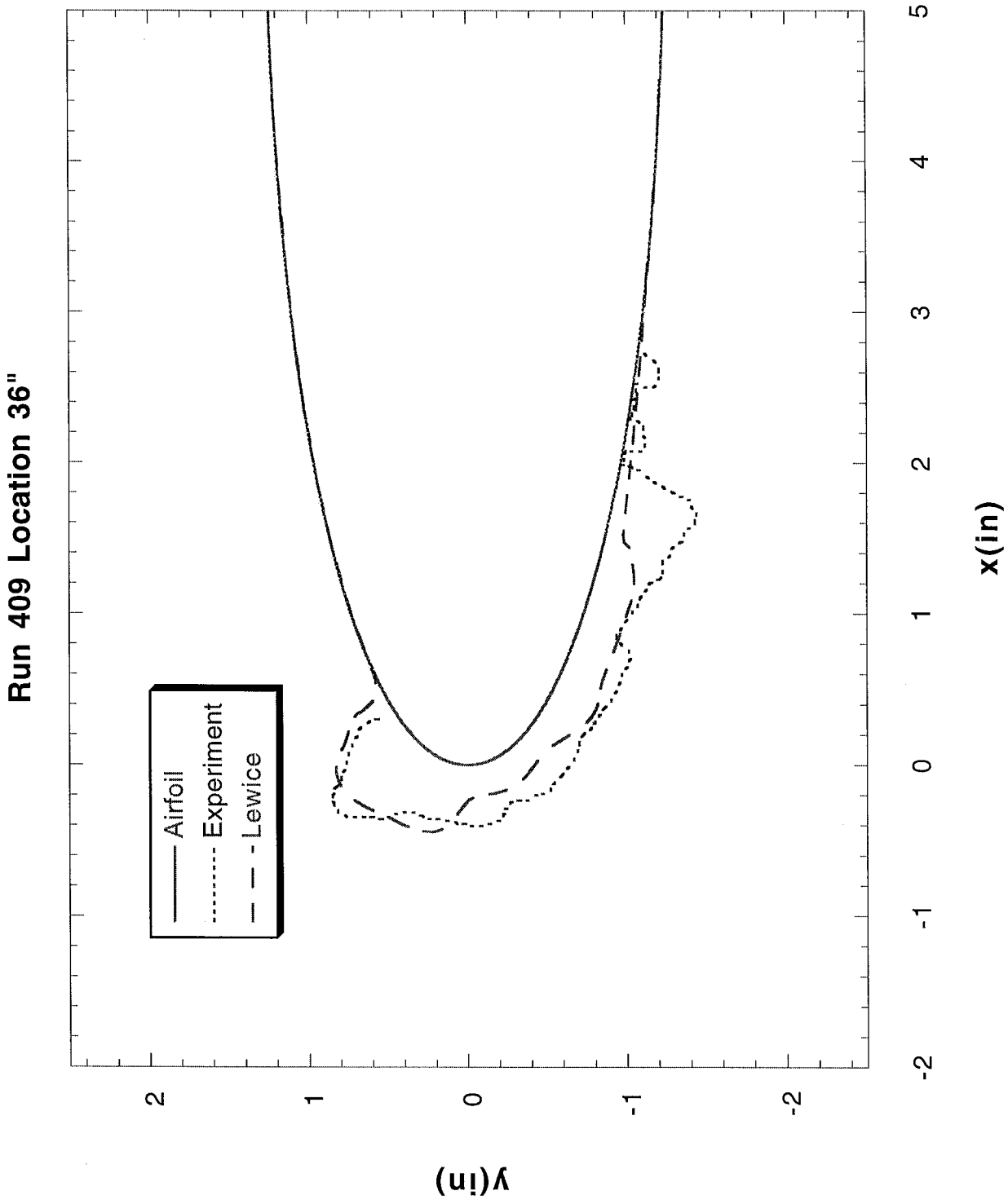
Run 409 Location 36"
Airfoil
Experiment
Lewice
y(in)
x(in)
2
1
0
-1
-2
-2
-1
0
1
2
3
4
5

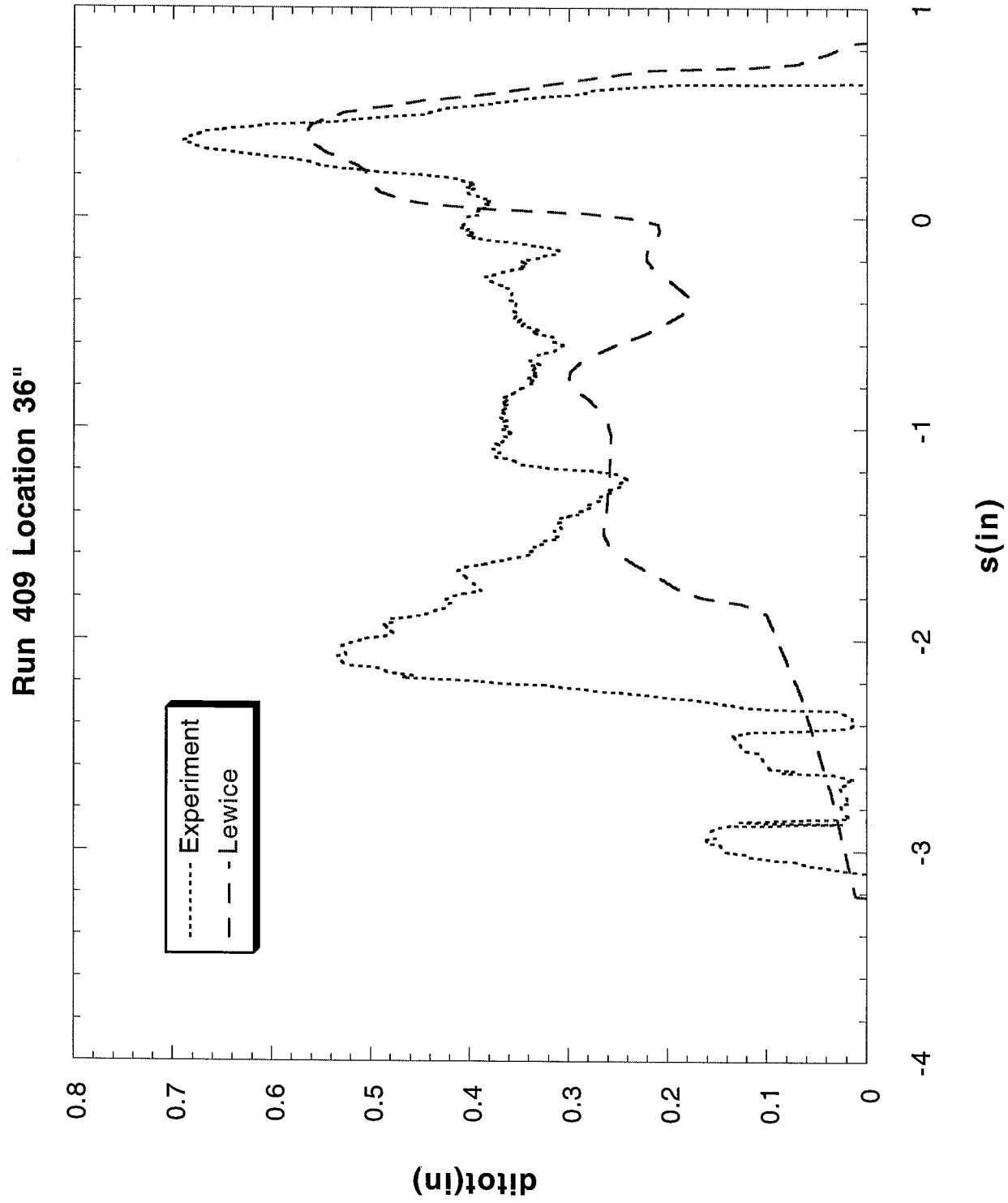
Run 409 Location 36"
Experiment
Lewice
dltot(in)
s(in)
0.8
0.7
0.6
0.5
0.4
0.3
0.2
0.1
0
-4
-3
-2
-1
0
1

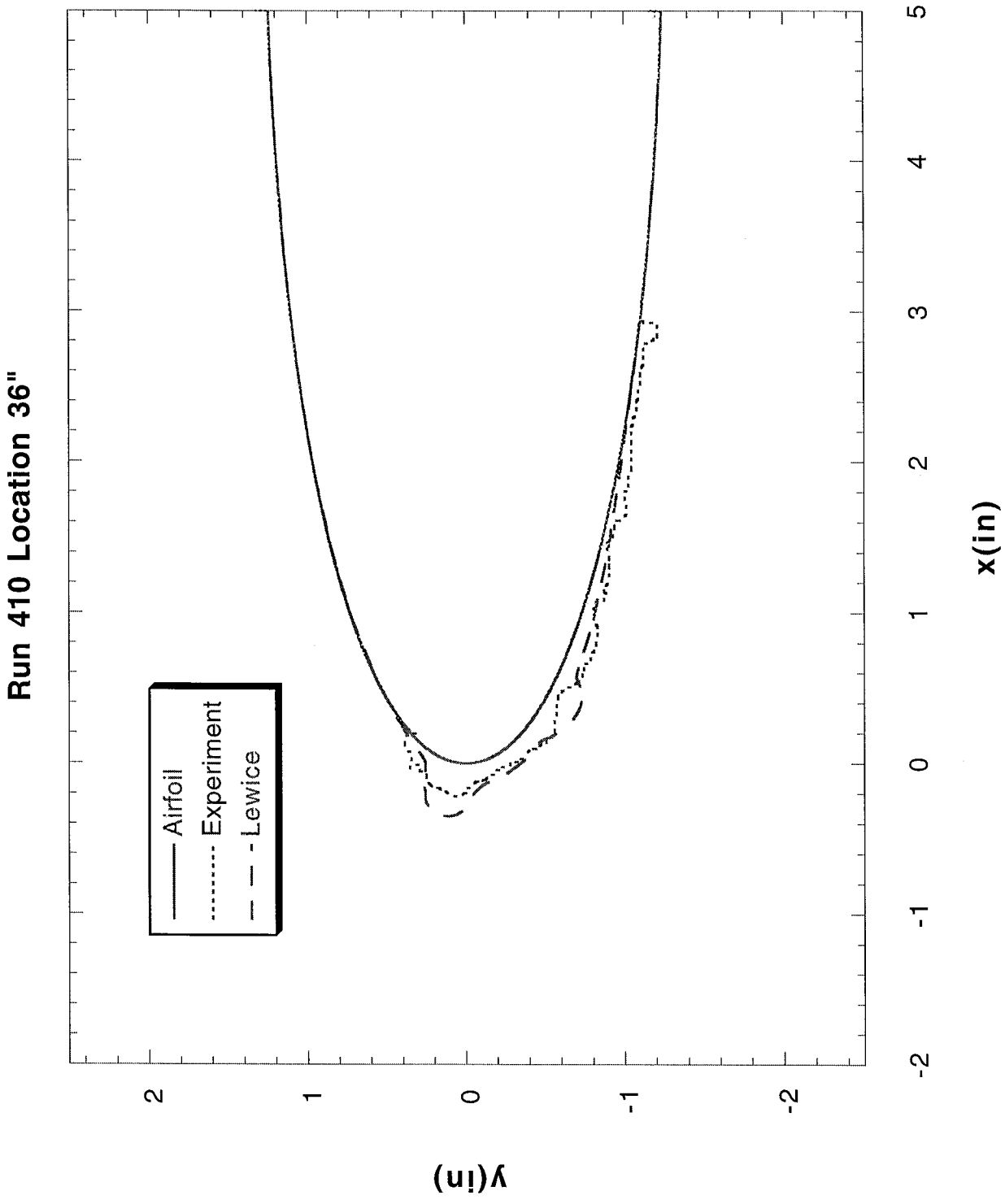
Run 410 Location 36"
Airfoil
Experiment
Lewice
y(in)
x(in)
2
1
0
-1
-2
-2
-1
0
1
2
3
4
5

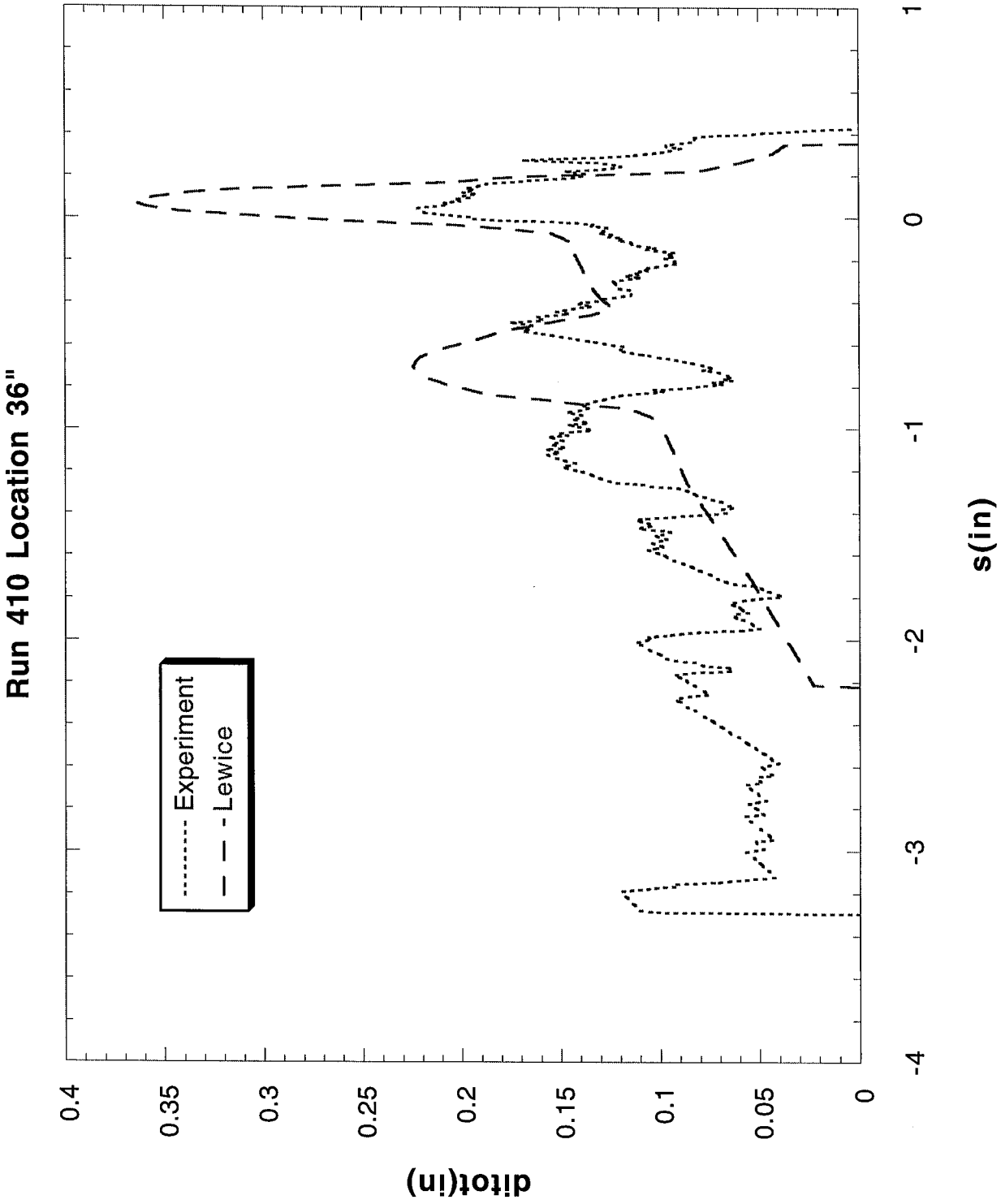
Run 410 Location 36"
Experiment
Lewice
ditot(in)
s(in)
0.4
0.35
0.3
0.25
0.2
0.15
0.1
0.05
0
-4
-3
-2
-1
0
1

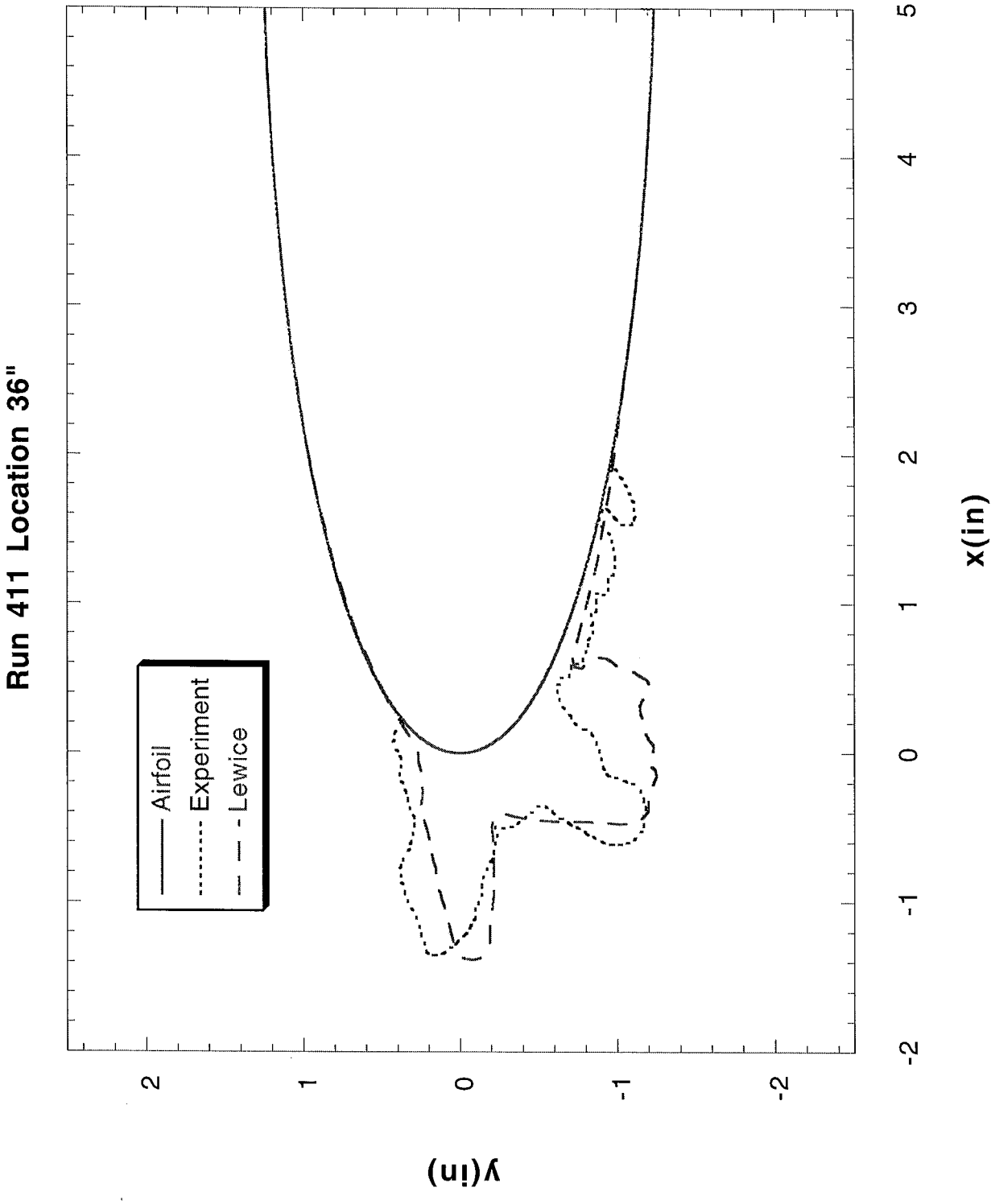
Run 411 Location 36"
Airfoil
Experiment
Lewice
y(in)
x(in)
2
1
0
-1
-2
-2
-1
0
1
2
3
4
5

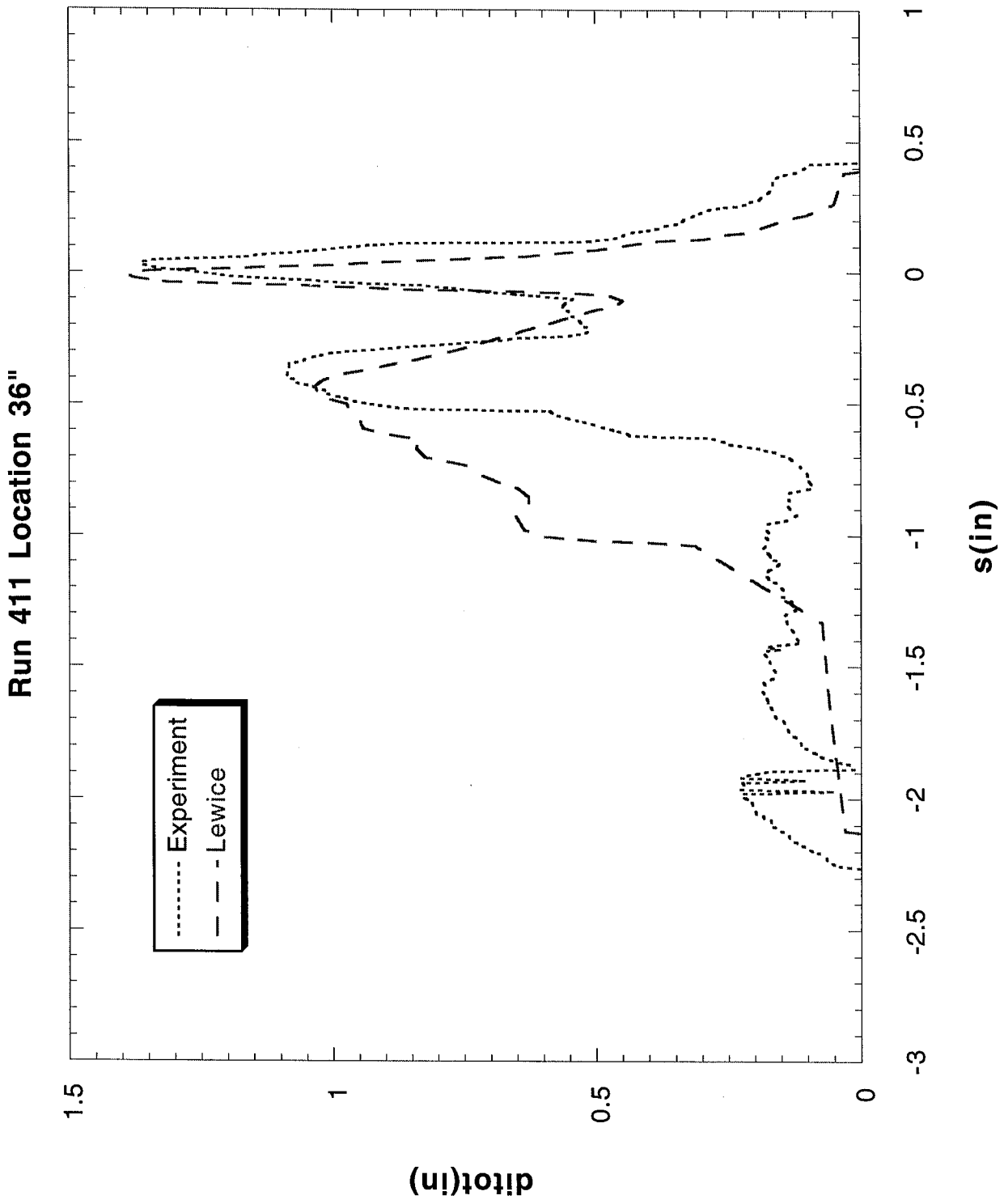
Run 411 Location 36"
Experiment
Lewice
ditot(in)
s(in)
1.5
1
0.5
0
-3
-2.5
-2
-1.5
-1
-0.5
0
0.5
1

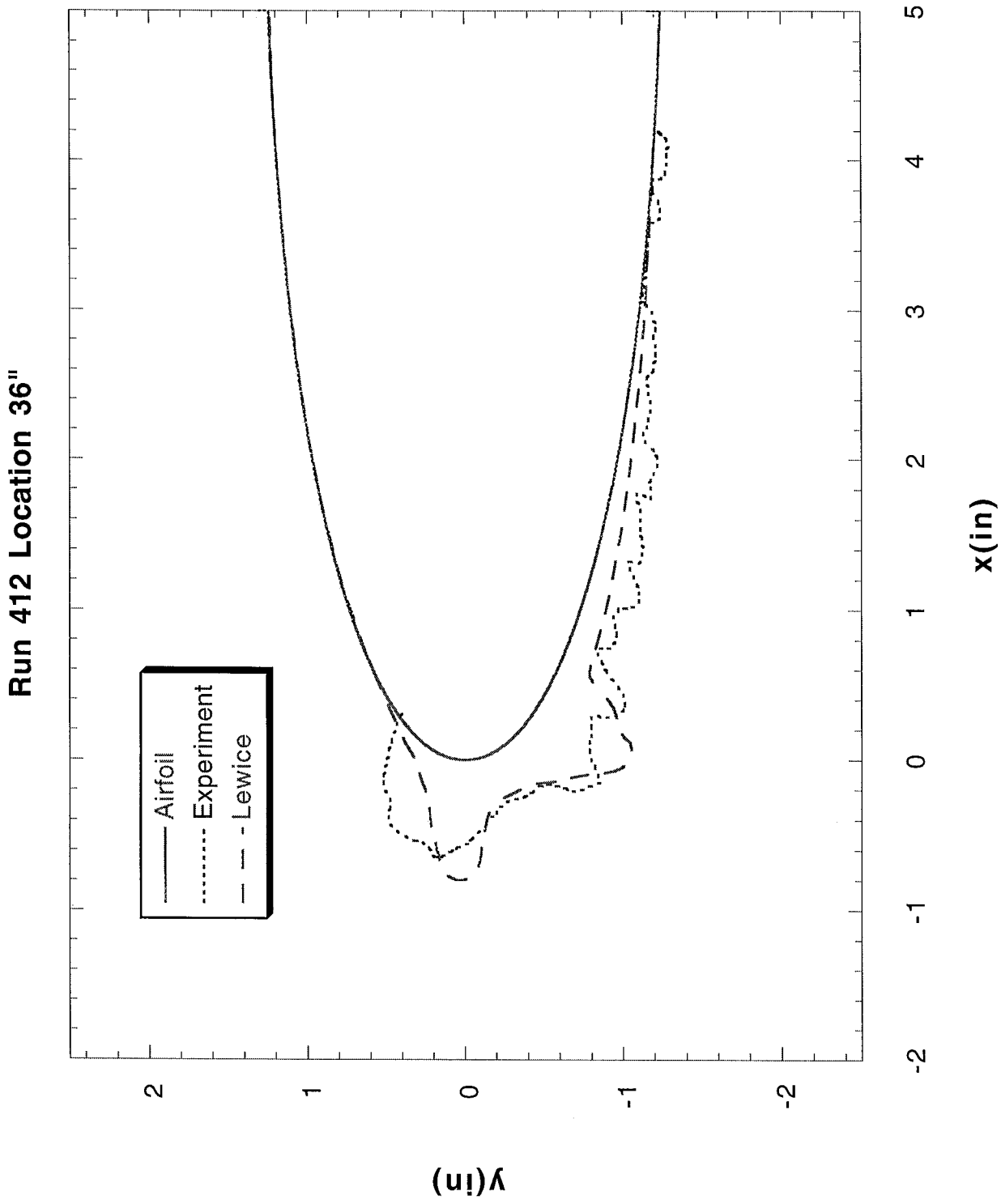
Run 412 Location 36"
Airfoil
Experiment
Lewice
y(in)
x(in)
2
1
0
-1
-2
-2
-1
0
1
2
3
4
5

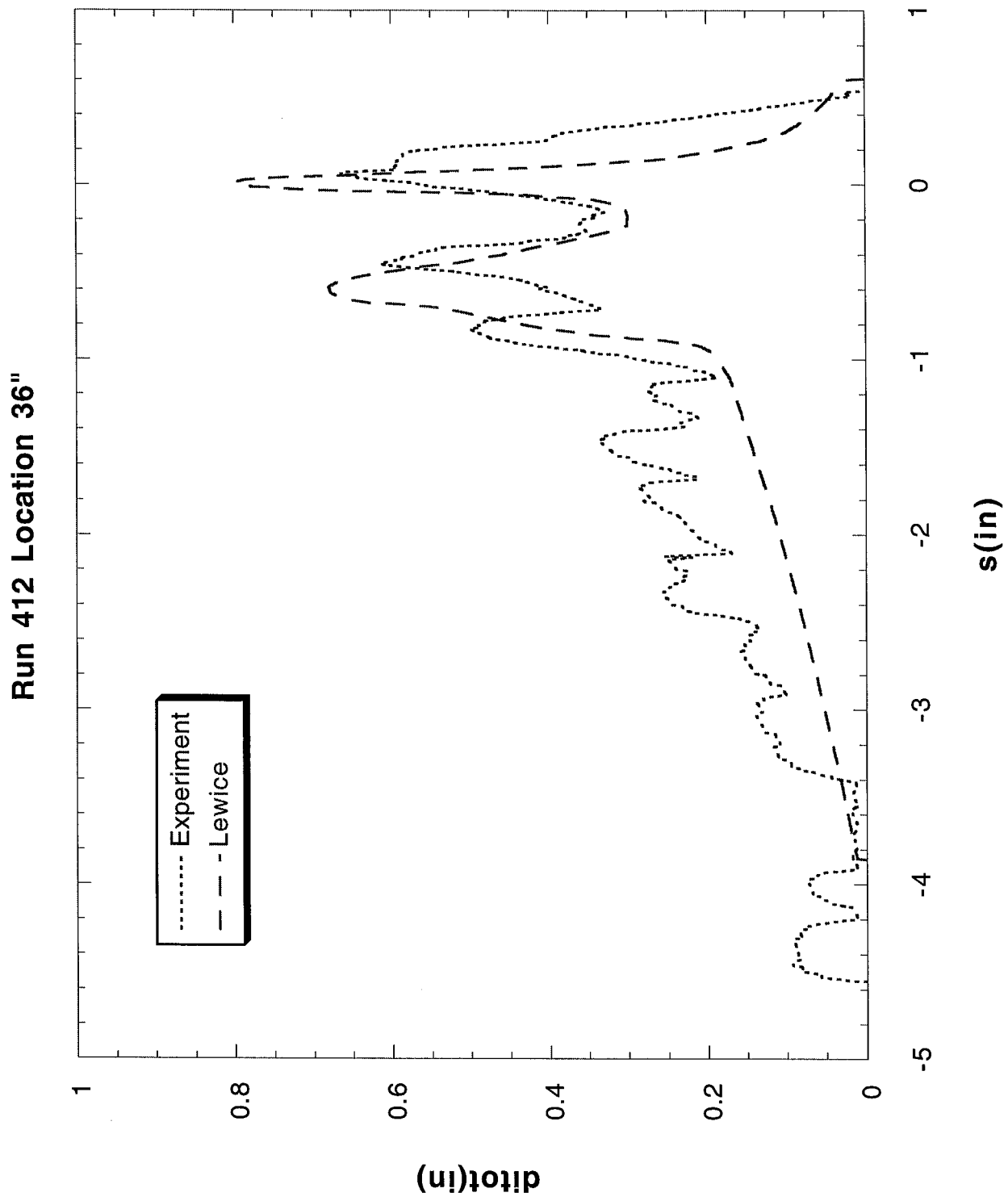
Run 412 Location 36"
Experiment
Lewice
ditot(in)
s(in)
1
0.8
0.6
0.4
0.2
0
-5
-4
-3
-2
-1
0
1

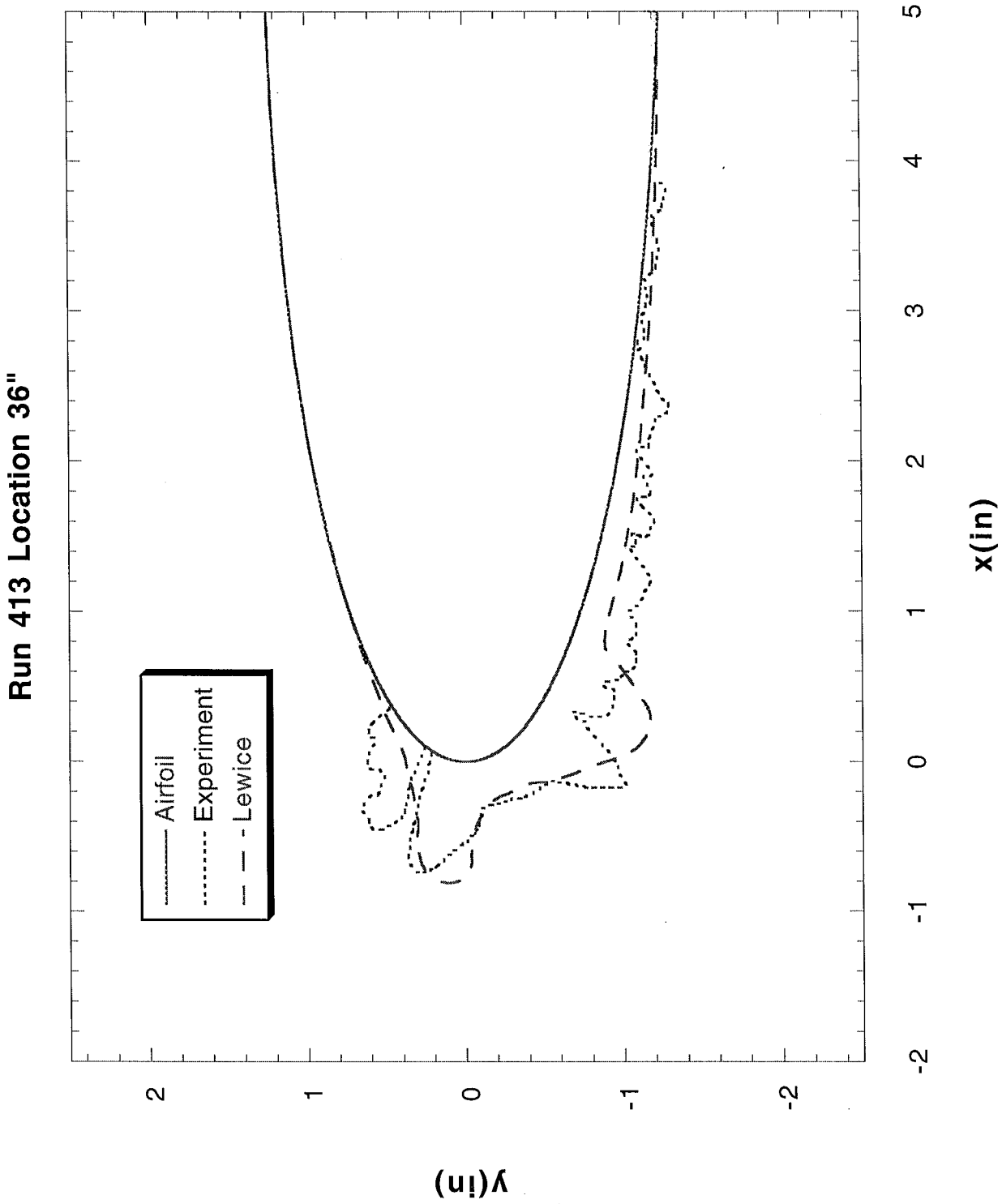
Run 413 Location 36"
Airfoil
Experiment
Lewice
y(in)
x(in)
2
1
0
-1
-2
-2
-1
0
1
2
3
4
5

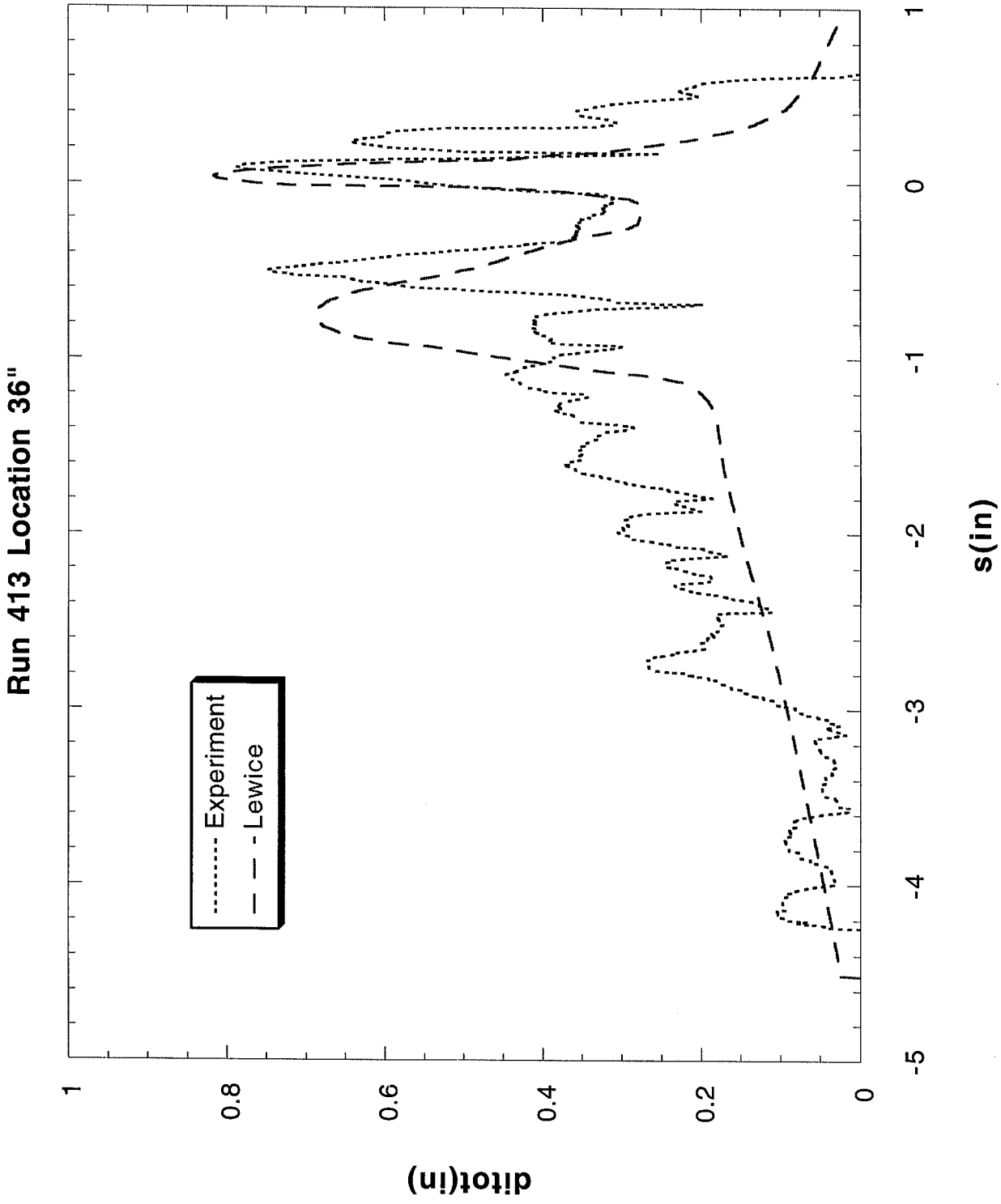
Run 413 Location 36"
Experiment
Lewice
dltot(in)
s(in)
1
0.8
0.6
0.4
0.2
0
-5
-4
-3
-2
-1
0
1

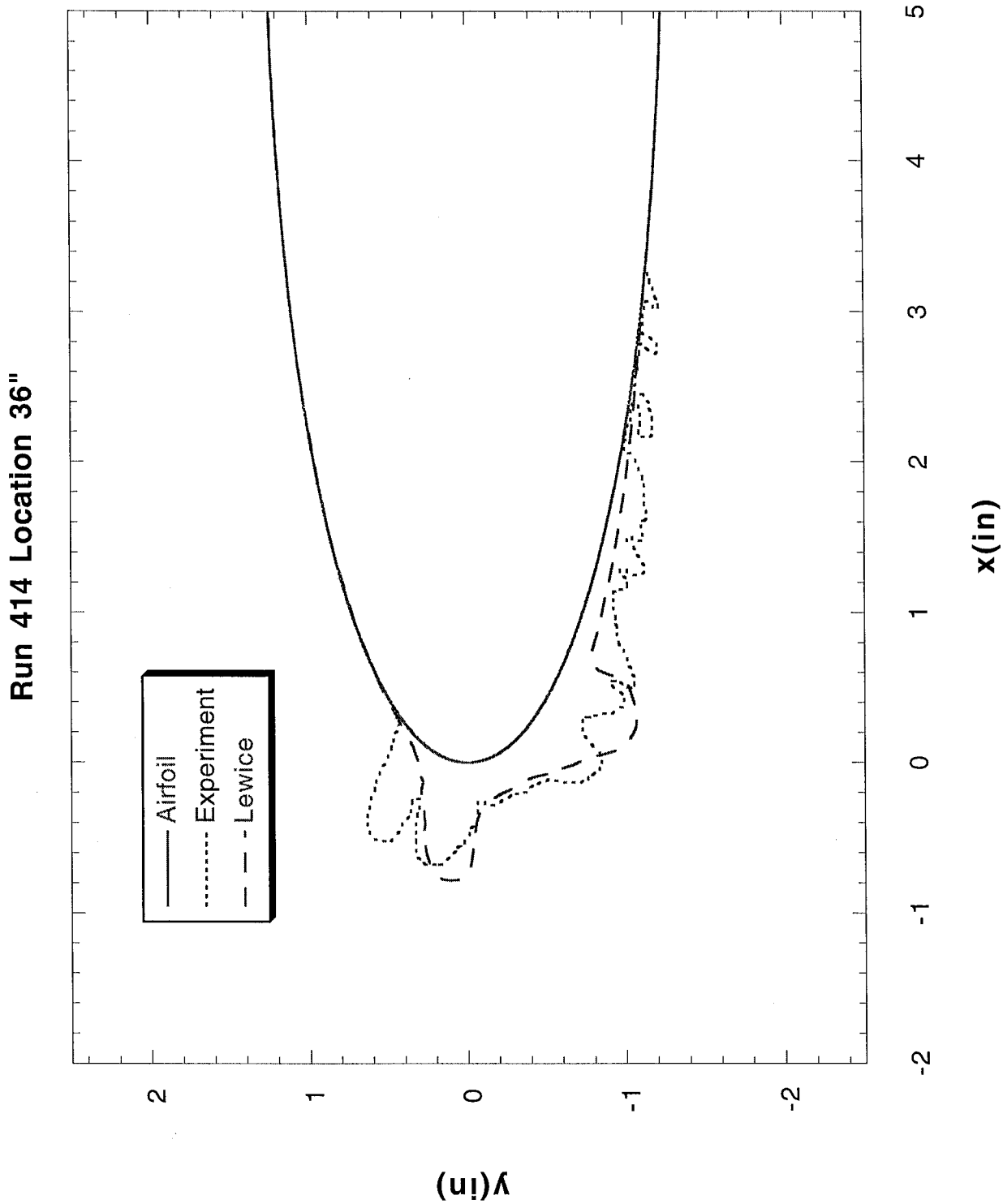
Run 414 Location 36"
Airfoil
Experiment
Lewice
y(in)
x(in)
2
1
0
-1
-2
-2
-1
0
1
2
3
4
5

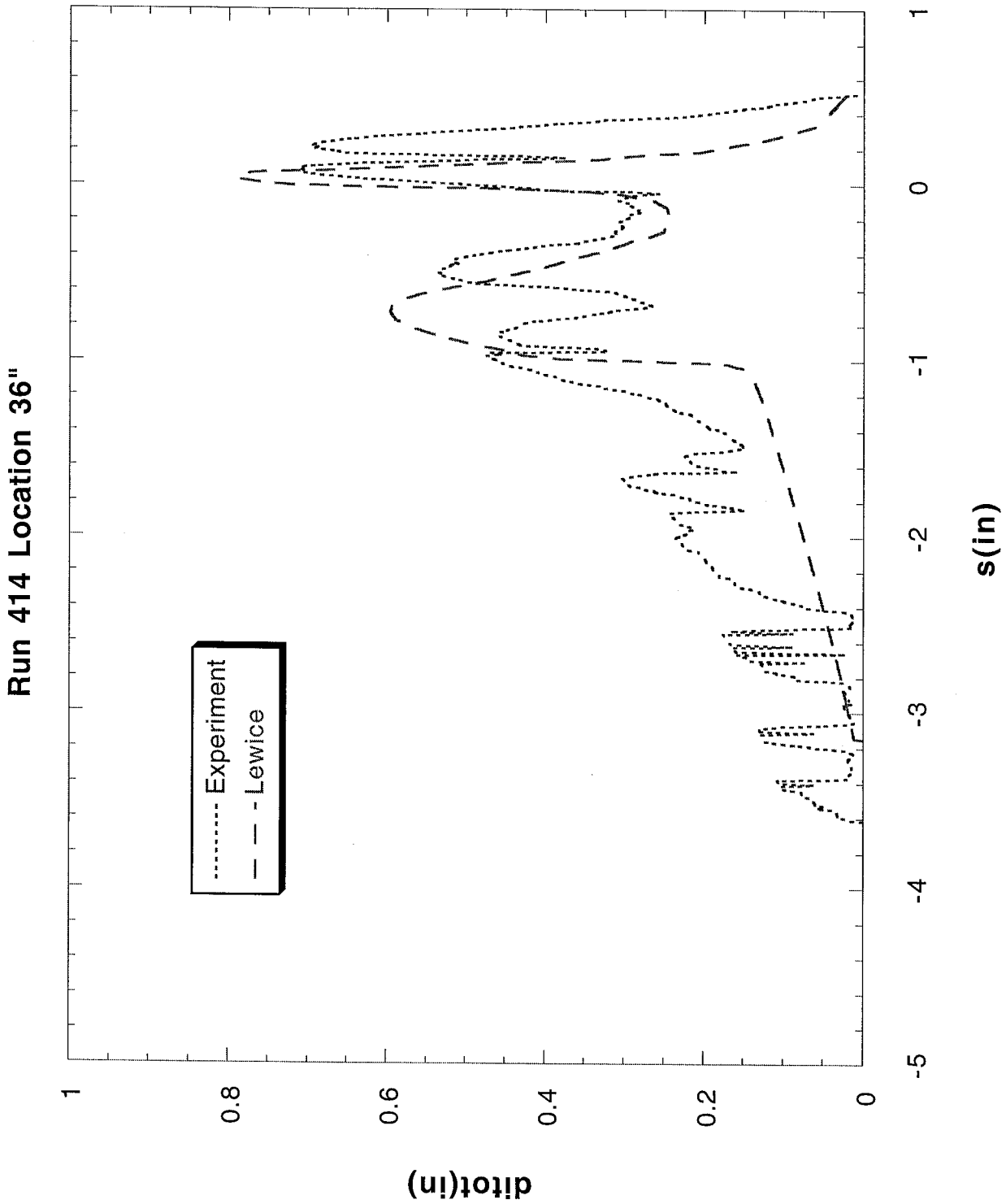
Run 414 Location 36"
Experiment
Lewice
dltot(in)
s(in)
1
0.8
0.6
0.4
0.2
0
-5
-4
-3
-2
-1
0
1

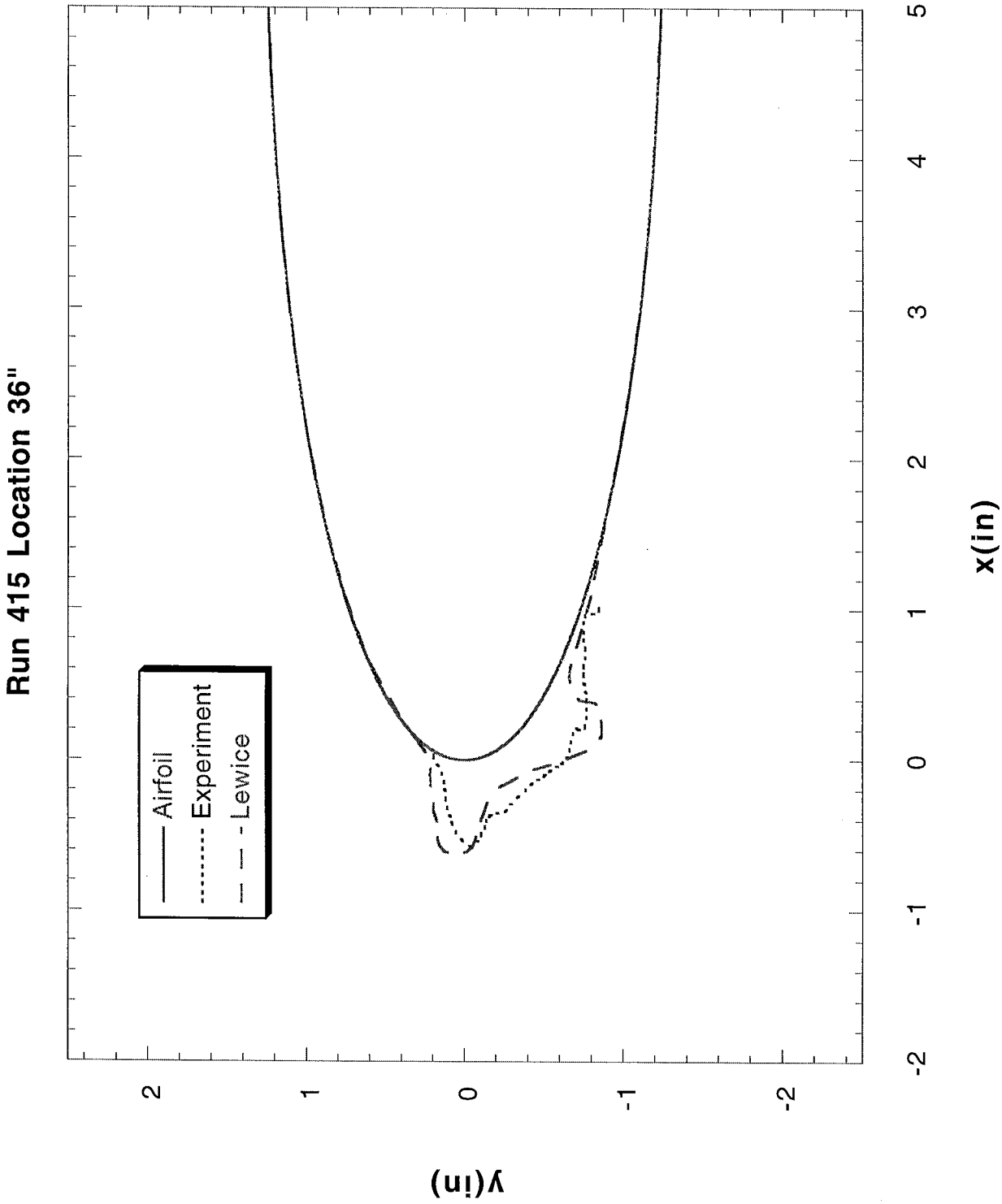
Run 415 Location 36"
Airfoil
Experiment
Lewice
y(in)
x(in)
2
1
0
-1
-2
-2
-1
0
1
2
3
4
5

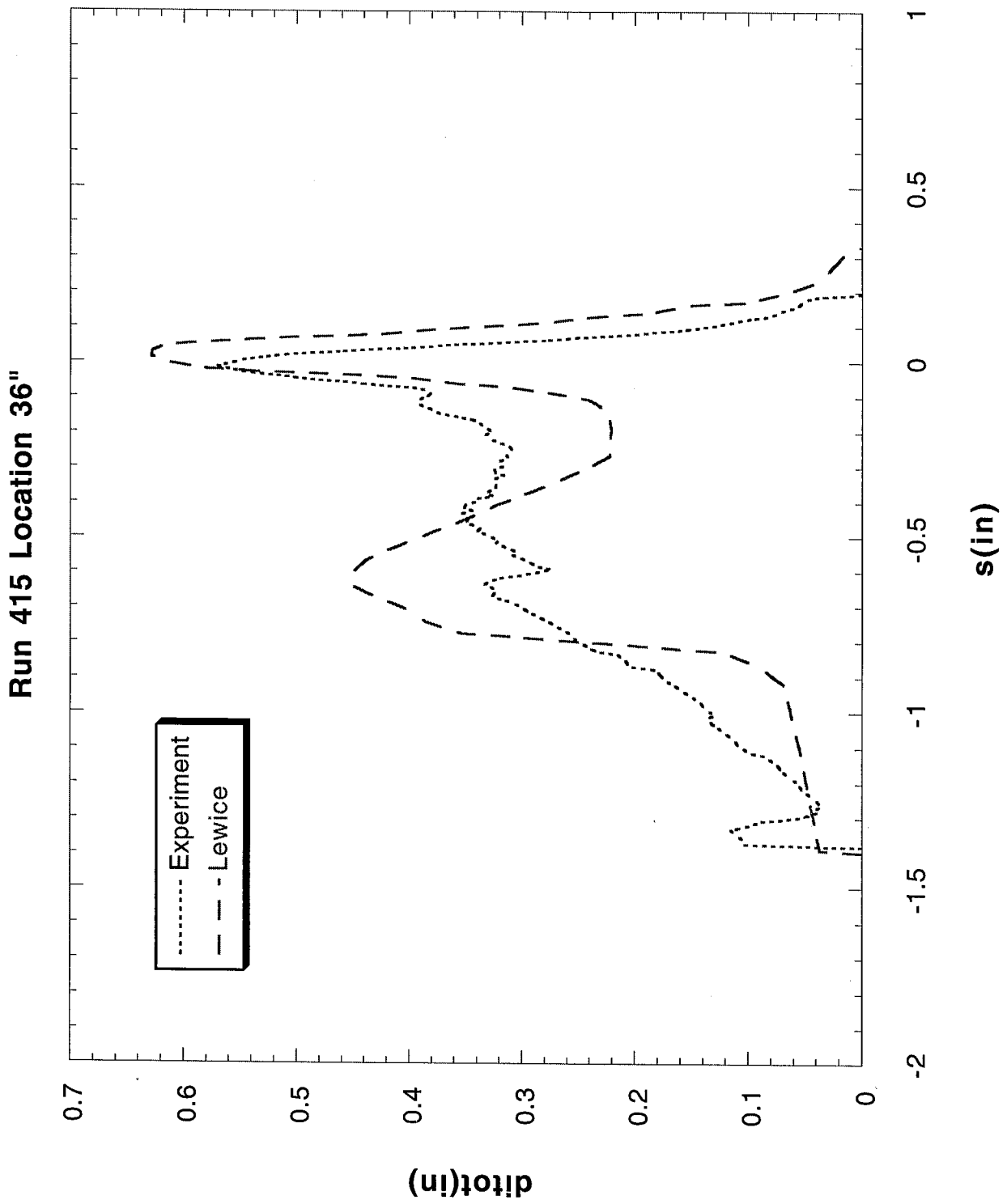
Run 415 Location 36"
Experiment
Lewice
dltot(in)
s(in)
0.7
0.6
0.5
0.4
0.3
0.2
0.1
0
-2
-1.5
-1
-0.5
0
0.5
1

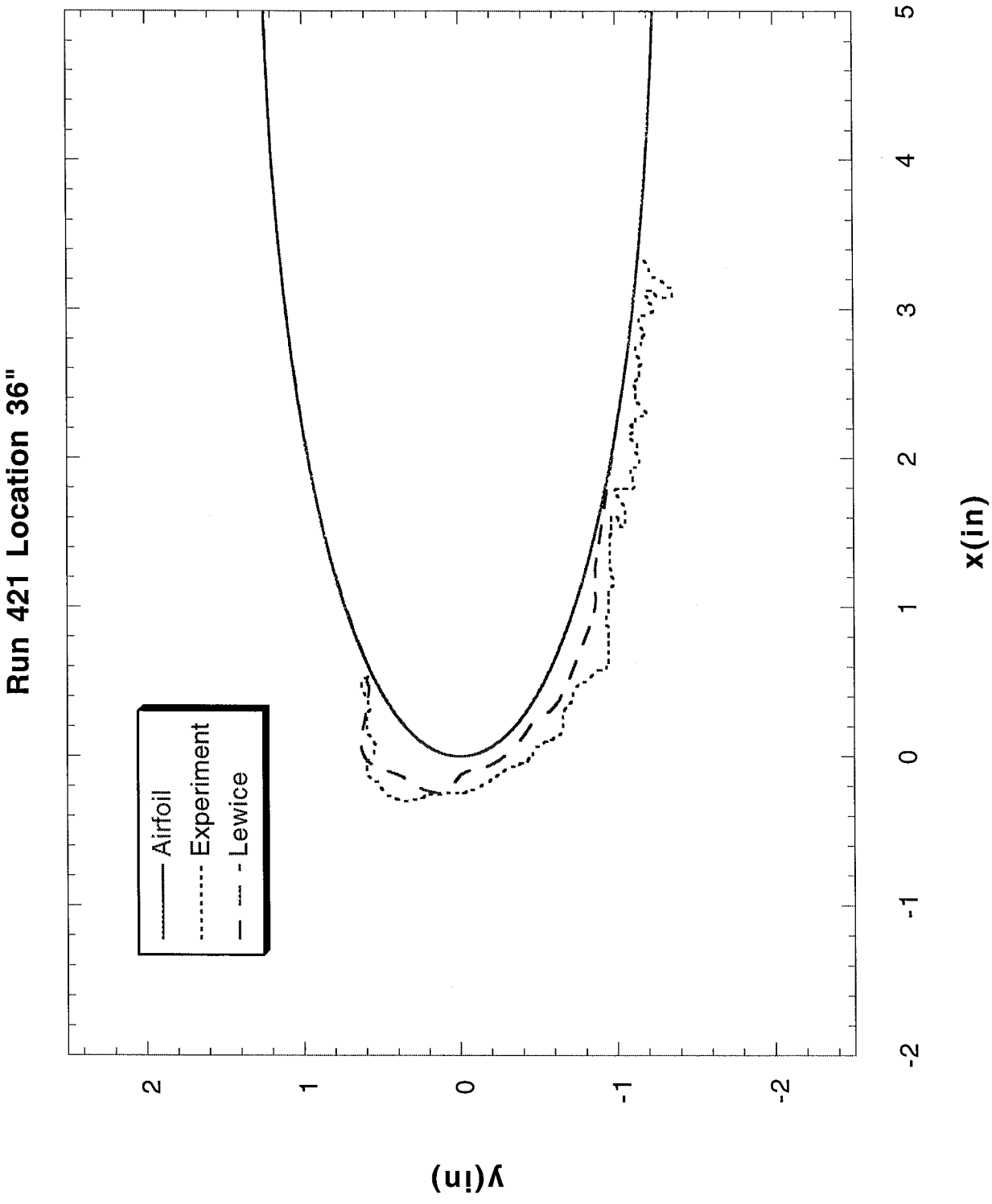
Run 421 Location 36"
Airfoil
Experiment
Lewice
y(in)
x(in)
2
1
0
-1
-2
-2
-1
0
1
2
3
4
5

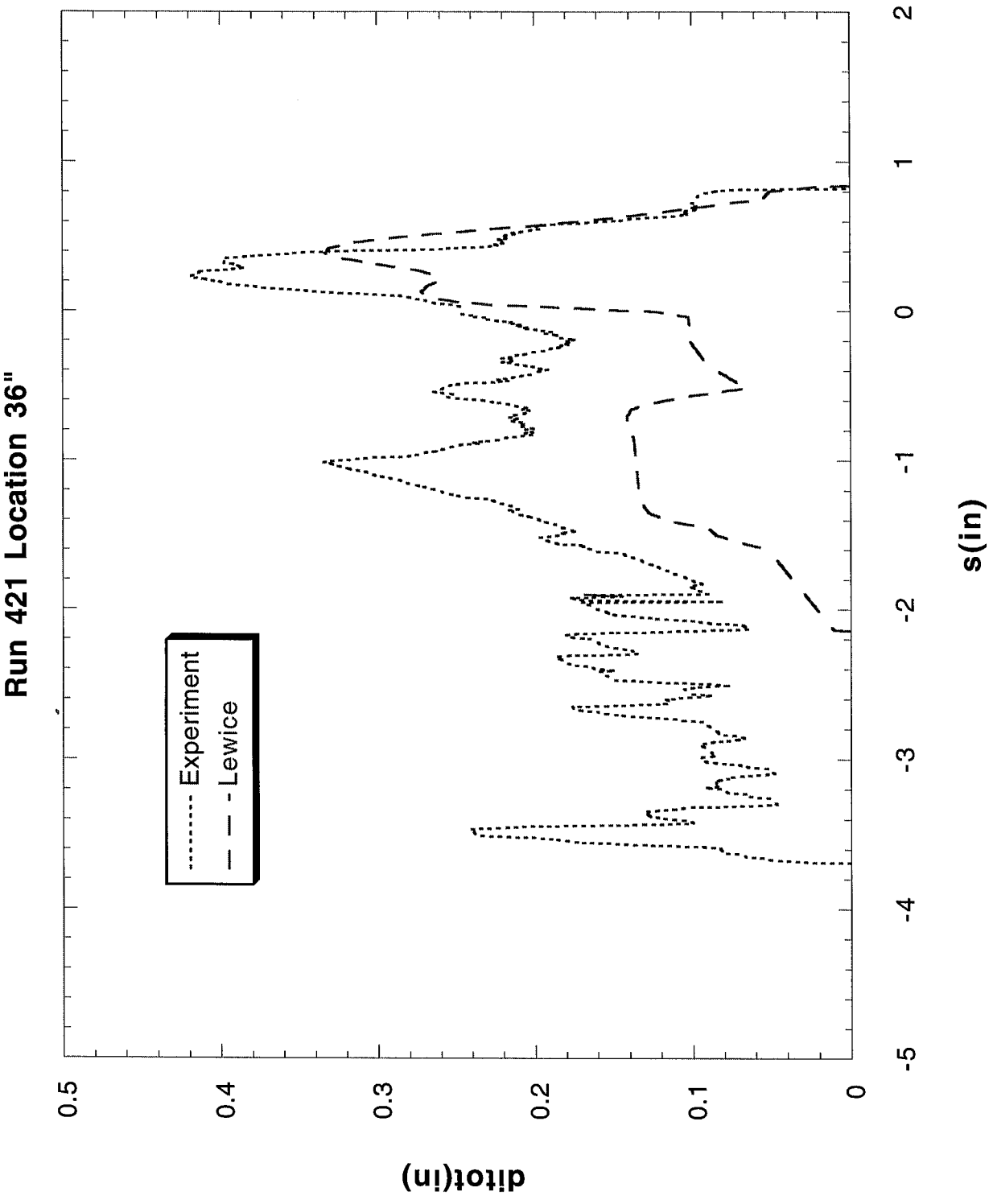
Run 421 Location 36"
Experiment
Lewice
dltot(in)
s(in)
0.5
0.4
0.3
0.2
0.1
0
-5
-4
-3
-2
-1
0
1
2

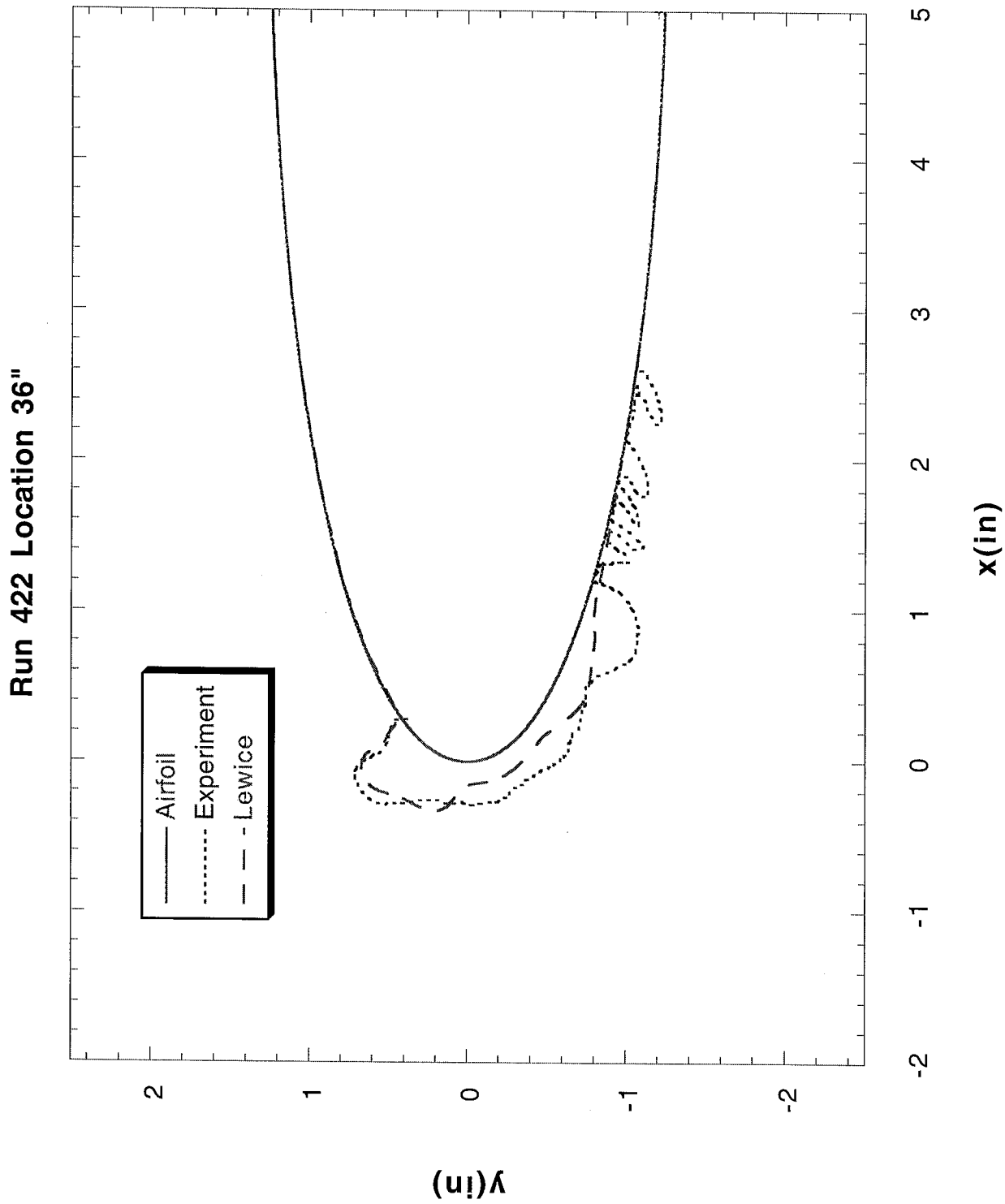
Run 422 Location 36"
Airfoil
Experiment
Lewice
y(in)
x(in)
2
1
0
-1
-2
-2
-1
0
1
2
3
4
5

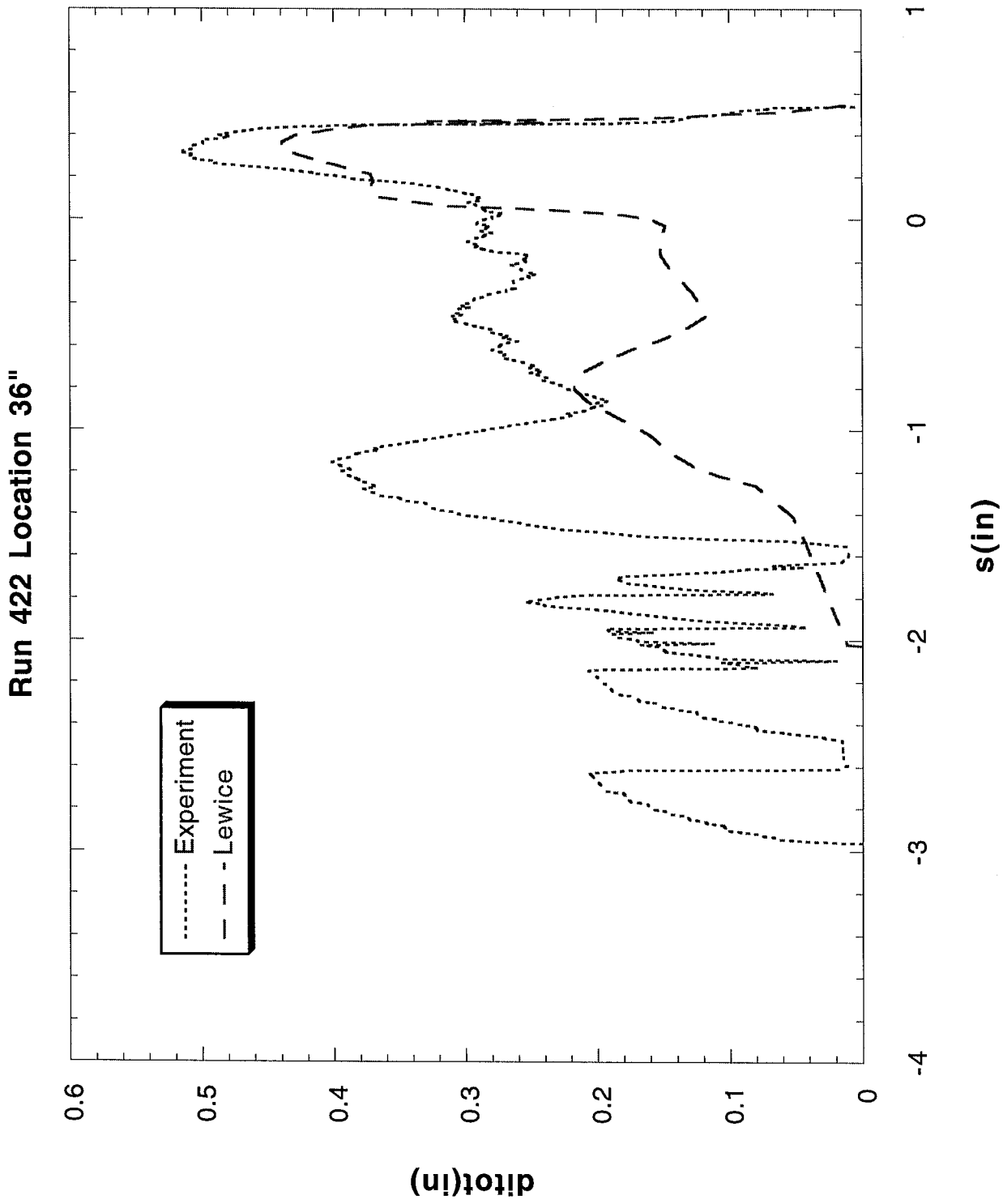
Run 422 Location 36"
Experiment
Lewice
dtot(in)
s(in)
0.6
0.5
0.4
0.3
0.2
0.1
0
-4
-3
-2
-1
0
1

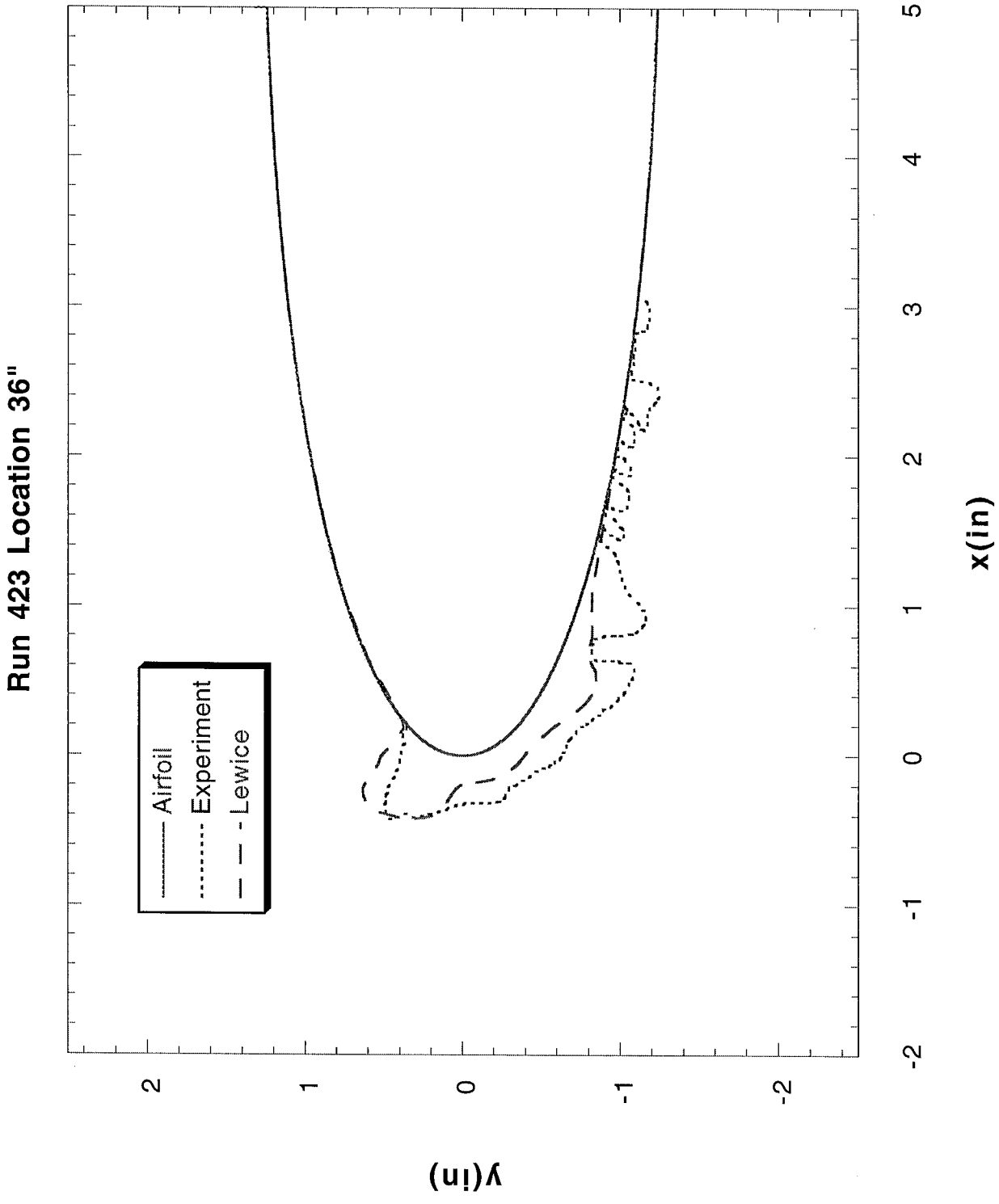
Run 423 Location 36"
Airfoil
Experiment
Lewice
y(in)
x(in)
2
1
0
-1
-2
-2
-1
0
1
2
3
4
5

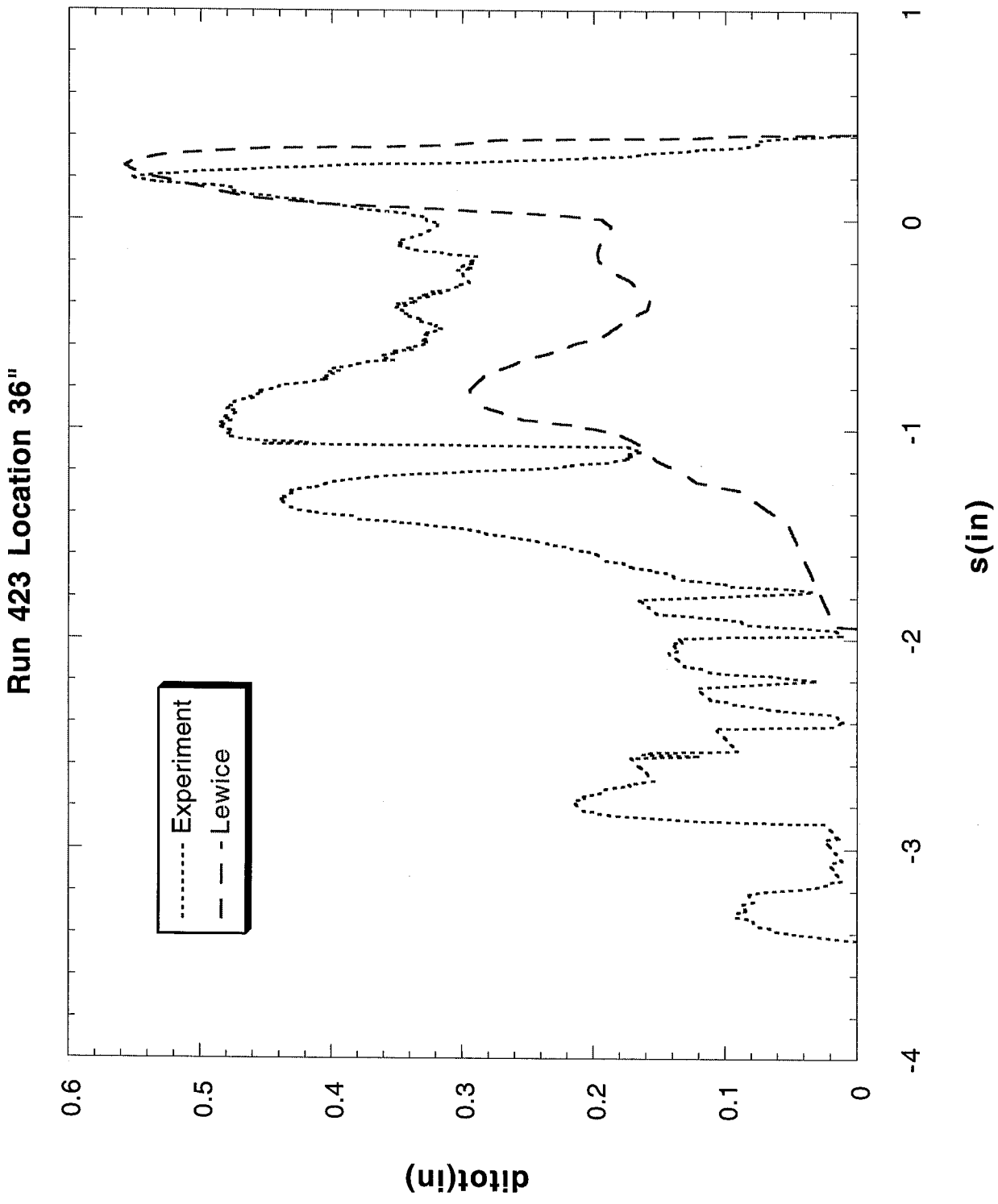
Run 423 Location 36"
Experiment
Lewice
dltot(in)
0.6
0.5
0.4
0.3
0.2
0.1
0
-4
-3
-2
-1
0
1
s(in)

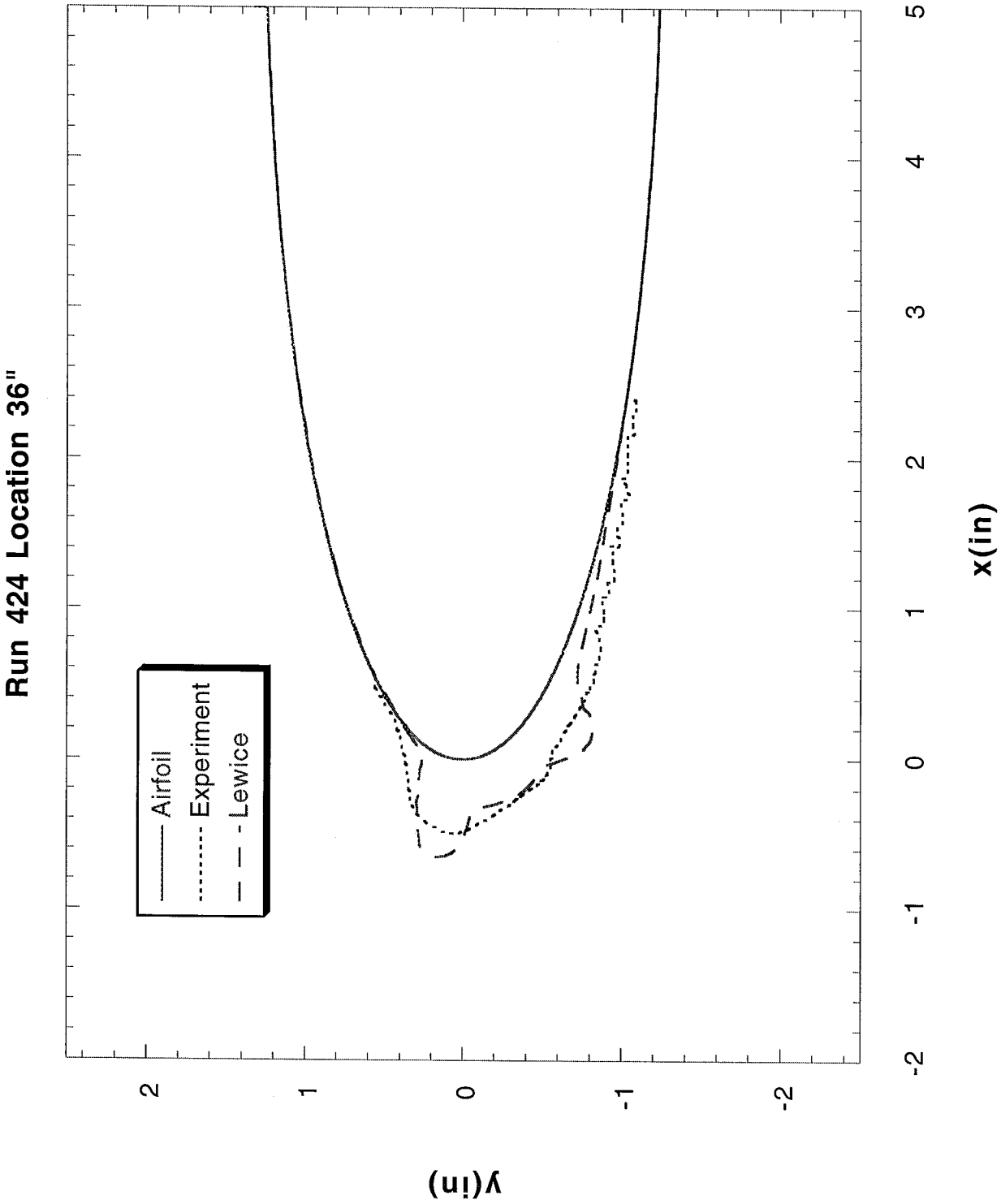
Run 424 Location 36"
Airfoil
Experiment
Lewice
y(in)
x(in)
2
1
0
-1
-2
-2
-1
0
1
2
3
4
5

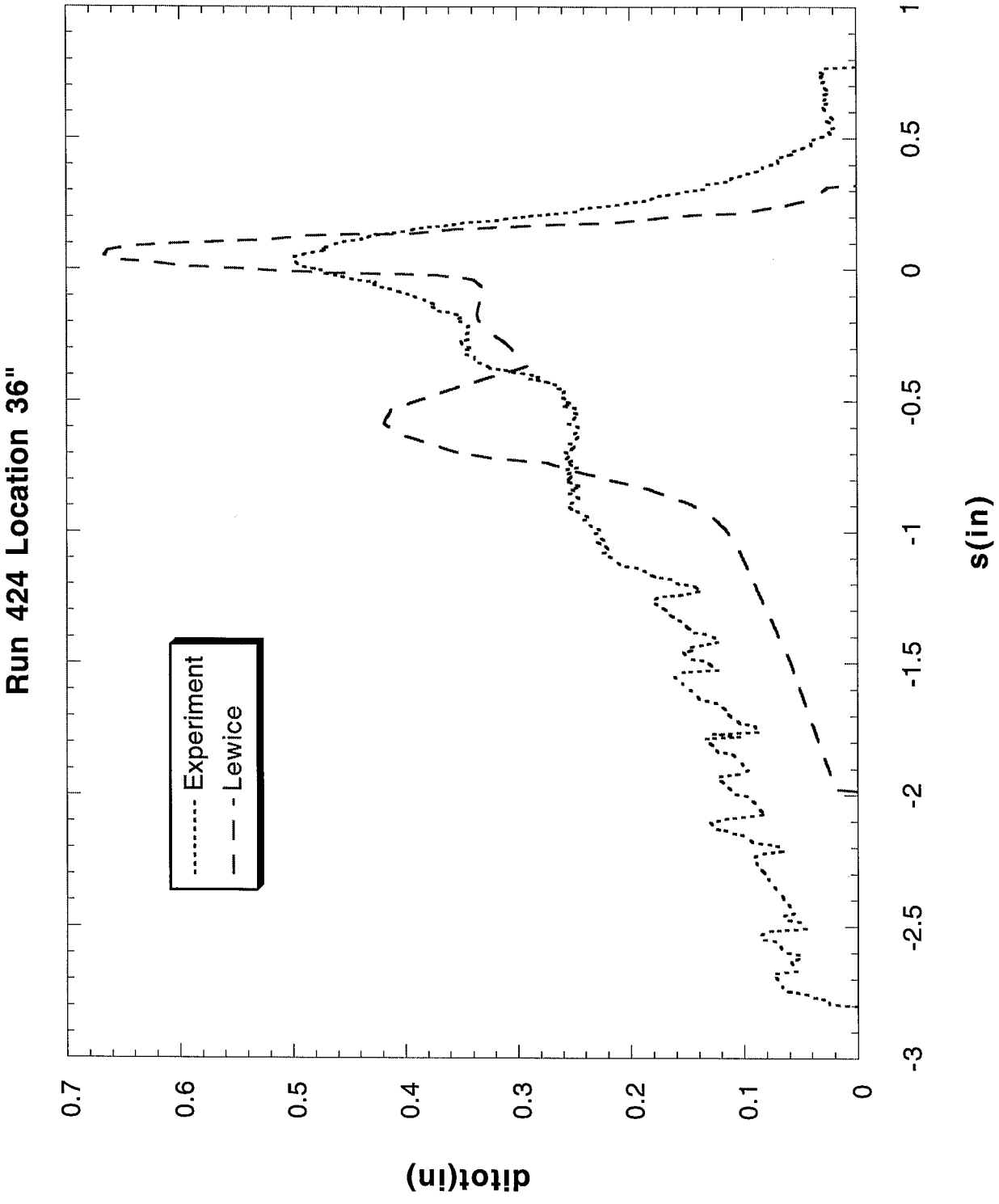
Run 424 Location 36"
Experiment
Lewice
dltot(in)
s(in)
0.7
0.6
0.5
0.4
0.3
0.2
0.1
0
-3
-2.5
-2
-1.5
-1
-0.5
0
0.5
1

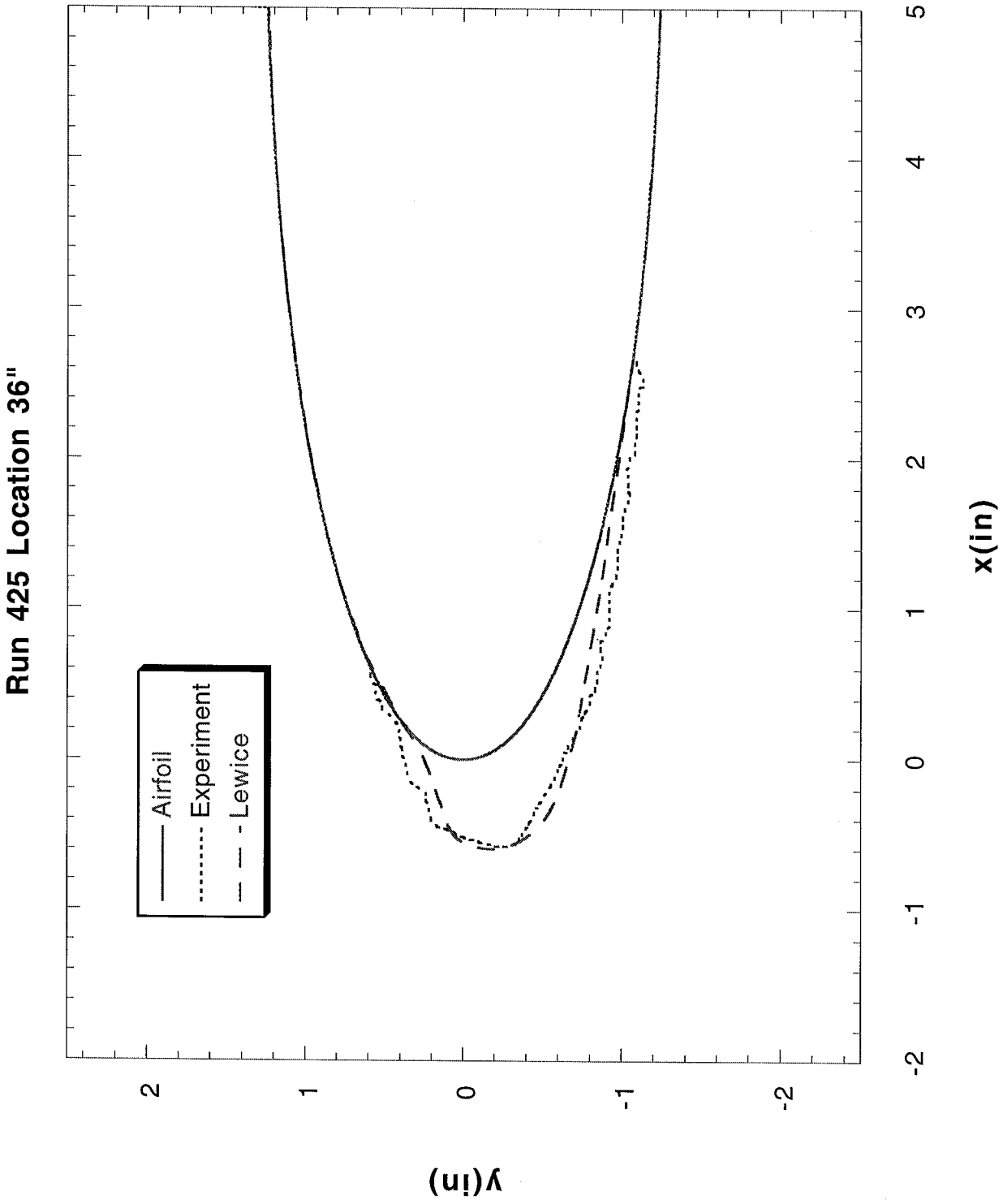
Run 425 Location 36"
Airfoil
Experiment
Lewice
y(in)
x(in)
2
1
0
-1
-2
-2
-1
0
1
2
3
4
5

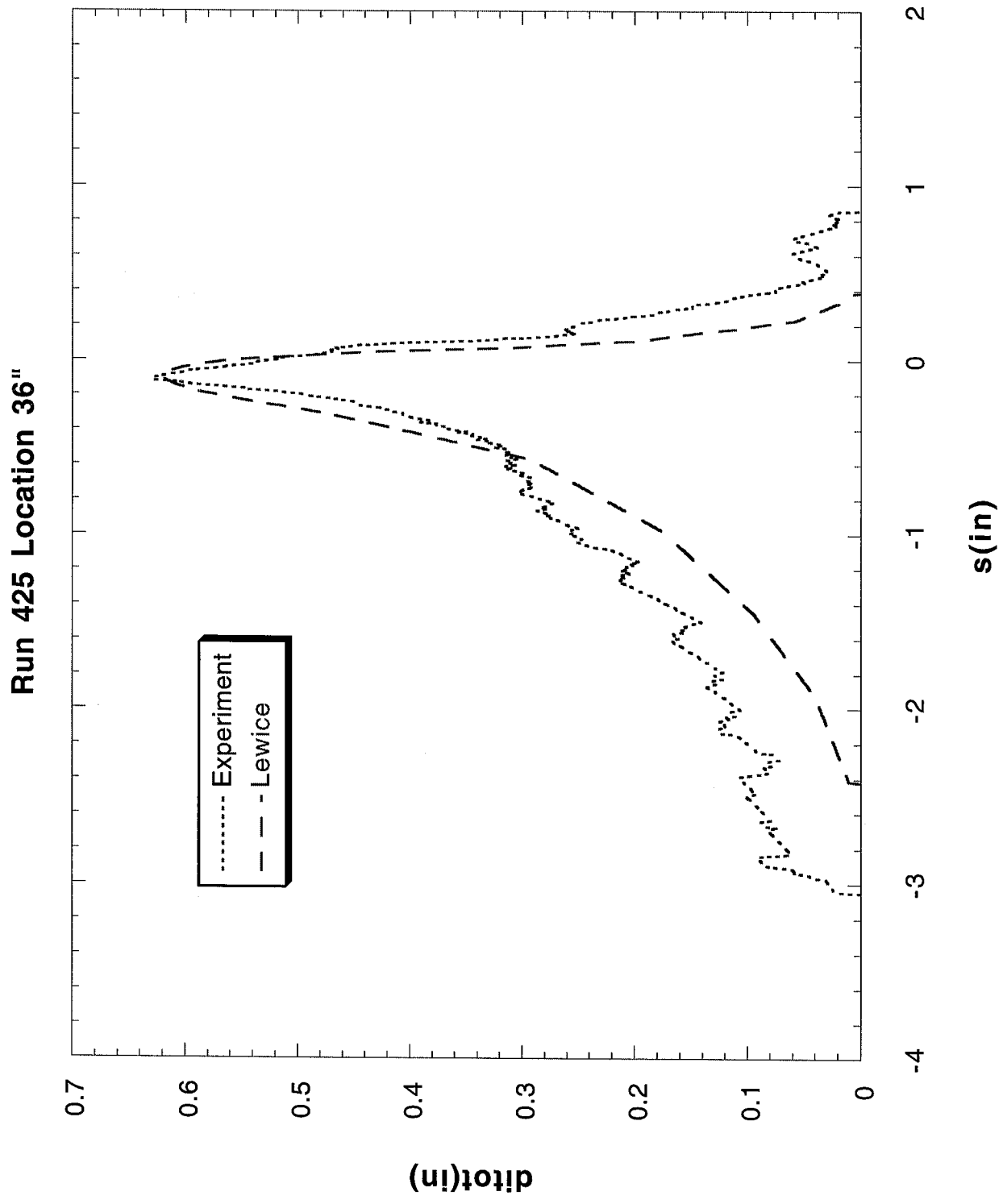
Run 425 Location 36"
Experiment
Lewice
dltot(in)
s(in)
0.7
0.6
0.5
0.4
0.3
0.2
0.1
0
-4
-3
-2
-1
0
1
2

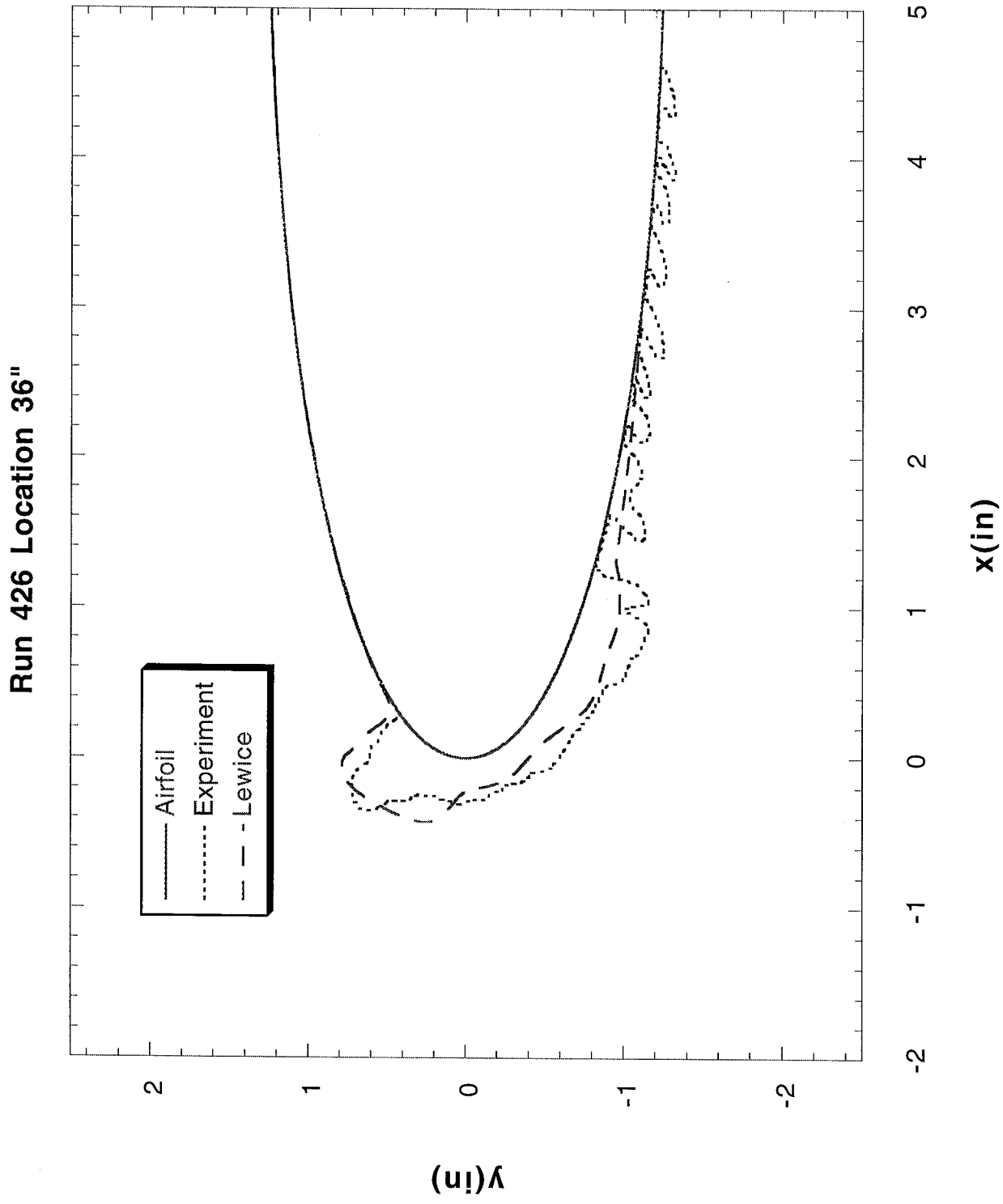
Run 426 Location 36"
Airfoil
Experiment
Lewice
y(in)
x(in)
2
1
0
-1
-2
-2
-1
0
1
2
3
4
5

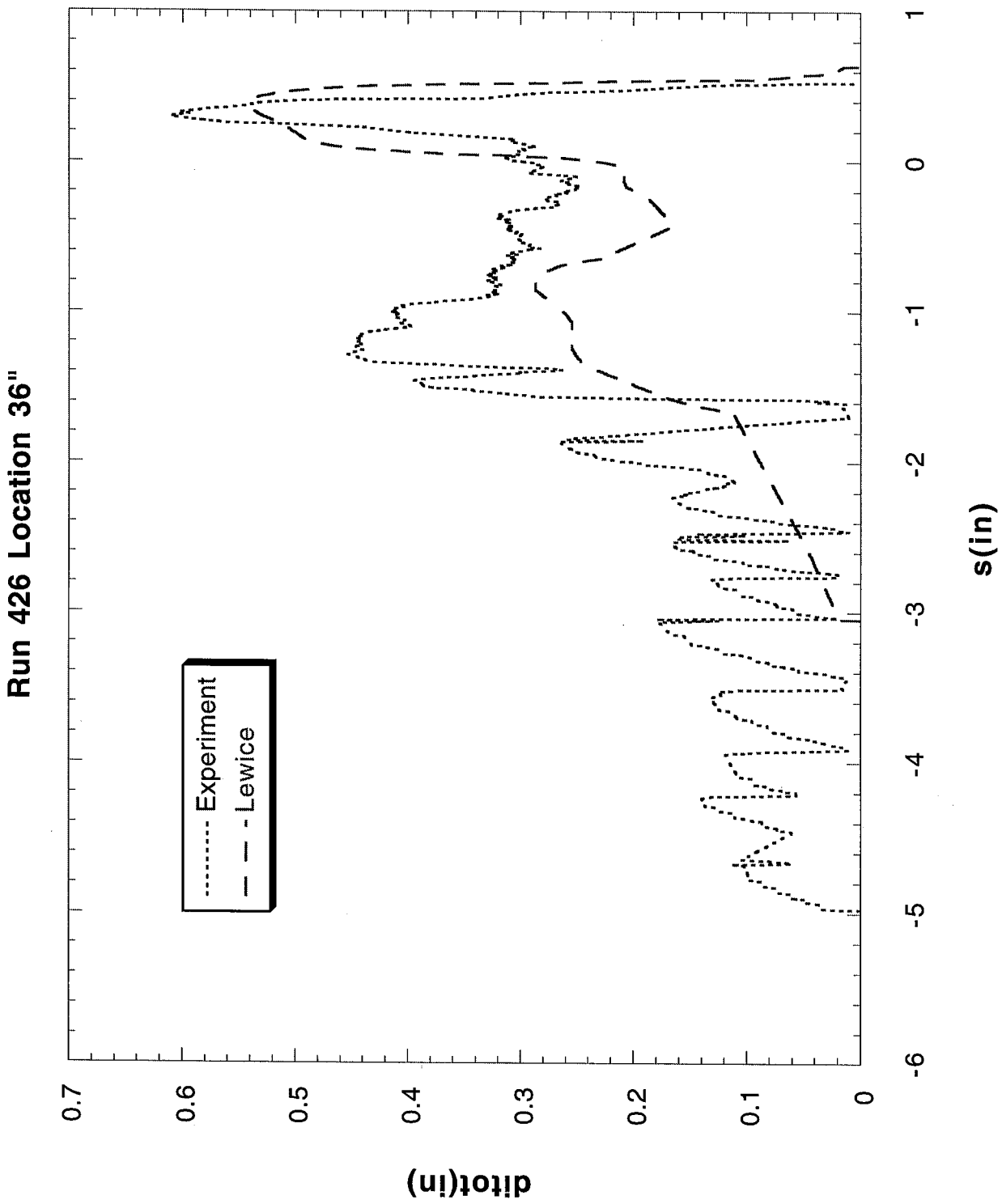
Run 426 Location 36"
Experiment
Lewice
dltot(in)
s(in)
0
0.1
0.2
0.3
0.4
0.5
0.6
0.7
-6
-5
-4
-3
-2
-1
0
1

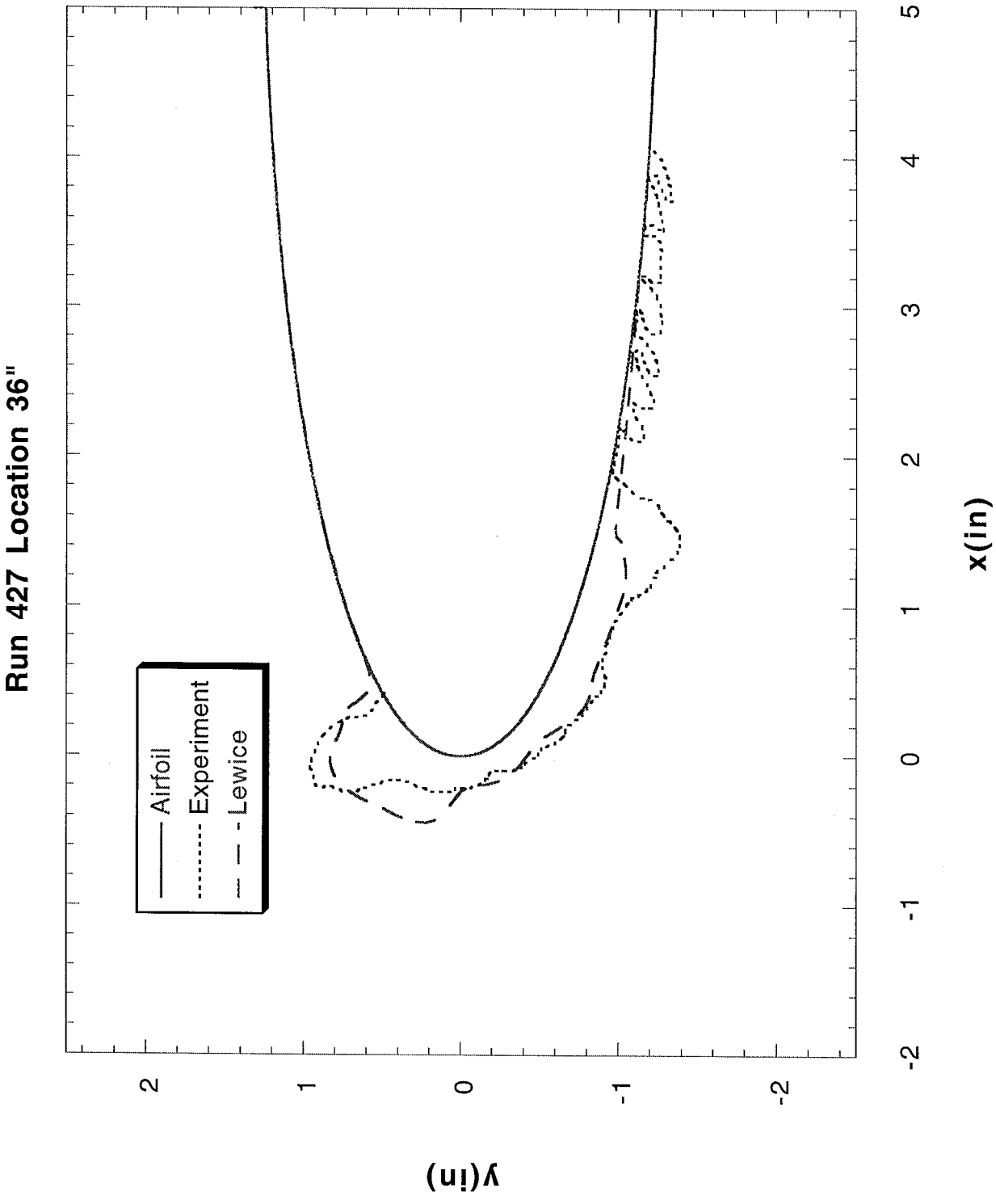
Run 427 Location 36"
Airfoil
Experiment
Lewice
y(in)
x(in)
2
1
0
-1
-2
-2
-1
0
1
2
3
4
5

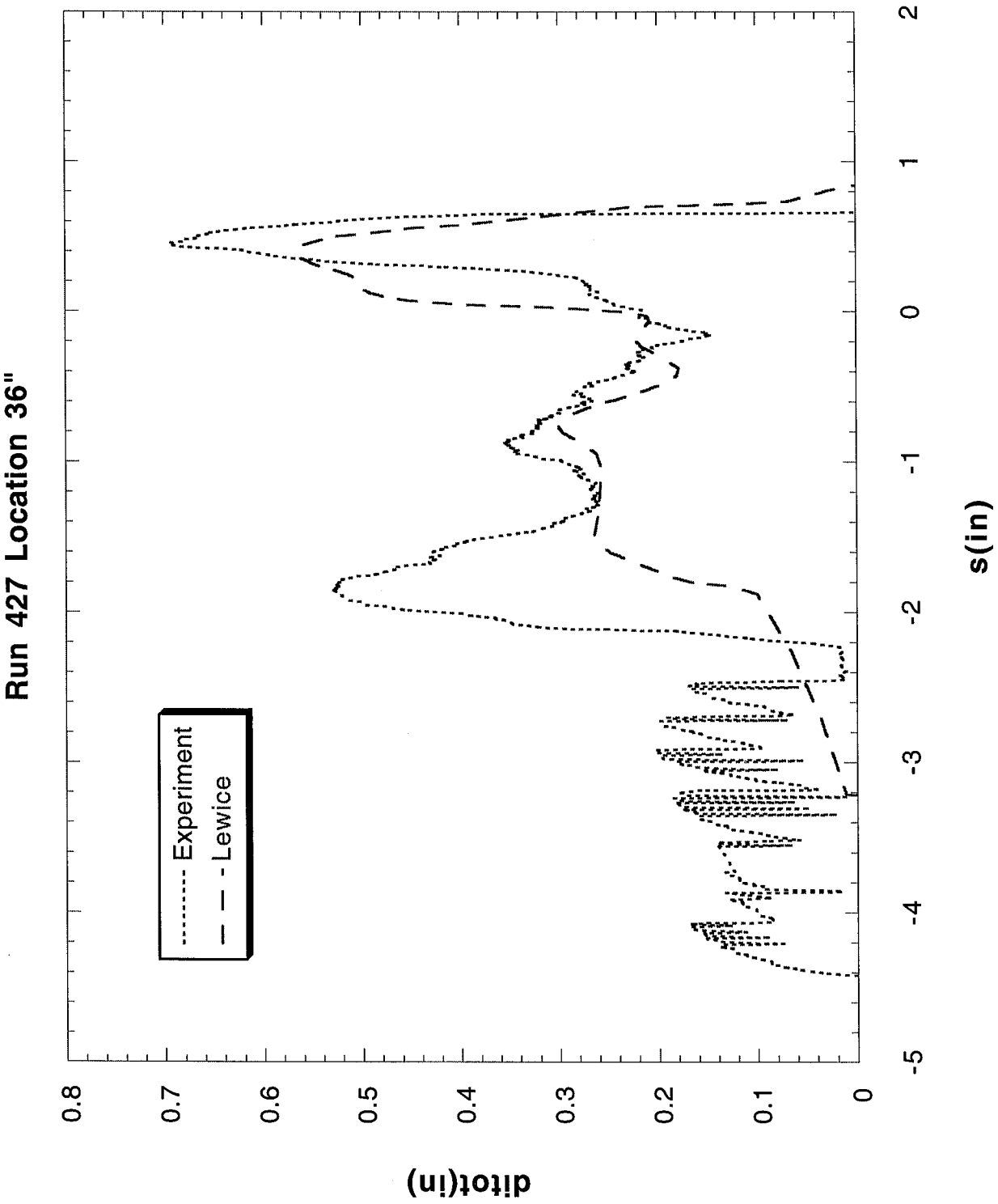
Run 427 Location 36"
Experiment
Lewice
dltot(in)
s(in)
0
0.1
0.2
0.3
0.4
0.5
0.6
0.7
0.8
-5
-4
-3
-2
-1
0
1
2

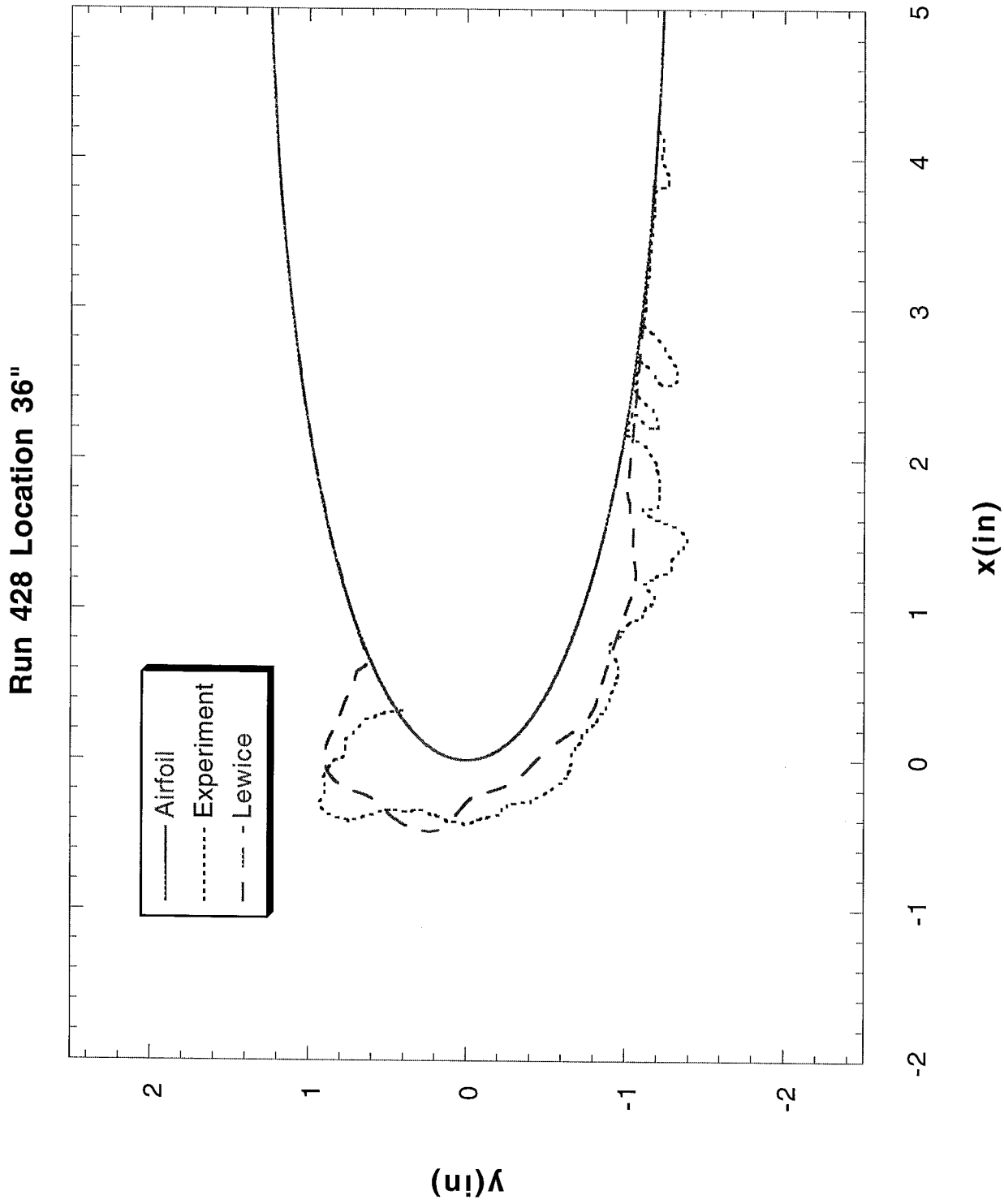
Run 428 Location 36"
Airfoil
Experiment
- Lewice
y(in)
x(in)
2
1
0
-1
-2
-2
-1
0
1
2
3
4
5

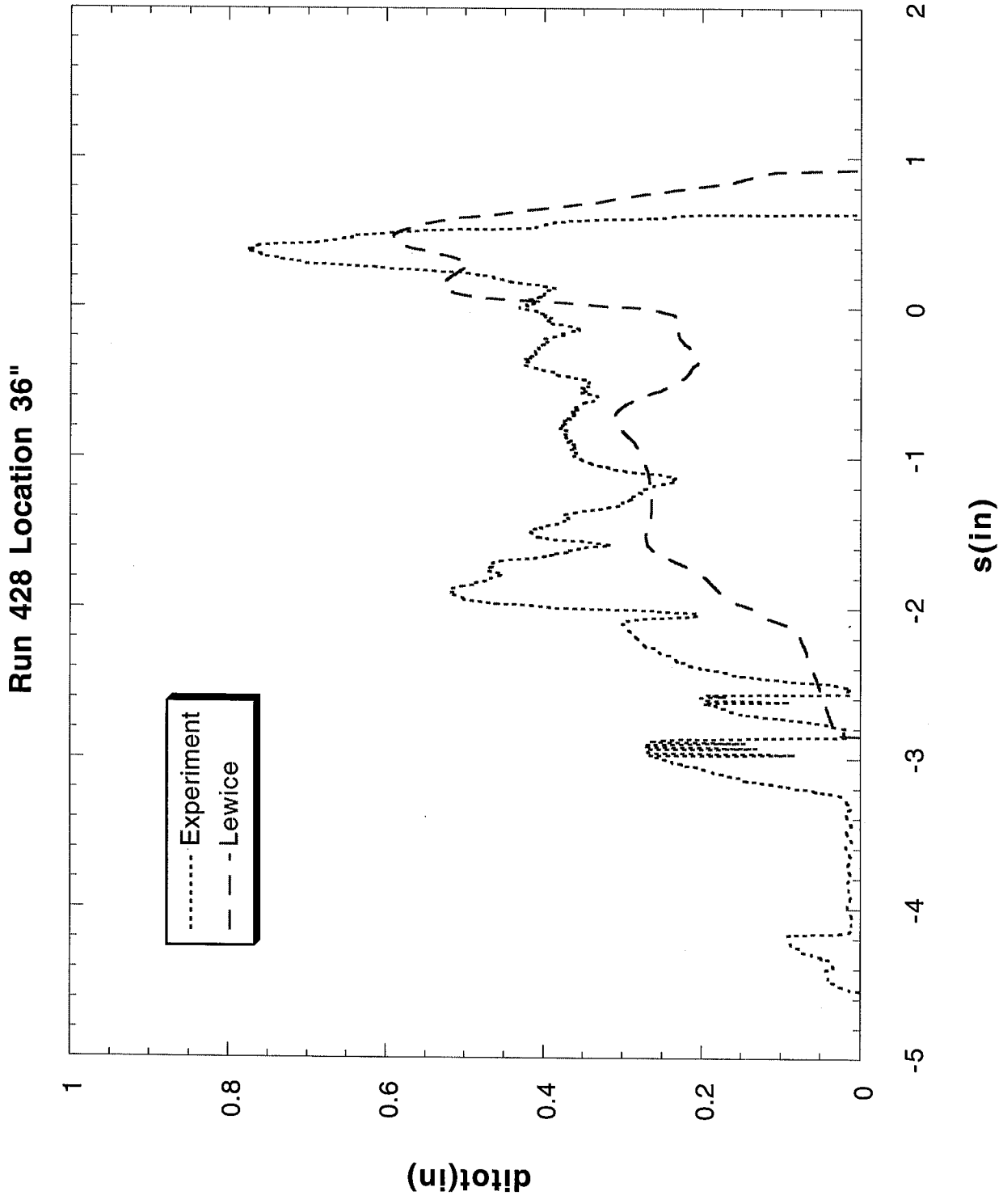
Run 428 Location 36"
Experiment
Lewice
dltot(in)
s(in)
1
0.8
0.6
0.4
0.2
0
2
1
0
-1
-2
-3
-4
-5

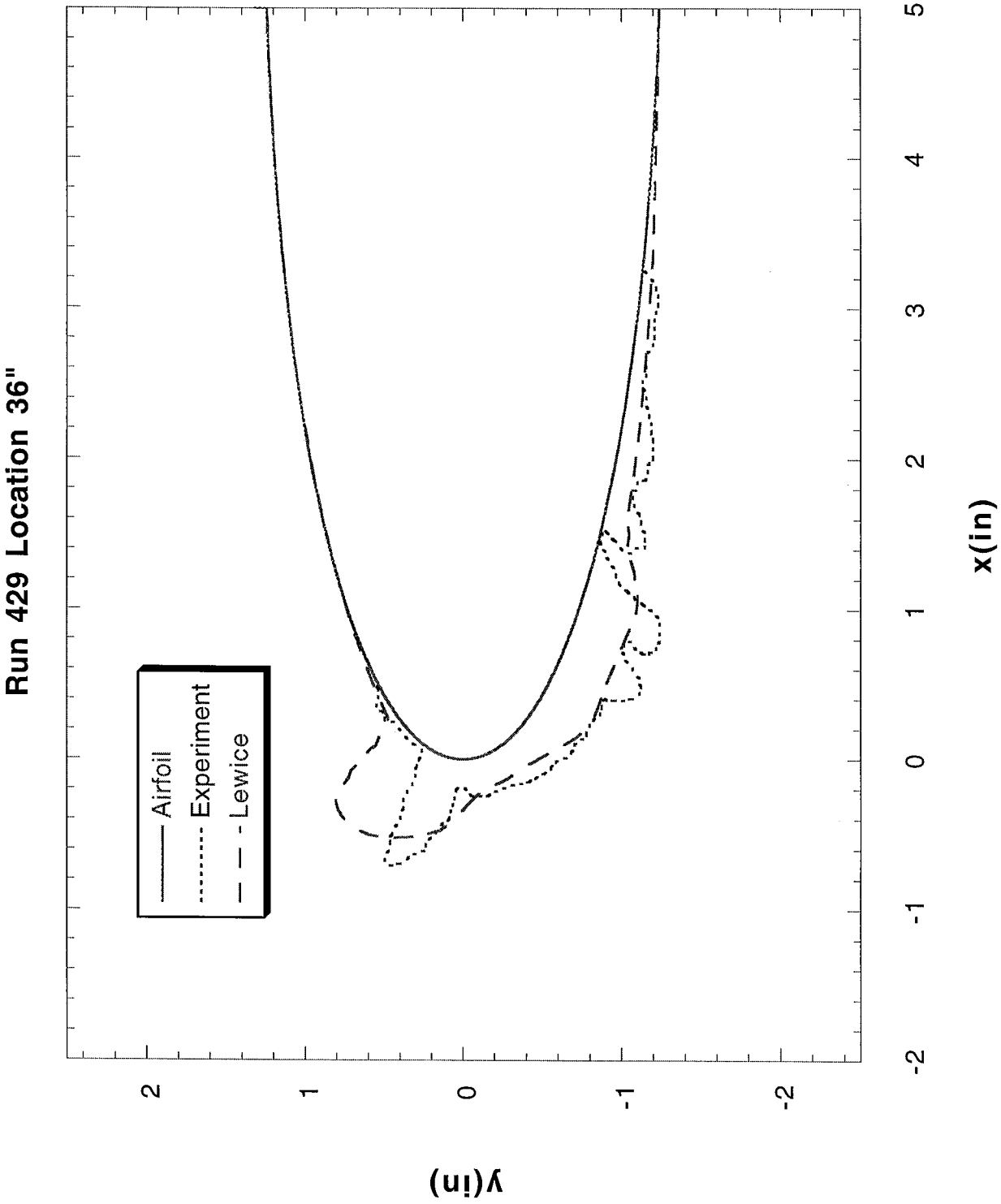
Run 429 Location 36"
Airfoil
Experiment
Lewice
y(in)
x(in)
2
1
0
-1
-2
-2
-1
0
1
2
3
4
5

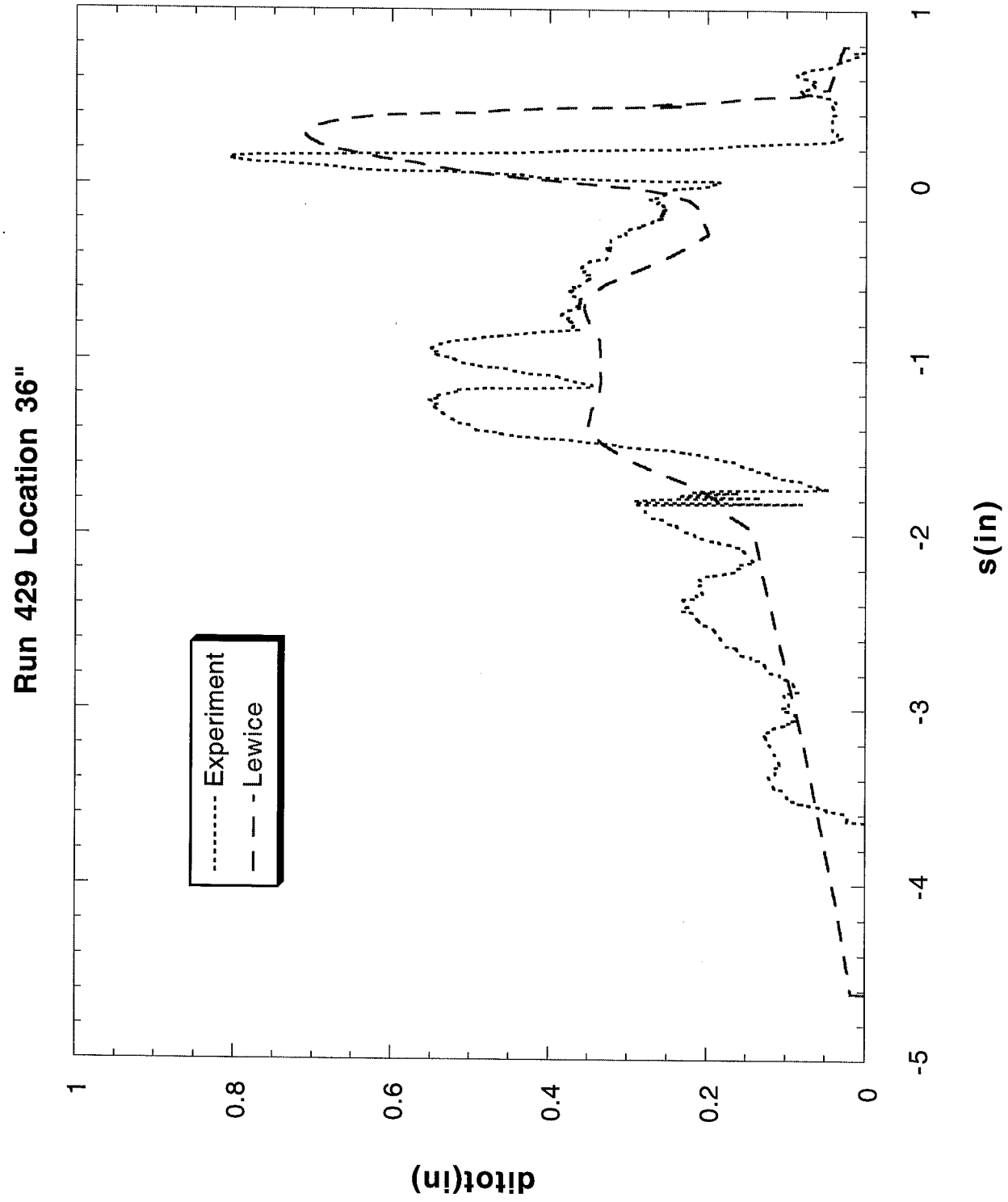
Run 429 Location 36"
Experiment
Lewice
ditot(in)
s(in)
1
0.8
0.6
0.4
0.2
0
-5
-4
-3
-2
-1
0
1

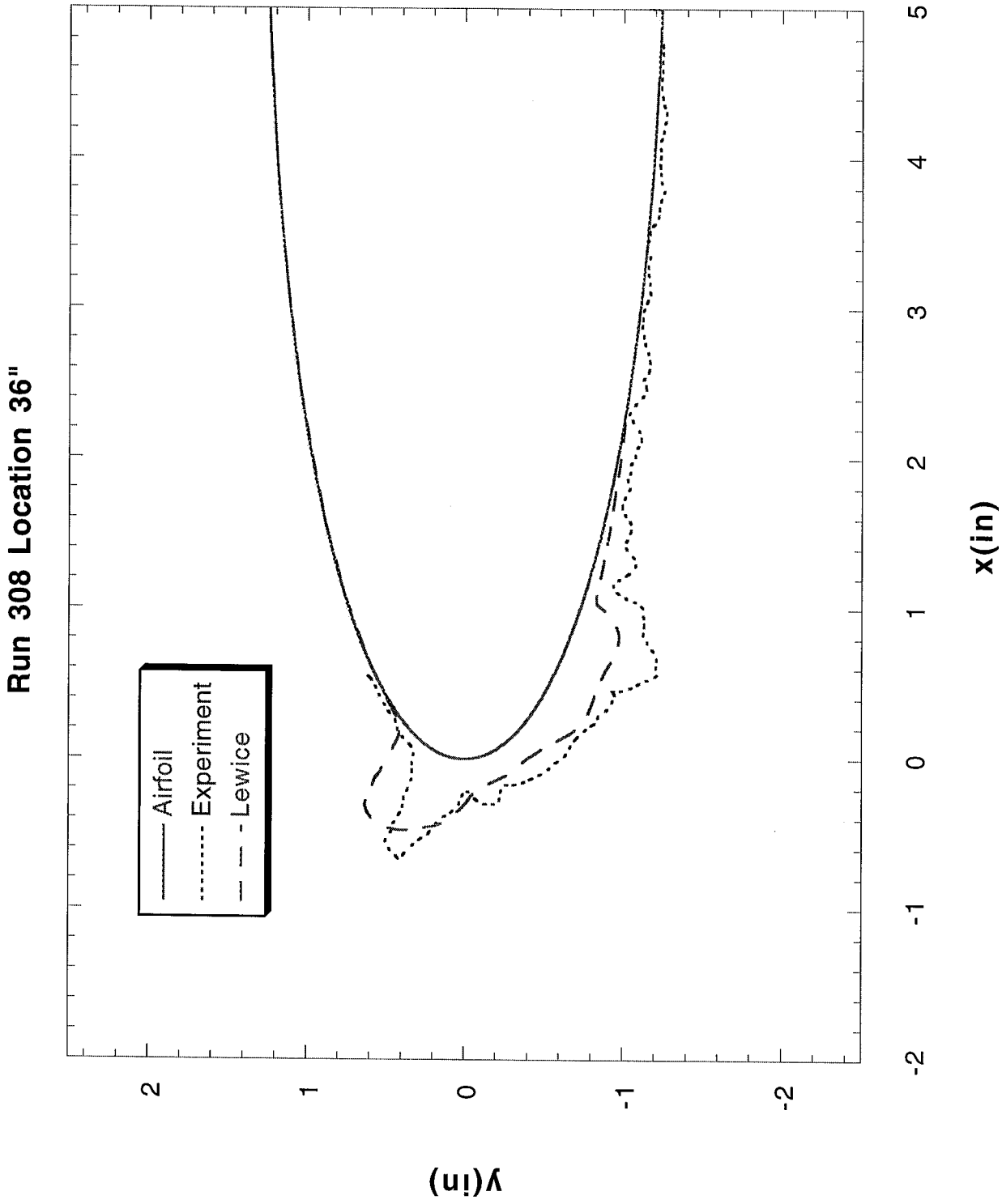
Run 308 Location 36"
Airfoil
Experiment
Lewice
y(in)
x(in)
2
1
0
-1
-2
-2
-1
0
1
2
3
4
5

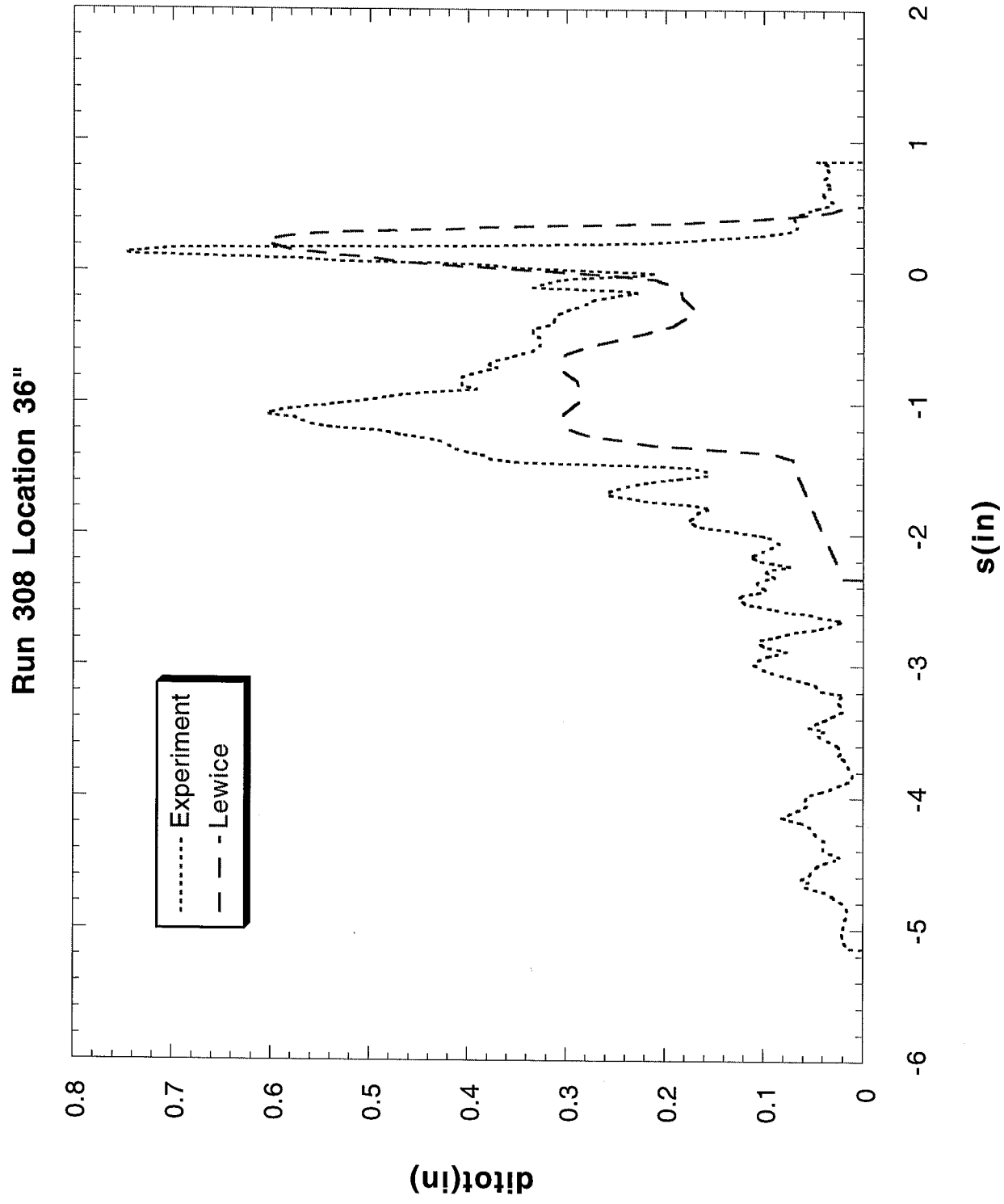
Run 308 Location 36"
Experiment
Lewice
dltot(in)
s(in)
0.8
0.7
0.6
0.5
0.4
0.3
0.2
0.1
0
-6
-5
-4
-3
-2
-1
0
1
2

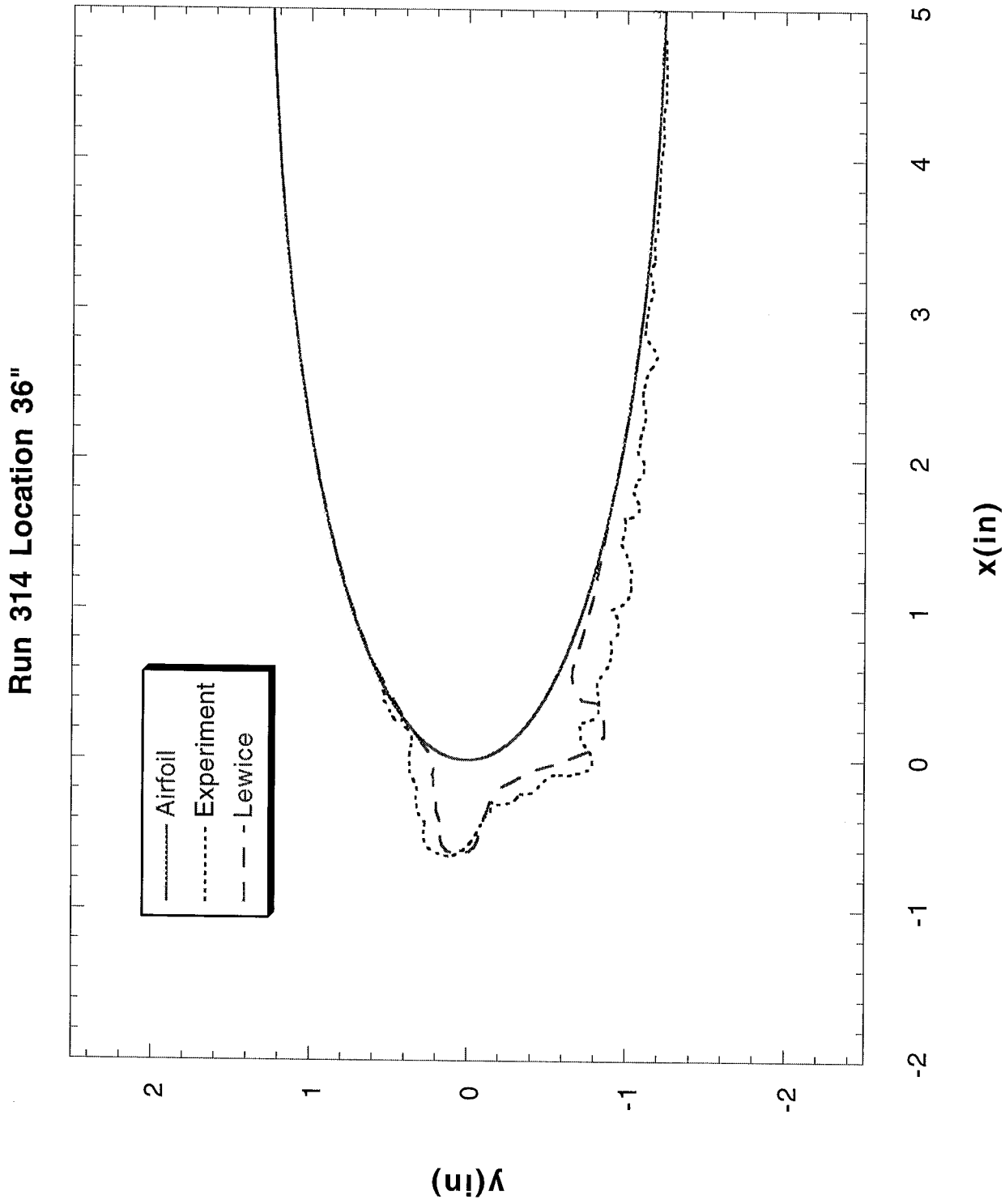
Run 314 Location 36"
Airfoil
Experiment
Lewice
y(in)
x(in)
2
1
0
-1
-2
-2
-1
0
1
2
3
4
5

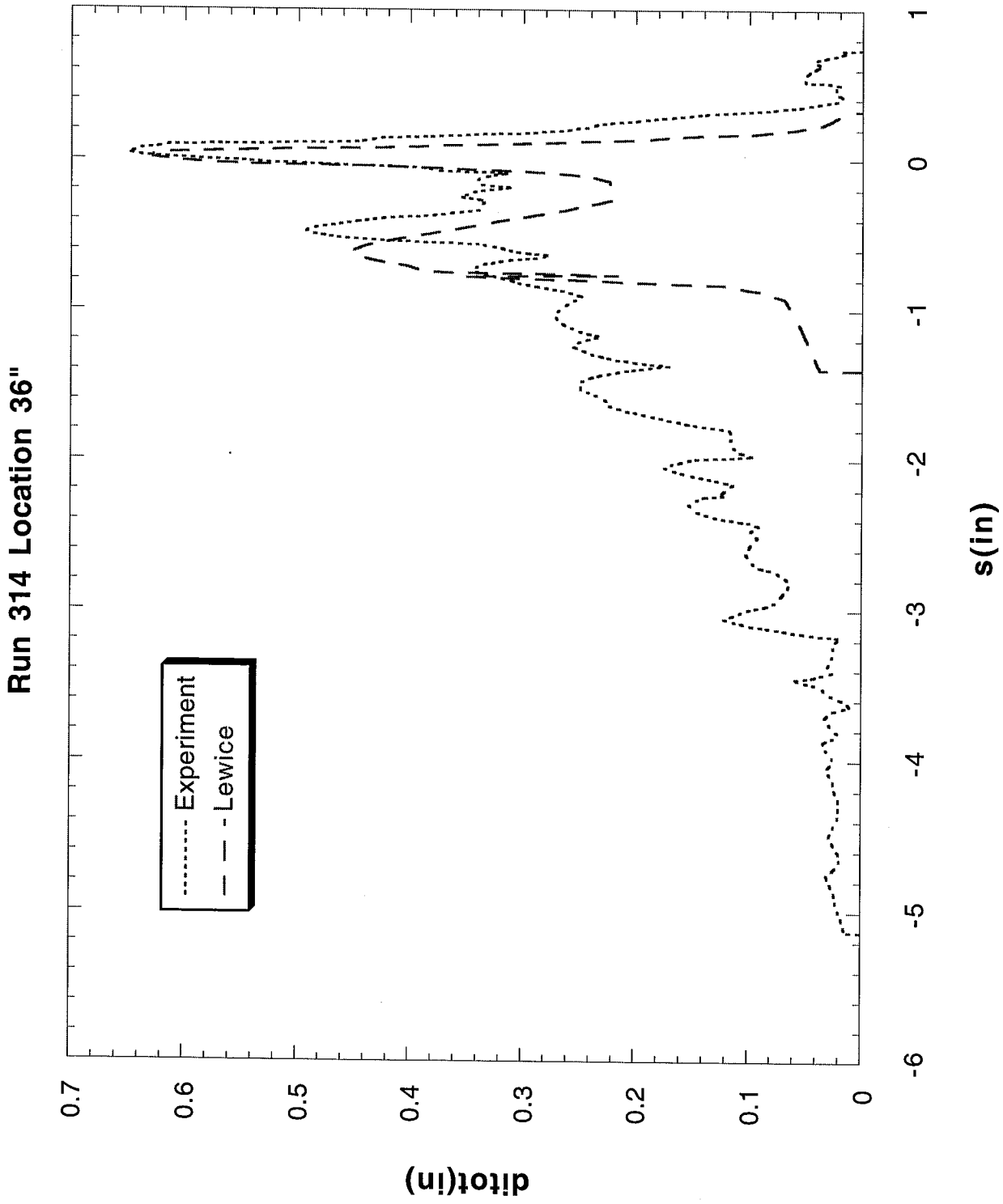
Run 314 Location 36"
Experiment
Lewice
dltot(in)
s(in)
0.7
0.6
0.5
0.4
0.3
0.2
0.1
0
1
0
-1
-2
-3
-4
-5
-6

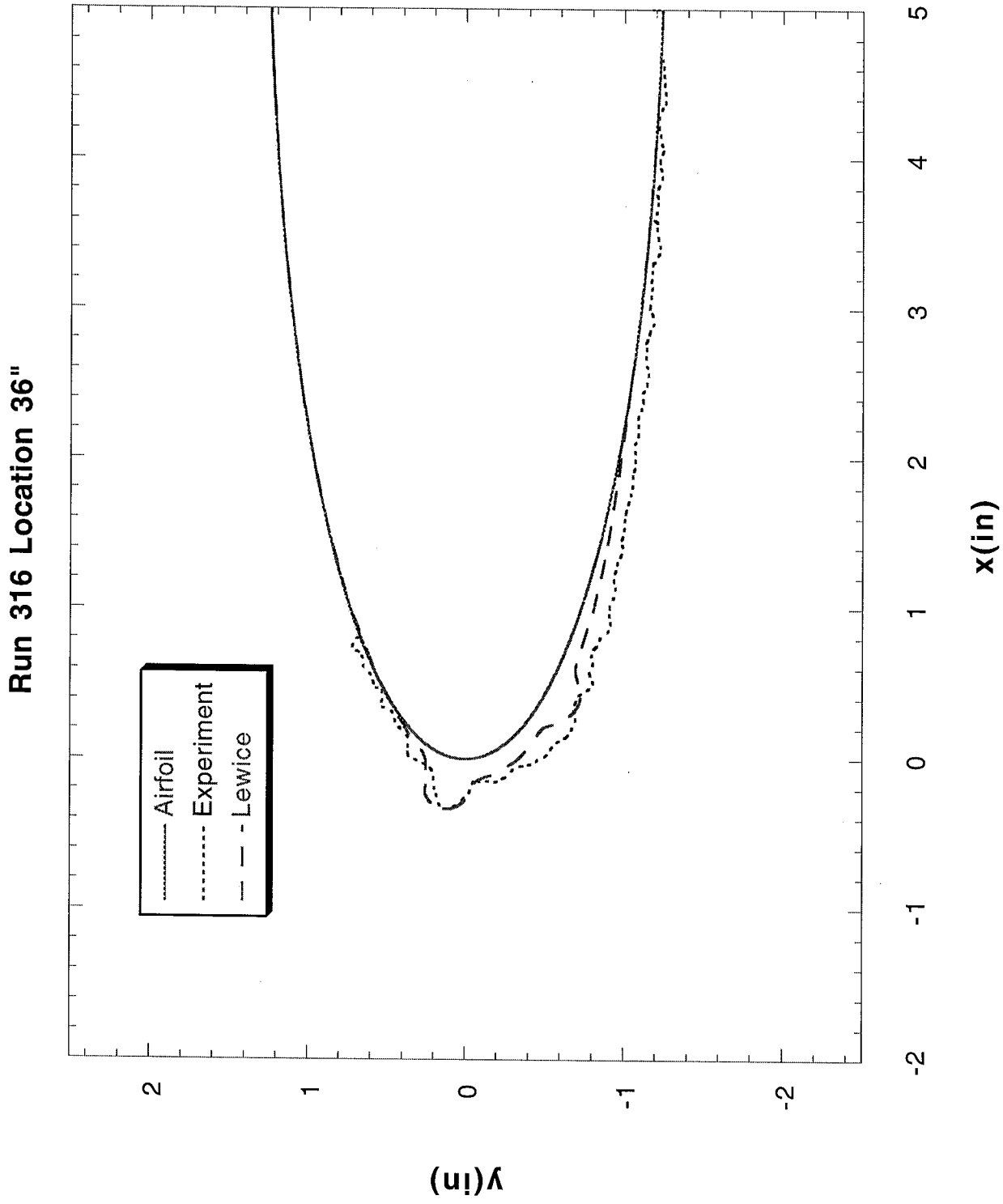
Run 316 Location 36"
Airfoil
Experiment
Lewice
y(in)
x(in)
2
1
0
-1
-2
-2
-1
0
1
2
3
4
5

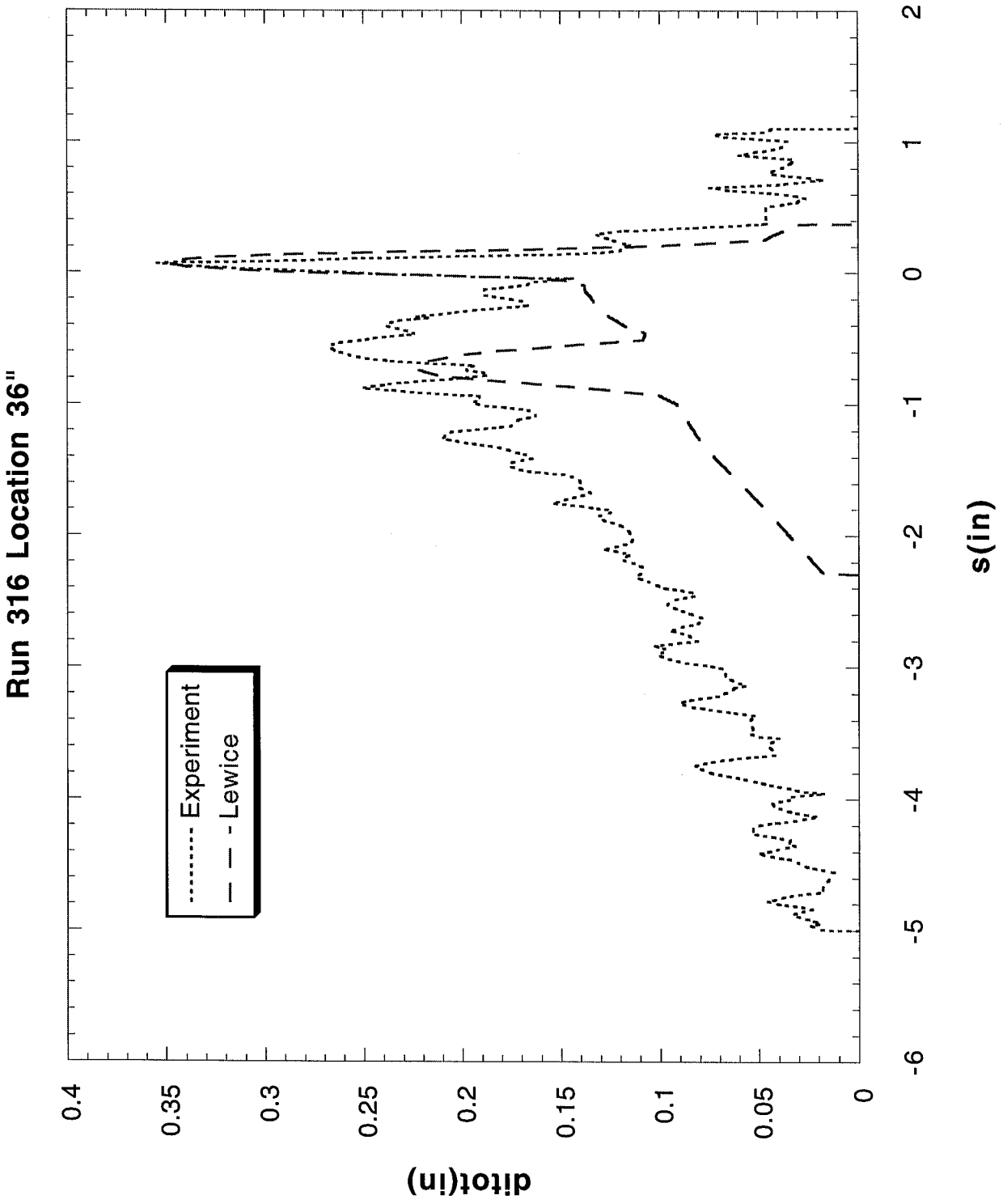
Run 316 Location 36"
Experiment
Lewice
dltot(in)
s(in)
0.4
0.35
0.3
0.25
0.2
0.15
0.1
0.05
0
-6
-5
-4
-3
-2
-1
0
1
2

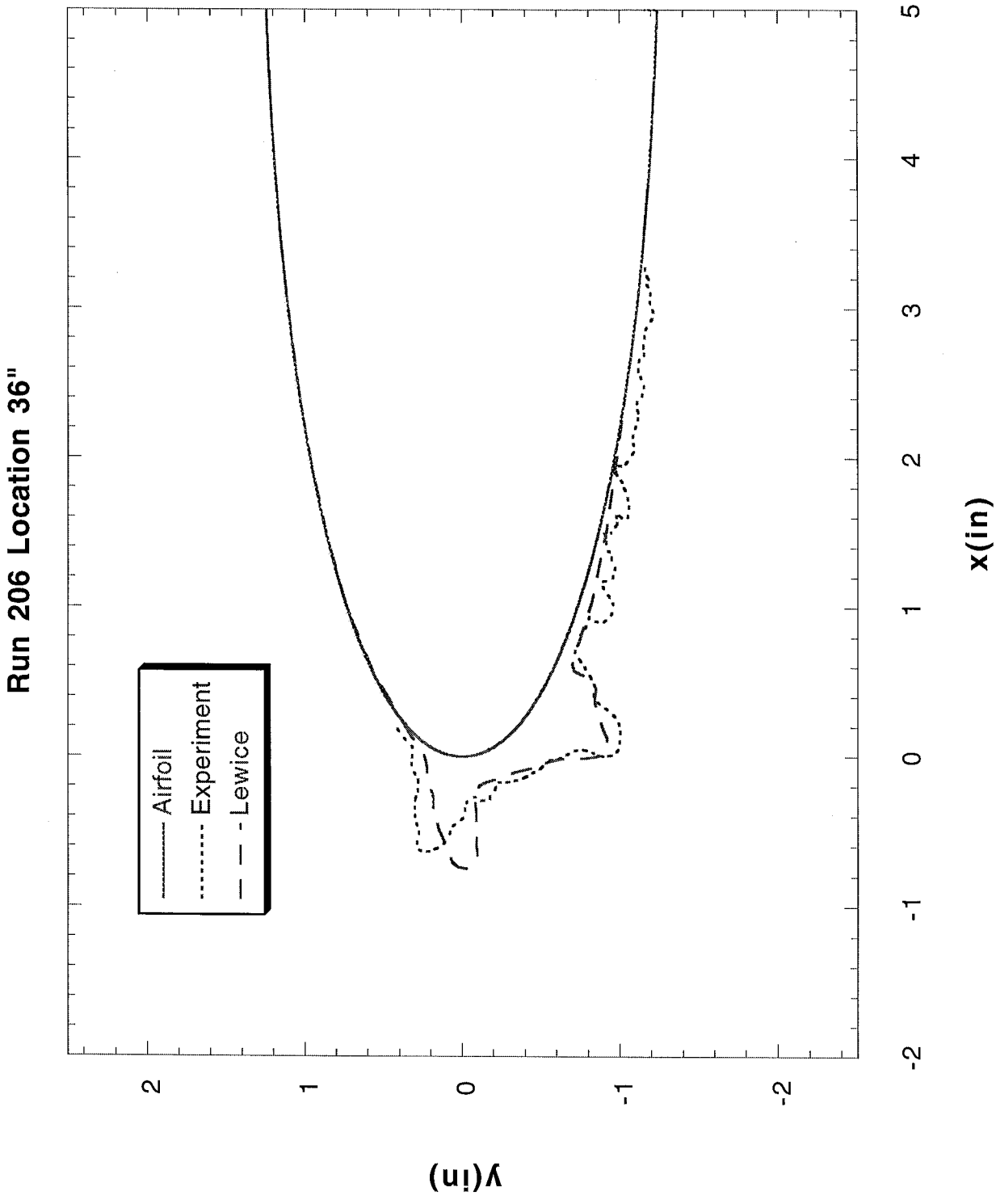
Run 206 Location 36"
Airfoil
Experiment
Lewice
y(in)
x(in)
2
1
0
-1
-2
-2
-1
0
1
2
3
4
5

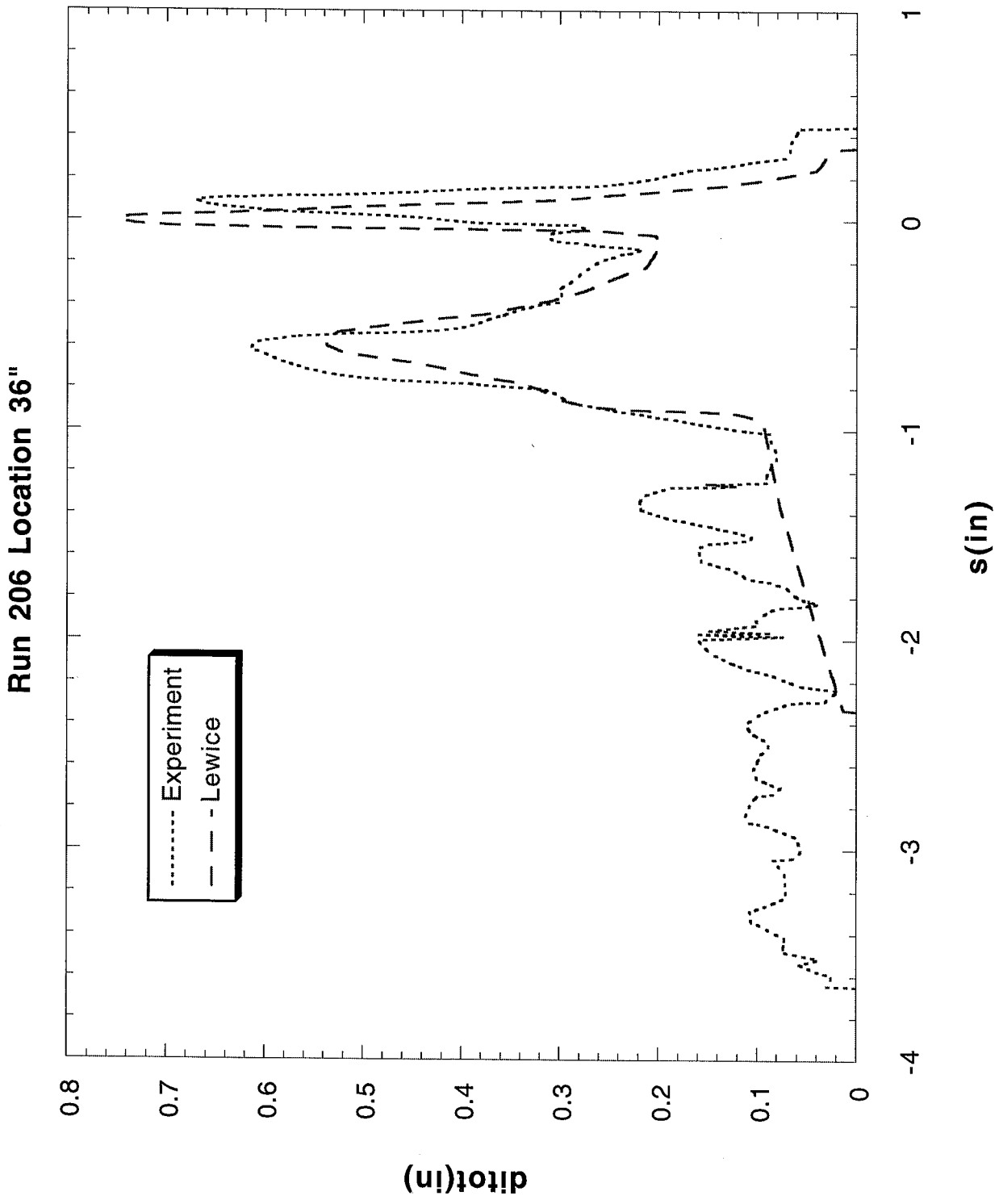
Run 206 Location 36"
Experiment
Lewice
dtot(in)
s(in)
0.8
0.7
0.6
0.5
0.4
0.3
0.2
0.1
0
-4
-3
-2
-1
0
1

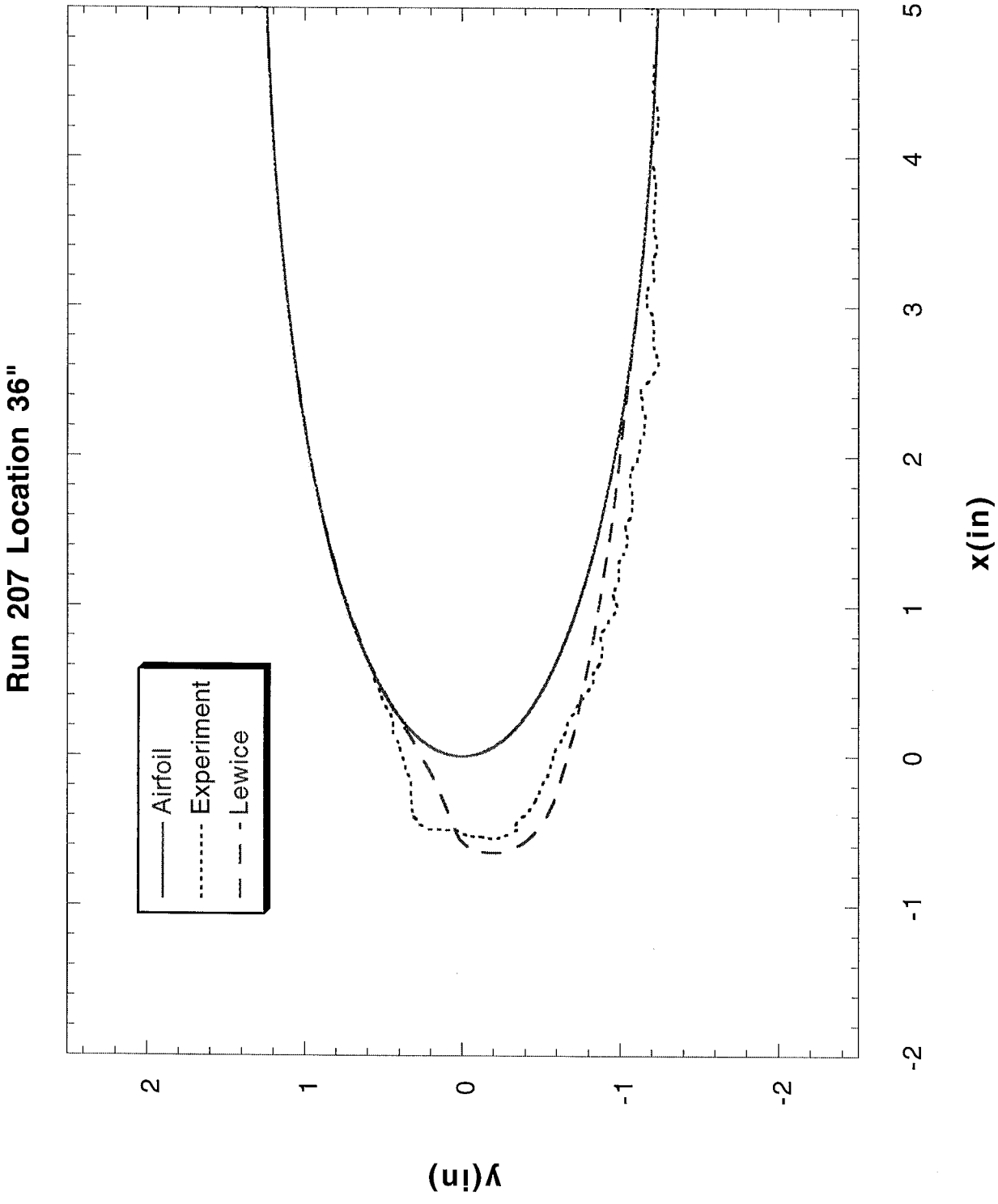
Run 207 Location 36"
Airfoil
Experiment
Lewice
y(in)
x(in)
2
1
0
-1
-2
-2
-1
0
1
2
3
4
5

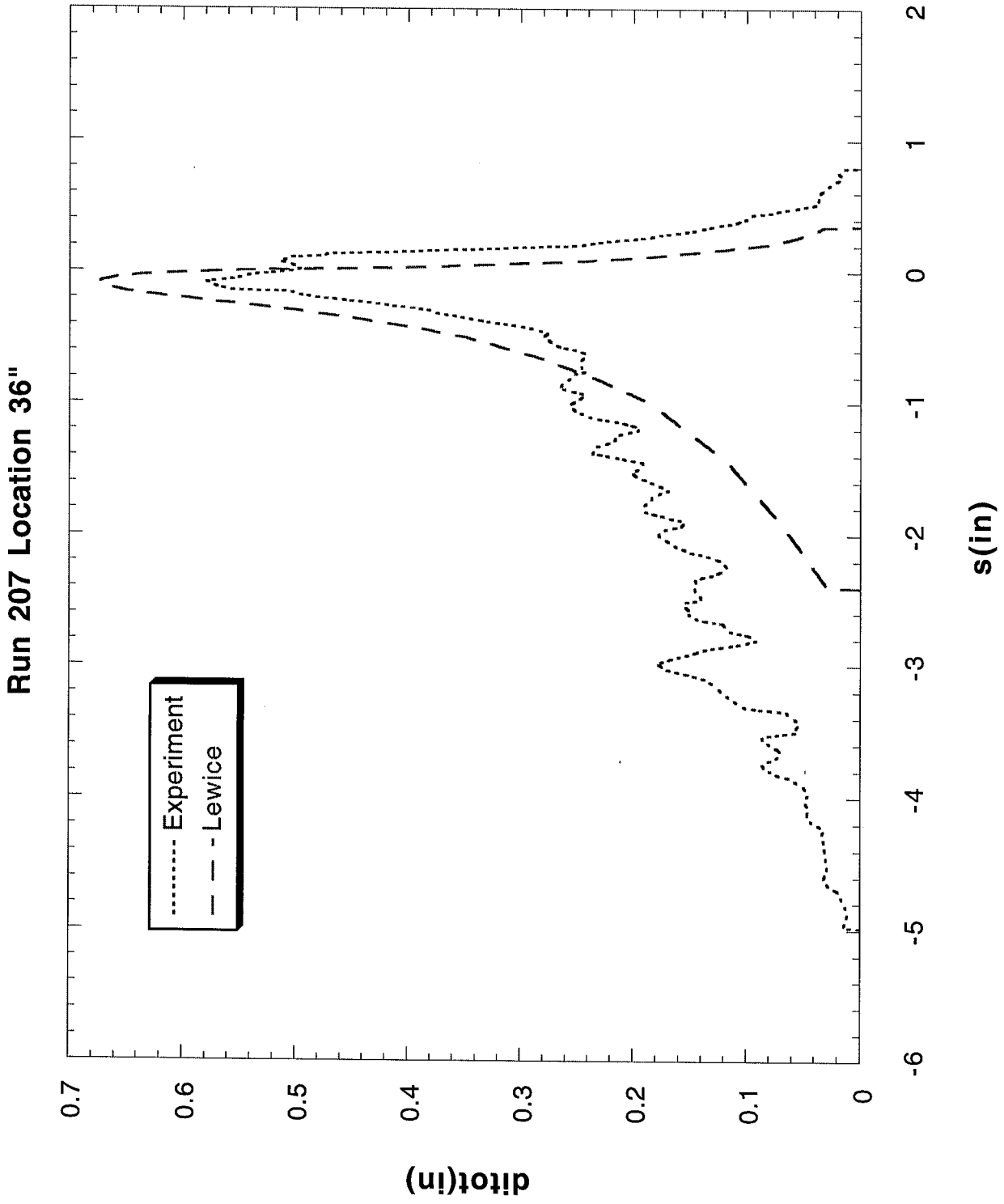
Run 207 Location 36"
Experiment
Lewice
dltot(in)
s(in)
0.7
0.6
0.5
0.4
0.3
0.2
0.1
0
2
1
0
-1
-2
-3
-4
-5
-6

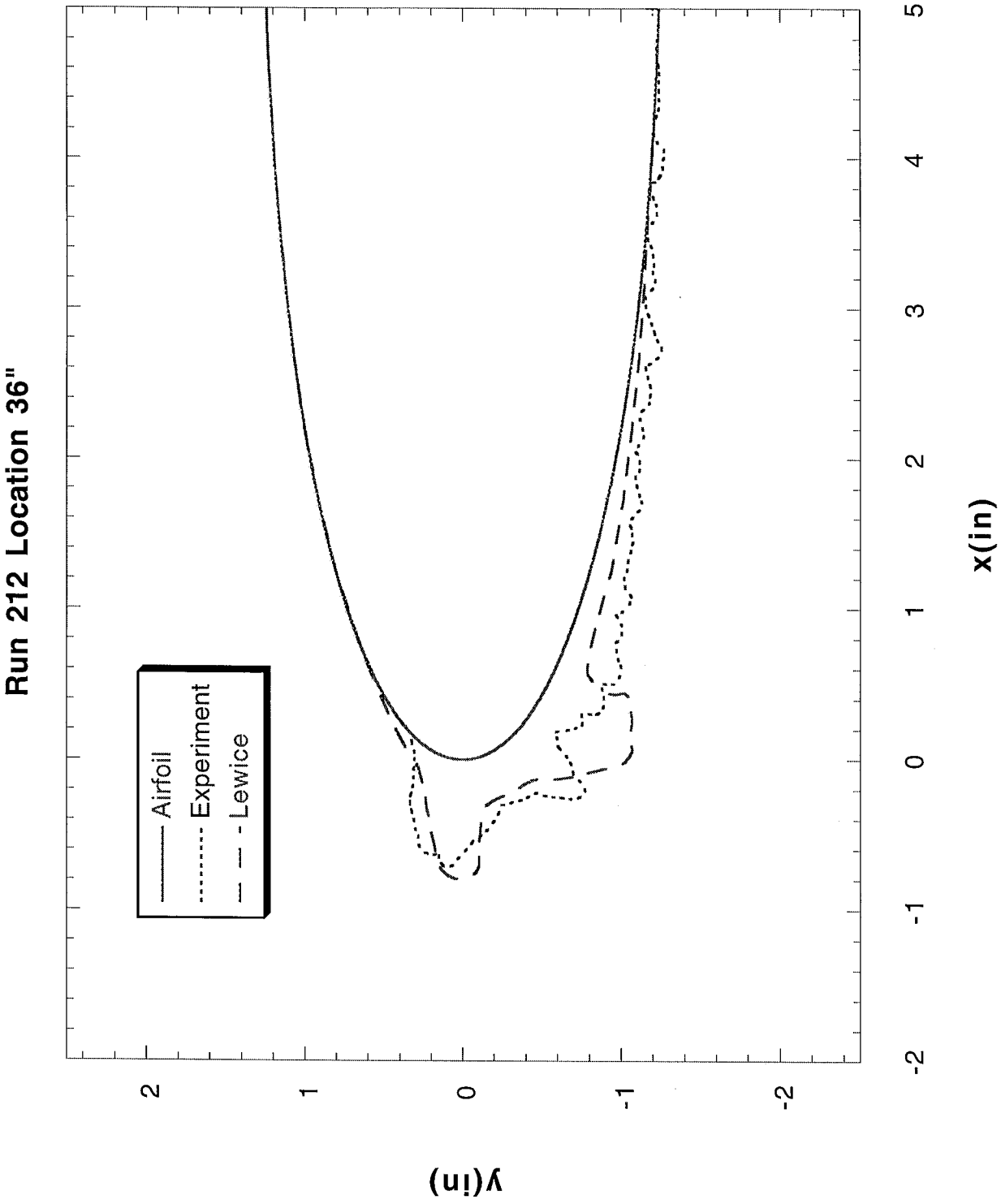
Run 212 Location 36"
Airfoil
Experiment
Lewice
y(in)
x(in)
2
1
0
-1
-2
-2
-1
0
1
2
3
4
5

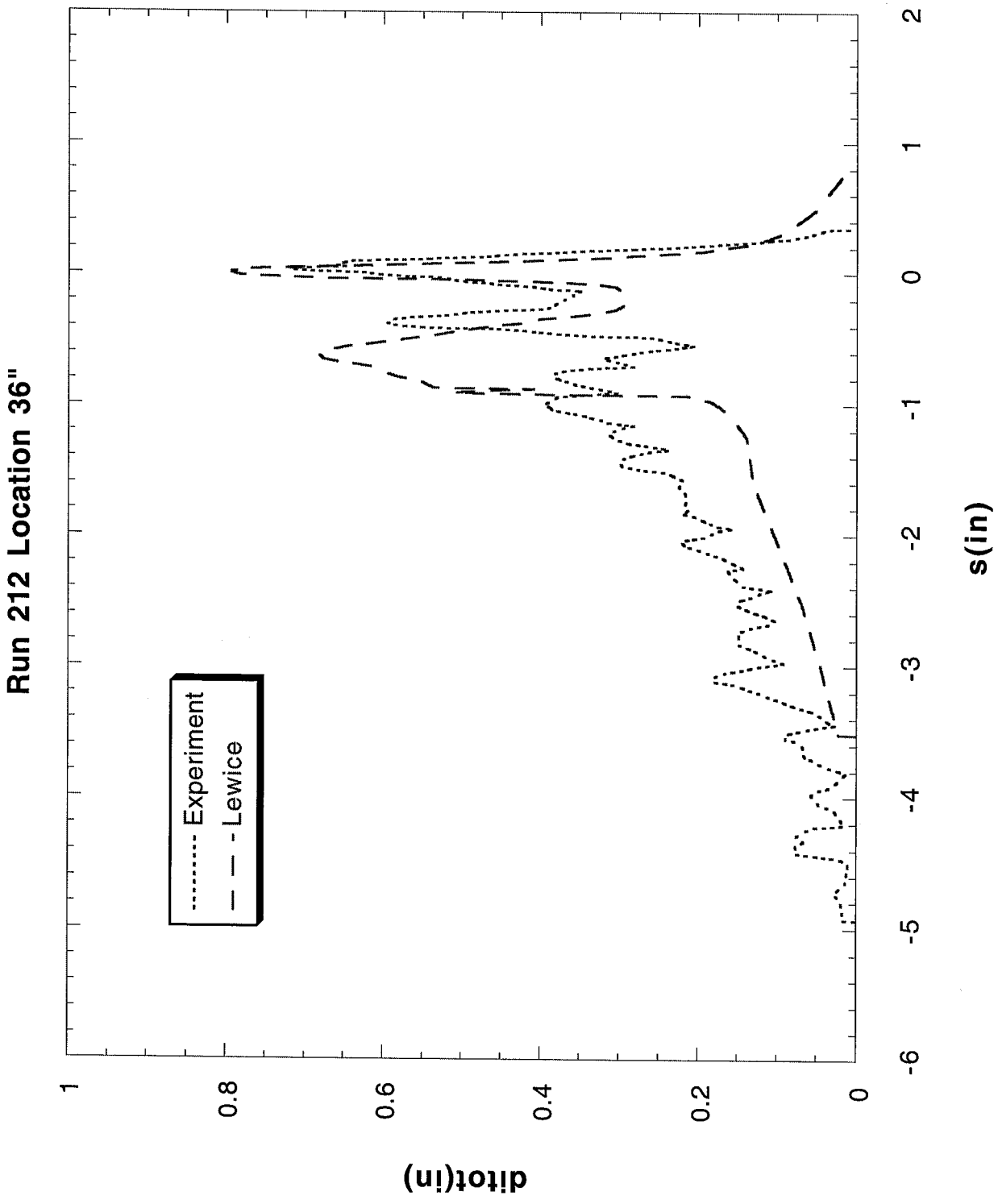
Run 212 Location 36"
Experiment
Lewice
dltot(in)
s(in)
1
0.8
0.6
0.4
0.2
0
2
1
0
-1
-2
-3
-4
-5
-6

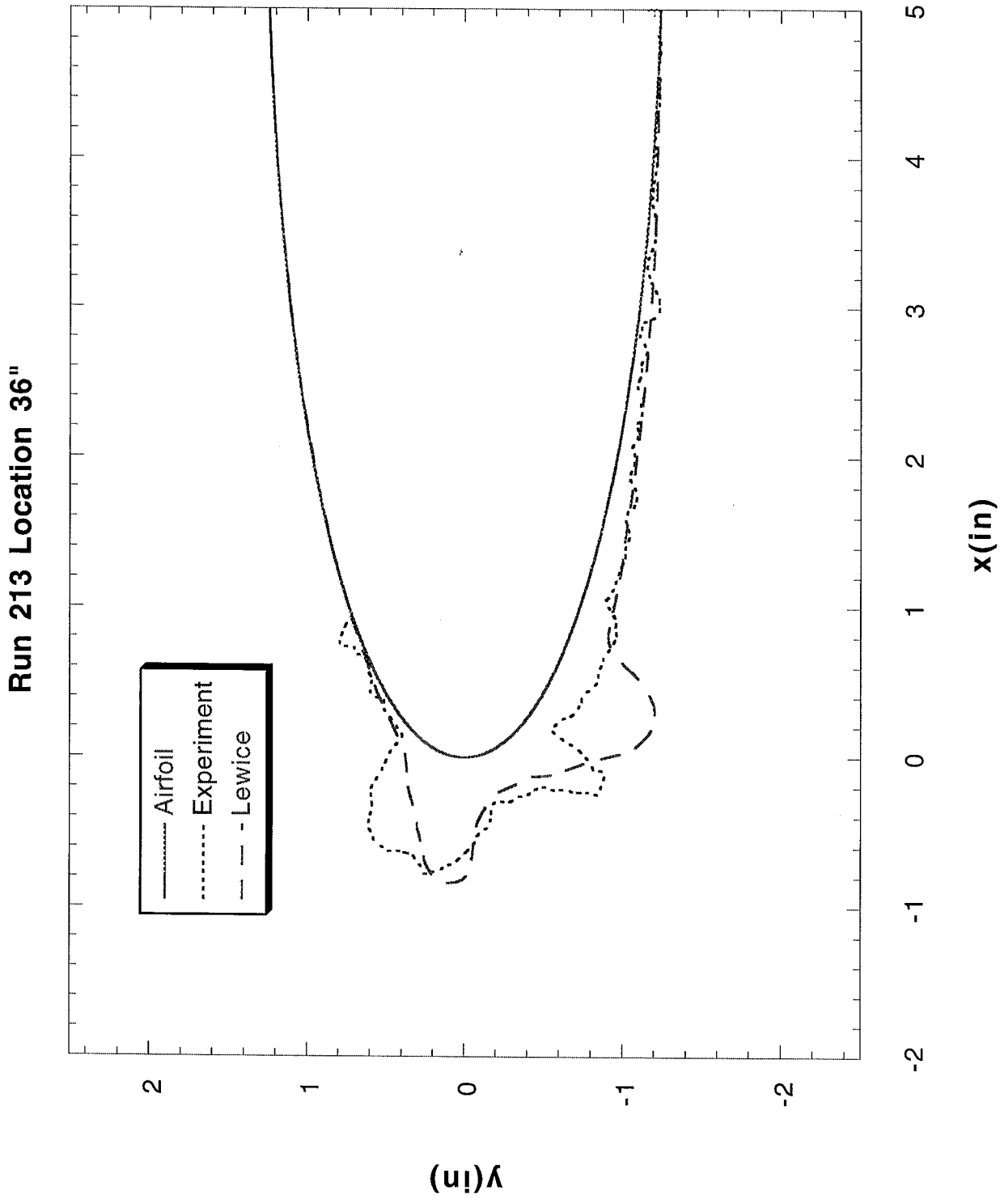
Run 213 Location 36"
Airfoil
Experiment
Lewice
y(in)
x(in)
2
1
0
-1
-2
-2
-1
0
1
2
3
4
5

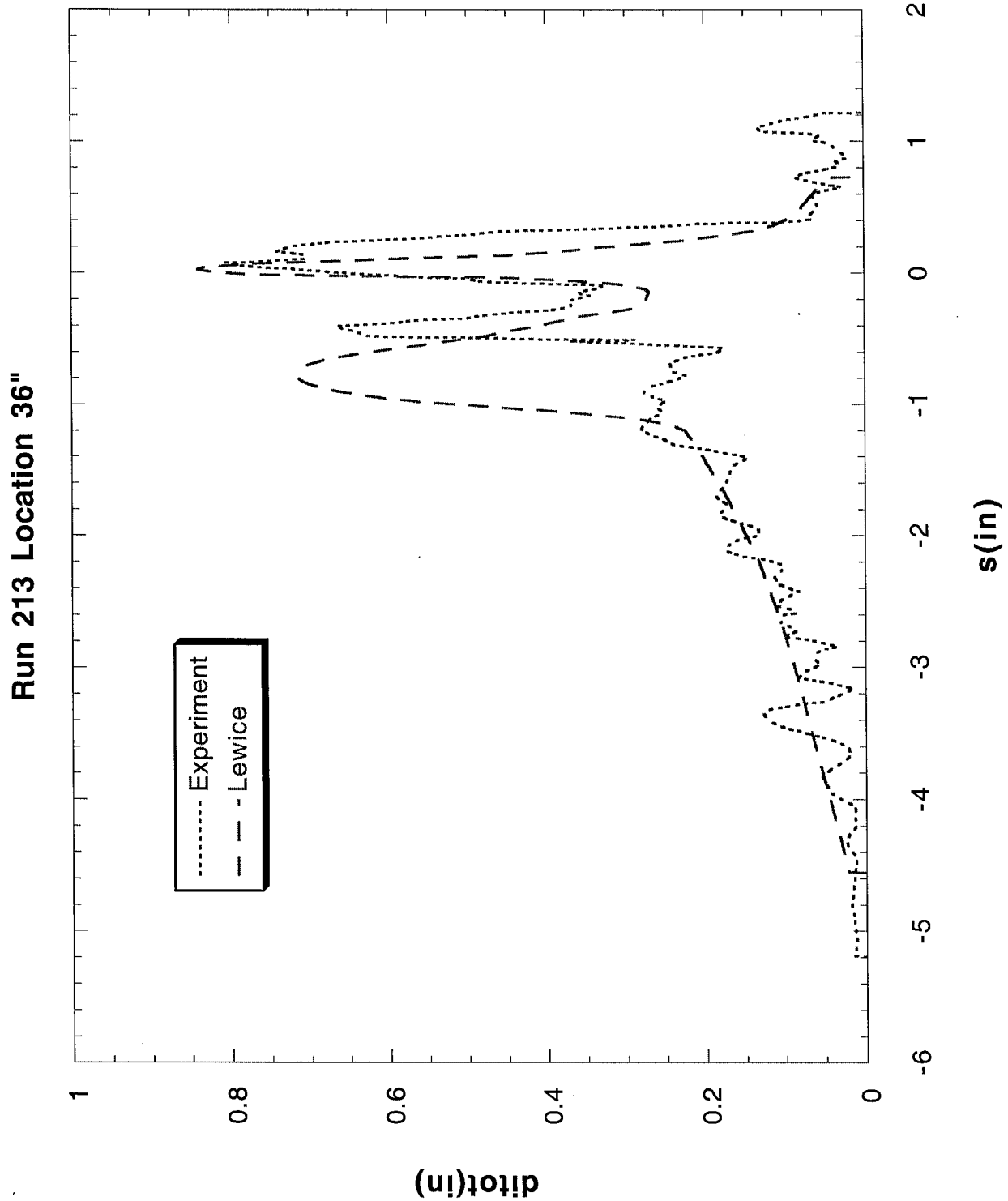
Run 213 Location 36"
Experiment
Lewice
dltot(in)
s(in)
1
0.8
0.6
0.4
0.2
0
-6
-5
-4
-3
-2
-1
0
1
2

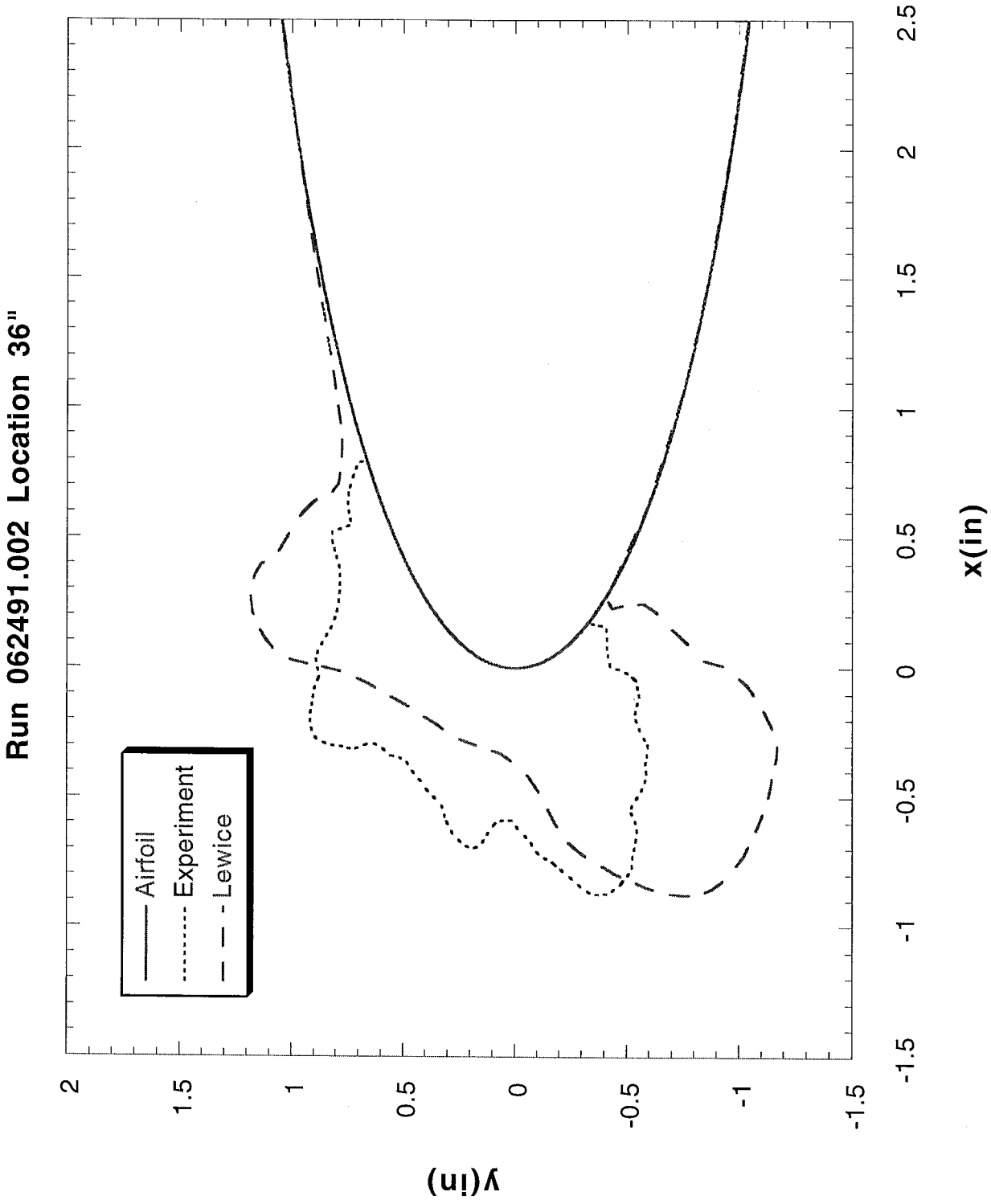
Run 062491.002 Location 36"
Airfoil
Experiment
Lewice
y(in)
x(in)
2
1.5
1
0.5
0
-0.5
-1
-1.5
2.5
2
1.5
1
0.5
0
-0.5
-1
-1.5

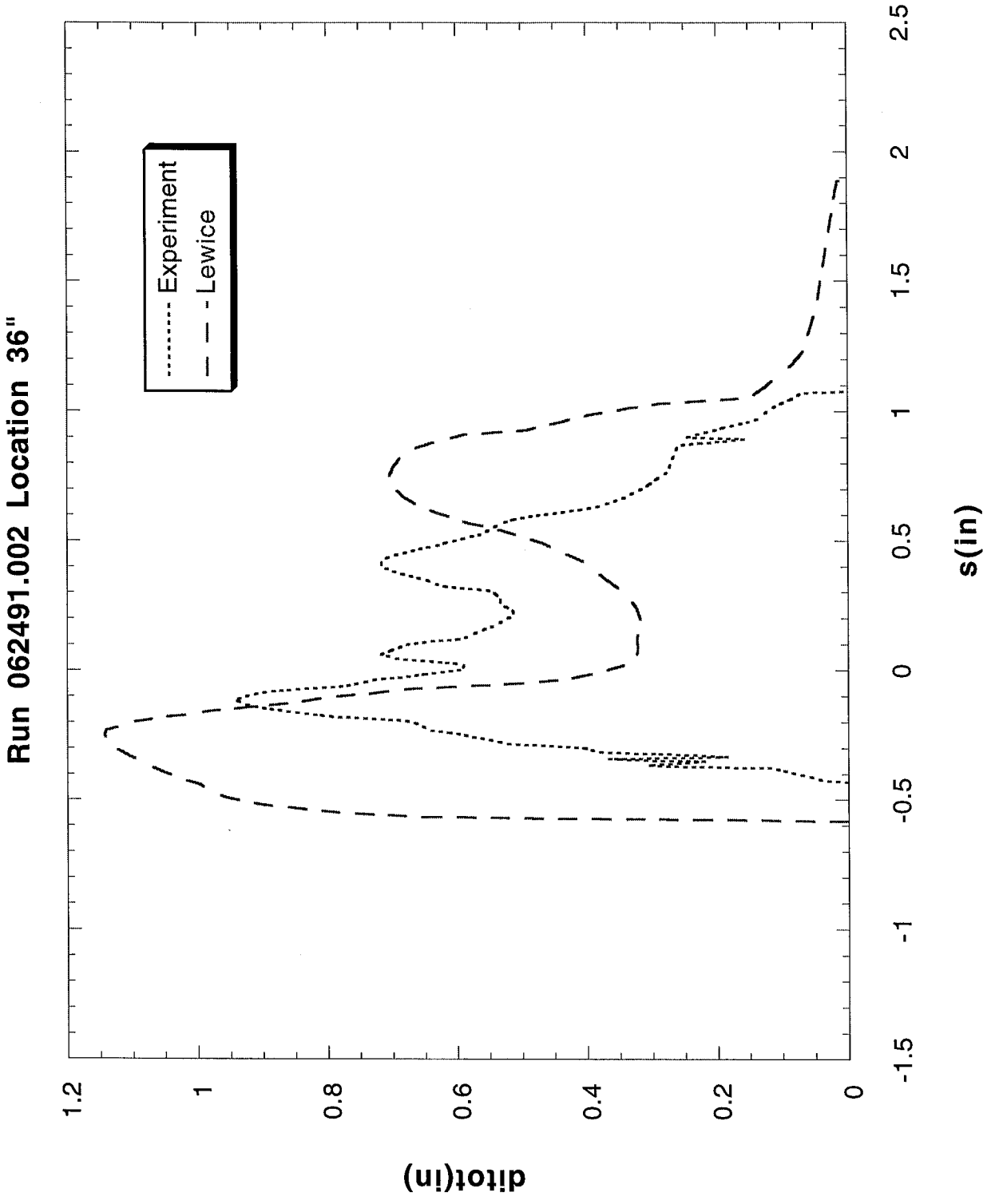
Run 062491.002 Location 36"
Experiment
Lewice
dltot(in)
s(in)
1.2
1
0.8
0.6
0.4
0.2
0
-1.5
-1
-0.5
0
0.5
1
1.5
2
2.5

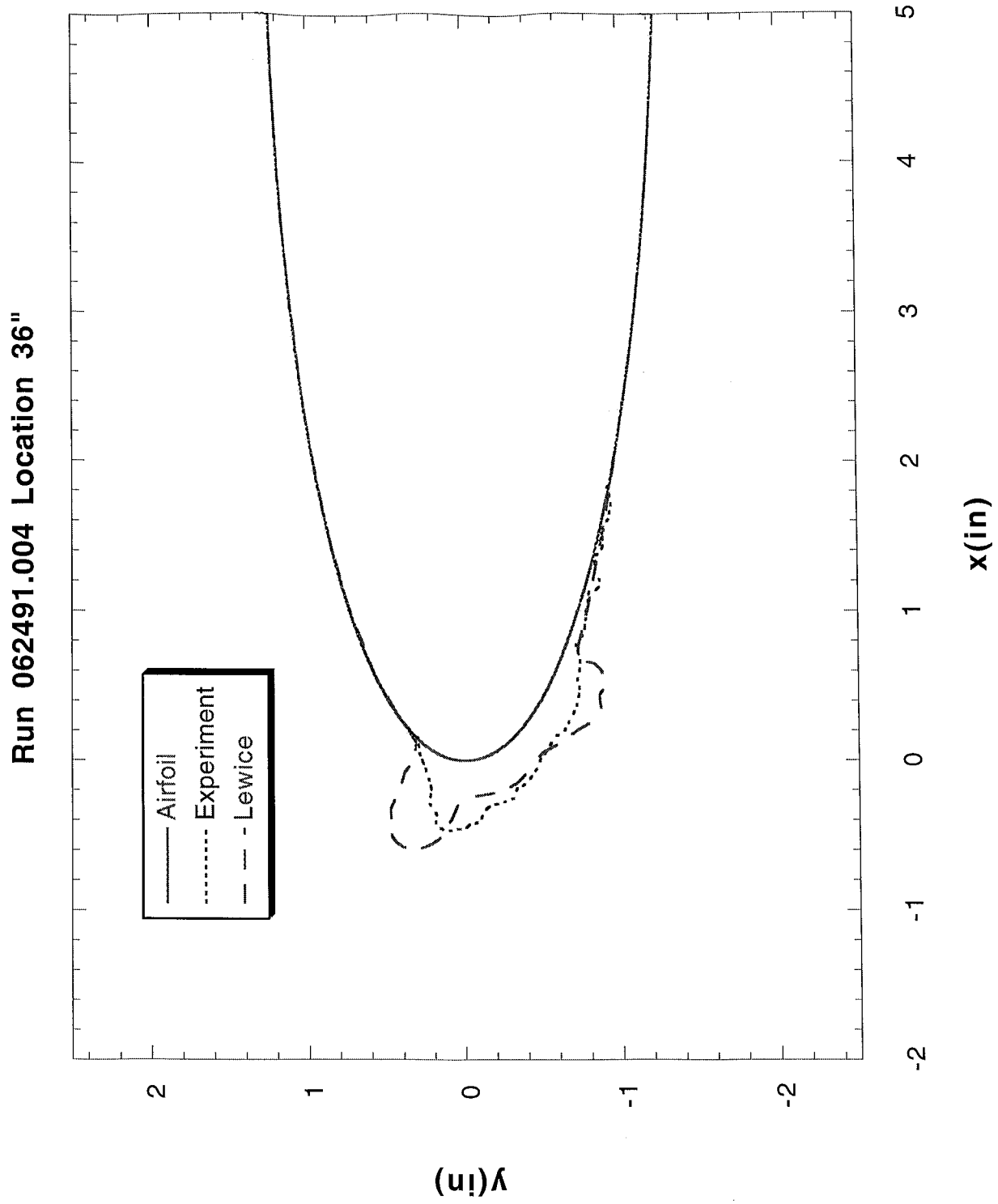
Run 062491.004 Location 36"
Airfoil
Experiment
Lewice
y(in)
x(in)
2
1
0
-1
-2
-2
-1
0
1
2
3
4
5

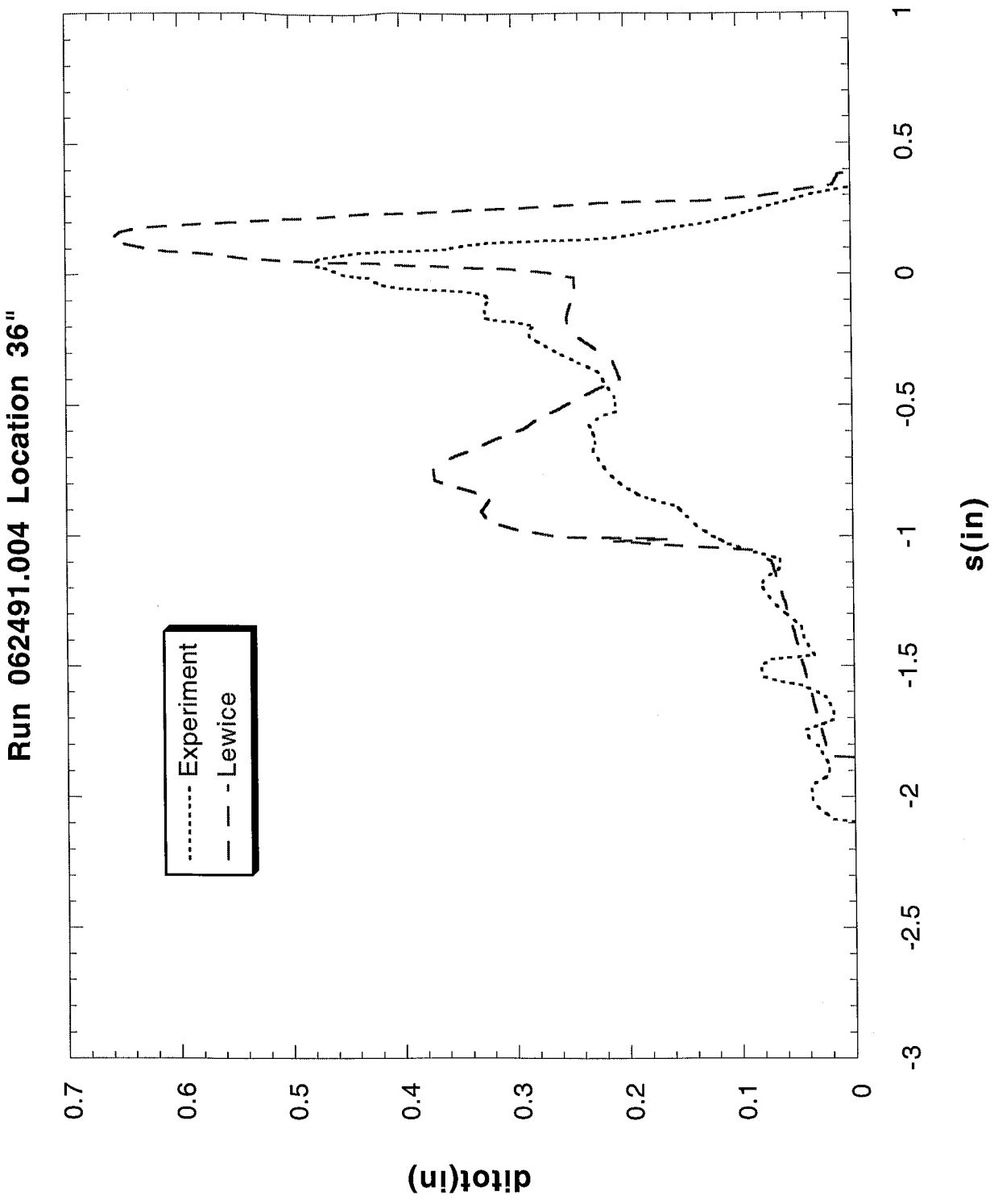
Run 062491.004 Location 36"
Experiment
Lewice
ditot(in)
s(in)
0.7
0.6
0.5
0.4
0.3
0.2
0.1
0
-3
-2.5
-2
-1.5
-1
-0.5
0
0.5
1

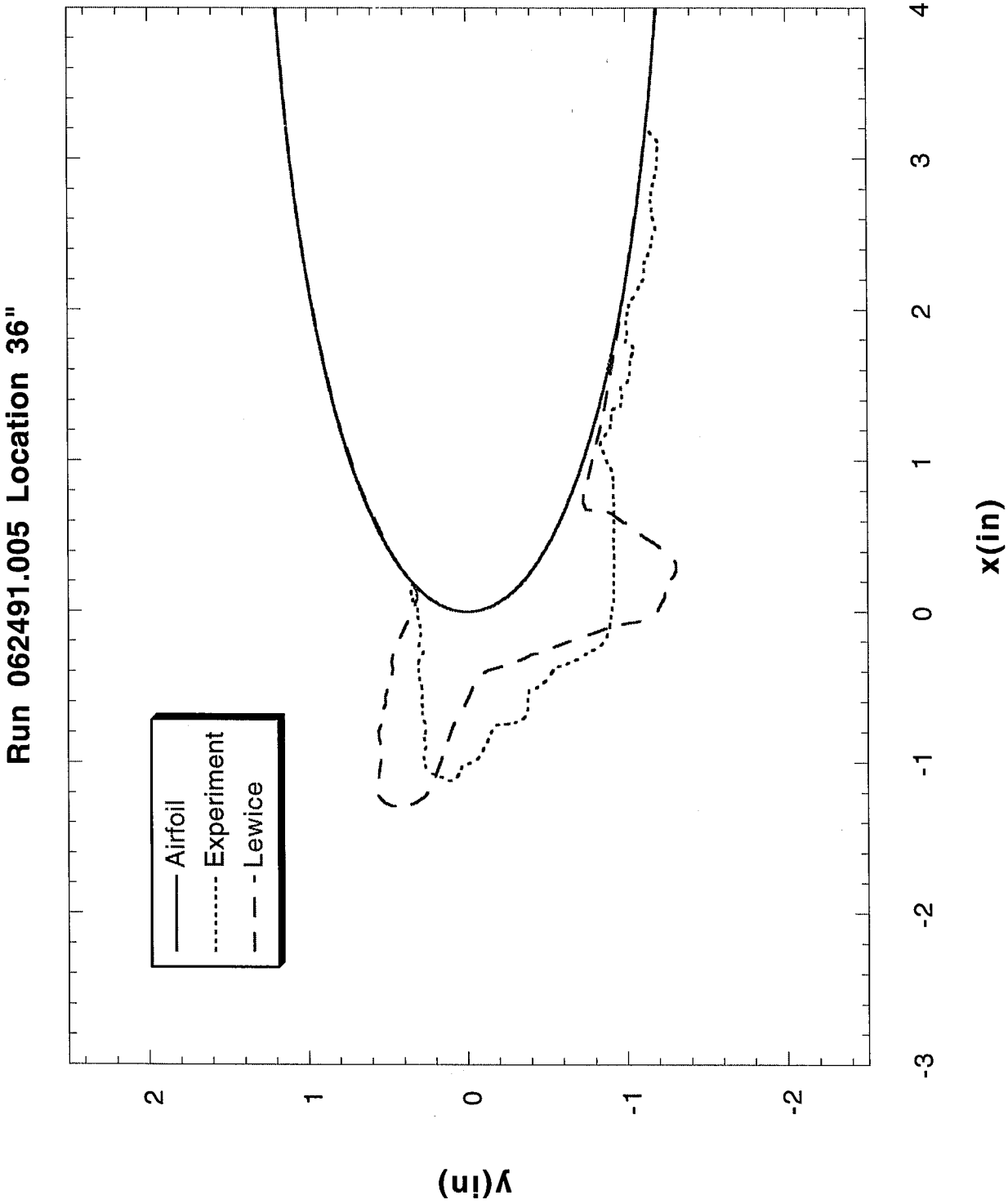
Run 062491.005 Location 36"
Airfoil
Experiment
Lewice
y(in)
x(in)
2
1
0
-1
-2
-3
-2
-1
0
1
2
3
4

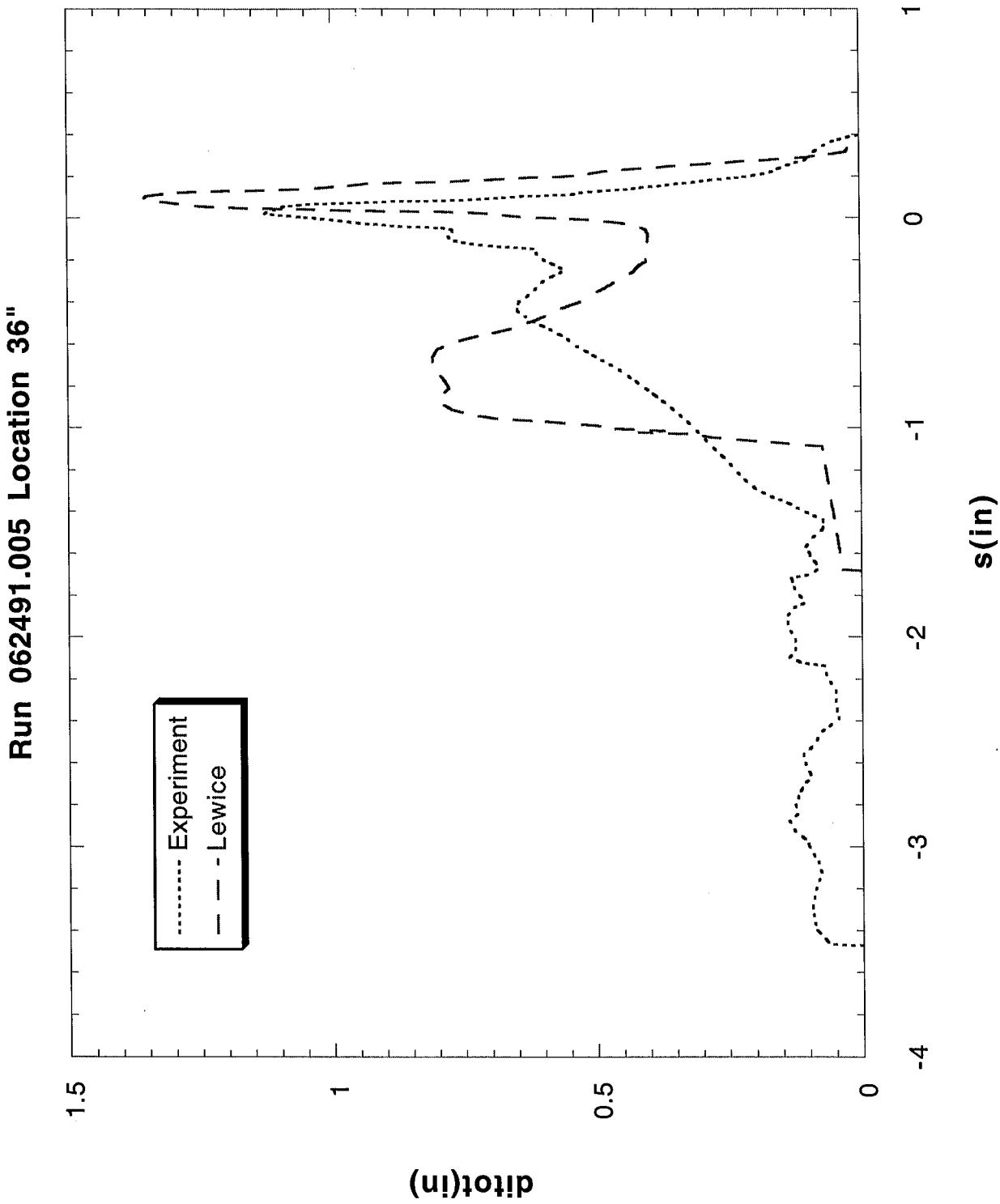
Run 062491.005 Location 36"
Experiment
Lewice
ditot(in)
s(in)
1.5
1
0.5
0
-4
-3
-2
-1
0
1

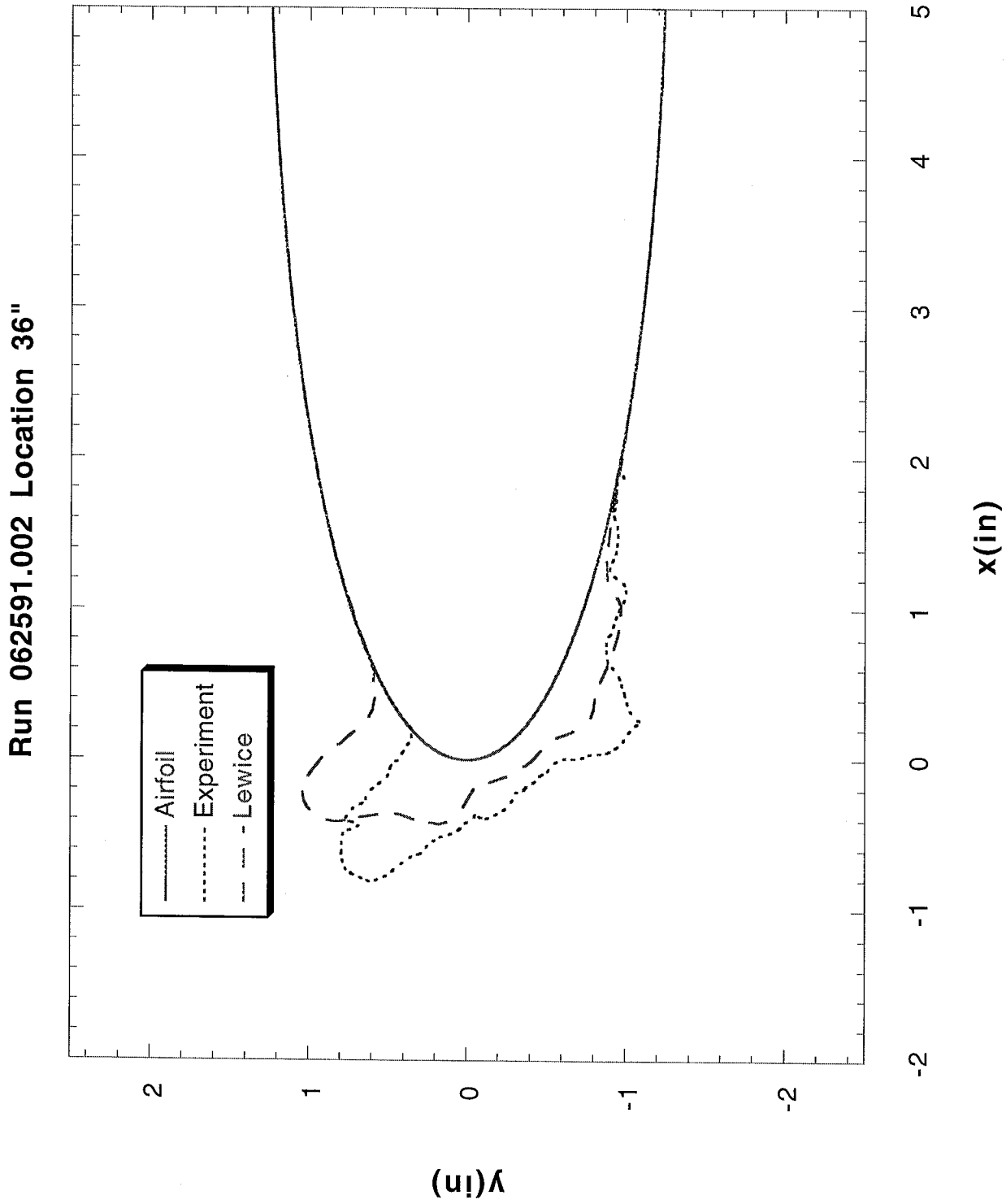
Run 062591.002 Location 36"
Airfoil
Experiment
- Lewice
y(in)
x(in)
2
1
0
-1
-2
-2
-1
0
1
2
3
4
5

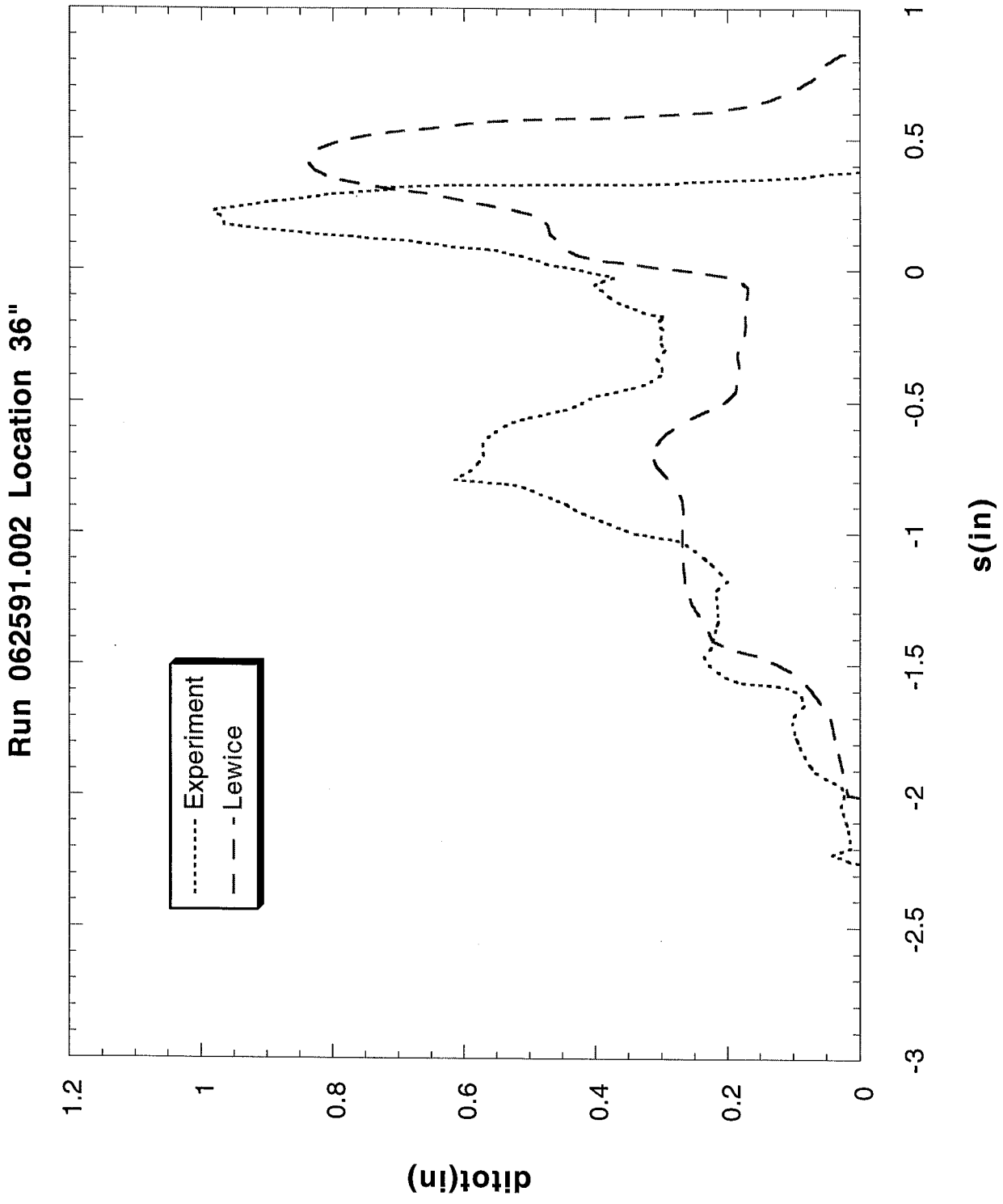
Run 062591.002 Location 36"
Experiment
Lewice
dltot(in)
s(in)
1.2
1
0.8
0.6
0.4
0.2
0
-3
-2.5
-2
-1.5
-1
-0.5
0
0.5
1

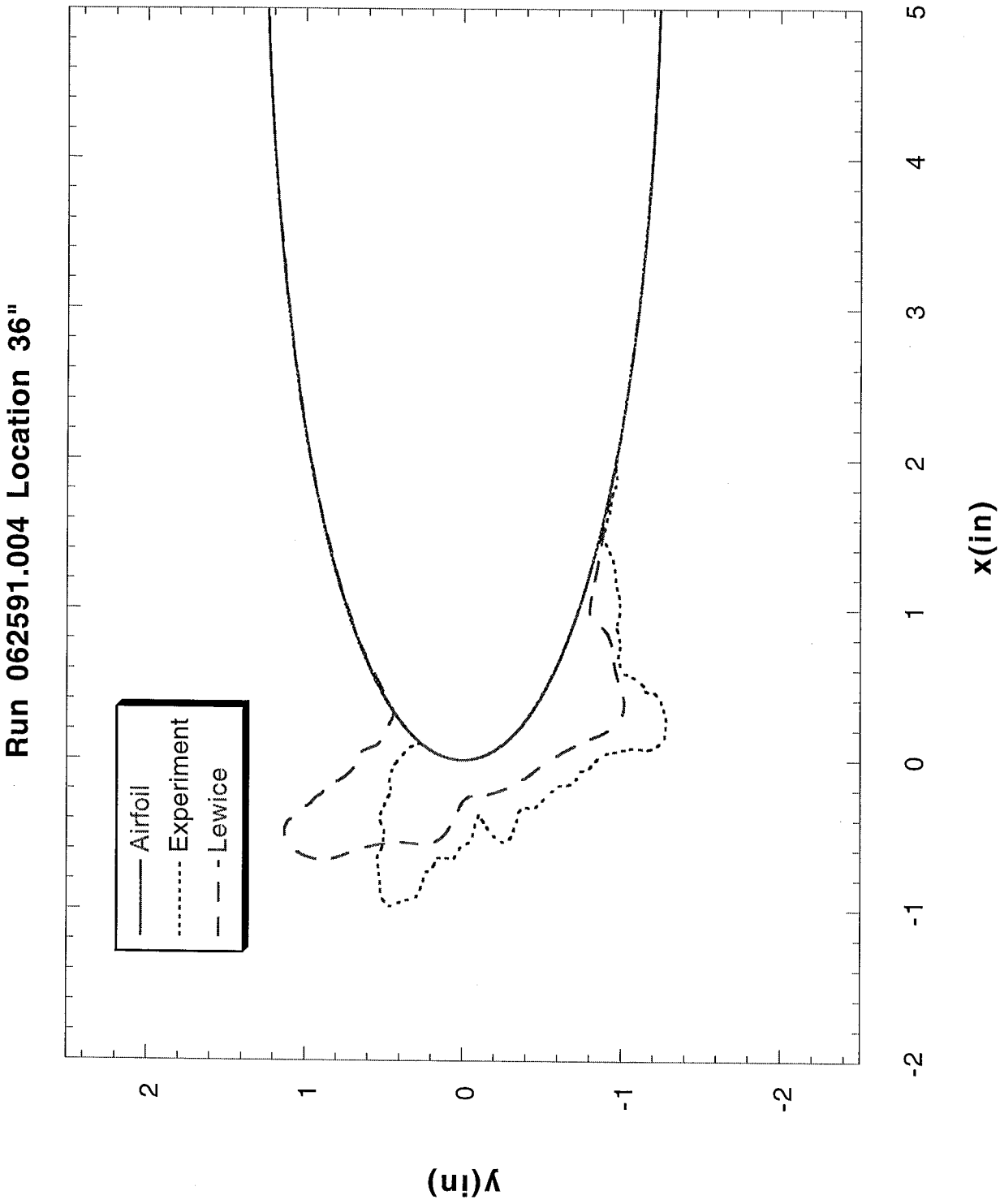
Run 062591.004 Location 36"
Airfoil
Experiment
Lewice
y(in)
x(in)
2
1
0
-1
-2
-2
-1
0
1
2
3
4
5

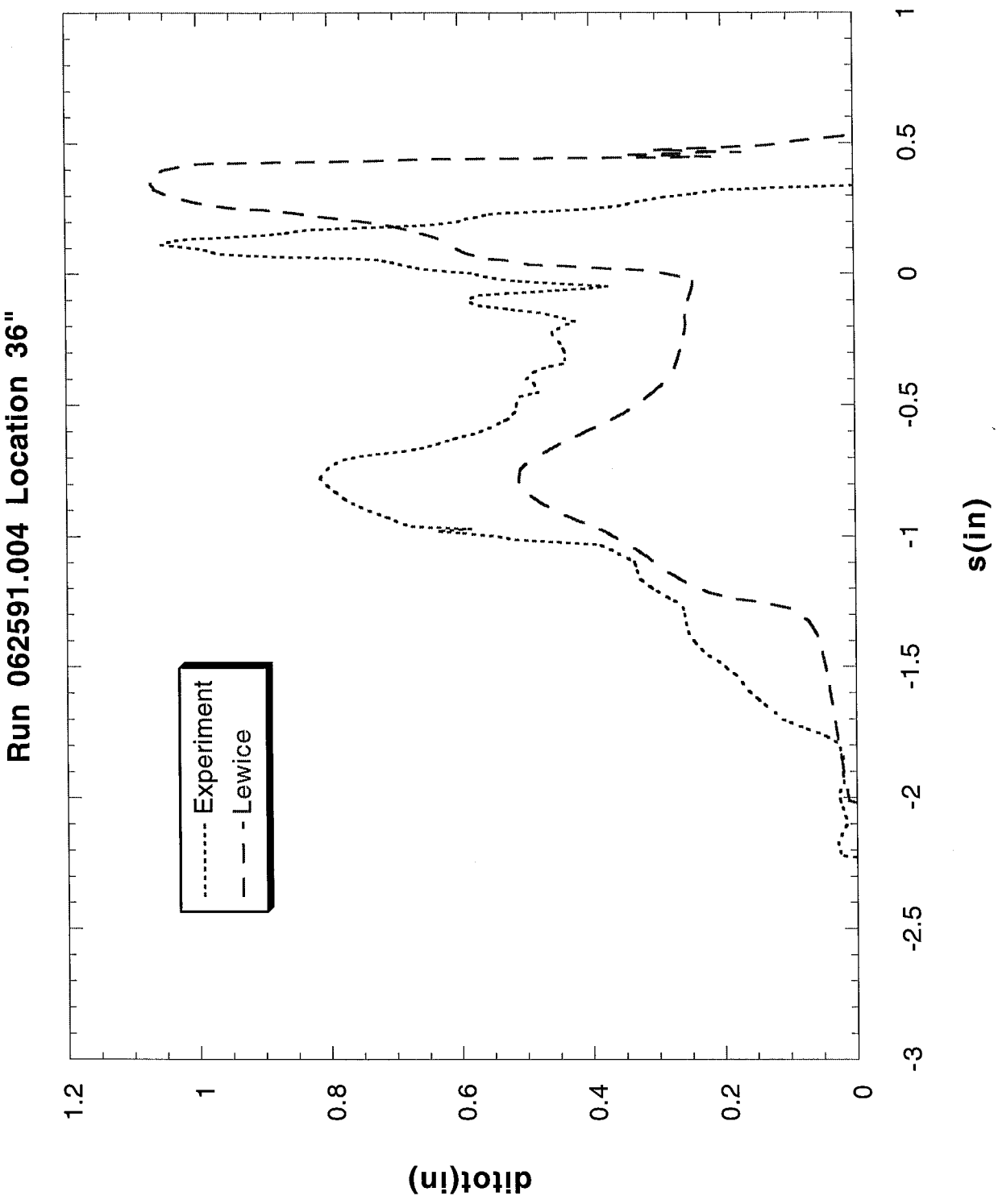
Run 062591.004 Location 36"
Experiment
Lewice
dltot(in)
s(in)
1.2
1
0.8
0.6
0.4
0.2
0
-3
-2.5
-2
-1.5
-1
-0.5
0
0.5
1

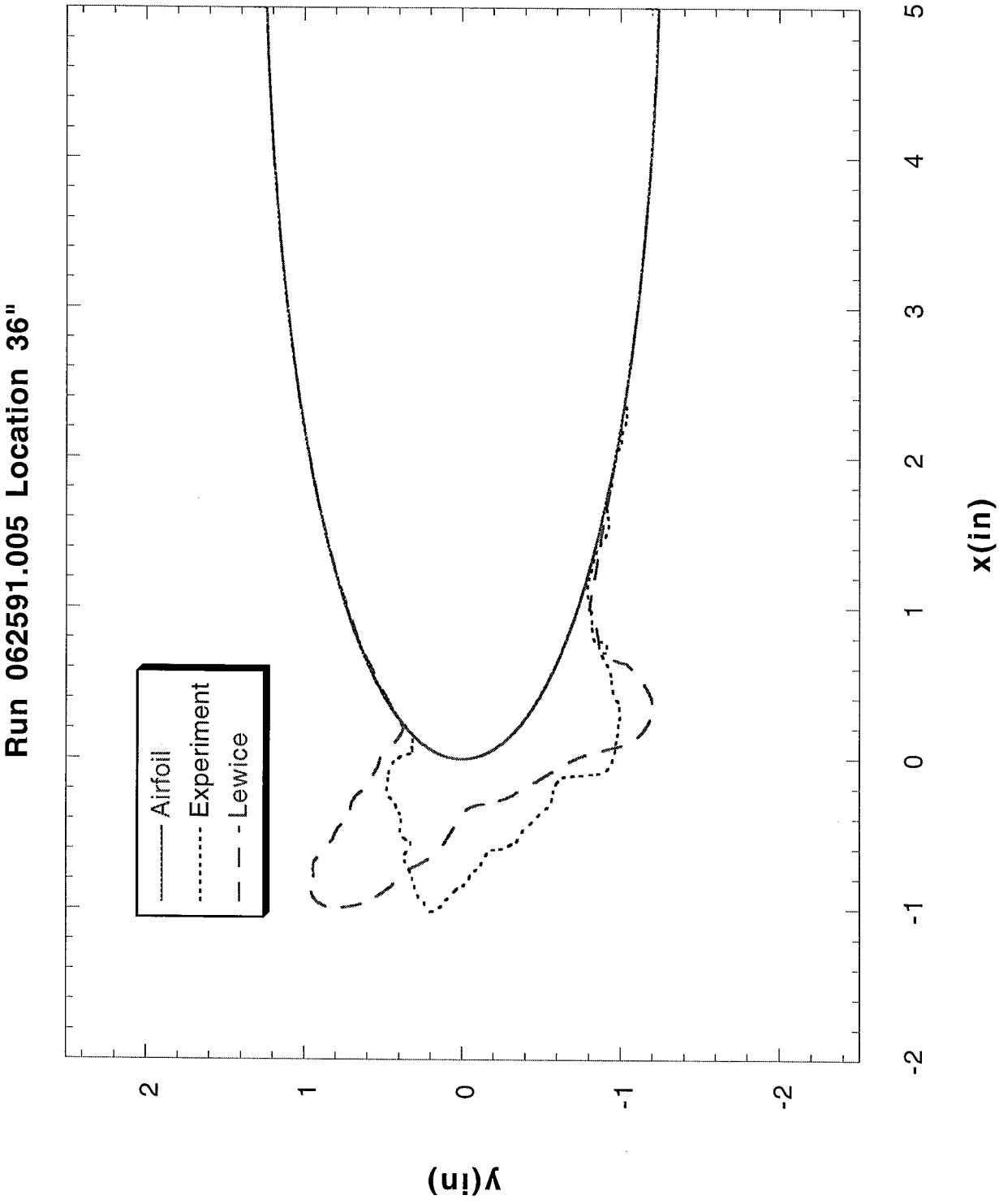
Run 062591.005 Location 36"
Airfoil
Experiment
Lewice
y(in)
x(in)
2
1
0
-1
-2
-2
-1
0
1
2
3
4
5

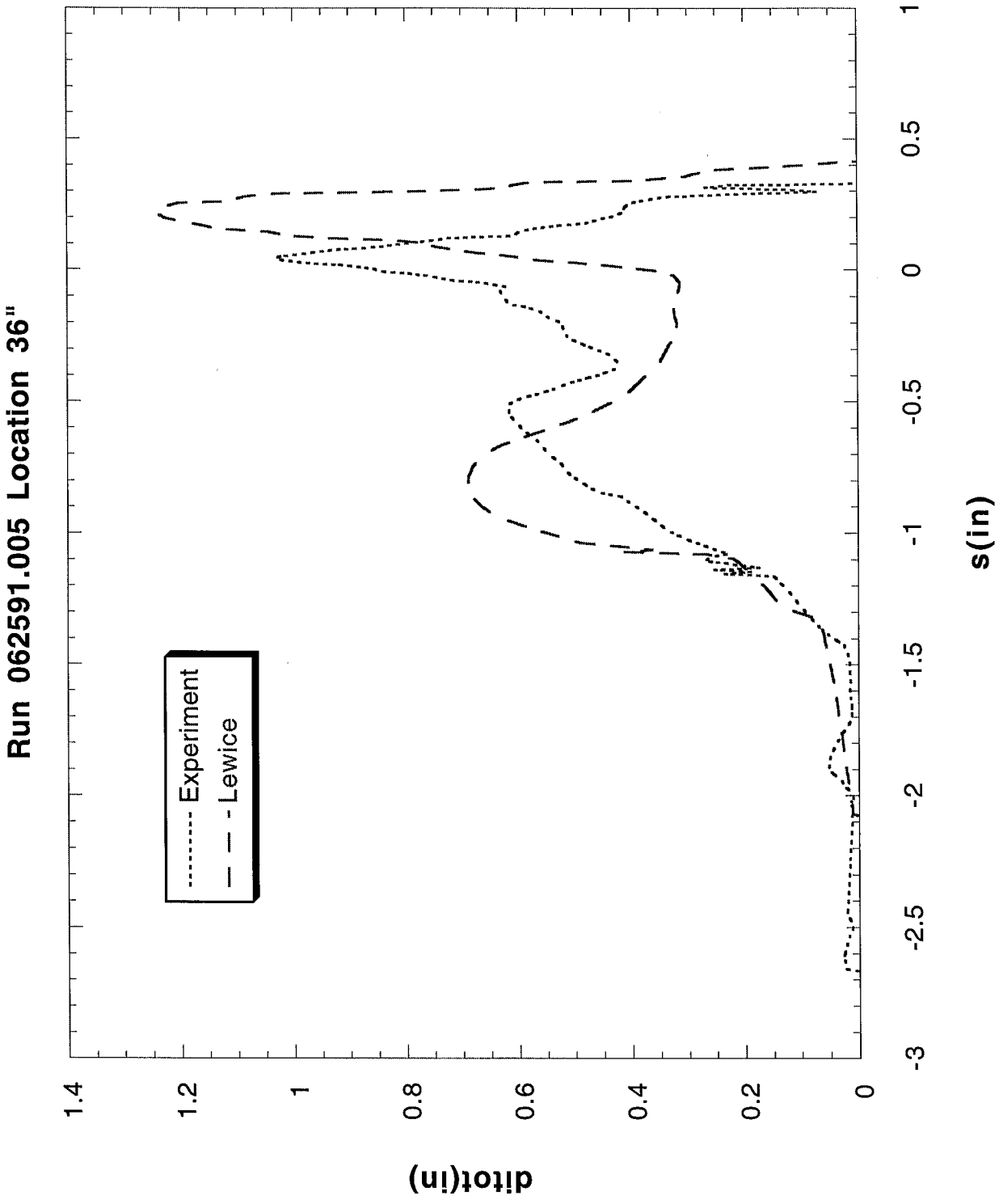
Run 062591.005 Location 36"
Experiment
Lewice
dltot(in)
s(in)
1.4
1.2
1
0.8
0.6
0.4
0.2
0
-3
-2.5
-2
-1.5
-1
-0.5
0
0.5
1

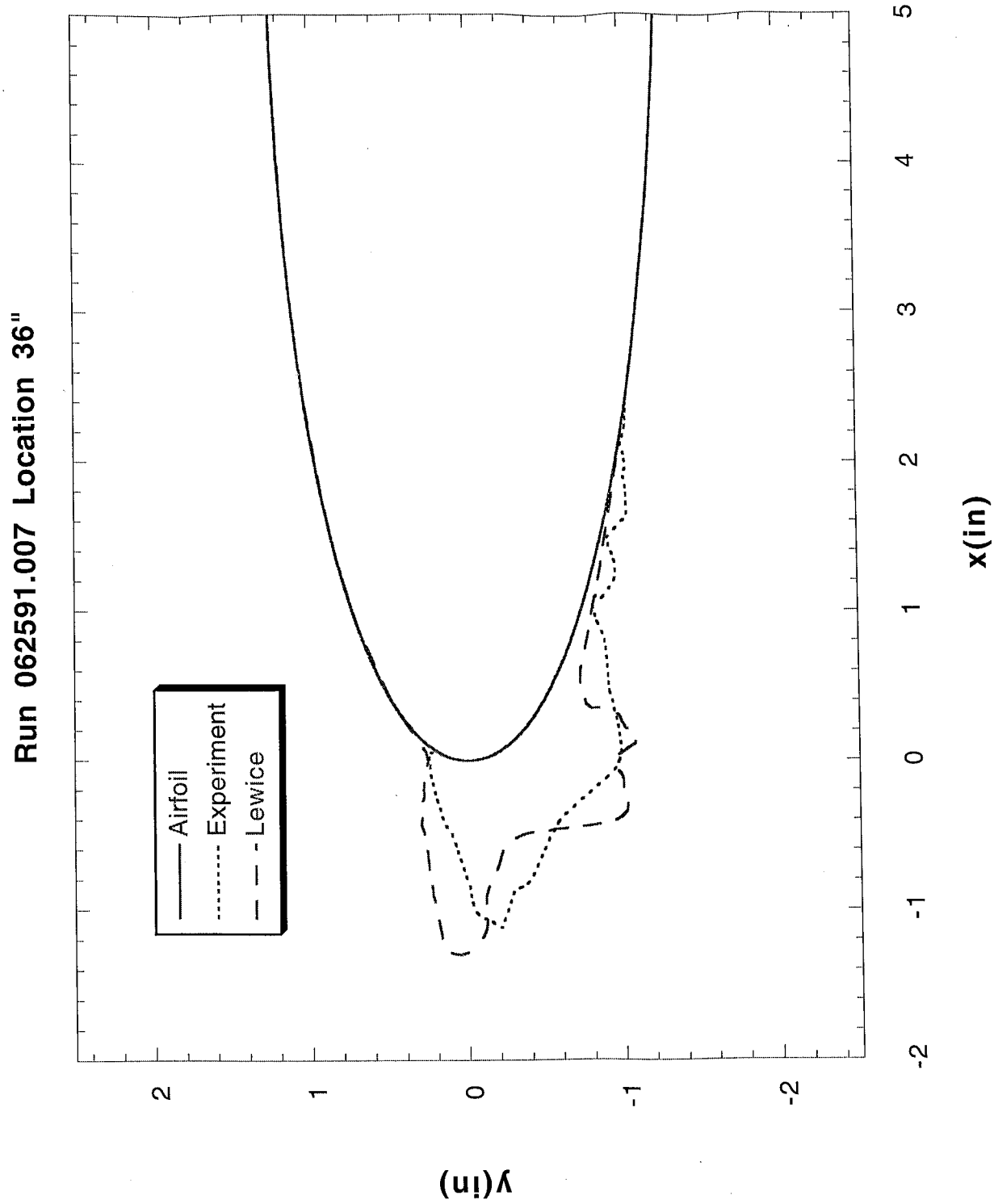
Run 062591.007 Location 36"
Airfoil
Experiment
Lewice
y(in)
x(in)
2
1
0
-1
-2
-2
-1
0
1
2
3
4
5

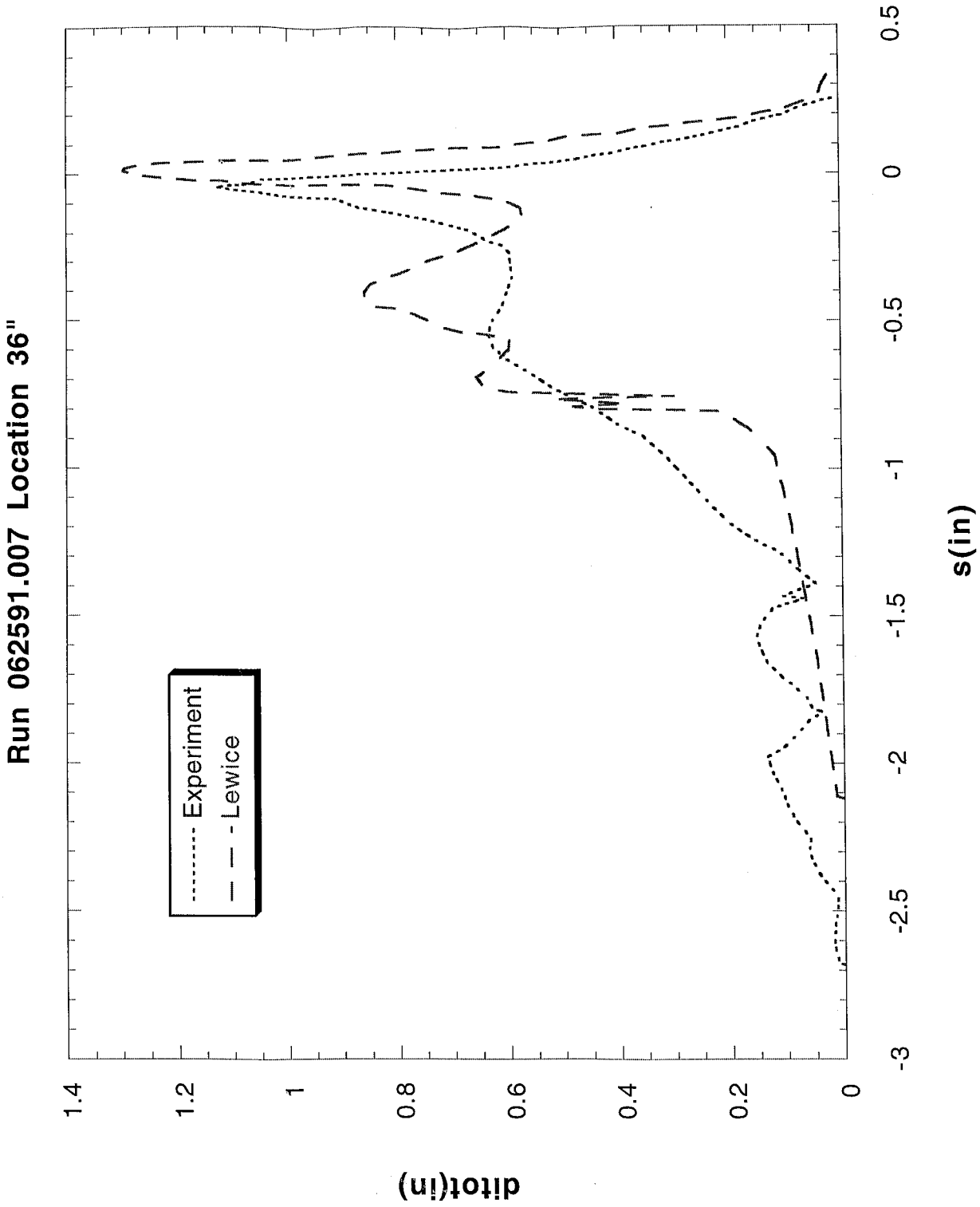
Run 062591.007 Location 36"
Experiment
Lewice
dltot(in)
s(in)
1.4
1.2
1
0.8
0.6
0.4
0.2
0
-3
-2.5
-2
-1.5
-1
-0.5
0
0.5

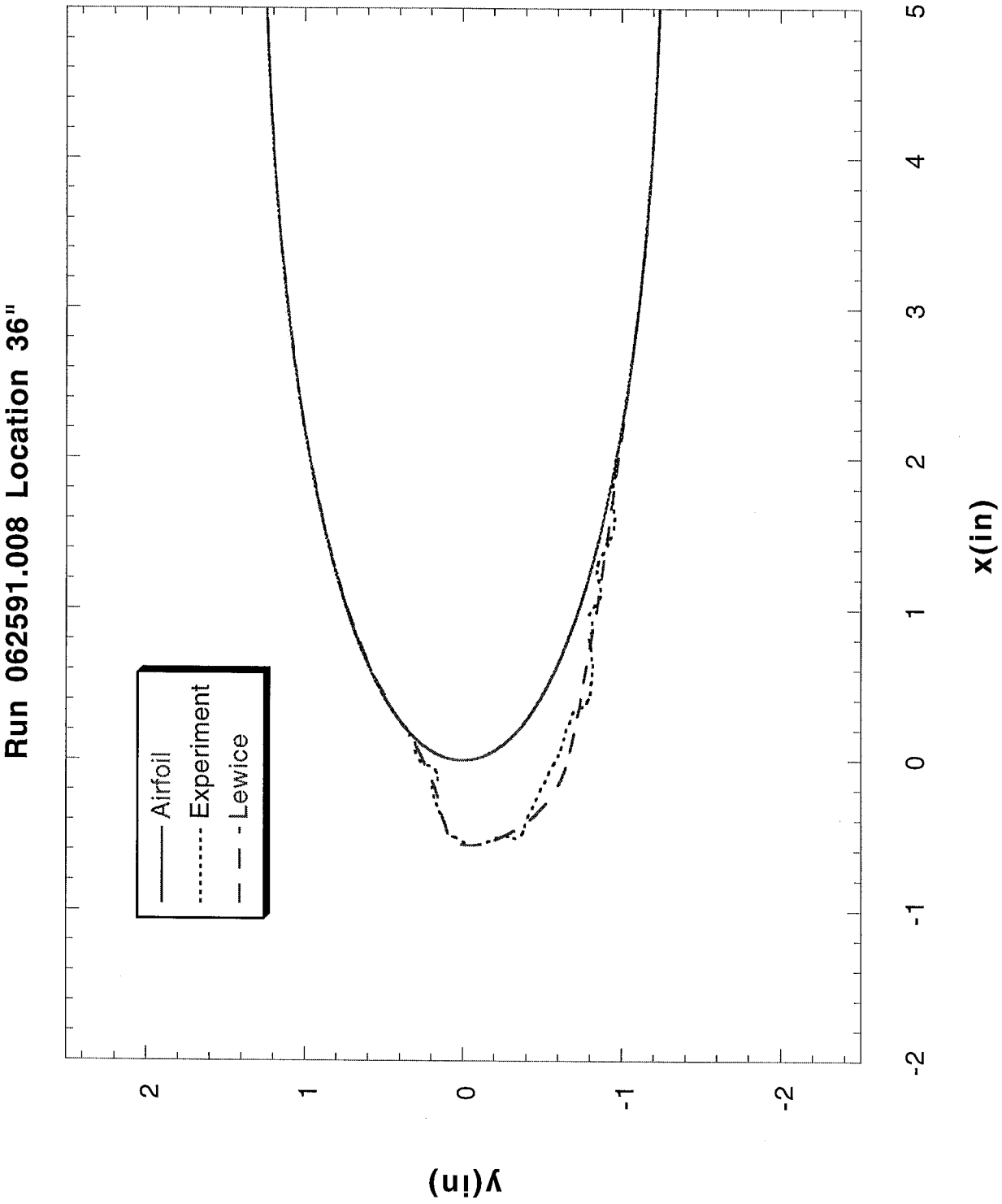
Run 062591.008 Location 36"
Airfoil
Experiment
Lewice
y(in)
x(in)
2
1
0
-1
-2
-2
-1
0
1
2
3
4
5

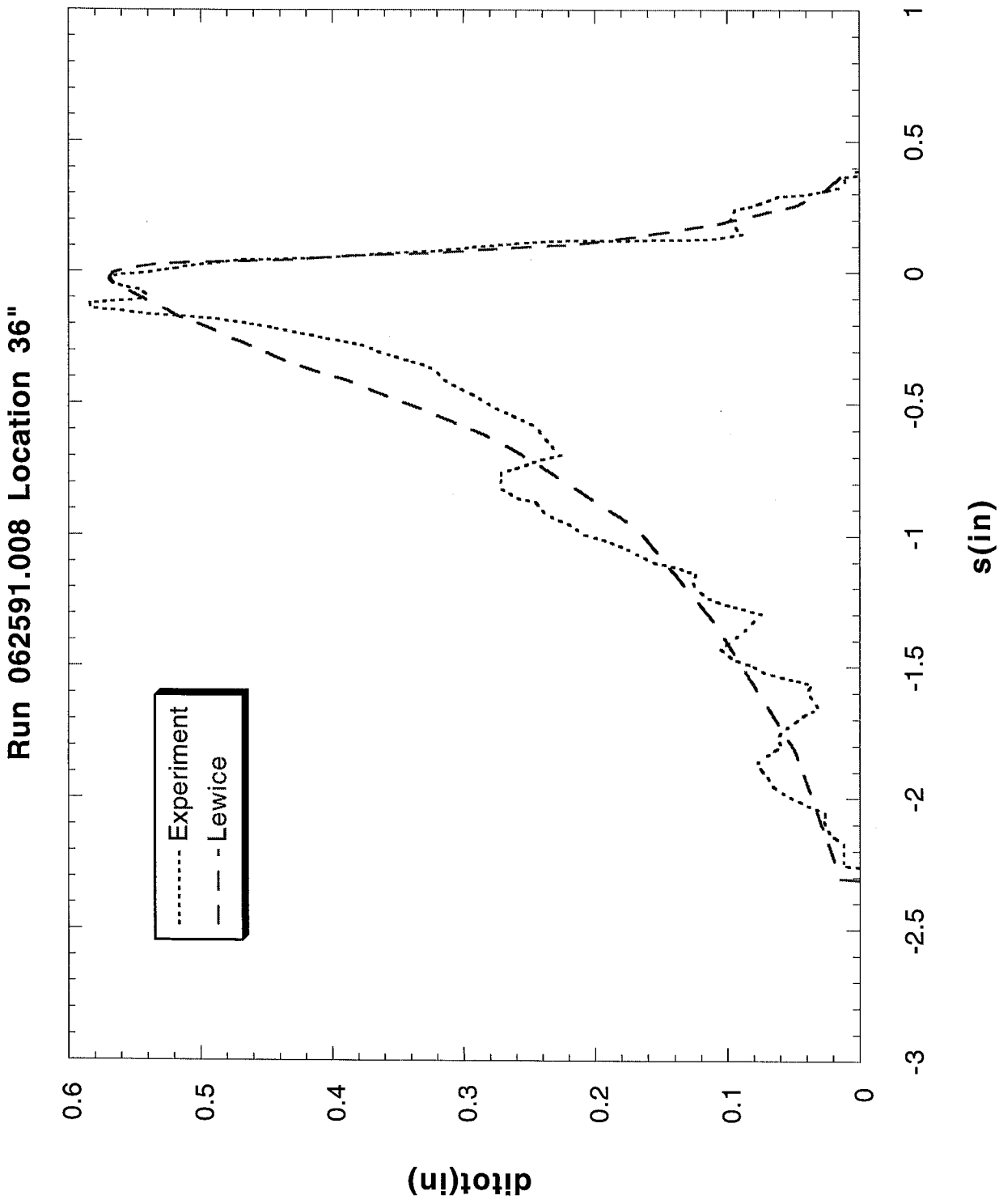
Run 062591.008 Location 36"
Experiment
Lewice
dltot(in)
s(in)
0.6
0.5
0.4
0.3
0.2
0.1
0
-3
-2.5
-2
-1.5
-1
-0.5
0
0.5
1

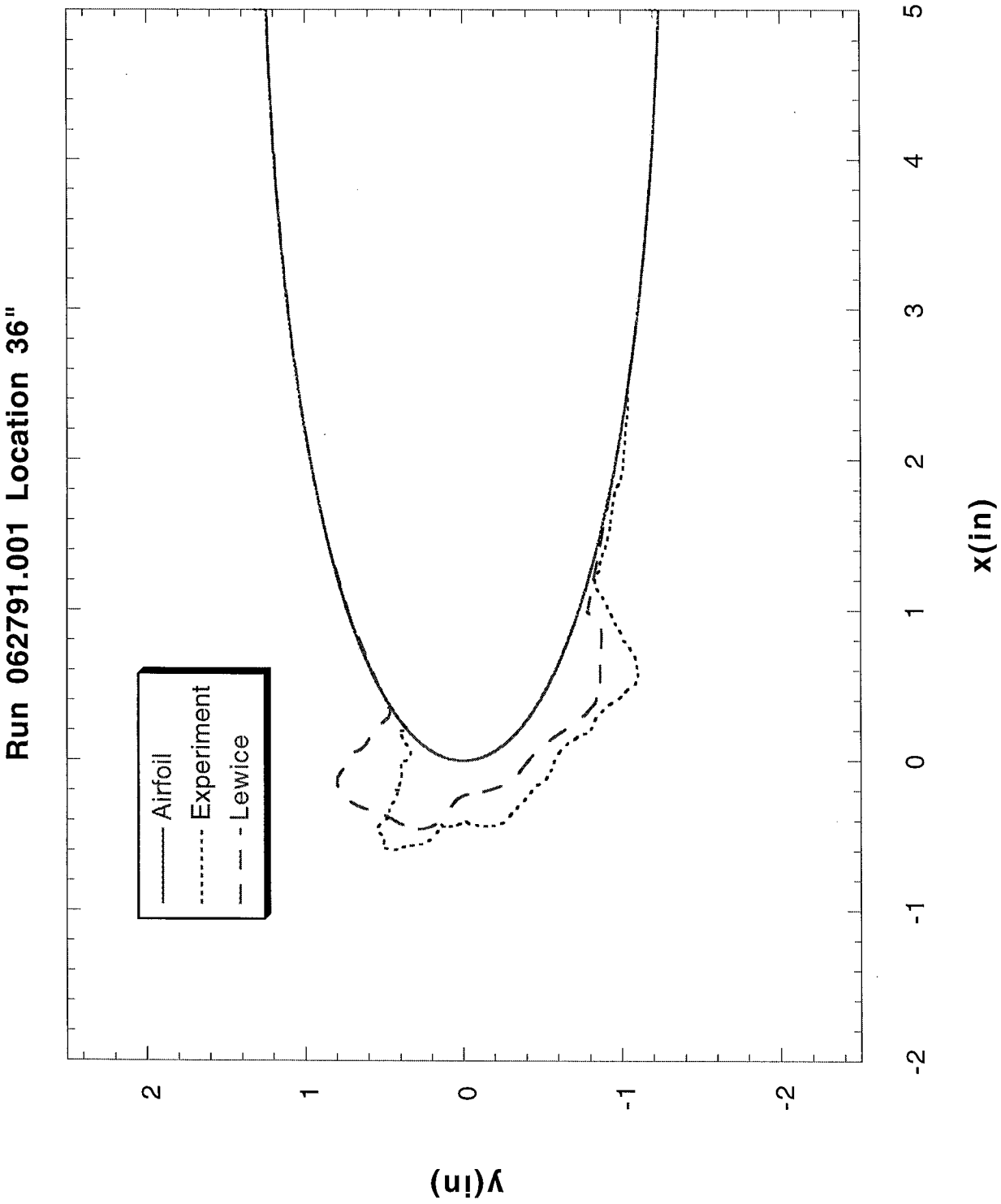
Run 062791.001 Location 36"
Airfoil
Experiment
Lewice
y(in)
x(in)
2
1
0
-1
-2
-2
-1
0
1
2
3
4
5

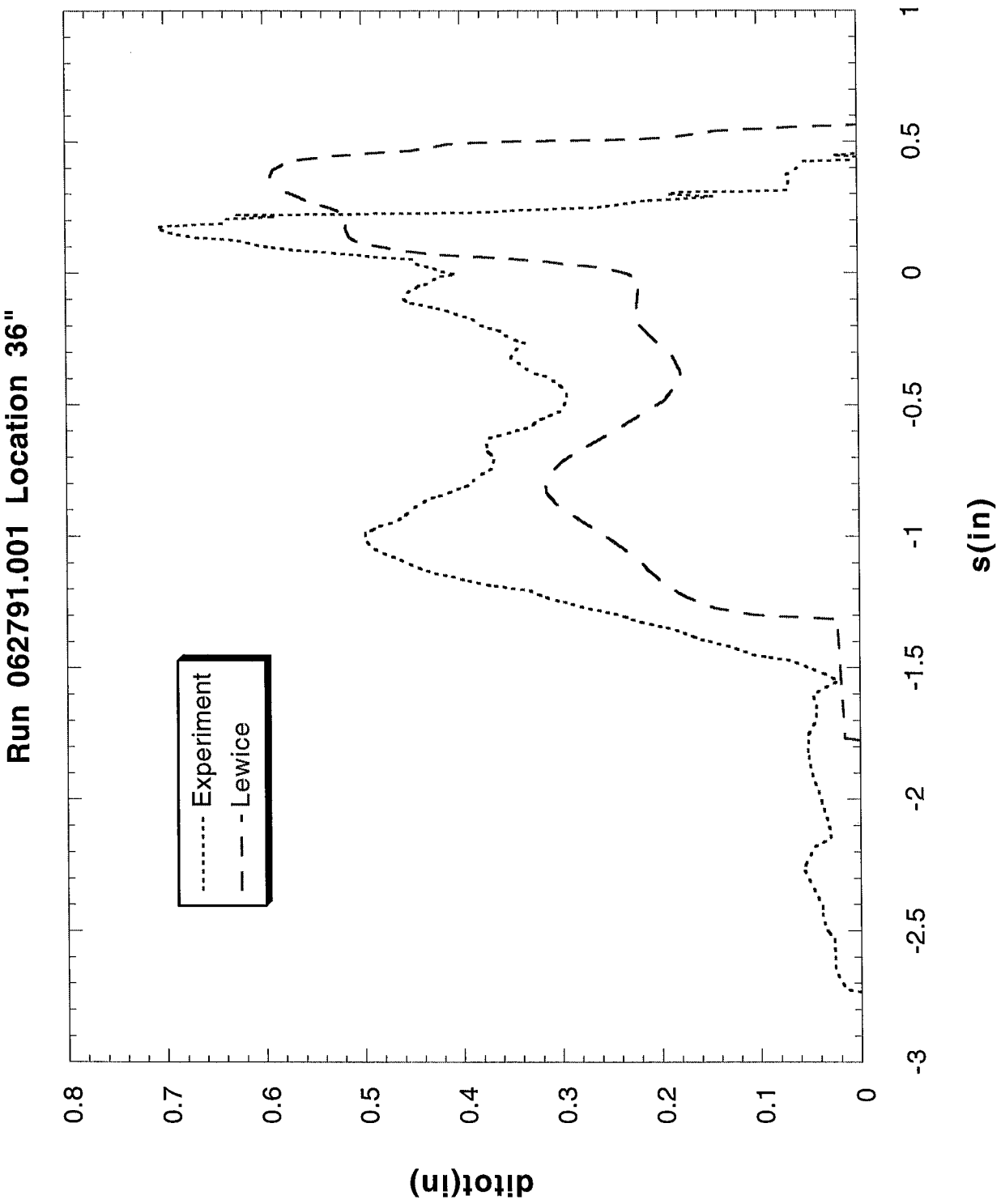
Run 062791.001 Location 36"
Experiment
Lewice
dltot(in)
s(in)
0
0.1
0.2
0.3
0.4
0.5
0.6
0.7
0.8
-3
-2.5
-2
-1.5
-1
-0.5
0
0.5
1

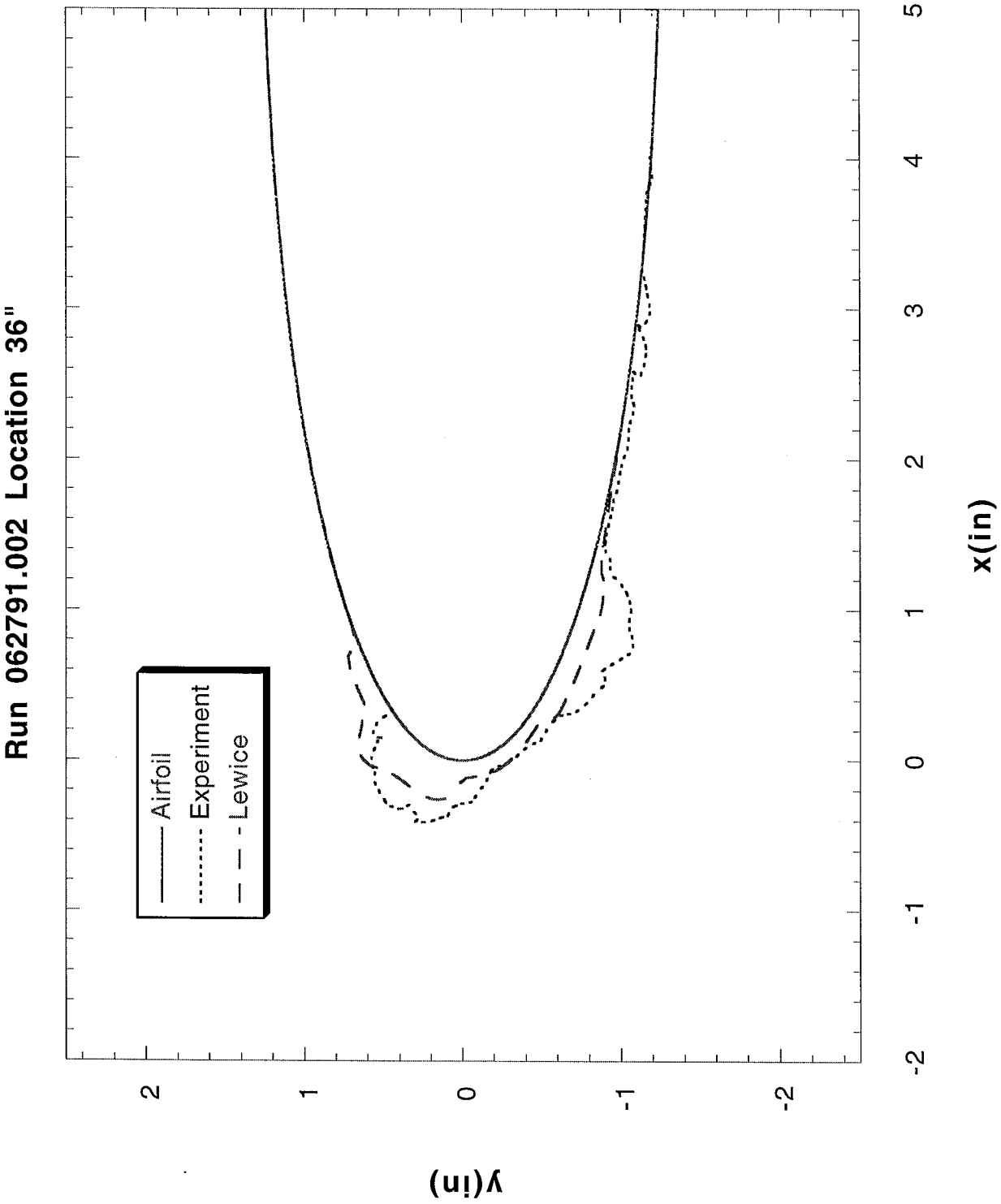
Run 062791.002 Location 36"
Airfoil
Experiment
Lewice
y(in)
x(in)
2
1
0
-1
-2
-2
-1
0
1
2
3
4
5

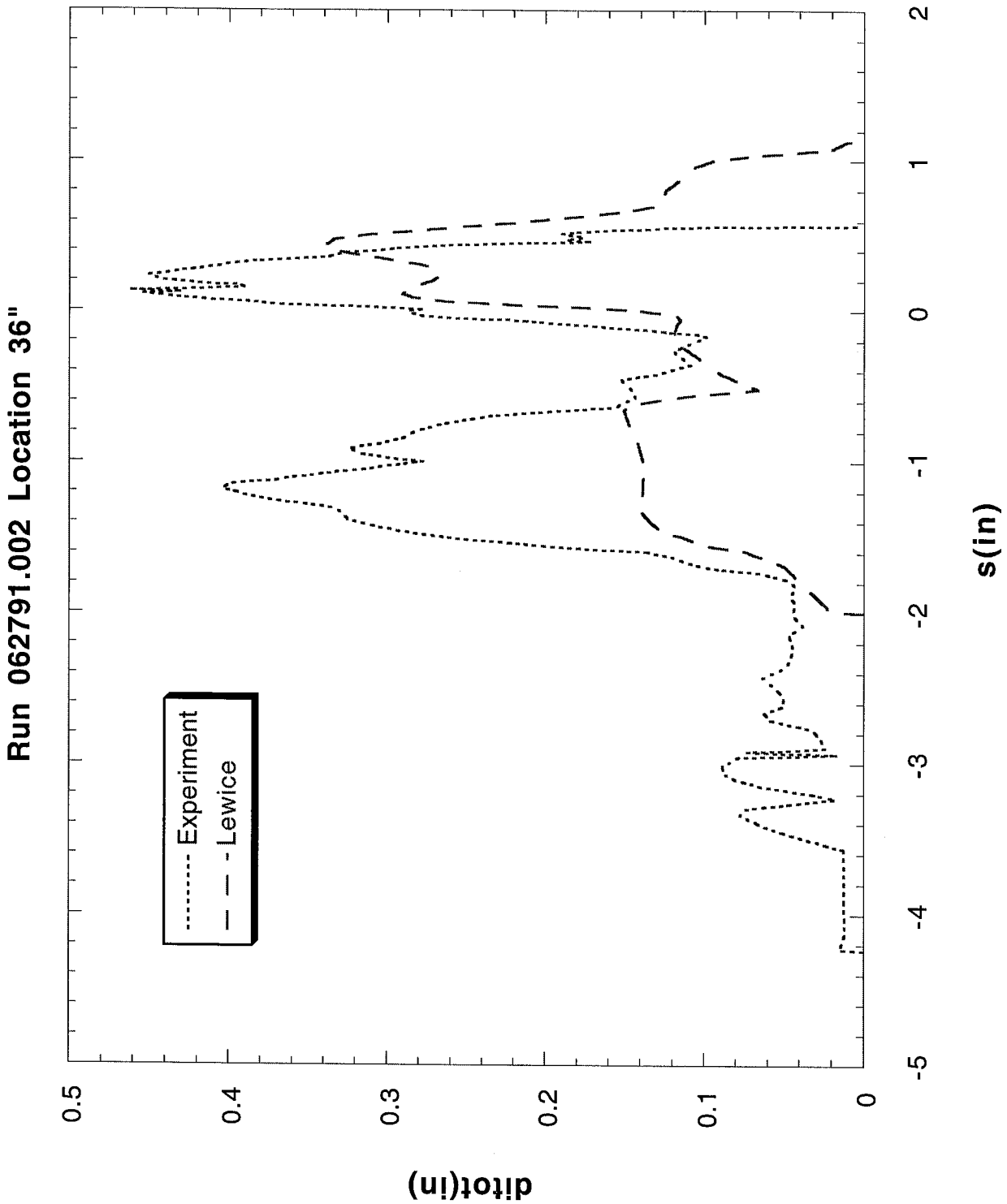
Run 062791.002 Location 36"
Experiment
Lewice
dltot(in)
s(in)
0.5
0.4
0.3
0.2
0.1
0
-5
-4
-3
-2
-1
0
1
2

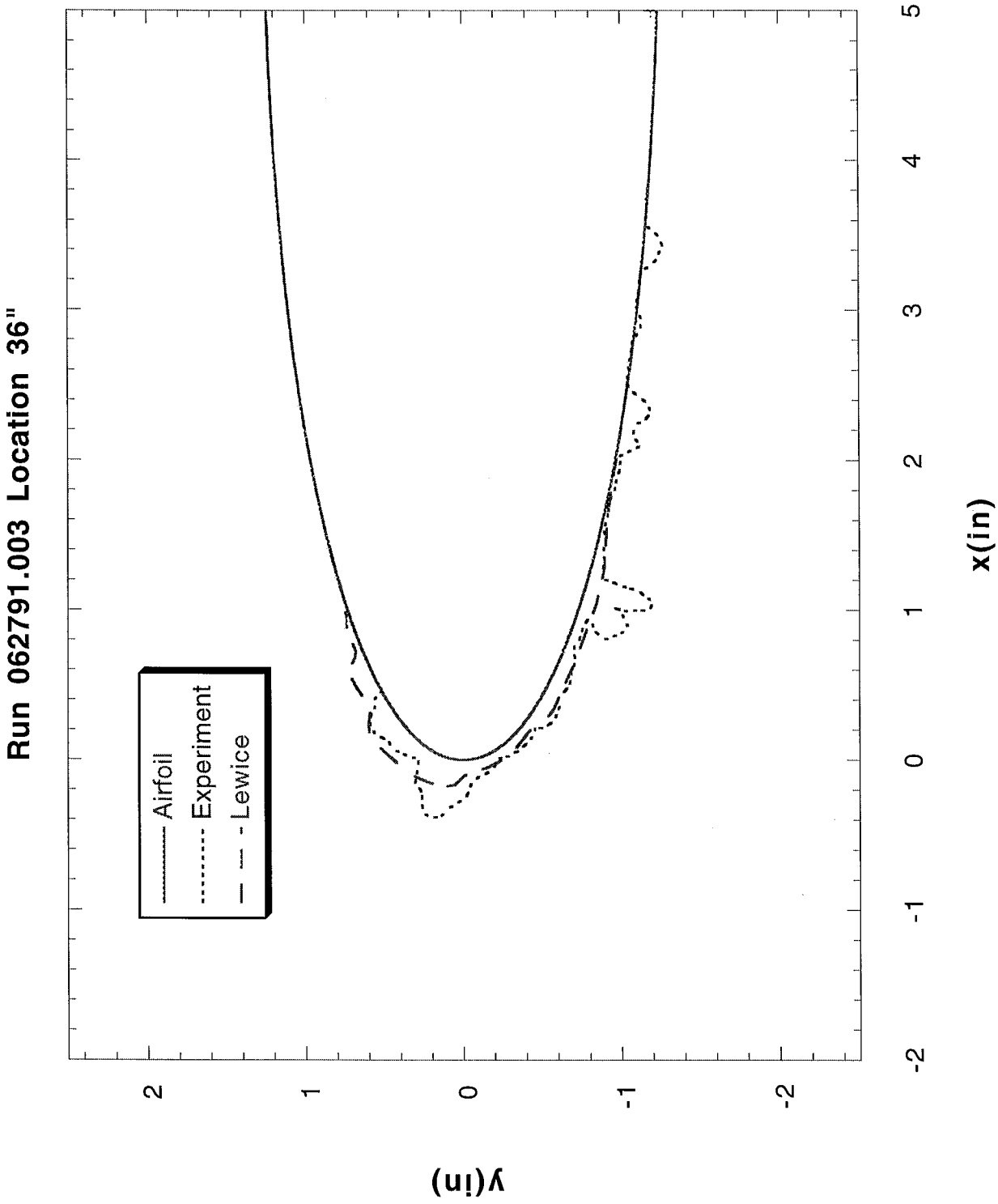
Run 062791.003 Location 36"
Airfoil
Experiment
Lewice
y(in)
x(in)
2
1
0
-1
-2
-2
-1
0
1
2
3
4
5

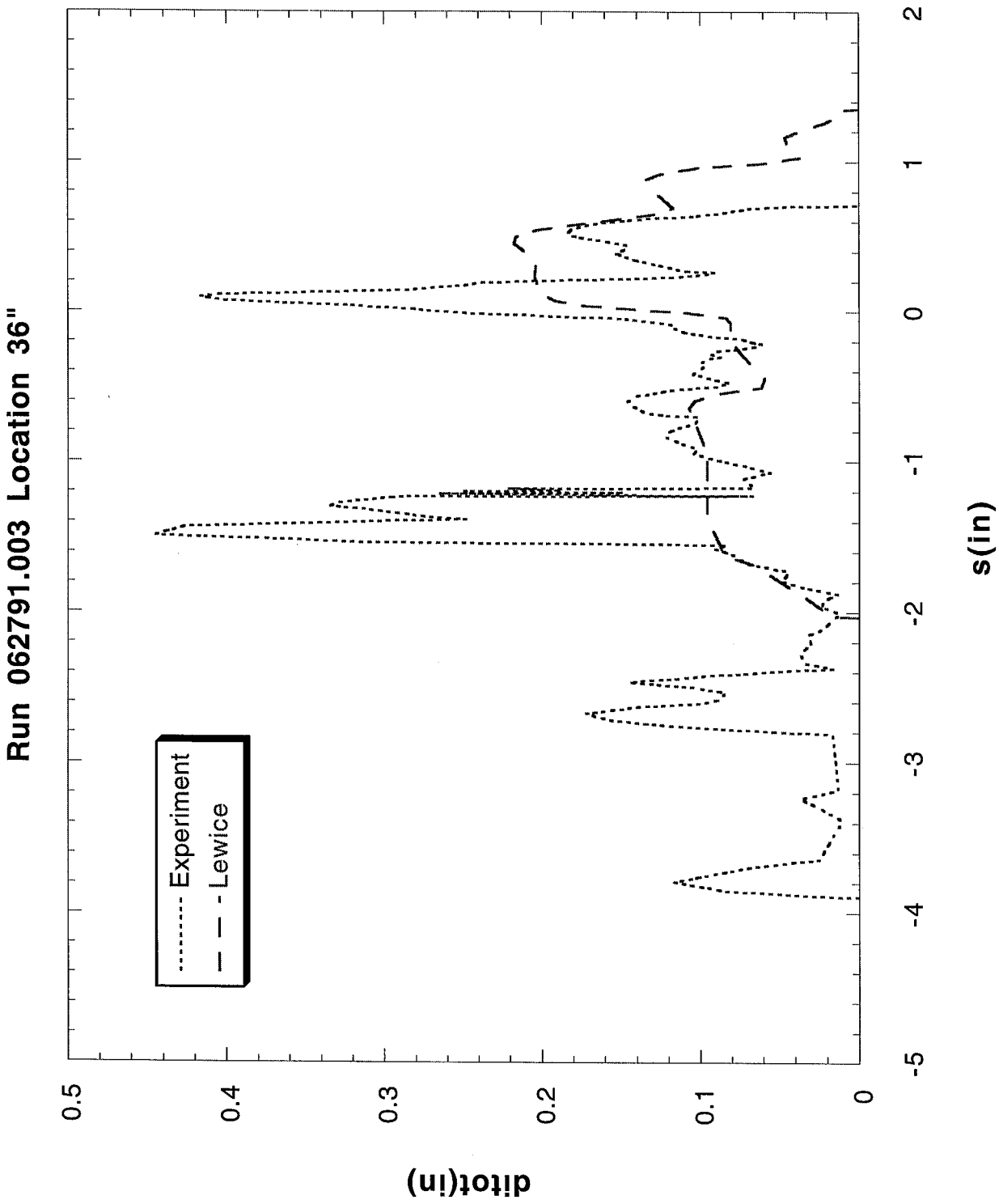
Run 062791.003 Location 36"
Experiment
Lewice
dltot(in)
s(in)
0.5
0.4
0.3
0.2
0.1
0
-5
-4
-3
-2
-1
0
1
2

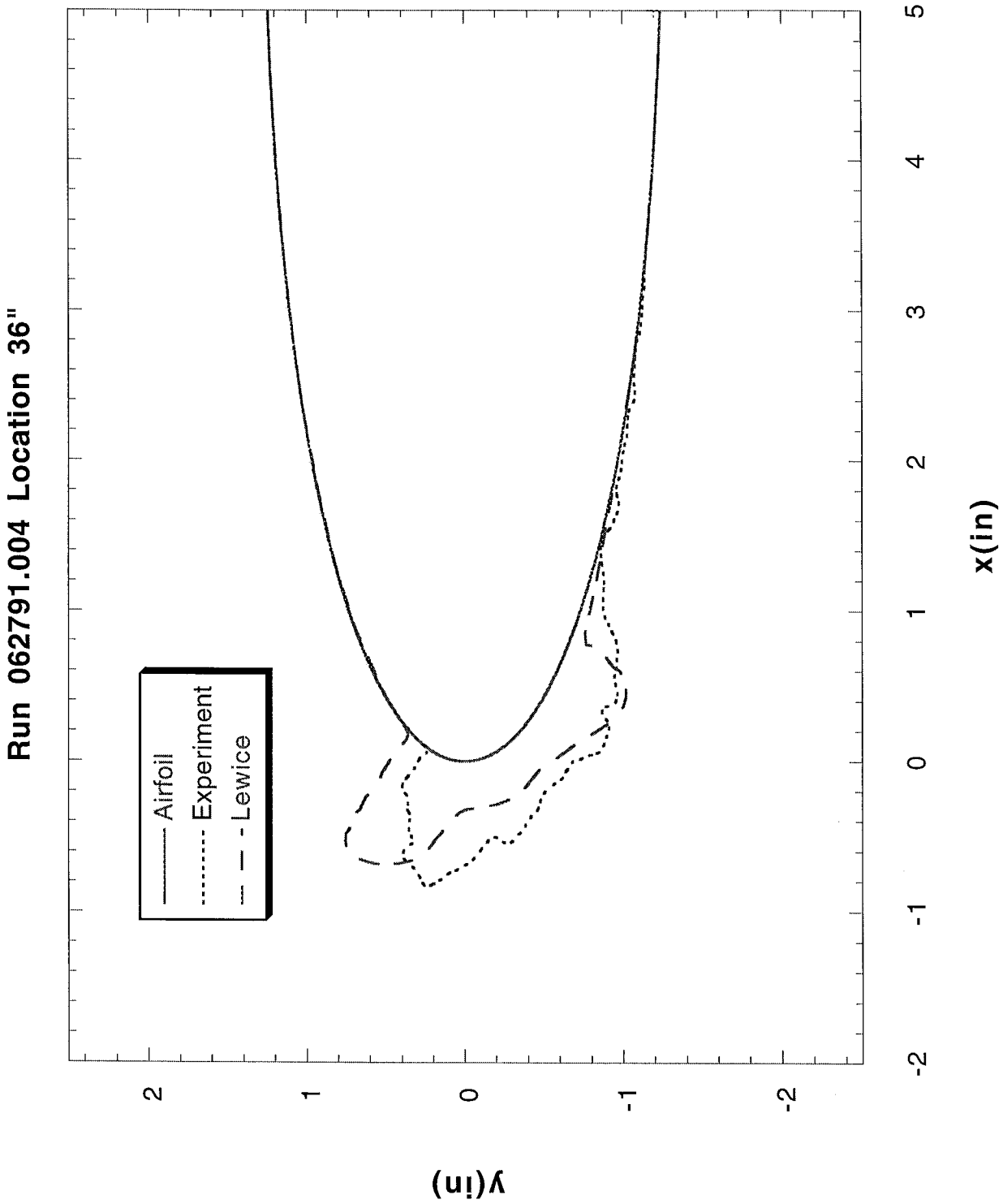
Run 062791.004 Location 36"
Airfoil
Experiment
Lewice
y(in)
x(in)
2
1
0
-1
-2
-2
-1
0
1
2
3
4
5

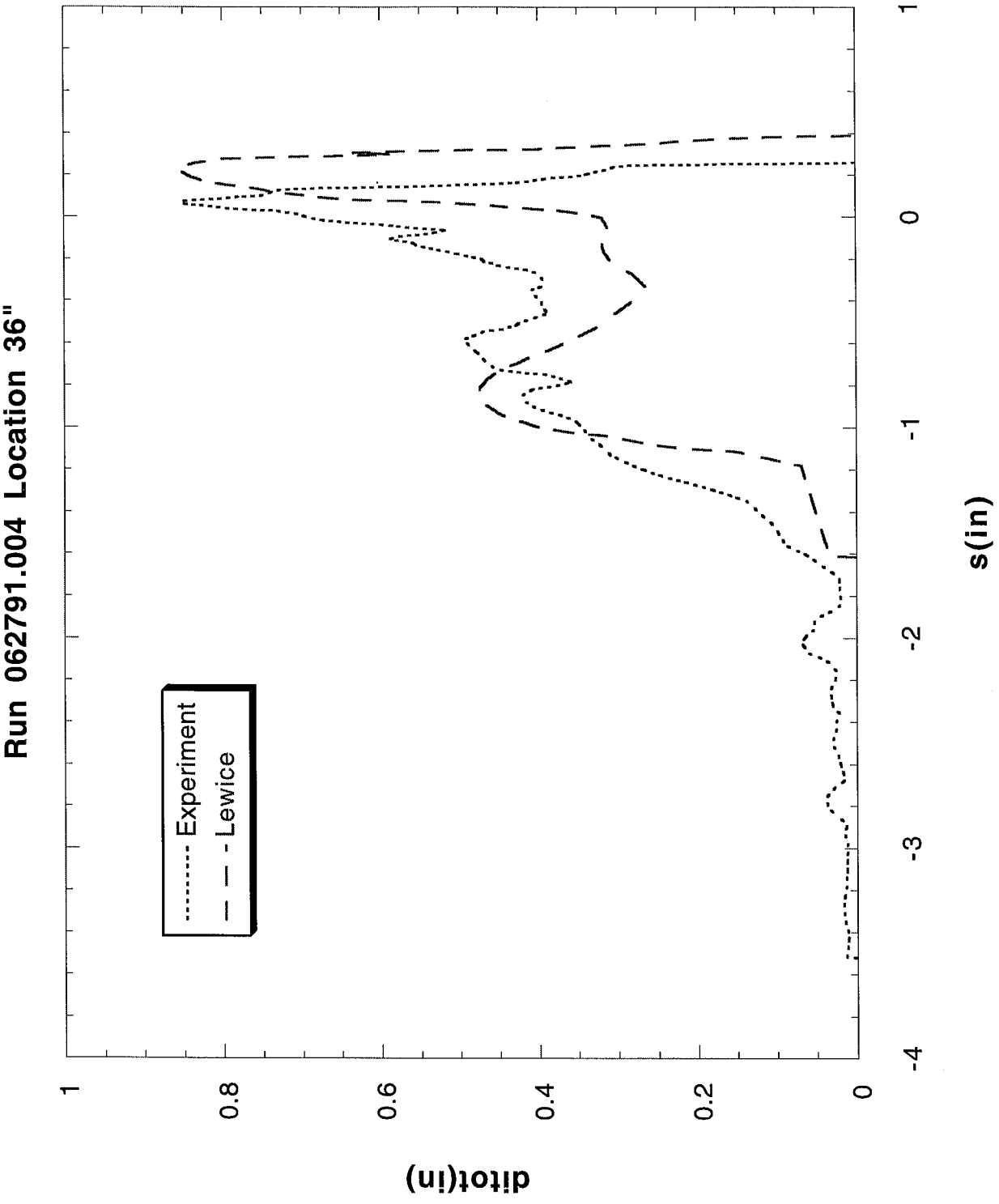
Run 062791.004 Location 36"
Experiment
Lewice
dltot(in)
s(in)
1
0.8
0.6
0.4
0.2
0
-4
-3
-2
-1
0
1

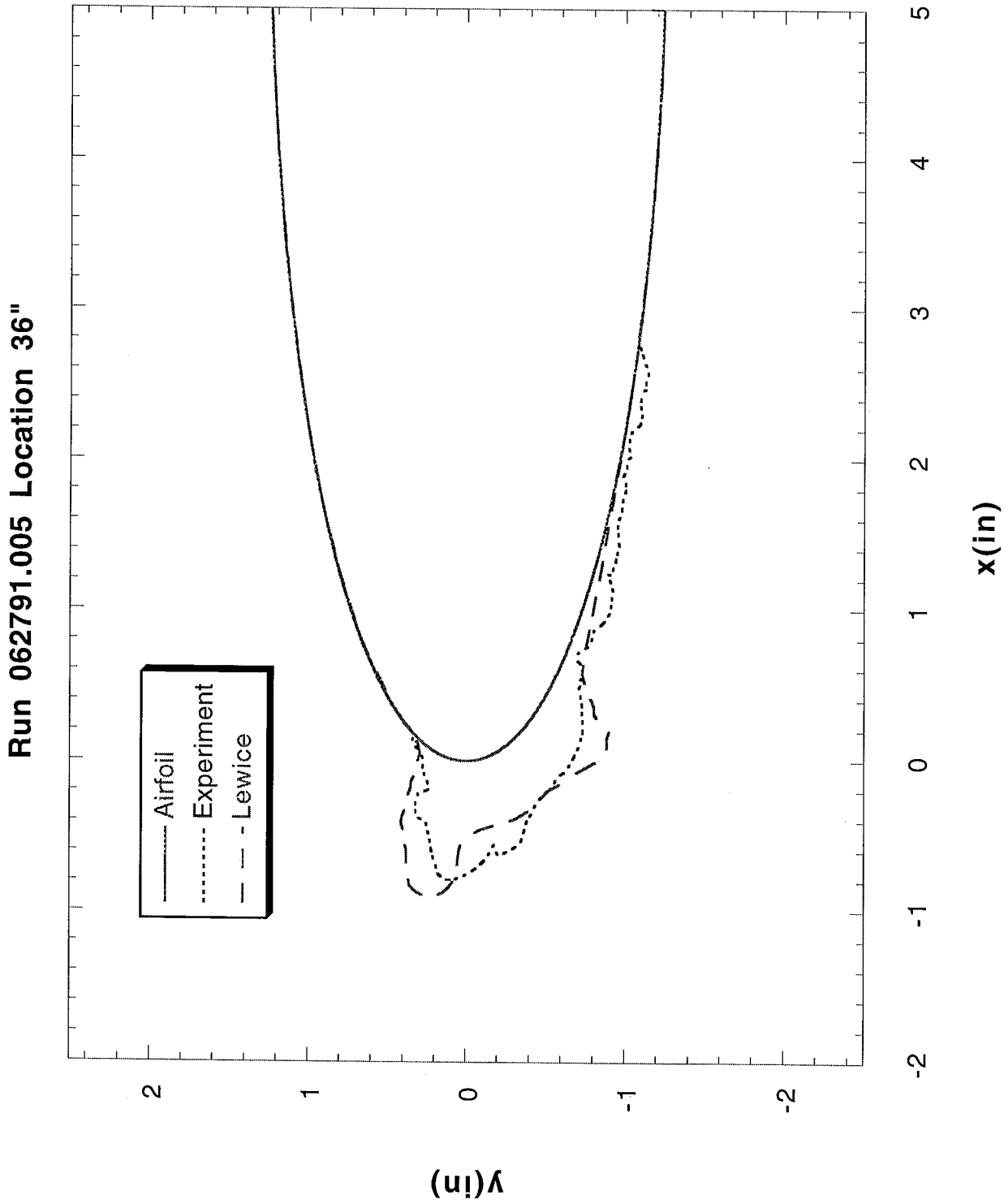
Run 062791.005 Location 36"
Airfoil
Experiment
Lewice
y(in)
x(in)
2
1
0
-1
-2
-2
-1
0
1
2
3
4
5

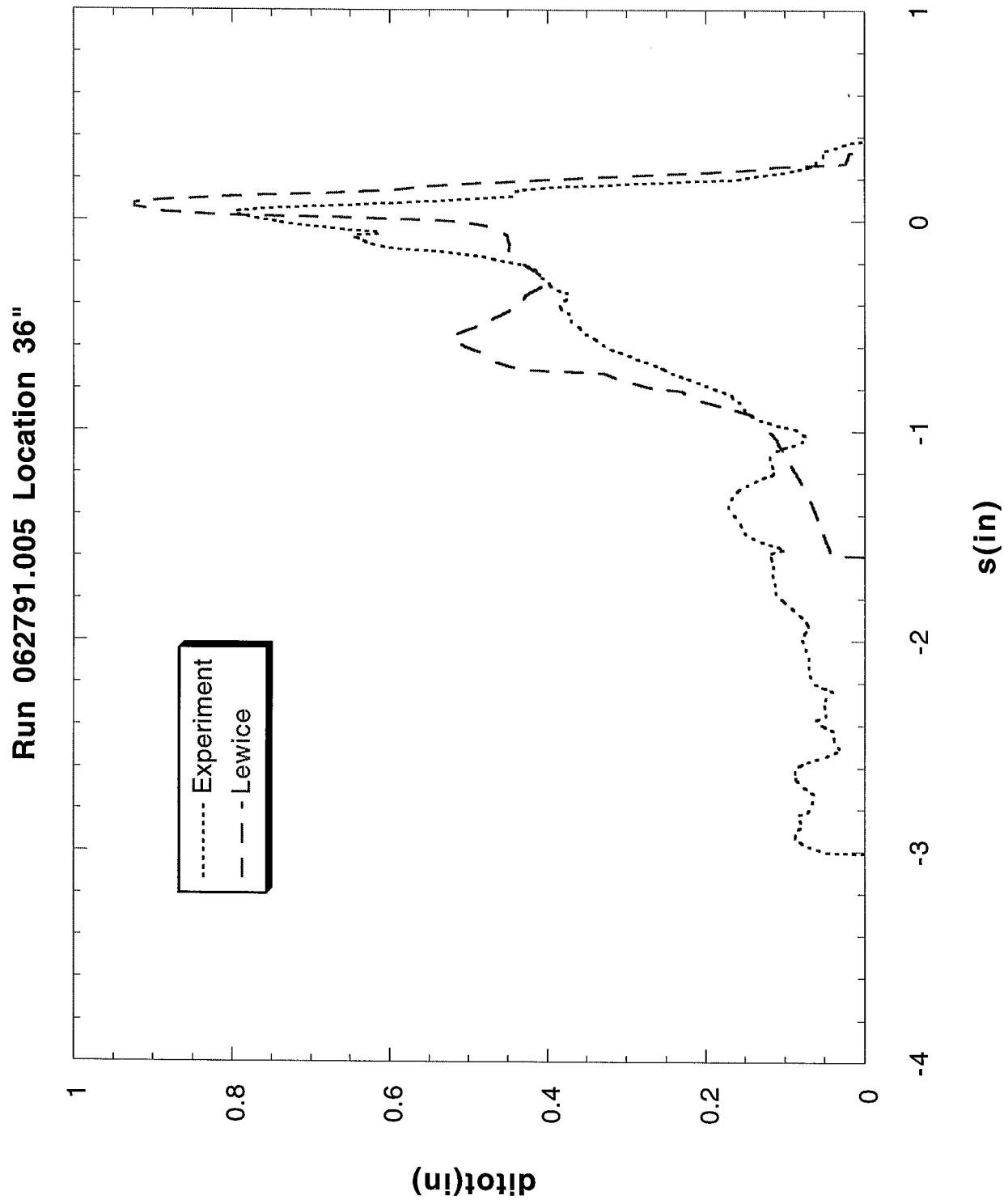
Run 062791.005 Location 36"
Experiment
Lewice
dltot(in)
s(in)
1
0.8
0.6
0.4
0.2
0
-4
-3
-2
-1
0
1

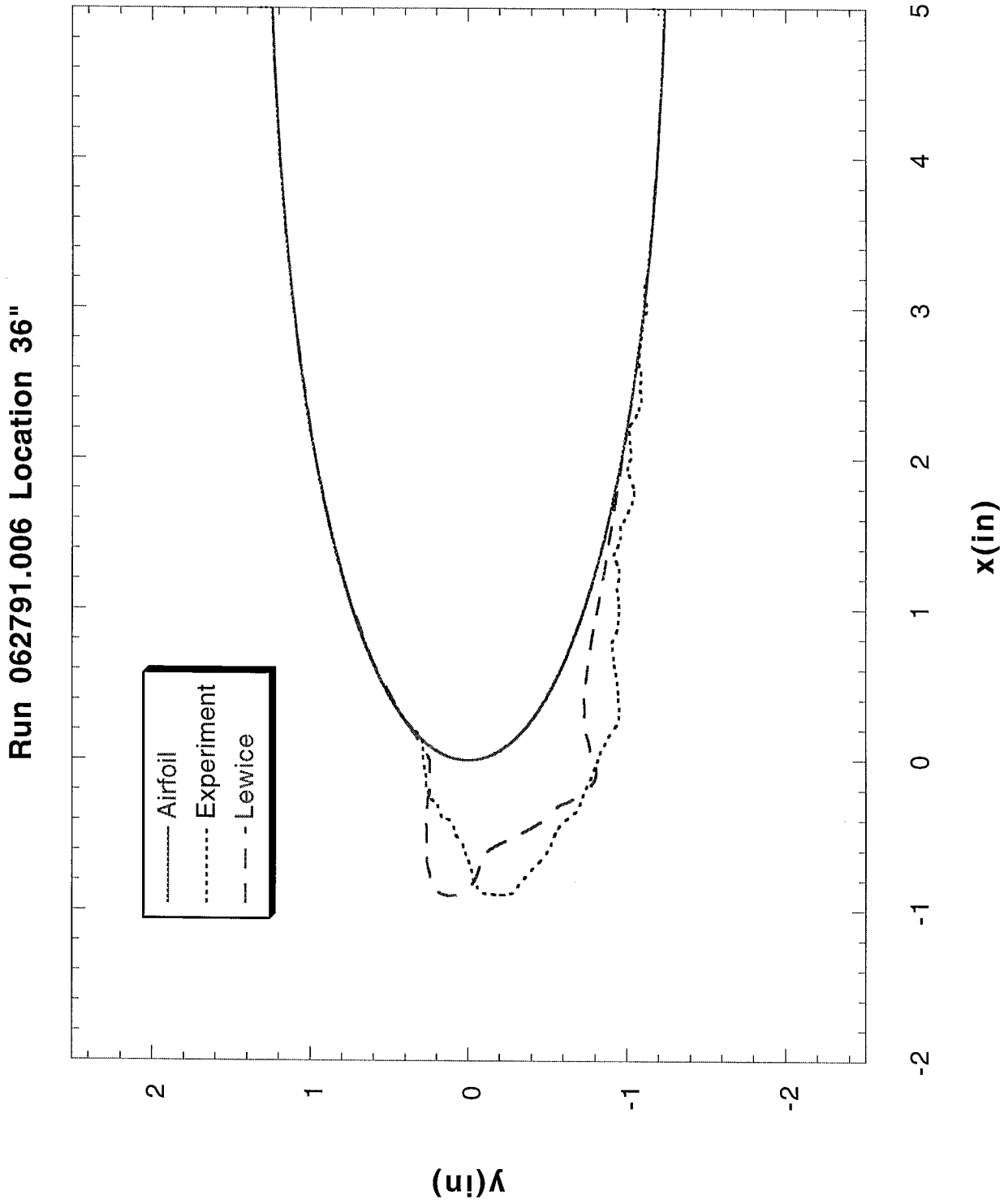
Run 062791.006 Location 36"
Airfoil
Experiment
Lewice
y(in)
x(in)
2
1
0
-1
-2
-2
-1
0
1
2
3
4
5

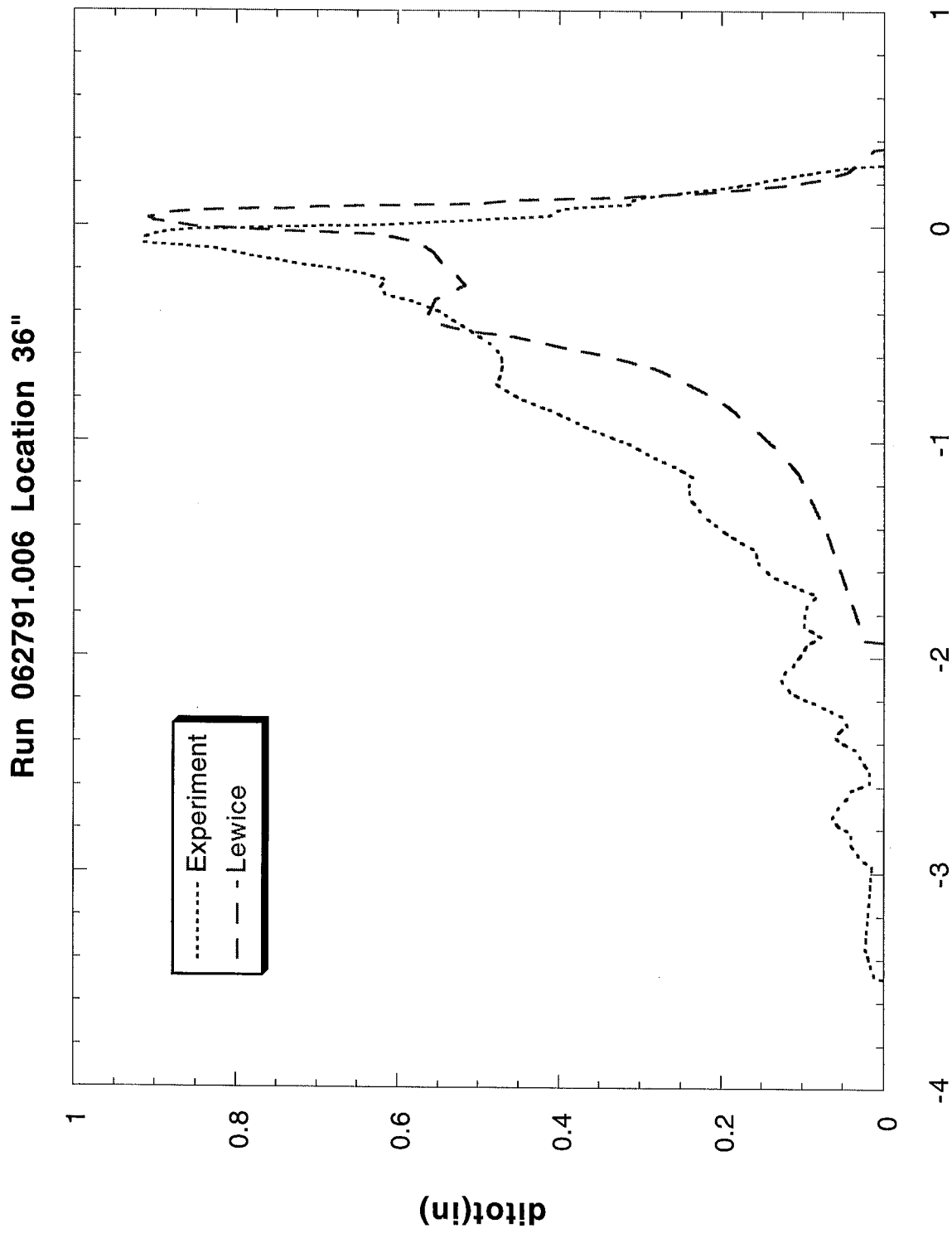
Run 062791.006 Location 36"
Experiment
Lewice
dltot(in)
s(in)
1
0.8
0.6
0.4
0.2
0
-4
-3
-2
-1
0
1

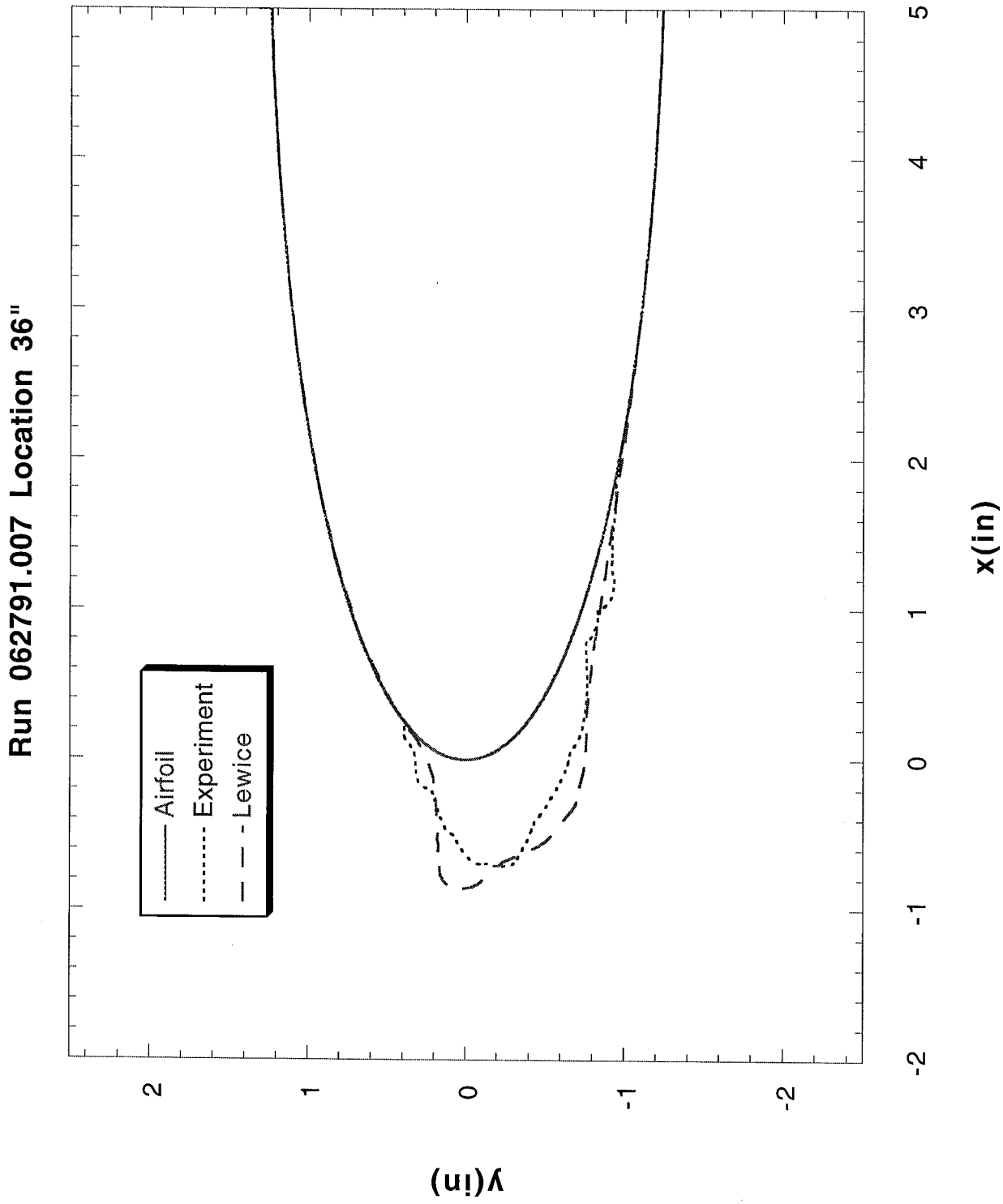
Run 062791.007 Location 36"
Airfoil
Experiment
- Lewice
y(in)
x(in)
2
1
0
-1
-2
-2
-1
0
1
2
3
4
5

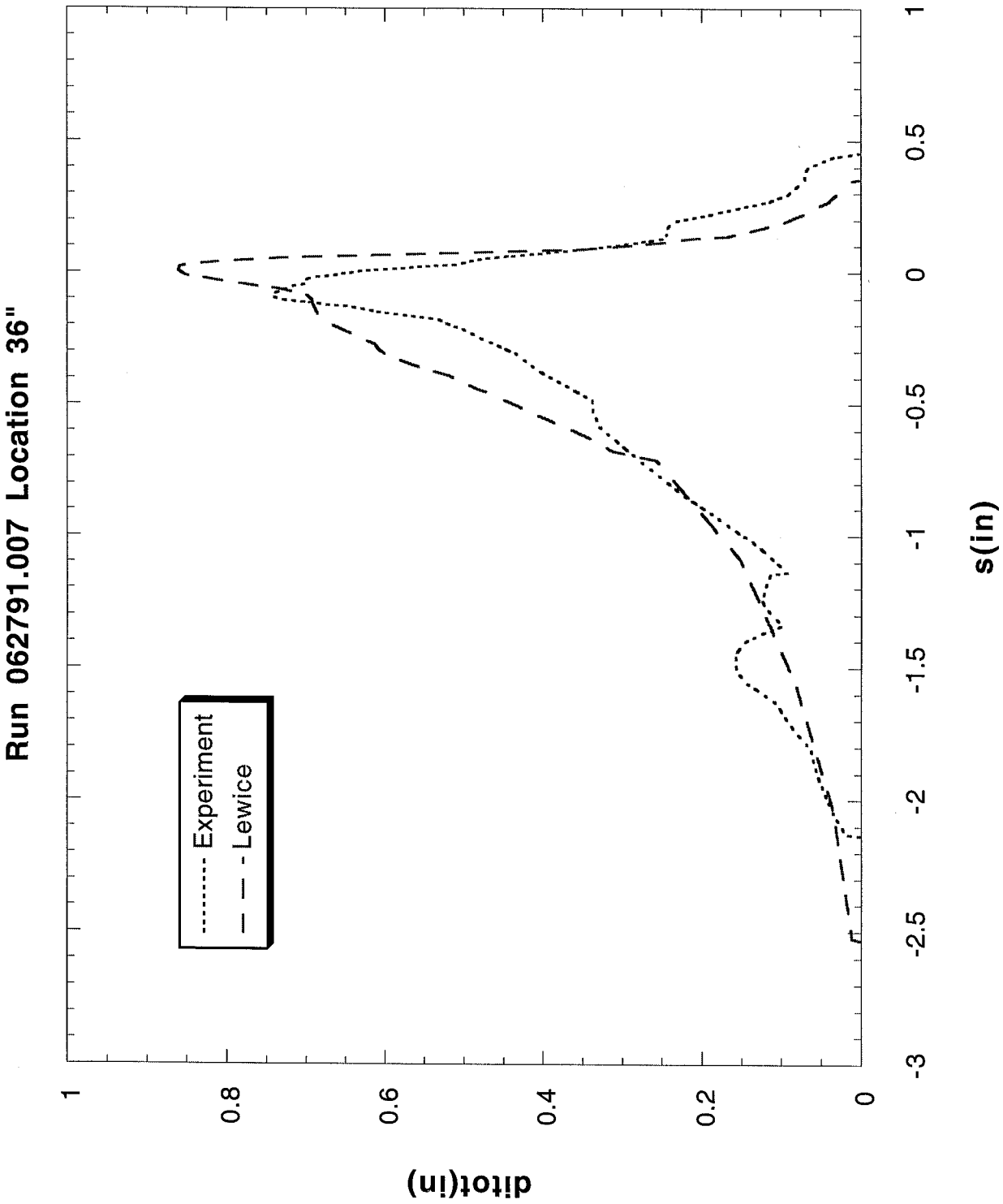
Run 062791.007 Location 36"
Experiment
Lewice
dltot(in)
s(in)
1
0.8
0.6
0.4
0.2
0
-3
-2.5
-2
-1.5
-1
-0.5
0
0.5
1

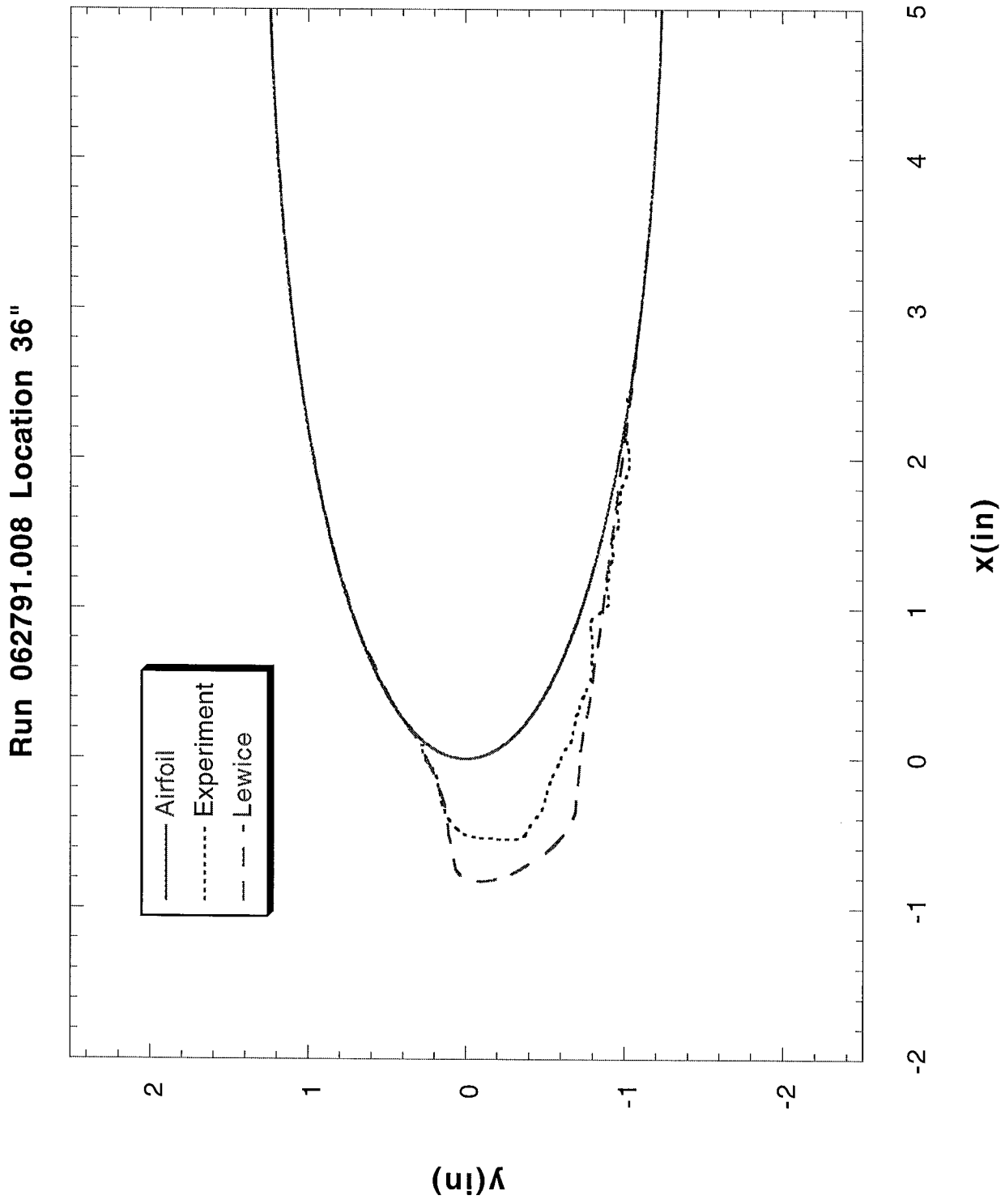
Run 062791.008 Location 36"
Airfoil
Experiment
Lewice
y(in)
x(in)
2
1
0
-1
-2
-2
-1
0
1
2
3
4
5

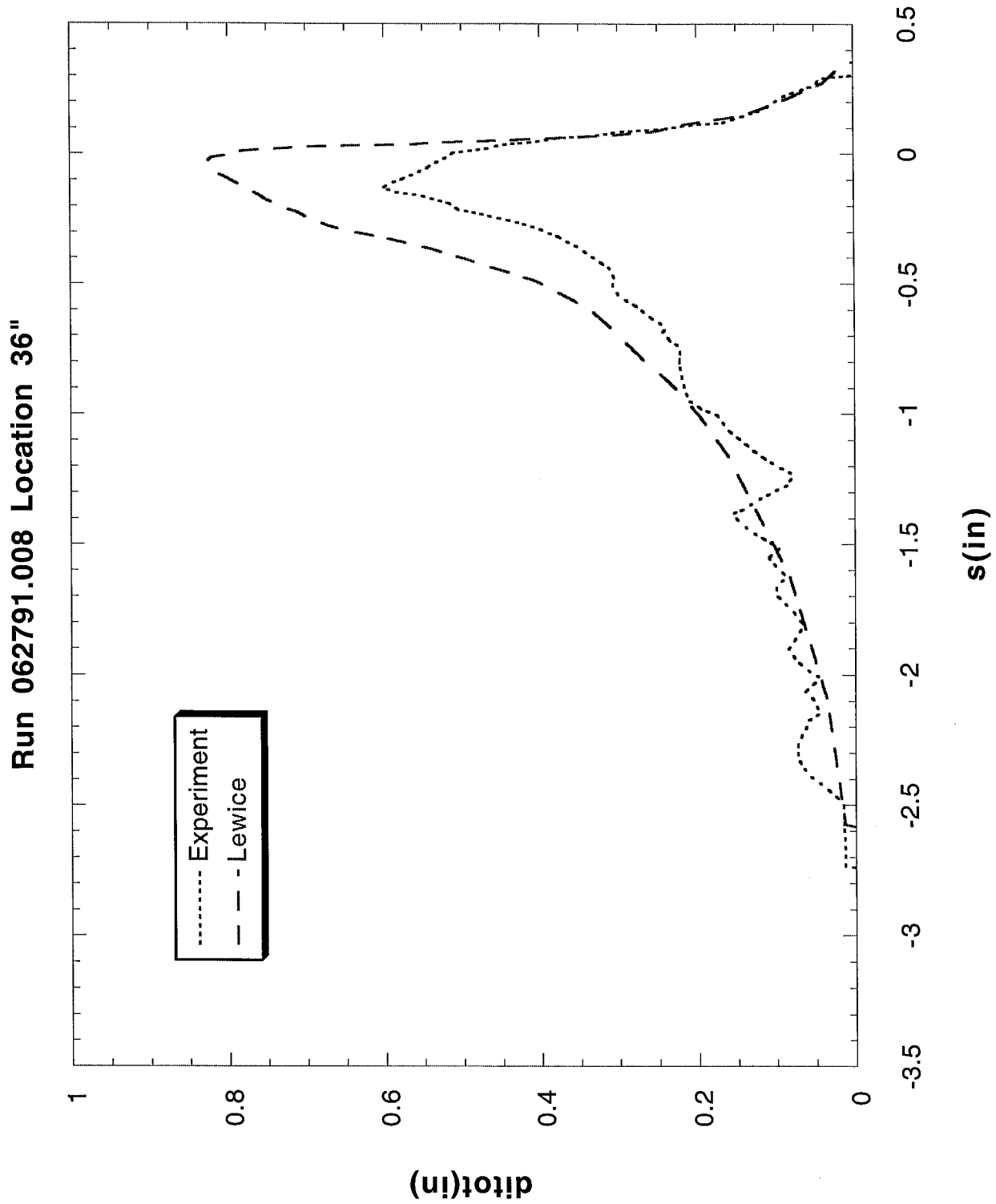
Run 062791.008 Location 36"
Experiment
Lewice
ditot(in)
s(in)
1
0.8
0.6
0.4
0.2
0
0.5
0
-0.5
-1
-1.5
-2
-2.5
-3
-3.5

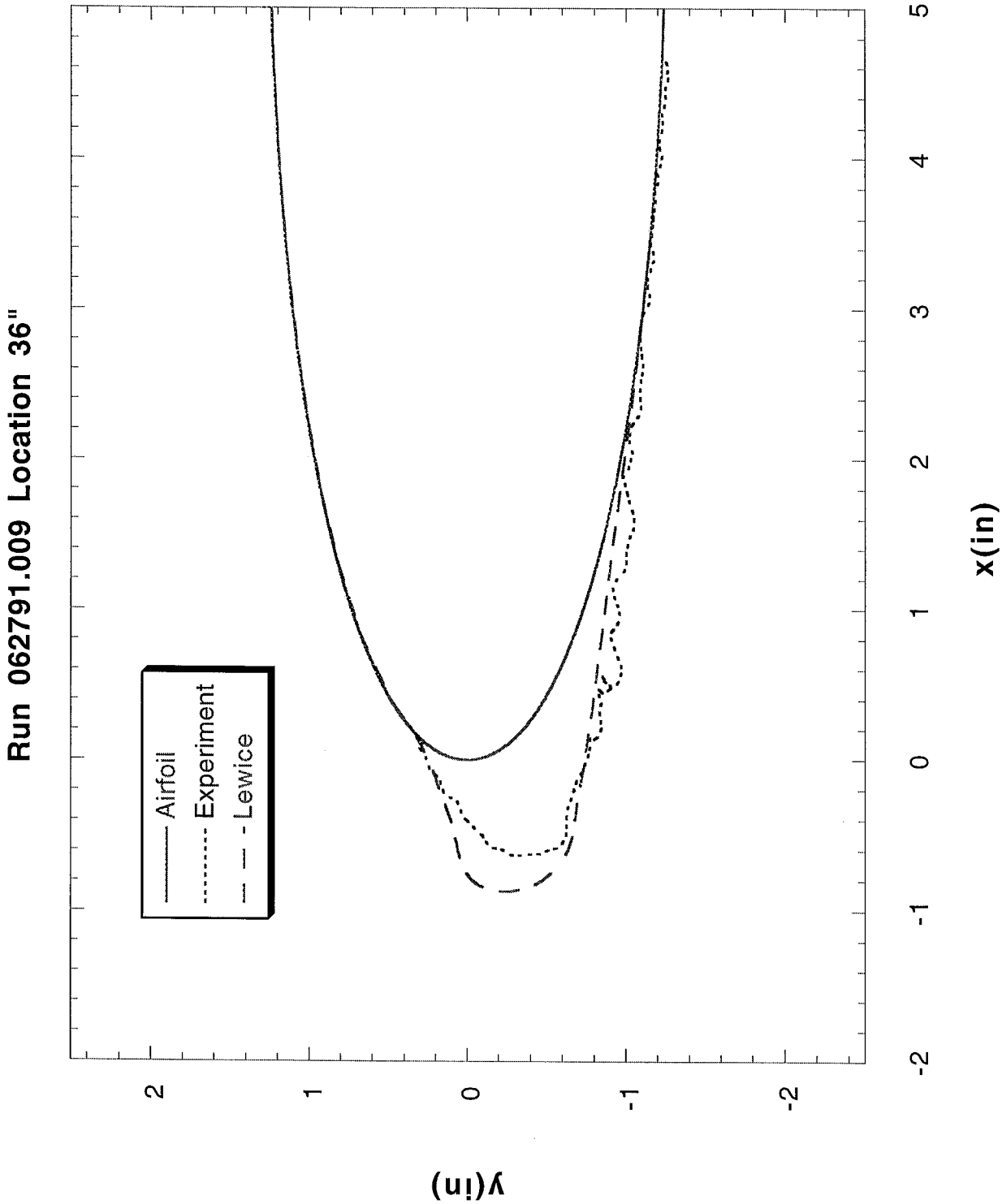
Run 062791.009 Location 36"
Airfoil
Experiment
Lewice
y(in)
x(in)
2
1
0
-1
-2
-2
-1
0
1
2
3
4
5

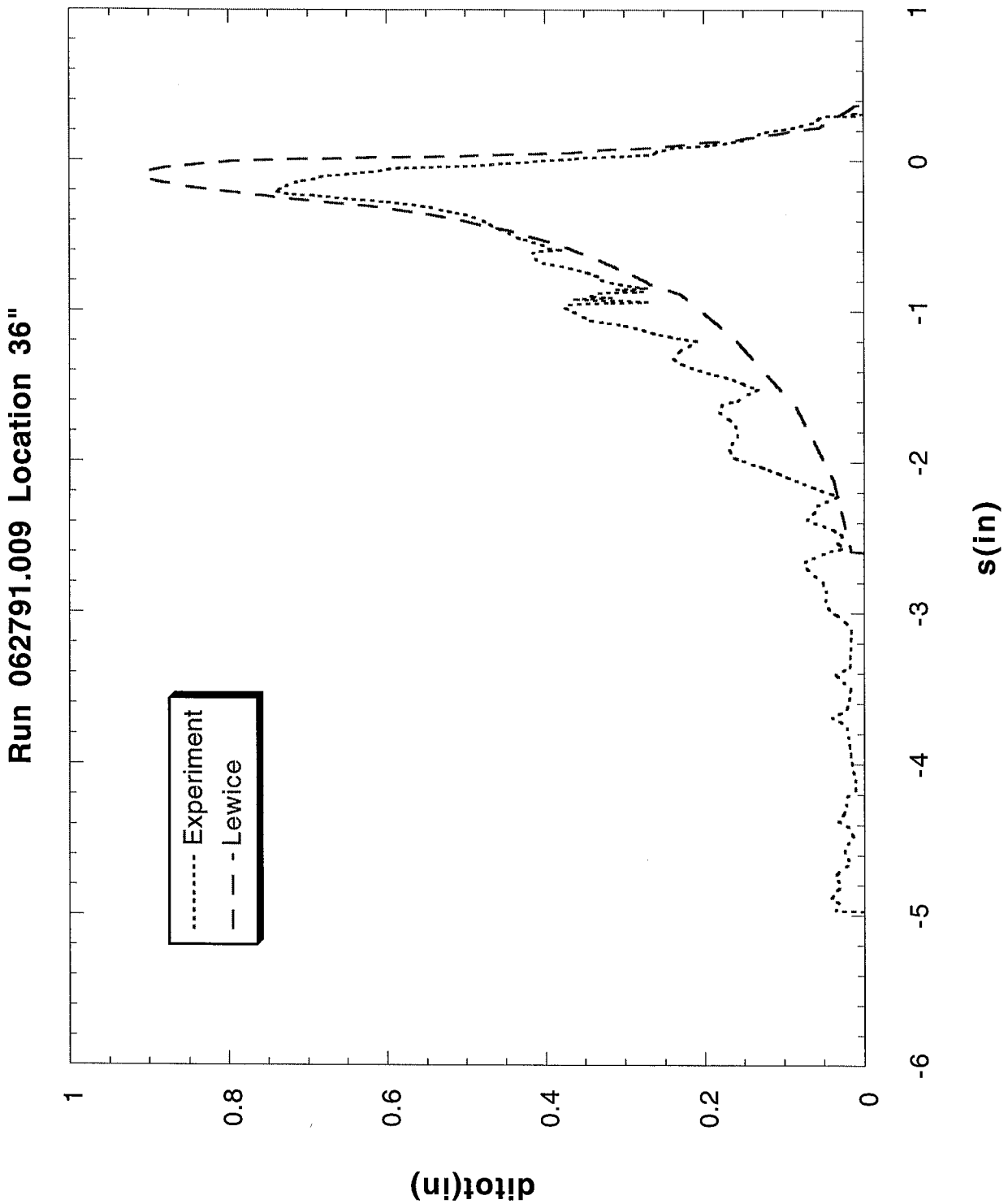
Run 062791.009 Location 36"
Experiment
Lewice
ditot(in)
s(in)
1
0.8
0.6
0.4
0.2
0
-6
-5
-4
-3
-2
-1
0
1

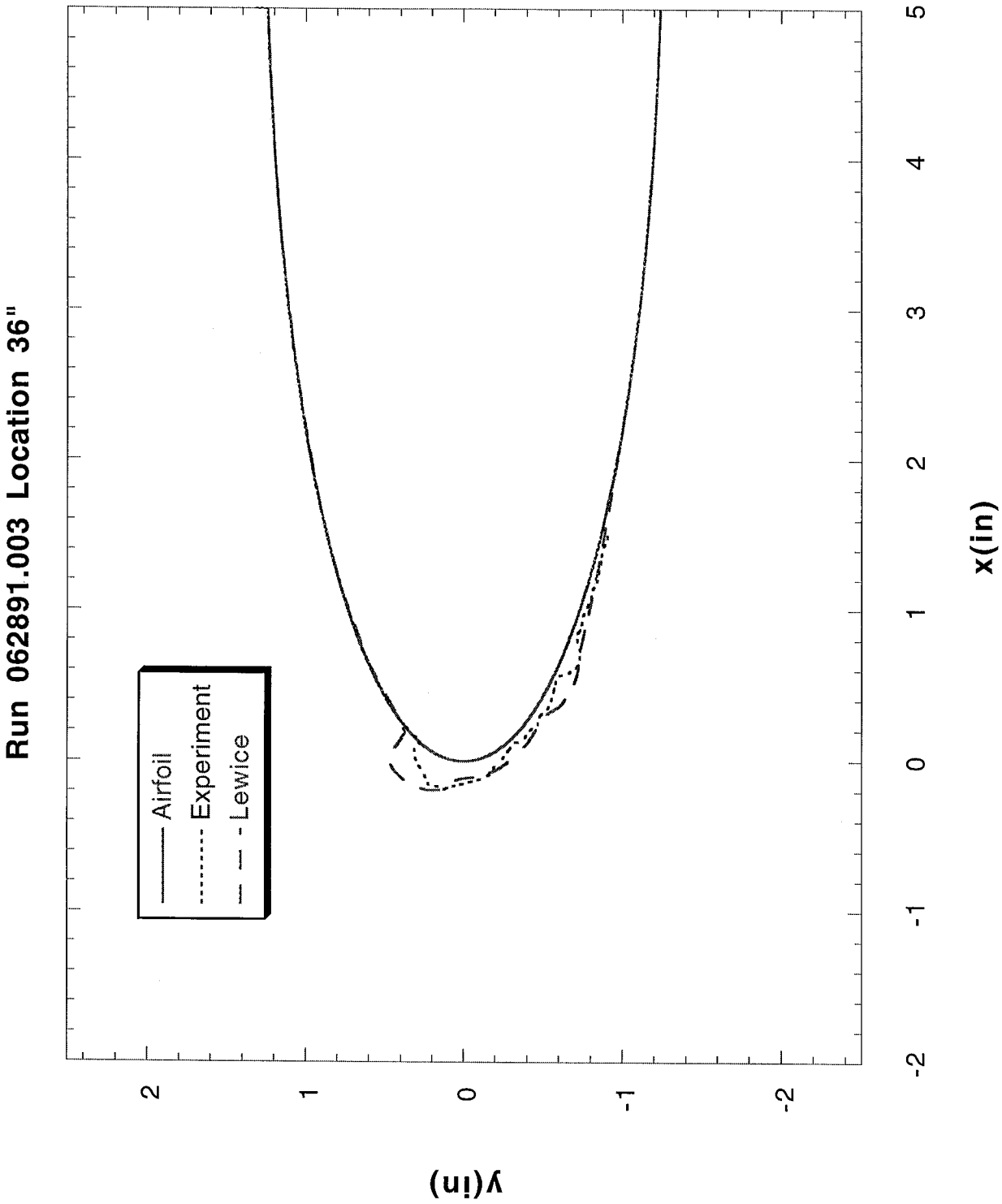
Run 062891.003 Location 36"
Airfoil
Experiment
Lewice
y(in)
x(in)
2
1
0
-1
-2
-2
-1
0
1
2
3
4
5

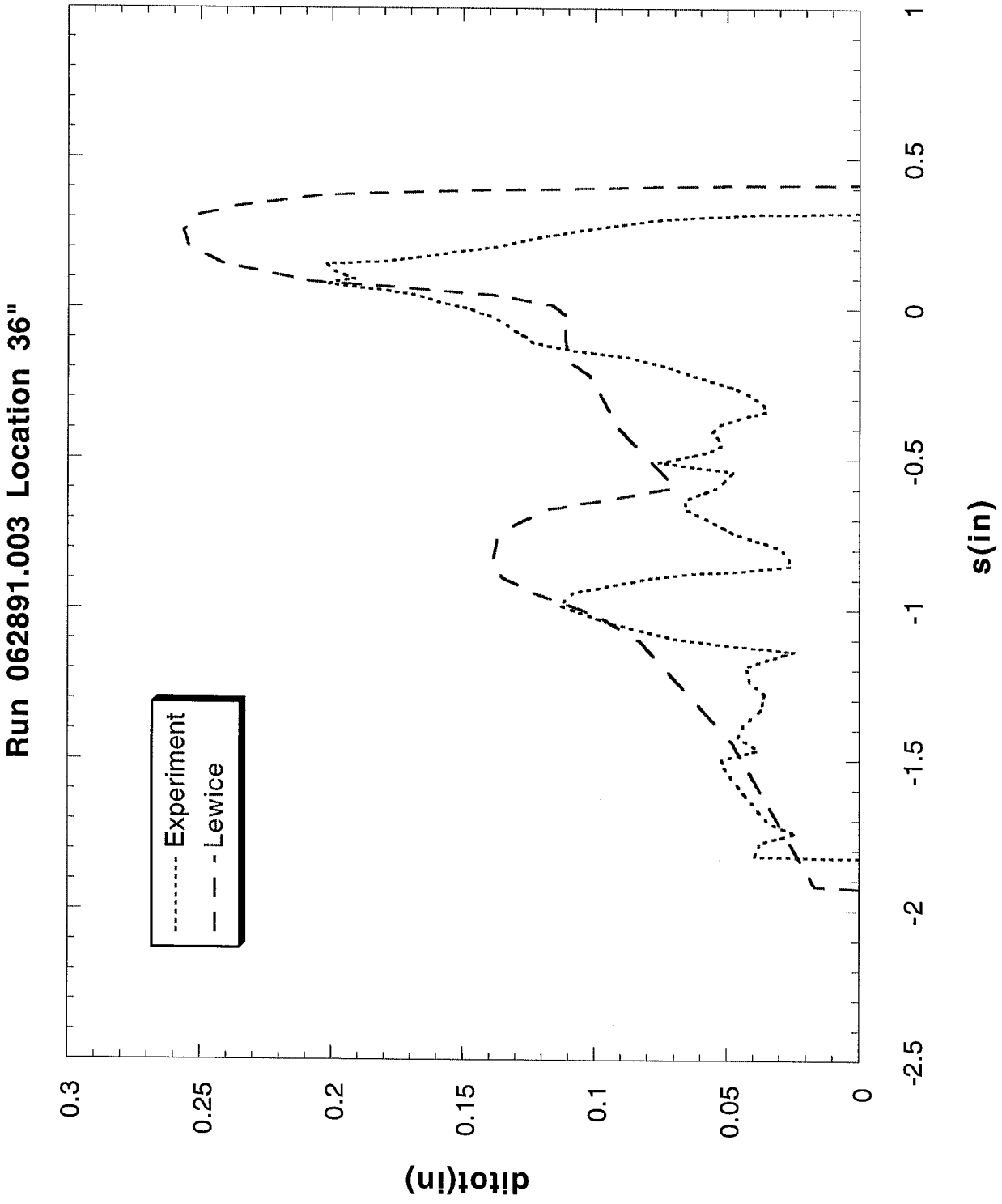
Run 062891.003 Location 36"
Experiment
Lewice
dltot(in)
s(in)
0.3
0.25
0.2
0.15
0.1
0.05
0
-2.5
-2
-1.5
-1
-0.5
0
0.5
1

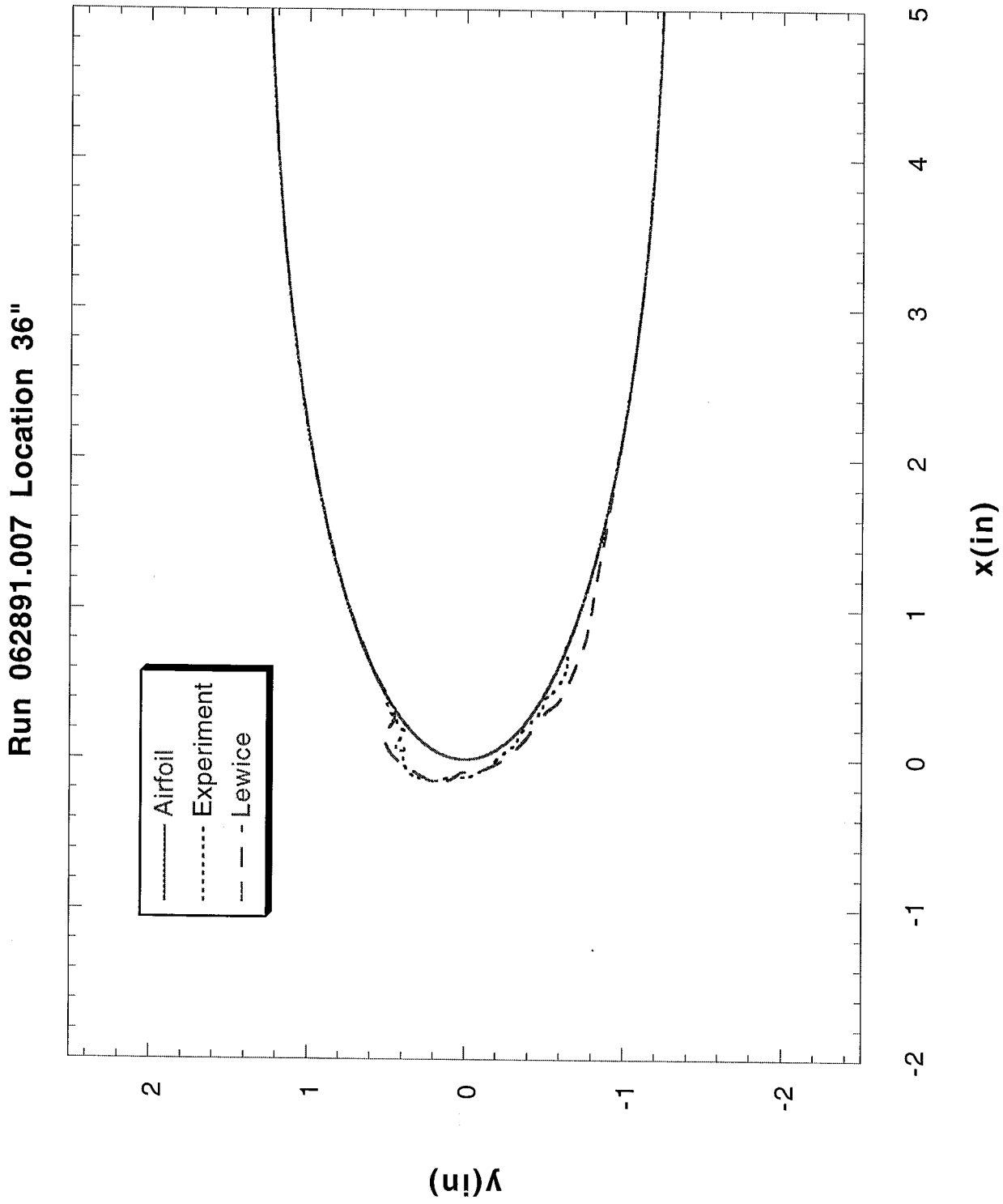
Run 062891.007 Location 36"
Airfoil
Experiment
Lewice
y(in)
x(in)
2
1
0
-1
-2
-2
-1
0
1
2
3
4
5

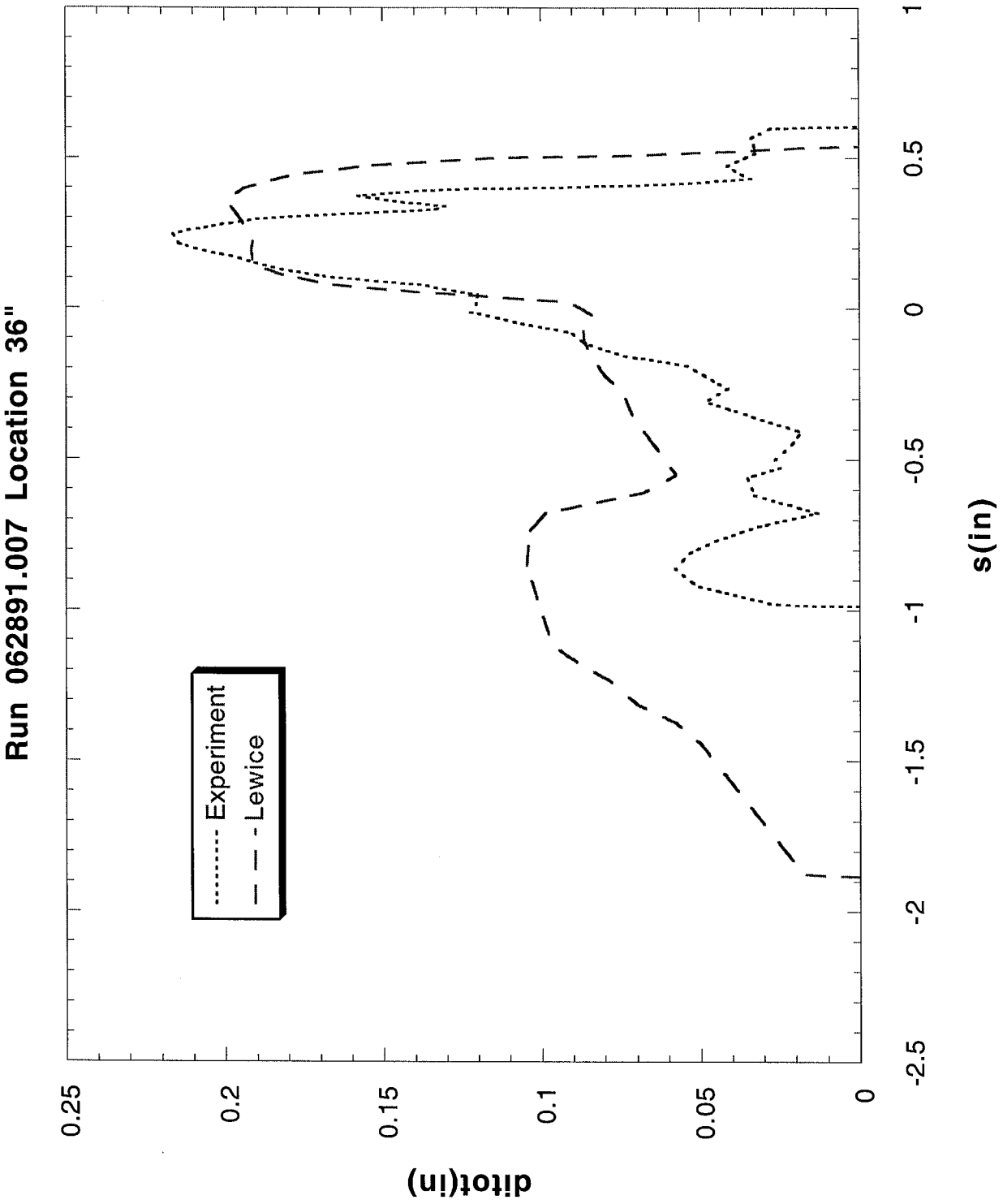
Run 062891.007 Location 36"
Experiment
Lewice
dltot(in)
s(in)
0.25
0.2
0.15
0.1
0.05
0
-2.5
-2
-1.5
-1
-0.5
0
0.5
1

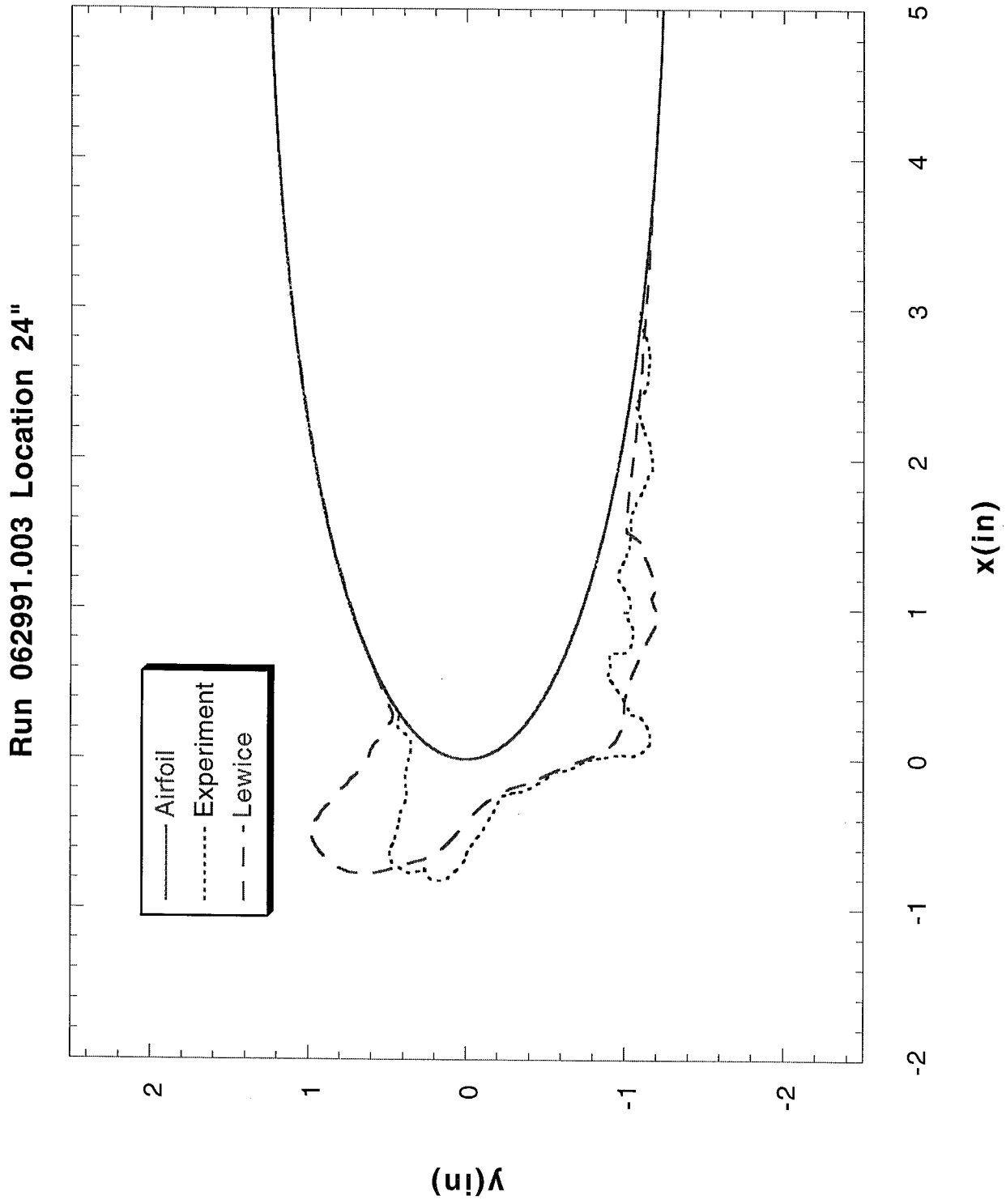
Run 062991.003 Location 24"
Airfoil
Experiment
Lewice
y(in)
x(in)
2
1
0
-1
-2
-2
-1
0
1
2
3
4
5

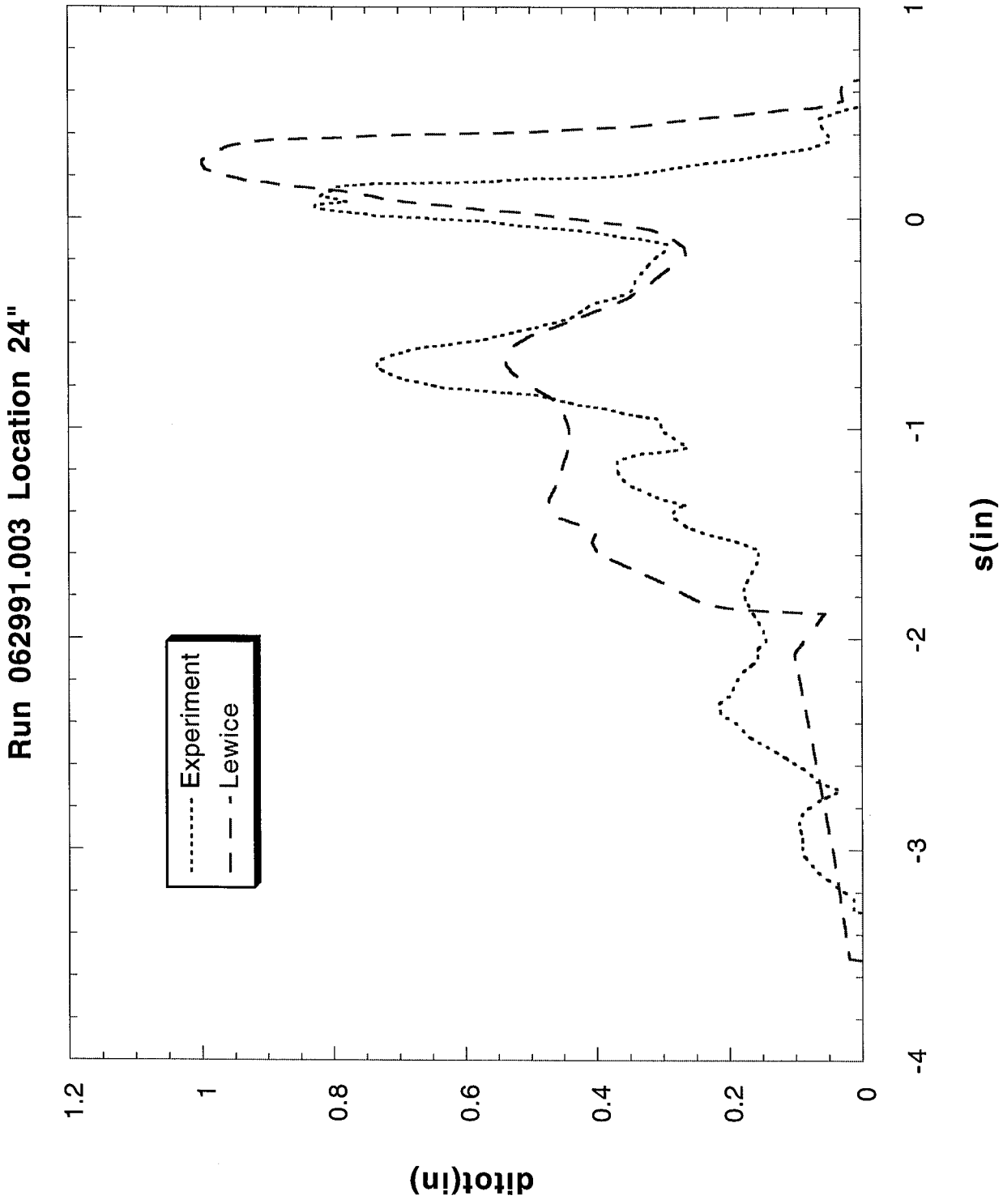
Run 062991.003 Location 24"
Experiment
Lewice
ditot(in)
s(in)
1.2
1
0.8
0.6
0.4
0.2
0
-4
-3
-2
-1
0
1

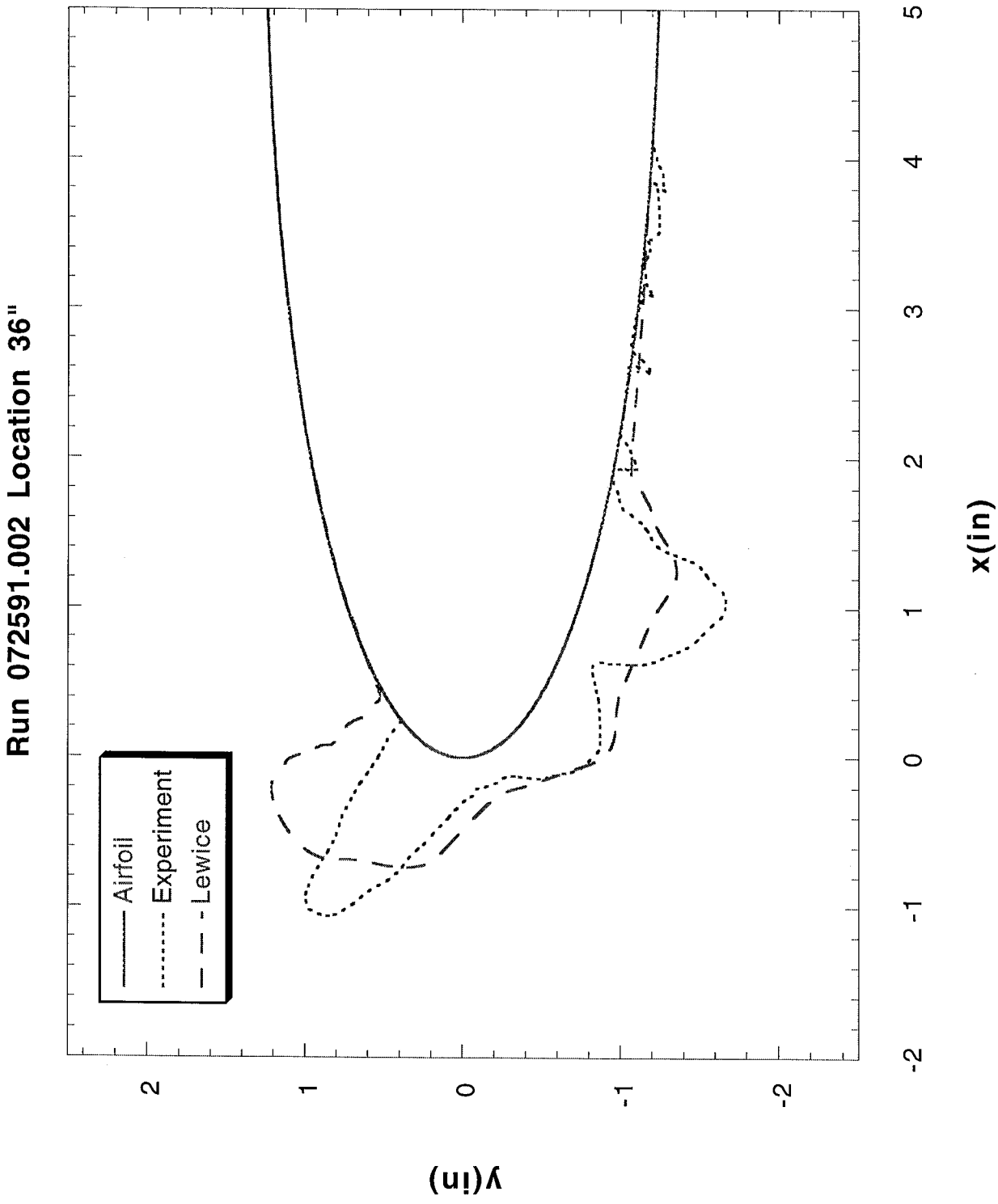
Run 072591.002 Location 36"
Airfoil
Experiment
Lewice
y(in)
x(in)
2
1
0
-1
-2
-2
-1
0
1
2
3
4
5

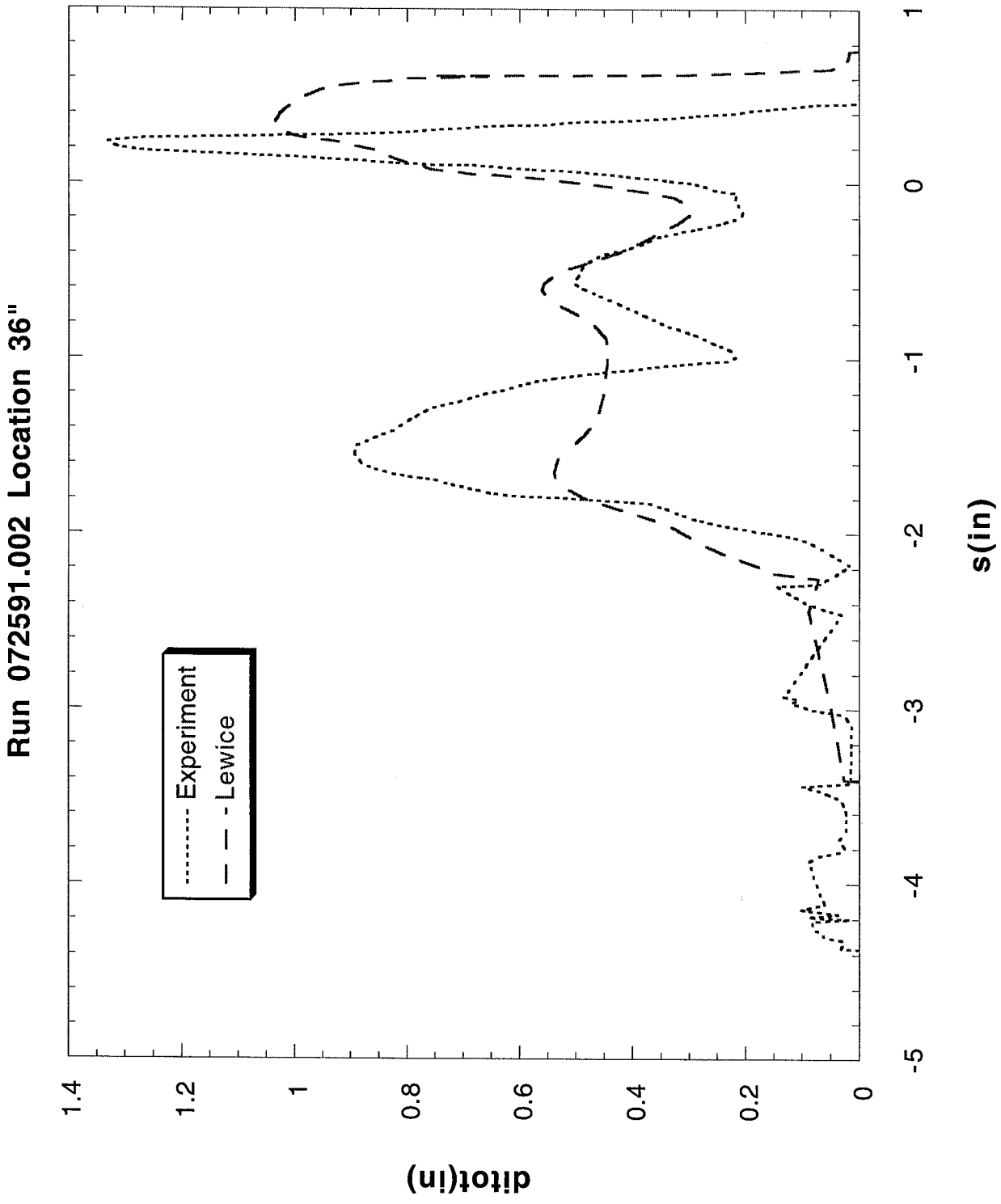
Run 072591.002 Location 36"
Experiment
Lewice
dltot(in)
s(in)
1.4
1.2
1
0.8
0.6
0.4
0.2
0
-5
-4
-3
-2
-1
0
1

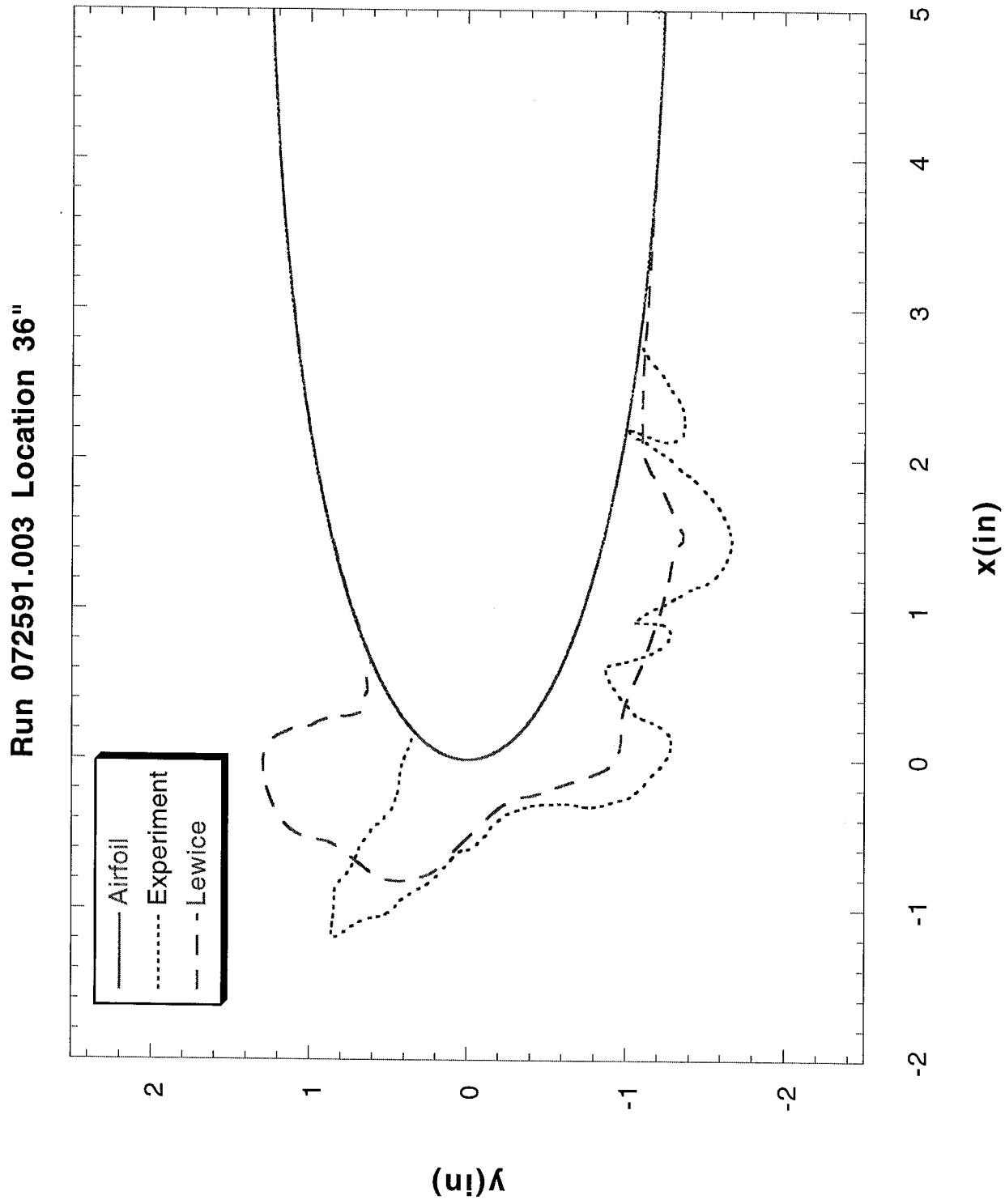
Run 072591.003 Location 36"
Airfoil
Experiment
Lewice
y(in)
x(in)
2
1
0
-1
-2
-2
-1
0
1
2
3
4
5

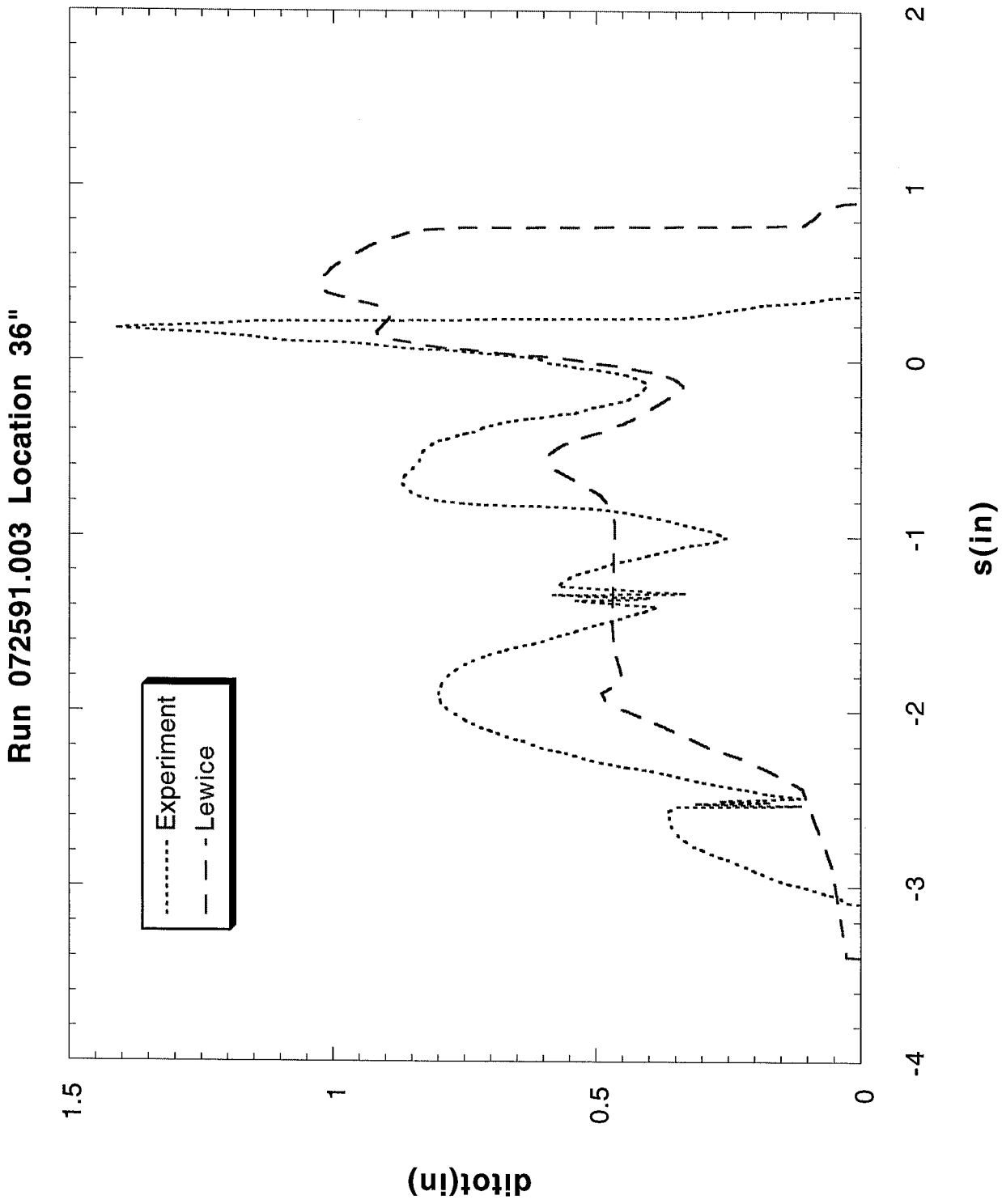
Run 072591.003 Location 36"
Experiment
Lewice
dltot(in)
s(in)
1.5
1
0.5
0
2
1
0
-1
-2
-3
-4

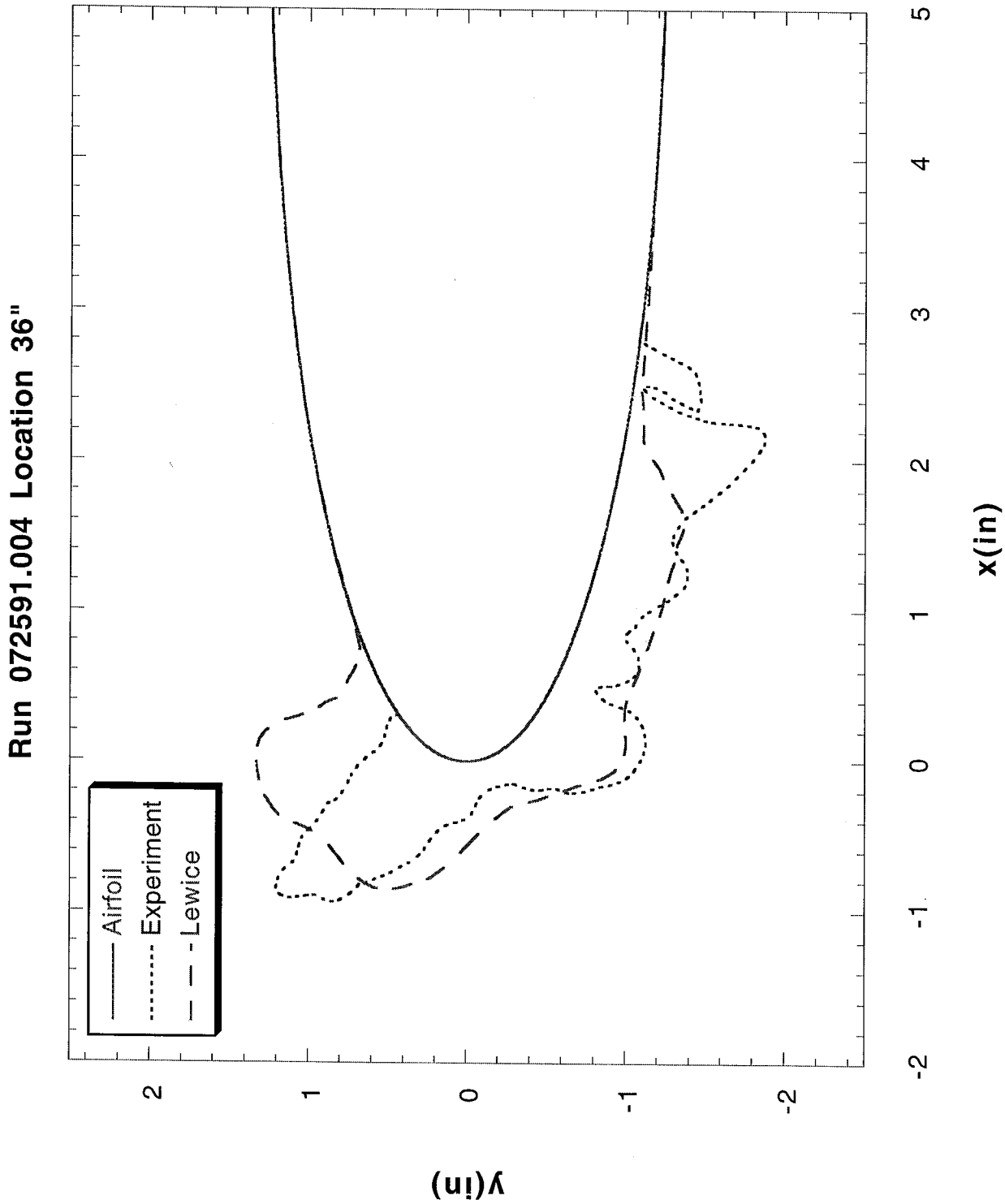
Run 072591.004 Location 36"
Airfoil
Experiment
Lewice
y(in)
x(in)
2
1
0
-1
-2
-2
-1
0
1
2
3
4
5

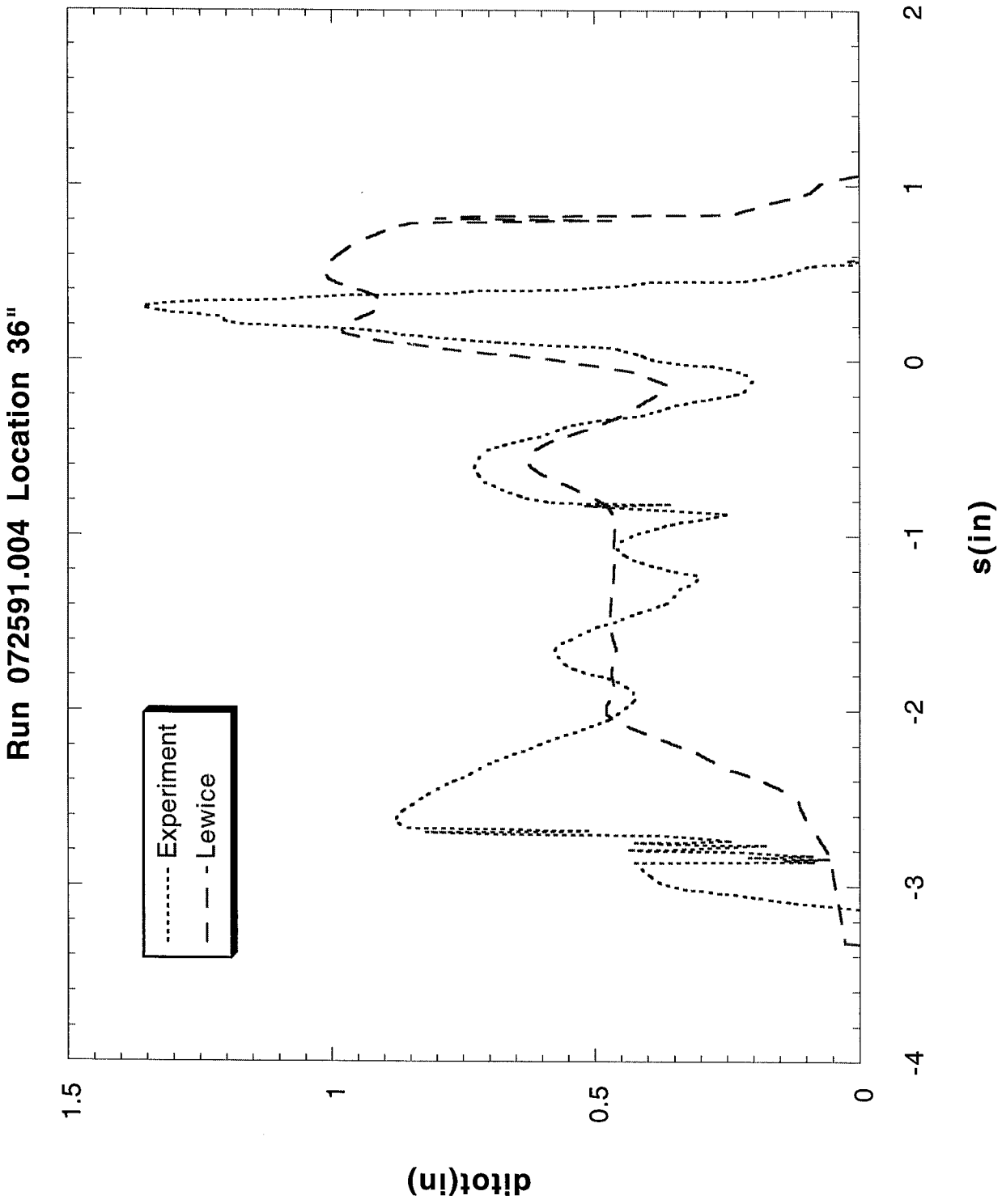
Run 072591.004 Location 36"
Experiment
Lewice
ditot(in)
s(in)
1.5
1
0.5
0
2
1
0
-1
-2
-3
-4

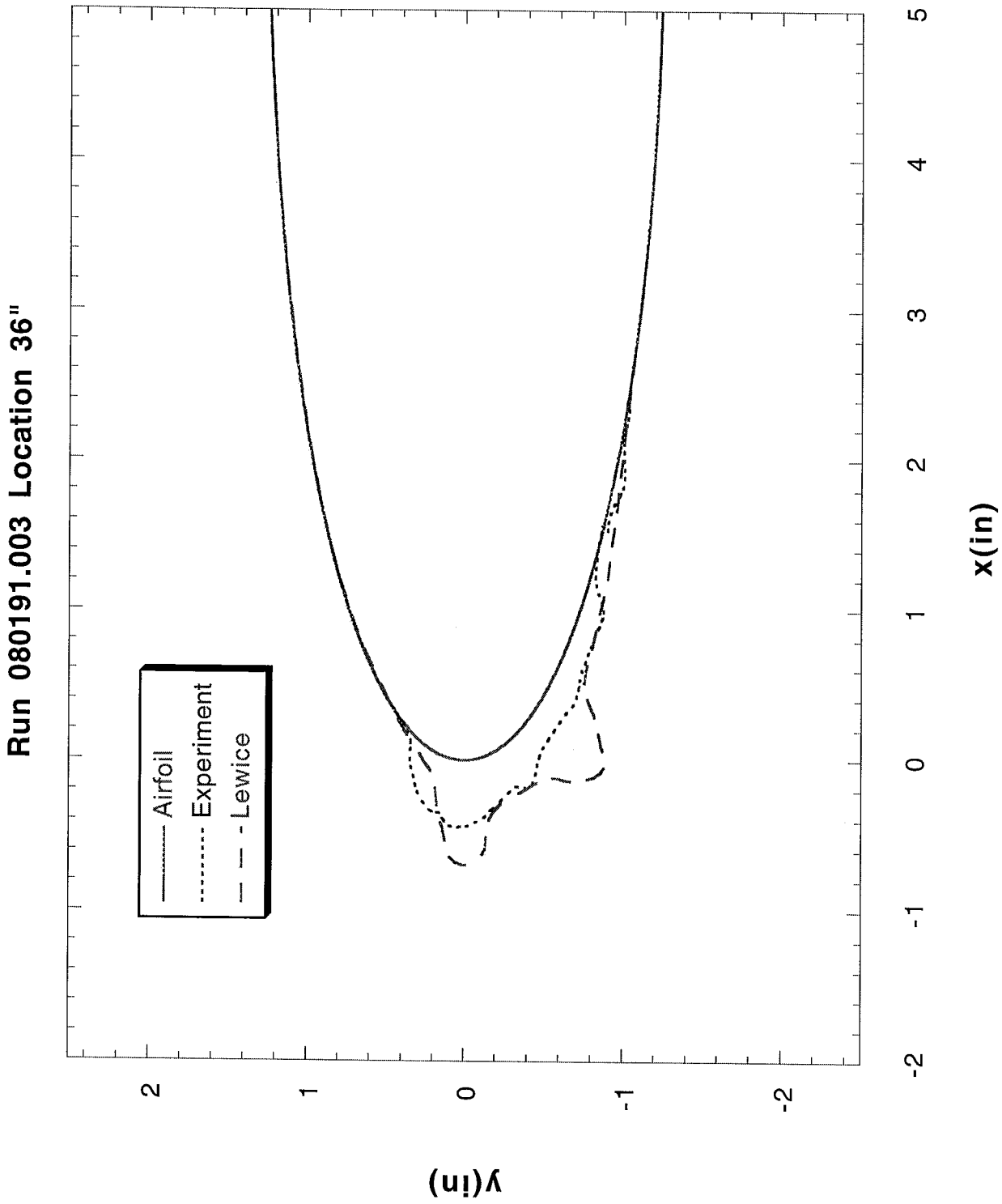
Run 080191.003 Location 36"
Airfoil
Experiment
Lewice
y(in)
x(in)
2
1
0
-1
-2
-2
-1
0
1
2
3
4
5

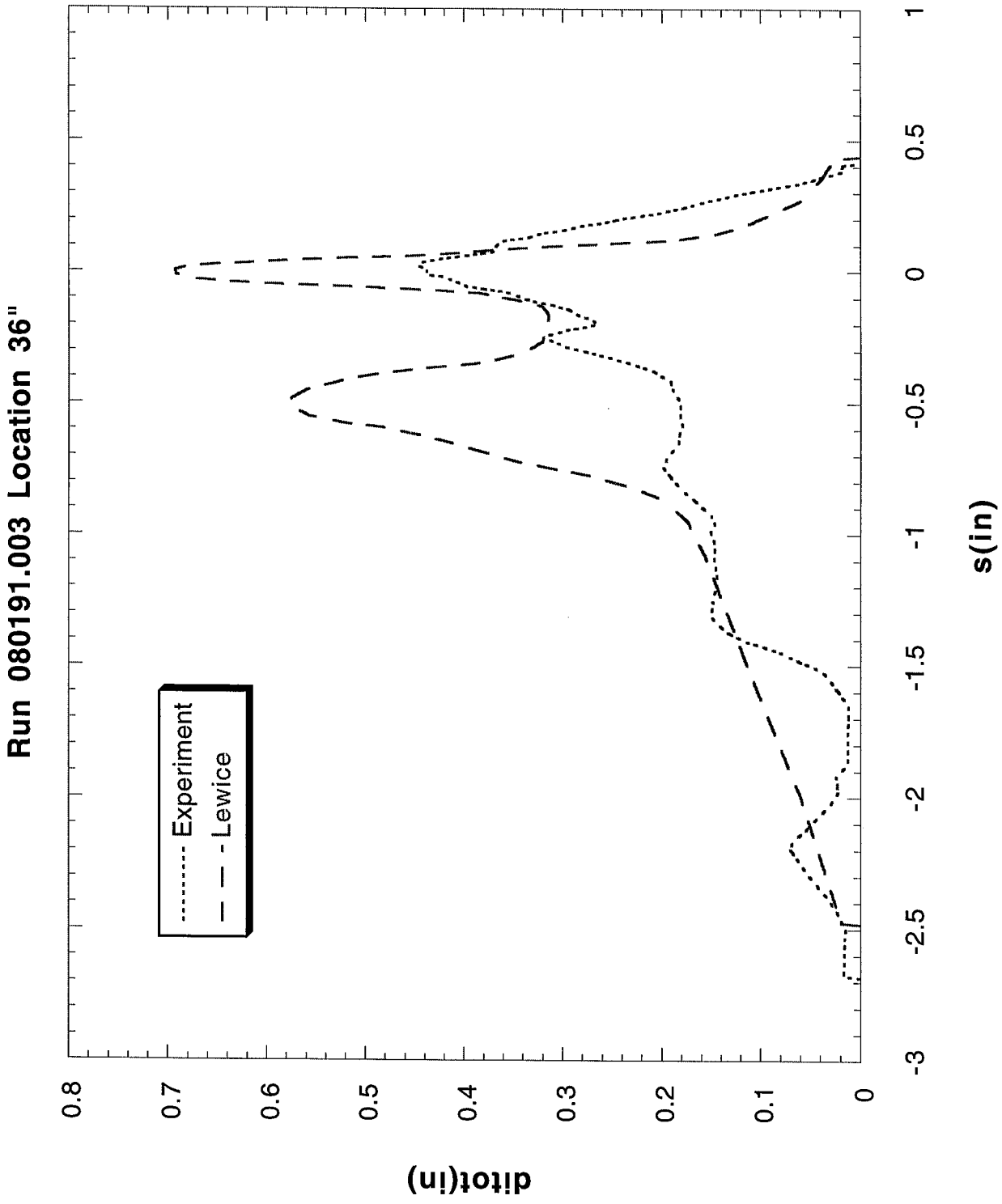
Run 080191.003 Location 36"
Experiment
Lewice
dtot(in)
s(in)
0.8
0.7
0.6
0.5
0.4
0.3
0.2
0.1
0
-3
-2.5
-2
-1.5
-1
-0.5
0
0.5
1

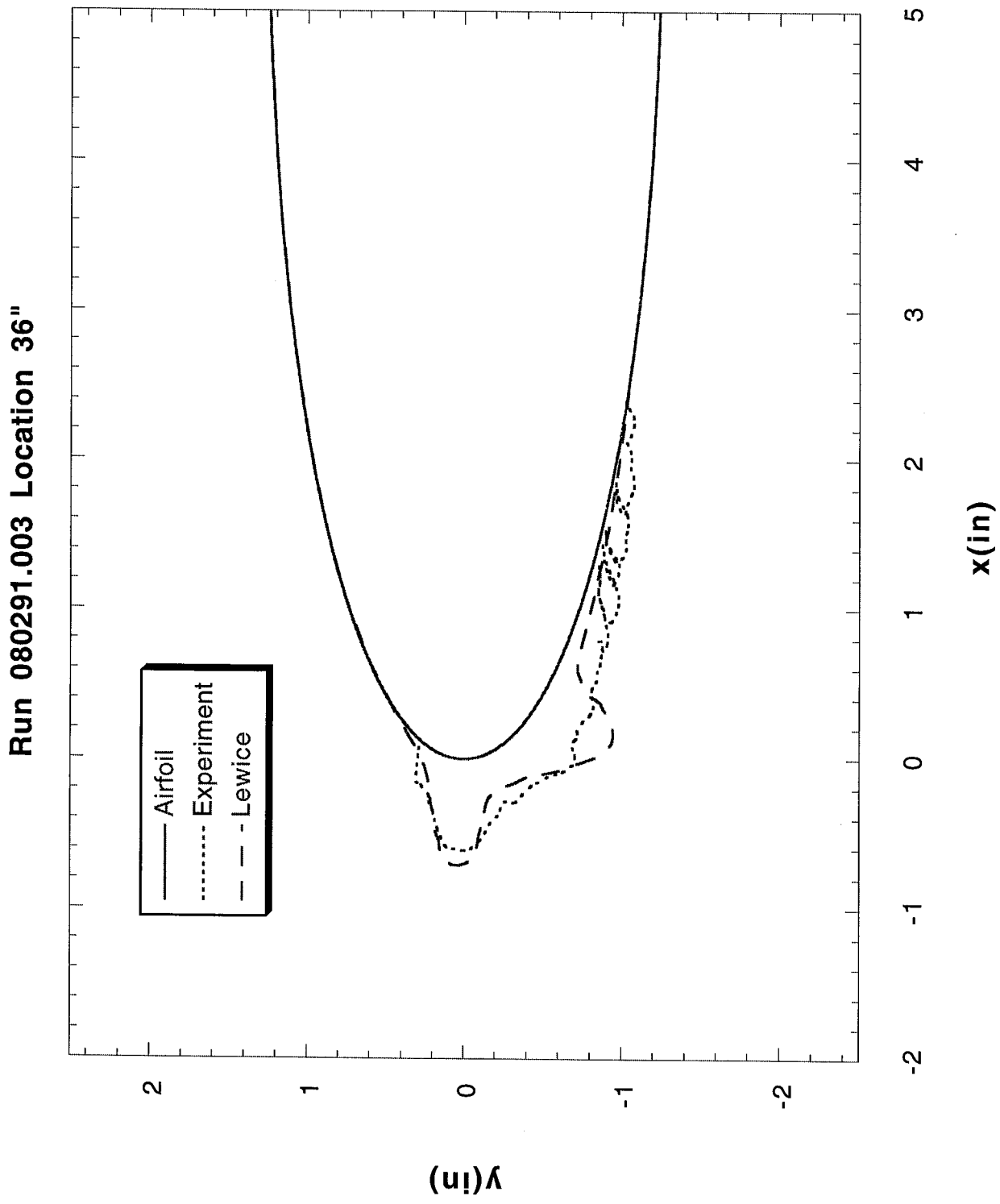
Run 080291.003 Location 36"
Airfoil
Experiment
Lewice
y(in)
x(in)
2
1
0
-1
-2
-2
-1
0
1
2
3
4
5

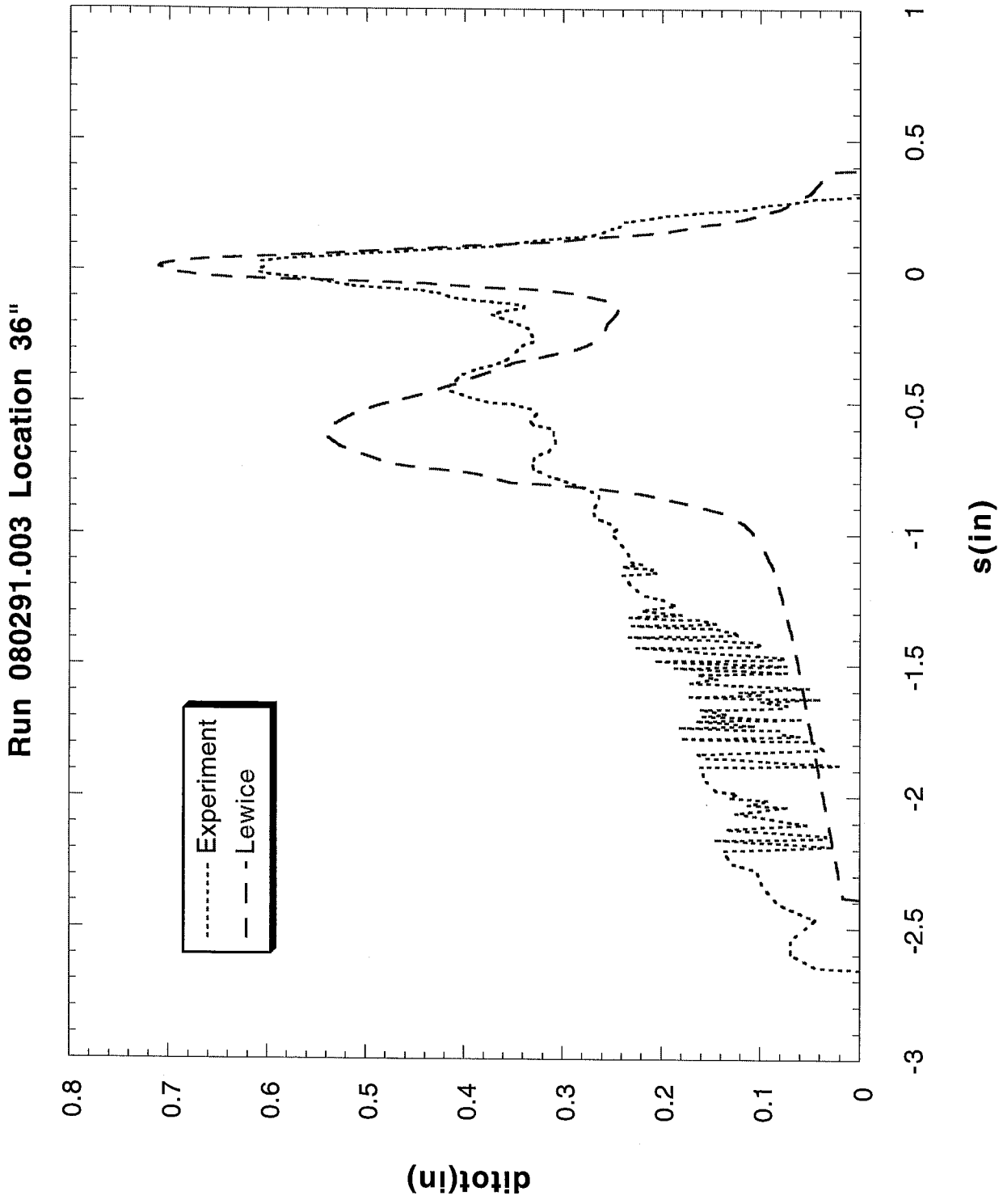
Run 080291.003 Location 36"
Experiment
Lewice
dltot(in)
s(in)
0.8
0.7
0.6
0.5
0.4
0.3
0.2
0.1
0
-3
-2.5
-2
-1.5
-1
-0.5
0
0.5
1

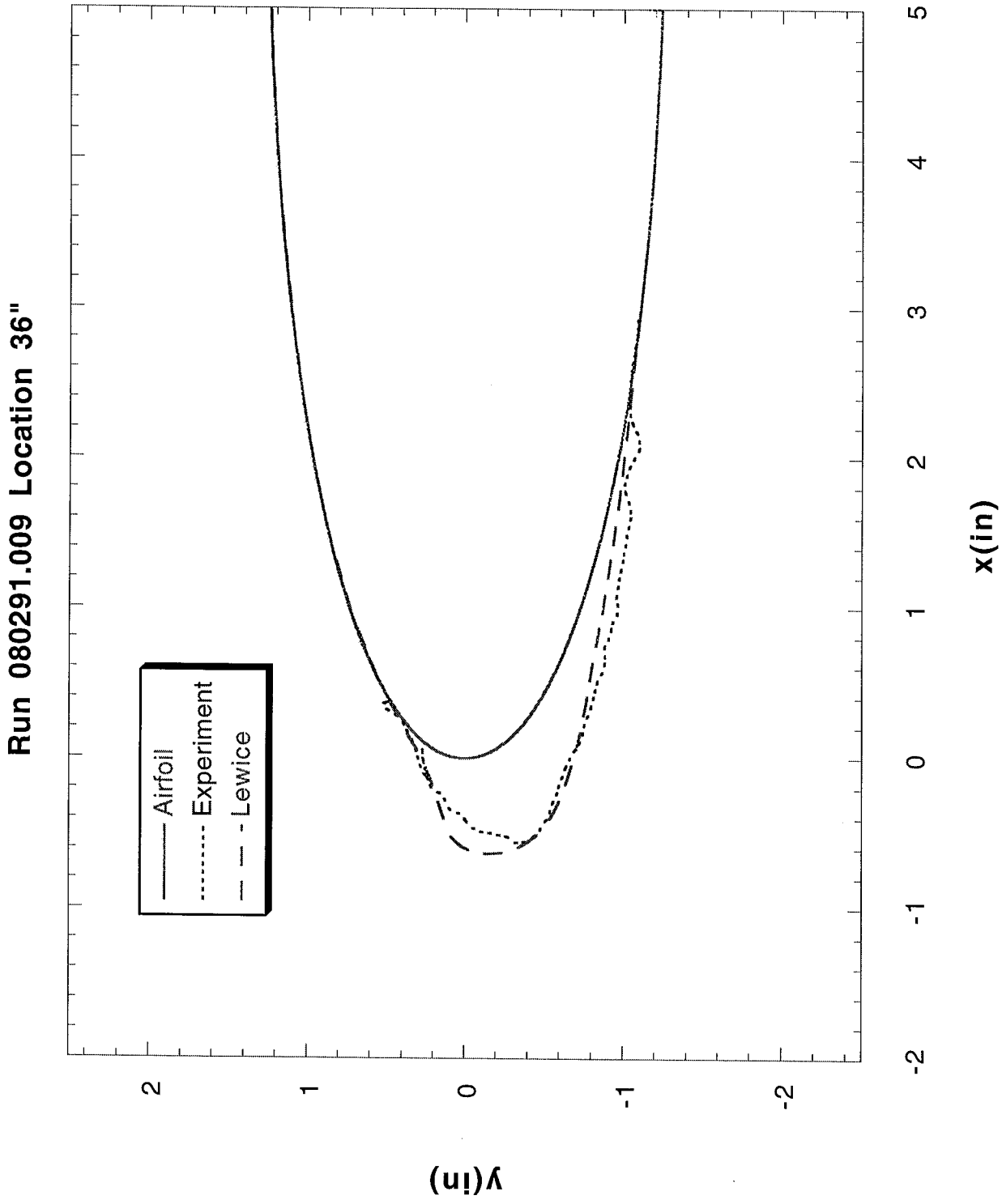
Run 080291.009 Location 36"
Airfoil
Experiment
- Lewice
y(in)
x(in)
2
1
0
-1
-2
-2
-1
0
1
2
3
4
5

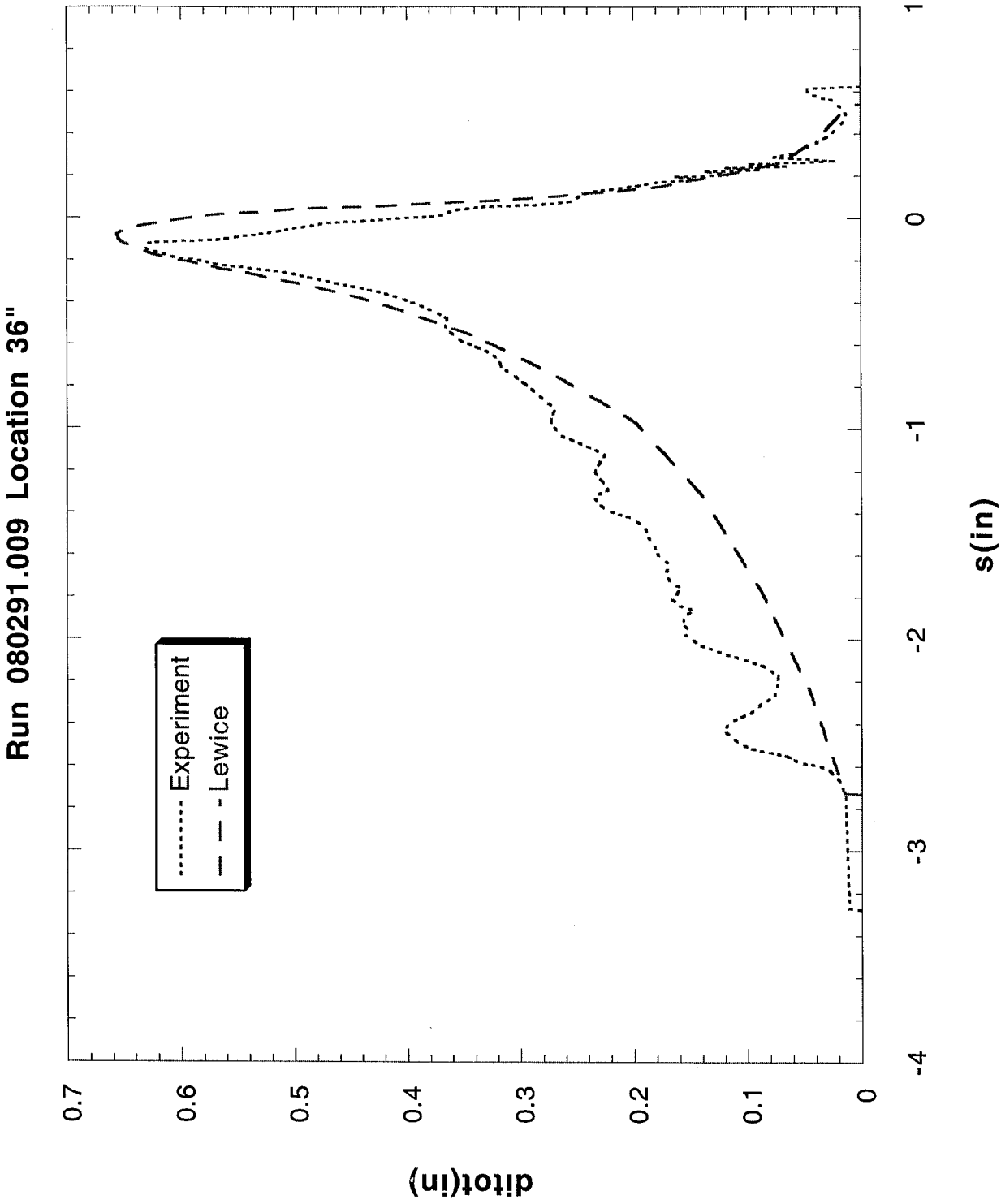
Run 080291.009 Location 36"
Experiment
Lewice
dltot(in)
s(in)
0.7
0.6
0.5
0.4
0.3
0.2
0.1
0
-4
-3
-2
-1
0
1

REPORT DOCUMENTATION PAGE

Form Approved
OMB No. 0704-0188

1. AGENCY USE ONLY (*Leave blank*)	2. REPORT DATE	3. REPORT TYPE AND DATES COVERED
	January 1999	Final Contractor Report

4. TITLE AND SUBTITLE

Validation Results for LEWICE 2.0

5. FUNDING NUMBERS

WU–548-20-23-00
NAS3–98022

6. AUTHOR(S)

William B. Wright and Adam Rutkowski

7. PERFORMING ORGANIZATION NAME(S) AND ADDRESS(ES)

Dynacs Engineering Company, Inc.
2001 Aerospace Parkway
Brookpark, Ohio 44142

8. PERFORMING ORGANIZATION REPORT NUMBER

E–11479

9. SPONSORING/MONITORING AGENCY NAME(S) AND ADDRESS(ES)

National Aeronautics and Space Administration
Lewis Research Center
Cleveland, Ohio 44135–3191

10. SPONSORING/MONITORING AGENCY REPORT NUMBER

NASA CR—1999-208690

11. SUPPLEMENTARY NOTES

Background data available on CD–ROM from the NASA Center for Aerospace Information or the first author. William B. Wright, Dynacs Engineering Company, Inc., (216) 433-2161; Adam Rutkowski, Case Western Reserve University, University Circle, Cleveland, Ohio 44106. Project Manager, Thomas H. Bond, Turbomachinery and Propulsion Systems Division, NASA Lewis Research Center, organization code 5840, (216) 433-3900.

12a. DISTRIBUTION/AVAILABILITY STATEMENT

Unclassified - Unlimited
Subject Category: 02 Distribution: Nonstandard

This publication is available from the NASA Center for AeroSpace Information, (301) 621–0390.

12b. DISTRIBUTION CODE

13. ABSTRACT ***(Maximum 200 words)***

A research project is underway at NASA Lewis to produce a computer code which can accurately predict ice growth under any meteorological conditions for any aircraft surface. This report will present results from version 2.0 of this code, which is called LEWICE. This version differs from previous releases due to its robustness and its ability to reproduce results accurately for different spacing and time step criteria across computing platform. It also differs in the extensive amount of effort undertaken to compare the results in a quantified manner against the database of ice shapes which have been generated in the NASA Lewis Icing Research Tunnel (IRT). The results of the shape comparisons are analyzed to determine the range of meteorological conditions under which LEWICE 2.0 is within the experimental repeatability. This comparison shows that the average variation of LEWICE 2.0 from the experimental data is 7.2% while the overall variability of the experimental data is 2.5%.

14. SUBJECT TERMS

Aircraft icing

15. NUMBER OF PAGES

680

16. PRICE CODE

A99

17. SECURITY CLASSIFICATION OF REPORT	18. SECURITY CLASSIFICATION OF THIS PAGE	19. SECURITY CLASSIFICATION OF ABSTRACT	20. LIMITATION OF ABSTRACT
Unclassified	Unclassified	Unclassified	